ROBOTICS, AUTONOMOUS SYSTEMS AND AI FOR NONURGENT/NONEMERGENT HEALTHCARE DELIVERY DURING AND AFTER THE COVID-19 PANDEMIC

EDITED BY: Mahdi Tavakoli, S. Farokh Atashzar, Ana Luisa Trejos, Simon DiMaio and Patrick M. Pilarski

PUBLISHED IN: Frontiers in Robotics and AI, Frontiers in Big Data, Frontiers in Artificial Intelligence and Frontiers in Neurorobotics

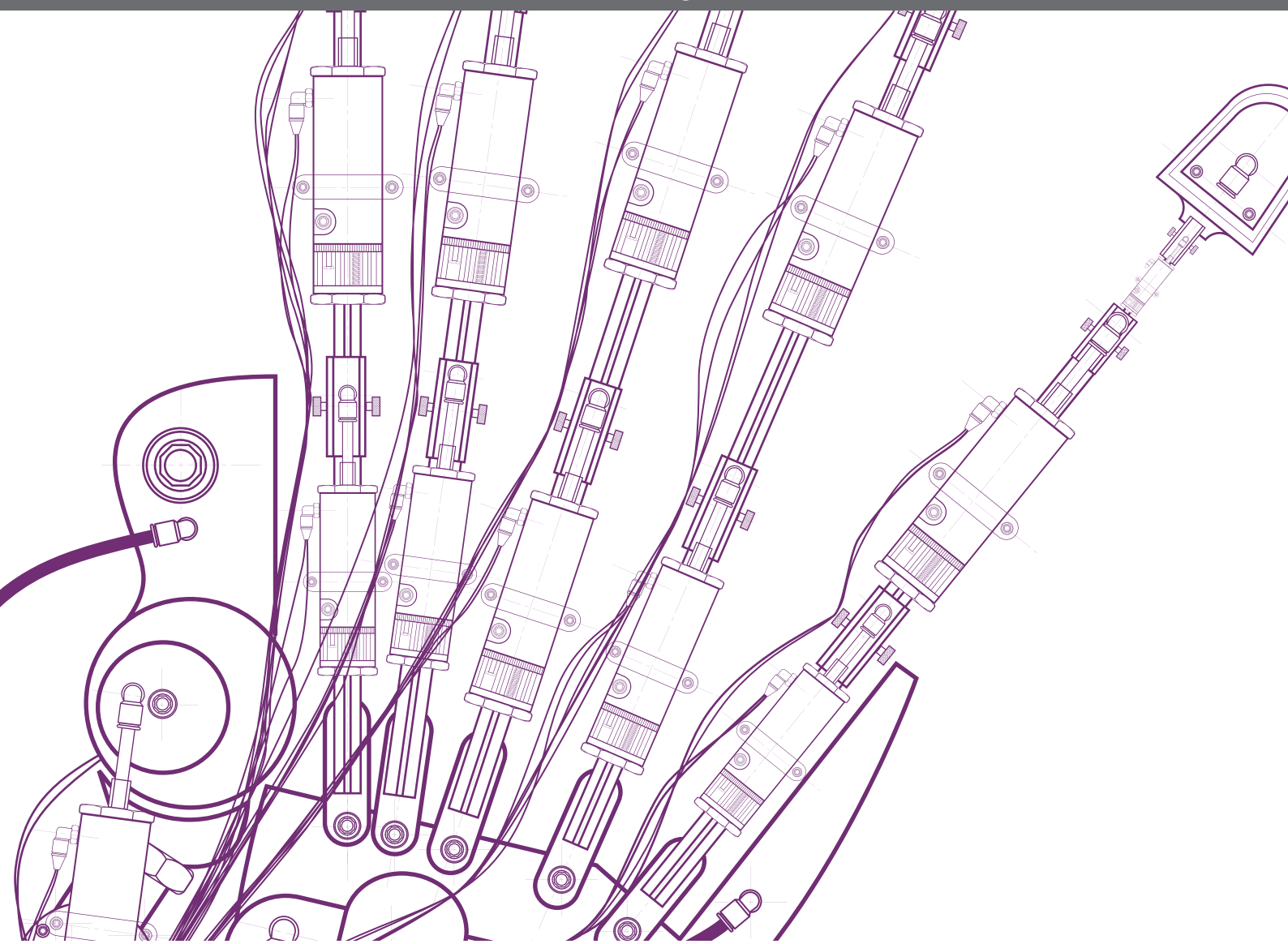

frontiers Research Topics

ISSN 1664-8714
ISBN 978-2-88976-473-0
DOI 10.3389/978-2-88976-473-0

About Frontiers

Frontiers is more than just an open-access publisher of scholarly articles: it is a pioneering approach to the world of academia, radically improving the way scholarly research is managed. The grand vision of Frontiers is a world where all people have an equal opportunity to seek, share and generate knowledge. Frontiers provides immediate and permanent online open access to all its publications, but this alone is not enough to realize our grand goals.

Frontiers Journal Series

The Frontiers Journal Series is a multi-tier and interdisciplinary set of open-access, online journals, promising a paradigm shift from the current review, selection and dissemination processes in academic publishing. All Frontiers journals are driven by researchers for researchers; therefore, they constitute a service to the scholarly community. At the same time, the Frontiers Journal Series operates on a revolutionary invention, the tiered publishing system, initially addressing specific communities of scholars, and gradually climbing up to broader public understanding, thus serving the interests of the lay society, too.

Dedication to Quality

Each Frontiers article is a landmark of the highest quality, thanks to genuinely collaborative interactions between authors and review editors, who include some of the world's best academicians. Research must be certified by peers before entering a stream of knowledge that may eventually reach the public - and shape society; therefore, Frontiers only applies the most rigorous and unbiased reviews.
Frontiers revolutionizes research publishing by freely delivering the most outstanding research, evaluated with no bias from both the academic and social point of view. By applying the most advanced information technologies, Frontiers is catapulting scholarly publishing into a new generation.

What are Frontiers Research Topics?

Frontiers Research Topics are very popular trademarks of the Frontiers Journals Series: they are collections of at least ten articles, all centered on a particular subject. With their unique mix of varied contributions from Original Research to Review Articles, Frontiers Research Topics unify the most influential researchers, the latest key findings and historical advances in a hot research area! Find out more on how to host your own Frontiers Research Topic or contribute to one as an author by contacting the Frontiers Editorial Office: frontiersin.org/about/contact

ROBOTICS, AUTONOMOUS SYSTEMS AND AI FOR NONURGENT/NONEMERGENT HEALTHCARE DELIVERY DURING AND AFTER THE COVID-19 PANDEMIC

Topic Editors:
Mahdi Tavakoli, University of Alberta, Canada
S. Farokh Atashzar, New York University, United States
Ana Luisa Trejos, Western University, Canada
Simon DiMaio, Intuitive Surgical, Inc, United States
Patrick M. Pilarski, University of Alberta, Canada

Citation: Tavakoli, M., Atashzar, S. F., Trejos, A. L., DiMaio, S., Pilarski, P. M., eds. (2022). Robotics, Autonomous Systems and AI for Nonurgent/Nonemergent Healthcare Delivery During and After the COVID-19 Pandemic. Lausanne: Frontiers Media SA. doi: 10.3389/978-2-88976-473-0

Table of Contents

frontiers | Frontiers in Robotics and AI

EDITORIAL
published: 08 June 2022
doi: 10.3389/frobt.2022.886926

Editorial: Robotics, Autonomous Systems and AI for Nonurgent/ Nonemergent Healthcare Delivery During and After the COVID-19 Pandemic

A. L. Trejos[1], S. F. Atashzar[2], S. P. DiMaio[3], P. M. Pilarski[4] and M. Tavakoli[4]*

[1]Western University, London, ON, Canada, [2]New York University, New York City, NY, United States, [3]Intuitive Surgical, Inc., Sunnyvale, CA, United States, [4]University of Alberta, Edmonton, AB, Canada

Keywords: robotics, autonomous systems, artificial intelligence, healthcare, COVID-19

Editorial on the Research Topic

Robotics, Autonomous Systems and AI for Nonurgent/Nonemergent Healthcare Delivery During and After the COVID-19 Pandemic

In an emergency, all resources are dedicated to ensuring survival. This was also true of the COVID-19 pandemic, in which, in an effort to keep people safe, research was directed to understanding the virus better and ensuring vaccines were developed. However, the vulnerability of our health care system was also exposed when we saw nonurgent and nonemergent cases fall through the cracks while resources were directed at addressing the emerging health crisis. This special issue aimed to capture novel research directions and perspectives on technological advances that can be put in place to support health care: from novel techniques for diagnosing and treating COVID-19 and preventing spread, to tools and procedures that support other aspects of our health during and after the pandemic. A total of 33 articles by 180 leading authors were accepted from around the world, demonstrating a significant effort from the robotics and artificial intelligence (AI) communities to help reduce the impact of the pandemic on our overall health. The articles have been divided into general themes, as described below.

OPEN ACCESS

Edited and reviewed by:
Elena De Momi,
Politecnico di Milano, Italy

****Correspondence:***
A. L. Trejos
atrejos@uwo.ca

Specialty section:
This article was submitted to Biomedical Robotics, a section of the journal Frontiers in Robotics and AI

Received: *01 March 2022*
Accepted: *21 April 2022*
Published: *08 June 2022*

Citation:
Trejos AL, Atashzar SF, DiMaio SP, Pilarski PM and Tavakoli M (2022) Editorial: Robotics, Autonomous Systems and AI for Nonurgent/ Nonemergent Healthcare Delivery During and After the COVID-19 Pandemic. Front. Robot. AI 9:886926. doi: 10.3389/frobt.2022.886926

PREVENTION OF COMMUNITY SPREAD

The first line of defense in a pandemic is to prevent the spread of the virus within the community, and a large component of prevention is proper cleaning and disinfection. Towards this end, the paper by Nasirian et al. proposes an end-to-end coverage path planning (CPP) method using a novel graph representation of the environment that can generate a continuous and uninterrupted collision-free path for an autonomous mobile robot. The proposed method is able to generate an optimal path that can reduce the disinfection task completion time and cost through shorter travel distances and a smaller number of turns than other approaches.

Complementary to disinfection are other ways to prevent the spread of the virus. The work by Michelin et al. aimed to prevent people from touching their faces. A convolutional neural network (CNN) algorithm using data from an inertial measurement unit (IMU) at the wrist was able to predict when a person was about to touch their face. The system then provided sensory feedback in various forms, with vibrotactile feedback providing the fastest response, the best success rate, and the best user experience.

Vicente et al. examine robotics and automation as an approach to reducing the transmissibility of COVID-19 in healthcare environments. Through modeling of temporal and spatial factors in geriatric units, they present a view into how robotic integration at key points in the care environment can have a large potential impact on the spread of pathogens in these units. To demonstrate the breadth of potential applications for robots to prevent viral spread, a review paper by Onaizah et al. evaluated the needs and challenges of designing robotic flexible endoscopes during a pandemic. By making a few minor adjustments to existing platforms, or by considering platforms in development, authors argue that significant benefits can be gained during infection control scenarios.

DIAGNOSTIC TECHNOLOGIES

Once the virus has spread, the second line of defense is to minimize exposure of healthy individuals by identifying and isolating those who are infected. For this purpose, a significant effort has been dedicated by the research community to identify better ways of diagnosing COVID-19 and the secondary effects that result from it. Given the potential health hazards during traditional swab sampling, a sensorized, self-administered oral swab is designed and fabricated by Kumar et al. using a closed-loop kinematic chain and a kirigami-based deployable telescopic tubular structure. Compared to traditional swabbing procedures and robot-assisted swab system, the proposed oral swab is simpler, less resource-intensive, and more convenient for self-administration. Also for swab sampling, Li et al. propose a flexible transoral robot in a teleoperated configuration and with a flexible mechanism. The proposed transoral robot realizes dexterous sampling and a tongue depressor is used to prevent the tongue's interference during the sampling. In an experiment with a human phantom, the usability of the robot is demonstrated. On the imaging side, the article by Deng and Li provides a comprehensive review of published work related to the use of AI and Deep Learning methods for segmentation, detection, diagnosis, and severity assessment for COVID-19 from X-RAY and computed tomography (CT) chest images. Ninety-six published studies are reviewed, with a discussion of future directions and thoughts on data fusion strategies for integrating multi-modality image data for COVID-19 examination. In order to better allocate clinical resources through early diagnosis, Heidarian et al. propose the use of capsule-network-based deep learning algorithms for interpreting CT data with increased spatial acuity, thanks in part to their use of capsule networks in place of more standard convolutional architectures. Their COVID-FACT framework was shown to require less manual intervention by domain experts while achieving accuracy, sensitivity, and specificity suitable for COVID-19 diagnosis. Similarly, in Tse et al., the authors survey the use of CT and its enhancements through methods from the field of artificial intelligence as an approach to COVID-19 diagnosis. They suggest further ways that the automation of CT through advanced computing technology can help combine with other existing approaches to COVID-19 assessment and mitigate risk factors in the supply and deployment of other gold-standard diagnostic approaches. Finally, McDermott et al. examine how lung ultrasound (LUS) is being used to diagnose COVID-19 and note difficulties in interpreting LUS by non-specialized operators. The authors survey algorithms that could potentially be used to automate the task of disease detection, severity classification, and patient triage. A comprehensive and critical review of image processing for lung ultrasound in the context of COVID-19 screening and diagnosis is presented.

COVID-19 PATIENT CARE

Once people are infected with the COVID-19 virus, treatment focuses on symptom management while the body heals; however, in many cases, patients have become severely ill with respiratory tract infections. When the respiratory illness is severe, some COVID-19 patients have required mechanical ventilation to support respiration while healing. Three papers in this special issue were related to the use of mechanical respirators. Mitros et al. presented the design of a 7-DOF robotic bronchoscope that allows accurate sampling of the distal lung in critical care mechanically ventilated patients, in order to improve diagnosis and treatment of lung disease. A prototype of a continuum robot is presented, as well as its mathematical model demonstrating high accuracy. In another paper by Xiao et al. a flexible trans-oral mini-robotic system incorporating a robotic needling technology is proposed to accurately access the cervical trachea in mechanically ventilated patients. Using an "inside-out" approach to the initial trachea puncture, the proposed system can cause fewer complications on the patient's neck and trachea. Finally, considering that the large ventilators that currently exist in intensive care units (ICU) cannot be controlled remotely, even for simple setting adjustments, the work by Vagvolgyi et al. reports on the development of a simple, low-cost telerobotic system to control ventilators using a small Cartesian robot. Engineering system tests and usability tests are reported as successful, and operation time was reduced from 271 to 109 s in a preliminary evaluation.

Other areas of patient care could also be supported by robotic technologies, although additional research is needed. Sierra Marín et al. present a systematic analysis of the perception of healthcare professionals regarding the benefits and uses of robotic systems at various levels in medicine. The paper discusses the design of a perception questionnaire to assess the acceptance and required education for using robots at scale, in order to fight the COVID-19 pandemic. The paper reports on the results obtained from a survey of 41 healthcare professionals, exposing a low level of knowledge about robots and their potential benefits. In addition, the survey highlights that the concern of "being replaced by robots" remains in the medical community. However, overall enthusiasm was reported regarding the use of robots for a crisis such as a pandemic.

TRAINING OF MEDICAL PROFESSIONALS

A large impact of the pandemic was felt in areas of healthcare that were not directly related to COVID-19. For example, teaching and education in healthcare was another area that suffered significantly as a result of closures and contact restrictions. For example, Motaharifar et al. focus on the use of virtual reality (VR), AI, and haptics for enhancing medical training during pandemics such as COVID-19 while reducing physical contact.

This paper specifically focuses on how such technologies can help novice surgeons receive the needed medical training without the need for in-person attendance, using VR, AI, and haptics. It also provides a comprehensive survey describing recent technologies that can be used for reducing physical contact in medical institutes while keeping the quality of training at a high level. Similarly, a deep learning solution for encoding the movement behavior of expert surgeons to be used for rendering is presented in Fekri et al. The work focuses on the development of technologies for training novice residents in the orthopedic surgical drilling procedure, and thus augmenting their educational system through the development of a skill transfer system. The proposed system uses virtual fixtures and haptic guidance for novice surgeons in order to provide timely training for clinicians whose education may be affected by COVID-19. Cheng et al. identify serious challenges to dentistry education and advanced training due to limitations to in-person learning as a result of public health protective measures. As a possible solution, they introduce DenTeach—a remote dental education solution in portable suitcase format that allows dentistry schools to move practical training content to a remote delivery format. They illustrate the feasibility of DenTeach through case study analysis and key performance indicator assessment of hands-on learner interactions with their training device. Also related to dentistry education, Maddahi et al. explore ethical considerations in the use of simulation and robotics in healthcare education. The authors illustrate the principles of "roboethics" with a case study in self-guided dentistry education using such technologies. They examine challenges related to cognitive, affective, and psychomotor learning.

NEUROMUSCULAR REHABILITATION

Regarding medical care, challenges created by the pandemic were particularly noticeable in neurorehabilitation, as the interruption of treatment resulted in critical problems, as highlighted by Lambercy et al. This paper presents the limitations in neurorehabilitation that occurred when the COVID-19 pandemic started and rehabilitation moved to a home setting, as well as some key directions to explore for providing neurorehabilitation from a distance. These include improvements in the usability of available technologies, the development of scalable rehabilitation technologies to account for the increasing number of patients, and clinically relevant and transparent AI to increase patients' trust in the technologies. These ideas are supported by a review by Atashzar et al. on the utility of intelligent robotic solutions for isolated adults with neuro-musculoskeletal conditions. The authors argue that smart robotics and wearable technology can play an important role in the timely delivery of assistance and support to individuals when it is most needed in their care pathway. They further support the perspective that such approaches allow physical distancing and other protective measures suitable for use during an ongoing public health crisis, providing a sound argument for the use of automation in the care of more isolated end users. Similarly, a review paper by Manjunatha et al. focuses on in-home rehabilitation robotics as a medium to deliver the needed therapy during COVID-19, addressing an increasing concern related to the need for rehabilitation therapy delivery during the pandemic. Specifically, the paper focuses on the overloading of the rehabilitation facilities by post-intensive-care patients (after COVID-19 infection) who have developed neurological and physical symptoms and require a wide range of rehabilitative care. This paper conducts a literature review of various telerehabilitation frameworks and robotic solutions that can be used in a hybrid model for providing rehabilitation and assessment. The paper also provides insight regarding the social support and engagement of patients to further improve the benefits of telerehabilitation systems. Finally, a perspective article by Ahmed provides a brief review and the author's opinion—as a neurologist—on how several routine protocols in healthcare may be improved using robotics and AI. The author indicates that such technologies can be merged with our home environments and various levels of healthcare delivery (from ambulance services to hospitalization and discharge) with a specific focus on how such technologies could potentially help the healthcare system during a health crisis such as the COVID-19 pandemic.

Various papers in this issue presented specific tools to aid neurorehabilitation. For example, arguing that early neurorehabilitation following a stroke cannot be delayed by the increased safety precautions resulting from the pandemic, Akbari et al. present a multi-agent framework for the development of intelligent rehabilitation systems for home use. They also provide a comprehensive review of existing devices that could be integrated into this framework for upper and lower-limb rehabilitation. The existing technologies for delivering mechanical tactile feedback (i.e., vibration, stretch, pressure, and mid-air stimulations) and those that can be integrated into home-based telerehabilitation practice are the special focus in a paper by Handelzalts et al. due to their low cost, compact size, and light weight. The advantages, opportunities, long-term challenges, and gaps with regard to practical implementations are discussed. Neurorehabilitation of gait using a social robot was presented in the work of Céspedes et al. In this study, the social robot monitored the patient's posture and provided motivation and feedback, while quantitative and qualitative metrics were collected. The results show that significant progress was possible, as reflected in improved spinal posture, while the technology allowed physical distancing from caregivers.

Motivated by raising concerns regarding the negative effect of COVID-19 on immobilization and lack of access to physical therapy due to home confinements, isolation, or infections, Akbas and Mummolo focus on balance control as an indicator of corresponding movement disorders. In this work, a new computational framework is proposed, which can be used for the assessment of balance control in the homes of the users and patients. The authors discussed the application of their technique for home-care rehabilitation and assessment of balance exercises. In a case report by Carriere et al., the authors examine the opportunities that machine learning and machine intelligence methods, specifically natural language processing, present for

delivering timely and appropriate acute and chronic rehabilitative care and assessment during an ongoing pandemic. As a concrete example, they discuss the deployment of a telehealth service called the Rehabilitation Advice Line (RAL) to address the immediate rehabilitation needs of patients. They then comment on how artificial intelligence and machine learning can be used to both enhance services like RAL, and leverage the data provided by such systems.

TELEMEDICINE AND REMOTE INTERACTIONS

Other important methods and tools have been proposed to enable remote interactions, particularly to reduce the risk of virus transmission while maintaining patient care. Wazir et al. present a proof of concept for an emergency, remote monitoring and control system that can be used to retrofit dialysis machines with telerobotic manipulators for safely supporting the treatment of patients with acute kidney disease. The approach allows a human caregiver to remotely control a dialysis session using existing dialysis equipment, thus reducing the use of personal protective equipment (PPE) while minimizing the risk of COVID-19 exposure for healthcare staff and their patients. Grasse et al. investigate the use of a delivery robot for reducing disease exposure to high-risk residents and staff within a care facility. The system uses a voice interface to avoid hands-on interactions and investigates the effects of face masks on speech recognition quality and robustness. Meinhold et al. highlight the accelerated rate of interest in telemedicine and telehealth and focus on designing new technology, i.e., smart tendon hammer, which can be used to remotely conduct deep tendon reflex exams, which is a critical part of routing neurological assessments. The system is also able to differentiate correct and incorrect tapping locations with high accuracy, which is imperative as feedback for the user to provide a high-quality assessment. The proposed technology can allow novices to be also able to conduct the exam remotely, which can be critically useful during shutdowns of medical facilities and infrastructure due to pandemics such as COVID-19. Mehrdad et al. provide a perspective into the role that networked wearable technologies can play in remotely viewing and acting on the unfolding symptoms and outcomes of individuals during a continuing pandemic. They reinforce in their survey the idea that a networked wearable device (Internet of Medical Things—IoMT) can allow the acquisition of critical data for advanced monitoring and predictive disease mitigation, potentially enhancing policy making by governments and global health regions. Finally, Work by Feizi et al. showcases the potential of robotics and artificial intelligence for teleoperation in surgical interventions and training during ongoing COVID-19-related public health measures. They specifically examine intelligent robotics in the areas of robotics-assisted surgery, tele-examination pre- and post-surgery, and surgical training. As one important contribution of their perspective article, they illustrate the role that smart teleoperation can play in reducing the potential for virus transmission in a surgical setting.

Of important consideration during these trying times has been the need for a more human approach to care delivery. Lima et al. present the design, development, and testing of a multimodal robotic framework for a more affective human-robot interaction to support dementia patients using telemedicine. A hybrid face robot design that combines digital facial expressions with static 3D facial features is reported, and a contextual virtual assistant is introduced that enables the robot to adapt its facial expressions to the user's speech in real time.

CONCLUSION

Based on the contributions included in this special issue, a comprehensive picture has emerged on the state of the art of robotics and AI to address healthcare needs resulting from the pandemic, highlighting new and impactful directions that may be explored in future work. These research directions have aimed to address several COVID-19 related issues, including techniques for preventing the spread of the virus via cleaning, disinfection and shielding; diagnostic technologies that include swabbing and new image processing techniques; and methods for improving mechanical ventilation of critically ill patients. Research has also aimed to address issues not directly related to COVID-19, but that resulted from closures and long periods of quarantine required throughout the pandemic. These include technologies for teaching medical skills in various disciplines, new advances that aim to address rehabilitation of neuromuscular disorders, and other innovations in telemedicine. Although new technologies and techniques have been developed, further research and development is needed in order to fully exploit the benefits of the field for supporting the healthcare system now and in the years to come.

AUTHOR CONTRIBUTIONS

All authors provided an editorial summary of the papers edited. PP provided an editorial summary of the articles edited by guest editors. AT organized the editorial by topic, wrote the connecting sections and formatted the document. All authors reviewed and edited the document.

Conflict of Interest: SPD is employed by Intuitive Surgical, Inc. PMP is employed by DeepMind, a subsidiary of Alphabet Inc., and on the board of directors of the Alberta Machine Intelligence Institute (Amii). SFA is an inventor of "Smart Wearable IOT Device for Health Tracking, Contact Tracing and Prediction of Health Deterioration" which is licensed by Tactile Robotics, Ltd. The remaining authors declare that the research was conducted in the absence of any commercial or financial relationships that could be construed as a potential conflict of interest.

frontiers in Robotics and AI

ORIGINAL RESEARCH
published: 27 November 2020
doi: 10.3389/frobt.2020.575445

Pilot Study of Trans-oral Robotic-Assisted Needle Direct Tracheostomy Puncture in Patients Requiring Prolonged Mechanical Ventilation

Xiao Xiao[1,2,3], *Howard Poon*[4], *Chwee Ming Lim*[4,5], *Max Q.-H. Meng*[1] *and Hongliang Ren*[2,3]*

[1] *Department of Electrical and Electronic Engineering, Southern University of Science and Technology, Shenzhen, China,* [2] *Department of Biomedical Engineering, National University of Singapore, Singapore, Singapore,* [3] *National University of Singapore (Suzhou) Research Institute, Suzhou, China,* [4] *Department of Otolaryngology-Head and Neck Surgery, National University Hospital, Singapore, Singapore,* [5] *Department of Otorhinolaryngology-Head and Neck Surgery, Singapore General Hospital, Singapore, Singapore*

OPEN ACCESS

Edited by:
Mahdi Tavakoli,
University of Alberta, Canada

Reviewed by:
Bernard Bayle,
Université de Strasbourg, France
Selene Tognarelli,
Sant'Anna School of Advanced Studies, Italy

***Correspondence:**
Hongliang Ren
ren@nus.edu.sg

Specialty section:
This article was submitted to Biomedical Robotics, a section of the journal Frontiers in Robotics and AI

Received: *23 June 2020*
Accepted: *27 October 2020*
Published: *27 November 2020*

Citation:
Xiao X, Poon H, Lim CM, Meng MQ-H and Ren H (2020) Pilot Study of Trans-oral Robotic-Assisted Needle Direct Tracheostomy Puncture in Patients Requiring Prolonged Mechanical Ventilation. Front. Robot. AI 7:575445. doi: 10.3389/frobt.2020.575445

COVID-19 can induce severe respiratory problems that need prolonged mechanical ventilation in the intensive care unit. While Open Tracheostomy (OT) is the preferred technique due to the excellent visualization of the surgical field and structures, Percutaneous Tracheostomy (PT) has proven to be a feasible minimally invasive alternative. However, PT's limitation relates to the inability to precisely enter the cervical trachea at the exact spot since the puncture is often performed based on crude estimation from anatomical laryngeal surface landmarks. Besides, there is no absolute control of the trajectory and force required to make the percutaneous puncture into the trachea, resulting in inadvertent injury to the cricoid ring, cervical esophagus, and vessels in the neck. Therefore, we hypothesize that a flexible mini-robotic system, incorporating the robotic needling technology, can overcome these challenges by allowing the trans-oral robotic instrument of the cervical trachea. This approach promises to improve current PT technology by making the initial trachea puncture from an "inside-out" approach, rather than an "outside-in" manner, fraught with several technical uncertainties.

Keywords: tracheostomy, minimally invasive surgery, flexible mini-robotic system, robotic needling technology, mechanical ventilation

1. INTRODUCTION

Tracheostomy, which creates an external opening to the trachea from the neck, is the most common surgical procedure performed in patients with respiratory diseases (e.g., COVID-19) needing prolonged mechanical ventilation (Hur et al., 2020; Mecham et al., 2020; Vargas et al., 2020). Other patients requiring this procedure frequently suffer from blockages in the upper airway, which may be due to the following reasons: subglottic stenosis, neck fractures, and presence of tumors in the head and neck (Gill-Schuster, 2016; Mieth et al., 2016). Other tracheostomy applications include

helping comatose patients expel secretions from their upper respiratory tract or, in the long term, for patients with severe chronic conditions, such as obstructive sleep apnea (Fray et al., 2018). Currently, there are two methods of tracheostomy: Open Tracheostomy (OT) and Percutaneous Tracheostomy (PT).

OT is also called a surgical tracheostomy, which involves making a horizontal or vertical incision approximately half-way between the cricoid cartilage and sternal notch. Dissection is then carried down through the subcutaneous tissues and the platysma muscles, creating a window between the second or third tracheal ring to allow the insertion of a tracheostomy tube for ventilation (Sanji et al., 2017; Kidane and Pierre, 2018). A shoulder roll may also position the patient with an optimal neck extension. Although OT allows excellent visualization of the surgical field and structures, it results in a risk of infection and bleeding, making it an unpopular choice among operators. In surgical tracheostomy, the incidence of local hemorrhage or stomal infection was around 37% (Cipriano et al., 2015; Hoseini et al., 2018).

While OT is still considered the gold standard, PT has proven to be a feasible minimally invasive alternative, gaining attention in recent years (Kannan et al., 2017; Rashid and Islam, 2017). PT remains an attractive option because of the ease of the procedure in carefully selected patients. It also avoids the transfer of critically ill patients to the operating room, implying stresses on the heavily utilized ICU setting resources. PT typically makes a small incision through which a guiding wire is advanced under direct bronchoscopic visualization, resulting in lesser bleeding and infection. The incision is then dilated using dilators until it is wide enough to fit the tracheostomy tube (Sandor and Shapiro, 2016).

However, there are risks involved, and no consensus on which techniques (OT or PT) minimizes complications in critically ill patients (Johnson-Obaseki et al., 2016). Although PT's complication rate is lower than that of OT, PT is more likely to cause serious and permanent complications (Guinot et al., 2012; Simon et al., 2013). It is hard to locate the drilling position as operators can only estimate from anatomical laryngeal surface landmarks. Only 9 out of 20 of the catheters entered the trachea in the correct space between the first and second cartilage rings with external punctures done blindly. One-third of 20 catheters punctured the thyroid, based on a study conducted on cadavers (Dexter, 1995).

Percutaneous procedures posed significant clinical and technical challenges due to the confined workspace, complex surrounding anatomical structures, constrained access to the surgical site, and incomplete exposure and visualization of the surgical field. As a result, complications, such as perforation of the esophagus, considerable vessel injury, the cricoid fracture may be encountered in PT, whereas these complications are not often in OT.

There remains an unmet need to develop novel percutaneous procedures that improve safety outcomes and allows better visualization for the primary puncture, though PTs are routine procedures. Current challenges associated with the use of PT can be summarized as below.

(1). A technician manually drives the introductory needle through tissue and cartilage. By manually driving the needle through tissue and cartilage, the technician risks puncturing through the trachea and esophagus in case of excessive force from the needle. This excessive force may lead to inadvertent perforation of the posterior trachea wall, and even the cervical esophagus, resulting in pneumomediastinum (Khandelwal et al., 2017).

(2). No guiding of aligning mechanism as the needle actuates through tissue. The absence of a guiding aligning mechanism may result in blood vessels being damaged and causing fatal bleeding. Typically, the source of bleeding is from the anterior jugular venous system, which, if encountered, is ligated and divided. Small venous branches can be a continued source of intraoperative and post-operative bleeding (Pilarczyk et al., 2016; Kruit et al., 2018; Sasane et al., 2020).

Besides, intubation and tracheotomy will produce an aerosol in treating pneumonia, which poses a great cross-infection risk to the medical staff.

The da Vinci surgical robot's success has proved that robotic-assisted minimally invasive surgery has great advantages over traditional surgery, such as less trauma, fewer complications, reduced hospital time, and improved surgical outcomes (Li et al., 2020). During the last decade, many specialized surgery robots with different functions have been developed. However, studies on robot-assisted intubation and tracheotomy are rare (Gu et al., 2019; Xiao et al., 2020). Hemmerling et al. (2012) presented the first human testing of a robotic intubation system called the Kepler intubation system for oral tracheal intubation. Do et al. (2016) proposed a mechatronic tracheostomy tube for automated tracheal suctioning. Wang et al. (2018) developed a remote robot-assisted intubation system to improve the success rate of the pre-hospital intubation and rescue model. Most of the studies on the tracheotomy system localize the position between the endotracheal tube and the carina. To the best of our knowledge, there is no tracheotomy robot reported in the literature.

To improve the current PT procedures and to reduce the infection risk of the medical staff in infectious disease unit, we proposed a flexible mini-robotic system incorporating a robotic needling technology, thereby allowing precise access to the cervical trachea. By creating the first puncture using an inside out technique, we believed the PT's current challenges could be potentially addressed. The proposed flexible mini-robotic system will provide new capabilities in the following areas: accurate identification of the proposed trachea puncture, controlled force to the introductory drill, and precision robotic needling puncturing technology as it actuates through tissue into the neck. No device is currently available on the market for performing internal-to-external (i.e., inside-out) punctures through multiple layers of tissue and cartilage. Based on our evaluation, there is presently no development of similar trans-oral tracheotomy puncture systems. This method could provide the basis for other percutaneous, for example, placement of suprapubic catheters and nephrectomies and cholangiostomies.

2. MATERIALS AND METHODS

Both endotracheal intubation and tracheostomy are used to improve respiratory function and facilitate ventilation support treatment. In endotracheal intubation, a flexible plastic tube is placed into the trachea through the patient's mouth. In tracheostomy, an opening is created on the patient's neck to place a curved tube.

By designing a robotic system that drills the hole from within the trachea and outwards, operators can see the drilling position using a camera. This system can cause fewer complications on the patient's neck and tracheae, such as excessive bleeding and the esophagus's possible damage. The proposed procedure is a combination of the endotracheal intubation and PT, which improves the current PT.

The size of the endotracheal tube and tracheostomy tube varies with age and gender. The commonly used measures for adults are listed in **Table 1**. The length from mouth to the trachea is about 21 and 23 cm long for female adults and male adults, respectively (Varshney et al., 2011). The trachea's average diameter for obese and non-obese adults is ∼2.1 and 2 cm, respectively. The puncture should be performed between the first and second or between the third and fourth tracheal rings (Al-Ansari and Hijazi, 2006; Lerner and Yarmus, 2018). These parameters provide a reference for our design.

TABLE 1 | Size of the endotracheal tube and tracheostomy tube.

Instrument	Diameter (female/male mm)	Length (cm)
Endotracheal tube	7.5/8.0	21–23
Tracheostomy tube	10/11	8

2.1. Design of the Flexible Robotic Needling System

A compact and miniature mechanism with variable curvature should be designed to deploy the flexible drill through the mouth to the trachea. The mechanism based on the traditional joint is composed of too many parts, and the rigid structure is not the first choice for safety consideration. Compliant mechanisms are usually monolithic, which transmit motion and force through the elastic deformation of the flexures (Xiao and Li, 2016; Xiao et al., 2017). Combining the concept of compliant mechanism with soft robot and continuum robot, we designed a flexible tube. A flexible tube is designed. To realize the tans-oral tracheostomy puncture, a flexible robotic needling system is proposed, as shown in **Figure 1**. The flexible robotic needling system consists of a linear displacement modular, a flexible tube, and an end tip.

The flexible tube has one bending degree of freedom (DoF); it has an outer diameter of 14.8 mm, length of 180 mm, and 2 mm thickness. The uniformly arranged notches are adopted to increase the tube's compliance to be blended smoothly. Besides, the notches can also let air into the trachea. At the end of the

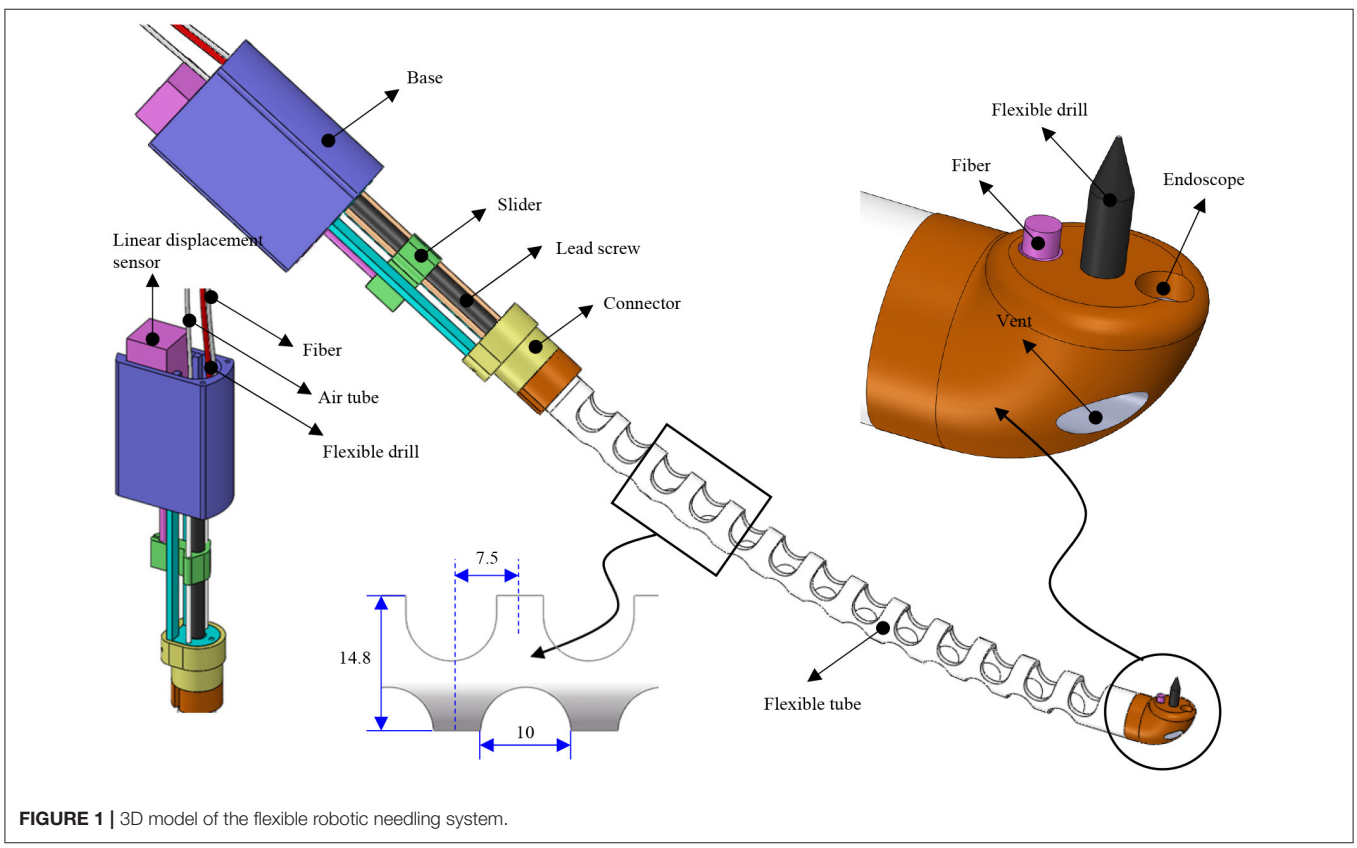

FIGURE 1 | 3D model of the flexible robotic needling system.

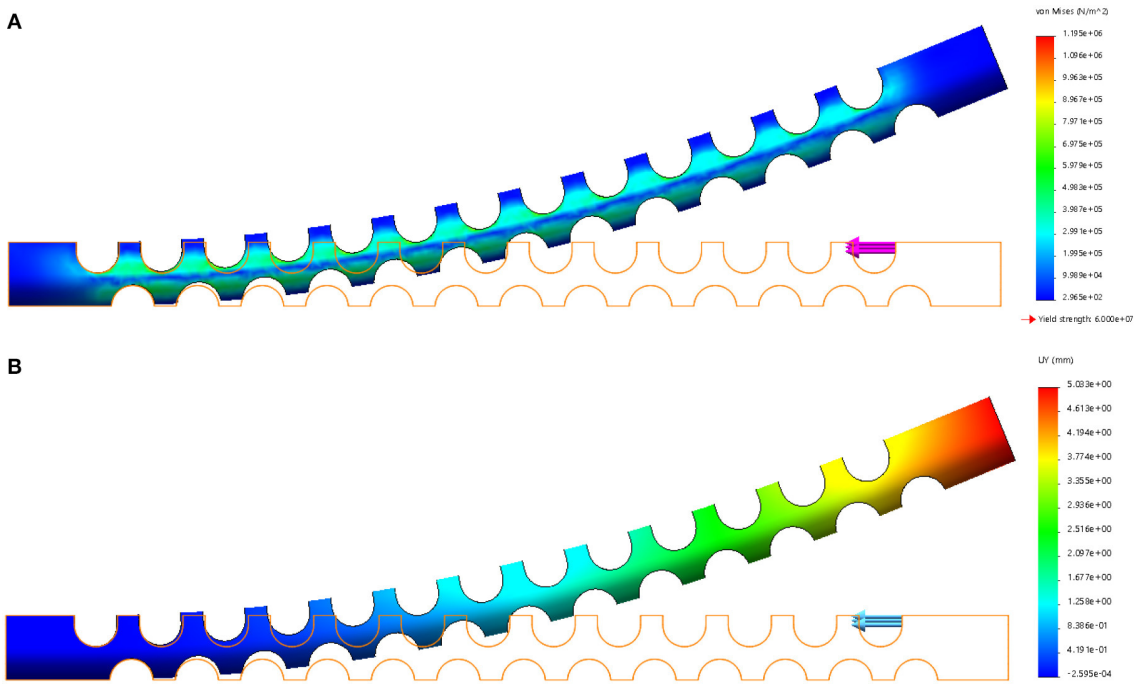

FIGURE 2 | FEA analysis of the flexible tube. **(A)** Strain results, **(B)** Displacement results.

tube, there is a rounded tip. The tip has five channels: flexible drill channel, camera channel, and fiber optic/tendon channel, respectively. The rests located on both sides are stabilization balloon channels, which decrease the vibration induced by the flexible drill. The tip's end surface is parallel to the centerline of the flexible tube so that the flexible drill can drill out vertically to the trachea. To control the bending of the flexible tube, tendon-driven is adopted. One end of the tendon is connected to the round tip, and another end is connected with the slider of the linear displacement modular.

FEA verification is carried out by using the Solidworks Simulation add-ins to validate the flexible tube's compliance. The left side of the flexible tube is fixed, and a 1 N force is applied at the right upper side of the flexible tube. The result is shown in **Figure 2**, the strain distribution is illustrated in **Figure 2A**, it can be observed that the strain mainly occurs around the notches. This is due to the local stretch (bottom layer) and compression (upper layer) during the bending. The displacement of the flexible tube is shown in **Figure 2B**. The largest displacement is 5.033 mm. The compliance can be calculated as 5.033 mm/N and used as a reference for choosing the tendon.

A 3D printed prototype of the flexible robotic needling system is developed, as shown in **Figure 3**. NinjaFlex (NinjaTek, Manheim, PA, USA) is chosen as the flexible tube material due to its superior flexibility and longevity compared to other non-polyurethane materials. The end tip is 3D printed with 3D printed PLA (Poly Lactic Acid).

The flexible drill is a sharped flexible shaft (Hagitec Co Ltd., Tokyo, Japan). The flexible shaft is made of hard steel wires adhesively coiling incrementally thicker steel around a central rod in alternating directions. It can transmit adequate torque to the drill tip. The flexible shaft's helix coils can provide thrust force like a screw when it is rotating.

Fiber optic/tendon (0.75 mm diameter) is introduced to bend the tube and illuminate the visual field. The flexible drill, fiber optic/tendon, and air supply silicone tubes are housed in the flexible tube's cavum. The ends are connected to a DC motor, the linear displacement modular, and a DC mini electric air pump.

2.2. Overview of the Robotic-Assisted Trans-oral Tracheostomy System

As shown in **Figure 4**, a prototype of the flexible mini-robotic tracheostomy system, is developed. The proposed system includes the following parts: a flexible robotic needling system, a stepper motor actuated linear displacement modules, a motion and control unit, DC power supply, and a manual test stand to support them. The flexible robotic needling system is fixed on the linear displacement module platform to pass through the curved oral cavity to the trachea. The working states of the system are demonstrated in **Figures 4B,C**.

The microcontroller used for our prototype is Arduino Due, which will be responsible for controlling the linear displacement module, two DC motors, and the air pump in controlling the vertical linear displacement of the prototype, actuating the tendon to achieve bending of the 3D printed notched tube, the drilling of the flexible shaft, and inflating the stabilization balloon, respectively.

The control diagram for the prototype, shown in **Figure 5**, is made up of relatively independent modules, which primarily guarantees the robustness and convenience of use. It can work

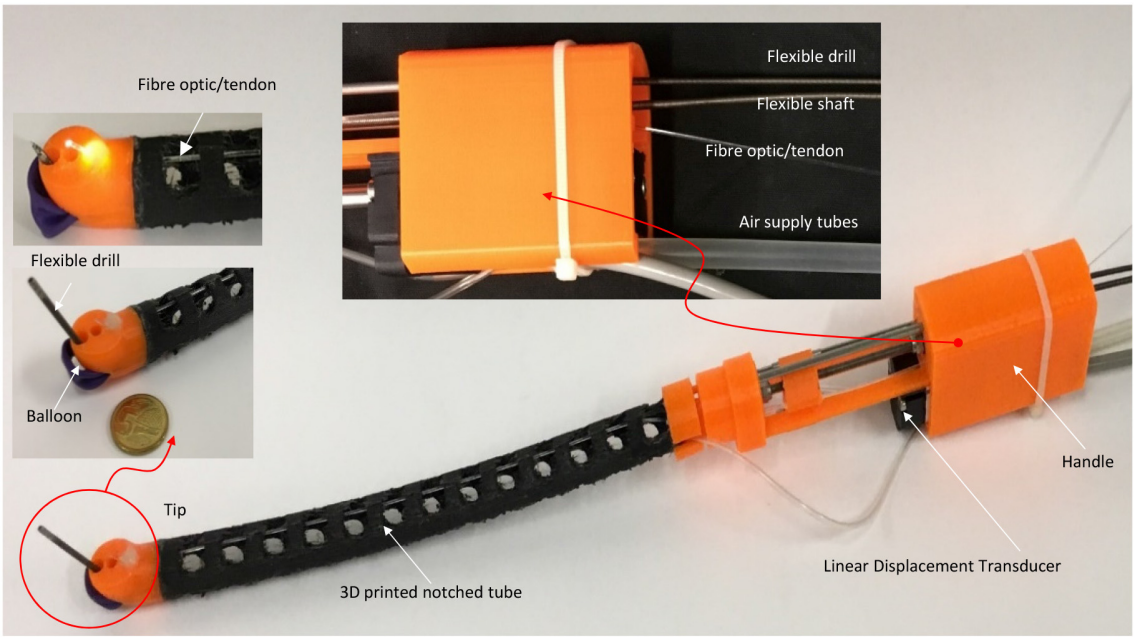

FIGURE 3 | Prototype of the flexible robotic needling system.

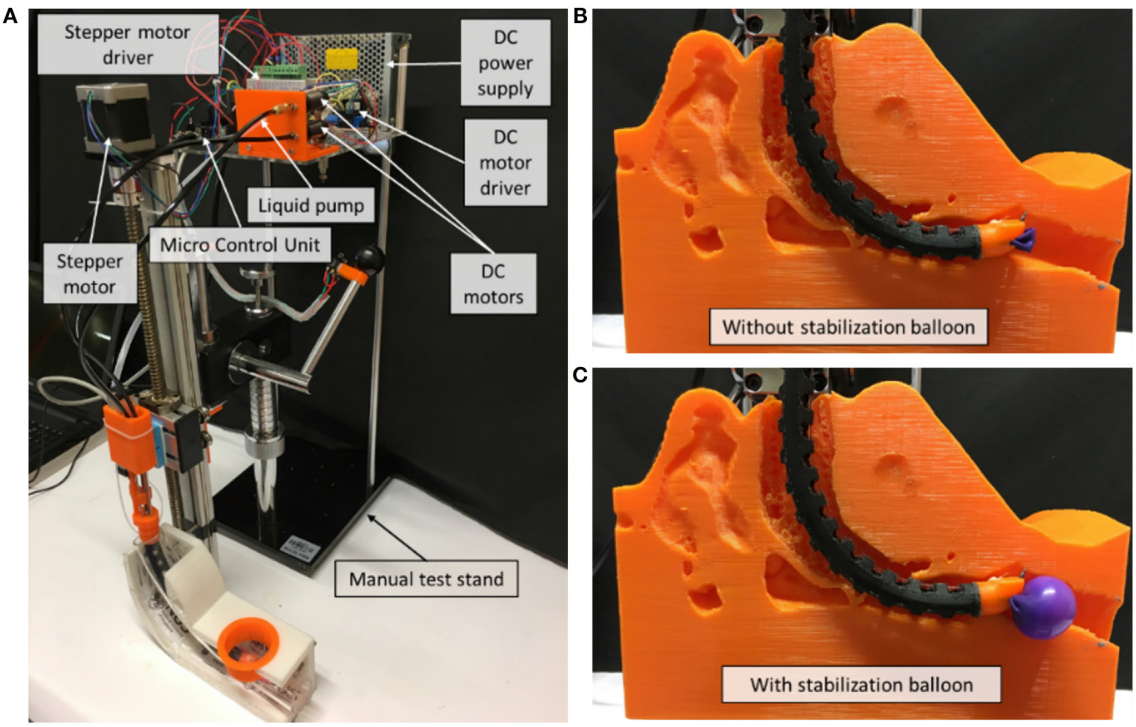

FIGURE 4 | Overview of the robotic system. **(A)** System overview, **(B)** Working state without stabilization balloon, **(C)** Working state with stabilization balloon.

in a passive or automated driven way under compliance control. Human visual feedback enables the closed-loop control of 3D printed notched tubes in adjusting the flexible drilling shaft position and orientation. The operator can control the puncture speed. The fiber optic/tendon displacement is real-time recorded by the linear displacement transducer (Teed KTM-V2-25 mm,

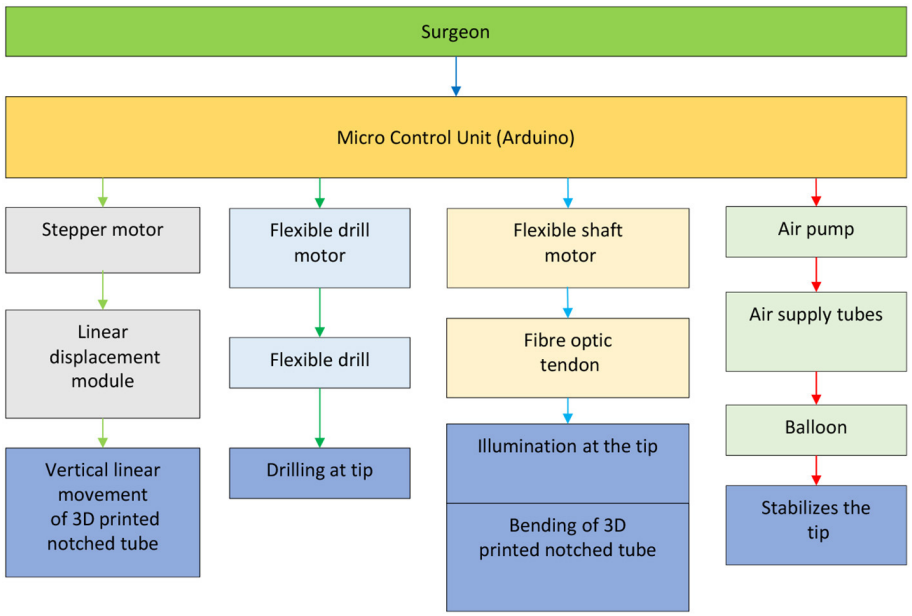

FIGURE 5 | The control diagram of the prototype.

Dongguan Jingbiao Electronic Technology Co. Ltd, China) it will not exceed the limit.

Our proposed design is to incorporate the following novel solutions: (1) a flexible variable curvature tube with a flexible drill; (2) an illumination source and a tendon mechanism to the point of interest; and (3) stability in drilling. The illumination incorporates an optic fiber, which also acts as a tendon in our design. This illumination allowed us to pinpoint precisely the drilling location as the optic fiber near the point of drilling. The balloon stent mechanism is to provide stability when drilling. The exact amount of air can be controlled, and the balloon's pressure can be controlled. Therefore, the amount of force exerted in the trachea wall can be controlled to ensure the least amount of discomfort.

3. RESULTS

3.1. Optic Fiber/Tendon Tensile Test

To measure the ultimate tensile strength of the fiber optic/tendon of the prototype, the monofilament/thread setup, shown in **Figure 6A**, was used. In this test, the optic fiber was placed over the center of the paper frame's slot with one end temporarily fixed with adhesive tape. Next, the same procedure was done to the other end of the optic fiber. A drop of superglue was then applied at both ends of the slots, which ensured that the optical fiber bonds firmly with the paper frame. The optic fiber, together with the frame, was then mounted onto the Instron machine. Before any load was applied, both sides of the paper frame were cut or burnt at mid-gauge (dotted line) with the paper frame unstrained. As shown in **Figure 6B**, the maximum tensile load the optic fiber could withstand, the tensile stress at full load experienced by the optical fiber, and the tensile strain at maximum load experienced by the optical fiber were 30.85 N, 120.88 MPa, and 0.05, respectively. According to the FEA analysis, the compliance of the flexible tube is 5.033 mm/N. A displacement of 50.33 mm can be achieved when 10 N force is applied at the end tip. Therefore, the fiber optic used was able to withstand the tension required to produce the prototype's bending motion.

3.2. Bending Without Load and With Load

The prototype was subject to bending without load, starting from a fully extended bending angle/reference line, as shown in **Figure 7A**. The fiber/optic tendon was controlled randomly in an increasing fashion to see how it corresponded to the bending angle. The slider is managed to pull the tendon to bend the flexible tube. The linear displacement transducer records the displacement of the slider. The displacement of the slide starts from 0 to 20 mm with a 2 mm interval. A camera is positioned perpendicularly to the experimental setup to capture the status of the flexible tube. The images were then uploaded into ImageJ, an open-source image processing program, and the bending angles were measured. The displacements and bending angles were plotted by MATLAB (MATLAB, The Mathworks Inc., Natick, MA, USA). The prototype exhibited an approximately linear relationship between the distance the tendon moved and the bending angle, as shown in **Figure 7B**. According to this result, we can obtain a certain bending angle by setting the tendon's movement. Next, the prototype was subjected to bending under loads, from 0 to 60 g, starting from a fully extended bending angle/reference line, as shown in **Figure 7C**. The loads were loaded at the tip and added in intervals of 10 g. Like the previous experiments, images were captured, analyzed by the image processor, and plotted on a graph. As shown in **Figure 7D**, it was observed that as the weights increase, the bending angle

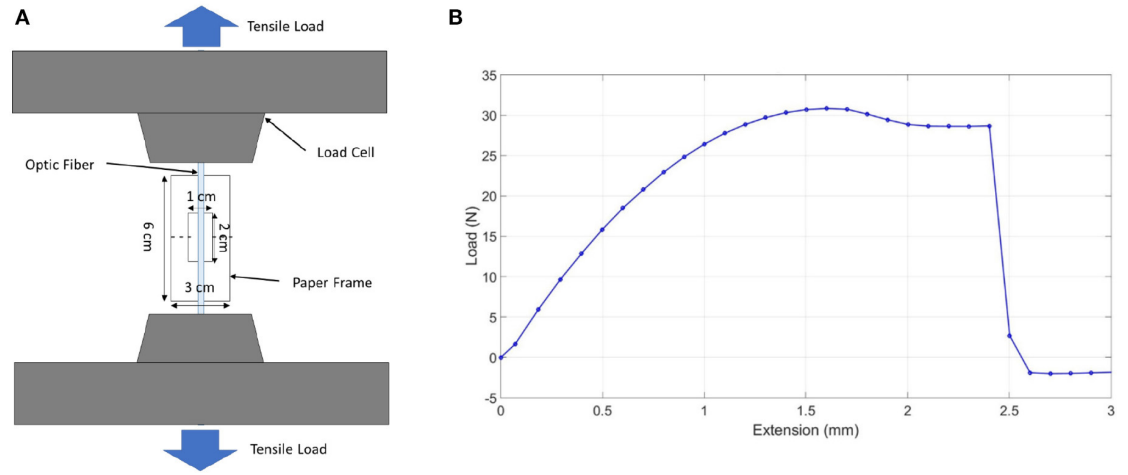

FIGURE 6 | Optic fiber tensile test. **(A)** Monofilament/thread tensile test setup. **(B)** Optic fiber tensile test graph.

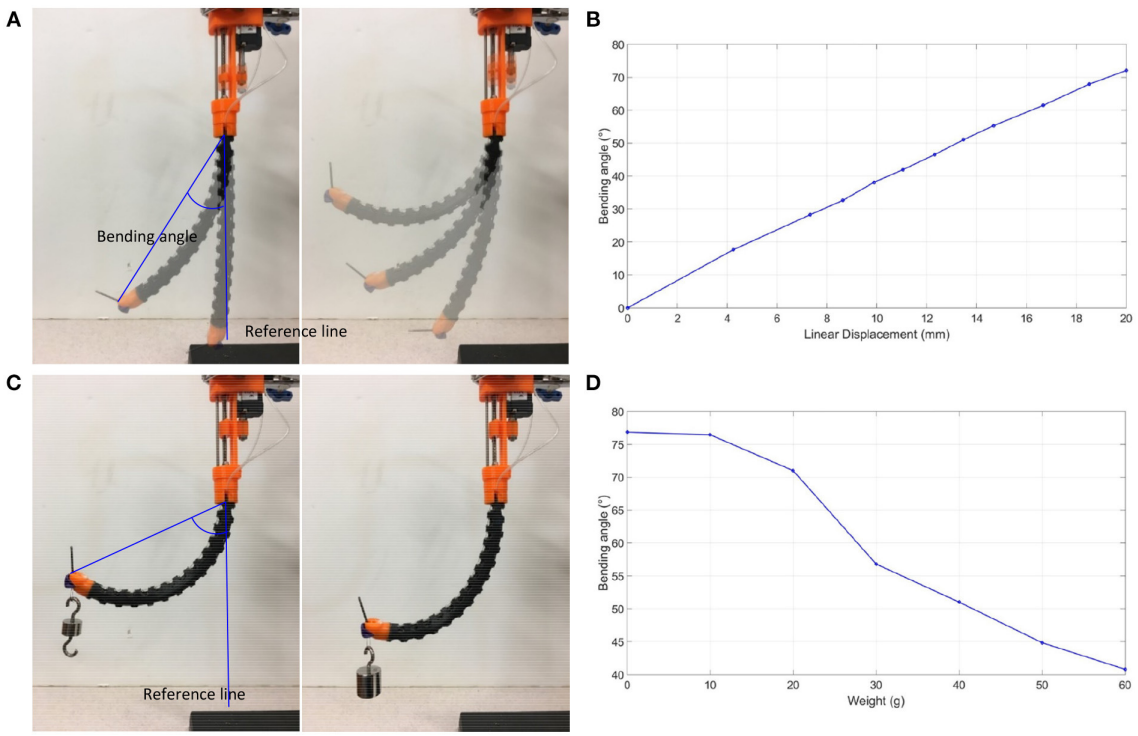

FIGURE 7 | Bending tests. **(A)** Bending angle measurement without loading, **(B)** Bending angle graph without loading, **(C)** Bending angle measurement under loading, **(D)** Bending angle graph under loading.

decreases. The relationship between the bending angle and the number of weights loaded at the tip highlights the importance of having the balloon stabilization method incorporated in our prototype. The drilling will bring counterforce on the tip.

3.3. Balloon Stability Test

The experiment in **Figure 8** involves inserting the prototype into a 2.2 cm diameter 20 cm long PVC tube and measuring the 3-dimensional forces produced by the balloon's expansion without drilling and during drilling. A tiny slot was made at the bottom of the transparent PVC tube to fit a 3D force sensor (Resolution: 2.5 mN, OMD-10-SE-10N, Optoforce Ltd.) and to capture the maximum forces exerted by the balloon during inflation. The maximum forces captured in the X-axis, Y-axis, and Z-axis direction during drilling, shown in **Figure 8B**, were 2.189, 3.916, and 1.496 N, respectively. There was a gradual

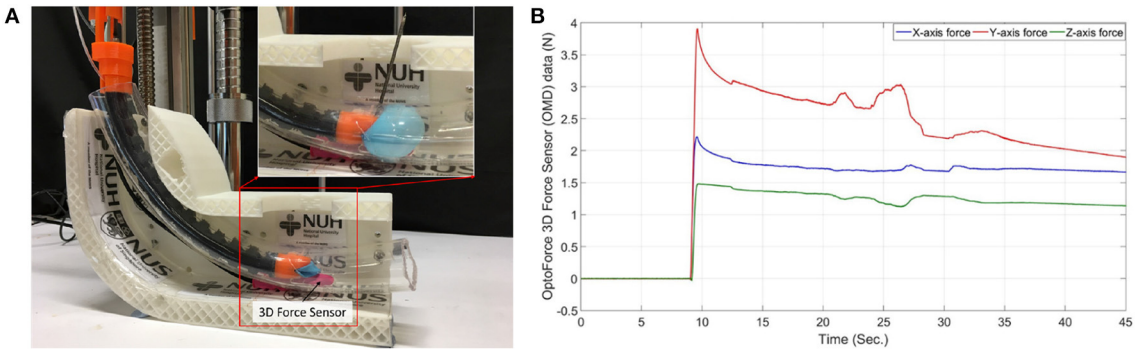

FIGURE 8 | Balloon stability test. **(A)** Balloon expansion force with drilling measurement method, **(B)** Balloon expansion force graph.

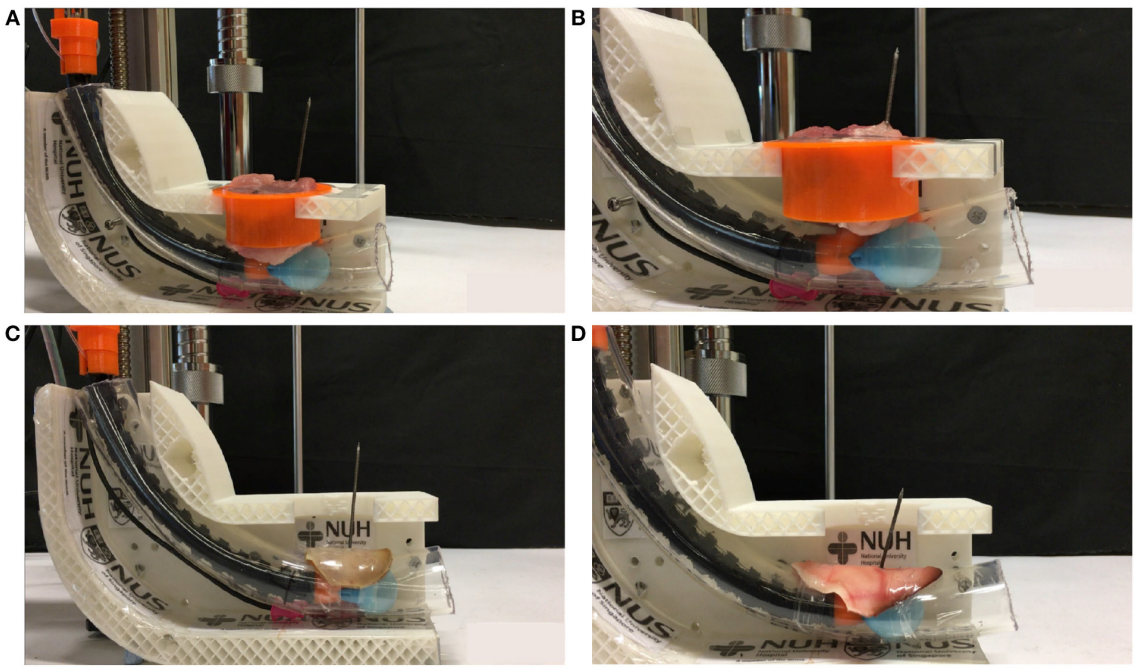

FIGURE 9 | Phantom tests. **(A)** Drilling through porcine lean meat, **(B)** Drilling through porcine lion, **(C)** Drilling through porcine smoked ear cartilage, **(D)** Drilling through porcine raw ear cartilage.

decline in the balloon's forces along time in the graphs, which is due to loose sealing. However, the fluctuations of the measured expansion forces during the drilling indicate the counterforce's existence. Therefore, a balloon to stabilize the drilling is necessary since it can produce a more accurate drilling process.

3.4. Phantom Tests

The prototype can drill through various porcine parts to simulate drilling through the human trachea using the same setup as the previous experiment. The parts were porcine loin and lean meat, shown in **Figures 9A,B**, respectively. Further validation experiments were on the porcine ear cartilage. The human ear's cartilage shares similar cartilage to the pig ear as three parts of the middle ear cavity in humans and pigs are broadly similar. Our prototype can drill through porcine ear cartilage that was smoked and raw, shown in **Figures 9C,D**, respectively. The prototype was able to pierce through the porcine loin, lean meat, and ear cartilage successfully. The porcine loin & lean meat was the least sturdy, followed by the smoked ear cartilage and raw ear cartilage. Our technology was able to drill through the ear cartilage, which bears a close resemblance to the human trachea.

4. DISCUSSION

We had tested our prototype to satisfy the basic requirements and mechanics of performing a trans-oral tracheostomy. The prototype will potentially decrease the time and errors of novice operators in reaching the target anatomical structures. However,

as a robotic medical system, some areas could be further optimized and improved. Currently, the control relies on human visual feedback. In the next prototype, closed-loop control of our prototype will be incorporated. Besides, shape and tip-tissue contact force sensing will be introduced, as this will enable us to introduce haptic feedback to the position, and orientate the needle, reducing surgical risks.

The existing air supply tubes could allow the different air entering the balloon, thus allowing our prototype to suit the patients' various applications and anatomical structures. A peristaltic pump could enable the air to inflate and deflate the balloon in a controlled manner and modulate the airflow. Besides, there is no oxygen supply channel in the current prototype, a channel to supply oxygen to the patient during the procedure will be added.

The precision of skin entry from the inside-out approach will be validated in comparative phantom and cadaver experiments. The performance of the prototype performance against conventional PT and OT will be evaluated. We plan to explore imaging techniques, such as ultrasound (US) and computed tomography (CT) imaging in our prototype. Additionally, we will also incorporate needle navigation and trajectory planning techniques into our prototype. These techniques are typically used with image guidance technologies to improve accuracy and efficiency and help preoperative planning and intraoperative planning procedures.

DATA AVAILABILITY STATEMENT

The raw data supporting the conclusions of this article will be made available by the authors, without undue reservation.

AUTHOR CONTRIBUTIONS

HR and CL conceived the project ideas and supervised the project. XX and HP established the experimental hardware setup and recorded the experimental results. MM, HR, CL, and XX were involved in the discussion and manuscript revisions. All authors carried out the experimental validations in the hospital setups and co-wrote the manuscript.

FUNDING

This work was supported by the National Key Research and Development Program, The Ministry of Science and Technology (MOST) of China (No. 2018YFB1307703), NMRC Bedside & Bench under grant R-397-000-245-511 awarded to HR, and NHIC I-to-develop Grant awarded to CL and HR.

REFERENCES

Al-Ansari, M. A., and Hijazi, M. H. (2006). Clinical review: percutaneous dilatational tracheostomy. *Crit. Care* 10, 202–202. doi: 10.1186/cc3900

Cipriano, A., Mao, M. L., Hon, H. H., Vazquez, D., Stawicki, S. P., Sharpe, R. P., et al. (2015). An overview of complications associated with open and percutaneous tracheostomy procedures. *Int. J. Crit. Illness Injury Sci*. 5, 179–188. doi: 10.4103/2229-5151.164994

Dexter, T. (1995). A cadaver study appraising accuracy of blind placement of percutaneous tracheostomy. *Anaesthesia* 67, 863–864. doi: 10.1111/j.1365-2044.1995.tb05852.x

Do, T. N., Seah, T. E. T., and Phee, S. J. (2016). Design and control of a mechatronic tracheostomy tube for automated tracheal suctioning. *IEEE Trans. Biomed. Eng.* 63, 1229–1237. doi: 10.1109/TBME.2015.2491327

Fray, S., Biello, A., Kwan, J., Kram, Y. A., Lu, K., and Camacho, M. (2018). Tracheostomy for paediatric obstructive sleep apnoea: a systematic review. *J. Laryngol. Otol*. 132, 680–684. doi: 10.1017/S0022215118001160

Gill-Schuster, D. (2016). Airway management–tracheotomy revisited. *Anasthesiol. Intensiv. Notfallmed. Schmerzther*. 51, 264–272. doi: 10.1055/s-0041-103154

Gu, X., Li, C., Xiao, X., Lim, C. M., and Ren, H. (2019). A compliant transoral surgical robotic system based on a parallel flexible mechanism. *Ann. Biomed. Eng.* 47, 1329–1344. doi: 10.1007/s10439-019-02241-0

Guinot, P.-G., Zogheib, E., Petiot, S., Marienne, J.-P., Guerin, A.-M., Monet, P., et al. (2012). Ultrasound-guided percutaneous tracheostomy in critically ill obese patients. *Crit. Care* 16, 1–8. doi: 10.1186/cc11233

Hemmerling, T. M., Taddei, R., Wehbe, M., Zaouter, C., Cyr, S., and Morse, J. (2012). First robotic tracheal intubations in humans using the kepler intubation system. *Br. J. Anaesth*. 108, 1011–1016. doi: 10.1093/bja/aes034

Hoseini, F., Zarankesh, S. M. Z., Alijanpour, E., and Gerdrodbari, M. G. (2018). Tracheostomy: complications and causes of complications. *Asian J. Pharma.* 12, 647–654. doi: 10.22377/ajp.v12i02.2410

Hur, K., Price, C. P. E., Gray, E. L., Gulati, R. K., Maksimoski, M., Racette, S. D., et al. (2020). Factors associated with intubation and prolonged intubation in hospitalized patients with COVID-19. *Otolaryngol. Head Neck Surg.* 163, 170–178. doi: 10.1177/0194599820929640

Johnson-Obaseki, S., Veljkovic, A., and Javidnia, H. (2016). Complication rates of open surgical versus percutaneous tracheostomy in critically ill patients. *Laryngoscope* 126, 2459–2467. doi: 10.1002/lary.26019

Kannan, D. S., Rajan, G. S., and Haridas, P. V. (2017). Comparative study of percutaneous dilatational tracheostomy versus standard operative tracheostomy. *J. Evol. Med. Dental Sci.* 6, 1066–1071. doi: 10.14260/Jemds/2017/231

Khandelwal, A., Kapoor, I., Goyal, K., Singh, S., and Jena, B. R. (2017). Pneumothorax during percutaneous tracheostomy–a brief review of literature on attributable causes and preventable strategies. *Anaesthesiol. Intensive Ther*. 49, 317–319. doi: 10.5603/AIT.a2017.0050

Kidane, B., and Pierre, A. F. (2018). From open to bedside percutaneous tracheostomy. *Thorac. Surg. Clin.* 28, 263–276. doi: 10.1016/j.thorsurg.2018.03.001

Kruit, N., Valchanov, K., Blaudszun, G., Fowles, J.-A., and Vuylsteke, A. (2018). Bleeding complications associated with percutaneous tracheostomy insertion in patients supported with venovenous extracorporeal membrane oxygen support: a 10-year institutional experience. *J. Cardiothorac. Vasc. Anesth*. 32, 1162–1166. doi: 10.1053/j.jvca.2017.08.010

Lerner, A. D., and Yarmus, L. (2018). Percutaneous dilational tracheostomy. *Clin. Chest Med*. 39, 211–222. doi: 10.1016/j.ccm.2017.11.009

Li, C., Gu, X., Xiao, X., Lim, C. M., and Ren, H. (2020). Flexible robot with variable stiffness in transoral surgery. *IEEE/ASME Trans. Mechatron*. 25, 1–10. doi: 10.1109/TMECH.2019.2945525

Mecham, J. C., Thomas, O. J., Pirgousis, P., and Janus, J. R. (2020). Utility of tracheostomy in patients with COVID-19 and other special considerations. *Laryngoscope* 130, 2546–2549. doi: 10.1002/lary.28734

Mieth, M., Schellhaass, A., Huettner, F. J., Larmann, J., Weigand, M. A., and Buechler, M. W. (2016). Tracheostomy techniques. *Chirurg* 87, 73–85. doi: 10.1007/s00104-015-0116-7

Pilarczyk, K., Haake, N., Dudasova, M., Huschens, B., Wendt, D., Demircioglu, E., et al. (2016). Risk factors for bleeding complications after percutaneous dilatational tracheostomy: a ten-year institutional analysis. *Anaesth. Intensive Care* 44, 227–236. doi: 10.1177/0310057X1604400209

Rashid, A. O., and Islam, S. (2017). Percutaneous tracheostomy: a comprehensive review. *J. Thorac. Dis*. 9, 1128–1138. doi: 10.21037/jtd.2017.09.33

Sandor, P. S., and Shapiro, D. S. (2016). *Percutaneous Dilatational Tracheostomy*. Cham: Springer International Publishing. 67–79. doi: 10.1007/978-3-319-25286-5_9

Sanji, R. R., Channegowda, C., and Patil, S. B. (2017). Comparison of elective minimally invasive with conventional surgical tracheostomy in adults. *Indian J. Otolaryngol. Head Neck Surg*. 69, 11–15. doi: 10.1007/s12070-016-0983-3

Sasane, S. P., Telang, M. M., Alrais, Z. F., Alrahma, A. H. N. S., and Khatib, K. I. (2020). Percutaneous tracheostomy in patients at high risk of bleeding complications: a retrospective single-center experience. *Indian J. Crit. Care Med*. 24, 90–94. doi: 10.5005/jp-journals-10071-23341

Simon, M., Metschke, M., Braune, S. A., Püschel, K., and Kluge, S. (2013). Death after percutaneous dilatational tracheostomy: a systematic review and analysis of risk factors. *Crit. Care* 17, 1–9. doi: 10.1186/cc13085

Vargas, M., Russo, G., Iacovazzo, C., and Servillo, G. (2020). Modified percutaneous tracheostomy in COVID-19 critically ill patients. *Head Neck* 42, 1363–1366. doi: 10.1002/hed.26276

Varshney, M., Sharma, K., Kumar, R., and Varshney, P. G. (2011). Appropriate depth of placement of oral endotracheal tube and its possible determinants in indian adult patients. *Indian J. Anaesth*. 55, 488–493. doi: 10.4103/0019-5049.89880

Wang, X., Tao, Y., Tao, X., Chen, J., Jin, Y., Shan, Z., et al. (2018). An original design of remote robot-assisted intubation system. *Sci. Rep*. 8, 1–9. doi: 10.1038/s41598-018-31607-y

Xiao, X., Gao, H., Li, C., Qiu, L., Kumar, K. S., Cai, C. J., et al. (2020). Portable body-attached positioning mechanism toward robotic needle intervention. *IEEE/ASME Trans. Mechatron*. 25, 1105–1116. doi: 10.1109/TMECH.2020.2974760

Xiao, X., and Li, Y. (2016). Development of an electromagnetic actuated microdisplacement module. *IEEE/ASME Trans. Mechatron*. 21, 1252–1261. doi: 10.1109/TMECH.2015.2510450

Xiao, X., Li, Y., and Xiao, S. (2017). Development of a novel large stroke 2-DOF micromanipulator for micro/nano manipulation. *Microsyst. Technol*. 23, 2993–3003. doi: 10.1007/s00542-016-2991-3

Conflict of Interest: The authors declare that the research was conducted in the absence of any commercial or financial relationships that could be construed as a potential conflict of interest.

frontiers in Robotics and AI

ORIGINAL RESEARCH
published: 20 January 2021
doi: 10.3389/frobt.2020.586707

Deep Learning-Based Haptic Guidance for Surgical Skills Transfer

Pedram Fekri[1]*, *Javad Dargahi*[1] and *Mehrdad Zadeh*[2]

[1] Mehchanical, Industrial, and Aerospace Engineering Department, Concordia University, Montreal, QC, Canada, [2] Electrical and Computer Engineering Department, Kettering University, Flint, MI, United States

Having a trusted and useful system that helps to diminish the risk of medical errors and facilitate the improvement of quality in the medical education is indispensable. Thousands of surgical errors are occurred annually with high adverse event rate, despite inordinate number of devised patients safety initiatives. Inadvertently or otherwise, surgeons play a critical role in the aforementioned errors. Training surgeons is one of the most crucial and delicate parts of medical education and needs more attention due to its practical intrinsic. In contrast to engineering, dealing with mortal alive creatures provides a minuscule chance of trial and error for trainees. Training in operative rooms, on the other hand, is extremely expensive in terms of not only equipment but also hiring professional trainers. In addition, the COVID-19 pandemic has caused to establish initiatives such as social distancing in order to mitigate the rate of outbreak. This leads surgeons to postpone some non-urgent surgeries or operate with restrictions in terms of safety. Subsequently, educational systems are affected by the limitations due to the pandemic. Skill transfer systems in cooperation with a virtual training environment is thought as a solution to address aforesaid issues. This enables not only novice surgeons to enrich their proficiency but also helps expert surgeons to be supervised during the operation. This paper focuses on devising a solution based on deep leaning algorithms to model the behavior of experts during the operation. In other words, the proposed solution is a skill transfer method that learns professional demonstrations using different effective factors from the body of experts. The trained model then provides a real-time haptic guidance signal for either instructing trainees or supervising expert surgeons. A simulation is utilized to emulate an operating room for femur drilling surgery, which is a common invasive treatment for osteoporosis. This helps us with both collecting the essential data and assessing the obtained models. Experimental results show that the proposed method is capable of emitting guidance force haptic signal with an acceptable error rate.

Keywords: deep learning, recurrent neural network, LSTM, haptic, force feedback, bone drilling, surgical skill transfer, COVID-19

OPEN ACCESS

Edited by:
S. Farokh Atashzar, New York University, United States

Reviewed by:
Fabien Danieau, InterDigital, France
Selene Tognarelli, Sant'Anna School of Advanced Studies, Italy

***Correspondence:**
Pedram Fekri
p_fekri@encs.concordia.ca

Specialty section:
This article was submitted to Biomedical Robotics, a section of the journal Frontiers in Robotics and AI

Received: *23 July 2020*
Accepted: *05 November 2020*
Published: *20 January 2021*

Citation:
Fekri P, Dargahi J and Zadeh M (2021) Deep Learning-Based Haptic Guidance for Surgical Skills Transfer. Front. Robot. AI 7:586707. doi: 10.3389/frobt.2020.586707

1. INTRODUCTION

Lack of having an appropriate medical training system may cause errors with adverse effects on patients. The practical intrinsic of medical education systems has led expert surgeons to transfer their skill to trainees via trial and error methods in the actual operating rooms. Evidently, novice surgeons have a minuscule chance of the repetition for improving their proficiency during the operation. Complications through surgical procedures have considerably raised, which signifies

young surgeons require to be more proficient. On the one hand, achieving hands-on skills in an actual operation room is a tedious and time-consuming process. On the other hand, training in operative rooms is extremely expensive so that estimations reveal a significant increase in operative time for training translated into about $53 million dollars per year (de Montbrun and MacRae, 2012). However, the National Health Service (NHS) has recommended a restriction in working hours for trainees (from 30,000 working hours to around 7,000 h) to increase the effective time of expert surgeons as well as improve the outcome of surgeries (Tan and Sarker, 2011). The aforementioned limitations accentuate the importance of having a proper educational system for surgeons other than the traditional methods.

Apart from the above challenging issues, the circumstances such as the recent global shutdown due to the COVID-19 pandemic cause a closure in the education system as well. In this case, trainees find it tough to attend the in-person sessions and operation rooms for educational purposes. On the one hand, most of operations are deferred in order to reduce the burden on the shoulders of hospitals' staff. On the other hand, enacting preventive rules and initiatives such as social distancing brings about encountering with the limitation in using surgical labs (Al-Jabir et al., 2020). To this end, in order to maintain surgical skills, the demands for using simulations and artificial intelligence methods have been soared. For instance, neurosurgical residents in New Orleans have been encouraged to utilize the aforementioned technologies so as to practice complex surgical task during the COVID-19 pandemic. The same concern has emerged from the community of orthopedics surgeons so that they have tended to use surgical simulation for their residents. Hence, it is necessary to equip the medical education system in such a way that the remote working become conceivable (Bernardi et al., 2020).

Although the above issues can be generalized to a wide range of surgical operations, for the sake of simplicity, this work exclusively concentrates on the hip fracture treatment. One of the most common health issues is hip fracture that is seen in elderly adults with a high mortality rate of 20 and 35% within 1 year (Goldacre et al., 2002; Thorngren, 2008). The cause, on the other hand, chiefly stems from osteoporosis so that 2–8% of males and 9–38% of females are diagnosed with this disease, which accounts for overall 30 million women and 8 million men around the United States and EU (Schapira and Schapira, 1992; Svedbom et al., 2013; Wade et al., 2014; Willson et al., 2015). Therefore, the hip fracture issue needs a precise and reliable treatment regardless of patients' gender.

Closed reduction percutaneous pinning (CRPP) is a typical treatment for supporting hip fractures, in which surgeons perform based on hands-on experiences in the operating room. This type of treatment is invasive and needs professional surgeons to do the task, thereby diminishing the presumable complications. Since the probability of making inadvertent mistakes is high, expert surgeons are mostly reluctant to operate and instruct novices simultaneously. With this in mind, having an auxiliary system is necessary so as to overcome the challenges and reduce the risk of medical errors as well as simplify the training in medical education systems. This leads to not only enhance the novice hands-on skills but also supervise expert surgeons during the surgery.

Skill transfer system is considered as a solution with the aim of addressing the aforesaid complications. As a matter of fact, the system models the performance of experts for a certain surgical procedure that culminates to a trained medical robot for fulfilling multiple goals such as more reliable assisting. An example of medical assistant robot is the human–robot interaction system, which has been introduced as a tool for improving human performance (Ramón Medina et al., 2012; Medina et al., 2015; Gil et al., 2019; Pezent et al., 2019). In general, a haptic device along with a simulation environment is deemed as an experimental setup for the human–robot interaction system in the surgical application. On the one hand, users manipulate the haptic device to complete a surgical task via a collaborative environment. On the other hand, haptic guidance signal is generated to correct or elevate the users' performance (Morris et al., 2006; Rozo et al., 2013). This setup can be utilized for the purpose of skill transfer in order to help experts to convey their knowledge in a safer environment.

In addition to the mechanical setup, it needs to elicit robust models from expert surgeons' demonstrations based on their dynamic and non-linear behaviors during the surgery. These behaviors are categorized into kinesthetic and kinematic demonstrations. Learning kinematic demonstrations is chiefly regarded as the process of extracting positional body movements of the expert during the operation (Abbott et al., 2007; Chipalkatty et al., 2011; Zahedi et al., 2017). Kinesthetic information can be obtained by a physical interaction between robots and users so that a surgeon directly works with the robot to perform a specified task (Rozo et al., 2013, 2016; Kronander and Billard, 2014).

All in all, the system comprises a perceptual part in conjunction with a robotic actuator in order to provide the realistic sense of surgery. In other words, this solution is an assistant human-in-the-loop system that consumes the data corresponding to either kinesthetic or kinematic demonstrations. The data are captured while the expert is manipulating the haptic end-effector to accomplish a specific task through a virtual environment. Then, the compiled dataset is used to train models for extracting experts' behaviors. Finally, the haptic guidance signal, which is emitted from the trained model, is employed as a reference signal for both trainees and experts. The trainees can correct their movements based on the provided signal through the virtual environment. The haptic guidance signal can be utilized as a supervisor for experts during a real operation as well.

Since the data related to both kinematic and kinesthetic demonstrations is time varying and also learning the performance of experts depends on modeling the dynamic behaviors over time, it is crucial to investigate the data with respect to the temporal characteristic. Statistical algorithms such as HMM and CRF have been used to extract the aforementioned features (Reiley and Hager, 2009; Ramón Medina et al., 2012; Tao et al., 2013; Zahedi et al., 2017, 2019). In addition, control algorithms have been applied to the human-in-the-loop system for guiding human via robots based on the model obtained from dynamic data (Chipalkatty et al., 2011; Safavi and Zadeh,

2015, 2017; Safavi et al., 2015). However, previous works have an impressive progress in modeling the dynamic data in the skill transfer system, advent of machine learning and deep learning algorithms is thought as a gigantic step toward developing more trustworthy predictive systems. For instance, a method has been proposed based on deep learning to predict the haptic feedback in percutaneous heart biopsy for decreasing delay in remote operations (Khatami et al., 2017). The temporal facet of data can help to enrich the throughput of the system whether in the data compilation or in the inference phase.

In this work, we seek to advance a solution for training novice residents in the orthopedic surgical drilling procedure by developing a skill transfer system using a deep learning method. The proposed system aims at contributing to the educational system of orthopedic residents during the COVID-19 pandemic. To this end, first, a simulation environment is used to visualize all components of a real operation room. The simulation creates a 3D visualization of the patient-specific bones from CT scan data. Moreover, it calculates an approximation of both bones' density and stiffness as physical properties of the tissue through the layers. As discussed in the next section, having these features helps to estimate the applied force feedback, when drill touches the bone. Using provided features, the system captures the essential data while expert surgeons perform a specific drilling task via the haptic device and simulation. Second, the solution aims to extract the model of expert surgeons' behaviors as a reference signal using the captured data. For this reason, a recurrent neural network with an LSTM architecture has been designed and implemented in order to be trained on force demonstrations as well as kinematic features and other effective data, which stems from either drill physics or bone tissues.

The main contributions of the proposed solution are summarized as follows: it investigates the influence of a deep recurrent neural network with an LSTM architecture on enhancing the quality of transfer skills in orthopedic surgical drilling. In contrast to the proposed solution in Khatami et al. (2017), our method incorporates multiple effective features, instead of utilizing force data solitary. In fact, in Khatami et al. (2017) the solution anticipates forces of X and Y directions using only the previously applied forces in the same directions and it does not engage other effective parameters in the estimation of force signals over time. Our proposed method, on the other hands, extracts the temporal behavior of force feedback data by fusing the data stemmed from multiple sources such as "bone's layer type," "penetration depth," "drill's temperature," and "drill's position." As a sensor fusion model, it will learn how to regulate the forces based on a fusion of data that impacts on the maneuver of the surgeon. Helping trainees to sense the guidance signal that stems from expert surgeons' hands-on skills along with other effective factors during surgery is another advantage of the proposed method. Also, since the force sensor is not utilized in this study, simulation aids to estimate forces as well as the other data.

The rest of the paper is organized as follows: the general explanation of proposed method along with experimental setup and data gathering are presented in section 2. Section 3 explains data preparation, computer experiments, result, and discussion. The paper concludes in the final section.

2. DEEP HAPTIC GUIDANCE GENERATOR

The proposed system provides a solution based on a deep learning algorithm for conveying experts' hands-on proficiency to novice surgeons, exclusively in orthopedic surgical drilling with the purpose of treating hip fractures (**Figure 1**). This is achieved by utilizing a simulation environment, which creates a virtual shape of the intended patient's bone using CT scan images. This shape preserves the most principal features of the bone such as stiffness of every layer. At the same time, a haptic device is used by a user to drill a specified path through the bone. To provide a realistic sense, physical features such as temperature and rotation speed are considered, while the drill touches bone. This setup has two main advantages for the proposed method: First, it helps to capture the requisite data from expert surgeons while accomplishing a predefined drilling task. Second, it aids to exploit the trained model virtually.

Subsequently, a deep neural network is fed by the attained data to generate models on the behaviors of experts in a predefined task. As with the behavior modeling, learning gestures occurs over time. With this in mind, a recurrent neural network with an LSTM architecture is employed to extract a dynamic model. The aforementioned network is trained by the data of multiple sources (explained in detail in section 2.2) and then the force feedback in three axes is expected in its output. In other words, the proposed method with a modified LSTM architecture attempts to identify the dynamic relationship between inputs and their corresponding outputs in a supervised manner, while they are not equal in terms of dimension size. Intuitively, the significant objective is to investigate the impact of physical properties emerged from the bone's tissues or drill on the performance of the skill transfer system. As a sensor fusion system, however, this method outputs force feedback in three axes, it combines multiple data such as drill temperature, the type of bone's layer, penetration depth, and drill position rather than only force feedback as the network's input.

It is worth noting that, because we do not utilize force sensor, the corresponding data are estimated using the physical properties of the patients' bone obtained from CT images. For simplicity, we call the proposed method "DHG" (Deep Haptic Guidance). **Figure 1** illustrates the structure of the DHG. Experimental setup, data gathering, and DHG are explained in the following sections.

2.1. Simulation and Experimental Setup for Bone Drilling Surgery

An experimental setup is used so as to capture the required data. It encompasses a haptic device (Phantom Omni, Geomagic Touch, USA) and a virtual environment (VE). The haptic device was set up on a movable and height adjustable table. The height of the table can be adjusted with respect to the convenience of the participants. The surgeons either experts or novices interact with the simulation system via the haptic device, a keyboard, and a computer mouse. A virtual drill can be manipulated to touch/drill the femur bone's shape through the stylus of the haptic device. The haptic device records motions of the end-effector, while it has been attached to a drill (**Figure 2**). It has 6 Degree of Freedom (DOF) positional sensing and capable of providing the user with

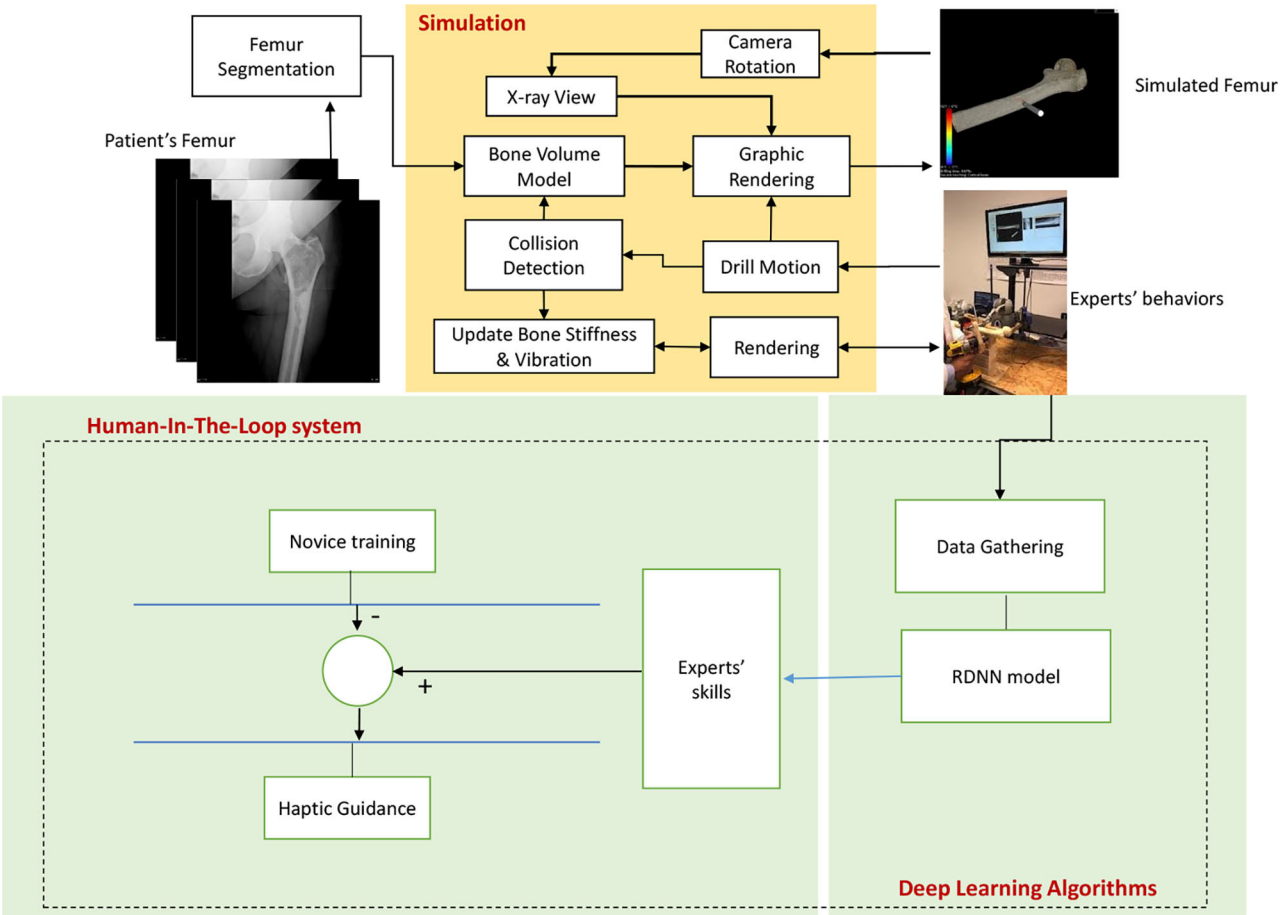

FIGURE 1 | The diagram depicts the structure of the Deep Haptic Guidance (DHG). The CT data corresponding to a patient enters for modeling, rendering, and determining the stiffness of the bone. The data are captured while an expert is completing the task. The obtained data are converted to a compatible dataset for training deep recurrent neural network. The trained model provides haptic force feedback based on the professional demonstrations. The guidance signal is generated by the difference between the DHG's prediction and force feedback of novice user. In fact, expert's skill implies DHG's prediction.

the force feedback in 3 DOF translational motions (the space of force feedback data). The sampling frequency for compiling data is 10 Hz. The estimation on stiffness of the bone's layer is updated every 20 ms. The tasks were completed by moving the end-effector in order to drill and penetrate through the bone along the pre-defined path.

In this setup, the simulation plays a crucial role in capturing data. Generally, simulated and virtual reality (VR) environments can be considered as an alternative of real operation rooms (Seymour, 2008; Kho et al., 2015; Van Duren et al., 2018). This enables trainers to define particular surgical task and drilling path for each patient separately. Here, we simulated attributes of the bone in order to gather data from experts during a surgery. For more precise explanations, four main parts of a required simulation, exclusively for bone drilling, are described as follows:

First, as shown in **Figure 1** it needs to simulate and render a patient's femur bone by considering physical properties. This is obtained by using the patient's specific CT images as the input of the simulation (**Figure 3**). Since the goal is to model the physical characteristics of the femur bone related to a patient with femoral head necrosis, CT is more useful than MRI images (Teo et al., 2006). Furthermore, as shown in **Figure 4**, a segmentation method ascertains different layers such as cortical bone, cancellous bone, and bone marrow in order to simulate their thickness, stiffness, and physical traits while interacting with a drill. The intensity values of the CT images are utilized to segment the bone's layers along with their mechanical properties. Namely, the bright part of a CT image is cortical bone, whereas the dark parts are cancellous bone.

Second, to make more actual sense of working with the simulator, a method is employed to change the virtual shape of the bone, whenever the drill touches or penetrates the tissue. In other words, the method models stiffness of tissues based on the bone's depth and then assigns a specific value to every voxel in each layer of the bone. Finding the relationship between intensity of voxels and density of the bone in the images helps the volume rendering operation to take an appropriate action. In fact, the rendering operation decides to keep or remove a voxel with respect to its density value and the drill status as well (Morris

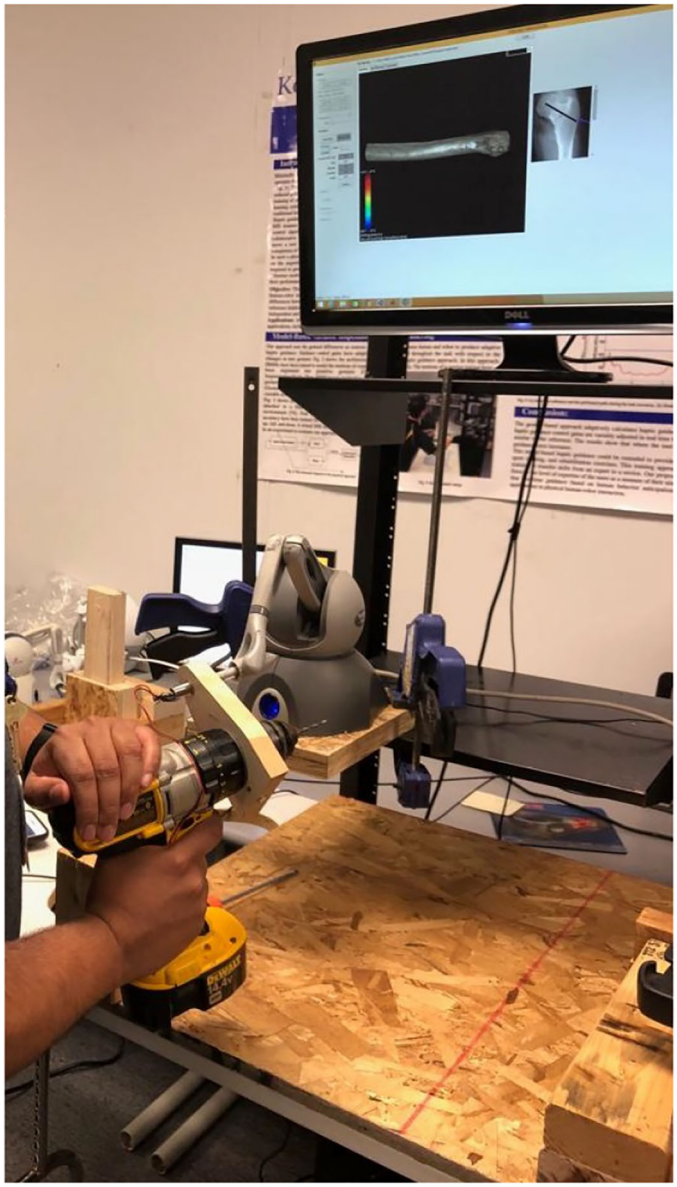

FIGURE 2 | Experimental setup: A volunteer is completing a required surgical drilling task while using a drill attached to the haptic device. It encompasses a haptic device, a keyboard, and a computer mouse interacting with a simulation.

et al., 2004; Liu and Laycock, 2009; Sofronia et al., 2012; Bogoni and Pinho, 2013).

Third, the mechanical traits of the obtained layers are involved to simulate haptic force feedback. As a result, cortical bone is much more stiffer that cancellous bone (Compere, 1980). On the other hand, the cancellous bone of the femur bone has a wide range of density that affects drilling forces. In Brown and Ferguson (1980), the distribution of stiffness and yield strength have been investigated. Accordingly, we estimate the force corresponding to each layer of the bone in order to provide users with a tangible force, while penetrating through the different layers. However, the acquired sense of the force is not equal to the actual bone stiffness, and it makes the sense of passing through the layers for users. It is worth to say that the determined stiffness for the bone's layers was limited to the haptic device capability. Therefore, since the discrepancy of estimated force feedback does not influence on the DHG, it can be considered as the scaled stiffness of the real value.

Fourth, as shown in **Figure 5**, it needs to enable the user to take X-ray images from different points of view. In other words, in the real operation room, surgeons capture X-ray images during a surgery to make sure whether the drill traverses through the correct pre-defined path or not. With this in mind, the simulation allows them to have the visualization of X-ray from

FIGURE 3 | The image shows a rendered bone obtained from the CT data. The user is able to touch or drill the shape, visually by moving the object sticked the bone.

the bone, analogs to the real operation room, from three views: the top, front, and the side. Eventually, a virtual environment is built to simulate the actual process in the operation room. Apart from provided facilities, the essential data are compiled via the experimental setup. In fact, the simulation strives to imitate real operation rooms as much as possible because it leads expert surgeons to function naturally, thereby capturing more meaningful data. It is good to say that the aforementioned setup in conjunction with the simulation has contributed in other studies in our research Lab at Kettering University (Safavi and Zadeh, 2017; Zahedi et al., 2017, 2019).

2.2. Data Preparation

To train the DHG on experts' behaviors, the aforesaid setup was exploited and a drilling path was determined between two points as a specific surgical task. The bone should be pierced from point A to B in the straight direction. Since it was not possible to invite surgeons, six engineering students who were familiar to the area were asked to pretend as our experts' reference and complete the task using the experimental setup. They were required to pass through all the layers of the bone and get to the target point. The participants were guided to perform the task and instructed to complete the task precisely and as quickly as possible. Every subject had 5 min to get acquainted with the experimental setup and then carry out the task. They were allowed to repeat the task as many times as they preferred. Then the best completed task of every attendee were selected based on his/her discretion. In the process of collecting data, the force feedback in x, y, and z axes as well as drill positions, drill penetration depth, the simulated temperature of the drill, and the type of layers in the bone were obtained in the format of a dataset. The data were collected with the frequency of 10 Hz. Eventually, the time-varying data were captured from six completed tasks and $D \in R^{n\times 9}$ constituted the dataset, where n is the number of data records. It is noteworthy that for the sake of preserving dynamic properties, the order of records for every task of the dataset was retained.

2.3. Creating Models Using Deep Learning Algorithm—DHG

By taking a closer look at the biological perception of human in performing tasks, it is evident that the action taken in the current time t has been concluded by the sequence of actions that happened in the past. This fact can be generalized to the current problem in such a way that "time" plays a significant role in learning expert surgeons' behaviors. On the other hand, learning process evolves during the time by retrying experiences.

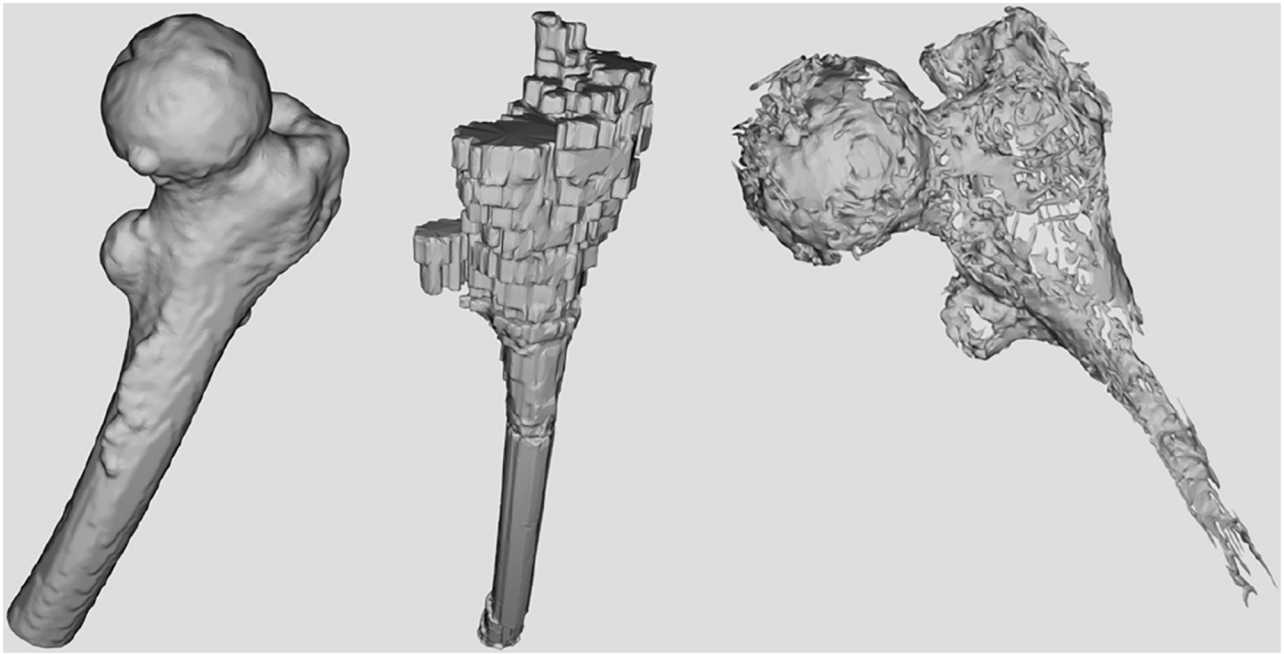

FIGURE 4 | The surfaces corresponding to the bone's layers extracted from CT data. From left to right: Cortical bone surface, bone marrow, and necrosis.

Accordingly, the DHG learns the experts' demonstrations by consuming the time-varying data, which has been gathered from multiple duplicate tasks (section 2.2). The DHG employs a recurrent neural network instead of a feed-forward one in order to extract the dynamic temporal behaviors of data. In fact, it models gestures of the surgeon in time t using a series of data with a specified length. This type of network includes a feedback signal as a loop to consider temporal effects of input data over time. Moreover, the LSTM is a popular architecture for RNNs, which has been proposed to address vanishing gradient problems in Vanilla RNNs (Hochreiter and Schmidhuber, 1997; Hochreiter et al., 2001). **Figure 6** depicts the internal structure of LSTM. The aforementioned architecture has been successfully applied in different applications such as the vehicle trajectory prediction for modeling temporal properties of data (Altché and de La Fortelle, 2018).

As mentioned in the previous section, the dataset $D \in R^{n\times 9}$ was prepared while surgeons were carrying out the task. Every feature of the dataset is deemed as an independent data stream, which has been emitted from a separate data source or sensor. From another point of view, as a sensor fusion method, the DHG receives a nine-dimensional vector of data and provides the prediction on force feedback in a three-dimensional vector in its output. Finally, the DHG uses an LSTM as the preferred architecture for the deep recurrent neural network to model the dynamic data.

The DHG is considered to have unequal inputs and outputs size because of the sensor fusion concept. To this end, as described in the following section, a partial modification was applied in the original structure of the LSTM by adding a linear layer (Equation 7). The LSTM's basic is explained in detail, although there are valuable sources in the literature as well.

As a recurrent neural network, the LSTM generates feedback signals via a loop to exert the impact of previous data in the current time instant t. Apart from the concept of hierarchical layers in deep neural networks, every unit of the LSTM has four exclusive layers (**Figure 6**). Cell state C_t keeps past experiences at time t and gets updated over time. Forget gate f_t removes data from the memory by using both input x_t and previous output h_{t-1}, while input gate i_t decides which value must be updated:

$$f_t = \sigma(W_f x_t + U_f h_{t-1} + b_f) \tag{1}$$

$$i_t = \sigma(W_i x_t + U_i h_{t-1} + b_i) \tag{2}$$

$$\tilde{C} = \tanh(W_{\tilde{c}} x_t + U_{\tilde{c}} h_{t-1} + b_{\tilde{c}}) \tag{3}$$

where σ is a sigmoid activation function, U_f and W_f are weight matrices, and b_f denotes the bias vector. A hyperbolic tangent layer calculates new values for update in cooperation with the input gate and then replaces memory C_t with the new values as follows:

$$C_t = f_t * C_{t-1} + i_t * \tilde{C}_t \tag{4}$$

where $*$ denotes the element-wise multiplication. Eventually, the output h_t is calculated by updated memory C_t and the previous output via output gate o_t as follows:

$$o_t = \sigma(W_o x_t + U_o h_{t-1} + b_o) \tag{5}$$

FIGURE 5 | The simulation was equipped with X-ray view for providing users an environment more analogous to the real operating room. Similar to the real operation room, it has three views: the top, front, and side.

$$h_t = o_t * \tanh(C_t) \tag{6}$$

It is worth to say that, input $x_t \in R^n$, weight matrices $W \in R^{h \times h}$ and $U \in R^{h \times h}$, and biases $b \in R^h$. n is the size of the input vector and h is the size of the internal memory or cell state, which is defined by designers.

Furthermore, the RNN should be unrolled to establish feedback signals in the internal structure and use the advantages of engaging previous input data in the current time t. So, we assume that the LSTM unit output h_t depends on $\{x_{t-e}, x_{t-e-1}, \ldots, x_{t-1}\}$ where e is the number of the dataset record used for unrolling the DNN. In another way, the loop of RNN is unrolled over e latest inputs. Thus, the prediction at time t relies on $0.1 \times e$ previous seconds of surgeons' behaviors. These unrolled units are defined as the system time steps.

As noted earlier, the DHG fuses multiple features and outputs only force feedback. With this in mind, the size of outputs in the network must be equal to the size of haptic force feedback vector,

whereas in the conventional LSTM both input and output vectors are equal in size. To this end, we add a linear output flattening layer with a linear activation function to map inputs into the output space as follows:

$$a = W_a h_t^l + b_a \tag{7}$$

By utilizing the above linear transition function, the output at last time step in the last layer is transferred to the force feedback output space. In contrast to classification problems, since the system attempts to generate force values in the output, transition from the feature space $d \in R^9$ to force feedback space $r_t^p \in R^3$ is accomplished by a linear regression, where r_t^p is the predicted force value in time t acquired from e previous number of the data records. **Figure 7** depicts the designed architecture for the DHG. In addition, RMSE is the objective function of the DNN, which attempts to learn the expected output r_t^{ex} in a supervised manner as follows:

$$e(r_t^p, r_t^{ex}) = \sqrt{\frac{\sum_{i=1}^{d}(r_{t,i}^p - r_{t,i}^{ex})}{d}} \tag{8}$$

To optimize the above objective function, different optimizer algorithms such as ADAM optimizer can be applied (Kingma and Ba, 2014).

3. EVALUATION AND DISCUSSION

The target of this section is preparing the data, which has been captured in section 2.2 for training models as well as assessing the performance of the DHG in predicting haptic force feedback. In section 3.1, we revise the format of the dataset (section 2.2)

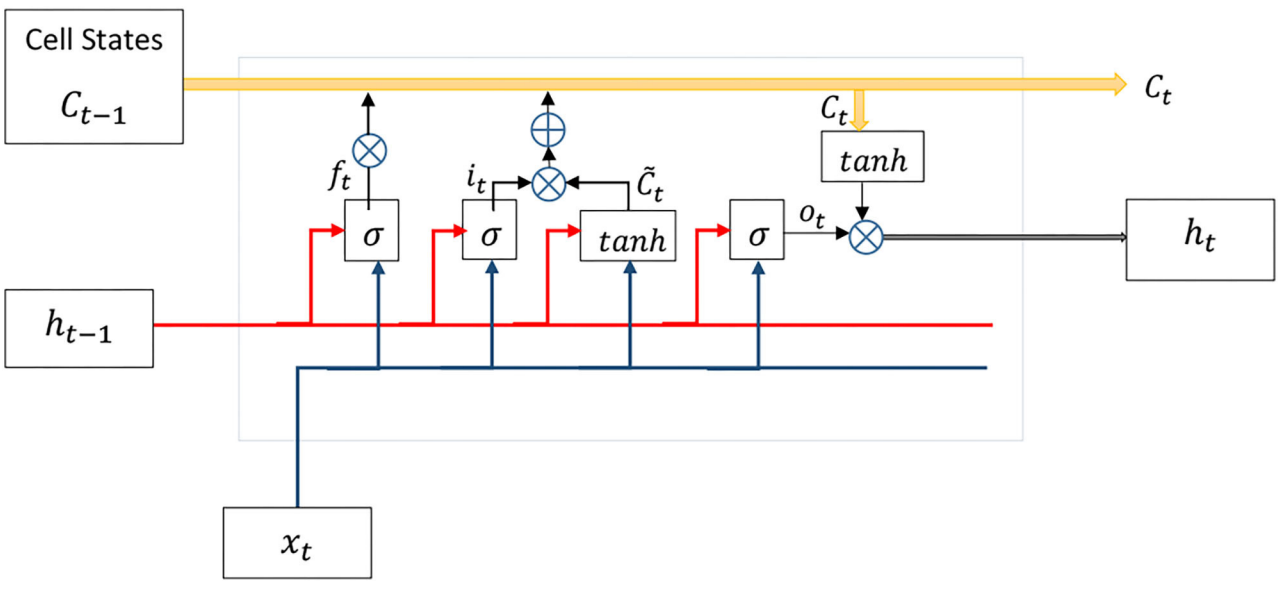

FIGURE 6 | The LSTM unit contains forget, input, and output gates along with cell state (further details in section 2.3).

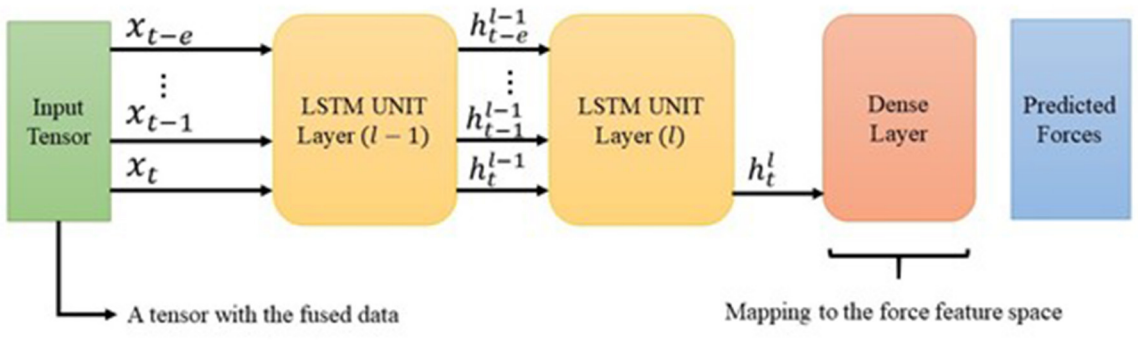

FIGURE 7 | The diagram shows the intended architecture for the DHG. The input is a tensor containing the data from different sources (section 2.2). The LSTM is unrolled over e previously generated data. The cell state h is the input of its corresponding unrolled unit in the next layer. However, using the latest LSTM unit's output, the DHG squeezes the prediction vector through a dense layer. Finally, the output of the network is a vector with three elements corresponding to forces in x, y, and z direction.

and make it compatible with the DHG's input. Finally, we investigate the result in the last subsection. In this work, we did not conduct a human factor study in experiments to examine the performance of the DHG. Instead, we evaluate the DHG based on common assessment methods such as RMSE to show the accuracy of predictions on the reference input. Obviously, haptic force feedback is the reference of the DHG model. It should be noted that we aim to thoroughly analyze the DHG with human-included experiments in a separate study in the future.

3.1. Dataset Revision and Model Configuration

As mentioned in the previous sections, we defined a drilling path in the virtual environment and asked six volunteers to drill through that path. As shown in **Figure 8**, haptic force feedback (**Figure 8A**), positions (**Figure 8B**), bone's layers (**Figure 8D**), depth of penetration (**Figure 8E**), and drill's temperature (**Figure 8F**) are the features of the dataset; "Drill's status" (**Figure 8C**) has not been involved in the dataset, though its correlation with drill temperature is comparable in the figure. This figure represents a time window of captured data from all sensors with 1,000 data records. The values corresponding to force feedback (**Figure 8A**), positions (**Figure 8B**), and penetration depth (**Figure 8E**) has been normalized; in other subplots, 0 means "deactivated" and 1 indicates "activated." For better visualization, the subplot related to bone's layers (**Figure 8D**) illustrates the presence of the drill's tip in different layers within a sequence of data with 30 records.

$r_i \in R^9$ is defined as the ith record of the prepared dataset, which is sorted by time. To convert the dataset records to a compatible format for an unrolled network, a modification is needed in such a way that every input in time instant t should be a set of e previous data records. Accordingly, the new dataset contains the records as follows:

$$nd = \{rn_1 = r_{1:e}, rn_2 = r_{2:e+1}, \ldots, rn_i = r_{i:e+i-1}\} \quad (9)$$

where $rn_i \in R^{e \times n}$, e is the time step and $t = ld - e + 1$ (ld is the length of dataset before conversion). It is worth to point that every input sample rn_i that encompasses data corresponding to e previous data should be mapped to the output space of $e + 1$. In this work, the dataset explained in section 2.2 was converted to the new format with the time step $e = 20$ with the aim of being compatible with the training phase. In fact, the system produced haptic force feedback in the current time using 20 previous data samples. Eventually, the dataset was divided into training and test sets without shuffling (**Table 1**).

3.2. Result and Discussion

We complied a dataset containing the demonstrations of six volunteers during accomplishing a drilling task. These data

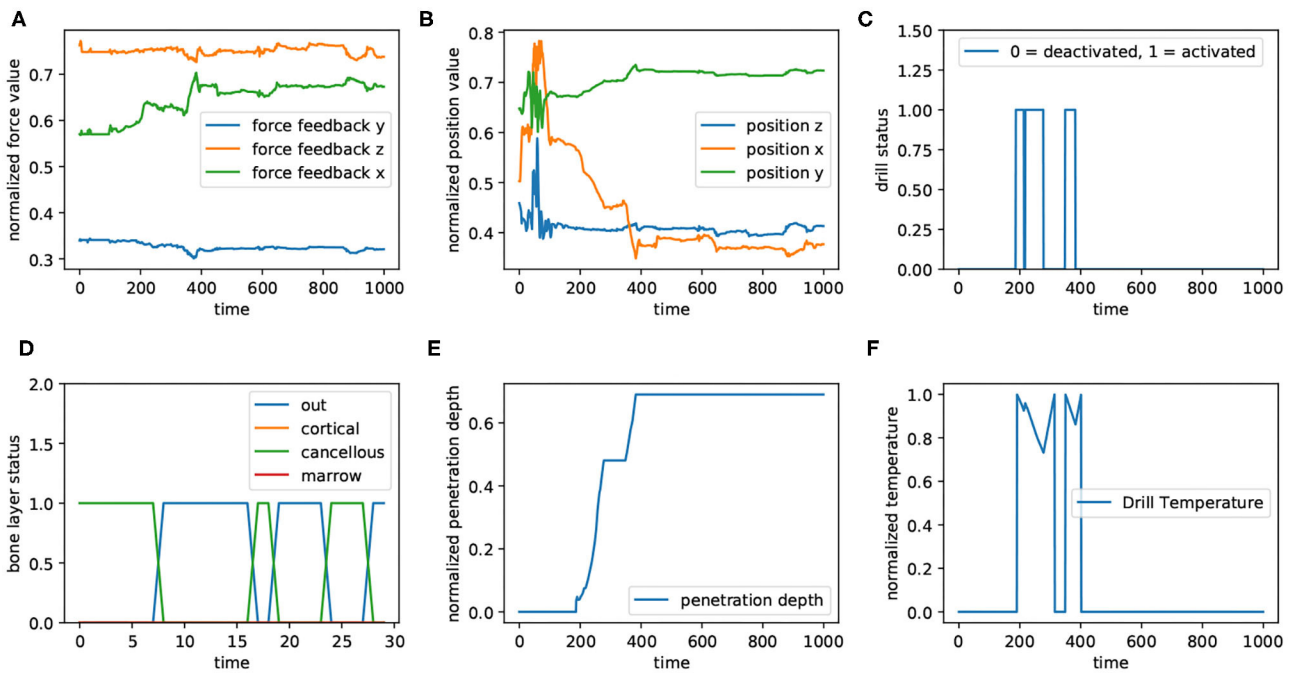

FIGURE 8 | The diagram shows the data captured from different sources in a window of 1,000 data samples. Panels **(A,B)** show the force feedback and positions, receptively. They have been plotted in 3 dimension (x, y, and z). In addition, all values corresponding to force feedback, positions, drill's temperature **(F)**, and penetration depth **(E)** have been normalized (between 0 and 1). Also, for both drilling status **(C)** and bone's layers **(D)**, 0 denotes "inactivated" and 1 means "activated." Panel **(D)** illustrates the layer of the bone, in which drill is located. For a better visualization in this subplot, the 30 first data corresponding to the aforementioned window are plotted.

TABLE 1 | The result obtained from different configurations of the DNN.

Configuration	Input size	Output size	Time steps	Layers	Memory	Training sample	Test sample	Batches	RMSE
1	9	3	20	1	128	9,133	1,442	50	0.0551
2	9	3	20	2	256	9,133	1,442	50	0.0249
3	3	3	20	2	256	9,133	1,442	50	0.0335
4	9	9	20	2	256	9,133	1,442	50	0.0626

The configuration related to the sensor fusion is shown in the first and second row. Increasing both memory and layer of the network caused to improve the DHG's performance. The superiority of the DHG with a sensor fusion setup (second row) is obvious in comparison with the third and last row. The third setup is the reproduction of the LSTM configuration used (Khatami et al., 2017).

are regarded as the reference behaviors for the input in the training phase. The DHG is supposed to mimic the gestures and act as a professional surgeon in that specific task. In other words, the DHG predicts appropriate force feedback signals in every time instant t. The more accurate prediction on the force feedback causes to obtain the more authentic discrepancy between the gestures of novices and experts (**Figure 1**). For better clarification, there are two types of signal: haptic force feedback and haptic guidance force. The DHG learns how to anticipate the haptic force feedback in different situations. In fact, it assumes that if the DHG is capable of imitating the reference force feedback properly, then it is possible to make a meaningful haptic guidance by extracting the difference between the output of the DHG and the emitted force feedback, while a user (novice) performs a task.

Hence, we set four different configurations of the DHG so as to evaluate the performance of predictions. **Table 1** represents the throughput of models. Also, we reproduced the proposed architecture of the LSTM in Khatami et al. (2017) in order to compare the DHG with one of the latest work in the literature. All configurations consumed a same training and test set and the networks were unrolled in 20 time steps with 50 samples of data in each data batch. The size of memory or neurons for the LSTM units is listed for every configuration. Moreover, all configurations were trained in 10,000 epochs and the learning rate was 0.004.

Configuration 1 had 128 memory size through a one-layer LSTM network. The aim of this setup was mapping the input vector of size nine to an output vector with three elements related to the haptic force feedback prediction. Configuration 2 is the intended architecture for the DHG. This setup reached to the best result in comparison with the others. **Figure 7** demonstrates the architecture of the DHG. The prepared data (section 3.1) is fed to an LSTM, which is unrolled over $e = 20$. Every hidden state of the unrolled unit enters to another LSTM unit in layer 2. In this unit, only the output of the hidden state in time t goes to a dense layer. Since the DHG aims at estimating the forces as a regression problem, the activation function for the dense layer is a linear one.

As mentioned earlier, to compare the influence of the sensor fusion (DHG) with the conventional multi-dimensional time series prediction in providing haptic force feedback, we set a DNN to anticipate force values in three axes while receiving the same feature vector (force feedback) solitary in the input. Configuration 2 is the implementation of with the same dataset and layers (Khatami et al., 2017). Comparing configurations 2 and 3 of **Table 1**, it can be seen that the sensor fusion setup has had a positive impact on reducing the error of force-feedback predictions. In fact, configuration 2 (Khatami et al., 2017) has hypothesized that the applied forces in the past is the only parameter, which influences on the currently yielded haptic force feedback. From that perspective, some effective parameters in the surgery such as time of completion, drilling speed, and tissue layer types should be assumed as fixed values or in some way, they have been overlooked.

In contrast, the DHG has attempted to include those parameters in the process of force estimation so as to investigate the effect related to not only physical properties of the bones but also the status of the actuator and its workspace environment on forces. In reality, the expert surgeons' maneuver in time t not only depends on the previously taken actions, but also is influenced by the status of the drill and environment it pierces through. The last row (configuration 4) shows the RMSE while the DHG was configured to predict features as same as the input vector. As mentioned before, this is the conventional multi-dimensional time series. Although the output vector contains force feedback, drill's positions, temperature, bone's layer, and penetration depth, the RMSE was computed just by using the elements of output vector related to the force feedback data. Finally, we showed that not only a deep recurrent neural network is capable of learning surgical gestures aptly but also having a sensor fusion mechanism through the network structure can impact on the prediction positively.

Figure 9 visualizes the performance of the DHG while using second configuration in **Table 1** to predict the unforeseen test data. There are two types of signals in the plot: reference and predicted. Every dimension of a force-feedback reference (x, y, z) was normalized. The plot demonstrates the prediction of the DHG for every reference of force-feedback dimensions in a specific time window with 1,000 sample. In other words, it was fed by 20 previous data samples for making anticipations on force feedback in every time t. Although the reference signal in

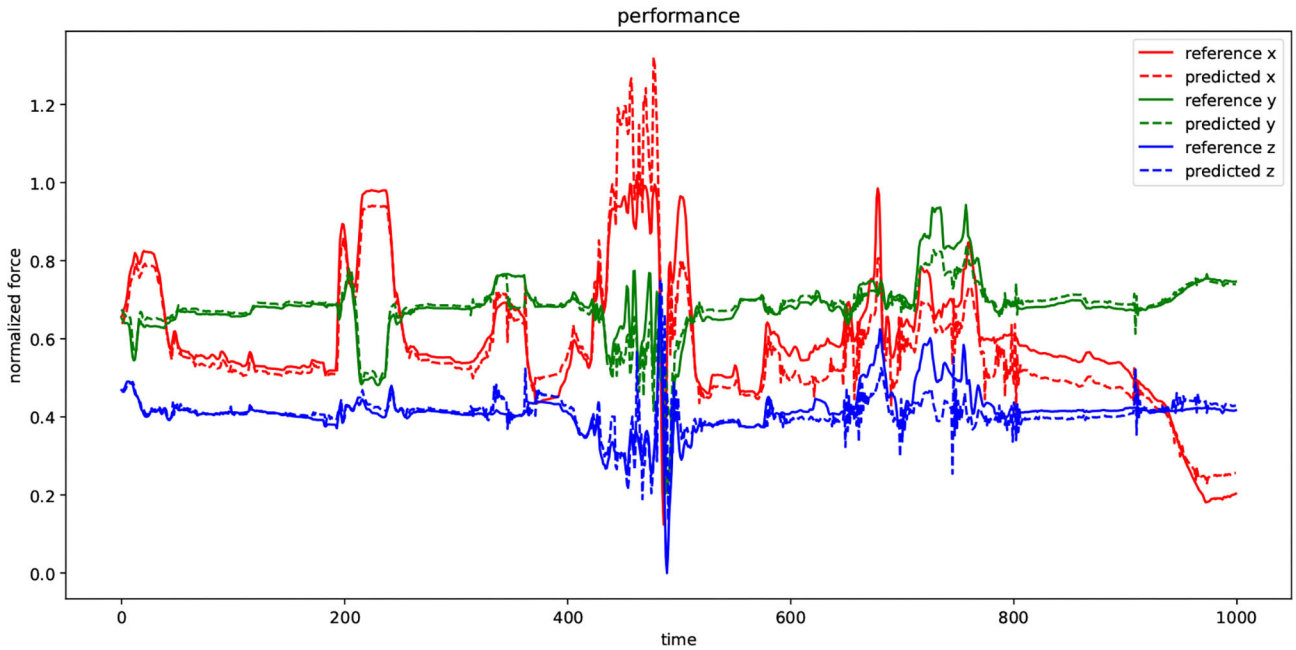

FIGURE 9 | The diagram depicts the performance of the DHG in a specified window with 1,000 data samples. Every dimension of force-feedback signals (x, y, and z) has a reference and a predicted demonstration. The value of the references has been normalized and also the model has been trained by normalized training set as well. The DHG makes predictions on force feedback in every time *t* using 20 previous data samples.

both test and training set was normalized, in some points the prediction has exceeded above 1 because of generalization that causes model to have margin around actual data and avoid facing with over-fitting.

It is worth noting that to use predicted guidance signals in the haptic device it should be denormalized regarding to the minimum and maximum of the samples in the dataset prior to dividing data into test and training sets. Estimating force feedback values in the data preparation phase along with normalization and denormalization process may cause to reduce the accuracy of trained models in practice. However, having a more precise guidance signal leads to effectively instruct trainees, but using directions of the force regardless of its value can make an acceptable feeling of haptic feedback, whenever a distraction occurs. All in all, the DHG is a modified version of RNNs with an LSTM architecture, which is a general solution for any problems using time-varying data. Since most of surgical tasks are carried out by surgeons' movements and their corresponding data has similar properties to our dataset, the DHG can be generalized to other specific surgical tasks as well.

4. CONCLUSION

In this work, we presented a deep learning based system in order to explore improvements in the performance of surgeons in surgical drilling operations. The proposed system strives to enhance the skill transfer system for instructing surgeons either the experts or novices via generating haptic guidance signals during the surgery. The system can address the limitations due to especial circumstances such as the COVID-19 pandemic, in which trainees cannot practice surgical tasks. This was achieved by designing a deep recurrent neural network with an LSTM architecture that models the behavior of experts. As a sensor fusion method, the DNN was trained using the data emitted from different sources such as drill's temperature, penetration depth, and the type of bone's layer. This led to have a robust model, which predicts demonstrations precisely. Since the experimental setup is not equipped with a force sensor, the simulation estimates different data values such as stiffness based on the physical properties of simulated bones. Finally, the experimental result showed that the proposed system was able to predict accurately haptic force feedback. Although the proposed method performed effectively in the evaluations, we did not apply the method in a human factor study. In fact, the significant purpose of this work was to inspect the possibility and performance, mostly by regular machine learning methods. Therefore, as a future work, we intend to exert the method in a practical experiment and examine it by surgeons.

DATA AVAILABILITY STATEMENT

The datasets presented in this article are not readily available because the data belongs to the Reach Lab at Kettering University. Requests to access the datasets should be directed to Mehrdad Zadeh, mzadeh@kettering.edu.

ETHICS STATEMENT

The studies involving human participants were reviewed and approved by The Kettering University Institutional Review Board (IRB protocol 2012.05). The patients/participants provided their written informed consent to participate in this study.

AUTHOR CONTRIBUTIONS

PF proposed and implemented the method and also wrote the paper. JD was the supervisor of the research lab as well as this project and defined the problem and contributed in the solution. MZ setup along with the data was provided by him. In parallel, he was the research co-supervisor and also contributed in the solution. All authors contributed to the article and approved the submitted version.

ACKNOWLEDGMENTS

The experiments of this research were approved by the Kettering University Institutional Review Board (IRB protocol 2012.05). The authors would like to thank the Kettering University students who volunteered to participate in the experiments and help with the experimental setup and data compilation.

REFERENCES

Abbott, J. J., Marayong, P., and Okamura, A. M. (2007). "Haptic virtual fixtures for robot-assisted manipulation," in *Robotics Research*, eds S. Thrun, R. Brooks, and H. Durrant-Whyte (Berlin; Heidelberg: Springer), 49–64. doi: 10.1007/978-3-540-48113-3_5

Al-Jabir, A., Kerwan, A., Nicola, M., Alsafi, Z., Khan, M., Sohrabi, C., et al. (2020). Impact of the coronavirus (covid-19) pandemic on surgical practice - Part 1. *Int. J. Surg.* 79, 168–179. doi: 10.1016/j.ijsu.2020.05.022

Altché, F., and de La Fortelle, A. (2018). An LSTM network for highway trajectory prediction. *CoRR abs/1801.07962*. Available online at: https://arxiv.org/abs/1801.07962

Bernardi, L., Germani, P., Del Zotto, G., Scotton, G., and de Manzini, N. (2020). Impact of covid-19 pandemic on general surgery training program: an Italian experience. *Am. J. Surg.* 220, 1361–1363. doi: 10.1016/j.amjsurg.2020.06.010

Bogoni, T. N., and Pinho, M. S. (2013). "Haptic technique for simulating multiple density materials and material removal," in *21st WSCG 2013* (Plzen), 151–160.

Brown, T. D., and Ferguson, A. B. (1980). Mechanical property distributions in the cancellous bone of the human proximal femur. *Acta Orthopaed. Scand.* 51, 429–437. doi: 10.3109/17453678008990819

Chipalkatty, R., Daepp, H., Egerstedt, M., and Book, W. (2011). "Human-in-the-loop: MPC for shared control of a quadruped rescue robot," in *2011 IEEE/RSJ International Conference on Intelligent Robots and Systems* (San Francisco, CA), 4556–4561. doi: 10.1109/IROS.2011.6094601

Compere, C. L. (1980). Manual of internal fixation: techniques recommended by the ao group. *JAMA*, 244(3):283. doi: 10.1001/jama.1980.03310030057038

de Montbrun, S. L., and MacRae, H. (2012). Simulation in surgical education. *Clin. Colon Rectal Surg.* 25, 156–165. doi: 10.1055/s-0032-1322553

Gil, G. D., Walker, J. M., Zemiti, N., Okamura, A. M., and Poignet, P. (2019). How to enhance learning of robotic surgery gestures? A tactile cue saliency investigation for 3d hand guidance. *CoRR abs/1904.00510*. doi: 10.31256/HSMR2019.9

Goldacre, M. J., Roberts, S. E., and Yeates, D. (2002). Mortality after admission to hospital with fractured neck of femur: database study. *BMJ* 325, 868–869. doi: 10.1136/bmj.325.7369.868

Hochreiter, S., Bengio, Y., Frasconi, P., and Schmidhuber, J. (2001). Gradient flow in recurrent nets: the difficulty of learning long-term dependencies. Available online at: https://pdfs.semanticscholar.org/2e5f/2b57f4c476dd69dc22ccdf547e48f40a994c.pdf

Hochreiter, S., and Schmidhuber, J. (1997). Long short-term memory. *Neural Comput.* 9, 1735–1780. doi: 10.1162/neco.1997.9.8.1735

Khatami, A., Tai, Y., Khosravi, A., Wei, L., Dalvand, M. M., Peng, J., et al. (2017). "A haptics feedback based-lstm predictive model for pericardiocentesis therapy using public introperative data," in *Neural Information Processing*, eds D. Liu, S. Xie, Y. Li, D. Zhao, and S. M. El-Alfy (Cham: Springer International Publishing), 810–818. doi: 10.1007/978-3-319-70139-4_82

Kho, J. Y., Johns, B. D., Thomas, G. W., Karam, M. D., Marsh, J. L., and Anderson, D. D. (2015). A hybrid reality radiation-free simulator for teaching wire navigation skills. *J. Orthop. Trauma* 29, e385–e390. doi: 10.1097/BOT.0000000000000372

Kingma, D. P., and Ba, J. (2014). Adam: a method for stochastic optimization. *CoRR abs/1412.6980*. Available online at: https://arxiv.org/abs/1412.6980

Kronander, K., and Billard, A. (2014). Learning compliant manipulation through kinesthetic and tactile human-robot interaction. *IEEE Trans. Hapt.* 7, 367–380. doi: 10.1109/TOH.2013.54

Liu, Y., and Laycock, S. D. (2009). "A haptic system for drilling into volume data with polygonal tools," in *Theory and Practice of Computer Graphics*, eds W. Tang and J. Collomosse (The Eurographics Association). doi: 10.2312/LocalChapterEvents/TPCG/TPCG09/009-016

Medina, J., Lorenz, T., and Hirche, S. (2015). Synthesizing anticipatory haptic assistance considering human behavior uncertainty. *IEEE Trans. Robot.* 31, 180–190. doi: 10.1109/TRO.2014.2387571

Morris, D., Sewell, C., Barbagli, F., Salisbury, K., Blevins, N. H., and Girod, S. (2006). Visuohaptic simulation of bone surgery for training and evaluation. *IEEE Comput. Graph. Appl.* 26, 48–57. doi: 10.1109/MCG.2006.140

Morris, D., Sewell, C., Blevins, N., Barbagli, F., and Salisbury, K. (2004). "A collaborative virtual environment for the simulation of temporal bone surgery," in *International Conference on Medical Image Computing and Computer-Assisted Intervention* (Berlin; Heidelberg: Springer), 319–327. doi: 10.1007/978-3-540-30136-3_40

Pezent, E., Fani, S., Clark, J., Bianchi, M., and O'Malley, M. K. (2019). Spatially separating haptic guidance from task dynamics through wearable devices. *IEEE Trans. Hapt.* 12, 581–593. doi: 10.1109/TOH.2019.2919281

Ramón Medina, J., Lee, D., and Hirche, S. (2012). "Risk-sensitive optimal feedback control for haptic assistance," in *2012 IEEE International Conference on Robotics and Automation* (Saint Paul, MN), 1025–1031. doi: 10.1109/ICRA.2012.6225085

Reiley, C. E., and Hager, G. D. (2009). "Task versus subtask surgical skill evaluation of robotic minimally invasive surgery," in *Medical Image Computing and Computer-Assisted Intervention – MICCAI 2009*, eds G.-Z. Yang, D. Hawkes, D. Rueckert, A. Noble, and C. Taylor (Berlin; Heidelberg: Springer), 435–442.

Rozo, L., Calinon, S., Caldwell, D. G., Jimenez, P., and Torras, C. (2016). Learning physical collaborative robot behaviors from human demonstrations. *IEEE Trans. Robot.* 32, 513–527. doi: 10.1109/TRO.2016.2540623

Rozo, L., Jiménez, P., and Torras, C. (2013). A robot learning from demonstration framework to perform force-based manipulation tasks. *Intell. Serv. Robot.* 6, 33–51. doi: 10.1007/s11370-012-0128-9

Safavi, A., Huynh, L., Rahmat-Khah, H., Zahedi, E., and Zadeh, M. H. (2015). "A novel MPC approach to optimize force feedback for human-robot shared control," in *2015 IEEE/RSJ International Conference on Intelligent Robots and Systems (IROS)* (Hamburg), 3018–3023. doi: 10.1109/IROS.2015.7353793

Safavi, A., and Zadeh, M. H. (2015). "Model-based haptic guidance in surgical skill improvement," in *2015 IEEE International Conference on Systems, Man, and Cybernetics* (Kowloon), 1104–1109. doi: 10.1109/SMC.2015.198

Safavi, A., and Zadeh, M. H. (2017). Teaching the user by learning from the user: personalizing movement control in physical human-robot interaction. *IEEE/CAA J. Automat. Sin.* 4, 704–713. doi: 10.1109/JAS.2017.7510634

Schapira, D., and Schapira, C. (1992). Osteoporosis: the evolution of a scientific term. *Osteoporos. Int*. 2, 164–167. doi: 10.1007/BF01623921

Seymour, N. (2008). VR to OR: a review of the evidence that virtual reality simulation improves operating room performance. *World J. Surg*. 32, 182–188. doi: 10.1007/s00268-007-9307-9

Sofronia, R. E., Davidescu, A., and Savii, G. G. (2012). Towards a virtual reality simulator for orthognathic basic skils. *Appl. Mech. Mater*. 162, 352–357. doi: 10.4028/www.scientific.net/AMM.162.352

Svedbom, A., Hernlund, E., Ivergård, M., Compston, J., Cooper, C., Stenmark, J., et al. (2013). Osteoporosis in the european union: a compendium of country-specific reports. *Arch. Osteoporos*. 8:137. doi: 10.1007/s11657-013-0137-0

Tan, S. S., and Sarker, S. (2011). Simulation in surgery: a review. *Scot. Med. J*. 56, 104–109. doi: 10.1258/smj.2011.011098

Tao, L., Zappella, L., Hager, G. D., and Vidal, R. (2013). "Surgical gesture segmentation and recognition," in *Medical Image Computing and Computer-Assisted Intervention – MICCAI 2013*, eds K. Mori, I. Sakuma, Y. Sato, C. Barillot, and N. Navab (Berlin; Heidelberg: Springer), 339–346.

Teo, J. C., Si-Hoe, K. M., Keh, J. E., and Teoh, S. H. (2006). Relationship between CT intensity, micro-architecture and mechanical properties of porcine vertebral cancellous bone. *Clin. Biomech*. 21, 235–244. doi: 10.1016/j.clinbiomech.2005.11.001

Thorngren, K.-G. (2008). National registration of hip fractures. doi: 10.1007/978-3-642-00966-2_2

Van Duren, B., Sugand, K., Wescott, R., Carrington, R., and Hart, A. (2018). Augmented reality fluoroscopy simulation of the guide-wire insertion in DHS surgery: a proof of concept study. *Med. Eng. Phys*. 55, 52–59. doi: 10.1016/j.medengphy.2018.02.007

Wade, S., Strader, C., Fitzpatrick, L., Anthony, M., and O'Malley, C. (2014). Estimating prevalence of osteoporosis: examples from industrialized countries. *Arch. Osteoporos*. 9:182. doi: 10.1007/s11657-014-0182-3

Willson, T., Nelson, S. D., Newbold, J., Nelson, R. E., and LaFleur, J. (2015). The clinical epidemiology of male osteoporosis: a review of the recent literature. *Clin. Epidemiol*. 7, 65–76. doi: 10.2147/CLEP.S40966

Zahedi, E., Dargahi, J., Kia, M., and Zadeh, M. (2017). Gesture-based adaptive haptic guidance: a comparison of discriminative and generative modeling approaches. *IEEE Robot. Automat. Lett*. 2, 1015–1022. doi: 10.1109/LRA.2017.2660071

Zahedi, E., Khosravian, F., Wang, W., Armand, M., Dargahi, J., and Zadeh, M. (2019). Towards skill transfer via learning-based guidance in human-robot interaction: an application to orthopaedic surgical drilling skill. *J. Intell. Robot. Syst*. 98, 667–678. doi: 10.1007/s10846-019-01082-2

Conflict of Interest: The authors declare that the research was conducted in the absence of any commercial or financial relationships that could be construed as a potential conflict of interest.

frontiers in Robotics and AI

CORRECTION
published: 05 May 2021
doi: 10.3389/frobt.2021.691570

Corrigendum: Deep Learning-Based Haptic Guidance for Surgical Skills Transfer

Pedram Fekri[1]*, *Javad Dargahi*[1] *and Mehrdad Zadeh*[2]

[1]Mechanical, Industrial, and Aerospace Engineering Department, Concordia University, Montreal, QC, Canada, [2]Electrical and Computer Engineering Department, Kettering University, Flint, MI, United States

Keywords: deep learning, recurrent neural network, LSTM, haptic, force feedback, bone drilling, surgical skill transfer, COVID-19

A Corrigendum on

Deep Learning-Based Haptic Guidance for Surgical Skills Transfer
by Fekri, P., Dargahi, J., and Zadeh, M., (2021). Front. Robot. AI 7:586707. doi:10.3389/frobt.2020.586707

OPEN ACCESS

Edited and reviewed by:
S. Farokh Atashzar,
New York University, United States

***Correspondence:**
Pedram Fekri
p_fekri@encs.concordia.ca

Specialty section:
This article was submitted to Biomedical Robotics, a section of the journal Frontiers in Robotics and AI

Received: *07 April 2021*
Accepted: *12 April 2021*
Published: *05 May 2021*

Citation:
Fekri P, Dargahi J and Zadeh M (2021) Corrigendum: Deep Learning-Based Haptic Guidance for Surgical Skills Transfer. Front. Robot. AI 8:691570. doi: 10.3389/frobt.2021.691570

In the original article, there was a mistake in **Figure 7** as published. The figure included "Dropout", which was not used in our reported results but can be applied to the "Dense Layers" before the output layer. Since we have not utilized "Dropout" in the reported results, the corresponding information has been removed from the caption of **Figure 7** and a correction has been made to the **Evaluation and Discussion** section, subsection **Result and Discussion, Paragraph 3**:

"Configuration 1 had 128 memory size through a one-layer LSTM network. The aim of this setup was mapping the input vector of size nine to an output vector with three elements related to the haptic force feedback prediction. Configuration 2 is the intended architecture for the DHG. This setup reached to the best result in comparison with the others. **Figure 7** demonstrates the architecture of the DHG. The prepared data (section 3.1) is fed to an LSTM, which is unrolled over $e = 20$. Every hidden state of the unrolled unit enters to another LSTM unit in layer 2. In this unit, only the output of the hidden state in time t goes to a dense layer. Since the DHG aims at estimating the forces as a regression problem, the activation function for the dense layer is a linear one."

The corrected Figure 7 and caption appear below.

The authors apologize for this error and state that this does not change the scientific conclusions of the article in any way. The original article has been updated.

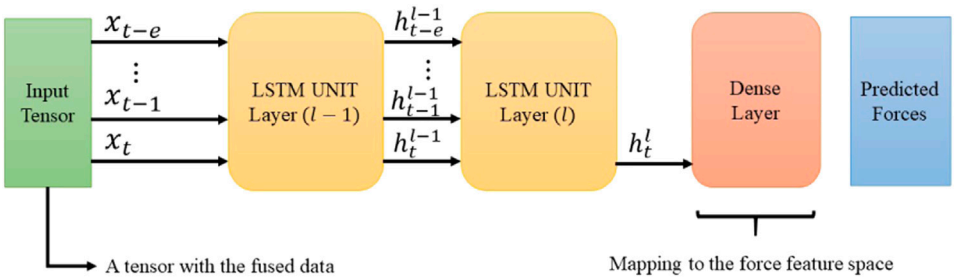

FIGURE 7 | The diagram shows the intended architecture for the DHG. The input is a tensor containing the data from different sources (section 2.2). The LSTM is unrolled over e previously generated data. The cell state h is the input of its corresponding unrolled unit in the next layer. However, using the latest LSTM unit's output, the DHG squeezes the prediction vector through a dense layer. Finally, the output of the network is a vector with three elements corresponding to forces in *x*, *y*, and *z* direction.

frontiers in Robotics and AI

ORIGINAL RESEARCH
published: 22 January 2021
doi: 10.3389/frobt.2020.611424

Application of DenTeach in Remote Dentistry Teaching and Learning During the COVID-19 Pandemic: A Case Study

Lingbo Cheng[1,2], *Maryam Kalvandi*[3], *Sheri McKinstry*[4], *Ali Maddahi*[5,6], *Ambika Chaudhary*[7], *Yaser Maddahi*[6] *and Mahdi Tavakoli*[2]*

[1]College of Control Science and Engineering, Zhejiang University, Zhejiang, China, [2]Department of Electrical and Computer Engineering, University of Alberta, Edmonton, AB, Canada, [3]Manitoba Dental Association, Winnipeg, MB, Canada, [4]College of Dentistry, University of Saskatchewan, Saskatchewan, SK, Canada, [5]Rady Faculty of Health Sciences, University of Manitoba, Winnipeg, MB, Canada, [6]Department of Research and Development, Tactile Robotics, Winnipeg, MB, Canada, [7]Dental Council of India and Indian Dental Association, Mumbai, India

OPEN ACCESS

Edited by:
Jungwon Yoon,
Gwangju Institute of Science and Technology, South Korea

Reviewed by:
Yue Chen,
University of Arkansas, United States
Hao Su,
City College of New York, United States

***Correspondence:**
Mahdi Tavakoli
mahdi.tavakoli@ualberta.ca

Specialty section:
This article was submitted to Biomedical Robotics, a section of the journal Frontiers in Robotics and AI

Received: 29 September 2020
Accepted: 22 December 2020
Published: 22 January 2021

Citation:
Cheng L, Kalvandi M, McKinstry S, Maddahi A, Chaudhary A, Maddahi Y and Tavakoli M (2021) Application of DenTeach in Remote Dentistry Teaching and Learning During the COVID-19 Pandemic: A Case Study. Front. Robot. AI 7:611424. doi: 10.3389/frobt.2020.611424

In December 2019, an outbreak of novel coronavirus pneumonia occurred, and subsequently attracted worldwide attention when it bloomed into the COVID-19 pandemic. To limit the spread and transmission of the novel coronavirus, governments, regulatory bodies, and health authorities across the globe strongly enforced shut down of educational institutions including medical and dental schools. The adverse effects of COVID-19 on dental education have been tremendous, including difficulties in the delivery of practical courses such as restorative dentistry. As a solution to help dental schools adapt to the pandemic, we have developed a compact and portable teaching-learning platform called DenTeach. This platform is intended for remote teaching and learning pertaining to dental schools at these unprecedented times. This device can facilitate fully remote and physical-distancing-aware teaching and learning in dentistry. DenTeach platform consists of an instructor workstation (DT-Performer), a student workstation (DT-Student), advanced wireless networking technology, and cloud-based data storage and retrieval. The platform procedurally synchronizes the instructor and the student with real-time video, audio, feel, and posture (VAFP). To provide quantitative feedback to instructors and students, the DT-Student workstation quantifies key performance indices (KPIs) related to a given task to assess and improve various aspects of the dental skills of the students. DenTeach has been developed for use in teaching, shadowing, and practice modes. In the teaching mode, the device provides each student with tactile feedback by processing the data measured and/or obtained from the instructor's workstation, which helps the student enhance their dental skills while inherently learning from the instructor. In the shadowing mode, the student can download the augmented videos and start watching, feeling, and repeating the tasks before entering the practice mode. In the practice mode, students use the system to perform dental tasks and have their dental performance skills automatically evaluated in terms of KPIs such that both the student and the instructor are able to monitor student's work. Most importantly, as DenTeach is packaged in a small portable suitcase, it can be used anywhere by connecting

to the cloud-based data storage network to retrieve procedures and performance metrics. This paper also discusses the feasibility of the DenTeach device in the form of a case study. It is demonstrated that a combination of the KPIs, video views, and graphical reports in both teaching and shadowing modes effectively help the student understand which aspects of their work needs further improvement. Moreover, the results of the practice mode over 10 trials have shown significant improvement in terms of tool handling, smoothness of motion, and steadiness of the operation.

Keywords: COVID-19, DenTeach, dental services, teaching and learning model, quantitative assessment

INTRODUCTION

The coronavirus disease 2019 (COVID-19) has been declared as a global pandemic by the World Health Organization (WHO). Globally, as of September 7, 2020, there have been 27,208,206 confirmed cases of COVID-19, including 889,989 deaths (WHO, 2020a). COVID-19 is estimated to have a mortality rate of approximately 4.05%. To slow the spread of COVID-19 at both national and community levels, various measures have been implemented such as COVID-19 testing, contact-tracing and quarantine, social and physical distancing, and international travel bans.

Social and physical distancing measures aim to slow the spread of COVID-19 by stopping chains of transmission of the SARS-CoV-2 virus (WHO, 2020b). Physical distancing measures include maintaining at least 2 m of physical distance between people and the reduction of non-essential personal interactions and reducing contact with potentially contaminated surfaces. Social distancing measures for the general public include flexible work arrangements such as teleworking, distance learning, cancellation of public events to prevent crowding, closure of non-essential facilities and services, local and national movement restrictions, staying-at-home measures, and coordinated reorganization of health care and social services networks to protect hospitals. During the time of the global pandemic, people are encouraged to sustain virtual social connections within families and communities.

COVID-19 social distancing policies led to a widespread lockdown of schools and universities, including dental education institutions (UNESCO, 2020). To a large degree, this has resulted in the extension of the study terms, and deferral of exams and graduation dates. COVID-19 lockdown has exhibited serious repercussions for dental education. While theoretical courses have still been delivered online during the COVID-19 pandemic, the delivery of hands-on courses such as restorative dentistry has been challenging while instructors and students self-isolate at home without access to dental equipment. The duration of this teaching interruption is still uncertain, and dental colleges must keep in mind the possibility of a second or third wave of COVID-19. Hence, it is necessary for dental colleges to look for a reliable and robust, yet inexpensive, solution to ensure the continuation of practical skills in dental education (Solana, 2020).

In this paper, we develop a novel portable teaching-learning platform for remote teaching and learning in dentistry (Maddahi et al., 2020). This new platform, DenTeach, provides an opportunity for dental schools to continue teaching and learning from a remote location (such as a home). This device can fill the existing gap for fully remote or physical-distancing-aware teaching and learning in dentistry. The DenTeach platform consists of an instructor workstation (DT-Performer), a student workstation (DT-Student), advanced wireless networking technology, and cloud-based data storage and retrieval. This platform has high efficiency and is able to procedurally synchronize the instructor and the student with real-time video, audio, feel, and posture (VAFP). As DenTeach is packaged in a small portable suitcase, it can be used anywhere by connecting to cloud-based data to retrieve procedures and performance metrics.

In this paper, we describe the available training and learning models, present the developed DenTeach platform, and demonstrate the feasibility of the DenTeach platform through a case study.

THE STATE OF DENTAL EDUCATION

In health sciences, the use of classroom and hands-on instructions by experts has been a training mechanism of choice for most educational programs. This training mechanism is also called the traditional novice-expert apprenticeship model (Collins et al., 1991). In this traditional model, dental students acquire technical dental skills through years of hands-on training in dental laboratories and clinics and receive supervision and feedback on performance skills. Specifically, mentors conduct a procedure that offers the students the opportunity of observing, then assisting, and finally performing that procedure under the supervision of their mentor. Students learn the nuances of required skills through working on artificial materials, cadaveric organs, animals, and case observations, and receive qualitative feedback on their performance from their mentor (Collins et al., 1991).

However, the traditional novice-expert model cannot be continued due to the continued lockdown of the dental school in the age of the COVID-19 pandemic, as students always require the presence of their mentor to practice and learn the key operation skills in a classroom setting. Additionally, in the field of dentistry, this traditional model is time-consuming, and the training process is slow and lacks quantitative

measures to assess aspects of technical skills. As a result, trial and error often constitute a major part of learning psychomotor skills for a student. To provide students with continued learning and training education in times of unprecedented crisis like COVID-19, decreased training hours, and increased training efficiency, there is an increasing demand to develop a portable intelligent teaching-learning platform capable of providing remote teaching and learning delivery and quantitative evaluation of dental performance.

Remote Teaching and Learning Delivery

The current teaching-learning method involves an instructor to provide visual instructions at a central point in the classroom, while students watch, listen, ask questions, and then imitate tasks. As all dental pieces of equipment are placed in dental schools, students do not have access to the equipment once they leave the classroom. However, if practice units and tools at both the instructor's and students' work areas are portable, the teaching and learning can be performed remotely (i.e., while self-isolating at home during the pandemic).

Dental Performance and Skills Assessment

In order to objectively assess technical dental skills (Schwibbe et al., 2016), it is implicit that one must first be able to measure and study essential aspects of dental performance. One important aspect of instrument handling is the ability to use the instrument (such as the dental handpiece) to effectively, yet safely, accomplish the dental goal. There are several tactile skills that should be understood and learned by students. Most importantly, a student should know how to hold the dental handpiece (orientation and position of the handpiece), comprehend how fast the drill should rotate, perceive the level of vibration produced by the handpiece during the performance of a dental task (acceleration and jerk) and receive adequate alerts once a task is performed improperly. The tactile skills listed above may vary depending on the type of tooth, the region of the oral cavity, or conducted tasks.

Dental Surgical Simulators

Understanding the tactile skills could be made possible through the incorporation of sensory and actuation systems onto a conventional tool such as a dental rotary handpiece in restorative dentistry.

A device for teaching and training dental treatment techniques has been developed that exerts a force on a tooth, preferably using tools, in order to examine or treat this tooth (Riener and Burgkart, 2013). The mandible or a tooth is coupled to a force measuring device in a manner that enables the forces applied to the tooth to be represented. By using force sensors, the force applied by the dentist is measured and used as a reference signal to be compared with the force applied by the student. Moreover, audible signal patterns are retrieved and audibly displayed utilizing an acoustic display unit such as loudspeakers, which means that screams of pain are played if the calculation shows that the tip of the drill invades the area of the nerve'. Additionally, the position of the force-application point of the tool is localized by means of a navigation system, such as a camera and other optical systems.

In the work of Ranta et al. (2007), a training system has been presented using haptic-enabled simulations of dental procedures to provide the sensorimotor involvement needed for dental training. To provide tactile feedback combined with a realistic visual experience, the system integrates an off-the-shelf haptic stylus interface for simulating the movement and feel of the tooltip with a 3D stereoscopic display. The haptic stylus enables the dental student to orient and to operate simulated dental tools. Working on a virtual model viewed in a stereo display, dental students can use a simulated pick to probe a tooth or a simulated drill to prepare a tooth for cavity repair. The touch feedback is simulated by representing these dental instruments as force-to-a-point tools, which map to haptic simulation procedures executed on a computer workstation that also provides the visual display.

Hayka and Eytan (1997) invented a visual-audio-feeling simulation system for dentistry that comprises a dental handpiece with a drill for drilling a cavity in a tooth. A 3D sensor, attached to the dental handpiece, provides the system with the position and orientation of the drill whereas a data processing unit and a display unit simulate the drill end. The system further controls the flow of compressed air operating the drill, and thus controls the drill's speed. This imitates the sound and hand-feeling associated when drilling through tooth layers of different hardness.

Kuchenbecker et al. (2017) developed a simulator to educate dental students in caries detection; the simulator allows dental faculty to share, record, and replay the tactile vibrations felt through a dental hand instrument. This simulation approach is assessed by asking experienced dental educators to evaluate the system's real-time and video playback modes. The simulator uses an accelerometer to sense instrument vibrations and a voice coil actuator to reproduce these vibrations on another tool.

Additionally, the Iowa dental surgical simulator unit focuses on tactile skill development (Johnson et al., 2000). The system consists of three hardware components: a computer, a monitor, and a force feedback device with software. Participants interact with the computer by grasping a joystick or explorer handle attached to the force feedback device. Teeth are displayed on the monitor, and the student can manipulate the joystick or explorer in such a way as to "feel" enamel, healthy dentin, and carious dentin. Different haptic responses are received when the joystick or explorer is manipulated over the appropriate areas of the tooth.

Virtual Reality and Augmented Reality

In addition to physical devices for dentistry training, some studies (Gal et al., 2011; Bakr et al., 2013; Bakr et al., 2014) also exist on the performance of available dental simulators that use the mechanical properties of teeth to simulate the oral cavity on which dental tasks are conducted. Among the developed dental simulators, the concept of virtual reality (VR) is widely used. As early as the 1990s, the concept of a VR dental training system was introduced to practice cavity preparation (Ranta and Aviles, 1999).

Research has assessed the perception of academic staff members on the realism of the Simodont® haptic 3D-VR dental trainer (Bakr et al., 2013) (MOOG Industrial Group,

Amsterdam). This simulator comprises a simulator unit, a panel, a stereo projection, a SpaceMouse, a handpiece, and a projector. The Simodont® courseware developed by the Academic Center for Dentistry in Amsterdam allows a variety of operative dental procedures to be practiced in a virtual oral and dental environment with force feedback. PerioSim© was developed for periodontal simulation, which can simulate three typical operations including pocket probing, calculus detection, and calculus removal (Kolesnikov et al., 2008; Luciano et al., 2009). Forsslund Dental system was developed by Forsslund Systems AB in 2008 to provide VR training for practicing dental drilling and wisdom tooth extraction (Forsslund et al., 2009). Rhienmora et al. (2011) designed a haptic VR crown preparation simulator, which includes a VR environment with haptic feedback for students to practice dental surgical skills, in the context of a crown preparation procedure. An individual dental education assistant (IDEA) used a PHANToM Omni haptic device that allowed for six degrees of freedom (DOF) for position sensing and generated three DOF for force feedback. The virtual dental handpiece was locked to the position and orientation of the haptic stylus (Gal et al., 2011).

A VR dental training system was presented to address limitations and to introduce new techniques such as 1) flexible learning with self-teaching not limited to formal training hours, thus increasing students' training time and reducing the overall future costs; 2) providing students with the opportunity to gain instant feedback and to practice assessment tasks using similar criteria used by examiners; 3) presenting tooth data as a 3D multi-resolution surface model, reconstructed from a patient's volumetric data to improve real-time performance; 4) collision detection and collision response algorithms used to handle a non-spherical tool such as a cylindrical one; 5) simulation of tooth surface exploration and cutting with a cylindrical burr by utilizing a surface displacement technique (Rhienmora et al., 2008).

Augmented reality (AR) haptic systems have also been used for dental surgical skills training. In the work of Rhienmora et al. (2010), a dental training simulator utilizing a haptic device was developed based on AR and VR technologies. This simulation utilizes volumetric force feedback computation and real-time modification of the volumetric data to overlay 3D models of the tooth operated on and tools used with the real-world view. The image overlay is delivered through a transparent head-mounted display, which is paired to a haptic device for simulation of virtual dental tools. The system allows dentists to practice using a probe to examine the surface of a tooth, to feel its hardness, and to drill or cut the tooth.

Quantitative Evaluation

Although a variety of dental surgical simulators for teaching and learning has been developed, the lack of quantitative key performance indices (KPIs) to assess aspects of dental skills is still a significant issue to be addressed. With decreasing operating hours and training resources, there is an increasing demand to improve training efficiency and to provide a quantitative evaluation of dental performance using KPIs.

In order to objectively assess technical dental skills, it is implicit that one must be able to measure and study essential aspects of dental performance (described in *Dental Surgical Simulators*) and quantify KPIs. Currently, in dental schools, dental laboratories, and clinics, this knowledge is often conveyed from the instructor to the apprentices through qualitative instructions, such as "be gentle," "go deeper" or "push harder". Quantitative vibrotactile data measured during the performance of dental tasks on human teeth remain largely unavailable. Therefore, in addition to developing advanced intelligent dental simulators to reform the traditional novice-expert apprenticeship model and improve teaching and learning performance, there is a strong demand for systematic quantitative evaluation of dental performance using KPIs. To this end, Wang et al. (2011) developed a haptic-based dental simulator, and preliminary user evaluations on its first-generation prototype have been carried out. Based on the detailed requirement analysis of periodontics procedures, a combined evaluation method including qualitative and quantitative analysis was designed.

Table 1 summarizes several existing commercial dental surgical simulators for teaching and learning and their characteristics. In comparison, the developed DenTeach system in this paper is shown in **Table 1** as well.

DenTeach System

The newly developed portable teaching-learning platform, DenTeach, complements traditional methods and is based on the latest industry technologies including smart sensors, advanced robotics, big data analysis, 3D printing, AR, and cloud-based computing. The system creates a real-life traditional teaching-learning experience by synchronizing an instructor and a student with real-time VAFP. The DenTeach portable platform consisting of a DT-Performer (Instructor's software), a DT-Student software (Student's software), advanced wireless networking technology, and cloud-based data storage and retrieval has been developed for use in teaching, shadowing, and practice modes. The data storage system stores VAFP data of the DT-Performer and the DT-Students in both modes, as well as KPIs, defined for evaluating students' performance. **Figure 1** provides an overall scheme of the system. An instructor workstation comprises a commercially available dental handpiece equipped with a wireless sensory system and a video recording system while each student workstation consists of a custom-made haptic-enabled dental handpiece augmented by another sensory system and an actuation system and a video recording system. There are processing systems and display units at each workstation, and a data transmission module to transfer commands between workstations through the cloud.

Physical Setup

DenTeach complements the traditional instructor and student working area by integrating into the existing working setup (which consists of a tabletop, dental unit, and dental instruments). For the instructor work area (**Figure 2**), the DenTeach platform integrates into a standard instructor work area and dental unit, and consists of DT-Performer software, DT-Rightway Articulator, DT-RealFeel sensors, and four mini

TABLE 1 | Comparison of dental simulators.

Simulators	Simodont®	PerioSim®	Forsslund	IDEA	DenTeach
Hardware	-Two projectors -Panel PC -3D glasses -Handpiece and mirror connected to force feedback sensors	-Two computer monitors with a haptic device -Crystal eyes stereo glasses™ and a crystal eyes workstation™ -A PHANToM haptic device with 3 DOFs - VR William's periodontal probe or periodontal explorer	- Polhem haptic device - Kobra oral surgery simulator with two screens - 3D glasses	A stylus with six DOFs position sensor and three DOFs force sensor attached to a stand PHANToM omni	- Two computer monitors with a haptic device - Handpiece connected to a custom-designed sensor
Software	Moog Simodont® dental trainer courseware software	Modified version of Ghost™	Kobra simulation software	ManualDexterity™, caries detection, scaling and Root-Planning™, OralMed™ and PreDenTouch™	DT-performer software
Ability to use off campus	No	Yes	No	Yes	Yes
Feedback sensory channels	Haptic-visual-auditory	Haptic-visual-auditory	Haptic-visual	Haptic-visual	Haptic-visual-auditory
Immediate feedback	No	No	Yes	Yes	Yes
Display type	3D	3D/AR	3D/VR	Monitor screen	Monitor screen
Haptic device	Moog haptic master	PHANToM desktop	PHANToM omni/ desktop	PHANToM omni	Custom-designed DT-RealFeel drill
Virtual drilling control	Foot pedal	No	Foot pedal	NA	Foot pedal
Sensor	Force sensor	Force sensors	NR	Position and force sensors	DT-RealFeel sensor
Automatic evaluation	Yes	Yes	Yes	Yes	Yes
Direct transfer data to tutor	Yes	No	No	Yes	Yes
Expert's database	No	Yes	Yes	No	Yes
Haptic-visual collocation	Yes	No	Yes	Yes	Yes
Practice/test simulation	Yes	Yes	Yes	No	Yes

cameras. Specifically, the DT-Performer software provides a full classroom view and selectable student profile and performance index. The DT-Rightway Articulator shown in **Figure 3** is a custom-designed system that supports upper and lower typodonts. The sensors are wirelessly attached to the standard dental drills to measure quantitative performance data. Each sensor is a state-of-the-art wireless sensor that records and streams the instructor's hand motion data to the cloud (recorded data will then be imported to each student workstation). DT-Performer interprets data in a real-time fashion and provides advanced statistical data analysis to quantitatively score students' performance. During each test, the orientation data and dynamic information are measured or calculated that include roll (axial), pitch (back-to-front) and yaw (side-to-side) angles, linear accelerations (3 DOFs), angular accelerations (3 DOFs), angular velocity (3 DOFs), jerk components (3 DOFs), and several KPIs.

To display and record the instructor's hand operation during teaching procedures, four mini cameras show the top view, two side views, and inside view. All videos are transmitted simultaneously onto the students' workstations. Additionally, DT-Performer software allows the instructor to select, record, and play over 30 psychomotor performance metrics to objectively measure effort, speed, accuracy, and learning curve.

For the student work area (**Figure 4**), the DT-Student consists of a fully integrated system with four selectable instructor videos, a student's drill model superimposed over the videos of the instructor's drill to enable effective imitation or mimicking, two typodonts affixed to the DT-Rightway Articulator, a student DT-RealFeel Handpiece synchronized to the instructor's movements while in teaching mode, and a DT-Student software that allows the student to select, record, and play recordings that demonstrate over psychomotor performance metrics to objectively measure effort, speed, accuracy and learning curve. To be more specific, the custom-designed DT-RealFeel Handpiece has a handle grip associated with its components including an actuation system to generate a vibrotactile feeling, a vibrator to apply an abrupt force to the student's hand as an alarm, and a set of sensory systems along with the data communication system. Besides, the processing unit of the Student's workstation is arranged to calculate a plurality of different performance indices in which each index is calculated using one or more operating characteristics detected by the sensory system of the DT-RealFeel Handpiece. Similar

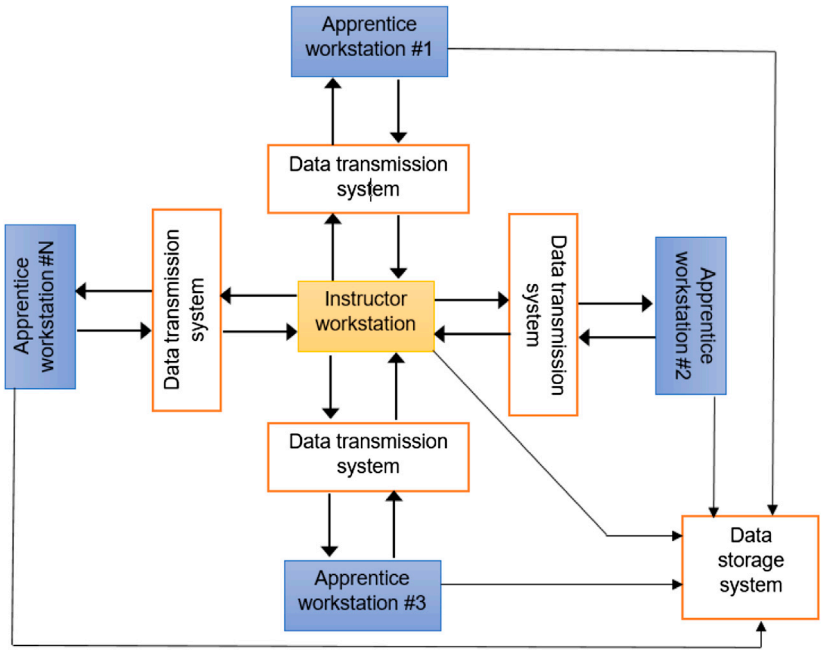

Figure 1 | The overall scheme of the DenTeach system comprising an instructor workstation, a number of student workstations, a data transmission system, and a data storage system along with the overall workflow of the main components of the device.

performance characteristics are calculated using the data from the DT-Performer at the instructor's station.

Education Modes

DenTeach allows learning activities in three modes namely teaching, shadowing, and practice.

Teaching Mode

In the teaching mode, similar to a general traditional teaching and learning mode, an instructor conducts dental tasks in the instructor's workstation and students mimic the tasks in the students' workstations. The main difference is that the DenTeach device uses a data transmission system to provide each student with tactile feedback by processing the data measured and/or obtained from the dental tool of the instructor's workstation. This helps students understand and perceive how their instructor is conducting the dental operation and tasks without their presence at the instructor's workplace. Moreover, the data storage system saves information such as data of sensory systems from the instructor and students' workstations as well as audiovisual

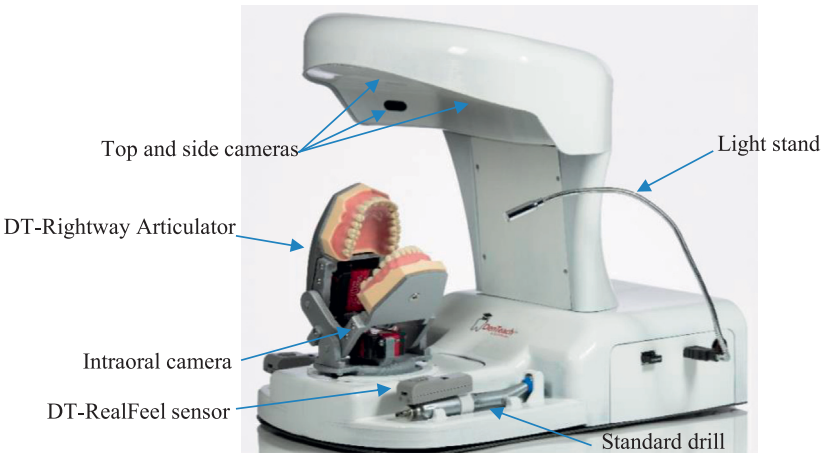

Figure 2 | Instructor workstation includes a dental unit, a rheostat, a processing unit, a tooth physical model, a dental handpiece, a set of sensory systems to measure vibrotactile data of the dental handpiece, a sensor to measure rheostat data, an audiovisual recording system, a software, and a display.

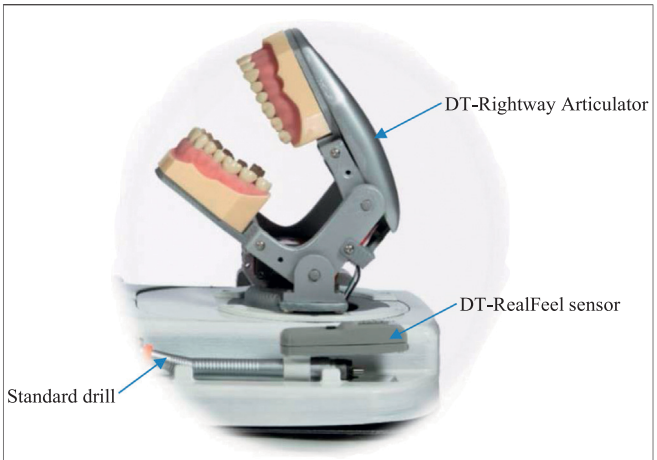

Figure 3 | DT-Rightway Articulator and DT-RealFeel sensor attached to a standard dental drill.

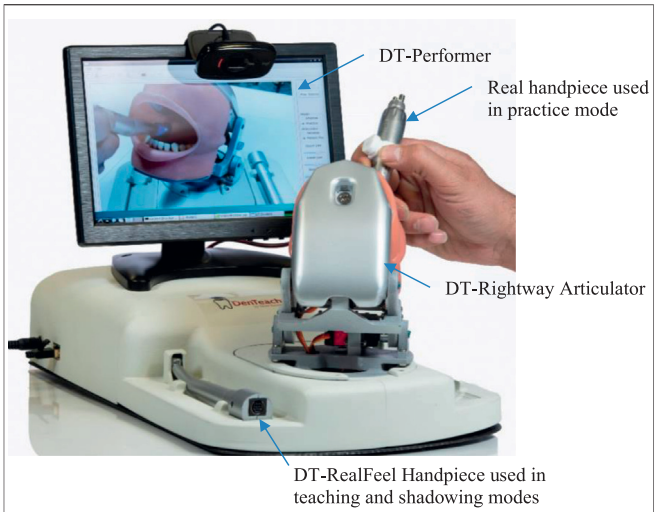

Figure 4 | The components of the DT-Student (apprentice workstation): DT-Rightway Articulator, DT-RealFeel Drill, and a monitor.

recordings taken from the instructor's workstation. This information can later be retrieved and used for various purposes, for example by students in the practice mode or by instructors for evaluation of student's performance in both teaching mode and practice mode.

A dental task is conducted by an instructor using a dental tool on a DT-Rightway Articulator. The instructor processing unit running DT-Performer software includes the main processor responsible for: 1) receiving and analyzing sensory systems data recorded during performance of a dental task by the instructor; 2) recording video and audio that are taken from the audiovisual recording system; 3) communicating with the students' workstations and the data storage system via the data transmission system; and 4) providing the instructor with user-friendly software designed for teaching different dental tasks that are screened on the display (see **Figure 5**).

The DT-Performer software enables the instructor to choose different options including the teaching session along with the time and date as well as the type of the dental task. Each set of students' KPIs is displayed graphically on the screen located at the instructor's workstation, which helps the instructor monitor student performance during a teaching session (**Figures 5A and 5B**). Additionally, the software can authenticate each student's access request when they enter the physical/online classroom.

In **Figure 6**, different components used in students' workstations are illustrated. A student holds a custom-designed DT-RealFeel Drill on a DT-Rightway Articulator, the same as the model used in the instructor's workstation. The DT-RealFeel Drill and DT-Rightway Articulator are mounted onto a platform for initialization and registration purposes. The student processing unit runs the DT-Performer software and provides each student with a user-friendly interface designed for the teaching mode.

In teaching mode, the student processing unit is responsible for: 1) receiving and analyzing data of the sensory system located inside the custom-designed training tool; 2) communicating with both instructor's workstation and the data storage system via the data transmission system; 3) generating control inputs for the vibrotactile actuation system and the vibrator that are located inside the custom-designed training tool, based on data received from the instructor's workstation through the data transmission system; 4) displaying video and audio recordings, which includes the instructor's hand, tool and tooth physical model received from the instructor's workstation through the data transmission system in real-time; 5) superimposing 3D model of the custom-designed training tool onto the video in an AR environment screened on the display (see the inset in **Figure 6**), and moving the 3D model using processed data of sensory system; 6) calculating KPIs for evaluation of each apprentice's performance during the teaching session based on the data taken from the sensory systems; 7) sending KPIs of each student to the instructor's workstation and data storage system via the data transmission system.

The DT-Student software of the student workstation enables each student to get access to data taken from the DT-Performer during the dental operation. Moreover, the student software helps the students monitor their own KPIs during the teaching session and receive detailed statistical reports on how well they could follow the dental task in teaching mode.

There are two factors that students can continuously monitor during the teaching sessions; these factors are plotted in a real-time fashion using 6-bar charts in DT-Performer, as seen in **Figure 6**.

(1) Tool handling ability is determined by the acceptable deviation set by the instructor. At the beginning of the experiment, the instructor sets the acceptable amount of the student's deviation to be less than 15° for the roll (ϕ), pitch (θ), and yaw (ψ) angles. Deviations are calculated by

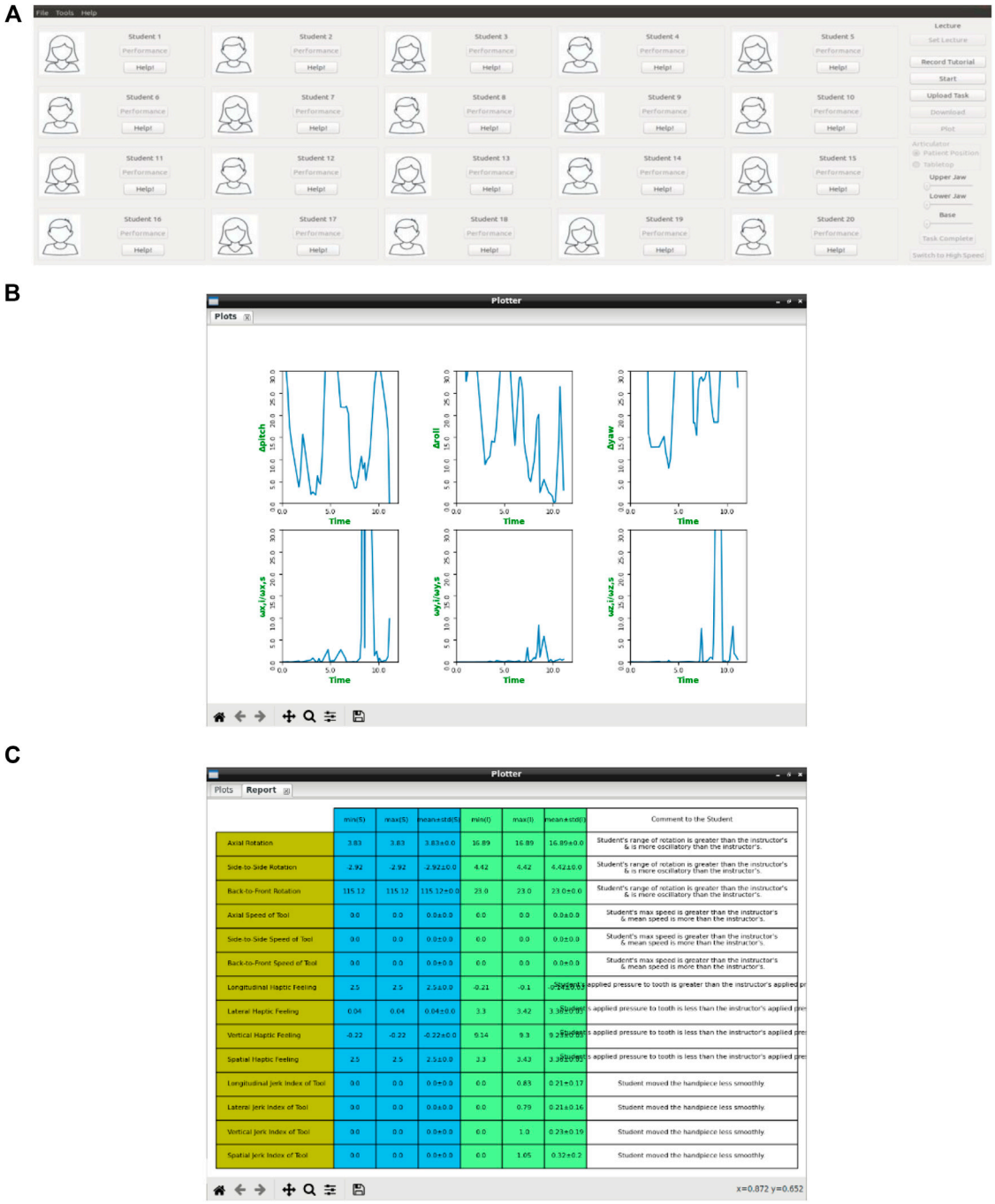

Figure 5 | The DT-Performer components and workflow in the teaching mode. **(A)** screenshot of the graphical user interface on the instructor's display unit. Each student can upload their photo to the system. Plotter is a feature that presents the KPIs in form of graphs **(B)** or tables **(C)**.

subtracting the angle of the student's tool from the corresponding angle of the instructor tool as follows:

$$\Delta\phi = \left|\phi_{instructor} - \phi_{student}\right|$$
$$\Delta\theta = \left|\theta_{instructor} - \theta_{student}\right| \quad (1)$$
$$\Delta\psi = \left|\psi_{instructor} - \psi_{student}\right|$$

(2) The smoothness of the motion or student's ability to move the tool at the same speed as the instructor, which is defined as:

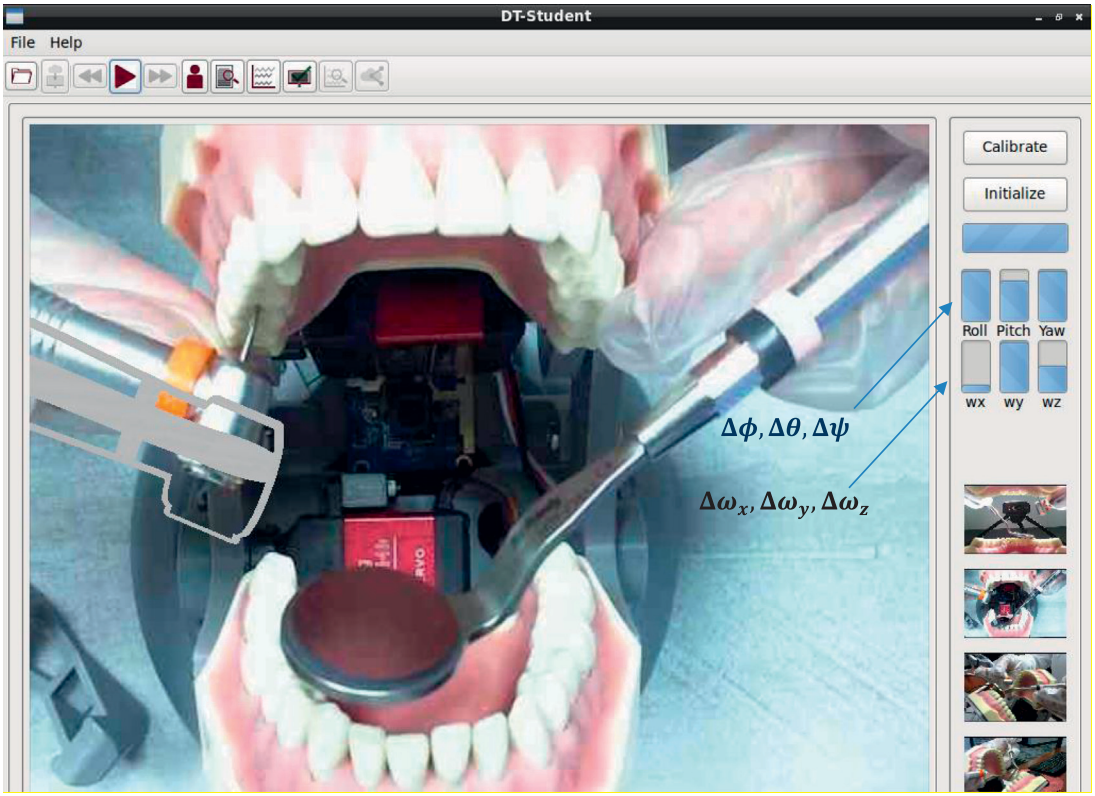

Figure 6 | The DT-Student components and workflow for teaching purposes. In addition to plotting the performance indices, the DT-Student allows students to switch between the four views streaming from the instructor workstation and choose the most discernable view to learn. A 3D model of the student's handpiece (DT-RealFeel Handpiece) is superimposed to the videos streaming from the instructor workstation and allows each student to visually monitor their tool handling. If the student's movement is not within the acceptable range of motion, in addition to the bar charts, the alarm inside the DT-RealFeel Handpiece will start vibrating to help the student to stay on track.

$$\Delta\omega_x = \frac{\omega_{x,instructor}}{\omega_{x,student}}$$
$$\Delta\omega_y = \frac{\omega_{y,instructor}}{\omega_{y,student}} \quad (2)$$
$$\Delta\omega_z = \frac{\omega_{z,instructor}}{\omega_{z,student}}$$

where ω_x, ω_y, and ω_z indicate the angular velocities about x, y, and z, respectively. Note that when the student is not performing the dental task as smoothly as the instructor (or moves the tool faster than the instructor) the numerator becomes much smaller than the denominator and the ratio will be close to zero, while the ratio of one means that the student is able to handle the tool as smoothly as the instructor.

Shadowing Mode

In shadowing mode, a student can download augmented videos (4 videos from the class session along with signals of sensory systems and values of KPIs) and start watching, feeling, and repeating the task before entering the practice mode. In the shadowing mode, a student uses the DT-RealFeel handpiece to shadow dental tasks taught by the instructor. In this operating mode, the video of the dental task - that has already been performed by the instructor–is displayed on the DT-Student monitor while superimposing a 3D model of the training tool (DT-RealFeel handpiece) onto the video, in an AR environment, when rehearsing the dental task.

Practice Mode

In practice mode, the setup components for a student are the same as the ones described in **Figure 6** except the training tool, which is the same as the dental tool used by the instructor in the teaching mode instead of the DT-RealFeel Handpiece. In practice mode, a student processing unit is responsible for: 1) receiving and analyzing data of sensory systems; 2) communicating with the data storage system via data transmission system and receiving sensory data already stored by the instructor during the teaching session and 3) calculating student's KPIs based on both data taken from sensory systems and data from instructor's workstation.

While a student is performing a dental task in practice mode, the DenTeach software displays KPIs of a student graphically. The software also generates statistical and graphical performance reports for dental tasks performed by a student in practice mode.

TABLE 2 | Performance measures and KPI signals.

Mode		KPI signal	Student	Instructor	Difference	Assessment purpose
Practice (48)	Teach and shadow (24)	Tool handling angulation	√	√	√	Assessment of the effort put by the student
		• Axial rotation of the tool	√	√	√	12 KPI signals in total
		• Side-to-side rotation of the tool	√	√	√	
		• Back-to-front rotation of the tool	√	√	√	
		• Overall tool handling skill				
		Tool handling smoothness	√	√	√	Assessment of the smoothness of student's tool handling skill
		• Axial speed of the tool	√	√	√	12 KPI signals in total
		• Side-to-side speed of the tool	√	√	√	
		• Back-to-front speed of the tool	√	√	√	
		• Overall smoothness in tool handling				
		Haptic sensation	√	√	√	Assessment of haptic feeling, i.e., the pressure applied to the tooth
		• Longitudinal haptic feeling	√	√	√	
		• Lateral haptic feeling	√	√	√	12 KPI signals in total
		• Vertical haptic feeling	√	√	√	
		• Spatial haptic feeling				
		Tool handling steadiness	√	√	√	Assessment of the steadiness of student's tool handling skill
		• Longitudinal jerk index of the tool	√	√	√	12 KPI signals in total
		• Lateral jerk index of the tool	√	√	√	
		• Vertical jerk index of the tool	√	√	√	
		• Spatial smoothness in tool handling				

These performance reports are uploaded to the data storage system via the data transmission system, and are made available to the instructor for evaluation purposes.

KPIs

In addition to the qualitative assessment of dental skills conducted by an instructor, the performance of each student is assessed quantitatively individually and comparatively. For quantitative evaluation, two sets of KPIs are used.

Table 2 shows the signals that are recorded and shown during the performance of the dental task that enable the student and the instructor to assess the performance of the student throughout teaching (24 KPI signals), shadowing (24 KPI signals), and practice modes (48 KPI signals). Each KPI signal is meant to assess a specific skill of the student that includes: 1) assessment of the effort put in by the student; 2) assessment of the smoothness factor of the student's tool handling skill; 3) assessment of haptic feeling, *i.e.*, pressure applied to the tooth; and 4) assessment of the steadiness factor of the student's tool handling skill. **Table 3** lists the second set of KPIs summarizes statistical indices of the signals presented in **Table 2** in an enumerative manner. Using the information provided by this set of KPIs, each student (and the instructor) can have an inclusive summary of the student's dental skills during teaching (40 PKIs), shadowing (40 PKIs), or practice (82 PKIs) modes. These numbers are also calculated for a task conducted during every trial; therefore, the student is able to monitor their progress over multiple trials.

CASE STUDY

Experimental Setup

DenTeach was used to measure the KPIs and the ability of the system to help an instructor and students teach and learn more effectively compared to existing traditional techniques. Plastic teeth were mounted onto the typodonts inside the DT-Rightway Dental Articulator. Three common dental tasks were completed by an experienced dentist as the instructor (MK), while a student (AM) mimicked the performance of dental tasks at the student workstation. The instructor used the sensor modified dental handpiece to perform a Class I, II, or V composite preparation, which involves different lesion sizes and caries, over an interval of active practicing on a plastic tooth that is characterized by rheostat engagement and drill operation. More detailed information on the procedures is given in Tam's work (Tam, 2020). A screenshot of the tasks is shown in **Figure 7**.

Teaching Mode

During the experiments, the outputs of the DT-Performer and DT-Student software were exported in this section. The software recorded, analyzed, and plotted real-time data from the instructor's dental handpiece. **Figure 8** depicts three Euler angles of the handpiece held by the instructor and the student as well as the deviations between their angulations, for Task 1. As observed in **Figure 8**, the instructor's motion was followed reasonably well by the student that held the DT-RealFeel Handpiece, as the student's motion deviations are within *a range expected by the instructor* (15 degrees of deviation). The amount of the deviation could change once the students become more experienced or if the instructor changes the deviation range. For this typical interval, the amount of angle deviation for roll angle was within the acceptable interval set by the instructor for most parts of the performance of the task, as depicted in **Figure 9**. However, a deviation of more than 15° was recorded 3 times during the teaching mode, one for the yaw angle and two for the pitch angle that accordingly received an excessive vibration signal reminding the student to keep the handpiece within the allowable zone. The number of deviations for Task 2 and 3 were 2 and 4,

TABLE 3 | Performance measures and KPI numbers.

Mode		Characteristics	Minimum	Maximum	Range	Average	Standard deviation	Purpose	
Practice (82)	Teach and shadow (40)	Tool handling angulation • Axial rotation of the tool • Side-to-side rotation of the tool • Back-to-front rotation of the tool • Overall tool handling skill	√ √ √ √	√ √ √ √	√ √ √ √	√ √ √ √	√ √ √ √	Assessment of the effort put by the student 20 KPIs in total	
		Tool handling smoothness • Axial speed of the tool • Side-to-side speed of the tool • Back-to-front speed of the tool • Overall smoothness in tool handling	√ √ √ √	√ √ √ √	√ √ √ √	√ √ √ √	√ √ √ √	Assessment of the smoothness of student's tool handling skill 20 KPIs in total	
		Haptic sensation • Longitudinal haptic feeling • Lateral haptic feeling • Vertical haptic feeling • Spatial haptic feeling	√ √ √ √	√ √ √ √	√ √ √ √	√ √ √ √	√ √ √ √	Assessment of haptic feeling, i.e., the pressure applied to the tooth 20 KPIs in total	
		Tool handling steadiness • Longitudinal jerk index of the tool • Lateral jerk index of the tool • Vertical jerk index of the tool • Spatial smoothness in tool handling	√ √ √ √	√ √ √ √	√ √ √ √	√ √ √ √	√ √ √ √	Assessment of the steadiness of student's tool handling skill 20 KPIs in total	
		Task completion time	√ (1 index)					Performance time	1 KPI in total
		Interruption index	√ (1 index)					Continuous motion	1 KPI in total

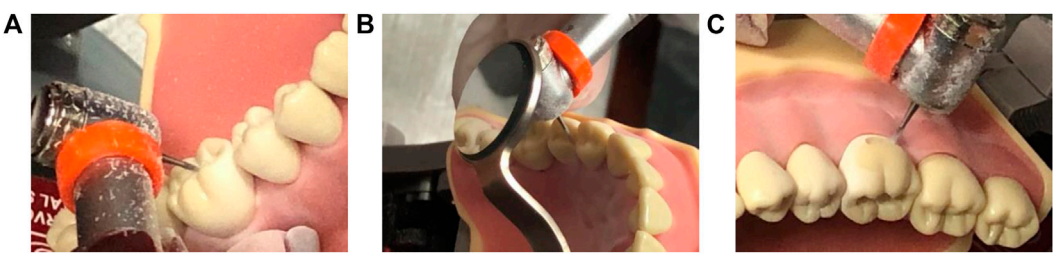

Figure 7 | Screenshots of the dental tasks - **(A)** Task 1: Class I composite preparation on tooth #46; **(B)** Task 2: Class II composite preparation on tooth number 45; **(C)** Task 3: Class V composite preparation on tooth number 46.

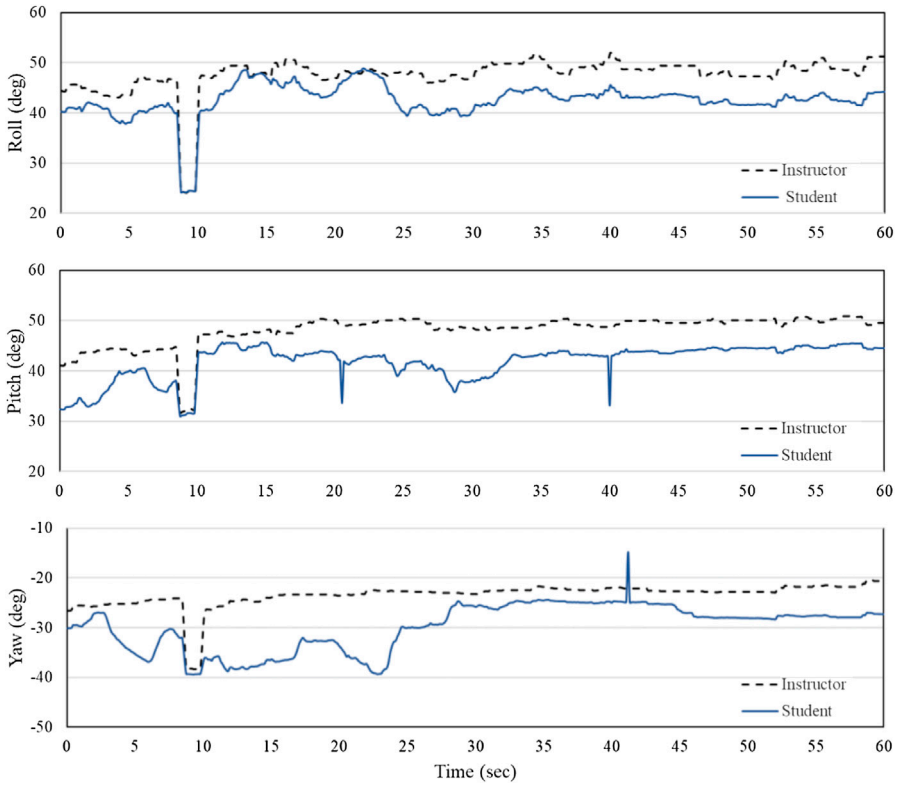

Figure 8 | Angulations of the instructor (blue line - solid) and the student's (black line - dashed) handpiece while performing task 1 over a typical time interval of 60 s - roll (ϕ), pitch (θ), and yaw (ψ).

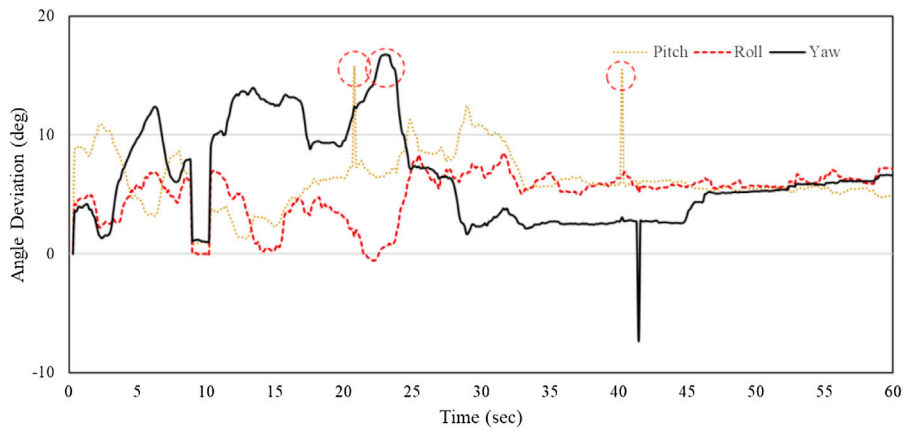

Figure 9 | Deviation of the student's tool handling from the instructor (roll: $\Delta\phi$, pitch: $\Delta\theta$ and yaw: $\Delta\psi$) while performing Task 1 over a typical time interval of 60 s.

respectively. The student took the handpiece back to the allowable range once the excessive signal was generated by the RealFeel handpiece. We expect to observe a decreased amount of deviation once the student is familiar with dental tasks, as shown in experiments.

Tables 4–6 show the values of select KPIs that are reported for the instructor and the student after the completion of Tasks 1, 2, 3, respectively. A combination of the KPIs, video views and graphical reports in both teaching and shadowing modes help the student understands which aspects of the work need further improvement. For example, in all KPIs reported, the standard deviation of the student is larger than the instructor's indicating that the student is required to work on the skill of tool handling (axial rotation, back-front motion, and side to side motion) and

TABLE 4 | Student and instructor KPIs while performing Task 1 in teaching mode.

Characteristics	Student					Instructor				
	Min	Max	Ran	Ave	Std	Min	Max	Ran	Ave	Std
• Axial rotation of the tool (ϕ) - deg	24.12	48.87	24.75	42.59	3.50	24.11	52.02	27.92	47.62	3.81
• Side-to-side rotation of the tool (ψ) - deg	–39.44	–14.75	24.69	–29.91	4.70	–38.31	–20.39	17.92	–23.42	2.48
• Back-to-front rotation of the tool (θ) - deg	30.97	45.72	14.75	41.91	3.53	31.73	51.01	19.28	48.10	3.17
• Axial speed of the tool ($\dot{\phi}$) - deg/s	0.05	13.33	13.28	2.16	1.58	–3.36	2.22	5.58	–0.23	3.47
• Side-to-side speed of the tool ($\dot{\psi}$) - deg/s	0.02	7.75	7.73	1.45	1.03	–1.75	1.64	3.39	–0.31	1.61
• Back-to-front speed of the tool ($\dot{\theta}$) - deg/s	0.01	15.20	15.19	1.64	1.91	–1.34	1.38	2.72	0.15	1.77

TABLE 5 | Deviation of the student's KPIs from the instructor's KPIs while performing Tasks 1, 2, and 3 in teaching mode.

Characteristics	Task 1					Task 2					Task 3				
	Min	Max	Ran	Ave	Std	Min	Max	Ran	Ave	Std	Min	Max	Ran	Ave	Std
Tool handling angulation															
• Axial rotation of the tool ($\Delta\phi$) - deg	–0.56	8.54	9.10	5.03	2.02	–0.76	2.13	2.90	2.01	2.12	–0.58	1.37	1.94	1.83	2.06
• Side-to-side rotation of the tool ($\Delta\psi$) - deg	–7.38	16.82	24.19	6.49	4.02	–1.84	33.63	35.47	5.19	3.24	–0.18	17.17	17.36	5.31	1.77
• Back-to-front rotation of the tool ($\Delta\theta$) - deg	0.77	15.80	15.04	6.20	2.28	0.19	4.74	4.55	10.22	2.16	0.22	2.13	1.91	17.38	1.84
Tool handling smoothness															
• Axial speed of the tool ($\Delta\phi$) - deg/s	0.05	13.33	13.28	2.16	1.58	0.04	8.53	8.49	1.19	1.91	0.05	12.88	12.83	0.83	3.05
• Side-to-side speed of the tool ($\Delta\dot{\psi}$) - deg/s	0.02	7.75	7.73	1.45	1.03	0.03	3.33	3.31	1.71	1.47	0.04	1.43	1.39	0.84	0.72
• Back-to-front speed of the tool ($\Delta\dot{\theta}$) - deg/s	0.01	15.20	15.19	1.64	1.91	0.00	13.83	13.83	1.68	2.95	0.01	12.17	12.17	2.44	3.74

TABLE 6 | Student's KPIs quantified while performing Task 1 in shadowing mode over trials 1 and 5.

Characteristics	Trial 1					Trial 5				
	Min	Max	Ran	Ave	Std	Min	Max	Ran	Ave	Std
Tool handling angulation										
• Axial rotation of the tool (ϕ) - deg	25.81	53.51	27.70	44.93	3.63	23.73	36.90	13.18	36.89	3.24
• Side-to-side rotation of the tool (ψ) - deg	–43.19	–14.90	28.29	–31.40	4.82	–34.58	–13.62	20.96	–24.48	4.64
• Back-to-front rotation of the tool (θ) - deg	31.28	45.95	14.67	42.96	3.56	31.17	29.01	2.16	40.95	3.39
Tool handling smoothness										
• Axial speed of the tool ($\dot{\phi}$) - deg/s	0.05	13.53	13.48	2.18	1.72	0.05	12.79	12.74	2.20	1.29
• Side-to-side speed of the tool ($\dot{\psi}$) - deg/s	0.02	8.02	8.00	1.52	1.04	0.02	5.31	5.29	1.22	0.96
• Back-to-front speed of the tool ($\dot{\theta}$) - deg/s	0.01	15.28	15.27	1.69	1.95	0.01	10.03	10.03	1.74	1.50

the speed of tool handling (axial rotation steadiness, back-front motion steadiness, side to side motion steadiness, and overall motion steadiness). The shaded cells in **Table 5** show that the student was out of range in terms of the tool handling and an alarming signal was applied to the handpiece to bring the hand back on the track.

Shadowing Mode

In shadowing mode, the student used the RealFeel handpiece to review the tasks taught by the instructor. In addition to acquiring more quantitative feedback on the tasks, this mode helps the student become confident and prepare for the practice mode to get hands-on practice with the actual dental handpiece. One advantage of the shadowing mode is to save material and time, with minimal supervision. Therefore, the student is not restricted to academic labs for extended hours, as the portable and compact unit can be used anywhere to practice dental operations over the Internet.

In this case study, the student performed five trials of task 1 in shadowing mode. This was assessed in terms of the three ϕ, θ, ψ angles and possible deviations from the instructor's angulation were monitored as well as the amount of the pressure to be exerted on the tooth 46. The results of the KPIs are presented in **Table 6** for trial 1 and trial 5. As observed, the range of motion in the last trials (#5) with respect to the first trial (#1) along axial, side-to-side, and back-to-front rotations decreased by 52.4%, 25.9%, and 74.9%, respectively. Moreover, the standard deviations in both angulation and speed components were reduced from trial 1 to trial 5, which shows that the improvement in student's ability to handle the tool in a more

TABLE 7 | KPIs quantified while performing Task 1 in practice mode over the first and the last trials (1 and 10).

Characteristics	Trial 1					Trial 10				
	Min	Max	Ran	Ave	Std	Min	Max	Ran	Ave	Std
Tool handling angulation										
• Axial rotation of the tool (ϕ) - deg	22.67	79.16	56.49	22.67	79.16	24.72	51.06	26.34	24.72	51.06
• Side-to-side rotation of the tool (ψ) - deg	−63.11	−15.93	47.17	−63.11	−15.93	−41.22	−15.34	25.87	−41.22	−15.34
• Back-to-front rotation of the tool (θ) - deg	30.25	72.24	41.99	30.25	72.24	31.90	47.78	15.88	31.90	47.78
Tool handling smoothness										
• Axial speed of the tool ($\dot{\phi}$) - deg/s	0.06	16.80	16.74	0.06	16.80	0.05	13.66	13.62	0.05	13.66
• Side-to-side speed of the tool ($\dot{\psi}$) - deg/s	0.03	13.18	13.14	0.03	13.18	0.02	7.83	7.81	0.02	7.83
• Back-to-front speed of the tool ($\dot{\theta}$) - deg/s	0.01	23.10	23.10	0.01	23.10	0.01	15.43	15.42	0.01	15.43
Haptic sensation										
• Longitudinal haptic feeling - deg/s^2	9.36	−5.80	15.16	0.16	7.73	9.11	−6.40	15.51	−0.74	7.18
• Lateral haptic feeling - deg/s^2	−1.12	−8.88	7.76	0.18	5.20	−2.12	−8.98	6.86	0.03	4.20
• Vertical haptic feeling - deg/s^2	−1.12	−5.80	4.68	−3.27	0.81	−1.47	−6.05	4.58	−3.77	−0.04
Tool handling steadiness										
• Longitudinal jerk index of the tool - deg/s^3	−7.14	7.63	14.77	0.02	1.01	−6.39	7.53	13.92	−1.63	0.64
• Lateral jerk index of the tool - deg/s^3	−2.61	2.16	4.77	0.00	0.59	−1.81	0.76	2.57	−1.20	0.40
• Vertical jerk index of the tool - deg/s^3	−2.75	2.52	5.27	0.00	0.10	−1.55	0.32	1.87	−0.80	−0.06
Task completion time - s	125					95.56				
Interruption index	16					9				

limited workspace and a smoother manner using the DenTeach setup. For example, the standard deviation of axial rotation changed from 3.63 to 3.24.

Practice Mode

In practice mode, the student used the actual dental handpiece to practice the three tasks. For this mode, a wireless sensory system that is identical to the sensors used by the instructor is used to measure the signals used for calculating the KPIs. The sensory system and camera then recorded and communicated the audiovisual vibrotactile information to the database to be compared with those of the instructor. Therefore, the student is able to submit the results of each trial to the instructor along with the audiovisual signals at the end of each trial. The KPIs of the first (#1) and last (#10) practice trials are listed in **Table 7**. As observed, the student improved the scores in most of the KPIs including the haptic jerk index that is used for assessing the steadiness of tool handling. Specifically, the maximum value of longitudinal, lateral, and vertical jerk indices decreased by 1.3%, 64.8%, and 25.8%, respectively, indicating the increase in the steadiness of hand's motion from the first trial to the last trial.

Figure 10 shows the variations of the task completion time and the interruption index (the number of rheostat engagements and disengagements). As observed, after 10 trials, the student could complete the task 25.5% faster than the first trial; however, the interruption index was improved by 43.7% showing that the student was more confident in handling the handpiece in the last trial compared to the first trial. The task completion time showed a mean ± standard deviation (std) of 109.13 + 8.88 and the interruption indices had a mean ± std of 11.7 + 2.26.

CONCLUSION

The COVID-19 pandemic response has resulted in remote and physical distancing restrictions to limit the spread and transmission of the novel coronavirus. This has caused significant adverse effects on dental education (i.e. difficulties

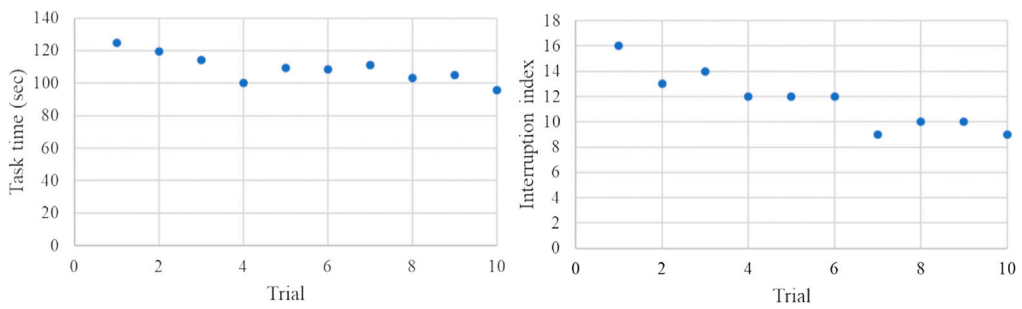

Figure 10 | Variations of the task completion time and the interruption index over 10 trials in the practice mode. The mean values and standard deviations of task completion time and interruption indices are 109.13 + 8.88 and 11.7 + 2.26, respectively.

in the delivery of practical courses such as restorative dentistry and deferral of exams). To help dental institutions continue delivering education remotely, a compact and portable teaching-learning platform, DenTeach, has been developed for remote teaching and learning. The platform includes an instructor workstation (DT-Performer), a student workstation (DT-Student), advanced wireless networking technology, and cloud-based data storage and retrieval. By providing real-time video, audio, feel, and posture (VAFP) information, the platform synchronizes the operations of the instructor and the student. Besides, the platform can provide quantitative KPIs of the student to both the instructor and the student to evaluate the student's skill level.

DenTeach follows and expands on the traditional novice-expert apprenticeship model of instruction to enhance dental training programs. It has been developed for use in teaching, shadowing, and practice modes. In teaching mode, the student can perceive how the instructor is conducting the dental operation through tactile feedback obtained from the dental tool of the instructor's workstation. In shadowing mode, the student can watch, feel, and repeat the tasks alone by downloading the augmented videos. In practice mode, students can use the system to perform dental tasks and have their dental performance skills automatically evaluated in terms of KPIs. A case study was performed to demonstrate the feasibility of the device, and the results show that a combination of KPIs, video views, and graphical reports in both teaching and shadowing modes can effectively help the student understand which aspects of their work need further improvement.

DenTeach is a useful invention for pedagogical and professional purposes, which can be used for training and educating students in both clinical/laboratory and remote (*i.e.*, home) settings due to its compact and portable size. This device facilitates both fully remote and physical-distancing aware teaching and learning in dentistry. Additionally, the DenTeach platform can be useful during the pandemic recovery phase, when dental schools are allowed to return to normal operations. Once dental schools are reopened, there will be a surge in teaching, practicing, and exams. DenTeach can be used to increase the efficiency of the training process, thus allowing dental schools to clear the backlog of activities faster. Before the second wave of COVID-19 hits, decision-makers at dental colleges may want to ensure they have adequate resources to continue teaching and testing from a remote location and minimize the backlog of deferred activities. DenTeach can be used as an effective remote training tool. Moreover, the application of DenTeach could be further extended to other fields of health sciences such as general surgery and neurosurgery where a drill is used to conduct a task.

DATA AVAILABILITY STATEMENT

The original contributions presented in the study and further inquiries can be directed to the corresponding author.

ETHICS STATEMENT

The studies involving human participants were reviewed and approved by University of Alberta. The patients/participants provided their written informed consent to participate in this study.

AUTHOR CONTRIBUTIONS

LC drafted the work including literature review, explanation of the platform and test procedure, and contributed to data analysis. MK, AC, and AM performed the experiments, and contributed to data analysis. SM and MK provided technical support for dentistry teaching and learning, validated the results and findings, and checked the compatibility of results with real-world dentistry. All authors contributed to revising the manuscript and ensuring the correctness of the content. MT and YM provided funding for developing and validating the platform. MT contributed to the further editing of the manuscript and provided guidance and valuable suggestions/discussions.

FUNDING

The Natural Sciences and Engineering Research Council (NSERC) of Canada under grant EGP 542825-19. The National Research Council Canada - Industrial Research Assistance Program (NRC-IRAP) under industrial grant 921303.

ACKNOWLEDGMENTS

The authors would like to thank Tactile Robotics Ltd. for providing experimental setup and technical support during the study. Also, the authors would like to thank the National Research Council of Canada - Industrial Research Assistance Program (NRC-IRAP) and Natural Sciences and Engineering Research Council (NSERC) for providing funding for the development and validation of the DenTeach™ platform.

REFERENCES

Bakr, M. M., Ward, L. M., and Alexander, H. (2013). Evaluation of Simodont® haptic 3D virtual reality dental training simulator. *Int. J. Dent. Clin.* 5, 4.

Bakr, M. M., Ward, L. M., and Alexander, H. (2014). Students' evaluation of a 3DVR haptic device (Simodont®). Does early exposure to haptic feedback during preclinical dental education enhance the development of psychomotor skills? *Int. J. Dent. Clin.* 6, 2.

Collins, A., Brown, J. S., and Holum, A. (1991). Cognitive apprenticeship: making thinking visible. *Am. Educat.* 15, 6–11.

Forsslund, J., Sallnas, E. L., and Palmerius, K. J. (2009). "A user-centered designed FOSS implementation of bone surgery simulations," in World haptics 2009-third joint EuroHaptics conference and symposium on haptic interfaces for

virtual environment and teleoperator systems, Salt Lake City, UT, March 18–20, 2009. New York, NY: IEEE, 391–392.

Gal, G. B., Weiss, E. I., Gafni, N., and Ziv, A. (2011). Preliminary assessment of faculty and student perception of a haptic virtual reality simulator for training dental manual dexterity. *J. Dent. Educ.* 75 (4), 496–504. doi:10.1002/j.0022-0337.2011.75.4.tb05073.x

Hayka, A., and Eytan, L. (1997). Image sound and feeling simulation system for dentistry. U.S. Patent 5,688,118 (Accessed November 16, 1997).

Johnson, L., Thomas, G., Dow, S., and Stanford, C. (2000). An initial evaluation of the Iowa dental surgical simulator. *J. Dent. Educ.* 64 (12), 847–853. doi:10.1002/j.0022-0337.2000.64.12.tb03385.x

Kolesnikov, M., Steinberg, A., Zefran, M., and Drummond, J. (2008). PerioSim: haptics-based virtual reality dental simulator. *Digital Dent. News* 331, 6–12.

Kuchenbecker, K. J., Parajon, R. C., and Maggio, M. P. (2017). Evaluation of a vibrotactile simulator for dental caries detection. *Simulat. Healthc. J. Soc. Med. Simulat.* 12 (3), 148–156. doi:10.1097/SIH.0000000000000201

Luciano, C., Banerjee, P., and DeFanti, T. S. (2009). Haptics-based virtual reality periodontal training simulator. *Virtual Reality* 13 (2), 69–85. doi:10.1007/s10055-009-0112-7

Maddahi, A., Bagheri, S., Mardan, M., Kalvandi, M., and Maddahi, Y. (2020). Vibrotactile method, apparatus and system for training and practicing dental procedures. WO Patent WO2020041879A1.

Ranta, J. F., Aviles, W. A., Donoff, R. B., and Nelson, L. P. (2007). Methods and apparatus for simulating dental procedures and for training dental students. U.S. Patent 7,249,952 (Accessed July 31, 2007).

Ranta, J. F., and Aviles, W. A. (1999). The virtual reality dental training system: simulating dental procedures for the purpose of training dental students using haptics. *Proc. PHANTOM* 4, 67–71.

Rhienmora, P., Haddawy, P., Suebnukarn, S., and Dailey, M. N. (2011). Intelligent dental training simulator with objective skill assessment and feedback. *Artif. Intell. Med.* 52 (2), 115–121. doi:10.1016/j.artmed.2011.04.003

Rhienmora, P., Gajananan, K., Haddawy, P., Dailey, M. N., and Suebnukarn, S. (2010). "Augmented reality haptics system for dental surgical skills training," in Proceedings of the 17th ACM symposium on virtual reality software and technology, Hong Kong, China, November 22–24, 2010. Beijing, China: ACM, 97–98.

Rhienmora, P., Haddawy, P., Dailey, M. N., Khanal, P., and Suebnukarn, S. (2008). Development of a dental skills training simulator using virtual reality and haptic device. *NEC Tech. J.* 8 (20), 140–147.

Riener, R., and Burgkart, R. (2013). Method and device for learning and training dental treatment techniques. U.S. Patent 8,376,753 (Accessed February 19, 2013).

Schwibbe, A., Kothe, C., Hampe, W., and Konradt, U. (2016). Acquisition of dental skills in preclinical technique courses: influence of spatial and manual abilities. *Adv. Health Sci. Educ. Theory Pract.* 21 (4), 841–857. doi:10.1007/s10459-016-9670-0

Solana, K. (2020). Dental schools take proactive steps in response to coronavirus outbreak. Available at: https://www.ada.org/en/publications/new-dentist-news/2020-archive/march/dental-schools-take-proactive-steps-in-response-to-coronavirus-outbreak (Accessed March 16, 2020).

Tam, L. (2020). Faculty of dentistry. Available at: https://www.google.com/search?client=firefox-b-d&q=class+I+composite+preparation (Accessed July 13, 2020).

UNESCO (2020). Education: from disruption to recovery. Available at: https://en.unesco.org/covid19/educationresponse (Accessed July 20, 2020).

Wang, D., Zhang, Y., Hou, J., Wang, Y., Lv, P., Chen, Y., et al. (2011). iDental: a haptic-based dental simulator and its preliminary user evaluation. *IEEE Trans. Haptics* 5 (4), 332–343. doi:10.1109/TOH.2011.59

WHO (2020a). WHO coronavirus disease (COVID-19) dashboard. Available at: https://covid19.who.int (Accessed July 3, 2020).

WHO (2020b). EPI-WIN: WHO information network for epidemics. Available at: https://www.who.int/teams/risk-communication (Accessed July 3, 2020).

Conflict of Interest: AM and YM work for the Department of Research and Development Tactile Robotics Company, the IP holder of the technology.

The remaining authors declare that the research was conducted in the absence of any commercial or financial relationships that could be construed as a potential conflict of interest.

frontiers in Artificial Intelligence

PERSPECTIVE
published: 12 February 2021
doi: 10.3389/frai.2021.613637

Case Report: Utilizing AI and NLP to Assist with Healthcare and Rehabilitation During the COVID-19 Pandemic

*Jay Carriere[1], Hareem Shafi[1], Katelyn Brehon[2], Kiran Pohar Manhas[3], Katie Churchill[4,5], Chester Ho[3,6] and Mahdi Tavakoli[1]**

[1]Department of Electrical and Computer Engineering, University of Alberta, Edmonton, AB, Canada, [2]School of Public Health, University of Alberta, Edmonton, AB, Canada, [3]Neurosciences, Rehabilitation, and Vision Strategic Clinical Network, Alberta Health Services, Calgary, AB, Canada, [4]Department of Occupational Therapy, University of Alberta, Edmonton, AB, Canada, [5]Cumming School of Medicine, University of Calgary, Calgary, AB, Canada, [6]Faculty of Medicine and Dentistry, University of Alberta, Edmonton, AB, Canada

OPEN ACCESS

Edited by:
Weida Tong,
National Center for Toxicological Research (FDA), United States

Reviewed by:
Mary Yang,
University of Arkansas at Little Rock, United States
Ruili Huang,
National Center for Advancing Translational Sciences (NCATS), United States

***Correspondence:**
Mahdi Tavakoli
mahdi.tavakoli@ualberta.ca

Specialty section:
This article was submitted to Medicine and Public Health, a section of the journal Frontiers in Artificial Intelligence

Received: 02 October 2020
Accepted: 08 January 2021
Published: 12 February 2021

Citation:
Carriere J, Shafi H, Brehon K, Pohar Manhas K, Churchill K, Ho C and Tavakoli M (2021) Case Report: Utilizing AI and NLP to Assist with Healthcare and Rehabilitation During the COVID-19 Pandemic. Front. Artif. Intell. 4:613637. doi: 10.3389/frai.2021.613637

The COVID-19 pandemic has profoundly affected healthcare systems and healthcare delivery worldwide. Policy makers are utilizing social distancing and isolation policies to reduce the risk of transmission and spread of COVID-19, while the research, development, and testing of antiviral treatments and vaccines are ongoing. As part of these isolation policies, in-person healthcare delivery has been reduced, or eliminated, to avoid the risk of COVID-19 infection in high-risk and vulnerable populations, particularly those with comorbidities. Clinicians, occupational therapists, and physiotherapists have traditionally relied on in-person diagnosis and treatment of acute and chronic musculoskeletal (MSK) and neurological conditions and illnesses. The assessment and rehabilitation of persons with acute and chronic conditions has, therefore, been particularly impacted during the pandemic. This article presents a perspective on how Artificial Intelligence and Machine Learning (AI/ML) technologies, such as Natural Language Processing (NLP), can be used to assist with assessment and rehabilitation for acute and chronic conditions.

Keywords: COVID-19, artificial intelligence, natural language processing, smart health, neuromusculoskeletal rehabilitation

1 INTRODUCTION

At the time this article was published, there were over 33 million confirmed COVID-19 patients globally, with 1 million deaths being reported (Johns Hopkins University, 2020) in over 188 countries and territories. The COVID-19 pandemic has had a profound effect on societies and healthcare systems worldwide. To address the pandemic, governments and healthcare providers have had to rethink how healthcare is delivered. COVID-19 spreads rapidly from direct or close human-to-human contact, and around 15–30% of infected individuals are asymptomatic with a large percentage of people having only mild symptoms (He et al., 2020; Tuli et al., 2020). Without a COVID-19 vaccine or proven antiviral treatment, public health policy has focused on social distancing to prevent and contain the spread of COVID-19. Healthcare systems have been forced to take drastic actions to mitigate the risk of infection and to ensure adequate healthcare system capacity. In-person treatment

and healthcare delivery has therefore been reduced, or canceled, for high-risk and vulnerable populations, particularly those with comorbidities.

This change in healthcare policies and priorities caused the treatment of non-emergent (chronic or non-life-threatening) conditions to be deferred into the future. While this shift has allowed for focusing healthcare resources to address the immediate needs of the pandemic, healthcare systems had to delay and defer non-emergent treatments to mitigate or reduce the risk of COVID-19 infection to vulnerable populations in healthcare settings. Some of the vulnerable populations, who have been identified as a high-risk category for developing more severe and life-threatening COVID-19 infections, include the elderly, those with disabilities, or multiple comorbidities (Bartolo et al., 2020). The COVID-19 pandemic forced healthcare providers and healthcare systems worldwide to reduce or limit less-urgent healthcare services, such as rehabilitation services for people with acute and chronic diseases and disorders (Prvu Bettger et al., 2020). For some patients, this delay in treatment is inconvenient but not substantially detrimental. For other patients, a delay or pause in treatment can significantly impair recovery and reduce effectiveness.

The deferral of rehabilitation therapies is undesirable due to diminished patient physical and psychological outcomes, and increases the burden on the healthcare system in the future to address this growing backlog (Prvu Bettger et al., 2020; Tavakoli et al., 2020). During the COVID-19 pandemic, rehabilitation has gained significant importance. Rehabilitation is required to address the needs of those with acute and chronic conditions and to support recovery for individuals who have had severe COVID-19 infections requiring long-term intensive care and respiration support. Rehabilitation for post-COVID patients has been shown to be taxing on healthcare systems, with the average cost of rehabilitation services for post-COVID patients being roughly twice the cost of rehabilitation services for non-COVID conditions (Iannaccone et al., 2020).

In this time, when healthcare resources are being strained due to the pandemic, artificial intelligence (AI) and machine learning (ML) methods can be utilized to assist healthcare workers and healthcare delivery (Tavakoli et al., 2020). This article will provide a brief review and perspective on the use of AI/ML technologies and systems that can aid in the assessment and treatment of acute and chronic musculoskeletal, neurological and other conditions. These AI/ML technologies can be used to complement in-person appointments with clinicians, occupational therapists, and physiotherapists. As an example of such a system, a case-study outline of our work on an AI/ML and Natural Language Processing (NLP) system for a telephone-based Rehabilitation Advice Line will also be presented. With future waves of the COVID-19 pandemic expected, these technologies can also provide continuity of care when in-person appointments present too much of a risk. Additionally, beyond the immediate needs of the pandemic, the deployment of these systems will continue to be of benefit for providing care for remote and rural populations.

This paper is laid out as follows. **Section 2** will cover an overview of AI and ML systems that have been applied to assisting with healthcare, including systems developed to address the COVID-19 pandemic. **Section 3** discusses the use of AI/ML methods, particularly natural language processing (NLP), for assisting with rehabilitation assessment and treatment. **Section 4** introduces our work using a combined ML-NLP system to analyze clinical data collected by a phone-based rehabilitation advice line during the pandemic. **Section 5** presents a brief decision about the utility and concerns when using AI/ML systems within healthcare, with concluding remarks given in **Section 6**.

2 ARTIFICIAL INTELLIGENCE FOR HEALTHCARE AND COVID-19

AI/ML techniques have been widely researched and deployed before the pandemic to aid clinicians, nurses, and healthcare workers in various healthcare tasks. Assisting with medical image based diagnosis and assessment is one such task that AI/ML technologies have been extensively researched and developed for. During the pandemic, existing and novel systems have been developed and deployed to address the particular challenges of COVID-19. These systems can provide predictions about the growth and spread of COVID-19 using AI/ML methods to assist with prevention/containment measures and can include the use of advanced robotic technologies (Tavakoli et al., 2020). **Figure 1** shows the relationship between clinical data that can be processed by AI/ML systems and example use cases for AI/ML systems during the COVID-19 pandemic.

2.1 Medical Image Processing

AI/ML algorithms have been widely used to aid in medical image processing. Several reviews in the literature, written before the pandemic, show the widespread interest, research, and adoption of AI/ML technologies for medical image processing for a variety of imaging modalities (Shen et al., 2017; Maier et al., 2019). Deep learning and deep neural network (DNN) methods have been explored to assist with segmentation of anatomical features (or areas of interest) in x-ray, CT, MR (Lundervold and Lundervold, 2019), and other medical imaging modalities. These segmented anatomical features can create and train diagnosis and health-outcome prediction systems for a large number of patient conditions.

AI/ML technologies can enhance medical images, giving physicians and healthcare workers superhuman vision by allowing them to detect patterns or small features in medical images, which would otherwise be imperceptible (Shen et al., 2017; Maier et al., 2019). AI/ML image enhancement tools can highlight or provide clearer visualization of diagnostically relevant structures in medical images. Assisting with interpretation of medical images, particularly for diagnostic purposes, obviously benefits the healthcare system. To address the need for rapid diagnosis of COVID-19 patients and to gauge the impact and severity of a patients' infection, these ML-based image enhancement and segmentation techniques were used to detect the presence of COVID-19 lung infections in x-ray and CT images (Panwar et al., 2020). By analyzing patterns and minute

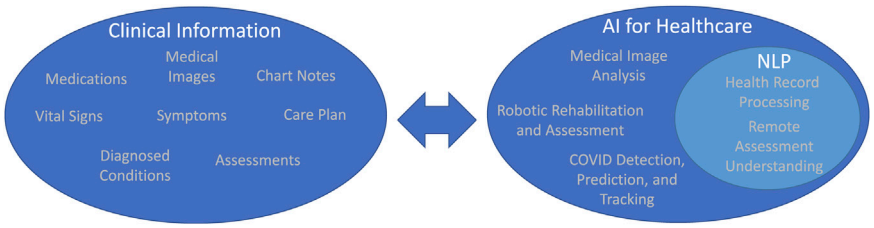

FIGURE 1 | Examples of clinical information that can be processed by AI algorithms and example AI use cases within healthcare.

differences in a large dataset of patient images, patterns can be found. These patterns could provide an early warning system for those coronavirus cases that will become the most serious.

2.2 COVID-19 Modeling, Prediction, and Tracking

Knowledge of the growth and trends of a pandemic are required for prevention and containment. AI/ML methods can intelligently use official data (such as from COVID-19 task forces) or indirect data (such as from wearable fitness trackers) to predict cases in different administrative regions.

Punn et al. (2020) used COVID-19 data from the John Hopkins database to train a predictive ML model. The dataset consisted of daily case reports and daily time series summary tables. Predictions were made about total cases for the next 10 days from attributes such as province/state, country/region, last update, last known confirmed cases, recovered cases, and deaths. The prediction will allow decision making based on transmission growth, such as increasing the period or extent of lockdown, executing sanitation procedures, or providing additional healthcare resources.

Aside from direct detection of COVID-19 infections using tests, it is known that acute infections can cause a measurable change to an individual's vital signs. For instance, resting heart rate trends in the population can indicate the presence of infection. (Radin et al., 2020) evaluated if population trends of seasonal respiratory infections, such as influenza, could be identified through wearable sensors (Fitbit) that collect resting heart rate and sleep data. Sensor data from Fitbit users in 5 US states was shown able to estimate the level of influenza-like illness rates at the state level (as reported by the CDC), using binomial and autoregressive models. The same methodology can be used to predict the spread of COVID-19 and future pandemics.

3 ARTIFICIAL INTELLIGENCE FOR REHABILITATION ASSESSMENT AND TREATMENT

There are a few modalities under which rehabilitation and assessment can be undertaken while allowing for adequate isolation and social-distancing. One of the primary advantages of these technologies is that they allow for hands-off treatment and assessment of persons with acute and chronic conditions, which is paramount with the social isolation restrictions during COVID-19.

3.1 Rehabilitation Robotics

One modality that has been explored in the literature is to use robotics for assisting with assessment and rehabilitation. The area of robotics for rehabilitation has seen significant development over the past three decades. Robots are able to provide the repetitive, high-intensity, interactions with patients necessary for rehabilitation (Voelker, 2005), without being subject to stress, fatigue, or injury like human beings. Robotic rehabilitation systems are highly sensorized, providing occupational and physiotherapists with high-quality objective data to assess the extent of a person's condition, disability, or monitor rehabilitation progress. A significant amount of research has been done on robotic rehabilitation systems to make them safe and provide effective and efficient rehabilitation.

Robotic systems for rehabilitation therapy were initially explored in the late 1980s (Voelker, 2005; Van der Loos et al., 2016). Robotic rehabilitation systems have been used to assist with upper-limb and lower-limb rehabilitation and assessment. (Khalili and Zomlefer, 1988) used two double-link planar robots that were coupled with a patient's lower limb to provide continuous passive motion for rehabilitation. In 1988, (Hogan et al., 1992) developed the MIT-MANUS, an upper-limb rehabilitation device for shoulder-and-elbow therapy. Development of upper-limb rehabilitation systems continued with devices such as the Mirror-Image Movement Enabler (MIME) robotic device, which improved muscle movements through mirror-image training (Lum et al., 2004), and the Assisted Rehabilitation and Measurement (ARM) Guide, which functions both as an assessment and rehabilitative tool (Reinkensmeyer et al., 2014). More general robotic rehabilitation systems, not limited to just upper-limb or lower-limb rehabilitation, began to emerge in the 2000s. These robotic devices allowed rehabilitation for areas such as the wrist (Williams et al., 2001), hand, and finger Worsnopp et al. (2007) for the upper-limb, and gait and ankle training (Colombo et al., 2000; Deutsch et al., 2001) for the lower limb. More recently, robots designed for training patients to perform activities of daily living (ADLs) have been developed (Guidali et al., 2011; Mehrholz et al., 2012). Newer work on robotic rehabilitation systems has focused on incorporating AI/ML technologies into these robotic systems to automatically tune the amount of assistance or resistance they provide during

rehabilitation therapy. (Najafi et al., 2020; Tao et al., 2020) used AI/ML technologies to provide more effective robotic rehabilitation by learning, and replicating, the amount of assistance a physiotherapist provides for an individual patient. The work of (Fong et al., 2020) incorporated machine learning to perform functional capacity evaluation and provide rehabilitation.

3.2 Natural Language Processing in Healthcare

Natural language processing (NLP) is the branch of ML focused on obtaining information representations by analyzing text and speech data. NLP, or speech processing and speech understanding technologies, have become ubiquitous in consumer products, particularly cell phones and smart speakers. Recent achievements of NLP include automatic speech recognition, information extraction, and image captioning (Esteva et al., 2019). These recent achievements are being applied to develop clinical voice assistants to transcribe patient visit information into their electronic health records (EHR). This technology is designed to reduce the amount of time a clinician spends on documentation, which can increase the time and capacity of a clinician to work with patients directly during the pandemic.

Another increasingly popular use is of NLP pipelines that preprocess EHR and then find and classify disease-relevant keywords for early detection of various diseases, most notably cancer, neural and cardiac ailments (Meystre and Haug, 2006; Jiang et al., 2017). ML is used to predict and analyze the performance of alternate treatment options for stroke patients and to predict the likely outcome for each patient given their medical history. (Melton and Hripcsak, 2005) used the NLP system MedLEE to analyze discharge summaries. This analysis predicted if a patient was likely to suffer from adverse effects, and this prediction was compared to the New York Patient Occurrence Reporting and Tracking System (NYPORTS). The system processed all inpatient cases with electronic discharge summaries for two years and was shown to outperform the traditional reporting system. Similarly, another NLP search approach was used to identify postoperative surgical complications from a comprehensive EHR containing clinical notes, microbiology reports, and discharge summaries at six Veteran Health Administration centers from 1999 to 2006 (Murff et al., 2011). NLP-based methods provide an additional surveillance opportunity, but utilizing information already present in clinical notes and discharge summaries. Using the same principle of clinical assistants, IntelliDoctor, an AI-based medical assistant android app, develops a profile of the user based on symptoms and medical history to predict future medical concerns (Gandhi et al., 2019). This concept is being extended to develop a comprehensive clinical assistant that can provide initial screening before referring patients to doctors to reduce patient-doctor interactions during the pandemic (Jensen et al., 2012). NLP methods can be employed to provide recommendations for specialized healthcare to those most at risk during pandemics using the text and information in their medical records. These predictions help increase the capacity of healthcare systems and can identify populations most at risk during the pandemic. An example of such a system was demonstrated by DeCaprio et al. (2020) utilizing existing medical datasets (e.g., pneumonia, influenza, acute bronchitis, upper respiratory infections) as COVID-19 proxies.

To further improve the accuracy of these clinical assistants, work has been done to reduce biomedical text ambiguity, through the use of context, such as in (Liu et al., 2001; Schuemie et al., 2005). Information extraction systems, when applied to EHRs, can consist of a tokenizer, sentence bound detector, POS tagger, morphological analyzer, shallow parser, deep parser, gazetteer, named entity recognizer, discourse module, template extractor and template combiner (Meystre et al., 2008). Using the same principle of clinical assistants, IntelliDoctor, an AI-based medical assistant android app, develops a profile of the user based on symptoms and medical history to predict future medical concerns.

4 REHABILITATION ADVICE LINE: DISCUSSION OF A CASE-STUDY

Alberta Health Services (the healthcare authority for the province of Alberta, Canada), has launched a novel telehealth service to address the rehabilitation needs of those with acute and chronic musculoskeletal, neurological, and other conditions impacted by the pandemic. This Rehabilitation Advice Line (RAL) is a telephone service that allows patients and caregivers to speak directly with rehabilitation clinicians and professionals. The RAL is the first of its kind in Canada, was launched on May 12, 2020, and is a free service for all Albertians over the age of 18.

The RAL is staffed by occupational therapists and physiotherapists to assist and assess persons remotely, and provides improved access and continuity of care during these uncertain times. Assistance provided by the RAL includes helping patients locate appropriate services in their geographical area, provide condition specific exercises, self management advice, or education to address their rehabilitation needs. This wayfinding is particularly helpful for individuals who had their rehabilitation treatment stopped due to COVID-19, or to individuals who were unable to start rehabilitation therapy due to the pandemic. The RAL system allows the clinicians to share referrals and clinical advice with other members of the person's healthcare team (e.g., primary care physicians). The RAL forms a part of a broader Health Link telephone service which provides free advice and health information within Alberta. The phone infrastructure and data storage for the RAL provided by Health Link.

While the RAL was implemented to address the immediate needs of patients with rehabilitation needs during the COVID-19 pandemic, the RAL aims to remain in place post-COVID. Long-term, the RAL will continue to act as a resource for patients to access immediate rehabilitation advice and guidance. Patients phoning the RAL will also be provided with referrals to available rehabilitation providers and services which are open for in-person and/or virtual visits. The RAL will continue to serve as an important resource post-COVID, particularly for the remote

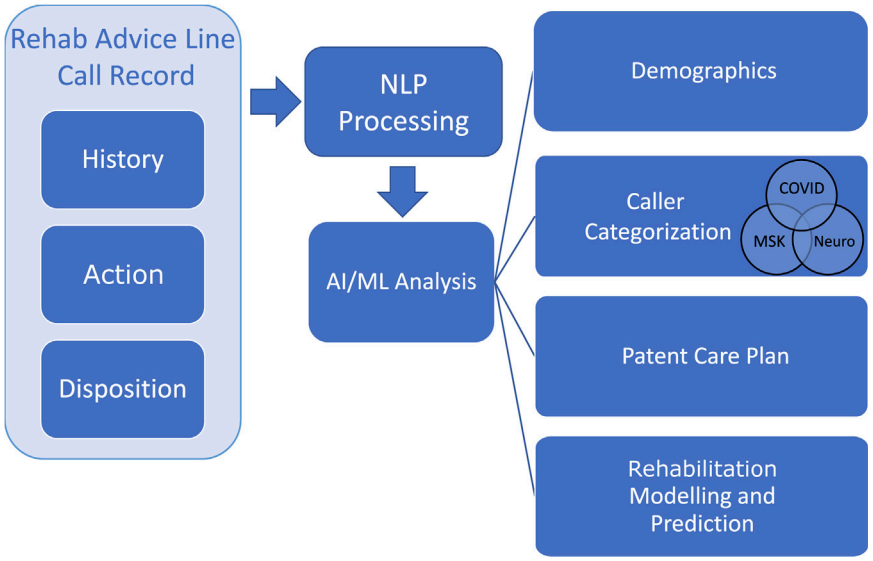

FIGURE 2 | Proposed NLP-ML processing pipeline for rehab advice line call records.

assistance it offers for patients in rural areas in Alberta and small urban centers with limited access to rehabilitation services.

4.1 Natural Language Processing Processing of RAL Clinical Notes

When a patient or caregiver phones into the RAL, clinical notes are entered into an online charting platform by the occupational and physiotherapists. These clinical notes contain key information about the patients, such as their age, location, and gender along detailing the patient's rehabilitation concerns. We propose the use of NLP and ML technologies to assist with analyzing the information contained in these clinical notes (after anonymization). The call notes consist of unstructured data that can be classified into three categories: History including previous patient diagnoses, medications, and existing symptoms; Action taken by the RAL advisor during the call including discussion of current symptoms (including pain, weakness, or difficulty performing ADLs, etc.), subjective over-the-phone assessment, and cause of the condition (if it was caused through injury); Disposition detailing the advice provided or service referrals given to the patient. By capturing this information, the RAL provides a means of monitoring and providing assistance to individual patients.

An NLP-ML system has been designed as a case-study to analyze the public health impact of the RAL, user engagement with the RAL, and to provide public health monitoring and prediction of future healthcare resource needs. Along with traditional rehabilitation assessment metrics that have been collected during patient calls and surveys, our NLP-ML system will provide deeper insight into the data collected by the RAL. This insight will include: automatically capturing demographic data; categorizing the reason for the call as resulting from musculoskeletal, neurological, COVID, or other conditions; analysis of the disposition to better understand the patient care plan; and predictive modeling of areas where rehabilitation services will be needed in the future. As shown in **Figure 2**, the NLP-ML system consists of two main components: the NLP-based preprocessing of clinical notes and an AI/ML-based system for modeling and analyzing the collected data. Apache cTakes (Savova et al., 2010) is being used for NLP processing of the clinical notes to convert them to a machine-readable format. cTAKES is able to process and provide context from these notes, including highlighting the patient's condition and medical history (including any injuries or medications), subjective assessment results, and the advice provided to them. Preliminary work has shown that the NLP system is capable can correctly identify salient keywords within the clinical notes (e.g., total knee replacement, multiple sclerosis, fractures, etc.). Our work on developing a ML system to distil salient public health information using a large set of these analyzed clinical notes is ongoing.

5 DISCUSSION AND FUTURE RESEARCH

We have provided a number of examples that show the utility of AI/ML systems, in theory, for assisting with healthcare. In practice however, there are a number of factors which must be addressed in the future to enable the adoption of AI/ML systems outside of research environments. One set of factors that should be addressed, are the safety and accuracy when using AI/ML systems for healthcare data analysis. For some healthcare tasks, such as medical image analysis, AI/ML systems have been widely explored and have become increasingly accurate, performing nearly as well as human clinicians (Shen et al., 2017; Lundervold and Lundervold, 2019; Maier et al., 2019). The success of AI/ML in the image analysis domain can be

attributed to the wide availability of high quality, comprehensive, and extensively annotated datasets. In other domains, such as NLP processing of electronic health records, there is an absence of publically available annotated datasets which can be used to develop and validate NLP systems (Kersloot et al., 2020). Due to this, there is limited information about the accuracy of NLP healthcare data analysis systems within the literature and it is difficult to compare the existing systems within the research (Kersloot et al., 2020). The development of publicly available challenge NLP healthcare datasets and better metrics for analyzing the accuracy of such systems is an area which should be worked on by researchers in the future.

In addition to the accuracy and safety of AI/ML systems, one other set of factors which should be carefully considered and discussed by researchers in the future are the ethics, privacy, and security when using AI/ML for healthcare data analysis. These factors are critical to consider when developing systems which work on identifying healthcare data, NLP systems for example. New technologies, like wearable/phone sensors, provide a wealth of new data which can be used to augment traditional clinical patient assessments, providing new insights into the day-to-day activities and symptoms of patients. The privacy and ethical use of this data needs to be discussed and addressed when developing novel healthcare AI/ML solutions. Within the COVID-19 pandemic, the balance between ethical/privacy concerns and public health assistance was a critical consideration for the various smartphone COVID-19 notification apps deployed across the world (Bradford et al., 2020).

6 CONCLUDING REMARKS

Healthcare systems and healthcare delivery have been significantly affected by the COVID-19 pandemic. With social distancing and isolation policies to continue until new treatment options and vaccines are widely deployed, there is a need to discuss how new and existing technologies can assist healthcare systems during this challenging time. In this perspective paper we have discussed the use of AI/ML technologies to assist with the assessment, diagnosis, and treatment of acute and chronic musculoskeletal, neurological, and other conditions during the COVID-19 pandemic. We have provided examples of AI/ML technologies applied to areas such as medical image analysis, robotic rehabilitation and assessment, and NLP systems which allow for remote, hands-off, treatment and assessment of persons with acute and chronic conditions. We have also provided an overview of our ongoing work to help the healthcare system better analyze, quantify, and understand information recorded during calls to a Rehabilitation Advice Line. As further waves of the pandemic are expected, it is important to highlight how using AL/ML technologies can be deployed to provide new public health insights using existing medical history data and new data captured during remote healthcare sessions during the pandemic.

DATA AVAILABILITY STATEMENT

The original contributions presented in the study are included in the article, further inquiries can be directed to the corresponding author.

AUTHOR CONTRIBUTIONS

The manuscript was prepared by JC and HS. JC, KB, KM, KC, CH, and MT contributed to the conception and outline of the perspective. All authors contributed to manuscript revision, read, and approved the submitted version.

ACKNOWLEDGMENTS

The authors wish to acknowledge the support of Alberta Health Services Neurosciences, Rehabilitation, and Vision Strategic Clinical Network, the University of Alberta Spinal Cord Injury Endowed Research Chair Funds, Canadian Institutes of Health Research, Natural Sciences and Engineering Research Council of Canada, and the Alberta Economic Development, Trade and Tourism Ministry's grant to Center for Autonomous Systems in Strengthening Future Communities.

REFERENCES

Bartolo, M., Intiso, D., Lentino, C., Sandrini, G., Paolucci, S., Zampolini, M., et al. (2020). Urgent measures for the containment of the coronavirus (covid-19) epidemic in the neurorehabilitation/rehabilitation departments in the phase of maximum expansion of the epidemic. *Front. Neurol.* 11, 423. doi:10.3389/fneur.2020.00423

Bradford, L., Aboy, M., and Liddell, K. (2020). COVID-19 contact tracing apps: a stress test for privacy, the GDPR, and data protection regimes. *J. Law Biosci.* 7 (1), lsaa034. doi:10.1093/jlb/lsaa034

Colombo, G., Joerg, M., Schreier, R., and Dietz, V. (2000). Treadmill training of paraplegic patients using a robotic orthosis. *J. Rehabil. Res. Dev.* 37, 693–700

DeCaprio, D., Gartner, J. A., Burgess, T., Kothari, S., Sayed, S., and McCall, C. J. (2020). Building a covid-19 vulnerability index. *medRxiv*. Available at: https://arxiv.org/abs/2003.07347.

Deutsch, J. E., Latonio, J., Burdea, G. C., and Boian, R. (2001). Post-stroke rehabilitation with the rutgers ankle system: a case study. *Presence Teleoperators Virtual Environ.* 10, 416–430. doi:10.1162/1054746011470262

Esteva, A., Robicquet, A., Ramsundar, B., Kuleshov, V., DePristo, M., Chou, K., et al. (2019). A guide to deep learning in healthcare. *Nat. Med.* 25, 24–29. doi:10.1038/s41591-018-0316-z

Fong, J., Ocampo, R., Gross, D. P., and Tavakoli, M. (2020). Intelligent robotics incorporating machine learning algorithms for improving functional capacity evaluation and occupational rehabilitation. *J. Occup. Rehabil.* 30, 362–370. doi:10.1007/s10926-020-09888-w

Gandhi, M., Singh, V. K., and Kumar, V. (2019). "Intellidoctor (AI) based medical assistant"' In 2019 fifth international conference on science technology engineering and mathematics (ICONSTEM), Chennai, India, March 29–30, 2019, Vol. 1, 162–168.

Guidali, M., Duschau-Wicke, A., Broggi, S., Klamroth-Marganska, V., Nef, T., and Riener, R. (2011). A robotic system to train activities of daily living in a virtual

environment. *Med. Biol. Eng. Comput.* 49, 1213. doi:10.1007/s11517-011-0809-0

He, J., Guo, Y., Mao, R., and Zhang, J. (2020). Proportion of asymptomatic coronavirus disease 2019: a systematic review and meta-analysis. *J. Med. Virol.* 93 (2), 820–830. doi:10.1002/jmv.26326

Hogan, N., Krebs, H. I., Charnnarong, J., Srikrishna, P., and Sharon, A. (1992). Mitmanus: a workstation for manual therapy and training. i. In Proceedings IEEE International Workshop on Robot and Human Communication, Tokyo, Japan, September 1–3, 1992 (New York, NY: IEEE), 161–165.

Iannaccone, S., Alemanno, F., Houdayer, E., Brugliera, L., Castellazzi, P., Cianflone, D., et al. (2020). Covid-19 rehabilitation units are twice as expensive as regular rehabilitation units. *J. Rehabil. Med.* 52 (6), jrm00073. doi:10.2340/16501977-2704

Jensen, P., Jensen, L., and Brunak, S. (2012). Mining electronic health records: toward better research applications and clinical care. *Nat. Rev. Genet.* 13, 395–405. doi:10.1038/nrg3208

Jiang, F., Jiang, Y., Zhi, H., Dong, Y., Li, H., Ma, S., et al. (2017). Artificial intelligence in healthcare: past, present and future. *Stroke Vasc Neurol* 2, 230–243. doi:10.1136/svn-2017-000101

Johns Hopkins University (2020). COVID-19 dashboard by the center for systems science and engineering (CSSE) at Hopkins university. Available at: https://coronavirus.jhu.edu/map.htm (Accessed August 27, 2020).

Kersloot, M. G., van Putten, F. J. P., Abu-Hanna, A., Cornet, R., and Arts, D. L. (2020). Natural language processing algorithms for mapping clinical text fragments onto ontology concepts: a systematic review and recommendations for future studies. *J. Biomed. Semant.* 11, 14. doi:10.1186/s13326-020-00231-z

Khalili, D., and Zomlefer, M. (1988). An intelligent robotic system for rehabilitation of joints and estimation of body segment parameters. *IEEE Trans. Biomed. Eng.* 35, 138–146. doi:10.1109/10.1352

Liu, H., Lussier, Y. A., and Friedman, C. (2001). Disambiguating ambiguous biomedical terms in biomedical narrative text: an unsupervised method. *J. Biomed. Inf.* 34, 249–261. doi:10.1006/jbin.2001.1023

Lum, P. S., Burgar, C. G., and Shor, P. C. (2004). Evidence for improved muscle activation patterns after retraining of reaching movements with the mime robotic system in subjects with post-stroke hemiparesis. *IEEE Trans. Neural Syst. Rehabil. Eng.* 12, 186–194. doi:10.1109/TNSRE.2004.827225

Lundervold, A. S., and Lundervold, A. (2019). An overview of deep learning in medical imaging focusing on MRI. *Zeitschrift für Medizinische Physik.* 29 (2), 102–127. doi:10.1016/j.zemedi.2018.11.002

Maier, A., Syben, C., Lasser, T., and Riess, C. (2019). A gentle introduction to deep learning in medical image processing. *Zeitschrift für Medizinische Physik.* 29 (2), 86–101. doi:10.1016/j.zemedi.2018.12.003

Mehrholz, J., Hädrich, A., Platz, T., Kugler, J., and Pohl, M. (2012). Electromechanical and robot-assisted arm training for improving generic activities of daily living, arm function, and arm muscle strength after stroke. *Cochrane Database Syst. Rev.* 13 (6), CD006876. doi:10.1002/14651858.CD006876.pub3

Melton, G. B., and Hripcsak, G. (2005). Automated detection of adverse events using natural language processing of discharge summaries. *J. Am. Med. Inf. Assoc.* 12, 448–457. doi:10.1197/jamia.M1794

Meystre, S., and Haug, P. J. (2006). Natural language processing to extract medical problems from electronic clinical documents: performance evaluation. *J. Biomed. Inf.* 39, 589–599. doi:10.1016/j.jbi.2005.11.004

Meystre, S. M., Savova, G. K., Kipper-Schuler, K. C., and Hurdle, J. F. (2008). Extracting information from textual documents in the electronic health record: a review of recent research. *Yearb Med Inform* 17 (01), 128–144. doi:10.1055/s-0038-1638592

Murff, H. J., FitzHenry, F., Matheny, M. E., Gentry, N., Kotter, K. L., Crimin, K., et al. (2011). Automated identification of postoperative complications within an electronic medical record using natural language processing. *JAMA* 306, 848–855. doi:10.1001/jama.2011.1204

Najafi, M., Rossa, C., Adams, K., and Tavakoli, M. (2020). Using potential field function with a velocity field controller to learn and reproduce the therapist's assistance in robot-assisted rehabilitation. *IEEE/ASME Trans. Mechatron.* 25, 1622–1633. doi:10.1109/tmech.2020.2981625

Panwar, H., Gupta, P. K., Siddiqui, M. K., Morales-Menendez, R., Bhardwaj, P., and Singh, V. (2020). A deep learning and grad-cam based color visualization approach for fast detection of covid-19 cases using chest x-ray and ct-scan images. *Chaos, Solit. Fractals* 140, 110190. doi:10.1016/j.chaos.2020.110190

Prvu Bettger, J., Thoumi, A., Marquevich, V., De Groote, W., Rizzo Battistella, L., Imamura, M., et al. (2020). Covid-19: maintaining essential rehabilitation services across the care continuum. *BMJ Glob Health* 5, e002670. doi:10.1136/bmjgh-2020-002670

Punn, N. S., Sonbhadra, S. K., and Agarwal, S. (2020). Covid-19 epidemic analysis using machine learning and deep learning algorithms. *medRxiv*. doi:10.1007/s10489-020-01900-3

Radin, J. M., Wineinger, N. E., Topol, E. J., and Steinhubl, S. R. (2020). Harnessing wearable device data to improve state-level real-time surveillance of influenza-like illness in the USA: a population-based study. *Lancet Digit Health* 2, e85–e93. doi:10.1016/S2589-7500(19)30222-5

Reinkensmeyer, D. J., Kahn, L. E., Averbuch, M., McKenna-Cole, A., Schmit, B. D., and Rymer, W. Z. (2014). Understanding and treating arm movement impairment after chronic brain injury: progress with the arm guide. *J. Rehabil. Res. Dev.* 37, 653–662.

Savova, G. K., Masanz, J. J., Ogren, P. V., Zheng, J., Sohn, S., Kipper-Schuler, K. C., et al. (2010). Mayo clinical text analysis and knowledge extraction system (cTAKES): architecture, component evaluation and applications. *J. Am. Med. Inf. Assoc.* 17, 507–513. doi:10.1136/jamia.2009.001560

Schuemie, M. J., Kors, J. A., and Mons, B. (2005). Word sense disambiguation in the biomedical domain: an overview. *J. Comput. Biol.* 12, 554–565. doi:10.1089/cmb.2005.12.554

Shen, D., Wu, G., and Suk, H.-I. (2017). Deep learning in medical image analysis. *Annu. Rev. Biomed. Eng.* 19, 221–248. doi:10.1146/annurev-bioeng-071516-044442

Tao, R., Ocampo, R., Fong, J., Soleymani, A., and Tavakoli, M. (2020). Modeling and emulating a physiotherapist's role in robot-assisted rehabilitation. *Advanced Intelligent Systems* 2, 1900181. doi:10.1002/aisy.201900181

Tavakoli, M., Carriere, J., and Torabi, A. (2020). Robotics, smart wearable technologies, and autonomous intelligent systems for healthcare during the covid-19 pandemic: an analysis of the state of the art and future vision. *Advanced Intelligent Systems* 2, 2000071. doi:10.1002/aisy.202000071

Tuli, S., Tuli, S., Tuli, R., and Gill, S. S. (2020). Predicting the growth and trend of COVID-19 pandemic using machine learning and cloud computing. *Internet of Things* 11, 100222. doi:10.1016/j.iot.2020.100222

Van der Loos, H. M., Reinkensmeyer, D. J., and Guglielmelli, E. (2016). *Rehabilitation and health care robotics* (New York, NY: Springer International Publishing), chap. 64. 1685–1728.

Voelker, R. (2005). Rehabilitation medicine welcomes a robotic revolution. *JAMA* 294, 1191–1195. doi:10.1001/jama.294.10.1191

Williams, D. J., Krebs, H. I., and Hogan, N. (2001). "A robot for wrist rehabilitation," In 2001 conference proceedings of the 23rd annual international conference of the ieee engineering in medicine and biology society, Istanbul, Turkey, October 25–28, 2001, Vol. 2, 1336–1339.

Worsnopp, T., Peshkin, M., Colgate, J., and Kamper, D. (2007). "An actuated finger exoskeleton for hand rehabilitation following stroke," In 2007 IEEE 10th international conference on rehabilitation robotics, Noordwijk, Netherlands, June 12–15, 2007, 896–901.

Conflict of Interest: The authors declare that the research was conducted in the absence of any commercial or financial relationships that could be construed as a potential conflict of interest.

frontiers in Neurorobotics

REVIEW
published: 17 February 2021
doi: 10.3389/fnbot.2021.617636

Integrating Tactile Feedback Technologies Into Home-Based Telerehabilitation: Opportunities and Challenges in Light of COVID-19 Pandemic

Shirley Handelzalts[1,2]*, *Giulia Ballardini*[3,4], *Chen Avraham*[5,6], *Mattia Pagano*[3,4], *Maura Casadio*[3,4] *and Ilana Nisky*[2,5,6]

[1] Department of Physical Therapy, Ben-Gurion University of the Negev, Be'er Sheva, Israel, [2] The Translational Neurorehabilitation Lab at Adi Negev Nahalat Eran, Ofakim, Israel, [3] Department of Informatics, Bioengineering, Robotics and Systems Engineering, University of Genoa, Genoa, Italy, [4] S.C.I.L Joint Lab, Department of Informatics, Bioengineering, Robotics and System Engineering (DIBRIS), Santa Corona Hospital, Pietra Ligure, Italy, [5] Department of Biomedical Engineering, Ben-Gurion University of the Negev, Be'er Sheva, Israel, [6] Zlotowski Center for Neuroscience, Ben-Gurion University of the Negev, Be'er Sheva, Israel

The COVID-19 pandemic has highlighted the need for advancing the development and implementation of novel means for home-based telerehabilitation in order to enable remote assessment and training for individuals with disabling conditions in need of therapy. While somatosensory input is essential for motor function, to date, most telerehabilitation therapies and technologies focus on assessing and training motor impairments, while the somatosensorial aspect is largely neglected. The integration of tactile devices into home-based rehabilitation practice has the potential to enhance the recovery of sensorimotor impairments and to promote functional gains through practice in an enriched environment with augmented tactile feedback and haptic interactions. In the current review, we outline the clinical approaches for stimulating somatosensation in home-based telerehabilitation and review the existing technologies for conveying mechanical tactile feedback (i.e., vibration, stretch, pressure, and mid-air stimulations). We focus on tactile feedback technologies that can be integrated into home-based practice due to their relatively low cost, compact size, and lightweight. The advantages and opportunities, as well as the long-term challenges and gaps with regards to implementing these technologies into home-based telerehabilitation, are discussed.

Keywords: haptic, training, stroke, neurorehabiliation, somatosensory, assessment

OPEN ACCESS

Edited by:
Mahdi Tavakoli,
University of Alberta, Canada

Reviewed by:
Bernhard M. Weber,
Helmholtz Association of German Research Centers (HZ), Germany
Serena Maggioni,
Hocoma, Switzerland

***Correspondence:**
Shirley Handelzalts
handelza@post.bgu.ac.il

Received: *15 October 2020*
Accepted: *07 January 2021*
Published: *17 February 2021*

Citation:
Handelzalts S, Ballardini G, Avraham C, Pagano M, Casadio M and Nisky I (2021) Integrating Tactile Feedback Technologies Into Home-Based Telerehabilitation: Opportunities and Challenges in Light of COVID-19 Pandemic. Front. Neurorobot. 15:617636. doi: 10.3389/fnbot.2021.617636

INTRODUCTION

The COVID-19 pandemic highlights the need to accelerate the development and implementation of innovative approaches for home-based rehabilitation (Simpson and Robinson, 2020). While in normal, non-pandemic times many individuals in need of rehabilitation services do not receive sufficient therapy due to difficulties posed by the need to travel to the location where the therapy is provided, a shortage of regional rehabilitation care, and poor adherence to assignments (Cramer et al., 2019), the COVID-19 pandemic is presenting new challenges to rehabilitation services. The restrictions imposed to contain the spread of infection further limit access to rehabilitation

services (Chaler et al., 2020) and challenge societal well-being. This may lead to long-term negative consequences by increasing functional impairments, and reducing participation and quality of life (Boldrini et al., 2020b). Telerehabilitation from home may partially mitigate these challenges, but state of the art telerehabilitation systems often only use visual or/and auditory feedback and lack somatosensory feedback (Navarro et al., 2018).

Somatosensory input is essential for accurate motor control and interactions with the external world (Pearson, 2000; Perez et al., 2003; Borich et al., 2015). The somatosensory impairment that is observed in many neurological disorders such as stroke, traumatic brain injury, and spinal cord injury can lead to impairments in adjusting the amount of force applied during grasping and fine manipulation of objects (Sullivan and Hedman, 2008; Doyle et al., 2010, 2014; Connell et al., 2014; Hill et al., 2014) and in performing tasks that require rapid dextrous movements (Goebl and Palmer, 2008), as well as in controlling more gross functions such as gait and posture (Maki and McIlroy, 1997; Horak, 2006).

In in-person rehabilitation intervention therapists frequently use touch to assist, and to provide and perceive information, as well as to comfort and encourage patients (Roger et al., 2002). In a survey regarding satisfaction with telerehabilitation during the COVID-19 pandemic, the absence of touch was reported by patients as a limitation (Tenforde et al., 2020). The current review focuses on tactile technologies that can be used as innovative solutions to support home-based telerehabilitation and addresses some challenges that have become more salient during the COVID-19 pandemic.

Previous reviews discussed telerehabilitation and wearable haptic devices; however, none has provided a comprehensive perspective on the variety of tactile stimulation technologies and the ways to exploit them for home-based telerehabilitation. An overview on tactile displays was conducted by Jones and Sarter (2008); however, since then significant developments in tactile technology have been presented. Culbertson et al. (2018b) reviewed the design, control, and general applications of haptic devices, but did not focus on rehabilitation applications. Several reviews focused on wearable technologies (not necessarily haptics) that can be used for remote monitoring of physiological and kinematic measurements, with a brief overview on the applications for home-based rehabilitation (Patel et al., 2012; Wang et al., 2017). Navarro et al. (2018) proposed features related to adaptive, multisensorial, physiological and social aspects that should be considered in the development process of the next generation of telerehabilitation systems. A systematic review of virtual reality technologies for rehabilitation examined the effect of haptic feedback on motor performance (Rose et al., 2018). Another review (Shull and Damian, 2015) examined wearable haptic applications for a variety of sensory impairments; however, the focus of that review was on stimulations to enhance motor performance. A previous narrative review focused on tactile technologies for hand rehabilitation in central nervous system disorders (Demain et al., 2013). In this work, we extend previous reviews by covering the development in tactile technologies over the last decade with an emphasis on wearable devices that potentially could be utilized at home. We also expand the scope to include the assessment of somatosensory deficits, in addition to various rehabilitative applications, and address the recent developments in mediation of social interaction. Specifically, we review: (1) clinical approaches for stimulating somatosensation in home-based rehabilitation, (2) tactile technologies that can be integrated into home-based rehabilitation, and (3) the challenges and gaps, as well as the opportunities, in this field.

CLINICAL APPROACHES FOR STIMULATING SOMATOSENSATION IN HOME-BASED NEUROREHABILITATION

Providing Tactile Augmented Feedback to Enhance Motor Control Performance and Learning

Somatosensory augmented feedback provides additional sensory cues that complement and/or replace native sensory input from the somatosensory, visual, and/or vestibular systems (Bach-y-Rita and Kercel, 2003). Tactile cues can guide patients on how to improve their movements (Bark et al., 2015) and may assist them in achieving their goals more quickly and/or more easily (Magill, 2004). A promising application of tactile feedback is to provide patients with guidance on how to improve their movements without the constant presence of a therapist (Bark et al., 2015; Bao et al., 2018), including when practicing on their own. The augmented feedback can be triggered by the participant's motor performance and can provide information continuously during the action or at specified times (Ferris and Sarter, 2011; Galambos, 2012; Kaul and Rohs, 2017). Compared with visual feedback, real time tactile feedback makes it possible for patients to receive information regarding movement errors without the need to shift visual attention, thus affording a more "natural" movement (Bark et al., 2015).

Tactile stimulation can also be beneficial even if it does not provide any information. For instance, subthreshold tactile stimulations (i.e., below the level at which a person can perceive the stimulation) add noise to proprioceptive signals and might help these signals to overcome the threshold of specific neural circuits. This phenomenon, also known as the stochastic resonance theory (Gammaitoni, 1995; Gammaitoni et al., 1998; Moss et al., 2004), facilitates more efficient detection of somatosensory information, and improves sensorimotor performance (Collins et al., 1996, 2003). As such, it could be used in the rehabilitation of individuals with sensorimotor deficits to improve motor functions (e.g., grasp, object manipulation, balance and gait) and tactile sensation (Enders et al., 2013; Seo et al., 2014, 2019).

Applying Tactile Stimulations to Improve/Restore Cutaneous Somatosensation

Somatosensory impairment is considered to have a negative prognostic impact on rehabilitation interventions and overall motor function recovery (Bowerman et al., 2012; Dietz and Fouad, 2014; Zandvliet et al., 2020). Although the current literature in this field is limited, a recent systematic review

and meta-analysis indicated positive effects in improving somatosensory impairments (Serrada et al., 2019). Specifically, sensory discrimination training by repeated practice to distinguish textures and localize tactile stimuli can influence the sensory system and drive recovery (Carey et al., 1993; Yekutiel and Guttman, 1993; Turville et al., 2019).

Presenting Tactile Feedback in Virtual Reality Environments

Telerehabilitation is often based on virtual reality systems and interactive video games that aim to facilitate repetitions of movements and to make the repetitive exercises more engaging, enjoyable and motivating (Standen et al., 2015). The virtual experience can be further enhanced by using tactile devices that can convey haptic interactions between the user and the virtual objects (Galambos, 2012; Culbertson et al., 2018b).

Conveying Social Tactile Interaction

Haptic feedback plays a critical role in emotional and social communication (Strong and Gaver, 1996; Brave and Dahley, 1997). During in-person rehabilitation sessions therapists often use touch to comfort and encourage patients (Roger et al., 2002). Recent developments in wearable tactile devices demonstrate very promising results in conveying sensations such as comfort and affection (Culbertson et al., 2018a; Nunez et al., 2019, 2020), attention (Baumann et al., 2010), playfulness (Mullenbach et al., 2014), or social presence (Baldi et al., 2020). The integration of social tactile aspects into telerehabilitation systems would open new possibilities for remote therapist-patient communication and may facilitate wider adoption of telerehabilitation from home by patients.

Assessing Tactile Impairments

In addition to the above training strategies, the use of measures to quantify somatosensory deficits could help therapists to understand patients' impairments beyond motor and functional status and assist in targeting appropriate interventions. The assessment of somatosensory functions, including proprioception and sensitivity to light touch, pressure, and temperature, cannot be done remotely in the traditional way where the therapist applies the stimulation and evaluates the performance using scales. Portable, and often wearable devices that apply multimodal stimulations have the potential to provide reliable and quantitative information regarding somatosensory impairments in a home-based setting (Rinderknecht et al., 2015, 2019). Such portable devices have already been used in some virtual reality systems for baseline measurements of activity and kinematics and for tracking changes over time (Patel et al., 2012; Chen et al., 2015; Bortone et al., 2018).

TACTILE STIMULATION TECHNOLOGIES

Over the last few decades, technologies that can provide versatile tactile stimulations have become very popular and many new devices continue to be developed. These devices can be integrated into wearable technologies and utilized for telerehabilitation due to their low cost, compact size, and lightweight. From the technological point of view, there is a variety of ways to apply tactile stimulation. These can be categorized according to the mechanism evoking the tactile sensation: mechanical, electrotactile, and thermal. In order to provide an in depth review of the technology and its applications, in this review we focus on mechanical tactile stimulations. However, it should be noted that electrotactile stimulation is also used for various assistive technologies and rehabilitation applications such as for people with visual (Bliss et al., 1970; Kajimoto et al., 2001) and auditory impairments (Weisenberger et al., 1989), as well as in prostheses, orthoses (Schweisfurth et al., 2016; Svensson et al., 2017) and stroke rehabilitation (for a review see Laufer and Elboim-Gabyzon, 2011).

Mechanical tactile stimulations can be further divided into vibration, skin deformation, and mid-air stimulations. Recently the idea of wearable tactile devices that combine vibration, stretch, and pressure for conveying multimodal haptic information was introduced (Aggravi et al., 2018; Sullivan et al., 2019; Dunkelberger et al., 2020), highlighting the importance of understanding the unique properties of each stimulation type and harnessing the advantages of each to design devices that are more than the sum of their parts. In the remainder of this section, we review the state of the art in mechanical tactile stimulation devices. For each type of device we review the technology, its applications for healthy and patient populations, and its advantages and disadvantages. The different devices and studies are summarized in **Tables 1**, **2**. **Table 1** summarizes the devices by stimulation type, actuator type, technological maturity level, and application. We rank the technological maturity level based on how extensively testing of the device has been reported in the literature, with the following levels: prototype demonstration ($N < 10$); healthy user studies ($N = 10$–100); extensive healthy user studies ($N > 100$); patient user studies ($N = 10$–100); extensive patient user studies ($N > 100$). **Table 2** summarizes the studies that were reviewed here that were tested on patient populations for different rehabilitation applications.

Vibration

Vibration is the simplest and most common tactile stimulation technology that has become ubiquitous and is used in a wide variety of devices such as phones, watches, games, and home appliances (Culbertson et al., 2018b). Typically, the actuators used in wearable devices produce vibration at frequencies above 100 Hz, which activates the Pacinian corpuscles mechanoreceptors (Culbertson et al., 2018b). The most common locations for applying the vibrotactile stimulation are the arm (Bark et al., 2008; Huisman et al., 2013; Krueger et al., 2017; Shah et al., 2018; Risi et al., 2019) and the torso (Van Erp et al., 2005; Lee et al., 2012; Ballardini et al., 2020). Other locations for stimulation include the hand (Jiang et al., 2009; Wan et al., 2016) and different locations on the lower limb (Chen B. et al., 2016; Shi et al., 2019). The design of the device and the stimulation patterns (e.g., frequency and amplitude of the vibration) need to take into account the targeted dermatomes and the density and size of the mechanoreceptors' receptive fields which vary across the body (Jones and Sarter, 2008; Johansson and Flanagan, 2009; Shah et al., 2019) and across the skin type

TABLE 1 | Tactile stimulation devices by type, maturity level, and applications in healthy individuals.

Stimulation type	Device type	Device maturity level	Applications	Commercial availability
Vibration	Single actuator	Extensive healthy and patient user studies	Improve walking pattern (Janssen et al., 2009)	BalanceFreedom of SwayStar system https://www.b2i.info/web/index.htm
			Improve force control accuracy (Ahmaniemi, 2012)	
			Convey proprioceptive information (Bark et al., 2008)	
	Multiple actuators	Extensive healthy and patient user studies	Enhance motor learning and performance (Lieberman and Breazeal, 2007; Bark et al., 2015; Kaul and Rohs, 2017; Van Breda et al., 2017; Shah et al., 2018)	
			Guide movement direction (Van Erp et al., 2005; Krueger et al., 2017; Risi et al., 2019)	
			Improve standing balance (Lee et al., 2012; Ma and Lee, 2017; Ballardini et al., 2020)	Vertiguard RT https://zeisberg.net/posturographie.html
			Improve walking pattern (Chen B. et al., 2016; Wan et al., 2016; Muijzer-Witteveen et al., 2017; Xu et al., 2017)	
			Convey various types of information (Ferris and Sarter, 2011; Cobus et al., 2018)	
			Convey affective touch (Israr and Abnousi, 2018)	
			Assess somatosensory impairments (Tommerdahl et al., 2019)	Brain Gauge https://www.corticalmetrics.com/howitworks
	Multiple actuators on a glove	Healthy and patient user studies	Convey virtual objects information (Muramatsu et al., 2012)	CyberTouch http://www.cyberglovesystems.com/cybertouch2
			Convey force information (Galambos, 2012)	
			Assess somatosensory impairments (Rinderknecht et al., 2015, 2019)	
	Single actuator with multiple probes	Healthy user studies	Assess somatosensory impairments (Holden et al., 2012; Puts et al., 2013; Mikkelsen et al., 2020)	
Skin deformation—tangential and stretch	Tactor	Extensive healthy user studies and patient studies	Alter mechanical properties of virtual objects (Sylvester and Provancher, 2007; Quek et al., 2013, 2014b; Schorr et al., 2013; Farajian et al., 2020a,b)	
			Convey direction information (Bark et al., 2010; Guinan et al., 2012, 2013a,b; Norman et al., 2014; Chinello et al., 2018; Kanjanapas et al., 2019)	
			Convey information about curvature (Frisoli et al., 2008; Prattichizzo et al., 2013), weight (Kato et al., 2016; Choi et al., 2017), and virtual objects information (Yem and Kajimoto, 2017; Wang et al., 2020)	
			Improve object manipulation (Leonardis et al., 2017; Schorr and Okamura, 2017b; Bortone et al., 2018), tracking (Quek et al., 2014b), insertion (Quek et al., 2015b), palpation (Schorr et al., 2015) and grasping (Westebring van der Putten et al., 2010; Kim and Colgate, 2012; Quek et al., 2015a; Choi et al., 2017; Stephens-Fripp et al., 2018; Avraham and Nisky, 2020; Bitton et al., 2020; Farajian et al., 2020b)	
			Guide movement direction (Bark et al., 2010; Guinan et al., 2012, 2013a,b; Norman et al., 2014; Chinello et al., 2018)	
			Improve standing balance (Hur et al., 2019)	

(Continued)

TABLE 1 | Continued

Stimulation type	Device type	Device maturity level	Applications	Commercial availability
			Convey affective touch (Nunez et al., 2019)	
			Assess somatosensory impairments (Ballardini et al., 2018)	
	Adhesive rings	Healthy user studies	Convey affective touch (Haynes et al., 2019)	
	Belt/Vest	Healthy user studies	Substitute and augment force and torque feedback (Pacchierotti et al., 2016), convey sensation of mass (Minamizawa et al., 2007), and sensation of virtual objects (Minamizawa et al., 2008),	
			Convey direction information (Bianchi, 2016)	
			Provide feedback about grasping force (Casini et al., 2015)	
			Guide movement direction (Stanley and Kuchenbecker, 2012; Pezent et al., 2019; Smith et al., 2020) and convey path information (Kumar et al., 2017)	
			General tactile stimulation (Nakamura and Jones, 2003; Wu et al., 2010)	
	Rocker and roller	Healthy user studies	Enhance virtual object manipulation (Provancher et al., 2005)	
			Convey proprioceptive information (Battaglia et al., 2017 and 2019; Colella et al., 2019) (Clark et al., 2018)	
	Mechanical cranks	Healthy user studies	General tactile stimulation (Stephens-Fripp et al., 2018)	
Skin deformation—pressure	Indentator	Healthy and patient user studies	General tactile stimulations (Chinello et al., 2015)	
			Convey sensations of softness (Frediani and Carpi, 2020), and holding a virtual object (Merrett et al., 2011)	
			Convey direction information (Raitor et al., 2017; Agharese et al., 2018)	
			Render shape information of remote and virtual objects (Chinello et al., 2019)	
			Convey affective touch (Culbertson et al., 2018a)	
			Assess somatosensory impairments (Jacobs et al., 2000)	
	Belt	Prototype demonstration	Convey affective touch (Prattichizzo et al., 2010)	
	Pin array	Healthy and patient user studies	Create 2D and 3D graphic display (Shimizu et al., 1993; Leo et al., 2016; Brayda et al., 2018)	
			General tactile stimulations (Caldwell et al., 1999),	
			Convey sensations of roughness (Kim et al., 2009), and texture (Sarakoglou et al., 2005; Kyung and Park, 2007; Garcia-Hernandez et al., 2011)	
Skin deformation or vibration ultrasound	Mid-air technology using phased arrays	Extensive healthy user studies	Create 3D haptic shapes (Long et al., 2014; Vo and Brewster, 2015; Makino et al., 2016)	UltraLeap https://www.ultraleap.com/
			Convey affective touch (Shakeri et al., 2017, 2018)	

Maturity level is ranked by the following levels: prototype demonstration (N < 10); healthy user studies (N = 10–100); extensive healthy user studies (N > 100); patient user studies (N = 10–100); extensive patient user studies (N > 100). Note that the applications column refers to studies in healthy individuals; for types of devices that were also tested on patients please refer to ***Table 2*** *for more detailed information about the specific studies. Commercial availability of devices that were reviewed in the current paper and tested either on healthy or patient populations.*

TABLE 2 | Tactile device applications for rehabilitation.

Application	Population	Tested in a home setting (Yes/No)	Type of stimulation	Type of device	Wearable/ Non-wearable	References
Enhance upper extremity function	Multiple Sclerosis (*N* = 24)	No	Vibration	Multiple actuators	Wearable	Jiang et al., 2009
	Stroke (*N* = 12)	No	Subthreshold vibration	Single actuator, (TheraBracelet)	Wearable	Seo et al., 2019
Enhance gait and balance control	Stroke (*N* = 8)	No	Vibration	Multiple actuators	Wearable	Afzal et al., 2019
	Stroke (*N* = 17)	No	Vibration	Multiple actuators	Wearable	Yasuda et al., 2017
	Stroke (*N* = 3)	No	Vibration	Platform (The Rutgers Ankle Haptic Interface)	Non-wearable	Boian et al., 2003
	Stroke (*N* = 20)	No	Vibration	Multiple actuators	Wearable	Jaffe et al., 2004
	Parkinson's disease (*N* = 43)	No	Vibration	Single actuator (VibroGait)	Wearable	Fino and Mancini, 2020
	Parkinson's disease (*N* = 20)	No	Vibration	Multiple actuators (BalanceFreedom)	Wearable	Nanhoe-Mahabier et al., 2012
	Parkinson's disease (*N* = 16)	No	Pressure	Steel stick	Non-wearable	Barbic et al., 2014
	Parkinson's disease (*N* = 10)	No	Vibration	Multiple actuators (Vertiguard)	Wearable	Rossi-Izquierdo et al., 2013
	Parkinson's disease (*N* = 9) and older adults at high risk for falls (*N* = 8) and older adults (*N* = 10)	No	Vibration	Multiple actuators	Wearable	High et al., 2018
	Parkinson's disease (*N* = 9) and older adults (*N* = 9)	No	Vibration	Multiple actuators	Wearable	Lee et al., 2018
	Older adults (*N*= 12)	Yes	Vibration	Multiple actuators	Wearable	Bao et al., 2018
	Peripheral Neuropathy (*N* = 4)	No	Pressure	Ballon arrays	Wearable	McKinney et al., 2014
	Vestibular disorder (*N* = 6)	No	Vibration	Multiple actuators	Wearable	Sienko et al., 2012
	Vestibular disorder (*N* = 7)	No	Vibration	Multiple actuators	Wearable	Sienko et al., 2013
	Vestibular disorder (*N* = 13)	No	Vibration	Multiple actuators (Vertiguard)	Wearable	Brugnera et al., 2015
	Vestibular disorder (*N* = 8)	No	Vibration	Multiple actuators	Wearable	Bao et al., 2019
	Vestibular disorder (*N* = 105)	No	Vibration	Multiple actuators, (Vertiguard)	Wearable	Basta et al., 2011
Enhance tactile sensation	Stroke (*N* = 5), diabetic neuropathy (*N* = 8) and older adults (*N* = 12)	No	Subthreshold vibration	Single actuator	Non-wearable	Liu et al., 2002
	Stroke (*N* = 10)	No	Subthreshold vibration	Single actuator	Wearable	Enders et al., 2013
	Stroke (*N* = 16)	Yes	Vibration	Multiple actuators on a glove	Wearable	Seim et al., 2020b
	Digital nerve injuries (*N* = 49)	No	Pressure	Rotating disk and a card	Non-wearable	Cheng, 2000
	Chronic pain (*N* = 13)	No	Pressure	Probe	Non-wearable	Moseley et al., 2008
	Spinal cord injury (*N* = 7)	Yes	Vibration	Multiple actuators on a glove (Mobile Music Touch)	Wearable	Estes et al., 2015
Somatosensory assessment	Stroke (*N*= 2)	No	Vibration	Multiple actuators on a glove (ReHaptic Glove)	Wearable	Rinderknecht et al., 2019
	Stroke (*N* = 3)	No	Skin stretch	Tactor	Non-wearable	Ballardini et al., 2018
	Brain injury (*N* = 1)	No	Vibration	Multiple actuators (Brain Gauge)	Non-wearable	King et al., 2018
Enhance interaction realism in virtual reality environment	Children with neuromotor impairments (*N* = 20)	No	Skin stretch and pressure	Tactor	Wearable	Bortone et al., 2018
	Spinal cord injury (*N* = 9)	No	Vibration	Multiple actuators on a glove (CyberTouch)	Wearable	Dimbwadyo-Terrer et al., 2016

(e.g., hairy skin has a reduced number of Pacinian corpuscles compared to glabrous skin) (Colgate and Brown, 1994; Ackerley et al., 2014). Skin type can also influence the quality of stimulation via its mechanical properties and its physical propagation of the vibration (Dandu et al., 2019; Hachisu and Suzuki, 2019).

Technology

Vibrotactile feedback can be conveyed by a single actuator, or by an array of actuators that create an oscillating movement. The choice of the actuator affects the size, shape, cost, availability, robustness, speed of response, input requirements, and power consumption of the device (Choi and Kuchenbecker, 2013). An overview of the different actuators can be found in Choi and Kuchenbecker (2013) and Kern (2009).

The stimulation patterns can be divided into two fundamental categories: (1) binary on-off state, and (2) continuous vibration, created by changing parameters of the vibration signals such as amplitude, frequency, duration, rhythm, and waveform (Brewster and Brown, 2004; Jones and Sarter, 2008). Binary feedback is not continuously provided but is triggered by specific events such as an alarm or event-cue related information (Ferris and Sarter, 2011; Galambos, 2012; Kaul and Rohs, 2017). The vibration intensity can be constant or may vary according to the event (Cobus et al., 2018). Continuous vibrotactile stimulation is used to convey various types of information to the users, including: (1) state feedback, encoding position and/or velocity of limbs (Ferris and Sarter, 2011; Krueger et al., 2017; Shah et al., 2018; Risi et al., 2019), (2) force feedback, encoding the amount of force exerted (Ahmaniemi, 2012), and (3) error feedback, encoding information regarding the goal of the task and the state of the end-effector (Wall et al., 2001; Cuppone et al., 2016; Krueger et al., 2017).

By controlling the shape and timing of the signals from multiple static actuators, it is also possible to display illusions of movement that can enrich the design space of tactile stimulation. Prominent examples are: (1) phi (or beta) movement, where a smooth apparent motion of a single stimulus is created by the periodic activation of two spatially separated stimuli (Sherrick and Rogers, 1966; Lederman and Klatzky, 2009), (2) saltatory (or rabbit) illusion, i.e., illusory sweeping movement of discrete taps that occur by activating actuators in sequence (Geldard and Sherrick, 1972; Lederman and Klatzky, 2009), and (3) the tendons vibration illusion, which is an illusory perception of movement that can be evoked by triggering the muscle spindle afferents through vibrations applied to the tendon (Goodwin et al., 1972; Taylor et al., 2017).

Applications for Enhancing Sensorimotor Performance and Learning

In healthy individuals, vibrotactile feedback is used to enhance motor control and learning (Lieberman and Breazeal, 2007; Van Breda et al., 2017; Shah et al., 2018). It has been demonstrated that state feedback regarding the force exerted improved the accuracy of force repetition (Ahmaniemi, 2012). Other studies used state and/or error feedback to guide upper limb reaching movements in the absence of visual information (Krueger et al., 2017; Shah et al., 2018; Risi et al., 2019) and to reach accuracy levels beyond the limits of natural proprioception (Risi et al., 2019). Results from a meta-analysis indicated that vibrotactile feedback was effective in reducing task completion times, but neither forces nor errors were significantly reduced (Nitsch and Färber, 2012). In addition, vibration feedback encoding center of mass or center of pressure motion was used to improve standing balance (Lee et al., 2012; Ma and Lee, 2017; Ballardini et al., 2020) and walking patterns (Janssen et al., 2009; Muijzer-Witteveen et al., 2017; Xu et al., 2017). Vibrotactile feedback based on stochastic resonance was applied for improving visuomotor temporal integration in hand control (Nobusako et al., 2019) and balance control (Magalhães and Kohn, 2011). Vibrations that informed the users about collisions with virtual objects in a virtual reality context added realism and improved performance (Galambos, 2012; Kaul and Rohs, 2017). Also, a vibrotactile glove interface has been used to convey sensations of virtual objects (Muramatsu et al., 2012).

Applications in Rehabilitation

In persons with multiple sclerosis, vibrotactile feedback applied to the fingernails of the contralateral hand improved the performance of a grasping and lifting task of the more impaired hand (Jiang et al., 2009). In addition, real time state vibrotactile cues reduced postural sway during standing balance tasks and improved gait parameters after stroke (Yasuda et al., 2017; Afzal et al., 2019), in people with Parkinson's disease (Nanhoe-Mahabier et al., 2012; High et al., 2018; Lee et al., 2018; Fino and Mancini, 2020) and with vestibular disorders (Sienko et al., 2012, 2013). However, in all of these studies improvements were observed during trials, and long-term effects were not tested. Vibrotactile stimulations were also used to enhance interaction realism in a rehabilitation system based on virtual reality (Boian et al., 2003; Dimbwadyo-Terrer et al., 2016), and to avoid collisions during walking in stroke survivors (Jaffe et al., 2004).

Several randomized controlled trials (RCTs) with small cohorts tested the effect of balance training programs with vibrotactile stimulations. Following a 2-week training program using vibrotactile feedback, individuals with Parkinson's disease improved their balance control parameters and performance-based measures and retained improvements 3 months after training (Rossi-Izquierdo et al., 2013). Additionally, adults with vestibular disorders improved their balance performance and felt more confident regarding their balance while performing daily activities after a training protocol with vibrotactile stimulations compared with a control group that trained without stimulations (Brugnera et al., 2015; Bao et al., 2019). Furthermore, balance improvements were retained at 6-month follow-up assessments (Bao et al., 2019). Also, reduced body sway and improved clinical outcome measures [e.g., Sensory Organization Test (SOT) (Franchignoni et al., 2010) and Dizziness Handicap Inventory (Jacobson and Newman, 1990)] were observed in a study with a large cohort of participants with vestibular disorders ($n = 105$) who trained with vibrotactile stimulations over 2-weeks (i.e., ten-sessions) compared with a control group that trained with a sham device (Basta et al., 2011).

Subthreshold vibrotactile stimulation improved somatosensation and motor function in persons with

sensorimotor impairments: stimulations applied at the wrist and dorsal hand improved the immediate fingertips light-touch sensation and grip ability of the paretic hand in stroke survivors (Enders et al., 2013). In addition, the vibrotactile detection threshold (i.e., the minimum level of vibration amplitude to be detected) at the tip of the middle finger in persons with diabetic neuropathy and stroke survivors was decreased (Liu et al., 2002). In persons with diabetic neuropathy the threshold was decreased at the foot as well (Liu et al., 2002; Khaodhiar et al., 2003). In a pilot randomized controlled trial, subthreshold vibratory stimulation was applied to the paretic wrist of stroke survivors during upper extremity task training (a total of 6 sessions provided in 2 weeks). The treatment group showed a significant improvement in hand motor function at the end of therapy, which was sustained 19 days after therapy, whereas the control group that practiced without stimulation did not improve from baseline performance (Seo et al., 2019).

While these studies were conducted in laboratory settings, few studies provided participants with vibrotactile devices to practice at home. Bao et al. (2018) tested the effect of long-term home-based balance training with vibrotactile sensory augmentation among community-dwelling healthy older adults. Participants were trained in static and dynamic standing and gait exercises for 8 weeks (3 sessions per week, 45-min each) using smartphone balance trainers that provided guidance while monitoring trunk sway. The experimental group received directional vibrotactile cues via actuators that were aligned around the torso in case the activation signal exceeded a pre-set threshold, while the control group practiced without supplemental feedback. Participants in the experimental group demonstrated significantly higher improvements in their SOT (Franchignoni et al., 2010) and Mini Balance Evaluation Systems Test scores (Clendaniel, 2000) compared with the control group at post training assessment. Seim et al. (2020a) designed a glove that provides subthreshold vibrotactile stimulation for stroke survivors to use at home and demonstrated the feasibility of wearing the glove for 3 h daily for 8 weeks. Also, in a double-blind RCT, chronic stroke survivors with impaired tactile sensation in the hand were given a glove to take home and asked to wear it during their normal daily routine (i.e., 3 h daily for 8 weeks) (Seim et al., 2020b). One group received a glove which provided vibrotactile stimulation to the hand and another group received a glove with the vibration disabled. Participants receiving tactile stimulations demonstrated significant improvement in tactile perception (assessed with monofilaments) in the affected hand. In another study, improvement in hand sensation was observed in participants with spinal cord injury after training with a glove providing vibration stimulations compared with participants who trained without stimulations (Estes et al., 2015). Vibration stimulations were applied during active practice sessions of playing piano in in-lab sessions (3 times a week for 30 min a session for 8 weeks) and during passive practice at home (2 h a day, 5 times a week). An illustration of a vibrotactile stimulation device is presented in **Figure 1**.

Applications for Conveying Social Tactile Cues

Gentle stroking touches resembling those of soft calming and caressing sensations are considered highly relevant in social interactions (Huisman et al., 2016). Using artificial means to convey such touches might enhance social presence in telecommunication or in virtual settings. Israr and Abnousi (2018), developed a vibrotactile device worn on the forearm that delivers stimuli which resemble caressing and calming sensations. Participants rated low frequency stimuli (<40 Hz) as pleasant sensations that feel like massaging and noted that they would be even more realistic with context. Huisman et al. (2013) developed a virtual agent setup that incorporates an augmented reality screen and a vibrotactile sleeve worn on the user's forearm. In this setup the forearm was placed under a tablet, thus allowing the user to see his/her forearm "through" the tablet. The vibrotactile stimulation combined with the visual

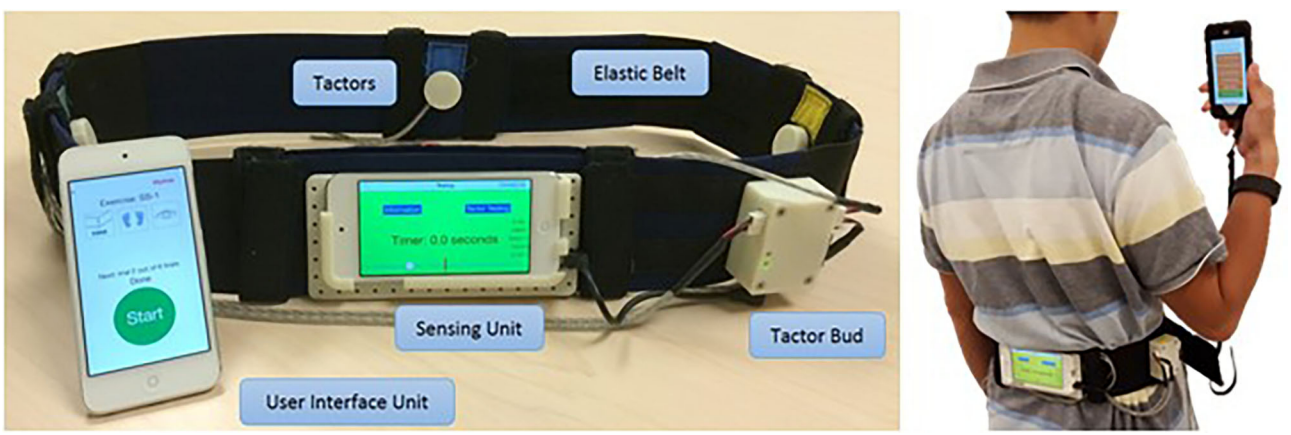

FIGURE 1 | Vibrotactile stimulation devices. The smartphone-based balance trainer used in Bao et al. (2018). The sensing unit is attached to an elastic belt worn around the torso to measure trunk sway. The four tactors are aligned over the anterior, posterior, and right and left sides of the torso to provide directional vibrotactile cues.

representation of a hand touching the user created a more realistic touching illusion.

Assessment of Tactile Impairments

Vibrotactile simulation can be used for assessment applications. In clinical settings the duration of vibration sensation and the perception threshold are commonly measured using a tuning fork (Perkins et al., 2001; Alanazy et al., 2018). However, results regarding its reliability are variable across studies (O'Neill et al., 2006; Lai et al., 2014; Lanting et al., 2020), and, most importantly, the assessment does not quantitatively provide the degree of dysfunction and depends on the level of clinical experience (Lanting et al., 2020).

To address limitations of clinical assessments, an automated approach to quantify topesthesia (i.e., the ability to recognize the location of a tactile stimulus) was developed (Rinderknecht et al., 2015). The system consists of two wearable gloves that can apply vibrations on the hand at 24 possible locations and a touchscreen to directly indicate with the non-tested hand the precise location of perception on the tested hand. The assessment provides a standardized, repeatable measurement as well as continuous outcome measures on ratio scales (Rinderknecht et al., 2015). It was tested on healthy individuals (Rinderknecht et al., 2015) and on stroke survivors (Rinderknecht et al., 2019).

In addition, a portable vibrotactile stimulator device was used to probe tactile function through a battery of tests assessing reaction time ("press the button when you feel the vibrotactile stimulation"), threshold detection (the weakest detectable stimulus), amplitude and frequency discrimination (discriminating between two stimuli that are simultaneously applied and discriminating between the frequency of two sequentially applied stimuli). The battery targets different mechanisms of somatosensory processing (Holden et al., 2012; Puts et al., 2013; King et al., 2018; Tommerdahl et al., 2019; Mikkelsen et al., 2020). These tests were used on healthy adults and children (Puts et al., 2013) for monitoring recovery from concussion (King et al., 2018) as well as a wide range of neurological disorders (Tommerdahl et al., 2019). There are also other specific tests that aim to independently evaluate only one of the aspects investigated by this paradigm; an overview of the tests assessing vibrotactile perception in healthy subjects can be found in Jones and Sarter (2008).

Advantages and Disadvantages

A major advantage of vibrotactile devices is that the actuators can be easily integrated into wearable devices because they are small, lightweight, low- power, and low-cost (Alahakone and Senanayake, 2009). On the other hand, disadvantages of vibrotactile feedback stem from the properties of the mechanoreceptors activated by vibration. First, it is difficult to accurately locate the source of the stimulations if they are placed close together, because of the propagation of the vibration (Sofia and Jones, 2013; Shah et al., 2019) and the large size of the mechanoreceptors' receptive fields (Johnson et al., 2000). Second, it is difficult to convey directional information, unless several actuators are used in a spatially and/or temporally coordinated mode (Rotella et al., 2012). Third, it has been suggested that the feedback coding of some vibrotactile devices may be less effective than of others in reducing applied forces i.e., if the vibration frequency or location varies, vibrotactile feedback may be less effective in conveying information on intensity or direction than a uniform signal that alerts the user of a required response (Nitsch and Färber, 2012). Fourth, prolonged exposure to continuous vibratory stimulation could result in an unpleasant sensation (Bark et al., 2008) and has been associated with long-term nerve and tissue damage (Takeuchi et al., 1986). Also, choosing the right type, number, and target location of the actuators for patients with possible degradation of perception due to aging or disease might be challenging (Jones and Sarter, 2008).

SKIN DEFORMATION

Tangential Force and Skin Stretch

Tangential skin deformation is evoked by pressure of the skin against a device, combined with a lateral movement of the entire device or a small part of it. Such deformation occurs naturally when touched by a therapist, when interacting with a real object, or when a device applies forces on a user, but it may also be elicited by technological solutions specifically designed to provide tactile stimulation (Bark et al., 2009; Quek et al., 2014b; Pan et al., 2017). The stimulation is detected by the Ruffini corpuscles which are slow adapting SA-II tactile afferents in the skin that are sensitive to tangential shear strain as well as the Meissner's corpuscles which are rapid adapting RA-I tactile afferents that are sensitive to dynamic skin deformation (Johansson and Flanagan, 2009). The detection resolution of the skin stretch at the fingertip is 0.1–0.2 mm, while the direction of the stretch can be accurately perceived with less than 1.0 mm of movement (Gould et al., 1979; Greenspan and Bolanowski, 1996).

Technology

There are different methods to render tangential and stretch forces, e.g., a roller (Provancher et al., 2005), a belt (Minamizawa et al., 2007), or a moving tactor (Quek et al., 2013). The most common location for applying the stimulation is the finger pad (Pasquero and Hayward, 2003; Drewing et al., 2005; Gleeson et al., 2010a; Solazzi et al., 2011; Tsetserukou et al., 2014), as it contains a very high density of mechanoreceptors (Abraira and Ginty, 2013). Other locations include the palm (Guzererler et al., 2016; Ballardini et al., 2018), the forearm (Bark et al., 2008; Kuniyasu et al., 2012; Chinello et al., 2016), the arm (Casini et al., 2015; Battaglia et al., 2017), and different locations on the lower limb (Chen D. K. Y. et al., 2016; Omori et al., 2019; Wang et al., 2020). The mechanism and actuation of the device can be tailored to the desired application (see Pacchierotti et al., 2017 for a review on wearable devices). By changing the magnitude and direction of the tactile stimulations it is possible to convey different types of information such as forces and directional guidance (Biggs and Srinivasan, 2002; Paré et al., 2002; Provancher et al., 2005; Guinan et al., 2014; Bianchi, 2016; Leonardis et al., 2017; Kanjanapas et al., 2019; Bitton et al., 2020).

Applications for Enhancing Sensorimotor Performance and Learning

Adding a skin stretch to force feedback has been shown to affect stiffness (Quek et al., 2013, 2014a,b; Schorr et al., 2013; Farajian et al., 2020a,b) and friction (Sylvester and Provancher, 2007; Provancher and Sylvester, 2009) perception. In addition, concurrent tangential and normal skin deformation can be used to substitute and/or augment upper extremity force and torque feedback in navigation, tracking, insertion and palpation tasks (Quek et al., 2014b, 2015b; Schorr et al., 2015; Pacchierotti et al., 2016; Clark et al., 2018), generating a high fidelity haptic feedback for the sensation of mass (Minamizawa et al., 2007; Kato et al., 2016) and virtual objects (Minamizawa et al., 2008). It can also be used to enhance perception and performance in object manipulation tasks (Leonardis et al., 2017; Schorr and Okamura, 2017b), and to deliver grasp force information (Casini et al., 2015).

Skin stretch feedback providing position information improved the movement accuracy of healthy participants who controlled the movement of a virtual arm (Bark et al., 2008). Compared with vibrotactile stimulation, skin stretch feedback provided superior results, particularly when the virtual arm was in a low-inertia configuration and at low velocity (Bark et al., 2008). Gleeson et al. demonstrated the ability of healthy participants to accurately identify the direction of tangential skin deformation at the fingertip, and highlighted the potential of using skin stretch cues to aid patients with balance control impairments (Gleeson et al., 2010b). Skin stretch stimulation was also found to be effective for improving performance in a curvature discrimination task (Frisoli et al., 2008; Prattichizzo et al., 2013).

Stretching the skin can affect not only perception, but also forces that are applied by the user for stabilization. Westebring van der Putten et al. (2010) explored the influence of skin stretch and tangential deformation feedback on grasp control and demonstrated a significant improvement in pinch force control for participants who received augmented tactile feedback. Bitton et al. (2020) showed that applying tactile stimulation of the fingertips increases grip force, even in a static force maintenance task. In addition, adding an artificial skin stretch to the finger pads in the same direction as force applied by a virtual object or a haptic device increased the applied grip force (Quek et al., 2015a; Avraham and Nisky, 2020; Farajian et al., 2020b), although this effect was not seen in Quek et al. (2015b), or in the case of skin-stretch that is in the opposite direction to the external force (Avraham and Nisky, 2020).

In addition, studies have shown the ability of participants to accurately produce motion according to haptic stimuli provided by a skin stretch device (Bark et al., 2010; Stanley and Kuchenbecker, 2012; Guinan et al., 2013b; Norman et al., 2014; Chinello et al., 2018; Pezent et al., 2019; Smith et al., 2020), including in gaming applications (Guinan et al., 2012, 2013a). Skin stretch feedback encoding the velocity of postural sway along the anterior-posterior direction enhanced standing balance with perturbed sensory systems (removed vision and unreliable vestibular systems) in healthy young adults compared with conditions without skin stretch feedback (Hur et al., 2019).

In virtual reality systems, skin stretch feedback has been applied at different body locations to simulate rich physical properties during the interaction with virtual environments and objects (Minamizawa et al., 2007, 2008; Choi et al., 2017; Yem and Kajimoto, 2017; Wang et al., 2020). For example, a leg-worn device that applies varied skin stretch profiles to induce an illusory force improved the realism and enjoyment of virtual reality applications (Wang et al., 2020).

Applications in Rehabilitation

To date, most applications of skin stretch stimulation were demonstrated in the context of prostheses or assistive devices. For example, a multimodal tactile stimulation device helped to improve the grip force control of an electromyographic-controlled virtual prosthetic hand that was operated by targeted reinnervation amputees (Kim and Colgate, 2012). Other examples conveyed proprioceptive (Battaglia et al., 2017, 2019; Colella et al., 2019), grasp force and position information to users of prosthetic hands (Casini et al., 2015; Stephens-Fripp et al., 2018), or path information to users of a powered-wheelchair (Kumar et al., 2017). Although it has not yet been tested directly in rehabilitation protocols for neurological populations, these technologies could potentially be used for tasks such as restoration of fine object manipulation. An example of such an application was demonstrated on children with neuromotor impairments who trained in performing upper limb movements, including reach to grasp, path tracking, and hand orientation, with a wearable haptic device rendering contact forces by deformation of the fingerpad (Bortone et al., 2018).

Applications for Conveying Social Tactile Cues

Recently, wearable devices that can generate pleasant tactile sensations have been developed (Haynes et al., 2019; Nunez et al., 2019). A skin slip technology was used to generate an illusory sensation of continuous lateral motion that could be used to convey social touch cues, such as comfort and affection, in which stroking motions are used (Nunez et al., 2019). The stimulation was perceived as pleasant when the speed was closer to 10 cm/s and applied on the volar side of the forearm.

Assessment of Tactile Impairments

The assessment of tactile directional sensitivity (i.e., the ability to identify the direction of an object's motion across the skin) is considered to be a sensitive screening test of sensory function after injuries in the central or peripheral nervous system (Wall and Noordenbos, 1977; Bender et al., 1982; Hankey and Edis, 1989; Norrsell and Olausson, 1992). However, to our knowledge, assessment properties (e.g., reliability) were not tested. Recently, a skin stretch device was developed to assess somatosensory impairments at different body areas (Ballardini et al., 2018). The system offers quantitative and reliable measures of tactile acuity (i.e., testing discrimination of the direction and amplitude of skin stretch stimuli) and was validated in healthy participants and in a small cohort of stroke survivors.

Advantages and Disadvantages

There are many advantages to skin stretch deformation. This stimulation provides a strong, quick, and accurate response to

changes in skin strain (Edin, 2004). In addition, skin stretch at low frequencies is attractive for wearable devices as it does not require much power (Bark et al., 2008). It can also convey direction even with a single actuator, does not suffer from adaptation effects, and is effective even at low velocities and with small movements (Bark et al., 2008). Moreover, skin stretch feedback is effective in inducing the perception of virtual textures and illusory forces and can be used to convey intuitive proprioceptive feedback (Chossat et al., 2019). Nevertheless, skin stretch stimulation has some disadvantages. The amount of skin deformation depends on the mechanical properties of the skin and the strength of the normal forces against the actuator, and thus partial or full slippage may occur. These and other factors contribute to large inter-participant variability in the perceptual effects of skin stretch (Quek et al., 2014b; Farajian et al., 2020b), while some individuals are not at all sensitive to stretch effects (Quek et al., 2014b). Also, this type of stimulation is commonly applied at the finger pad where there is a limited area for applying the stretch. Finally, although skin stretch devices are usually safe, when developing the device, one should carefully consider unpleasant sensations and abrasion. Illustrations of tangential and stretch stimulation devices are presented in **Figure 2**.

Pressure

Pressure triggers a response in the low frequency range of the slow adapting afferents SA-I, innervating the Merkel cells (Johansson and Flanagan, 2009). Technologies that provide this type of feedback deliver forces that cause deformation, and the strength of the stimulus is determined based on sensitivity thresholds, which vary across the body.

Technology

Pressure stimulation is commonly provided by devices that contact the skin with a single end-effector that can: (1) change its properties, such as the shape in soft actuators (Koehler et al., 2020) or the viscosity in electrorheological or magnetorheological fluids (Taylor et al., 1997; Jungmann and Schlaak, 2002; Jansen et al., 2010; Yang et al., 2010; Kim et al., 2016), (2) tighten a band around a body location, like the fingertip (Merrett et al., 2011), wrist (Stanley and Kuchenbecker, 2012) or forearm (Meli et al., 2018), and (3) press on the skin with a servomotor (Quek et al., 2015b; Schorr and Okamura, 2017a) or a hydraulic, or pneumatic actuator (Franks et al., 2008; Yem et al., 2015; Talhan and Jeon, 2018). For the latter solution, it is also possible to enlarge the area of stimulation by increasing the number of end-effectors in contact with the skin using a pin array matrix, i.e., a matrix of actuators that can be activated separately. In order to provide efficient tactile stimulation it is also important to consider the size and density of the contact points, since these will affect the cost and weight of the device, as well as its perceptual effect.

Applications for Enhancing Sensorimotor Performance and Learning

Using force indentation at different orientations makes it possible to display contact forces for multiple applications. Already in 1993, the technology was used to produce 2D and 3D graphic display for haptic recognition of familiar objects and was tested in blind and sighted participants (Shimizu et al., 1993; Leo et al., 2016; Brayda et al., 2018). Since then, multiple tactile devices with lightweight and compact mechanisms have been developed to produce pressure stimulation, thereby providing a range of tactile sensations including natural touch (Caldwell et al., 1999; Chinello et al., 2015; Culbertson et al., 2018a), roughness (Kim et al., 2009), softness (Frediani and Carpi, 2020), and texture (Sarakoglou et al., 2005; Kyung and Park, 2007; Kim et al., 2009; Garcia-Hernandez et al., 2011). In addition, pressure stimulation was used for conveying directional cues (Raitor et al., 2017; Agharese et al., 2018), and for rendering shape in virtual and remote environments (Chinello et al., 2019).

Applications in Rehabilitation

In patients with digital nerve injury, stroking, and pressing a pocket tactile stimulator and contacting the rotating disc of a tactile stimulator improved functional sensitivity measured by the smallest perceivable force using Semmes-Weinstein monofilaments (Semmes et al., 1960), and the shortest perceivable distance using a standardized two-point discrimination test instrument (Dellon et al., 1987; Cheng, 2000). In patients with complex regional pain syndrome of one limb, tactile stimulation was shown to decrease pain and increase tactile acuity when patients were required to discriminate between the type and location of tactile stimuli (Moseley et al., 2008). Skin pressure stimulation at the hallux and first metatarsal joint of the feet applied to participants with Parkinson's disease increased step length and gait velocity and reduced cadence compared with baseline measurements (Barbic et al., 2014). A wearable tactile feedback system that was originally developed for sensory augmentation of prosthetic limbs has been adapted for individuals with bilateral peripheral neuropathy (McKinney et al., 2014). Using thigh cuffs (one per leg) with silicone balloons for conveying sensory information specific to each foot, participants could modify their gait in real time (i.e., increase walking speed, step cadence and step length). Although not tested in populations undergoing rehabilitation, tactile vests worn on the torso have been shown to create a variety of tactile stimuli that could potentially be useful in applications such as balance control training (Nakamura and Jones, 2003; Wu et al., 2010). Also, pressure applied simultaneously to the thumb and index fingers generated a perception of holding an object, exhibiting the potential to provide a realistic haptic sensation in virtual reality based rehabilitation (Merrett et al., 2011).

Applications for Conveying Social Tactile Cues

Culbertson et al. developed a device that creates a stroking sensation using a linear array of voice coil actuators embedded in a fabric sleeve worn around the arm. The voice coils were controlled to indent the skin in a linear pattern to create the sensation of a stroking motion even though only normal force was applied (Culbertson et al., 2018a). As indicated from participants' ratings, to create a continuous and pleasant sensation the device should be controlled with a short delay and long pulse width (800 ms, 12.5% delay). Another system, the RemoTouch (Prattichizzo et al., 2010), was designed to provide experiences of remote touch. The user perceives force

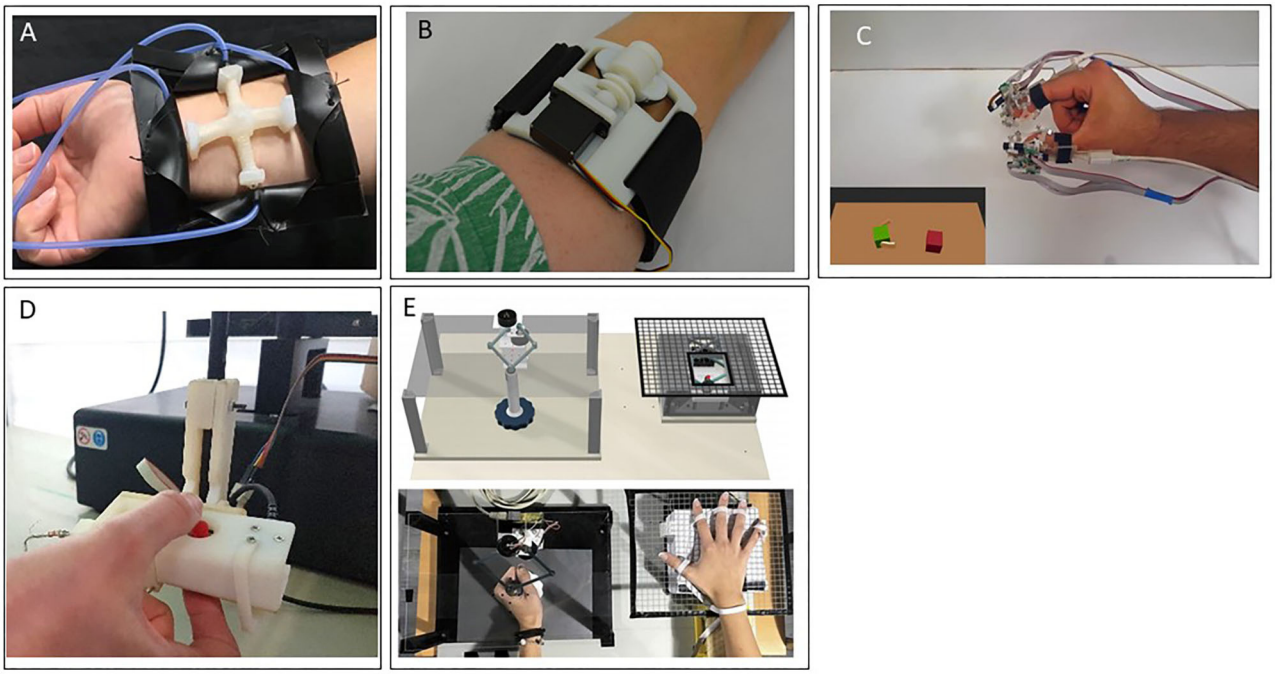

FIGURE 2 | Skin deformation—tangential and stretch stimulation devices. **(A)** A wearable device that is comprised of pneumatic actuators to guide motion direction (Kanjanapas et al., 2019). **(B)** The Rice Haptic Rocker that was designed to convey proprioceptive information to users of prostheses (Battaglia et al., 2019). **(C)** A wearable device that was used to render virtual environment forces (Schorr and Okamura, 2017b). **(D)** An aperture and tactor skin-stretch device that was used to study the contribution of tactile stimulation of the fingertips to motor adaptation (Avraham and Nisky, 2020). **(E)** The Tactile-STAR, a skin brushing stimulator (top right) and a recorder (top left) that were used to assess and train tactile perception acuity. The device was specifically designed to be appropriate for use with stroke survivors who may have difficulty in maintaining contact with an aperture and tactor type of a device (Ballardini et al., 2018).

feedback recorded by a human that wears a glove equipped with force sensors. The measured contact force at the remote interaction is fed back to the user through wearable tactile displays for each finger. Preliminary tests show that the realism of this remote experience largely improved with the tactile feedback.

Assessment of Tactile Impairments

Sensitivity to pressure is often used as a measure of absolute tactile sensitivity (for more details see Demain et al., 2013). The most commonly used method to assess pressure sensation is the Semmes–Weinstein monofilaments that are calibrated to apply predetermined forces to the skin (Semmes et al., 1960; Bell-Krotoski, 1984). Jacobs et al., suggested another approach for examining the psychophysical detection threshold of pressure stimulation of a prosthetic and a normal limb (Jacobs et al., 2000). Stimulations were applied using a computer connected to a probe and to a remote control that was operated by the patient. The patient could control the amplitude of the pushing force by pressing the remote control. To measure the detection threshold the up-down method was used (i.e., the amplitude of the pushing force was decreased until the patient did not feel the stimulation and stopped pressing the remote control). Then, the amplitude was increased until 16 reversals were obtained. This setup can be modified for home-based assessment, possibly by using a smaller controller instead of the computer.

Advantages and Disadvantages

Pressure stimulation enables rendering perceptual properties such as shape, curvature, orientation, and texture (Gabardi et al., 2016). However, sensitivity to pressure is largely dependent on the area of stimulation (Stevens, 1982). In addition, while multiple actuation approaches are available for applying pressure to the skin, each approach is suitable for a different application. Therefore, one should carefully consider the specifications of the design that would be appropriate for the desired application. Illustrations of pressure stimulation devices are presented in **Figure 3**.

Mid-air

All the technologies described above require physical contact between the device and the body to provide somatosensory feedback, and the energy produced by the actuators is transferred to the skin through a solid medium. This allows efficient energy transduction, creating natural haptic sensations with the aid of appropriate contactors to the skin. However, these solutions present some limitations: (1) they do not exploit arbitrary body locations, i.e., can deliver feedback only at a location close to the device's end effector, (2) they may cause undesired effects due to the continuous contact between the skin and the devices, and (3) if used by different individuals, they require cleaning and disinfecting, especially in light of the recent COVID-19 related recommendations (Thomas et al., 2020). Several recent

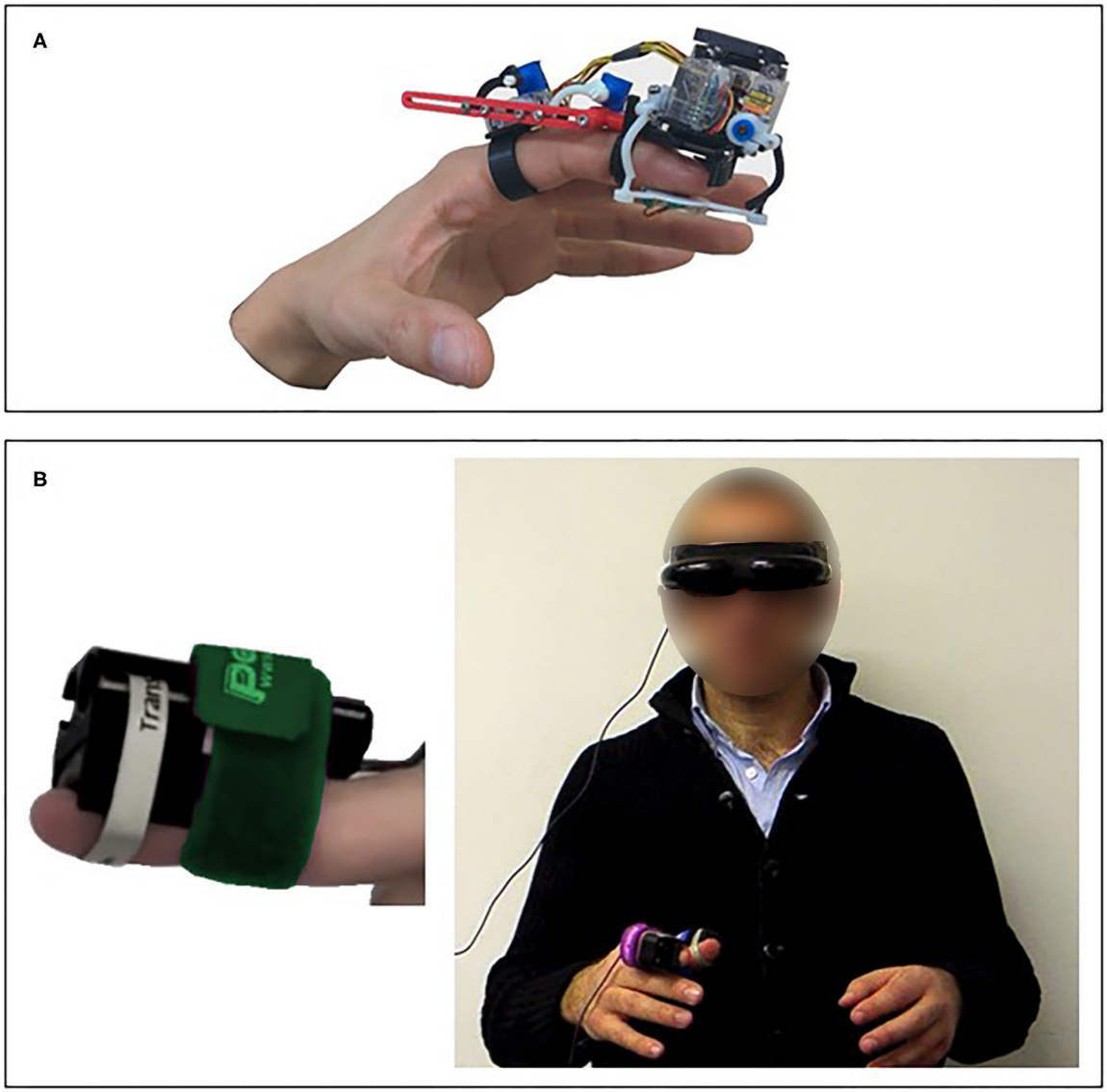

FIGURE 3 | Skin deformation—pressure stimulation devices. **(A)** A wearable finger device that was designed and tested in virtual reality applications (Chinello et al., 2019). **(B)** The RemoTouch system that provides experience of remote touch (Prattichizzo et al., 2010).

developments address these limitations by proposing mid-air technologies. They transmit the energy of the stimulus through air, avoiding the direct contact with the skin.

Technology

One of the main approaches to creating mid-air stimulation relies on ultrasonic waves, typically at 40 or 70 kHz frequencies (for survey see Rakkolainen et al., 2019). In this type of mid-air tactile stimulation the sensation is caused by a non-linear effect of focused ultrasound called acoustic radiation force, which induces a shear wave in the skin, creating a displacement, which triggers the mechanoreceptors within the skin and evoking mainly a pressure sensation (Gavrilov and Tsirulnikov, 2002). Most ultrasound haptic systems targeting the hand trigger the Lamellar corpuscles (Rakkolainen et al., 2019). In other body locations ultrasound can trigger other mechanoreceptors, such as Meissner corpuscles on the face (Gil et al., 2018), and Ruffini corpuscles or Merkel disks on the upper limb (Suzuki et al., 2018).

The most widely used technological solution to evoke tactile sensation with ultrasound is based on phased arrays of transducers, i.e., multiple transducers whose phase and intensity can be controlled individually, with a defined timing. In this way, the focused ultrasound waves can generate one or more localized regions of pressure in the 3D space, called focal points, without moving or turning the device. These focal points cannot be fully singular because of secondary peaks and wavelength limitations (Rakkolainen et al., 2019). However, several focal points can be controlled together to create shapes (Long et al., 2014) or textures

(Monnai et al., 2015; Freeman et al., 2017). If the radiation force is modulated at the 1–1 kHz range the ultrasound waves can also evoke a vibratory sensation in addition to the pressure sensation (Hasegawa and Shinoda, 2013; Howard et al., 2020; Rutten et al., 2020).

Applications for Enhancing Sensorimotor Performance and Learning

The use of focused ultrasound as a non-invasive method of stimulation has been studied since the early 1970s (Gavrilov et al., 1977). Recently, this technology was used for several proof-of-concept applications, including creating floating 2D icons (Gavrilov, 2008) and 3D haptic shapes (Long et al., 2014; Monnai et al., 2014; Vo and Brewster, 2015; Makino et al., 2016), interacting in a virtual reality environment (Romanus et al., 2019; Howard et al., 2020), and gesture interaction (Shakeri et al., 2017, 2018). To the best of our knowledge, mid-air haptic devices have not yet been used for rehabilitative purposes or for somatosensory assessment.

Applications for Conveying Social Tactile Cues

The communication of emotions through a haptic system that uses tactile stimulation in mid-air communication was explored by Obrist et al. and showed promising results of interpretability of emotions (Obrist et al., 2015). Despite these promising results the application of ultrasound devices for conveying emotions and social interaction has not yet been extensively investigated.

Advantages and Disadvantages

The major advantage of this emerging technology is its not requiring contact with the body, while easily and efficiently creating static or dynamic textures and volumetric shapes. Another important advantage is that commercial devices are available that use this technology, even at this early stage. In its current state, this technology has some inherent limitations that may have an impact on potential applications, including the size and the weight of the transducers (Rakkolainen et al., 2019) and the low intensity of the force conveyed to the user, which is at most 160 mN (Tsalamlal et al., 2013), and so does not allow the rendering of real-word interaction forces. Nevertheless, we anticipate that mid-air solutions will develop in the next few years, and we foresee that they will be designed for rehabilitation purposes and clinical assessments. Illustrations of mid-air stimulation devices are presented in **Figure 4**.

DISCUSSION

The COVID-19 pandemic is currently placing significant pressure on health services including rehabilitation services, worldwide. The reduced access to rehabilitation care due to restrictions as well as the reduction in rehabilitation services as a consequence of reassignment of rehabilitation professionals to acute care and the transformation of rehabilitation facilities into makeshift inpatient wards (Boldrini et al., 2020a; Chaler et al., 2020) are expected to lead to long-lasting negative consequences for individuals with disabilities (Boldrini et al., 2020b). In fact, these are only the tip of the iceberg when considering the long-standing and more severe problem of limited resources in hospital care together with the rising number of individuals with chronic diseases (Koh et al., 2015; Steihaug et al., 2016; Dodakian et al., 2017).

Remote communication technologies, as well as technologies developed for home-based telerehabilitation, have the potential to support neurorehabilitation care and make breakthroughs in treatment by facilitating continuous and intensive training. The emerging technological solutions reviewed in the current paper highlight the promise of wearable tactile stimulation devices to enhance home-based rehabilitation training gains by the provision of tactile feedback and haptic interactions. These technologies seem propitious and attractive for home-based rehabilitation: the devices are wearable, portable, and relatively low cost (estimated cost between tens and hundreds of dollars). Moreover, some of these technologies can easily be integrated into virtual/telerehabilitation environments (Feintuch et al., 2006; Bortone et al., 2018; Wang et al., 2020).

However, despite technological advantages and great potential for home-based practice, to date, tactile feedback devices have not yet evolved into common solutions for rehabilitation. There are still challenges that need to be met in a joint effort between sensorimotor neuroscientists, technology developers and clinicians in order to successfully integrate tactile technologies into neurorehabilitation programs. We review these challenges in the remainder of this section.

Testing Training Effects on Large Patient Populations

Most tactile device prototypes were tested on healthy individuals or on small cohorts of patients and their effects need to be further examined: (1) on larger patient populations, ideally in randomized controlled trials, (2) over longer training periods, and with long-term follow up assessments to evaluate whether improvements observed immediately post training have been retained after training is completed and (3) with respect to outcome measures relevant to the daily life function of the patients. Studies conducted on healthy individuals often focus on laboratory parameters, while in patients undergoing rehabilitation exploring whether training effects have transferred to daily life activities is of clinical significance. As was demonstrated above, few such examples exist in the literature; however, these are the exception and not the rule, and more studies are needed. Several factors contribute to the difficulty of overcoming this challenge. First, the lack of collaborations between technology developers, researchers, clinicians, and rehabilitation facilities. Second, it is difficult to secure funding for such large-scale studies. Third, the facts that most tactile devices are not commercially available and do not have medical device safety approval limits the ability to easily test them on patient populations.

Translation Into Clinical Practice

To integrate tactile stimulations into rehabilitation training it is critical to identify the optimal method to provide the feedback and the patients that would benefit from such training. The feedback provided by some common devices might be difficult to interpret and integrate. Also, the tactile stimuli patterns might not be intuitive or might be too complex for the user, due to

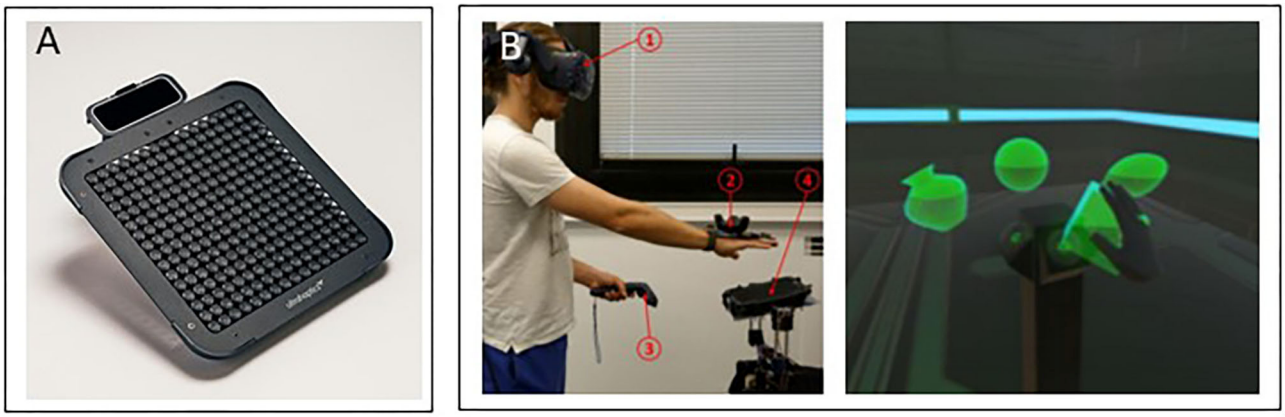

FIGURE 4 | Mid-air devices. **(A)** The Ultraleap device (https://www.ultraleap.com/). **(B)** Its application to interaction with a virtual reality environment (Howard et al., 2020).

either the number of tactile motors forcing the user to process a redundant set of signals, or to the encoding methods that may require specific attention (Brewster and Brown, 2004; Ballardini et al., 2020). This is especially important for patients undergoing rehabilitation training, who are often at the initial stages of learning that already require a relatively high degree of cognitive effort and attention (Fitts and Posner, 1967). Moreover, some neurological patients suffer from cognitive and attention deficits, and hence, to benefit from added information, the feedback must be simple (Van Vliet and Wulf, 2006). Additionally, the cognitive load of interpreting tactile cues in applications where the patient's attention is divided among multiple tasks, and how this might reduce the saliency of the cues, should be further explored (Gleeson et al., 2010b; Shah et al., 2018).

The optimal timing of providing somatosensory feedback also needs to be examined. For example, providing feedback for the entire duration of training can improve short term performance, but may limit motor learning. Conversely, providing feedback for only portions of training might produce poor initial performance, but improve motor skill retention (Winstein and Schmidt, 1990). Moreover, the conditions under which tactile feedback is most effective at improving task performance should be examined (e.g., whether it is most effective when supplementing another modality), as well as the temporal and spatial patterns and the location for applying the stimulation.

In addition, affective haptic feedback, used to render realistic feelings, has the potential to enhance remote patient-therapist communication. It can also be applied to reinvigorate the patient's interest when he/she is bored or frustrated during practice (Eid and Al Osman, 2015). While wearable haptic devices were designed to replicate a specific interaction or gesture such as comfort and affection (Culbertson et al., 2018a; Nunez et al., 2019, 2020), attention (Baumann et al., 2010) or social presence (Baldi et al., 2020), further exploration is needed in order to gain a better understanding of how to create realistic sensations, how to display them in complete synchronization with other display modalities (i.e., visual, auditory, olfactory, etc.), and how to integrate them in the right context during remote rehabilitation sessions. Other important challenges relate to touch etiquette in social interaction and how to incorporate social, cultural and individual differences with respect to the acceptance and meaning of affective touch (Eid and Al Osman, 2015).

Using the Technology at Home

Although the devices seem promising for home use and some have already been tested in at-home practice (Bao et al., 2018; Seim et al., 2020a,b) some gaps still need to be bridged in this regard. First, further studies are needed to explore the feasibility of using tactile devices by patients undergoing home-based telerehabilitation: whether patients can correctly wear and operate the device without assistance, whether the form of the device is compatible for patients with different impairments, the adherence of using or wearing the device (Seim et al., 2020a), and safety and technical problems that may arise when using it during the training period (Seo et al., 2020). Second, tactile devices need to be integrated into already existing or new telerehabilitation/virtual reality systems to provide the whole framework of sensorimotor training (Feintuch et al., 2006).

Rehabilitation platforms that are capable of intelligent, adaptable tactile feedback configurations, adjustable in terms of difficulty level, capable of measuring performance and progression and of providing exercises relevant to daily living activities as well as motivating the user's engagement could provide a more tailored training intervention to maximize improvements (Shull and Damian, 2015; Navarro et al., 2018). Additionally, there are other important issues related to telerehabilitation in general, such as web communication between the therapist and the patient, information security, and data storing that are beyond the technical-clinical outlook of our review.

CONCLUSIONS

The COVID-19 pandemic has highlighted the need for home-based telerehabilitation and at the same time has accelerated the adoption of a digital culture worldwide. Exploiting this opportunity together with the rapid developments in wearable haptic technologies offers a time window to advance sensorimotor neurorehabilitation, elevating it to innovative

solutions for home-based therapies. Although there remain gaps and challenges that still need to be addressed jointly by scientists, technology developers and clinicians, wearable haptic devices, if correctly adapted, could potentially turn into cost-effective medical devices for use at home by individuals in need of rehabilitation treatments. The integration of tactile devices into home-based telerehabilitation practice has the potential to enhance patients' functional gains and quality of life through practice in an enriched environment with augmented tactile feedback and tactile interactions.

AUTHOR CONTRIBUTIONS

All authors contributed to the article (drafting and writing) and approved the submitted version.

FUNDING

This study was supported by the Israel-Italy virtual lab on Artificial Somatosensation for Humans and Humanoids grant from the Israeli Ministry of Science and Technology, the Israeli Science Foundation (grant 327/20) and both the Agricultural, Biological and Cognitive Robotics Initiative and the Marcus Endowment Fund (at Ben-Gurion University of the Negev). SH was supported by the Yitzhak Shamir scholarship for returning scientists from the Israeli Ministry of Science and Technology, Israel. CA was supported by the Besor Fellowship and the Planning and Budgeting Committee Fellowship. MP was supported by the operative program Por FSE Regione Liguria 2014-2020 RLOF18ASSRIC/15/1.

REFERENCES

Abraira, V. E., and Ginty, D. D. (2013). The sensory neurons of touch. *Neuron* 79, 618–639. doi: 10.1016/j.neuron.2013.07.051

Ackerley, R., Carlsson, I., Wester, H., Olausson, H., and Backlund Wasling, H. (2014). Touch perceptions across skin sites: differences between sensitivity, direction discrimination and pleasantness. *Front. Behav. Neurosci.* 8:54. doi: 10.3389/fnbeh.2014.00054

Afzal, M. R., Lee, H., Eizad, A., Lee, C. H., Oh, M. K., and Yoon, J. (2019). Effects of vibrotactile biofeedback coding schemes on gait symmetry training of individuals with stroke. *IEEE Trans. Neural Syst. Rehabil. Eng.* 27, 1617–1625 doi: 10.1109/TNSRE.2019.2924682

Aggravi, M., Pausé, F., Giordano, P. R., and Pacchierotti, C. (2018). Design and evaluation of a wearable haptic device for skin stretch, pressure, and vibrotactile stimuli. *IEEE Robot. Autom. Lett.* 3, 2166–2173. doi: 10.1109/LRA.2018.2810887

Agharese, N., Cloyd, T., Blumenschein, L. H., Raitor, M., Hawkes, E. W., Culbertson, H., et al. (2018). "HapWRAP: soft growing wearable haptic device," in *IEEE International Conference on Robotics and Automation (ICRA)* (Brisbane, QLD), 5466–5472.

Ahmaniemi, T. (2012). Effect of dynamic vibrotactile feedback on the control of isometric finger force. *IEEE Trans. Haptics* 6, 376–380. doi: 10.1109/TOH.2012.72

Alahakone, A. U., and Senanayake, S. M. N. A. (2009). "Vibrotactile feedback systems: Current trends in rehabilitation, sports and information display," *Paper presented at the IEEE/ASME International Conference on Advanced Intelligent Mechatronics, AIM* (Singapore: IEEE), 1148–1153. doi: 10.1109/AIM.2009.5229741

Alanazy, M. H., Alfurayh, N. A., Almweisheer, S. N., Aljafen, B. N., and Muayqil, T. (2018). The conventional tuning fork as a quantitative tool for vibration threshold. *Muscle Nerve* 57, 49–53. doi: 10.1002/mus.25680

Avraham, C., and Nisky, I. (2020). The effect of tactile augmentation on manipulation and grip force control during force-field adaptation. *J. Neuroeng. Rehabil.* 17, 1–19. doi: 10.1186/s12984-020-0649-y

Bach-y-Rita, P. W., and Kercel, S. (2003). Sensory substitution and the human–machine interface. *Trends Cogn. Sci.* 7, 541–546. doi: 10.1016/j.tics.2003.10.013

Baldi, T. L., Paolocci, G., Barcelli, D., and Prattichizzo, D. (2020). Wearable haptics for remote social walking. *IEEE Trans. Haptics* 13, 761–776. doi: 10.1109/TOH.2020.2967049

Ballardini, G., Carlini, G., Giannoni, P., Scheidt, R. A., Nisky, I., and Casadio, M. (2018). Tactile-STAR: a novel tactile STimulator and recorder system for evaluating and improving tactile perception. *Front. Neurorobot.* 12:12. doi: 10.3389/fnbot.2018.00012

Ballardini, G., Florio, V., Canessa, A., Carlini, G., Morasso, P., and Casadio, M. (2020). Vibrotactile feedback for improving standing balance. *Front. Bioeng. Biotechnol.* 8:94. doi: 10.3389/fbioe.2020.00094

Bao, T., Carender, W. J., Kinnaird, C., Barone, V. J., Peethambaran, G., Whitney, S. L., et al. (2018). Effects of long-term balance training with vibrotactile sensory augmentation among community-dwelling healthy older adults: a randomized preliminary study. *J. Neuroeng. Rehabil.* 15:5. doi: 10.1186/s12984-017-0339-6

Bao, T., Klatt, B. N., Carender, W. J., Kinnaird, C., Alsubaie, S., Whitney, S. L., et al. (2019). Effects of long-term vestibular rehabilitation therapy with vibrotactile sensory augmentation for people with unilateral vestibular disorders–A randomized preliminary study. *J. Vestib. Res.* 29, 323–334. doi: 10.3233/VES-190683

Barbic, F., Galli, M., Dalla Vecchia, L., Canesi, M., Cimolin, V., Porta, A., et al. (2014). Effects of mechanical stimulation of the feet on gait and cardiovascular autonomic control in parkinson's disease. *J. Appl. Physiol.* 116, 495–503. doi: 10.1152/japplphysiol.01160.2013

Bark, K., Hyman, E., Tan, F., Cha, E., Jax, S. A., Buxbaum, L. J., et al. (2015). Effects of vibrotactile feedback on human learning of arm motions. *IEEE Trans. Neural Syst. Rehabil. Eng.* 23, 51–63. doi: 10.1109/TNSRE.2014.2327229

Bark, K., Wheeler, J., Lee, G., Savall, J., and Cutkosky, M. (2009). "A wearable skin stretch device for haptic feedback," in *World Haptics 2009-Third Joint EuroHaptics conference and Symposium on Haptic Interfaces for Virtual Environment and Teleoperator Systems* (Salt Lake City, UT), 464–469. doi: 10.1109/WHC.2009.4810850

Bark, K., Wheeler, J., Shull, P., Savall, J., and Cutkosky, M. (2010). Rotational skin stretch feedback: a wearable haptic display for motion. *IEEE Trans. Haptics* 3, 166–176. doi: 10.1109/TOH.2010.21

Bark, K., Wheeler, J. W., Premakumar, S., and Cutkosky, M. R. (2008). "Comparison of skin stretch and vibrotactile stimulation for feedback of proprioceptive information," in *Haptics Interfaces for Virtual Environment and Teleoperator Systems Symposium* (Reno, NV), 71–78. doi: 10.1109/HAPTICS.2008.4479916

Basta, D., Rossi-Izquierdo, M., Soto-Varela, A., Greters, M. E., Bittar, R. S., Steinhagen-Thiessen, E., et al. (2011). Efficacy of a vibrotactile neurofeedback training in stance and gait conditions for the treatment of balance deficits: a double-blind, placebo-controlled multicenter study. *Otol. Neurotol.* 32, 1492–1499. doi: 10.1097/MAO.0b013e31823827ec

Battaglia, E., Clark, J. P., Bianchi, M., Catalano, M. G., Bicchi, A., and O'Malley, M. K. (2017). "The rice haptic rocker: skin stretch haptic feedback with the Pisa/IIT SoftHand," in *2017 IEEE World Haptics Conference (WHC)*, 7–12.

Battaglia, E., Clark, J. P., Bianchi, M., Catalano, M. G., Bicchi, A., and O'Malley, M. K. (2019). Skin stretch haptic feedback to convey closure information in anthropomorphic, under-actuated upper limb soft prostheses. *IEEE Trans. Haptics* 12, 508–520. doi: 10.1109/TOH.2019.2915075

Baumann, M. A., MacLean, K. E., Hazelton, T. W., and McKay, A. (2010). "Emulating human attention-getting practices with wearable haptics," in *2010 IEEE Haptics Symposium* (Waltham, MA), 149–156.

Bell-Krotoski, J. A. (1984). "Light touch-deep pressure testing using Semmes-Weinstein monofilaments. in *Rehabilitation of the Hand, 3rd Edn*," eds J. M.

Hunter, L. H. Schnieder, E. J. Mackin, and J. A. Bell JA (St. Louis, MO: CV Mosby), 585–593.

Bender, M. B., Stacy, C., and Cohen, J. (1982). Agraphesthesia. A disorder of directional cutaneous kinesthesia or a disorientation in cutaneous space. *J. Neurol. Sci.* 53, 531–555.

Bianchi, M. (2016). A fabric-based approach for wearable haptics. *Electronics* 5:44. doi: 10.3390/electronics5030044

Biggs, J., and Srinivasan, M. A. (2002). "Tangential versus normal displacements of skin: Relative effectiveness for producing tactile sensations," in *Proceedings 10th Symposium on Haptic Interfaces for Virtual Environment and Teleoperator Systems. HAPTICS* (Orlando, FL), 121–128.

Bitton, G., Nisky, I., and Zarrouk, D. (2020). A novel grip force measurement concept for tactile stimulation mechanisms - design, validation, and user study. *arXiv Preprint* arXiv:2006.04053.

Bliss, J. C., Katcher, M. H., Rogers, C. H., and Shepard, R. P. (1970). Optical-to-tactile image conversion for the blind. *IEEE Trans. Man Mach. Syst.* 11, 58–65.

Boian, R. F., Deutsch, J. E., Burdea, G. C., and Lewis, J. (2003). "Haptic effects for virtual reality-based post-stroke rehabilitation," in *11th Symposium on Haptic Interfaces for Virtual Environment and Teleoperator Systems, HAPTICS. Proceedings* (Los Angeles, CA), 247–253.

Boldrini, P., Bernetti, A., Fiore, P., and SIMFER Executive Committee (2020a). Impact of COVID-19 outbreak on rehabilitation services and Physical and Rehabilitation Medicine physicians' activities in Italy. An official document of the Italian PRM Society (SIMFER). *Eur. J. Phys. Rehabil. Med.* 56, 316–318. doi: 10.23736/S1973-9087.20.06256-5

Boldrini, P., Garcea, M., Brichetto, G., Reale, N., Tonolo, S., Falabella, V., et al. (2020b). Living with a disability during the pandemic. "instant paper from the field" on rehabilitation answers to the COVID-19 emergency. *Eur. J. Phys. Rehabil. Med.* 56, 331–334. doi: 10.23736/S1973-9087.20.06373-X

Borich, M. R., Brodie, S. M., Gray, W. A., Ionta, S., and Boyd, L. A. (2015). Understanding the role of the primary somatosensory cortex: opportunities for rehabilitation. *Neuropsychologia* 79(Pt B), 246–255. doi: 10.1016/j.neuropsychologia.2015.07.007

Bortone, I., Leonardis, D., Mastronicola, N., Crecchi, A., Bonfiglio, L., Procopio, C., et al. (2018). Wearable haptics and immersive virtual reality rehabilitation training in children with neuromotor impairments. *IEEE Trans. Neural Syst. Rehabil. Eng.* 26, 1469–1478. doi: 10.1109/TNSRE.2018.2846814

Bowerman, C. C., Semrau, J. A., Kiss, Z., and Dukelow, S. P. (2012). "The importance of somatosensory deficits in neurological disease," in *International Functional Electrical Stimulation Society (IFESS) Conference* (Banff, AB), 2–5.

Brave, S., and Dahley, A. (1997). "inTouch: a medium for haptic interpersonal communication, in *CHI '97: CHI '97 Extended Abstracts on Human Factors in Computing Systems* (New York, NY: ACM Press), 363–364.

Brayda, L., Leo, F., Baccelliere, C., Ferrari, E., and Vigini, C. (2018). Updated tactile feedback with a pin array matrix helps blind people to reduce self-location errors. *Micromachines* 9:351. doi: 10.3390/mi9070351

Brewster, S. A., and Brown, L. M. (2004). "Tactons: structured tactile messages for non-visual information display," in *Proc. Fifth Australasian User Interface Conference (AUIC2004)*, ed A. Cockburn (Dunedin: ACS), 15–23.

Brugnera, C., Bittar, R. S. M., Greters, M. E., and Basta, D. (2015). Effects of vibrotactile vestibular substitution on vestibular rehabilitation - preliminary study. *Braz. J. Otorhinolaryngol.* 81, 616–621. doi: 10.1016/j.bjorl.2015.08.013

Caldwell, D. G., Tsagarakis, N., and Giesler, C. (1999). "An integrated tactile/shear feedback array for stimulation of finger mechanoreceptor," in *Proceedings 1999 IEEE International Conference on Robotics and Automation (Cat. No. 99CH36288C) Vol. 1* (IEEE), 287–292.

Carey, L. M., Matyas, T. A., and Oke, L. E. (1993). Sensory loss in stroke patients: effective training of tactile and proprioceptive discrimination. *Arch. Phys. Med. Rehabil.* 74, 602–611.

Casini, S., Morvidoni, M., Bianchi, M., Catalano, M., Grioli, G., and Bicchi, A. (2015). "Design and realization of the CUFF - clenching upper-limb force feedback wearable device for distributed mechano-tactile stimulation of normal and tangential skin forces," in *2015 IEEE/RSJ International Conference on Intelligent Robots and Systems (IROS)* (Hamburg). doi: 10.1109/IROS.2015.7353520

Chaler, J., Gil Fraguas, L., Gómez García, A., Laxe, S., Luna Cabrera, F., Llavona, R., et al. (2020). Impact of coronavirus disease 2019 outbreak on rehabilitation services and physical rehabilitation medicine and rehabilitation physicians' activities: perspectives from the spanish experience. *Eur. J. Phys. Rehabil. Med.* 56, 369–371. doi: 10.23736/S1973-9087.20.06304-2

Chen, B., Feng, Y., and Wang, Q. (2016). Combining vibrotactile feedback with volitional myoelectric control for robotic transtibial prostheses. *Front. Neurorobot.* 10:8. doi: 10.3389/fnbot.2016.00008

Chen, D. K. Y., Anderson, I. A., Walker, C. G., and Besier, T. F. (2016). Lower extremity lateral skin stretch perception for haptic feedback. *IEEE Trans. Haptics* 9, 62–68. doi: 10.1109/TOH.2016.2516012

Chen, Y., Garcia-Vergara, S., and Howard, A. M. (2015). Effect of a home-based virtual reality intervention for children with cerebral palsy using super pop VR evaluation metrics: a feasibility study. *Rehabil. Res. Pract.* 2015:812348. doi: 10.1155/2015/812348

Cheng, A. S. (2000). Use of early tactile stimulation in rehabilitation of digital nerve injuries. *Am. J. Occup. Ther.* 54, 159–165. doi: 10.5014/ajot.54.2.159

Chinello, F., Malvezzi, M., Pacchierotti, C., and Prattichizzo, D. (2015). "Design and development of a 3RRS wearable fingertip cutaneous device.," in *IEEE International Conference on Advanced Intelligent Mechatronics (AIM)* (Busan), 293–298.

Chinello, F., Malvezzi, M., Prattichizzo, D., and Pacchierotti, C. (2019). A modular wearable finger interface for cutaneous and kinesthetic interaction: control and evaluation. *IEEE Trans. Indus. Electron.* 67, 706–716. doi: 10.1109/TIE.2019.2899551

Chinello, F., Pacchierotti, C., Bimbo, J., Tsagarakis, N. G., and Prattichizzo, D. (2018). Design and evaluation of a wearable skin stretch device for haptic guidance. *IEEE Robot. Autom. Lett.* 3, 524–531. doi: 10.1109/LRA.2017.2766244

Chinello, F., Pacchierotti, C., Tsagarakis, N. G., and Prattichizzo, D. (2016). "Design of a wearable skin stretch cutaneous device for the upper limb. in *IEEE Haptics Symposium (HAPTICS)* (Philadelphia, PA), 14–20.

Choi, I., Culbertson, H., Miller, M. R., Olwal, A., and Follmer, S. (2017). "Grabity: a wearable haptic interface for simulating weight and grasping in virtual reality," in *Proceedings of the 30th Annual ACM Symposium on User Interface Software and Technology* (Québec City, QC), 119–130.

Choi, S., and Kuchenbecker, K. J. (2013). Vibrotactile display: perception, technology, and applications. *Proc. IEEE* 101, 2093–2104. doi: 10.1109/JPROC.2012.2221071

Chossat, J. B., Chen, D. K. Y., Park, Y. L., and Shull, P. B. (2019). Soft wearable skin-stretch device for haptic feedback using twisted and coiled polymer actuators. *IEEE Trans. Haptics* 12, 521–532. doi: 10.1109/TOH.2019.2943154

Clark, J. P., Kim, S. Y., and O'Malley, M. K. (2018). "The rice haptic rocker: comparing longitudinal and lateral upper-limb skin stretch perception," in *International Conference on Human Haptic Sensing and Touch Enabled Computer Applications* (Pisa), 125–134.

Clendaniel, R. A. (2000). Outcome measures for assessment of treatment of the dizzy and balance disorder patient. *Otolaryngol. Clin. North Am.* 33, 519–533. doi: 10.1016/s0030-6665(05)70225-5

Cobus, V., Ehrhardt, B., Boll, S., and Heuten, W. (2018). "Vibrotactile alarm display for critical care," in *Proceedings of the 7th ACM International Symposium on Pervasive Displays* (Munich), 1–7.

Colella, N., Bianchi, M., Grioli, G., Bicchi, A., and Catalano, M. G. (2019). A novel skin-stretch haptic device for intuitive control of robotic prostheses and avatars. *IEEE Robot. Autom. Lett.* 4, 1572–1579. doi: 10.1109/LRA.2019.2896484

Colgate, J. E., and Brown, J. M. (1994). "Factors affecting the z-width of a haptic display," in *Proceedings of the IEEE International Conference on Robotics and Automation* (San Diego, CA), 3205–3210.

Collins, J. J., Imhoff, T. T., and Grigg, P. (1996). Noise-enhanced tactile sensation. *Nature* 383:770.

Collins, J. J., Priplata, A. A., Gravelle, D. C., Niemi, J., Harry, J., and Lipsitz, L. A. (2003). Noise-enhanced human sensorimotor function. *IEEE Eng. Med. Biol. Mag.* 22, 76–83. doi: 10.1109/memb.2003.1195700

Connell, L. A., McMahon, N. E., and Adams, N. (2014). Stroke survivors' experiences of somatosensory impairment after stroke: an interpretative phenomenological analysis. *Physiotherapy* 100, 150–155. doi: 10.1016/j.physio.2013.09.003

Cramer, S. C., Dodakian, L., Le, V., See, J., Augsburger, R., McKenzie, A., et al. (2019). Efficacy of home-based telerehabilitation vs in-clinic therapy for adults after stroke: a randomized clinical trial. *JAMA Neurol.* 76, 1079–1087. doi: 10.1001/jamaneurol.2019.1604

Culbertson, H., Nunez, C. M., Israr, A., Lau, F., Abnousi, F., and Okamura, A. (2018a). "A social haptic device to create continuous lateral motion using sequential normal indentation," in *2018 IEEE Haptics Symposium (HAPTICS)* (San Francisco, CA). doi: 10.1109/HAPTICS.2018.8357149

Culbertson, H., Schorr, S. B., and Okamura, A. M. (2018b). Haptics: the present and future of artificial touch sensation. *Annu. Rev. Control Robot. Auton. Syst.* 1, 385–409. doi: 10.1146/annurev-control-060117-105043

Cuppone, A. V., Squeri, V., Semprini, M., Masia, L., and Konczak, J. (2016). Robot-assisted proprioceptive training with added vibro-tactile feedback enhances somatosensory and motor performance. *PLoS ONE* 11:e0164511. doi: 10.1371/journal.pone.0164511

Dandu, B., Shao, Y., Stanley, A., and Visell, Y. (2019). "Spatiotemporal haptic effects from a single actuator via spectral control of cutaneous wave propagation," in *IEEE World Haptics Conference (WHC)* (Tokyo), 425-430.

Dellon, A. L., Mackinnon, S. E., and Crosby, P. M. (1987). Reliability of two-point discrimination measurements. *J. Hand Surg.* 12(5 Pt 1), 693–696. doi: 10.1016/s0363-5023(87)80049-7

Demain, S., Metcalf, C. D., Merrett, G. V., Zheng, D., and Cunningham, S. (2013). A narrative review on haptic devices: relating the physiology and psychophysical properties of the hand to devices for rehabilitation in central nervous system disorders. *Disab. Rehabil. Assist. Technol.* 8, 181–189. doi: 10.3109/17483107.2012.697532

Dietz, V., and Fouad, K. (2014). Restoration of sensorimotor functions after spinal cord injury. *Brain* 137(Pt 3), 654–667. doi: 10.1093/brain/awt262

Dimbwadyo-Terrer, I., Trincado-Alonso, F., de los Reyes-Guzmán, A., Aznar, M. A., Alcubilla, C., Pérez-Nombela, S., et al. (2016). Upper limb rehabilitation after spinal cord injury: a treatment based on a data glove and an immersive virtual reality environment. *Disabil. Rehabil. Assist. Technol.* 11, 462–467. doi: 10.3109/17483107.2015.1027293

Dodakian, L., McKenzie, A. L., Le, V., See, J., Pearson-Fuhrhop, K., Burke Quinlan, E., et al. (2017). A home-based telerehabilitation program for patients with stroke. *Neurorehabil. Neural Repair* 31, 923–933. doi: 10.1177/1545968317733818

Doyle, S., Bennett, S., Fasoli, S. E., and McKenna, K. T. (2010). Interventions for sensory impairment in the upper limb after stroke. *Cochrane Database Syst. Rev.* 6:CD006331. doi: 10.1002/14651858.CD006331.pub2

Doyle, S. D., Bennett, S., and Dudgeon, B. (2014). Upper limb post-stroke sensory impairments: the survivor's experience. *Disabil. Rehabil.* 36, 993–1000. doi: 10.3109/09638288.2013.825649

Drewing, K., Fritschi, M., Zopf, R., Ernst, M. O., and Buss, M. (2005). First evaluation of a novel tactile display exerting shear force via lateral displacement. *ACM Trans. Appl. Percept.* 2, 118–131. doi: 10.1145/1060581.1060586

Dunkelberger, N., Sullivan, J. L., Bradley, J., Manickam, I., Dasarathy, G., Baraniuk, R. G., et al. (2020). A multi-sensory approach to present phonemes as language through a wearable haptic device. *IEEE Trans. Haptics*. doi: 10.1109/TOH.2020.3009581

Edin, B. B. (2004). Quantitative analyses of dynamic strain sensitivity in human skin mechanoreceptors. *J. Neurophysiol.* 92, 3233–3243. doi: 10.1152/jn.00628.2004

Eid, M. A., and Al Osman, H. (2015). Affective haptics: current research and future directions. *IEEE Access* 4, 26–40. doi: 10.1109/ACCESS.2015.2497316

Enders, L. R., Hur, P., Johnson, M. J., and Seo, N. J. (2013). Remote vibrotactile noise improves light touch sensation in stroke survivors' fingertips via stochastic resonance. *J. Neuroeng. Rehabil.* 10:105. doi: 10.1186/1743-0003-10-105

Estes, L. T., Backus, D., and Starner, T. (2015). "A wearable vibration glove for improving hand sensation in persons with spinal cord injury using passive haptic rehabilitation," in *2015 9th International Conference on Pervasive Computing Technologies for Healthcare (PervasiveHealth)* (Istanbul), 37–44.

Farajian, M., Kossowsky, H., Leib, R., and Nisky, I. (2020a). Visual feedback weakens the augmentation of perceived stiffness by artificial skin stretch. *bioRxiv* 2020.07.22.215715. doi: 10.1101/2020.07.22.215715

Farajian, M., Leib, R., Kossowsky, H., Zaidenberg, T., Mussa-Ivaldi, F. A., and Nisky, I. (2020b). Stretching the skin immediately enhances perceived stiffness and gradually enhances the predictive control of grip force. *Elife* 9:e52653. doi: 10.7554/eLife.52653

Feintuch, U., Raz, L., Hwang, J., Josman, N., Katz, N., Kizony, R., et al. (2006). Integrating haptic-tactile feedback into a video-capture-based virtual environment for rehabilitation. *Cyberpsychol. Behav.* 9, 129–132. doi: 10.1089/cpb.2006.9.129

Ferris, T. K., and Sarter, N. (2011). Continuously informing vibrotactile displays in support of attention management and multitasking in anesthesiology. *Hum. Factors* 53, 600–611. doi: 10.1177/0018720811425043

Fino, P. C., and Mancini, M. (2020). Phase-dependent effects of closed-loop tactile feedback on gait stability in parkinson's disease. *IEEE Trans. Neural Syst. Rehabil. Eng.* 28, 1636–1641. doi: 10.1109/TNSRE.2020.2997283

Fitts, P. M., and Posner, M. I. (1967). *Human Performance*. Belmont, CA: Brooks/Cole.

Franchignoni, F., Horak, F., Godi, M., Nardone, A., and Giordano, A. (2010). Using psychometric techniques to improve the balance evaluation systems test: the mini-BESTest. *J. Rehabil. Med.* 42, 323–331. doi: 10.2340/16501977-0537

Franks, J., Culjat, M., King, C. H., Franco, M., Bisley, J., Grundfest, W., et al. (2008). Pneumatic balloon actuators for tactile feedback in robotic surgery. *Indus. Robot.* 35, 449–455.

Frediani, G., and Carpi, F. (2020). Tactile display of softness on fingertip. *Sci. Rep.* 10:20491. doi: 10.1038/s41598-020-77591-0

Freeman, E., Anderson, R., Williamson, J., Wilson, G., and Brewster, S. A. (2017). "Textured surfaces for ultrasound haptic displays," in *Proceedings of the 19th ACM International Conference on Multimodal Interaction* (Glasgow), 491–492.

Frisoli, A., Solazzi, M., Salsedo, F., and Bergamasco, M. (2008). A fingertip haptic display for improving curvature discrimination. *Presence Teleoperators Virtual Environ.* 17, 550–561. doi: 10.1162/pres.17.6.550

Gabardi, M., Solazzi, M., Leonardis, D., and Frisoli, A. (2016). "A new wearable fingertip haptic interface for the rendering of virtual shapes and surface features," in *2016 IEEE Haptics Symposium (HAPTICS)* (Philadelphia, PA). doi: 10.1109/HAPTICS.2016.7463168

Galambos, P. (2012). Vibrotactile feedback for haptics and telemanipulation: survey, concept and experiment. *Acta Polytech. Hung.* 9, 41–65.

Gammaitoni, L. (1995). Stochastic resonance and the dithering effect in threshold physical systems. *Phys. Rev. E.* 52:4691. doi: 10.1103/PhysRevE.52.4691

Gammaitoni, L., Hänggi, P., Jung, P., and Marchesoni, F. (1998). Stochastic resonance. *Rev. Mod. Phys.* 70:223. doi: 10.4249/scholarpedia.1474

Garcia-Hernandez, N., Sarakoglou, I., Tsagarakis, N., and Caldwell, D. (2011). "Orientation discrimination of patterned surfaces through an actuated and non-actuated tactile display," in *IEEE World Haptics Conference* (Istanbul), 599–604. doi: 10.1109/WHC.2011.5945553

Gavrilov, L. R. (2008). The possibility of generating focal regions of complex configurations in application to the problems of stimulation of human receptor structures by focused ultrasound. *Acoust. Phys.* 54, 269–278. doi: 10.1134/S1063771008020152

Gavrilov, L. R., Gersuni, G. V., Ilyinski, O. B., Tsirulnikov, E. M., and Shchekanov, E. E. (1977). A study of reception with the use of focused ultrasound. I. effects on the skin and deep receptor structures in man. *Brain Res.* 135, 265–277. doi: 10.1016/0006-8993(77)91030-7

Gavrilov, L. R., and Tsirulnikov, E. M. (2002). Mechanisms of stimulation effects of focused ultrasound on neural structures: role of nonlinear effects. *Nonlinear Acoust.* 445–448.

Geldard, F. A., and Sherrick, C. E. (1972). The cutaneous "rabbit": a perceptual illusion. *Science* 178, 178–179. doi: 10.1126/science.178.4057.178

Gil, H., Son, H., Kim, J., and Oakley, I. (2018). "Whiskers: exploring the use of ultrasonic haptic cues on the face," in *Proceedings of the CHI Conference on Human Factors in Computing Systems* (Montréal, QC), 1–13.

Gleeson, B. T., Horschel, S. K., and Provancher, W. R. (2010a). Design of a fingertip-mounted tactile display with tangential skin displacement feedback. *IEEE Trans. Haptics* 3, 297–301. doi: 10.1109/TOH.2010.8

Gleeson, B. T., Horschel, S. K., and Provancher, W. R. (2010b). Perception of direction for applied tangential skin displacement: effects of speed, displacement, and repetition. *IEEE Trans. Haptics* 3, 177–188. doi: 10.1109/TOH.2010.20

Goebl, W., and Palmer, C. (2008). Tactile feedback and timing accuracy in piano performance. *Exp. Brain Res.* 186, 471–479. doi: 10.1007/s00221-007-1252-1

Goodwin, G. M., McCloskey, D. I., and Matthews, P. B. (1972). Proprioceptive illusions induced by muscle vibration: contribution by muscle spindles to perception? *Science* 175, 1382–1384. doi: 10.1126/science.175.4028.1382

Gould, W. R., Vierck, C. J., and Luck, M. M. (1979). "Cues supporting recognition of the orientation or direction of movement of tactile stimuli," in *Sensory Functions of the Skin of Humans* (Boston, MA: Springer), 63–78.

Greenspan, J. D., and Bolanowski, S. J. (1996). "Chapter 2 - The psychophysics of tactile perception and its peripheral physiological basis," in *Pain and Touch, Handbook of Perception and Cognition*, ed L. Kruger (San Diego, CA: Academic Press), 25–103. doi: 10.1016/B978-012426910-1/50004-2

Guinan, A. L., Caswell, N. A., Drews, F. A., and Provancher, W. R. (2013a). "A video game controller with skin stretch haptic feedback," in *IEEE International Conference on Consumer Electronics (ICCE)* (Las Vegas, NV), 456–457.

Guinan, A. L., Hornbaker, N. C., Montandon, M. N., Doxon, A. J., and Provancher, W. R. (2013b). "Back-to-back skin stretch feedback for communicating five degree-of-freedom direction cues," in *World Haptics Conference (WHC)* (Daejeon), 13–18.

Guinan, A. L., Montandon, M. N., Caswell, N. A., and Provancher, W. R. (2012). "Skin stretch feedback for gaming environments," in *IEEE International Workshop on Haptic Audio Visual Environments and Games (HAVE) Proceedings* (Munich), 101–106.

Guinan, A. L., Montandon, M. N., Doxon, A. J., and Provancher, W. R. (2014). "Discrimination thresholds for communicating rotational inertia and torque using differential skin stretch feedback in virtual environments," in *IEEE Haptics Symposium (HAPTICS)* (Houston, TX), 277–282.

Guzererler, A., Provancher, W. R., and Basdogan, C. (2016). "Perception of skin stretch applied to palm: effects of speed and displacement," in *Haptics: Perception, Devices, Control, and Applications, Lecture Notes in Computer Science,* eds F. Bello, H. Kajimoto, and Y. Visel (Cham: Springer International Publishing), 180–189. doi: 10.1007/978-3-319-42321-0_17

Hachisu, T., and Suzuki, K. (2019). Representing interpersonal touch directions by tactile apparent motion using smart bracelets. *IEEE Trans. Haptics* 12, 327–338. doi: 10.1109/TOH.2019.2929810

Hankey, G. J., and Edis, R. H. (1989). The utility of testing tactile perception of direction of scratch as a sensitive clinical sign of posterior column dysfunction in spinal cord disorders. *J. Neurol. Neurosurg. Psychiatry* 52, 395–398.

Hasegawa, K., and Shinoda, H. (2013). "Aerial display of vibrotactile sensation with high spatial-temporal resolution using large-aperture airborne ultrasound phased array," in *World Haptics Conference (WHC)* (Daejeon), 31–36.

Haynes, A., Simons, M. F., Helps, T., Nakamura, Y., and Rossiter, J. (2019). A wearable skin-stretching tactile interface for Human–Robot and Human–Human communication. *IEEE Robot. Autom. Lett.* 4, 1641–1646. doi: 10.1109/LRA.2019.2896933

High, C. M., McHugh, H. F., Mills, S. C., Amano, S., Freund, J. E., and Vallabhajosula, S. (2018). Vibrotactile feedback alters dynamics of static postural control in persons with parkinson's disease but not older adults at high fall risk. *Gait Posture* 63, 202–207. doi: 10.1016/j.gaitpost.2018.05.010

Hill, V. A., Fisher, T., Schmid, A. A., Crabtree, J., and Page, S. J. (2014). Relationship between touch sensation of the affected hand and performance of valued activities in individuals with chronic stroke. *Top. Stroke Rehabil.* 21, 339–346. doi: 10.1310/tsr2104-339

Holden, J. K., Nguyen, R. H., Francisco, E. M., Zhang, Z., Dennis, R. G., and Tommerdahl, M. (2012). A novel device for the study of somatosensory information processing. *J. Neurosci. Methods* 204, 215–220. doi: 10.1016/j.jneumeth.2011.11.007

Horak, F. B. (2006). Postural orientation and equilibrium: what do we need to know about neural control of balance to prevent falls? *Age Ageing* 35(Suppl. 2), ii7–ii11. doi: 10.1093/ageing/afl077

Howard, T., Marchal, M., Lécuyer, A., and Pacchierotti, C. (2020). PUMAH: pan-tilt ultrasound mid-air haptics for larger interaction workspace in virtual reality. *IEEE Trans. Haptics* 13, 38–44. doi: 10.1109/TOH.2019.2963028

Huisman, G., Bruijnes, M., Kolkmeier, J., Jung, M., Frederiks, A. D., and Rybarczyk, Y. (2013). "Touching virtual agents: embodiment and mind," in *International Summer Workshop on Multimodal Interfaces* (Lisbon), 114–138.

Huisman, G., Frederiks, A. D., van Erp, J. B., and Heylen, D. K. (2016). "Simulating affective touch: Using a vibrotactile array to generate pleasant stroking sensations," in *International Conference on Human Haptic Sensing and Touch Enabled Computer Applications* (London), 240–250.

Hur, P., Pan, Y., and DeBuys, C. (2019). Free energy principle in human postural control system: Skin stretch feedback reduces the entropy. *Sci. Rep.* 9:16870. doi: 10.1038/s41598-019-53028-1

Israr, A., and Abnousi, F. (2018). "Towards pleasant touch: vibrotactile grids for social touch interactions," in *Extended Abstracts of the* 2018 *CHI Conference on Human Factors in Computing Systems* (Montréal, QC), 1–6.

Jacobs, R., Brånemark, R., Olmarker, K., Rydevik, B., Steenberghe, D., and van, Brånemark, P. (2000). Evaluation of the psychophysical detection threshold level for vibrotactile and pressure stimulation of prosthetic limbs using bone anchorage or soft tissue support. *Prosthet. Orthot. Int.* 24, 133–142. doi: 10.1080/03093640008726536

Jacobson, G. P., and Newman, C. W. (1990). The development of the dizziness handicap inventory. *Arch. Otolaryngol. Head Neck Surg.* 116, 424–427.

Jaffe, D. L., Brown, D. A., Pierson-Carey, C. D., Buckley, E. L., and Lew, H. L. (2004). Stepping over obstacles to improve walking in individuals with poststroke hemiplegia. *J. Rehabil. Res. Dev.* 41, 283–292. doi: 10.1682/jrrd.2004.03.0283

Jansen, Y., Karrer, T., and Borchers, J. (2010). "MudPad: localized tactile feedback on touch surfaces," in *Adjunct Proceedings of the 23nd Annual ACM Symposium on User Interface Software and Technology*, 385–386.

Janssen, L. J. F., Verhoeff, L. L., Horlings, C. G. C., and Allum, J. H. J. (2009). Directional effects of biofeedback on trunk sway during gait tasks in healthy young subjects. *Gait Posture* 29, 575–581. doi: 10.1016/j.gaitpost.2008.12.009

Jiang, L., Cutkosky, M. R., Ruutiainen, J., and Raisamo, R. (2009). Using haptic feedback to improve grasp force control in multiple sclerosis patients. *IEEE Trans. Robot.* 25, 593–601. doi: 10.1109/TRO.2009.2019789

Johansson, R. S., and Flanagan, J. R. (2009). Coding and use of tactile signals from the fingertips in object manipulation tasks. *Nat. Rev. Neurosci.* 10, 345–359. doi: 10.1038/nrn2621

Johnson, K. O., Yoshioka, T., and Vega-Bermudez, F. (2000). Tactile functions of mechanoreceptive afferents innervating the hand. *J. Clin. Neurophysiol.* 17, 539–558. doi: 10.1097/00004691-200011000-00002

Jones, L. A., and Sarter, N. B. (2008). Tactile displays: guidance for their design and application. *Hum. Factors* 50, 90–111. doi: 10.1518/001872008X250638

Jungmann, M., and Schlaak, H. F. (2002). "Miniaturised electrostatic tactile display with high structural compliance," in *Proceedings of Eurohaptics* (Edingburgh), 12–17.

Kajimoto, H., Kawakami, N., Maeda, T., and Tachi, S. (2001). Electro-tactile display with force feedback. In *Proc. World Multiconference on Systemics, Cybernetics and Informatics (SCI2001),* 11, 95-99.

Kanjanapas, S., Nunez, C. M., Williams, S. R., Okamura, A. M., and Luo, M. (2019). Design and analysis of pneumatic 2-DoF soft haptic devices for shear display. *IEEE Robot. Autom. Lett.* 4, 1365–1371. doi: 10.1109/LRA.2019.2895890

Kato, G., Kuroda, Y., Nisky, I., Kiyokawa, K., and Takemura, H. (2016). Design and Psychophysical Evaluation of the HapSticks: a novel non-grounded mechanism for presenting tool-mediated vertical forces. *IEEE Trans. Haptics* 10, 338–349. doi: 10.1109/TOH.2016.2636824

Kaul, O. B., and Rohs, M. (2017). "HapticHead: a spherical vibrotactile grid around the head for 3D guidance in virtual and augmented reality," in *Proceedings of the CHI Conference on Human Factors in Computing Systems* (Denver, CO), 3729–3740.

Kern, T. A. (2009). *Engineering Haptic Devices: A Beginner's Guide for Engineers*. New York, NY: Springer-Verlag. doi: 10.1007/978-3-540-88248-0

Khaodhiar, L., Niemi, J. B., Earnest, R., Lima, C., Harry, J. D., and Veves, A. (2003). Enhancing sensation in diabetic neuropathic foot with mechanical noise. *Diabetes Care* 26, 3280–3283. doi: 10.2337/diacare.26.12.3280

Kim, K., and Colgate, J. E. (2012). Haptic feedback enhances grip force control of sEMG-controlled prosthetic hands in targeted reinnervation amputees. *IEEE Trans. Neural Syst. Rehabil. Eng.* 20, 798–805. doi: 10.1109/TNSRE.2012.2206080

Kim, S., Kim, C., Yang, G., Yang, T., Han, B., Kang, S., et al. (2009). "Small and lightweight tactile display(SaLT) and its application," in *World Haptics -Third Joint EuroHaptics conference and Symposium on Haptic Interfaces for Virtual Environment and Teleoperator Systems* (Salt Lake City, UT), 69–74.

Kim, S., Kim, P., Park, C., and Choi, S. (2016). A new tactile device using magneto-rheological sponge cells for medical applications: experimental investigation. *Sensors Actuat. A Phys.* 239, 61–69. doi: 10.1016/j.sna.2016.01.016

King, D. A., Hume, P., and Tommerdahl, M. (2018). Use of the Brain-Gauge somatosensory assessment for monitoring recovery from concussion: a case study. *J. Physiother. Res.* 2:13.

Koehler, M., Usevitch, N. S., and Okamura, A. M. (2020). Model-based design of a soft 3-D haptic shape display. *IEEE Trans. Robot.* 36, 613–628. doi: 10.1109/TRO.2020.2980114

Koh, G. C., Yen, S. C., Tay, A., Cheong, A., Ng, Y. S., De Silva, D. A., et al. (2015). Singapore tele-technology aided rehabilitation in stroke (STARS) trial: protocol of a randomized clinical trial on tele-rehabilitation for stroke patients. *BMC Neurol.* 15:161. doi: 10.1186/s12883-015-0420-3

Krueger, A. R., Giannoni, P., Shah, V., Casadio, M., and Scheidt, R. A. (2017). Supplemental vibrotactile feedback control of stabilization and reaching actions of the arm using limb state and position error encodings. *J. Neuroeng. Rehabil.* 14:69. doi: 10.1186/s12984-017-0281-7

Kumar, N. A., Yoon, H. U., and Hur, P. (2017). "A user-centric feedback device for powered wheelchairs comprising a wearable skin stretch device and a haptic joystick," in *IEEE Workshop on Advanced Robotics and its Social Impacts (ARSO)* (Austin, TX), 1–2.

Kuniyasu, Y., Sato, M., Fukushima, S., and Kajimoto, H. (2012). "Transmission of forearm motion by tangential deformation of the skin," in *Proceedings of the 3rd Augmented Human International Conference* (Megève), 1–4.

Kyung, K. U., and Park, J. S. (2007). "Ubi-Pen: Development of a compact tactile display module and its application to a haptic stylus," in Second *Joint EuroHaptics Conference and Symposium on Haptic Interfaces for Virtual Environment and Teleoperator Systems (WHC'07)* (Tsukaba), 109–114.

Lai, S., Ahmed, U., Bollineni, A., Lewis, R., and Ramchandren, S. (2014). Diagnostic accuracy of qualitative vs. quantitative tuning forks: outcome measure for neuropathy. *J. Clin. Neuromuscul. Dis.* 15:96. doi: 10.1097/CND.0000000000000019

Lanting, S. M., Spink, M. J., Tehan, P. E., Vickers, S., Casey, S. L., and Chuter, V. H. (2020). Non-invasive assessment of vibration perception and protective sensation in people with diabetes mellitus: inter-and intra-rater reliability. *J. Foot Ankle Res.* 13, 1–7. doi: 10.1186/s13047-020-0371-9

Laufer, Y., and Elboim-Gabyzon, M. (2011). Does sensory transcutaneous electrical stimulation enhance motor recovery following a stroke? A systematic review. *Neurorehabil. Neural Repair* 25, 799–809. doi: 10.1177/1545968310397205

Lederman, S. J., and Klatzky, R. L. (2009). Haptic perception: a tutorial. *Attent. Percept. Psychophys.* 71, 1439–1459. doi: 10.3758/APP

Lee, B., Fung, A., and Thrasher, T. A. (2018). The effects of coding schemes on vibrotactile biofeedback for dynamic balance training in parkinson's disease and healthy elderly individuals. *IEEE Trans. Neural Syst. Rehabil. Eng.* 26, 153–160. doi: 10.1109/TNSRE.2017.2762239

Lee, B. C., Martin, B. J., and Sienko, K. H. (2012). Directional postural responses induced by vibrotactile stimulations applied to the torso. *Exp. Brain Res.* 222, 471–482. doi: 10.1007/s00221-012-3233-2

Leo, F., Cocchi, E., and Brayda, L. (2016). The effect of programmable tactile displays on spatial learning skills in children and adolescents of different visual disability. *IEEE Trans. Neural Syst. Rehabil. Eng.* 25, 861–872. doi: 10.1109/TNSRE.2016.2619742

Leonardis, D., Solazzi, M., Bortone, I., and Frisoli, A. (2017). A 3-RSR haptic wearable device for rendering fingertip contact forces. *IEEE Trans. Haptics* 10, 305–316. doi: 10.1109/TOH.2016.2640291

Lieberman, J., and Breazeal, C. (2007). "Development of a wearable vibrotactile feedback suit for accelerated human motor learning," in *Proceedings IEEE International Conference on Robotics and Automation* (Roma), 4001–4006.

Liu, W., Lipsitz, L. A., Montero-Odasso, M., Bean, J., Kerrigan, D. C., and Collins, J. J. (2002). Noise-enhanced vibrotactile sensitivity in older adults, patients with stroke, and patients with diabetic neuropathy. *Arch. Phys. Med. Rehabil.* 83, 171–176. doi: 10.1053/apmr.2002.28025

Long, B., Seah, S. A., Carter, T., and Subramanian, S. (2014). Rendering volumetric haptic shapes in mid-air using ultrasound. *ACM Trans. Graph* 33, 1–10. doi: 10.1145/2661229.2661257

Ma, C. Z. H., and Lee, W. C. C. (2017). A wearable vibrotactile biofeedback system improves balance control of healthy young adults following perturbations from quiet stance. *Hum. Mov. Sci*, 55, 54–60. doi: 10.1016/j.humov.2017.07.006

Magalhães, F. H., and Kohn, A. F. (2011). Vibratory noise to the fingertip enhances balance improvement associated with light touch. *Exp. Brain Res.* 209, 139–151. doi: 10.1007/s00221-010-2529-3

Magill, R. A. (2004). *Motor Learning and Control: Concepts and Applications*, *7th Edn*. New York, NY: McGraw-Hill.

Maki, B. E., and McIlroy, W. E. (1997). The role of limb movements in maintaining upright stance: the "change-in-support" strategy. *Phys. Ther.* 77, 488–507. doi: 10.1093/ptj/77.5.488

Makino, Y., Furuyama, Y., Inoue, S., and Shinoda, H. (2016). "HaptoClone (Haptic-Optical Clone) for mutual tele-environment by real-time 3D image transfer with midair force feedback," in *CHI* (San Jose, CA), 1980–1990.

McKinney, Z., Heberer, K., Nowroozi, B. N., Greenberg, M., Fowler, E., and Grundfest, W. (2014). "Pilot evaluation of wearable tactile biofeedback system for gait rehabilitation in peripheral neuropathy," in *2014 IEEE Haptics Symposium (HAPTICS)* (Houston, TX: IEEE), 135–140.

Meli, L., Hussain, I., Aurilio, M., Malvezzi, M., O'Malley, M. K., and Prattichizzo, D. (2018). The hBracelet: a wearable haptic device for the distributed mechanotactile stimulation of the upper limb. *IEEE Robot. Autom. Lett.* 3, 2198–2205. doi: 10.1109/LRA.2018.2810958

Merrett, G. V., Metcalf, C. D., Zheng, D., Cunningham, S., Barrow, S., and Demain, S. H. (2011). "Design and qualitative evaluation of tactile devices for stroke rehabilitation," in *IET Seminar on Assisted Living* (London), 1–6. doi: 10.1049/ic.2011.0025

Mikkelsen, M., He, J., Tommerdahl, M., Edden, R. A., Mostofsky, S. H., and Puts, N. A. (2020). Reproducibility of flutter-range vibrotactile detection and discrimination thresholds. *Sci. Rep.* 10, 1–14. doi: 10.1038/s41598-020-63208-z

Minamizawa, K., Fukamachi, S., Kajimoto, H., Kawakami, N., and Tachi, S. (2007). "Gravity grabber: wearable haptic display to present virtual mass sensation," in *ACM SIGGRAPH 2007 Emerging Technologies* (San Diego, CA), 8-es.

Minamizawa, K., Kamuro, S., Fukamachi, S., Kawakami, N., and Tachi, S. (2008). "GhostGlove: haptic existence of the virtual world," in *ACM SIGGRAPH 2008 New Tech Demos* (Los Angeles, CA), 18.

Monnai, Y., Hasegawa, K., Fujiwara, M., Yoshino, K., Inoue, S., and Shinoda, H. (2014). "HaptoMime: mid-air haptic interaction with a floating virtual screen," in *User Interface Software and Technology Symposium (UIST)* (Honolulu, HA), 663–667. doi: 10.1145/2642918.2647407

Monnai, Y., Hasegawa, K., Fujiwara, M., Yoshino, K., Inoue, S., and Shinoda, H. (2015). "Adding texture to aerial images using ultrasounds," in *Haptic Interaction* (Tokyo: Springer), 59–61.

Moseley, G. L., Zalucki, N. M., and Wiech, K. (2008). Tactile discrimination, but not tactile stimulation alone, reduces chronic limb pain. *Pain* 137, 600–608. doi: 10.1016/j.pain.2007.10.021

Moss, F., Ward, L. M., and Sannita, W. G. (2004). Stochastic resonance and sensory information processing: a tutorial and review of application. *Clin. Neurophysiol.* 115, 267–281. doi: 10.1016/j.clinph.2003.09.014

Muijzer-Witteveen, H. J. B., Nataletti, S., Agnello, M., Casadio, M., and Van Asseldonk, E. H. F. (2017). "Vibrotactile feedback to control the amount of weight shift during walking - a first step towards better control of an exoskeleton for spinal cord Injury subjects," in *IEEE International Conference on Rehabilitation Robotics* (London: IEEE), 1482–1487. doi: 10.1109/ICORR.2017.8009457

Mullenbach, J., Shultz, C., Colgate, J. E., and Piper, A. M. (2014). "Exploring affective communication through variable-friction surface haptics," in *Proceedings of the SIGCHI Conference on Human Factors in Computing Systems* (Toronto, ON), 3963–3972.

Muramatsu, Y., Niitsuma, M., and Thomessen, T. (2012). "Perception of tactile sensation using vibrotactile glove interface," in *2012 IEEE 3rd International Conference on Cognitive Infocommunications (CogInfoCom)* (Kosice: IEEE), 621–626.

Nakamura, M., and Jones, L. (2003). "An actuator for the tactile vest - a torso-based haptic device," in *11th Symposium on Haptic Interfaces for Virtual Environment and Teleoperator Systems. HAPTICS. Proceedings* (Los Angeles, CA), 333–339.

Nanhoe-Mahabier, W., Allum, J. H., Pasman, E. P., Overeem, S., and Bloem, B. R. (2012). The effects of vibrotactile biofeedback training on trunk sway in Parkinson's disease patients. *Parkinson. Relat. Disord.* 18, 1017–1021. doi: 10.1016/j.parkreldis.2012.05.018

Navarro, E., González, P., López-Jaquero, V., Montero, F., Molina, J. P., and Romero-Ayuso, D. (2018). Adaptive, multisensorial, physiological and social: the next generation of telerehabilitation systems. *Front. Neuroinform.* 12:43. doi: 10.3389/fninf.2018.00043

Nitsch, V., and Färber, B. (2012). A meta-analysis of the effects of haptic interfaces on task performance with teleoperation systems. *IEEE Trans. Haptics* 6, 387–398. doi: 10.1109/TOH.2012.62

Nobusako, S., Osumi, M., Matsuo, A., Furukawa, E., Maeda, T., Shimada, S., et al. (2019). Subthreshold vibrotactile noise stimulation immediately improves manual dexterity in a child with developmental coordination disorder: a single-case study. *Front. Neurol.* 10:717. doi: 10.3389/fneur.2019.00717

Norman, S. L., Doxon, A. J., Gleeson, B. T., and Provancher, W. R. (2014). Planar hand motion guidance using fingertip skin-stretch feedback. *IEEE Trans. Haptics* 7, 121–130. doi: 10.1109/TOH.2013.2296306

Norrsell, U., and Olausson, H. (1992). Human, tactile, directional sensibility and its peripheral origins. *Acta Physiol. Scand.* 144, 155–161.

Nunez, C. M., Huerta, B. N., Okamura, A. M., and Culbertson, H. (2020). "Investigating social haptic illusions for tactile stroking (SHIFTS)," in *IEEE Haptics Symposium (HAPTICS)*, 629–636.

Nunez, C. M., Williams, S. R., Okamura, A. M., and Culbertson, H. (2019). Understanding continuous and pleasant linear sensations on the forearm from a sequential discrete lateral skin-slip haptic device. *IEEE Trans. Haptics* 12, 414–427. doi: 10.1109/TOH.2019.2941190

Obrist, M., Subramanian, S., Gatti, E., Long, B., and Carter, T. (2015). "Emotions mediated through mid-air haptics," in *Proceedings of the 33rd Annual ACM Conference on Human Factors in Computing Systems* (Seoul), 2053–2062.

Omori, R., Kuroda, Y., Yoshimoto, S., and Oshiro, O. (2019). "A wearable skin stretch device for lower limbs: investigation of curvature effect on slip," in *IEEE World Haptics Conference (WHC)* (Tokyo), 37–42. doi: 10.1109/WHC.2019.8816129

O'Neill, J., McCann, S. M., and Lagan, K. M. (2006). Tuning fork (128 Hz) versus neurothesiometer: a comparison of methods of assessing vibration sensation in patients with diabetes mellitus. *Int. J. Clin. Pract.* 60, 174–178. doi: 10.1111/j.1742-1241.2005.00650.x

Pacchierotti, C., Salvietti, G., Hussain, I., Meli, L., and Prattichizzo, D. (2016). "The hRing: a wearable haptic device to avoid occlusions in hand tracking," in *Presented at the IEEE Haptics Symposium (HAPTICS)* (Philadelphia, PA), 134–139. doi: 10.1109/HAPTICS.2016.7463167

Pacchierotti, C., Sinclair, S., Solazzi, M., Frisoli, A., Hayward, V., and Prattichizzo, D. (2017). Wearable haptic systems for the fingertip and the hand: taxonomy, review, and perspectives. *IEEE Trans. Haptics* 10, 580–600. doi: 10.1109/TOH.2017.2689006

Pan, Y. T., Yoon, H. U., and Hur, P. (2017). A portable sensory augmentation device for balance rehabilitation using fingertip skin stretch feedback. *IEEE Trans. Neural Syst. Rehabil. Eng.* 25, 31–39. doi: 10.1109/TNSRE.2016.2542064

Paré, M., Carnahan, H., and Smith, A. (2002). Magnitude estimation of tangential force applied to the fingerpad. *Exp. Brain Res.* 142, 342–348. doi: 10.1007/s00221-001-0939-y

Pasquero, J., and Hayward, V. (2003). "STReSS: a practical tactile display system with one millimeter spatial resolution and 700 Hz refresh rate," in *Proc. Eurohaptics* (Dublin), 94–110.

Patel, S., Park, H., Bonato, P., Chan, L., and Rodgers, M. (2012). A review of wearable sensors and systems with application in rehabilitation. *J. Neuroeng. Rehabil.* 9:21. doi: 10.1186/1743-0003-9-21

Pearson, K. G. (2000). Plasticity of neuronal networks in the spinal cord: modifications in response to altered sensory input. *Prog. Brain Res.* 128, 61–70. doi: 10.1016/S0079-6123(00)28007-2

Perez, M. A., Field-Fote, E. C., and Floeter, M. K. (2003). Patterned sensory stimulation induces plasticity in reciprocal ia inhibition in humans. *J. Neurosci.* 23, 2014–2018. doi: 10.1523/JNEUROSCI.23-06-02014.2003

Perkins, B. A., Olaleye, D., Zinman, B., and Bril, V. (2001). Simple screening tests for peripheral neuropathy in the diabetes clinic. *Diabetes Care* 24, 250–256. doi: 10.2337/diacare.24.2.250

Pezent, E., Fani, S., Clark, J., Bianchi, M., and O'Malley, M. K. (2019). Spatially separating haptic guidance from task dynamics through wearable devices. *IEEE Trans. Haptics* 12, 581–593. doi: 10.1109/TOH.2019.2919281

Prattichizzo, D., Chinello, F., Pacchierotti, C., and Malvezzi, M. (2013). Towards wearability in fingertip haptics: a 3-DoF Wearable Device for Cutaneous Force Feedback. *IEEE Trans. Haptics* 6, 506–516. doi: 10.1109/TOH.2013.53

Prattichizzo, D., Chinello, F., Pacchierotti, C., and Minamizawa, K. (2010). "RemoTouch: a system for remote touch experience," in *Presented at the 19th International Symposium in Robot and Human Interactive Communication* (Viareggio), 676–679. doi: 10.1109/ROMAN.2010.5598606

Provancher, W. R., Cutkosky, M. R., Kuchenbecker, K. J., and Niemeyer, G. (2005). Contact location display for haptic perception of curvature and object motion. *Int. J. Robot. Res.*, 24, 691–702. doi: 10.1177/0278364905057121

Provancher, W. R., and Sylvester, N. D. (2009). Fingerpad skin stretch increases the perception of virtual friction. *IEEE Trans. Haptics* 2, 212–223. doi: 10.1109/TOH.2009.34

Puts, N. A. J., Edden, R. A. E., Wodka, E. L., Mostofsky, S. H., Tommerdahl, M. (2013). A vibrotactile behavioral battery for investigating somatosensory processing in children and adults. *J. Neurosci. Methods* 218, 39–47. doi: 10.1016/j.jneumeth.2013.04.012

Quek, Z. F., Schorr, S. B., Nisky, I., Okamura, A. M., and Provancher, W. R. (2013). "Sensory augmentation of stiffness using fingerpad skin stretch," in *Presented at the World Haptics Conference (WHC)* (Daejeon), 467–472. doi: 10.1109/WHC.2013.6548453

Quek, Z. F., Schorr, S. B., Nisky, I., Okamura, A. M., and Provancher, W. R. (2014a). Augmentation of stiffness perception with a 1-degree-of-freedom skin stretch device. *IEEE Transactions on Human-Machine Systems* 44, 731–742. doi: 10.1109/THMS.2014.2348865

Quek, Z. F., Schorr, S. B., Nisky, I., Provancher, W. R., and Okamura, A. M. (2014b). "Sensory substitution using 3-degree-of-freedom tangential and normal skin deformation feedback," in *Pesented at the IEEE Haptics Symposium (HAPTICS)* (Houston, TX), 27–33. doi: 10.1109/HAPTICS.2014.6775429

Quek, Z. F., Schorr, S. B., Nisky, I., Provancher, W. R., and Okamura, A. M. (2015a). Sensory substitution and augmentation using 3-degree-of-freedom skin deformation feedback. *IEEE Trans. Haptics* 8, 209–221. doi: 10.1109/TOH.2015.2398448

Quek, Z. F., Schorr, S. B., Nisky, I., Provancher, W. R., and Okamura, A. M. (2015b). "Sensory substitution of force and torque using 6-DoF tangential and normal skin deformation feedback," *Presented at the IEEE International Conference on Robotics and Automation (ICRA)* (Seattle, WA), 264–271. doi: 10.1109/ICRA.2015.7139010

Raitor, M., Walker, J. M., Okamura, A. M., and Culbertson, H. (2017). "WRAP: Wearable, restricted-aperture pneumatics for haptic guidance," in *2017 IEEE International Conference on Robotics and Automation (ICRA)* (Singapore), 427–432.

Rakkolainen, I., Sand, A., and Raisamo, R. (2019). "A survey of mid-air ultrasonic tactile feedback," in *IEEE International Symposium on Multimedia (ISM)* (San Diego, CA), doi: 10.1109/ISM46123.2019.00022

Rinderknecht, M. D., Dueñas, J. A., Held, J. P., Lambercy, O., Conti, F. M., Zizlsperger, L., et al. (2019). Automated and quantitative assessment of tactile mislocalization after stroke. *Front. Neurol.* 10:593. doi: 10.3389/fneur.2019.00593

Rinderknecht, M. D., Gross, R., Leuenberger, K., Lambercy, O., and Gassert, R. (2015). "Objective assessment of vibrotactile mislocalization using a haptic glove," in *IEEE International Conference on Rehabilitation Robotics (ICORR)* (Singapore), 145–150.

Risi, N., Shah, V., Mrotek, L. A., Casadio, M., and Scheidt, R. A. (2019). Supplemental vibrotactile feedback of real-time limb position enhances precision of goal-directed reaching. *J. Neurophysiol.* 122, 22–38. doi: 10.1152/jn.00337.2018

Roger, J., Darfour, D., Dha, A., Hickman, O., Shaubach, L., and Shepard, K. (2002). Physiotherapists' use of touch in inpatient settings. *Physiother. Res. Int.* 7, 170–186. doi: 10.1002/pri.253

Romanus, T., Frish, S., Maksymenko, M., Frier, W., Corenthy, L., and Georgiou, O. (2019). "Mid-air haptic bio-holograms in mixed reality," in *Adjunct Proceedings of the 2019 IEEE International Symposium on Mixed and Augmented Reality, ISMAR-Adjunct 2019* (Beijing). doi: 10.1109/ISMAR-Adjunct.2019.00-14

Rose, T., Nam, C. S., and Chen, K. B. (2018). Immersion of virtual reality for rehabilitation-Review. *Appl. Ergon.* 69, 153–161. doi: 10.1016/j.apergo.2018.01.009

Rossi-Izquierdo, M., Ernst, A., Soto-Varela, A., Santos-Pérez, S., Faraldo-García, A., Sesar-Ignacio, A., et al. (2013). Vibrotactile neurofeedback balance training in patients with parkinson's disease: reducing the number of falls. *Gait Posture* 37, 195–200. doi: 10.1016/j.gaitpost.2012.07.002

Rotella, M. F., Guerin, K., He, X., and Okamura, A. M. (2012). "Hapi bands: a haptic augmented posture interface," in *IEEE Haptics Symposium (HAPTICS)* (Vancouver, BC), 163–170.

Rutten, E., Van Den Bogaert, L., and Geerts, D. (2020). From initial encounter with mid-air haptic feedback to repeated use: the role of the novelty effect in user experience. *IEEE Trans. Haptics*. doi: 10.1109/TOH.2020.3043658. [Epub ahead of print].

Sarakoglou, I., Tsagarakis, N., and Caldwell, D. G. (2005). "A portable fingertip tactile feedback array - transmission system reliability and modelling," in *First Joint Eurohaptics Conference and Symposium on Haptic Interfaces for Virtual Environment and Teleoperator Systems. World Haptics Conference* (Pisa), 547–548.

Schorr, S. B., and Okamura, A. (2017a). Three-dimensional skin deformation as force substitution: Wearable device design and performance during haptic exploration of virtual environments. *IEEE Trans. Haptics*. 10, 418–430. doi: 10.1109/TOH.2017.2672969

Schorr, S. B., and Okamura, A. M. (2017b). "Fingertip tactile devices for virtual object manipulation and exploration," in *Proceedings of the 2017 CHI Conference on Human Factors in Computing Systems* (Denver), 3115–3119.

Schorr, S. B., Quek, Z. F., Nisky, I., Provancher, W. R., and Okamura, A. M. (2015). Tactor-induced skin stretch as a sensory substitution method in teleoperated palpation. *IEEE Trans. Hum. Mach. Syst.* 45, 714–726. doi: 10.1109/THMS.2015.2463090

Schorr, S. B., Quek, Z. F., Romano, R. Y., Nisky, I., Provancher, W. R., and Okamura, A. M. (2013). "Sensory substitution via cutaneous skin stretch feedback," *Presented at the 2013 IEEE International Conference on Robotics and Automation (ICRA)* (Karlsruhe), 2341–2346.

Schweisfurth, M. A., Markovic, M., Dosen, S., Teich, F., Graimann, B., and Farina, D. (2016). Electrotactile EMG feedback improves the control of prosthesis grasping force. *J. Neural Eng.* 13:056010. doi: 10.1088/1741-2560/13/5/056010

Seim, C. E., Ritter, B., Starner, T. E., Flavin, K., Lansberg, M. G., and Okamura, A. M. (2020a). Perspectives on the design and performance of upper-limb wearable stimulation devices for stroke survivors with hemiplegia and spasticity. *bioRxiv [Preprint]*. doi: 10.1101/2020.08.20.260000

Seim, C. E., Wolf, S. L., and Starner, T. E. (2020b). Wearable vibrotactile stimulation for upper extremity rehabilitation in chronic stroke: clinical feasibility trial using the VTS Glove. *arXiv preprint* arXiv:2007.09262.

Semmes, J., Weinstein, S., Ghent, L., and Teuber, H. L. (1960). *Somatosensory Changes After Penetrating Brain Wounds in Man*. Commonwealth Fund. Cambridge, MA: Harvard University Press.

Seo, N. J., Enders, L. R., Fortune, A., Cain, S., Vatinno, A. A., Schuster, E., et al. (2020). Phase I safety trial: extended daily peripheral sensory stimulation using a wrist-worn vibrator in stroke survivors. *Transl. Stroke Res.* 11, 204–213. doi: 10.1007/s12975-019-00724-9

Seo, N. J., Kosmopoulos, M. L., Enders, L. R., and Hur, P. (2014). Effect of remote sensory noise on hand function post stroke. *Front. Hum. Neurosci.* 8:934. doi: 10.3389/fnhum.2014.00934

Seo, N. J., Woodbury, M. L., Bonilha, L., Ramakrishnan, V., Kautz, S. A., Downey, R. J., et al. (2019). TheraBracelet stimulation during task-practice therapy to improve upper extremity function after stroke: a pilot randomized controlled study. *Phys. Ther.* 99, 319–328. doi: 10.1093/ptj/pzy143

Serrada, I., Hordacre, B., and Hillier, S. L. (2019). Does sensory retraining improve sensation and sensorimotor function following stroke: a systematic review and meta-analysis. *Front. Neurosci.* 13, 402. doi: 10.3389/fnins.2019.00402

Shah, V. A., Casadio, M., Scheidt, R. A., and Mrotek, L. A. (2019). Vibration propagation on the skin of the arm. *Appl. Sci.* 9:4329. doi: 10.3390/app9204329

Shah, V. A., Risi, N., Ballardini, G., Mrotek, L. A., Casadio, M., and Scheidt, R. A. (2018). "Effect of dual tasking on vibrotactile feedback guided reaching – a pilot study," in *Haptics: Science, Technology, and Applications: 11th International Conference, EuroHaptics* (Pisa), 10893, 3–14. doi: 10.1007/978-3-319-93445-7_1

Shakeri, G., Williamson, J. H., and Brewster, S. (2017). "Novel multimodal feedback techniques for in-car mid-air gesture interaction," in *AutomotiveUI 2017 - 9th International ACM Conference on Automotive User Interfaces and Interactive Vehicular Applications, Proceedings* (Oldenburg). doi: 10.1145/3122986.3123011

Shakeri, G., Williamson, J. H., and Brewster, S. (2018). "May the force be with you: ultrasound haptic feedback for mid-air gesture interaction in cars," in *Proceedings - 10th International ACM Conference on Automotive User Interfaces and Interactive Vehicular Applications* (Toronto, ON: AutomotiveUI). doi: 10.1145/3239060.3239081

Sherrick, C. E., and Rogers, R. (1966). Apparent haptic movement. *Percept. Psychophys.* 1, 175–180. doi: 10.3758/BF03215780

Shi, S., Leineweber, M. J., and Andrysek, J. (2019). Exploring the tactor configurations of vibrotactile feedback systems for use in lower-limb prostheses. *J. Vibr. Acoust.* 141: 051009. doi: 10.1115/1.4043610

Shimizu, Y., Saida, S., and Shimura, H. (1993). Tactile pattern recognition by graphic display: importance of 3-D information for haptic perception of familiar objects. *Percept. Psychophys.* 53, 43–48. doi: 10.3758/BF03211714

Shull, P. B., and Damian, D. D. (2015). Haptic wearables as sensory replacement, sensory augmentation and trainer - a review. *J. Neuroeng. Rehabil.* 12:59. doi: 10.1186/s12984-015-0055-z

Sienko, K. H., Balkwill, M. D., Oddsson, L. I. E., and Wall, C. (2013). The effect of vibrotactile feedback on postural sway during locomotor activities. *J. Neuroeng. Rehabil.* 10:93. doi: 10.1186/1743-0003-10-93

Sienko, K. H., Balkwill, M. D., and Wall, C. (2012). Biofeedback improves postural control recovery from multi-axis discrete perturbations. *J. Neuroeng. Rehabil.* 9:53. doi: 10.1186/1743-0003-9-53

Simpson, R., and Robinson, L. (2020). Rehabilitation after critical illness in people with COVID-19 infection. *Am. J. Phys. Med. Rehabil.* 99, 470–474. doi: 10.1097/PHM.0000000000001443

Smith, C., Pezent, E., and O'Malley, M. K. (2020). "Spatially separated cutaneous haptic guidance for training of a virtual sensorimotor task," in *Presented at the IEEE Haptics Symposium (HAPTICS)* (Crystal City, VA), 974–979. doi: 10.1109/HAPTICS45997.2020.ras.HAP20.11.2032900c

Sofia, K. O., and Jones, L. (2013). Mechanical and psychophysical studies of surface wave propagation during vibrotactile stimulation. *IEEE Trans. Haptics* 6, 320–329. doi: 10.1109/TOH.2013.1

Solazzi, M., Provancher, W. R., Frisoli, A., and Bergamasco, M. (2011). "Design of a SMA actuated 2-DoF tactile device for displaying tangential skin displacement," *Presented at the IEEE World Haptics Conference* (Istanbul), 31–36. doi: 10.1109/WHC.2011.5945457

Standen, P. J., Threapleton, K., Connell, L., Richardson, A., Brown, D. J., Battersby, S., et al. (2015). Patients' use of a home-based virtual reality system to provide rehabilitation of the upper limb following stroke. *Phys. Ther.* 95, 350–359. doi: 10.2522/ptj.20130564

Stanley, A. A., and Kuchenbecker, K. J. (2012). Evaluation of tactile feedback methods for wrist rotation guidance. *IEEE Trans. Haptics* 5, 240–251. doi: 10.1109/TOH.2012.33

Steihaug, S., Lippestad, J., and Werner, A. (2016). Between ideals and reality in home-based rehabilitation. *Scand. J. Prim. Health Care* 34, 46–54. doi: 10.3109/02813432.2015.1132888

Stephens-Fripp, B., Mutlu, R., and Alici, G. (2018). "Applying mechanical pressure and skin stretch simultaneously for sensory feedback in prosthetic hands," in *7th IEEE International Conference on Biomedical Robotics and Biomechatronics (Biorob)* (Enschede), 230–235.

Stevens, J. C. (1982). Temperature can sharpen tactile acuity. *Percept. Psychophys.* 31, 577–580. doi: 10.3758/BF03204192

Strong, R., and Gaver, B. (1996). Feather, scent and shaker: supporting simple intimacy. *Proc. CSCW* 96, 29–30.

Sullivan, J. E., and Hedman, L. D. (2008). Sensory dysfunction following stroke: incidence, significance, examination, and intervention. *Top. Stroke Rehabil.* 15, 200–217. doi: 10.1310/tsr1503-200

Sullivan, J. L., Dunkelberger, N., Bradley, J., Young, J., Israr, A., Lau, F., et al. (2019). Multi-sensory stimuli improve distinguishability of cutaneous haptic cues. *IEEE Trans. Haptics*? 13, 286–297. doi: 10.1109/TOH.2019.2922901

Suzuki, S., Takahashi, R., Nakajima, M., Hasegawa, K., Makino, Y., and Shinoda, H. (2018). "Midair haptic display to human upper body," in *Proc. Soc. Instrument and Control Engineers Japan (SICE'18)* (Nara), 848–853.

Svensson, P., Wijk, U., Björkman, A., and Antfolk, C. (2017). A review of invasive and non-invasive sensory feedback in upper limb prostheses. *Expert Rev. Med. Dev.* 14, 439–447. doi: 10.1080/17434440.2017.1332989

Sylvester, N. D., and Provancher, W. R. (2007). "Effects of longitudinal skin stretch on the perception of friction," in *Second Joint EuroHaptics Conference and Symposium on Haptic Interfaces for Virtual Environment and Teleoperator Systems (WHC'07)* (Tsukaba), 373–378.

Takeuchi, T., Futatsuka, M., Imanishi, H., and Yamada, S. (1986). Pathological changes observed in the finger biopsy of patients with vibration-induced white finger. *Scand. J. Work Environ. Health* 12, 280–283. doi: 10.5271/sjweh.2140

Talhan, A., and Jeon, S. (2018). Pneumatic actuation in haptic-enabled medical simulators: a review. *IEEE Access* 6, 3184–3200. doi: 10.1109/ACCESS.2017.2787601

Taylor, M. W., Taylor, J. L., and Seizova-Cajic, T. (2017). Muscle vibration-induced illusions: review of contributing factors, taxonomy of illusions and user's guide. *Multisens. Res.* 30, 25–63. doi: 10.1163/22134808-00002544

Taylor, P. M., Hosseini-Sianaki, A., Varley, C. J., and Pollet, D. M. (1997). *Advances in an Electrorheological Fluid Based Tactile Array*. IEE Colloquium on Developments in Tactile Display. London: IET.

Tenforde, A. S., Borgstrom, H., Polich, G., Steere, H., Davis, I. S., Cotton, K., et al. (2020). Outpatient physical, occupational, and speech therapy synchronous telemedicine: a survey study of patient satisfaction with virtual visits during the COVID-19 pandemic. *Am. J. Phys. Med. Rehabil.* 99, 977–981. doi: 10.1097/PHM.0000000000001571

Thomas, P., Baldwin, C., Bissett, B., Boden, I., Gosselink, R., Granger, C. L., et al. (2020). Physiotherapy management for COVID-19 in the acute hospital setting: clinical practice recommendations. *J. Physiother.* 66, 73–82. doi: 10.1016/j.jphys.2020.03.011

Tommerdahl, M., Lensch, R., Francisco, E., Holden, J., and Favorov, O. (2019). The brain gauge: a novel tool for assessing brain health. *J. Sci. Med.* 1, 1–19. doi: 10.37714/josam.v1i1.4

Tsalamlal, M. Y., Ouarti, N., and Ammi, M. (2013). "Psychophysical study of air jet based tactile stimulation," in *World Haptics Conference (WHC)* (Daejeon), 639–644.

Tsetserukou, D., Hosokawa, S., and Terashima, K. (2014). "LinkTouch: a wearable haptic device with five-bar linkage mechanism for presentation of two-DOF force feedback at the fingerpad," in *IEEE Haptics Symposium (HAPTICS)* (Houston, TX), 307–312.

Turville, M. L., Cahill, L. S., Matyas, T. A., Blennerhassett, J. M., and Carey, L. M. (2019). The effectiveness of somatosensory retraining for improving sensory function in the arm following stroke: a systematic review. *Clin. Rehabil.* 33, 834–846. doi: 10.1177/0269215519829795

Van Breda, E., Verwulgen, S., Saeys, W., Wuyts, K., Peeters, T., and Truijen, S. (2017). Vibrotactile feedback as a tool to improve motor learning and sports performance: a systematic review. *BMJ Open Sport Exerc. Med.* 3:e000216. doi: 10.1136/bmjsem-2016-000216

Van Erp, Jan, B. F., Van, V.een, Hendrik, A. H. C., Jansen, C., and Dobbins, T. (2005). Waypoint navigation with a vibrotactile waist belt. *ACM Trans. Appl. Percept.* 2, 106–117. doi: 10.1145/1060581.1060585

Van Vliet, P. M., and Wulf, G. (2006). Extrinsic feedback for motor learning after stroke: what is the evidence? *Disabil. Rehabil.* 28, 831–840. doi: 10.1080/09638280500534937

Vo, D., and Brewster, S. A. (2015). "Touching the invisible: localizing ultrasonic haptic cues," in *IEEE World Haptics Conference (WHC)* (Evanston, IL), 368–373.

Wall, C., Weinberg, M. S., Schmidt, P. B., and Krebs, D. E. (2001). Balance prosthesis based on micromechanical sensors using vibrotactile feedback of tilt. *IEEE Trans. Biomed. Eng.* 48, 1153–1161. doi: 10.1109/10.951518

Wall, P. D., and Noordenbos, W. (1977). Sensory functions which remain in man after complete transection of dorsal columns. *Brain* 100, 641–653.

Wan, A. H., Wong, D. W., Ma, C. Z., Zhang, M., and Lee, W. C. (2016). Wearable vibrotactile biofeedback device allowing identification of different floor conditions for lower-limb amputees. *Arch. Phys. Med. Rehabil.* 97, 1210–1213. doi: 10.1016/j.apmr.2015.12.016

Wang, C., Huang, D. Y., Hsu, S. W., Lin, C. L., Chiu, Y. L., Hou, C. E., et al. (2020). "Gaiters: exploring skin stretch feedback on legs for enhancing virtual reality experiences," in *Proceedings of the CHI Conference on Human Factors in Computing Systems* (Honolulu, HI), 1–14.

Wang, Q., Markopoulos, P., Yu, B., Chen, W., and Timmermans, A. (2017). Interactive wearable systems for upper body rehabilitation: a systematic review. *J. Neuroeng. Rehabil.* 14, 1–21. doi: 10.1186/s12984-017-0229-y

Weisenberger, J. M., Broadstone, S. M., and Saunders, F. A. (1989). Evaluation of two multichannel tactile aids for the hearing impaired. *J. Acoust. Soc. Am.* 86, 1764–1775.

Westebring van der Putten, E. P., van den Dobbelsteen, J. J., Goossens, R. H. M., Jakimowicz, J. J., and Dankelman, J. (2010). The effect of augmented feedback on grasp force in laparoscopic grasp control. *IEEE Trans. Haptics* 3, 280–291. doi: 10.1109/TOH.2010.23

Winstein, C. J., and Schmidt, R. A. (1990). Reduced frequency of knowledge of results enhances motor skill learning. *J. Exp. Psychol. Learn. Mem. Cogn.* 16, 677–691. doi: 10.1037/0278-7393.16.4.677

Wu, S. W., Fan, R. E., Wottawa, C. R., Fowler, E. G., Bisley, J. W., Grundfest, W. S., et al. (2010). "Torso-based tactile feedback system for patients with balance disorders," in *2010 IEEE Haptics Symposium* (Waltham, MA), 359–362.

Xu, J., Bao, T., Lee, U. H., Kinnaird, C., Carender, W., Huang, Y., et al. (2017). Configurable, wearable sensing and vibrotactile feedback system for real-time postural balance and gait training: proof-of-concept. *J. Neuroeng. Rehabil.* 14:102. doi: 10.1186/s12984-017-0313-3

Yang, T. H., Kwon, H. J., Lee, S. S., An, J., Koo, J. H., Kim, S. Y., et al. (2010). Development of a miniature tunable stiffness display using MR fluids for haptic application. *Sensors Actuators A Phys.* 163, 180–190. doi: 10.1016/j.sna.2010.07.004

Yasuda, K., Kaibuki, N., Harashima, H., and Iwata, H. (2017). The effect of a haptic biofeedback system on postural control in patients with stroke: an experimental pilot study. *Somatosensory Motor Res.* 34, 65–71. doi: 10.1080/08990220.2017.1292236

Yekutiel, M., and Guttman, E. (1993). A controlled trial of the retraining of the sensory function of the hand in stroke patients. *J. Neurol. Neurosurg. Psychiatr.* 56, 241–244.

Yem, V., and Kajimoto, H. (2017). "Wearable tactile device using mechanical and electrical stimulation for fingertip interaction with virtual world," in *IEEE Virtual Reality (VR)*, 99–104. doi: 10.1109/VR.2017.7892236

Yem, V., Otsuki, M., and Kuzuoka, H. (2015). Development of a wearable out-covering haptic display using ball effector for hand motion guidance. *Lecture Notes Electric. Eng.* 277, 85–89. doi: 10.1007/978-4-431-55690-9

Zandvliet, S. B., Kwakkel, G., Nijland, R. H. M., van Wegen Erwin, E., H., and Meskers, C. G. M. (2020). Is recovery of somatosensory impairment conditional for upper-limb motor recovery early after stroke? *Neurorehabil. Neural Repair* 34, 403–416. doi: 10.1177/1545968320907075

Conflict of Interest: The authors declare that the research was conducted in the absence of any commercial or financial relationships that could be construed as a potential conflict of interest.

frontiers in Neurorobotics

ORIGINAL RESEARCH
published: 23 February 2021
doi: 10.3389/fnbot.2021.612034

Long-Term Social Human-Robot Interaction for Neurorehabilitation: Robots as a Tool to Support Gait Therapy in the Pandemic

*Nathalia Céspedes, Denniss Raigoso, Marcela Múnera and Carlos A. Cifuentes**

Departament of Biomedical Engineering, Colombian School of Engineering Julio Garavito, Bogotá, Colombia

COVID-19 pandemic has affected the population worldwide, evidencing new challenges and opportunities for several kinds of emergent and existing technologies. Social Assistive Robotics could be a potential tool to support clinical care areas, promoting physical distancing, and reducing the contagion rate. In this context, this paper presents a long-term evaluation of a social robotic platform for gait neurorehabilitation. The robot's primary roles are monitoring physiological progress and promoting social interaction with human distancing during the sessions. A clinical validation with ten patients during 15 sessions were conducted in a rehabilitation center located in Colombia. Results showed that the robot's support improves the patients' physiological progress by reducing their unhealthy spinal posture time, with positive acceptance. 65% of patients described the platform as helpful and secure. Regarding the robot's role within the therapy, the health care staff agreed (>95%) that this tool can promote physical distancing and it is highly useful to support neurorehabilitation throughout the pandemic. These outcomes suggest the benefits of this tool to be further implemented in the pandemic.

Keywords: COVID-19, gait rehabilitation, Lokomat, long-term human-robot interaction, biofeedback, socially assistive robotics

OPEN ACCESS

Edited by:
Ana Luisa Trejos, Western University, Canada

Reviewed by:
Chung Hyuk Park, George Washington University, United States
Wellington Pinheiro dos Santos, Federal University of Pernambuco, Brazil

****Correspondence:***
Carlos A. Cifuentes
carlos.cifuentes@escuelaing.edu.co

Received: *30 September 2020*
Accepted: *27 January 2021*
Published: *23 February 2021*

Citation:
Céspedes N, Raigoso D, Múnera M and Cifuentes CA (2021) Long-Term Social Human-Robot Interaction for Neurorehabilitation: Robots as a Tool to Support Gait Therapy in the Pandemic. Front. Neurorobot. 15:612034. doi: 10.3389/fnbot.2021.612034

1. INTRODUCTION

In light of the rapid spread of COVID-19, several healthcare services are looking for strategies to promote physical distancing and enhance healthcare procedures. Physical distancing and isolation measures are adopted worldwide (WHO, 2020). Studies highlight the importance of these actions to decrease the transmission rate (Jarvis et al., 2020), reduce the peak incidence, delay the epidemic (Zhang et al., 2020), and minimize the intrahospital interactions (Aymerich-Franch, 2020). For instance, there is a concern to seek adaptive strategies to continue offering neurorehabilitation services during the COVID-19 pandemic, as the people with disabilities and chronic progressive diseases require constant monitoring and care (Leocani et al., 2020; Russo and Trabacca, 2020). the exploration of new technologies to support the general population's health is studied (Sakel et al., 2020).

In this context, Social Assistive Robotics (SAR) can play a critical role in real environments, mainly to promote physical distancing and support the rehabilitation's continuity. SAR shares with Assistive Robotics (AR), not only the goal of providing physical assistance to patients, but also to aid users through cognitive support, and social interaction. Thus, social robots need to

perform high degree autonomy tasks to achieve natural interaction (Duffy et al., 1999; Feil-Seifer and Mataric, 2011). SAR based applications have been developed in multiple clinics (Cifuentes et al., 2020), home-based (Campa and Campa, 2016), and educational (Heerink et al., 2016) areas. The outcomes of these studies show positive effects regarding the motivation (Winkle et al., 2018), adherence to medical treatments (Fasola and Matarić, 2010; Heerink et al., 2016), social interaction (Agrigoroaie and Tapus, 2016), among others. Within the COVID-19 pandemic, several researchers highlight the use of SAR through two main tasks: (i) monitoring the patients, and (ii) connecting doctors (who are exposed to a high risk of contagion) with patients using teleoperation (Aymerich-Franch, 2020; Hollander and Carr, 2020). Scassellati and Vázquez (2020) proposed using SAR to sustain social distancing and serve as health monitoring tools in high-risk areas. Khaleghi et al. (2020) remarked on social robots' opportunities to provide services remotely and aid the healthcare staff. Furthermore, some studies proposed SAR to interact in hospital environments and deal with mental health and well-being (Tavakoli et al., 2020).

In this study, a social robotic platform for neurorehabilitation with Lokomat for during and after the COVID-19 pandemic is presented. Lokomat is a device that combines a bodyweight support system and a robotic orthosis to assist the gait using repetitive specific tasks and the principle of neuroplasticity (Swinnen et al., 2017). This platform allows the measurement of different parameters: the patients' strength, mechanical stiffness, and the range of motion during the walking. These parameters enable the physiotherapist to straighten the therapy according to the objective of each patient (Gittler M, 2018). However, some parameters not detected by the Lokomat are essential during the rehabilitation (e.g., heart rate, the patient's posture, and the patient's fatigue level). In this sense, clinicians measure those parameters directly using external equipment (heart rate), visually (posture), and asking the patient (level of fatigue) verbally. Monitoring the heart rate enables the observation of the physical progress in terms of cardiovascular functioning, and correcting the spinal posture to maintain it healthy, promotes back health, allows muscles to work correctly, and decrease muscle fatigue (Sante, 2012; Daroff, 2016; Weaver and Ferg, 2020). Thus, SAR can be a complementary tool to automatize these parameters, provide feedback, interact with the patients during the therapy, and promote physical distancing.

This paper presents the long-term evaluation of a social robotic platform in neurorehabilitation with Lokomat. The patients performed a repeated measures study (due to the heterogeneity of the pathologies) during 15 sessions, where two conditions were established (i.e., control and robot-assisted therapy). The robot's primary roles were to assist the patient through physiological parameter feedback (e.g., posture correction and heart rate and perceived exertion monitoring) and motivational approaches. Furthermore, the platform's assessment seeks to observe the patient's progress through the therapies and their perception toward the robot. This platform can represent an opportunity to provide rehabilitation safely during and after the COVID-19 pandemic.

This paper is organized as follows. Section 2 presents the related work of social robotic platforms implemented in healthcare and rehabilitation areas. Section 3 describes the social robotic platform and the assessment methods used to evaluate its functionality and effectiveness in a neurorehabilitation scenario. Section 4 introduces the long-term results observed during the session regarding the physiological parameters and the patients' perception of social robots. Finally, the results and conclusions are presented at the end of this paper.

2. RELATED WORK

Although robot-assisted therapies as Lokomat are successful, cognitive approaches to enhance the treatment are also essential to provide care and physical assistance. SAR is currently being used in different areas (Yang et al., 2015; Heerink et al., 2016; Peleka et al., 2018). In healthcare, several studies are focused on measure the effects of social robots during rehabilitation procedures in terms of adherence to the treatments, assistance and perception (Matarić et al., 2007; Casas et al., 2019).

Different studies show the capabilities of SAR in post-stroke patients to support rehabilitation procedures regarding the cognitive approach. Robinson et al. (2013), proposed a social care robotic platform to aid post-stroke patients through contactless assistance. The system was tested in a pilot study, where the mobile robot supports the therapy through encouragement and reminders. The researchers found that welfare robots were well-received by stroke survivors and positively impacted willingness to undergo rehabilitation plans. In Libin and Libin (2004), a social robot was designed to create a relationship with the user using extroversion and introversion techniques. The robot also offers an adaptive behavior, capable of adjusting social interaction (e.g., interaction/proxemic distances, personalized speed, and vocal content) based on the users' personality traits and task performance. The reported results provide evidence of the user's preference for the personality matching robot and its benefits over rehabilitation performance. Currently, Polak and Levy-Tzedek (2020) presented a Pepper robot aimed at supporting upperlimb rehabilitation in a long-term study. The design of SAR based therapy considered the clinician's experience and perception. The robot was capable of promoting different skills and gives the patients trust to perform the games.

In contrast, social robots can also assist patients in employing physiological parameters monitoring and providing feedback. For instance, Kozyavkin et al. (2014) use a humanoid robot to help cerebral palsy patients during motor training activities. The primary role of the robot was supporting the children. The results indicate that patients like to interact with the robot and even suggest integrating them in other rehabilitation scenarios. The outcomes also show that the social robot has a positive effect on the patients regarding their motivation and their willingness to complete the health procedures. Similarly, in pediatric rehabilitation, researchers have highlighted the potential use of robots to actively engage the children to the rehabilitation and increase the commitment to perform the exercises (Carrillo et al., 2017; Pulido et al., 2017). Martín et al. (2020) developed

a physical therapy assisted by a humanoid robot to guide the patients through imitation of several postures. Depending on the patients' performance, the robot congratulates or corrects the users. The system was implemented in real environment set-ups, showing that the system was reliable and could improve the therapist's and patient's tasks during rehabilitation procedures.

Furthermore, social robots are being used in alternative rehabilitation areas. For instance, in cardiac rehabilitation, a humanoid robot was implemented to monitor and support patients with cardiovascular diseases (Casas et al., 2020). The robot gives the clinicians alerts to warn emergency events, provide motivation and correct the patient's physical activity performance. The outcomes highlight the robot's potential in this scenario and the positive effects on cardiovascular physiology.

Finally, in our previous work (Cespedes et al., 2020), the development of a SAR interface was presented. The social robot's roles were to support and encourage patients with neurological diseases during gait rehabilitation with Lokomat. These patients perform two sessions (one assisted by the robot and one conventional therapy). Preliminary findings show that patients tend to improve their posture with the use of the robot. Overall, the results regarding social robots in rehabilitation are positive. However, few studies assess SAR's effects in long-term periods, avoiding the fact that the novelty effect can decrease with time (Kasap and Magnenat-Thalmann, 2012), and social interaction could be affected. Most of these studies also integrate social robotics in conventional therapies rather than robot-assisted therapies as Lokomat rehabilitation. In this context, it is crucial to assess the effects of a complementary tool (SAR) that support rehabilitation from other approaches.

3. METHODOLOGY

This section describes the methodology carried out to evaluate the social robot effect during a long-term study in neurorehabilitation with Lokomat. Within the method, three steps were followed: (i) social robotic platform architecture, (ii) the experimental protocol, and (iii) data analysis.

3.1. Social Robotic Platform Architecture

Figure 1, shows the architecture of the social robotic platform proposed for neurorehabilitation with the Lokomat Scenario. The system is composed of three main modules: (i) the sensory module, which allows the acquisition and processing of the physiological data, (ii) the social robot module, in charge of the social interaction and the assistance of the patients, and (iii) the graphical user interface used to visualize the parameters of the parameters and control the therapy flow.

Sensory module: As mentioned previously in the sensory module, the physiological data are acquired and processed. The system's physiological parameters are the spinal posture (*thoracic and cervical posture*), the *heart rate*, and the *Borg scale*. The interface performs downsampling (1 Hz) to obtain simultaneous data from the sensors, then the data are stored on the database. *Cervical and Thoracic postures* are measured by an IMU BNO055 (Adafruit, USA), and inclination angles in the sagittal, coronal and traversal planes are obtained. A Zephyr HxM sensor (Medtronic, New Zealand) measures the heart rate. The sensor is located in the patient's chest to monitor cardiovascular functioning. Finally, the Borg Scale is a subjective measurement commonly used in rehabilitation to measure the patients' perceived exertion during the exercise (Compagnant et al., 2017). The robot asks the scale in a frequency of 5 min across the session. The therapist records the scale in the database.

Social robot module: A NAO V6 robot (Softbank Robotics, France) was used to achieve the interaction. The primary robot's role is to provide feedback to the patient of physiological parameters (i.e., cervical and thoracic posture, heart rate) and motivate them during therapy development. Additionally, the robot supports the therapists while they perform other tasks during the session. The robot is located in front of the patient during the exercise, guiding their performance by imitating healthy postures (**Figure 2**). Thus, the platform enables the physical distancing between the clinicians and the patient. The feedback given by the robot includes non-verbal and verbal gestures. Three feedback categories are proposed: (i) Heart rate feedback, provide alerts regarding the patient's high heart rate during the gait rehabilitation. (ii) Posture feedback, where the robot uses a verbal phrase to indicate the patient the performance of an unhealthy posture, and body gestures to show the patient how to correct and maintain a proper posture. This type of feedback is given to correct cervical and thoracic spinal postures. Finally, (iii) motivational feedback supports the patients through encouraging phrases. The non-verbal gestures and the conversation scheme designed for the robot is developed with a rule-based algorithm. This algorithm depends on the events triggered during the sessions and the types of feedback presented previously. For instance, the motivational phrases are performed when the patient accomplish a healthy posture. The conversation contents include a set of phrases (e.g., *"you are doing ok," "We almost finished the sessions," "Great!, you are improving the posture"*) that are performed randomly.

Graphical User Interface: This interface is in charge of visualizing the therapy's data and control the session flow (**Figure 3**). A tablet Surface Pro (Windows, USA) was used to display the interface. This tool also allows therapists to interact with the patient and manage the session.

3.2. Experimental Protocol

A total of 10 patients were recruited during the study. These patients performed actively Neurological Rehabilitation with Lokomat at Mobility Group Rehabilitation Center located in Bogota, Colombia. These patients voluntarily agreed to perform the rehabilitation assisted by the robot during 15 sessions (approx. 5 months, where 1 session was conducted per week[1], the sessions lasted between 40 and 60 min) (Bickmore and Picard, 2005; Sabelli et al., 2011). However, within this study, only 60% of the patients finished rehabilitation with Lokomat. **Table 1** shows the demographic data of the patients and their pathologies.

[1]Some patients begun 3 weeks after the study beginning due the recruitment in the rehabilitation center.

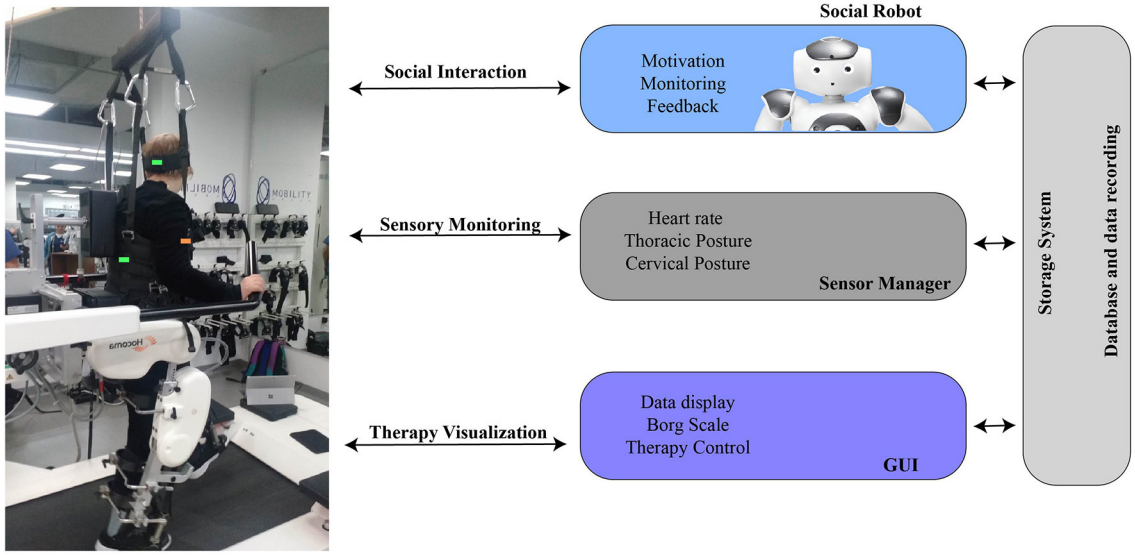

FIGURE 1 | Social robotic platform architecture for neurological rehabilitation with Lokomat.

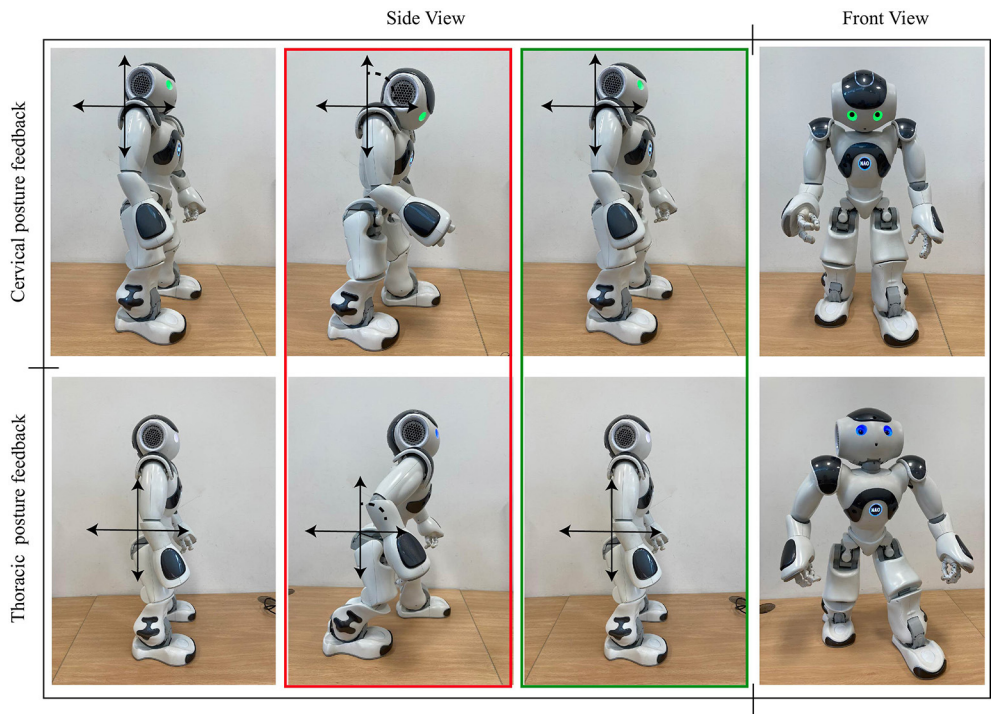

FIGURE 2 | Robot's behaviors regarding the posture feedback provided to the patient during Lokomat sessions.

3.2.1. Experimental Design

Due to the patient's heterogeneity, a repeated measures study was performed to evaluate the patient's progress during neurological Rehabilitation with Lokomat. Two conditions were established: a control condition and a robot condition (**Figure 4**); during both conditions the patients also received support from the healthcare staff. **Figure 5** shows the design of the study. *Test sessions* are performed at the beginning, in the middle, and at the end of the study. Within these *Test sessions*, only physiological parameters were measured and were taken as a baseline. Then, the patients were assigned randomly to start with one condition (either control or robot) during six sessions (one session per week). Finally, considering the start condition, the patients changed the scenario during another six sessions (one session per week).

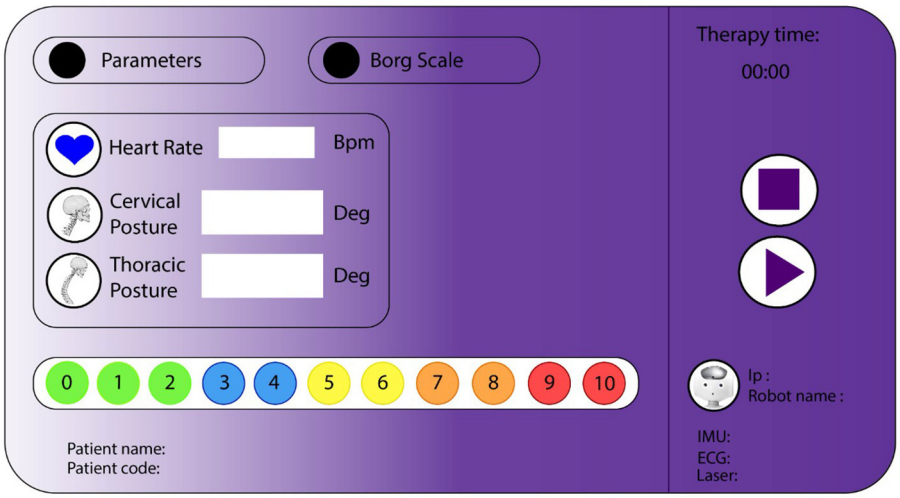

FIGURE 3 | Graphical user interface for neurological rehabilitation with Lokomat. The visualization area contains labels that show physiological parameters and patients' information. The control flow area has buttons to start and stop the therapy.

TABLE 1 | Demographic data of the patients within the study.

	Patients' data	
Participants	10	
Gender	3 females	7 males
Age (years), mean ± SD	35.5 ± 9.98	
Weight (Kg), mean ± SD	71.7 ± 7.60	
Pathology (%)	Stroke (60%)	
	Spinal cord injury (40%)	

FIGURE 4 | The diagram illustrates the robot condition performed in the experimental design.

Control Condition: Within this condition, the participants performed a conventional session of neurological rehabilitation with Lokomat. However, to measure the physiological data and compare them to the other conditions, the patients were monitored through the sensory module. The patients received assistance and assessment from the healthcare staff.

Robot Condition: Within this condition, the participants performed the sessions assisted by the social robot. As was explained in the section that describes the architecture, the robot's role was focused on providing motivational feedback and support patients' rehabilitation throughout the monitoring of physiological parameters (e.g., cervical, thoracic posture, and heart rate). Furthermore, the healthcare staff was supervising the therapy and gave additional feedback to the patient (e.g., ankle gait patterns correction).

3.2.2. Experimental Criteria

Inclusion Criteria: The patients considered in this study were those who actively perform neurorehabilitation therapies with Lokomat. Overall, the patients had to be able to understand and follow the robot instructions. The pathologies considered in the study were: spinal cord injury (hemiplegia, paraplegia) and stroke.

Exclusion Criteria: Patients with neurodegenerative diseases such as Multiple sclerosis, Alzheimer's Parkinson's, among others, were not included in the study. Additionally, patients who had invasive electronic devices (e.g., pacemakers) cannot perform the study due to the interference that can cause the system's sensors.

3.3. Data Analysis

Two types of variables were analyzed to evaluate the robot assistance: on the one hand, quantitative variables included the unhealthy posture time, the Borg scale, and the heart rate at training. On the other hand, qualitative variables integrate the UTAUT questionnaire to observe the patient's perceptions of the robot's role.

PPt [%]: This value describe the time during which the patient presents an unhealthy spinal posture (i.e., thoracic and cervical posture) in the Lokomat sessions. First the values

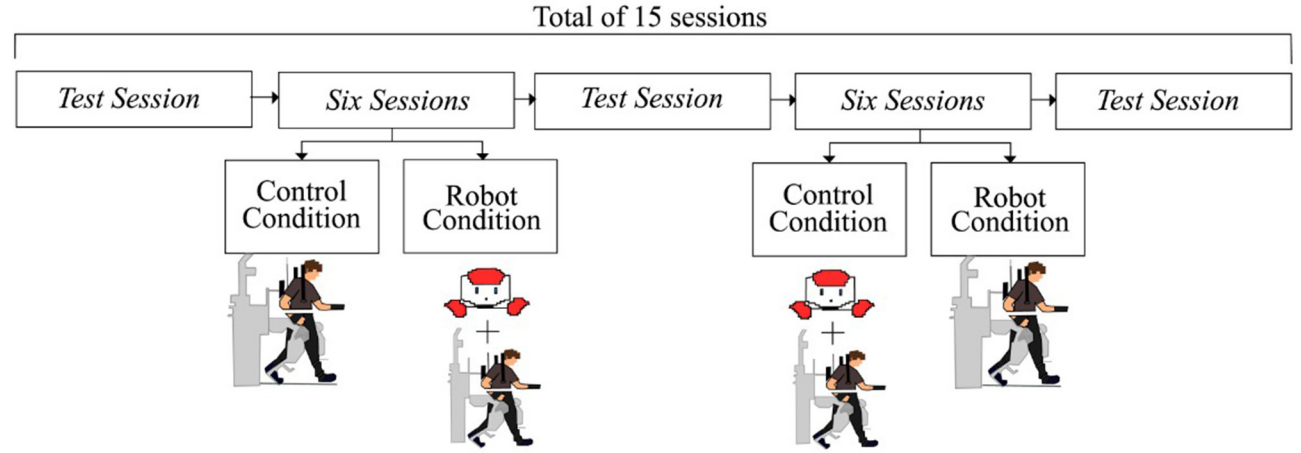

FIGURE 5 | The diagram illustrates the experimental design. *Test sessions* and six therapy sessions are developed to evaluate the robot's effects over the patients.

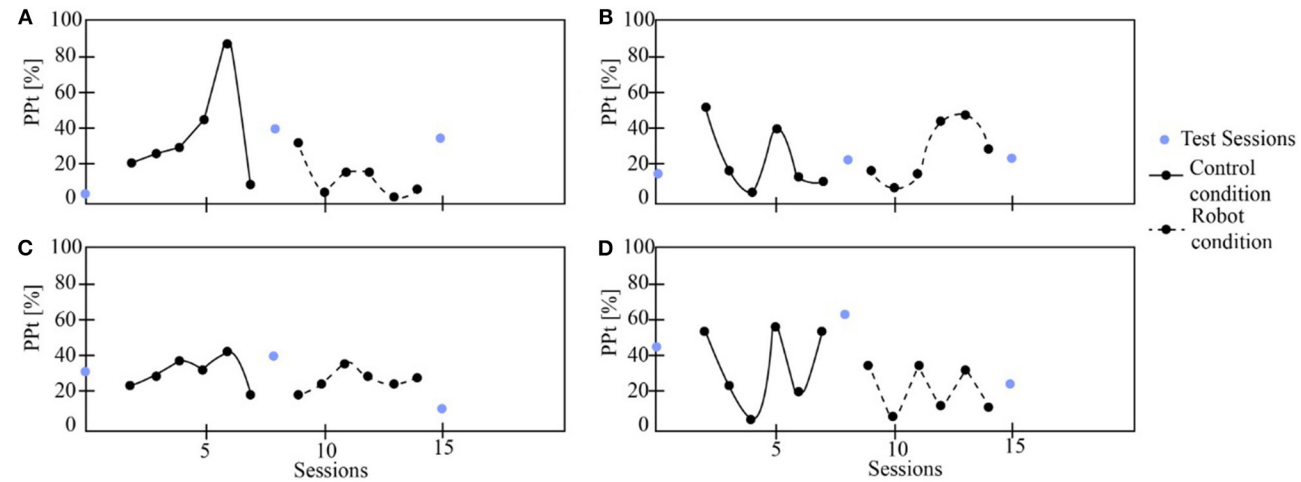

FIGURE 6 | The patient's physiological progress starts with the control condition. **(A)** Cervical PP_t (sagittal plane), **(B)** Cervical PP_t (coronal plane), **(C)** Thoracic PP_t (sagittal plane), **(D)** Thoracic PP_t (coronal plane).

considered as a healthy posture were calibrated for each patient to measure this parameter. With these values, a threshold was determined to calculate the unhealthy posture (i.e., 10 degrees over/under the threshold). Finally, the time of this event was calculated and normalized with the test sessions. Equation (1), where PPt_{norm}, is the time of unhealthy spinal posture; $PPt_{n-session}$ is the time of unhealthy spinal posture in the current session, and $PPt_{test-session}$ is the time of unhealthy spinal posture in the test session.

$$PPt_{norm} = \frac{(PPt_{n-session} - PPt_{test-session})}{PPt_{test-session}} * 100 \qquad (1)$$

Heart Rate [Bpm]: This parameter corresponds to the heart rate acquired during the rehabilitation. The parameter was averaged in each session.

Borg Scale: This parameter corresponds to the exertion perceived during the exercise. The scale used in the rehabilitation center varies between 0 (i.e., rest) and 10 (i.e., exertion perceived as high). This value was averaged in each session.

UTAUT questionnaire: A UTAUT questionnaire was applied at the end of the rehabilitation to measure the clinicians' perception and attitudes to the social robot. This measurement is based on the Almere model (Heerink et al., 2010), which evaluates the perception through different constructs: Social Presence (SP), Perceived Sociability (PS), Perceived Trust (PT), Ease of Use (EU), Safety (S), Perceived Utility (PU), and Usefulness (U). A total of 26 closed questions (answered by a Likert scale) and two open items were implemented in the questionnaire (**Supplementary Table 1**).

COVID-related questionnaire: A short-questionnaire was implemented to the clinicians' to measure their perception toward the robot during the pandemic. For instance, the

questions were related to the usability of the robot in the pandemic and how it can be a tool to support neurorehabilitation (**Supplementary Table 2**). The questionnaire was composed of six closed questions and three open questions.

A Wilcoxon Signed-Rank test was applied to compare the patient's progress in both conditions. The Wilcoxon Signed Rank is a non-parametric test used to compare two related samples (i.e., in this case compare the robot and control condition performed by the same patient) to assess whether their population mean rank differ (Wilcoxon, 1945). A descriptive analysis was performed for the closed questions in the qualitative parameters, and a textual data analysis test was performed for the open items.

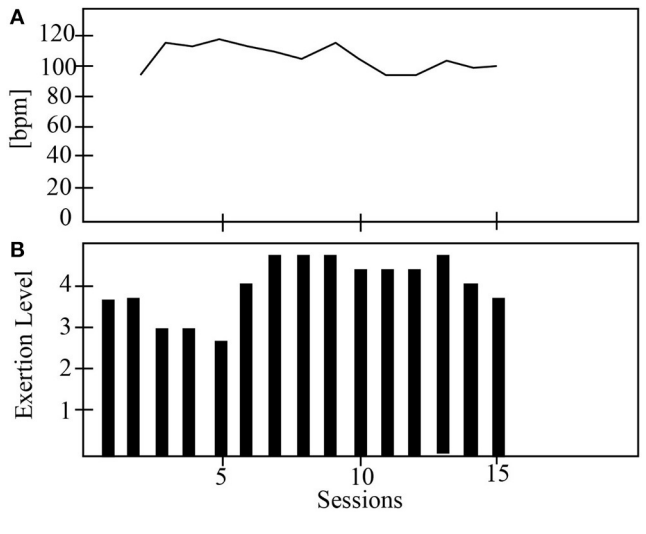

FIGURE 7 | The physiological progress of a patient that starts with the control condition. **(A)** Heart rate and **(B)** Borg scale.

4. RESULTS

As mentioned in the methodology section, two types of variables were observed (i.e., qualitative and quantitative). This section presents the results of patients who participated in the study during 15 sessions of neurorehabilitation with Lokomat.

Figures 6–9 show the patient's physiological progress regarding the cervical and thoracic posture, the heart rate, and the Borg scale. **Figure 6** shows one patient's physiological parameter that starts the study with the control condition. In the cervical posture (**Figures 6A,B**), for both planes (sagittal and coronal) the percentage of PP_t decreases when the patient performs the session with the robot. The same result can be seen for the thoracic posture (**Figures 6C,D**). Moreover, the heart rate was maintained in a healthy range considering the exercise performed during the session. Also, the Borg scale was at low-perceived level (**Figure 7**).

On the other hand, **Figure 8** presents one patient's physiological data who started the study with the robot. The cervical PP_t (sagittal and coronal planes) was lower with the social robot-assisted therapy (**Figures 8A,B**). An impressive result is that the patient tends to maintain the posture after the robot intervention (**Figure 8A**). This result could initially indicate that the patient learns how to control the cervical posture on the sagittal plane. This task corresponds to looking straight while performing the gait therapy with the Lokomat. In the case of thoracic posture (**Figures 8C,D**), it can be seen that the percentage of PP_t in this area was lower when using the robot. Finally, both the heart rate and the Borg scale were performed in healthy ranges (**Figure 9**).

Table 2 shows the *p*-values obtained after applied the Wilcoxon Signed-Rank test to the physiological data (i.e., PP_t). There is a significant difference between the control and the robot condition regarding the PP_t for sagittal and coronal plane in both spinal areas. For instance, in the robot condition the percentages where the patients maintain an unhealthy posture are lower than the control condition (**Figure 10**). This outcome

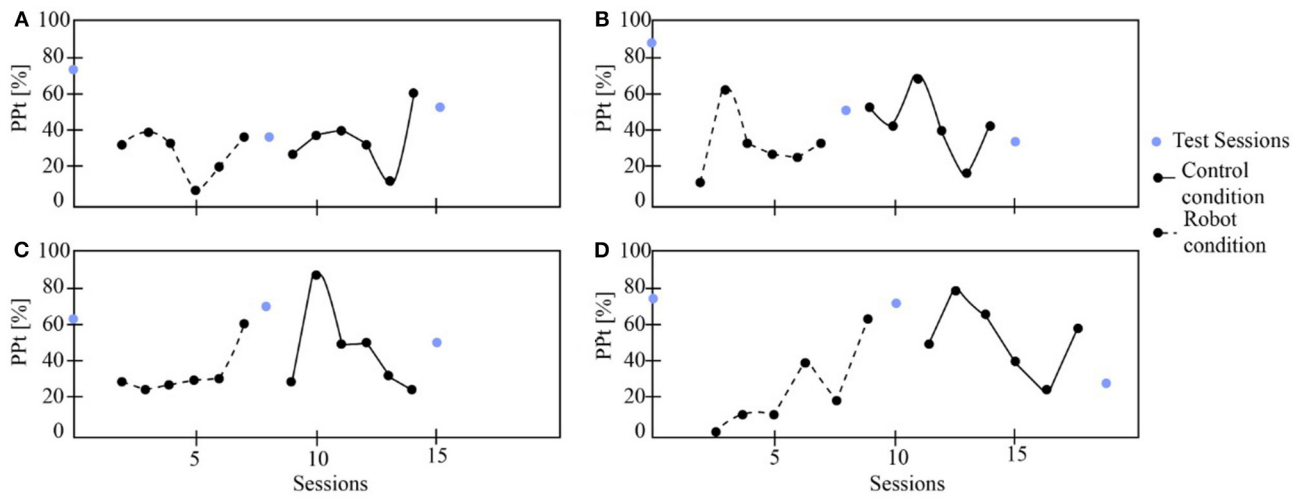

FIGURE 8 | The patient's physiological progress who starts with the robot condition. **(A)** Cervical PP_t (sagittal plane), **(B)** Cervical PP_t (coronal plane), **(C)** Thoracic PP_t (sagittal plane), **(D)** Thoracic PP_t (coronal plane).

demonstrates the positive impact of the robot during the sessions, this effect could be related to the constant feedback provided to the patients and their willingness to achieve and maintain a healthy posture during the sessions. Furthermore, the heart rate and the Borg scale parameters, do not show differences between groups. This result can be due to the high dependence of the heart rate and the Borg scale of the patient's exercise during the therapy with Lokomat.

The qualitative data analysis was performed to measure patient's interaction and attitudes toward the robot role during Lokomat therapy. **Figure 11** shows the percentage on the Likert scale regarding each construct. It can be observed, that the patients have a positive perception of the robot in most of the constructs (U, PU, S, EU, and PT). In contrast, for the social presence (SP) construct a negative perception was elucidated by the participants.

Two open questions were analyzed using the frequency of the answers regarding the essential social robot's aspects (**Figure 12**). Question 1, reflects the clinicians' perceptions regarding the social robot. The answer elucidates the platform produces feelings of *help* (28.32%) and *trust* (36.47%) to the participants. The patients also use the words *posture* (15.42%) and *motivation* (21.46%) to describe the robot. Question 2 is focused on evaluating which factors could be improved in the therapy assisted by the robot; 68.21% of the patients' answer that the robot's dialogues could be less repetitive and 33.17% recommend inserting more *sensors* to improve reliability.

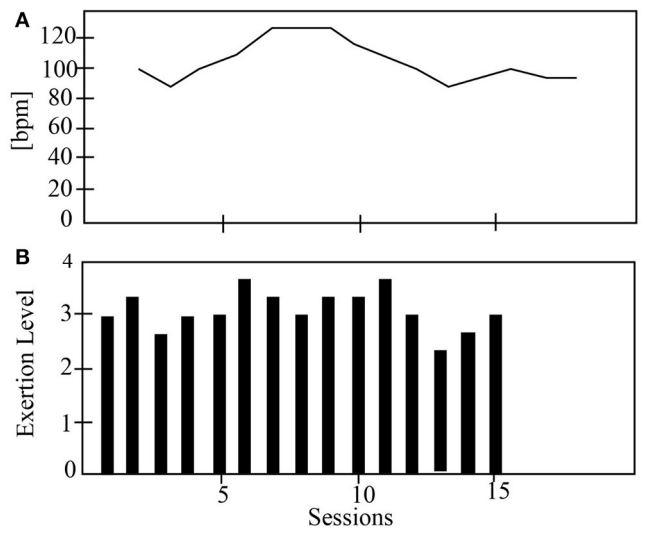

FIGURE 9 | The physiological progress of a patient starts with the robot condition. **(A)** Heart rate and **(B)** Borg scale.

Furthermore, **Figure 13** shows the results of the clinicians' perception regarding the robot's role in neurorehabilitation during the pandemic. In general, the healthcare personnel will *agree* (50%) and *totally agree* to use the robot during the pandemic, and recommend the robot to other colleagues to use the robot (Question 6). On the other hand, most clinicians agree with the fact that the robot can promote the physical distancing between the healthcare personnel and the patients. Within Question 4, a small percentage of clinicians answer that they disagree with the capability of the robot to support all of the tasks during the pandemic carried out in rehabilitation procedures. This result can be due to the limitations of the robot and highlighted in the open questions of the UTAUT questionnaire (**Figure 12**).

In the case of the open questions, the clinicians remarked on several advantages of the robot during the pandemic (e.g., *" During the pandemic using robots could promote the distancing, the visual and hearing feedback,"* *" Continuous feedback and motivation,"* *" It allows distancing, greater interaction of the patients, the robot does not condition the answers.'*). As disadvantages the health care commentaries were: *" There are limitations regarding some verbal feedback of the robot,"* and *" If the robot does not coordinate properly with the team's feedback, it can generate dispersion of attention, confusion in the orders of the therapist and the team."* Finally, as additional features the therapists suggest to increase the robot's mobility in the scenario, and add the robot's behaviors at the end of the session to give some recommendations regarding the COVID-19 pandemic.

5. DISCUSSION

This article presents a long-term study that involves ten patients who perform actively in Lokomat gait rehabilitation.

TABLE 2 | Wilcoxon ranked signed test results.

Measurement	*p*-value	PP_t Mean control condition [%]	PP_t SD Control condition [%]	PP_t Mean Robot condition [%]	PP_t SD Robot condition [%]
Cervical PP_t (sagittal plane)	**0.01**	39.18	23.05	20.41	13.18
Cervical PP_t (coronal plane)	***p*<0.01**	36.56	22.61	23.01	15.29
Thoracic PP_t (sagittal plane)	***p*<0.01**	39.31	18.70	29.10	14.39
Thoracic PP_t (coronal plane)	***p*<0.01**	46.9	19.71	30.8	17.88

Robot and control conditions comparison for intra-subject analysis. Bold values are the p-values obtained after the Wilcoxon Signed-Rank test. They are bolding as they show significant differences between the conditions applied.

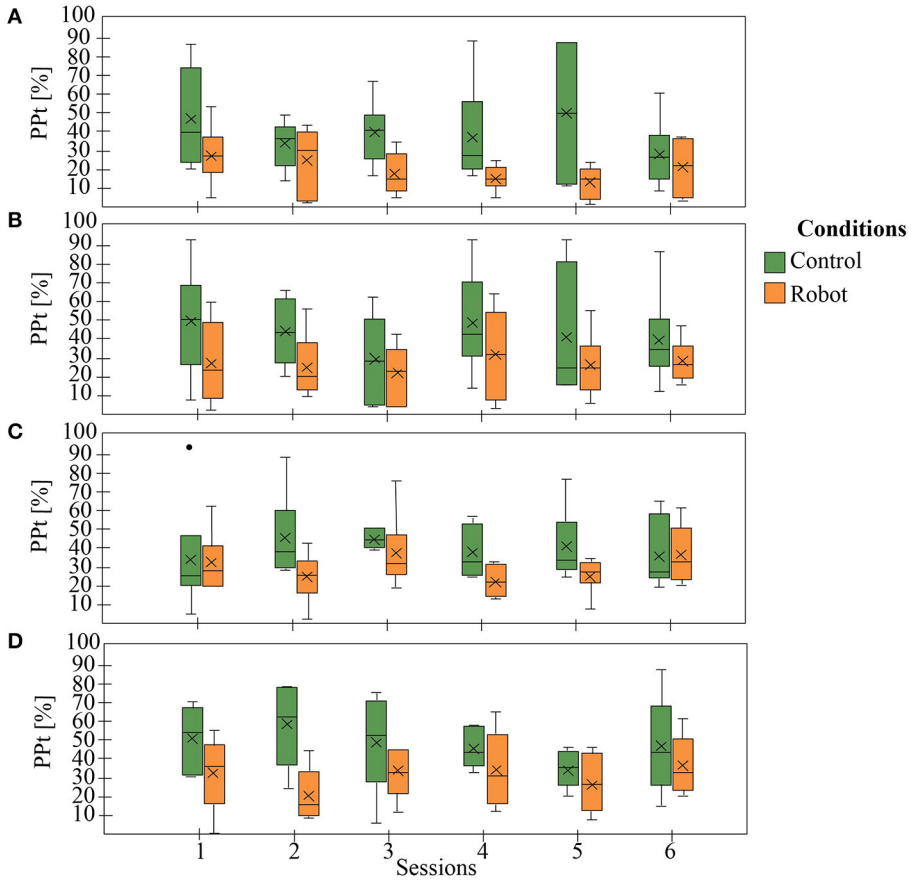

FIGURE 10 | General patient's physiological progress. **(A)** Cervical PP_t (sagittal plane), **(B)** Cervical PP_t (coronal plane), **(C)** Thoracic PP_t (sagittal plane), **(D)** Thoracic PP_t (coronal plane).

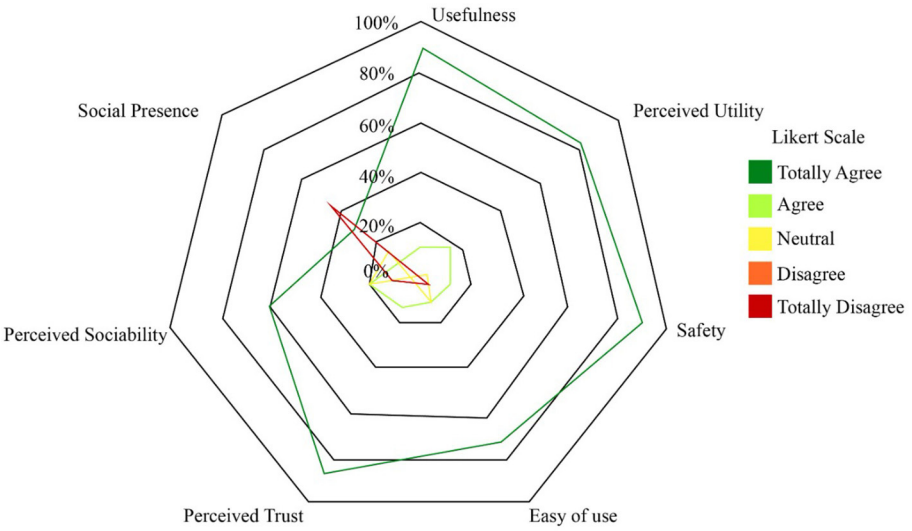

FIGURE 11 | Chart of the percentage of the number of responses for each category. Social Presence (SP), Perceived Sociability (PS), Perceived Trust (PT), Ease of Use (EU), Safety (S), Perceived Utility (PU), and Usefulness (U).

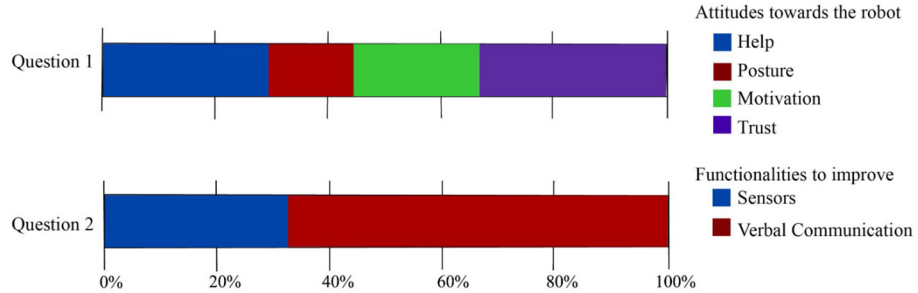

FIGURE 12 | Results regarding the open questions of the UTAUT questionnaires. Attitudes toward the robot's role in neurorehabilitation and functionalities to improve were assessed.

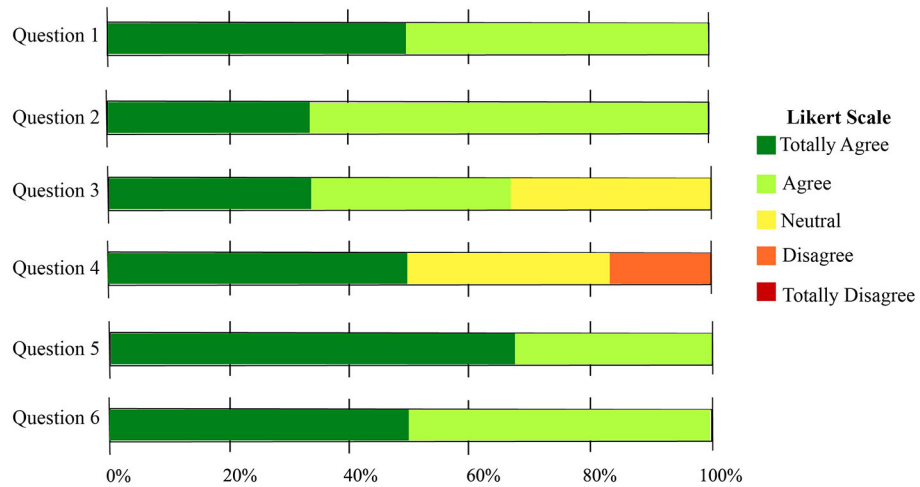

FIGURE 13 | Results regarding the closed questions of the COVID related questionnaire. The usability of the robot in a rehabilitation scenario was assessed.

A social robot supported these patients. The roles were to provide feedback and monitor the physiological progress of the patient. Two main variables were included in the study: (i) quantitative variables to measure the physiological progress, and (ii) qualitative variables to measure the interaction and patient's perception of the patients toward the robot.

The results show that the posture improves with the robot's assistance in the thoracic and cervical areas. Also, there is a statistical difference between the robot and the control condition. These results are very encouraging, as they show the robot's positive impact on the patient's physiological behavior. The feedback provided by the robot allows the patient to maintain a healthy posture and promote full gait rehabilitation. Moreover, the medical team also benefits from the robot's support, as the patient is continuously monitored and their ability to perform other tasks during the session increases. Within the study it was observed that the clinicians do not interfere with the robot's work and trust in the platform. Hence, in the COVID-19 pandemic, this tool could be handy as it allows the clinicians to complete the rehabilitation sustaining the social distancing with the patients, and decrease the contagion rate.

On the other hand, the system enables continuous monitoring of the patient. For instance, the heart rate is not measured in conventional therapies. With the system and the robot's interaction the clinicians could be warned by the robot and take action during the therapy if the patient has a high heart rate. Additionally, at the end of the rehabilitation, the clinicians could evaluate the patient progress, not only in the gait behavior but also in their cardiovascular functioning and the exertion perceived during each session. Through the questionnaire, the clinicians highlight that they trust in the system as a complementary tool in rehabilitation. Regarding the robot's role during the COVID-19 pandemic, the clinicians have a positive perception of the robot to use it as a tool to manage the rehabilitation procedures. Most of the healthcare personnel will use the robot during the pandemic, as they consider this tool can promote physical distancing and it is a secure device to carry out the healthcare protocol. Also, another encouraging result is that the clinicians will recommend the robot to other colleagues and institutions to support rehabilitation during the COVID-19 pandemic.

The qualitative results highlight the positive patient's perception and acceptance of the social robot. The patients perceived that the robot helped give feedback on the physiological parameters and maintain their healthy posture. Additionally, they considered that the system was very safe and secure as

they were continuously monitored. Within the conventional Lokomat sessions, the cardiovascular response is not measured. In this case, the clinicians and patients consider this parameter fundamental to perform a safe therapy. In contrast, the patients have a neutral perception of the social presence and robot sociability. This result can be due to the repeatability of the dialogues and the robot's behaviors during the session. The patient's commentaries suggest that a fluid speech and conversation with the robot could improve the patient-robot interaction and sociability. This limitation could be enhanced by implementing strategies (e.g., face recognition and speech recognition) in subsequent studies. For example, in Libin and Libin (2004) the use of adaptive behaviors regarding the user personality increases motivation and quality of the interaction. Furthermore, the clinicians remark to add behaviors at the end of the session where the robot can make recommendations to the patients over the COVID-19 pandemic. For instance, washing hand protocols, correct use of the mask, among others.

Although the robot's sociability was perceived as lower, the patients highlight the platform's potential in Lokomat therapy. At the end of the sessions, most of the patients suggest using the robot with other patients, due to its reliability and help during the rehabilitation procedures. Also, some patients answer that the robot could enhance the health personnel tasks, and consequently, their trust in the sessions was higher.

6. CONCLUSIONS AND FUTURE WORK

This paper presents the evaluation of a social robotic platform for neurorehabilitation with Lokomat. A total of 10 patients were evaluated during 15 sessions. The patients perform conventional and robot-assisted therapy starting the conditions randomly, to assess their performance in both scenarios.

Overall, the results evidence a positive effect of the social robot in the patient's physiological progress and interaction. The study's primary outcomes show that the patients improved their spinal posture (cervical and thoracic) when the social robot assisted them. The platform also allowed the on-line monitoring of patients' gait performance and cardiovascular functioning.

Regarding the perception, most of the patients highlight the platform's capability to aid their rehabilitation procedures and enhance the therapy for the patients and the clinicians. In contrast, they suggest that the sociability of the robot could increase using communicative and speech techniques. Thus, in future works a system that includes strategies to promote long-term interaction will be implemented. On the other hand, most of the assistive platforms as Lokomat are focused on assist the patients in a physiological way, however, the cognitive support it is essential to achieve a comprehensive procedure and adhere the patients to the treatment. In this way, SAR can be a potential tool to offer a cognitive approach and support clinicians in their tasks. These outcomes became more relevant with the COVID-19 pandemic, where clinicians need tools to assist patients in a safer manner; and the continuity of the rehabilitation is essential to maintain the patient's quality of life.

DATA AVAILABILITY STATEMENT

The raw data supporting the conclusions of this article will be made available by the authors, without undue reservation.

ETHICS STATEMENT

The studies involving human participants were reviewed and approved by The ethics committee at Colombian School of Engineering. The patients/participants provided their written informed consent to participate in this study.

AUTHOR CONTRIBUTIONS

NC developed the social robotic platform and the UTAUT questionnaires. DR performed the clinical validation of the interface and process the study's data and including the statistical analysis. NC and DR led the manuscript writing. MM developed the experimental protocol. CC proposed and supervised the structure of the paper. MM and CC were involved in the revising and correcting the manuscript. All authors contributed to the article and approved the submitted version.

FUNDING

This work was financially supported by the *Ministerio de Ciencia, Tecnología e Innovación* (Grant 801-2017) and the Royal Academy of Engineering - Pandemic Preparedness (Grant EXPP20211\1\183).

ACKNOWLEDGMENTS

This work was carried out in collaboration with the Mobility group rehabilitation center, where the experiments and protocols were performed. The authors acknowledge the work of patients and therapist who were involved in this study.

SUPPLEMENTARY MATERIAL

The Supplementary Material for this article can be found online at: https://www.frontiersin.org/articles/10.3389/fnbot.2021.612034/full#supplementary-material

REFERENCES

Agrigoroaie, R. M., and Tapus, A. (2016). "Developing a healthcare robot with personalized behaviors and social skills for the elderly," in *International Conference on Human Robot Interaction* (Christchurch). doi: 10.1109/HRI.2016.7451870

Aymerich-Franch, L. (2020). Why it is time to stop ostracizing social robots. *Nat. Mach. Intell.* 2:364. doi: 10.1038/s42256-020-0202-5

Bickmore, T. W., and Picard, R. W. (2005). Establishing and maintaining long-term human- computer relationships. *ACM Trans. Comput. Hum. Interact.* 2, 617–638. doi: 10.1145/1067860.1067867

Campa, R., and Campa, R. (2016). The rise of social robots: a review of the recent literature. *J. Evol. Technol.* 26, 106–113.

Carrillo, F. M., Butchart, J., Knight, S., Scheinberg, A., Wise, L., Sterling, L., et al. (2017). Adapting a general purpose social robot for paediatric rehabilitation through *in-situ* design. *ACM Trans. Hum. Robot Interact.* 7, 1–30. doi: 10.1145/3203304

Casas, J., Senft, E., Gutierrez, L., Rincon-Roncancio, M., Munera, M., Belpaeme, T., et al. (2020). Social assistive robots: assessing the impact of a training assistant robot in cardiac rehabilitation. *Int. J. Soc. Robot.* 12, 1–15. doi: 10.1007/s12369-020-00708-y

Casas, J. A., Céspedes, N., Cifuentes, C. A., Gutierrez, L. F., Rincón-Roncancio, M., and Múnera, M. (2019). Expectation vs. reality: attitudes towards a socially assistive robot in cardiac rehabilitation. *Appl. Sci.* 9:4651. doi: 10.3390/app9214651

Cespedes, N., Munera, M., Gomez, C., and Cifuentes, C. A. (2020). Social human-robot interaction for gait rehabilitation. *IEEE Trans. Neural Syst. Rehabil. Eng.* 18, 1299–1307. doi: 10.1109/TNSRE.2020.2987428

Cifuentes, C. A., Pinto, M. J., Céspedes, N., and Múnera, M. (2020). Social robots in therapy and care. *Curr. Robot. Rep.* 28, 1–16. doi: 10.1007/s43154-020-00009-2

Compagnant, M., Daviet, J. C., Mandigout, S., Lcroix, J., Vuillerme, N., and Salle, J. Y. (2017). Reliability of the rating of perceived exertion (Borg Scale) in post-stroke during 2 tasks of daily life. *Ann. Phys. Rehabil. Med.* 60, e1–e2. doi: 10.1016/j.rehab.2017.07.017

Daroff, R. (2016). *Bradley's Neurology in Clinical Practice*. London: Elsevier.

Duffy, B. R., Rooney, C. F. B., Hare, G. M. P. O., and Donoghue, R. P. S. O. (1999). "What is a social robot?" in *10th Irish Conference on Artificial Intelligence Cognitive Science* (Ireland), 1–3.

Fasola, J., and Matarić, M. J. (2010). "Robot exercise instructor: a socially assistive robot system to monitor and encourage physical exercise for the elderly," in *Proceedings - IEEE International Workshop on Robot and Human Interactive Communication* (Viareggio), 416–421. doi: 10.1109/ROMAN.2010.5598658

Feil-Seifer, D., and Matarić, M. J. (2011). Socially assistive robotics. *IEEE Robot. Automat. Mag.* 18, 24–31. doi: 10.1109/MRA.2010.940150

Gittler, M., and Andrew, M. D. (2018). Guidelines for adult stroke rehabilitation and recovery. *JAMA* 319, 820–821. doi: 10.1001/jama.2017.22036

Heerink, M., Kröse, B., Evers, V., and Wielinga, B. (2010). Assessing acceptance of assistive social agent technology by older adults: the almere model. *Int. J. Soc. Robot.* 2, 361–375. doi: 10.1007/s12369-010-0068-5

Heerink, M., Vanderborght, B., Broekens, J., and Albo-Canals, J. (2016). New friends: social robots in therapy and education. *Int. J. Soc. Robot.* 8, 443–444. doi: 10.1007/s12369-016-0374-7

Hollander, J. E., and Carr, B. G. (2020). Virtually perfect? Telemedicine for Covid-19. *N. Engl. J. Med.* 382, 1679–1681. doi: 10.1056/NEJMp2003539

Jarvis, C. I., Van Zandvoort, K., Gimma, A., Prem, K., Auzenbergs, M., O'Reilly, K., et al. (2020). Quantifying the impact of physical distance measures on the transmission of COVID-19 in the UK. *BMC Med.* 18:124. doi: 10.1186/s12916-020-01597-8

Kasap, Z., and Magnenat-Thalmann, N. (2012). Building long-term relationships with virtual and robotic characters: the role of remembering. *Vis. Comput.* 28, 87–97. doi: 10.1007/s00371-011-0630-7

Khaleghi, A., Mohammadi, M. R., Jahromi, G. P., and Zarafshan, H. (2020). New ways to manage pandemics: using technologies in the era of COVID-19, a narrative review. *Iran J. Psychiatry* 15, 236–242. doi: 10.18502/ijps.v15i3.3816

Kozyavkin, V., Kachmar, O., and Ablikova, I. (2014). "Humanoid social robots in the rehabilitation of children with cerebral palsy," in *Proceedings - REHAB 2014* (Tomar), 430–431. doi: 10.4108/icst.pervasivehealth.2014.255323

Leocani, L., Diserens, K., Moccia, M., and Caltagirone, C. (2020). Disability through COVID-19 pandemic: neurorehabilitation cannot wait. *Eur. J. Neurol.* 27, 50–51. doi: 10.1111/ene.14320

Libin, A. V., and Libin, E. V. (2004). Person-robot interactions from the robopsychologists' point of view: the robotic psychology and robotherapy approach. *Proc. IEEE* 92, 1789–1803. doi: 10.1109/JPROC.2004.835366

Martín, A., Pulido, J. C., González, J. C., García-Olaya, Á., and Suárez, C. (2020). A framework for user adaptation and profiling for social robotics in rehabilitation. *Sensors* 20, 1–23. doi: 10.3390/s20174792

Matarić, M. J., Eriksson, J., Feil-Seifer, D. J., and Winstein, C. J. (2007). Socially assistive robotics for post-stroke rehabilitation. *J. Neuroeng. Rehabil.* 4:5. doi: 10.1186/1743-0003-4-5

Peleka, G., Kargakos, A., Skartados, E., Kostavelis, J., Giakoumis, D., Sarantopoulos, I., et al. (2018). "RAMCIP - a service robot for MCI patients at home," in *2018 IEEE/RSJ International Conference on Intelligent Robots and Systems (IROS)* (Madrid), 1–9.

Polak, R. F., and Levy-Tzedek, S. (2020). "A social robot for rehabilitation: expert clinicians and post-stroke patients' evaluation following a long-term intervention," in *ACM/IEEE International Conference on Human-Robot Interaction* (New York, NY: IEEE Computer Society), 151–160.

Pulido, J. C., González, J. C., Suárez-Mejías, C., Bandera, A., Bustos, P., and Fernández, F. (2017). Evaluating the child-robot interaction of the NAOTherapist platform in pediatric rehabilitation. *Int. J. Soc. Robot.* 9, 343–358. doi: 10.1007/s12369-017-0402-2

Robinson, H., MacDonald, B., Kerse, N., and Broadbent, E. (2013). The psychosocial effects of a companion robot: a randomized controlled trial. *J. Am. Med. Direct. Assoc.* 14, 661–667. doi: 10.1016/j.jamda.2013.02.007

Russo, L., and Trabacca, A. (2020). The ethic of care, disability and rehabilitation during the Covid-19 pandemic. *Pediatr. Neurol.* 111:39. doi: 10.1016/j.pediatrneurol.2020.06.006

Sabelli, A., Way, M., and Hagita, N. (2011). "A conversational robot in an elderly care center: an ethnographic study," in *HRI 2011 - Proceedings of the 6th ACM/IEEE International Conference on Human-Robot Interaction* (Lausanne), 37–44. doi: 10.1145/1957656.1957669

Sakel, M., Saunders, K., Chandi, J., Haxha, S., and Faruqui, R. (2020). Neuro-rehabilitation service during COVID-19 pandemic: best practices from UK. *J. Pakistan Med. Assoc.* 70, S136–S140. doi: 10.5455/JPMA.33

Sante, H. A. D. (2012). *Accident Vasculaire Cerebral: Methodes de Reeducation de la fonction Motrice chez l'adulte*. Haute Autorite de Sante, Saint-Denis La Plaine Cedex.

Scassellati, B., and Vázquez, M. (2020). The potential of socially assistive robots during infectious disease outbreaks. *Sci. Robot.* 5:eabc9014. doi: 10.1126/scirobotics.abc9014

Swinnen, E., Lefeber, N., Willaert, W., De Neef, F., Bruyndonckx, L., Spooren, A., et al. (2017). Motivation, expectations, and usability of a driven gait orthosis in stroke patients and their therapists. *Top. Stroke Rehabil.* 24, 299–308. doi: 10.1080/10749357.2016.1266750

Tavakoli, M., Carriere, J., and Torabi, A. (2020). Robotics, smart wearable technologies, and autonomous intelligent systems for healthcare during the COVID-19 pandemic: an analysis of the state of the art and future vision. *Adv. Intell. Syst.* 2:2000071. doi: 10.1002/aisy.202000071

Weaver, L. J., and Ferg, A. L. (2020). *Therapeutic measurement and testing*. Clifton Park, NY: Delmar Cengage Learning.

WHO (2020). *Coronavirus Disease 2019, Situation Report-192*. doi: 10.1213/XAA.0000000000001218

Wilcoxon, F. (1945). Individual comparisons by ranking methods. *Biometr. Bull.* 1:80. doi: 10.2307/3001968

Winkle, K., Caleb-Solly, P., Turton, A., and Bremner, P. (2018). "Social robots for engagement in rehabilitative therapies: design implications from a study with therapists," in *Proceedings of the 2018 ACM/IEEE International Conference on Human-Robot Interaction (HRI '18)* (New York, NY: Association for Computing Machinery), 289–297. doi: 10.1145/3171221.3171273

Yang, L., Cheng, H., Hao, J., Ji, Y., and Kuang, Y. (2015). "A survey on media interaction in social robotics," in *Lecture Notes in Computer Science* (Gwangju: Springer Verlag), 181–190. doi: 10.1007/978-3-319-24078-7_18

Zhang, J., Litvinova, M., Liang, Y., Wang, Y., Wang, W., Zhao, S., et al. (2020). Changes in contact patterns shape the dynamics of the COVID-19 outbreak in China. *Science* 368, 1481–1486. doi: 10.1126/science.abb8001

Conflict of Interest: The authors declare that the research was conducted in the absence of any commercial or financial relationships that could be construed as a potential conflict of interest.

frontiers in Robotics and AI

MINI REVIEW
published: 25 February 2021
doi: 10.3389/frobt.2021.612852

Guidelines for Robotic Flexible Endoscopy at the Time of COVID-19

Onaizah Onaizah[1], Zaneta Koszowska[1], Conchubhair Winters[2], Venkatamaran Subramanian[2], David Jayne[2], Alberto Arezzo[3], Keith L. Obstein[4,5] and Pietro Valdastri[1]**

[1]School of Electronic and Electrical Engineering, University of Leeds, Leeds, United Kingdom, [2]Leeds Institute of Medical Research, University of Leeds, Leeds, United Kingdom, [3]Department of Surgical Sciences, University of Torino, Torino, Italy, [4]Department of Gastroenterology, Hepatology, Nutrition, Vanderbilt University Medical Center, Nashville, TN, United States, [5]Department of Mechanical Engineering, Vanderbilt University, Nashville, TN, United States

Flexible endoscopy involves the insertion of a long narrow flexible tube into the body for diagnostic and therapeutic procedures. In the gastrointestinal (GI) tract, flexible endoscopy plays a major role in cancer screening, surveillance, and treatment programs. As a result of gas insufflation during the procedure, both upper and lower GI endoscopy procedures have been classified as aerosol generating by the guidelines issued by the respective societies during the COVID-19 pandemic—although no quantifiable data on aerosol generation currently exists. Due to the risk of COVID-19 transmission to healthcare workers, most societies halted non-emergency and diagnostic procedures during the lockdown. The long-term implications of stoppage in cancer diagnoses and treatment is predicted to lead to a large increase in preventable deaths. Robotics may play a major role in this field by allowing healthcare operators to control the flexible endoscope from a safe distance and pave a path for protecting healthcare workers through minimizing the risk of virus transmission without reducing diagnostic and therapeutic capacities. This review focuses on the needs and challenges associated with the design of robotic flexible endoscopes for use during a pandemic. The authors propose that a few minor changes to existing platforms or considerations for platforms in development could lead to significant benefits for use during infection control scenarios.

Keywords: robotic flexible endoscopy, endoscopes, gastrointestinal, infection control, aerosol generating procedure, COVID-19

OPEN ACCESS

Edited by:
Mahdi Tavakoli, University of Alberta, Canada

Reviewed by:
J. Micah Prendergast, Delft University of Technology, Netherlands
Antonia Tzemanaki, University of Bristol, United Kingdom

****Correspondence:***
Pietro Valdastri
p.valdastri@leeds.ac.uk
Onaizah Onaizah
o.onaizah@leeds.ac.uk

Specialty section:
This article was submitted to Biomedical Robotics, a section of the journal Frontiers in Robotics and AI

Received: *30 September 2020*
Accepted: *20 January 2021*
Published: *25 February 2021*

Citation:
Onaizah O, Koszowska Z, Winters C, Subramanian V, Jayne D, Arezzo A, Obstein KL and Valdastri P (2021) Guidelines for Robotic Flexible Endoscopy at the Time of COVID-19. Front. Robot. AI 8:612852. doi: 10.3389/frobt.2021.612852

ENDOSCOPY DURING COVID-19

COVID-19

On March 11th, the WHO (World Health Organization) declared COVID-19 caused by the SARS-CoV-2 virus a pandemic. There have been over 94 million cases reported and over two million fatalities worldwide (Johns Hopkins University Coronavirus Center, 2020) as of January 2021. The main symptoms include fever, cough, change in smell or taste, breathlessness, and weakness with many people also reporting gastrointestinal symptoms such as abdominal pain, diarrhoea and vomiting. A small percentage develop acute respiratory distress syndrome (ARDS) which can be fatal. Human-to-human transmission primarily occurs through direct contact or droplets (Repici et al., 2020), with smaller droplets (often called aerosols) having the potential to remain airborne for an extended period of time and thus travel

much larger distances. This means they cannot be tackled simply by physical distancing measures employed whereas larger particles are immediately pulled down due to gravity and risks can be mitigated with physical distancing measures.

Endoscopy is considered a high-risk procedure due to the proximity of health care workers (HCW) to patients and the potential for aerosol generation. Recent work has shown that endoscopists without proper face protection such as a face visor could be at an increased risk to bacterial pathogens (Johnston et al., 2019). Many studies have since shown that a face visor is also not adequate face protection from droplets (Akagi et al., 2020). Studies from the SARS-CoV-2 outbreak have shown that droplets could easily reach 6 ft (~2 m) from an infected patient thereby putting HCW in endoscopy units at risk (Wong et al., 2004).

Conventional Endoscopy

Endoscopy is a procedure where organs and tissues inside the body can be imaged and monitored using an endoscope. An endoscope is a thin tube with a light source and camera, often with additional tools, for example ultrasound or a working channel for introduction of biopsy forceps or therapeutic equipment. Endoscopy can be used for diagnostic (visualisation and sampling) and therapeutic purposes such as removing cancer tissue. An endoscope can be either rigid or flexible; with flexible endoscopes offering a multitude of advantages for navigation to target sites. Endoscopes can be inserted through natural orifices like the mouth, anus or urethra or via incisions made in the body. Flexible endoscopy is often used as a diagnostic tool for many types of cancer and diseases and thus plays a vital role in the management of multiple malignancies. There are many different types of endoscopy from bronchoscopy (monitoring the lungs) to hysteroscopy (monitoring the uterus) and cystoscopy (monitoring the bladder); however, for the purposes of this review we will limit our focus to flexible gastrointestinal (GI) endoscopy. There are a range of flexible GI endoscopies including esophagogastroduodenoscopy (EGD–for assessing esophagus, stomach, and duodenum), colonoscopy (for assessing the large bowel), sigmoidoscopy (for the rectum and sigmoid colon), endoscopic retrograde cholangiopancreatography (ERCP–for assessing the biliary tree and pancreatic ducts), and enteroscopy (for assessing the small intestine).

Colorectal cancer is the third most common cancer in the world in terms of mortality and fourth most common in terms of incidence reaching nearly two million cases and one million fatalities in 2018 according to some projections (Rawla et al., 2019). Colonoscopy can detect and remove pre-cancerous tissue in the colon, thus preventing the development of colorectal cancers. GI endoscopies are also the gold standard investigative method in the diagnosis and surveillance of a large variety of conditions such as celiac disease, and inflammatory bowel diseases. In 2014, it was projected that there will be over 75 million gastrointestinal endoscopic procedures performed by 2020 in Europe and the United States alone (Lau, 2014). There were more than two million total GI procedures in the United Kingdom in 2019 (Ravindran et al., 2020) and over 17 million total GI procedures in the United States in 2013 (Peery et al., 2019).

Conventional endoscopy uses a semi-rigid tube and manoeuvring the endoscope is performed manually by rotation of a set of wheels on the handle and by pushing, pulling, and torqueing the insertion tube of the endoscope. Many procedures are uncomfortable or painful, requiring analgesia and sedation. A typical GI endoscopy process requires multiple HCW inside the room–an endoscopist, an assistant/technician, and a nurse to monitor the patient. For general anaesthetic and fluoroscopic procedures, this could potentially include anaesthesiologists and radiographers. Typical pre-pandemic personal protective equipment (PPE) for these processes consisted of gloves, gown/apron, and eye protection.

COVID-19 Related Risks During Flexible GI Endoscopy

Some endoscopic procedures are considered aerosol generating procedures (AGPs). Aerosols are small particles/droplets below 5 μm that can remain airborne for an extended period of time. One of the postulated sources of aerosol generation during endoscopy procedures is related to gas insufflation. Positive insufflation is used to visualize the lumen and create space to move the instrument forward. The potential generation of aerosols during endoscopy could pose a risk to HCW.

Evidence of aerosols generated during different endoscopic procedures varies and there is no homogeneity of evidence. Endoscopic procedures such as bronchoscopy have been shown to be aerosol generating along with several other patient care and operating room procedures (Mittal et al., 2020; Thamboo et al., 2020; Wahidi et al., 2020). However, for GI endoscopic procedures, no current evidence exists of aerosol generation and advice from respective societies around infection control (IC) is based on expert opinion (Chai et al., 2020; Mahadev et al., 2020; Repici et al., 2020; Tse et al., 2020). A well-designed study is needed to address this knowledge gap in the field that would allow tailored advice for specific endoscopic procedures.

Upper GI procedures are considered a greater risk during the current pandemic because the virus has been shown to be transmissible through airway secretions. The risk for lower GI procedures (e.g. colonoscopy and sigmoidoscopy) is less clear, although SARS studies have shown the presence of coronavirus in stool samples and in intestinal biopsy samples (Isakbaeva et al., 2004; Pan et al., 2020) and there is some data regarding the dispersion of microorganisms throughout an endoscopy suite during colonoscopy (Vavricka et al., 2010). There has also been some focus on identifying a COVID-19 outbreak through wastewater at several institutions in the United States, which would suggest either the presence of the virus or viral RNA in stool samples (Cahill and Morris, 2020). For now, most guidelines from gastroenterology societies have classified all GI endoscopic procedures as AGPs (Chai et al., 2020; Mahadev et al., 2020; Repici et al., 2020; Tse et al., 2020). Therefore, PPE has been enhanced during the COVID-19 pandemic to include a full sleeve

TABLE 1 | Examples of robotic flexible endoscopy (RFE) platforms.

Device	Actuation and features	Outcome of clinical studies
Aer-O-Scope system (GI view, ramat Gan, Israel) (Pfeffer et al. (2006); Gluck et al. (2016))	Two cameras, one front viewing and second giving a 360° panoramic view that can see behind folds, disposable, tip-pulling locomotion, computer aided control, no steering or instrument channel	Cecal intubation was successful in 55/56 recruited patients (98.2%). System detected 87.6% of polyps. No mucosal damage or adverse events were reported. *Available on the market.*
Neo-guide endoscopy system (NeoGuide endoscopy system Inc., Los Gatos, CA, United States) (Eickhoff et al. (2007))	Electromechanical actuation of 2 independent 2 DOF segments to achieve snake - like motion, shape retention, instrument channel, 3D map of the device, computer-aided control, reusable so requires cleaning, large diameter	Cecal intubation was successful in 10 patients in the time range 24–60 min. No longer available on the market.
Invedosacope TMSC40 (Invendo medical GmbH, Weinheim, Germany and AMBU A/S, Copenhagen, Denmark) (Rosch et al. (2008); Groth et al. (2011); Yeung et al. (2019))	Disposable colonoscope (10 mm in diameter, with a 3.1-mm working channel), controlled electro-hydraulically by actuators placed outside the patient, operator controlled with a joystick interface, disposable, instrument channel, diameter similar to a colonoscope	Cecal intubation was successful in 98.4%, reported to be painless in 92% of patients. No longer available on the market.
Endotics (ERA endoscopy SRL, Peccioli, Italy) (Cosentino et al. (2009); Tumino et al. (2010); Tumino et al. (2017))	Inchworm movements, disposable, steerable tip with integrated camera and light source, computer-aided control, thin tip, no instrument channel, and procedure times longer than colonoscopy	Significantly lower patient discomfort and was also able to complete 93% of colonoscopies that were left incomplete through conventional colonoscopy Available on the market.
Consis medical (Beer'Sheva, Israel) (Yeung et al. (2019))	Consists of an inverted sleeve that self-propels through the colon using hydraulic aided propulsion. The sleeve is disposable, while the device head is a capsule that can be sterilised.	No available clinical studies
NaviCam® (Ankon technologies co, Ltd. Wuhan, Shanghai, China) (Liao et al. (2016))	A wireless capsule endoscope that can be actuated internally by an external magnetic field.	Mean duration of examination was 25 ± 7 min. Anxiety, discomfort and pain scores (worst-best = 0–10) were 1 ± 0, 1.3 ± 0.6, and 1 ± 0 respectively.
Magnetic flexible endoscope (MFE)(STORM Lab, Leeds, United Kingdom/Nashville, TN, United States) (Martin et al. (2020))	Relies on actuation using a permanent magnet manipulated by a robot that is external to the patient; no push activation, instrument channel, large one-time robot cost and complexities around magnetic control	Currently undergoing human trials

gown, an FFP3/N95 mask, gloves, face visor or goggles, shoe covers, and a surgical hair cap.

Potential for Innovation

Despite significant advances in the imaging capabilities of endoscopes, the controls remain largely unchanged in the last 60 years. The rear steering approach of conventional colonoscopy for example stretches the bowel and surround mesentery which makes it uncomfortable and often requires sedation or analgesia. While many new devices are being developed to attempt to address the shortfalls of conventional endoscopy (**Table 1**), COVID-19 has further highlighted the need for innovation in the field of flexible endoscopy. One such improvement is the use of disposable endoscopes that have already gained popularity due to concerns around duodenoscope related infection and infected biofilm in endoscope channels (Rauwers et al., 2018; Balan et al., 2019). There is also a considerable argument for a single use endoscope in reducing the running costs of departments by preventing the need for costly decontamination facilities and supplies (Larsen et al., 2020). The current pandemic has increased the awareness of IC, and the time has come to explore single use endoscopes further.

Another avenue of improvement in endoscopy is through robotic advancements, which have the potential to reduce pain and widen the availability of procedures as they often place a lower cognitive and physical (improved ergonomics) burden on the operator and thus require less training. Robotic flexible endoscopy (RFE) can offer many advantages in general and specifically when dealing with IC related to aerosol generation. During the time of COVID-19, these include introducing physical distancing between HCW and patients (enabled as a result of teleoperation) as well as reduce the number of HCW in the endoscopy suite. In this review, we explore the impact of COVID-19 on GI endoscopy processes and how robotic flexible endoscopic platforms can be designed to minimize these impacts and improve IC mechanisms.

IMPACT OF COVID-19 ON FLEXIBLE GI ENDOSCOPY

Reduction of GI Endoscopic Capacity and Its Long-Term Implication

Due to COVID-19 guidance, endoscopic procedures were significantly reduced during the pandemic to acute, urgent cases. In Europe, the volume of these procedures fell to 15% of previous capacity between February to May 2020 during the peak of the pandemic, while in North America, these levels were at 10% (Parasa et al., 2020). The National Endoscopy Database (The National Endoscopy Database, 2020) shows that endoscopic procedures fell to about 5% of normal levels in the United Kingdom. They were down from about 35,000 reported procedures per week to 1,700 for the week ending April 13th, 2020. When compared to 2019 levels in the

United Kingdom, 51% more people were waiting for colonoscopies, 46% more for flexible sigmoidoscopies and 44% more patients were waiting for gastroscopies as of July 2020 (Cancer Research UK, 2020). While these numbers are specifically focused on the United Kingdom, a similar trend was seen worldwide in almost every national healthcare system. The statistics in this review are sometimes focused on the United Kingdom and United States as these are just a result of easily accessible data. It is estimated that for every week that screening is paused, 7,000 people are not being referred for further tests and 380 cancers are not being diagnosed through screening programs in the United Kingdom (Roberts, 2020).

Avoidable deaths due to suspended screening and treatment are expected to rise significantly with an estimated increase of more than 6,000 excess deaths in the United Kingdom and more than 33,000 excess deaths in the US (Lai et al., 2020). Endoscopic capacity has still not been restored to pre-pandemic levels (at 80% in September 2020) and with a second wave imminent, it becomes important to set the scene for future IC measures and to understand how RFE can service this need.

Current endoscopic procedures rely on PPE (enhanced during COVID-19), comprehensive room and equipment cleaning and of course air circulation (Garbey et al., 2020) which can vary for endoscopy suites. Despite concerns around patient exposure to the virus due to contaminated endoscopes, evidence suggests that reprocessing agents with viricidal activity will remove the SARS-CoV-2 virus (Kampf et al., 2020; Rai, 2020). In the past, certain bacteria were not successfully removed from duodenoscopes (Rauwers et al., 2018; Balan et al., 2019), starting a push for disposable endoscopes. There is some evidence of bronchoscope contamination (Ofstead et al., 2020), and therefore single-use endoscopes are considered safer, with potential cost savings in the long run from not having large-scale cleaning facilities on premises.

Other Infection Control Measures

Another IC technique has been to adapt the current facilities such as the endoscopy suite to increase safety during the COVID-19 pandemic. Modified face masks or boxes have been developed as mechanical barriers (Narwani et al., 2020; Tsui, 2020). Paired with CO_2 extractors or suction mechanism, they create negative pressure zones with the potential of eliminating (or significantly reducing) aerosols escaping the procedure site and travelling around the suite. None of the mentioned risk minimizing techniques have been quantified and the evidence around aerosol dispersion while using these methods has not been published. There is a clinical need to quantify aerosol generation during standard flexible endoscopic procedures as well as robot assisted approaches. Apart from that, there is a need for evaluation of mechanical barriers and extractors currently employed in the hospitals to provide best and uniform guidelines for clinicians working during a pandemic. Air filtration is another key aspect in reducing HCW exposure to any potential aerosols (Garbey et al., 2020).

The Ideal RFE

A flexible robotic endoscopic platform must be able to meet certain needs during COVID-19. A teleoperated platform would allow physical distancing between the patient and HCW. A simple and easy to use robotic platform could reduce the number of people in the room allowing reallocation of staff at a crucial time and putting fewer HCW at risk during each procedure. A less painful procedure which does not require sedation would also reduce the number of people in the room. More intuitive navigation will reduce training times for future endoscopists. A RFE platform would preferably have higher degrees-of-freedom (DOF) than current commercial platforms and improved control. In addition, AI systems can be used for improved navigation and localization of endoscopes using data from both imaging and on-board sensing. This increased control and better visibility of the intestine would improve detection rates while allowing procedures such as tissue sampling and cancer removal to be performed. By reducing the force and torque exerted on the luminal wall, patient discomfort can be reduced in addition to sedation requirements thus lowering risk and recovery times. Finally, it is important to consider the environmental impacts of single-use endoscopes and using recyclable materials would be beneficial for future platforms.

ROBOTIC FLEXIBLE GI ENDOSCOPY

The motivation for developing robotic platforms in endoscopy is similar to the motivation in other biomedical areas such as robotically assisted surgery. These robotic platforms allow HCW to overcome the current limitations of standard endoscopic devices for diagnostic and therapeutic procedures. These platforms can be used to improve the precision and safety of the tools thus making them more reliable and effective (Boškoski and Costamagna, 2019). The challenges for these platforms are around locomotion of endoscopes and instrument control as well as their applicability to a wide variety of clinical applications. RFE has the potential to increase safety of procedures by lowering risk of tissue damage due to human error and lower the rates of complications.

RFE has the potential to meet the needs of enhanced IC measures during COVID-19 and future pandemics. Remotely controlled devices increase the distance between patient and operator, hence less aerosol and droplet contact and reduced infection risk for HCW (Wong et al., 2004). Easy to operate robotic platforms could also help to reduce the HCWs in the room and reduce training times. It could also be extremely useful in cases where precise fine motor skills are required and cannot be met by normal human dexterity by improving the control and precision of endoscopes in robotic platforms (Lucarini et al., 2015). This will improve the speed and accuracy of procedures which will reduce adverse effects and discomfort during the procedure. Both will result in patients spending less time in the endoscopy suite.

Advantages of RFE

With the potential advantage of lowering discomfort for patients, RFE can be used in cases where the patient is unable to tolerate conventional endoscopy or in cases where frailty and co-morbidity rule out the use of sedation during conventional

endoscopy procedures. This will be achieved by having precise control over the force and torque applied to the luminal walls through force feedback. It will be hugely beneficial in cases where patients require repeated and regular procedures (e.g. surveillance in those with inflammatory bowel disease, or hereditary colorectal cancer) where using a less painful procedure will enhance surveillance uptake. It can also help to improve detection rates as more control and more comfort means better visibility. Another gap that RFE could fill is in cases where conventional endoscopes are unable to complete an examination.

While RFE is a potential solution for diagnostic endoscopy and therapeutic procedures in the GI tract, challenges remain due to the limited DOF of such platforms. Therefore, current RFE research focuses on increasing the manoeuvrability and control of the tools to enable more complex and varied interventions. Flexible endoscope manipulations common to most systems are shaft insertion and tip steering. These complex movements add difficulty in developing robot-assisted flexible endoscopes.

Examples of RFE

Over the years many researchers have developed RFE platforms focused on various actuation and control approaches. There are several recent reviews (Li et al., 2007; Ciuti et al., 2016; Tapia-Siles et al., 2016; Li and Chiu, 2018; Boskoski and Costamagna, 2019; Ciuti et al., 2020; Visconti et al., 2020) that cover these technologies and other cutting-edge platforms in depth which is not the remit of this paper. A selection of them are listed in **Table 1**. The Bellowscope is another promising device not included in the table since it is not strictly a robotic platform but is a low-cost disposable endoscope. Its working principle is based on pistons and bellow actuators which are controlled by multi-DOF handheld controller (Garbin et al., 2018a; Garbin et al., 2018b; Garbin et al., 2019; Chandler et al., 2020).

Wireless endoscopes (capsules) are a great tool for diagnostic purposes and providing painless inspection of the GI tract. Introduction through the mouth and lack of wiring makes them ideal for diagnostic applications (Liao et al., 2016). The less invasive a procedure is; the less risk it carries, more so in the current climate. Currently available capsules can visualize the small bowel (such as the PillCam (Li et al., 2007)) and therefore have good diagnostic capabilities but lack therapeutic capabilities. Capsules for upper GI tract are more difficult but some devices with handheld magnetic control have shown some promise, again solely for diagnostic use. The best technical solution at the moment is the NaviCam® (Ankon Technologies Co, Ltd. Wuhan, Shanghai, China), with a wireless capsule endoscope steered magnetically inside the stomach filled with water (Jiang et al., 2019). This can be classified as a robotic solution as there is a robotic arm moving the magnetic field generator. This is in use in almost every large hospital in China. The colon capsule, however, is less successful. Without the ability to clean the stool coating the mucosa the views are limited. In addition, up to 50% of people will have a pathology requiring biopsy and therefore, many end up requiring conventional colonoscopy anyway. While capsule endoscopes would have major advantages in the case of aerosolized particles (Slawinski et al., 2015; Ciuti et al., 2016); they still have severe limitations for GI endoscopy. They lack the ability to take biopsy samples or perform therapeutic procedures. The requirements for a perfect capsule would include enhanced locomotion, location, vision, telemetry, energy, and diagnostic and therapeutic tools. A further limitation is including all these technologies in a capsule that is small enough to safely traverse the GI tract (Kwack and Lim, 2016; Singeap et al., 2016).

CHALLENGES FOR ROBOTIC FLEXIBLE GI ENDOSCOPY TO OVERCOME DURING COVID-19

RFE can introduce physical distancing into the endoscopy units. However, one of the main challenges is related to feeding and manoeuvring the flexible endoscope. Endoscopists can be severely limited due to a lack of manoeuvrability when manually operating the endoscopes during both diagnostic and therapeutic procedures. It has been documented that during the removal of abnormal tissue (polyps) during colonoscopies, even well-experienced endoscopists can miss up to 20% of the tissue (van Rijn et al., 2006). Robotic platforms use various actuation mechanisms for endoscopes with varying levels of manoeuvrability. In fact, in many review papers, robotic endoscopes are classified based on their actuation principles which typically fall into one of the following categories: 1) magnetic, 2) electric or 3) hydraulic or pneumatic with many devices using a combination of these principles. For example: a legged robotic endoscope has recently been developed (Lee et al., 2017; Lee et al., 2019) that can be operated with an electric motor connected to reel-based mechanism that is both simple and reliable. By using soft materials for the legs, a high degree of manoeuvrability was achieved with no scratches or perforations on a porcine tissue. This is just one example of how robotic endoscopes in development can solve some of the current challenges.

Another challenge is related to operating an endoscopic instrument through the working channel, making sure that no aerosols come back from that channel. The working channel of the endoscopes can be responsible for releasing aerosols or droplets into the suite during standard operating procedure (Vavricka et al., 2010). However, very little quantifiable data exists around whether this is an issue and how big of a challenge it could be. A study that measures the aerosol levels in GI endoscopy suites during procedures would be a welcome addition to the field as well as a follow-up comparison with robotic platforms.

Introducing robotic platforms to endoscopic systems simplifies the procedure. Teleoperation allows clinicians to control the endoscope from a safe distance or/and behind mechanical barriers, with reduced need for direct contact with the patient. Reduced discomfort means less monitoring is required and no need for additional anaesthesiologists or nursing staff, thus reducing the risk to HCW as can be seen in **Figure 1**.

Following evidence of transmission of infection despite decontamination, via infected biofilm in endoscopes (Rauwers et al., 2018; Balan et al., 2019), single use endoscopes are

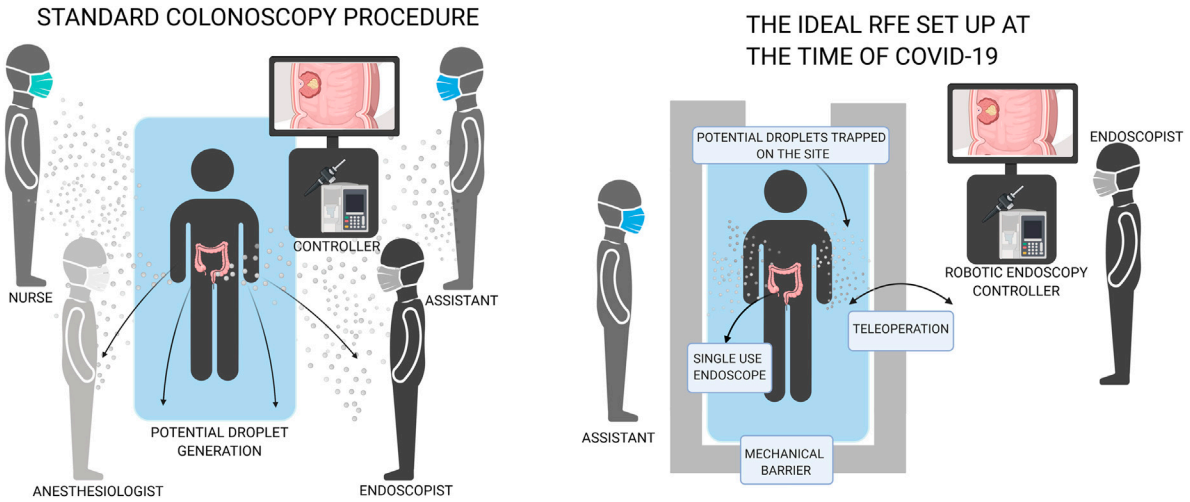

FIGURE 1 | Comparison of conventional endoscopy with robotic flexible endoscopy which can increase distance and decrease number of people in the room.

gaining popularity (Pfeffer et al., 2006; Rosch et al., 2008; Cosentino et al., 2009; Tumino et al., 2010; Groth et al., 2011; Gluck et al., 2016; Tumino et al., 2017; Yeung et al., 2019). For example: the Aer-O-Scope proposes RFE with disposable rectal introducer and supply cables for colonoscopy (Pfeffer et al., 2006; Gluck et al., 2016). Research on fully disposable endoscopes with robotic platforms should be prioritized to implement these solutions in hospitals during the COVID-19 pandemic or future airborne virus pandemics. Single use conventional endoscopes are becoming commercially available. An alternative to disposable endoscopes is tool protection (e.g. protective sheet) which can be disposed of after the procedure, followed by routine sterilisation of the remaining part. However, decontamination of endoscopy equipment is costly, and additionally places more HCW at risk of contraction of infections such as coronavirus during the decontamination process. There is evidence that some tools, such as bronchoscopes (Ofstead et al., 2020) and duodenoscopes (Rauwers et al., 2018; Balan et al., 2019), might still be contaminated with bacteria after routine sterilization. Recurrent passing of instruments down the working channel of the scope leads to damage, that damage leads to accumulation of biofilm which can become infected (Alfa and Singh, 2020; Bouiller et al., 2020; Santos et al., 2020).

DISCUSSION

RFE procedures have the potential to be completed with increased speed and without sedation and fewer complications, leading to a shorter recovery time, freeing space in endoscopy suites at a crucial time where endoscopic capacity has still not recovered to pre-pandemic levels. GI endoscopic procedures have been deemed high risk of contact and droplet formation with the potential to be aerosol generating. Despite little evidence as of now as to the true aerosol generating potential of GI endoscopic procedures, enhanced IC measures are likely to continue.

The ideal RFE during COVID-19 would combine teleoperation, single-use endoscopes and mechanical barriers/seals. Teleoperation allows for physical distancing between patients and HCW, single-use endoscopes would reduce the risk of contaminated scopes. A mobile device would also be extremely useful at a time when the endoscopy suite capacity is limited to make space for COVID-19 patients. RFE has significant potential in diagnostic and therapeutic endoscopy, but some challenges remain to developing the ideal pandemic-secure RFE. There is a significant need for a study to define the aerosol generation during GI endoscopy in order to tailor future guidance for both patients and HCW and maintaining capacity levels in order to avoid devastating long term implications. Even with the hope of a successful vaccine rollout, we have learned that healthcare technologies should be resilient to pandemics in general, so we believe this review will still be relevant in the future.

AUTHOR CONTRIBUTIONS

OO, ZK and CW contributed to conception, literature review, manuscript preparation and revisions. VS, DJ, AA, KO and PV contributed scientific support, coordination, layout, and revision support for the manuscript preparation. All authors contributed to the article.

FUNDING

Research reported in this article was supported by the Royal Society, by Cancer Research United Kingdom (CRUK) Early Detection and Diagnosis Research Committee under Award Number 27744, by the Engineering and Physical Sciences Research Council (EPSRC) under grants #EP/R045291/1 and #EP/P027938/1, by the National Institute of Biomedical Imaging and Bioengineering of the National Institutes of Health (NIH) under Award Number R01EB018992, by the

European Research Council (ERC) under the European Union's Horizon 2020 research and innovation program (grant agreement no. 818045), and by the Italian Ministry of Health funding programme "Ricerca Sanitaria Finalizzata 2013-Giovani Ricercatori" project n. PE-2013-02359172. OO is a winner of the NSERC Canada PDF Award (PDF-546133-2020). Any opinions, findings, and conclusions, or recommendations expressed in this article are those of the authors and do not necessarily reflect the views of the Royal Society, CRUK, EPSRC, NIH, ERC, NSERC or the Italian Ministry of Health. We acknowledge support from the European Union's Horizon 2020 Research and Innovation Programme under grant agreement no. 952118 (AUTOCAPSULE)

REFERENCES

Akagi, F., Haraga, I., Inage, S. I., and Akiyoshi, K. (2020). Effect of sneezing on the flow around a face shield. *Phys. Fluids* 32 (12), 127105. doi:10.1063/5.0031150

Alfa, M. J., and Singh, H. (2020). Impact of wet storage and other factors on biofilm formation and contamination of patient-ready endoscopes: a narrative review. *Gastrointest. Endosc.* 91 (2), 236–247. doi:10.1016/j.gie.2019.08.043

Balan, G. G., Sfarti, C. V., Chiriac, S. A., Stanciu, C., and Trifan, A. (2019). Duodenoscope-associated infections: a review. *Eur. J. Clin. Microbiol. Infect. Dis.* 38 (12), 2205–2213. doi:10.1007/s10096-019-03671-3

Boskoski, I., and Costamagna, G. (2019). Endoscopy robotics: current and future applications. *Dig. Endosc.* 31 (2), 119–124. doi:10.1111/den.13270

Boškoski, I., and Costamagna, G. (2019). Endoscopy robotics: current and future applications. *Dig. Endosc.* 31 (2), 119–124. doi:10.1111/den.13270

Bouiller, K., Ilic, D., Wicky, P. H., Cholley, P., Chirouze, C., and Bertrand, X. (2020). Spread of clonal linezolid-resistant Staphylococcus epidermidis in an intensive care unit associated with linezolid exposure. *Eur. J. Clin. Microbiol. Infect. Dis.* 39 (7), 1271–1277. doi:10.1007/s10096-020-03842-7

Cahill, N., and Morris, D. (2020). Recreational waters – a potential transmission route for SARS-CoV-2 to humans?. *Sci. Total Environ.* 740, 140122. doi:10.1016/j.scitotenv.2020.140122

Cancer Research UK (2020). *44% rise in patients waiting for tests to diagnose bowel, stomach, bladder and oesophageal cancer*. London, United Kingdom: Cancer Research UK.

Chai, N., Mei, Z., Zhang, W., Du, C., Wang, X., Li, L., et al. (2020). Endoscopy works during the pandemic of coronavirus COVID-19: recommendations by the Chinese Society of Digestive Endoscopy. *United European Gastroenterol. J.* 8 (7), 798–803. doi:10.1177/2050640620930632

Chandler, J. H., Chauhan, M., Caló, S., Aruparayil, N., Garbin, N., Campisano, F., et al. (2020). Tu1964 usability of a novel disposable endoscope for gastric cancer screening in low-resource settings: results from rural India. *Gastroenterology* 158 (6), 1235. doi:10.1016/S0016-5085(20)33749-5

Ciuti, G., Caliò, R., Camboni, D., Neri, L., Bianchi, F., Arezzo, A., et al. (2016). Frontiers of robotic endoscopic capsules: a review. *J. Microbio. Robot.* 11 (1), 1–18. doi:10.1007/s12213-016-0087-x

Ciuti, G., Skonieczna-Żydecka, K., Marlicz, W., Iacovacci, V., Liu, H., Stoyanov, D., et al. (2020). Frontiers of robotic colonoscopy: a comprehensive review of robotic colonoscopes and technologies. *J. Clin. Med.* 9 (6), 1648. doi:10.3390/jcm9061648

Cosentino, F., Tumino, E., Passoni, G. R., Morandi, E., and Capria, A. (2009). Functional evaluation of the endotics system, a new disposable self-propelled robotic colonoscope: *in vitro* tests and clinical trial. *Int. J. Artif. Organs* 32 (8), 517–527. doi:10.1177/039139880903200806

Eickhoff, A., van Dam, J., Jakobs, R., Kudis, V., Hartmann, D., Damian, U., et al. (2007). Computer-assisted colonoscopy (the NeoGuide Endoscopy System): results of the first human clinical trial ("PACE study"). *Am. J. Gastroenterol.* 102 (2), 261–266. doi:10.1111/j.1572-0241.2006.01002.x

Garbey, M., Joerger, G., and Furr, S. (2020). Gastroenterology procedures generate aerosols: an air quality turnover solution to mitigate COVID-19's propagation risk. *Int. J. Environ. Res. Publ. Health* 17 (23), 8780. doi:10.3390/ijerph17238780

Garbin, N., Mamunes, A. P., Sohn, D., Hawkins, R. W., Valdastri, P., and Obstein, K. L. (2019). Evaluation of a novel low-cost disposable endoscope for visual assessment of the esophagus and stomach in an *ex-vivo* phantom model. *Endosc. Int. Open* 7 (9), E1175–E1183. doi:10.1055/a-0914-2749

Garbin, N., Wang, L., Chandler, J. H., Obstein, K. L., Simaan, N., and Valdastri, P. (2018a). "A disposable continuum endoscope using piston-driven parallel bellow actuator," in International symposium on medical robotics (ISMR), Atlanta, GA, March 1–3, 2018 (Piscataway, NJ: IEEE), 1–6.

Garbin, N., Wang, L., Chandler, J. H., Obstein, K. L., Simaan, N., and Valdastri, P. (2018b). Dual-Continuum design approach for intuitive and low-cost upper gastrointestinal endoscopy. *IEEE Trans. Biomed. Eng.* 66 (7), 1963–1974. doi:10.1109/TBME.2018.2881717

Gluck, N., Melhem, A., Halpern, Z., Mergener, K., and Santo, E. (2016). A novel self-propelled disposable colonoscope is effective for colonoscopy in humans (with video). *Gastrointest. Endosc.* 83 (5), 998. doi:10.1016/j.gie.2015.08.083

Groth, S., Rex, D. K., Rösch, T., and Hoepffner, N. (2011). High cecal intubation rates with a new computer-assisted colonoscope: a feasibility study. *Am. J. Gastroenterol.* 106 (6), 1075–1080. doi:10.1038/ajg.2011.52

Isakbaeva, E. T., Khetsuriani, N., Beard, R. S., Peck, A., Erdman, D., Monroe, S. S., et al. (2004). SARS-associated coronavirus transmission, United States. *Emerg. Infect. Dis.* 10 (2), 225–231. doi:10.3201/eid1002.030734

Jiang, X., Pan, J., Li, Z. S., and Liao, Z. (2019). Standardized examination procedure of magnetically controlled capsule endoscopy. *Video* 4 (6), 239–243. doi:10.1016/j.vgie.2019.03.003

Johns Hopkins University Coronavirus Center (2020). Available at: https://coronavirus.jhu.edu/ (Accessed September 29, 2020).

Johnston, E. R., Habib-Bein, N., Dueker, J. M., Quiroz, B., Corsaro, E., Ambrogio, M., et al. (2019). Risk of bacterial exposure to the endoscopist's face during endoscopy. *Gastrointest. Endosc.* 89 (4), 818–824. doi:10.1016/j.gie.2018.10.034

Kampf, G., Todt, D., Pfaender, S., and Steinmann, E. (2020). Persistence of coronaviruses on inanimate surfaces and their inactivation with biocidal agents. *J. Hosp. Infect.* 104 (3), 246–251. doi:10.1016/j.jhin.2020.01.022

Kwack, W. G., and Lim, Y. J. (2016). Current status and research into overcoming limitations of capsule endoscopy. *Clin. Endosc.* 49 (1), 8–15. doi:10.5946/ce.2016.49.1.8

Lai, A. G., Pasea, L., Banerjee, A., Denaxas, S., Katsoulis, M., Chang, W. H., et al. (2020). Estimating excess mortality in people with cancer and multimorbidity in the COVID-19 emergency. *medRxiv*. doi:10.1101/2020.05.27.20083287

Larsen, S., Kalloo, A., and Hutfless, S. (2020). The hidden cost of colonoscopy including cost of reprocessing and infection rate: the implications for disposable colonoscopes. *Gut* 69 (2), 197. doi:10.1136/gutjnl-2019-319108

Lau, C. (2014). *$4.4 billion gastrointestinal endoscopic market in the United States and Europe projected for 2020. Vancouver, B.C., Canada: Globe Newswire*.

Lee, D., Joe, S., Kang, H., An, T., and Kim, B. (2019). A reel mechanism-based robotic colonoscope with high safety and maneuverability. *Surg. Endosc.* 33 (1), 322–332. doi:10.1007/s00464-018-6362-2

Lee, D., Joe, S., Jung, J.-H., Kim, J.-U., and Kim, B. (2017). A simple and reliable reel mechanism-based robotic colonoscope for high mobility. *Proc. IME C J. Mech. Eng. Sci.* 232 (16), 2753–2763. doi:10.1177/0954406217723941

Li, F., Leighton, J. A., and Sharma, V. K. (2007). Capsule endoscopy: a comprehensive review. *Minerva Gastroenterol. Dietol.* 53 (3), 257–272. doi:10.5772/23120

Li, Z., and Chiu, P. W. (2018). Robotic endoscopy. *Visc. Med.* 34 (1), 45–51. doi:10.1159/000486121

Liao, Z., Hou, X., Lin-Hu, E. Q., Sheng, J. Q., Ge, Z. Z., Jiang, B., et al. (2016). Accuracy of magnetically controlled capsule endoscopy, compared with conventional gastroscopy, in detection of gastric diseases. *Clin. Gastroenterol. Hepatol.* 14 (9), 1266–e1. doi:10.1016/j.cgh.2016.05.013

Lucarini, G., Ciuti, G., Mura, M., Rizzo, R., and Menciassi, A. (2015). A new concept for magnetic capsule colonoscopy based on an electromagnetic system. *Int. J. Adv. Rob. Syst.* 12 (3), 25. doi:10.5772/60134

Mahadev, S., Aroniadis, O. C., Barraza, L. H., Agarunov, E., Smith, M. S., Goodman, A. J., et al. (2020). Gastrointestinal endoscopy during the coronavirus pandemic in the New York area: results from a multi-institutional survey. *Endosc. Int. Open* 8 (12), E1865–E1871. doi:10.1055/a-1264-7599

Martin, J. W., Scaglioni, B., Norton, J. C., Subramanian, V., Arezzo, A., Obstein, K. L., et al. (2020). Enabling the future of colonoscopy with intelligent and autonomous magnetic manipulation. *Nat. Mach. Intell.* 2, 595–606. doi:10.1038/s42256-020-00231-9

Mittal, R., Ni, R., and Seo, J.-H. (2020). The flow physics of COVID-19. *J. Fluid Mech.* 894, F2. doi:10.1017/jfm.2020.330

Narwani, V., Kohli, N., and Lerner, M. Z. (2020). Application of a modified endoscopy face mask for flexible laryngoscopy during the COVID-19 pandemic. *Otolaryngology-Head Neck Surg. (Tokyo)* 163 (1), 107–109. doi:10.1177/0194599820928977

National Endoscopy Database (2020). Available at: www.ned.jets.nhs.uk (Accessed September 1, 2020).

Ofstead, C. L., Hopkins, K. M., Binnicker, M. J., and Poland, G. A. (2020). Potential impact of contaminated bronchoscopes on novel coronavirus disease (COVID-19) patients. *Infect. Control Hosp. Epidemiol.* 41, 862–864. doi:10.1017/ice.2020.102

Pan, Y., Zhang, D., Yang, P., Poon, L. L. M., and Wang, Q. (2020). Viral load of SARS-CoV-2 in clinical samples. *Lancet Infect. Dis.* 20 (4), 411–412. doi:10.1016/S1473-3099(20)30113-4

Parasa, S., Reddy, N., Faigel, D. O., Repici, A., Emura, F., and Sharma, P. (2020). Global impact of the COVID-19 pandemic on endoscopy: an international survey of 252 centers from 55 countries. *Gastroenterology* S0016-5085, 34761–34762. doi:10.1053/j.gastro.2020.06.009

Peery, A. F., Crockett, S. D., Murphy, C. C., Lund, J. L., Dellon, E. S., Williams, J. L., et al. (2019). Burden and cost of gastrointestinal, liver, and pancreatic diseases in the United States: update 2018. *Gastroenterology* 156 (1), 254. doi:10.1053/j.gastro.2018.08.063e211

Pfeffer, J., Grinshpon, R., Rex, D., Levin, B., Rösch, T., Arber, N., et al. (2006). The Aer-O-Scope: proof of the concept of a pneumatic, skill-independent, self-propelling, self-navigating colonoscope in a pig model. *Endoscopy* 38 (2), 144–148. doi:10.1055/s-2006-925089

Rai, P. (2020). Disinfection of endoscopy and reusability of accessories. *J. Dig. Endosc.* 11 (1), 61–66. doi:10.1055/s-0040-1712238

Rauwers, A. W., Voor In 't Holt, J. G., de Groot, W., Hansen, B. E., Bruno, M. J., and Vos, M. C. (2018). High prevalence rate of digestive tract bacteria in duodenoscopes: a nationwide study. *Gut* 67 (9), 1637. doi:10.1136/gutjnl-2017-315082

Ravindran, S., Bassett, P., Shaw, T., Dron, M., Broughton, R., Johnston, D., et al. (2020). National census of UK endoscopy services in 2019. *Front. Gastroenter.* doi:10.1136/flgastro-2020-101538

Rawla, P., Sunkara, T., and Barsouk, A. (2019). Epidemiology of colorectal cancer: incidence, mortality, survival, and risk factors. *Przeglad Gastroenterol.* 14 (2), 89–103. doi:10.5114/pg.2018.81072

Repici, A., Maselli, R., Colombo, M., Gabbiadini, R., Spadaccini, M., Anderloni, A., et al. (2020). Coronavirus (COVID-19) outbreak: what the department of endoscopy should know. *Gastrointest. Endosc.* 14, 192–197. doi:10.1016/j.gie.2020.03.019

Roberts, K. (2020). *Over 2 million people waiting for cancer screening, tests and treatments*. London, United Kingdom: Cancer Research UK.

Rösch, T., Adler, A., Pohl, H., Wettschureck, E., Koch, M., Wiedenmann, B., et al. (2008). A motor-driven single-use colonoscope controlled with a hand-held device: a feasibility study in volunteers. *Gastrointest. Endosc.* 67 (7), 1139–1146. doi:10.1016/j.gie.2007.10.065

Santos, L. C. S., Parvin, F., Huizer-Pajkos, A., Wang, J., Inglis, D. W., Andrade, D., et al. (2020). Contribution of usage to endoscope working channel damage and bacterial contamination. *J. Hosp. Infect.* 105 (2), 176–182. doi:10.1016/j.jhin.2020.03.007

Singeap, A. M., Stanciu, C., and Trifan, A. (2016). Capsule endoscopy: the road ahead. *World J. Gastroenterol.* 22 (1), 369–378. doi:10.3748/wjg.v22.i1.369

Slawinski, P. R., Obstein, K. L., and Valdastri, P. (2015). Emerging issues and future developments in capsule endoscopy. *Tech. Gastrointest. Endosc.* 17 (1), 40–46. doi:10.1016/j.tgie.2015.02.006

Tapia-Siles, S. C., Coleman, S., and Cuschieri, A. (2016). Current state of micro-robots/devices as substitutes for screening colonoscopy: assessment based on technology readiness levels. *Surg. Endosc.* 30 (2), 404–413. doi:10.1007/s00464-015-4263-1

Thamboo, A., Lea, J., Sommer, D. D., Sowerby, L., Abdalkhani, A., Diamond, C., et al. (2020). Clinical evidence based review and recommendations of aerosol generating medical procedures in otolaryngology - head and neck surgery during the COVID-19 pandemic. *J. Otolaryngol. Head Neck Surg.* 49 (1), 28. doi:10.1186/s40463-020-00425-6

Tse, F., Borgaonkar, M., and Leontiadis, G. I. (2020). COVID-19: advice from the Canadian association of gastroenterology for endoscopy facilities, as of March 16, 2020. *J. Can. Assoc. Gastroenterol.* 3 (3), 147–149. doi:10.1093/jcag/gwaa012

Tsui, B. C. H. (2020). Re-purposing a face tent as a disposable aerosol evacuation system to reduce contamination in COVID-19 patients: a simulated demonstration. *Can. J. Anaesth.* 30, 1–3. doi:10.1007/s12630-020-01687-4

Tumino, E., Parisi, G., Bertoni, M., Bertini, M., Metrangolo, S., Ierardi, E., et al. (2017). Use of robotic colonoscopy in patients with previous incomplete colonoscopy. *Eur. Rev. Med. Pharmacol. Sci.* 21 (4), 819–826. .

Tumino, E., Sacco, R., Bertini, M., Bertoni, M., Parisi, G., and Capria, A. (2010). Endotics system vs colonoscopy for the detection of polyps. *World J. Gastroenterol.* 16 (43), 5452–5456. doi:10.3748/wjg.v16.i43.5452

van Rijn, J. C., Reitsma, J. B., Stoker, J., Bossuyt, P. M., van Deventer, S. J., and Dekker, E. (2006). Polyp miss rate determined by tandem colonoscopy: a systematic review. *Am. J. Gastroenterol.* 101 (2), 343–350. doi:10.1111/j.1572-0241.2006.00390.x

Vavricka, S. R., Tutuian, R., Imhof, A., Wildi, S., Gubler, C., Fruehauf, H., et al. (2010). Air suctioning during colon biopsy forceps removal reduces bacterial air contamination in the endoscopy suite. *Endoscopy* 42 (9), 736–741. doi:10.1055/s-0030-1255615

Visconti, T. A. C., Otoch, J. P., and Artifon, E. L. A. (2020). Robotic endoscopy. A review of the literature. *Acta Cir. Bras.* 35 (2), e202000206. doi:10.1590/s0102-865020200020000006

Wahidi, M. M., Shojaee, S., Lamb, C. R., Ost, D., Maldonado, F., Eapen, G., et al. (2020). The use of bronchoscopy during the COVID-19 pandemic: CHEST/AABIP guideline and expert panel report. *Chest* 158 (3), 1268–1281. doi:10.1016/j.chest.2020.04.036

Wong, T. W., Lee, C. K., Tam, W., Lau, J. T., Yu, T. S., Lui, S. F., et al. (2004). Cluster of SARS among medical students exposed to single patient, Hong Kong. *Emerg. Infect. Dis.* 10 (2), 269–276. doi:10.3201/eid1002.030452

Yeung, C. K., Cheung, J. L., and Sreedhar, B. (2019). Emerging next-generation robotic colonoscopy systems towards painless colonoscopy. *J. Dig. Dis.* 20 (4), 196–205. doi:10.1111/1751-2980.12718

Conflict of Interest: The authors declare that the research was conducted in the absence of any commercial or financial relationships that could be construed as a potential conflict of interest.

frontiers in Robotics and AI

ORIGINAL RESEARCH
published: 05 March 2021
doi: 10.3389/frobt.2021.612959

Deployable Telescopic Tubular Mechanisms With a Steerable Tongue Depressor Towards Self-Administered Oral Swab

*Kirthika Senthil Kumar[1,2], Tuan Dung Nguyen[3], Manivannan Sivaperuman Kalairaj[1], Vishnu Mani Hema[1,4], Catherine Jiayi Cai[1,2], Hui Huang[2], Chwee Ming Lim[5,6] and Hongliang Ren[1,7]**

[1]Department of Biomedical Engineering, Faculty of Engineering, National University of Singapore, Singapore, [2]Singapore Institute of Manufacturing Technology, A*STAR Singapore, Fusionopolis Two, Singapore, [3]Department of Mechanical Engineering, Faculty of Engineering, National University of Singapore, Singapore, [4]Department of Mechanical Engineering, National Institute of Technology, Tiruchirappalli, India, [5]Department of Otolaryngology-Head and Neck Surgery, Singapore General Hospital, Singapore, [6]Duke-NUS Graduate Medical School, Singapore, [7]Department of Electronic Engineering, Faculty of Engineering, Chinese University of Hong Kong, Hong Kong

OPEN ACCESS

Edited by:
Mahdi Tavakoli,
University of Alberta, Canada

Reviewed by:
Mohsen Khadem,
University of Edinburgh,
United Kingdom
Abed Soleymani,
University of Alberta, Canada

***Correspondence:**
Hongliang Ren
hlren@ieee.org

Specialty section:
This article was submitted to Biomedical Robotics, a section of the journal Frontiers in Robotics and AI

Received: 01 October 2020
Accepted: 28 January 2021
Published: 05 March 2021

Citation:
Kumar KS, Nguyen TD, Kalairaj MS, Hema VM, Cai CJ, Huang H, Lim CM and Ren H (2021) Deployable Telescopic Tubular Mechanisms With a Steerable Tongue Depressor Towards Self-Administered Oral Swab. Front. Robot. AI 8:612959. doi: 10.3389/frobt.2021.612959

Swabbing tests have proved to be an effective method of diagnosis for a wide range of diseases. Potential occupational health hazards and reliance on healthcare workers during traditional swabbing procedures can be mitigated by self-administered swabs. Hence, we report possible methods to apply closed kinematic chain theory to develop a self-administered viral swab to collect respiratory specimens. The proposed sensorized swab models utilizing hollow polypropylene tubes possess mechanical compliance, simple construction, and inexpensive components. In detail, the adaptation of the slider-crank mechanism combined with concepts of a deployable telescopic tubular mechanical system is explored through four different oral swab designs. A closed kinematic chain on suitable material to create a developable surface allows the translation of simple two-dimensional motion into more complex multi-dimensional motion. These foldable telescopic straws with multiple kirigami cuts minimize components involved in the system as the characteristics are built directly into the material. Further, it offers a possibility to include soft stretchable sensors for realtime performance monitoring. A variety of features were constructed and tested using the concepts above, including 1) tongue depressor and cough/gag reflex deflector; 2) changing the position and orientation of the oral swab when sample collection is in the process; 3) protective cover for the swabbing bud; 4) a combination of the features mentioned above.

Keywords: COVID-19, swab, self-administered, oropharangeal swab, low-cost, tongue depressor, stretchable sensors

INTRODUCTION

With the spread of the COVID-19 pandemic throughout the world, mass testing of the population has proved to be an effective method to contain and control the disease. The testing of the patient involves the collection of respiratory specimens through two modes of swab tests – a nasopharyngeal swab and an oropharyngeal swab (Petruzzi et al., 2020). Between the two modes, the oropharyngeal is often preferred by patients as it causes less pain or discomfort (Wyllie et al., 2020). The procedure of oropharyngeal swab is as follows: 1) a tongue depressor used to depress the tongue, allowing

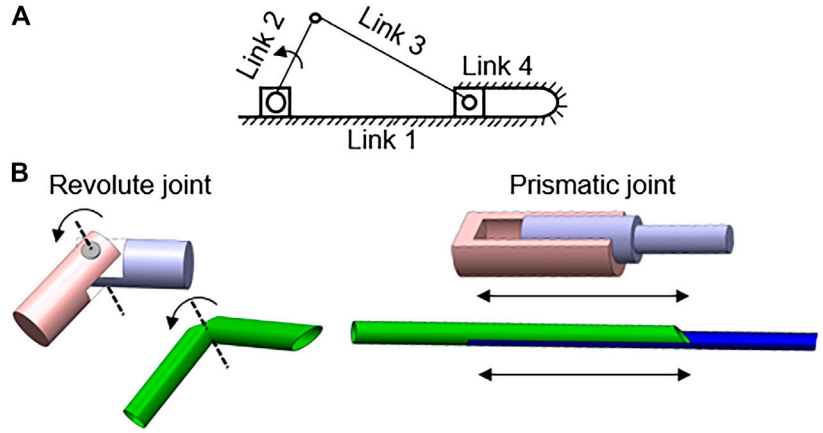

FIGURE 1 | Combination of slider-crank linkage and kirigami-based deployable telescopic tubular mechanical designs **(A)** Variation of slider-crank mechanism with link 1 grounded; **(B)** Replication of joints on polypropylene tubes with simple cuts.

examination of the throat and suppress gag reflex; 2) a swab directed towards the rear wall of the oropharynx near the tonsils and is rotated a few times before removal. Due to the complexity of hand-eye coordination in the swabbing process, the oropharyngeal swab is carried out mainly by healthcare workers at present. However, this practice limits the testing capacity based on access to swabs, workforce availability, increased rate of infection risks, psychological distress, and workload to healthcare workers (Greenberg et al., 2020; World Health Organization, 2020; Schwartz et al., 2020; Shechter et al., 2020).

Currently, the most common solution to counter this issue is to adopt a robotics system to replace healthcare workers during the swabbing process (Yang et al., 2020). This system prevents cross-infection and collects the patient's respiratory samples through automation or remote-controlled actuation (Hunt et al., 2008; Li et al., 2020; Robotics, 2020). These designs, while being novel and effective in a modern testing facility, are still rather resource-intensive for applications such as at-home sample collection or testing in remote, rural areas. Hence, it is important to develop a simple and effective self-administered oropharyngeal swab for the particular group of patients with the difficulty of oropharynx exposure.

Herein, we explore new designs of the oral swab equipped with stretchable sensors which are more suitable for self-administered compared to the rigid and inflexible traditional swabbing methods. At the same time, it is also simpler and less resource-intensive compared to a robot-assisted swab system. In particular, we are interested in swabs that are: 1) "cooperative" (i.e., safe to operate in contact with humans); 2) simple to construct, inexpensive (suitable for the single-use purpose); 3) intuitive to use (to be self-administered by patients); 4) effective (despite natural reaction such as cough, sneeze, and gag by the patient). Without resorting to complex systems, the simplest method to achieve cooperativity is to embed this characteristic straight into the material property of the swab by constructing them out of lightweight materials that are mechanically compliant to external forces (Hartenberg and Danavit, 1964; Gaiser et al., 2012). We also seek to achieve cooperativity by focusing on applying deployable telescopic tubular techniques to create a complaint mechanism with closed kinematic chains.

MATERIALS AND METHODS

Actuation Mechanism

To develop a suitable design for an oral swab, deployable and foldable telescopic tubular mechanical designs were explored to fabricate a slider-crank linkage. A traditional in-line slider-crank mechanism consists of one sliding pair and three revolute pairs. It allows the translation of linear sliding motion to rotatory motion or vice versa (Nemiroski et al., 2017). In the proposed designs, an inversion of the closed slider-crank chain is utilized, similar to a reciprocating-engine mechanism except that link 1 is fixed (**Figure 1A**). The four links in this mechanism are connected by 3 revolute joints and 1 prismatic joint with 1 degree of freedom (DoF) each. Traditionally, slider-crank linkage comprises rigid bodies made from a hard material which is rather bulky and un-cooperative. To address this, we achieved a slider-crank mechanism by applying kirigami techniques to a soft material (polypropylene tube) to alter its material property directly. A kirigami-based mechanical system allows us to create sophisticated three-dimensional (3D) motion from a 2D surface (Felton et al., 2014). A kirigami-based compliant mechanism also has a compact mechanical footprint and volumes while having high cooperativity with humans (Nelson et al., 2019).

To fabricate a compliant slider-crank linkage from deployable telescopic tubes, kirigami cuts of size ~2.3–5 mm, are made to form the hinges/joints (**Figure 1B**). The type of cut determines the compliance of the bending motion. To ensure the motion of the links and joints follow the desired path, diamond shape opening has been cut to promote either inward or outward folding as seen in (**Figure 2**). Through experiments, it is realized that a curvilinear cut retains its structural rigidity

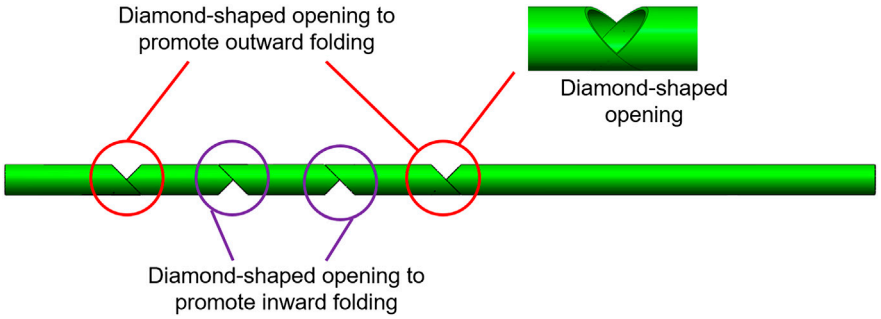

FIGURE 2 | Detailed schematic of the design of the kirigami cuts to promote inward and outward folding.

ptduring bending motion, making it controlled and smooth. Also, the load-bearing capacity is higher with the curvilinear cut than a simple linear cut for joints. The continuum sliding pair is fabricated by inserting two straws of different diameters. Rigid links are formed using adhesive tapes. These slider-crank linkages are attractive as the basis for a new design of self-administered oral swab for three reasons; 1) easily accomplished joint/link to a structure by cutting a notch at the desired point of flexure, 2) complex actuation such as multi-directional or rotatory motion achieved by simple linear translational sliding, 3) placements of constraints through links and joints allowing precise control of equipment in operation.

Straw Swab Designs

Bistable Swab With Tongue Depressor (BSTD)

Bistable swab with tongue depressor (BSTD) and its components are shown in **Figure 3A**. The construction of three revolute joints to a slider-crank mechanism allows developing a monostable swab with a tongue depressor. This design contains four linkages with 2 DoF. The Linear translation motion of link 4 deploys links 2 and 3 in the *Y*-axis. However, this structure has a possibility of retraction upon resultant force from the tongue. By adding an extra link and joint, a bistable system can be produced to create a planar closed kinematic chain. The closed kinematic chain has 5 links and 5 lower pairs, giving it 2 DoF. Linear translation motion of link 5 deploys link 3. By additional DoF to the system, link 3 deploys vertically (*Y*-axis) while remaining parallel to the main body axis. This allows link 3 to act as an effective tongue depressor and remains compact.

Figure 3B demonstrates the motions of the linkages from initiation to motion to finish. While in operation, BSTD can be placed in the patient mouth with the undeployed depressor facing downward toward the tongue. Once placed in the desired position, the depressor can be activated by sliding the control handle, causing the closed kinematic chain to pop down. Once activated in the patient mouth, the collection swab can be controlled with 2 DoF – sliding and rolling. Upon completion, the tongue depressor can be brought back to the idle state by retracting the control handle.

Side Swab Actuator (SSA)

Side swab actuator (SSA) takes another approach where the closed kinematic chain is used to change the direction of the motion of the swabbing bud. **Figure 4** demonstrates SSA at a different stage of its motion. Similar to the monostable design, three revolute joints are added to the slider-crank mechanism. Additionally, link 3 is extended with a T-tip to accommodate for the swab bud, normal to the slider. The linear sliding motion of link 4 is translated into rotating motion through the one DoF closed kinematic chain. This SSA design allows the patient to hold the swab perpendicularly to their mouth, instead of parallel. They are thus providing a more convenient hand position for the user. Also, this swab design, when operated by healthcare workers, allow them to stand facing away from the patients while still being able to collect the sample effectively.

Rotational Swab With Tongue Depressor (RSTD)

Rotational swab with tongue depressor (RSTD) has four linkages, the main shaft to hold the swab bud, T-tip for rotational motion control,

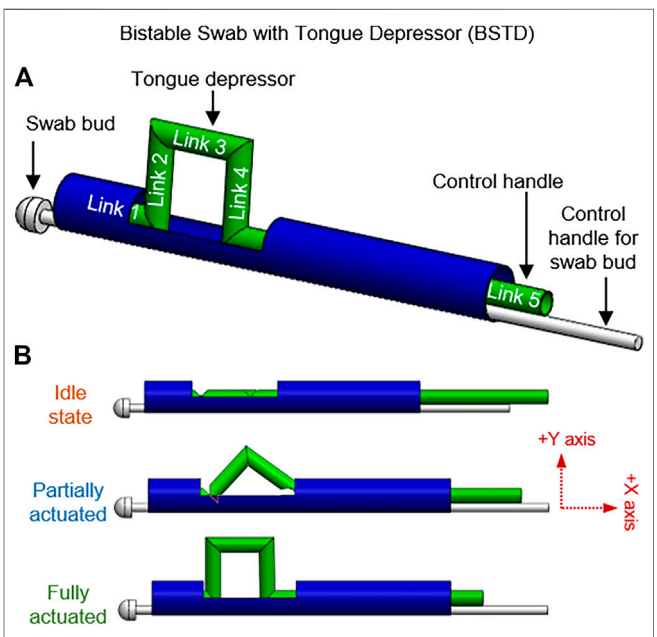

FIGURE 3 | Bistable swab with tongue depressor (BSTD); **(A)** Annotations of the links and various components of the BSTD design, **(B)** BSTD at different stages of actuation.

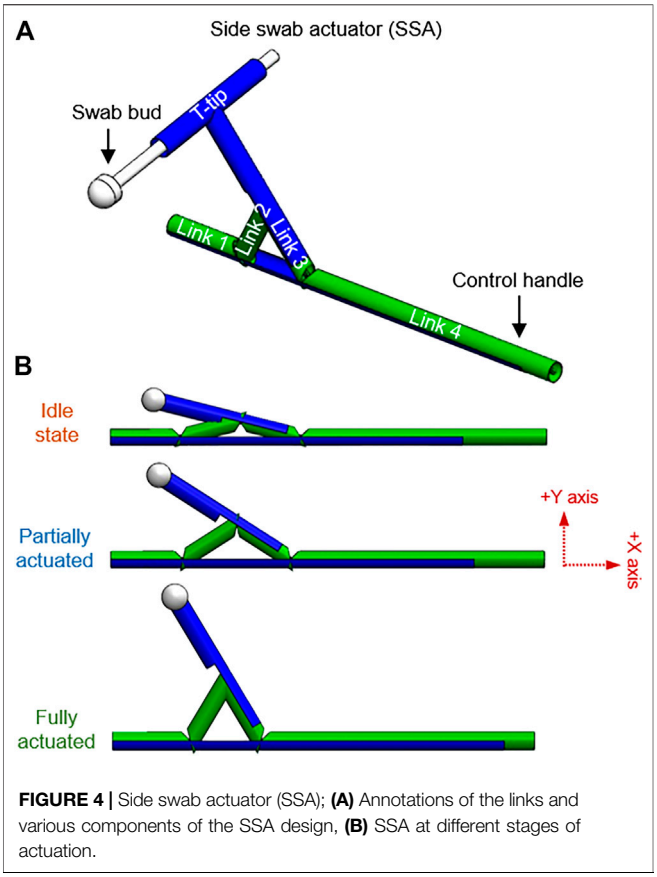

FIGURE 4 | Side swab actuator (SSA); **(A)** Annotations of the links and various components of the SSA design, **(B)** SSA at different stages of actuation.

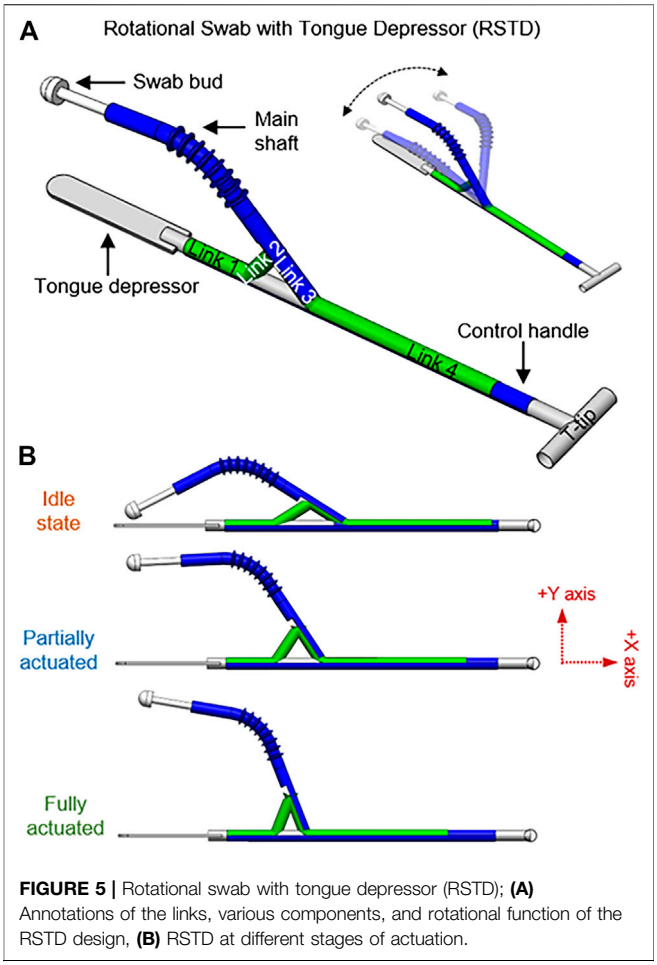

FIGURE 5 | Rotational swab with tongue depressor (RSTD); **(A)** Annotations of the links, various components, and rotational function of the RSTD design, **(B)** RSTD at different stages of actuation.

and a tongue depressor to minimize gag reflex (**Figure 5**). RSTD possesses 2 DoF; 1) sway in medial-lateral axis translated from the sliding motion of link 4 through the slider-crank linkage, 2) *X*-axis roll of the main shaft of the swab through the T-tip attached to link 4. During operation, this design allows the user to adjust the angle of the swab bud in the lateral axis through the slider. Once the desired angle is obtained, the swab bud can be rotated to facilitate the swabbing process.

Tendon-Driven Swab With Tongue Depressor (TSTD)

In the Tendon-driven Swab with Tongue Depressor (TSTD) design, the 1 DoF slider-crank linkage is equipped with four features: tongue depressor, swab cover, stretchable elastomer, and tendon at the proximal end. **Figure 6** shows the swab at a relaxed state where the tongue depressor is deactivated, and the swab bud is enclosed in the swab cover. The swab device can be actuated by retracting the tendon that runs through links 2,3, and 4. Upon actuation, the swab moves linearly towards the proximal end, exposing the swab bud. This linear motion also activates links 3 and 4 to be deployed as a tongue depressor. After the sample is collected, the depressor is retracted, and the cover is closed simultaneously by applying pressure on link 4. Alternatively, the storage elasticity in the stretchable elastomer between links 2 and 4 allows automatic retraction.

Sensorization

Self-administered swabs pose a potential for injuries as the user is not a trained professional like a healthcare worker. Besides, most of the swabs rely on direct vision to understand the placement or orientation of the swab. The actuation in a constrained environment thereby restricts the visualization of the swab. Others depend on their hand guidance to approximately sense the alignment of the swab. This efficiency of sensing is gained through experience and practice. However, in most cases, self-administered swabbing is performed for the first time by the user without prior experience. Hence, it is important to make self-administered swabs more intuitive and provide full information to the user during the process. This sensing information creates more awareness and provides a sense of control and confidence to the user. Therefore, a means of feedback would provide accurate identification of the deployment stage, improve the control, employ safety with better precision, and enhance the effectiveness of the swabbing process.

Directly mounting sensors on the self-administered swabs can help to evaluate their dynamic actuation. However, the sensors are required to possess good mechanical compliance that does not hinder the actuation mechanism. Hence, soft stretchable strain sensors hold the potential for this application. Hydrogel-based stretchable strain sensors possess good mechanical compliance, biocompatibility, and sensitivity. The sensor responds to tensile strains (ε) in the longitudinal direction by reflecting a change in electrical resistance(ΔR), acting on a piezoresistive principle. Its

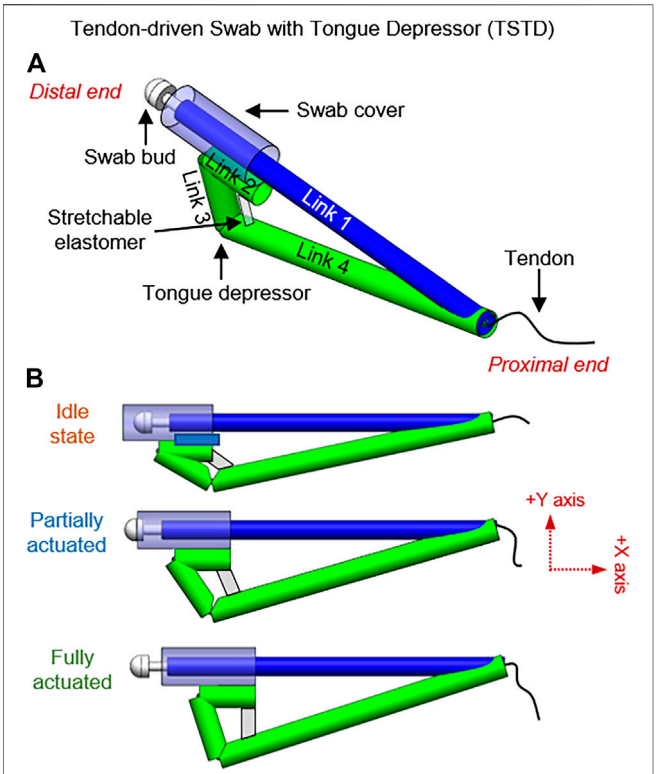

FIGURE 6 | Tendon-driven swab with tongue depressor (TSTD); **(A)** Annotations of the links and various components of the TSTD design, **(B)** TSTD at different stages of actuation.

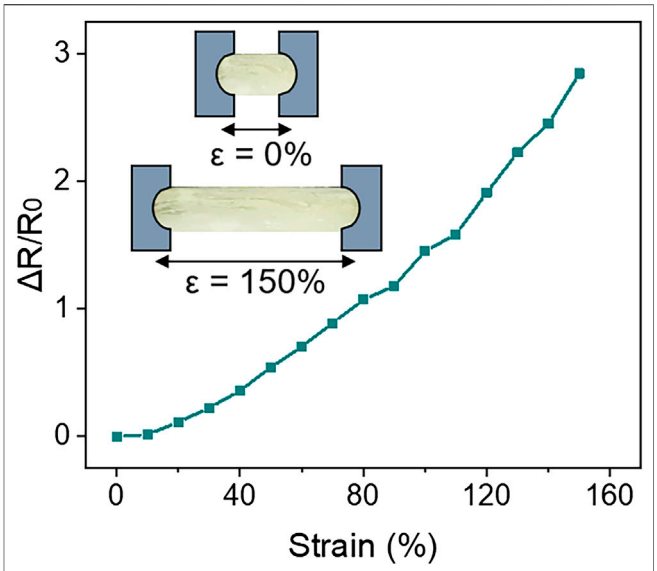

FIGURE 7 | Strain profile of soft stretchable hydrogel-based strain sensor for strains up to 150%.

sensitivity can be represented through gauge factor (GF) where $GF = (\Delta R/R_0)/\varepsilon$, R_0 is the initial resistance. The hydrogel-based strain sensor has a GF of 1.96 for strains up to 150%, as displayed in **Figure 7**.

Further, these sensors have the potential to behave as a restoring spring. The stored elastic energy upon stretching can be used as a medium of actuation, making them multi-purpose. This property is demonstrated in the TSTD design (**Figure 6**).

RESULTS

Experiments were conducted to understand the trajectory, complete workspace, amount of force required to actuate the swabs, force applied by the tongue depressor in each design, realtime performance monitoring using soft stretchable sensors, and the performance of the swabs on a human phantom.

Motion and Workspace Analysis

The behaviour of the swab designs is investigated using the simulation of the computer-aided design (CAD) models. The trajectories and workspace are analyzed for all 4 swab designs as the manipulators are driven to their limit positions (**Figure 8**). For the BSTD design, since link 3 is responsible for the gag deflecting feature, trajectories of the joint connected to it (link 2 and 4) are examined. The motion of link 5 (control handle-slider) is also recorded to compare the input linear sliding motion to the vertical output displacement of link 3. The trajectories in 3D space are shown in **Figure 8A**. Overall, it is observed that with an input of 31.2 mm linear sliding displacement in the –X-axis, a vertical displacement of 15.6 mm in the +*Y*-axis is achieved. For SSA design, the point of interest in motion analysis is at the tip of the swab bud and joint between link 2-3. The trajectories and workspace are recorded (**Figure 8B**) as the control handle is linearly displaced for 14 mm. Overall, an angular displacement of 17.7° in the +*Y*-axis is attained for the swab bud with the 14 mm linear displacement input.

To examine the movement and evaluate the workspace of the swab for RSTD design, motion analysis is performed (**Figure 8C**). A constraint is placed on the rotary motion to limit the roll axis to 90° (45° in the +*Z*-axis and – *Z*-axis) and a linear sliding distance of 11 mm. These boundaries are chosen to set a realistic range of motion for the 3D model based on the oral cavity. The trajectory of the slider and the swab bud are presented in **Figure 8C**. At extreme points, it is observed that an 11 mm linear displacement in the –X-axis of the slider results in a 14.7° angular displacement in the –Y-axis of the swab bud. The entire workspace of the swab bud is also displayed in **Figure 8C**. In the TSTD design, to understand the simultaneous motion between the tongue depressor and the swab cover, link 2 and the joint between link 1 and link 4 are focused for investigation. The trajectories and workspace of these two subjects can be seen in **Figure 8D**. It is observed that a 13 mm linear displacement of the swab cover in the + *X*-axis is translated to a 7.5-degree angular displacement between link 1 and link 4 in the –Y-axis, which is responsible for the actuation of the tongue depressor.

Force Analysis

The force required to actuate the straw mechanisms to perform swabbing is measured. The applied force depends on the

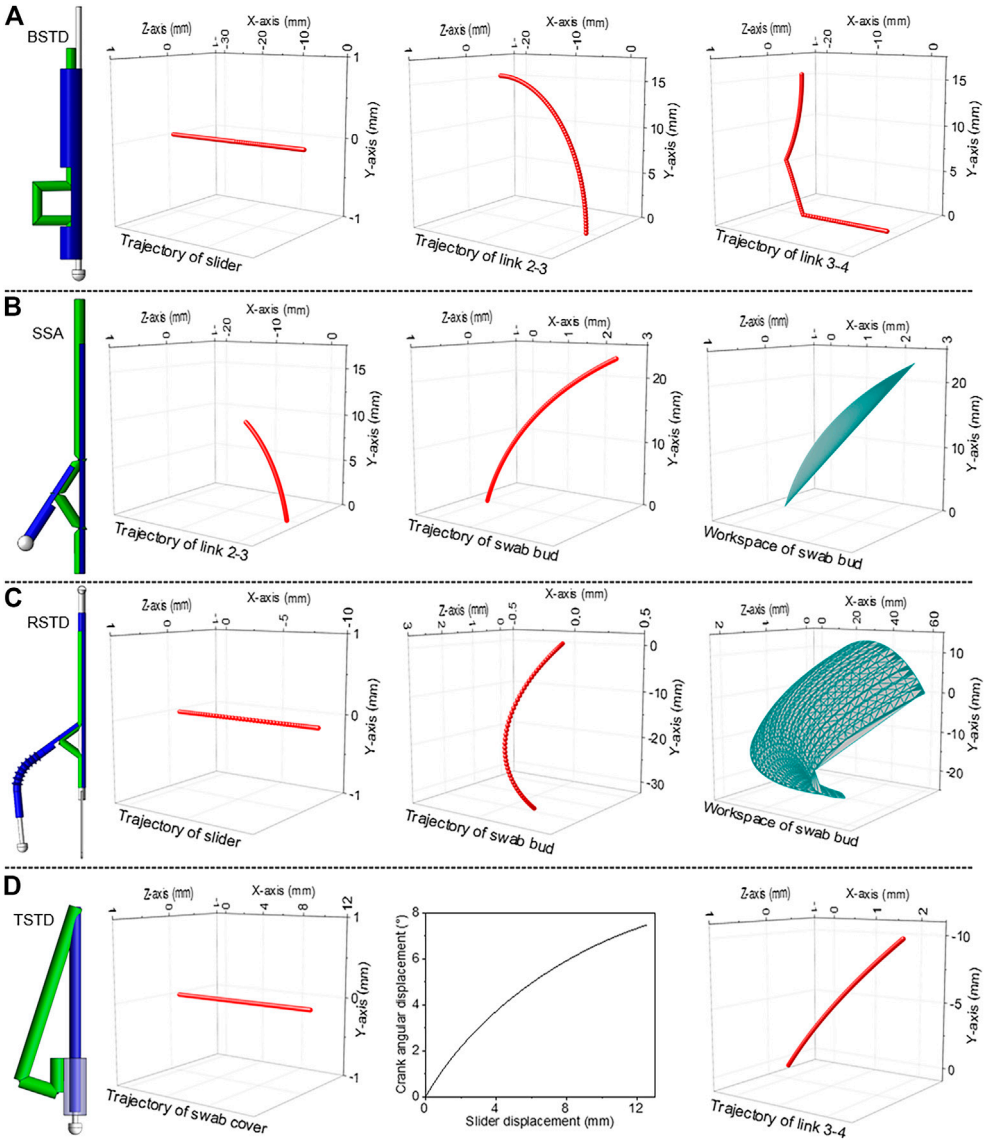

FIGURE 8 | Trajectories and workspace analysis of the oral swab designs **(A)** BSTD, **(B)** SSA, **(C)** RSTD), **(D)** TSTD.

functional capability of the mechanisms, resistance between the polypropylene tubes, and the opposing force from the tongue depressor as it comes in contact with the tongue. The forces are measured using a semi-spherical 3axis force sensor (OMD-10-SE-10N, Optoforce Ltd.) with a sensing head (D = 10 mm) and resolution of 200mN. The sensor is placed in a plane normal to the swab models. For BSTD design (**Figure 9A**), an incremental force of 0.9N is required to initiate the actuation and land in a monostable position. A higher force ~2.8N is required to deploy completely due to the resistance from the tongue on link 3.

Further, during the relaxation phase, two peaks occur as the process is done in two phases, monostable and bistable. The first peak occurs at 1.43N, and the second peak occurs while relaxing the slider-crank linkage at about 0.97N. Activating the mechanism on average requires much higher force than deactivating it.

The SSA design requires an average force of 1.35N to activate and deactivate the mechanism (**Figure 9B**). This value is similar to the maximum force required to initiate the slider-crank mechanism using the polypropylene tubes. Similar to BSTD, the RSTD design is operated with a constraint mimicking the tongue. The force profile gradually increases from the idle state to a fully actuated state, reaching a maximum value of 2.19N (**Figure 9C**), which is lower than the BSTD maximum force as the tongue depressor is isolated from the swab deploying mechanism. The force analysis for this design is done in 2 separate cases similar to design 1 due to the presence of a tongue depressor. When operating without external influence, the force profile gradually increases from the idle state to fully actuated until reaching a maximum value of 3N when the device is fully actuated. The second peak is received while relaxing the

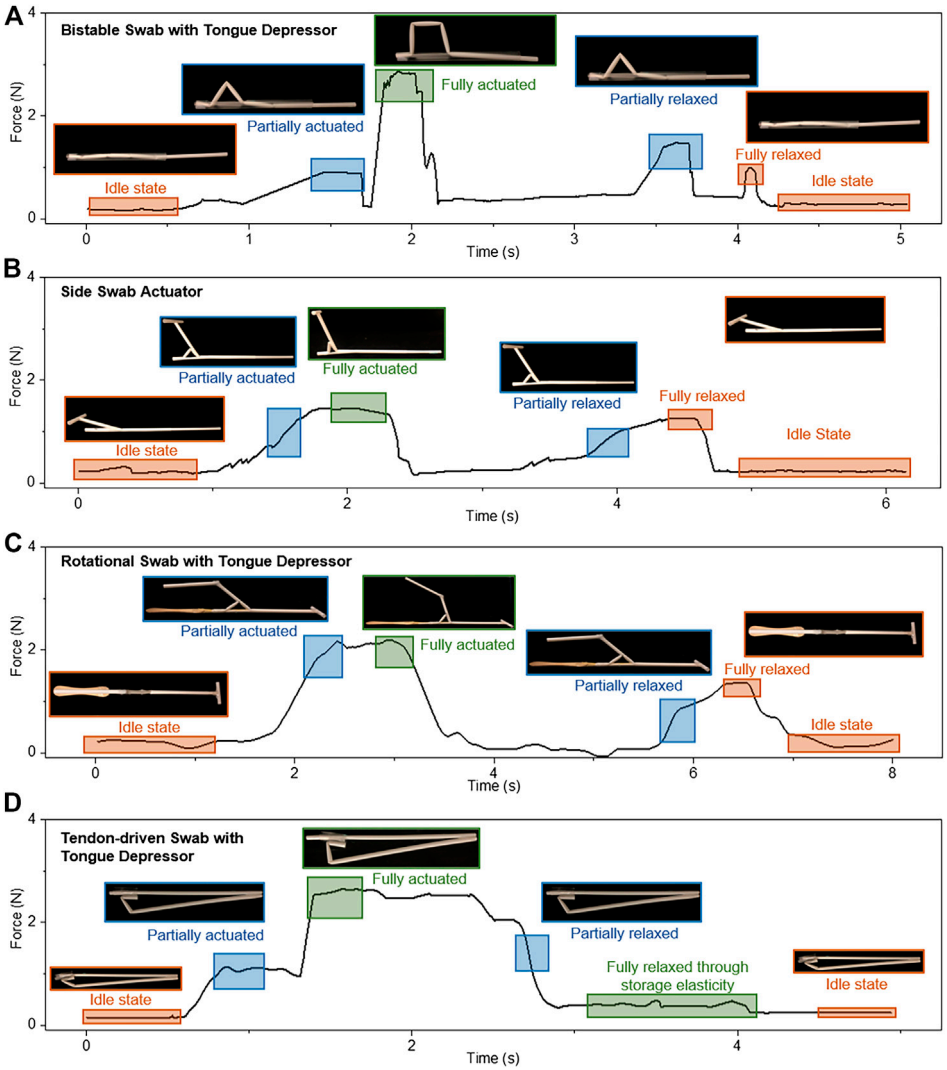

FIGURE 9 | Force analysis of **(A)** BSTD, **(B)** SSA, **(C)** RSTD, **(D)** TSTD.

device at about 1.5N. It is observed that the force needed to relax the mechanism is approximately half of the force needed to actuate it. The retracting force is similar to the SSA design of ~1.5N.

Further, the TSTD design creates a different force profile (**Figure 9D**). Force is applied for the deployment of the tongue depressor and removal of the swab cover simultaneously. During which, the stretchable elastomer stretches to its maximum. Summing to a maximum force of 2.64N, including the opposing force from the tongue constrain and the stored elasticity of the stretchable elastomer. This force has to be retained during the swabbing process, and a decline in the force allows automatic retraction due to the storage elasticity of the stretchable elastomer.

The most conventional way to depress the tongue is by using a simple wooden flat stick (tongue depressor). When using the wooden tongue depressor, a common technique to prevent unconscious tongue slippage is by applying pressure on the tongue through the tip/frontal areas of the stick. Likewise, the tongue depressor proposed can be used. The amount of force/pressure applied on the tongue by the tongue depressor for each design is quantified using the semi-spherical 3axis force sensor (OMD-10-SE-10N, Optoforce Ltd.). The minimum and maximum force applied by the swabs is plotted in **Figure 10**. In most cases, the initial force of the tongue depressor is due to the deployment mechanism. However, the maximum force is still controlled by the user during the self-administered swabbing process. The maximum force applied by the BSTD design is 3.28N, whereas the RSTD design can apply 3.9N as the control is still with the user. The TSTD design applies a force of 2.98N upon deployment. It is essential to apply enough pressure to suppress the tongue. It is also advisable to avoid applying too much pressure, damaging the tissues {Ponraj, 2018 #22}. The amount of force that can be applied by the proposed tongue depressors are in the ranges of ~2.9–3.9 N. Unconscious motion of the tongue will be restricted by this amount of force. Moreover,

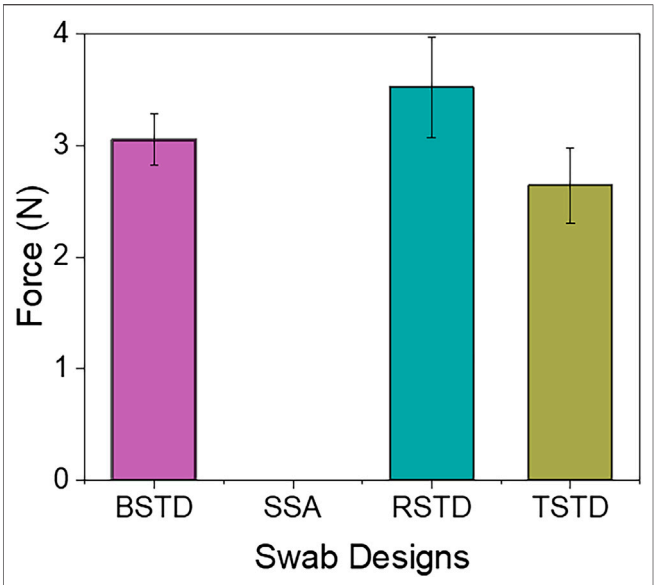

FIGURE 10 | Force applied on tongue by the tongue depressor in the swab designs

in the case of tongue slipping into the throat, the ultimate control lies with the user as it is self-administered swabbing. It is thereby enabling the user to stabilize the swab immediately.

Realtime Performance Monitoring

The determination of strategic locations for sensor placement is by identifying the prominent links with maximum movements. For the BSTD, SSA, and RSTD design, the diagonal length between the links upon actuation is smaller than the point-to-point length in the idle state. Hence, the stretchable strain sensors are mounted at a fully actuated state. The RSTD design of the sensor is mounted between link 2, and link 3 is shown in **Figure 11A**. However, the initial distance between the link 2 and link 4 for the TSTD design is smaller. Hence the sensors are mounted in an idle state. The sensor's elastic storage property helps to relax the TSTD design from the fully actuated stage to the idle stage. The sensor response is exclusive to each swab design, which requires one-time calibration using the optical tracker before realtime monitoring for each swab design. The two orange points on the sensor are used to visually track the strains evolved to cross-validate the sensor performance with the angles. The optical tracking software (Tracker 5.0 (Douglas Brown©) is utilized for the same. The strains experienced by the stretchable sensor at various deployment stages are presented in **Figure 11B**. Further, the $\Delta R/R_0$ response of the sensor to various strains allows the determination of the change of angles between the mentioned links **Figure 11C**. Combining the data from the tracker software, strains of the sensors, and $\Delta R/R_0$ values, the deployment stages and angles between the links of the swab designs are determined in **Figure 11D**.

Demonstration on Human Phantom

The self-administered swabbing process is demonstrated on a human phantom for all the four proposed swab designs, as shown in **Figure 12**. An endoscope (OVS1 Video System Portable Hysteroscopy System, Olive Medical Corporation) is mounted on the swab designs to validate the maximum reach of the swab towards the rear wall of the oropharynx near the tonsils. The effect of cough or sneeze during swabbing procedures are tested on the human phantom. During cough or sneeze, an impact is

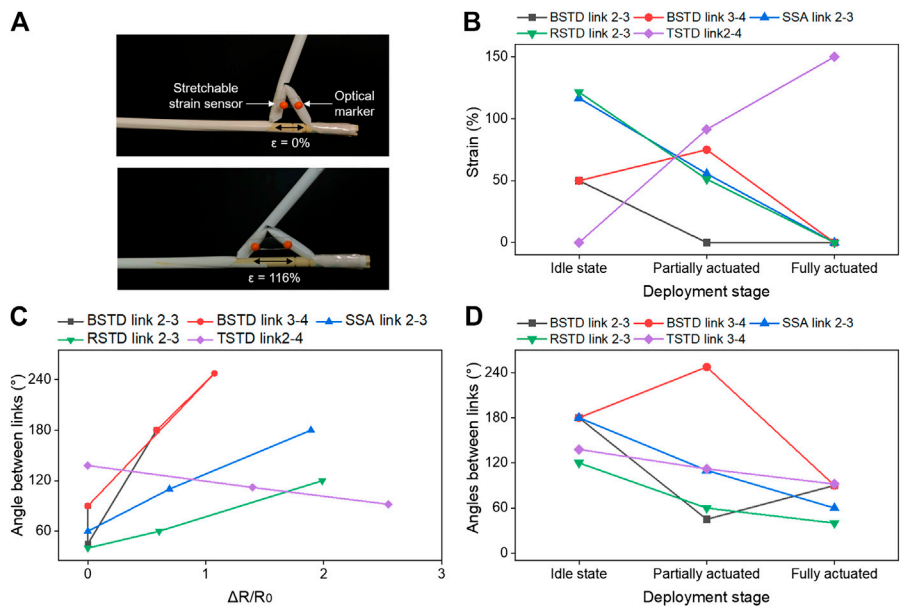

FIGURE 11 | Realtime performance monitoring **(A)** Stretchable sensor placement on the swab design, **(B)** Strains experienced on sensors at various deployment stages, **(C)** $\Delta R/R_0$ response of the sensor and the determined angle between the links, **(D)** Angles formed between the links at various deployment stages.

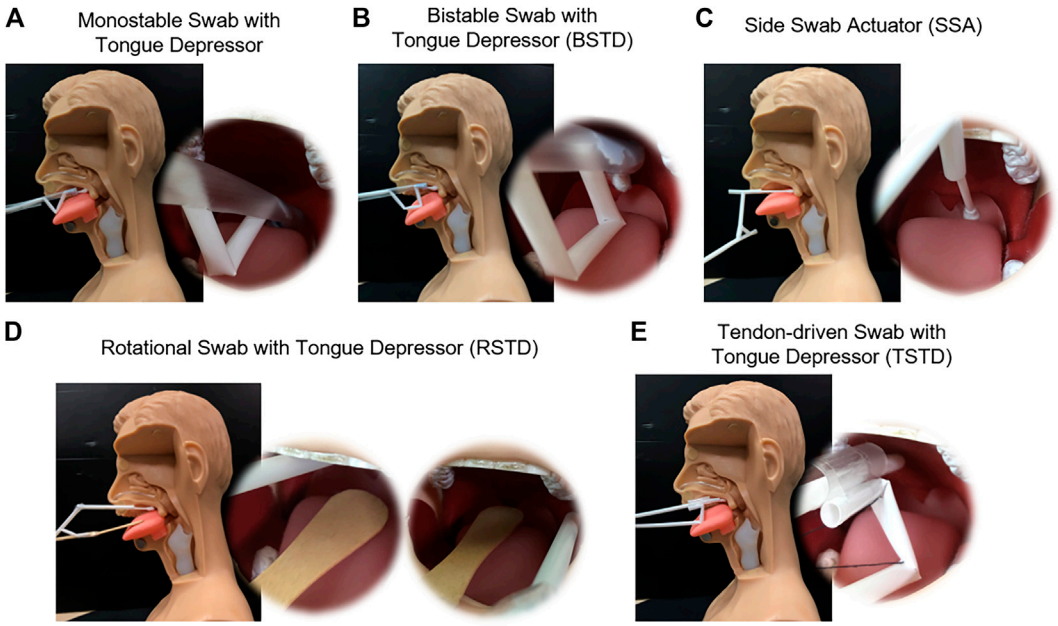

FIGURE 12 | Demonstration of the proposed swab designs on the human phantom in the sagittal plane and endoscopic view **(A)** Monostable swab with a tongue depressor, **(B)** Bistable swab with tongue depressor (BSTD), **(C)** Side swab actuator (SSA), **(D)** Rotational swab with tongue depressor (RSTD), **(E)** Tendon-driven swab with tongue depressor (TSTD).

generated from the throat towards the oral opening and air is forcefully expelled. This impact applied an angular force on the swab which immediately reverts it to its more complaint partially actuated position.

DISCUSSION

A simple strategy to design and fabricate a sensorized self-administered oral swab using a closed-loop kinematic chain and kirigami-based deployable telescopic tubular structure is presented to address the potential occupational health hazard and reduce the workload to healthcare workers during the swabbing process. The central idea lies in the adaptation of the slider-crank mechanism to employ on a mechanically compliant structure. The combination of the tongue depressor with the swab aims to make this swabbing process compact, simpler, faster, and minimize gagging or choking of the patient. The four proposed designs demonstrate the opportunity to fulfil the three criteria set out for a self-administered swab 1) simple and inexpensive. They can be easily fabricated using readily available materials, suitable for the single-use nature of the oral swab. 2) designs equipped with sufficient features to offset potential hindrance such as natural response to oral swab and ensure the effectiveness of the collection of respiratory specimens. 3) cooperative designs (suitable to use with a human) made of soft materials. Additionally, the swab designs show the potential to be sensorized using soft stretchable strain sensors, allowing realtime monitoring of the swab performance and intuitive control. However, the future work is steered towards developing a golden ratio for the swab designs that could accommodate various dimension changes between the users. Also, the development of home-based swabbing kits could be a wise way to spend the resources.

DATA AVAILABILITY STATEMENT

The original contributions presented in the study are included in the article/Supplementary Material, further inquiries can be directed to the corresponding author.

AUTHOR CONTRIBUTIONS

HR and CL initiated and designed the project. KK, ND, MK, CL and HR contributed to developing the project, analysis, and preparation of the manuscript. CJ and VH assisted in testing and editing the manuscript. HR, CL and HH guided and mentored the project.

FUNDING

This work is supported by Singapore NMRC Bedside and Bench grant R-397-000-245-511 awarded to HR and CL.

ACKNOWLEDGMENTS

We would like to thank the students from department bioengineering design module for the discussions and trials.

REFERENCES

Felton, S., Tolley, M., Demaine, E., Rus, D., and Wood, R. (2014). Applied origami. A method for building self-folding machines. *Science* 345 (6197), 644–646. doi:10.1126/science.1252610

Gaiser, I., Wiegand, R., Ivlev, O., Andres, A., Breitwieser, H., Schulz, S., et al. (2012). "Compliant robotics and automation with flexible fluidic actuators and inflatable structures" In Smart Actuation and Sensing Systems-Recent Advances and Future Challenges. Editor G. Berselli, London, UK: IntechOpen, Chap. 22, 567–608. doi:10.5772/51866

Greenberg, N., Docherty, M., Gnanapragasam, S., and Wessely, S. (2020). Managing mental health challenges faced by healthcare workers during COVID-19 pandemic. *BMJ* 368, m1211. doi:10.1136/bmj.m1211

Hartenberg, R., and Danavit, J. (1964). *Kinematic synthesis of linkages*: New York: McGraw-Hill.

Hunt, S., Witus, G., and Ellis, D. (2008). *Computer assisted robotic examination swab sampling (CARESS)* In Unmanned Systems Technology X. Bellingham, Washington United States: International Society for Optics and Photonics, Vol. 6962, p. 69620O. doi:10.1117/12.783229

Li, S.-Q., Guo, W.-L., Liu, H., Wang, T., Zhou, Y.-Y., Yu, T., et al. (2020). Clinical application of an intelligent oropharyngeal swab robot: implication for the COVID-19 pandemic. *Eur. Respir. J.* 56 (2), 2001912. doi:10.1183/13993003.01912-2020

Nelson, T. G., Zimmerman, T. K., Magleby, S. P., Lang, R. J., and Howell, L. L. (2019). Developable mechanisms on developable surfaces. *Sci. Robot* 4 (27), eaau5171. doi:10.1126/scirobotics.aau5171

Nemiroski, A., Shevchenko, Y. Y., Stokes, A. A., Unal, B., Ainla, A., Albert, S., et al. (2017). Arthrobots. *Soft Robotics* 4 (3), 183–190. doi:10.1089/soro.2016.0043

Petruzzi, G., De Virgilio, A., Pichi, B., Mazzola, F., Zocchi, J., Mercante, G., et al. (2020). COVID-19: nasal and oropharyngeal swab. *Head & Neck* 42 (6), 1303–1304. doi:10.1002/hed.26212

Robotics, L. (2020). *World's first automatic swab robot*. Available at: https://www.lifelinerobotics.com/.

Schwartz, J., King, C.-C., and Yen, M.-Y. (2020). Protecting healthcare workers during the coronavirus disease 2019 (COVID-19) outbreak: lessons from Taiwan's severe acute respiratory syndrome response. *Clin. Infect. Dis.* 71 (15), 858–860. doi:10.1093/cid/ciaa255

Shechter, A., Diaz, F., Moise, N., Anstey, D. E., Ye, S., Agarwal, S., et al. (2020). Psychological distress, coping behaviors, and preferences for support among New York healthcare workers during the COVID-19 pandemic. *Gen. Hosp. Psychiatry* 66, 1–8. doi:10.1016/j.genhosppsych.2020.06.007

World Health Organization (2020). *Coronavirus disease 2019 (COVID-19) Situation Report*. Available at: https://www.who.int/docs/default-source/coronaviruse/situation-reports/20200411-sitrep-82-covid-19.pdf?sfvrsn=74a5d15_2. (Accessed April 11, 2020).

Wyllie, A. L., Fournier, J., Casanovas-Massana, A., Campbell, M., Tokuyama, M., Vijayakumar, P., et al. (2020). Saliva or nasopharyngeal swab specimens for detection of SARS-CoV-2. *New Engl. J. Med.* 383, 1283–1286. doi:10.1056/NEJMc2016359

Yang, G.-Z., Nelson, B. J., Murphy, R. R., Choset, H., Christensen, H., Collins, S. H., et al. (2020). Combating COVID-19—the role of robotics in managing public health and infectious diseases. *Sci. Robotics* 5, eabb5589. doi:10.1126/scirobotics.abb5589

Conflict of Interest: The authors declare that the research was conducted in the absence of any commercial or financial relationships that could be construed as a potential conflict of interest.

frontiers in Big Data

REVIEW
published: 09 March 2021
doi: 10.3389/fdata.2021.612561

Sonographic Diagnosis of COVID-19: A Review of Image Processing for Lung Ultrasound

*Conor McDermott[1], Maciej Łącki[1], Ben Sainsbury[2], Jessica Henry[2], Mihail Filippov[2] and Carlos Rossa[1]**

[1]Faculty of Engineering and Applied Science, Ontario Tech University, Oshawa, ON, Canada, [2]Marion Surgical, Toronto, ON, Canada

The sustained increase in new cases of COVID-19 across the world and potential for subsequent outbreaks call for new tools to assist health professionals with early diagnosis and patient monitoring. Growing evidence around the world is showing that lung ultrasound examination can detect manifestations of COVID-19 infection. Ultrasound imaging has several characteristics that make it ideally suited for routine use: small hand-held systems can be contained inside a protective sheath, making it easier to disinfect than X-ray or computed tomography equipment; lung ultrasound allows triage of patients in long term care homes, tents or other areas outside of the hospital where other imaging modalities are not available; and it can determine lung involvement during the early phases of the disease and monitor affected patients at bedside on a daily basis. However, some challenges still remain with routine use of lung ultrasound. Namely, current examination practices and image interpretation are quite challenging, especially for unspecialized personnel. This paper reviews how lung ultrasound (LUS) imaging can be used for COVID-19 diagnosis and explores different image processing methods that have the potential to detect manifestations of COVID-19 in LUS images. Then, the paper reviews how general lung ultrasound examinations are performed before addressing how COVID-19 manifests itself in the images. This will provide the basis to study contemporary methods for both segmentation and classification of lung ultrasound images. The paper concludes with a discussion regarding practical considerations of lung ultrasound image processing use and draws parallels between different methods to allow researchers to decide which particular method may be best considering their needs. With the deficit of trained sonographers who are working to diagnose the thousands of people afflicted by COVID-19, a partially or totally automated lung ultrasound detection and diagnosis tool would be a major asset to fight the pandemic at the front lines.

Keywords: COVID-19, lung ultrasound, image processing, machine learning, diagnosis, segmentation, classification

OPEN ACCESS

Edited by:
Simon DiMaio, Intuitive Surgical, Inc., United States

Reviewed by:
Maria F. Chan, Memorial Sloan Kettering Cancer Center, United States
Tina Kapur, Harvard Medical School, United States

****Correspondence:***
Carlos Rossa
carlos.rossa@ontariotechu.ca

Specialty section:
This article was submitted to Medicine and Public Health, a section of the journal Frontiers in Big Data

Received: *30 September 2020*
Accepted: *14 January 2021*
Published: *09 March 2021*

Citation:
McDermott C, Łącki M, Sainsbury B, Henry J, Filippov M and Rossa C (2021) Sonographic Diagnosis of COVID-19: A Review of Image Processing for Lung Ultrasound. Front. Big Data 4:612561. doi: 10.3389/fdata.2021.612561

1 INTRODUCTION

Severe acute respiratory syndrome coronavirus 2 is the third pathogenic human coronavirus to be identified with a predilection for causing severe pneumonia in 15–20% of infected individuals and 5–10% of all cases requiring critical care. First emerged in Wuhan, China, it has quickly spread across the world Buonsenso et al. (2020). Severe forms of the infection are commonly characterized by

pneumonia, lymphopenia, exhausted lymphocytes, and a cytokine release syndrome. As the COVID-19 epidemic develops, there is a strong desire for fast and accurate methods to assist in diagnosis and decision making Huang et al. (2020), Born et al. (2020a). The outward symptoms are similar to that of influenza and thus laboratory testing is required for diagnosis. The most common techniques that have been employed include ribonucleic acid analysis from sputum or nasopharyngeal swab alongside chest radiographs. However, these tests are not always able to detect this disease.

COVID-19 preparedness and response critically rely upon rapid diagnosis and contact tracking to prevent further spread of the infection. With a surge in new cases, particularly those requiring critical care, monitoring the disease can help healthcare professionals make important management decisions. While CT is a proven tool for diagnosing COVID-19, it has limitations that make routine use impractical: CT is not widely available, turnaround times are long, and it requires patients to be moved outside of their unit Hope et al. (2020) and reported sensitivities vary, as per Hope et al. (2020). Safely using CT machines during the pandemic is logistically challenging and can overwhelm available resources. Even with proper cleaning protocols, CT scanners could become a source of infection to other patients who require imaging.

Amidst the rush to use CT scans and develop image processing algorithms to detect COVID-19 in CT images, researchers seem to have given little attention to a much more convenient and simpler imaging method: Lung ultrasound (LUS), Buonsenso et al. (2020). LUS has been used for decades for diagnoses and patient monitoring in a variety of respiratory diseases including pneumonia and acute respiratory distress syndrome, as per Staub et al. (2018) and Lichtenstein (2009). Very recently, it has been proven to also have the ability to detect manifestations of COVID-19 in the images when the examination is performed accurately as shown by Huang et al. (2020), Thomas et al. (2020), and Buonsenso et al. (2020). LUS has many appealing features that make its application to COVID-19 diagnosis and monitoring quite advantageous. It uses basic technology available at a much larger volume than CT scans and is free of ionizing radiation. It is also non-invasive, repeatable, cost-effective, and unlike CT-scan, LUS can be performed at a patient's bedside. Furthermore, the issue of viral cross-contamination with LUS machines is nearly nonexistent. Sterilizing ultrasonography equipment is quite easy and is currently done hundreds if not thousands of times per week in a single hospital. More subtly, thanks to the prompt availability of LUS, patients may benefit from a lower threshold for performing LUS examination than what is required for CT tests. Thus, earlier and more frequent lung examinations can be offered, even in COVID-19 assessment centers outside of hospitals. Furthermore, infected but discharged patients could be evaluated with lung imaging directly in their homes. This is particularly important with respect to long-term care homes and in regions experiencing a deficit of available hospital beds.

With the completion of a reliable diagnostic algorithm and handheld tool, it will be possible to diagnose patients where there is an absence or limited number of practitioners, such as in rural and isolated communities. This can assist in better managing medical resources by providing a quick and reliable way to triage patients.

Early diagnosis allows for timely infection prevention and control measures. Patients with mild disease do not require hospitalization, unless there is concern for rapid deterioration. Thus, in the short term, a more systematic way to help healthcare professionals identify cases and assess the risk of progression to severe or critical conditions, or from acute to subacute conditions, can help better manage scarce resources in hospitals. Thus, routine use of LUS can help the fight against COVID-19 in several ways:

- LUS offers a supplementary screening tool available in any healthcare center. It can allow for a first screening to discriminate between low and high-risk patients. Routine LUS is much easier to implement as a screening tool than other imaging methods and thus earlier and more frequent lung examinations can be offered, even directly in COVID-19 assessment centers outside of hospitals.
- In the absence of sufficient COVID-19 testing kit availability, LUS can assist in diagnosing patients;
- LUS images can be obtained directly at bedside reducing the number of health workers potentially exposed to the patient. Currently, the use of chest X-Ray or CT scan requires the patient to be moved to the radiology unit, potentially exposing several people to the virus. With LUS, the same clinician can visit the patient and perform all required tests. This is a primary point since recent data shows that in severely affected countries about 3–10% of infected patients are health workers, worsening the serious problem of health professionals' shortage Buonsenso et al. (2020);
- Discharged patients can be actively monitored with LUS imaging directly in their homes. This is crucial in long-term care homes and in regions with saturation of admission in hospital beds;
- Portable ultrasound machines are easier to sterilize due to smaller surface areas than CT scans;
- LUS is radiation free and can be performed every 12–24 h, allowing close monitoring of clinical conditions and also detecting very early change in lung involvement;
- LUS can be easily performed in the outpatient setting by general practitioners. This would also allow a better pre-triage to determine which patients should be sent to a hospital;
- Lastly, LUS is an inexpensive instrument and can be easily deployed in resource-deprived settings. In case of a massive spread, traditional imaging such as CT scan is much more difficult to be performed compared to LUS.

A database of LUS ultrasound images is being collected by researchers worldwide Born et al. (2020a), Roy et al. (2020). Reports issued from this data have identified common structures seen in LUS on patients with confirmed cases of COVID-19. The data has revealed trends in LUS images that provide markers for the disease. However, these indicators have also been seen in other respiratory infections, but COVID-19 has some unique distinguishing features. Some of these investigations have drawn

from limited datasets: 1 case in Thomas et al. (2020) and 20 in Huang et al. (2020), to over 60,000 images in Soldati et al. (2020). Although there is strong evidence that LUS can diagnose and monitor COVID-19, it is important to acknowledge that there is a spectrum of clinical manifestations of the virus in LUS images during the clinical course of the infection. Even though image-based patterns are intuitively recognisable, they may be mistaken with manifestations of other respiratory diseases. Furthermore, according to the standardized protocol for point-of-care LUS and grading score system proposed in Italy by Soldati et al. (2020), a lung examination requires multiple LUS scans obtained at different locations on the chest. It becomes hard to reconstruct a mental map of a required set of up to 14 scans, and image quality and interpretation are largely operator-dependent. These issues suggest that LUS diagnosis would benefit from a standardized approach, common language, and uniform training, which may not be feasible in the time of pandemic. Thus, there is an urgent need to develop computer-aided methods to assist with sonographic diagnosis of COVID-19.

This paper provides a review of contemporary methods for both the segmentation and classification of LUS and is organized as follows: The next section provides a review of existing manual diagnostic techniques currently being employed around the world. **Section 3** delivers a narrative on proven techniques on LUS image segmentation found in literature. **Section 4** does the same but with classification. Lastly, the paper discusses parallels between different methods and allow readers to decide which particular method may be best for their needs. With the deficit of trained sonographers who are working to diagnose the thousands of people afflicted by COVID-19, a partially or totally automated LUS detection and diagnosis tool can have a tremendous impact in the battle against COVID-19. Let us start with narrative on how conventionally COVID-19 and other lung diseases are examined and diagnosed using LUS. It is important to note, however, that not all of the methods presented in this paper have been specifically used as a diagnostic tool for COVID-19, but they have the potential to be used as such. As COVID-19 is a new virus, little work has been done to develop detection tools. This paper is meant to act as a guide for methods that have been proven to diagnose pneumonia and other respiratory pathologys indicative of COVID-19.

2 THE BASES OF LUNG ULTRASOUND DIAGNOSIS OF COVID-19

Since the end goal is to at least partially automate the process of LUS diagnosis, an understanding of how LUS images are acquired is necessary.

2.1 LUS Examination Protocol

Before moving any further, it is important to outline the basic principles of LUS and how it is being applied to COVID-19. LUS images offer real-time insight into the state of eration of the lung, i.e., the air to fluid ratio in the lung, which distinguishes normal eration from respiratory illnesses.

Normally erated lung: Since ultrasonic energy is rapidly dissipated in the air, in a normally erated lung the only detectable structure is the pleura, observed as a hyperechoic horizontal line (see **Figure 1**, green lines). The pleural line moves synchronously with respiration—this is called lung sliding. In addition, successive hyperechoic horizontal lines appear below the pleural: the A-lines (blue). These artifacts along with lung sliding represent a sign of normal content of air in the lung by Gargani and Volpicelli (2014). See **Figure 1A**.

Interstitial lung disease: When the state of eration decreases due to the accumulation of fluid or cells, the ultrasound beam travels deeper in the lung. This phenomenon creates vertical reverberation lines known as B-lines (comet-tail artifacts outlined by yellow lines in **Figure 1A**). Hyperechoic B-lines start at the pleural line, extend to the bottom of the image without fading, and move with lung sliding. The lower the air content in the lung, the more B-lines are visible in the image. Multiple B-lines in certain regions indicate lung interstitial syndrome.

Lung consolidation: When the air content further decreases to the point of absence of air, with some abuse of terminology, the lung becomes a continuous medium where ultrasound waves cannot reverberate. The LUS image appears as a solid parenchyma, like the liver or the spleen. Consolidation is the result of an infectious process, a pulmonary embolism, obstructive atelectasis, or a contusion in thoracic trauma. Additional sonographic signs are needed to determine the cause of the consolidation in order to attribute it to COVID-19 such as the quality of the deep margins or the presence of air or fluid bronchogram Huang et al. (2020). In **Figure 1A**, consolidation is indicated by the presence of the C-lines highlighted in red.

The recommended acquisition protocol for COVID-19, as proposed by Soldati et al. (2020), screening includes 14 intercostal scans in 3 posterior, 2 lateral, and 2 anterior areas, currently considered "hot areas" for COVID-19 (**Figure 1B**). Each scan is 10 s long so that lung sliding can be visualized. For patients who are not able to maintain the sitting position the echographic assessment may start from landmark number 7, as per Soldati et al. (2020). Once the images are acquired, each scan is analyzed and classified following the 3-point score summarized below Huang et al. (2020). Practically, the device to do this would need to be robust, cheap, and easily cleanable. The software would need to be able to be used by non-professional sonographers (i.e., nurses, etc.).

Specific manifestations of COVID-19 include:

- COVID-19 foci are mainly observed in the posterior fields in both lungs, especially in the posterior lower fields;
- Fused B lines and waterfall signs are visible under the pleura. The B lines are in fixed position;
- The pleural line is unsmooth, discontinuous and interrupted;
- The subpleural lesions show patchy, strip, and nodule consolidation;
- Air bronchogram sign or air bronchiologram sign can be seen in the consolidation; and

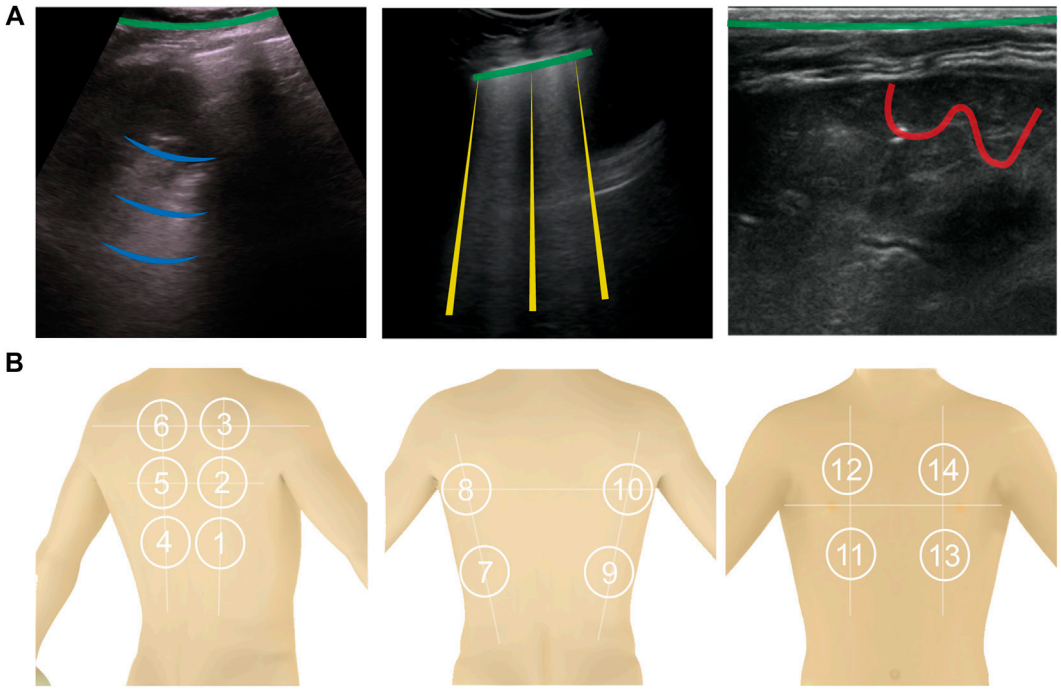

FIGURE 1 | (A): Shows the four types of lines found in LUS images. A-lines are shown in blue, B-lines are yellow, C-lines red, and the pleural line is green. **(B)**: 14 anatomical scanning locations for LUS diagnosis. From left to right are scanning locations on the back [with the vertical paravertebral line, spine of shoulder blade (upper horizontal line) and interior angle of shoulder blade (lower horizontal line)], sides (showing the mid-axillary lines on the left and right sides and internipple line), and front of a torso (showing the internipple line).

- The involved interstitial tissues have localized thickening and edema, and there is localized pleural effusion around the lesions;

2.2 Diagnosis

After the images are taken from the 14 intercostal positions, they can be analyzed to determine the presence of COVID-19 pneumonia. Depending on the results from the sonographer, a score is assigned to the LUS images to indicate the severity of the disease present, if any. The score is from 0 to 3, 0 indicating a healthy lung and 3 indicating a heavily diseased lung.

- Score 0: The pleural line is continuous and A-lines are present indicating a normally erated lung;
- Score 1: The pleural line is indented and below the indent B-lines are visible. These are due to the replacement of volumes previously occupied by air in favor of intercostal tissue;
- Score 2: The pleural line is severely broken and consolidated areas appear below the breaking point (C-lines and darker areas). The C-lines signal the loss of eration and the transition;
- Score 3: The scanned area shows dense and largely extended white lung with or without C-lines. At the end of the procedure, the clinician classifies each area according to the highest score obtained. Huang et al. (2020) further suggests that COVID-19 has other specific manifestations in LUS, mainly observed in the posterior area: Fused B-lines; the pleural line is unsmooth, discontinuous or interrupted; and the subpleural lesions show patchy, strip, and nodule consolidation in which air bronchogram can be seen. The interstitial tissues show obvious thickening and edema, the pleura shows localized thickening, and there is localized pleural effusion around the lesions.

There are numerous methods, presented in the following sections, which give medical researchers the tools required to pre-process, segment, and classify LUS images (**Figure 2**).

3 SEGMENTATION OF COVID-19 MANIFESTATIONS IN LUS

Segmentation divides an LUS image into smaller classifiable sections. This means identifying the pleuralline and the presence of A-lines, B-lines, or consolidated regions of the image. Thus, segmentation plays the role of interpreting what manifestations are held within the LUS image. Pre-processing is necessary as raw LUS images can be noisy and difficult to interpret.

3.1 Image Pre-Processing

Ultrasound images are noisy, often lack contrast, and contain artifacts such as attenuation speckles, shadows, and signal

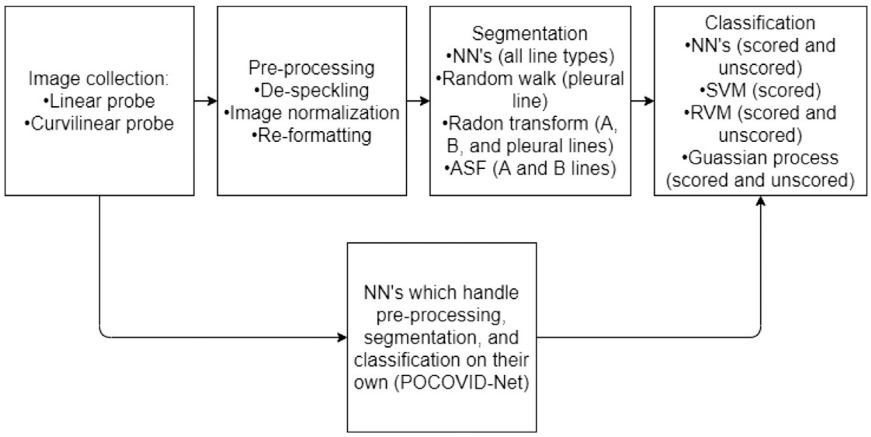

FIGURE 2 | A flow chart representing a normal work flow for LUS images processing. The flowchart has two parallel components, illustrating that typically the stages of image collection, processing, segmentation, and classifications are performed in a linear fashion. However, the parallel component is to illustrate that some neural network methods can be trained in order to handle the entire process (from collection to classification) as one black-box solution.

dropouts [Noble and Boukerroui (2006)], making image segmentation a difficult task. Furthermore, images collected using an ultrasound machine will differ between different models and types of probes. Pre-processing is almost always done on LUS images to enhance their quality and prepare them for further processing. One of the most common pre-processing operations is binarization. It converts pixels in a gray scale image into a black and white image (with pixels either on or off) based on the intensity of the pixel and a threshold value Correa et al. (2018). The choice of the threshold value changes the features that will be visible in the processed image.

Image normalization is required to offset any scaling differences between different images caused by gain adjustments on the ultrasound device. In case the gain settings are not known, Brattain et al. (2013) propose the use of the image peak approach for enhancing the image which minimizes the potential for differences in gain during the recording process from affecting the algorithm. Image reformatting may be necessary depending on the method used. In Cristiana et al. (2020), all images were reformatted to be in a consistent rectilinear format so no matter what transducer was used in order to take the images, they could be processed in the same way. Brattain et al. (2013) performs a similar operation where each frame in a video was reformatted and normalized so that difference in gain setting during the original recording was reduced. This further minimizes discrepancies between data sets.

3.2 Pleural Line Detection

The first set of segmentation methods focuses on the detection of the pleural. This first step is typically to exclude the area above the pleural (e.g.,: noise from the rib bones) from segmentation as it has no diagnostic importance aside from acting as a reference point.

The method presented in Moshavegh et al. (2016) and Moshavegh et al. (2018) employs the random walk technique to automatically detect the pleural line. A classical random walk algorithm, introduced by Grady (2006), is a method for image segmentation that can be either interactive or automatic. In this method a set of pixels called seeds is selected and given a label. Random walkers are then used to identify regions containing the labeled seeds. The method was adapted to ultrasound imaging in Karamalis et al. (2012). Since the ultrasound images contains artifacts and noise, the walkers are constrained using a confidence map constructed based on the image quality. This simple method is easy to implement as it uses a well-known image segmentation technique. One notable consideration is that a starting point must be chosen carefully Moshavegh et al. (2016), Moshavegh et al. (2018). Additionally, it remains unknown if this method is suitable for identifying the pleuralline in patients with score greater than 2, as in severe cases where the pleuralline can be discontinuous.

In Moshavegh et al. (2016) random walk is combined with alternate sequential filtering to detect the presence of pleurallines. A similar approach was proposed by Carrer et al. (2020) but instead of random walk, the method uses Hidden Markov Model (HMM) and Viterbi Algorithm (VA). It can detect discontinuous pleural lines, which is a direct advantage over the random walk method. Based on experimental evaluation, the algorithm can detect the pleuralline in a heterogeneous data set collected from various sources. Another method proposed in Correa et al. (2018) finds the pleuralline using in two steps. First, the image is binarized and divided into narrow vertical slices. Each slice is then divided in half by a line, which is moved such that the number of *on* pixels is equal above and below it. A curve is then fitted along to the points on each of the lines such giving the approximate location of the pleuralline.

One of the most common methods for line detection is the Radon transform, which projects the density of an object in an angular coordinate system Anantrasirichai et al. (2016), Anantrasirichai et al. (2017). The Radon transform can be used to identify the pleuralline by searching for the brightest horizontal line which they define as one with the $90^\circ \pm 20^\circ$. An improved version of this method presented in Karakus et al. (2020) was tested in LUS images of COVID-19 patients. One of

the main advantages of this method is its simplicity. The pleuralline can be easily identified as it is always the brightest object in the image. As a major shortcoming, detectable lines are straight, meaning that this method can only approximate the actual position of the pleuralline and is more suitable for detecting A and B lines.

3.3 A and B Line Detection

Finding pleurallines is an important aspect of LUS imaging, however often times medical professionals are more interested in locating and segmenting the A and B lines that are characteristic of healthy and unhealthy lung conditions. This section describes some of these methods.

In a Radon transform A-lines can be identified as horizontal lines, ones with an angle $90^\circ \pm 20^\circ$, with a lower brightness than that of the pleuralline. Similarly, B-lines can be identified by searching for horizontal lines with angle $0^\circ \pm 20^\circ$. Anantrasirichai et al. (2016) and Anantrasirichai et al. (2017) proved that using such a method can indeed differentiate between these different lines.

Brattain et al. (2013) presented one of the first methods used to identify B-lines in LUS. The method converts the conic ultrasound image into a rectangle and divides it into columns. The B-lines are identified by finding columns through analyzing the brightness profile of each column, and searching for columns with a high, uniform intensity, spanning the length of the column. This method, though simple, requires the detection parameters to be tuned depending on the model of the ultrasound machine and the probe used to detect images. This method was later improved upon by applying a series of morphological operations and filters to the image to more accurately segment B-lines. Moshavegh et al. (2016), Moshavegh et al. (2018), and Brusasco et al. (2019) all used alternate sequential filtering[1] (ASF) with an axial-line structuring element to consolidate regions containing disjointed elements of the B-lines into continuous vertical shapes. Moshavegh et al. (2016) applied the Top-Hat filter to distinguish between connected B-lines, while Brusasco et al. (2019) scans the image laterally in search of long columns that contain mostly bright pixels. The location of the B-Lines can be adjusted using Gaussian model fitting method, as shown in Moshavegh et al. (2018).

A similar approach in Correa et al. (2018) has been shown to aid in the identification of A-lines. Like in the previous methods, only the region below the pleuralline is considered. A procedure named *close method* is applied to the image to emphasize the shape of regions possibly containing A-lines. A-lines are identified by adding the brightness values of each row.

3.4 C-Lines (Consolidations)

There presently are no methods provided in literature specifically tailored for segmenting lung consolidations for LUS. However, there is potential for doing so. In Nazerian et al. (2015), a method for manually imaging pneumonia consolidations in LUS was presented. In this paper, recommendations for what to look for are included. The consolidations due to pneumonia usually contain dynamic echogenic structures that move with breathing. They may also contain multiple hyperechogenic spots, due to air trapped in the small airways, with associated focal B-lines. This is typically characterized by a large dark spot in the LUS, caused by pleura breakdown, as shown by Volpicelli et al. (2010). Lung consolidations are superficial and relatively easy to spot by lung ultrasound, as per Lichtenstein (2015). The methods presented by Correa et al. (2018) or Brattain et al. (2013) could potentially be applied to properly segment LUS images with lung consolidations present. A tool for identifying lung consolidations is important as C-lines are required for LUS diagnoses.

3.5 Neural Networks Based Segmentation

A more modern approach to segmenting LUS images involves using neural networks and deep learning. Convolutional Neural networks (CNNs) are a type of neural network (NN) specifically designed for processing, identifying, and detecting features in images or sounds tracks. These networks use deep learning methods and require hundreds or thousands of images with features labeled. To this end, large datasets are required for training and testing of CNNs. To this date, there are mainly two datasets of LUS images of COVID-19 patients. First, Roy et al. (2020) presented the Italian COVID-19 LUS DataBase (ICLUS-DB) composed of 277 LUS videos from 35 patients, 17 of whom were diagnosed with COVID-19, four were suspected, and 14 were healthy, with a total of 58,924 frames. Each image was labeled using the scoring system proposed by Soldati et al. (2020), seen earlier in **Section 2.2**. Second, the lung point-of-care ultrasound (POCUS), Born et al. (2020b) dataset Born et al. (2020a) contains 39 videos of COVID-19 patients, 14 videos of patients with bacterial pneumonia, and 11 healthy individuals for a total of 64 videos and 1,103 images. Both data sets were collected using a variety of ultrasound scanners and probes by sonographers in multiple different hospitals. The dataset includes ultrasound images of patients with bacterial pneumonia which is an important distinction when attempting to diagnose a patient with COVID-19. On the other hand, ICLUS-DB does only consider COVID-19 patients, but the data is labeled with the severity of the infection.

CNNs have been used previously to detect B-lines in patients with pneumonia. One weakly-supervized network built to detect B-lines in real-time was proposed by van Sloun and Demi (2019). The CNN uses 12 convolutional layers and incorporates a gradient-weight class-activation mapping (grad-CAM) which identifies the regions where B-lines are located. More importantly, the network learns how to identify B-lines based on data labels that only indicate if B-lines are present. Since the network does not need a labeled dataset for training, it is easy to implement and use. Note, however, that this network is not able to count the number of B-lines in an image, though the number of lines is an indication of the state of eration of the lung. Due to layer pooling, the output map highlighting the regions containing B-lines has low resolution. Wang et al. (2019) presents a four layer, semi-supervized CNN capable of measuring the number of

[1]A sequence of two morphological operations, opening and closing, that closes small gaps, see Sternberg (1986) for details.

B-lines in the images. The network was trained on dataset labeled with only the number of visible B-lines without specifying their location. The network can count the number of B-lines, but it is not able to identify their location. A similar approach is used to analyze brightness profiles from LUS data with artificial neural networks (ANN) in Barrientos et al. (2016), Correa et al. (2018).

Another CNN-based method that does not share the limitations described earlier has been proposed by Kulhare et al. (2018), who uses a Single Shot Detector (SSD) to identify the locations of the pleural, A, B, and C-lines. SSDs, introduced by Liu et al. (2016), are a fast and accurate method used to identify objects in pictures. The method uses feature maps generated by a 16 layer CNN presented in Simonyan and Zisserman (2014) to fit bounding boxes around the features. The network training requires training data with ultrasound images with target features locations fully annotated. This supervised algorithm has a sensitivity of 85% on animal specimens but cannot be used for COVID-19 until the two available datasets are annotated.

In contrast, the approach presented by Roy et al. (2020) uses a CNN with a Spatial Transform Network proposed by Jaderberg et al. (2015). It applies linear transformations to the feature maps of the image allowing features to be identified in any orientation. This enables the network to identify the regions of interest by itself. As a result, the network can provide feature localization without great level of supervision. Based on experimental validation, Roy et al. (2020) claim that this approach outperforms the one proposed in van Sloun and Demi (2019).

4 IMAGE CLASSIFICATION

After LUS images have been segmented, they must be classified to provide diagnosis. Using the presence of B-lines, consolidation, etc., a classifier can assign a label to the previously segmented images which can then be used as a basis for diagnosis and prognosis Correa et al. (2018). There are two main methods of classifying LUS images: 1) Feature-based classification where segmented features are analyzed stochastically, and 2) learning-based methods such as NN's which act more as a black box solution. They are trained to classify images based on geometric patterns that are present in certain diseases in the LUS images. This section discusses some available methods for segmented LUS image classification.

4.1 Neural Network Classification

There are mainly two NN methods used to classify images, firstly using pre-segmented images, where regions of interest are segmented by an expert and then fed into a NN, or secondly, a NN may be trained to do both segmentation and classification. Some of the networks discussed in **Section 3.5** are CNN's focused on finding and segmenting features in LUS images.

An interesting manipulation of data is the brightness profile of vectors method presented by Correa et al. (2018). In this method, LUS images of healthy lungs and with pneumonia are distinguished from one another by the brightness profile of the raw LUS data. The brightness profile being the profile that represents a single vector of ultrasound data as strong reflected ultrasound waves are interpreted as "bright". The brightness profile of healthy lung tissue is characterized by smooth, exponentially decaying brightness, whereas unhealthy lung tissue has erratic brightness and non-exponential decay. Rib bones have an abrupt drop on brightness right below the pleuralline.

Cristiana et al. (2020) proposed a direct improvement to Correa et al. (2018) where a secondary NN was trained using softmax activation as a multiclass classifier. The method classifies whether B-lines are present and the multiclass classification network scores the images based on the scoring system presented by Soldati et al. (2020). The two models, binary and multiclass, were trained separate from one another. The binary classifier had a sensitivity of 93% and a specificity of 96%[2] as compared to a medical expert classifying the same images. Agreement between the multiclass severity scoring system and a medical expert was 93% ± 1.

Similarly, Born et al. (2020a) presents POCOVID-Net, the first CNN for identifying COVID-19 through LUS, which uses VGG-16, as established CNN, pre-trained on ImageNet (Krizhevsky et al., 2012) for image feature extraction. It uses a pre-trained 16 layer CNN from Simonyan and Zisserman (2014) to extract lower level features such as textures and shapes. The last three layers of the network were further trained using POCUS dataset to differentiate between patients who were diagnosed with COVID-19, bacterial pneumonia, and healthy individuals. The network uses softmax activation to classify images and had an overall accuracy of 89%. It's sensitivity and specificity for detecting COVID-19 in particular was 96 and 79%. van Sloun and Demi (2019) outline a method for CNN's to segment and classify LUS images for B-lines. This method is one of the few which is capable of real time classification by exploiting GPU acceleration. It had an *in-vitro* accuracy of 91.7%, and an *in-vivo* accuracy of 83.9 when using the ULA-Op transducer, a research platform, and 89.2% using a Toshiba transducer. The network, with six layers, used softmax activation, just as Correa et al. (2018) and Cristiana et al. (2020). The greater accuracy in *in-vitro* data was due to analyzing *in-vitro* images, while the *in-vivo* data were videos as the videos are more complex and variable than the images to analyze as even the breathing of a patient is enough to make B-lines more difficult to detect. Further the presence of intercostal tissue, not present in the *in-vitro* data further complicates its processing. Therefore, a loss of resolution and classification accuracy is expected. van Sloun and Demi (2019) used imagenet a popular CNN architecture, as a basis for their pre-trained neural network, therein easier to train to perform particular tasks.

In Kulhare et al. (2018) a binary classifier, indicating presence or lack thereof, based off the Inception V3 SSD Convolutional Neural Network architecture. The system was trained to classify LUS images with A, B, and pleural lines as well as lung tissue

[2]Specificity is defined as true negatives/(true negatives + false positives), sensitivity is defined as true positive/(true positive + false negative), accuracy is defined as (true positive + true negative)/(all positives + all negatives).

TABLE 1 | Comparison of LUS image classification methods.

Method	Author	Objective	Accuracy	Sensitivity	Specificity
Supervised feed forward ANN (2018)	Correa et al.	Pediatric Pneumonia	—	90.9%	100%
ANN (2016)	Barrientos et al.	Pneumonia	—	91.5%	100%
CNN (2020)	Born et al.	COVID-19	92%	96%	79%
CNN (2020)	Cristiana et al.	B-lines (presence)	94%	—	—
CNN (2020)	Cristiana et al.	B-line (severity)	54%	—	—
CNN (2019)	van Sloun and Demi	B-lines (*in-vitro*)	91.7%	91.5%	91.8%
CNN (2019)	van Sloun and Demi	B-lines (*in-vivo*)	89.2%	87.1%	93%
CNN (2018)	Kulhare et al.	Multiple Abnormalities	—	¿85%	¿85%
SVM Classifier (2020)	Carrer et al.	COVID-19	88–94%	—	—
RVM Classifier (binary) (2016)	Veeramani and Muthusamy	Healthy lung	100%	100%	100%
RVM Classifier (multiclass) (2016)	Veeramani and Muthusamy	Multiple Abnormalities	100%	100%	100%
Stochastic Method (2013)	Brattain et al.	B-lines	100%	—	—

consolidation. Overall, its pleuralline classification was 89% accurate.

Despite the suitability of NN's for LUS image classification, they are often computationally heavier and require greater training sets than other methods. Stochastic methods provide a lighter option which are just as accurate which may be better suited for a portable LUS device.

4.2 Stochastic Classification

Stochastic classifiers are purpose-built classifiers which use statistical regression and image filtering to analyze the segmented images which are fed to them and then classify the image contents.

Brusasco et al. (2019) proposed an off-line method to segment and classify the quantity of B-lines, similar to the CNN model proposed by Wang et al. (2019), in LUS images. The end goal was to create an automated method of determining extravascular lung water. The algorithm scored the segmented gray-scale LUS images. B-lines are classified when the filtered images are scanned and white pixels are measured to make up ¿50% of the total vertical length of the image. Using statistical regression on the segmented LUS images, the total number of B-lines present can be quantified. However, classifying images when many B-lines are present is difficult as they coalesce and are imaged as singular B-lines as opposed to multiple, close-by B-lines.

In Carrer et al. (2020) a support vector machine (SVM) classifies and scores pleural lines. The SVM is fed segmented partitioned United States images whose features were fed into Gaussian radial basis function kernel, a type of SVM classifier known to have a better convergence time than polynomial kernels. The SVM classifier was chosen over an NN as it requires significantly less data to train, which is pertinent as COVID-19 training data is presently lacking. The classifier was applied to linear United States probe and convex United States probe data separately, and the accuracy for the linear and convex probes were 94 and 88%.

A similar method described by Veeramani and Muthusamy (2016) is to use two Relevance Vector Machines, a Bayesian framework for achieving the sparse linear model as per Babaeean et al. (2008), to classify the LUS images as healthy or unhealthy, and if unhealthy what disease is present. RVM's provide a probabilistic diagnosis, as opposed to the discrete diagnose obtained with SVM's. The method offered better accuracy, sensitivity, and specificity than SVM and NN methods. While first RVM classifier was a binary, the second RVM classifier was a multiclass classifier capable of noting which diseases are present in the lung including: respiratory distress syndrome, transient tachypnea of the newborn, meconium aspiration syndrome, pneumothorax, bronchiolitis, pneumonia, and lung cancer. Both the binary and multiclass classifiers had classifying accuracies of 100%.

Brattain et al. (2013) use Gaussian or statistical operations to either score or classify LUS. Gaussian operations are convenient because of their low computational weight. However, they do not share the same level of generality as NN's and as such they are trained on narrower data sets and are prescribed in narrower conditions. In Brattain et al. (2013), a statistical B-line scoring system was developed. Depending on the severity of the B-lines presented, the images were given a score between 0 and 4 using angular features and thresholding. This method analyzed segmented features and determines the severity of the B-lines depending on five conditions: 1) Mean of a B-line column; 2) Column length above half-maximum; 3) Value of the last row of a column; 4) Ratio of the value of the last row over maximum for that column; and 5) Ratio of the value for the midsection of a column over maximum for that column. If these five features exceeded predefined thresholds, the image column is a B-line severity associated with it. However, as per Anantrasirichai et al. (2016) this method is not robust as it is prone to being greatly affected by noise and image intensity meaning the threshold values must be changed depending on the quality of the images being analyzed.

Table 1 provides a comparison of the accuracies of assorted classification methods found in literature.

5 DISCUSSION

The previous sections discussed different methods to identify manifestations of COVID-19 in lung ultrasound images. Several challenges exist in order to implement these methods in a useful clinical setting that can effectively assist healthcare professionals during the course of the pandemic, autonomously identify

manifestations of COVID-19 in LUS images, and assess the severity of the infection according to the grading scale proposed in Soldati et al. (2020). The most important practical considerations are related to the quality of the ultrasound images. This means that the system must guide healthcare professionals during LUS examinations and ensure appropriate image quality is obtained regardless of the operator's experience and hardware, and the image processing method must be integrated into a portable ultrasound system.

5.1 Augmented LUS Images for Operator Guidance

Providing health care practitioners with an alternative to the time consuming and ionizing CT and X-ray scans would reduce the loading on the current medical system. However, the increasing need for lung imaging in hospitals, long-term care homes, and clinics, can lead to a shortage of sonographers. A reduction in that additional load can be sought in the form of a device to be used by personnel other than trained sonographers to either assist in triaging incoming patients or be used as a bedside monitoring tool.

The biggest challenge in LUS is that image segmentation and classification requires quality images. One possible way to assist the operation in this regard is to overlay processed images on top of the original LUS images. For example, one can consider presenting diagnostic information and a real time assessment of the image quality over the original image to intuitively guide the operator as in Moshavegh et al. (2016) and Moshavegh et al. (2018). Image overlay on top of the LUS image can indicate the current state of the image and how the operator can target specific features in the images. Further, following the recommendations outlined in the LUS-based diagnosis of COVID-19 standardization protocol proposed in Soldati et al. (2020), such a software may guide the operator to ensure that:

1. The focal point of the image is set on the pleural line. Using a single focal point and setting it at the right location has the benefit of optimizing the beam shape for sensing the lung surface. At the focus, the beam has the smallest width and is therefore set to best respond to the smallest details.
2. The mechanical index is kept below 0.7. Mechanical index is an indication of an ultrasonic pressure ability to cause micromechanical damage to the tissue. The mechanical index decreases as the focal zone moves further away from the transducer, hence it can become a concern given the previous point, in particular for a long observation time as it is required for LUS. The mechanical index can be changed with the frequency of the beam.
3. The image is not saturated. Saturation occurs when the signal strength of the echo signals is too high making the pressure/echo relationship no longer linear. This has the effect of distorting the signals images, giving rise to completely white areas in the image, which can be easily identified in the software. Control gain and mechanical index can be adjusted to prevent saturation.
4. The ultrasound probe is properly oriented to provide oblique scans. The image features needed in the image processing algorithm are clear.

5.2 Integration With a Portable Hand-Held Ultrasound

High frequency linear array probe is suggested to be used for minor subpleural lesions, as it can provide rich information and improve diagnostic accuracy. In the setting of COVID-19, experts suggest that wireless ultrasound transducers and tablets are the most appropriate ultrasound equipment for diagnosis, Soldati et al. (2020). These devices can easily be wrapped in single-use plastic covers, reducing the risk of viral contamination and making sterilization procedures easy. Furthermore, such devices can range between $4,000 and $8,000, which is a fraction of the cost of regular ultrasound machines. In cases of unavailability of these devices, portable machines dedicated to use for patients with COVID-19 can be still used, although more care for sterilization is necessary.

On a software front, the QLUSS and RVM classification methods presented in **Section 4.2**, respectively, seem well suited for a handheld solution. The QLUSS system has a low computational weight attached to it and is able to operate in real time, which is an asset for front line workers. The RVM method is capable of classifying which lung disease from a list of potentials is present in the LUS images and for processing of images off line. These methods also have the added benefit of requiring small databases, which could be stored in the handheld device itself or on a nearby computer. Using an off-line, i.e., a method which segments and classifies images after they are taken, solution is critical in certain parts of the world due to the possibility of data breach. Or online solutions—i.e., a solution that attempts to segment and classify images live as they are being taken—are simply not feasible due to lack of infrastructure. A portable hand-held United States device would require local storage which could be updated when new data was made available. An alternative option would be to access a database stored online via the Internet, as in Born et al. (2020a), if the infrastructure is available.

5.3 Probe Tracking

Probe tracking, a well documented and researched field Bouget et al. (2017), gives the sonographer the ability to see in real-time the position and orientation of the ultrasound probe. It can be done by integrating a motion sensor into the probe itself. By putting a position stamp on each United States frame would assist in identifying and mapping intercostal tissue and bones which may inadvertently cause black spots in the images, which are of no use. Further, the ability to know each United States images relative location to one another would allow the creation of 3D maps to assist in diagnosis.

6 CONCLUSION

Current advancements in ultrasound image processing provides health care practioners a means of imaging lungs to

diagnose COVID-19. The methods presented in this article may aid in interpreting LUS images autonomously or semi-autonomously, thus allowing doctors without sonographic training to diagnose COVID-19. Integration of image processing for COVID-19 diagnosis into handheld ultrasound machines can be used for beside monitoring, as a triaging tool for quickly diagnosing the severity of COVID-19 present.

As the COVID-19 pandemic and its characteristic traits are so new to medical research, there is a severe lacking of databases with significant resources. But as with every disease that has come before, those resources will come with time. Further, those databases combined with LUS will allow for more in-depth, greater diagnostic tools.

AUTHOR CONTRIBUTIONS

CM wrote **Sections 4–6**, ML wrote **Section 3**, BS, JH, and MF edited the manuscript, and CR wrote **Sections 1**, **2** and edited the manuscript.

FUNDING

We acknowledge the support of Marion Surgical and the Natural Sciences and Engineering Research Council of Canada (NSERC) (funding reference number ALLRP 550307-20). Cette recherche a été menée en collaboration avec Marion Surgical et a été financée par le Conseil de recherches en sciences naturelles et en génie du Canada (CRSNG) (numéro de référence ALLRP 550307-20).

REFERENCES

Anantrasirichai, N., Hayes, W., Allinovi, M., Bull, D., and Achim, A. (2017). Line detection as an inverse problem: application to lung ultrasound imaging. *IEEE Trans. Med. Imag.* 36, 2045–2056. doi:10.1109/TMI.2017.2715880

Anantrasirichai, N., Allinovi, M., Hayes, W., and Achim, A. (2016). "Automatic b-line detection in paediatric lung ultrasound," in 2016 IEEE International Ultrasonics Symposium (IUS), Tours, France, September 18–21, 2016 (New York, NY: IEEE), 1–4.

Babaeean, A., Tashk, A. B., Bandarabadi, M., and Rastegar, S. (2008). "Target tracking using wavelet features and rvm classifier," in 2008 Fourth International Conference on Natural Computation, Jinan, China, October 18–20, 2008 (New York, NY: IEEE) 4, 569–572.

Barrientos, R., Roman-Gonzalez, A., Barrientos, F., Solis, L., Correa, M., Pajuelo, M., et al. (2016). "Automatic detection of pneumonia analyzing ultrasound digital images," in 2016 IEEE 36th Central American and Panama Convention (CONCAPAN XXXVI), San Jose, CA, November 9–11, 2016, (New York, NY: IEEE), 1–4.

Born, J., Brändle, G., Cossio, M., Disdier, M., Goulet, J., Roulin, J., et al. (2020a). Pocovid-net: automatic detection of covid-19 from a new lung ultrasound imaging dataset (pocus). Preprint: arXiv:2004.12084.

Born, J., Wiedemann, N., Brändle, G., Buhre, C., Rieck, B., and Borgwardt, K. (2020b). Accelerating covid-19 differential diagnosis with explainable ultrasound image analysis. Preprint: arXiv:2009.06116.

Bouget, D., Allan, M., Stoyanov, D., and Jannin, P. (2017). Vision-based and marker-less surgical tool detection and tracking: a review of the literature. *Med. Image Anal.* 35, 633–654. doi:10.1016/j.media.2016.09.003

Brattain, L. J., Telfer, B. A., Liteplo, A. S., and Noble, V. E. (2013). Automated b-line scoring on thoracic sonography. *J. Ultrasound Med.* 32, 2185–2190. doi:10.7863/ultra.32.12.2185

Brusasco, C., Santori, G., Bruzzo, E., Trò, R., Robba, C., Tavazzi, G., et al. (2019). Quantitative lung ultrasonography: a putative new algorithm for automatic detection and quantification of b-lines. *Crit. Care.* 23, 288–297. doi:10.1186/s13054-019-2569-4

Buonsenso, D., Piano, A., Raffaelli, F., Bonadia, N., de Gaetano Donati, K., and Franceschi, F. (2020). Point-of-Care Lung Ultrasound findings in novel coronavirus disease-19 pnemoniae: a case report and potential applications during COVID-19 outbreak. *Eur. Rev. Med. Pharmacol. Sci.* 24, 2776–2780. doi:10.26355/eurrev_202003_20549

Carrer, L., Donini, E., Marinelli, D., Zanetti, M., Mento, F., Torri, E., et al. (2020). Automatic pleural line extraction and covid-19 scoring from lung ultrasound data. *IEEE Trans. Ultrason. Ferroelectr. Freq. Control.* 67, 2207–2217. doi:10.1109/TUFFC.2020.3005512

Correa, M., Zimic, M., Barrientos, F., Barrientos, R., Román-Gonzalez, A., Pajuelo, M. J., et al. (2018). Automatic classification of pediatric pneumonia based on lung ultrasound pattern recognition. *PLoS One.* 13, e0206410. doi:10.1371/journal.pone.0206410

Cristiana, B., Grzegorz, T., Seungsoo, K., Katelyn, M., Rachel, L., Shaw, M. M., et al. (2020). Automated lung ultrasound b-line assessment using a deep learning algorithm. *IEEE Trans. Ultrason. Ferroelectr. Freq. Control.* 67, 2312–2320. doi:10.1109/TUFFC.2020.3002249

Gargani, L., and Volpicelli, G. (2014). How i do it: lung ultrasound. *Cardiovasc. Ultrasound.* 12, 25. doi:10.1186/1476-7120-12-25

Grady, L. (2006). Random walks for image segmentation. *IEEE Trans. Pattern Anal. Mach. Intell.* 28, 1768–1783. doi:10.1109/TPAMI.2006.233

Hope, M. D., Raptis, C. A., Amar, S., Hammer Mark, M., and Henry Travis, S. (2020). A role for ct in covid-19? what data really tell us so far. *Lancet.* 395, 1189–1190. doi:10.1016/S0140-6736(20)30728-5

Huang, Y., Wang, S., Liu, Y., Zhang, Y., Zheng, C., Zheng, Y., et al. (2020). A preliminary study on the ultrasonic manifestations of peripulmonary lesions of non-critical novel coronavirus pneumonia (covid-19). doi:10.21203/rs.2.24369/v1

Jaderberg, M., Simonyan, K., Zisserman, A., and Kavukcuoglu, K. (2015). Spatial transformer networks. *Adv. Neural Inf. Process. Syst.*, 2017–2025.

Karakus, O., Anantrasirichai, N., Aguersif, A., Silva, S., Basarab, A., and Achim, A. (2020). Detection of line artefacts in lung ultrasound images of covid-19 patients via non-convex regularization. *IEEE Trans. Ultrason. Ferroelectr. Freq. Control.* 67, 2218–2229. doi:10.1109/TUFFC.2020.3016092

Karamalis, A., Wein, W., Klein, T., and Navab, N. (2012). Ultrasound confidence maps using random walks. *Med. Image Anal.* 16, 1101–1112. doi:10.1016/j.media.2012.07.005

Krizhevsky, A., Sutskever, I., and Hinton, G. E. (2012). Imagenet classification with deep convolutional neural networks. *Adv. Neural Inf. Process. Syst.* 25, 1097–1105. doi:10.1145/3065386

Kulhare, S., Zheng, X., Mehanian, C., Gregory, C., Zhu, M., Gregory, K., et al. (2018). "Ultrasound-based detection of lung abnormalities using single shot detection convolutional neural networks," in *Simulation, image processing, and ultrasound systems for assisted diagnosis and navigation.* (Springer), 65–73.

Lichtenstein, D. A. (2015). Blue-protocol and falls-protocol: two applications of lung ultrasound in the critically ill. *Chest.* 147, 1659–1670. doi:10.1378/chest.14-1313

Lichtenstein, D. A. (2009). Ultrasound examination of the lungs in the intensive care unit. *Pediatr. Crit. Care Med.* 10, 693–698. doi:10.1097/PCC.0b013e3181b7f637

Liu, W., Anguelov, D., Erhan, D., Szegedy, C., Reed, S., Fu, C.-Y., et al. (2016). "Ssd: single shot multibox detector," in European conference on computer vision, Amsterdam, Netherlands, October 8–16, 2016 (Springer), 21–37. doi:10.1007/978-3-319-46448-0_2

Moshavegh, R., Hansen, K. L., Møller-Sørensen, H., Nielsen, M. B., and Jensen, J. A. (2018). Automatic detection of b-lines in lung ultrasound. *IEEE Trans. Ultrason. Ferroelectr. Freq. Control.* 66, 309–317. doi:10.1109/TUFFC.2018.2885955

Moshavegh, R., Hansen, K. L., Sørensen, H. M., Hemmsen, M. C., Ewertsen, C., Nielsen, M. B., et al. (2016). "Novel automatic detection of pleura and b-lines (comet-tail artifacts) on *in vivo* lung ultrasound scans," in Medical Imaging

2016: Ultrasonic Imaging and Tomography (International Society for Optics and Photonics) 9790, 97900K.

Nazerian, P., Volpicelli, G., Vanni, S., Gigli, C., Betti, L., Bartolucci, M., et al. (2015). Accuracy of lung ultrasound for the diagnosis of consolidations when compared to chest computed tomography. *Am. J. Emerg. Med.* 33, 620–625. doi:10.1016/j.ajem.2015.01.035

Noble, J. A., and Boukerroui, D. (2006). Ultrasound image segmentation: a survey. *IEEE Trans. Med. Imaging.* 25, 987–1010. doi:10.1109/tmi.2006.877092

Roy, S., Menapace, W., Oei, S., Luijten, B., Fini, E., Saltori, C., et al. (2020). Deep learning for classification and localization of covid-19 markers in point-of-care lung ultrasound. *IEEE Trans. Med. Imaging.* 37, 2676–2687. doi:10.1109/TMI.2020.2994459

Simonyan, K., and Zisserman, A. (2014). Very deep convolutional networks for large-scale image recognition. Preprint: arXiv:1409.1556.

Soldati, G., Smargiassi, A., Inchingolo, R., Buonsenso, D., Perrone, T., Briganti, D. F., et al. (2020). Proposal for international standardization of the use of lung ultrasound for patients with covid-19: a simple, quantitative, reproducible method. *J. Ultrasound Med.* 39, 1413–1419. doi:10.1002/jum.15285

Staub, L. J., Biscaro, R. R. M., and Maurici, R. (2018). Accuracy and applications of lung ultrasound to diagnose ventilator-associated pneumonia: a systematic review. *J. Intensive Care Med.* 33, 447–455. doi:10.1177/0885066617737756

Sternberg, S. R. (1986). Grayscale morphology. *Comput. Vis. Graph. Image Process.* 35, 333–355. doi:10.1016/0734-189x(86)90004-6

Thomas, A., Haljan, G., and Mitra, A. (2020). Lung ultrasound findings in a 64-year-old woman with covid-19. *CMAJ.* 192, E399. doi:10.1503/cmaj.200414

van Sloun, R. J. G., and Demi, L. (2020). Localizing b-lines in lung ultrasonography by weakly supervised deep learning, *in-vivo* results. *IEEE J. Biomed. Health Inform.* 24, 957–964. doi:10.1109/JBHI.2019.2936151

Veeramani, S. K., and Muthusamy, E. (2016). Detection of abnormalities in ultrasound lung image using multi-level rvm classification. *J. Matern. Fetal Neonatal. Med.* 29, 1844–1852. doi:10.3109/14767058.2015.1064888

Volpicelli, G., Silva, F., and Radeos, M. (2010). Real-time lung ultrasound for the diagnosis of alveolar consolidation and interstitial syndrome in the emergency department. *Eur. J. Emerg. Med.* 17, 63–72. doi:10.1097/mej.0b013e3283101685

Wang, X., Burzynski, J. S., Hamilton, J., Rao, P. S., Weitzel, W. F., and Bull, J. L. (2019). Quantifying lung ultrasound comets with a convolutional neural network: initial clinical results. *Comput. Biol. Med.* 107, 39–46. doi:10.1016/j.compbiomed.2019.02.002

Conflict of Interest: The authors declare that the research was conducted in the absence of any commercial or financial relationships that could be construed as a potential conflict of interest.

frontiers in Robotics and AI

ORIGINAL RESEARCH
published: 15 March 2021
doi: 10.3389/frobt.2021.624333

Efficient Coverage Path Planning for Mobile Disinfecting Robots Using Graph-Based Representation of Environment

B. Nasirian[1], *M. Mehrandezh*[1] *and F. Janabi-Sharifi*[2]*

[1]*Faculty of Engineering and Applied Science, University of Regina, Regina, SK, Canada,* [2]*Robotics, Mechatronics and Automation Laboratory (RMAL), Department of Mechanical and Industrial Engineering, Ryerson University, Toronto, ON, Canada*

The effective disinfection of hospitals is paramount in lowering the COVID-19 transmission risk to both patients and medical personnel. Autonomous mobile robots can perform the surface disinfection task in a timely and cost-effective manner, while preventing the direct contact of disinfecting agents with humans. This paper proposes an end-to-end coverage path planning technique that generates a continuous and uninterrupted collision-free path for a mobile robot to cover an area of interest. The aim of this work is to decrease the disinfection task completion time and cost by finding an optimal coverage path using a new graph-based representation of the environment. The results are compared with other existing state-of-the-art coverage path planning approaches. It is shown that the proposed approach generates a path with shorter total travelled distance (fewer number of overlaps) and smaller number of turns.

Keywords: coverage path planning, disinfection, optimization, deep reinforcement learning, autonomous mobile robots

OPEN ACCESS

Edited by:
Mahdi Tavakoli,
University of Alberta, Canada

Reviewed by:
Cosmin Copot,
University of Antwerp, Belgium
Hongjun Xing,
Harbin Institute of Technology, China

***Correspondence:**
F. Janabi-Sharifi
fsharifi@ryerson.ca

Specialty section:
This article was submitted to Biomedical Robotics, a section of the journal Frontiers in Robotics and AI

Received: *31 October 2020*
Accepted: *07 January 2021*
Published: *15 March 2021*

Citation:
Nasirian B, Mehrandezh M and Janabi-Sharifi F (2021) Efficient Coverage Path Planning for Mobile Disinfecting Robots Using Graph-Based Representation of Environment. Front. Robot. AI 8:624333. doi: 10.3389/frobt.2021.624333

INTRODUCTION

Surfaces contaminated with COVID-19 pathogens in hospitals introduce significant risk to the safety of medical personnel and patients. Disinfection routines are among critical measures that hospitals are taking to minimize the spread of COVID-19. To reduce the workload of the hospitals' cleaning teams and to avoid the direct contact of disinfecting agents such as chemicals or UV-C disinfectants with human body, autonomous mobile robots would provide a favorable solution. The autonomous robots can potentially perform the disinfection task more precisely and in a timely and cost-effective fashion. Central to robotic disinfection routines is the coverage path planning.

Coverage Path Planning (CPP) will lead to an improvement in the efficiency of operations in terms of cost, time, and job quality. It is defined as: generating a continuous and un-interrupted path that covers an area of interest, while avoiding obstacles (Galceran and Carreras, 2013). The efficiency of a CPP algorithm is usually determined by the total coverage ratio, completion time, total travelled path length, and the number of turns (Khan et al., 2017).

Some CPP works cited in the literature are based on heuristics or randomized approaches, where the coverage path is determined based on a set of simple behaviors (e.g., Mackenzie and Balch, 1993) or randomized search through the environment (e.g., Palacin et al., 2005). These methods, however, do not guarantee a complete coverage of the free space (Choset, 2001) while coverage completeness is essential to guarantee that all COVID-19 pathogens are killed during the robotic disinfection tasks.

Complete CPP methods decomposed the free space into smaller regions (cells) in which optimal path planning could be simply formulated (Choset, 2001). A complete coverage was achieved by ensuring that the robot visited all cells in the decomposed environment at least once (Choset, 2001). Among the decomposition methods cited in the literature, an exact environment decomposition method would stand out specially in environments with un-even-shape boundaries and in presence of concave-shape obstacles since the re-union of the cells under this decomposition method would fully represent the free space (Cabreira et al., 2019). In the pertinent literature, three topics are given special attention: 1) the environment decomposition techniques, 2) the optimal coverage path in each cell generated via environment decomposition, and 3) the optimal coverage sequences (Cabreira et al., 2019). In this paper we formulate a complete coverage path planning in the environment that leads to a minimal travelled distance (cost).

The operational environment would generally consist of obstacles, free space, and the mobile robot. In the Boustrophedon decomposition, as the most commonly-used exact cellular decomposition approach, the free space was divided into smaller regions (cells) by sweeping a line through the whole target area in one direction (Choset and Pignon, 1998; Choset et al., 2000). In order to traverse from one cell to another, the robot might need to transit through a part of a third cell. This causes overlaps, thus, extra travelled distance. This is mainly due to the fact that no mechanism has been considered for transition from one cell to another in present exact cellular decomposition methods. To avoid the unnecessary cost associated with this transition, a modified version of the Boustrophedon-based decomposition has been proposed by us. Three transition cells have been added to the decomposed environment at each critical point. This allows the robot to either expand or shrink the original cells around the critical point to avoid the overlaps of inter-cell traversals and cell coverage paths (further explained in Section *Modified Graph Considering the Modified Environment Decomposition (to Avoid Overlaps)*).

Under classical CPP approaches (e.g., Choset and Pignon, 1998; Choset et al., 2000), an adjacency graph was built based on the topology of the decomposition, where the nodes of the graph represented the cells and the edges of the graph connected the nodes with adjacent corresponding cells in the decomposed environment. The problem of finding the optimal coverage sequence was equivalent to finding the shortest path within the adjacency graph that visits each node (cell) at least once, which was equivalent to the Traveling Salesman Problem. The problem of finding the optimal path over the adjacency graph is an NP-complete problem. A depth-first graph search algorithm was proposed to find an exhaustive walk through the adjacency graph. However, the depth-first search solution was not optimal, was computationally expensive, and required huge memory storage for problems with a large adjacency graph (i.e., environments with a large number of cells). Later works on CPP (e.g., Jimenez et al., 2007; Hameed et al., 2013; Tung and Liu, 2019) utilized Genetic Algorithm (GA) optimization techniques to find an efficient coverage sequence over larger adjacency graphs in a shorter computational time and with less required memory space. However, in the coverage path found using the adjacency graphs the robot usually needs to traverse through the middle of the cells to transit from one cell to another, which results in overlaps (extra travelled distance). The shortest path that visits all nodes of the adjacency graph is not necessarily equivalent to the shortest path travelled by robot since the graph does not consider the overlaps of the transition paths with coverage back-and-forth straight-line motions in the cell.

Another approach to find the traversal sequences was to create a Reeb graph of the environment, where the nodes denoted the critical points, and the edges represented the cells (Mannadiar and Rekleitis, 2010). In order to find the most efficient coverage sequence, the Chinese Postman Problem was solved over the graph, that was to find the shortest tour that traversed over every edge at least once (Mannadiar and Rekleitis, 2010). In (Mannadiar and Rekleitis, 2010; Xu et al., 2011; Xu et al., 2014), the Reeb graph was modified to an Eulerian graph by duplicating selected edges of the graph. The edge duplication referred to a situation, where the cell corresponding to the duplicated edge in graph was divided into two different cells, which further leaded to extra turns to make in the middle of the original cell. Since performing a turn in the path takes more time and energy than that in a straight-line motion, an efficient coverage path should be generated such that the total number of turns is minimized and consequently the total operational time and cost of the CPP is decreased (Galceran and Carreras, 2013).

In this work, a CPP approach is proposed that works based on a new graph representation of environment. In order to avoid the costly turns in the middle of the cells, which is the case in (Mannadiar and Rekleitis, 2010; Xu et al., 2011; Xu et al., 2014), and transition path overlaps through the middle of the cells, which is the case in (Jimenez et al., 2007; Hameed et al., 2013; Tung and Liu, 2019), two different possible actions have been considered for the robot in a cell: 1) back-and-forth straight-line motion with turns at the end of the lines for covering the cell, and 2) environment/obstacle contour-following motion to adjust the robot position for starting the cell coverage. At those cells, which had their corresponding Reeb graph edge duplicated in (Mannadiar and Rekleitis, 2010; Xu et al., 2011; Xu et al., 2014), the robot will have the option to follow some parts of the cell's contour in the first traversal, and then cover the cell by back-and-forth straight-line motion in the second traversal without any overlaps with the covered parts of the cell's contour in first traversal. This would lead to a new form of graph in which the Eulerian cycle/path needs to be determined leading to a minimum travelled distance (overlaps). The number of turns would be also less than that cited in literature, (e.g., Xu et al., 2014), since the turns in the middle of the cells are eliminated (this will be further explained in Section *Modified Graph Considering Contour-Following Motion*).

Another contribution of this research is that it evaluates the inter-cell traversals at a low-level as well. The travelled distance depends on both current-cell-coverage end point and next-cell-coverage start point. Most of the previous works on CPP (e.g., Choset and Pignon, 1998; Jimenez et al., 2007; Xu et al., 2014) did not consider the current position of the robot in the current cell to choose the next cell in the coverage sequence. In (Chen et al.,

2019), a corner model was utilized to find the shortest path between the current cell and the next cell which would not necessarily lead to an optimal path that robot can take. Their technique did not choose the corner that cell coverage should be started from, hence, the corner information was not included in their graph representation of the environment. In (Hameed et al., 2013; Tung and Liu, 2019), entrance and exit points have been considered for each cell which resulted in multiple inter-cell paths for each cell. In this work, four corners have been considered at each cell as the candidates for the cell coverage start and/or end points. Contrary to the case in a Reeb graph, where the nodes represent the critical points, in the proposed graph by us, the nodes represent the cell corner points at the critical points. Some extra edges get added to the graph, which facilitate inter-cell traversal paths at each critical point. To perform a complete coverage, some edges are required to be traversed (cell coverage edges), while some other will remain optional (i.e., contour-following, and inter-cell traversal edges) (for further explanation see Section *Modified Graph Considering Cell Coverage Start and End Points*).

The problem of finding the efficient cell coverage sequence can be solved by finding a path over the proposed graph in which a required subset of the edges is needed to be traversed with minimal cost. In this work, the cell coverage sequence optimization problem has been considered as a Markov Decision Process (MDP), and the efficient sequence within the graph has been found using a double Deep Q Network (DQN) approach. Double DQN is a Deep Reinforcement Learning (DRL) method which utilizes two identical deep neural networks to estimate Q-values where each of the networks is used to update the other. The efficient coverage sequence of the cells is equivalent to the optimal policy found via the double DQN. In addition to finding shortest travelled distance, the path generated through this method is robust to changes in the start and/or end positions of the disinfection task and works for coverage of any arbitrary subset of the cells in the target space (further explained in Section *Coverage Optimization Over the Proposed Graph*).

The aim of this work is to decrease the disinfection task cost by adopting a new graph-based representation of the environment. More specifically, the contributions are:

- A new graph representation of the environment has been proposed based on the following modifications which facilitate finding an efficient coverage path for disinfection task.

    1) Proposing a modified version of the Boustrophedon environment decomposition with three transition cells added at each critical point to allow the original cells expansion or shrinkage;
    2) Programming two different actions for the robot in a cell: 1) back-and-forth straight-line motion, and 2) contour-following motion to adjust the robot position for starting the cell coverage with no extra travelled distance (overlaps); and
    3) Considering the corners of the cells (as the candidates for the cell coverage start and/or end points) as graph nodes to minimize the inter-cell traversal path overlaps at each critical point.
- The optimization problem over the proposed graph has been solved using a Double DQN technique which trains a model over the environment to find an efficient coverage path for any start and/or end positions of the disinfection task and any arbitrary subset of the cells in the environment.

The results of the proposed approach are compared with other complete CPP approaches cited in literature for indoor environments (see Section *Results and Discussion*). It is shown that the proposed approach outperforms the previous techniques in terms of the total travelled distance. In addition, the total number of turns are reduced in comparison with the work in (Xu et al., 2014). Also, the proposed method is robust to changes in the start and/or end positions of the robot used for the disinfection task, and that it generates coverage path for any arbitrary set of the cells in the decomposed environment. This will reduce the overall cost of repetitive disinfection tasks in large hospitals drastically.

METHODOLOGY

In order to decrease the travelled distance and the number of turns in the hospital disinfection task, a complete CPP based on a new graph representation of the decomposed environment has been proposed. In this section the steps and approaches of environment decomposition, constructing the graph, and solving the optimization problem over the graph are described.

Environment Decomposition

CPP in environments comprised of non-convex boundaries and obstacles renders itself as a complex problem. A commonly-used technique in most CPP approaches is to decompose the environment using exact cellular decomposition into smaller regions (cells) in which optimal path planning can be formulated (Choset, 2001). Boustrophedon decomposition is one of the most commonly-used exact cellular decomposition methods for CPP problem over planar environments. The Boustrophedon decomposition assumes the environment boundaries are polygonal and known a priori. In this method, a line segment (called a slice) is swept through the whole target area in one direction to determine the critical points. Critical points are the vertices of the environment boundaries where the sweeping slice connectivity changes (Choset and Pignon, 1998). One or two new cells are formed whenever the slice arrives at a critical point, as shown in **Figure 1**. The decomposition can be done in different directions (i.e., different slice sweeping directions) resulting in different cell decomposition configurations. One can also optimize the coverage by finding the best decomposition direction over a particular environment which leads to a cost-efficient coverage path (Oksanen and Visala, 2009).

After decomposing the environment into cells, the optimal coverage path inside each cell can be determined separately by

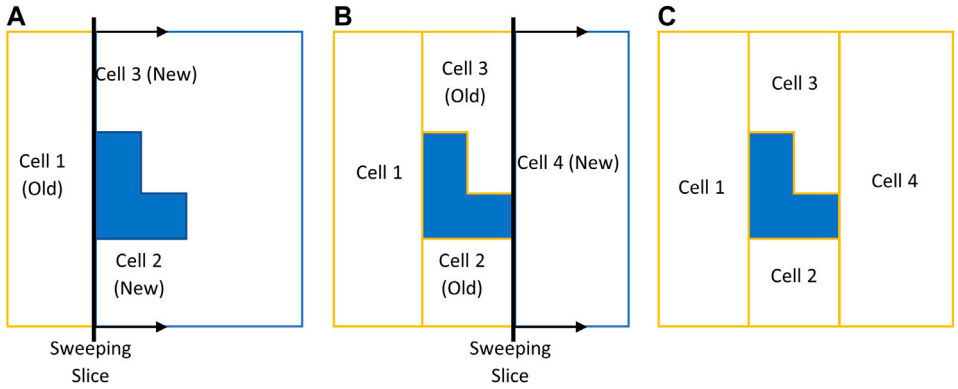

FIGURE 1 | Boustrophedon decomposition technique with a slice sweeping from left to right. **(A)** Slice connectivity changes from one to two which results in two new cells. **(B)** Slice connectivity changes from two to one which results in one new cell. **(C)** Decomposed environment.

minimizing a coverage cost function. The direction of the back-and-forth straight-line motions can be determined in a way that the total number of turns is minimized and consequently the total operational time of the CPP is decreased (Galceran and Carreras, 2013).

Graph Representation of Decomposed Environments

In order to find an efficient sequence in traversing all the cells in a decomposed environment, a commonly-used approach is to build a graph that captures the topology of the cells. The problem of finding the minimum cost coverage sequence is then equivalent to finding the shortest path over this graph. In this work, we have proposed a new graph representation of the environment which leads to a more efficient coverage path. More details are provided in the following sub-sections.

Mobile Robot

The proposed CPP technique in this work focuses on finding the efficient sequence of cells coverage and the inter-cell paths connecting the cells using a graph representation of the environment. Similar to some other suggested CPP-based techniques cited in the literature (e.g., Choset and Pignon, 1998; Mannadiar and Rekleitis, 2010; Hameed et al., 2013; Chen et al., 2019), the proposed CPP technique in general is not limited to a particular robot and is implementable on most of the mobile disinfecting robots available in the market. However, some assumptions have been made on the mobile robot shape, disinfection system, and the drive mechanism when in designing the proposed graph representation and the coverage path over the environment.

The mobile robot is assumed to have a disk shape (i.e., the robot is presented as a circle that circumscribes the robot footprint entirely). Also, we assume that the robot is equipped with a UV-C disinfection system. In order to avoid collision with environment boundaries, the diameter of the circle circumscribing the robot (L) should be known while generating the proposed graph and the coverage path (equivalent to constructing the configuration space). Furthermore, disinfection diameter (D) denotes the diameter of the area that the robot can disinfect using its onboard probes, e.g., the maximum range of the onboard UV-C lamp array can be considered as the disinfection radius. Disinfection diameter (D) is always greater than or equal to the diameter of the largest circle that circumscribes the entire robot (L). It is also assumed that the disinfecting robot is of a differential-drive type, which is capable of turning on the spot. Therefore, the robot does not need any extra space to perform turns at the end of the straight-lines in the planned path.

In order to disinfect things such as the beds, walls, shelves, and other equipment in the hospitals, the disinfection coverage diameter (W) is assumed to be always smaller than or equal to the disinfection diameter (D). Please note that, in the coverage path, the distance between the stripes and the distance of the robot's center point to the boundaries of the obstacles are equal to W and W/2, respectively. This means that the free space will get disinfected based on the disinfection coverage diameter (W), while a depth of (D/2-W/2) of the walls and obstacles are being disinfected (note that $D \geq W \geq L$). All the items within the range (i.e., at the D/2 distance from the center of the robot) along the path will be disinfected. We also assume that, in addition to vertical UV-C emitters, there are circumferential emitters to disinfect blind spots immediately under and/or surrounding the robot. If there are goods covered by other objects, they will likely be missed due to the nature of radiation-based disinfection. Since W is always greater than or equal to L, it is guaranteed that the robot will not collide with the environment boundaries (equivalent to constructing an automaton representation of a point robot within its configuration space). Robot diameter (L) and disinfection diameter (D) depend on the mobile robot used for the disinfection task while the disinfection coverage diameter (W) can be selected by a user based on the required obstacles disinfection depth (D/2-W/2). The disinfection coverage diameter (W) is an input to the proposed algorithm in this work, and it can be adjusted by the user. In all figures and results presented in this paper, the default

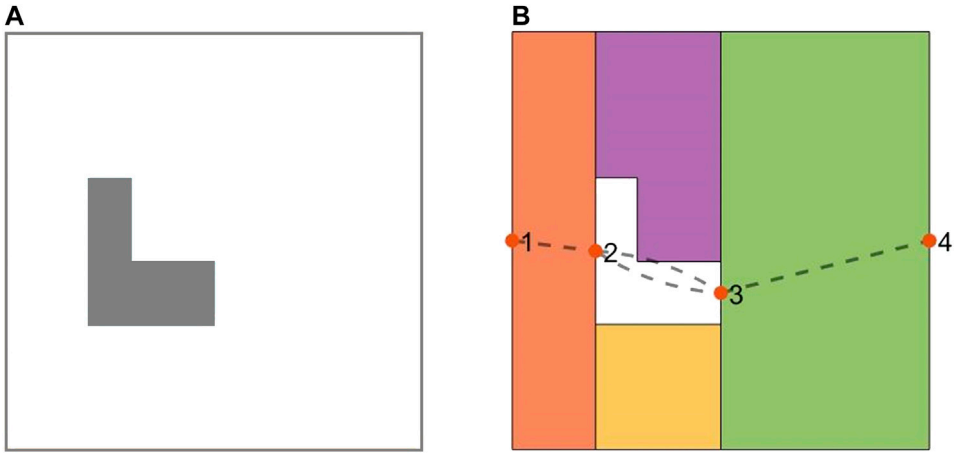

FIGURE 2 | (A) The planar map of a simple indoor environment in presence of a convex obstacle. **(B)** The Boustrophedon decomposition and Reeb graph representation of the environment. The numbered solid points represent the nodes, and the dashed lines denote the edges in the Reeb graph.

value of W is assumed to be equal to 1 m. The algorithms would allow different W values, however.

Reeb Graph

One of the approaches that has been utilized in the literature is based on generating a Reeb graph representation of the environment and to solve the Chinese Postman Problem over that graph (Mannadiar and Rekleitis, 2010). Under this, the nodes denote the critical points, and the edges represent the cells connecting two neighboring critical points. **Figure 2** illustrates the Boustrophedon decomposition and Reeb graph representation of a simple environment in presence of a convex-shape obstacle. In **Figure 2**, the Reeb graph contains four nodes (critical points) and four edges (cells).

In order to find the best coverage sequence of the cells, one needs to solve the Chinese Postman Problem on the graph, which translates to: finding the shortest tour that traverses every edge on the Reeb graph at least once. If the Reeb graph of the environment is an Eulerian graph, all its Euler tours will be solutions to the Chinese Postman Problem (Mannadiar and Rekleitis, 2010). For non-Eulerian Reeb graphs, a standard approach to solve the Chinese Postman Problem is to modify the graph to an Eulerian one by duplicating selected edges in the graph. The challenge is to choose duplicated edges such that the total cost (the sum of the individual costs of all the edges) of the Euler tour be minimized (Mannadiar and Rekleitis, 2010). Different strategies such as linear programming and matching theory algorithms can be utilized to determine which edges to duplicate (Edmonds and Johnson, 1973).

However, the generated paths in (Mannadiar and Rekleitis, 2010; Xu et al., 2011; Xu et al., 2014) include a high number of turns in the middle of the environment because of dividing the cells with duplicated edges into two parts. In addition, the travelled distance can decrease by applying some modifications to the Reeb graph. Our proposed approach to resolve these short comings by modifying the Reeb graph is described in the following sections.

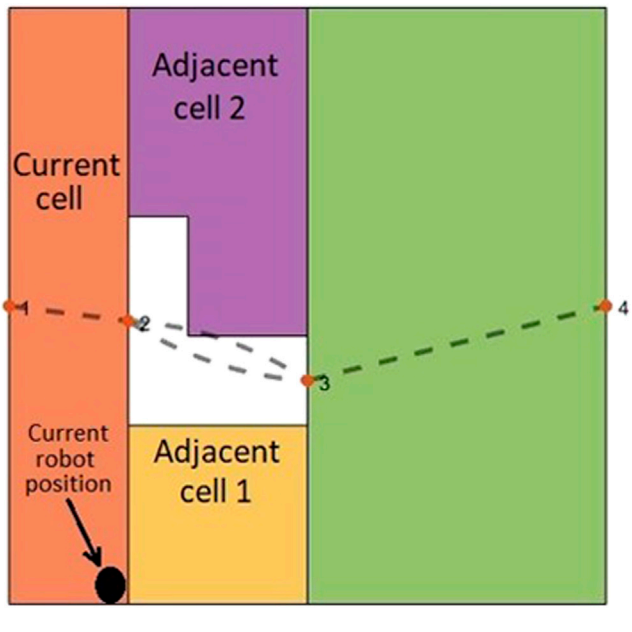

FIGURE 3 | The position of the mobile robot along the common boundary is an important factor in choosing one of the adjacent cells as the next cell in the coverage sequence.

Modified Graph Considering Cell Coverage Start and End Points

Most of the previous works on CPP did not consider the position of the mobile robot in the current cell to choose the next cell in the coverage sequence. As shown in **Figure 3**, if the mobile robot is at the common boundary of the current cell (already covered cell) and two adjacent cells (not covered yet), the position of the mobile robot along the common boundary would be an important factor to account for when choosing the next cell in the coverage sequence. For example, when the robot is at the position shown in **Figure 3**, the adjacent cell one would be a

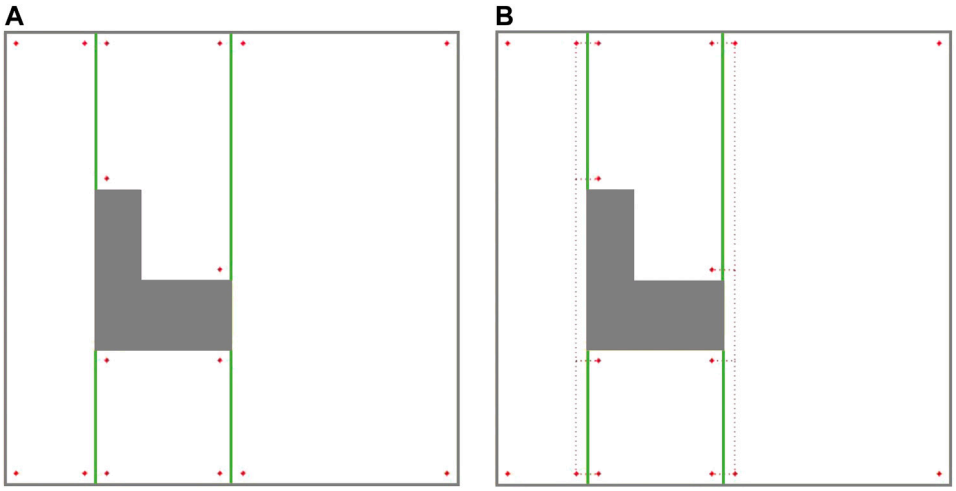

FIGURE 4 | (A) The candidate cell coverage with start and end points at each cell. **(B)** The inter-cell transition options for mobile robot at each corner of the cells. The dashed red lines show the inter-cell transition paths.

better candidate, than adjacent cell 2, to be the next cell in the coverage sequence. In (Chen et al., 2019), the shortest path between the current cell and the next cell is obtained by using a corner model. However, the shortest path between them is not always the best path. Graph-search approaches under CPP do not consider this point because graphs, particularly Reeb graphs, do not contain any information about the position of the robot at the critical points.

The Reeb graph representation of the environment needs to be modified to include the information on position of the robot at the critical points. As illustrated in **Figure 4A**, four corners are being considered for every cell as the potential cell coverage start and end points. There are two critical points at two sides of a cell (left critical point and right critical point). In each cell, two corners are located on the right side of the left critical point (left-top and left-bottom), and two corners are located on the left side of the right critical point (right-top and right-bottom).

As it can be seen in **Figure 4A**, corners have an offset of W/2 from critical points horizontal position and environment boundaries, with W being the robot coverage diameter. This offset ensures that: 1) the robot does not collide with the environment boundaries (equivalent to constructing an automaton representation of a point robot within its configuration space) of the environment and 2) the covered areas at the common boundary of two adjacent cells do not overlap.

Figure 4B shows that the robot located at each corner of the current cell will have four optional paths to traverse to reach one of the four adjacent-cell corners. One should note that corners at the most left and most right critical points of the environment are exceptions. These optional paths can be added to the Reeb graph as some extra edges, which facilitate the inter-cell traversal at each critical point.

In the proposed modified graph, nodes denote the cell corners (not the critical points), and some optional edges are added to the graph representing the paths between the corners. In addition to the nodes, the Reeb graph edges need to be modified as well. Traversing each edge of the Reeb graph is equivalent to the corresponding cell coverage. However, as it is shown in **Figure 5**, the cell coverage can be done under two different options. Under the first cell-coverage option, if the robot starts the cell coverage from the left-bottom corner (corner 4) of the current cell, it will finish the coverage in one of the two right corners depending on the cell width and disinfection coverage diameter. In **Figure 5A**, the cell coverage finishes at the right-bottom corner (corner 3). The coverage path is undirected, so the coverage can start from corner three and end at corner 4. Under the second cell-coverage option, if the robot starts the cell coverage from the left-top corner (corner 1) of the same cell, the end corner on the right side (right-top corner or corner two in **Figure 5B**) would be different than the end corner in the first cell coverage option. Therefore, each edge of the Reeb graph should be replaced with a pair of coverage edges, where traversing only one of these edges will suffice for cell coverage.

This would lead to a new graph-search problem in which some edges are required to be traversed (one of the two cell coverage edges at each cell), while some other edges will remain optional (inter-cell traversal edges in **Figure 4B**). Closest problem cited in the literature to this setup would be the Rural Chinese Postman Problem, where a subset of the edges from the graph are required to be traversed at a minimal cost. Since this required subset does not form a weakly-connected network, the Rural Chinese Postman Problem would constitute an NP-complete problem (Pearn and Wu, 1995). As opposed to that in the original Rural Chinese Postman Problem, there is a pair of coverage edges associated to each cell in the graph, and only one of these coverage edges is required to be traversed in our case. This means that there are no edges that are required to be traversed; however, there are pairs of edges that remain essential to be traversed. When one of the edges in a pair is traversed, that pair is considered to be complete. The graph representation of the simple environment

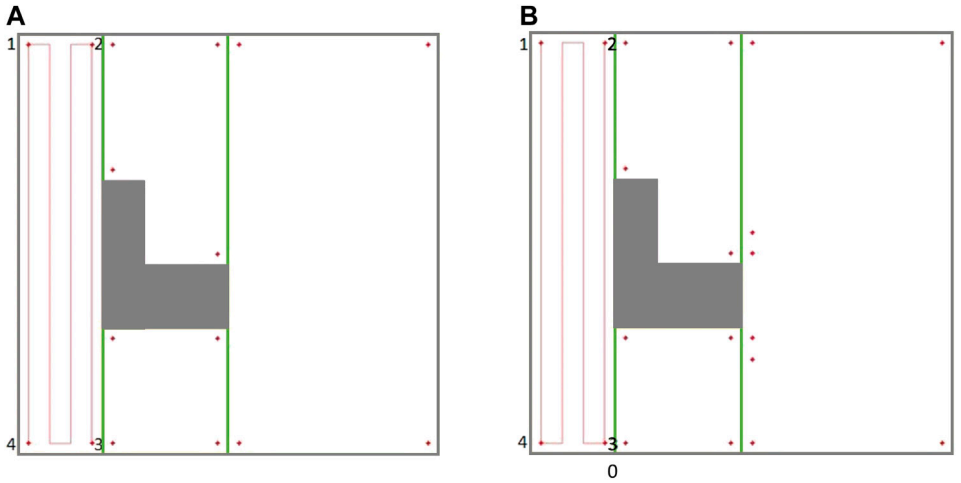

FIGURE 5 | The coverage paths of a cell starting from different corners. **(A)** Cell coverage started from corner 4 ending at corner 3, and vice versa. **(B)** Cell coverage started from corner 1 ending at corner 2, and vice versa.

seen in **Figure 2**, with coverage edge pairs and inter-cell traversal edges at each critical point (CP) is shown in **Figure 6**. The environment boundaries and cell decomposition have been removed from that in **Figure 6** to illustrate that the cell coverage sequence problem can be solved as a solely graph-search problem indeed. In **Figure 6A**, all the quotients in dividing cells' widths based on the coverage diameter (W) in this environment are even numbered. Therefore, the coverage edges' end points are adjacent to their start points. **Figure 6B** shows a case where the quotient in dividing cell 4's width by the coverage diameter (W) is odd numbered. As it can be seen in **Figure 6B**, the coverage edges in cell four start and end corners are not adjacent. It should be noted that the proposed graph representation of environment is undirected; therefore, both coverage and inter-cell traversal edges do not have a direction.

Modified Graph Considering Contour-Following Motion

As it can be seen in **Figure 6A**, in order to find a route over the graph which traverses all coverage edge pairs, some of the coverage edges would be required to be duplicated or at some cases both coverage edges in the same pair have to be traversed. In (Mannadiar and Rekleitis, 2010; Xu et al., 2011; Xu et al., 2014), in order to avoid covering the cells with duplicated edges twice, the graph-search algorithm was modified to cover the top (or bottom) part of the cell in the first traversal and the bottom (or top) part of the cell in the second traversal. However, as **Figure 7** shows, the generated path includes a high number of turns right in the middle of the environment because of splitting cells. One should note that turns are more costly, so they have to be avoided. The travelled distance is also increased under this algorithm because of the extra distance travelled to make those turns.

Instead of splitting the cells into two, we have defined a contour-following option for the mobile robot. It allows the robot to adjust its position in a cell, or cross a cell, without traversing cell coverage edges. This will result in a reduced number of turns and travelled distance. Two different actions are considered for the robot inside each cell: 1) back-and-forth straight-line motion with turns at the end of the lines (cell coverage edges pair), and 2) contour-following motion to adjust the robot position for starting the cell coverage (contour-following edges).

In this approach, instead of duplicating the coverage edges or traversing both cell coverage edges in the same pair, the mobile robot follows some parts of the cell's contour in the first traversal to get to a favorable corner node to start the cell coverage from. Then, it covers the rest of the cell by back-and-forth straight-line motions in the second traversal. An optimal coverage path over the environment in **Figure 2** has been represented in **Figure 8**. A contour-following motion has been performed by the mobile robot in cell 3. As it can be seen in **Figure 8**, there would be no overlaps between the back-and-forth straight-line motions and the path taken by robot to adjust its position for starting cell three coverage which was not the case in CPP techniques (Jimenez et al., 2007; Hameed et al., 2013; Tung and Liu, 2019) that utilized adjacency graph to find the coverage sequence.

There are four possible contour-following paths at each cell connecting the adjacent cell corners to each other. The contour-following paths have been added to the graph (see **Figure 6C**). In CPP problem, traversing of the contour-following edges is not required.

Modified Graph Considering the Modified Environment Decomposition (to Avoid Overlaps)

The ellipse shown in **Figure 8** represents a part of the optimal path over the environment, where the most left stripe of cell 4 has been covered separately while the robot was traversing from cell two to cell three and from cell two to cell four. Cell four coverage has started from the second stripe of the cell. The

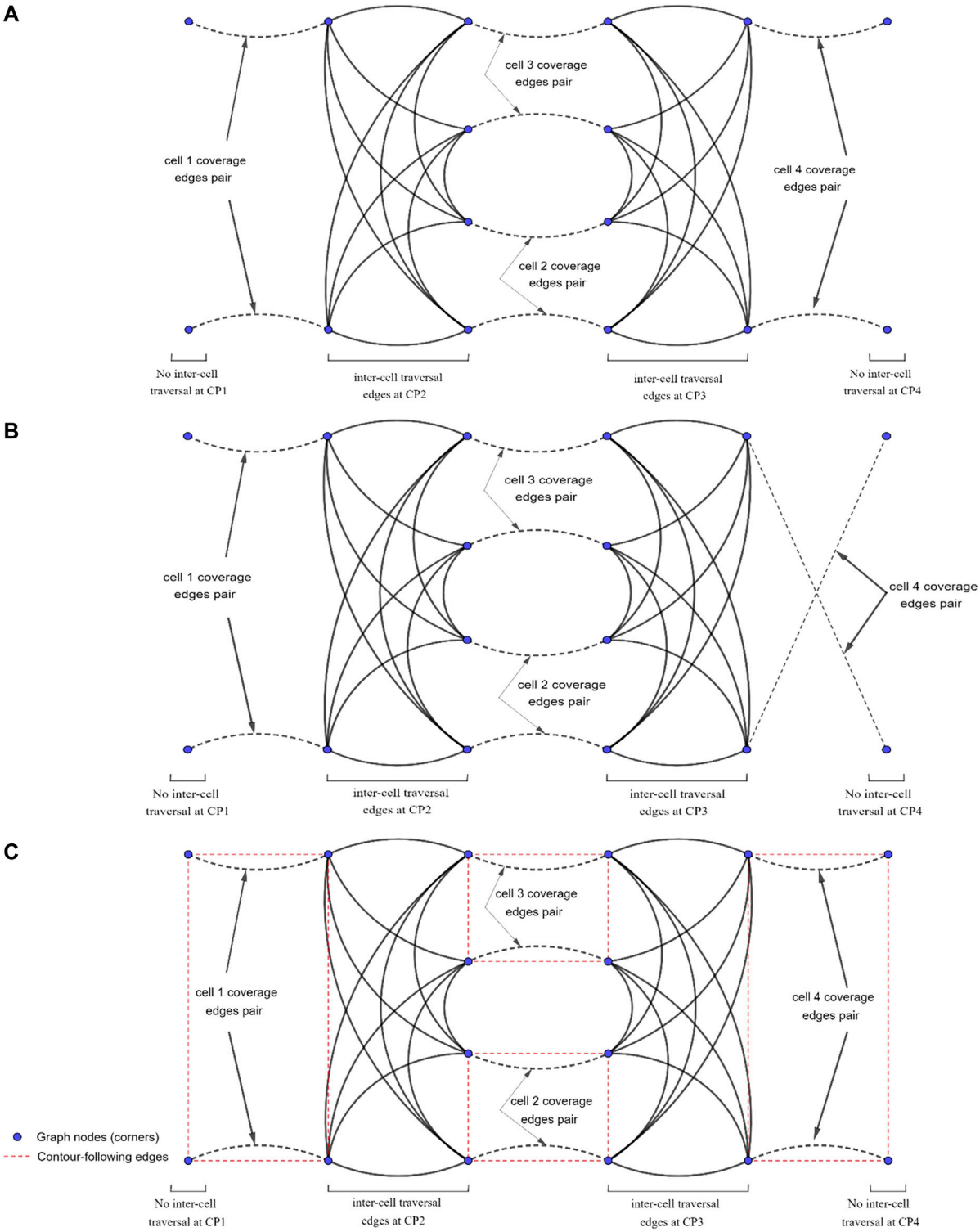

FIGURE 6 | The graph representation of the simple environment of **Figure 2** with coverage edges pairs and inter-cell traversal edges at critical points (CPs). **(A)** The quotient in dividing cell 4's width by the coverage diameter (W) is even numbered. **(B)** The quotient in dividing cell 4's width by the coverage diameter (W) is odd numbered. **(C)** Contour-following edges are added to the graph.

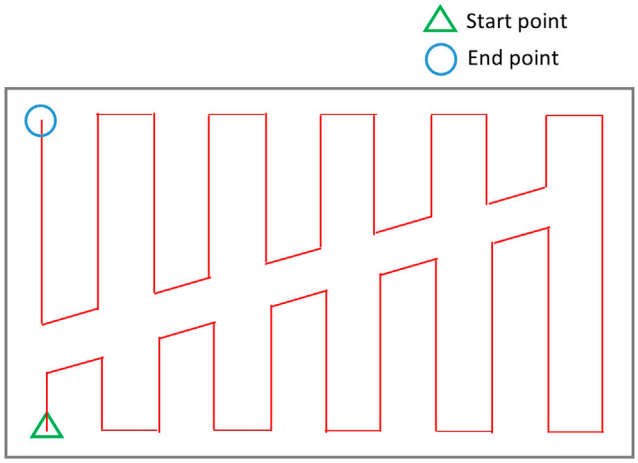

FIGURE 7 | Coverage of a single cell in (Mannadiar and Rekleitis, 2010).

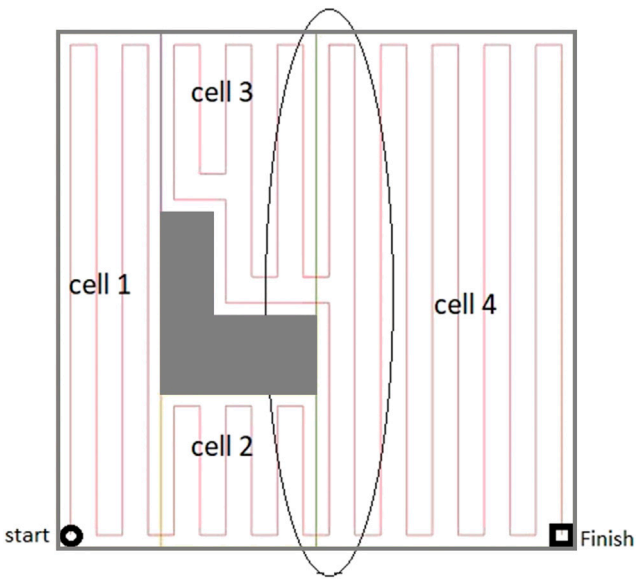

FIGURE 8 | The optimal coverage path for the simple environment of **Figure 2**. The ellipse shows the first stripe of cell four which has been covered apart from the rest of the cell area.

graph does not contain enough information to consider skipping the first stripe. When the robot is traversing a cell coverage edge, it is covering the whole cell. As a result, there would be a coverage overlap in the first stripe of the cell four. This overlap increases the travelled distance and consequently the cost of operation. To avoid this, the graph has been modified based on a more flexible environment decomposition method. Three transition cells are added to the cellular decomposition of the environment at each critical point. This allows the robot to expand or shrink the cells around the critical points to avoid the overlaps of inter-cell traversals and cell coverage paths. **Figure 9** illustrates the

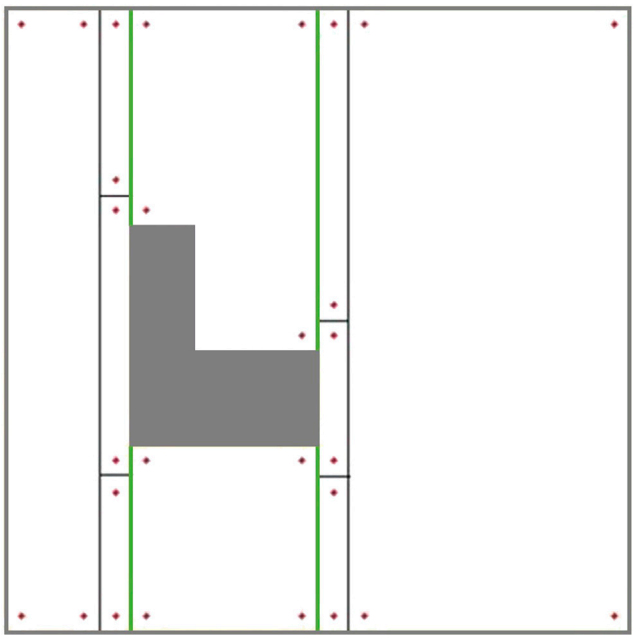

FIGURE 9 | The modified cellular decomposition with transition cells. Each transition cell has only two corners.

transition cells and their associated corners which are added to the graph nodes. The transition cells have a width of W (coverage diameter) and include two corners (top and bottom). The modified graph of the simple environment of **Figure 2** has been shown in **Figure 10**. In **Figure 10A**, the graph is represented over the environment. The environment boundaries are removed in **Figure 10B** to illustrate that the coverage sequence problem can be considered as a solely graph-search problem. Those edges of the graph that are equivalent to coverage of transition cells should be added to the list of required edges to be traversed for complete coverage. All other added inter-cell traversal edges at the end of the transition cells are optional.

Coverage Optimization Over the Proposed Graph

As explained in Section *Graph Representation of Decomposed Environments*, a new graph representation of environment was constructed, where the graph nodes represent corners of the cells, and the edges represent cell coverage, contour-following, or inter-cell traversal. For a complete coverage, all cells including primary and transition cells are required to be covered by the robot at least once. This is equivalent to going through all cell coverage edges (transition cells) or edge pairs (primary cells) in the graph at least once. Since cell coverage edges or edge pairs are not connected, the robot should connect these coverage edges together using contour-following or inter-cell traversal edges. To find an efficient sequence of covering the cells, an optimization problem over the graph was formulated that targets to minimize the distance

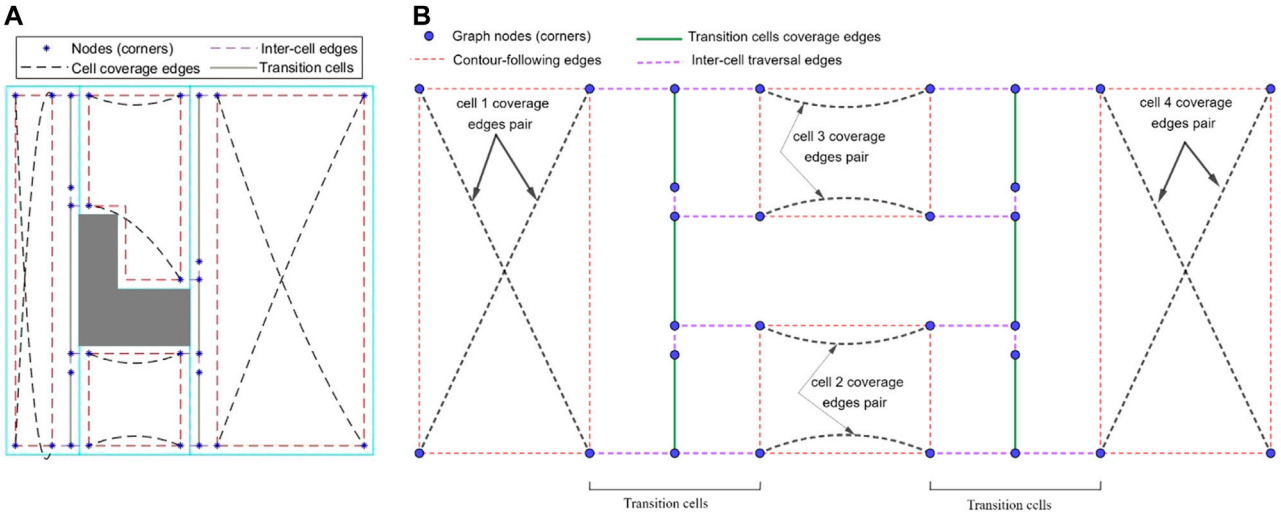

FIGURE 10 | The graph representation of the simple environment of **Figure 2**, which can be utilized to find an efficient cell coverage sequence. **(A)** The environment boundaries are shown to present how the graph is constructed. **(B)** The environment boundaries are removed to show that the coverage sequence problem can be solved as a solely graph problem.

travelled by the robot for transitioning between the cells. Similar to the Rural Chinese Postman Problem (Pearn and Wu, 1995), the optimization problem would be an NP-complete combinatorial problem since the subset of required edges does not form a weakly-connected network.

In this work, the optimization problem was solved using a double DQN technique (Van Hasselt et al., 2015). As represented in **Algorithm 1**, double DQN trains a deep Q network (Q_θ) to approximate the action values through a DRL process. The reason that a DRL has been chosen over RL techniques is that the state space for coverage problem is generally large, and consequently there would be a large number of state-action pairs. Therefore, a function (deep network) would be required to approximate the action values (Q values). Two identical deep networks, online Q network (Q_θ) and target Q network ($Q_{\theta'}$), are utilized in the double DQN learning process. The purpose of using the target Q network is to reduce Q-values overestimation (Van Hasselt et al., 2015). Through this DRL-based technique, the robot interacts with the environment defined based on the proposed graph and learns how to choose the starting corner of the next cell in the coverage sequence. A pseudocode is provided in **Table 1**, which illustrates how the environment in DRL framework has been constructed based on the proposed graph information. When Q_θ is trained over the graph environment, the efficient coverage sequence of the cells would be equivalent to the optimal policy found by double DQN. The optimal action that the robot takes at each step of the coverage process is computed by **Eq. 1**.

$$a_t^* = \underset{a}{\text{argmax}}\ Q_\theta(S_t, a), \tag{1}$$

where $a$represents all possible actions that the robot can take at state S_t, which are the integer numbers in the set: [0, number of nodes), and a_t^* is the optimal action taken by the agent at each state S_t, which is the largest Q-value approximated by Q_θ. It is an integer number in the set: [0, number of nodes) that represents the starting corner of the next cell in the optimal coverage sequence.

Algorithm 1. | Double DQN (Van Hasselt et al., 2015).

Initialize online network Q_θ, target network $Q_{\theta'}$, experience replay memory D

repeat

for each environment step:

Select some action a_t at state S_t

Execute a_t and observe next state S_{t+1} and reward r_t

Add (S_t, a_t, S_{t+1}, r_t) to D

for each online network update step:

Sample a random mini-batch of (S_t, a_t, S_{t+1}, r_t) from D

Compute the target: $Y_t^Q = r_t + \gamma Q_\theta(S_{t+1}, \underset{a}{\text{argmax}} Q_{\theta'}(S_{t+1}, a))$

Update the online network weight θ based on the error $(Q_\theta(S_{t+1}, a_t) - Y_t^Q)^2$

for each target network update step:

Update the target network weight: $\theta' = \theta$

In the following, the DRL framework in this context is explained. More details on the definitions and steps are provided in the pseudocode of **Table 1**.

Episodes of the learning process start with a robot at a random node (corner) and a list of already covered cells which is created randomly. The state changes through interactions of the agent and the environment, which is defined based on our proposed graph representation of the environment. An episode ends when the agent reaches the goal (final) state. The agent is at the goal state when all the cell coverage edges are covered, and the robot is at the end node (corner) of the episode, which is also selected randomly. If the episode is

TABLE 1 | Pseudocode for the python class *graphEnvironment* which includes details on how the methods for episode reset, transition and reward model, and creating the observation image are coded. The environment in DRL framework is constructed based on the proposed graph information.

```
class graphEnvironment:
  def __init__(graph, start_corner, end_corner, max_steps):
    episode_step ← 0
    reward ← 0
    done ← False
    SIZE ← ceil ( sqrt (graph.num_corners))
    episode_actions ← empty array
    current_corner ← start_corner
    state ← a list of 0s and 1s representing the robot current corner and already covered cells
    final_state ← a list of 0s and 1s representing the robot end corner and required cells to be covered
    final_reward ← 1
    double_coverage_reward ← - 0.5
    primary_cell_coverage_reward ← 0.05
    transition_cell_coverage_reward ← 0.005
    cost_scale ← 0.1
    coverage_overlap_scale = 2
  def reset():
    episode_step ← 0
    reward ← 0
    done ← False
    start_corner ← a random integer number in the set [0, graph.num_corners)
    end_corner ← a random integer number in the set [0, graph.num_corners)
    current_corner ← start_corner
    state ← a list of 0s and 1s representing the robot current corner and a random set of already covered cells
    final_state ← a list of 0s and 1s representing the robot end corner and a random set of required cells to be covered
    episode_actions ← empty array
    observation ← get_image()
    return observation
  def step(action):
    episode_step ← episode_step + 1
    if action belongs to a cell that has not been covered:
      action_sequence ← graph.actionSequence (current_corner, action)
      episode_actions ← concatenate (episode_actions, actionSequence)
      reward ← 0
      for act in action_sequence:
        new_pos ← graph.nextCorner (current_corner, act)
        cost ← graph.transitionCost (current_corner, act)/max_cost×cost_scale
        reward ← reward - cost
        if current_corner is in a primary cell:
          if act is equivalent to cell coverage:
            state ← update state by adding the current cell to the list of covered cells
            reward ← reward + primary_cell_coverage_reward
          if act is equivalent to contour-following and cell has already been covered or the contour-following is parallel to the coverage direction:
            reward ← reward - cost×coverage_overlap_scale
        else:
          if act is equivalent to cell coverage:
            if action != current_corner:
              reward ← reward - cost×coverage_overlap_scale
            else:
              state ← update state by adding the current cell to the list of covered cells
              reward ← reward + transition_cell_coverage_reward
        current_corner ← new_pos
        state ← update the robot current corner
      else:
        done ← False
        if state==final_state or episode_step >= max_steps:
          done ← True
        new_observation ← get_image()
        reward ← double_coverage_reward
        return new_observation, reward, done
      if all required cells have been covered:
        final_path_cost ← graph.transitionCost (current_corner, end_corner)/max_cost×cost_scale ×(coverage_overlap_scale+1)
        reward ← reward + final_reward - final_path_cost
        action_sequence ← graph.actionSequence (current_corner, end_corner)
        episode_actions ← concatenate (episode_actions, actionSequence)
```

(Continued on following page)

TABLE 1 | (*Continued*) Pseudocode for the python class *graphEnvironment* which includes details on how the methods for episode reset, transition and reward model, and creating the observation image are coded. The environment in DRL framework is constructed based on the proposed graph information.

```
        current_corner ← end corner
      done ← False
      if state==final_state or episode_step >= max_steps:
        done ← True
      new_observation ← get_image()
      return new_observation, reward, done
  def get_image():
    env ← 3-dimensional array with size of (SIZE, SIZE, 3) # equivalent to an image with 3 channels and width×height of SIZE×SIZE
    env ← update the first channel to indicate the robot current corner
    env ← update the second channel to indicate the already covered cells
    env ← update the third channel to indicate the robot end corner
    img ← convert env to an RGB image
    return img
```

not converging to the goal state, it will be forced to stop when the number of steps reaches a pre-defined maximum number of steps.

State includes 1) the robot's current node (corner), 2) the list of already covered cells, and 3) the episode's end node (corner). Since the model considered for the Q networks is a convolutional neural network, the state, *S*, at each step of the episode is a three-channel image created based on the observation made on the above three parameters, where the first channel has a nonzero value in the pixel corresponding to the robot's current node number, the second channel has nonzero values in the pixels corresponding to the already covered cell numbers, and the third channel has a nonzero value in the pixel corresponding to the robot's end node number. The size of this square image is calculated based on the total number of nodes.

Action, *a*, is an integer number in the set: [0, number of nodes) that represents a node number. Having access to its current state, the agent selects a node number from which the robot should start covering the next cell. There are four options (nodes) for starting coverage from at each primary cell and two options (nodes) for starting coverage from at each transition cell.

Transition is the process of applying the selected action at the current state and updating the state after observing the changes in the environment. If the selected action by agent is a node in an uncovered cell, the robot takes the shortest path from the current node to the selected node (as its action) over the graph. When the robot arrives at the selected node (as its action), it starts covering the cell and ends at another corner of the cell. This covered cell is added to the list of already covered cells in the new state. The robot's current node (corner) is updated in the new state as well. If the selected action by agent is a node in an already covered cell, the state does not change, and a negative reward is assigned to that state-action pair.

Rewards are defined in a way that they would encourage the robot to take an efficient path for traversing all cell coverage edges in the proposed graph. The reward function is defined in a way that it would reward the agent for reaching the goal state with minimum travelled distance. The following is a description of the reward function. The pseudocode of **Table 1** provides more detail on how these rewards are applied at each step of an episode.

- If the agent at a particular state selects a node to travel to (as its action) which belongs to an already covered cell, meaning that it decides to cover a cell that has already been covered before, the state (robot's current node and the list of already covered cells) will not change and a large negative *double-coverage* reward of $R_{dc} = -0.5$ will be assigned to that state-action pair. R_{dc} has a large negative value since covering an already covered cell (area) of the environment results in a large amount of unnecessary cost (extra travelled distance) while not helping the coverage task completion at all. The magnitude of R_{dc} has been chosen to be much larger than the magnitude of the cost of transition (C_T in **Eq. 2**) for travelling from current node to a node in an adjacent uncovered cell. This encourages the agent to avoid covering a cell more than once and try covering the uncovered cells in the environment instead. The exact value of R_{dc} has been found by tuning the DRL hyperparameters over several sample indoor environments based on speed of convergence, *and not getting stuck in local minima.*

- If the agent at a particular state selects a node to travel to (as its action) which belongs to an uncovered cell, the transition model has two parts: 1) transition part which constitutes travelling from the current node to the selected node (as an action) using contour-following and inter-cell traversal edges, and 2) coverage part which constitutes covering the destination cell starting from the selected node (as an action). Therefore, the *coverage* reward assigned to the state-action pair, R_c, has two parts that encourages the agent to select nodes in the uncovered cells while minimizing the travelled distance for transition to the selected node.

$$R_c = C_T + R_{cc}. \tag{2}$$

Cost of transition, C_T, and *cell-coverage* reward, R_{cc}, are described below:

1) Cost of transition (C_T) is a negative reward assigned for the cost of travelling from current node to the selected node (as an action). The total cost of transition is the summation of cost of traversing all edges in the graph path from current node to the selected node:

$$C_T = \sum_i C_{T_i}. \tag{3}$$

The cost of travelling from one node to an adjacent node in the graph has already been calculated offline and is included in the graph edge weights. The graph edge weights, W_{T_i}, are obtained based on the shortest distances between adjacent nodes of the graph. A primary cell coverage edge weight is zero since there is no extra travelled distance for covering a single primary cell. To find C_{T_i} associated to every two nodes, the edge weight (W_{T_i}), is normalized and then scaled based on a trial and error process while tuning the DRL framework rewards definition.

$$C_{T_i} = -0.1\left(\frac{W_{T_i}}{W_{T_{\max}}}\right), \tag{4}$$

where $W_{T_{\max}}$ is the maximum edge weight in the entire graph.

2) A positive *cell-coverage* reward of $R_{cc} = 0.05$ for covering an uncovered primary cell or a positive cell coverage reward of $R_{cc} = 0.05 \times 0.1 = 0.005$ for covering an uncovered transition cell is assigned to the coverage part. This positive R_{cc} reward has been utilized to allow the agent learn if it is gradually getting closer to the goal state. The magnitude of R_{cc} is in the order of the magnitude of the cost of transition (C_T in **Eq. 2**) for travelling from current node to another node in an uncovered cell. This helps the agent to learn how to select the next cell in a way that the total episode reward is maximized instead of selecting the closest uncovered cell. R_{cc} for covering an uncovered transition cell is smaller (by a factor of 10) than the corresponding parameter for a primary cell since the transition cells are always smaller than the primary cells. The exact values of R_{cc} for both primary and transition cells have been found by trial and error through implementing the DRL optimization over several sample indoor environments. Improper values of R_{cc} would increase the optimization convergence time and/or even lead to getting stuck in local minima.

- When the transition path includes a contour-following, the edge transition cost (C_{T_i}) is calculated similar to that in **Eq. 4** as if the contour-following happens in an uncovered cell, and that it is not parallel to the cell coverage direction. However, if the contour-following happens in a covered cell or the contour-following path is parallel to the cell coverage direction, the cost would increase since coverage overlaps would be inevitable in those parts. For those cases, the transition cost is multiplied by a factor of 3 (obtained based on trial and error) to penalize the agent for the coverage overlaps (extra travelled distances) as it is indicated in **Eq. 5**.

$$C_{T_i} = -0.1\,(3)\left(\frac{W_{T_i}}{W_{T_{\max}}}\right). \tag{5}$$

- The magnitude of this transition cost should not be much larger than the magnitude of transition cost in **Eq. 4** since the agent should still have a chance to take a contour-following path in a covered cell if it leads to a maximized total episode reward at the end.

- If applying an action at the current state results in reaching the goal state, where all the cells are covered and the robot is at the end corner of the episode, a large positive *final* reward of $R_f = 1$ will be assigned to the current state-action pair. This large positive reward encourages the agent to continue taking transition paths and covering the cells to reach the goal state.

This double DQN approach, like many other Deep learning techniques, is slow at the training step since a large number of possible interactions with the environment needs to be fed to the learning networks. However, once the agent is trained on the environment, the execution speed would be fast. The agent would be capable of generating an efficient coverage path for any arbitrary start and/or end positions immediately (i.e., via a transfer learning). The user can determine which cells need to be covered (which could be equivalent to selecting the rooms that need to be disinfected), and the agent will generate the coverage path using the already trained model without wasting time to solve the problem for the new setting. The training step used in the DRL can be done offline on a more powerful processor and then the trained network can be uploaded onto the robot onboard hardware. At the execution step, the required computational power is not expensive, therefore, most of the commonly-used processors on the mobile robots will be able to run it in real time.

Similar to some other CPP works cited in the literature (e.g., Hameed et al., 2013; Xu et al., 2014; Lewis et al., 2017; Chen et al., 2019), our proposed technique considers a global path planning that finds an efficient sequence for covering different regions (cells) of the static and known environment, while minimizing the travelled distance (overlap) in the coverage path. Therefore, we assume that the hospital floor plans would be static and known in advance, and the DRL-based coverage planning can be carried out offline. The proposed Double DQN optimization technique is applicable for hospital disinfection since it is fast enough at the execution phase and suitable for transfer learning (i.e., it can manage new start/end corners, arbitrary areas of the environment selected for disinfection). The environment uncertainties such as unknown obstacles, dynamic objects, etc. and the robot constraints are usually considered in a local path planning algorithm, which needs to constantly acquire sensory information on the environment. Development of a local path planning method constitutes our future work through which we will compute a collision-free trajectory in real time based on the coverage path generated by our proposed global CPP technique.

RESULTS AND DISCUSSION

The proposed graph can be automatically created for any environment based on the steps described in Section *Environment Decomposition* and Section *Graph Representation*

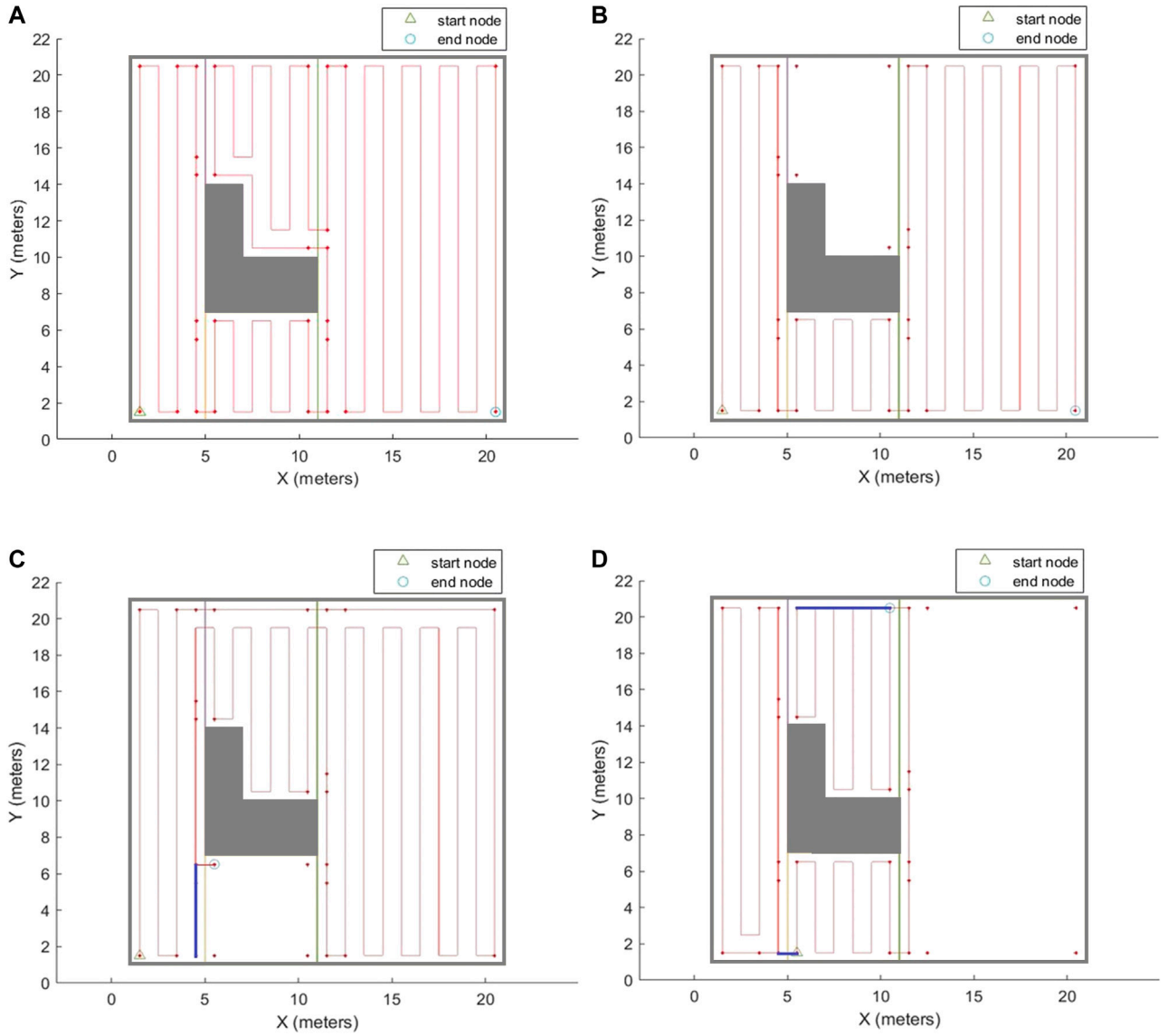

FIGURE 11 | The complete coverage path generated by the proposed CPP technique based on the graph representation of environment. **(A)** Whole free space has been covered. **(B)** Cell 3 has been excluded from the area of interest. **(C)** Cell 2 has been excluded from the area of interest, and end corner position has changed. **(D)** Cell 4 has been excluded from the area of interest, and both start and end corner positions have changed. The blue lines represent the overlapped parts of the path.

of Decomposed Environments. The environment data including the planar map of the environment is passed as input to a MATLAB script written by our team. The proposed algorithm creates and saves a file which contains all the information about the graph representation of the environment including nodes, edges, and transition costs and action sequences of travelling from one node to another. The time required for this process is in the order of seconds (using an OMEN HP laptop running Windows 10 with an Intel Core i7-9750H CPU @ 2.60 GHZ and 16 GB of RAM). The constructed graph is passed to a Python code, where the environment of the DRL framework has been created based on the information of the graph. The pseudocode for the Python class of the environment constructed based on the proposed graph is provided in **Table 1**. The Double DQN agent provided in the GitHub repository of keras-rl package has been utilized to create the Keras model and run the reinforcement learning episodes. The sequential model initialized for both online and target Q networks includes three convolutional layers followed by two dense layers. An epsilon-greedy policy and an Adam optimizer with learning rate of 25e-5 are considered for the training step.

After the agent is trained over the graph environment, it would be able to generate an efficient traversal sequence over the graph for different configurations of the input environment. Different configurations can be created by selecting different: 1) start and/or end positions for

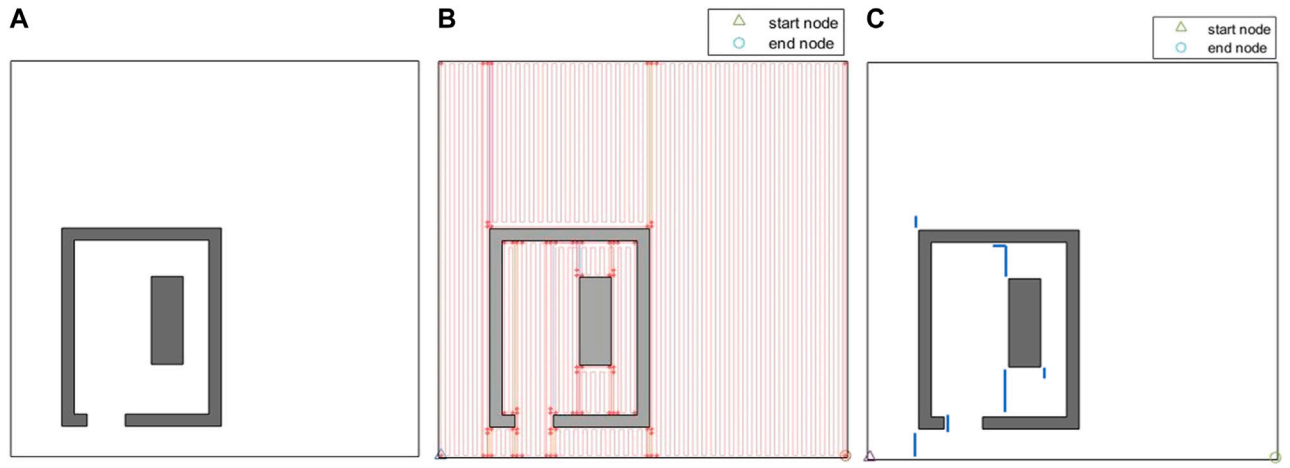

FIGURE 12 | (A) An indoor environment with a single room and a single obstacle inside the room. **(B)** The complete coverage path generated by the CPP technique based on the graph representation of environment. The path stripes are shown by solid red lines. **(C)** The extra travelled distances (overlaps) in the generated coverage path. The overlapping parts of the path are shown by solid blue lines.

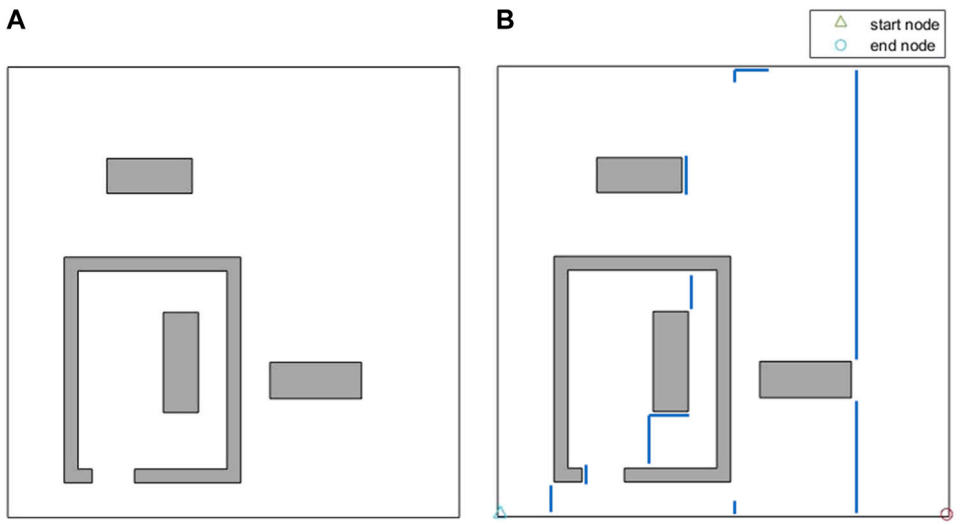

FIGURE 13 | (A) An indoor environment including a single room with a single obstacle inside and two obstacles outside. **(B)** The extra travelled distances (overlaps) in the generated coverage. The overlapping parts of the path are shown by solid blue lines.

disinfection task, and/or 2) sets of the environment cells that need to be covered. In order to evaluate the performance of the proposed CPP technique, the coverage path has been generated in several environments. The environment shown in **Figure 2**, with modified cell decomposition shown in **Figure 9**, and the graph representation shown in **Figure 10**, has been chosen to demonstrate the performance of our proposed method. This simple environment has been chosen as the testbench evaluation environment since the optimal coverage path for different configurations of this environment is manually attainable. In the first scenario, the entire free space is required to be covered. The coverage planning is set to start from cell one and to end at cell four. **Figure 11A** shows the calculated coverage path. As it can be seen, there are no overlaps (extra travelled distance). The robot performs a contour-following motion in cell three to adjust the cell coverage start corner. The disinfection coverage diameter (W) in this scenario was set at 1 m. It should be noted that all cell coverage paths are assumed to be in vertical direction (parallel to the Y-axis).

As it was mentioned in Section *Coverage Optimization Over the Proposed Graph*, the coverage path planner can generate paths for different configurations of the environment which it has been trained for. It means that users can select any arbitrary area of interest in the environment to be covered (**Figure 11B**). They can also choose any arbitrary combination of the start and end corners for the disinfection task (**Figures 11C,D**). As it can be seen in **Figure 11**, the generated paths for different configurations

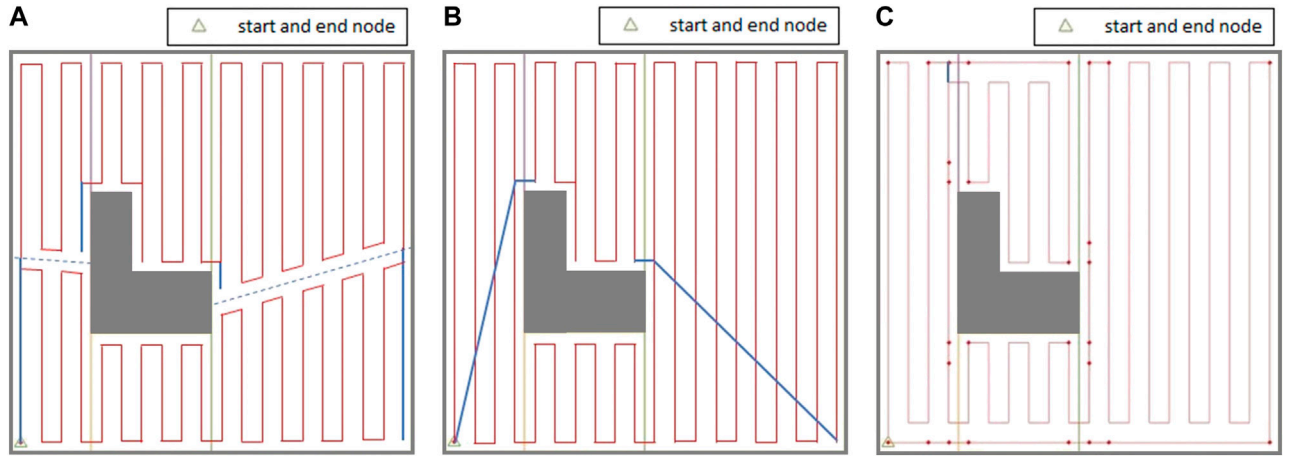

FIGURE 14 | The complete coverage path generated by: **(A)** the CPP technique proposed in (Xu et al., 2014), **(B)** the CPP technique proposed in (Tung and Liu, 2019), and **(C)** the proposed CPP technique based on the graph representation of environment. The solid red lines represent the generated path, and the solid blue lines represent the overlapped parts of the path. The dashed blue lines show the common boundaries of the divided cells.

of the environment are optimal, i.e., the extra travelled distance (overlap) is minimal.

Figure 12A represents another indoor environment that comprises of a single room and a single obstacle. The generated path is shown in **Figure 12B**. Since the environment is larger than the simple environment in **Figure 11**, and that there is a higher number of path stripes over the environment, **Figure 12C** has been also generated to show the extra travelled distances (overlaps) in the generated coverage path. **Figure 13A** shows another environment that comprises of the same room, but two obstacles are added to the environment. The extra travelled distances (overlaps) in the generated path are shown in **Figure 13B**. The extra travelled distance (overlap) is the optimization metric used in the CPP problem. If two different CPP approaches generate two different complete coverage paths with no overlaps, the travelled distances of those two approaches will be equal, and the extra travelled distance will be zero in both cases. As the coverage overlap increases, the extra travelled distance increases. Therefore, the extra travelled distance (overlap) can be considered as the evaluation metric in the CPP problem. The complete coverage paths generated for both cases in **Figures 12**, **13** environments are quite efficient in terms of extra travelled distance since the ratios of their extra travelled distance to their total travelled distance are quite low (less than 2%).

In the next step of the evaluation, the performance of the proposed CPP technique based on our proposed graph representation of environment has been compared with two well-known state-of-the-art CPP techniques suggested in the literature over two indoor environments. The CPP technique proposed in (Mannadiar and Rekleitis, 2010; Xu et al., 2011; Xu et al., 2014) duplicated selected edges of the Reeb Graph to make it Eulerian, and then solved a Chinese Postman Problem over the graph to find the efficient sequence of cell coverage with minimal travelled distance. **Figure 14A** shows the coverage path generated by the CPP technique proposed in (Xu et al., 2014) on the simple environment shown in **Figure 2**. As it can be seen in **Figure 14A**, there are many turns in the middle of cell one and cell four that happen because of splitting these two cells into two parts (dashed blue lines). The extra travelled distances (overlaps) are represented by solid blue lines. The generated coverage path is not optimal over this simple environment since the technique does not consider the start and end points of coverage for each cell. In their CPP technique, the robot has to return to the starting cell at the end of the coverage (**Figure 14A**).

The CPP technique proposed in many of the previous attempts (e.g., Jimenez et al., 2007; Hameed et al., 2013; Tung and Liu, 2019) utilized Genetic Algorithm (GA) optimization to find an efficient coverage sequence over the adjacency graph of the environment that visits each node (cell) at least once by solving a Traveling Salesman Problem. The coverage path generated by the CPP technique proposed in (Tung and Liu, 2019) is shown in **Figure 14B**. As it can be seen in **Figure 14B**, the robot needs to traverse through the middle of the cells one and four to get back to the starting point which results in extra travelled distances (overlaps) represented by solid blue lines in cells one and four. In their CPP technique, the robot has to return to the starting point at the end of the coverage.

A coverage path has been also generated using our proposed method on the same environment with the exact same start and end position. Results are given in **Figure 14C**. Our proposed method outperforms the CPP techniques in (Xu et al., 2014) and (Tung and Liu, 2019) in terms of total travelled distance. The extra travelled distance in the path generated by our approach is about 5% and 3.6% of the extra travelled distance resulted by applying the CPP technique in (Xu et al., 2014) and (Tung and Liu, 2019), respectively. The robot takes contour-following paths to adjust its position for starting the cell coverage at each cell. After arriving at the cell coverage start point found through the optimization, the robot covers the cell with no overlaps with the previously covered part of the cell contour. This can be seen in all the cells in **Figure 14C**. The number of turns in the path

TABLE 2 | A comparison of the extra travelled distance and number of turns resulted in the proposed CPP technique based on the graph representation of environment and CPP techniques proposed in (Xu et al., 2014) and (Tung and Liu, 2019).

CPP technique proposed in other works	**CPP technique proposed in (Xu et al., 2014)**		**CPP technique proposed in (Tung and Liu, 2019)**	
Environment	Environment of **Figure 14**	Environment of **Figure 15**	Environment of **Figure 14**	Environment of **Figure 15**
Extra travelled distance ratio ×100	5%	42%	3.6%	43%
Number of turns ratio ×100	65%	45%	≈100%	≈100%

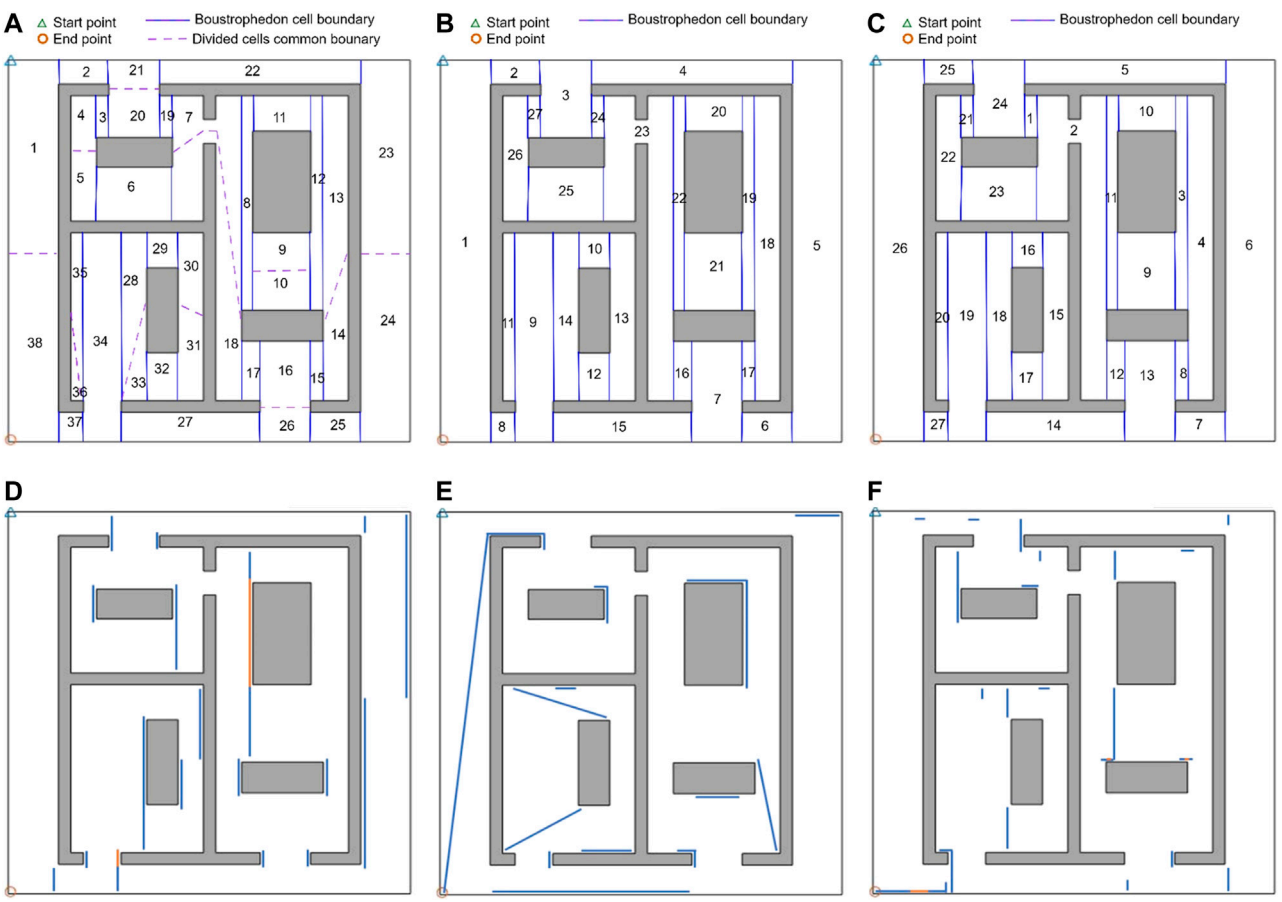

FIGURE 15 | The cell coverage sequence by: **(A)** the CPP technique proposed in (Xu et al., 2014), **(B)** the CPP technique proposed in (Tung and Liu, 2019), and **(C)** the proposed CPP technique based on the graph representation of environment The extra travelled distances (overlaps) in the generated coverage path by: **(D)** the CPP technique given in (Xu et al., 2014), **(E)** the CPP technique proposed in (Tung and Liu, 2019), and **(F)** the proposed CPP technique based on the graph representation of environment. The overlapping parts of the path are shown by solid blue lines. The solid orange lines.

generated by our approach is about 65% of the number of turns resulted by applying the CPP technique in (Xu et al., 2014) since the robot does not need to split the cells to get back to the starting cell, and it takes contour following paths instead. The technique proposed in (Tung and Liu, 2019) produced similar number of turns to that in our proposed technique. A comparison of the extra travelled distance and number of turns is shown in **Table 2**. In **Table 2**, the extra travelled distance ratio is defined as the extra travelled distance using our proposed technique divided by the extra travelled distance utilizing other techniques in (Xu et al., 2014; Tung and Liu, 2019). Similarly, the number of turns ratio is defined as the number of turns produced through the use of our proposed technique divided by the number of those from other techniques in (Xu et al., 2014; Tung and Liu, 2019). The smaller extra travelled distance ratio or number of turns ratio are in **Table 2**, the better our technique has worked in comparison with other techniques.

The proposed CPP technique based on the graph representation of environment and other techniques (Xu et al., 2014; Tung and Liu, 2019) have been applied to generate a complete coverage path on a more complicated indoor environment, as shown in **Figure 15**. The sequences of

covering the cells using the proposed techniques in (Xu et al., 2014) and (Tung and Liu, 2019) are shown in **Figures 15A,B** respectively. The extra travelled distances (overlaps) in the path generated by the other techniques in (Xu et al., 2014) and (Tung and Liu, 2019) are depicted in **Figures 15D,E**, respectively.

The proposed CPP technique based on the graph representation of the environment has been applied over the same environment with same start and end points. The sequence of covering the cells and the extra travelled distance (overlaps) in the path generated by our proposed method are shown in **Figures 15C,F** respectively. A comparison of the extra travelled distance and number of turns has been shown in **Table 2**. As it can bee seen in **Figure 15F**, the extra travelled distance (overlap) has been decreased in the generated coverage path by our proposed method. The extra travelled distance in the path generated by our proposed approach is about 42% and 43% of the extra travelled distance resulted by applying the other CPP technique in (Xu et al., 2014) and (Tung and Liu, 2019), respectively. This cost reduction is a result of utilizing the proposed graph representation of the environment, which was created considering three modifications described in Section *Graph Representation of Decomposed Environments*. This improvement can decrease the disinfection cost dramatically since the hospital disinfection is a repetitive task which should be done based on certain routines. The decrease in the cost is more significant when our proposed method is applied over larger indoor environments like hospitals.

In addition to the extra travelled distance (overlap), the number of turns in the path generated for environment of **Figure 15** is 45% of the total number of turns resulted by applying the CPP technique in (Xu et al., 2014). The number of turns is decreased because the proposed graph representation of the environment makes it possible for the robot to take a contour-following edge for adjusting each cell coverage start point or crossing a cell. The CPP technique in (Xu et al., 2014) split the duplicated edges, so the robot performed extra turns at each side of the splitting edges. This decrease in the number of turns decreases the disinfection task completion time and cost. The number of turns in the path generated by applying our technique is similar to the number of turns produced by applying the technique proposed in (Tung and Liu, 2019).

At the execution step, the required computational power was not expensive. Therefore, most of the commonly-used processors on the mobile robots will be able to run it in real time. For example, using an OMEN HP laptop running Windows 10 with an Intel Core i7-9750H CPU @ 2.60 GHZ and 16 GB of RAM, the execution of the algorithm for the environment of **Figure 15** took about 30 s.

CONCLUSION

Mobile robots make the hospital disinfection process safer and more effective. Central to the autonomous disinfection, a CPP technique was presented in this paper which decreases the time and cost for robotic disinfection of hospitals. The proposed technique utilizes a new graph representation of the environment. This graph representation of the environment is created offline considering a more flexible version of Boustrophedon cell decomposition method, taking both contour-following paths in cells, and the corners of cells as start and end points of cell coverage into account. The efficient cell coverage sequence is found by solving an optimization problem over the graph using a double DQN technique. The generated coverage path by the proposed technique has been compared with those generated by two state-of-the-art CPP approaches over two indoor environments. The results indicate that the travelled distance and number of turns are reduced when using our proposed method. In particular, the extra travelled distance in the path generated by the proposed approach was in the range of 3.6% to 43% of the extra travelled distance resulted from applying other CPP techniques cited in the literature, (Xu et al., 2014; Tung and Liu, 2019), depending on the complexity of the environment. Furthermore, the number of turns was 45% to 65% of the total number of turns resulted when applying one of the CPP techniques cited in the literature, (Xu et al., 2014). This will lead to an improved completion time and cost for disinfecting hospitals using unmanned systems.

The learning time in the double DQN is in the order of hours which indicates that the agent should be trained offline. However, once the agent is trained over an environment, the in-field execution time will be in the order of seconds (with an Intel Core i7-9750H CPU @ 2.60 GHZ and 16 GB of RAM). Additionally, the trained model by double DQN technique is robust to changes in the start and/or end states of the robot used for the disinfecting task. It is also robust to excluding some cells from the disinfection target area, so regions of interest to disinfect can be prioritized on the fly. For future works, we will apply other DRL techniques over our proposed graph to decrease the training time. To further our research, we intend to extend this work to scenarios, where multiple disinfecting robots are employed for doing the task collectively. This will decrease the total operation time significantly due to the division of workload over all robots, which can be incorporated to the current problem formulation under the DRL method. Also, further works needs to be done on adding constraints and uncertainties to the problem formulation, for instance, uncertainties in the obstacles position (including unknown static obstacles and dynamic obstacles), constraints and uncertainties in mobile robot motion, constraints on the battery capacity and access to the charging stations will be considered.

DATA AVAILABILITY STATEMENT

The raw data supporting the conclusions of this article will be made available by the authors, without undue reservation.

AUTHOR CONTRIBUTIONS

BN developed the algorithms, conducted the simulations and was the main author of the manuscript. MM helped with the development of the idea, led the graph representation work, and helped with authoring the paper. FJ-S helped with the

development of the planning algorithm, reinforcement learning, and helped with the paper authorship and organization.

FUNDING

This work was financially supported by Natural Sciences and Engineering Research Council of Canada under Discovery Grant # 2017-06930 and Ryerson Dean of Engineering and Architectural Science Research Fund (DRF). The funding from NSERC was used partially to support the first author, the research activities including computing system and simulation software. The second source was used to support the computing facility and field trips. The work was also partially funded through MITACS Accelerate to support the first author.

REFERENCES

Cabreira, T., Brisolara, L., and Ferreira, P. R., Jr (2019). Survey on coverage path planning with unmanned aerial vehicles. *Drones* 3 (1), 4. doi:10.3390/drones3010004

Chen, X., Tucker, T. M., Kurfess, T. R., and Vuduc, R. (2019). "Adaptive deep path: efficient coverage of a known environment under various configurations," in Proceedings of 2019 IEEE/RSJ International Conference on Intelligent Robots and Systems (IROS), Macau, China, November 3–8, 2019 (Piscataway, NY: IEEE), 3549–3556.

Choset, H., Acar, E., Rizzi, A. A., and Luntz, J. (2000). "Exact cellular decompositions in terms of critical points of morse functions," in *Proceedings of 2000 IEEE international conference on robotics & automation* (Symposia Proceedings), 2270–2277.

Choset, H. (2001). Coverage for robotics–a survey of recent results. *Ann. Math. Artif. Intell.* 31 (1-4), 113–126. doi:10.1023/a:1016639210559

Choset, H., and Pignon, P. (1998). "Coverage path planning: the boustrophedon cellular decomposition," in *Field and Service Robotics* Editor A. Zelinsky (London, United Kingdom: Springer), 203–209.

Edmonds, J., and Johnson, E. L. (1973). Matching, Euler tours and the Chinese postman. *Math. Program.* 5 (1), 88–124. doi:10.1007/bf01580113

Galceran, E., and Carreras, M. (2013). A survey on coverage path planning for robotics. *Robot. Autonom. Syst.* 61 (12), 1258–1276. doi:10.1016/j.robot.2013.09.004

Hameed, I. A., Bochtis, D., and Sørensen, C. A. (2013). An optimized field coverage planning approach for navigation of agricultural robots in fields involving obstacle areas. *Int. J. Adv. Rob. Syst.* 10 (5), 231. doi:10.5772/56248

Jimenez, P. A., Shirinzadeh, B., Nicholson, A., and Alici, G. (2007). "Optimal area covering using genetic algorithms," in Proceedings of 2007 IEEE/ASME International Conference on Advanced Intelligent Mechatronics, Zurich, Switzerland, September 4–7, 2007 (Piscataway, NY: IEEE), 1–5.

Khan, A., Noreen, I., and Habib, Z. (2017). On complete coverage path planning algorithms for non-holonomic mobile robots: survey and challenges. *J. Inf. Sci. Eng.* 33 (1), 101–121. doi:10.6688/JISE.2017.33.1.7

Lewis, J. S., Edwards, W., Benson, K., Rekleitis, I., and O'Kane, J. M. (2017). "Semi-boustrophedon coverage with a dubins vehicle," in Proceedings of 2017 IEEE/RSJ International Conference on Intelligent Robots and Systems (IROS), Vancouver, BC, September 24–28, 2017 (Piscataway, NY: IEEE), 5630–5637.

Mackenzie, D., and Balch, T. (1993). "Making a clean sweep: behavior based vacuuming," in Proceedings of AAAI 1993 fall symposium series: Instantiating Real-World Agents, Washington, DC, October 22–24, 1993 (Menlo Park, CA: AAAI), 93–98.

Mannadiar, R., and Rekleitis, I. (2010). "Optimal coverage of a known arbitrary environment," in Proceedings of 2010 IEEE International Conference on Robotics and Automation, Anchorage, AK, May 3–7, 2010 (Piscataway, NY: IEEE), 5525–5530.

Oksanen, T., and Visala, A. (2009). Coverage path planning algorithms for agricultural field machines. *J. Field Robot.* 26 (8), 651–668. doi:10.1002/rob.20300

Palacin, J., Palleja, T., Valganón, I., Pernia, R., and Roca, J. (2005). "Measuring coverage performances of a floor cleaning mobile robot using a vision system," in Proceedings of 2005 IEEE International Conference on Robotics and Automation, Barcelona, Spain, May 18–22, 2005 (Piscataway, NY: IEEE), 4236–4241.

Pearn, W. L., and Wu, T. C. (1995). Algorithms for the rural postman problem. *Comput. Oper. Res.* 22 (8), 819–828. doi:10.1016/0305-0548(94)00070-o

Tung, W. C., and Liu, J. S. (2019). Solution of an integrated traveling salesman and coverage path planning problem by using a genetic algorithm with modified operators. *IADIS Int. J. Comput. Sci. Inf. Syst.* 14 (2). 95–114.

Van Hasselt, H., Guez, A., and Silver, D. (2015). Deep reinforcement learning with double q-learning. https://arxiv.org/abs/1509.06461.

Xu, A., Viriyasuthee, C., and Rekleitis, I. (2014). Efficient complete coverage of a known arbitrary environment with applications to aerial operations. *Aut. Robots* 36 (4), 365–381. doi:10.1007/s10514-013-9364-x

Xu, A., Viriyasuthee, C., and Rekleitis, I. (2011). "Optimal complete terrain coverage using an unmanned aerial vehicle," in Proceedings of 2011 IEEE International Conference on Robotics and Automation, Shanghai, China, May 9–13, 2011 (Piscataway, NY: IEEE), 2513–2519.

Conflict of Interest: The authors declare that the research was conducted in the absence of any commercial or financial relationships that could be construed as a potential conflict of interest.

frontiers in Robotics and AI

BRIEF RESEARCH REPORT
published: 16 March 2021
doi: 10.3389/frobt.2021.618656

A Smart Tendon Hammer System for Remote Neurological Examination

Waiman Meinhold[1], Yoshinori Yamakawa[2], Hiroshi Honda[2], Takayuki Mori[3], Shin-ichi Izumi[3] and Jun Ueda[1]*

[1]Biorobotics and Human Modeling Laboratory, Woodruff School of Mechanical Engineering, Georgia Institute of Technology, Atlanta, GA, United States, [2]NITI-ON Co. Ltd., Funabashi, Japan, [3]Graduate School of Biomedical Engineering, Tohoku University, Sendai, Japan

The deep tendon reflex exam is an important part of neurological assessment of patients consisting of two components, reflex elicitation and reflex grading. While this exam has traditionally been performed in person, with trained clinicians both eliciting and grading the reflex, this work seeks to enable the exam by novices. The COVID-19 pandemic has motivated greater utilization of telemedicine and other remote healthcare delivery tools. A smart tendon hammer capable of streaming acceleration measurements wirelessly allows differentiation of correct and incorrect tapping locations with 91.5% accuracy to provide feedback to users about the appropriateness of stimulation, enabling reflex elicitation by laypeople, while survey results demonstrate that novices are reasonably able to grade reflex responses. Novice reflex grading demonstrates adequate performance with a mean error of 0.2 points on a five point scale. This work shows that by assisting in the reflex elicitation component of the reflex exam via a smart hammer and feedback application, novices should be able to complete the reflex exam remotely, filling a critical gap in neurological care during the COVID-19 pandemic.

Keywords: remote diagnosis, neurology, IoT, reflex, COVID-19 pandemic

OPEN ACCESS

Edited by:
S. Farokh Atashzar, New York University, United States

Reviewed by:
Soroosh Shahtalebi, Concordia University, Canada
Ying Feng, South China University of Technology, China

****Correspondence:***
Waiman Meinhold
wmeinhold@gatech.edu

Specialty section:
This article was submitted to Biomedical Robotics, a section of the journal Frontiers in Robotics and AI

Received: *17 October 2020*
Accepted: *27 January 2021*
Published: *16 March 2021*

Citation:
Meinhold W, Yamakawa Y, Honda H, Mori T, Izumi S and Ueda J (2021) A Smart Tendon Hammer System for Remote Neurological Examination. Front. Robot. AI 8:618656. doi: 10.3389/frobt.2021.618656

1 INTRODUCTION

The deep tendon reflex (DTR) is a critically important diagnostic tool for multiple upper and lower neuron neurological illnesses Chardon et al. (2014); Walker et al. (1990). Assessment of the DTR is often the first step toward localization of a neurological lesion. Crucially, the DTR exam requires physical interaction with a patient, and is thus limited when in-person healthcare delivery is reduced.

The COVID-19 pandemic has strained existing healthcare resources while simultaneously providing significant impetus for the development and implementation of remote diagnostic and therapeutic systems for healthcare delivery Chauhan et al. (2020). The development of a system for smart delivery of tendon tapping stimulation will aid in the remote assessment of deep tendon reflexes (DTRs) with future potential for therapeutic applications as well. Although there have been reported neurological symptoms of COVID-19 Ottaviani et al. (2020); Pezzini and Padovani (2020), the primary effect to neurological diagnosis and treatment is likely the backlog of urgent, non-COVID-19 related healthcare needs.

Examination of the DTR is a standard part of the neurological exam, but one that requires both physical contact between the clinician and patient, and the use of a non-disposable medical hammer. The assessment of DTRs requires two main steps, 1) delivery of adequate stimulus via tendon tapping, and 2) grading of the reflex response. Clinicians receive training in both of these skills, but

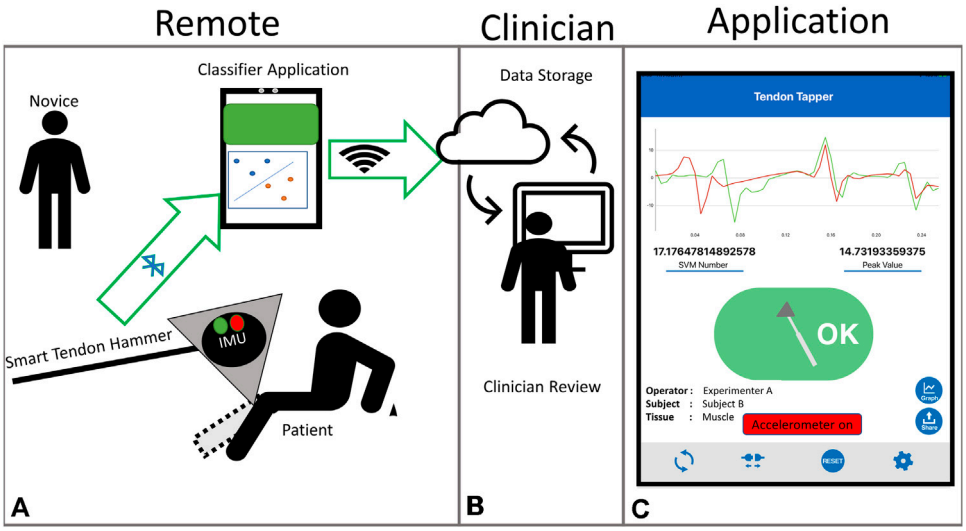

FIGURE 1 | Proposed remote deep tendon reflex exam system **(A)** Remote portion with smart hammer assisted reflex elicitation and grading, **(B)** Clinical portion, with clinician receiving assessed scores and communicating with patient, **(C)** Tapping application screen.

the stimulus delivery is the component that must be performed in close physical proximity to the patient.

The DTR involves afferent neurons in the muscle that synapse directly onto the motor neurons of that muscle. The reflex is stimulated via the application of an impact from a reflex hammer. The hammer impact displaces the tendon, lengthening the muscle tendon complex, and stretching the afferent neurons in the muscle fibers Walker et al. (1990). This stretching of the neurons activates the reflex loop, causing a rapid contraction of the muscle and rotation of the joint. The reflex response is then graded on a numerical scale, either five point (National Institute of Neurological Disorders and Stroke), or nine point (Mayo) Manschot et al. (1998).

A number of conditions such as hypothyroidism, peripheral neuropathy, myoclonus and parkinsonism affect the reflex response Chardon et al. (2014); Walker et al. (1990); Eslamian et al. (2011). Efforts to quantify the dynamics of various DTR's are ongoing Shaik et al. (2020); Mamizuka et al. (2007); Manschot et al. (1998); Kim et al. (2002); Chardon et al. (2014); Stam and Tan (1987); Frijns et al. (1997), however, typical diagnostic use is as a screening tool to indicate the presence of lesion and aid in localization in either the upper or lower reflex arc, Walker et al. (1990).

While laypeople may be able to accurately grade reflexes, stimulation of the tendon with a reflex hammer is more difficult. To that end, this work involves the development of a smart tendon hammer and accompanying application for the immediate assessment of tendon tapping stimulus. By measuring hammer acceleration during tapping, it is possible to characterize the stimulus as appropriate or inappropriate (in terms of tapping location) after each individual tap. Implementation of this categorization in a mobile application enables tendon stimulus delivery by a layperson, as the skilled component of the procedure then becomes the response grading. The reflex grading portion of the proposed remote tendon exam is validated through a video response survey in which both novice and expert participants grade reflexes from video segments.

2 MATERIALS AND METHODS

All of the work, experiments and results reported here aim to provide motivation and validation of the remote DTR evaluation workflow and smart hammer system shown in **Figure 1**. The system is intended to enable physical separation between patient and clinician, with a patient's caretaker or family member serving as the novice participant delivering the tendon tapping and grading the reflex response. A smart hammer streams tapping accelerations to the mobile application, which then provides feedback to the operator about the tapping location. Once grades are recorded, they can be sent along with the associated tapping data to a clinician for review.

This method of remote tapping contains key differences from the standard tapping procedure that clinicians perform. In the traditional clinical tapping by an expert, this characterization of stimulus is done through experience and "feel", primarily based on visual location of the impact site and the rebounding of the hammer in the clinician's hand. The proposed system utilizes the smart hammer to collect and analyze the hammer acceleration in order to provide the same characterization of stimulus to a novice who lacks the experience and training of an expert.

First, tapping classification via acceleration is assessed for feasibility and performed via support vector machine (SVM). Next, the design and development of an assistive application for tendon tapping feedback is presented. Novice tapping variability is compared to expert performance in terms of impact acceleration viability. Finally, novice reflex grading is

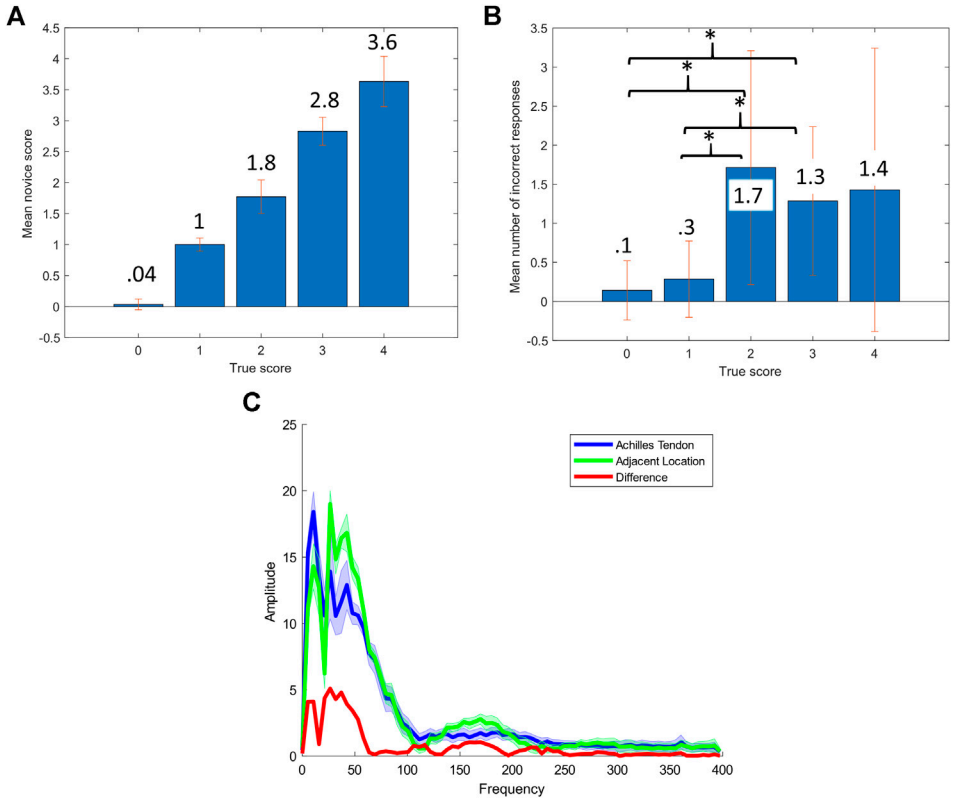

FIGURE 2 | Survey and automated tapping results **(A)** Mean score for each true score, **(B)** Mean number of errors for each true score, * represents $p < 0.05$. **(C)** Mean amplitude spectrum of robotic tapping on two human subjects, shaded portions represent one standard deviation.

compared to expert grading through the use of an online video reflex grading task.

2.1 Tapping Classification

The primary aim of the technical developments reported here is the accurate classification of tendon tapping from hammer acceleration measurements. It is essential that the information to discriminate between correct and incorrect stimulation is contained within the readily measurable hammer acceleration. In the case of the wireless instrumented hammer and mobile application, Bluetooth communication is the primary limiting factor for the sample rate. To evaluate the practicality of classification via streamed acceleration measurements (limited to 200 Hz), human tapping data was collected at 800 Hz using a previously developed automated tapping device Meinhold and Ueda (2018). 50 taps were analyzed from two locations on each of the two subjects, the apex of the right Achilles tendon, and an adjacent location. All data collection occurred under an institutionally approved protocol (GT# H17264).

The frequency content of each tap was ascertained by discrete Fourier transform (*fft*, MATLAB, MathWorks Inc., United States). Mean results for both subjects, along with the difference between locations, are shown in **Figure 2C**. Clear separation between the tendon and incorrect location is apparent up to about 50 Hz, which indicates that the 200 Hz sampling rate may be sufficient for tapping classification. A *t*-test confirmed ($p < 0.001$) that the mean power of the first 50 Hz of the spectrum was significantly different between the on tendon and off tendon conditions. There was a significant difference ($p < 0.01$) in the mean power from 50 to 400 Hz, but not from 100 to 400 Hz ($p > 0.05$). For the statistical tests, power in the respective bandwidths was computed for each tap, then the groups of 100 were tested against the null hypothesis that there was not a difference in the population means. The results of a χ^2 test for the full frequency range are shown in the **Supplementary Material**. Although the reported results pertain only to the Achilles tendon, it is expected that other tendons produce similar acceleration profiles and frequency spectra.

Both the waveform and amplitude of the frequency response contain important information for differentiating the two locations. The waveform most likely contains differences in frequency dependent damping, while differences in amplitude are most likely due to the level of impedance matching between the hammer and tissues. These properties are each individually viable choices for location classification, while acceleration time series contains both frequency and amplitude information, such that any classifier utilizing acceleration time series inherently leverages both domains.

2.2 Tendon Hammer Design and Evaluation

A previously developed smart tendon hammer Meinhold et al. (2017) was used in the course of this work. The hammer is a modified commercially available reflex hammer (NITI-ON, Chiba, Japan) with a silicone head, stainless steel handle and wireless Inertial Measurement Unit (IMU) (Mbient Labs, San Francisco, CA, United States) situated in a polymer case in the head. The IMU records 3-axis acceleration at up to 800 Hz for data logged to the onboard memory, or up to 200 Hz for data streamed directly to a mobile device. The addition of the IMU to the commercial hammer requires only the removal of a disc of material out of the silicone head and inserting the IMU case, which can be done without any precision machining. More details on the construction and operation of the instrumented hammer can be found in the previous study Meinhold et al. (2017), as well as the **Supplementary Material** documentation.

2.3 Tapping Variability Comparison

As described above, the force applied by the tendon hammer to the tendon is the mechanism for eliciting the DTR. Stimulation variability is a confounding factor for the diagnostic utility of the procedure. In order to ascertain the potential for laypeople to perform this procedure remotely, manual stimulation variability was compared between an expert and a non-trained operator.

A trained clinician performed a series of 50 taps with the instrumented medical hammer to a latex rubber tendon analog. The tendon analog was used to eliminate variability due to human subject movement or physiological factors. Acceleration was recorded from the embedded sensor at 100 Hz. The repeatability of stimulation intensity was measured and compared. The relative standard deviation (RSD) of peak deceleration during impact was the metric used for comparison.

The performance of a novice operator in the same simulated tapping experiment was also assessed. A series of 50 taps to the surface of the latex rubber tendon was conducted, with the RSD of peak tapping acceleration again being the primary metric of comparison.

2.4 Materials Cost and Distribution

The Achilles tapping results and the associated statistical analysis in **Section 2.1** demonstrate that sufficient information for classification is contained in the 100 Hz acceleration signal. This has significant benefits for a distributed and remote method of DTR assessment. The 200 Hz bandwidth allows for the use of relatively cheap (61 USD) IMUs as well as standard mobile phone data collection. The process of retrofitting a standard silicone Taylor hammer with an IMU requires only the coarse removal of silicone material to accommodate the IMU case, without any high tolerance machining operations. The ideal tool for communicating with the wireless IMU is a mobile application, as this is easily distributed, and does not require hardware beyond common mobile devices. With distribution of the devices to individuals requiring a DTR exam, physical proximity between patient and clinician is precluded, and sterilization of the hammer between uses is not necessary, because the low cost enables a one device per patient paradigm.

2.5 Application Design and Functionality

A preliminary version of this application was previously reported Meinhold et al. (2017). In the past, this application was designed primarily for research users, the version presented here has been adapted to aid novice users. The interface has been streamlined and simplified to avoid confusion. In addition to the tablet interface, LED indicators on the hammer body itself now indicate the success or failure of the prior tap. A diagram of the intended use is shown in **Figure 1**. The main function of the application is to stream acceleration data from the tendon hammer, detect and classify tendon strikes, then provide binary feedback in the form of a red or green indicator. Although much more information can be recorded, classification results are of the most use to a novice attempting DTR evaluation. The application allows user input of physiological information, as well as import of trained classifiers. These SVM classifiers take the form of a string of parameters defining a hyperplane, that are then used to classify each tap as either on target or incorrect.

2.6 SVM Classifier

To evaluate the classification of tendon tapping location from streamed acceleration data, an additional set of human trials were carried out. Each subject underwent 100 taps from the tendon hammer described in **Section 2.2**, 50 taps to the right Achilles tendon, and 50 taps to a laterally adjacent location. A total of eight healthy adult subjects participated in the experiments (mean age 36.5, 5 F), following an approved human subjects research protocol (GT# H20531).

The large amount of sample points and classification problem associated with traditional stimulus delivery during tendon tapping lends itself to SVM based classification. Although a large number of additional classification methods exist, SVM was chosen due to the portability of the model and the training speed. In order to evaluate the suitability of SVM classification of the tapping location, eight different test/train datasets were produced, with a single subject comprising the test set and the remaining seven making up the training set. The feature vector used consisted of the acceleration at each sample taken by the IMU. A segment of acceleration consisting of the period after impact was used, 0.25 s in length, for a total of 51 samples, a representative feature vector is shown in the **Supplementary Material** document. Each acceleration time series (feature vector) was standardized prior to training of the model. The models were trained in MATLAB (fitsvm), with a linear kernel. Accuracy of the models was assessed as the accuracy in correctly classifying the 100 taps on the held out subject.

The linear SVM classification method produces a simple model of coefficient weights and an offset, which allows for easy transfer to the mobile application. Classification also can take place in near realtime, because of the computational simplicity.

2.7 Layperson Grading

Human subjects (N = 9, 2 Expert, 7 Novice) were recruited to validate the ability of laypeople to grade reflex responses accurately, and to compare to trained expert performance. Experts had both formal training and clinical experience in DTR assessment, for more information, see the **Supplementary**

TABLE 1 | Classification accuracy for each subject. The bold is meant to emphasize the average location accuracy.

Subject	1	2	3	4	5	6	7	8	Mean
Location classification accuracy (%)	100	98	86	90	98	100	67	93	**91.5**

TABLE 2 | Novice survey results by reflex grade.

Ground truth	0	1	2	3	4
Correct responses (%)	97	94	69	71	71
Median selection accuracy (%)	100	100	71	86	86
Mean selection accuracy (%)	100	100	86	86	86
Responses error ≤1 point (%)	100	100	100	100	97

Material. Reflex grading took place in a virtual environment, with video training and evaluation. All training and testing took place in an online, remote format. Participants were first given a training video with three repeated examples of a tap and a response, the impact location of the tendon hammer on the bicep tendon was obscured in all cases. The rating scale employed was the National Institute of Neurological Disorders and Stroke (NINDS) 0–4 numerical scale. After reviewing the training video, participants were given 25 unlabelled tap videos to score, five for each of the five grades. Mean and median scores for each of the five were tabulated for each participant. All data collection took place under an institutionally approved protocol (GT# H20393).

3 RESULTS

3.1 Expert and Novice Tendon Tapping Variability

Expert impact deceleration RSD was 18% while the novice acceleration RSD was 25%. The variability in acceleration indicates that similar levels of variability in tapping force should be expected for expert tendon tapping. Novice impact acceleration variability was larger than the expert's, but still suitable for tendon reflex elicitation. Full results are shown in the **Supplementary Material** documentation.

3.2 SVM Classification Accuracy

The accuracy of the trained SVM model for the achilles tendon is shown in **Table 1** Classification accuracy for each subject. Overall classification accuracy was 91.5% with a range of 67% when subject seven was held out for testing to 100% on subjects 1 and 6. With the relatively small subject pool, the high accuracy demonstrates the suitability of the SVM based classification method for determining tapping impact location from streamed (200 Hz) acceleration data.

3.3 Layperson Grading Results

Aggregate results for each reflex grade from the reflex grading survey are shown in **Table 2**. The mean error across all seven of the novice participants and 25 reflex videos graded was 0.205 on the five point scale. However, mean error provides only one descriptor of the results. A more clinically relevant statistic may be the number of instances in which multiple trials would still result in an incorrect grade. In that case, taking the mean and median of all five trials for each participant results in an incorrect grade in just three and four of the 35 cases respectively. Both experts who completed the survey did not have any errors. Results are shown in **Figure 2** and **Table 2**. There was a significant difference ($p < 0.05$), between the number of errors in the 0 and 1 reflex grades and the 2 and 3 grades.

4 DISCUSSION

Taken together, the results shown demonstrate the potential viability of the remote deep tendon reflex exam. Tapping data on human subjects shows that 68% of the power difference between tapping locations is contained in acceleration signals below 100 Hz, and that the signals below 50 Hz are significantly different, allowing the combined use of readily available wireless IMUs and support vector machine classifiers to provide DTR elicitation feedback. The SVM classifier is shown to be capable of detecting tapping location on the Achilles tendon with 91.5% accuracy from streamed acceleration measurements enabling instant feedback to novices attempting to elicit reflex responses. With the developed application, remote users know when they have hit the tendon correctly, and can then grade the response.

Although novice performance is not perfect, the results indicate grading errors after a number of trials are relatively rare. Most importantly, out of a total of 175 novice graded reflexes, only a single response was more than 1 point away from the ground truth. The significant difference between errors in the 0 and 1 groups and the 2 and 3 groups indicates that areflexia or below normal reflexes are easier for novices to catch than the normal range. Although a larger sample size is needed, it is important to consider the range of conditions that can cause reflex responses to be on the lower end of the scale. Only a single reflex, the bicep tendon reflex, was evaluated, however it is expected that the novice performance in grading other reflexes would be similar.

Although this work has centered on the reflex exam being performed in a completely remote manner, with both tapping and grading done by novices, an important result emerged from the survey results. Both experts were capable of grading reflexes from video with 100% accuracy. An alternative procedure where the novice provides the elicitation via smart hammer and assistive application, and a video of the response is sent to the clinician may deserve further study and development. As the COVID-19 pandemic continues to dictate the use of telemedicine, this work provides experimental indications that remote implementation of the tendon reflex examination is possible.

DATA AVAILABILITY STATEMENT

The raw data supporting the conclusions of this article will be made available by the authors, without undue reservation.

ETHICS STATEMENT

The studies involving human participants were reviewed and approved by Georgia Tech Institutional Review Board. The patients/participants provided their written informed consent to participate in this study.

AUTHOR CONTRIBUTIONS

WM worked on an initial prototype application, experimental data collection, data analysis and manuscript writing. JU contributed analysis and manuscript editing, as well as experimental conceptualization and development. YY and HH worked on the design and development of the tapping application. SI and TM contributed clinical insights, as well as assistance with survey preparation and data collection.

FUNDING

YY and HH were supported in part by Medical Device Development Grant, Fukushima Prefecture, Japan, Title: Smart tendon reflex hammer for early diagnosis of diabetic neuropathy (Main contractor: NITI-ON, Inc., Japan, Technical advisor: JU).

ACKNOWLEDGMENTS

Evan Kaplan of Georgia Institute of Technology aided initial application development.

SUPPLEMENTARY MATERIAL

The Supplementary Material for this article can be found online at: https://www.frontiersin.org/articles/10.3389/frobt.2021.618656/full#supplementary-material.

REFERENCES

Chardon, M. K., Rymer, W. Z., and Suresh, N. L. (2014). Quantifying the deep tendon reflex using varying tendon indentation depths: applications to spasticity. *IEEE Trans. Neural Syst. Rehabil. Eng.* 22, 280–289. doi:10.1109/TNSRE.2014.2299753

Chauhan, V., Galwankar, S., Arquilla, B., Garg, M., Di Somma, S., El-Menyar, A., et al. (2020). Novel coronavirus (Covid-19): leveraging telemedicine to optimize care while minimizing exposures and viral transmission. *J. Emerg. Trauma Shock* 13, 20. doi:10.4103/jets.jets_151_20

Eslamian, F., Bahrami, A., Aghamohammadzadeh, N., Niafar, M., Salekzamani, Y., Behkamrad, K., et al. (2011). Electrophysiologic changes in patients with untreated primary hypothyroidism. *J. Clin. Neurophysiol.* 28 (3), 323–328. doi:10.1097/WNP.0b013e31821c30d9

Frijns, C., Laman, D., Van Duijn, M., and Van Duijn, H. (1997). Normal values of patellar and ankle tendon reflex latencies. *Clin. Neurol. Neurosurg.* 99, 31–36. doi:10.1016/s0303-8467(96)00593-8

Kim, K.-J., Hwang, I.-K., and Wertsch, J. J. (2002). Development of a quantitative reflex hammer for measurement of tendon stretch reflex. *IEEE Trans. Neural Syst. Rehabil. Eng.* 10, 165–169. doi:10.1109/TNSRE.2002.802864

Mamizuka, N., Sakane, M., Kaneoka, K., Hori, N., and Ochiai, N. (2007). Kinematic quantitation of the patellar tendon reflex using a tri-axial accelerometer. *J. Biomech.* 40, 2107–2111. doi:10.1016/j.jbiomech.2006.10.003

Manschot, S., van Passel, L., Buskens, E., Algra, A., and van Gijn, J. (1998). Mayo and ninds scales for assessment of tendon reflexes: between observer agreement and implications for communication. *J. Neurol. Neurosurg. Psychiatry* 64, 253–255. doi:10.1136/jnnp.64.2.253

Meinhold, W., Kaplan, E., Ueda, J., Mori, T., and Izumi, S.-I. (2017). "An instrumented medical hammer with diagnostic, therapeutic and pedagogical applications," in Dynamic systems and control conference, Tysons, Virginia, October 11–13, 2107 (New York, NY: American Society of Mechanical Engineers), 58271, V001T38A001.

Meinhold, W., and Ueda, J. (2018). "Tendon tapping stimulus charecterization through contact modeling," in ASME 2018 dynamic systems and control conference, Atlanta, Georgia, September–October 30–3, 2018 (New York, NY: American Society of Mechanical Engineers), 6.

Ottaviani, D., Boso, F., Tranquillini, E., Gapeni, I., Pedrotti, G., Cozzio, S., et al. (2020). Early guillain-barré syndrome in coronavirus disease 2019 (Covid-19): a case report from an Italian COVID-hospital. *Neurol. Sci.* 41, 1351–1354. doi:10.1007/s10072-020-04449-8

Pezzini, A., and Padovani, A. (2020). Lifting the mask on neurological manifestations of covid-19. *Nat. Rev. Neurol.* 16, 1–9. doi:10.1038/s41582-020-0398-3

Shaik, K., Kamaldeen, D., Maruthy, K., Johnson, P., and Kumar, A. S. (2020). A newer approach for quantitative assessment of patellar tendon reflex response using biomechanical data of foot movement by a digital method. *Sports Orthop. Traumatol.* 36, 271–277. doi:10.1016/j.orthtr.2020.04.010

Stam, J., and Tan, K. (1987). Tendon reflex variability and method of stimulation. *Electroencephalogr. Clin. Neurophysiol.* 67, 463–467. doi:10.1016/0013-4694(87)90010-1

Walker, H., Hall, W., and Hurst, J. (1990). *Deep tendon reflexes–clinical methods: the history, physical, and laboratory examinations*. 2nd Edn. Boston: Butterworths, 365–367.

Conflict of Interest: YY and HH are employees of NITI-ON Co. a company that develops, manufactures and sells medical devices and software.

The remaining authors declare that the research was conducted in the absence of any commercial or financial relationships that could be construed as a potential conflict of interest.

frontiers in Robotics and AI

ORIGINAL RESEARCH
published: 18 March 2021
doi: 10.3389/frobt.2021.618866

Robotic Telemedicine for Mental Health: A Multimodal Approach to Improve Human-Robot Engagement

*Maria R. Lima[1], Maitreyee Wairagkar[1], Nirupama Natarajan[2], Sridhar Vaitheswaran[2] and Ravi Vaidyanathan[1]**

[1]Department of Mechanical Engineering, Imperial College London, and UK Dementia Research Institute—Care Research and Technology Centre, London, United Kingdom, [2]Schizophrenia Research Foundation (SCARF), Chennai, India

COVID-19 has severely impacted mental health in vulnerable demographics, in particular older adults, who face unprecedented isolation. Consequences, while globally severe, are acutely pronounced in low- and middle-income countries (LMICs) confronting pronounced gaps in resources and clinician accessibility. Social robots are well-recognized for their potential to support mental health, yet user compliance (i.e., trust) demands seamless affective human-robot interactions; natural 'human-like' conversations are required in simple, inexpensive, deployable platforms. We present the design, development, and pilot testing of a multimodal robotic framework fusing verbal (contextual speech) and nonverbal (facial expressions) social cues, aimed to improve engagement in human-robot interaction and ultimately facilitate mental health telemedicine during and beyond the COVID-19 pandemic. We report the design optimization of a hybrid face robot, which combines digital facial expressions based on mathematical affect space mapping with static 3D facial features. We further introduce a contextual virtual assistant with integrated cloud-based AI coupled to the robot's facial representation of emotions, such that the robot adapts its emotional response to users' speech in real-time. Experiments with healthy participants demonstrate emotion recognition exceeding 90% for happy, tired, sad, angry, surprised and stern/disgusted robotic emotions. When separated, stern and disgusted are occasionally transposed (70%+ accuracy overall) but are easily distinguishable from other emotions. A qualitative user experience analysis indicates overall enthusiastic and engaging reception to human-robot multimodal interaction with the new framework. The robot has been modified to enable clinical telemedicine for cognitive engagement with older adults and people with dementia (PwD) in LMICs. The mechanically simple and low-cost social robot has been deployed in pilot tests to support older individuals and PwD at the Schizophrenia Research Foundation (SCARF) in Chennai, India. A procedure for deployment addressing challenges in cultural acceptance, end-user acclimatization and resource allocation is further introduced. Results indicate strong promise to stimulate human-robot psychosocial interaction through the hybrid-face robotic system. Future work is targeting deployment for telemedicine to mitigate the mental health impact of COVID-19 on older adults and PwD in both LMICs and higher income regions.

Keywords: social robots, COVID-19, human-robot interaction, intelligent virtual assistant, multimodal interaction, dementia, telemedicine, low- and middle-income countries

OPEN ACCESS

Edited by:
Mahdi Tavakoli,
University of Alberta, Canada

Reviewed by:
Abdul Rauf Anwar,
University of Engineering and Technology, Lahore, Pakistan
Wajid Mumtaz,
National University of Sciences and Technology (NUST), Pakistan
Sanja Dogramadzi,
The University of Sheffield, United Kingdom

****Correspondence:***
Ravi Vaidyanathan
r.vaidyanathan@imperial.ac.uk

Specialty section:
This article was submitted to Biomedical Robotics, a section of the journal Frontiers in Robotics and AI

Received: *18 October 2020*
Accepted: *01 February 2021*
Published: *18 March 2021*

Citation:
Lima MR, Wairagkar M, Natarajan N, Vaitheswaran S and Vaidyanathan R (2021) Robotic Telemedicine for Mental Health: A Multimodal Approach to Improve Human-Robot Engagement. Front. Robot. AI 8:618866. doi: 10.3389/frobt.2021.618866

INTRODUCTION

Dementia is a leading cause for disability and dependence across the world. As a chronic neurodegenerative condition, demands for care increase over time. Many people with dementia require social support, day care or assisted residence facilities with advancing illness. A staggering one in four United Kingdom hospital admissions is due to a dementia-related condition (Alzheimer's Research UK, 2020)[1]. Global care costs are projected to exceed $2 trillion/annum demanding 40 million new care workers, which could easily overwhelm medical and social care systems as they stand today (Alzheimer's Research UK, 2020)[1]. Prevalence of dementia is further skyrocketing in LMICs; 63% of PwD already live in LMICs, where 70% of new cases occur (Prince et al., 2007; Prince et al., 2013). In India, the treatment gap today is a staggering 90% (Dias and Patel, 2009). Lower-income nations will have comparable or even worse rates. Availability of resources, including human resource capacity, are major contributing factors to this gap (Prince et al., 2007; Shaji et al., 2010). Recent industrialization, migration, and urbanization in Asia have also impacted traditional family structures such that older people face less family support and more isolation today than ever before (Dias and Patel, 2009).

This global health crisis has become even more critical during the COVID-19 pandemic. However, planning and response to public health emergencies (i.e., COVID-19 outbreak) often do not directly address mental health, in particular for vulnerable groups such as older adults and PwD (Vaitheswaran et al., 2020). Dementia is already an emerging pandemic (Wang et al., 2020) with more than 50 million cases worldwide and a new case occurring every 3 s (Alzheimer's Disease International, 2019)[2]. The combined strain of COVID-19 and dementia pandemics is severely increasing suffering of PwD and their caregivers. COVID-19 has caused unprecedented stress, fear and agitation among the seniors, especially those with cognitive impairment or dementia (Mehra and Grover, 2020), who are considered to be more vulnerable to COVID-19 (Wang et al., 2020). Isolation and confinement measures imposed to prevent infection of high-risk populations have undercut essential sources of support. Care is reduced or, in some cases, completely removed and important face-to-face contact lost, which may have long-lasting psychosocial and cognitive consequences in PwD. Caregivers for PwD are also in dire need of mental health support and many older adults without specific mental health diagnosis are also suffering pronounced psychological consequences due to isolation. Furthermore, the level of anxiety and exhaustion among staff in care residence facilities has increased during COVID-19 (Wang et al., 2020). There is immediate, urgent and desperate call for greater mental health support in this arena.

The need for mental health and psychosocial support of PwD and their carers worldwide is well-documented (Wang et al., 2020) both during and prior to the COVID-19 pandemic. The effect of COVID-19 on healthcare infrastructure in LMICs, however, is arguably more extreme due to the health system capacity and deeper dependency on families for support of PwD (Walker et al., 2020). A recent study conducted with caregivers in South India (Vaitheswaran et al., 2020) highlights a clear need for more services and support of PwD and caregivers for the post-pandemic, including stronger adoption of technology. Affordable, accessible and scalable solutions to monitor mental health, improve independence, increase quality of life, and reduce caregiver burden are urgently needed both in the immediate situation, as well as beyond the current global lockdowns.

Socially assistive robots (SAR) are well-documented for promise to support dementia and mental health (Tapus et al., 2007), with strong potential specifically to mitigate COVID-19 impact on PwD. Prior to the COVID-19 pandemic, a range of tools from simple voice interfaces to interactive social robots have been introduced with the aim of providing stimulation, entertainment, personal assistance, monitoring and safety for older adults and PwD (Inoue et al., 2012; Martín et al., 2013; Mordoch et al., 2013; Joranson et al., 2015; Moyle et al., 2017; Falck et al., 2020); see (Abdi et al., 2018) for a recent review. Exemplary cases such as the humanoid robot NAO (Agüera-Ortiz et al., 2015), PaPeRo (Inoue et al., 2012), Bandit (Tapus et al., 2009), Eva (Cruz-Sandoval and Favela, 2016), and robot alternatives to animal assisted therapy such as AIBO, the robotic dog (Tamura et al., 2004), NeCoRo, the robotic cat (Libin and Cohen-Mansfield, 2004), and the well-known Paro, the robotic seal (Wada and Shibata, 2007) have shown the possibility of improving patient engagement, reducing agitation, improving mood and communication, and decreasing stress (Inoue et al., 2011; Petersen et al., 2017), though comparable results have been argued with a simple stuffed animal (Moyle et al., 2017). Recent literature (Martín et al., 2013; Valenti Soler et al., 2015; Rouaix et al., 2017) has argued social robots can help improve irritability, global neuropsychiatric symptoms, and PwD's emotional responses with robot assisted therapies. The neuropsychological effects of interaction with robots has also shown increased cortical neuron activity (Wada et al., 2005a). Social robots hold specific promise in the COVID-19 crisis by providing older adults and PwD with complementary support to alleviate anxiety and loneliness, improve engagement, and reduce caregiver burden. Social robots can also provide clinicians with an alternative platform to deliver remote therapies and support PwD, especially at a time when nonemergency clinical appointments are increasingly shifting to remote alternatives.

There are several verbal and nonverbal interaction modes used by SAR to engage with humans—such as facial expressions, speech, gestures, or behavior—but the most effective communication mode in human-robot interaction (HRI) is largely considered to be speech (Fong et al., 2003). Intelligent virtual assistants (IVA), also known as conversational agents, chatbots, or virtual assistants, are AI-powered systems that understand user intents in natural language and generate relevant responses using machine learning (ML) algorithms. Despite benefits in feasibility of implementation and commercial availability, virtual assistants and voice-enabled smart speakers (e.g., Amazon Alexa, Google Home) alone have limited flexibility to adapt for mental health care applications,

[1]https://www.dementiastatistics.org/statistics/hospitals/

[2]https://www.alz.co.uk/research/WorldAlzheimerReport2019.pdf

particularly to support PwD. Emerging social robots, on the contrary, can use a multimodal approach with combined social and emotional nonverbal cues, such as facial expressions or gestures, in addition to verbal communication. The integration of affective communicative modalities and implementation in social robots can ultimately lead to improved engagement in HRI in demanding healthcare contexts, such as dementia care, during and beyond the COVID-19 pandemic. Social robots can be used as a means of telemedicine and remote therapy delivery for mental health monitoring and psychosocial support of high-risk populations, particularly older adults and PwD. By providing companionship and enhancing independent living, such robotic technologies could also give carers some respite time and relieve the caregiver burden especially faced during lockdowns.

The high cost of such complex interactive systems is oftentimes a barrier for deployment, especially in LMICs. While SAR have shown great potential to support PwD in clinical and residential environments, no research to date has developed and pilot tested mechanically simple and low-cost robotic solutions to support dementia care in challenging scenarios imposed by the COVID-19 outbreak in LMICs, particularly in India.

The goal of this investigation is to design, develop, and test the feasibility of a social robotic platform to support people with dementia, during and following the COVID-19 pandemic. We are particularly interested in surmounting cost constraints and ease of use demands for utility in LMICs. In our previous work (Bazo et al., 2010) we introduced a 'hybrid face' robot with combined static physical features and a digital face that simulates facial expressions based on mathematical affect space emotion mapping. We further quantified the neurophysiological response to the robot and initiated work to translate a simplified version of it as a consumer product (Wairagkar et al., 2020). In this study, we:

(1) Propose a new multimodal robotic framework that integrates animated representation of emotions with a voice system supported by a cloud-based AI conversational engine for enhanced engagement in HRI.
(2) Test human-robot multimodal interactions with healthy participants in the United Kingdom demonstrating the robot's ability to adapt facial expressions to users' speech in real-time and a strong user preference for multimodal vs. pure voice communication.
(3) Introduce a user-centred procedure for cultural validation addressing telemedicine acceptance of robotic mental health support of older individuals and PwD. Modifications to our robotic platform based on this procedure as implemented in South India are presented, and the procedure is offered as a broader method for introduction of such technology in new cultural arenas and demographics.
(4) Present a pilot study introducing the robot into practice for dementia support in LMICs through experiments conducted with people with dementia at the Schizophrenia Research Foundation (SCARF) in Chennai, India.

Results demonstrate the capacity to deliver telemedicine cognitive engagement and mental health support through the hybrid face robot. Current work is targeting trials in South India with planned investigations on deployment in LMICs as well as wealthier nations.

RELATED WORK

The ability to recognize, understand, and show emotions plays a fundamental role in the development of SAR capable of meaningful interactions (Breazeal, 2009). Facial expressions, speech, and body language are proved to carry essential affective information for social interactions (Breazeal, 2003). According to (Schiano et al., 2000) facial expressions are the primary means of communicating emotions. Ekman introduced the facial action coding system (FACS) (Donato et al., 1999) and posits that all human expressions are a combination of the primary expressions: happiness, sadness, anger, fear, disgust, and surprise.

Robotics researchers are faced with the question of whether to design physically embodied, fully actuated robots, or simpler and cheaper virtual agents. Literature has argued the level of a robot's embodiment is key to develop trust and rapport, and may affect human judgements of the robot as a social partner (Wainer et al., 2006; Bainbridge et al., 2011). (Ghazali et al., 2018) have suggested trust toward robotic agents is also influenced by its facial characteristics. Though it remains unclear how robot's gender shapes human trust, in this experimental study, gender did not affect user trust and a higher psychological reactance was observed in participants during interactions with a robot of opposite gender. Embodiment is also an influencing factor of users' expectations of the robot's abilities and autonomy (Clabaugh and Matarić, 2019). However, the mechatronic complexity in the development of embodied, fully actuated robots with the desired expressive ability is associated with high costs. This in turn constitutes a barrier for real-world deployment beyond academic research, especially in LMICs. The implementation of expressive robotic faces on LCD screens has recently been applied in different SAR platforms, which allows easy customization, adaptability to users' preferences and culture, higher accessibility and scalability (Abdollahi et al., 2017; Portugal et al., 2019); this may be especially relevant for human-robot engagement with older adults with and without dementia, as the screen can also be used for interactive activities, visualization of the robot's speech, or as an additional user input. Regardless of the social robot level of embodiment, facial characteristics, or gender, care should be taken to avoid reaching the uncanny valley, graphically represented by a sudden negative drop in human's emotional response toward robots when shifting from non-human/artificial faces toward optimal human faces (Mori et al., 2012). Additionally, when designing social robots to effectively interact with older citizens and cognitive impaired individuals, researchers must consider ethical concerns that may limit the deployment of such technologies. These include increased use by vulnerable populations, reduced human contact, loss of privacy,

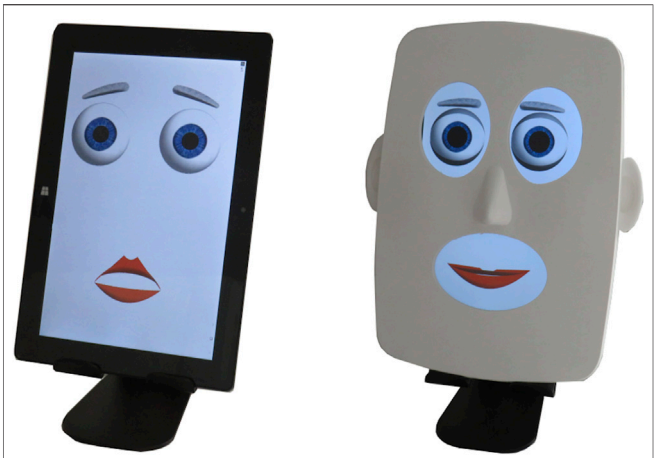

FIGURE 1 | Hybrid face robot running on a tablet PC with option to add a 3D printed faceplate for realism and depth.

emotional deception, which occurs when users' expectations of the robot are not met, and attachment to the robot, which may cause emotional distress (Van Maris et al., 2020; Van Patten et al., 2020). In a longitudinal study with older citizens, (Van Maris et al., 2020) highlight the need for research metrics to analyze emotional attachment to social robots, people's behaviors, and speech patterns.

The field of ML has recently experienced extraordinary progress in the development of IVA. These AI-powered systems interact with users using natural language and are able to generate relevant responses in the form of text, speech, or both. This technology started in the 1960s with ELIZA (Weizenbaum, 1966), which held text-based conversations with users acting as a psychotherapist. A recent body of work (Romero et al., 2017; Harms et al., 2018) has provided novel approaches for the development of conversational agents for increased user engagement. Along similar lines, there has been work on the development of embodied conversational agents—virtual animated characters, usually with the appearance of a human-like avatar, capable of understanding multimodal utterances, such as voice, gestures, and emotion (Griol et al., 2019). These systems aim to provide a more empathetic response based on dialogue and behavior (Merdivan et al., 2019), yet they often cause a sense of discomfort explained by the uncanny valley (Ciechanowski et al., 2019).

Intelligent virtual assistants have been deployed in healthcare for delivering cognitive behavior therapy (Fitzpatrick et al., 2017) or assist older people in the living environment; see (Laranjo et al., 2018) for a recent review. Yet, evidence of efficacy and safety of conversational agents to reliably support healthcare is limited (Laranjo et al., 2018); prior research has reported inconsistent responses even when user statements explicitly contained risk or harm (e.g., "I want to commit suicide," "I am depressed") (Miner et al., 2016). To assist those with cognitive impairments, (Wolters et al., 2016) have explored the use of virtual assistants with PwD, highlighting the importance of adapting voice and interaction style to each user's preferences and expectations, but importantly, to cognitive decline. One interesting observation that deserves more introspection is that people with dementia questioned the acceptability of a voice system without a face. Furthermore, the COVID-19 outbreak has spurred greater interest in the use of voice assistants and chatbots as a tool to support high-risk populations, such as older individuals and PwD; if designed effectively, these may support patients in need for routine care via conversations, provide up-to-date information, and alleviate the mental health burden (Miner et al., 2020; Sezgin et al., 2020).

METHODS

Development of Multimodal Robotic System

Affective Hybrid Face Robot

The hybrid face robot integrates a digital face capable of showing facial expressions and a 3D printed faceplace to convey realism and depth, which can be flexibly added to the robot (**Figure 1**). The robot's software was programmed using Max 8 (Cycling '74, San Francisco, CA, United States) and was implemented on a tablet PC, building upon our previous work (Bazo et al., 2010).

The robotic face is simply made of four facial features: eyebrows, eyelids, eyes, and lips, with a total of 13 degrees of freedom (DoF) illustrated in **Figure 2**. Realism features, such as constant motion of the face, random blinking of the eyes, and pupil dilation (Bazo et al., 2010; Craig et al., 2010; Wairagkar et al., 2020) can be controlled and may lead to more dynamic HRIs. Our choice of a simplistic three-dimensional design for the robotic face aims to avoid the uncanny valley effect. Ideally, this mechanically simple robot would elicit human-like trust and engagement in HRIs, yet without the mechatronic complexity and associated high-costs of a fully actuated face.

The robot's software design is based on a mathematical approach for emotion mapping, in which the robot's expression state, $\vec{e}\,(t)$, for any given time, t, is defined as the weighted linear combination of a set of basis expressions $B = \{\vec{b}_1, \vec{b}_2, \ldots, \vec{b}_n\}$. Each vector contains 13 values, one for each degree of freedom of the digital face. In our previous work (Bazo et al., 2010), this set has been defined with the following expressions: $B = \{\vec{b}_{happy}, \vec{b}_{sad}, \vec{b}_{angry}, \vec{b}_{stern}, \vec{b}_{surprised}, \vec{b}_{disgusted}, \vec{b}_{afraid}, \vec{b}_{tired}\}$. The intensity vector $\vec{w} = [w_1, w_2, \ldots, w_n]^T$, $w_i \in [0,1]$, symbolizes the amount by which an expression $\vec{b}_i$ contributes to $\vec{e}\,(t)$. Hence, any expression state is the weighted sum of variances of each basis expression, $\vec{b}_i$, from the neutral expression, $\vec{b}_N$, and then added to the neutral expression along the following equation (time is omitted from notation for simplicity):

$$\vec{e} = \sum_{i=1}^{n} \left(\vec{b}_i - \vec{b}_N \right) \vec{w}_i + \vec{b}_N \qquad (1)$$

Following this approach, the modeling of emotions can be manually and remotely controlled by selecting each expression's intensity, which is in turn converted into a 13-value vector, defining the DoF of the desired facial expression (**Figure 3**). Additionally, the robot's mouth is animated and synchronized with the audio input's amplitude, in decibel (dB), in such a way

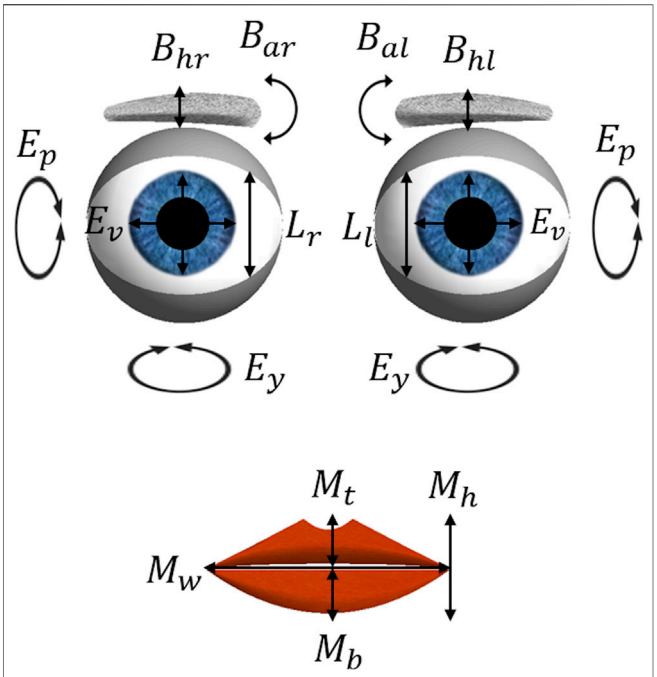

FIGURE 2 | The 13 degrees of freedom of the expressive face: eyebrow angles (B_{al} and B_{ar}) and vertical height (B_{hl} and B_{hr}); eyelid openness (L_l and L_r); eye vergence (E_v), pitch (E_p) and yaw (E_y); mouth corner vertical height (M_h), width (M_w), top lip openness (M_t) and bottom lip openness (M_b).

that when it surpasses a cut-off dB value the DoF correspondent to the top and bottom lips (M_t and M_b, respectively) open and close simultaneously, while the mouth width, M_w, changes by 30% to simulate the elastic movement of a human mouth.

The design of robot's facial expressions and its control system were optimized in this work. This optimization included: 1) creating an interface with Python to enable automatic and remote control of facial expressions integrated with autonomous speech (see Section *Intelligent Virtual Assistant*); 2) optimizing the voice stream synchronization parameters in Max software; 3) modifying DoF for some expressions to improve recognition rates. Taken together, these improvements allowed us to:

(1) Integrate the robot's speech capacity with facial expressions for adaptable emotion in response to users' speech in real-time.
(2) Introduce the robot into practice for aging and dementia support in LMICs; a pilot study was conducted at SCARF India using the hybrid face robot as a telemedicine tool for remote cognitive engagement with a person with dementia through repeated sessions, in the form of Wizard of Oz experiment [see (Natarajan et al., 2019) for our recent work].

Our aim is to enhance engagement in HRI by endowing the robot with a set of multimodal affective cues (i.e., verbal and nonverbal, through facial expressions), and further validate the cultural acceptability and usefulness of such robotic tool as a telemedicine solution for mental health support of older adults and people with dementia in India. This may be of special interest (but not limited to) in the context of COVID-19, particularly in LMICs.

Figure 4 shows the optimized design of different facial expressions simulated by the robot. Importantly, the disgusted expression, which as pointed by Ekman in (Donato et al., 1999) features a peculiar wrinkling of the nose impossible to simulate with the current face design, was redesigned following psychology and robotics literature (Donato et al., 1999; Breazeal, 2003): the eyes were narrowed, by decreasing L_l and L_r and adjusting the eyelid asymmetry; eyebrows were lowered, with a significant change in the right angle, B_{al}; upper and lower lips

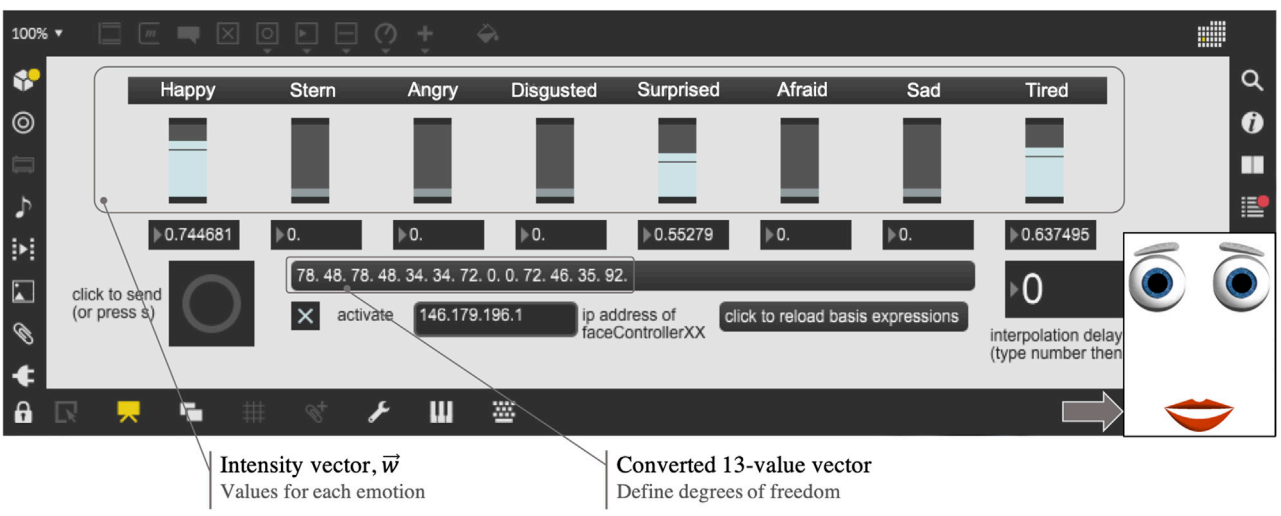

FIGURE 3 | Front-end control of robotic animated facial expressions.

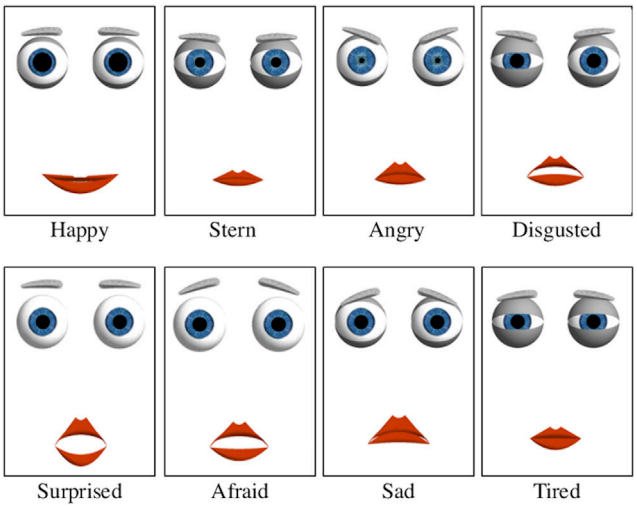

FIGURE 4 | Optimized design of facial expressions simulated by the robot. Major modifications were made for the disgusted, surprised, and afraid robotic expressions with the aim of improving emotion recognition rates.

were raised, and the mouth was slightly opened, by adjusting M_t and M_b; lastly, the mouth width, M_w, was increased. Afraid and surprised expressions were modified to avoid past confusion between one another (Bazo et al., 2010), as both feature raised eyebrows, opened eyes and mouth. Major modifications included: for surprised, the DoF M_t and M_b were increased to their maximum values and M_w decreased to the minimum; for afraid, the eyebrows vertical height was raised (DoF B_{hl} and B_{hr}) and the angles were slightly rotated (DoF B_{al} and B_{ar}). Other expressions were used as in previous work (Bazo et al., 2010; Craig et al., 2010).

Intelligent Virtual Assistant

In order to extend the social robot's autonomous interactive capabilities and explore multimodal affective HRI, we developed a virtual assistant powered by state-of-the-art IBM Watson (IBM, New York, United States) cloud-based AI capabilities. These AI cloud services have been used in past research in robotics and computer science (Chozas et al., 2017; Novoa et al., 2018; Di Nuovo et al., 2019). Overall, the implementation of the multimodal architecture described below allows the robot to emotionally interact with humans through voice, in addition to simulated facial expressions, and adapt the displayed emotion depending on users' speech in real-time.

System Architecture

The system uses speech recognition algorithms, natural language understanding (NLU), and the training data provided to simulate a natural conversation. The cloud-based AI conversational system was designed to interact with users through speech, text, or both, maintaining a conversation in four different domains of knowledge, i.e., skills, atomic programs that represent a capability in a specific domain. The implemented skills enhance the flow of conversation and lead the system to:

- Converse about the user's emotional state.
- Entertain the user with a quiz on selected topics.
- Provide definitions of any concept the user asks about (integration with Wikipedia[3]).
- Give local weather forecasts if requested (integration with The Weather Company[4]).

To create natural, believable interactions between intelligent virtual assistants and humans, understanding the context of conversations is of utmost importance (Harms et al., 2018). Therefore, for each dialogue skill designed several context variables were programmed (i.e., information that is stored during the dialogue), such as the user's name, mood, time of day, or location. These allowed a certain degree of personalization, in that for each interaction the system dynamically tailors responses to user preferences and mood. **Figure 5** shows an extract of a human-robot conversation, including different dialogue skills, context variables and the interface with the affective hybrid face robot (see Section *Implementation* for further details). Our principal aim in this investigation was to integrate the IVA system with the robot's affective framework and address feasibility of acceptance and deployment. In future work we intend to introduce a knowledge base with user profiles and implement machine learning to personalize interactions over time.

Implementation

Several APIs were programmable combined and integrated with the robot's affective capabilities in the back-end system by an orchestrator coded in Python. The main cloud-based services used include: 1) IBM Watson Assistant to create a dialogue flow, context variables, and provide training data—intents and entities, the user goal and its context, respectively; 2) IBM Tone Analyzer, which detects sentiment from text; 3) Google Speech to Text to perform speech recognition; 4) Google Text to Speech to generate the robot's voice with a relevant response.

The interface created in Python between the hybrid-face robot and the IVA takes as input 13-integer strings via sockets UDP and local IP address, which represent the 13 degrees of freedom for each facial expression simulated by the robot. The default facial expression simulated by the robot was defined as happy. The orchestrator is therefore responsible to manage the flow of conversation by 1) controlling the jump between several dialogue skills and 2) adapting the robot's facial expression depending on users' responses in real-time, which are analyzed by IBM Tone Analyzer and sent to the robot's software (e.g., if the user says "I had a bad day" the robot will verbally reply while displaying a sad expression). To trigger a conversation 'skill' and subsequently a dialogue node, the IVA algorithm evaluates intents, entities, and context variables included in the user response. This process is done based on the confidence level, i.e., the probability that the variable was correctly identified, with

[3]https://en.wikipedia.org/wiki/Main_Page
[4]https://www.ibm.com/weather

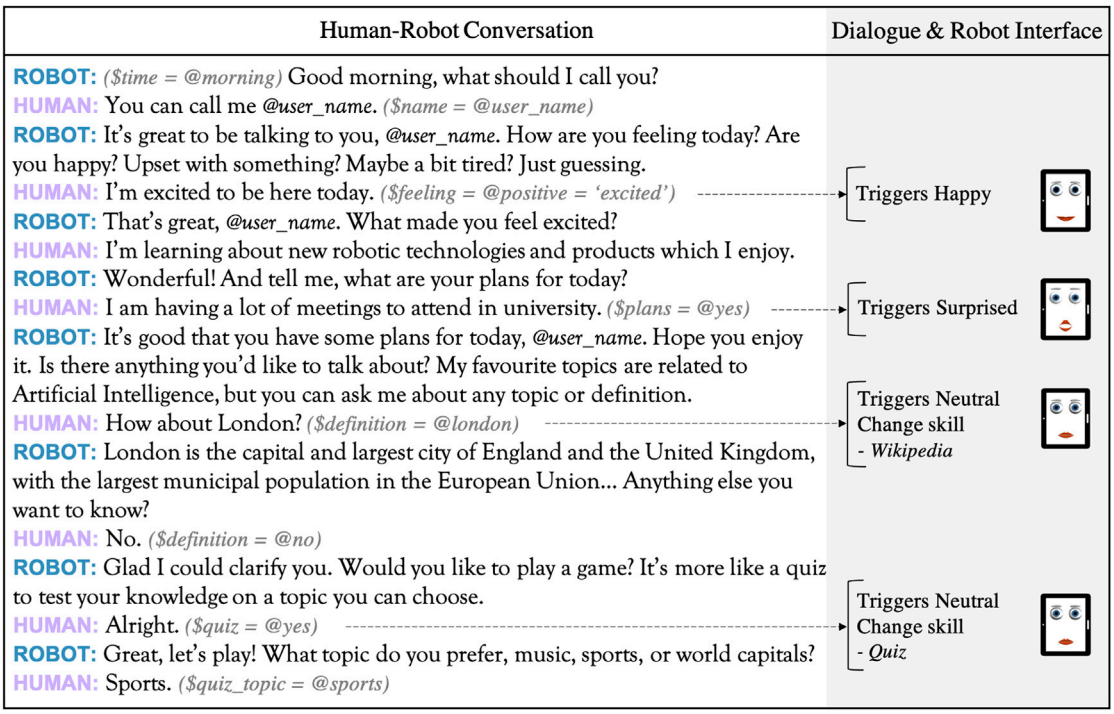

FIGURE 5 | Section of a human-robot conversation transcript from testing with healthy participants in the United Kingdom. Various context variables ($) and entities (@) are identified. These allow to 1) change dialogue skills (e.g., gather definitions from Wikipedia, start a quiz to entertain the user), and 2) simultaneously adapt the robot's facial representation of emotion according to the sentiment in user response, ultimately leading to more engaging and personalized interactions.

regards to the examples given when training the algorithm. The confidence scoring (decimal in the range 0–1) is done independently of previous utterances and its default threshold is 0.3[5].

Figure 6 illustrates the four layers coordinated by the orchestrator, which were designedly integrated to enhance engagement in multimodal HRIs. The *interface layer* includes APIs for communication (speech and text), the interface with the robot's software and control of facial expressions; it receives input from the *cognitive layer*, which comprises the cognitive process of understanding user inputs through NLU. This is algorithmically achieved by recognizing intents, entities and context variables, and by analyzing the emotion in user responses. Further, the *enrichment layer* establishes communication with external services to get information about the current weather (The Weather Company and Python library geopy were used to locate coordinates and provide weather forecasts), or general definitions provided by Wikipedia. Lastly, the *support layer* is responsible for all links with external services and APIs, i.e., config files, and stores all the cognitive processes involved in interactions, indicating intents, entities and context variables recognized for each user response, their confidence level, or possible errors encountered (i.e., application logs). The latter were utilized for algorithm training using the Watson Assistant platform so that the system could understand different natural language syntaxes, adapt its responses, and retrain itself in case the wrong intent was identified.

Evaluation of Human-Robot Interactions with Healthy Participants

In order to evaluate interactions with the multimodal robotic system proposed, we conducted a user study to assess emotion recognition of simulated facial expressions and the user experience in human-robot multimodal interactions. Ethics clearance was obtained by Imperial College London Science, Engineering and Technology Research Ethics Committee (SETREC). Written informed consent was obtained from participants.

Emotion Recognition Experiments

Recognition of Ekman's basic expressions is a standard test to assess the emotional abilities of an expressive robotic face (Schiano et al., 2000; Breazeal, 2003). Therefore, an expression recognition task was conducted with N = 15 healthy participants (23–49 years, 3 female, 12 male) in the United Kingdom to qualitatively assess the optimized design (Section *Affective Hybrid Face Robot*) of the affective robotic face, particularly the disgusted, afraid and surprised facial expressions. Participants were given a list with the eight facial expressions and were shown a sequence of the robot's eight expressions (see **Figure 4**) of approximately 5 s each. After each facial expression observed, participants chose the best match from the given list, following a

[5]https://cloud.ibm.com/docs/assistant?topic=assistant-expression-language

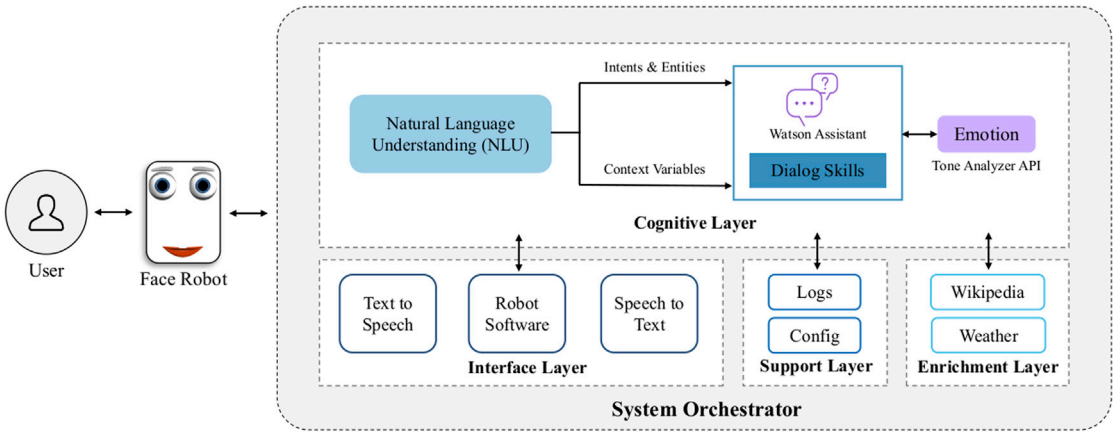

FIGURE 6 | Proposed architecture design of the intelligent virtual assistant for engagement in multimodal HRI. Multiple cloud-based AI services were combined and integrated with the robot's affective capabilities in the back-end system by an orchestrator coded in Python. The orchestrator manages the flow of conversation and adapts the robot's facial representation of emotion in response to users' speech in real-time. The orchestrator coordinates the interface, cognitive, support and enrichment layers.

forced-choice paradigm in line with research (Breazeal, 2003). The hybrid face robot was shown both with and without the 3D faceplate (see **Figure 1**) to address its likeability. After the task, qualitative feedback was gathered from in-depth interviews to understand how the design of robot's facial expressions could be adjusted for further experiments and address the overall impression of the robot.

User Experience Experiments

A user experience questionnaire (UEQ) was used to evaluate the multimodal robotic system. The UEQ matched those deployed for measuring the user experience of interactive products (Schrepp, 2015; Memeti and Pllana, 2018). Our testing was completed with N = 10 healthy volunteers (21–59 years, 5 female, 5 male) who had never interacted with the hybrid face robot but had previous experience with interactive technologies. This study was implemented as a new experiment drawing on findings from the emotion recognition task (Section *Emotion Recognition Experiments*). It was conducted independently with a different set of users to obtain entirely unbiased user experience feedback. For instance, the additional 3D faceplate was not used in this study as it was not perceived favourably in previous human-robot interaction experiments, suggesting a potential uncanny valley effect, induced when the faceplate was added to the digital face (see Section *Emotion Recognition*). The main goal of the UEQ is to evaluate the interaction and engagement between participants and the robotic system. The UEQ used in this study considers five aspects: *attractiveness* evaluates the overall impression of the robot; *perspicuity* assesses the difficulty level to get familiar with the robotic tool; *efficiency* relates to the effort required to understand the robot's emotional responses; *stimulation* evaluates how motivating and exciting is to interact with the robot; lastly, *novelty* judges how innovative and creative the robotic system was perceived by users.

Participants were seated in front of the robot and interacted with it, through speech and visualization of simulated facial expressions. The IVA system was activated in one laptop, and a speaker was placed behind the tablet PC, where the robot's software runs. This allowed a better synchronization of the robot's mouth animation and the audio signal (dB), in such a way that the robot is assumed to be the one speaking. Following human-robot interactions, participants answered the UEQ. **Table 1** lists the questions used for each aspect in this UEQ analysis. The Likert scale system (Boone and Boone, 2012) was used in this method with a scale range from 1 to 5 (1 represents the most negative answer, 3 a neutral answer, and five the most positive answer). For the novelty aspect, participants were asked to choose between two terms with opposite meaning, using the same scale. Afterward, we conducted a short in-depth interview with the aim of qualitatively understanding benefits of multimodal vs. pure face or voice interactions. Specifically, participants were asked whether they would prefer to verbally interact with the virtual assistant (voice only), or with the multimodal robotic system instead (speech integrated with facial expressions).

Robotic Telemedicine for Mental Health Support

The overarching goal in this study is to facilitate introduction of the robot into practice for mental health and PwD support in LMICs. We introduce a user-centred procedure for cultural adaptation of the robot in the context of South India and describe the infrastructure to deploy it as a telemedicine tool to deliver regular cognitive engagement. The pilot study here described is the first of its nature to explore the feasibility and cultural acceptability of robotic telemedicine for mental health and dementia support in India. This may be of particular interest during and following the COVID-19 context to alleviate end-user anxiety and loneliness, improve engagement, and reduce the caregiver burden especially faced during lockdowns.

TABLE 1 | Questions selected for the user experience questionnaire (UEQ) evaluating response to the multimodal robotic system. Questions were grouped to evaluate five aspects: attractiveness evaluates the overall impression of the robot; perspicuity assesses the difficulty level to get familiar with the robotic tool; efficiency addresses the effort required to understand the robot's emotional responses; stimulation judges how motivating and exciting human-robot interactions are perceived; novelty relates to how innovative and creative the robot was perceived by end-users.

Aspect	Id	Question
Attractiveness	a1	What is your overall impression of the proposed robotic system?
	a2	How useful do you find the possibility to communicate with voice?
	a3	How attractive and friendly do you find the robot's facial expressions?
Perspicuity	p1	How intuitive are the robot's emotions?
	p2	How clear are the robot's responses?
	p3	How easy is it to communicate with the robotic system?
Efficiency	e1	How efficient is the robot to convey emotion through speech and expressive faces?
	e2	How practical are the robot's answers or suggestions?
Stimulation	s1	How exciting is to communicate with this robotic system?
	s2	How interesting was the conversation/interaction?
	s3	How much does the robot motivate you to have new interactions?
Novelty	n1	Dull/creative
	n2	Conventional/Inventive
	n3	Usual/leading edge
	n4	Conservative/innovative

Designing Infrastructure

Due to regional language barriers, the AI voice system integration (Section *Intelligent Virtual Assistant*) was not suitable for clinical experiments conducted at SCARF India. Hence, we designed a test infrastructure to use the hybrid face robot as an assistive tool to deliver meaningful cognitive engagement with PwD and healthy older adults in Chennai, India. This infrastructure gives medical professionals the remote control of robot's animated facial expressions and speech. The proposed experimental approach may provide clinicians with an alternative platform for remote therapy delivery and enhanced mental health support of PwD, in particular that meets the cost constraints and ease of use demands for utility in LMICs.

Figure 7 illustrates the experimental setup to conduct remote cognitive engagement using the hybrid face robot, in the form of Wizard of Oz experiments. PwD and clinicians were located in separate rooms to emulate a remote therapy session. PwD was seated in front of the hybrid face robot which was placed on the table. An external webcam was placed right under the robot to record PwD's expressions and gaze, which will be used for further analysis; video of the whole session was recorded to capture all human-robot interactions. In a separate room, a laptop was used by the clinician to remotely control the robot's facial expressions (see front-end control in **Figure 3**). The clinician spoke audio over a Bluetooth wireless microphone connected with the tablet running the robotic face to allow synchronization of the robot's mouth animation with the clinician's speech. The two-way verbal communication between PwD and clinician during cognitive engagement sessions took place via an additional phone call connection due to unreliable internet connectivity for smooth voice over IP. The mobile phone in PwD's room was placed out of sight behind the hybrid face robot as shown in **Figure 7** such that participants assumed the voice came from the robot (Wizard of Oz approach). This additional voice connection for two-way communication was required because the robot's ability to communicate autonomously could not be used, as the regional language in Chennai, India (Tamil) is not yet supported by the IVA. Furthermore, we aimed to provide clinicians with an alternative robotic platform to deliver meaningful cognitive engagement to PwD remotely, which may be of special utility in the COVID-19 era. However, our experimental approach is applicable to other scenarios where in-person meetings with clinicians are not feasible, necessary or desirable.

LMIC Pilot Testing in India

This study protocol: "Use of a Hybrid Face Humanoid Robot in Dementia Care: A preliminary study of feasibility and acceptability" was reviewed and approved by the Institutional Ethics Committee (IEC) of the Schizophrenia Research Foundation (SCARF) in Chennai, India. It was executed as a part of ongoing experiments conducted at Dementia Care (DEMCARES), a geriatric outpatient mental health service run by SCARF. All participants were required to provide informed consent before recruitment.

Cultural Acceptability and Emotion Recognition in Target Population

The acceptability and cultural appropriateness of the hybrid face robot was explored in South India through qualitative interviewing techniques, such as focus group discussions and in-depth interviews with people with dementia and caregivers, professionals with experience in dementia care, and robotics researchers. We present a user-centred procedure for successful introduction of the new affective robot in different cultures, which involves iterative adjustments based on a set of user studies with healthy older adults and people diagnosed with dementia. We further validate the robot and its facial representation of emotions specifically in the cultural context of South India.

We conducted a series of emotion recognition tasks with a total of N = 14 PwD and N = 26 healthy older adults to assess cultural appropriateness and recognition of robotic facial expressions in South India. Two types of emotion recognition tasks were used. Participants were first shown a sequence of culturally validated

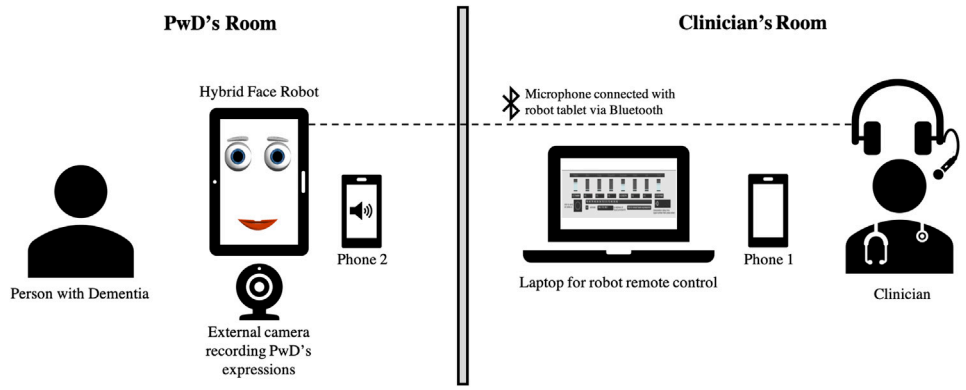

FIGURE 7 | Setup for using the hybrid face robot as a telemedicine interface to deliver cognitive engagement to PwD in the cultural context of South India. PwD's room includes: tablet with hybrid face robot, webcam to capture participant's emotions; Clinician's room includes: laptop with robot's control, Bluetooth wireless microphone; phone 1 and phone 2 were used to troubleshoot two-way voice communication.

pictures of Indian people displaying facial expressions (Mandal, 1987), corresponding to those simulated by the hybrid face robot (see **Figure 4**). After each emotion observed, participants selected the best match from the given list, following a forced-choice paradigm. Then, the same procedure was followed using the animated facial expressions displayed by the hybrid face robot. The recognition of robot's emotive responses was compared with the recognition of validated Indian photographs of the corresponding emotions for the two cohorts in India: healthy older citizens and people diagnosed with dementia.

Application of Hybrid Face Robot in Dementia Care

Finally, beyond use for social engagement with older adults, we wish to target feasibility of using the robotic platform as a telemedicine system to support mental health, dementia care, and eventually therapeutic intervention. As a basis for this utility, three repeated sessions of remote cognitive engagement using the hybrid face robot, of 30 min each, were conducted with a person with dementia [67 years, male, vascular dementia diagnosis, CDR rating 1 (mild) (Morris, 1991)] at SCARF in Chennai, India. The aim was twofold:

(1) Exploration of the feasibility of such robotic system to be used for cognitive engagement with PwD with regard to end-user acceptance and clinician ease-of-use.
(2) Test system infrastructure in clinical settings to troubleshoot potential technical problems, prior to planned trials and larger scale deployment beyond the COVID-19 pandemic.

The test infrastructure (Section *Designing Infrastructure*) was applied in a set of three robot-assisted cognitive engagement sessions to a person with dementia using the telemedicine interface. Beyond demonstrating the feasibility of the clinician-robot-patient interface in telemedicine for mental health in LMIC setting, we wish to generate initial data on the hybrid face robot as an engagement tool with PwD in the cultural context of South India. A Wizard of Oz approach was used during the three sessions. Hence, a clinician located in a separate room controlled the robot's range of facial expressions and spoke with the participant 'through' the robot (**Figure 7**). In a separate room, the participant was seated in front of the hybrid face robot. Interactions between the robot and participant included: presentation of the robot, discussion of newspaper articles, and listening to music. The following pre- and post-measures were used to understand the effect of robot-assisted cognitive engagement sessions on mood and engagement, respectively: the face scale (7-item modified version) (Lorish and Maisiak, 1986; Wada et al., 2005b) and the observational measure of engagement (OME) modified (Cohen-Mansfield et al., 2009), a tool to assess direct observations of engagement in people with dementia. The measures were observed by a trained nursing assistant who was present with the participant during experiments. This follows the standard technique described in (Cohen-Mansfield et al., 2009). Repeated sessions were used to acclimatize the participant to the robotic system and develop a level of familiarity. Together with the pre- and post-measures, this enabled a comprehensive comparison of user behavior and engagement in repeated human-robot sessions. After each session, qualitative feedback was collected from the person with dementia, the nursing assistant, caregiver, and clinician.

RESULTS

Findings of Human-Robot Interactions with Healthy Participants

Emotion Recognition

Table 2 shows the results obtained in a confusion matrix of expression recognition accuracies. The values on each row represent, for a single facial expression, the percentage of responses of the forced-choice. Results showed improved recognition rates compared to our past experiments [see (Bazo et al., 2010; Wairagkar et al., 2020)] All facial expressions showed high recognition rates above 70%. Participants perfectly identified the emotions for happy and tired. Disgusted and stern showed the

TABLE 2 | Expression confusion matrix for the hybrid face robot (% of total per presented expression). Bolded values indicate the % of correctly identified emotions.

	Happy	Stern	Angry	Disgusted	Surprised	Afraid	Sad	Tired
Happy	**100**	0	0	0	0	0	0	0
Stern	0	**73.3**	0	20	0	0	0	6.7
Angry	0	0	**93.3**	6.7	0	0	0	0
Disgusted	0	20	6.7	**73.3**	0	0	0	0
Surprised	0	0	0	0	**93.3**	6.7	0	0
Afraid	0	0	0	0	6.7	**86.7**	6.7	0
Sad	0	0	0	0	0	6.7	**93.3**	0
Tired	0	0	0	0	0	0	0	**100**

lowest recognition rates (73.3%) and were often confused between one another, which is in line with our past results. Notably, the recognition rate for disgusted rose from 18.4% (Bazo et al., 2010) to 73.3%. To a lesser degree, afraid was slightly confused with surprised and sad. Afraid shared the elevated eyebrows and opened eyelids of surprise, as well as the sparse downward-curving mouth of sad, which may explain the confusion. Nevertheless, recognition rates were high. In particular, afraid showed an increase to approximately double the recognition rate previously obtained, from 44% (Bazo et al., 2010) to 86.7%.

Qualitative data from interviews indicates the need to adjust some features for the happy expression to increase its likeability, namely increase the eyebrows' vertical height (B_{hl} and B_{hr}) and show an open mouth (increase M_t and M_b). Though the tired expression showed 100% recognition, participants reported some confusion with stern and disgusted, which can be due to their similarity of partially-closed eyelids and low eyebrows. Despite the added human features, participants' feedback indicated the addition of the faceplate was perceived unfavourably and the physical depth was poorly perceived. The majority (13 out of 15 participants) disliked the robot and its capacity to show facial expressions when the faceplate was added. We hypothesize our experiments lie on the downslope of the uncanny valley; at this negative gradient, an increase in human likeness (e.g., added faceplate) worsens the human response toward the robot as its partial human appearance moves toward the minimum in the valley. Adding the 3D faceplate to the robot's digital face appears in this context to induce a stronger uncanny valley effect, which we have considered in subsequent human-robot experiments.

User Experience of Multimodal Human-Robot Interactions

Results from UEQ analysis are shown in **Figure 8**. An overall positive impression of the multimodal robotic system by healthy participants is shown. On average, the novelty and stimulation aspects have received the most positive ratings. Notably, all respondents consistently considered the robot as a creative and inventive robotic platform (n1 and n2) and showed enthusiasm in having new interactions with the robot (s3). The attractiveness aspect showed positive responses. Particularly, 70% of respondents found the possibility to interact with voice extremely useful (a2). The lowest rate within this aspect corresponded to the robot's design (a3 with 20% neutral answers), which may suggest that our design choice of a simplistic robotic face (with only four facial features) is not sufficient to elicit trust and acceptability in HRI. Regarding questions about perspicuity, there was an overall easiness in interacting and getting familiar with the robot and 90% of participants found the robotic platform easy to use (p3). The efficiency aspect showed the less positive answers (e1, e2) and 20% of participants claimed difficulty identifying the emotion conveyed by the combination of robotic speech and facial expression. In post experimental interviews, all 10 participants reported a strong preference for the multimodal system over pure voice communication, which turned interactions and the overall user experience more "enthusiastic". Particularly, the robot's ability to adapt its animated facial representation of emotion in response to user speech in real-time stood out.

Cross-Cultural Pilot Testing

Cultural Acceptability and Emotion Recognition

We have investigated cultural acceptability and feasibility of using the hybrid face robot to support dementia care in India. The overall perception of stakeholders was positive. The preliminary indications are promising as the robot was considered a viable, low-cost and culturally appropriate tool to assist in clinical cognitive engagement with healthy older adults (healthy control—"HC") and PwD in India. Stakeholders concurred that the possibility of using a hybrid face robot for remote cognitive engagement can potentially help in meaningful engagement of people with dementia at home and also alleviate the perils of social isolation. Plans to deploy the robot as a remote platform to deliver regular cognitive engagement with more participants are underway. Ultimately, these findings suggest the use of this mechanically simple robotic platform for remote cognitive engagement may enhance mental health care and mitigate the impact of COVID-19 on people with dementia.

Emotion recognition experiments with healthy older adults and PwD aimed to assess cultural appropriateness of the hybrid face robot's simulated facial expressions. Recognition rates of human pictures were similarly high for PwD and HC for all emotions except for afraid, which was well recognized by HC but showed an accuracy below 50% for PwD. We found accuracies for all robot's simulated facial expressions were lower than expected (between 14 and 62%), with similar values for both PwD and HC. Afraid, angry and disgusted expressions showed the lowest accuracies (between 14 and 20%) for both testing cohorts. Emotions with subtle differences such as surprised and afraid

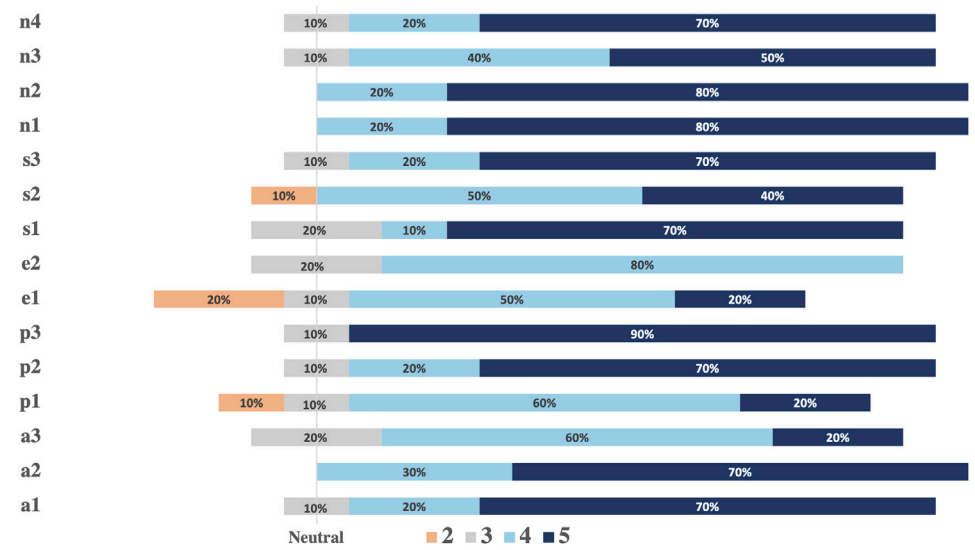

FIGURE 8 | Analysis of the user experience questionnaire. The vertical line marks neutral answers. All positive answers of the 5-point Likert scale are shown on the right with correspondent %. Negative answers and each % are shown on the left side.

were regularly transposed in user perception. The major difference between the two control groups was observed for the happy expression: double recognition value was obtained for HC. Hence, a discrepancy was observed between cultural recognition of human emotions vs. robotic simulated expressions, however both PwD and healthy older participants perceived the robot's facial representation of emotion comparably. Results from recognition of robot's simulated emotions in Chennai, India are in contrast to the high emotion recognition rates obtained with healthy, younger participants in the United Kingdom (Section *Emotion Recognition*). Recognition may show differences due to age, cultural context, and cognitive state. Hence, expressions of the hybrid face robot should be adapted accordingly for use in South India to maximize long-term user engagement and compliance.

Pilot Testing Remote Cognitive Engagement for Dementia Support

We piloted repeated sessions with one person diagnosed with dementia as a test of the infrastructure to deliver cognitive engagement in regular sessions. We investigated feasibility of using a mechanically simple, low-cost robotic platform as a robotic telemedicine system to support mental health, particularly in the cultural context of South India. The participant enjoyed interacting with the robot in all three sessions and his mood was rated "very happy" on the pre and post measures of the modified face scale before and after each session, respectively. As shown in **Table 3**, results from the OME showed a trend of longer duration of engagement with the robot from session 1 (9 min 35 s) to session 3 (18 min 1 s). The participant had no difficulty talking to the robot as assessed by OME "Talking to robot" measure, which received the highest possible score of engagement in all three sessions. Furthermore, the participant was never disruptive during any of the sessions as shown by the lowest possible score received on OME "Disruptive" measure (**Table 3**).

We identified the main areas of technical difficulties and potential improvements for the next planned trials: 1) network connection, which resulted in lags and distortion of voice during remote human-robot sessions; 2) dependency of same network for clinician and PwD; 3) problems in streaming music; 4) lack of a synthetically generated robot's voice instead of a recognizable human one, which may interfere with participants' acceptability of the robot. As observed by the nursing assistant, these technical issues often resulted in distraction, impacting participant's engagement, yet the advantages of robot-assisted cognitive engagement with PwD were acknowledged. The caregiver reported a positive impression of using the hybrid face robot as a telemedicine tool for cognitive engagement and perceived it

TABLE 3 | Results from the observational measure of engagement (OME) modified, which considered the following parameters to assess engagement during robot-assisted clinical sessions: participant's *attention* on a scale of 1 (very disruptive) to 7 (very attentive); *attitude* to stimulus rated on a scale of 1 (very negative) to 7 (very positive); *duration of engagement* (time until not interested); frequency rate, 0 (none) to 3 (most or all the session), of *talking to the robot*, *talking about the robot* with the nursing assistant, being *disruptive* or *distracted*. The measures were observed by a trained nursing assistant.

Measure		Session 1	Session 2	Session 3
Attention	Average	7	6	5
	Highest	7	7	7
Attitude	Average	4	4	3
	Highest	6	4	4
Duration of engagement		9 min 35 s	10 min 47 s	18 min 1 s
Talking to the robot		3	3	3
Talking about the robot		0	0	0
Disruptive		0	0	0
Distracted		0	1	2

as a technology to help with her husband's condition. The clinicians who conducted cognitive engagement sessions commented that the use of affective robotic platforms for engaging persons with dementia, who otherwise are unable to participate in many activities due to the restrictions imposed by pandemic scenarios, holds significant promise. Further work will be necessary to identify factors that will facilitate the use of robotic platforms as a means of telemedicine and develop methods to overcome potential barriers.

Overall, our results demonstrate remote cognitive engagement is feasible with PwD in India using the hybrid face robot as a telemedicine tool. The user-centred design and testing procedure followed with 14 PwD and 26 older adults interacting with the robot, in addition to repeated trials of remote cognitive engagement with one PwD through repeated sessions, provides a basis for deployment with larger participant cohorts. The robotic system may be used as an alternative platform to assist clinicians and support dementia care, which may be especially useful in times when social and medical support of PwD is limited, such as during and beyond the COVID-19 pandemic.

DISCUSSION

We have introduced a multimodal affective robotic framework to enhance engagement in HRI with capacity to deliver robotic telemedicine to support mental health and dementia care during and beyond the COVID-19 context. We summarize the main findings of the study, their implication for future research and larger scale telemedicine deployment. We also outline the limitations of our investigation and highlight future directions.

Summary of Findings

At a time of unprecedented overwhelming of global health systems in face of the COVID-19 outbreak, limited social and medical support is delivered to older adults and people living with dementia, who face greater isolation than ever before. Social robots hold significant promise to support mental health and may provide end-users with complementary assistance to stimulate interaction, alleviate anxiety and loneliness, in addition to reducing the caregiver burden, which is a critical need during and after the COVID-19 context. While user trust, complexity and expense of socially assistive robots is a challenge in any setting, we believe there is a larger gap of both resources and targeted research in LMICs. Cultural differences—which influence compliance—as well as technical challenges and cost need to be addressed. In this work, we make progress toward these challenges. In summary, contributions of this investigation include: 1) the robot's software design optimization; 2) emotion modeling; 3) integration of autonomous conversation capability; 4) testing of the multimodal robotic system with healthy participants in the United Kingdom; 5) validation of the modified robot and its telemedicine interface with older adults with and without dementia in the cultural context of South India.

Our study demonstrates feasibility and cultural appropriateness of robotic telemedicine for mental health support in India. One of the major findings of our study is that cultural adaptation of a social robot is critical—we propose a user-centred procedure that may be followed for successful introduction of a new affective robot in different cultural backgrounds, which involves iterative adjustments based on a set of validation experiments with target users (Section *Robotic Telemedicine for Mental Health Support*). The user-centred procedure followed with 14 PwD and 26 healthy older adults interacting with the robot in South India, in addition to a set of repeated cognitive engagement pilot sessions with one person with dementia, provides a strong foundation for subsequent clinical use.

Our approach for robotic affective communication offers novelty in its mechanically simple, low-cost and multimodal design. We propose it as clinically useful and culturally appropriate technology to deliver cognitive engagement for dementia support in LMICs, particularly in India. Therefore, this social robotic platform may result in a potential telemedicine solution for mental health support of vulnerable populations, not only in the COVID-19 era—which presents a unique opportunity to introduce the robotic system, bringing familiarity with the technology, which may enhance acceptability and compliance in the near future—but also in scenarios where in-person patient-clinician sessions are not logistically feasible or desirable.

Design Implication and Cultural Adaptation

We optimized the software design and control system of a hybrid face robot comprising an animated digital face that simulates facial expressions based on mathematical affect space emotion mapping with a 3D faceplate to convey realism and depth. This led to considerably higher emotion recognition accuracies than earlier implementations of this style of robot (Section *Emotion Recognition*). More specifically, accuracies above 90% were obtained for happy, tired, sad, angry, surprised and stern/disgusted robotic simulated facial expressions. When separated, stern and disgusted were occasionally mistaken for one another (70%+ accuracy overall) but were easily distinguishable from all other simulated emotions. Furthermore, we have ported the entire robotic system to an inexpensive tablet platform. This highlights the flexibility and adaptability in design of the hybrid face robot, which we have identified as a key feature for cultural usefulness in India. By integrating the robot's facial expressions with an autonomous conversational engine, we demonstrated real-time adaptable emotion of the robot in response to users' speech in HRI experiments with healthy participants in the United Kingdom. Although participants did not interact with the robot with different modalities (i.e., speech with and without integration of the robotic expressive face), there was a strong user preference for multimodal over pure voice communication.

To understand the cultural differences in recognition of robot's simulated emotions, we conducted a series of expression recognition tasks with PwD and healthy older citizens in South India. Despite the increased recognition accuracies obtained from younger participants in the United Kingdom, we observed lower recognition rates for all facial expressions simulated by the robot in India. One potential explanation is the fact that young participants might be more

familiar with robotic faces and digital characters, such as emoticons, than older adults tested in India. These findings are very intriguing as a basis for direct comparison between cultural perception of affective emotion. Testing on a wider cohort with parallel controls on subject age, experience with interactive technologies, and possibly education represents a very promising area for future work. In our experiments, we further observed differences between healthy older adults and PwD in India were marginal except for the happy expression, for which double recognition was obtained for the healthy control group. These results inform the cultural acceptability of the robot. As PwD are from the same culture, this allows us to infer that problems with acceptability are unlikely due to the cultural influences but rather due to the effects of cognitive impairment in dementia. Regardless of the current precision of facial expression recognition, stakeholders were positively disposed toward using the robot.

Although further investigation is needed, these studies suggest that emotion recognition of affective robots and the overall effectiveness of HRI are influenced by culture, age, cognitive ability and familiarity with similar technologies. We argue the expressiveness of social robots must be adapted to the culture they will be deployed to following a user-centred and iterative approach to ensure effectiveness, user acceptability and compliance.

Robotic Telemedicine Beyond COVID-19

While our investigation of human-robot multimodal interactions with healthy participants in the United Kingdom yielded promising results, the AI voice system would need to support regional languages for fully autonomous use in India. Hence, we have designed an alternative test infrastructure to deploy the hybrid face robot as a telemedicine interface to deliver cognitive engagement in regular sessions (Section *Designing Infrastructure*). In our set of user-centred validation studies, including focus group discussions with stakeholders and emotion recognition experiments with 14 PwD and 26 healthy older adults, we identified the hybrid face robot as a feasible, culturally appropriate, and low-cost telemedicine system to support mental health in India. Additionally, we have piloted repeated sessions with one person with dementia as a test of the infrastructure to deliver cognitive engagement in regular sessions. Finally, we have proposed a protocol to introduce the robot for use with PwD and acclimatize the participant to the robot which, through repeated sessions, was received favourably by the participant in experiments, paving the way for further use.

We argue remote cognitive engagement assisted by such robotic platform is feasible with PwD in the cultural context of South India. We observed a trend of increased duration of engagement with the robot from the first to last session, and no alterations in PwD's mood before and after each session. Positive feedback was obtained from the caregiver and clinician present in robot-assisted sessions. Particularly, the clinician indicated strong promise in using social robotic platforms as a means of telemedicine for dementia support; the caregiver also perceived the robot as a technological tool to help with her husband's condition. As no similar study has been previously conducted in the literature, this work may provide useful insights into testing and adjusting a hybrid social robot for cognitive engagement with PwD in the cultural context of India and lay the foundation for future telemedicine deployment. This technology may be of special utility, but not limited to dementia support in the COVID-19 era. While the system could be used for other psychological disorders, we wish to establish some veracity through dementia and mental health support of older adults, who are facing more isolation than ever before.

Limitations and Future Work

Limitations of the AI conversational system integration were acknowledged pointing toward the need for a more natural and unstructured dialogue, and adaptation for mental health applications, e.g., to guide cognitive stimulation therapies for older individuals and PwD. One potential way of increasing trust and acceptability of the AI voice system among the target population is to include different voices and speaking styles. Future improvements of the system architecture should include more training data, i.e., intents, entities and context variables, in the attempt to step beyond a conversational flow. This is a common drawback of existing dialogue systems (Fitzpatrick et al., 2017; Harms et al., 2018). Nevertheless, great efforts are being made in this promising research field to create natural 'human-like' conversations (Harms et al., 2018; Griol et al., 2019)[6], including the exploration of conversational robots and voice-based systems for supporting cognitive impaired individuals (Cruz-Sandoval et al., 2020; Pou-Prom et al., 2020; Salichs et al., 2020). A possibility for future work is to use the camera of the tablet PC running the robot's software to automatically recognize user emotions. A thorough analysis combining emotion detected from camera, speech and natural language processing could ultimately allow the robot to sense the user's mood, behavior and personality traits and adapt its response (verbal and nonverbal) in the most appropriate way based on that multimodal feedback, in real-time. Future studies may also use machine learning to adapt behavior to each user over time, which is key for long-term compliance.

One fundamental limitation of the pilot study conducted in India using the robotic telemedicine interface was that only one person with dementia participated. These experiments were logistically very challenging; one of the major drawbacks identified was the screening of patients due to the resources and time available. The main limitation of the experimental setup created for remote cognitive engagement (Section *Designing Infrastructure*) is that both PwD and clinician are required to be connected to the same internet network. We identified lags and distortion of voice during remote clinical sessions as the main technical issue to solve for next trials, in order to ensure maximum engagement. Although the nursing assistant indicated distraction of PwD when technical issues occurred, the participant was overall attentive and enjoyed interacting with the robot. Future experiments could quantify engagement with the robot, with more participants, different types and stages of

[6]https://www.research.ibm.com/artificial-intelligence/project-debater/

dementia. Furthermore, for a more direct and rigorous assessment of cultural differences in recognition of robot's simulated emotions, stricter controls would be needed for subject age, experience with interactive technologies, and cognitive ability. Education level of participants, which may impact acceptability and compliance, could also be used as a metric to be monitored in larger testing cohorts. Future clinical trials and wider deployment could also include end-user training sessions to fully judge the system capability, which may improve its performance.

Finally, aiming to improve robustness, ease of use, availability and scalability of the current system, we have also developed a mobile app working in a similar fashion to the hybrid face robot, as a digital affective robotic platform. Our new mobile-based face robot will allow communication between clinicians and PwD via mobile, without restrictions on location. Even in its current form, our robotic framework provides a more accessible tool to deliver cognitive engagement in LMICs, with potential for positive impact in mental health and dementia care, during and beyond the COVID-19 pandemic. Plans for deployment in India are underway, specifically through robot-assisted telemedicine sessions with older adults and PwD.

CONCLUSION

The major contributions of this paper are the development, implementation and pilot testing of a multimodal robotic framework that emotionally interacts through facial expressions and speech to enhance engagement in human-robot interactions. We qualitatively identified the benefits in user engagement of multimodal vs. pure voice communication. We modified this robot further to provide clinicians with a telemedicine interface to deliver regular cognitive engagement, which may be of great utility during and beyond the COVID-19 era. We followed a user-centred design of the robot to ensure it meets the cost constraints and ease of use demands for utility in LMICs, in addition to cultural acceptability. We found cultural validation of a social robot is paramount and introduced a procedure that may inform future studies for engaging human-robot interactions in local cultures. We successfully introduced the modified hybrid face robot into practice for dementia support in LMICs through a pilot study. Results revealed robot-assisted cognitive engagement sessions are feasible in India (and more broadly LMICs), and a trend of longer duration of engagement with the robot was observed through our protocol to introduce the robot to people with dementia in the cultural context of South India. Moreover, clinicians, PwD and caregivers indicated strong promise in the use of this social robotic platform as a means of telemedicine for dementia support in India. Hence, we propose it as an alternative or complementary technological solution to deliver cognitive engagement and enhanced mental health support to older citizens or PwD, during and beyond COVID-19. Plans for deployment in telemedicine sessions specifically motivated by the pandemic are currently underway.

DATA AVAILABILITY STATEMENT

The original contributions presented in the study are included in the article, further inquiries can be directed to the corresponding author.

ETHICS STATEMENT

The studies involving human participants were reviewed and approved by the Imperial College London Science, Engineering and Technology Research Ethics Committee (SETREC) and the Schizophrenia Research Foundation (SCARF), Chennai, India. This study protocol: "Use of a Hybrid Face Humanoid Robot in Dementia Care: A preliminary study of feasibility and acceptability" was reviewed and approved by the Institutional Ethics Committee of the SCARF in Chennai, India. It was executed as a part of ongoing experiments conducted at Dementia care (DEMCARES), a geriatric outpatient mental health service run by the SCARF, with the approval granted on 26 Jan 2019. The patients/participants provided their written informed consent to participate in this study.

AUTHOR CONTRIBUTIONS

ML designed, developed, and implemented the robotic system, analyzed and interpreted data, and drafted the presented work. ML, MW, and NN developed the robot's infrastructure for experiments conducted in India. MW contributed to the conceptualization of the system and revised the manuscript critically. NN carried out experiments at SCARF, analyzed clinical data, and revised the work for clinical content. SV developed the concept, planned trials, and revised the work critically for clinical merit. RV developed the concept, drove the focus of this research, revised the work critically for intellectual content, and revised the manuscript. All authors read and gave final approval of the submitted manuscript.

FUNDING

This work was supported by Research England Grand Challenge Research Fund (GCRF) through Imperial College London, the Dementia Research Institute Care Research & Technology Center (DRI-CRT) (UKDRI-7003), the Imperial College London's President's PhD Scholarships, and the United Kingdom MedTech SuperConnector (MTSC).

ACKNOWLEDGMENTS

We thank all participants involved in the evaluation of human-robot interactions, both at Imperial College London and SCARF India. We thank Professor Suresh Devasahayam and team from the Christian Medical College, Vellore (CMC) for the valuable feedback when designing experiments to be conducted in India.

REFERENCES

Abdi, J., Al-Hindawi, A., Ng, T., and Vizcaychipi, M. P. (2018). Scoping review on the use of socially assistive robot technology in elderly care. *BMJ Open* 8, e018815. doi:10.1136/bmjopen-2017-018815

Abdollahi, H., Mollahosseini, A., Lane, J. T., and Mahoor, M. H. (2017). "A pilot study on using an intelligent life-like robot as a companion for elderly individuals with dementia and depression," in 2017 IEEE-RAS 17th international conference on humanoid robotics (Humanoids), Birmingham, United Kingdom, November 15–17, 2017 (United Kingdom: IEEE), 541–546.

Agüera-Ortiz, L., Pérez, R., Ruiz, F., and Jm, C. P. (2015). Social robots in advanced dementia. *Front. Aging Neurosci.* 7, 133. doi:10.3389/fnagi.2015.00133

Alzheimer's Disease International (2019). World alzheimer report 2019 attitudes to dementia. Available at: https://www.alz.co.uk/research/WorldAlzheimerReport2019.pdf (Accessed September 1 2020)

Bainbridge, W. A., Hart, J. W., Kim, E. S., and Scassellati, B. (2011). The benefits of interactions with physically present robots over video-displayed agents. *Int. J. Soc. Robotics* 3, 41–52. doi:10.1007/s12369-010-0082-7

Bazo, D., Vaidyanathan, R., Lentz, A., and Melhuish, C. (2010). "Design and testing of a hybrid expressive face for a humanoid robot," in 2010 IEEE/RSJ international conference on intelligent robots and systems, Taipei, Taiwan, October 18–22, 2010, 5317–5322.

Boone, H. N., and Boone, D. A. (2012). Analyzing likert data. *J. extension* 50, 1–5.

Breazeal, C. (2003). Emotion and sociable humanoid robots. *Int. J. human-computer Stud.* 59, 119–155. doi:10.1016/s1071-5819(03)00018-1

Breazeal, C. (2009). Role of expressive behaviour for robots that learn from people. *Phil. Trans. R. Soc. B* 364, 3527–3538. doi:10.1098/rstb.2009.0157

Chozas, A. C., Memeti, S., and Pllana, S. (2017). Using cognitive computing for learning parallel programming: an IBM Watson solution. *Procedia Comput. Sci.* 108, 2121–2130. doi:10.1016/j.procs.2017.05.187

Ciechanowski, L., Przegalinska, A., Magnuski, M., and Gloor, P. (2019). In the shades of the uncanny valley: an experimental study of human–chatbot interaction. *Future Generation Comp. Syst.* 92, 539–548. doi:10.1016/j.future.2018.01.055

Clabaugh, C., and Matarić, M. (2019). Escaping oz: autonomy in socially assistive robotics. *Annu. Rev. Control. Robot. Auton. Syst.* 2, 33–61. doi:10.1146/annurev-control-060117-104911

Cohen-Mansfield, J., Dakheel-Ali, M., and Marx, M. S. (2009). Engagement in persons with dementia: the concept and its measurement. *Am. J. Geriatr. Psychiatry* 17, 299–307. doi:10.1097/jgp.0b013e31818f3a52

Craig, R., Vaidyanathan, R., James, C., and Melhuish, C. (2010). "Assessment of human response to robot facial expressions through visual evoked potentials," in 2010 10th IEEE-RAS international conference on humanoid robots, Nashville, TN, December 6–8, 2010 (IEEE), 647–652.

Cruz-Sandoval, D., and Favela, J. (2016). "Human-robot interaction to deal with problematic behaviors from people with dementia," in Proceedings of the 10th EAI international conference on pervasive computing technologies for healthcare, Cancun, Mexico, May 16–19, 2016 (ICST Institute for Computer Sciences, Social-Informatics and Telecommunications Engineering). doi:10.4108/eai.16-5-2016.2263873

Cruz-Sandoval, D., Morales-Tellez, A., Sandoval, E. B., and Favela, J. (2020). "A social robot as therapy facilitator in interventions to deal with dementia-related behavioral symptoms," in Proceedings of the 2020 ACM/IEEE international conference on human-robot interaction, Cambridge, March 23–26, 2020, 161–169.

Di Nuovo, A., Varrasi, S., Lucas, A., Conti, D., Mcnamara, J., and Soranzo, A. (2019). *Assessment of cognitive skills via human-robot interaction and cloud computing*. Berlin, Germany: Springer

Dias, A., and Patel, V. (2009). Closing the treatment gap for dementia in India. *Indian J. Psychiatry* 51, 93–97.

Donato, G., Bartlett, M. S., Hager, J. C., Ekman, P., and Sejnowski, T. J. (1999). Classifying facial actions. *IEEE Trans. Pattern Anal. Machine Intell.* 21, 974–989. doi:10.1109/34.799905

Falck, F., Doshi, S., Tormento, M., Nersisyan, G., Smuts, N., Lingi, J., et al. (2020). Robot DE NIRO: a human-centered, autonomous, mobile research platform for cognitively-enhanced manipulation. *Front. Robotics AI* 7, 66. doi:10.3389/frobt.2020.00066

Fitzpatrick, K. K., Darcy, A., and Vierhile, M. (2017). Delivering cognitive behavior therapy to young adults with symptoms of depression and anxiety using a fully automated conversational agent (Woebot): a randomized controlled trial. *JMIR Ment. Health* 4, e19. doi:10.2196/mental.7785

Fong, T., Nourbakhsh, I., and Dautenhahn, K. (2003). A survey of socially interactive robots. *Robotics autonomous Syst.* 42, 143–166. doi:10.1016/s0921-8890(02)00372-x

Ghazali, A. S., Ham, J., Barakova, E. I., and Markopoulos, P. (2018). Effects of robot facial characteristics and gender in persuasive human-robot interaction. *Front. Robotics AI* 5, 73. doi:10.3389/frobt.2018.00073

Griol, D., Sanchis, A., Molina, J. M., and Callejas, Z. (2019). Developing enhanced conversational agents for social virtual worlds. *Neurocomputing* 354, 27–40. doi:10.1016/j.neucom.2018.09.099

Harms, J.-G., Kucherbaev, P., Bozzon, A., and Houben, G.-J. (2018). Approaches for dialog management in conversational agents. *IEEE Internet Comput.* 23, 13–22. doi:10.1109/mic.2018.2881519

Inoue, K., Wada, K., and Ito, Y. (2012). "Effective application of Paro: seal type robots for disabled people in according to ideas of occupational therapists," in *Computers helping people with special needs. ICCHP 2008. Lecture notes in computer science*. Editors K. Miesenberger, J. Klaus, W. Zagler, and A. Karshmer (Berlin, Germany: Springer), 1321–1324.

Inoue, T., Nihei, M., Narita, T., Onoda, M., Ishiwata, R., Mamiya, I., et al. (2011). Field-based development of an information support robot for persons with dementia. *Everyday Tech. Independence Care* 29, 534–541.

Joranson, N., Pedersen, I., Rokstad, A. M., and Ihlebaek, C. (2015). Effects on symptoms of agitation and depression in persons with dementia participating in robot-assisted activity: a cluster-randomized controlled trial. *J. Am. Med. Dir. Assoc.* 16, 867–873. doi:10.1016/j.jamda.2015.05.002

Laranjo, L., Dunn, A. G., Tong, H. L., Kocaballi, A. B., Chen, J., Bashir, R., et al. (2018). Conversational agents in healthcare: a systematic review. *J. Am. Med. Inform. Assoc.* 25, 1248–1258. doi:10.1093/jamia/ocy072

Libin, A., and Cohen-Mansfield, J. (2004). Therapeutic robocat for nursing home residents with dementia: preliminary inquiry. *Am. J. Alzheimers Dis. Other Demen.* 19, 111–116. doi:10.1177/153331750401900209

Lorish, C. D., and Maisiak, R. (1986). The face scale: a brief, nonverbal method for assessing patient mood. *Arthritis Rheum.* 29, 906–909. doi:10.1002/art.1780290714

Mandal, M. K. (1987). Decoding of facial emotions, in terms of expressiveness, by schizophrenics and depressives. *Psychiatry* 50, 371–376. doi:10.1080/00332747.1987.11024368

Martín, F., Agüero, C. E., Cañas, J. M., Valenti, M., and Martínez-Martín, P. (2013). Robotherapy with dementia patients. *Int. J. Adv. Robotic Syst.* 10, 10. doi:10.5772/54765

Mehra, A., and Grover, S. (2020). COVID-19: a crisis for people with dementia. *J. Geriatr. Ment. Health* 7, 1. doi:10.4103/jgmh.jgmh_6_20

Memeti, S., and Pllana, S. (2018). PAPA: a parallel programming assistant powered by IBM Watson cognitive computing technology. *J. Comput. Sci.* 26, 275–284. doi:10.1016/j.jocs.2018.01.001

Merdivan, E., Singh, D., Holzinger, A., Merdivan, E., Hanke, S., and Holzinger, A. (2019). Dialogue systems for intelligent human computer interactions MAKEpatho-machine learning and knowledge extraction for digital pathology view project memento view project sten hanke fachhochschule joanneum. *Electron. Notes Theor. Comput. Sci.* 343, 57–71. doi:10.1016/j.entcs.2019.04.010

Miner, A. S., Laranjo, L., and Kocaballi, A. B. (2020). Chatbots in the fight against the COVID-19 pandemic. *NPJ Digital Med.* 3, 1–4. doi:10.1038/s41746-020-0280-0

Miner, A. S., Milstein, A., Schueller, S., Hegde, R., Mangurian, C., and Linos, E. (2016). Smartphone-based conversational agents and responses to questions about mental health, interpersonal violence, and physical health. *JAMA Intern. Med.* 176, 619–625. doi:10.1001/jamainternmed.2016.0400

Mordoch, E., Osterreicher, A., Guse, L., Roger, K., and Thompson, G. (2013). Use of social commitment robots in the care of elderly people with dementia: a literature review. *Maturitas* 74, 14–20. doi:10.1016/j.maturitas.2012.10.015

Mori, M., Macdorman, K. F., and Kageki, N. (2012). The uncanny valley [from the field]. *IEEE Robot. Automat. Mag.* 19, 98–100. doi:10.1109/mra.2012.2192811

Morris, J. C. (1991). The clinical dementia rating (CDR): current version and. *Young* 41, 1588–1592.

Moyle, W., Jones, C. J., Murfield, J. E., Thalib, L., Beattie, E. R. A., Shum, D. K. H., et al. (2017). Use of a robotic seal as a therapeutic tool to improve dementia symptoms: a cluster-randomized controlled trial. *J. Am. Med. Dir. Assoc.* 18, 766–773. doi:10.1016/j.jamda.2017.03.018

Natarajan, N., Vaitheswaran, S., De Lima, M. R., Wairagkar, M., and Vaidyanathan, R. (2019). P4-630: use of a hybrid face robot in dementia care: understanding feasibility in India. *Alzheimer's Demen.* 15, P1569. doi:10.1016/j.jalz.2019.08.179

Novoa, J., Wuth, J., Escudero, J. P., Fredes, J., Mahu, R., and Yoma, N. B. (2018). *DNN-HMM based automatic speech recognition for HRI scenarios*. Tokyo, Japan: IEEE Computer Society

Petersen, S., Houston, S., Qin, H., Tague, C., and Studley, J. (2017). The utilization of robotic pets in dementia care. *J. Alzheimers Dis.* 55, 569–574. doi:10.3233/JAD-160703

Portugal, D., Alvito, P., Christodoulou, E., Samaras, G., and Dias, J. (2019). A study on the deployment of a service robot in an elderly care center. *Int. J. Soc. Robotics* 11, 317–341. doi:10.1007/s12369-018-0492-5

Pou-Prom, C., Raimondo, S., and Rudzicz, F. (2020). A conversational robot for older adults with alzheimer's Disease. *J. Hum.-Robot Interact.* 9, 1–25. doi:10.1145/3380785

Prince, M., Guerchet, M., and Prina, M. (2013). Policy brief: the global impact of dementia 2013–2050. *Alzheimer's Dis. Int.* 28 (7), 728–737.

Prince, M., Livingston, G., and Katona, C. (2007). Mental health care for the elderly in low-income countries: a health systems approach. *World Psychiatry* 6, 5–13.

Romero, O. J., Zhao, R., and Cassell, J. (2017). "Cognitive-inspired conversational-strategy reasoner for socially-aware agents," in 2017 International joint conference on artificial intelligence, Melbourne, VIC, August 19–25, 2017, 3807–3813. doi:10.24963/ijcai.2017/532

Rouaix, N., Retru-Chavastel, L., Rigaud, A. S., Monnet, C., Lenoir, H., and Pino, M. (2017). Affective and engagement issues in the conception and assessment of a robot-assisted psychomotor therapy for persons with dementia. *Front. Psychol.* 8, 950. doi:10.3389/fpsyg.2017.00950

Salichs, M. A., Castro-González, Á., Salichs, E., Fernández-Rodicio, E., Maroto-Gómez, M., Gamboa-Montero, J. J., et al. (2020). Mini: a new social robot for the elderly. *Int. J. Soc. Robotics* 18, 1–19. doi:10.1007/s12369-020-00687-0

Schiano, D. J., Ehrlich, S. M., Rahardja, K., and Sheridan, K. (2000). "Face to interface: facial affect in (hu) man and machine," in Proceedings of the SIGCHI conference on human factors in computing systems, Netherlands, April, 2000, 193–200.

Schrepp, M. (2015). User experience questionnaire handbook. *All You Need To Know To Apply The UEQ Successfully In Your Project* 86, 105. doi:10.13140/RG.2.1.2815.0245

Sezgin, E., Huang, Y., Ramtekkar, U., and Lin, S. (2020). Readiness for voice assistants to support healthcare delivery during a health crisis and pandemic. *NPJ Digital Med.* 3, 1–4. doi:10.1038/s41746-020-00332-0

Shaji, K. S., Jotheeswaran, A. T., Girish, N., Bharath, S., Dias, A., and Pattabiraman, M. (2010). The dementia India report: prevalence, impact, costs and services for dementia. *Alzheimer's Relat. Disord. Soc. India* 60, 44–52.

Tamura, T., Yonemitsu, S., Itoh, A., Oikawa, D., Kawakami, A., Higashi, Y., et al. (2004). Is an entertainment robot useful in the care of elderly people with severe dementia? *J. Gerontol. A. Biol. Sci. Med. Sci.* 59, 83–85. doi:10.1093/gerona/59.1.m83

Tapus, A., Mataric, M. J., and Scassellati, B. (2007). Socially assistive robotics [Grand challenges of robotics]. *IEEE Rob. Autom. Mag.* 14 (1), 35–42. doi:10.1109/mra.2007.339605

Tapus, A., Tapus, C., and Mataric, M. J. (2009). "The use of socially assistive robots in the design of intelligent cognitive therapies for people with dementia," in 2009 IEEE international conference on rehabilitation robotics, Kyoto, Japan, June 23–26, 2009 (IEEE), 924–929.

Vaitheswaran, S., Lakshminarayanan, M., Ramanujam, V., Sargunan, S., and Venkatesan, S. (2020). Experiences and needs of caregivers of persons with dementia in India during the COVID-19 pandemic—a qualitative study. *Am. J. Geriatr. Psychiatry* 28 (11), 1185–1194. doi:10.1016/j.jagp.2020.06.026

Valenti Soler, M., Aguera-Ortiz, L., Olazaran Rodriguez, J., Mendoza Rebolledo, C., Perez Munoz, A., Rodriguez Perez, I., et al. (2015). Social robots in advanced dementia. *Front. Aging Neurosci.* 7, 133. doi:10.3389/fnagi.2015.00133

Van Maris, A., Zook, N., Caleb-Solly, P., Studley, M., Winfield, A., and Dogramadzi, S. (2020). Designing ethical social robots-A longitudinal field study with older adults. *Front. Robotics AI* 7, 1. doi:10.3389/frobt.2020.00001

Van Patten, R., Keller, A. V., Maye, J. E., Jeste, D. V., Depp, C., Riek, L. D., et al. (2020). Home-based cognitively assistive robots: maximizing cognitive functioning and maintaining independence in older adults without dementia. *CIA* 15, 1129. doi:10.2147/cia.s253236

Wada, K., and Shibata, T. (2007). Living with seal robots—its sociopsychological and physiological influences on the elderly at a care house. *IEEE Trans. Robot.* 23, 972–980. doi:10.1109/tro.2007.906261

Wada, K., Shibata, T., Musha, T., and Kimura, S. (2005a). "Effects of robot therapy for demented patients evaluated by EEG," in 2005 IEEE/RSJ international conference on intelligent robots and systems, Edmonton, AB, August 2–6, 2005, 1552–1557.

Wada, K., Shibata, T., Saito, T., Sakamoto, K., and Tanie, K. (2005b). "Psychological and social effects of one year robot assisted activity on elderly people at a health service facility for the aged," in Proceedings of the 2005 IEEE international conference on robotics and automation, Barcelona, Spain, August 2–6, 2005 (IEEE), 2785–2790.

Wainer, J., Feil-Seifer, D. J., Shell, D. A., and Mataric, M. J. (2006). The role of physical embodiment in human-robot interaction," in ROMAN 2006-The 15th IEEE International Symposium on Robot and Human Interactive Communication, Hatfield, United Kingdom, September 6–8, 2006, (IEEE), 117–122.

Wairagkar, M., Lima, M. R., Bazo, D., Craig, R., Weissbart, H., Etoundi, A. C., et al. (2020). Emotive response to a hybrid-face robot and translation to consumer social robots. arXiv preprint arXiv:2012.04511

Walker, P. G. T., Whittaker, C., Watson, O. J., Baguelin, M., Winskill, P., Hamlet, A., et al. (2020). The impact of COVID-19 and strategies for mitigation and suppression in low- and middle-income countries. *Science* 369, 413–412. doi:10.1126/science.abc0035

Wang, H., Li, T., Barbarino, P., Gauthier, S., Brodaty, H., Molinuevo, J. L., et al. (2020). Dementia care during COVID-19. *The Lancet* 395, 1190–1191. doi:10.1016/s0140-6736(20)30755-8

Weizenbaum, J. (1966). ELIZA—a computer program for the study of natural language communication between man and machine. *Commun. ACM* 9, 36–45. doi:10.1145/365153.365168

Wolters, M. K., Kelly, F., Kilgour, J., and Kilgour, J. (2016). *Designing a spoken dialogue interface to an intelligent cognitive assistant for people with dementia*. Newbury Park, CA: SAGE Publications Ltd.

Conflict of Interest: The authors declare that the research was conducted in the absence of any commercial or financial relationships that could be construed as a potential conflict of interest.

frontiers in Robotics and AI

PERSPECTIVE
published: 25 March 2021
doi: 10.3389/frobt.2021.617426

Covid, AI, and Robotics—A Neurologist's Perspective

*Syed Nizamuddin Ahmed**

Division of Neurology, Department of Medicine, University of Alberta, Edmonton, AB, Canada

Two of the major revolutions of this century are the Artificial Intelligence and Robotics. These technologies are penetrating through all disciplines and faculties at a very rapid pace. The application of these technologies in medicine, specifically in the context of Covid 19 is paramount. This article briefly reviews the commonly applied protocols in the Health Care System and provides a perspective in improving the efficiency and effectiveness of the current system. This article is not meant to provide a literature review of the current technology but rather provides a personal perspective of the author regarding what could happen in the ideal situation.

Keywords: artificial intelligence, robotics, COVID-19, telemedicine, neurology, AI, neurologist

OPEN ACCESS

Edited by:
S. Farokh Atashzar, New York University, United States

Reviewed by:
Yunze Zeng, Robert Bosch, United States
Alexandru Burlacu, Grigore T. Popa University of Medicine and Pharmacy, Romania

***Correspondence:**
Syed Nizamuddin Ahmed
snahmed@ualberta.ca

Specialty section:
This article was submitted to Biomedical Robotics, a section of the journal Frontiers in Robotics and AI

Received: *14 October 2020*
Accepted: *03 March 2021*
Published: *25 March 2021*

Citation:
Ahmed SN (2021) Covid, AI, and Robotics—A Neurologist's Perspective. Front. Robot. AI 8:617426. doi: 10.3389/frobt.2021.617426

INTRODUCTION

Despite being one of the best healthcare systems in the world, our healthcare system is still highly inefficient, suboptimal, and redundant. From the time a person enters the hospital to the time he gets discharged, inefficiencies can be noted at every nook and corner. These inefficiencies lead to poor patient care, creation of scut work for the caregivers, poor infection control, guess work in medical management, inaccuracies in test reporting, waste of resources and very poor judgement when it comes to spending the health care dollars.

If the working machinery is of poor quality, no matter how good an operator you hire, the productivity of the machines will still be as good as the machinery employed. Unfortunately, this applies to the health care system not only in Canada but around the world. Instead of changing the machinery we keep replacing the operators. That's the big reason we have not been able to revolutionize health care. All we have kept doing is presenting the same machines in newer and more attractive packaging. The machines are still the same.

Case Study

Let me start with a story. This is not a real story but brings you very close to reality. This is the story of so many patients that I see in the hospital. Being a neurologist, I will mold the story to fit a patient coming in for a neurological condition. For the understanding of the lay public let's start with a diagnosis familiar to most people—a seizure. So, this is the story of a patient who presents to the hospital with a new onset seizure.

Case Review

Nora's husband got woken up at 2 a.m. on July 29th, 2020 when he heard "a deep scream" and found that Nora was convulsing, foaming from her mouth and unresponsive. She appeared gray and started breathing heavily. He called 911. Emergency Medical Team (EMT) were there within 10 min and after providing urgent care took her to the nearest emergency room. Nora was awake but somewhat disoriented by the time she arrived at the emergency room. She was triaged within 10 min but waited for another 2 h before seeing a physician. She followed simple commands, but

her husband said that she was still "off and not back to the baseline." The doctor from the rural emergency room called the neurologist on call who suggested a computerized tomography (CT) scan of the head, a spinal tap and a load of 1,000 mg of intravenous Phenytoin. CT scan was done after 2 h followed by the spinal tap. It was 4 p.m. the next day before the tests results were available and reported normal. Nora had another witnessed seizure. The emergency room (ER) physician loaded her with another 500 mg of Phenytoin and transferred her to the University Hospital. Patient was seen within an hour by the casualty officer (CO). She did not seem to have any obvious seizures. Neurology resident was consulted at 11 p.m. the next day and completed the consult by midnight the following morning.

Patient was reviewed by the staff neurologist the following morning. Although she was awake and partially responsive, she was still confused and disoriented. An urgent electroencephalogram (EEG) was requested which showed that the patient was in non-convulsive status epilepticus. At this time the patient was given an extra load of Phenytoin and the intensive care unit (ICU) ICU team was consulted. EEG was still running and showed recurrent electrographic seizures. Patient was given a load of Propofol and admitted to ICU. Since there were no respiratory symptoms and the chest Xray was normal she was not isolated. Blood was sent for CBC, LFTs, COVID PCR, CRP, and electrolytes. An MRI was requested for the morning. The COVID test came back positive. The neurologist, neurology resident and five other medical house staff were asked to self-isolate for the next 14 days due to exposure to a patient who tested positive for Covid.

The next day Propofol was tapered off and Nora was alert and oriented. She stayed in the hospital for an additional 4 days. During the hospital stay she got daily CBC and electrolytes, vital signs and neurochecks were done twice a day, she had two additional chest x-rays in the context of the positive COVID. Her MRI came back normal. On a daily basis she was seen by her nurses every shift, seen by the neurology resident and staff, met personnel from the dietary service who provided the food, and was once evaluated by the physiotherapy service. She was finally discharged on August 6th with instructions about safety and driving and a follow-up by a neurologist in 3 months.

While writing the above case I have significantly simplified the course taken by a usual patient. A typical patient will go through a way more tedious process to get the above care and typically significantly more health resources are used to provide the above care. Now before I share my thoughts on how to improve the status quo I invite the reader to pause right here and write down a list of changes they would like to see in the care of this patient. I specifically suggest imagining the applications of artificial intelligence and robotics not only because of the new reality of Covid but also to better streamline the healthcare system, optimize health delivery, ensure safety of the health providers and best use of all the information collected on this patient.

DISCUSSION

As I look at this case and hundreds of cases that are triaged, investigated and managed all over the country on a daily basis, I ponder "if things could be different" had we used artificial intelligence, machine learning, and robotics much more wisely. Let me be more specific. We cannot improve a system if we are unable to measure the success of that system. The definition of success is a philosophical one and in general success is defined as success based on the community norms. For our healthcare system, in-part, I define success of a system based on whether the following quantitative and qualitative outcomes are achieved:

1. Reducing morbidity and mortality related to specific diagnosis.
2. Reducing healthcare costs within affordable budgets.
3. Patient and family satisfaction.
4. Sustainability of the system.
5. Reducing wait times.

A paradigm shift in health delivery requires resources, and resources can come from proper budgeting. For long term benefits we will have to start thinking about the cumulative costs over decades rather than getting overwhelmed by instantaneous expenses. In the following few paragraphs, I would like to present an alternative to the current model and propose that such a change can make our healthcare system significantly more efficient and effective. Please be mindful that due to space and time constraints, I have significantly abbreviated and simplified my suggestions and thoughts.

HOME HEALTH MONITORS/PERSONALIZED MEDICAL ROBOTS

Compact devices could easily be designed, where a single device monitors your blood pressure, heart rate, blood glucose, reads and reports your electrocardiogram (ECG), detects heart attacks and cardiac arrhythmias, monitors your oxygen saturation, identifies and classifies dysarthria or aphasia based on machine learning and even assesses your gait with a smart camera. The device would also be able to provide first aid instructions. This robotic device would come to you on wheels if it detects any concern linked to your wearable device. These devices will have a Bluetooth or Wi-Fi connection with your cell phone and will enable you to call 911 and immediately transfer critical medical data to the EMS who are en route to your home. This will save significant time and help EMT make proper triaging and urgent plans.

Medical Ambulances

Getting ambulances to rural settings in time is always a challenge. This issue can be potentially resolved by creating rural ambulance sub-stations with self-driving ambulances that will carry patients to a main ambulance station staffed with humans. This will cut down the commute to the hospitals. Because of low traffic in rural

communities, self- driving ambulances will be useful for patients who can be accompanied by a family member or friend.

With Covid or any other contagious disease, the safety of paramedics is essential. This can be compromised if the EMT sits too close to the patient monitoring the vitals during the ride to the hospital. Medical robots can easily monitor cardiac functions and vitals while the EMT can sit in a separate chamber avoiding exposure to any contagion.

CT scans have already been deployed in ambulances. What if the scanners are equipped with AI technology for identifying potentially salvageable tissue in stroke patients? This will significantly shorten the door to needle time, saving, and improving more lives.

Triaging in the Emergency Rooms Using AI Technology

One of the worst nightmares of many patients in the emergency rooms is the never-ending wait time. AND the reason for the waits is lack of personnel. The question is, do we really need a human interface to triage patients in the emergency rooms? This could be very easily done by self-serving kiosks as are seen on airports for checking-in. These kiosks could be equipped with statistical learning technology to properly triage and prioritize patients and inform the attending physicians about the urgency of the situation. At the same time the specialist on call can be kept up to date about the ER visits of patients related to their fields of expertise. IMAGINE how much time can be saved if the triage monitors in the ER communicate directly to the monitors in the on-call rooms.

When Patients Are Admitted

People/patients get hospitalized for one or combination of the following reasons: To make a diagnosis, for investigations, treatment and supportive care and placement in a safe setting. Once the patient is admitted, there can be a lot of roadblocks for timely investigations and discharge planning. The triaging of requests for investigations is subjective to some extent. Developing AI based algorithms that are reviewed by radiologists may provide a more objective way to order tests. Routine blood work these days has become random blood work. If all investigations that are ordered on a daily basis were to be justified, the ordering physicians will be in serious trouble. And this adds up to the costs of the healthcare system. There have to be AI monitored statistical protocols for ordering investigations that will ensure that appropriate investigations get carried out on a timely basis and inappropriate redundant investigations are eliminated.

In the context of infection control, robotics can play a significant role in patient care. Daily patient rounds can be easily carried out by robots with a screen that shows the doctors face to the patients. It is a short distance telemedicine. Telemedicine does not have to be distant locations. Telemedicine can be used across the hall to maintain social distancing.

Discharge Planning

AI can play an excellent role in discharge planning. Instead of writing random clinic notes, the healthcare providers will be required to provide object-oriented notes. This information will be fed into a master database that will provide a daily update on the roadblocks to discharging a patient.

Patients who may require a long-term care or placement will be identified earlier instead at the time of discharge.

Clinic Visits

One of the shortcomings of the clinical care system is that in this day and age humans are still involved in data collection that could be easily done otherwise. We need to have a system in place where all relevant clinical information is collected by an automated system that also uses the tools necessary to make a diagnosis and devices a treatment plan based on evidence-based medicine. Humans will play a role in ensuring that there are no shortfalls to the system. The automated system will be able to counsel patients and can even be designed to show empathy at the right time. All follow ups will be at the patient's own home if they operate a computer or to digital clinics if they require technical help. Humans can still play a role in clinical examination until that time that proven technologies also overcome this barrier.

APPLICATIONS OF AI AND ROBOTICS IN CURRENT USE

Although the current use of AI and Robotics is far from ideal, there are already many frontiers which have successfully employed these technologies and are striving for an optimal model. In the following two paragraphs I will discuss some literature pertaining to this subject, briefly touching on our own work in the use of AI in diagnostic radiology.

A complex experiment always starts from a simple one. In order to identify complex pathologies in neuroimaging one has to be able to identify the normal anatomy. This was the basis of our initial experiments to segment and identify corpus callosum on the mid-sagittal sections of the brain MRI (Li et al., 2013). We subsequently worked with different classification techniques to automatically identify various epileptogenic lesions on the MRI of the brain including focal cortical dysplasia (Wang et al., 2020), cavernous malformations (Wang et al., 2018), and mesial temporal sclerosis (Wang et al., 2019). These techniques can be potentially be implemented in remote settings where there is no access to neuroradiologists for timely interpretation of the studies. The same technique can be expanded to other regions of the human body to compliment the radiologist for an expedited reporting system. Pathologists have also been using AI techniques to classify and identify cancerous cells as a pre-screen before a more thorough and meticulous review (Brinker et al., 2021).

Robotics have dramatically changed the landscape of diagnostic and therapeutic applications of stereotaxic neurosurgery. Robotic frameless neurosurgery has exponentially cut down the time employed to completing the procedure and also minimizing the contact between the surgeon and the patient as well as with the other support staff. Robotic stereotactic surgery has become a routine in many affluent north American hospitals with excellent results and in fact with improved accuracy (Dorfer et al., 2020).

Robotic telerounding employs a wheeled robot controlled by the physician. The face of the robot is visible on the robotic screen. Such robots have been employed for rounding in the Intensive Care Units and acute stroke units (Garingo et al., 2016). My vision will be to have such robots in each and every hospital, specifically in wards that deal with contagious and infectious diseases such as COVID. With the existing commercially available devices this would be an expensive undertaking. However, cheaper models can easily be manufactured on a large scale. I believe the lives of hundreds of health care workers could have been saved if such robots were already available during the COVID pandemic.

FANTASY VS. REALITY

One of the biggest impediments in progress is the idea that "it cannot be done." If you can imagine it, you can do it. Execution only follows imagination but otherwise is merely a random motion. The kind of medical progress that we have seen in the past 50 years would have also sounded like a sci-fi movie to those before those times. MRI scanning, functional MRI, gamma knife, stroke ambulance, clot retrieval after a stroke, laser epilepsy surgery, functional brain mapping, robotic stereotactic brain surgery, monoclonal antibodies for cancer treatment, capsule endoscopy, deep brain stimulation for movement disorders, exoskeletons for paraplegics, bionics, vagas nerve stimulators for epilepsy, artificial heart, organ transplantation, cardiac defibrillator device, cardiac pacemakers, artificial plasma, plasmapheresis, treatment with IVIG are just a few of hundreds of other examples.

If self-driving cars are possible, self-driving ambulances are just a step forward. When I was in the medical school almost 30 years ago, there was not much that could be done if a person had a stroke. Just see how much things have changed. Starting from intravenous tissue plasminogen activator, to intra-arterial treatment, then from intra-arterial treatments to clot extraction. People who would have been disabled for life are now walking out of the hospital in a few days.

I ask the readers to attend to this article with an open mind that looks at the light ahead of us. If we close our eyes, all we will see is darkness and hopelessness.

CONCLUSION

A well-known saying goes that if you keep doing the same thing over and over again, you cannot expect a different result. To improve our health care system during Covid 19 and once the pandemic is over, we need to implement some dramatic measures, and we need to start thinking about a workable strategy immediately. AI, robotics and telemedicine provides a unique platform to device change. To bring about a universal change we need to start thinking at the highest administrative levels with well-defined timelines and achievable milestones.

DATA AVAILABILITY STATEMENT

The original contributions presented in the study are included in the article/supplementary material, further inquiries can be directed to the corresponding author.

AUTHOR CONTRIBUTIONS

This article was conceived, written, and formatted by SNA.

REFERENCES

Brinker, T. J., Schmitt, M., Krieghoff-Henning, E. I., Barnhill, R., Beltraminelli, H., Braun, S. A., et al. (2021). Diagnostic performance of artificial intelligence for histologic melanoma recognition compared to 18 international expert pathologists. *J. Am. Acad. Dermatol.* doi: 10.1016/j.jaad.2021.02.009. [Epub ahead of print].

Dorfer, C., Rydenhag, B., Baltuch, G., Buch, V., Blount, J., Bollo, R., et al. (2020). How technology is driving the landscape of epilepsy surgery. *Epilepsia* 61, 841–855. doi: 10.1111/epi.16489

Garingo, A., Friedlich, P., Chavez, T., Tesoriero, L., Patil, S., Jackson, P., et al. (2016). "Tele-rounding" with a remotely controlled mobile robot in the neonatal intensive care unit. *J. Telemed. Telecare* 22, 132–138. doi: 10.1177/1357633X15589478

Li, Y., Mandal, M., and Ahmed, S. N. (2013). Fully automated segmentation of corpus callosum in midsagittal Brain MRIs. *Annul. Int. Conf. IEEE Eng. Med. Biol. Soc.* 2013:5111–5114.

Wang, H., Ahmed, S. N., and Mandal, M. (2018). Computer-aided diagnosis of cavernous malformations in brain MR images. *Comput. Med. Imaging Graph.* 66, 115–123. doi: 10.1016/j.compmedimag.2018.03.004

Wang, H., Ahmed, S. N., and Mandal, M. (2019). Computer aided detection of mesial temporal sclerosis based on hippocampal and CSF features in MR images. *Biocybernet. Biomed. Eng.* 39, 122–132. doi: 10.1016/j.bbe.2018.10.005

Wang, H., Ahmed, S. N., and Mandal, M. (2020). Automated detection of focal cortical dysplasia using a deep convolutional neural network. *Comput. Med. Imaging Graph.* 79:101662. doi: 10.1016/j.compmedimag.2019.101662

Conflict of Interest: The author declares that the research was conducted in the absence of any commercial or financial relationships that could be construed as a potential conflict of interest.

frontiers in Robotics and AI

ORIGINAL RESEARCH
published: 08 April 2021
doi: 10.3389/frobt.2021.612392

FaceGuard: A Wearable System To Avoid Face Touching

*Allan Michael Michelin[1], Georgios Korres[1], Sara Ba'ara[1], Hadi Assadi[1], Haneen Alsuradi[1], Rony R. Sayegh[2], Antonis Argyros[3] and Mohamad Eid[1]**

[1]*Applied Interactive Multimedia Lab, Engineering Division, New York University Abu Dhabi, Abu Dhabi, United Arab Emirates,*
[2]*Clinical Associate Professor, Cornea and Refractive Surgery, Cleveland Clinic Abu Dhabi, Abu Dhabi, United Arab Emirates,*
[3]*Professor at the Computer Science Department (CSD), University of Crete (UoC), Crete, Greece*

Most people touch their faces unconsciously, for instance to scratch an itch or to rest one's chin in their hands. To reduce the spread of the novel coronavirus (COVID-19), public health officials recommend against touching one's face, as the virus is transmitted through mucous membranes in the mouth, nose and eyes. Students, office workers, medical personnel and people on trains were found to touch their faces between 9 and 23 times per hour. This paper introduces FaceGuard, a system that utilizes deep learning to predict hand movements that result in touching the face, and provides sensory feedback to stop the user from touching the face. The system utilizes an inertial measurement unit (IMU) to obtain features that characterize hand movement involving face touching. Time-series data can be efficiently classified using 1D-Convolutional Neural Network (CNN) with minimal feature engineering; 1D-CNN filters automatically extract temporal features in IMU data. Thus, a 1D-CNN based prediction model is developed and trained with data from 4,800 trials recorded from 40 participants. Training data are collected for hand movements involving face touching during various everyday activities such as sitting, standing, or walking. Results showed that while the average time needed to touch the face is 1,200 ms, a prediction accuracy of more than 92% is achieved with less than 550 ms of IMU data. As for the sensory response, the paper presents a psychophysical experiment to compare the response time for three sensory feedback modalities, namely visual, auditory, and vibrotactile. Results demonstrate that the response time is significantly smaller for vibrotactile feedback (427.3 ms) compared to visual (561.70 ms) and auditory (520.97 ms). Furthermore, the success rate (to avoid face touching) is also statistically higher for vibrotactile and auditory feedback compared to visual feedback. These results demonstrate the feasibility of predicting a hand movement and providing timely sensory feedback within less than a second in order to avoid face touching.

Keywords: face touching avoidance, IMU-based hand tracking, sensory feedback, vibrotactile stimulation, wearable technologies for health care

OPEN ACCESS

Edited by:
Ana Luisa Trejos,
Western University, Canada

Reviewed by:
Zhihan Lv,
Qingdao University, China
Tommaso Lisini Baldi,
University of Siena, Italy
Domen Novak,
University of Wyoming, United States

****Correspondence:***
Mohamad Eid
mohamad.eid@nyu.edu

Specialty section:
This article was submitted to Biomedical Robotics, a section of the journal Frontiers in Robotics and AI

Received: *30 September 2020*
Accepted: *08 February 2021*
Published: *08 April 2021*

Citation:
Michelin AM, Korres G, Ba'ara S, Assadi H, Alsuradi H, Sayegh RR, Argyros A and Eid M (2021) FaceGuard: A Wearable System To Avoid Face Touching. Front. Robot. AI 8:612392. doi: 10.3389/frobt.2021.612392

1 INTRODUCTION

Coronavirus disease (COVID-19), caused by severe acute respiratory syndrome coronavirus 2 (SARS-CoV-2), has spread worldwide, with more than 88 million cases and 1.9 million fatalities as of January, 2021 WHO (2020). Maintaining social distancing, washing hands frequently, avoiding touching the face including eyes, nose, and mouth, are the major methods associated with preventing

COVID-19 transmission Chu et al. (2020). Contaminated hands have the potential to disseminate COVID-19 especially if associated with touching the face Macias et al. (2009). Face touching is an act that can happen without much thought, and in fact, happens with such a high occurrence that reducing it could mitigate a heavy source of transmission. Beyond simple skin irritations, face touching has been linked to emotional and cognitive processes Barroso et al. (1980), Mueller et al. (2019), increasing with attentiveness while tasks are being performed, as well as with increasing pressure and anxiety Harrigan (1985). For such common underlying motives, it is no surprise to see that on average a person touches their face 23 times in an hour Kwok et al. (2015). Given that the primary source of COVID-19 transmission is through contact with respiratory droplets [via the nose, mouth, or eyes, either directly from another individual or picked up from a surface Pisharady and Saerbeck (2015)], avoiding face touching is of a great value.

Developing a system to avoid face touching outright by stopping hand movement raises two main challenges. First of all, a system must predict rather than detect when a hand movement will result in face touching well before the hand reaches the face. Secondly, once a hand movement is predicted to result in face touching, a sensory feedback must be presented immediately in order to stop the hand movement and thus avoid face touching. Note that the prediction and response components are evaluated separately to better analyze the capabilities/limits of each component.

1.1 Predicting Hand Movement

Predicting face touching requires precise hand tracking. Two common approaches for tracking hand movement are vision-based approaches Al-Shamayleh et al. (2018) and wearable sensor-based approaches Jiang X. et al. (2017), Mummadi et al. (2018). A combination of these have also shown potential for enhanced accuracy Jiang S. et al. (2017), Siddiqui and Chan (2020). Vision-based hand tracking utilizes camera networks Pisharady and Saerbeck (2015), and as mentioned, can be supplemented with wearable devices such as motion sensor systems placed along the body, to map either whole body or hand movement Liu et al. (2019). One particular wearable device often used is the inertial measurement unit (IMU), capable of collecting data along six degrees of freedom, with three additional angular sensors to enable a total of nine inputs. Found in many smart watches, the IMU is equipped with an accelerometer and gyroscope, providing an inexpensive option that is not only accurate, taking measures along all three dimensions for each of its components, but also one that does not require complementary infrastructure to operate. This allows the IMU to be versatile yet effective in the context in which it is implemented.

Paired with an appropriate machine learning model, the data from an IMU can be used to notify a user how often they are touching their face, as well as whether they have done so after each movement. IMUs have been used to correctly identify a completed face touch with high accuracy Fu and Yu (2017), Rivera et al. (2017). Even though detecting face touching greatly supports awareness training, it does not prevent face touching from happening. The motivation of the proposed system is to apply machine learning in order to predict face touching and provide vibrotactile feedback to prevent it rather than detecting it.

1.2 Sensory Feedback for Motor Control

Along with the development of hand tracking, the user must also be notified of their impending action before it is committed, with ample time for them to react. The notification must be delivered through a medium that will elicit the fastest response time. The three feedback modalities of relevance are visual, auditory, and vibrotactile, and it has been shown that vibrotactile feedback produces the fastest response times Ng and Chan (2012). Vibrotactile feedback systems can be used to achieve this, with benefits similar to that of an IMU, being cost-effective, and easily implemented into a wearable device.

A low-cost wearable system that prevents people from touching their face, and in the long run, assist people in becoming more aware of their face-touching, is proposed. The system exploits widespread and off-the-shelf smartwatches to track the human hand and provide timely notification of hand movement in order to stop touching the face. The decision to build the system with just a smartwatch makes it immediately available to people, without the requirement of building or wearing additional hardware. The system assumes a smartwatch with an IMU module and a vibration motor; a reasonable assumption as most commercial smartwatches are equipped with such hardware. Although preventing the spread of COVID-19 is the most evident, the system can be adapted for other applications such as habit reversal therapy (HRT) Bate et al. (2011) and treatment of chronic eye rubbing McMonnies (2008). The main contributions of this paper are summarized as follows:

1. Proposing a conceptual approach that utilizes IMU data to predict if a hand movement would result in face touching and provides real-time sensory feedback to avoid face touching.
2. Developing a model for tracking hand movement and predicting face touching using convolutional neural networks based on IMU data. To train the model, a database of 4,800 hand motion trials recording with 40 users under three conditions, sitting, standing, and walking is built.
3. Presenting a psychophysical study with 30 participants to compare the effectiveness of sensory feedback modalities, namely visual, auditory, and vibrotactile, to stop the hand while already in motion before reaching the face. The response time and success rate were used as the evaluation metrics for the comparison.

2 RELATED WORK

2.1 Understanding Hand Movement

The detection and classification of body activity is a major area of research, with applications and techniques ranging from wearable electrocardiogram recorders to classify body movements in

patients with cardiac abnormalities Pawar et al. (2007), recognition and 3D reconstruction of the face using computer vision Chen et al. (2017), Zhao et al. (2018), Lv (2020), Yang and Lv (2020), to activity tracking of remote workers through sensory systems Ward et al. (2006), Manghisi et al. (2020). For instance, a system named HealthSHIELD utilized Microsoft Kinect Azure D-RGB camera to detect high/low risk face touching in order to monitor compliance with behavioral protection practices. Results demonstrated an overall accuracy of 91%. Inertial Measurement Units (IMU) are another particularly common alternative that although can be used in tandem with other systems Corrales et al. (2008), can provide exceptional results on its own Olivares et al. (2011).

In connection to real-time hand movement recognition in virtual reality games, a wearable IMU has been investigated as an alternative to simple button presses on a controller to identify player action intent Fu and Yu (2017). Similar to the IMU implementation of our own study, an accelerometer, gyroscope, and magnetometer are used as the sensor inputs for classification. Once a user moves their hand in a predetermined pattern, a trained long short term memory (LSTM) model identifies the movement, and the relevant in-game controls are carried out.

Detecting the touching of one's face using an IMU has been examined recently Christofferson and Yang (2020). A convolutional neural network is used to identify whether a user had touched their face at the end of a gesture. Once a user made their move, the collected data from the nine data modes of the IMU are passed through a trained model, with a face touch classification provided simply as true or false. This approach resulted in a 99% accuracy rate.

As is seen in previous studies, the deep learning model used alongside the IMU varies. Requiring a time series based solution, recurrent neural networks, particularly LSTM, and convolutional neural network (CNN) models have been implemented with significant success Rivera et al. (2017), Christian et al. (2019). Combinations of CNN layers with LSTM models have also been effective in processing IMU data Silva do Monte Lima et al. (2019). However, in related works where classification time is relevant, a standalone CNN has shown great promise Huang et al. (2017).

2.2 Real-Time Sensory Feedback

In order to provide a real-time sensory feedback to stop the hand movement and avoid face touching, multiple feedback sensory modalities can be utilized. Sensory feedback is usually presented through visual, auditory, and tactile modalities. Visual modality stimuli such as flashing is common in several warning systems, such as road transport industries Solomon and Hill (2002) and crosswalk warning systems Hakkert et al. (2002). In addition to the use of vision, auditory modality is widely used in transport, heath care, and industrial environments as it has an immediate arousing effect Sanders (1975). For instance, a previous study showed that auditory alarms used in helicopter environments conveyed urgency Arrabito et al. (2004). Comparing the two modalities, it was found that the response time to visual and auditory stimuli is approximately 180–200 and 140–160 ms,

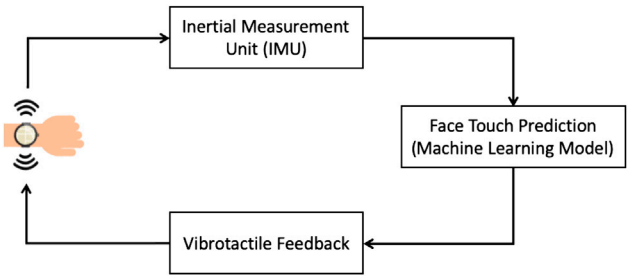

FIGURE 1 | The application scenario involves a smartwatch with Inertial Measurement Unit to detect hand movement, a machine learning model to predict when a movement results in touching the face, and a vibration motor to alert the user in order to stop the hand movement.

respectively Thompson et al. (1992). This is based on a previous finding that an auditory stimulus takes only 8–10 ms to reach the brain whereas visual stimulus takes 20–40 ms Kemp (1973). However, there are several factors that influence the average human response time include age, gender, hand orientation, fatigue, previous experience, etc. Karia et al. (2012).

Vibrotactile modality has also been found to improve the reaction time for several applications such as drone tele-operation Calhoun et al. (2003), Macchini et al. (2020), collision avoidance while driving Scott and Gray (2008), and alteration of motor command in progress (such as altering a reach in progress) Godlove et al. (2014). The temporal aspects of visual and vibrotactile modalities, as sources of feedback about movement control, are examined in Godlove et al. (2014). A modified center-out reach task where the subject's hand movement was occasionally interrupted by a stimulus that instructed an immediate change in reach goal is utilized. Results demonstrated that the response for tactile stimuli was significantly faster than for visual stimuli.

Utilizing vibrotactile feedback for alarming the user about face touching has recently been studied. A commercial product, named IMMUTOUCH, utilized a smart wristband that vibrates every time the user touches their face Immutouch (2020). A recent research study presented a wearable system that utilizes a smartwatch to provide vibrotactile feedback and a magnetic necklace to detect when the hand comes to a close proximity to the face D'Aurizio et al. (2020). Even though these solutions are a great step forward to reducing the number of face touches and their duration, they do not consider real-time touch avoidance. Furthermore, these studies did not perform any systematic studies to determine the most effective sensory feedback modality to stop the hand movement and eventually avoid face touching. Aside from differences in the type and architecture of the deep learning model used for classification, our study employs a wearable IMU not just to classify a gesture, but to predict a gesture before it happens. The motion input data therefore will not include the final portion of an individual's hand movement, placing a limit on the available data for training. In examining feasibility of success under such constraints, optimal sensory feedback thus plays a significant role.

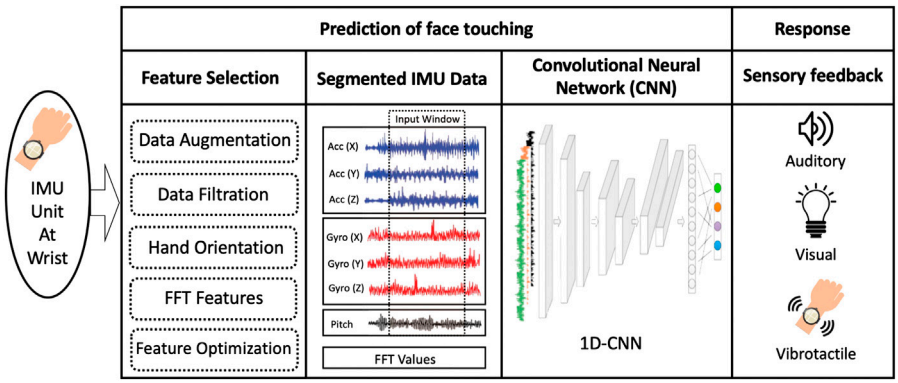

FIGURE 2 | Overview of the FaceGuard system. Abreviations: FFT (Fast Fourier Transform), IMU (Inertial Measurement Unit), CNN (Convolutional Neural Network).

3 PROPOSED APPROACH

A high-level description of the system is visualized in **Figure 1**. The system utilizes IMU data to measure hand movement, convolutional neural networks to predict, in real time, whether a hand movement will involve touching the face, and vibrotactile feedback to alert the user so they stop their hand movement before touching their face. Note that the system must perform in real time in order to generate response to stop the hand movement before it reaches the face.

A more detailed description of the system is shown in **Figure 2** while a technical description of the system is further analyzed in **Section 4**. The prediction component involves a sequence of three processes, namely feature selection, data segmentation, and a Convolutional Neural Network (CNN). Three sensory feedback modalities are considered for the response component, namely visual, auditory, and vibrotactile. **Section 5** presents a psychophysical experiment to compare these modalities and inform the decision about using vibrotactile feedback.

A wearable device with an embedded IMU recording nine different types of hand motion data (x, y, and z components for accelerometer and gyroscope, and rotational pitch, roll, and yaw) makes the input to the prediction component. In the feature selection process, features are extracted and evaluated for relevance to predicting face touching hand movement. These features are used to improve the performance of the prediction model. Feature selection included several data pre-processing procedures such as data augmentation (to increase the size of training data), data filtration to enhance the signal-to-noise ratio, hand orientation calculation, Fast Fourier Transform (FFT) features extraction, and optimization of the combined features.

Once the features are identified, the time-series of the selected features are segmented according to a time window. The window size is an extremely important parameter to optimize in this process since it controls the tradeoff between response time and prediction accuracy. Once the time series data are segmented, all the features are fed into a one dimensional convolutional neural network (1D-CNN) model. 1D-CNNs are generally excellent in automatically detecting temporal relationships in multi-channel time-series data with minimal feature engineering. Using the 1D-CNN kernels allows an automatic extraction of the temporal features in IMU data, which is deemed important in recognizing hand movement towards the face through its corresponding IMU data. The model is trained and evaluated with data generated for this purpose that is recorded from 40 participants. Each participant went through a data collection session that consisted of two runs. In each run, the participant had to perform 10 face-touching hand movements during each of the following everyday activities (standing, walking, sitting) as well as 10 non-face touching hand movements during the same activities. Thus, each participant contributed 120 trials, yielding a total of 4,800 trials. The CNN model provides a binary output, whether the respective hand movement is predicted to result in face touching or not.

As soon as a prediction of face touching event is made, the response component renders a sensory feedback to alert the user, while the hand is in motion, to immediately stop the hand movement in order to avoid face touching. Based on the findings of **Section 5**, vibrotactile feedback is utilized as the sensory feedback modality as it provided superior performance (measured using the response time and success rate of avoiding face touching), compared to visual or auditory.

4 PREDICTION OF FACE TOUCHING

4.1 Data Collection

The data collection procedure combines computer and smartwatch interfaces to collect the needed participant data. The hardware used to collect the IMU data is an Esp32-powered, M5Stack development watch known as M5StickC. It has six degrees of freedom consisting of a 3-axis accelerometer and a 3-axis gyroscope, with pitch, yaw, and roll being calculated internally.

Using an Arduino IDE, the M5StickC is programmed to read the IMU data and store it into a file through a serial connection to a computer. It relies on input from two buttons: the main button used to start and stop the recording of IMU data, and the side button used for user error correction related to trial invalidation and repetition. The program runs for a predetermined number of

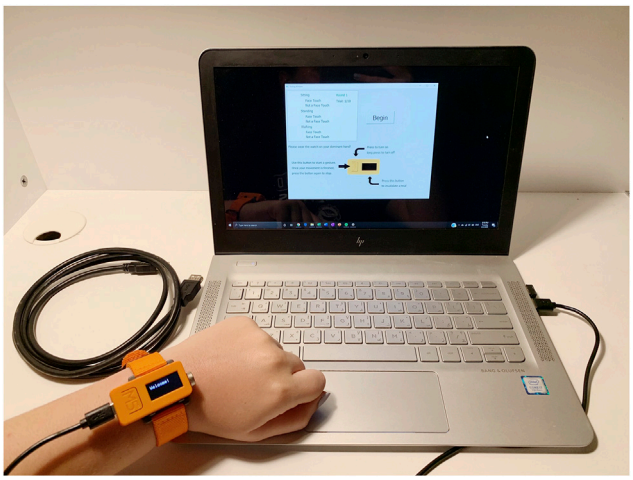

FIGURE 3 | The general setup of the participation. The user is provided with a Windows laptop, the M5StickC watch, a USB-C cable, as well as a USB extension cable to be used for the walking trials.

trials per session before sending an end signal to the computer that saves all the data to a file. The participation protocol in a session consists of two runs, with 60 trials each (30 face-touching and 30 non-face touching hand movements), that are repeated twice to gather a total of 120 trials. As can be seen in **Figure 3**, *sitting*, *standing*, and *walking* are considered as the three main activity types due to them being the most common positions taken in our daily lives. Thus, gathering data for *touching* and *not touching the face* for each of those stances would allow the trained model to make accurate predictions regardless of the user's position.

The M5StickC is used in conjunction with a computer GUI application developed to ensure a holistic, user-friendly collection protocol. Its main purpose is to guide users through the participation and to store auxiliary user information that may be useful in optimizing the prediction model, including height, arm length, and age group. Users are first asked to fill out the aforementioned optional information fields. Then, the application window displays a list of the different sessions to be completed and their associated number of trials, with instructions on the watch's hardware as well as the next steps. Both interfaces rely on a communication of signals to control the start and end of the data collection process. The M5StickC starts recording the moment the main button on the watch is pressed and stops recording when the same button is pressed again by the participant. A single gesture is recorded in this fashion.

The data are then stored into a file. To prevent the loss of data that may occur if the serial connection is interrupted, the user is provided with the option to save their data at any point during the participation upon exiting the computer application.

The general protocol for collecting the data relies on remote participation in compliance with global social-distancing and safety procedures. Users first receive a consent form and statement containing information and instructions pertaining to the participation. If consent is provided, they are given the watch, a compatible laptop, and all needed accessories to complete the required number of sessions in their own homes, as can be seen in **Figure 3**. The equipment is then sanitized properly before being passed on to the next participant. To ensure overall user anonymity, no identifying information is asked for or stored. Additionally, the protocol is asynchronous, which provides users with the freedom to complete the participation at their own pace as it is not compulsory to complete all trails and sessions in one run, rather users are encouraged to take a break at any point and return later to finish.

Overall, 40 sessions were recorded by 40 participants collecting 4,800 trials in total as elaborated in **Section 3**. Of the information disclosed to us, 15 of the 40 participants were female, 15 were male, and 10 undisclosed. Additionally, most of the participants were young adults, with the most common age range being 16–20 years followed by 21–25 years.

4.2 Data Preparation and Inputs

Once data collection is completed, data are prepared for the training and testing of the CNN-based prediction model. Each gesture lasts varying amounts of time, and therefore, requires a select window size to ensure prediction before a face touch has occurred. However, during data collection, users are able to begin their gestures at any point once the start button has been pressed. As such, each trial recording includes a static component (the duration before the hand movement starts), potentially shifting relevant data outside of the determined window. A script that produces plots displaying averaged sensor values over time identifies the lengths of these gestures. The script is applied to each file individually, providing plots for each feature (IMU sensory data)—split into sub plots for each stance (sitting, standing, and walking). The lengths of the static component of every plot at the beginning of the gesture are recorded and averaged, with the resulting values to be referenced for trimming during data preparation. These plots are also used to observe data trends among each feature. It is observed that the roll and yaw did not yield a discriminative pattern for the hand touch condition and thus they are excluded from the analysis. Further confirmation is obtained during the training process of the model; removing these two features improved the accuracy of the model. Furthermore, it is observed that it takes around 1,200 ms to complete a hand movement that involves face touching, which marks the upper limit for the total response time of the proposed system (prediction and motor response).

From the total number of gestures (4,800), the training and testing data sets are formed, randomly split 80–20% (3,840/960 gestures), respectively, and the two 3D input matrices are constructed. Splitting was done by participants; data from a single participant exist either in the training or the test set. This is to ensure the model is resilient to behavioral differences among participants. Filtration is also undergone, where gestures that finish before reaching the time required for the allotted window size are removed. In other words, gestures with very short duration (shorter than the window size of the 1D-CNN) are omitted from the dataset.

One challenge for developing a robust prediction model comes from the lack of large-scale data samples (40 participants with 120

trial repetition). To overcome this problem, data augmentation is introduced to prevent overfitting and improve generalization of the model. Augmentation is done by creating copies of the training data set and shifting it in time with 'N' number of steps while maintaining a constant window size. Augmentation is a great tool for populating the training data such that they share the same characteristics of the original set (representing the events of touching or not touching the face).

Frequency domain signature of hand movement toward the face can be obtained by taking the Fourier transform of the chosen IMU signals. Frequencies of noise can be learnt and discarded once the frequency domain features are obtained. The fast Fourier transform algorithm which is readily available in NumPy library in python was used toward the calculation of the FFT coefficients for all the gestures. Raw and FFT IMU data are then stacked to form 3D matrices, both for the training and testing data sets. Both sets are also standardized, with the testing data set standardized in reference to the training data set statistics. In other words, the data are transformed to have a mean of zero and a standard deviation of one across each feature. This is done in response to differing scales between the components of the IMU, particularly between the accelerometer, gyroscope, and pitch angle. The dimensions of the training and testing matrices are thus 41808×W×14, and 844×W×14.

One dimensional output matrices are constructed to provide the desired output of the model, aligned with each hand movement in the testing and training matrices. The output of the prediction model is set to binary, designating a face touch to (1), or not a face touch to (0).

4.3 CNN-Based Prediction Model Architecture

The input data used to train the model is arranged into a three-dimensional matrix: the first dimension represents the number of trials in the dataset, the second dimension is the time length of the gesture (each index represents a time step of 11 ms, in accordance to the 90.9 Hz IMU sampling rate), and the third dimension is the number of features. The number of features is defined by 6 degrees of freedom from the IMU (acceleration and gyroscope data), as well as the pitch angle value, and corresponding FFT coefficients to form a total depth of 14 features. These data are used to train and test the model, where first a convolution layer (conv1D) is applied, comprising 64 filters of kernel size 8. This is followed by a rectified linear unit (ReLu) activation function applied to the previous output, a batch normalization layer (BN), and a max-pooling layer with a pool size of 2. A dropout layer of value 0.8 is then applied. A second convolution layer is used, consisting of 128 filters also of kernel size 8, followed by another ReLu activation function. Batch normalization is utilized once more, along with a dropout layer of value 0.9, after which the input at its current state is passed through a flatten layer. Finally, two fully connected layers separated by a third dropout layer of value 0.8 are applied. The first fully connected layer has a dimensional unit of 256, with a softmax activation function, and the second has a dimensional unit of 2, with a ReLu activation function. The last fully-connected layer outputs two probabilities, one for each class (Not a face touch, face touch). The architecture for the CNN-based prediction model is shown in **Figure 4**.

4.4 Training and Performance Measures

The model shown in **Figure 4** was trained using a categorical cross-entropy cost function with a default learning rate of 0.001, batch size of 512, and 300 epochs. The model was optimized (weights adjustment) using Adam optimizer Kingma and Ba (2014) during the training process. Batch normalization layers (BN) were used after each of the convolutional layers which basically re-centers and re-scales the input data leading to a faster and more stable training process. To avoid overfitting and prevent co-adaptation of the network weights, a dropout ratio (0.8–0.9) was used in the model. This high dropout ratio proved to work well with our study due to the relatively limited dataset which makes the model more prone to overfitting. The training accuracy reached 96.2% with a loss of 0.1. **Table 1** shows the normalized confusion matrix of the results. The trained model has a sensitivity of 0.929 and a specificity of 0.935. This 1D-CNN model was finalized after many optimization rounds for the different hyper-parameters including the number of layers, filters and dropout ratios. An accuracy of 87.89, 89.7, 87.31% was obtained for a model with 3, 4, and 5 1D-convolutional layers respectively and thus, a model with 2 layers proved to be more efficient. Reducing the dropout ration to 0.5 reduces the classification accuracy to 90%. Thus, an optimized ratio of 0.8 or 0.9 was used.

4.5 Results

With a focus on prediction rather than classification, the period for data collection in real time becomes a significant parameter to select. This window size limits the collection of data from the IMU during a hand movement. **Figure 5** displays the resulting prediction accuracy as this window size is varied.

A shown in **Figure 5**, the prediction accuracy increases as the window size increases, with 95.7% test accuracy reported at around 935 ms. As expected, increasing the window size provides the CNN-based model with further information about the hand movement and thus improves the prediction accuracy. However, increasing the window sacrifices how fast a sensory feedback is presented to the user. When fully implemented, this prediction delay will also be extended by the inference time of the model. At a window size of 700 ms, the average inference time, in which the trained model classifies a single gesture, is 0.313 ms, and at a window size of 990 ms, is 0.446 ms. These values are small enough that they become negligible to the total time delay, effectively reducing time delay before prediction to depend only on window size.

The significance of this delay depends on the application of this device. In a case where it is crucial to keep the user from touching their face, a smaller window size will reduce the time delay before a prediction is made (and before the user can be warned sooner), thereby maximizing time for reaction. This increases the probability that the user will indeed be able to stop their hand movement and avoid touching their face. As is shown in **Figure 5**, the consequence of this is a reduced prediction

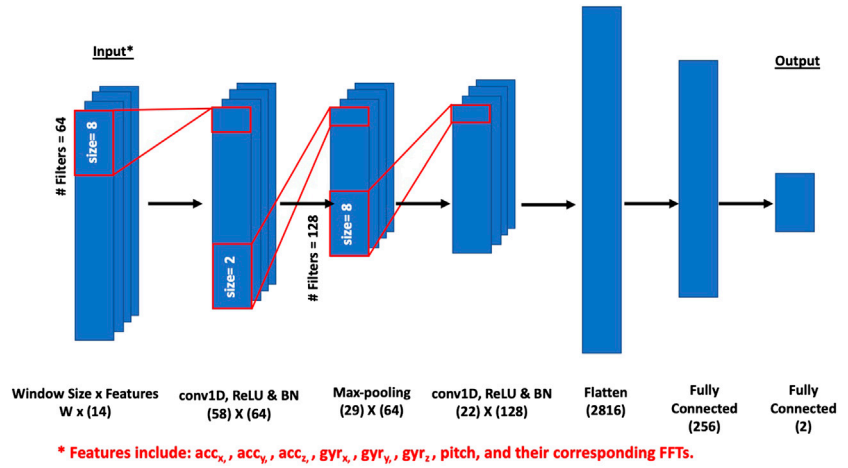

FIGURE 4 | The architecture of the CNN-based prediction model. Note that W represents window size for the input matrix.

TABLE 1 | Normalized confusion matrix of the face touching/not face touching classification.

True label	Predicted label	
	Not face touching	Face touching
Not face touching	0.97	0.03
Face touching	0.11	0.89

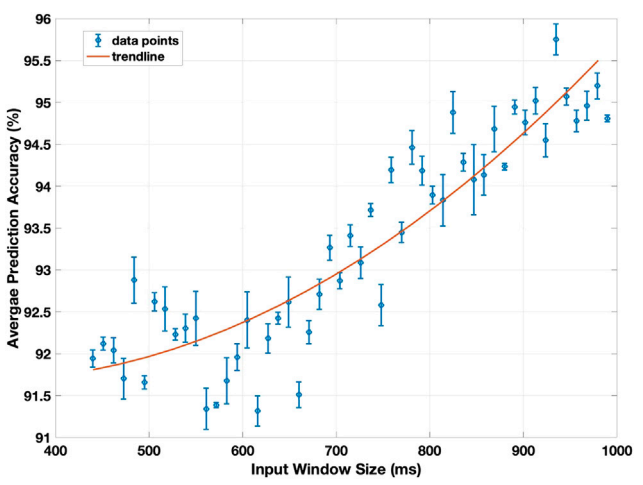

FIGURE 5 | The prediction accuracy of the model against the input window size, averaged for the three conditions (sitting, standing, and walking). The input window size range is 440–990 ms, in increments of 11 ms, out of the 1,200 ms average time needed to touch the face.

accuracy, as reducing the size of the time window reduces the amount of information about the hand movement. With urgency being prioritized, however, false-positives along with ample time to react is still more favorable. In a case where the device is meant to act as a reminder and perhaps a non-essential deterrent, such as may be the case during the COVID-19 pandemic, a larger window size may be excused to achieve higher accuracy. Therefore, finding an optimum trade-off between response time and prediction accuracy through the window size depends largely on the application.

5 SENSORY FEEDBACK FOR MOTOR CONTROL

A psychophysical experiment is presented to compare the effectiveness of three different sensory modalities, visual, auditory, and vibrotactile, as sources of feedback to stop the hand movement. The ability of a subject to stop their hand movement when confronted with sensory information is quantified by comparing the response time and success rate (percentage of times the user succeeds in avoiding face touching) for the three sensory modalities ($p < 0.05$). Finally, a questionnaire was introduced to the participants at the end of the experiment to subjectively evaluate their quality of experience.

5.1 Participant

Thirty participants (15 female, 15 male, ages 25–50 years) are recruited for the experiment. None of the participants have any known sensorimotor, developmental or cognitive disorders at the time of testing. Written informed consent is obtained from all participants. The study is approved by the Institutional Review Board for Protection of Human Subjects at New York University Abu Dhabi (Project # HRPP-2020-108).

5.2 Experimental Setup

A custom wristband is developed to provide the three sensory modalities, shown in **Figure 6**. A strip of five 3 mm LED's is attached along the top face of the wristband to provide blinking visual feedback. On the bottom face of the wristband a coin type vibration motor is attached to provide vibrotactile feedback (Pico Vibe 310-177, Precision Microdrives vibration motor). At the middle of the top face, a 9 Degrees of freedom (DoF) IMU is

placed in order to sense any movements (displacements and rotations) when the wristband is strapped on a hand. The wristband is connected to a control box which hosts the driving circuit of the vibration motor. A 1 kHz piezoelectric buzzer is utilized to provide auditory feedback. An ATMEGA328 microcontroller unit to control and acquire data from all of the aforementioned hardware components is used. The experimental setup is connected to a laptop through a serial connection over a USB cable.

Participants sit around 2 m in front of the experimenter where they could make unrestricted arm movements. Participants are asked to wear the wristband at their dominant hand and keep their hand in a resting position (on the table). The experimenter instructs the participants through the experiment verbally.

5.3 Experimental Task and Protocol

In this experiment, participants complete a face touching task. Participants are instructed to move their dominant hand to touch their face, during which the hand movement is occasionally interrupted by a stimulus cue that informs the subject to stop the movement in order to avoid touching the face. Each participant completes a total of 100 trials, with 30% of these trials provide sensory feedback while the other 70% of the trials have no sensory feedback and thus result in touching the face. Among the 30% with sensory feedback, 10% are visual, 10% are auditory, and 10% are vibrotactile. To minimize the learning effects that influence the response time, the trials are presented in a counterbalanced fashion.

A trial starts with the experimenter asking the participant to rest their dominant hand on the table with tactile sensing capability to detect the start of the hand movement. The experimenter instructs the participant to move their dominant hand and touch their face. During the hand movement, the sensory cue is applied at the wristband. The hand movement is analyzed based on the recorded IMU data. At the end of the trial, the experimenter prompts the participant to confirm whether they touched their face or not. The sensory stimulus is given at a random time during the movement. The visual stimulus is a blinking red light that shines around the wristband to make it clearly visible, and lasts for 500 ms. The auditory stimulus is a beeping sound at 1,000 Hz for 500 ms. The vibrotactile stimulus has a vibration frequency of 200 Hz and lasts for 500 ms. The intensity of vibration is set to be readily detected (defined as > 95% correct in stimulus detection). After completing the experiment, participants fill a questionnaire in order to evaluate their subjective experience.

The main quantification is the response time, which indicates how rapidly a subject can respond to a stimulus as a source of feedback and stop the ongoing hand movement. The response time is measured as the time between the onset of the sensory feedback stimulus and the time when the hand reaches a complete stop or reverses the direction of motion. The success rate—the percentage of times the participants succeeds to respond timely to the sensory feedback stimulus and avoid touching their face—is also recorded. The data are analyzed using repeated measures ANOVA (Analysis Of Variance) after confirming normal distribution (D'Agostino-Pearson normality test).

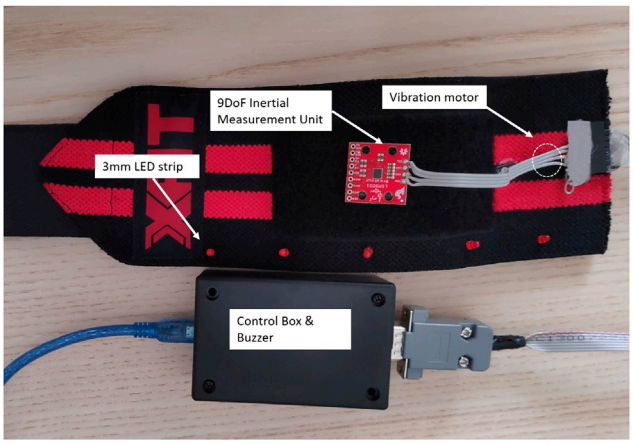

FIGURE 6 | The wristband used in this study with all its components labeled.

It is also worth noting that the experimental protocol followed COVID-19 preventive measures in terms of social distancing, symptom check for all participants, disinfection of study visit area before, and wearing personal protective equipment (surgical mask and gloves).

5.4 Results

The average response time for vibrotactile stimulus is 427.3 ms with standard deviation of 110.88 ms. The average response time for visual stimuli is 561.70 ms with standard deviation of 173.15 ms. With regards to auditory stimulus, the average response time is 520.97 ms with standard deviation of 182.67 m. Response time to vibrotactile stimulus is found to be significantly shorter than that to auditory stimulus ($p < 0.01$) and visual stimulus ($p < 0.01$). Furthermore, the response time to auditory stimulus is found to be significantly shorter than that to visual stimulus ($p < 0.05$). A summary of these findings is shown in **Figure 7**.

Another important performance parameter to compare is the success rate. The average success rate for vibrotactile stimulus is found to be statistically larger than that of visual stimulus ($p < 0.05$). Furthermore, the average success rate for auditory stimulus is found to be statistically larger than that of visual stimulus ($p < 0.05$). However, there is no significant differences between vibrotactile stimulus and auditory stimulus ($p = 0.07$). **Figure 8** shows the differences in success rate among the three groups.

The questionnaire is designed to capture the participant's quality of experience. Participants are asked about their favorite modality for feedback, which modality provides the most pleasant experience, whether vibrotactile feedback creates any fatigue or discomfort, and the chance to provide any further feedback. As for preference, 25 participants (83.34%) selected vibrotactile as their favorite modality for feedback, 3 (10%) selected auditory feedback, and 2 (6.67%) preferred visual. 29 participants (96.67%) reported that they clearly perceived the vibrotactile stimulation. 28 participants (93.34%) selected

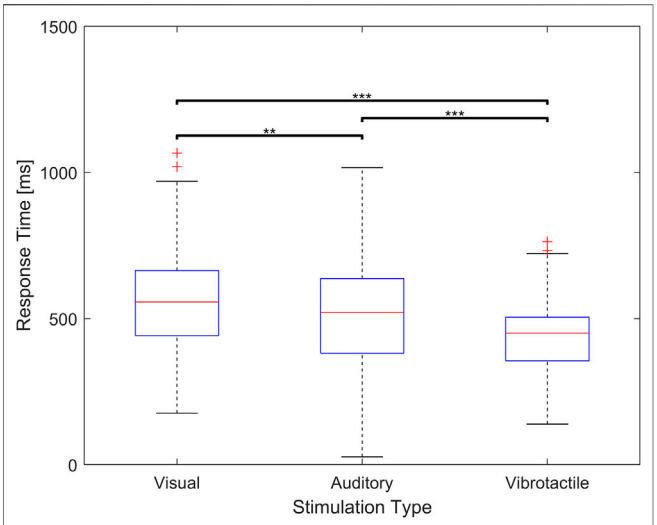

FIGURE 7 | Response time for visual, auditory, and vibrotactile feedback. The middle red line of the blue box indicate a median value and the bottom and top edges indicate the 25th and 75th percentiles respectively (** means $p < 0.05$, *** means $p < 0.01$).

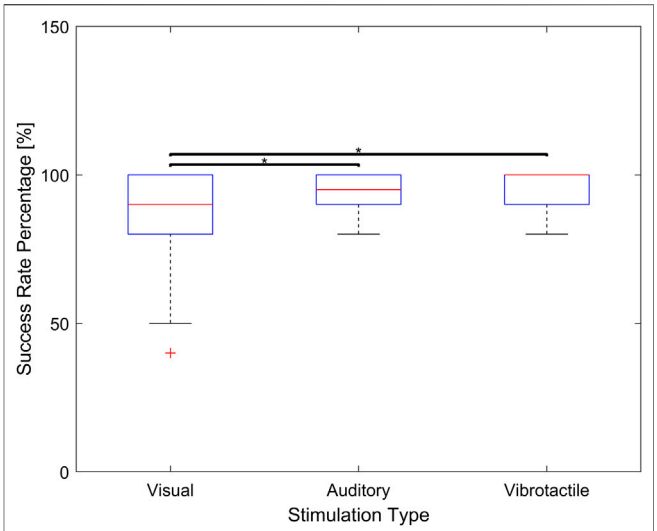

FIGURE 8 | Success rate associated with visual, auditory, and vibrotactile feedback. The middle red line of the blue box indicate a median value and the bottom and top edges indicate the 25th and 75th percentiles respectively (* means $p < 0.05$).

vibrotactile feedback as the most pleasant among the three modalities. Finally, none of the participants reported significant fatigue or discomfort during the experiment.

6 DISCUSSION

The CNN-based prediction model requires less than 550 ms of IMU data to predict face touching events with an accuracy greater than 92%. Furthermore, the sensory feedback experiment showed that around 427 ms is needed to stop the hand movement using vibrotactile feedback. Therefore, it will take less than a second from the start of the hand movement until complete stop. Meanwhile, our study suggests that the average time for a hand to reach and touch the face is 1,200 m. Therefore, the proposed system is capable of providing timely response to avoid face touching within less than 1 s. It is worth noting that there is a tradeoff between the prediction accuracy and the response time. In order to improve the prediction accuracy, the input window size must increase, which implies that it will take more time to stop the hand movement, which causes a decrease in chances to avoid face touching.

Another important factor is the relationship between prediction accuracy and practical usefulness of the system: an increase in the number of false positives would create unnecessary buzzing which may distract/annoy the user while an increase in false negatives would not prevent face touching entirely. Therefore, while the current prediction system is based solely on the IMU data, fusing other sensory modalities into the CNN-based model that are relevant to face touching and hand movement would significantly improve the prediction accuracy. For instance, gender, arm length, hand size, and age group may provide complementary information to improving the prediction accuracy. This involves recruiting a significantly larger number of participants to generate enough data points to train the model. In situations where camera data are available, such as when the user is sitting in front of a PC, computer vision approaches can be applied in order to fine-tune the model for improved performance.

A major source for false positives stems from the lack of information about the head posture in reference to the hand movement. Therefore, it would be interesting to augment the current CNN-based prediction model with the head position and/or orientation. With appropriate sensors or camera systems, the head posture can be continuously monitored and used as an auxiliary input to the prediction model to further improve the prediction accuracy. This is an interesting direction for future work. Furthermore, collecting hand movements that are likely to cause false positives (such as eating where the hand movement is very similar to that of face touching) and training the model with such data would significantly reduce the false positives.

Although the findings of the present study demonstrate the feasibility of developing a system to avoid face touching, a few limitations should be mentioned. First, the dataset utilized to train the CNN-based prediction model is rather limited. A larger dataset improves the prediction accuracy, including false positives and negatives, which allows for a reduced window size and improved system response. Furthermore, running the CNN model is computationally expensive. Therefore, the inference about the prediction of face touching may have to be performed on a computationally powerful machine such as a smart phone or even the cloud. This adds further delays to the overall system response. Additionally, the current study focused on preventing face touching through the dominant hand. It might be desirable for several applications to avoid touching the face with both hands, and thus evaluating the performance of the

system while tracking both hands is necessary for such applications.

Another very important limitation is that the collected IMU data were pre-segmented such that each trial is known to have a single hand gesture. As the IMU signals are continuous streaming data, a sliding window must be used to segment the raw data to individual pieces in real time, each of which is the input of the CNN model. The length and moving step of the sliding window are hyper-parameters that need to be carefully tuned to achieve satisfactory performance. This problem is present not only in tasks that require constant gesture recognition, but also in other fields such as continuous speech recognition. Finally, the participants' behavior or activities could modulate the hand movement and thus may impact the accuracy of the prediction model. More data must be collected while participants are engaged in various activities/behavior in order to enhance the resilience of the classifications against users' activities/behavior.

7 CONCLUSION

This paper presented a system that utilizes IMU data to predict hand movement that results in face touching and provide sensory feedback to stop the hand movement before touching the face. A 1D-CNN-based prediction model, capable of automatically extracting temporal features of the IMU data through 1D-CNN filters, was developed and trained with IMU data collected from 4,800 trials recorded from 40 participants. Results demonstrated a prediction accuracy of more than 92% with less than 550 ms of IMU time series data. Compared to visual and auditory modalities, it was found that vibrotactile feedback results in statistically faster response, better success rate, and improved quality of user experience.

As for future work, it is of an importance to evaluate the combined prediction/response system as a whole in a realistic experimental environment (while performing everyday life activities). Furthermore, the authors plan to develop a light-weight CNN-based prediction model that optimizes computational power in order to run the prediction model on a wearable device (with limited computational power). Improving the dataset by collecting more data can immensely improve the model training and performance. In particular, collecting data from tasks that exhibit similar hand movements to face touching but do not involve face touching (such as eating) will improve the system robustness, particularly against false positives.

DATA AVAILABILITY STATEMENT

The dataset used to train the CNN-based prediction model can be found in the Applied Interactive Multimedia research lab directory using this link: https://drive.google.com/drive/folders/13ffsGBzL_6-5bmFgIJhdLiVkC3VWIs3A.

ETHICS STATEMENT

The studies involving human participants were reviewed and approved by the Institutional Review Board for Protection of Human Subjects at New York University Abu Dhabi (Project \# HRPP-2020-108). The patients/participants provided their written informed consent to participate in this study.

AUTHOR CONTRIBUTIONS

AM, SB, HA, and HA developed the prediction component, including the data collection protocol and the CNN model development and evaluation, GK, AA, and ME developed the sensory feedback psychophysical study. RRS, AA, and ME contributed to the conceptualization of the solution.

FUNDING

This project is supported by New York University Abu Dhabi.

REFERENCES

Al-Shamayleh, A. S., Ahmad, R., Abushariah, M. A. M., Alam, K. A., and Jomhari, N. (2018). A systematic literature review on vision based gesture recognition techniques. *Multimed. Tools Appl.* 77, 28121–28184. doi:10.1007/s11042-018-5971-z

Arrabito, G. R., Mondor, T. A., and Kent, K. J. (2004). Judging the urgency of non-verbal auditory alarms: a case study. *Ergonomics* 47, 821–840. doi:10.1080/00140130420001932 82

Barroso, F., Freedman, N., and Grand, S. (1980). Self-touching, performance, and attentional processes. *Percept. Mot. Skills* 50, 1083–1089. doi:10.2466/pms.1980.50.3c.1083

Bate, K. S., Malouff, J. M., Thorsteinsson, E. T., and Bhullar, N. (2011). The efficacy of habit reversal therapy for tics, habit disorders, and stuttering: a meta-analytic review. *Clin. Psychol. Rev.* 31, 865–871. doi:10.1016/j.cpr.2011.03.013

Calhoun, G., Draper, M., Ruff, H., Fontejon, J., and Guilfoos, B. (2003). "Evaluation of tactile alerts for control station operation,"in Proceedings of the human factors and ergonomics society Annual Meeting, Denver, Colorado, October 13–17, 2003 (Los Angeles, CA: SAGE Publications Sage CA). 47, 2118–2122.

Chen, Z., Huang, W., and Lv, Z. (2017). Towards a face recognition method based on uncorrelated discriminant sparse preserving projection. *Multimed. Tools Appl.* 76, 17669–17683. doi:10.1007/s11042-015-2882-0

Christian, M., Uyanik, C., Erdemir, E., Kaplanoglu, E., Bhattacharya, S., Bailey, R., et al. (2019). "Application of deep learning to imu sensor motion,"in 2019 SoutheastCon, Huntsville, AL, April 11–14, 2019 (New York, NY: IEEE). 1–6.

Christofferson, K., and Yang, R. (2020). FaceSpace–apple watch application. Tech. rep., DEVOPS, FaceSpace Application. Available at: https://facespace.app/ (Accessed March 9, 2021)

Chu, D. K., Akl, E. A., Duda, S., Solo, K., Yaacoub, S., Schünemann, H. J., et al. (2020). Physical distancing, face masks, and eye protection to prevent person-to-person transmission of sars-cov-2 and covid-19: a systematic review and meta-analysis. *Lancet* 395, 1973–1987. doi:10.1016/S0140-6736(20)31142-9

Corrales, J. A., Candelas, F., and Torres, F. (2008). "Hybrid tracking of human operators using imu/uwb data fusion by a kalman filter,"in 2008 3rd ACM/IEEE International Conference on Human-Robot Interaction (HRI). Amsterdams, Netherland, March 12–15, 2008 (New York, NY: IEEE).

D'Aurizio, N., Baldi, T. L., Paolocci, G., and Prattichizzo, D. (2020). Preventing undesired face-touches with wearable devices and haptic feedback. *IEEE Access* 8, 139033–139043. doi:10.1109/ACCESS.2020.3012309

Fu, A., and Yu, Y. (2017). Real-time gesture pattern classification with imu data. FaceSpace Application. Available at: https://facespace.app/ (Accessed March 9, 2021)

Godlove, J. M., Whaite, E. O., and Batista, A. P. (2014). Comparing temporal aspects of visual, tactile, and microstimulation feedback for motor control. *J. Neural Eng.* 11, 046025. doi:10.1088/1741-2560/11/4/046025

Hakkert, A. S., Gitelman, V., and Ben-Shabat, E. (2002). An evaluation of crosswalk warning systems: effects on pedestrian and vehicle behaviour. *Transp. Res. Part F: Traffic Psychol. Behav.* 5, 275–292. doi:10.1016/s1369-8478(02)00033-5

Harrigan, J. A. (1985). Self-touching as an indicator of underlying affect and language processes. *Soc. Sci. Med.* 20, 1161–1168. doi:10.1016/0277-9536(85)90193-5

Huang, J., Huang, Z., and Chen, K. (2017). "Combining low-cost inertial measurement unit (IMU) and deep learning algorithm for predicting vehicle attitude," in 2017 IEEE Conference on Dependable and Secure Computing, Taipei, China, August 7–10, 2017 (New York, NY: IEEE), 237–239.

Immutouch (2020). Immutouch wearable device. Available at: https://immutouch.com/ (Accessed September 03, 2020).

Jiang, S., Lv, B., Guo, W., Zhang, C., Wang, H., Sheng, X., et al. (2017). Feasibility of wrist-worn, real-time hand, and surface gesture recognition via semg and imu sensing. *IEEE Trans. Ind. Inform.* 14, 3376–3385. doi:10.1109/TII.2017.2779814

Jiang, X., Merhi, L.-K., and Menon, C. (2017). Force exertion affects grasp classification using force myography. *IEEE Trans. Human-Machine Syst.* 48, 219–226. doi:10.1109/THMS.2017.2693245

Karia, R. M., Ghuntla, T. P., Mehta, H. B., Gokhale, P. A., and Shah, C. J. (2012). Effect of gender difference on visual reaction time: a study on medical students of bhavnagar region. *IOSR J. Pharm.* 2, 452–454. doi:10.9790/3013-0230452454[

Kemp, B. J. (1973). Reaction time of young and elderly subjects in relation to perceptual deprivation and signal-on versus signal-off conditions. *Develop. Psychol.* 8, 268. doi:10.1037/h0034147

Kingma, D. P., and Ba, J. (2014). Adam: a method for stochastic optimization. Preprint: arXiv:1412.6980.

Kwok, Y. L. A., Gralton, J., and McLaws, M.-L. (2015). Face touching: a frequent habit that has implications for hand hygiene. *Am. J. Infect. Control* 43, 112–114. doi:10.1016/j.ajic.2014.10.015

Liu, Y., Li, Z., Liu, Z., and Wu, K. (2019). "Real-time arm skeleton tracking and gesture inference tolerant to missing wearable sensors,"in Proceedings of the 17th Annual International Conference on Mobile Systems, Applications and Service, Seoul, Republic of Korea, June, 2019, 287–299.

Lv, Z. (2020). Robust3d: a robust 3d face reconstruction application. *Neural Comput. Appl.* 32, 8893–8900. doi:10.1007/s00521-019-04380-w

Macchini, M., Havy, T., Weber, A., Schiano, F., and Floreano, D. (2020). Hand-worn haptic interface for drone teleoperation. Preprint: arXiv:2004.07111.

Macias, A. E., De la Torre, A., Moreno-Espinosa, S., Leal, P. E., Bourlon, M. T., and Ruiz-Palacios, G. M. (2009). Controlling the novel A (H1N1) influenza virus: don't touch your face!. *J. Hosp. Infect.* 73, 280–281. doi:10.1016/j.jhin.2009.06.017

Manghisi, V. M., Fiorentino, M., Boccaccio, A., Gattullo, M., Cascella, G. L., Toschi, N., et al. (2020). A body tracking-based low-cost solution for monitoring workers' hygiene best practices during pandemics. *Sensors* 20, 6149.doi:10.3390/s20216149

McMonnies, C. W. (2008). Management of chronic habits of abnormal eye rubbing. *Cont. Lens Anterior Eye* 31, 95–102. doi:10.1016/j.clae.2007.07.008

Mueller, S. M., Martin, S., and Grunwald, M. (2019). Self-touch: contact durations and point of touch of spontaneous facial self-touches differ depending on cognitive and emotional load. *PLoS One* 14, e0213677. doi:10.1371/journal.pone.0213677

Mummadi, C. K., Leo, F. P. P., Verma, K. D., Kasireddy, S., Scholl, P. M., Kempfle, J., et al. (2018). Real-time and embedded detection of hand gestures with an imu-based glove. *Inform.* 5, 28. doi:10.3390/informatics5020028

Ng, A. W., and Chan, A. H. (2012). "Finger response times to visual, auditory and tactile modality stimuli," in Proceedings of the international multiconference of engineers and computer scientists, Kowloon, Hongkong, March 14–16, 2012. 2, 1449–1454.

Olivares, A., Olivares, G., Mula, F., Górriz, J. M., and Ramírez, J. (2011). Wagyromag: wireless sensor network for monitoring and processing human body movement in healthcare applications. *J. Syst. Archit.* 57, 905–915. doi:10.1016/j.sysarc.2011.04.001

Pawar, T., Chaudhuri, S., and Duttagupta, S. P. (2007). Body movement activity recognition for ambulatory cardiac monitoring. *IEEE Trans. Biomed. Eng.* 54, 874–882. doi:10.1109/tbme.2006.889186

Pisharady, P. K., and Saerbeck, M. (2015). Recent methods and databases in vision-based hand gesture recognition: a review. *Comput. Vis. Image Underst.* 141, 152–165. doi:10.1016/j.cviu.2015.08.004

Rivera, P., Valarezo, E., Valarezo, E., Choi, M.-T., and Kim, T.-S. (2017). Recognition of human hand activities based on a single wrist imu using recurrent neural networks. *Int. J. Pharma Med. Biol. Sci.* 6, 114–118. doi:10.18178/ijpmbs.6.4.114-118

Sanders, A. F. (1975). The foreperiod effect revisited. *Q. J. Exp. Psychol.* 27, 591–598. doi:10.1080/14640747508400522

Scott, J. J., and Gray, R. (2008). A comparison of tactile, visual, and auditory warnings for rear-end collision prevention in simulated driving. *Hum. Factors* 50, 264–275. doi:10.1518/001872008x250674

Siddiqui, N., and Chan, R. H. (2020). Multimodal hand gesture recognition using single iMU and acoustic measurements at wrist. *PLoS One* 15, e0227039. doi:10.1371/journal.pone.0227039

Silva do Monte Lima, J. P., Uchiyama, H., and Taniguchi, R.-i. (2019). End-to-end learning framework for imu-based 6-dof odometry. *Sensors (Basel)* 19, 3777. doi:10.3390/s19173777

Solomon, S. S., and Hill, P. F. (2002). *Emergency vehicle accidents: Prevention, reconstruction, and survey of state law*. Tucson, AZ: Lawyers & Judges Publishing.

Thompson, P. D., Colebatch, J. G., Brown, P., Rothwell, J. C., Day, B. L., Obeso, J. A., et al. (1992). Voluntary stimulus-sensitive jerks and jumps mimicking myoclonus or pathological startle syndromes. *Mov. Disord.* 7, 257–262. doi:10.1002/mds.870070312

Ward, J. A., Lukowicz, P., Troster, G., and Starner, T. E. (2006). Activity recognition of assembly tasks using body-worn microphones and accelerometers. *IEEE Trans. Pattern Anal. Mach. Intell.* 28, 1553–1567. doi:10.1109/tpami.2006.197

WHO (2020). World health organization. Avaliable at: https://covid19.who.int/ (Accessed June 09, 2020).

Yang, C., and Lv, Z. (2020). Gender based face aging with cycle-consistent adversarial networks. *Image Vis. Comput.* 100, 103945. doi:10.1016/j.imavis.2020.103945

Zhao, J.-L., Wu, Z.-K., Pan, Z.-K., Duan, F.-Q., Li, J.-H., Lv, Z.-H., et al. (2018). 3D face similarity measure by fréchet distances of geodesics. *J. Comput. Sci. Technol.* 33, 207–222. doi:10.1007/s11390-018-1814-7

Conflict of Interest: The authors declare that the research was conducted in the absence of any commercial or financial relationships that could be construed as a potential conflict of interest.

frontiers in Robotics and AI

ORIGINAL RESEARCH
published: 08 April 2021
doi: 10.3389/frobt.2021.612750

Speech Interaction to Control a Hands-Free Delivery Robot for High-Risk Health Care Scenarios

Lukas Grasse[†]*, *Sylvain J. Boutros*[†] *and Matthew S. Tata*

[1]*Canadian Centre for Behavioural Neuroscience, Department of Neuroscience, University of Lethbridge, Lethbridge, AB, Canada*

The Covid-19 pandemic has had a widespread effect across the globe. The major effect on health-care workers and the vulnerable populations they serve has been of particular concern. Near-complete lockdown has been a common strategy to reduce the spread of the pandemic in environments such as live-in care facilities. Robotics is a promising area of research that can assist in reducing the spread of covid-19, while also preventing the need for complete physical isolation. The research presented in this paper demonstrates a speech-controlled, self-sanitizing robot that enables the delivery of items from a visitor to a resident of a care facility. The system is automated to reduce the burden on facility staff, and it is controlled entirely through hands-free audio interaction in order to reduce transmission of the virus. We demonstrate an end-to-end delivery test, and an in-depth evaluation of the speech interface. We also recorded a speech dataset with two conditions: the talker wearing a face mask and the talker not wearing a face mask. We then used this dataset to evaluate the speech recognition system. This enabled us to test the effect of face masks on speech recognition interfaces in the context of autonomous systems.

Keywords: speech recognition, assistive robotics, COVID-19, medical robotics, human-robot interaction

OPEN ACCESS

Edited by:
Simon DiMaio,
Intuitive Surgical, Inc., United States

Reviewed by:
Hendrik Santosa,
University of Pittsburgh, United States
Ryan Corey,
University of Illinois at Urbana-Champaign, United States

***Correspondence:**
Lukas Grasse
lukas.grasse@uleth.ca

[†]*These authors have contributed equally to this work*

Specialty section:
This article was submitted to Biomedical Robotics, a section of the journal Frontiers in Robotics and AI

Received: *30 September 2020*
Accepted: *04 February 2021*
Published: *08 April 2021*

Citation:
Grasse L, Boutros SJ and Tata MS (2021) Speech Interaction to Control a Hands-Free Delivery Robot for High-Risk Health Care Scenarios. Front. Robot. AI 8:612750. doi: 10.3389/frobt.2021.612750

INTRODUCTION

On March 11th, 2020, the World Health Organization (WHO) declared Covid-19 to be a global pandemic (Huang et al., 2020), however the transmission and impact of the virus has varied tremendously across regional, racial, and socioeconomic boundaries. Of particular importance and concern is the role of front-line health care workers in spreading the virus (Casini et al., 2019) and the extra burden placed on those workers in situations of high transmission risk. For example in China, a study that surveyed health care workers in hospitals found that half of the employees were depressed (50.7%), close to half of them had anxiety (44.7%), over a third of them suffered from insomnia (36.1%) (Li et al., 2020), and a little under three quarter of them were facing psychological distress (Tomlin et al., 2020).

This burden faced by health-care workers is compounded when those workers are responsible for the mental and physical health of aging patients. Although the Covid-19 pandemic has affected people all over the globe, it has had a disproportionately strong effect on the aging population and their care givers. For example, as of September 2020 there have been just over 146,000 cases in Canada. Of these, 10,549 cases were staff at long-term care facilities and 18,940 were residents of such facilities. Since senior citizens account for 77% of the deaths related to SARS-CoV-2 (NIA, 2020), there was an immediate need early in the pandemic to reduce the rate of transmission to people who live in care facilities for the elderly and the care-givers who work with them. One common strategy

has been near-complete lockdown of such facilities. Although effective at reducing the risk of transmission into the resident population, this approach has the unwanted consequence of isolating residents from loved ones at a profoundly stressful time. The longer-term consequences of this physical and social isolation on the mental wellness of the aging population is not yet known. Here we describe an end-to-end robotics solution to break the physical isolation of lockdown in long-term care and similar facilities.

Robotics is a promising area of research that can contribute to an effective response to pandemic across a variety of health care scenarios. Uses have been proposed and developed ranging from assistance during Ebola outbreaks (Yang et al., 2020) to supporting children during their stay in a hospital (Joseph et al., 2018). Robotics and other autonomous systems offer the distinct advantage of uncoupling physical interactions between people by providing the option of interaction-at-a-distance. This enables robots to act as a physical link between people who cannot come into close contact. Widespread use of such systems could act as a surrogate in place of real physical interaction during periods of high risk of disease transmission.

One barrier to adoption of robotics in health care environments is the human-robot interaction (HRI) component. The research performed in this paper uses speech as a modality for interaction, in order to lower the learning curve for end users interacting with robots. Speech is an intuitive and powerful means of interaction between humans and robots, and speech recognition is increasingly being adopted for HRI in humanoid robotics (Stiefelhagen et al., 2004; Higy et al., 2018; Kennedy et al., 2017). However, speech still remains underexplored in industrial collaborative robotics. A goal of this paper was to provide insight into the scientific and technical challenges of audio HRI in complex collaborative robotics.

According the World Health Organization, the coronavirus that causes COVID-19 is transmitted by various modes, but mainly during one of two classes of interactions between individuals: either close contact that allows direct exposure to respiratory droplets, or contact with contaminated surfaces enabling the virus to be transported to the nose or mouth by the hands. Robots cannot contract respiratory diseases and do not cough or sneeze, so using robotic systems as a physical link between individuals breaks the direct respiratory transmission mode. However, most robotic systems employ at least some degree of hands-on operation so that human users can provide instructions to the robot (e.g., via a keyboard or tablet computer). This interaction exposes the risk of transmission via contaminated surfaces. A hands-free solution is needed. Here we present an end-to-end system for robotic delivery of items from a visitor to a resident of a care facility. The proposed system can operate without supervision by a facility worker thus reducing their workload and diminishing their exposure and spread of the virus. Importantly, it is controlled entirely by audio interaction for hands-free use so that both direct respiratory and indirect surface transmission modes are broken.

One novel contribution this paper makes is the evaluation of the effect masks and accented speech have on speech recognition interfaces for robotics in real-world environments. The demonstration of an end-to-end self-sanitizing delivery system is also a unique demonstration that can provide a useful starting point for roboticists looking to build such systems for real world environments. Our system demonstrates how speech control can be integrated into a robotics project, enabling users to directly communicate with robots naturally. This paper has two intended audiences. The first is speech recognition researchers who are curious about the distortion effects of masks, and will find our analysis of speech recognition performance under different mask conditions to be informative. Secondly, roboticists who are trying to develop automated delivery systems will find the technical implementation of the end-to-end solution to be one path to solve the typical problems that arise in this scenario.

MATERIALS AND METHODS

The goal of this research was to improve the quality of life and reduce the isolation of residents in facilities with a high risk of disease transmission during the pandemic. We sought to develop a system that can deliver items from visitors to residents using end-to-end voice interaction to prevent physical contact with surfaces. The robot makes use of a custom speech recognition interface to interact with humans at a distance, thus reducing the transmission of pathogens. This section begins by outlining the robotics hardware platform on which the system was demonstrated, then delves into the speech recognition interface used to control the robot, and finally outlines the implementation of a human-robot interaction workflow using a state machine. All custom software was developed using the *Python* programming language.

0.1 Robotics Platform

This section outlines the robotics platform and other hardware used to demonstrate the system in this paper. The robotics platform used was a Turtlebot 2 mobile base consisting of a Kobuki base with proximity sensors, and an Orbbec Astra Pro Depth Camera for mapping, navigation, and obstacle avoidance. The Turtlebot 2 uses an Acer netbook to run the mapping, navigation, and other aspects of the mobile base. We mounted a Raspberry Pi 3 Model B to the base of the turtlebot and attached microphones from a Logitech C920 webcam to the top of the robot. This raspberry pi was used to run the speech recognition interface described below. All communication between components of the Turtlebot 2 as well as the speech recognition system on the Raspberry Pi ran through Robot Operating System (ROS) modules. Importantly, by using ROS as a middle layer, the system is scalable to larger ROS-based rover platforms in the case that the Turtlebot 2 is insufficient for a particular use case.

0.2 Depth Camera

The depth camera was the Orbbec Astra with a depth image size of 640 × 480 (VGA) 16 bit @ 30 FPS. It has a scanning range from

0.4 to 8 m. The field of view consists of 60°horizontally, 49.5°vertically and 73°diagonally. It also has an infrared and RGB sensor (Astra, 2020).

0.3 Mapping and Navigation

The mapping was created using Robot Operating System 3D Robot Visualizer (RVIZ) (Dave Hershberger and Gossow, 2020) and gmapping (Gerkey, 2020a) packages. The gmapping package provided the turtlebot with the laser-based simultaneous localization and mapping (SLAM) node using the depthimage_to_laserscan package. Since it was impossible during the 2020 pandemic to work within the setting of a care facility, we demonstrated our system in a typical academic research building. To control which rooms we wanted to map, we used the turtlebot_teleop package, created by Wise (2020), which provided us with manual control of teleoperation using a keyboard. During this pre-mapping phase, we achieved a better map by occasionally stopping and slowly rotating the robot to draw an accurate representation of the objects and obstacles around it. We used the publish point feature in RVIZ and manually integrated the waypoints in a python dictionary to obtain the coordinates of the rooms that we wanted to include in the turtlebot's database. Each waypoint consisted of five different entries: the exact coordinates, and four nearest neighbours. The nearest neighbours were intended to be used as a fallback option. In the event that the turtlebot could not properly plan a trajectory to one set of coordinates, it fell back to the next set until a proper plan was made available to be followed. The map was stored using the map_server package, created by Brian Gerkey (2020), this produced two files (.pgm and .yaml) that were used later with the AMCL package. The AMCL package created by Gerkey (2020b) was used with the previously generated map to allow the turtlebot to navigate to specified waypoints provided by the audio interaction interface.

0.4 Sanitization Pod

Another technology that has shown promise for reducing virus transmission rates is Ultraviolet (UV) light sanitization. A recent study on UV light has shown it to be effective on killing Covid-19 virus (Kitagawa et al., 2020) in their study, the authors have demonstrated that a 222 nm Ultraviolet C (UV-C) irradiation for 30 s resulted in 99.7% decrease of SARS-CoV-2 virus. The combination of UV light sanitization and robotics is a powerful combination for fighting the war against Covid-19. An example of this combination is a robot developed by MIT and Ava Robotics that can sanitize warehouses through the use of UV-C light (Gordon, 2020). Robots can assist health care employees with trivial tasks that reduce human exposure to and the spreading of the SARS-CoV-2 pathogen.

Our system as conceived in this context is not fool-proof, for example if the robot encountered an infectious individual while navigating through the space, it is possible that it could transmit pathogens. Since many transmissible pathogens can live on surfaces for minutes to hours, we included an intermediate behaviour for the robot in which it brings the item to be delivered to a location where it can be cleaned. For our demonstration, we built a custom enclosure with an opening to represent a station for either automatic or manual sanitization of the to-be-delivered item. We envision a more elaborate future implementation that might involve automatic UV-C or similar systems.

An important aspect of voice communication is acknowledgement that the receiver is indeed listening to the speaker's instructions. Humans use behaviours such as head-turning and sometimes subtle facial gestures to convey attentiveness. To provide acknowledgement of voice commands, we used a voice-activity detection algorithm (provided by WebRTC) with an LED indicator to show that the robot was triggered to be in listening mode.

0.5 Speech Recognition Interface

The speech recognition interface consisted of multiple components that record and understand the speech of the person using the delivery robot. The following section gives a high-level overview of the speech recognition interface. The process started with voice activity detection (VAD) and speech recognition. We compared two commonly used open source speech recognition systems in our research, Mozilla DeepSpeech and Kaldi. Each speech recognition system used a custom language model with a vocabulary that was restricted to the specifics of the delivery task. Once a sentence was recognized the user intent was parsed from the sentence using simple rules. Next, we consider the specifics of each component of the system.

0.5.1 Speech Recognition and Custom Language Model

The first speech recognition system was implemented using WebRTC (Google, 2020b) for voice activity detection (VAD) and used the DeepSpeech architecture demonstrated by Hannun et al. (2014) for speech recognition. Specifically, we used the implementation from Mozilla (2020). This implementation contains a model that runs using Tensorflow Lite (Google, 2020a). This allowed us to run the speech recognition system on a raspberry pi in real-time. The system started by performing VAD on each audio frame using WebRTC and then added each incoming audio frame to a ring buffer. If the ratio of frames containing speech exceeded a threshold, the existing frames from the buffer were fed to the speech recognition system. New frames were continuously fed to both the speech recognition system and the ring buffer until the ratio fell back below the threshold. Some adjustment of the voice activity threshold were required, but once the correct threshold was determined the system was quite effective at identifying the onset of a voice.

Mozilla Deepspeech uses KenLM (Heafield, 2011) as the language model used during decoding the speech from the neural network. In this research we trained a custom KenLM language model that was used to recognize specific sentences related to initiating the robot to deliver a package, confirmation of a correct delivery location, confirmation of receipt of a package, etc. Using a reduced custom model substantially increases the accuracy of the speech recognition system's performance in real-world environments. The custom language model was a 3°g KenLM model trained with example sentences. During inference we set the language model alpha value to 0.931,289

and the beta value to 1.183,414 as these were the default values used in DeepSpeech.

The second speech recognition system we used was Kaldi (Povey et al., 2011), and the Vosk API (Cephei, 2020). For this system we used the built in voice activity detection and the *vosk-model-small-en-us* model, which was lightweight and can run on small single board computers. This model also uses the Kaldi Active Grammar feature, which enabled us to dynamically change the vocabulary of the model to only include words relevant to the delivery task. We used the same set of sentences and words used to train the previously described custom language model for DeepSpeech.

0.5.2 Intent Parsing

The next step in the speech recognition system was parsing the user's intent from the recognized speech. This was greatly simplified due to the use of the restricted language model described previously. The main type of intent parsing that occurred was detecting when a user intended to initiate a delivery, and then parsing out the location of the delivery. The first step in achieving this was to ensure a recognized sentence started with the word "robot", which implied that the user was addressing the robot. Once a sentence that started with the word robot had been recognized, the next step was parsing the location from the string. The language model was restricted such that all the delivery sentences contained the phrase "deliver this package to" as part of the sentence. An example of this is the sentence "hey robot please deliver this package to room A". The fixed structure of these sentences enabled us to split the recognized string on the words "package to" and take the remaining part of the string as the selected room for delivery.

Another type of intent parsing that occurred in our speech interface was to obtain confirmation from a user: either confirmation of a correct intended delivery location, or confirmation of successful package delivery. The first confirmation happened after the selected room identifier was parsed out of the recognized sentence. The robot used the Text-To-Speech system described in the next section to confirm with the user as to whether the room was correctly understood. The user then confirmed the location as correct or rejected the location. To do this, the language model contained multiple sentences containing various confirming statements such as "yes", "yes that is correct" etc. and other rejection statements such as "no", "no that's wrong", etc. The confirmation intent parsing step then performed keyword spotting over the recognized string to see if any of the rejection statements were present. If they were present the robot rejected the selected location and informed the user. If the sentence contained confirmation statements such as "yes" the robot then performed the delivery. The final case is one in which the perceived sentence did not contain any of the keywords, in which case the system continued listening for a confirmation or rejection.

0.5.3 Text-To-Speech

The system included a Text-To-Speech (TTS) functionality that enables it to speak to users. This is an important component of the Human-Robot Interaction as it is the primary method through which the robot communicates after parsing the delivery location and during delivery confirmation. The TTS system used was the Ubuntu say command, which uses the GNUstep speech engine created by Hill (2008). The TTS system operated using a ROS python script; when a string was published to a TTS topic the TTS system executed the say command using the subprocess library. This enabled the TTS system to be easily triggered via ROS from any device connected to roscore over the network.

0.6 State Machine for Human-Robot Interaction

All of the components demonstrated so far were connected together into a complete system using a state machine that communicated over ROS and coordinated the various aspects of the human-robot interaction. The state machine and interaction process are outlined in **Figure 1**.

The state machine facilitated an interaction scenario in which a visitor to a long-term care facility wishes to deliver a package to an at-risk individual that resides in the facility. The visitor initiated the interaction with the robot by placing a package in the robot's delivery basket and then speaking to the robot. Then the visitor instructs the robot on which room to deliver the package to by saying a sentence such as "Hey robot, please deliver this package to room E3". Once the robot has successfully parsed a delivery sentence the state machine advances to the confirmation state. In this state the robot repeats the room number to the human and asks if the room number is correct.

Once the robot received verbal confirmation, the state machine proceeded to the next state, which sent the room id over ROS to the navigation system. The navigation system then mapped the name to coordinates using the turtlebot's database. Next, the robot sanitized itself by navigating into the UV-c sanitization pod. Once the robot had waited for the correct amount of time in the pod it navigated to the coordinates for the target room. Arrival at the delivery target waypoint triggered the delivery confirmation state. In this state the robot used the TTS system to inform the recipient that they have a package and should remove it from the basket. After a time delay to account for the removal of the package the robot asked for confirmation that the package has been removed. Once the robot received this verbal confirmation, the state machine entered the final state, in which the robot navigated back to the home position.

The state machine included an error state. The error state communicated to the user that the robot did not understand a command and then returned to the initial command recognition state. This error state was specifically used during the command recognition and confirmation stages to provide a way for the robot to reset itself if instructions were unclear.

Methodology

Our tests of the implemented system consisted of a test of the delivery scenario from start to finish, and an in-depth test of the

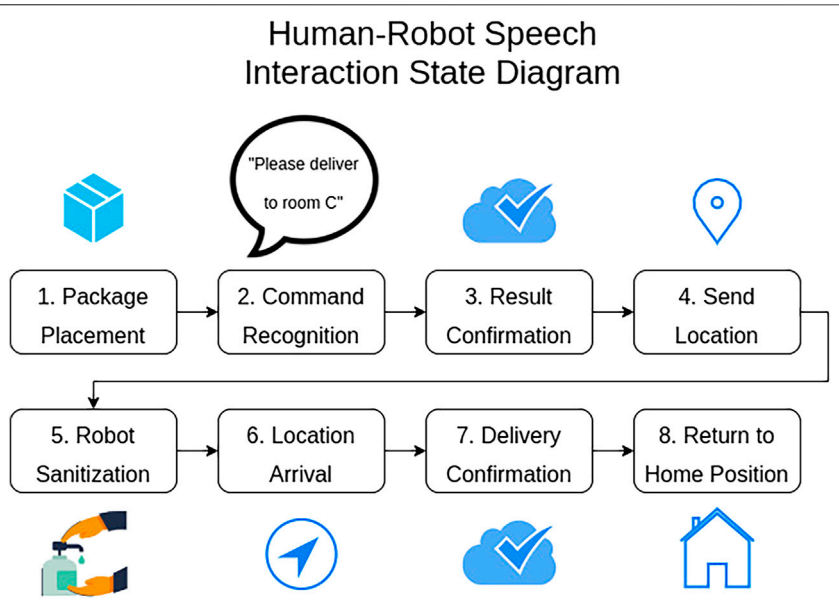

FIGURE 1 | The Human-Robot Interaction Workflow. Delivery was triggered and confirmed by speech interaction between a visitor and the robot. The robot navigated to the delivery target waypoint, with a stop to clean the item with UV-C light. At the target waypoint the robot used speech to confirm delivery and then returned to its home position. Note that the entire interaction required no physical interaction with surfaces on the robot and, except for placing and retrieving the item in the basket, could be conducted from a distance of as much as several meters away.

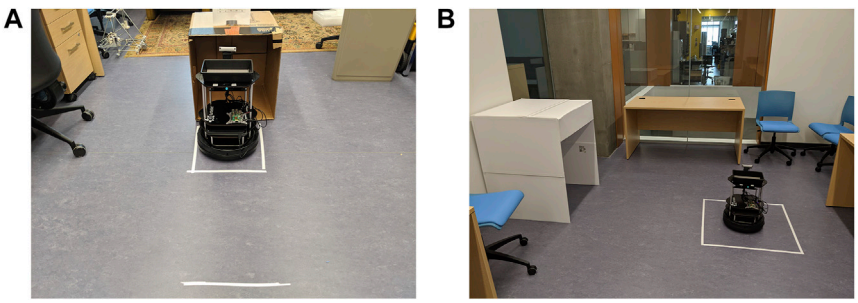

FIGURE 2 | Experimental setup for speech recognition evaluation and delivery scenario evaluation.

speech recognition component. The setups of these experiments are described below.

0.6.1 Delivery Scenario Evaluation

We verified the system's functionality by completing an end-to-end speech-controlled delivery using all of the components described in the implementation section. We envisioned a scenario in which a visitor to a care home would want a small item such as a note or gift to be delivered to a resident in a lock-down situation. Thus the test ran between two labs at the Canadian Centre for Behavioural Neuroscience at the University of Lethbridge. One lab was designated as the start point where the visitor would give the item to the robot and provide voice instructions about where to deliver it. This space also contained a designated parking area for the robot and a box intended to simulate the sanitization pod. This lab was labelled lab c (see **Figure 2**). The destination for the delivery was set to a second lab that was in the same building and connected by a hallway to the first lab. This lab was labelled lab t. The hallway contained garbage/recycling bins which provided a realistic real-world environment for navigation. Both rooms were on the same floor, as our robotics platform cannot navigate between floors. This is a critical challenge that would be important for future research in developing delivery systems.

The speech recognition system used in the test had a language model that recognised sentences such as *robot please deliver this package to room c* or *robot take this package to room t*, where *room c* and *room t* were the only valid room names. During the test a light package was placed in the delivery basket in lab c and removed in lab t upon successful delivery.

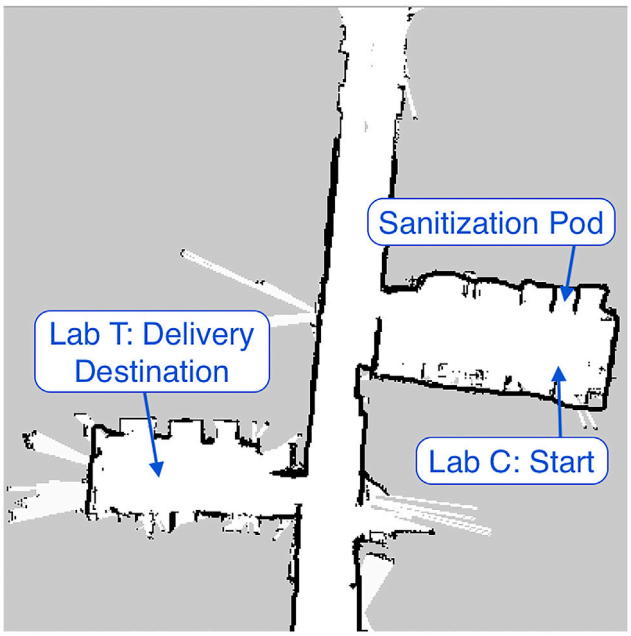

FIGURE 3 | Map generated for turtlebot navigation using the ROS gmapping package and an astra depth camera.

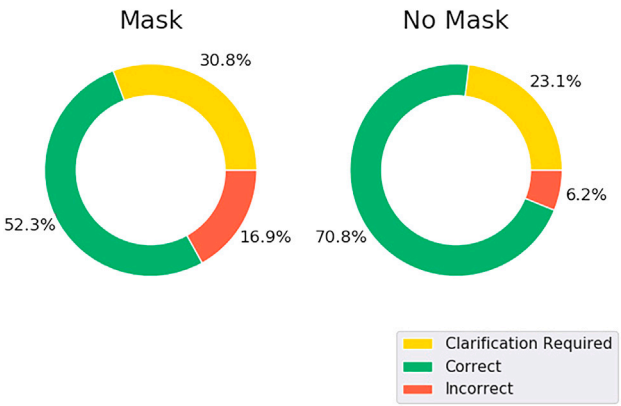

FIGURE 4 | First-pass outcomes of each recognition system with **(left)** and without **(right)** a face mask. Recognition was scored as *correct* when the intended target room was successfully recognized the first try. Recognition was scored as *clarification required* when the state machine needed to enter the error state and ask the user to repeat the instruction. Recognition was scored as *incorrect* when the system recognized the wrong room. This mode would require the user to reject the recognized room during the confirmation step and repeat the instruction.

0.6.2 Speech Recognition Evaluation

To evaluate the performance of the speech recognition system in real-world conditions, we recorded audio from 13 participants asking the robot to deliver a package to a room they selected from a list of 30 possible rooms. Audio was recorded in a typical office space with background heating/ventilation as the main source of noise (the RT60 of the room was 0.33 @ 1,000 Hz and the average SNR was 10.92 dB). Each possible room was a randomly generated combination of a single letter and single numerical digit, e.g., E4. The audio was recorded using microphones mounted on the turtlebot. Since viruses cannot be transmitted to a robot, the visitor need not maintain any particular distance from the robot. Thus, participants stood facing the turtlebot behind a line marked on the ground 61 cm back from the robot's position to speak the commands. The recording setup is shown in **Figure 2**.

A hallmark of the COVID-19 pandemic was the widespread requirement to wear a face mask in public spaces. Since such masks are known to impart a low-pass filter to speech (Corey et al., 2020), we considered whether our speech recognition system would be negatively affected if users were wearing masks. We therefore recorded speech using two conditions, one with the participant wearing a face mask and another with the face mask removed. This enabled us to calculate whether or not a face mask would impede the accuracy of each speech recognition system. For each condition we recorded five trials for a total of 10 trials per participant. Each participant wore their own personal mask. The masks consisted of a variety of cloth, disposable polyester, and other masks.

RESULTS

0.7 Experiment 1: Delivery Scenario Evaluation

The first evaluation we performed of the delivery robot was an end-to-end test delivery of a package from a starting location to an end location, as outlined in Section 0.6.1. The first step in this test was the manual generation of a map using the ROS gmapping package. The turtlebot was manually navigated using the teleop package and the generated map was saved for use during navigation. The map is shown in **Figure 3**. The coordinates of the starting point, sanitization pod, and delivery destination, were then recorded and added to the python dictionary described in Section 0.3. The command recognition component of the state machine was configured such that the recognition of the phrase *Room T* triggered a delivery to lab T and *Room C* triggered a delivery to lab C. The previously described DeepSpeech system was used for this step. The coordinates of the starting point in lab C were also used as the location of the home position.

A package was placed in the robot's delivery basket. After receiving a verbal delivery command, the robot successfully recognized and parsed the sentence asking it to deliver the package to room T. The robot then navigated into the sanitization box, waited for the correct amount of time, and then autonomously navigated to lab T. Once the package was removed and the robot received verbal confirmation it returned to the initial starting point in lab C. A video demonstration is available at[1].

[1]https://youtu.be/-LCqVXyjT1k.

TABLE 1 | First-pass Recognition Accuracy compared between participants who learned English as their first language vs. English as a second language. The best performance is highlighted in bold. Accuracy is averaged over all five recordings for each condition from all 13 participants.

Delivery Location Recognition Accuracy %				
Mask Condition	No Mask		Mask	
Approach	DeepSpeech	Kaldi/Vosk	DeepSpeech	Kaldi/Vosk
English is First language	**75.0**	**75.0**	62.5	70.0
English is second language	64.0	72.0	36.0	44.0

0.8 Experiment 2: Evaluation of Delivery Location Recognition System

The use of audio interaction to achieve hands-free autonomy for the delivery robot was a key goal of this research. We explored factors related to the success of potential failure of each speech interaction system. We were particularly interested in two factors that might influence the usefulness of audio interaction in this use case: the use of a protective face mask, and the challenge of recognizing the speech of users whose first language is not English. Specifically, we evaluated each system's delivery location recognition component as described in Section 0.6.2. Thirteen participants contributed five audio samples for each experimental condition: with and without a protective cloth mask covering the mouth and nose. The audio was recorded using the microphones on the robot. We recorded audio from both native English speakers and non-native speakers.

We measured accuracy to choose the correct target room by running each speech recognition system on the pre-recorded audio and parsing the results using the same approach as the command recognition step of the state machine. Accuracy was then calculated across all trials for each condition as the percentage of destinations that were parsed and determined successfully. The results of the experiment are shown in **Figure 4**. The mask-off condition outperformed the mask-on condition for both systems, correctly recognizing **70.8** and **73.8%** of the destinations as opposed to **52.3** and **60.0%** for the mask-on case for the DeepSpeech and Kaldi/Vosk systems respectively. We also compared the results between participants who learned English as a first language and non-native speakers of English. The results are shown in **Table 1**. We found that the speech recognition system performed poorly with non-native English, particularly when the speaker was wearing a mask.

DISCUSSION

The Covid-19 pandemic has put an enormous strain on front-line medical workers and threatened the lives of millions worldwide. The widespread effects of the virus have also disproportionately effected our aging population, who account for 77% of Covid-19 related deaths. The social and mental health impacts of lockdown measures in long-term and assisted-living care facilities for seniors, even for those who never experience the disease, are not yet known but are likely to be severe. We sought to develop an end-to-end autonomous delivery system that could break the physical isolation of care-home residents by delivering physical items (such as gifts, letters, etc.) from visitors to residents. The system needed to meet two criteria: 1) break the direct respiratory transmission pathway by using a mobile rover platform and 2) break the surface transmission pathway by providing an end-to-end hands-free speech control system. The system needed to be intuitive to use and good at trapping errors.

We built a successful system based on a ROS-controlled Turtlebot2 mobile base and free-field microphones. In ideal conditions the system demonstrated good first-pass accuracy (75% for native English speakers without masks) at understanding the target destination for the delivery. In the first-pass failure mode, 21% of outcomes were cases of the robot failing to understand any target instruction and, thus, asking for the instruction to be repeated. Only 6% of first-pass interactions resulted in the robot understanding the wrong target destination. Coupled with simple error-trapping in the confirmation step, we believe the system could perform quite well under ideal conditions.

One goal of this work was to compare commonly used speech recognition packages (DeepSpeech vs. Kaldi/VOSK). Whereas the two approaches performed identically given the hypothetically ideal case of native English speakers without masks, we found that Kaldi/VOSK handled the less-ideal case of users wearing masks. In that case Kaldi/VOSK showed a lower tendency to have high confidence in the wrong room (16.9% for DeepSpeech vs. 1.5% for Kaldi/VOSK).

There are, however, a number of challenges that were uncovered by this research. First, it is evident that face masks cause problems for automatic speech recognition. This is unsurprising given that they effectively low-pass filter the acoustic signal (Corey et al., 2020). One solution might involve training a custom acoustic model for the speech recognition system trained on audio that is recorded from people wearing masks. Alternatively, an existing speech dataset could be modified to simulate the acoustic effect of a mask. A second important challenge is that speech recognition systems may perform worse for non-native speakers of English. This is a known problem of speech recognition systems in general trained with speech from native English speakers (Hou et al., 2019; Derwing et al., 2000). Importantly though, the problem of recognizing non-native English speech and the problem of recognizing speech with a face mask seem to be interactive (such that only 36% for DeepSpeech and 44% for Kaldi/Vosk of first-pass recognitions were successful in this worst-case scenario). Creation of a more robust acoustic model could increase the reliability and widespread usefulness of the system.

Here we demonstrated the usefulness and some of the challenges associated with hands-free audio control of

robotics. By building the system around a set of ROS modules, the system is both scalable and portable to other robot systems that make use of the ROS platform. Although this research is described entirely within the context of autonomous delivery in a health-care isolation scenario, it is easy to imagine related use cases in which hands-free control of a mobile robot platform might be advantageous. It is our hope that the present study draws attention to the important contribution that audio AI can make to sound-aware robots across a wide-range of use cases.

DATA AVAILABILITY STATEMENT

The datasets for this study have not been published, as they contain personally identifiable human data. They can be made available on request.

ETHICS STATEMENT

The studies involving human participants were reviewed and approved by University of Lethbridge Institutional Review Board. The patients/participants provided their written informed consent to participate in this study.

AUTHOR CONTRIBUTIONS

LG contributed to the development of the speech recognition interface, human-robot interaction state machine, analysis, and testing, and writing. SB contributed to the development of the navigation system, sanitization pod, testing, and writing. MT contributed to the supervision of the project, writing, review, analysis, and project administration. All authors approved the final version of the submitted article.

FUNDING

The research was funded by an NSERC Canada Discovery Grant (No. #05659) and a Government of Alberta Centre for Autonomous Systems in Strengthening Future Communities grant to MT and an Alberta Innovates Graduate Student Scholarship to LG.

ACKNOWLEDGMENTS

The authors would like to thank the Agility Innovation Zone at the University of Lethbridge Learning Centre for supporting this project.

REFERENCES

Astra, O. (2020). Orbbec astra specifications. Available at: https://www.roscomponents.com/en/cameras/76-orbbec.html (Accessed October, 2020).

Brian Gerkey, T. P. (2020). Map server package. Available at: http://wiki.ros.org/map_server (Accessed October, 2020).

Casini, B., Tuvo, B., Cristina, M. L., Spagnolo, A. M., Totaro, M., Baggiani, A., et al. (2019). Evaluation of an ultraviolet c (uvc) light-emitting device for disinfection of high touch surfaces in hospital critical areas. *Int. J. Environ. Res. Public Health* 16, 3572. doi:10.3390/ijerph16193572

Cephei, A. (2020). Vosk offline speech recognition API. Available at: https://alphacephei.com/vosk/ (Accessed October, 2020).

Corey, R. M., Jones, U., and Singer, A. C. (2020). Acoustic effects of medical, cloth, and transparent face masks on speech signals. *J. Acous. Soc. America* 148 (4), 2371–2375. doi:10.1121/10.0002279

Dave Hershberger, J. F., and Gossow, D. (2020). RVIZ visualization package. Available: http://wiki.ros.org/rviz (Accessed October, 2020).

Derwing, T. M., Munro, M. J., and Carbonaro, M. (2000). Does popular speech recognition software work with esl speech? *TESOL Q.* 34, 592–603. doi:10.2307/3587748

Gerkey, B. (2020a). GMapping package. Available: http://wiki.ros.org/gmapping (Accessed October, 2020).

Gerkey, B. P. (2020b). AMCL package. Available: http://wiki.ros.org/amcl (Accessed October, 2020).

Google (2020a). Tensorflow Lite. Available: https://www.tensorflow.org/lite. (Accessed October, 2020)

Google (2020b). WebRTC. Available: https://webrtc.org/ (Accessed October, 2020).

Gordon, R. (2020). CSAIL robot disinfects greater boston food bank. Available: https://news.mit.edu/2020/csail-robot-disinfects-greater-boston-food-bank-covid-19-0629 (Accessed October, 2020).

Hannun, A., Case, C., Casper, J., Catanzaro, B., Diamos, G., Elsen, E., et al. (2014). Deep speech: Scaling up end-to-end speech recognition. Available at: http://arxiv.org/abs/1412.5567 (Accessed October, 2020).

Heafield, K. (2011). "Kenlm: Faster and smaller language model queries," in Proceedings of the sixth workshop on statistical machine translation (Edinburgh, Scotland: Association for Computational Linguistics), 187–197.

Higy, B., Mereta, A., Metta, G., and Badino, L. (2018). Speech recognition for the icub platform. *Front. Robotics AI* 5, 10. doi:10.3389/frobt.2018.00010

Hill, D. (2008). Gnuspeech: Articulatory speech synthesis. Available at: http://www.gnu.org/software/gnuspeech/ (Accessed August 23 2015).

Hou, J., Guo, P, Sun, S., Soong, F. K., Hu, W., and Xie, L. (2019). "Domain adversarial training for improving keyword spotting performance of esl speech," in ICASSP 2019-2019 IEEE International conference on acoustics, speech and signal processing (ICASSP), Brighton, UK, May 12 2019-May 17 2019 (Brighton, United Kingdom: IEEE), 8122–8126.

Huang, C., Wang, Y., Li, X., Ren, L., Zhao, J., Hu, Y., et al. (2020). Clinical features of patients infected with 2019 novel coronavirus in wuhan, China. *The lancet* 395, 497–506. doi:10.1016/s0140-6736(20)30183-5

Joseph, A., Christian, B., Abiodun, A. A., and Oyawale, F. (2018). A review on humanoid robotics in healthcare. *MATEC Web Conf.* 153, 02004. doi:10.1051/matecconf/201815302004

Kennedy, J., Lemaignan, S., Montassier, C., Lavalade, P., Irfan, B., Papadopoulos, F., et al. (2017). "Child speech recognition in human-robot interaction: evaluations and recommendations," in Proceedings of the 2017 ACM/IEEE International conference on human-robot interaction, Vienna, Austria, March 06 2017 (New York, NY, USA: ACM Press), 82–90. Available at: http://hdl.handle.net/1854/LU-8528353 (Accessed November 13, 2018).

Kitagawa, H., Nomura, T., Nazmul, T., Keitaro, O., Shigemoto, N., Sakaguchi, T., et al. (2020). Effectiveness of 222-nm ultraviolet light on disinfecting sars-cov-2 surface contamination. *Am. J. Infect. Control.*49 (3), 299–301. doi:10.1016/j.ajic.2020.08.022

Li, W., Yang, Y., Liu, Z.-H., Zhao, Y.-J., Zhang, Q., Zhang, L., et al. (2020). Progression of mental health services during the covid-19 outbreak in China. *Int. J. Biol. Sci.* 16, 1732. doi:10.7150/ijbs.45120

Mozilla (2020). mozilla/DeepSpeech. Available at: https://github.com/mozilla/DeepSpeech (Accessed October, 2020).

NIA (2020). National Institute of Ageing. Available at: https://ltc-covid19-tracker.ca (Accessed September, 2020).

Povey, D., Ghoshal, A., Boulianne, G., Burget, L., Glembek, O., Goel, N., et al. (2011). "The kaldi speech recognition toolkit," in IEEE 2011 workshop on automatic speech recognition and understanding, December 11 2011–December 15 2011, Hawaii, US, (Big Island, Hawaii: IEEE Signal Processing Society).

Stiefelhagen, R., Fugen, C., Gieselmann, R., Holzapfel, H., Nickel, K., and Waibel, A. (2004). "Natural human-robot interaction using speech, head pose and gestures," in IEEE/RSJ International Conference on Intelligent Robots and Systems, Sendai, Japan, September 28-October 2 2004, Vol. 3, 2422–2427.

Tomlin, J., Dalgleish-Warburton, B., and Lamph, G. (2020). Psychosocial support for healthcare workers during the covid-19 pandemic. *Front. Psychol.* 11, 1960. doi:10.3389/fpsyg.2020.01960

Wise, M. (2020). Turtlebot teleop package. Available at: http://wiki.ros.org/turtlebot_teleop (Accessed October, 2020).

Yang, G.-Z., Nelson, J. B., Murphy, R. R., Choset, H., Christensen, H., Collins, H. S., et al. (2020). Combating covid-19—the role of robotics in managing public health and infectious diseases. *Sci. Robot.* 5, eabb5589. doi:10.1126/scirobotics.abb5589

Conflict of Interest: The authors (LG and MT) disclose an affiliation with Reverb Robotics Inc., which develops audio AI solutions for robotics.

The remaining author declares that the research was conducted in the absence of any commercial or financial relationships that could be construed as a potential conflict of interest.

frontiers in Robotics and AI

ORIGINAL RESEARCH
published: 12 April 2021
doi: 10.3389/frobt.2021.612167

A Flexible Transoral Robot Towards COVID-19 Swab Sampling

Changsheng Li[1,2,3,4], *Xiaoyi Gu*[3,4], *Xiao Xiao*[5], *Chwee Ming Lim*[6,7], *Xingguang Duan*[1,2] *and Hongliang Ren*[3,4,8]*

[1]School of Mechatronical Engineering, Beijing Institute of Technology, Beijing, China, [2]Beijing Advanced Innovation Center for Intelligent Robots and Systems, Beijing Institute of Technology, Beijing, China, [3]Department of Biomedical Engineering, National University of Singapore, Singapore, Singapore, [4]NUS (Suzhou) Research Institute (NUSRI), Suzhou, China, [5]Department of Electrical and Electronic Engineering, Southern University of Science and Technology, Shenzhen, China, [6]Department of Otolaryngology-Head and Neck Surgery, Singapore General Hospital, Singapore, Singapore, [7]Duke-NUS Graduate Medical School, Singapore, Singapore, [8]Department of Electronic Engineering, The Chinese University of Hong Kong (CUHK), Hong Kong, China

There are high risks of infection for surgeons during the face-to-face COVID-19 swab sampling due to the novel coronavirus's infectivity. To address this issue, we propose a flexible transoral robot with a teleoperated configuration for swab sampling. The robot comprises a flexible manipulator, an endoscope with a monitor, and a master device. A 3-prismatic-universal (3-PU) flexible parallel mechanism with 3 degrees of freedom (DOF) is used to realize the manipulator's movements. The flexibility of the manipulator improves the safety of testees. Besides, the master device is similar to the manipulator in structure. It is easy to use for operators. Under the guidance of the vision from the endoscope, the surgeon can operate the master device to control the swab's motion attached to the manipulator for sampling. In this paper, the robotic system, the workspace, and the operation procedure are described in detail. The tongue depressor, which is used to prevent the tongue's interference during the sampling, is also tested. The accuracy of the manipulator under visual guidance is validated intuitively. Finally, the experiment on a human phantom is conducted to demonstrate the feasibility of the robot preliminarily.

Keywords: COVID-19, swab sampling, transoral robot, Flexible robot, sampling robot, Flexible parallel mechanism, surgical robotics, medical robotics

OPEN ACCESS

Edited by:
Mahdi Tavakoli,
University of Alberta, Canada

Reviewed by:
Christos Bergeles,
King's College London,
United Kingdom
Shuangyi Wang,
Institute of Automation (CAS), China

***Correspondence:**
Hongliang Ren
hlren@ieee.org

Specialty section:
This article was submitted to Biomedical Robotics, a section of the journal Frontiers in Robotics and AI

Received: *30 September 2020*
Accepted: *11 February 2021*
Published: *12 April 2021*

Citation:
Li C, Gu X, Xiao X, Lim CM, Duan X and Ren H (2021) A Flexible Transoral Robot Towards COVID-19 Swab Sampling. Front. Robot. AI 8:612167. doi: 10.3389/frobt.2021.612167

1 INTRODUCTION

Coronavirus disease 2019 (COVID-19) transmitted through respiratory droplets is spreading rapidly (Chaolin et al., 2020). The widely used diagnose method is the oropharyngeal-swab (OP-swab) sampling (Chen et al., 2020). This sampling is suggested to be performed by a healthcare professional, while other possible approaches such as nasal mid-turbinate swab could be self-collection under supervised (Kim et al., 2020). The healthcare workers who perform swab sampling face high infection risks caused by the testees' aerosol during the sampling, as close person to person contact is the main way for the transmission of the virus (Jin et al., 2020). Besides, the sample's quality depends on the operators' skills, which is inconsistent and may cause misdiagnosis (Li et al., 2020b). As highlighted in (Yang et al., 2020), one of the effective solutions is using the teleoperated robot that can keep the operators safe by avoiding close contact with the testees (Navid et al., 2021; Xiao et al., 2021).

Accurate swab delivery to the target region with reasonable force is essential for the teleoperated robot-assisted swab sampling (Gu et al., 2019; Hosokawa-Muto et al., 2019). Enough dexterity for the robot with at least three degrees of freedom is required to ensure that the robot can reach the target

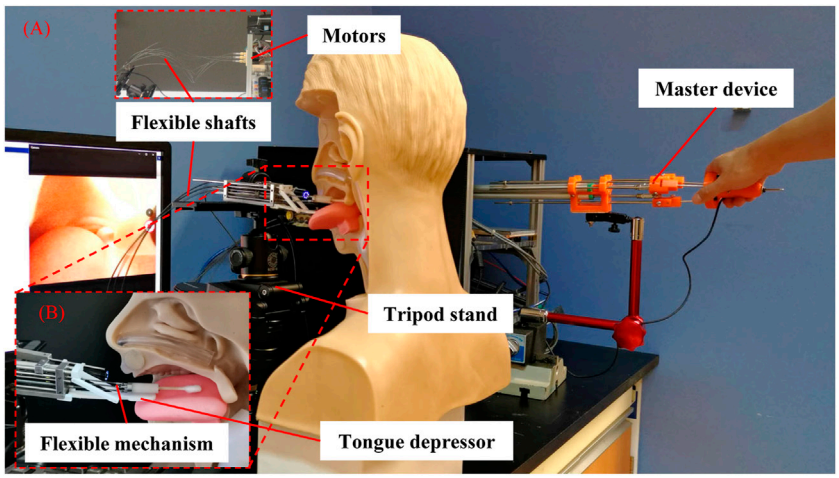

FIGURE 1 | Flexible transoral robot. **(A)** The robotic system; **(B)** The flexible manipulator.

region and to wipe through the mouth. The typical configurations are two bending DOFs with one translational DOF, or one bending DOF, one rotational DOF with one translational DOF. The workspace of the robot needs to cover the area of throat with a maximum size of 23 mm × 20 mm. The anteroposterior length of the tongue is less than 75 mm (Miguel et al., 2007). As the applied force determined the keenly feel of the testees, the robot is recommended to be compliant enough through there is no quantitation standard currently. Teleoperation is usually carried out under visual guidance. In this situation, the operator stands by the master console and teleoperates the slave robot. During the operation, the swab sampling's safety is an indispensable factor that can be achieved by a flexible mechanism or control algorithm (Park, 2007; Ren et al., 2013). As the potential irritation of the swab sampling for the testee, the operator should consider how to prevent the tongue to block the view (Sahin and Dogan, 2019). Besides, the sterilizability of the robot to prevent cross-infection should also be considered (Porter et al., 2020). Currently, the swab sampling robots are under development around the world (Wang et al., 2020), with some of them being preliminarily applied in the clinic (Li et al., 2020b). However, due to the research activities' limitation, most of the robots are still incomplete with a simple structure.

This paper proposes a flexible transoral robot towards COVID-19 swab sampling, aiming to reduce the risks of infection for the healthcare workers during the sampling. The contributions can be detailed as follows:

- A robotic system with a flexible mechanism is proposed, achieving a dexterity sampling with flexibility.
- The tongue depressor is designed for safe operation.
- The experiments, including the parameter and the performance tests of the robot, are conducted.

The rest of this paper is organized as follows. In **Section 2**, the robotic system with the workspace and the operation procedure is introduced in detail. The experimental evaluation is demonstrated. **Section 3** presents the results of the experiments. Finally, the discussion is presented in **Section 4**.

2 MATERIALS AND METHODS

2.1 System Description

2.1.1 Robotic System

The robotic system consists of a flexible manipulator with a tongue depressor mounted on a tripod stand, an endoscope (Diameter: 5.5 mm, Resolution: 1280 × 720, HL-5520, Hlisen Inc.) with a monitor for the guidance of the operation, and a master console with a master device and a controller (**Figure 1A**). To achieve the sampling, the surgeon stands by the master console and operates the master device to control the manipulator's motion under the guidance of vision obtained from the endoscope.

As shown in **Figure 1B**, the flexible parallel mechanism is designed as the manipulator's terminal. The super-elastic Ni-Ti rods (Diameter: 0.78 mm, Young's modulus: 20 Gpa, Suzuki-Sumiden Wire Products Co., Ltd.) with universal joints (MAASS-1.0, Misumi South East Asia Pte Ltd.) are used as the chains to construct a 3-prismatic-universal (3-PU) mechanism. The chains are driven by motors placed far away from the manipulator via thread rods and flexible shafts. To be specific, the motors are connected to the thread rods via flexible shafts. The thread rods are used to drive the motion of the flexible mechanism by translating the rotational motion of the flexible shafts to the translational motion of the Ni-Ti rods. The manipulator diameter is 8 mm. There are three DOFs, including two bending DOFs and one translational DOF. More details about this flexible parallel mechanism including the kinematic, stiffness analysis, evaluation, and master-slave operative performance can be found in our previous work (Li et al., 2019a; Li et al., 2019b). In brief, the manipulator can be operated stably and

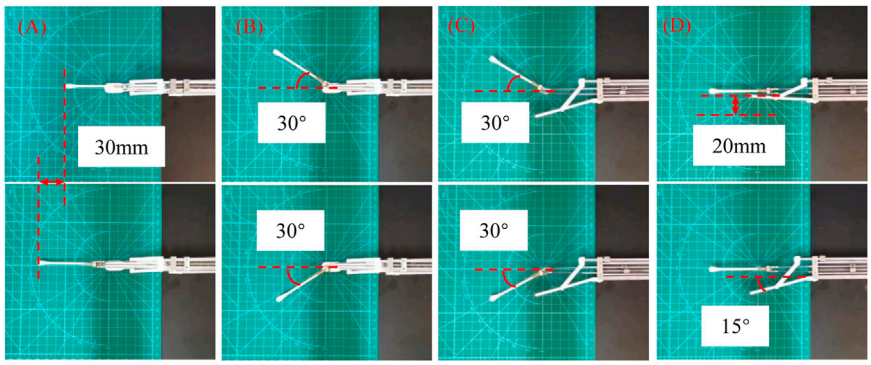

FIGURE 2 | Workspace demonstration of the robot. **(A)** The maximum displacement; **(B)** The maximum bending angle in top view; **(C)** The maximum bending angle in side view; **(D)** The motion range of the tongue depressor.

accurately with proper flexibility by combining the parallel mechanism and the flexible mechanism. The swab stick for sampling can be attached or removed from the manipulator's terminal via its mechanical interface. As the swab stick is in contact with the tissue of testee during the sampling, the compliance of the manipulator is helpful to alleviate the testee' pain and increase their safety. In our design, it is achieved via the Ni-Ti rods with super-elastic characteristic. The level of the compliance is determined by the stiffness of the rods, which is related with the sizes of their diameters.

During the sampling, there is a possibility that the swab stick would be disturbed by the spontaneous action of the tongue caused by the irritation of the throat, leading to the failure of the sampling or even additional injuries. So the tongue depressor composed by a linkage mechanism is designed to restrict the motion of the tongue. The tongue depressor can be controlled to rotate in real-time during the sampling and reset to the initial state when the manipulator inserts or retreats from the oral cavity.

The master device is mainly composed of a parallel mechanism with three prismatic-revolute-spherical (3-PRS) chains, similar to the flexible manipulator in structure. This kind of design plays an active role in decreasing the learning curve for less experienced surgeons (Li et al., 2020a). Three displacement sensors (LPZ-200, Fiaye Electric Co., Ltd.) are attached to the chains to detect the pose of the master device. Another displacement sensor (LPZ-20, Fiaye Electric Co., Ltd.) is connected to the master device terminal to control the motion of the tongue depressor. Three DOFs are achieved, including two bending DOFs and one translational DOF. The flexible manipulator's movement can be amplified by five times, allowing the operator's delicate operation. The time delay of the master-slave control has been tested in our previous work (Li et al., 2019a; Li et al., 2019b).

The personal computer (PC) with SimLab boards (Zeltom LLC.) running Matlab/Simulink programs is used as a controller. The input pose signals of the master device and the tongue depressor's control signals are obtained from the displacement sensors. The output signals are used to control the motion of the flexible manipulator via flexible shafts (Diameter: 1.7 mm, Hagitec Co., Ltd.) and screws (Diameter: 3 mm, lead: 0.5 mm) driven by direct current (DC) motors (RE13, Maxon motor Inc.).

2.1.2 Workspace Characterization

The workspace of the robot is evaluated by driving the manipulator to its limit positions, which is shown in **Figure 2**. The maximum displacement of the manipulator is 30 mm (**Figure 2A**), and the maximum bending angles of the manipulator in its top view and its side view are both 30° (**Figures 2B,C**). The displacement and the manipulator's bending angle are determined by both of the mechanical structure of the manipulator and the master device. The results show that if the swab stick's length is 60 mm, the workspace of the robot covers a cylinder space with a diameter of 60 mm and a height of 30 mm, which is large enough for the swab sampling compared with the size of the throat. As the manipulator can be placed close the throat before sampling, the translational distance of the manipulator is allowed to be shorter than the length of the anteroposterior length of the tongue. The tongue depressor's maximum moving distance is 20 mm, with a bending angle of 15° (**Figure 2D**).

2.1.3 Operation Procedure

The operation procedure is described as follows. Before the operation, the sterilized wraps are attached to the flexible manipulator, and the plastic wrap with high light transmittance are covered on the endoscope to prevent the possibility of cross-infection. After that, the robotic system is set to the initial state. The operator stands by the master console in the isolated condition. The testee faces to the mechanical design and opens the mouth. When the tongue's tip props up the tongue depressor, the operator begins to operate the flexible manipulator. The tongue depressor is controlled to hold down the tongue and allows the swab stick to reach the throat. The secret can be collected by quickly wiping the palatal arch, pharynx, and tonsil. After the operation, the swab stick and the tongue are retrieved.

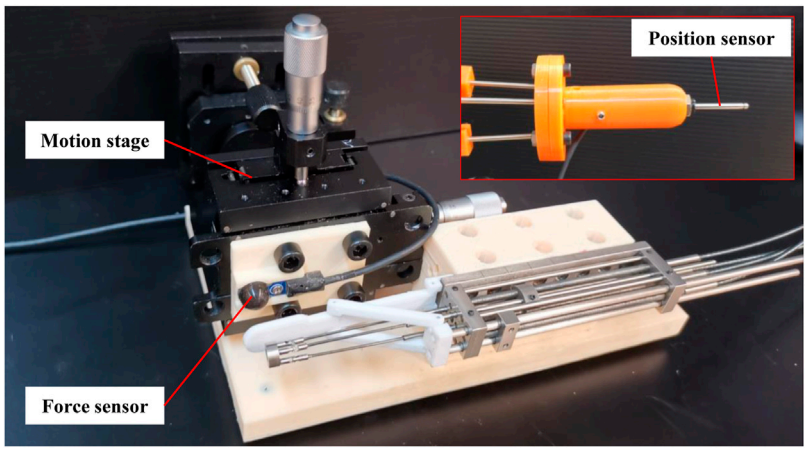

FIGURE 3 | Setup for the pressure tests of the tongue depressor.

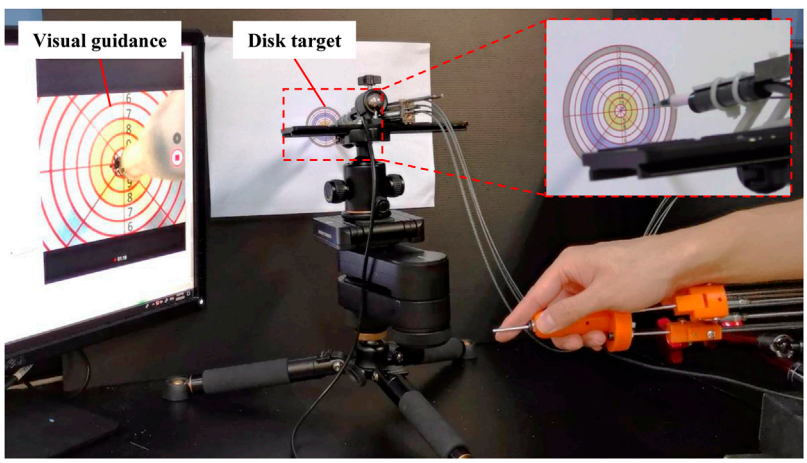

FIGURE 4 | Setup for the accuracy tests of master-slave operation under the visual guidance.

2.2 Experimental Evaluation

Three experiments were conducted to test the pressure of the tongue depressor, the accuracy of the manipulator under visual guidance, and the robotic system's performance on the human phantom (see videos in **Supplementary Materials**).

2.2.1 Pressure Tests of the Tongue Depressor

The pressure on the tongue provided by the tongue depressor should be larger than the forward force of tongue to prevent the tongue's disturbance. Nevertheless, overload pressure may lead to the increased risks of tongue injuries. So the maximum pressure of the tongue depressor is tested in this section. As shown in **Figure 3**, the force sensor (Resolution: 2.5 mN, OMD-10-SE-10N, Optoforce Ltd.) and the manipulator were attached to the motion stage via the 3D printed support. The tongue depressor was driven to rotate under the control of the position sensor attached to the master device. The force sensor detected the pressure from the terminal of the tongue depressor. This process was repeated ten times, and the pressure data from the force sensor were recorded.

2.2.2 Accuracy Tests Under Visual Guidance

The efficiency of sampling and the validity of the samples are highly related with the operative accuracy, especially for the master-slave operation under visual guidance. The tests of the master-slave operation with following the reciprocating motion and circle trajectory tracking have been conducted in our previous work (Li et al., 2019a; Li et al., 2019b). As a result, the accuracy of the master-slave operation under visual guidance was tested by a simple method as follows. As shown in **Figure 4**, the disk target with ten concentric and equally distributed circles was designed. The diameters of the first and 10th circles were 50 and 5mm, close to the diameters of the opened mouth and the uvula. A ballpoint pen refill was attached to the terminal of the manipulator instead of the swab stick. The disk target was placed in front of the manipulator with a distance of 20 mm. Under the guidance of the real-time video from the camera,

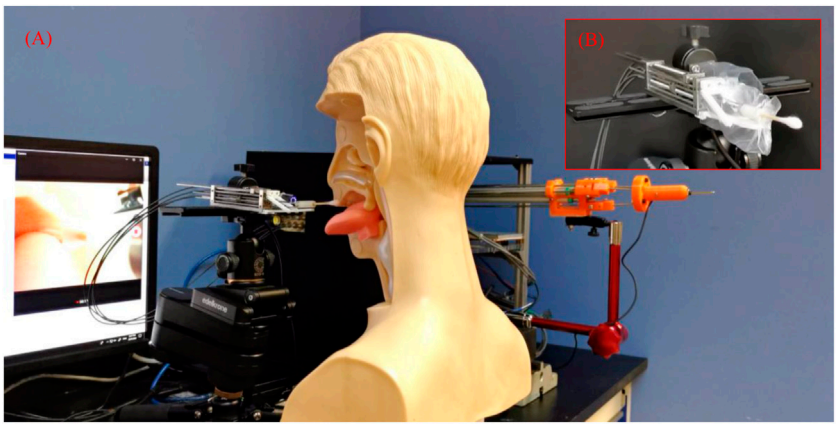

FIGURE 5 | Setup for the performance tests of the robot, **(A)** The setup of the robot, **(B)** The flexible manipulator with sterilized wraps.

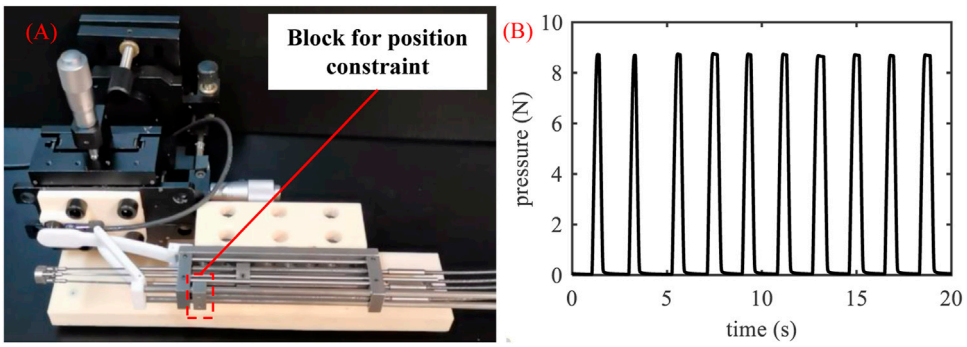

FIGURE 6 | Pressure tests of the tongue depressor, **(A)** Process of the tests, **(B)** The pressure of the tongue depressor with time.

the manipulator was driven to move towards the center of the disk target by operating the master device with an average speed of more than 6 mm/s. This process was repeated ten times.

2.2.3 Performance Tests on the Human Phantom

The performance of the robot was preliminarily tested on a human phantom to demonstrate the feasibility of sampling. As shown in **Figure 5A**, the human phantom with a ratio of 1:1 to the human body was placed in front of the robot. The manipulator with a swab stick was controlled by the operator under the visual guidance, aiming to reach the throat and swab it via a swab stick. This process was repeated three times. The method that prevents the robot from being polluted by the virus was shown in **Figure 5B**. The manipulator was covered with sterilized wraps, and the endoscope was covered with transparent preservative film for a clear vision.

3 RESULTS

3.1 Pressure of the Tongue Depressor

The results of the pressure test of the tongue depressor are shown in **Figure 6**. **Figure 6A** shows the state of the tongue depressor when it contacts the force sensor. The deformation of the tongue is caused by the elastic of the polylactic acid (PLA) material. For the safety consideration, the block that drives the tongue depressor is restricted within the manipulator frame to ensure that the rotation of the tongue depressor ranges is in a defined region. **Figure 6B** shows that the pressure is stable in each test. The average pressure of 10 trials is 8.72 ± 0.03 N. As the pressure is used to prevent the disturbance of the tongue under normal conditions, it should be much larger than the average forward force of the tongue with 2.2 N (Milazzo et al., 2019) in consideration of the individual differences and the stress reaction of the testees. According to the force transmission, the pressure of the tongue depressor is determined by the power of the driving motor, which means it can be further adjusted for practical application if it is not applicable.

3.2 Accuracy Under Visual Guidance

As shown in **Figure 7**, all the points drawn by the terminal of the flexible manipulator are located in the 10th circle, which means the accuracy of the manipulator under visual guidance is higher than 2.5 mm during the teleoperation. It is satisfied for sampling because the target region's diameter is more than 20 mm, which is

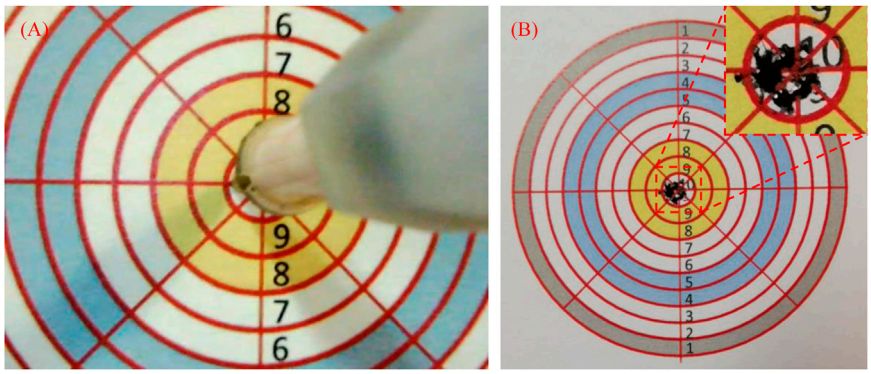

FIGURE 7 | Accuracy tests' results of master-slave operation under the visual guidance, **(A)** The process of the tests, **(B)** The results.

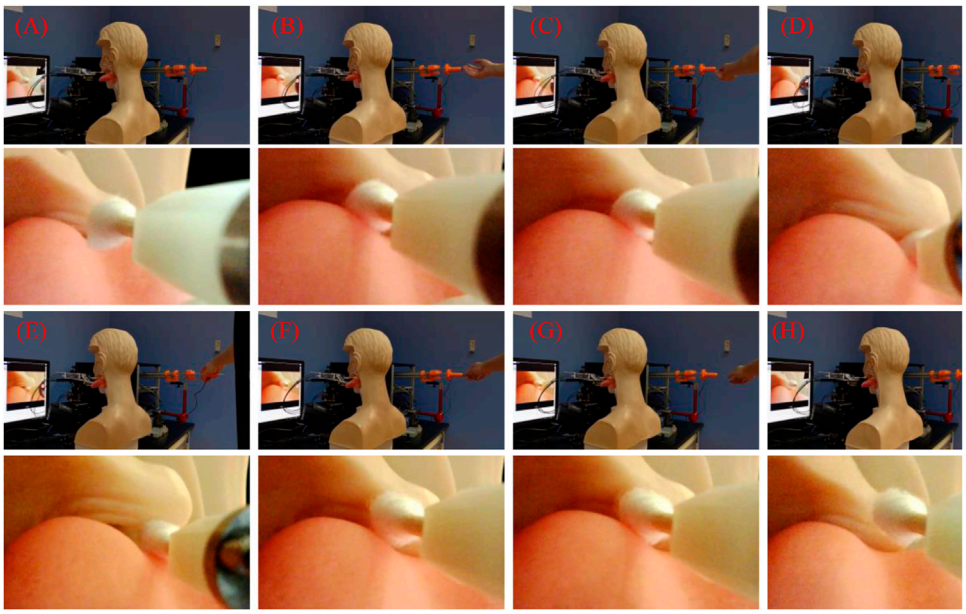

FIGURE 8 | The performance tests' results of the robot, **(A)** The flexible manipulator was set to the initial state and put on the table, **(B)** The human phantom was pushed forward with the tongue contact to the tongue depressor, **(C)** The tongue depressor was controlled to press the tongue, **(D)** The flexible manipulator was controlled to reach to the target region, **(E)** The flexible manipulator was controlled to get sample via the swab stick, **(F)** The flexible manipulator was controlled to retrieve from the throat, **(G)** The tongue depressor was retrieved, **(H)** The human phantom was pulled back.

eight times more than the maximum error. This test is practical and effective as the trial process is close to the sampling operation, though the method is simple without using precision measuring equipment.

3.3 Performance on the Human Phantom

As the operation process of the tests is similar each time, we take one as an example, which is shown in **Figure 8**. The followings are the procedure:

- The flexible manipulator was set to the initial state and put on the table (**Figure 8A**, time: 3 s).
- The human phantom was pushed forward with the tongue contact to the tongue depressor (**Figure 8B**, time: 4 s).
- The tongue depressor was controlled to press the tongue (**Figure 8C**, time: 3 s).
- The flexible manipulator was controlled to reach the target region (**Figure 8D**, time: 4 s).
- The flexible manipulator was manipulated to get a sample via the swab stick (**Figure 8E**, time: 6 s).
- The flexible manipulator was controlled to retrieve from the throat (**Figure 8F**, time: 6 s).
- The tongue depressor was retrieved (**Figure 8G**, time: 2 s).
- The human phantom was pulled back (**Figure 8H**, time: 6 s).

After this operation, the operator completed all the procedures, which lasted for 34 s. During the process, c) to g) are conducted under visual guidance. As key steps, the tongue depressor pressed the tongue effectively, and the swab stick was operated dexterously, which is satisfied for the operator. This is only a preliminary test to shown the possible procedure of the operation. More tests on human will be involved in the future to further evaluate the performance of the robot.

4 DISCUSSION

A flexible transoral robot with a teleoperated configuration is proposed to address the surgeons' risks during the face-to-face COVID-19 swab sampling due to the novel coronavirus's high infectivity. The manipulator with a 3-PU flexible parallel mechanism allows it to achieve proper flexibility, improving testees' safety. The master device is similar to the manipulator in structure, which is easy to use for operators. Under the guidance of the vision from the endoscope, the surgeon can operate the master device to control the swab's motion attached to the manipulator for sampling. As a key feature of this robot, the tongue depressor is used because there is a possibility that the tongue blocks the view to swab the back of the throat during the sampling. Hence, the tongue depressor is useful to provide a counterforce. Sterilizability is essential for surgical robotics, especially the sampling robot. Cross infection to testee should be avoided. The common methods, such as sterilized wraps, ultrasonic washing, and pasteurization, are applicable for this robot. As a quick and easy solution, we cover the sterilized wraps manually to the robot. The terminal compliance is combined by the swab with long and thin shaft and the manipulator. As the manipulator is operated under visual guidance, the deformation of the swab can be observed in real-time that indicates the contact force between the swab and the tissue as the safety assurance passively.

In this paper, the robotic system, the workspace, and the operation procedure are described in detail. The experiments are conducted to demonstrate the preliminary feasibility of the robot. The pressure tests of the tongue depressor show that proper pressure can be provided. With visual guidance, the flexible manipulator's accuracy under the master-slave configuration is acceptable for the sampling operation. The performance tests on the human phantom show the basic operation procedure, providing a reference for application. In practical application, the operator can stand far away from the slave manipulator by extend the cables connecting the controlled and the computer to avoid the face to face sampling. Besides, this robot can also be used for self-testing. The master-slave configuration under visual guidance makes the test easier. And the disturbance of the tongue can be reduced by the tongue depressor.

As a surgical robot, many difficulties need to be overcome before its clinical deployments. More experiments will be conducted to evaluate the performance of the robot, such as the success rate of sampling and the testee's adverse reaction. The fully autonomous operation will be taken into consideration.

DATA AVAILABILITY STATEMENT

The original contributions presented in the study are included in the article/**Supplementary Material**, further inquiries can be directed to the corresponding author.

AUTHOR CONTRIBUTIONS

HR and CML initiated and supervised the project. CL contributed to the development of the hardware and preparation of the manuscript. All attended and contributed to the research discussion and manuscript revisions.

FUNDING

This work is supported by the National Key R&D Program of China 2018YFB1307700 (including the associated subprogram 2018YFB1307703), The Ministry of Science and Technology (MOST) of China, and Singapore NMRC Bedside & Bench under grant R-397-000-245-511 awarded to HR, and National Natural Science Foundation of China (No. 62003045, No. 62073043) awarded to CL and XD.

ACKNOWLEDGMENTS

We would like to thank Dr. Yusheng Yan for his enthusiastic help.

SUPPLEMENTARY MATERIAL

The Supplementary Material for this article can be found online at: https://www.frontiersin.org/articles/10.3389/frobt.2021.612167/full#supplementary-material.

REFERENCES

Chaolin, H., Yeming, W., Xingwang, L., Lili, R., Jianping, Z., Yi, H., et al. (2020). Clinical features of patients infected with 2019 novel coronavirus in wuhan China. *Lancet* 395, 497–506. doi:10.1016/S0140-6736(20)30183-5

Chen, N., Zhou, M., Dong, X., Qu, J., Gong, F., Han, Y., et al. (2020). Epidemiological and clinical characteristics of 99 cases of 2019 novel coronavirus pneumonia in wuhan, China: a descriptive study. *Lancet* 395, 507–513. doi:10.1016/s0140-6736(20)30211-7

Gu, X., Li, C., Xiao, X., Lim, C. M., and Ren, H. (2019). A compliant transoral surgical robotic system based on a parallel flexible mechanism. *Ann. Biomed. Eng.* 47, 1329–1344. doi:10.1007/s10439-019-02241-0

Hosokawa-Muto Qiu, J., Sakai, H., Sassa, Y., Fujinami, Y., and Nakahara, H. (2019). Rapid detection of pathogenic virus genome sequence from throat and nasal swab samples using an exhaustive gene amplification method. *Forensicence, Med. Pathol.* 15, 399–403. doi:10.1007/s12024-019-00128-z

Jin, Y., Cai, L., Cheng, Z., Cheng, H., Deng, T., Fan, Y., et al. (2020). A rapid advice guideline for the diagnosis and treatment of 2019 novel coronavirus (2019-

ncov) infected pneumonia (standard version). *Mil. Med. Res.* 7, 1. doi:10.1186/s40779-020-0233-6

Kim, S. B., Huh, K., Heo, J. Y., Joo, E. J., and Yeom, J. S. (2020). Interim guidelines on antiviral therapy for covid-19. *Infect Chemother*. 52, 281–304. doi:10.3947/ic.2020.52.2.281

Li, C., Gu, X., Xiao, X., Lim, C. M., and Ren, H. (2019b). A robotic system with multichannel flexible parallel manipulators for single port access surgery. *IEEE Trans. Ind. Inf.* 15, 1678–1687. doi:10.1109/tii.2018.2856108

Li, C., Gu, X., Xiao, X., Lim, C. M., and Ren, H. (2020a). Cadaveric feasibility study of a teleoperated parallel continuum robot with variable stiffness for transoral surgery. *Med. Biol. Eng. Comput.* 58, 2063–2069. doi:10.1007/s11517-020-02217-6

Li, C., Gu, X., Xiao, X., Lim, C. M., and Ren, H. (2019a). Flexible robot with variable stiffness in transoral surgery. *IEEE/ASME Trans. Mechatronics PP* 23, 120–128. doi:10.1109/TMECH.2019.2945525

Li, S.-Q., Guo, W.-L., Liu, H., Wang, T., Zhou, Y.-Y., Yu, T., et al. (2020b). Clinical application of intelligent oropharyngeal-swab robot: implication for covid-19 pandemic. *Eur. Respir. J.* 56 (2), 2001912. doi:10.1183/13993003.01912-2020

Miguel, D. M., CecÃ, L. M., Costa, L. C. D., and Geraldo, L. F. (2007). Pharyngeal dimensions in healthy men and women. *Clinics* 62, 5–10. doi:10.1590/s1807-59322007000100002

Milazzo, M., Panepinto, A., Sabatini, A. M., and Danti, S. (2019). Tongue rehabilitation device for dysphagic patients. *Sensors* 19, 4657. doi:10.3390/s19214657

Navid, F., Mahdi, T., Rajnikant, P., and Atashaz, S. F. (2021). Robotics and ai for teleoperation, tele-assessment, and tele-training for surgery in the era of covid-19: existing challenges, and future vision. *Front Robot Al.* 8, 16. doi:10.3389/frobt.2021.610677

Park, S. (2007). "Safety strategies for human-robot interaction in surgical environment," in 2006 SICE-ICASE international joint conference, Busan, South Korea, October 18–21, 2006.

Porter, J., Blau, E., Gharagozloo, F., Martino, M., Cerfolio, R., Duvvuri, U., et al. (2020). Society of robotic surgery review: recommendations regarding the risk of covid-19 transmission during minimally invasive surgery. *BJU Int.* 126, 225–234. doi:10.1111/bju.15105

Ren, H., Lim, C. M., Wang, J., Liu, W., Song, S., Li, Z., et al. (2013). Computer-assisted transoral surgery with flexible robotics and navigation technologies: a review of recent progress and research challenges. *Crit. Rev. Biomed. Eng.* 41, 365–391. doi:10.1615/critrevbiomedeng.2014010440

Sahin, C., and Dogan, B. (2019). The development of a new medical instrument: modified tongue depressor. *J. Craniofac. Surg.* 30 (7), e595–e597. doi:10.1097/scs.0000000000005596

Wang, S., Wang, K., Liu, H., and Hou, Z. (2020). Design of a low-cost miniature robot to assist the covid-19 nasopharyngeal swab sampling. *IEEE Trans. Med. Robot. Bionics.* 2020, 1–5. doi:10.1109/TMRB.2020.3036461

Xiao, X., Poon, H., Lim, C. M., Meng, M. Q.-H., and Ren, H. (2021). Pilot study of trans-oral robotic-assisted needle direct tracheostomy puncture in patients requiring prolonged mechanical ventilation. *Front. Robot. Al.* 7, 575445. doi:10.3389/frobt.2020575445

Yang, G. Z., Nelson, B. J., Murphy, R. R., Choset, H., and Mcnutt, M. (2020). Combating covid-19–the role of robotics in managing public health and infectious diseases. *Science Robot.*. 5 (40), eabb5589. doi:10.1126/scirobotics.abb5589

Conflict of Interest: The authors declare that the research was conducted in the absence of any commercial or financial relationships that could be construed as a potential conflict of interest.

frontiers in Robotics and AI

REVIEW
published: 12 April 2021
doi: 10.3389/frobt.2021.610529

Review: How Can Intelligent Robots and Smart Mechatronic Modules Facilitate Remote Assessment, Assistance, and Rehabilitation for Isolated Adults With Neuro-Musculoskeletal Conditions?

S. Farokh Atashzar[1]*, *Jay Carriere*[2] *and Mahdi Tavakoli*[2]

[1]Department of Electrical and Computer Engineering, Department of Mechanical and Aerospace Engineering, New York University, New York, NY, United States, [2]Department of Electrical and Computer Engineering, University of Alberta, Edmonton, AB, Canada

OPEN ACCESS

Edited by:
Elena De Momi,
Politecnico di Milano, Italy

Reviewed by:
Salih Ertug Ovur,
Politecnico di Milano, Italy
Matteo Sposito,
Italian Institute of Technology (IIT), Italy

***Correspondence:**
S. Farokh Atashzar
f.atashzar@nyu.edu

Specialty section:
This article was submitted to Biomedical Robotics, a section of the journal Frontiers in Robotics and AI

Received: 26 September 2020
Accepted: 08 February 2021
Published: 12 April 2021

Citation:
Atashzar SF, Carriere J and Tavakoli M (2021) Review: How Can Intelligent Robots and Smart Mechatronic Modules Facilitate Remote Assessment, Assistance, and Rehabilitation for Isolated Adults With Neuro-Musculoskeletal Conditions?. Front. Robot. AI 8:610529. doi: 10.3389/frobt.2021.610529

Worldwide, at the time this article was written, there are over 127 million cases of patients with a confirmed link to COVID-19 and about 2.78 million deaths reported. With limited access to vaccine or strong antiviral treatment for the novel coronavirus, actions in terms of prevention and containment of the virus transmission rely mostly on social distancing among susceptible and high-risk populations. Aside from the direct challenges posed by the novel coronavirus pandemic, there are serious and growing secondary consequences caused by the physical distancing and isolation guidelines, among vulnerable populations. Moreover, the healthcare system's resources and capacity have been focused on addressing the COVID-19 pandemic, causing less urgent care, such as physical neurorehabilitation and assessment, to be paused, canceled, or delayed. Overall, this has left elderly adults, in particular those with neuromusculoskeletal (NMSK) conditions, without the required service support. However, in many cases, such as stroke, the available time window of recovery through rehabilitation is limited since neural plasticity decays quickly with time. Given that future waves of the outbreak are expected in the coming months worldwide, it is important to discuss the possibility of using available technologies to address this issue, as societies have a duty to protect the most vulnerable populations. In this perspective review article, we argue that intelligent robotics and wearable technologies can help with remote delivery of assessment, assistance, and rehabilitation services while physical distancing and isolation measures are in place to curtail the spread of the virus. By supporting patients and medical professionals during this pandemic, robots, and smart digital mechatronic systems can reduce the non-COVID-19 burden on healthcare systems. Digital health and cloud telehealth solutions that can complement remote delivery of assessment and physical rehabilitation services will be the subject of discussion in this article due to their potential in enabling more effective and safer NMSDK rehabilitation, assistance, and assessment service delivery. This article will hopefully lead to an interdisciplinary dialogue between the

medical and engineering sectors, stake holders, and policy makers for a better delivery of care for those with NMSK conditions during a global health crisis including future pandemics.

Keywords: COVID19, Medical Robotics, neuro-musculoskeletal disorders, telerehabilitation, smart digital health

1 INTRODUCTION

Worldwide, over 127 million cases of patients with a confirmed link to COVID-19 and about 2.78 million deaths have been reported at the time this article was written (Johns Hopkins University. (2020)). With limited access to vaccine or strong antiviral treatment for the novel coronavirus, actions in terms of prevention and containment of the virus transmission rely mostly on social distancing among susceptible and high-risk populations (Block et al. (2020); Lewnard and Lo (2020); World Health Organization. (2020)). Also, mitigation strategies among suspicious and positively tested populations again rely on isolation measures, with the exception of those who are sufficiently ill to be hospitalized (Jawaid (2020); Tripathy (2020)). This review paper focuses on elderly adults with acute or chronic neuro-musculoskeletal disorders and disabilities.

Aside from the direct challenges posed by the novel coronavirus pandemic, there are serious and growing secondary consequences (explained below) caused by physical distancing, isolation guidelines, and by focusing the healthcare resources almost only on COVID-19 (Bartolo et al. (2020)). Related to the mentioned consequences, it should be noted that the healthcare system's resources and capacity have been focused on addressing the COVID-19 pandemic, causing less urgent care, (e.g. physical neurorehabilitation and assessment) to be paused, canceled, or delayed, resulting in non-COVID health-related concerns for patients suffering from other conditions, such as post-stroke disabilities (for which intense and immediate rehabilitation is needed). However, In many jurisdictions, in-person visits to rehabilitation clinics were prohibited with the exception of serious emergency cases; thus, at best, non-emergency assessment and rehabilitation were transitioned to remote delivery via verbal or visual teleconferencing (please see Caso and Federico (2020); Ferini-Strambi and Salsone (2020); Leocani et al. (2020); Ng et al. (2020); Seiffert et al. (2020); Srivastav and Samuel (2020); Venketasubramanian (2020)). As a result, this has left the elderly and adults with acute and chronic conditions, in particular those in need of receiving neuromusculoskeletal rehabilitation services, without the required support resulting in serious delays for therapeutic and rehabilitation services (Schirmer et al. (2020)). This has also resulted in delays between the appearance of symptoms of a non-COVID life-threatening condition (such as stroke or heart attack) and when patients seek urgent care (Lange et al. (2020); Kansagra et al. (2020)). Unfortunately, in many cases, such as stroke, fast initiation of treatment and prompt followup rehabilitation services are critical, since 1) late initiation of therapy can result in vaster damage, and 2) neural plasticity after stroke decays very quickly with time. In addition, in many cases, care for non-life-threatening chronic disabilities and illnesses has been deferred to the future, creating a backlog that will take years to clear. All of these put an excessive amount of pressure on the infrastructure of society including healthcare systems in various domains which are now serving for the fight against the virus among the society.

Given that multiple waves of the outbreak are expected (Stefana et al. (2020); Xu and Li. (2020)) in the coming months worldwide, it is important to address this issue as societies have a duty to protect the most vulnerable populations. The actions which are being taken during this process will be imperative to boost up our healthcare system and make it prepared not only for future waves of this pandemic but also for future pandemics. The COVID-19 pandemic has shown that our current healthcare system and model of healthcare delivery are far more unprepared (King. (2020)) than anticipated and require rethinking and substantial future preparation in order to provide continuity of care throughout the second and third waves of COVID-19 and for potential future pandemics.

In this article, we provide a detailed and targeted analysis of the literature based on which we argue that intelligent robotics and smart wearable technologies can help with extended, accessible, and remote delivery of assessment and rehabilitation services while physical distancing and isolation measures are in place to curtail the spread of the virus. We will also discuss that through supporting patients and medical professionals during this pandemic, robots, and smart mechatronic systems (such as telerobotic rehabilitation platforms), which have been designed in the literature and can be exploited here, have the potential to reduce the non-COVID-19 burden on healthcare systems so that the hospitalization and treatment of COVID-19 patients can remain the top priority.

This article conducts a literature survey supporting the use of robotics technologies and AI for enhancing the quality of care delivery specially for patients with NMSK conditions. This is motivated by the fact that, in times of deep health crises such as during the novel coronavirus pandemic, medical robotic and smart wearable systems can play a positive role by assisting the healthcare system and safeguarding public health in various ways. Within this review we define smart wearable systems as wearable IoT type devices, (e.g. a FitBit) which contain various sensors and can provide feedback (through visual or other means) to the patient. We will discuss exoskeletons separately, given their utility for rehabilitation and assistance. Another robotic modality we will discuss are telerobots, which can enable closed-loop, autonomous, and semi-autonomous kinesthetic interaction between an in-home patient and in-clinic therapies for rehabilitation exercises of stroke patients (Atashzar et al. (2016a); Shahbazi et al. (2016); Atashzar et al. (2018); Hooshiar et al. (2019); Panesar et al. (2019); Fong et al.

(2020a); Fong et al. (2020b); Sharifi et al. (2020)). In addition, robots and telerobots can be used to help in preventing the spread of COVID-19 by making it possible for frontline healthcare workers to screen, triage, evaluate, monitor, and even treat patients from a safe distance (please see Tavakoli et al. (2020) for a high-level review of how robotics can aid the healthcare workers, and society). In this regard, digital health and telehealth solutions that integrate assessment and physical rehabilitation of people with chronic NMSK conditions are the focus of this review article and will be the subject of discussion below due to their potential in enabling more effective and safer NMSK rehabilitation and assessment service delivery. We will present examples of robotic systems that aid and complement remote delivery of assessment and physical rehabilitation services for adults with chronic conditions.

It should be highlighted that this paper is written based on the lessons we learned from COVID-19, in particular the deficiency of remote rehabilitation and assessment for patients considering a wide demographics. COVID-19 has proven that our healthcare system is not prepared for taking such an unprecedented challenge. This paper examines not only the current activities but also the future horizon of technology and investigates how can intelligent robots and smart mechatronic modules facilitate remote assessment, assistance, and rehabilitation for isolated adults with NMSK conditions. The last sentence is indeed the title of the paper to show that we not only consider direct challenges caused by COVID-19 but also we look beyond COVID-19 to broaden the knowledge on the potentials for the existing technologies to martialize the health care of tomorrow.

In addition to discussing existing rehabilitation and assistive technologies for a more efficient delivery of care for individuals with NMSK disabilities, we also discuss where there is potential for further use of this technology to improve the quality of life among this population. This will hopefully lead to an interdisciplinary dialogue between the medical and engineering communities in addition to the end-users of these technologies, i.e., people in long-term or home care with chronic NMSK conditions. This article also attempts to open a line of conversation, supported by strong literature, between the public, stakeholders, and policymakers about the real, practical, and life-saving benefits that can be achieved in a short-term future with the use and fusion of existing robotic, telerobotic, and wearable technologies in the healthcare system.

It should be highlighted that, before the pandemic era, robotics and automation were often tagged in several analyses as a force that can eliminate jobs and damage humanity and society. This article represents a targeted and focused literature review to impress upon the fact that at this time, more than ever, we need to invest in and investigate the life-saving potentials of robotics and AI to better serve our society and reduce the burden on healthcare systems during such unprecedented situation. A science-based ethics-centered shift of culture toward more advanced use of technology to assist delivery of healthcare services (and in particular those related to NMSK conditions) requires increasing the awareness about the features of existing technologies, besides, dialogue, and collaboration. This perspective review article aims to be one step in that direction.

2 POPULATION AGING BEFORE COVID-19: AN UNDERLYING COMPOUNDED PROBLEM

Based on official numbers and statistics, the population of senior adults worldwide over the age of 60 is expected to more than double by 2050. It is anticipated that by 2047, the number of senior adults will exceed the number of children. This trend is expected to continue due to increased life expectancy and reduced fertility rates. An aging society can become a global public health challenge in the near future and have significant social and economic effects on healthcare systems worldwide (Christensen et al. (2009); Chatterji et al. (2015); Suzman et al. (2015); World Health Organization (2015)). The rapid aging of societies worldwide is likely to increase the incidence rate of age-related neuromuscular and sensorimotor degeneration and corresponding disabilities. These age-related neuro-muscular disabilities are caused by various factors such as normal degeneration, stroke, and musculoskeletal conditions, resulting in sensorimotor dysfunction (Degardin et al. (2011)), impaired mobility (Wesselhoff et al. (2018)), and long-lasting motor disabilities (Alawieh et al. (2018)), directly affecting the quality of life of senior adults (Almkvist Muren et al. (2008)). In addition to the deleterious effect on the quality of life, these disabilities can reduce life expectancy, increase the risk of injuries (particularly fall-related injuries), and result in further cognitive and sensorimotor deterioration.

Stroke is the leading cause of significant age-related neuromuscular and sensorimotor impairment (Mukherjee and Patil (2011); Prince et al. (2015); Mozaffarian et al. (2015)) and causes excessive pressure on healthcare systems. This has been a major concern even before the substantial extra pressure due to the pandemic. Many stroke survivors experience permanent or long-lasting motor disabilities and often require labor-intensive sensorimotor rehabilitation therapies and progress monitoring during the golden time of recovery, the acute post-stroke phase, and an extended period of time afterward (Dimyan and Cohen (2011); Teasell and Hussein (2016)). The need to rapidly begin treatment after a stroke and the extended duration of treatment for stroke patients (Arias and Smith (2007); Cumming et al. (2008); Cumming et al. (2011); Yen et al. (2020)), places a significant burden on the healthcare system. The likely outcome is that, with a healthcare system that is already under-resourced, many patients suffering from a significant functional deficit would not receive sufficient rehabilitation and progress monitoring services during the pandemic, when the healthcare system is extensively loaded with managing (and preparing for) COVID-19 patients.

For a broad range of NMSK disabilities, it has been shown that rehabilitation technologies, including multimodal biofeedback, functional electrical stimulation therapy, and intelligent robotic rehabilitation systems can significantly help patients in regaining some of the lost sensorimotor functionalities (please see Takeda et al. (2017); Atashzar et al. (2019); Yang. et al. (2019b) and references therein). These rehabilitation technologies have been seen as an adjunct to traditional rehabilitation therapies, and may potentially replace traditional therapies for accelerating neural

plasticity and regaining lost sensorimotor function, which results in increasing functional capacity, quality of life, and ultimately patient independence. The concern of societal aging and age-related NMSK disorders is more pronounced due to the current pandemic. Most of the patients in need of urgent and long-term NMSK rehabilitation services are senior adults who are in the vulnerable category considering the demographics related to COVID19. The question is, "how can we deliver rehabilitation services to this population during, and after COVID19 pandemic?" This question has raised in a serious international conversations on how to deliver acute stroke rehabilitation during the pandemic (please see the following citations and references therein Lyden. (2020); Rudilosso et al. (2020); Smith et al. (2020); Wang et al. (2020)). The problem is that a long delay can result in losing major motor functionality, which would not happen if rehabilitation was delivered in a timely manner, minimizing permanent damages. A systematic literature-based investigation on this question to find alternative solutions can highlight the use of Robotics and AI technologies for rehabilitation, which is the focus of this article and can help with addressing the excessive pressure on the healthcare systems resulting in interruption of neurorehabilitation for patients in need.

3 CATEGORIES OF ROBOTIC SYSTEMS FOR BOOSTING CARE DELIVERY

Figure 1 demonstrates the overall design of the paper and shows how various modalities of robotics can be used for three main modalities of the healthcare spectrum (rehabilitation, assessment, and assistance) needed for patients with NMSK disabilities during and after a pandemics. In **Figure 1**, we categorize various robotic systems and various modalities of care. Some robots can be used for multiple modalities of care. For example, an exoskeleton can be used to retrain a post-stroke patient when the patient performs a wide range of robotics-enabled treadmill based task in a virtual reality environment so that gradually the patient's nervous system can be retrained and the patient can walk better out of the robot. For this, the physical, intensity, and temporal characteristics of robotic therapy should be designed in a way that maximizes the engagement of the patient and stimulation f the nervous systems. An example of this technology is Locomat from Hocoma (Switzerland). In addition, the exoskeleton can be used as an advanced wheelchair in the format of an assistive device, the primary function of which is to help the patient to perform the activities of daily living with the use of the robot without being too concerned about retraining the brain. In this regard, the robot should be able to detect the intention of the patient and help to perform the task for the patient. Another example is social robotic systems for kids with cerebral palsy, which has shown potential for helping this population to better engage in sensorimotor learning activities over time of aging as a rehabilitative device. Also, social robots are used for elderlies to assist them in managing isolation in long-term care facilities (as an assistive device). **Figure 1** shows the overall concept of the paper when we classify the modalities of robotic systems and modalities of care services, emphasizing

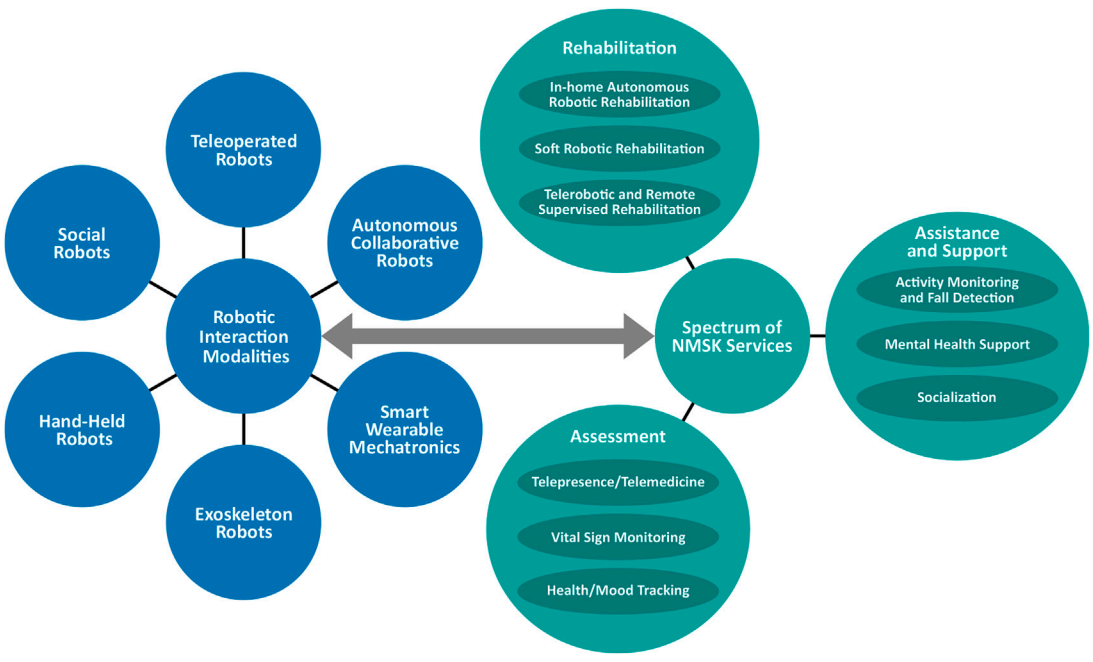

FIGURE 1 | Categories of robotic interaction and example remote rehabilitation, assessment, assistance, and support tasks for adults with neuro-musculoskeletal conditions.

that robotic systems can be used in a variety of health care application, while some format of robotic systems can have multiple health care application and some may have one or few applications. In this paper, based on the concept shown in **Figure 1**, we will discuss different robotic modalities which have been used for a wide range of spectrum of care for patients with NMSK conditions. In the current section, categories of robotic systems are introduced for boosting the care delivery, while **Sections 4**, **5** and **6** will provide relevant discussions about the use of robots for addressing the mentioned spectrum during and after COVID-19 with the focus on patients living with NMSK.

In the literature, a wide range of robotic systems and wearable technologies have been introduced to help people with NMSK conditions. In order to establish an efficient discussion about the existing technologies and how they can be adapted to help with the current pandemic situation, it is advantageous to discuss a number of definitions and ways to classify such technologies. Categories can be defined according to either 1) *mechanical structure* or 2) *modality of human-robot interaction (HRI)*. The former explained the mechanical characteristics of the robots regardless of how it interacts with humans, while the latter focuses on how these systems physically and intelligently interact with humans to deliver the needed care. In this article, the modality of interaction is considered to be the primary distinguishing factor between various robotic and wearable systems. The resulting categories can be defined as *Telerobots, Autonomous Collaborative Robots, Exoskeleton Robots, Smart Wearable Mechatronic Systems, Hand-held Robots, and Social Robots*. The proposed categorization (which takes into account the interaction, intelligence, and control) helps to lead the discussion on how particular styles of robotic systems can assist with the three core modalities of the spectrum of healthcare for NMSK patients, during the COVID19 pandemic, namely, *assessment, rehabilitation, assistance*.

The intersections between various human-robot interaction modalities and the spectrum of healthcare delivery are shown in **Figure 1**. In this article, we provide literature-based discussion

TABLE 1 | Summary of advantages and limitations of robotic interaction modalities.

		Advantages	Limitations
Robotic interaction modalities	Teleoperated robots	Remote operation; sensory augmentation through data fusion; motor augmentation; bypassing the barrier of distance; computerized interaction to log the performance metrics of both users at the two terminals	Minimum to no autonomy; concerns regarding transparency of reflected force field; susceptibility of system stability to network time delay and the variation in the delays which may challenge safety; relatively high cost due to the need for two robots; synchronization challenges
	Autonomous collaborative robots	High level of autonomy; need for minimum-to-no intervention from human; allowing for higher level of distancing; possibility of infinite work space (for mobile systems); can be integrated with existing mechanical and mechanic systems such as wheelchairs; securing a high level of sensor-based situational awareness; minimizing possible human error (depending on the context) relying on the past data and cloud computation	Totally removing the human domain knowledge from the loop which can raise safety risks for unseen situations and under unstructured conditions; susceptibility to sensor failure; susceptibility to biases in the data sets based on which a behavior is trained; need for extra and redundant sensors with high speed which can increase the cost and accessibility
	Exoskeleton robots	Joint-space operation for augmenting the natural motor ability of users; augmenting the mechanical power of the wearer and enhancing the safety; ability to serve as both assistive and rehabilitative system; reducing the mechanical load on the joints, skeleton, and muscles of the users (such as workers) supporting a high level of musculoskeletal health	Need for high power; increasing the weight and battery size; major concerns of safety due to the several point of physical contacts with the user and due to the secured contacts with the user; a high level of safety risk in the case of sensor failure; high cost; low accessibility; low level of compatibility (the current state) with various unstructured environments
	Smart wearable mechatronic systems	Ability to be worn and measure body signals; ability to provide biofeedback through due to close skin contact; augmenting sensory awareness (haptics and proprioception); ability to measure body motion for monitoring and rehabilitation in the context of supervised or unsupervised telemedicine; ability to contact tracing and localization for navigation and for medical purposes; ability to communicate with cloud over internet (in the context of IoT)	Low battery life and need for recharge in case of high functionality due to limited space; possibility of errors in measurement due to the small and variable surface contact (such as due to hair blockage or sweating) resulting in false-positive and false-negative alarms/reports; susceptibility to hacking and attacks when communicating biological signals and location information over cloud; limited actuation ability due to the limited power and size
	Hand-held robots	Being light-weight while powered; providing active assistance to delicate manual tasks; application in helping people with hand tremor as an eating assistive device for higher independence	Limitation complex mechatronic design of sensors and actuators due to the small size and limited acceptable weight; relatively high cost; limited degrees of freedom; limited number of tasks which can benefit
	Social robots	Interact socially with humans including patients with cognitive disorders or those in isolation; providing sense of social engagements; supporting education and development for kids with autism; possibility of multiple recording during social engagement (including mood, stress and vital signs)	Limited actuation and degrees of freedom needed for a natural social interaction; challenges to adapt to complex cognitive-related factors affecting social interaction; requirement for a very high level of intelligence to promote social engagement

and our perspective on how HRI categorizations can help the healthcare system during and after the COVID-19 pandemic. In this section, we also offer some examples corresponding to a subset of possible robotic solutions existing at these intersections. The hope is that this review of existing technologies starts an in-depth discussion and inspires others to quickly find new and innovative solutions using existing systems in the literature that can be applied across the healthcare spectrum and using all possible modalities of human-robot interaction in the era of the current crisis and to prepare for future waves and future pandemics. To help the reader we have created **Table 1**, which is a summary of the following section. **Table 2** contains selected references from the literature to show which type of robotic systems are commonly applied to the three healthcare tasks covered in this review, (i.e. Rehabilitation, Assessment, and Assistance/Support).

3.1 Teleoperated Robots

These systems are composed of two synchronized robotic systems (often called as leader-follower robotic systems, or leader and follower robotic consoles) that communicate over a communication channel (see Avgousti et al. (2016); Niemeyer et al. (2016); Farooq et al. (2017); Evans et al. (2018); Hooshiar et al. (2019) and references therein). An extension of these technologies are multilateral telerobotic systems (see Shahbazi et al. (2018) and references therein) which have multiple robots interacting over a multiport network, realizing collaborative tasks by operators or robots or both. The communication channel can be a hard line, or satellite, or the internet. The purpose of such technology is to transfer the agency and motor control of the human operator(s) over a barrier and allow remote operation while receiving sensory awareness feedback from the remote environment(s) for the operator(s). Four main examples of barriers are distance, danger, safety, and scale. A successful example of a translational telerobotic technology in a totally different medical application, (i.e. surgery) is the da Vinci surgical robotic system.

In the context of NMSK, emerging telerobotic rehabilitation systems which recently have attracted a great deal of interest (Atashzar et al. (2016a); Shahbazi et al. (2016); Atashzar et al. (2018); Hooshiar et al. (2019); Panesar et al. (2019); Fong et al. (2020a); Fong et al. (2020b); Sharifi et al. (2020)) allow remote access of patients to kinesthetic rehabilitation and remote monitoring under telemedicine, maximizing accessibility regardless of geographical barrier and minimizing the risk associated with commuting to healthcare centers. This topic is discussed in details later in this paper (under **Sections 4.3**, and **4.4**).

3.2 Autonomous Collaborative Robots

These technologies are designed particularly to physically conduct a task with the need for a high level of autonomy, and situational awareness, and in collaboration with human operators. Several examples and the literature can be found in (Ajoudani et al. (2018); Chen. et al. (2018a); Saenz et al. (2018); Haidegger. (2019); Hentout et al. (2019); Gualtieri et al. (2020)). These robots sometimes have fixed bases, sometimes have mobile

TABLE 2 | Categorization of selected articles from the literature.

		Healthcare services		
		Rehabilitation	**Assistance and support**	**Assessment**
Robotic systems	Teleoperated robots	Atashzar et al. (2016a); Shahbazi et al. (2016); Atashzar et al. (2018); Panesar et al. (2019), Fong et al. (2020b); Sharifi et al. (2020)	Pernalete et al. (2002); Pernalete et al. (2003); Atashzar et al. (2017a); Reis et al. (2018); Hooshiar et al. (2019); Mehrdad et al. (2021)	Brennan et al. (2009); Fong et al. (2020a); Kim et al. (2020)
	Autonomous collaborative robots	Krebs et al. (1998); Krebs and Hogan. (2006); Brewer et al. (2007); Blank et al. (2014); Maciejasz et al. (2014); Pehlivan et al. (2016); Díaz et al. (2018); Atashzar et al. (2019); BionikLabs. (2020); Nicholson-Smith et al. (2020)	Chow and Xu. (2006); Parikh et al. (2007); Leaman and La. (2017); Chen et al. (2018a); Wu et al. (2019); Azad et al. (2020)	Balasubramanian et al. (2012); Debert et al. (2012); Lambercy et al. (2012); Nordin et al. (2014); Otaka et al. (2015); Kuczynski et al. (2016); Kuczynski et al. (2017); Simbaña et al. (2019); Simmatis et al. (2019); Simmatis et al. (2020)
	Exoskeleton robots	Mao and Agrawal (2012); Proietti et al. (2016); Bernocchi et al. (2018); Rehmat et al. (2018); Bao et al. (2019); Shi et al. (2019); Hocoma. (2020)	Chen et al. (2013); Pazzaglia and Molinari (2016); Randazzo et al. (2017); Shore et al. (2018); Di Natali et al. (2019); Lyu et al. (2019); Kapsalyamov et al. (2020); Settembre et al. (2020)	Ball et al. (2007); Rocon et al. (2007); Fitle et al. (2015); Simmatis et al. (2017); Rose et al. (2018); Mochizuki et al. (2019)
	Smart wearable mechatronic systems	Bonato (2005); Polygerinos et al. (2015); Simon et al. (2015); Yang et al. (2018); Bisio et al. (2019); Kos and Umek (2019); Wei et al. (2019)	Shull and Damian (2015); Katzschmann et al. (2018); Sweeney et al. (2019); Gathmann et al. (2020); Alva et al. (2020); Seshadri et al. (2020)	Šlajpah et al. (2014); Qiu et al. (2018); Qiu et al. (2019); Carnevale et al. (2019); Cerqueira et al. (2020); Oubre et al. (2020)
	Hand-held mechatronic systems and robots	Rinne et al. (2016); Hussain et al. (2017); Mace et al. (2017)	MacLachlan et al. (2011); Pathak et al. (2012); Yang et al. (2014); Pathak et al. (2014); Sabari et al. (2019); Ripin et al. (2020)	Rinne et al. (2016); Hussain et al. (2017); Mace et al. (2017)
	Social robots	Fasola and Mataric (2012); Calderita et al. (2013); Malik et al. (2016); Céspedes et al. (2020); Martín et al. (2020)	Broekens et al. (2009); Belpaeme et al. (2018); van den Berghe et al. (2019); Scoglio et al. (2019); Armitage and Nellums (2020)	Pennisi et al. (2016); Chen et al. (2018b); Do et al. (2020)

bases, and sometimes they are equipped with arms. In addition, hybrid collaborative arm systems exist, having one end fixed to a mobile base, which is free to perform tasks in an environment dexterously (these are often called mobile manipulators). Mobile manipulators allow for a theoretically infinite workspace for the manipulator (see the following citations for more information about the modern application of this technology: Zhao et al. (2018); Wu et al. (2019); Balatti et al. (2020)). Such hybrid robotic systems can be used in healthcare centers for manipulating and moving materials, and even can assist with delivering physical assistance for patients, reducing physical interaction between personnel and between patients and caregivers. Autonomous collaborative robots have been used frequently in industry, and more recently in health care systems (motivated by the need to such technologies for handling COVID-19-related issues), to reduce the load of repetition and precision when collaboratively conducting tasks with humans. There are a wide range of examples, but one particular example is handling samples of COVID-19 and being part of the testing pipeline, making the whole testing chain faster and more reliable (please see Yang et al. (2020) for more details). In addition to the above, mobile platforms (typically without manipulators), including smart wheelchairs, are not fixed in a position and instead use a wheeled platform or walking mechanism to move in an environment (Chow and Xu (2006); Parikh et al. (2007); Leaman and La. (2017)). This technology can be used for various applications, including 1) mobility of patients with physical NMSK disability and those with reduced cognitive strength caused by COVID-19, reducing the need for physical assistance by human, and maximizing patients' independence; 2) as an inherent part of telemedicine which can be used for delivering care remotely and checking vital signals in isolated centers (such as nursing homes); and 3) interaction between isolated patients and their families and personnel of the facility.

3.3 Exoskeleton Robots

These robots are external actuated mechanisms worn by humans for motor augmentation, strengthening the users' capabilities, or to rehabilitate a human's lost abilities and function (Gopura et al. (2016); Proietti et al. (2016); Young and Ferris (2016); Hill et al. (2017); Rehmat et al. (2018); Di Natali et al. (2019); Settembre et al. (2020)). Using such technical aspects of rehabilitation and mobility can be realized with minimum human-based intervention. Exoskeletons have been used in industries to reduce the mechanical load on workers. With the same functionality, they have been proposed to be used for assisting patients with extreme mobility problems, and in this regard, they have been often seen as the next revolutionary generation of wheelchairs (Pazzaglia and Molinari. (2016); Hill et al. (2017)). They have been designed in various formats, including upper-limb and lower limb, and combined. Using exoskeleton patients with NMSK disabilities can be rehabilitated during walking and mobility exercises while finely tuning the characteristics of exercise (including the speed, step length, joint trajectories, posture). This will significantly reduce the need to have multiple therapists closely interacting with a patient to deliver the mobility exercises.

3.4 Smart Wearable Mechatronics

These technologies are human-worn devices that measure body signals and display information to the user through biofeedback to support, assist, or augment the capabilities of the user. Smart wearables can also provide haptic-, vibro-, and electro-feedback stimulation to users (see the following citations for examples and more details: Polygerinos et al. (2015); Chen et al. (2017); Maisto et al. (2017); Yang. et al. (2019a); Alva et al. (2020); Cerqueira et al. (2020); Gathmann et al. (2020)). These technologies have been used to enhance the sensory capability of patients with NMSK disabilities (such as Simon et al. (2015); Lopes and Baudisch (2017); Bisio et al. (2019); Alva et al. (2020); Gathmann et al. (2020)). These technologies have also been categorized under the umbrella of the Internet of Medical Things (IoMT) (Bisio et al. (2019))) and smart environments. Related to COVID-19, recently, researchers are utilizing wearable technologies for following the time-series of symptoms of patients, especially those with NMSK disabilities which may degrade the ability to monitor the symptoms through traditional means, and evaluate the evolution and dynamics in bio-markers. These wearable sensor technologies have the potential to provide early diagnosis of those who may be in a sensitive age range or with underlying conditions; also for monitoring of those who have shown some symptoms but not serious enough to be hospitalized. With the use of artificial intelligence, the collected data can be processed on the cloud, and any health anomaly can be detected using computational models (see examples: Saglia et al. (2019); Ding et al. (2020); Seshadri et al. (2020); Weizman et al. (2020); Tripathy et al. (2020)). As mentioned, these technologies can be equipped with the tactile actuator to provide sensory feedback for the user, for example when they move their hand close to their face (D'Aurizio et al. (2020)), or when they do not follow guidelines for washing the hands for a long enough duration; providing an additional layer of situational awareness. These technologies can also be used to track the spread of the virus by tracking the mobility of those with comorbidities. In this regard, recently, there have been several conversations about data security and privacy of the users, which are all ongoing topics at the moment, to make sure that these technologies follow the ethical guidelines and privacy of the users (Arias et al. (2015); He et al. (2018); Tseng et al. (2019); Stoyanova et al. (2020)).

3.5 Hand-Held Robots

This is a relatively small category of assistive robotic systems. These technologies are light-weight powered robotic systems designed to be held in a user's hand and typically assist with performing tasks. Initial uses of hand-held robotics were in surgery to help a surgeon stabilize physiological hand tremors when performing delicate surgical operations, such as retinal surgery (MacLachlan et al. (2011); Becker et al. (2013); Yang et al. (2014)). Recently, the same concept has been utilized to assist patients with NMSK disabilities, in particular, assisting users with severe NMSK disabilities when eating. This reduces the need for interaction with nurses and other helpers (family members), enhancing the independence and quality of life of users. An example of such a robot is a smart-spoon, which counteracts hand tremors in those with Parkinson's disease to allow them to eat

more easily with more confidence and without the need for someone to feed them (Pathak et al. (2014); Stamford et al. (2015); Sabari et al. (2019)). Such technology not only helps with a patient's self-confidence and mental state but also, during the COVID-19 pandemic, it will reduce the need to have close and long physical interaction with nurses and helpers for feeding (as one example).

3.6 Social Robots

These technologies are robots that interact socially with humans (Campa. (2016)) and have been used for a variety of applications that benefit from social interaction, such as for education (see Belpaeme et al. (2018) and references therein), for language learning (see van den Berghe et al. (2019) and references therein), for elderly care (see Broekens et al. (2009) and references therein), for helping people with autism (see Pennisi et al. (2016) and references therein), and depression (see Chen. et al. (2018b) and references therein). Social robots may be actuated or have speech capabilities and can measure the user's mood, temperature, stress, and vital signs via various embedded sensors. Smart social robots have shown good potential in engaging the users in interactive social exercises. Social robotics systems have been shown to successfully benefit kids living with autism (Pennisi et al. (2016)), and elderly living with mild cognitive impairments, Alzheimer's disease, and dementia (Valentí Soler et al. (2015); Góngora Alonso et al. (2019)). This technology can be a major benefit, especially during the COVID-19 pandemic, when the elderly are isolated due to the concerns over disease spread. Long term isolation for patients who are already having cognitive disorders may have very serious consequences, and any technology which can engage these persons in interactive social exercises, while reducing the risk of human-human contact, can be significantly beneficial.

4 REHABILITATION ROBOTICS

4.1 Rehabilitation During the COVID-19 Pandemic and Post-COVID Era

As mentioned earlier, the COVID-19 pandemic has put high pressure on healthcare systems. Due to the inability of patients to visit rehabilitation centers, or the risk of patients when going to rehabilitation centers, the delivery of NMSK rehabilitation has been distorted. It should be noted that most patients who have experienced stroke(s) have an age greater than 65. This means that the population of stroke patients is categorized as at-high-risk, and it is critical for those patients to minimize situations that may result in human contact, in particular visits to health care systems. Concern has been raised, since the delivery of rehabilitation is a time-sensitive treatment (as mentioned in the introduction). A delay, or long pause, in treatment can result in permanent loss of major sensorimotor functionality. Recent literature strongly suggests very early mobilization and intense therapy right after stroke to secure a high degree of functional recovery, during the short golden time (right after the stroke) when brain plasticity is at its maximum (Arias and Smith (2007); Yen et al. (2020); Cumming et al. (2008); Cumming et al. (2011)). However, currently, COVID-19 is the main (if not sole) focus of healthcare systems in many countries. Thus, while there are many patients who experience a stroke during this very challenging time, access to healthcare facilities is strictly limited. Also, as mentioned in the introduction, not only has the pressure of COVID-19, and corresponding concerns about disease transfer to the elderly, resulted in delays in delivery (and consistency of delivery) of rehabilitation services, but also the fear of COVID-19 has caused delays where patients are holding off in seeking emergency care after stroke symptoms. It should also be pointed out that family members, who usually play a central role as the regular caregiver (or helper) for the post-stroke process, are usually partners of an age that also likely falls within the high-risk category for COVID-19. Thus, it would be highly risky (if not impossible) for patients and their immediate families to travel repeatedly to healthcare centers to receive frequent rehabilitation services. At the same time, it is highly risky for post-stroke patients to remain in the hospital as in-patients, due to the risk of pneumonia, which can be significant for those with suppressed immune systems. Thus, now, the question is how we can use the existing intelligent robotic and mechatronic technologies, and how we can expand and exploit them to deliver a high degree of care while maximizing patients' safety.

4.2 Conventional Robotic Rehabilitation

A solution suggested in the literature, before the current COVID-19 pandemic, for reducing pressure on the healthcare system to deliver labor-intensive rehabilitation was to develop in-clinic robotic technologies that provide repetitive, multimodal, rehabilitation exercises (such as active assist robot, and exoskeletons for both upper and lower limbs). Examples of such robots are InteractiveArm (which is an upper limb end-point robotic system from BionikLabs, Toronto, Canada (BionikLabs. (2020))), ArmeoPower (which is an upper limb exoskeleton from Hocoma, Switzerland (Hocoma. (2020))). Robotic rehabilitation technologies are designed to promote multimodal stimulation of neural and muscle activities, while patients perform tasks in a virtual-reality environment. Functionality, effectiveness, and various formats of robotic rehabilitation are explained in our recent literature survey, published in (Atashzar et al. (2019)). Conventional robotic rehabilitation technologies utilize various modalities of interaction, mainly being collaborative robots (Peternel et al. (2017)) and exoskeletons (examples can be found in Proietti et al. (2016); Rehmat et al. (2018); Lv et al. (2018); Lefeber et al. (2019)). Commercial robotic rehabilitation technologies are composed of three components:

a) A sensorized robotic module which is an active medical device and can provide multi-directional and high bandwidth kinesthetic force fields (such as assistive, coordinative, and resistive forces) and vibrotactile haptic feedback, to enable the delivery of various types of rehabilitation for patients with a wide range of biomechanics, motor deficits, and levels of muscle tone, spasticity, and involuntary motions. A core design factor is to make the robots responsive to allow for rendering a

highly transparent and agile interaction with the patient's biomechanics, which is an imperative factor for an efficient rehabilitation regimen. Rehabilitation robotic systems have been equipped with a variety of sensors, which can measure eye motion, quality of hand-eye coordination, force and motion, grasp pressure profile, and neuromuscular activities such as electromyography (EMG) and electroencephalography (EEG).

b) A task-oriented visual game-like virtual reality environment, which is an inherent component designed to provide patients with multimodal cues during tasks, with the goal of enhancing the engagement and participation needed for promoting plasticity.

c) Programmable virtual therapist algorithms that are coded to provide intervention, and are responsible for quantifying the performance of the patients (based on the recorded multimodal data) and, accordingly, designing therapeutic reactions for delivery by the interface.

There are several advantages with the use of robotic technologies and they have shown potential in accelerating neural recovery. These technologies have been shown to enhance the quality of motor performance for stroke patients with mild-to-moderate disabilities. The contributing factors are as follows:

a) Power: Robots are powerful and precise, so they can generate accurate high- and low-intensity assistive and resistive force fields and vibrotactile haptic feedback to deliver therapy for a wide range of patients with various biomechanics over a long period of time.

b) Repeatability: Robots can be programmed to repeat an interactive task for as many iterations as are needed.

c) Objective assessment and progress tracking: Robots are computerized and can measure and log multimodal data, such as kinematic and kinesthetic factors (such as motion and force profiles in different joints), eye motion, quality of hand-eye coordination, biological signals (such as EMG and EEG); with the recording of all these modalities synced and saved for each session during rehabilitation. This enables precise and repeatable objective assessment that is imperative for clinicians to tune the dose, strategy, type, and intensity of therapy while monitoring the progress of motor enhancement.

d) Multimodal Stimulation for Engagement: Using VR environments coupled with robotic systems, visual, haptics, and auditory cues can be fused with kinesthetic rehabilitation, enabling multimodal goal-oriented sensorimotor tasks which can help to keep patients engaged and urge them to use their decision-making capabilities, which is a critical factor for stimulating neural recovery, in comparison to passive limb movement therapy.

Please see: Jimenez-Fabian and Verlinden. (2012); Chen et al. (2013); Tucker et al. (2015); Atashzar et al. (2019), for more details on these technologies. The effectiveness of robotic rehabilitation systems in enhancing neural recovery has been widely studied and attracted a great deal of interest in the literature (Krebs and Hogan. (2006); Atashzar et al. (2019); Bao et al. (2019); Simbaña et al. (2019); Shi et al. (2019)). There are several journals, societies, and conferences focusing on this topic to raise awareness regarding new robotic solutions, algorithms, technologies, and industries. However, despite the proven potential, there exist several challenges limiting the performance, efficacy, accessibility, compatibility, and usability of this technology. This has resulted in conflicting clinical studies with contradictory conclusions on the topic (Atashzar et al. (2019)). Based on the literature mentioned, among the limitations are 1) the restricted interpersonal interaction between the patient and the therapist, 2) a homogeneous response (with minimum flexibility) of a programmed robot over the workspace to a heterogeneous symptom space of the pathology, 3) non-standard strategies to tune the intensity, dose, and parameters of robotic therapy, 4) conservative constraints limiting the performance of the robot due to basic patient-robot safety features, 5) cost, accessibility and portability of robotic rehabilitation.

4.3 In-Home Robots for Delivering Rehabilitation During the COVID-19 Pandemic

Considering the current pandemic and the above-mentioned risks associated with visiting rehabilitation centers for post-stroke patients, while considering the imperative need for early rehabilitation, existing robotic systems can play a central role if their use is managed systematically. During the last decade, there has been an active scientific movement to make robotic systems home compatible (Huang et al. (2016); Bernocchi et al. (2018); Díaz et al. (2018); Washabaugh et al. (2018); Lyu et al. (2019)). For this, the three main factors to be met are safety, portability, and cost. Current commercial robotic rehabilitation systems are not primarily designed to be used in patient's homes. Therefore, the existing commercial robotic rehabilitation systems are mostly expensive, bulky, and may not be safe enough to be used at home (with minimal supervision of an expert or trained operator). Safety is a major concern due to the ability of these technologies to generate very large forces while tightly connected to patients' biomechanics (Zhang and Cheah. (2015); Atashzar et al. (2016b); Atashzar et al. (2017b); Atashzar et al. (2020)). In order to address these issues, two categories of suggestions have been made and implemented in the literature, 1) hardware solutions and 2) algorithmic solutions. Suggestions regarding hardware solutions have resulted in the design and implementation of novel robotic systems with inherent safety. In this regard, soft robots (please see Chu and Patterson. (2018); Cianchetti et al. (2018) and references therein) and mobile robots (see examples: Avizzano et al. (2011); Yurkewich et al. (2015); Germanotta et al. (2018)) are two suggestions in the literature, which be explained below. It should be noted that both soft rehabilitation robotic systems and mobile robotic systems can be made in very compact sizes at a low cost. One major reason for this is that both of these

technologies drop the need for the use of heavy, expensive, motors in a rigid link format, which was previously required for delivering high-torque therapeutic forces.

a) Soft Robots: Soft robotic systems are composed of soft actuators, soft bodies, and possibly soft sensors. These robots are inherently safe due to their particular physics. Soft robotic systems are also usually inexpensive and can be made in small sizes, in particular in the format of soft exo-suits, which are soft exoskeleton robotic systems. These robotic systems can be operated with minimal concerns about safety (due to their compliant design) and can be used for a variety of rehabilitative tasks (Chu and Patterson (2018); Cianchetti et al. (2018)). These systems have great potential to be used in the homes of patients with NMSK disabilities, allowing them to have inexpensive rehabilitation therapy and minimizing the need for frequent visits to clinic.
b) Mobile Robots: Mobile wheeled robotic systems have been recently been considered as another potential solution to enhance safety and portability while reducing costs (Germanotta et al. (2018); Avizzano et al. (2011); Yurkewich et al. (2015)). The actuation principal of these robots is based on the friction between the wheels of a mobile platform and a table-top surface (instead of a robotic-links rigidly connected to a structure). Because these robots are not connected rigidly affixed to a base, they can provide a high degree of safety. In addition, since these systems do not require long arms and have indirect power transmission, they can be designed in a very compact size for maximum portability, while reducing the cost of the system.

In terms of algorithms, it should be noted that there has been active research on designing intelligent stabilizers (such as those designed based on the Strong Passivity Theory) which can guarantee the safety and stability of mechanisms by monitoring and updating the amount of energy which can be delivered and absorbed by patients' biomechanics when conducting rehabilitation exercises (Zhang and Cheah. (2015); Atashzar et al. (2016b); Atashzar et al. (2017b); Atashzar et al. (2020)). These algorithms mainly function by monitoring the mechanical energy flow between patient and robot. By analyzing system stability conditions on the fly, these systems allow for initiation and tuning of interventions (through immediate injection of damping factors) whenever stability conditions are about to be violated. With the use of such intelligent observational algorithms, the safety and stability of HRI is guaranteed, adding one more layer of safety in addition to mechanical safety, as explained before. It can be envisioned that with the use of existing soft and mobile robotic systems, that have embedded intelligent stabilizers, we can have in-home robotic technologies to deliver a highly transpicuous kinesthetic therapy for patients in the home and minimize the need for visits and therapist-patient physical contacts. Considering the need for urgent rehabilitation post-stroke, and due to the extensive research and available mechanical and algorithmic supports, implementing such composite technologies on a large scale can be envisioned to address the lack of rehabilitation services for post-stroke patients in isolation due to the concerns related to COVID-19. Achieving this goal requires a focused interaction between industries, designing robotic systems, and healthcare systems, to make such technologies widely available for the public and maximizing the accessibility of rehabilitation services. This section provides the needed facts and scientific perspective of such discussion.

4.4 Telerobotic Rehabilitation: A Potential Transformative Paradigm for Delivering Supervised Remote Therapy

Telerobotic rehabilitation systems (under the category of teleoperated robotic systems) are the result of a natural extension of conventional robotic rehabilitation systems and have been seen as a novel paradigm within telemedicine, can maximize equal opportunity regardless of geographical constraints (Atashzar et al. (2016a); Shahbazi et al. (2016); Atashzar et al. (2018); Panesar et al. (2019); Hooshiar et al. (2019); Fong et al. (2020a); Fong et al. (2020b); Sharifi et al. (2020)) and restrictions caused by COVID-19. Telerobotic rehabilitation systems are composed of two synchronized robotic systems that communicate over a communication channel, (e.g., internet). One robot is at the patient's side and one robot is at the therapist's side. A virtual reality environment is shared between the therapist and the patient. As a result, the patient can perform tasks (like what he/she would do using conventional robotic systems), but at the same time, the motions are sent to the clinician's side where the therapist can feel all the motions provided by the patients (since the two robots are synchronized in the position-force domain) and can react by applying forces. The forces generated by the therapist are logged using the sensory systems of robotic system while being sent back to the patient-side robot. The patient can move the robot, and the forces relayed to patient-side robot allow for the patient's motion to be corrected and guided if needed. This technology can be a core solution for patients at home, since a remote therapist can interact with a patient not only through vision and audio channels (conventional telemedicine modalities) but also through kinesthetic and haptic interaction, which is imperative in the rehabilitation domain. With the use of this new paradigm, patients can benefit in-home from remote multimodal and tele-kinesthetic interaction with in-hospital therapists. This enables supervised and remote motor assessment and delivery of rehabilitation. This technology can realize the immersive experience of teletherapy and interpersonal interaction between the patient and the therapist. At the time of the COVID-19 crisis, the need for this technology is pronounced, which can significantly enhance the current state of telemedicine. Such technology enables wide-range interaction between clinicians and patients across the country with a specific focus on patients in nursing homes, those with co-morbidities, and those in areas with highly pressurized healthcare systems. This offers a transformation to equal access of healthcare services and is a major global need, especially during this crisis. Besides

accessibility, telerobotic rehabilitation can significantly increase the duration in which a patient can receive rehabilitation services in-home since the involvement in a rehabilitation program would no longer be linked to physical visits to care centers.

It should be emphasized that although the concept of telerobotic rehabilitation has been proposed and investigated during the last decade, there were some restrictions, in the past, for realizing such technology at large scale, mainly due to the sensitivity of the quality of therapy to the quality of service (QoS) of communication networks. This includes issues related to reliability and resiliency of communication and security of data transfer. In this regard, latency, jitter, and packet loss not only deteriorate the fidelity of therapy rendered for the remote patient, but can also result in "non-passive coupling" between the two robots, adding to concerns about safety (as this can potentially cause asynchronous growing of interactional trajectories). This concern has been addressed in the literature to a reasonable extent, mainly 1) through the use of passivity stabilizers (mentioned earlier) and 2) accessibility to secure, highly reliable, and an agile internet connection, such as 5G and beyond Aijaz et al. (2016).

It should be noted it is imperative for therapists and clinicians to feel the kinesthetic actions and reactions of patients. This is needed for two major interconnected purposes 1) rehabilitation, 2) assessment, as explained below.

First, it should be mentioned that in the field of motor learning and rehabilitation sciences, it is known that a successful rehabilitative therapy needs to provide the therapist with the on-the-fly awareness of 1) the user-specific motor capability, kinematics, and biomechanical characteristics of the patient, 2) the specific characteristics of the neuromuscular deficits, and 3) the rate and pattern of motor improvement. These three factors are identified in the literature of rehabilitation as the three critical factors of motor retraining, which basically require physical interaction between therapists and patients. Thus it can be mentioned that although in-home autonomous robotic systems can deliver programmed rehabilitation therapy for patients in the home, without a telerobotic paradigm, these robots block the interpersonal interaction between a human therapist and the patients.

Second, it should be noted that interpersonal interaction is also known to be an imperative need, beyond rehabilitation, and specifically for long-term assessment of the severity of the condition and any changes in motor performance potentially correlated to the delivered regimen of rehabilitation.

Considering this note, the importance of telerobotic rehabilitation and assessment systems is further underscored. Thanks to the high speed, reliability, and accessibility of modern internet in many parts of the world, telerobotic rehabilitation can multiply the use potential of a therapist's time by bypassing the obstacles due to distance and challenges due to isolation/quarantine situations caused by COVID-19. These technologies minimize actual human-human contact through virtualization, while still allowing computerized physical interaction. Considering the available communications backbone and robotic technologies, telerobotic rehabilitation can be envisioned as part of the response to the COVID-19 pandemic and to prepare healthcare systems for future pandemics. This section displayed the imperative need and feasibility of such telerobotic rehabilitation systems, with the hope of increasing public and scientific awareness on the topic.

Remark: It should be noted that one of the challenges which should be addressed for a fluent translation of telerobotic rehabilitation technology into practice is the cost and portability of robotic systems for use in the patient's home (as one terminal of the telerobotic system). This is an active line of research and can be considered as the current limitation. However, due to the accelerated trend of improvement regarding in-expensive robotic systems, such as soft and mobile robotic technologies, which can be used in the context of rehabilitation to reduce the cost and improve the portability (as mentioned in the previous section), it can be envisioned that the mentioned limitations can be addressed in the near future. However, this would require further research, development, and investment in the future of telerobotic rehabilitation systems.

5 ASSISTIVE TECHNOLOGIES

As mentioned in the previous section, robotic systems have transformed the delivery of rehabilitation therapies, assisting with the gradual recovery of patients with sensorimotor disabilities. The other related, yet different, category of robotic systems developed to help patients with NMSK deficits are assistive robotic technologies. The primary difference is that assistive technologies are designed to immediately augment the sensorimotor capacity of NMSK patients and help them in performing activities of daily living. As a result, a gradual recovery is not the primary focus of assistive technologies. Assistive technologies are realized in various modalities of interaction, including smart wearable mechatronics (Simon et al. (2015); Chen et al. (2017); Lopes and Baudisch (2017); Maisto et al. (2017); Bisio et al. (2019); Yang et al. (2019a); Alva et al. (2020); Cerqueira et al. (2020); Gathmann et al. (2020)), handheld robots (Pathak et al. (2014); Stamford et al. (2015); Sabari et al. (2019)), exoskeletons (Gopura et al. (2016); Pazzaglia and Molinari (2016); Young and Ferris (2016); Hill et al. (2017); Settembre et al. (2020)), and smart wheelchairs (under autonomous robots) (Chow and Xu (2006); Parikh et al. (2007); Leaman and La. (2017)). Assistive technologies can be as simple as smart IoT-based fall protection devices (Saadeh et al. (2019)), smart gait-aid goggles for Parkinson's patients (Ahn et al. (2017)) and active canes (Lachtar et al. (2019)); they can be also be more complex, such as exoskeletons (Gopura et al. (2016); Pazzaglia and Molinari (2016); Young and Ferris (2016); Hill et al. (2017); Settembre et al. (2020)). In this regard, it should be noted that falls are a major concern for the aged population (Terroba-Chambi et al. (2019); Silva de Lima et al. (2020)) and can result in critical bone fractures (which heal slowly, if at all) and other deteriorating secondary conditions. On the other hand, mobility is essential for aged individuals to maintain cardiovascular and musculoskeletal health, particularly after recovery from NMSK conditions. This is an addition to the normal needs for situational awareness and navigation in daily

living environments and manipulation of objects (such as doorknobs, food, etc.). Addressing this need to enable mobility without the use of advanced technologies would call for more interaction with care providers for the delivery of assistance, which increases the risk of infection transmission among this vulnerable population. The main outcome of the use of assistive systems is enhanced situational awareness (i.e., perceptual augmentation), enhanced independence, empowered mobility, and increased manipulability for individuals with degraded sensorimotor competence, (i.e. motor augmentation).

Common use cases of assistive robots to improve the motor performance of patients living with NMSK are 1) exoskeletons for patients with spinal cord injuries, stroke, and gait deficits, 2) smart motorized wheelchairs for patients with severe lack of mobility, 3) wheelchair-mounted arms for patients with the lack of manipulability (such as those aging with severe cerebral palsy), 4) smart motorized walking supports for patients with limited mobility and those with a high risk of fall, and 5) handheld tremor compensators for patients with pathological hand tremors such as Parkinson's disease and essential tremor.

In addition to the above-mentioned examples, which mainly focused on augmenting the motor performance of users, the second category of assistive mechatronic technologies are designed to augment the sensory perception of the patients. These active smart-technologies aim to boost up the perceptual awareness of users, to improve perception of sensory input. These technologies ultimately help with activities of daily living and tracking the health status of patients. Sensory perception enhancing systems may be in the format of wearable suits, (e.g. armbands) and may provide auditory, vibrotactile, or visual cues for the patients. One example of such a systems are wearable vibrotactile suits for helping individuals with degraded vision and sensory awareness, so they can navigate safely in daily environments while protecting them when encountering unexpected contacts, which may result in falls (Bharadwaj et al. (2019)). Another example is technologies that provide cues to the user regarding their posture during walking to maintain a safer balance (Viseux et al. (2019)). These technologies have been used to enhance sensory awareness of people with degraded vision and perceptual capability. Another important example is closed loop and open loop sensory cueing systems for patients with freezing of gait caused by Parkinson's disease (Mancini et al. (2018); Sweeney et al. (2019)). Freezing of gait can result in danger and major challenges during daily navigation (such as crossing a street, navigating in a home, walking to the bathroom, etc.), resulting in limited mobility and independence. With the use of sensory augmentation technologies, patients with Parkinson's disease have shown to have significantly enhanced mobility and have recovered a high degree of gait fluency. This is believed to be caused through the opening of a redundant neural sensory processing pathway, which may be less affected by degenerated neurons. The above-mentioned technologies will enhance the mobility and independence of patients with NMSK conditions, minimizing reliance on caregivers, which reduces concerns of disease transfer. Additionally, new assistive and wearable technologies have been recently proposed to increase gesture awareness to alert individuals about hand-face contact to reduce the risk of COVID-19 infection (D'Aurizio et al. (2020)). Although some of these technologies may not be directly categorized as robotic systems, they are smart mechatronic modules that can enhance sensorimotor functionality of people, while minimizing the risk of infection and maximizing the patient's cognitive awareness about the possible risky situations (which should be strictly avoided for NMSK patients with co-morbidity).

Enhancing motor performance and situational awareness, offered by assistive technologies, is particularly critical during the COVID-19 pandemic, as the increasing a person's independence during daily activities decreases their need for interaction with helpers, nurses, and care providers. In other words, using assistive technologies, patients with sensorimotor deficits require a lower amount of supervision and physical interaction with care providers for conducting activities of daily living. This can also reduce the need for having a high number of nurses and helpers in long term care facilities, which is a significant concern at the moment with concerns related to bilateral disease transfer between patients and between patients and care providers. Besides cognitive aspects, there are several mobility/manipulability restrictions that are associated with normal aging or age-related NMSK deficits. This includes gait control problems, balance problems, dexterity deficits, lack of motor power, affected precision in targeting, perceptual deficits, and involuntary movements.

Thanks to the use of advanced assistive technologies, the need for interpersonal interaction between elderly and care givers can be significantly reduced. This shows an unmet need to boost the performance, and availability, of assistive technologies to help patients with conducting many activities of daily living. With the use of advanced smart assistive robotic and mechatronic technologies, it is possible to enhance mobility and manipulability during the daily lives of senior individuals; ultimately improving their independence and increasing their situational awareness while minimizing the risk of COVID-19 infection. By employing several assistive technologies, the need for care providers in the living environment of senior individuals will be reduced, minimizing the risk of infection transmission to this vulnerable population during and after the COVID-19 pandemic era. Due to the strong literature and successful implementation of assistive technologies, short and long-term investment in this field of research and development can make the healthcare system more prepared for future pandemics.

6 ROBOTS FOR ASSESSMENT AND SUPPORT

In this section, we discuss the use of robotic and mechatronic technologies for 1) delivering assessment for monitoring, evaluating, and diagnosing NMSK disabilities and 2) for providing mental, social, cognitive, and emotional support to isolated NMSK individuals. Support and assessment technologies can be implemented in a number of ways through robotic and

wearable technologies. These technologies are grouped together here as many supportive technologies require some manner of real-time monitoring or assessment of an individual.

6.1 Social Robots for Support

It should be noted that due to COVID-19-related guidelines and concerns, the elderly, particularly those with age-related NMSK disabilities and mobility issues, are affected by extra social distancing and prolonged isolation policies. This leads to secondary challenges such as depression, anxiety, and stress, caused by excessive and prolonged isolation in this population (Armitage and Nellums. (2020)). Seniors are being isolated from their families and caregivers, with some long term facilities around the world reducing or restricting patient/physician visits. Given this, robotic and wearable technologies can be used to compensate in part for this lack of direct physician, caregiver, and family interaction. Social robots, for instance, are designed to interact and communicate with humans and their surrounding environment. Social robots have been constructed in a range of form factors from pet-like toys (e.g., Paro) to humanoids (e.g., Sophia). Social robots have been shown to be particularly effective at helping with the mental health and well-being of elderly persons with dementia or other NMSK conditions in healthcare and long-term care settings (see Pu et al. (2019); Scoglio et al. (2019)). Social robots can provide or act as a companion to help people with NMSK conditions feel less lonely, feel more socially engaged, and interactive. Social robotics has primarily been used in assisting with the treatment of elderly patients, particularly those with dementia, and have been shown to have a positive benefit in improving mood, reducing anxiety, and reducing depression.

The mood-boosting effects of social robotics can be particularly helpful during the COVID-19 pandemic, as social robots can help to bring a sense of comfort and interaction to isolated elderly persons, and can be used to create a sense or routine or order without the need for caregiver interaction. From its inception, social robotics research traditionally has been focused on robotics for elderly care and those with NMSK disabilities. Social robots have gained new relevance during the pandemic, with many seniors, group, and long-term care homes no longer allowing family members (or with extreme restricted care and reduced frequency and physical contact), social workers, and support workers to visit. Due to the low-cost and substantial research that has already been done with social robotics, they are among the technologies that can be quickly deployed to healthcare and long-term care settings during the COVID-19.

6.2 Mechatronic Assessment Technologies

Smart wearable mechatronic technologies refer to smart body-worn devices that can measure, analyze, display, and transmit information and are among other smart mechatronic technologies which can significantly reduce the burden on the healthcare system. Due to the close physical contact with the body, these devices have been used to measure several biomarkers of users, including heart rate, oxygen saturation level, temperature, and mobility. Monitoring these biomarkers is imperative for remotely supervising the health status of isolated seniors and, in particular, those in long term care facilities. These technologies can help to find, diagnose, track, and trace COVID-19 symptoms and infections. They can directly assist the healthcare system to more optimally distribute resources and act quickly to 1) avoid the worsening of the symptoms, 2) avoid transmission of COVID-19 among elderly adults, especially in long care facilities. Due to the computational power available to modern cloud processing modules, data collected using wearables can be processed on the fly with machine learning systems. Thus, such technologies have been suggested for detecting and tracking COVID-19 symptoms and alerting of any anomalies (Seshadri et al. (2020)). They have also been used for contact tracing and activity tracking of patients during the COVID-19 pandemic to monitor adherence to guidelines for protecting individuals and reducing the spread of infection (Pépin et al. (2020); Seshadri et al. (2020)).

Besides being used for monitoring and assessment of health status and searching for COVID-19 symptoms/infections, such technologies can be used to remotely monitor the physical performance of patients with NMSK conditions (Venkataraman et al. (2017); Noorian et al. (2018); Noorian et al. (2019); Sanders et al. (2020); Venkataraman et al. (2020)). Using such technologies, the need for frequent visits to clinics for (subjective) recording of patient performance would be minimized, further reducing the risk of disease transfer during the pandemic. A classic example of these devices is those that monitor (and encourage) physical activity (for instance a Fitbit watch). More complicated wearable devices can monitor patients physiotherapy exercises in-home as part of telemedicine services. They may also monitor vital signs, or report if a person is in distress through the detection of serious conditions such as fall(s) and monitoring of mobility status. For elderly people with NMSK conditions, there is a clear benefit to using wearable technologies to keep track of rehabilitation progress and quality of life measures without requiring hands-on contact with a clinician or rehabilitation specialist. Many of the interfacing sensors (such as EMG, MMG, and EEG) can be built into wearable devices opening an unobtrusive neurophysiological window to the underlying biomarkers. Thus allowing for a truly remote and objective assessment of patients with NMSK conditions in their homes, while relaxing the need for in-person visits (please see Maceira-Elvira et al. (2019) and references therein). This is a critical factor to be considered that can allow the clinician to monitor the progress of and recovery after a NMSK condition, such as stroke.

Research in both fields of social robotics and smart wearable monitoring mechatronics have had significant progress during the last decade resulting in a wide range of available, inexpensive, technologies which can be exploited by the healthcare system in the short-term future to further support patients. Particularly those in need of NMSK rehabilitation, supervision, and monitoring. Thus with systematic planning and involvement of stakeholders, such technologies can be utilized to fight the primary and secondary challenges imposed by the COVID-19 pandemic for serving patients with underlying NMSK conditions. The proven potential for such technologies calls for further investigation and development to provide a range of

"standardized" devices to lift the pressure on healthcare systems in future potential waves of the COVID-19 pandemic and potential future pandemics.

7 CONCLUDING REMARKS

The COVID-19 pandemic has significantly affected the healthcare systems and has raised several questions about its capacity and preparedness to serve under heavy pressure. Based on the significant advancements in various fields of engineering, it is widely accepted that the current unprecedented pressure could have been eased if available technologies, developed during decades of research and investment, had been channeled through a standardized pipeline to tackle the many challenges presented by existing conditions before the pandemic. Among these challenges, there is a growing concern regarding services needed for patients with NMSK conditions, many of which are halted, whilst treatment is still extremely time-sensitive (such as rehabilitation post stroke). In this perspective review article, we have provided a detailed analysis of existing technologies and literature, and discussed the corresponding capacity and how they can help to serve patients, particularly those in the three critical domains of NMSK care (namely rehabilitation, assessment, and assistance). Supported by current literature, we believe that there exists significant technological advancements that could have been established and deployed to deliver a much higher quality of care for NMSK patients during the COVID-19 pandemic. We have provided a detailed discussion of several examples of such technologies and introduced their capacity. This article provides an in-depth and focused look at the existing literature and provides a platform, and the needed information, to initiate a conversation between stakeholders, engineers, policy makers, researchers, and healthcare providers to discuss various aspects of intelligent robotics and smart mechatronic technologies to augment the delivery of care through a systematic investigation, investment, and development for NMSK patients. We believe that the existing technologies have the ability, and are ready, to assist with healthcare delivery during the current and upcoming future waves of the pandemic, if much needed awareness is raised. In addition, this article strongly suggests that a continual conversation be struck, so that for future pandemics, healthcare systems can be equipped with the power and intelligence of robotics and mechatronics technologies to ensure patients with NMSK conditions receive the same high level of care comparable with the that received during the pre-pandemic era.

AUTHOR CONTRIBUTIONS

The three authors (SA, JC, and MT) collaborated on to conceptualization of this article, conducting the literature review and demographic study, analysing the existing technologies, and writing and editing the paper.

FUNDING

This study is supported by United States National Science Foundation: Awards 2031594, and 2037878.

REFERENCES

Ahn, D., Chung, H., Lee, H.-W., Kang, K., Ko, P.-W., Kim, N. S., et al. (2017). Smart gait-aid glasses for Parkinson's disease patients. *IEEE Trans. Biomed. Eng.* 64, 2394–2402. doi:10.1109/tbme.2017.2655344

Aijaz, A., Dohler, M., Aghvami, A. H., Friderikos, V., and Frodigh, M. (2016). Realizing the tactile internet: haptic communications over next generation 5g cellular networks. *IEEE Wireless Commun.* 24, 82–89. doi:10.1109/MWC.2016.1500157RP

Ajoudani, A., Zanchettin, A. M., Ivaldi, S., Albu-Schäffer, A., Kosuge, K., and Khatib, O. (2018). Progress and prospects of the human-robot collaboration. *Auton. Robot* 42, 957–975. doi:10.1007/s10514-017-9677-2

Alawieh, A., Zhao, J., and Feng, W. (2018). Factors affecting post-stroke motor recovery: implications on neurotherapy after brain injury. *Behav. Brain Res.* 340, 94–101. doi:10.1016/j.bbr.2016.08.029

Almkvist Muren, M., Hütler, M., and Hooper, J. (2008). Functional capacity and health-related quality of life in individuals post stroke. *Top. stroke Rehabil.* 15, 51–58. doi:10.1310/tsr1501-51

Alva, P. G. S., Muceli, S., Atashzar, S. F., William, L., and Farina, D. (2020). Wearable multichannel haptic device for encoding proprioception in the upper limb. *J. Neural Eng.* 17, 056035. doi:10.1088/1741-2552/aba6da

Arias, M., and Smith, L. N. (2007). Early mobilization of acute stroke patients. *J. Clin. Nurs.* 16, 282–288. doi:10.1111/j.1365-2702.2005.01488.x

Arias, O., Wurm, J., Hoang, K., and Jin, Y. (2015). Privacy and security in internet of things and wearable devices. *IEEE Trans. Multi-scale Comp. Syst.* 1, 99–109. doi:10.1109/tmscs.2015.2498605

Armitage, R., and Nellums, L. B. (2020). Covid-19 and the consequences of isolating the elderly. *The Lancet Public Health* 5, e256. doi:10.1016/s2468-2667(20)30061-x

Atashzar, S. F., Huang, H.-Y., Duca, F. D., Burdet, E., and Farina, D. (2020). Energetic passivity decoding of human hip joint for physical human-robot interaction. *IEEE Robot. Autom. Lett.* 5, 5953–5960. doi:10.1109/lra.2020.3010459

Atashzar, S. F., Jafari, N., Shahbazi, M., Janz, H., Tavakoli, M., Patel, R. V., et al. (2017a). Telerobotics-assisted platform for enhancing interaction with physical environments for people living with cerebral palsy. *J. Med. Robot. Res.* 02, 1740001. doi:10.1142/s2424905x17400013

Atashzar, S. F., Polushin, I. G., and Patel, R. V. (2016a). A small-gain approach for nonpassive bilateral telerobotic rehabilitation: stability analysis and controller synthesis. *IEEE Trans. Robotics* 33, 49–66.

Atashzar, S. F., Shahbazi, M., and Patel, R. V. (2019). Haptics-enabled interactive neurorehabilitation mechatronics: classification, functionality, challenges and ongoing research. *Mechatronics* 57, 1–19. doi:10.1016/j.mechatronics.2018.03.002

Atashzar, S. F., Shahbazi, M., Tavakoli, M., and Patel, R. V. (2018). A computational-model-based study of supervised haptics-enabled therapist-in-the-loop training for upper-limb poststroke robotic rehabilitation. *Ieee/asme Trans. Mechatron.* 23, 563–574. doi:10.1109/tmech.2018.2806918

Atashzar, S. F., Shahbazi, M., Tavakoli, M., and Patel, R. V. (2017b). A grasp-based passivity signature for haptics-enabled human-robot interaction: application to design of a new safety mechanism for robotic rehabilitation. *Int. J. Robotics Res.* 36, 778–799. doi:10.1177/0278364916689139

Atashzar, S. F., Shahbazi, M., Tavakoli, M., and Patel, R. V. (2016b). A passivity-based approach for stable patient–robot interaction in haptics-enabled rehabilitation systems: modulated time-domain passivity control. *IEEE Trans. Control. Syst. Tech.* 25, 991–1006. doi:10.1109/TCST.2016.2594584

Avgousti, S., Christoforou, E. G., Panayides, A. S., Voskarides, S., Novales, C., Nouaille, L., et al. (2016). Medical telerobotic systems: current status and future trends. *Biomed. Eng. Online* 15, 96. doi:10.1186/s12938-016-0217-7

Avizzano, C. A., Satler, M., Cappiello, G., Scoglio, A., Ruffaldi, E., and Bergamasco, M. (2011). Motore: a mobile haptic interface for neuro-rehabilitation. *RO-MAN (IEEE)* 2011, 383–388. doi:10.1109/ROMAN.2011.6005238

Azad, A., Tavakoli, R., Pratik, U., Varghese, B., Coopmans, C., and Pantic, Z. (2020). A smart autonomous wpt system for electric wheelchair applications with free-positioning charging feature. *IEEE J. Emerg. Sel. Top. Power Electron.* 8, 3516–3532. doi:10.1109/JESTPE.2018.2884887

Balasubramanian, S., Colombo, R., Sterpi, I., Sanguineti, V., and Burdet, E. (2012). Robotic assessment of upper limb motor function after stroke. *Am. J. Phys. Med. Rehabil.* 91, S255–S269. doi:10.1097/phm.0b013e31826bcdc1

Balatti, P., Fusaro, F., Villa, N., Lamon, E., and Ajoudani, A. (2020). A collaborative robotic approach to autonomous pallet jack transportation and positioning. *IEEE Access* 8, 142191–142204. doi:10.1109/access.2020.3013382

Ball, S. J., Brown, I. E., and Scott, S. H. (2007). A planar 3dof robotic exoskeleton for rehabilitation and assessment. *Conf. Proc. IEEE Eng. Med. Biol. Soc.* 2007, 4024–4027. doi:10.1109/IEMBS.2007.4353216

Bao, G., Pan, L., Fang, H., Wu, X., Yu, H., Cai, S., et al. (2019). Academic review and perspectives on robotic exoskeletons. *IEEE Trans. Neural Syst. Rehabil. Eng.* 27, 2294–2304. doi:10.1109/TNSRE.2019.2944655

Bartolo, M., Intiso, D., Lentino, C., Sandrini, G., Paolucci, S., Zampolini, M., et al. (2020). Urgent measures for the containment of the coronavirus (covid-19) epidemic in the neurorehabilitation/rehabilitation departments in the phase of maximum expansion of the epidemic. *Front. Neurol.* 11, 423. doi:10.3389/fneur.2020.00423

Becker, B. C., MacLachlan, R. A., Lobes, L. A., Hager, G. D., and Riviere, C. N. (2013). Vision-based control of a handheld surgical micromanipulator with virtual fixtures. *IEEE Trans. Robot.* 29, 674–683. doi:10.1109/tro.2013.2239552

Belpaeme, T., Kennedy, J., Ramachandran, A., Scassellati, B., and Tanaka, F. (2018). Social robots for education: a review. *Sci. robotics* 3, eaat5954. doi:10.1126/scirobotics.aat5954

Bernocchi, P., Mulè, C., Vanoglio, F., Taveggia, G., Luisa, A., and Scalvini, S. (2018). Home-based hand rehabilitation with a robotic glove in hemiplegic patients after stroke: a pilot feasibility study. *Top. stroke Rehabil.* 25, 114–119. doi:10.1080/10749357.2017.1389021

Bharadwaj, A., Shaw, S. B., and Goldreich, D. (2019). Comparing tactile to auditory guidance for blind individuals. *Front. Hum. Neurosci.* 13, 443. doi:10.3389/fnhum.2019.00443

BionikLabs (2020). *BionikLabs* (Accessed September 01, 2020).

Bisio, I., Garibotto, C., Lavagetto, F., and Sciarrone, A. (2019). When ehealth meets iot: a smart wireless system for post-stroke home rehabilitation. *IEEE Wireless Commun.* 26, 24–29. doi:10.1109/mwc.001.1900125

Blank, A. A., French, J. A., Pehlivan, A. U., and O'Malley, M. K. (2014). Current trends in robot-assisted upper-limb stroke rehabilitation: promoting patient engagement in therapy. *Curr. Phys. Med. Rehabil. Rep.* 2, 184–195. doi:10.1007/s40141-014-0056-z

Block, P., Hoffman, M., Raabe, I. J., Dowd, J. B., Rahal, C., Kashyap, R., et al. (2020). Social network-based distancing strategies to flatten the covid-19 curve in a post-lockdown world. *Nat. Hum. Behav.* 4, 588–596. doi:10.1038/s41562-020-0898-6

Bonato, P. (2005). Advances in wearable technology and applications in physical medicine and rehabilitation. *J. Neuroeng. Rehabil.* 2, 2. doi:10.1186/1743-0003-2-2

Brennan, D. M., Mawson, S., and Brownsell, S. (2009). Telerehabilitation: enabling the remote delivery of healthcare, rehabilitation, and self management. *Stud. Health Technol. Inform.* 145, 231.

Brewer, B. R., McDowell, S. K., and Worthen-Chaudhari, L. C. (2007). Poststroke upper extremity rehabilitation: a review of robotic systems and clinical results. *Top. stroke Rehabil.* 14, 22–44. doi:10.1310/tsr1406-22

Broekens, J., Heerink, M., and Rosendal, H. (2009). Assistive social robots in elderly care: a review. *Gerontechnology* 8, 94–103. doi:10.4017/gt.2009.08.02.002.00

Calderita, L. V., Bustos, P., Suarez-Mejias, C., Ferrer-González, B., and Bandera, A. (2013). Rehabilitation for children while playing with a robotic assistant in a serious game. *NEUROTECHNIX*, 89–96. doi:10.5220/0004646700890096

Campa, R. (2016). The rise of social robots: a review of the recent literature. *J. Evol. Tech.* 26, 106–113.

Carnevale, A., Longo, U. G., Schena, E., Massaroni, C., Presti, D. L., Berton, A., et al. (2019). Wearable systems for shoulder kinematics assessment: a systematic review. *BMC Musculoskelet. Disord.* 20, 546. doi:10.1186/s12891-019-2930-4

Caso, V., and Federico, A. (2020). No lockdown for neurological diseases during covid19 pandemic infection. *Neurol Sci.* 41, 999–1001. doi:10.1007/s10072-020-04389-3

Cerqueira, S. M., Silva, A. F. D., and Santos, C. P. (2020). Smart vest for real-time postural biofeedback and ergonomic risk assessment. *IEEE Access* 8, 107583–107592. doi:10.1109/access.2020.3000673

Céspedes, N., Múnera, M., Gómez, C., and Cifuentes, C. A. (2020). Social human-robot interaction for gait rehabilitation. *IEEE Trans. Neural Syst. Rehabil. Eng.* 28, 1299–1307. doi:10.1109/TNSRE.2020.2987428

Chatterji, S., Byles, J., Cutler, D., Seeman, T., and Verdes, E. (2015). Health, functioning, and disability in older adults-present status and future implications. *The lancet* 385, 563–575. doi:10.1016/s0140-6736(14)61462-8

Chen, G., Chan, C. K., Guo, Z., and Yu, H. (2013). A review of lower extremity assistive robotic exoskeletons in rehabilitation therapy. *Crit. Review^{TM} Biomed. Eng.* 41. doi:10.1615/critrevbiomedeng.2014010453

Chen, J. Y. C., Lakhmani, S. G., Stowers, K., Selkowitz, A. R., Wright, J. L., and Barnes, M. (2018a). Situation awareness-based agent transparency and human-autonomy teaming effectiveness. *Theor. Issues Ergon. Sci.* 19, 259–282. doi:10.1080/1463922x.2017.1315750

Chen, M., Ma, Y., Li, Y., Wu, D., Zhang, Y., and Youn, C.-H. (2017). Wearable 2.0: enabling human-cloud integration in next generation healthcare systems. *IEEE Commun. Mag.* 55, 54–61. doi:10.1109/mcom.2017.1600410cm

Chen, S. C., Jones, C., and Moyle, W. (2018b). Social robots for depression in older adults: a systematic review. *J. Nurs. Scholarship* 50, 612–622. doi:10.1111/jnu.12423

Chow, H. N., and Xu, Y. (2006). Learning human navigational skill for smart wheelchair in a static cluttered route. *IEEE Trans. Ind. Electron.* 53, 1350–1361. doi:10.1109/tie.2006.878296

Christensen, K., Doblhammer, G., Rau, R., and Vaupel, J. W. (2009). Ageing populations: the challenges ahead. *The lancet* 374, 1196–1208. doi:10.1016/s0140-6736(09)61460-4

Chu, C.-Y., and Patterson, R. M. (2018). Soft robotic devices for hand rehabilitation and assistance: a narrative review. *J. neuroengineering Rehabil.* 15, 9. doi:10.1186/s12984-018-0350-6

Cianchetti, M., Laschi, C., Menciassi, A., and Dario, P. (2018). Biomedical applications of soft robotics. *Nat. Rev. Mater.* 3, 143–153. doi:10.1038/s41578-018-0022-y

Cumming, T. B., Thrift, A. G., Collier, J. M., Churilov, L., Dewey, H. M., Donnan, G. A., et al. (2011). Very early mobilization after stroke fast-tracks return to walking. *Stroke* 42, 153–158. doi:10.1161/strokeaha.110.594598

Cumming, T., Collier, J., Thrift, A., and Bernhardt, J. (2008). The effect of very early mobilisation after stroke on psychological well-being. *J. Rehabil. Med.* 40, 609–614. doi:10.2340/16501977-0226

Debert, C. T., Herter, T. M., Scott, S. H., and Dukelow, S. (2012). Robotic assessment of sensorimotor deficits after traumatic brain injury. *J. Neurol. Phys. Ther.* 36, 58–67. doi:10.1097/npt.0b013e318254bd4f

Degardin, A., Devos, D., Cassim, F., Bourriez, J.-L., Defebvre, L., Derambure, P., et al. (2011). Deficit of sensorimotor integration in normal aging. *Neurosci. Lett.* 498, 208–212. doi:10.1016/j.neulet.2011.05.010

Di Natali, C., Poliero, T., Sposito, M., Graf, E., Bauer, C., Pauli, C., et al. (2019). Design and evaluation of a soft assistive lower limb exoskeleton. *Robotica* 37, 2014–2034. doi:10.1017/s0263574719000067

Díaz, I., Catalan, J. M., Badesa, F. J., Justo, X., Lledo, L. D., Ugartemendia, A., et al. (2018). Development of a robotic device for post-stroke home tele-rehabilitation. *Adv. Mech. Eng.* 10, 1687814017752302. doi:10.1177/1687814017752302

Dimyan, M. A., and Cohen, L. G. (2011). Neuroplasticity in the context of motor rehabilitation after stroke. *Nat. Rev. Neurol.* 7, 76–85. doi:10.1038/nrneurol.2010.200

Ding, X.-R., Clifton, D., Nan, J., Lovell, N. H., Bonato, P., Chen, W., et al. (2020). Wearable sensing and telehealth technology with potential applications in the coronavirus pandemic. *IEEE Rev. Biomed. Eng.* 2020, 2992838. doi:10.1109/RBME.2020.2992838

Do, H. M., Sheng, W., Harrington, E. E., and Bishop, A. J. (2020). Clinical screening interview using a social robot for geriatric care. *IEEE Trans. Automat. Sci. Eng.* 1, 1–14. doi:10.1109/TASE.2020.2999203

D'Aurizio, N., Baldi, T. L., Paolocci, G., and Prattichizzo, D. (2020). Preventing undesired face-touches with wearable devices and haptic feedback. *IEEE Access* 99, 1. doi:10.1109/ACCESS.2020.3012309

Evans, C. R., Medina, M. G., and Dwyer, A. M. (2018). Telemedicine and telerobotics: from science fiction to reality. *Updates Surg.* 70, 357–362. doi:10.1007/s13304-018-0574-9

Farooq, U., Gu, J., El-Hawary, M. E., Asad, M. U., Abbas, G., and Luo, J. (2017). A time-delayed multi-master-single-slave non-linear tele-robotic system through state convergence. *IEEE Access* 6, 5447–5459. doi:10.1109/ACCESS.2017.2782178

Fasola, J., and Mataric, M. J. (2012). Using socially assistive human-robot interaction to motivate physical exercise for older adults. *Proc. IEEE* 100, 2512–2526. doi:10.1109/JPROC.2012.2200539

Ferini-Strambi, L., and Salsone, M. (2020). Covid-19 and neurological disorders: are neurodegenerative or neuroimmunological diseases more vulnerable? *J. Neurol.* 268, 19. doi:10.1007/s00415-020-10070-8

Fitle, K. D., Pehlivan, A. U., and O'Malley, M. K. (2015). A robotic exoskeleton for rehabilitation and assessment of the upper limb following incomplete spinal cord injury. IEEE Int. Conf. Robotics Automation (Icra) *(Ieee)* 2015, 4960–4966. doi:10.1109/ICRA.2015.7139888

Fong, J., Ocampo, R., Gross, D. P., and Tavakoli, M. (2020a). Intelligent robotics incorporating machine learning algorithms for improving functional capacity evaluation and occupational rehabilitation. *J. Occup. Rehabil.* 30, 362–370. doi:10.1007/s10926-020-09888-w

Fong, J., Ocampo, R., and Tavakoli, M. (2020b). *Intelligent robotics and immersive displays for enhancing haptic interaction in physical rehabilitation environments*. In *Haptic interfaces for accessibility, health, and enhanced quality of life*. Berlin, Germany: Springer, 265–297. doi:10.1007/978-3-030-34230-2_10

Gathmann, T., Atashzar, S. F., Alva, P. G. S., and Farina, D. (2020). Wearable dual-frequency vibrotactile system for restoring force and stiffness perception. *IEEE Trans. Haptics* 13, 191–196. doi:10.1109/toh.2020.2969162

Germanotta, M., Cruciani, A., Pecchioli, C., Loreti, S., Spedicato, A., Meotti, M., et al. (2018). Reliability, validity and discriminant ability of the instrumental indices provided by a novel planar robotic device for upper limb rehabilitation. *J. neuroengineering Rehabil.* 15, 39. doi:10.1186/s12984-018-0385-8

Góngora Alonso, S., Hamrioui, S., de la Torre Díez, I., Motta Cruz, E., López-Coronado, M., and Franco, M. (2019). Social robots for people with aging and dementia: a systematic review of literature. *Telemed. e-Health* 25, 533–540. doi:10.1089/tmj.2018.0051

Gopura, R. A. R. C., Bandara, D. S. V., Kiguchi, K., and Mann, G. K. I. (2016). Developments in hardware systems of active upper-limb exoskeleton robots: a review. *Robotics Autonomous Syst.* 75, 203–220. doi:10.1016/j.robot.2015.10.001

Gualtieri, L., Rauch, E., and Vidoni, R. (2020). Emerging research fields in safety and ergonomics in industrial collaborative robotics: a systematic literature review. *Robot. Com.Int. Manuf.* 67, 101998. doi:10.1016/j.rcim.2020.101998

Haidegger, T. (2019). Autonomy for surgical robots: concepts and paradigms. *IEEE Trans. Med. Robot. Bionics* 1, 65–76. doi:10.1109/tmrb.2019.2913282

He, D., Ye, R., Chan, S., Guizani, M., and Xu, Y. (2018). Privacy in the internet of things for smart healthcare. *IEEE Commun. Mag.* 56, 38–44. doi:10.1109/mcom.2018.1700809

Hentout, A., Aouache, M., Maoudj, A., and Akli, I. (2019). Human-robot interaction in industrial collaborative robotics: a literature review of the decade 2008-2017. *Adv. Robotics* 33, 764–799. doi:10.1080/01691864.2019.1636714

Hill, D., Holloway, C. S., Morgado Ramirez, D. Z., Smitham, P., and Pappas, Y. (2017). What are user perspectives of exoskeleton technology? a literature review. *Int. J. Technol. Assess. Health Care* 33, 160–167. doi:10.1017/s0266462317000460

Hocoma (2020). *Hocoma* (Accessed September 01, 2020).

Hooshiar, A., Najarian, S., and Dargahi, J. (2020). Haptic telerobotic cardiovascular intervention: a review of approaches, methods, and future perspectives. *IEEE Rev. Biomed. Eng.* 13, 32–50. doi:10.1109/RBME.2019.2907458

Huang, J., Tu, X., and He, J. (2016). Design and evaluation of the rupert wearable upper extremity exoskeleton robot for clinical and in-home therapies. *IEEE Trans. Syst. Man. Cybern, Syst.* 46, 926–935. doi:10.1109/tsmc.2015.2497205

Hussain, A., Balasubramanian, S., Roach, N., Klein, J., Jarrassé, N., Mace, M., et al. (2017). Sitar: a system for independent task-oriented assessment and rehabilitation. *J. Rehabil. assistive Tech. Eng.* 4, 2055668317729637. doi:10.1177/2055668317729637

Jawaid, A. (2020). Protecting older adults during social distancing. *Science* 368, 145. doi:10.1126/science.abb7885

Jiménez-Fabián, R., and Verlinden, O. (2012). Review of control algorithms for robotic ankle systems in lower-limb orthoses, prostheses, and exoskeletons. *Med. Eng. Phys.* 34, 397–408. doi:10.1016/j.medengphy.2011.11.018

Johns Hopkins University (2020). *Covid-19 dashboard by the center for systems science and engineering (csse) at hopkins university*, Baltimore, MD: Johns Hopkins University. (Accessed September 01, 2020).

Kansagra, A. P., Goyal, M. S., Hamilton, S., and Albers, G. W. (2020). Collateral effect of covid-19 on stroke evaluation in the United States. *New Engl. J. Med.* 383 (4), 400–401. doi:10.1056/NEJMc2014816

Kapsalyamov, A., Hussain, S., and Jamwal, P. K. (2020). State-of-the-art assistive powered upper limb exoskeletons for elderly. *IEEE Access* 8, 178991–179001. doi:10.1109/access.2020.3026641

Katzschmann, R. K., Araki, B., and Rus, D. (2018). Safe local navigation for visually impaired users with a time-of-flight and haptic feedback device. *IEEE Trans. Neural Syst. Rehabil. Eng.* 26, 583–593. doi:10.1109/TNSRE.2018.2800665

Kim, J., Sin, M., Kim, W.-S., Min, Y.-S., Kim, W., Paik, N.-J., et al. (2020). Remote assessment of post-stroke elbow function using internet-based telerobotics: a proof-of-concept study. *Front. Neurol.* 11. doi:10.3389/fneur.2020.583101

King, J. S. (2020). Covid-19 and the need for health care reform. *New Engl. J. Med.* 382 (26), e104. doi:10.1056/NEJMp2000821

Kos, A., and Umek, A. (2019). Wearable sensor devices for prevention and rehabilitation in healthcare: swimming exercise with real-time therapist feedback. *IEEE Internet Things J.* 6, 1331–1341. doi:10.1109/JIOT.2018.2850664

Krebs, H. I., Hogan, N., Aisen, M. L., and Volpe, B. T. (1998). Robot-aided neurorehabilitation. *IEEE Trans. Rehab. Eng.* 6, 75–87. doi:10.1109/86.662623

Krebs, H. I., and Hogan, N. (2006). Therapeutic robotics: a technology push. *Proc. IEEE* 94, 1727–1738. doi:10.1109/jproc.2006.880721

Kuczynski, A. M., Dukelow, S. P., Semrau, J. A., and Kirton, A. (2016). Robotic quantification of position sense in children with perinatal stroke. *Neurorehabil. Neural Repair* 30, 762–772. doi:10.1177/1545968315624781

Kuczynski, A. M., Semrau, J. A., Kirton, A., and Dukelow, S. P. (2017). Kinesthetic deficits after perinatal stroke: robotic measurement in hemiparetic children. *J. neuroengineering Rehabil.* 14, 13. doi:10.1186/s12984-017-0221-6

Lachtar, A., Val, T., and Kachouri, A. (2019). Elderly monitoring system in a smart city environment using lora and mqtt. *IET Wireless Sensor Syst.* 10, 70–77. doi:10.1049/iet-wss.2019.0121

Lambercy, O., Lünenburger, L., Gassert, R., and Bolliger, M. (2012). Robots for measurement/clinical assessment. *Neurorehabil. Technol. (Springer)*, 443–456. doi:10.1007/978-1-4471-2277-7_24

Lange, S. J., Ritchey, M. D., Goodman, A. B., Dias, T., Twentyman, E., Fuld, J., et al. (2020). Potential indirect effects of the COVID-19 pandemic on use of emergency departments for acute life-threatening conditions - United States, january-may 2020. *MMWR Morb. Mortal. Wkly. Rep.* 69, 795. doi:10.15585/mmwr.mm6925e2

Leaman, J., and La, H. M. (2017). A comprehensive review of smart wheelchairs: past, present, and future. *IEEE Trans. Human-mach. Syst.* 47, 486–499. doi:10.1109/THMS.2017.2706727

Lefeber, N., De Keersmaecker, E., Troch, M., Lafosse, C., de Geus, B., Kerckhofs, E., et al. (2019). Robot-assisted overground walking: physiological responses and perceived exertion in nonambulatory stroke survivors. *IEEE Robotics Automation Mag.* 27, 22–31. doi:10.1109/MRA.2019.2939212

Leocani, L., Diserens, K., Moccia, M., and Caltagirone, C. (2020). Disability through covid-19 pandemic: neurorehabilitation cannot wait. *Eur. J. Neurol.* 27 (9), e50–e51. doi:10.1111/ene.14320

Lewnard, J. A., and Lo, N. C. (2020). Scientific and ethical basis for social-distancing interventions against COVID-19. *Lancet Infect. Dis.* 20, 631. doi:10.1016/s1473-3099(20)30190-0

Lopes, P., and Baudisch, P. (2017). Immense power in a tiny package: wearables based on electrical muscle stimulation. *IEEE Pervasive Comput.* 16, 12–16. doi:10.1109/mprv.2017.2940953

Lv, G., Zhu, H., and Gregg, R. D. (2018). On the design and control of highly backdrivable lower-limb exoskeletons: a discussion of past and ongoing work. *IEEE Control. Syst.* 38, 88–113. doi:10.1109/mcs.2018.2866605

Lyden, P. (2020). Temporary emergency guidance to us stroke centers during the covid-19 pandemic on behalf of the aha/asa stroke council leadership. *Stroke* 51, 1910–1912. doi:10.1161/STROKEAHA.120.030023

Lyu, M., Chen, W., Ding, X., Wang, J., Pei, Z., and Zhang, B. (2019). Development of an emg-controlled knee exoskeleton to assist home rehabilitation in a game context. *Front. neurorobotics* 13, 67. doi:10.3389/fnbot.2019.00067

Mace, M., Rinne, P., Liardon, J.-L., Uhomoibhi, C., Bentley, P., and Burdet, E. (2017). Elasticity improves handgrip performance and user experience during visuomotor control. *R. Soc. Open Sci.* 4, 160961. doi:10.1098/rsos.160961

Maceira-Elvira, P., Popa, T., Schmid, A.-C., and Hummel, F. C. (2019). Wearable technology in stroke rehabilitation: towards improved diagnosis and treatment of upper-limb motor impairment. *J. neuroengineering Rehabil.* 16, 142. doi:10.1186/s12984-019-0612-y

Maciejasz, P., Eschweiler, J., Gerlach-Hahn, K., Jansen-Troy, A., and Leonhardt, S. (2014). A survey on robotic devices for upper limb rehabilitation. *J. neuroengineering Rehabil.* 11, 3. doi:10.1186/1743-0003-11-3

MacLachlan, R. A., Becker, B. C., Tabarés, J. C., Podnar, G. W., Lobes, L. A., and Riviere, C. N. (2011). Micron: an actively stabilized handheld tool for microsurgery. *IEEE Trans. Robot* 28, 195–212. doi:10.1109/TRO.2011.2169634

Maisto, M., Pacchierotti, C., Chinello, F., Salvietti, G., De Luca, A., and Prattichizzo, D. (2017). Evaluation of wearable haptic systems for the fingers in augmented reality applications. *IEEE Trans. Haptics* 10, 511–522. doi:10.1109/toh.2017.2691328

Malik, N. A., Hanapiah, F. A., Rahman, R. A. A., and Yussof, H. (2016). Emergence of socially assistive robotics in rehabilitation for children with cerebral palsy: a review. *Int. J. Adv. Robotic Syst.* 13, 135. doi:10.5772/64163

Mancini, M., Smulders, K., Harker, G., Stuart, S., and Nutt, J. G. (2018). Assessment of the ability of open-and closed-loop cueing to improve turning and freezing in people with Parkinson's disease. *Scientific Rep.* 8, 1–9. doi:10.1038/s41598-018-31156-4

Mao, Y., and Agrawal, S. K. (2012). Design of a cable-driven arm exoskeleton (carex) for neural rehabilitation. *IEEE Trans. Robot.* 28, 922–931. doi:10.1109/TRO.2012.2189496

Martín, A., Pulido, J. C., González, J. C., García-Olaya, Á., and Suárez, C. (2020). A framework for user adaptation and profiling for social robotics in rehabilitation. *Sensors* 20, 4792. doi:10.3390/s20174792

Mehrdad, S., Liu, F., Pham, M. T., Lelevé, A., and Atashzar, S. F. (2021). Review of advanced medical telerobots. *Appl. Sci.* 11, 209. doi:10.3390/app11010209

Mochizuki, G., Centen, A., Resnick, M., Lowrey, C., Dukelow, S. P., and Scott, S. H. (2019). Movement kinematics and proprioception in post-stroke spasticity: assessment using the kinarm robotic exoskeleton. *J. neuroengineering Rehabil.* 16, 146. doi:10.1186/s12984-019-0618-5

Mozaffarian, D., Benjamin, E. J., Go, A. S., Arnett, D. K., Blaha, M. J., Cushman, M., et al. (2015). Executive summary: heart disease and stroke statistics-2015 update. *Circulation* 131, 434–441. doi:10.1161/cir.0000000000000157

Mukherjee, D., and Patil, C. G. (2011). Epidemiology and the global burden of stroke. *World Neurosurg.* 76, S85–S90. doi:10.1016/j.wneu.2011.07.023

Ng, J. J., Ho, P., Dharmaraj, R. B., Wong, J. C. L., and Choong, A. M. T. L. (2020). The global impact of covid-19 on vascular surgical services. *J. Vasc. Surg.* 71, 2182–2183. doi:10.1016/j.jvs.2020.03.024

Nicholson-Smith, C., Mehrabi, V., Atashzar, S. F., and Patel, R. V. (2020). A multi-functional lower- and upper-limb stroke rehabilitation robot. *IEEE Trans. Med. Robot. Bionics* 2, 549–552. doi:10.1109/TMRB.2020.3034497

Niemeyer, G., Preusche, C., Stramigioli, S., and Lee, D. (2016). Telerobotics. *Springer handbook of robotics*. Berlin, Germany: Springer, 1085–1108.

Noorian, A. R., Bahr Hosseini, M., Avila, G., Gerardi, R., Andrle, A.-F., Su, M., et al. (2019). Use of wearable technology in remote evaluation of acute stroke patients: feasibility and reliability of a google glass-based device. *J. Stroke Cerebrovasc. Dis.* 28, 104258. doi:10.1016/j.jstrokecerebrovasdis.2019.06.016

Noorian, A. R., Bahr Hosseini, M., Avilda, G., Gerardi, R., Andrle, A.-F., Su, M., et al. (2018). Abstract WP243: use of wearable technology in remote evaluation of acute stroke patients: feasibility and reliability of xpert eye: a google glass based solution. *Stroke* 49, AWP243. doi:10.1161/str.49.suppl_1.wp243

Nordin, N., Xie, S., and Wünsche, B. (2014). Assessment of movement quality in robot- assisted upper limb rehabilitation after stroke: a review. *J. neuroengineering Rehabil.* 11, 137. doi:10.1186/1743-0003-11-137

Otaka, E., Otaka, Y., Kasuga, S., Nishimoto, A., Yamazaki, K., Kawakami, M., et al. (2015). Clinical usefulness and validity of robotic measures of reaching movement in hemiparetic stroke patients. *J. neuroengineering Rehabil.* 12, 66. doi:10.1186/s12984-015-0059-8

Oubre, B., Daneault, J.-F., Jung, H.-T., Whritenour, K., Miranda, J. G. V., Park, J., et al. (2020). Estimating upper-limb impairment level in stroke survivors using wearable inertial sensors and a minimally-burdensome motor task. *IEEE Trans. Neural Syst. Rehabil. Eng.* 28, 601–611. doi:10.1109/TNSRE.2020.2966950

Panesar, S. S., Volpi, J. J., Lumsden, A., Desai, V., Kleiman, N. S., Sample, T. L., et al. (2019). Telerobotic stroke intervention: a novel solution to the care dissemination dilemma. *J. Neurosurg.* 132, 971–978. doi:10.3171/2019.8.JNS191739

Parikh, S. P., Grassi, V., Kumar, V., and Okamoto, J. (2007). Integrating human inputs with autonomous behaviors on an intelligent wheelchair platform. *IEEE Intell. Syst.* 22, 33–41. doi:10.1109/mis.2007.36

Pathak, A., Luntz, J., Brei, D., Shen, T., Napier, S., Ghosh, R., et al. (2012). Tremor stabilizing system for handheld devices. *US Patent* 8 (308), 664.

Pathak, A., Redmond, J. A., Allen, M., and Chou, K. L. (2014). A noninvasive handheld assistive device to accommodate essential tremor: a pilot study. *Mov Disord.* 29, 838–842. doi:10.1002/mds.25796

Pazzaglia, M., and Molinari, M. (2016). The embodiment of assistive devices-from wheelchair to exoskeleton. *Phys. Life Rev.* 16, 163–175. doi:10.1016/j.plrev.2015.11.006

Pehlivan, A. U., Losey, D. P., and OMalley, M. K. (2016). Minimal assist-as-needed controller for upper limb robotic rehabilitation. *IEEE Trans. Robot.* 32, 113–124. doi:10.1109/TRO.2015.2503726

Pennisi, P., Tonacci, A., Tartarisco, G., Billeci, L., Ruta, L., Gangemi, S., et al. (2016). Autism and social robotics: a systematic review. *Autism Res.* 9, 165–183. doi:10.1002/aur.1527

Pépin, J. L., Bruno, R. M., Yang, R.-Y., Vercamer, V., Jouhaud, P., Escourrou, P., et al. (2020). Wearable activity trackers for monitoring adherence to home confinement during the covid-19 pandemic worldwide: data aggregation and analysis. *J. Med. Internet Res.* 22, e19787. doi:10.2196/19787

Pernalete, N. P., Wentao Yu, W., Dubey, R. V., and Moreno, W. A. (2002). Augmentation of manipulation capabilities of persons with disabilities using scaled teleoperation. *IEEE/RSJ Int. Conf. Intell. Robots Syst.* 2, 1517–1522. doi:10.1109/IRDS.2002.1043970

Pernalete, N., Wentao Yu, W., Dubey, R., and Moreno, W. A. (2003). Telerobotic haptic system to assist the performance of occupational therapy tests by motion-impaired users. *IEEE Int. Conf. Robotics Automation (Cat. No.03CH37422)* 1, 1247–1252. doi:10.1109/ROBOT.2003.1241763

Peternel, L., Tsagarakis, N., and Ajoudani, A. (2017). A human-robot co-manipulation approach based on human sensorimotor information. *IEEE Trans. Neural Syst. Rehabil. Eng.* 25, 811–822. doi:10.1109/tnsre.2017.2694553

Polygerinos, P., Wang, Z., Galloway, K. C., Wood, R. J., and Walsh, C. J. (2015). Soft robotic glove for combined assistance and at-home rehabilitation. *Robotics Autonomous Syst.* 73, 135–143. doi:10.1016/j.robot.2014.08.014

Prince, M. J., Wu, F., Guo, Y., Gutierrez Robledo, L. M., O'Donnell, M., Sullivan, R., et al. (2015). The burden of disease in older people and implications for health policy and practice. *The Lancet* 385, 549–562. doi:10.1016/s0140-6736(14)61347-7

Proietti, T., Crocher, V., Roby-Brami, A., and Jarrasse, N. (2016). Upper-limb robotic exoskeletons for neurorehabilitation: a review on control strategies. *IEEE Rev. Biomed. Eng.* 9, 4–14. doi:10.1109/rbme.2016.2552201

Pu, L., Moyle, W., Jones, C., and Todorovic, M. (2019). The effectiveness of social robots for older adults: a systematic review and meta-analysis of randomized controlled studies. *The Gerontologist* 59, e37–e51. doi:10.1093/geront/gny046

Qiu, S., Liu, L., Wang, Z., Li, S., Zhao, H., Wang, J., et al. (2019). Body sensor network-based gait quality assessment for clinical decision-support via multi-sensor fusion. *IEEE Access* 7, 59884–59894. doi:10.1109/ACCESS.2019.2913897

Qiu, S., Wang, Z., Zhao, H., Liu, L., and Jiang, Y. (2018). Using body-worn sensors for preliminary rehabilitation assessment in stroke victims with gait impairment. *IEEE Access* 6, 31249–31258. doi:10.1109/ACCESS.2018.2816816

Randazzo, L., Iturrate, I., Perdikis, S., and Millán, J. D. R. (2017). mano: a wearable hand exoskeleton for activities of daily living and neurorehabilitation. *IEEE Robotics Automation Lett.* 3, 500–507. doi:10.1109/LRA.2017.2771329

Rehmat, N., Zuo, J., Meng, W., Liu, Q., Xie, S. Q., and Liang, H. (2018). Upper limb rehabilitation using robotic exoskeleton systems: a systematic review. *Int. J. Intell. Robot Appl.* 2, 283–295. doi:10.1007/s41315-018-0064-8

Reis, A., Xavier, R., Barroso, I., Monteiro, M. J., Paredes, H., and Barroso, J. (2018). The usage of telepresence robots to support the elderly. *(TISHW) (IEEE)* 2018, 8559549. doi:10.1109/TISHW.2018.8559549

Rinne, P., Mace, M., Nakornchai, T., Zimmerman, K., Fayer, S., Sharma, P., et al. (2016). Democratizing neurorehabilitation: how accessible are low-cost mobile-gaming technologies for self-rehabilitation of arm disability in stroke? *PLoS one* 11, e0163413. doi:10.1371/journal.pone.0163413

Ripin, Z. M., Chan, P. Y., and Alisah, I. (2020). Preliminary evaluation of active tremor cancellation spoon for patients with hand tremor. *IOP Conf. Ser. Mater. Sci. Eng.* 815, 012002. doi:10.1088/1757-899X/815/1/012002

Rocon, E., Belda-Lois, J. M., Ruiz, A. F., Manto, M., Moreno, J. C., and Pons, J. L. (2007). Design and validation of a rehabilitation robotic exoskeleton for tremor assessment and suppression. *IEEE Trans. Neural Syst. Rehabil. Eng.* 15, 367–378. doi:10.1109/tnsre.2007.903917

Rose, C. G., Pezent, E., Kann, C. K., Deshpande, A. D., and O'Malley, M. K. (2018). Assessing wrist movement with robotic devices. *IEEE Trans. Neural Syst. Rehabil. Eng.* 26, 1585–1595. doi:10.1109/TNSRE.2018.2853143

Rudilosso, S., Laredo, C., Vera, V., Vargas, M., Renú, A., Llull, L., et al. (2020). Acute stroke care is at risk in the era of covid-19: experience at a comprehensive stroke center in barcelona. *Stroke* 120, 1991–1995. doi:10.1161/STROKEAHA.120.030329

Saadeh, W., Butt, S. A., and Altaf, M. A. B. (2019). A patient-specific single sensor iot-based wearable fall prediction and detection system. *IEEE Trans. Neural Syst. Rehabil. Eng.* 27, 995–1003. doi:10.1109/tnsre.2019.2911602

Sabari, J., Stefanov, D. G., Chan, J., Goed, L., and Starr, J. (2019). Adapted feeding utensils for people with Parkinson's-related or essential tremor. *Am. J. Occup. Ther.* 73, 7302205120p1–7302205120p9. doi:10.5014/ajot.2019.030759

Saenz, J., Elkmann, N., Gibaru, O., and Neto, P. (2018). Survey of methods for design of collaborative robotics applications-why safety is a barrier to more widespread robotics uptake. *Proceedings of the 2018 4th International Conference on Mechatronics and Robotics Engineering*, 95–101. doi:10.1145/3191477.3191507

Saglia, J. A., Luca, A., Squeri, V., Ciaccia, L., Sanfilippo, C., Ungaro, S., et al. (2019). Design and development of a novel core, balance and lower limb rehabilitation robot: hunova®. *IEEE Int. Conf. Rehabil. Robot*, 2019, 417–422. doi:10.1109/ICORR.2019.8779531

Sanders, Q., Chan, V., Augsburger, R., Cramer, S. C., Reinkensmeyer, D. J., and Do, A. H. (2020). Feasibility of wearable sensing for in-home finger rehabilitation early after stroke. *IEEE Trans. Neural Syst. Rehabil. Eng.* 2020, 2988177. doi:10.1109/TNSRE.2020.2988177

Schirmer, C. M., Ringer, A. J., Arthur, A. S., Binning, M. J., Fox, W. C., James, R. F., et al. (2020). Delayed presentation of acute ischemic strokes during the covid-19 crisis. *J. Neurointervent Surg.* 12, 639–642. doi:10.1136/neurintsurg-2020-016299

Scoglio, A. A., Reilly, E. D., Gorman, J. A., and Drebing, C. E. (2019). Use of social robots in mental health and well-being research: systematic review. *J. Med. Internet Res.* 21, e13322. doi:10.2196/13322

Seiffert, M., Brunner, F. J., Remmel, M., Thomalla, G., Marschall, U., L'Hoest, H., et al. (2020). Temporal trends in the presentation of cardiovascular and cerebrovascular emergencies during the covid-19 pandemic in Germany: an analysis of health insurance claims. *Clin. Res. Cardiol.* 109, 1540–1548. doi:10.1007/s00392-020-01723-9

Seshadri, D. R., Davies, E. V., Harlow, E. R., Hsu, J. J., Knighton, S. C., Walker, T. A., et al. (2020). Wearable sensors for covid-19: a call to action to harness our digital infrastructure for remote patient monitoring and virtual assessments. *Front. Digital Health* 2, 8. doi:10.3389/fdgth.2020.00008

Settembre, N., Maurice, P., Paysant, J., Theurel, J., Claudon, L., Hani, H., et al. (2020). The use of exoskeletons to help with prone positioning in the intensive care unit during covid-19. *Ann. Phys. Rehabil. Med.* 63 (4), 379–382. doi:10.1016/j.rehab.2020.05.004

Shahbazi, M., Atashzar, S. F., and Patel, R. V. (2018). A systematic review of multilateral teleoperation systems. *IEEE Trans. Haptics* 11, 338–356. doi:10.1109/toh.2018.2818134

Shahbazi, M., Atashzar, S. F., Tavakoli, M., and Patel, R. V. (2016). Robotics-assisted mirror rehabilitation therapy: a therapist-in-the-loop assist-as-needed architecture. *Ieee/asme Trans. Mechatron.* 21, 1954–1965. doi:10.1109/tmech.2016.2551725

Sharifi, M., Behzadipour, S., Salarieh, H., and Tavakoli, M. (2020). Assist-as-needed policy for movement therapy using telerobotics-mediated therapist supervision. *Control. Eng. Pract.* 101, 104481. doi:10.1016/j.conengprac.2020.104481

Shi, B., Chen, X., Yue, Z., Yin, S., Weng, Q., Zhang, X., et al. (2019). Wearable ankle robots in post-stroke rehabilitation of gait: a systematic review. *Front. neurorobotics* 13, 63. doi:10.3389/fnbot.2019.00063

Shore, L., Power, V., De Eyto, A., and O'Sullivan, L. (2018). Technology acceptance and user-centred design of assistive exoskeletons for older adults: a commentary. *Robotics* 7, 3. doi:10.3390/robotics7010003

Shull, P. B., and Damian, D. D. (2015). Haptic wearables as sensory replacement, sensory augmentation and trainer–a review. *J. neuroengineering Rehabil.* 12, 59. doi:10.1186/s12984-015-0055-z

Silva de Lima, A. L., Smits, T., Darweesh, S. K. L., Valenti, G., Milosevic, M., Pijl, M., et al. (2020). Home-based monitoring of falls using wearable sensors in Parkinson's disease. *Mov Disord.* 35, 109–115. doi:10.1002/mds.27830

Simbaña, E. D. O., Baeza, P. S.-H., Huete, A. J., and Balaguer, C. (2019). Review of automated systems for upper limbs functional assessment in neurorehabilitation. *IEEE Access* 7, 32352–32367. doi:10.1109/ACCESS.2019.2901814

Simmatis, L., Atallah, G., Scott, S. H., and Taylor, S. (2019). The feasibility of using robotic technology to quantify sensory, motor, and cognitive impairments associated with als. *Amyotroph. Lateral Scler. Frontotemporal Degeneration* 20, 43–52. doi:10.1080/21678421.2018.1550515

Simmatis, L. E. R., Jin, A. Y., Keiski, M., Lomax, L. B., Scott, S. H., and Winston, G. P. (2020). Assessing various sensorimotor and cognitive functions in people with epilepsy is feasible with robotics. *Epilepsy Behav.* 103, 106859. doi:10.1016/j.yebeh.2019.106859

Simmatis, L., Krett, J., Scott, S. H., and Jin, A. Y. (2017). Robotic exoskeleton assessment of transient ischemic attack. *PLoS one* 12, e0188786. doi:10.1371/journal.pone.0188786

Simon, T. M., Thomas, B. H., and Smith, R. T. (2015). Low-profile jamming technology for medical rehabilitation. *IT Prof.* 17, 28–34. doi:10.1109/mitp.2015.87

Šlajpah, S., Kamnik, R., and Munih, M. (2014). Kinematics based sensory fusion for wearable motion assessment in human walking. *Comp. Methods Programs Biomed.* 116, 131–144.

Smith, E. E., Mountain, A., Hill, M. D., Wein, T. H., Blacquiere, D., Casaubon, L. K., et al. (2020). Canadian stroke best practice guidance during the covid-19 pandemic. *Can. J. Neurol. Sci.* 47, 474–478. doi:10.1017/cjn.2020.74

Srivastav, A. K., and Samuel, A. J. (2020). E-rehabilitation: one solution for patients with Parkinson's disease in covid-19 era. *Parkinsonism Relat. Disord.* 75, 128–129. doi:10.1016/j.parkreldis.2020.05.021

Stamford, J. A., Schmidt, P. N., and Friedl, K. E. (2015). What engineering technology could do for quality of life in Parkinson's disease: a review of current needs and opportunities. *IEEE J. Biomed. Health Inform.* 19, 1862–1872. doi:10.1109/jbhi.2015.2464354

Stefana, A., Youngstrom, E. A., Hopwood, C. J., and Dakanalis, A. (2020). The covid-19 pandemic brings a second wave of social isolation and disrupted services. *Eur. Arch. Psychiatry Clin. Neurosci.* 270, 785. doi:10.1007/s00406-020-01137-8

Stoyanova, M., Nikoloudakis, Y., Panagiotakis, S., Pallis, E., and Markakis, E. K. (2020). A survey on the internet of things (iot) forensics: challenges, approaches and open issues. *IEEE Commun. Surv. Tutorials* 2019, 2962586. doi:10.1109/COMST.2019.2962586

Suzman, R., Beard, J. R., Boerma, T., and Chatterji, S. (2015). Health in an ageing world-what do we know? *The Lancet* 385, 484–486. doi:10.1016/s0140-6736(14)61597-x

Sweeney, D., Quinlan, L., Browne, P., Richardson, M., Meskell, P., and ÓLaighin, G. (2019). A technological review of wearable cueing devices addressing freezing of gait in Parkinson's disease. *Sensors* 19, 1277. doi:10.3390/s19061277

Takeda, K., Tanino, G., and Miyasaka, H. (2017). Review of devices used in neuromuscular electrical stimulation for stroke rehabilitation. *Mder.* 10, 207. doi:10.2147/mder.s123464

Tavakoli, M., Carriere, J., and Torabi, A. (2020). Robotics, smart wearable technologies, and autonomous intelligent systems for healthcare during the COVID-19 pandemic: an analysis of the state of the art and future vision. *Adv. Intell. Syst.* 2, 2000071. doi:10.1002/aisy.202000071

Teasell, R., and Hussein, N. (2016). General concepts: therapies for rehabilitation and recovery. *Ischemic stroke therapeutics*. Berlin, Germany: Springer, 195–201.

Terroba-Chambi, C., Bruno, V., Millar-Vernetti, P., Bruce, D., Brockman, S., Merello, M., et al. (2019). Design and validation of a new instrument to assess fear of falling in Parkinson's disease. *Mov Disord.* 34, 1496–1504. doi:10.1002/mds.27820

Tripathy, A. K., Mohapatra, A. G., Mohanty, S. P., Kougianos, E., Joshi, A. M., and Das, G. (2020). Easyband: a wearable for safety-aware mobility during pandemic outbreak. *IEEE Consumer Elect. Mag.* 2020, 2992034. doi:10.1109/MCE.2020.2992034

Tripathy, S. (2020). The covid-19 pandemic and the elderly patient: review of current literature and knowledgebase. *J. Geriatr. Care Res.* 7, 79–83.

Tseng, T. W., Wu, C. T., and Lai, F. (2019). Threat analysis for wearable health devices and environment monitoring internet of things integration system. *IEEE Access* 7, 144983–144994. doi:10.1109/access.2019.2946081

Tucker, M. R., Olivier, J., Pagel, A., Bleuler, H., Bouri, M., Lambercy, O., et al. (2015). Control strategies for active lower extremity prosthetics and orthotics: a review. *J. neuroengineering Rehabil.* 12, 1. doi:10.1186/1743-0003-12-1

Valentí Soler, M., Agüera-Ortiz, L., Olazarán Rodríguez, J., Mendoza Rebolledo, C., Pérez Muñoz, A., Rodríguez Pérez, I., et al. (2015). Social robots in advanced dementia. *Front. Aging Neurosci.* 7, 133. doi:10.3389/fnagi.2015.00133

van den Berghe, R., Verhagen, J., Oudgenoeg-Paz, O., Van der Ven, S., and Leseman, P. (2019). Social robots for language learning: a review. *Rev. Educ. Res.* 89, 259–295. doi:10.3102/0034654318821286

Venkataraman, K., Amis, K., Landerman, L. R., Caves, K., Koh, G. C., and Hoenig, H. (2020). Teleassessment of gait and gait aids: validity and interrater reliability. *Phys. Ther.* 100, 708–717. doi:10.1093/ptj/pzaa005

Venkataraman, K., Morgan, M., Amis, K. A., Landerman, L. R., Koh, G. C., Caves, K., et al. (2017). Tele-assessment of the berg balance scale. *Arch. Phys. Med. Rehabil.* 98, 659–664. doi:10.1016/j.apmr.2016.10.019

Venketasubramanian, N. (2020). Stroke care services in Singapore during covid-19 pandemic—a national perspective. *Front. Neurol.* 11, 780. doi:10.3389/fneur.2020.00780

Viseux, F., Lemaire, A., Barbier, F., Charpentier, P., Leteneur, S., and Villeneuve, P. (2019). How can the stimulation of plantar cutaneous receptors improve postural control? review and clinical commentary. *Neurophysiologie Clinique* 49, 263–268. doi:10.1016/j.neucli.2018.12.006

Wang, C.-C., Chao, J.-K., Wang, M.-L., Yang, Y.-P., Chien, C.-S., Lai, W.-Y., et al. (2020). Care for patients with stroke during the covid-19 pandemic: physical therapy and rehabilitation suggestions for preventing secondary stroke. *J. Stroke Cerebrovasc. Dis.* 29, 105182. doi:10.1016/j.jstrokecerebrovasdis.2020.105182

Washabaugh, E., Guo, J., Chang, C. K., Remy, D., and Krishnan, C. (2019). A portable passive rehabilitation robot for upper-extremity functional resistance training. *IEEE Trans. Biomed. Eng.* 66, 496–508. doi:10.1109/TBME.2018.2849580

Wei, W. X. J., Fong, K. N. K., Chung, R. C. K., Cheung, H. K. Y., and Chow, E. S. L. (2019). "Remind-to-Move" for promoting upper extremity recovery using wearable devices in subacute stroke: a multi-center randomized controlled study. *IEEE Trans. Neural Syst. Rehabil. Eng.* 27, 51–59. doi:10.1109/TNSRE.2018.2882235

Weizman, Y., Tan, A. M., and Fuss, F. K. (2020). Use of wearable technology to enhance response to the coronavirus (covid-19) pandemic. *Public Health* 185, 221–222. doi:10.1016/j.puhe.2020.06.048

Wesselhoff, S., Hanke, T. A., and Evans, C. C. (2018). Community mobility after stroke: a systematic review. *Top. stroke Rehabil.* 25, 224–238. doi:10.1080/10749357.2017.1419617

World Health Organization (2020). *Coronavirus disease (covid-19) advice for the public*. Geneva, Switzerland: World Health Organization.

World Health Organization (2015). *World report on ageing and health*. Geneva, Switzerland: World Health Organization.

Wu, Y., Balatti, P., Lorenzini, M., Zhao, F., Kim, W., and Ajoudani, A. (2019). A teleoperation interface for loco-manipulation control of mobile collaborative robotic assistant. *IEEE Robot. Autom. Lett.* 4, 3593–3600. doi:10.1109/lra.2019.2928757

Xu, S., and Li, Y. (2020). Beware of the second wave of covid-19. *The Lancet* 395, 1321–1322. doi:10.1016/s0140-6736(20)30845-x

Yang, G.-Z., Nelson, B. J., Murphy, R. R., Choset, H., Christensen, H., Collins, S. H., et al. (2020). Combating covid-19—the role of robotics in managing public health and infectious diseases. 5 (40), eabb5589. doi:10.1126/scirobotics.abb5589

Yang, G., Deng, J., Pang, G., Zhang, H., Li, J., Deng, B., et al. (2018). An iot-enabled stroke rehabilitation system based on smart wearable armb and machine learning. *IEEE J. Transl. Eng. Health Med.* 6, 1–10. doi:10.1109/JTEHM.2018.2822681

Yang, J.-D., Liao, C.-D., Huang, S.-W., Tam, K.-W., Liou, T.-H., Lee, Y.-H., et al. (2019b). Effectiveness of electrical stimulation therapy in improving arm function after stroke: a systematic review and a meta-analysis of randomised controlled trials. *Clin. Rehabil.* 33, 1286–1297. doi:10.1177/0269215519839165

Yang, J., Zhou, J., Tao, G., Alrashoud, M., Mutib, K. N. A., and Al-Hammadi, M. (2019a). Wearable 3.0: from smart clothing to wearable affective robot. *IEEE Netw.* 33, 8–14. doi:10.1109/mnet.001.1900059

Yang, S., MacLachlan, R. A., and Riviere, C. N. (2014). Manipulator design and operation for a six-degree-of-freedom handheld tremor-canceling microsurgical instrument. *IEEE ASME Trans. Mechatron* 20, 761–772. doi:10.1109/TMECH.2014.2320858

Yen, H.-C., Jeng, J.-S., Chen, W.-S., Pan, G.-S., Chuang, Pt, Bs, W.-Y., Lee, Y.-Y., et al. (2020). Early mobilization of mild-moderate intracerebral hemorrhage patients in a stroke center: a randomized controlled trial. *Neurorehabil. Neural Repair* 34, 72–81. doi:10.1177/1545968319893294

Young, A. J., and Ferris, D. P. (2016). State of the art and future directions for lower limb robotic exoskeletons. *IEEE Trans. Neural Syst. Rehabil. Eng.* 25, 171–182. doi:10.1109/TNSRE.2016.2521160

Yurkewich, A., Atashzar, S. F., Ayad, A., and Patel, R. V. (2015). A six-degree-of-freedom robotic system for lower extremity rehabilitation. *IEEE (ICORR)* 2015, 810–815. doi:10.1109/ICORR.2015.7281302

Zhang, J., and Cheah, C. C. (2015). Passivity and stability of human-robot interaction control for upper-limb rehabilitation robots. *IEEE Trans. Robot.* 31, 233–245. doi:10.1109/tro.2015.2392451

Zhao, T., Deng, M., Li, Z., and Hu, Y. (2018). Cooperative manipulation for a mobile dual-arm robot using sequences of dynamic movement primitives. *IEEE Trans. Cogn. Dev. Syst.* 2018, 2868921. doi:10.1109/TCDS.2018.2868921

Conflict of Interest: The authors declare that the research was conducted in the absence of any commercial or financial relationships that could be construed as a potential conflict of interest.

frontiers in Robotics and AI

PERSPECTIVE
published: 14 April 2021
doi: 10.3389/frobt.2021.610653

Perspective: Wearable Internet of Medical Things for Remote Tracking of Symptoms, Prediction of Health Anomalies, Implementation of Preventative Measures, and Control of Virus Spread During the Era of COVID-19

Sarmad Mehrdad[1], *Yao Wang*[1,2] *and S. Farokh Atashzar*[1,3]*

[1] Department of Electrical and Computer Engineering, New York University, New York, NY, United States, [2] Department of Biomedical Engineering, New York University, New York, NY, United States, [3] Department of Mechanical and Aerospace Engineering, New York University, New York, NY, United States

OPEN ACCESS

Edited by:
Sanja Dogramadzi,
The University of Sheffield,
United Kingdom

Reviewed by:
Luis Gomez,
University of Las Palmas de Gran Canaria, Spain
Alessandro Di Nuovo,
Sheffield Hallam University,
United Kingdom

***Correspondence:**
S. Farokh Atashzar
f.atashzar@nyu.edu

Specialty section:
This article was submitted to Biomedical Robotics, a section of the journal Frontiers in Robotics and AI

Received: 26 September 2020
Accepted: 11 March 2021
Published: 14 April 2021

Citation:
Mehrdad S, Wang Y and Atashzar SF (2021) Perspective: Wearable Internet of Medical Things for Remote Tracking of Symptoms, Prediction of Health Anomalies, Implementation of Preventative Measures, and Control of Virus Spread During the Era of COVID-19. Front. Robot. AI 8:610653. doi: 10.3389/frobt.2021.610653

The COVID-19 pandemic has highly impacted the communities globally by reprioritizing the means through which various societal sectors operate. Among these sectors, healthcare providers and medical workers have been impacted prominently due to the massive increase in demand for medical services under unprecedented circumstances. Hence, any tool that can help the compliance with social guidelines for COVID-19 spread prevention will have a positive impact on managing and controlling the virus outbreak and reducing the excessive burden on the healthcare system. This perspective article disseminates the perspectives of the authors regarding the use of novel biosensors and intelligent algorithms embodied in wearable IoMT frameworks for tackling this issue. We discuss how with the use of smart IoMT wearables certain biomarkers can be tracked for detection of COVID-19 in exposed individuals. We enumerate several machine learning algorithms which can be used to process a wide range of collected biomarkers for detecting (a) multiple symptoms of SARS-CoV-2 infection and (b) the dynamical likelihood of contracting the virus through interpersonal interaction. Eventually, we enunciate how a systematic use of smart wearable IoMT devices in various social sectors can intelligently help controlling the spread of COVID-19 in communities as they enter the reopening phase. We explain how this framework can benefit individuals and their medical correspondents by introducing Systems for Symptom Decoding (SSD), and how the use of this technology can be generalized on a societal level for the control of spread by introducing Systems for Spread Tracing (SST).

Keywords: COVID-19, IoMT, smart wearables, spread control, AI for health, smart connected health, telemedicine, symptom tracking

1. INTRODUCTION

SARS-CoV-2, also known as COVID-19, is a novel coronavirus that initiated a pandemic outbreak in December 2019. Due to the high infection rate and relatively low mortality rate, as well as the long incubation period, COVID-19 spread through more than 19 countries by late-January 2020 (Adhikari et al., 2020; Tang et al., 2020; Zhai et al., 2020). The aggressive nature of the virus besides the limited knowledge has resulted in high pressure on the healthcare systems (Wang C. et al., 2020). As the initial waves of this virus is being passed in some countries (Leung et al., 2020), many nations and states are going through phases of reopening (Ainslie et al., 2020; Olagnier and Mogensen, 2020), which suggests that active monitoring of symptom development and spread should be conducted more robustly while preventive measures are implemented in a multifaceted manner to mitigate (if not possible to prevent) the following waves of the pandemic.

In the absence of widely-available vaccine for different variants of the virus, and approved treatment during any pandemic, the only available solution is to implement preventive measures to be taken in an attempt to mitigate the virus' damage as much as possible until a reliable cure is found (Le et al., 2020). As of the time of writing this paper, no approved cure for COVID-19 has been found, and the research for finding a solution to end this pandemic is still ongoing (Li X. et al., 2020) with some limited access to vaccines for initial variants of the virus. A wide range of tests has been introduced for diagnosing infected cases such as CT Scans (Li and Xia, 2020) and Polymerase Chain Reaction (PCR) (Li Y. et al., 2020; Long et al., 2020). Research centers are acquiring knowledge about the virus to understand the infection mechanism (Zheng et al., 2020), alarming early symptoms (Sun et al., 2020), silent symptoms (e.g., "happy hypoxemia Guo et al., 2020; Tobin et al., 2020"), and the virus' function in the body (Chen et al., 2020).

Any possible solution that can facilitate faster and more accurate preventative actions (Adhikari et al., 2020), means of diagnosis (Wynants et al., 2020; Zhai et al., 2020), development of predictive models (for identifying symptoms' progress) (Liu et al., 2020), tracing, and monitoring (Hellewell et al., 2020) is highly beneficial and essentially needed by several policymakers and stakeholders (Ransing et al., 2020). These activities concern hospitalized patients, out-patients, and those who have not been diagnosed.

This article provides the authors' perspectives about the functionality of smart wearable IoMT technologies for early diagnosis of COVID-19 symptoms (including silent symptoms) at the individual level and for tracking the interpersonal interaction using which the spread of the virus within the society can be modeled. We argue that the same technology can be used beyond COVID-19 and for detection and tracking of any infectious disease which results in respiratory symptoms. We will discuss the existing techniques and technologies and will explain the existing technical challenges to be addressed. We explain the functionality of state-of-the-art biosensors and machine intelligence which can be fused in the context of wearable IoMT technology to address several "unmet needs."

In this paper we categorize IoMT technologies as (a) Systems for Symptom Decoding (SSD), and (b) Systems for Spread Tracing (SST). IoMT-based SSD are those systems which assist with early diagnosis and tracing of the symptoms at the individual level while coupled with certain algorithms and additional hardware, SST technology are those technologies to model not only the individual symptoms but also the dynamics of symptom evolution in clusters of population based on interaction models and tracing of interpersonal interaction for better management of the spread in a cluster and on a larger scale in society.

In this perspective article, we disseminate our perspective about the challenges and potentials for the use of SSD technologies to continuously and autonomously monitor the vital signs of patients can be to alert the individual and the care providers about any upcoming potentially-major health anomalies so that proper medical care can be planned. We will discuss the imperative role of machine intelligence in particular health-related anomaly detection algorithms which can be used to not only detect but also predict the flares of symptoms. We will also highlight that how with the use of SSD technologies objective telemedicine sessions have been conducted, and how this can be further promoted to enhance telemedicine quality and reduce the need for in-person visits, and to avoid interpersonal contacts.

It should be noted that, continual monitoring allows for detecting infrequent flares of symptoms which may not be feasible based on infrequent discrete visits (Joyia et al., 2017; Khan et al., 2020). This is a major benefit of IoMT technologies which can significantly help with the fight against a pandemic, if low-cost, and highly-accessible wearable IoMT can be made available. This will not only help with a faster and more efficient assessment of the symptoms, but it also will help to distribute the healthcare resources optimally based on data collected from the affected patients. To further motivate more investment and investigation in this field it should be noted that SSD systems can also significantly help to monitor individuals before the infection and promote early diagnosis, planning, and management under remote access. This will be possible due to the available infrastructures for a smart and connected healthcare model which should be further enhanced to prepare the system for future waves of the pandemic and future pandemics.

The authors would like to emphasize their opinion that the use of IoMT devices can be extended to a higher level, for example, for clusters of patients in clinics or in small and then larger societies. This will be challenging but will allow monitoring not only the symptoms of individuals but also the spread of the symptoms. This concept has already been evaluated using smartphones in some couturiers (such as South Korea, India, Iceland) and some states in the United States (such as Utah), using GPS data of smartphones to monitor COVID-19 spread. However, GPS is not precise enough to gauge short distances, especially for in-door interactions. Thus, other forms of technologies such as Bluetooth Low-Energy (BLE) have been suggested (for example, by Google and Apple) on smartphones.

Based on the literature review conducted in this paper (explained later), despite the benefit of existing systems, such as BLE, the current technology has major limitations, among which we can highlight sensitivity to dynamic motions of

the two carriers, sensitivity to a dynamic environment, the difficulty of calibration and need for re-calibration in a cluttered environment, and sensitivity to angle of arrival and location of the sender and receiver. This highlights a list of challenges that should be investigated for the higher performance of wearable IoMT on a large scale. Addressing these challenges, IoMT-based SST can implement preventive measures such as social distancing guidelines (SDG) based on the gathered multimodal information about (a) the symptoms evolution in a cluster of population and (b) interpersonal interaction in the clusters, especially in crowded indoor environments. Examples are medical facilities (such as dialysis clinics and neurorehabilitation clinics) and non-medical facilities, such as nursing homes, senior homes, drug rehabilitation facilities. On a larger scale, SST technology can enable medical providers to have a broader symptom monitoring over the society (and clusters of the population) in terms of the pandemic spread, and thereby manage the distribution of hospitalizations and medical supplies. It can be mentioned that the extended surveillance that SST technology grants can help policymakers to detect and react to the main causes of the spread by enacting more accurate laws to fight against the spread. SST technologies also raise awareness among the people about the dangerous areas of the city in regard to COVID-19 spread.

In this perspective article, we will also disseminate our opinion that both SST and SSD technologies can be embodied as a personal smart wearable device to help process the related bio-signals for diagnosis, tracking, and prevention. However, this would require significant optimization of electronics and investigation of means of reducing the cost to maximize accessibility and wide-use of such technology among the society regardless of the economic strength. This is a challenge to be addressed since most of the existing wearable systems either rely on connection with smartphones or have a very high cost, challenging the usability and feasibility of widely-used in societies with a low economy. In addition, despite all exciting benefits, data security, and reliability of data transmission can raise concerns and should be investigated thoroughly (Zhang Z. K. et al., 2014; Dorri et al., 2017; Khan and Salah, 2018; Noor and Hassan, 2019).

This article aims to initiate an in-depth conversation between different sectors, including researchers, technology designers, providers, hospitals, and policymakers to not only examine ways that can be implemented rapidly to adopt the existing technology and improve the health care system's diagnostic and preventative power using IoMTs but also to examine the challenges, and future directions of such technology in particular when the use is scaled-up to a societal level in order to fight possible future waves of COVID-19 pandemic and future pandemics. The authors would like to acknowledge that this article is written as a "perspective article type" to provide the opinion of the authors on the specific topic of the paper, i.e., the potentials of IoMT for COVID-19 response. Our intention in writing this article is to initiate discussions between researchers, policymakers, and stakeholders to further investigate the use of IoMT solutions for empowering the healthcare systems under the severe restrictions imposed by COVID-19 and considering the unfortunate current and future waves of this pandemic and future pandemics.

2. INTERNET OF (MEDICAL) THINGS IN THE ERA OF COVID19

IoMT has exponentially become more popular during the past decade due to the benefits for creating smart environments that can autonomously function to provide various services (Bélissent, 2010; Sundmaeker et al., 2010; Gubbi et al., 2013). IoMT wearable devices have been increasingly used for medical purposes, such as monitoring health of elderly (Liang and Yuan, 2016), physical activity monitoring (Wang and Tang, 2020), and orthopedic care (Singh et al., 2020). However, most of the pre-COVID-19 uses of IoMT devices were for small-scale application and in many cases when the cost and scalability were not an issue. Given the large-scale challenges caused by COVID-19 pandemic, autonomous services, and remote conduction of service (telepresence) have become of higher importance, in particular in the context of telemedicine (Singh et al., 2020) calling for large-scale use of affordable and accessible technology which can be used in remote areas and in regions with limited economic power. Several governmental funding agencies are now supporting research proposals across the world for designing low-cost scalable IoMT devices to enhance the health care system during the fight with COVID-19. Examples are funded NSF RAPID grants (Atashzar and Wang, 2020; Rogers, 2020), in addition to numerous calls for proposals, such as NRC (2020). This shows the imperative unmet need for having very low cost and effective IoMT devices for telemedicine which requires addressing a wide range of technical challenges including the accuracy, wearability, ease-of-use (specially for aged population) in unstructured dynamic environments and with minimum to no re-calibration needs. For this there is a need for discussing the building block of an IoMT framework in the context of COVID-19. IoMT frameworks are composed of two cores, namely, hardware and middleware (Gubbi et al., 2013).

2.1. Hardware

Hardware includes all the sensors that monitor biomarkers and symptoms. To choose the best sensors for tracking symptoms of COVID-19, first, we should have an in-depth insight into the symptoms of COVID-19 infection. Then we should choose the most appropriate sensors for tracking the symptoms, considering the cost for large scale deployment, need for calibration, re-calibration, and the ease of use in the context of a wearable system for the society.

Current identified symptoms of COVID-19 are predominantly fever (Huang et al., 2020; Roser et al., 2020; Wang D. et al., 2020), dry cough (Chen et al., 2020; Huang et al., 2020; Roser et al., 2020; Wang D. et al., 2020), fatigue (Huang et al., 2020; Roser et al., 2020; Wang D. et al., 2020), a drop of SpO2 with minimum signs (happy hypoxemia) (Guo et al., 2020; Tobin et al., 2020), and other symptoms that are less frequent, though can be more serious, e.g., shortness of breath (Chen et al., 2020; Roser et al., 2020), headache (Chen et al., 2020; Huang et al., 2020; Roser et al., 2020; Wang D. et al., 2020), and muscle pain (Chen et al., 2020; Roser et al., 2020).

Since COVID-19 is still known to be a respiratory disease, achieving information about blood oxygen saturation level is

essential. It should be highlighted that happy hypoxemia is an unconventional situation because of which patients who have critical oxygen saturation do not feel unwell for a long period of time during which the infection gets worse, while patients do not show serious symptoms resulting in delayed delivery of care. This shows the importance of detecting such a condition as early as possible. Pulse oximeter sensors measure pulse rate and the level of oxygen saturation in reduced hemoglobin (Hb), based on the light absorption characteristic (Vandecasteele et al., 2017).

Challenges for using Spo2 is the sensitivity of such sensor to the contact quality and possibility blockage issues (such as due to body hair) affecting the reflective light, also sensitivity to movements. Thus choosing the best number of sensors (to conduct redundant recording) and the best location on the body are imperative topics to be investigated when designing the wearable for a large scale. One solution is to use the multichannel recording to reduce the chance of blockage and increase the signal to noise ratio by fusing the recording. However, this would increase the cost, size, and computational load. A comprehensive analysis is needed to test various locations on the body, which can provide a robust recording. The most successful wearable systems in the market are smartwatches. However, due to the complexity of the physiology at the wrist, recording SPo2 has been a major challenge for smartwatch companies. A limited number of very recent smartwatches in the marker offer SPo2 recording; however, they require a very steady posture for a prolonged duration, which will be a challenge for patients or elderly users. Also, these systems are not able to provide continual recording, limiting the chance of picking up the dynamic changes.

Another challenge of existing IoMT devices is the need for being paired with a smartphone. This significantly increases the cost and reduces accessibility, especially for remote areas and for areas with a low economy. Thus there is an unmet need for having an IoMT device that can not only accurately measure the symptoms but also be independent of any edge device and can operate as a stand-alone technology with minimum cost. As mentioned before, some grant agencies are calling for new proposals to generate stand-alone IoMT devices under 50$. Of course, the accuracy cannot be sacrificed, especially since the recordings are very sensitive. For example, a SPo2 of 91 out of 100 may require immediate attention, and this cannot be within the range of error of the hardware.

In addition to Spo2, respiratory rate (RR) can be achieved by various means, such as advanced processing of ECG (Shen et al., 2017) or through the use of an array of piezoresistive films placed non-invasively around an individual's chest to sense the frequency of the chest motion (Loriga et al., 2006; Pacelli et al., 2006a,b; Witt et al., 2011; Fiedler et al., 2012; Atalay et al., 2014; Subbe and Kinsella, 2018). The challenge with measuring RR is the very low-frequency content, which makes it computationally difficult to estimate based on bioelectrical recording such as ECG. There are also specific challenges with any bioelectric recording, as explained below. Using pressure belts can provide a measure of RR, but it would challenge the wearability and usability of the system and makes it difficult for large-scale uses. The topic of calculating RR is an accelerated field of research, and more recent efforts are focused on using other modalities (such as optical PPG) to extract RR.

Body temperature is the most important information for COVID-19 (Roser et al., 2020). In order to measure this modality, contact sensors and IR sensors have been used. IR-based temperature sensors provide better performance in rejecting the ambient noise and less sensitivity to contact conditions (Stavem et al., 1997; Liang and Yuan, 2016) when compared with contact sensors (Sibinski et al., 2010), thus it is suggested for smart wearables.

For detecting functionality of cardiovascular system besides symptoms of fatigue, muscle soreness, stress, and heart rate (and possibly RR), bioelectrical signals (such as EEG, EMG, and ECG) can be used as information rich markers (Gazendam and Hof, 2007; Jap et al., 2009; Craven et al., 2014; Rechy-Ramirez and Hu, 2015; Acharya et al., 2018; Xia et al., 2018). Bioelectrical recording however may face challenges such as being affected by the electromagnetic noise of the household devices, or changes in electrical impedance and connectivity stemming from sweating and other physiological causes. Substitutional sensing modalities have been used in wearable IoMT devices. For monitoring heart rate, PPG may replace ECG while relaxing the dependency to electrical contact, and for monitoring muscle activities, mechanomyography, or force-myography may replace EMG (Castillo et al., 2020). Besides sensors, communication, and power electronics are other modules of hardware in a wearable IoMT, the complexity of which depends on the bandwidth needed and power consumption.

From a communication standpoint, in wearable IoMT devices, near field connection (NFC) (Neefs et al., 2010; Opperman and Hancke, 2011; Timalsina et al., 2012; Duregger et al., 2015), Bluetooth connection (Lee et al., 2007; Dementyev et al., 2013), and WiFi (Lee et al., 2007; Curone et al., 2010; Kim et al., 2015) are used based on their data transfer rate, range of communication capability, power consumption, and availability. Some of these communication modalities are also used for localization, as explained later. It should be added that the communication module of wearable systems has been seen as a potential solution for addressing the contact tracing problem. For example, there is a wide range of studies on the use of Bluetooth low energy. Later in this document, we provide our perspectives on the benefits and challenges of the use of such a solution for detecting interpersonal contact between the wearers.

Thus, it can be mentioned that despite a wide range of available sensing technologies, particular investigations are needed to minimize the cost while maximizing the accuracy and wearability. In the above, a range of challenges with existing technologies is provided, which shows the roadmap that can be taken to realize a scalable solution.

2.2. Middleware

Middleware administrates storing the information and evaluating the collected data to extract meaningful features that can be assessed on the fly to (a) provide biofeedback to the user (Sundmaeker et al., 2010), and (b) provide information from a cluster of users for analysis by medical workers, policymakers, and other public sectors, which helps to monitor the effects of

healthcare and guidelines at the societal level. There are different architectures of IoMT middleware that are utilized based on the expected functionality of the framework. These architectures can be categorized mainly as service-based (Papazoglou and Georgakopoulos, 2003), cloud-based (Ngu et al., 2016), and actor-based (Soldatos et al., 2015) modules. As a part of middleware, diagnostic IoMT technologies can be equipped with means of artificial intelligence to predict health-related anomalies. In the rest of this article, we provide our perspective on this important topic as well.

2.2.1. Security and Privacy

Privacy is a significant concern and must be addressed before any potential large-scale use of IoMT devices for contact tracing and symptom tracking. Without a systematic solution which provides a very high degree of protection on patient's data, IoMT devices can only be used up to a limited scale, such as for in a hospital uses or for clusters of the high-risk population in a closed space (such as nursing homes to track symptom evolution in the population), or as part of telemedicine and individual uses. These are examples of limited scale uses for which the important matter of privacy and security can be addressed using existing infrastructures. For any large-scale use of the device, a serious concern that needs to be addressed is the matter of large scale security and privacy of the information. Relevant important discussions can be found in Subashini and Kavitha (2011), Zhang Z. K. et al. (2014), Dorri et al. (2017), Gatouillat et al. (2018), Khan and Salah (2018), Hatzivasilis et al. (2019), Noor and Hassan (2019), and Kagita et al. (2020).

The authors also believe that one additional issue related to this topic is the reliability of data storage and data transmission and accessibility of the medical sector to such data. Since internet-based architectures that handle personal information can be a subject of different attacks, there is an imperative need for utilizing security algorithms. Examples can be found in the literature focusing on the maintenance of the safety of such systems (Sicari et al., 2015). In addition to compromising information confidentiality, large-scale uses of IoMT architectures can increase the susceptibility to malicious cyber-physical attacks that are aiming to hinder the processing of the data and causing failures, false-positive alarms, and false-negative reports (Khan and Salah, 2018). These attacks can range from low-level (Xu et al., 2005) to intermediate-level (Zhang K. et al., 2014) and high-level (Conzon et al., 2012). For addressing this issue, there is a need for implementing defense mechanisms. Several defense techniques have been proposed in the literature for each type of attack, which should be investigated before a large-scale IoMT can be deployed (Xiao et al., 2009; Bhattasali and Chaki, 2011; Khan and Salah, 2018).

3. IoMT WEARABLE TECHNOLOGIES

Due to the potential benefit of IoMT devices, there have been an accelerated range of recent efforts that envision the use for fighting against COVID-19 spread and future pandemics. These aim at the conduction of early diagnosis, tracking the spread, and monitoring the infected and susceptible individuals (Atashzar and Wang, 2020; Dong et al., 2020; Garg, 2020; Roser et al., 2020; Sohrabi et al., 2020; Wu and McGoogan, 2020). The trend (Ng et al., 2020) is motivated with the imperative need to prevent the spread of the COVID-19 on different societal levels. In order to discuss various functionality of IoMT wearable technologies, in this prespective article, authors have categorized IoMT wearables into SSD and SST.

3.1. Systems for Symptom Decoding

Technologies, which are called Systems for Symptom Decoding (SSD) in this paper, are designed for diagnosis, monitoring, analyzing the evolution of signs of infection at an individual level. Upon achieving the biomarkers via the hardware in an SSD, the information can be sent to the (cloud-based) middleware to be processed using various AI-based anomaly detection algorithms, which are machine learning modules that process the distribution of multidimensional data and detect health-related anomalies.

The authors would like to highlight that based on conventional machine-learning-based anomaly detection approaches, subtle multidimensional changes in the well-being of an individual can be tracked to inform the medical correspondent about the malevolent alterations in the biomarkers, to promote early diagnosis of COVID-19 infection, fighting the prolonged incubation period of COVID-19 (Zhai et al., 2020).

In terms of the type of algorithm for detecting infection-related health anomalies, gray box and black box artificial intelligence models can be used (see examples in the literature; Khan and Khan, 2012), some of which rely on probabilistic distributions of the data, and some rely on underlying labeled patterns in the healthy data to be modeled. Based on probabilistic algorithms, the likelihood of infection for an individual can be calculated. In this regard, we can highlight two main subcategories for health-related anomaly detection, which can be used in IoMT wearable for COVID-19, namely (a) clustering-based techniques, (b) classification-based techniques.

In this regard, the K-means clustering approach (Tan et al., 2016), K-medoids approach (Garg et al., 2020), and Expectation-Maximization-based clustering approaches such as mixture models (Bublitz et al., 2017; Qi et al., 2018) are among the candidates for clustering techniques. These machine learning modules try to detect the underlying clusters of multidimensional data and predict an anomaly if the new data does not show a high probability of belonging to one of the clusters.

In addition, the Fuzzy logic approach (Hamamoto et al., 2018), genetic algorithm (Chen et al., 2018), naïve Bayes networks (Zhen et al., 2017), neural networks (Amarasinghe et al., 2018; Chalapathy and Chawla, 2019), and support vector machines (Erfani et al., 2016) are among classification algorithms used for anomaly detection, which can be used for detecting COVID-19 anomalies in the symptom space of patients.

The authors' perspective about the context of detecting the health anomalies of COVID-19 based on multidimensional data collected by wearables is as follows. Despite the great success and advancements in the field, the anomaly detection algorithms suffer from several issues which are pronounced for COVID-19, including (a) the sensitivity of the accuracy to the amount of available labeled data (this is concerning in the context of

COVID-19 since the data is limited due to the novelty of the virus and limited knowledge and consistent data collection), (b) variation in the normal behavior of the data and the definition of normal behavior (which is questionable due to the very different and unpredictable behavior of the virus for different individuals), (c) noise in data (which is a challenge for any wearable and in-home technologies), (d) similarity between advanced anomalies and normal data (which is a problem due to heterogeneity of symptoms of COVID-19). Some of the aforementioned concerns are rooted in existing issues of health-related and more information in this regard can be found in Papazoglou and Georgakopoulos (2003), Xu et al. (2005), Xiao et al. (2009), Bhattasali and Chaki (2011), Conzon et al. (2012), Zhang K. et al. (2014), Agrawal and Agrawal (2015), Rechy-Ramirez and Hu (2015), Sicari et al. (2015), Soldatos et al. (2015), Ngu et al. (2016), and Khan and Salah (2018).

Our perspective about the near future of AI-based diagnostic techniques for COVID-19 and other infectious disease is that the SSD technologies can be augmented by algorithms which can facilitate prediction-in-time (beyond monitoring) the "evolution" of symptom biosignals. This can significantly augment the versatility of the system. In this regard, machine learning algorithms that can predict a possible near future adverse event over a given prediction horizon can be significantly beneficial as it would allow for early diagnosis and planning. The longer the prediction horizon, the more complex yet more beneficial the algorithms will be. This is a challenging task; however, the authors believe that it can be realized in the near future using state of the art neural network architectures, specifically LSTM or GRU (which are two modern formats of recurrent neural networks for processing time series). However, these models are supervised techniques and require heavy data collection. A new variant of neural network architecture that can help with addressing this issue is shallow neural networks. Thus, the authors believe that a combination of a shallow neural network and a recurrent neural network architecture can provide the needed temporal resolution in terms of the prediction horizon for diagnosing infection for COVID-19 symptoms. The use of shallow architectures reduces the need for heavy data collection, and the use of advanced modules such as GRU, which is designed to be more efficient, allows for underlying modeling patterns of symptom evolution that can be decoded for early prediction of infection progress.

Thus, it can be summarized that thanks to the advances in the last decade on neural network architectures, the next generation of wearable IoMT devices can be augmented with cloud computation allowing for accessing strong machine intelligence for early detection and possibly prediction (with a tunable horizon) for health-related anomalies. However, this requires widespread and fast access to cloud computation infrastructure. There exists a rich literature for detecting general health anomalies to be adopted in COVID-19 IoMT wearables; however, there exist several challenges that should be investigated, as discussed in the above. This would call for investment and investigation to empower wearable technologies of tomorrow with means of predictive diagnosis intelligence. This can significantly enhance the protocols and diagnostic workflow. For example, results of the anomaly assessment can be forwarded to the medical correspondent to accordingly schedule hospitalization and online visits or suggest guidelines to the possibly infected person. **Figure 1** shows the overall concept of SSD.

3.2. Systems for Spread Tracing

In this paper, we categorize SST as technologies that will take the analyzed information from multiple SSD systems to monitor the aggregation of information from a cluster of users to assess the current status of the spread of COVID-19 and suggest guidelines for the communities (including users and non-users of SSDs) to help avoid the contraction of the COVID-19 especially for high-risk populations and plan for minimizing the risk of infections for non-affected groups.

The authors would like to highlight that SST can be identified as the more general IoMT surveillance system for a population cluster as it evaluates both medical biomarkers (those collected by SSD) and non-medical information regarding the interpersonal interaction between individuals. As an example, our perspective is that in an in-patient non-COVID clinic in a hospital where there are clusters of patients, clinicians, and visitors, deployment of an SST technology (such as smart tags) can allow for monitoring the evolution of symptoms among the under surveillance population to minimize the risk of confrontation and detecting early spread and hotspots of infection. This will be imperative for (a) controlling the spread, (b) isolating the non-infected individuals, and (c) planning for implementation of a more efficient SDG.

It is of high importance to track and backtrace the path that led to an infection, to monitor the early or recovered cases, and to collect data for future analyses. This requires significant human resources, clinical resources, and time which are all in shortage currently in healthcare systems (Boulos and Geraghty, 2020; Dong et al., 2020; Emanuel et al., 2020; Fauci et al., 2020; Menni et al., 2020). Here, "tracking" is defined as gathering information about (a) the history of an individual's locations, (b) people that the individual has visited, and (c) tracking back to the infection source. The authors would like to highlight that currently, still in many couturiers (not all), this process has been done by subjective surveys, which are very costly, non-objective, time-consuming, and not necessarily accurate as in many cases, an individual in the chain of interaction may have mild or happy symptoms (which exist but are not felt as mentioned before). This shows the importance of objective tracking of the trace of the virus by (a) collecting multidimensional symptom markers and (b) history of interaction, and (c) compliance to the SDG. This topic is discussed in detail in section 3.2, and the authors have introduced recent efforts by industries such as Google and Apple and some governments to use advanced technologies such as GPS and BLE to promote objective contact tracking using smartphone technologies. This highlights the ongoing accelerated effort, which further supports the use of wearable IoMT technologies (equipped with contact tracking technologies) for COVID-19.

It should be noted that the benefit of augmenting sensorized wearable technologies with biomarker and contact tracking features is that the technology is able to not only track the location

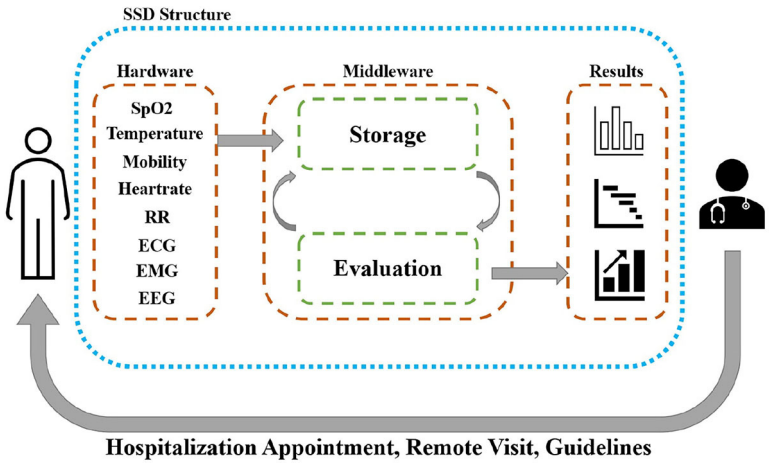

FIGURE 1 | Functionality of SSD.

but also concurrently the symptoms of the user to generate a better model of infection spread in society and to better protect the wearer and the visitors to the hotspots and estimate the infection severity in various regions.

However, we should highlight that there is a wide range of technical bottlenecks. Among the existing challenges, we would light to highlight (a) localization accuracy and resolution in a dynamic, unstructured, and cluttered environment and (b) the security and privacy of the wearers. Regarding outdoor localization, it can be mentioned that although GPS accuracy may not be at the ideal level to detect interpersonal interaction, it is sufficient for detecting whether an individual has been in a crowded or infected hotspot zone or if a region is showing flares of symptoms. It can also be used to detect whether an individual has been following SDG. The use of such an advanced approach allows for the generation of density heatmaps of the cluster of crowds and that of symptoms and analysis of the interaction between the two clusters.

Regarding indoor localization, however, the state of the art techniques are designed based on the use of Bluetooth Low Energy (BLE) (Ng et al., 2020; Sadowski et al., 2020; Spachos and Plataniotis, 2020a,b), Ultra High-Frequency RFID (Li et al., 2019), WiFi (Wang et al., 2017), and hybrid systems (Guo et al., 2019; Monica and Bergenti, 2019). Our perspective is that using these technologies; a wearable IoMT device can be equipped with cloud-based signal triangulation techniques and advanced filtering, data fusion, and estimation approaches (such as Kalman-based sensor fusion and machine learning techniques) to locate the wearer with respect to the known locations of signal transmitters installed in an indoor infrastructure. The technical challenges are (a) accuracy needed for detecting interpersonal interactions, (b) high sensitivity to dynamical movements within the unstructured under-surveillance environment and movement artifacts from the wearers, (c) the cost of the systematic infrastructure needed for signal triangulation, and (d) patient privacy.

The authors would like to highlight that with the use of SST, it can be inferred if an under-surveillance society is following the preventive guidelines and how the symptom activity is spreading among the population. In addition, we believe that optimizing the effort to treat hotspots detected by wearable systems can help the policymakers to reevaluate the regulations based on the real-time status of symptom spread. Thus it can be mentioned that SST can help the sectors in charge to smartly alter the intensity of the public regulations for controlling the COVID-19 spread to manage the spatiotemporal aspect of the reopening process while ascertaining the public compliance with preventive guidelines. The authors' opinion is that the use of wearable technologies can help to better predict upcoming waves in various zones and to objectively plan for sourcing medical supplies to avoid urgent shortages. As an additional feature, symptom activities in various clusters can be shared on a common platform with the society to let commuters avoid facing hotspots with a higher risk of infection. **Figure 2** shows a schematic view of SST's functionality.

The authors would like to highlight that the topic of contact tracing using advanced proximity sensing, such as using Bluetooth low energy (BLE) technology, is an active field of research and recently is more accelerated due to the benefit of tracking and backtracing contacts between individuals with a positive history of COVID-19 infection and other users of the technology. The use of BLE is motivated due to the availability of it in smartphones and because of the functionality for indoor locations to track interpersonal contacts. In this regard, it should be noted that some governments are suggesting the use of this technology for current waves of the pandemic. As mentioned in Servick (2020) (the following quoted text is taken from Servick, 2020); currently, "GPS data from phones can identify potential hot spots and indicate who has been exposed.

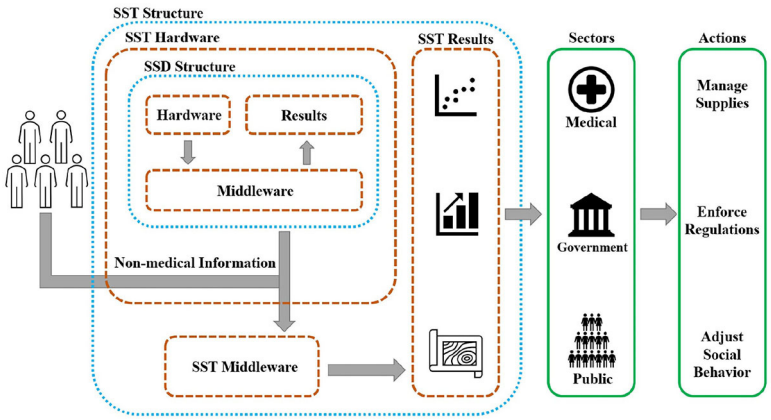

FIGURE 2 | Functionality of SST.

Government programs in South Korea, India, Iceland, and U.S. states, including North Dakota and Utah, are using phone location data to monitor COVID-19 spread. But GPS technology is not precise enough to gauge short distances between two phones to determine which encounters are most risky." This is the motivation for using other platforms such as BLE to detect interpersonal interaction. Please see more details in Ng et al. (2020), Servick (2020), and Zastrow (2020) for an explanation of the use of BLE technology on smartphone applications for tracking COVID-19 infection and some recent efforts such as those by Google and Apple for releasing an application for doing this. Also please see Wang et al. (2017), Guo et al. (2019), Li et al. (2019), Monica and Bergenti (2019), Mackey et al. (2020), Sadowski et al. (2020), Spachos and Plataniotis (2020a), and Spachos and Plataniotis (2020b) for more details on technologies that can be used for indoor tracking. However, there is a wide range of challenges to be addressed for the use of such technology. The challenges are mainly related to the achievable accuracy of such a technique for an unstructured, cluttered, and dynamic environment. Also, the need for calibration, the sensitivity to angle of arrival, and the location of the sensor, and the motion of the wearer further challenge the use of such a system. The current efforts are toward (a) developing new machine intelligence algorithms to further enhance the accuracy of the system, (b) fusion with other modalities while keeping the cost low to enhance the resolution.

The authors believe that the wearable technologies of tomorrow will be able to estimate social distancing without reliance on communication with smartphones to minimize the cost and maximize accessibility while providing the needed accuracy and resolution. This calls for an extensive investigation and investment related to the field of IoMT wearables and can significantly reform the future of the modern healthcare system through more objective telemedicine.

It should be noted that a situation that can potentially challenge this technology is the large-scale acceptability of the society for the use of the proposed approach. The high-scale use can be affected by the resistance of different groups for the adoption of this technology and the lack of compliance. These are open challenges facing large-scale use of any new technology, which may initially limit the feasibility at the societal level. A gradual adoption may be suggested starting from smaller populations such as people in nursing homes and those with co-morbidities, then scaling it to higher volumes. The aforementioned challenges call for an active discussion with and involvement of social scientists and policymakers, who can help to investigate the underlying reasons for the potential rejection of large-scale uses, and thus implement the needed training and deliver accurate information to allow for a higher volume of use and higher compliance at the societal level.

4. CONCLUSION

In this paper, the authors disseminate their perspective on the use, functionality, and challenges of Wearable IoMT technologies coupled with artificial intelligence for changing the picture of telehealth during a global pandemic in which remoteness, cost, accessibility, efficacy, and versatility are crucial to managing the infection symptoms at the individual level, in clusters of high-risk populations, and ultimately in society. The authors believe that to deploy this technology and benefit from its multifaceted objective features, and several sectors should be informed and agree on terms of operation. This perspective article aims at providing insight on various aspects of wearable IoMT, elucidating existing advances and challenges while highlighting the potential benefit for managing the future waves of COVID-19 pandemic and future pandemics. We emphasize how this technology can help to conduct early diagnosis at individual levels and how it can help with optimizing the governmental regulations based on the interaction between high-risk population clusters and symptom spread. This article aims at increasing the awareness of the society, governments, medical correspondents, and industries about this new smart

way of surveillance of infection and spread to act accordingly by enacting regulatory laws, providing medical supports, optimizing plans for testing and hospitalization, and monitoring the compliance. There are several technical and technological challenges to be addressed, listed in this paper, calling for extensive investigation and investment on the topic of IoMT Wearable Technologies.

DATA AVAILABILITY STATEMENT

The original contributions presented in the study are included in the article/supplementary material, further inquiries can be directed to the corresponding author/s.

AUTHOR CONTRIBUTIONS

SM, YW, and SA collaborated on the conceptualization of this perspective article, conducting the literature review and demographic study, analyzing the existing technologies, and writing and editing the paper. All authors contributed to the article and approved the submitted version.

FUNDING

This work was supported by the National Science Foundation of the USA, grant number: 2031594, under the NSF COVID-19 Research program.

REFERENCES

Acharya, U. R., Oh, S. L., Hagiwara, Y., Tan, J. H., and Adeli, H. (2018). Deep convolutional neural network for the automated detection and diagnosis of seizure using EEG signals. *Comput. Biol. Med.* 100, 270–278. doi: 10.1016/j.compbiomed.2017.09.017

Adhikari, S. P., Meng, S., Wu, Y.-J., Mao, Y.-P., Ye, R.-X., Wang, Q.-Z., et al. (2020). Epidemiology, causes, clinical manifestation and diagnosis, prevention and control of coronavirus disease (COVID-19) during the early outbreak period: a scoping review. *Infect. Dis. Pov.* 9, 1–12. doi: 10.1186/s40249-020-00646-x

Agrawal, S., and Agrawal, J. (2015). Survey on anomaly detection using data mining techniques. *Proc. Comput. Sci.* 60, 708–713. doi: 10.1016/j.procs.2015.08.220

Ainslie, K. E., Walters, C. E., Fu, H., Bhatia, S., Wang, H., Xi, X., et al. (2020). Evidence of initial success for china exiting COVID-19 social distancing policy after achieving containment. *Wellcome Open Res.* 5, 1–14. doi: 10.12688/wellcomeopenres.15843.2

Amarasinghe, K., Kenney, K., and Manic, M. (2018). "Toward explainable deep neural network based anomaly detection," in *2018 11th International Conference on Human System Interaction (HSI)* (Gdansk), 311–317. doi: 10.1109/HSI.2018.8430788

Atalay, O., Kennon, W. R., and Demirok, E. (2014). Weft-knitted strain sensor for monitoring respiratory rate and its electro-mechanical modeling. *IEEE Sens. J.* 15, 110–122. doi: 10.1109/JSEN.2014.2339739

Atashzar, S. F., and Wang, Y. (2020). *NSF Rapid: SCH: Smart Wearable COVID19 Biotracker Necklace: Remote Assessment and Monitoring of Symptoms for Early Diagnosis, Continual Monitoring, and Prediction of Adverse Event*. Alexandria, VI: US National Science Foundation. Available online at: https://www.nsf.gov/awardsearch/showAward?AWD_ID=2031594&HistoricalAwards=false

Bélissent, J. (2010). *Getting Clever About Smart Cities: New Opportunities Require New Business Models*. (Cambridge, MA), 244–277.

Bhattasali, T., and Chaki, R. (2011). "A survey of recent intrusion detection systems for wireless sensor network," in *International Conference on Network Security and Applications* (Chennai: Springer), 268–280. doi: 10.1007/978-3-642-22540-6_27

Boulos, M. N. K., and Geraghty, E. M. (2020). Geographical tracking and mapping of coronavirus disease COVID-19/severe acute respiratory syndrome coronavirus 2 (SARS-CoV-2) epidemic and associated events around the world: how 21st century GIS technologies are supporting the global fight against outbreaks and epidemics. *Int. J. Health Geogr.* 19:8. doi: 10.1186/s12942-020-00202-8

Bublitz, C. F., Ribeiro-Teixeira, A. C., Pianoschi, T. A., Rochol, J., and Both, C. B. (2017). "Unsupervised segmentation and classification of snoring events for mobile health," in *GLOBECOM 2017-2017 IEEE Global Communications Conference* (Singapore), 1–6. doi: 10.1109/GLOCOM.2017.8255031

Castillo, C. S. M., Atashzar, S. F., and Vaidyanathan, R. (2020). "3D-mechanomyography: accessing deeper muscle information non-invasively for human-machine interfacing," in *2020 IEEE/ASME International Conference on Advanced Intelligent Mechatronics (AIM)* (Boston, MA), 1458–1463. doi: 10.1109/AIM43001.2020.9159036

Chalapathy, R., and Chawla, S. (2019). Deep learning for anomaly detection: a survey. *arXiv preprint arXiv:1901.03407*.

Chen, N., Zhou, M., Dong, X., Qu, J., Gong, F., Han, Y., et al. (2020). Epidemiological and clinical characteristics of 99 cases of 2019 novel coronavirus pneumonia in Wuhan, china: a descriptive study. *Lancet* 395, 507–513. doi: 10.1016/S0140-6736(20)30211-7

Chen, S., Wen, P., Zhao, S., Huang, D., Wu, M., and Zhang, Y. (2018). "A data fusion-based methodology of constructing health indicators for anomaly detection and prognostics," in *2018 International Conference on Sensing, Diagnostics, Prognostics, and Control (SDPC)* (Xi'an), 570–576. doi: 10.1109/SDPC.2018.8664723

Conzon, D., Bolognesi, T., Brizzi, P., Lotito, A., Tomasi, R., and Spirito, M. A. (2012). "The virtus middleware: an XMPP based architecture for secure IOT communications," in *2012 21st International Conference on Computer Communications and Networks (ICCCN)* (Munich), 1–6. doi: 10.1109/ICCCN.2012.6289309

Craven, D., McGinley, B., Kilmartin, L., Glavin, M., and Jones, E. (2014). Compressed sensing for bioelectric signals: a review. *IEEE J. Biomed. Health Inform.* 19, 529–540. doi: 10.1109/JBHI.2014.2327194

Curone, D., Secco, E. L., Tognetti, A., Loriga, G., Dudnik, G., Risatti, M., et al. (2010). Smart garments for emergency operators: the proetex project. *IEEE Transactions on Information Technology in Biomed* 14, 694-701. doi: 10.1109/TITB.2010.2045003

Dementyev, A., Hodges, S., Taylor, S., and Smith, J. (2013). "Power consumption analysis of bluetooth low energy, zigbee and ant sensor nodes in a cyclic sleep scenario," in *2013 IEEE International Wireless Symposium (IWS)* (Beijing), 1–4. doi: 10.1109/IEEE-IWS.2013.6616827

Dong, E., Du, H., and Gardner, L. (2020). An interactive web-based dashboard to track COVID-19 in real time. *Lancet Infect. Dis.* 20, 533–534. doi: 10.1016/S1473-3099(20)30120-1

Dorri, A., Kanhere, S. S., Jurdak, R., and Gauravaram, P. (2017). "Blockchain for IOT security and privacy: The case study of a smart home," in *2017 IEEE International Conference on Pervasive Computing and Communications Workshops (PerCom Workshops)* (Kona, HI), 618–623. doi: 10.1109/PERCOMW.2017.7917634

Duregger, K., Hayn, D., Morak, J., Ladenstein, R., and Schreier, G. (2015). "An mHealth system for toxicity monitoring of paediatric oncological patients using near field communication technology," in *2015 37th Annual International Conference of the IEEE Engineering in Medicine and Biology Society (EMBC)* (Milan), 6848–6851. doi: 10.1109/EMBC.2015.7319966

Emanuel, E. J., Persad, G., Upshur, R., Thome, B., Parker, M., Glickman, A., et al. (2020). Fair allocation of scarce medical resources in the time of Covid-19. *N. Engl. J. Med.* 382, 2049–2055. doi: 10.1056/NEJMsb2005114

Erfani, S. M., Rajasegarar, S., Karunasekera, S., and Leckie, C. (2016). High-dimensional and large-scale anomaly detection using a linear

one-class SVM with deep learning. *Pattern Recogn.* 58, 121–134. doi: 10.1016/j.patcog.2016.03.028

Fauci, A. S., Lane, H. C., and Redfield, R. R. (2020). Covid-19-navigating the uncharted. *N. Engl. J. Med*. 382, 1268–1269. doi: 10.1056/NEJMe2002387

Fiedler, P., Biller, S., Griebel, S., and Haueisen, J. (2012). "Impedance pneumography using textile electrodes," in *2012 Annual International Conference of the IEEE Engineering in Medicine and Biology Society* (San Diego, CA), 1606–1609. doi: 10.1109/EMBC.2012.6346252

Garg, S. (2020). *Hospitalization Rates and Characteristics of Patients Hospitalized With Laboratory-Confirmed Coronavirus Disease 2019-COVID-Net, 14 States, March 1-30, 2020*. MMWR. Morbidity and Mortality Weekly Report, 69. Centers for Disease Control and Prevention.

Garg, S., Kaur, K., Batra, S., Kaddoum, G., Kumar, N., and Boukerche, A. (2020). A multi-stage anomaly detection scheme for augmenting the security in iot-enabled applications. *Fut. Gener. Comput. Syst*. 104, 105–118. doi: 10.1016/j.future.2019.09.038

Gatouillat, A., Badr, Y., Massot, B., and Sejdić, E. (2018). Internet of medical things: a review of recent contributions dealing with cyber-physical systems in medicine. *IEEE Intern. Things J*. 5, 3810–3822. doi: 10.1109/JIOT.2018.2849014

Gazendam, M. G., and Hof, A. L. (2007). Averaged EMG profiles in jogging and running at different speeds. *Gait Posture* 25, 604–614. doi: 10.1016/j.gaitpost.2006.06.013

Gubbi, J., Buyya, R., Marusic, S., and Palaniswami, M. (2013). Internet of things (IOT): a vision, architectural elements, and future directions. *Fut. Gener. Comput. Syst*. 29, 1645–1660. doi: 10.1016/j.future.2013.01.010

Guo, G., Chen, R., Ye, F., Peng, X., Liu, Z., and Pan, Y. (2019). Indoor smartphone localization: a hybrid wifi RTT-RSS ranging approach. *IEEE Access* 7, 176767–176781. doi: 10.1109/ACCESS.2019.2957753

Guo, L., Ren, L., Yang, S., Xiao, M., Chang, D., Yang, F., et al. (2020). Profiling early humoral response to diagnose novel coronavirus disease (COVID-19). *Clin. Infect. Dis*. 71, 778–785. doi: 10.1093/cid/ciaa310

Hamamoto, A. H., Carvalho, L. F., Sampaio, L. D. H., Abrão, T., and Proença, M. L. Jr. (2018). Network anomaly detection system using genetic algorithm and fuzzy logic. *Expert Syst. Appl*. 92, 390–402. doi: 10.1016/j.eswa.2017.09.013

Hatzivasilis, G., Soultatos, O., Ioannidis, S., Verikoukis, C., Demetriou, G., and Tsatsoulis, C. (2019). "Review of security and privacy for the internet of medical things (IoMT)," in *2019 15th International Conference on Distributed Computing in Sensor Systems (DCOSS)* (Santorini), 457–464. doi: 10.1109/DCOSS.2019.00091

Hellewell, J., Abbott, S., Gimma, A., Bosse, N. I., Jarvis, C. I., Russell, T. W., et al. (2020). Feasibility of controlling COVID-19 outbreaks by isolation of cases and contacts. *Lancet Glob. Health* 8, E488–E496. doi: 10.1016/S2214-109X(20)30074-7

Huang, C., Wang, Y., Li, X., Ren, L., Zhao, J., Hu, Y., et al. (2020). Clinical features of patients infected with 2019 novel coronavirus in Wuhan, china. *Lancet* 395, 497–506. doi: 10.1016/S0140-6736(20)30183-5

Jap, B. T., Lal, S., Fischer, P., and Bekiaris, E. (2009). Using EEG spectral components to assess algorithms for detecting fatigue. *Expert Syst. Appl*. 36, 2352–2359. doi: 10.1016/j.eswa.2007.12.043

Joyia, G. J., Liaqat, R. M., Farooq, A., and Rehman, S. (2017). Internet of medical things (IoMT): applications, benefits and future challenges in healthcare domain. *J. Commun*. 12, 240–247. doi: 10.12720/jcm.12.4.240-247

Kagita, M. K., Thilakarathne, N., Gadekallu, T. R., and Maddikunta, P. K. R. (2020). A review on security and privacy of internet of medical things. *arXiv preprint arXiv:2009.05394*.

Khan, M. A. and Salah, K. (2018). IoT security: review, blockchain solutions, and open challenges. *Fut. Gener. Comput. Syst*. 82, 395–411. doi: 10.1016/j.future.2017.11.022

Khan, M. E., and Khan, F. (2012). A comparative study of white box, black box and grey box testing techniques. *Int. J. Adv. Comput. Sci. Appl*. 3, 12–15. doi: 10.14569/IJACSA.2012.030603

Khan, S. R., Sikandar, M., Almogren, A., Din, I. U., Guerrieri, A., and Fortino, G. (2020). Iomt-based computational approach for detecting brain tumor. *Fut. Gener. Comput. Syst*. 109, 360–367. doi: 10.1016/j.future.2020.03.054

Kim, Y., Lee, S., and Lee, S. (2015). Coexistence of Zigbee-based WBAN and Wifi for health telemonitoring systems. *IEEE J. Biomed. Health Inform*. 20, 222–230. doi: 10.1109/JBHI.2014.2387867

Le, T. T., Andreadakis, Z., Kumar, A., Roman, R. G., Tollefsen, S., Saville, M., et al. (2020). The COVID-19 vaccine development landscape. *Nat. Rev. Drug Discov*. 19, 305–306. doi: 10.1038/d41573-020-00151-8

Lee, J.-S., Su, Y.-W., and Shen, C.-C. (2007). "A comparative study of wireless protocols: bluetooth, UWB, Zigbee, and Wi-fi," in *IECON 2007-33rd Annual Conference of the IEEE Industrial Electronics Society* (Taipei), 46–51. doi: 10.1109/IECON.2007.4460126

Leung, K., Wu, J. T., Liu, D., and Leung, G. M. (2020). First-wave COVID-19 transmissibility and severity in china outside HUBEI after control measures, and second-wave scenario planning: a modelling impact assessment. *Lancet*. 395, 1382–1393. doi: 10.1016/S0140-6736(20)30746-7

Li, C., Mo, L., and Zhang, D. (2019). Review on uhf RFID localization methods. *IEEE J. Radio Freq. Identif*. 3, 205–215. doi: 10.1109/JRFID.2019.2924346

Li, X., Geng, M., Peng, Y., Meng, L., and Lu, S. (2020). Molecular immune pathogenesis and diagnosis of COVID-19. *J. Pharm. Anal*. 10, 102–108. doi: 10.1016/j.jpha.2020.03.001

Li, Y., and Xia, L. (2020). Coronavirus disease 2019 (COVID-19): role of chest CT in diagnosis and management. *Am. J. Roentgenol*. 214, 1280–1286. doi: 10.2214/AJR.20.22954

Li, Y., Yao, L., Li, J., Chen, L., Song, Y., Cai, Z., et al. (2020). Stability issues of RT-PCR testing of SARS-CoV-2 for hospitalized patients clinically diagnosed with COVID-19. *J. Med. Virol*. 92, 903–908. doi: 10.1002/jmv.25786

Liang, T., and Yuan, Y. J. (2016). Wearable medical monitoring systems based on wireless networks: a review. *IEEE Sens. J*. 16, 8186–8199. doi: 10.1109/JSEN.2016.2597312

Liu, F., Xu, A., Zhang, Y., Xuan, W., Yan, T., Pan, K., et al. (2020). Patients of COVID-19 may benefit from sustained lopinavir-combined regimen and the increase of eosinophil may predict the outcome of COVID-19 progression. *Int. J. Infect. Dis*. 95, 183–191. doi: 10.1016/j.ijid.2020.03.013

Long, C., Xu, H., Shen, Q., Zhang, X., Fan, B., Wang, C., et al. (2020). Diagnosis of the coronavirus disease (COVID-19): rRT-PCR or CT? *Eur. J. Radiol*. 2020:108961. doi: 10.1016/j.ejrad.2020.108961

Loriga, G., Taccini, N., De Rossi, D., and Paradiso, R. (2006). "Textile sensing interfaces for cardiopulmonary signs monitoring," in *2005 IEEE Engineering in Medicine and Biology 27th Annual Conference* (Shanghai), 7349–7352. doi: 10.1109/IEMBS.2005.1616209

Mackey, A., Spachos, P., Song, L., and Plataniotis, K. N. (2020). Improving BLE beacon proximity estimation accuracy through Bayesian filtering. *IEEE Intern. Things J*. 7, 3160–3169. doi: 10.1109/JIOT.2020.2965583

Menni, C., Valdes, A. M., Freidin, M. B., Sudre, C. H., Nguyen, L. H., Drew, D. A., et al. (2020). Real-time tracking of self-reported symptoms to predict potential COVID-19. *Nat. Med*. 26, 1037–1040. doi: 10.1038/s41591-020-0916-2

Monica, S., and Bergenti, F. (2019). Hybrid indoor localization using Wifi and UWB technologies. *Electronics* 8:334. doi: 10.3390/electronics8030334

Neefs, J., Schrooyen, F., Doggen, J., and Renckens, K. (2010). "Paper ticketing vs. electronic ticketing based on off-line system'tapango," in *2010 Second International Workshop on Near Field Communication* (Monaco), 3–8. doi: 10.1109/NFC.2010.24

Ng, P. C., Spachos, P., and Plataniotis, K. (2020). COVID-19 and your smartphone: BLE-based smart contact tracing. *arXiv preprint arXiv:2005.13754*. doi: 10.1109/JSYST.2021.3055675

Ngu, A. H., Gutierrez, M., Metsis, V., Nepal, S., and Sheng, Q. Z. (2016). IoT middleware: a survey on issues and enabling technologies. *IEEE Intern. Things J*. 4, 1–20. doi: 10.1109/JIOT.2016.2615180

Noor, M. M., and Hassan, W. H. (2019). Current research on internet of things (IoT) security: a survey. *Comput. Netw*. 148, 283–294. doi: 10.1016/j.comnet.2018.11.025

NRC (2020). *COVID-19 Challenge: Low-Cost Sensor System for COVID-19 Patient Monitoring*. NRC.

Olagnier, D., and Mogensen, T. H. (2020). The COVID-19 pandemic in Denmark: big lessons from a small country. *Cytokine Growth Fact. Rev*. 53, 1–12. doi: 10.1016/j.cytogfr.2020.05.005

Opperman, C. A., and Hancke, G. P. (2011). "A generic NFC-enabled measurement system for remote monitoring and control of client-side equipment," in *2011 Third International Workshop on Near Field Communication* (Hagenberg), 44–49. doi: 10.1109/NFC.2011.11

Pacelli, M., Caldani, L., and Paradiso, R. (2006a). "Textile piezoresistive sensors for biomechanical variables monitoring," in *2006 International Conference of the IEEE Engineering in Medicine and Biology Society* (New York, NY), 5358–5361. doi: 10.1109/IEMBS.2006.259287

Pacelli, M., Loriga, G., Taccini, N., and Paradiso, R. (2006b). "Sensing fabrics for monitoring physiological and biomechanical variables: E-textile solutions," in *2006 3rd IEEE/EMBS International Summer School on Medical Devices and Biosensors* (Cambridge, MA), 1–4. doi: 10.1109/ISSMDBS.2006.360082

Papazoglou, M. P., and Georgakopoulos, D. (2003). Introduction: Service-oriented computing. *Commun. ACM* 46, 24–28. doi: 10.1145/944217.944233

Qi, J., Yang, P., Waraich, A., Deng, Z., Zhao, Y., and Yang, Y. (2018). Examining sensor-based physical activity recognition and monitoring for healthcare using internet of things: a systematic review. *J. Biomed. Inform.* 87, 138–153. doi: 10.1016/j.jbi.2018.09.002

Ransing, R., Adiukwu, F., Pereira-Sanchez, V., Ramalho, R., Orsolini, L., Teixeira, A. L. S., et al. (2020). Mental health interventions during the COVID-19 pandemic: a conceptual framework by early career psychiatrists. *Asian J. Psychiatry* 51, 102085–102085. doi: 10.1016/j.ajp.2020.102085

Rechy-Ramirez, E. J., and Hu, H. (2015). Bio-signal based control in assistive robots: a survey. *Digital Commun. Netw.* 1, 85–101. doi: 10.1016/j.dcan.2015.02.004

Rogers, J. (2020). *Rapid: Collaborative Research: Data Analytics for Mechano-Acoustic and Physiological Monitoring of COVID19 Symptoms*. National Science Foundation.

Roser, M., Ritchie, H., Ortiz-Ospina, E., and Hasell, J. (2020). *Coronavirus Disease (COVID-19)-Statistics and Research*. Our World in data.

Sadowski, S., Spachos, P., and Plataniotis, K. N. (2020). Memoryless techniques and wireless technologies for indoor localization with the internet of things. *IEEE Intern. Things J.* 7, 10996–11005. doi: 10.1109/JIOT.2020.2992651

Servick, K. (2020). COVID-19 contact tracing apps are coming to a phone near you. How will we know whether they work? *Science*. doi: 10.1126/science.abc9379

Shen, C.-L., Huang, T.-H., Hsu, P.-C., Ko, Y.-C., Chen, F.-L., Wang, W.-C., et al. (2017). Respiratory rate estimation by using ECG, impedance, and motion sensing in smart clothing. *J. Med. Biol. Eng.* 37, 826–842. doi: 10.1007/s40846-017-0247-z

Sibinski, M., Jakubowska, M., and Sloma, M. (2010). Flexible temperature sensors on fibers. *Sensors* 10, 7934–7946. doi: 10.3390/s100907934

Sicari, S., Rizzardi, A., Grieco, L. A., and Coen-Porisini, A. (2015). Security, privacy and trust in internet of things: the road ahead. *Comput. Netw.* 76, 146–164. doi: 10.1016/j.comnet.2014.11.008

Singh, R. P., Javaid, M., Haleem, A., Vaishya, R., and Al, S. (2020). Internet of medical things (IoMT) for orthopaedic in COVID-19 pandemic: roles, challenges, and applications. *J. Clin. Orthop. Trauma.* 11, 713–717. doi: 10.1016/j.jcot.2020.05.011

Sohrabi, C., Alsafi, Z., O'Neill, N., Khan, M., Kerwan, A., Al-Jabir, A., et al. (2020). World health organization declares global emergency: a review of the 2019 novel coronavirus (COVID-19). *Int. J. Surg.* 76, 71–76. doi: 10.1016/j.ijsu.2020.02.034

Soldatos, J., Kefalakis, N., Hauswirth, M., Serrano, M., Calbimonte, J.-P., Riahi, M., et al. (2015). "Openiot: Open source internet-of-things in the cloud," in *Interoperability and Open-Source Solutions for the Internet of Things*, eds I. Podnar Žarko, K. Pripužić, and S., Martin (Split; Cham: Springer International Publishing), 13–25. doi: 10.1007/978-3-319-16546-2_3

Spachos, P., and Plataniotis, K. (2020a). BLE beacons in the smart city: applications, challenges, and research opportunities. *IEEE Intern. Things Mag.* 3, 14–18. doi: 10.1109/IOTM.0001.1900073

Spachos, P., and Plataniotis, K. N. (2020b). BLE beacons for indoor positioning at an interactive IoT-based smart museum. *IEEE Syst. J.* 14, 3483–3493. doi: 10.1109/JSYST.2020.2969088

Stavem, K., Saxholm, H., and Smith-Erichsen, N. (1997). Accuracy of infrared ear thermometry in adult patients. *Intens. Care Med.* 23, 100–105. doi: 10.1007/s001340050297

Subashini, S., and Kavitha, V. (2011). A survey on security issues in service delivery models of cloud computing. *J. Netw. Comput. Appl.* 34, 1–11. doi: 10.1016/j.jnca.2010.07.006

Subbe, C. P., and Kinsella, S. (2018). Continuous monitoring of respiratory rate in emergency admissions: evaluation of the respirasense-sensor in acute care compared to the industry standard and gold standard. *Sensors* 18:2700. doi: 10.3390/s18082700

Sun, P., Lu, X., Xu, C., Sun, W., and Pan, B. (2020). Understanding of COVID-19 based on current evidence. *J. Med. Virol.* 92, 548–551. doi: 10.1002/jmv.25722

Sundmaeker, H., Guillemin, P., Friess, P., and Woelfflé, S. (2010). "Vision and challenges for realising the internet of things," in *Cluster of European Research Projects on the Internet of Things* (Brussels: European Commision), 34–36.

Tan, P.-N., Steinbach, M., and Kumar, V. (2016). *Introduction to Data Mining*. New Delhi; London: Pearson Education India.

Tang, Y.-W., Schmitz, J. E., Persing, D. H., and Stratton, C. W. (2020). Laboratory diagnosis of COVID-19: current issues and challenges. *J. Clin. Microbiol.* 58:e00512-20. doi: 10.1128/JCM.00512-20

Timalsina, S. K., Bhusal, R., and Moh, S. (2012). "NFC and its application to mobile payment: overview and comparison," in *2012 8th International Conference on Information Science and Digital Content Technology (ICIDT2012)*, *Vol. 1* (Jeju), 203–206.

Tobin, M. J., Laghi, F., and Jubran, A. (2020). Why COVID-19 silent hypoxemia is baffling to physicians. *Am. J. Respir. Crit. Care Med.* 202, 356–360. doi: 10.1164/rccm.202006-2157CP

Vandecasteele, K., De Cooman, T., Gu, Y., Cleeren, E., Claes, K., Paesschen, W. V., et al. (2017). Automated epileptic seizure detection based on wearable ECG and PPG in a hospital environment. *Sensors* 17:2338. doi: 10.3390/s17102338

Wang, C., Horby, P. W., Hayden, F. G., and Gao, G. F. (2020). A novel coronavirus outbreak of global health concern. *Lancet* 395, 470–473. doi: 10.1016/S0140-6736(20)30185-9

Wang, D., Hu, B., Hu, C., Zhu, F., Liu, X., Zhang, J., et al. (2020). Clinical characteristics of 138 hospitalized patients with 2019 novel coronavirus-infected pneumonia in Wuhan, china. *JAMA* 323, 1061–1069. doi: 10.1001/jama.2020.1585

Wang, X., Gao, L., and Mao, S. (2017). BiLoc: Bi-modal deep learning for indoor localization with commodity 5GHZ Wifi. *IEEE Access* 5, 4209–4220. doi: 10.1109/ACCESS.2017.2688362

Wang, Z., and Tang, K. (2020). Combating COVID-19: health equity matters. *Nat. Med.* 26, 458–458. doi: 10.1038/s41591-020-0823-6

Witt, J., Narbonneau, F., Schukar, M., Krebber, K., De Jonckheere, J., Jeanne, M., et al. (2011). Medical textiles with embedded fiber optic sensors for monitoring of respiratory movement. *IEEE Sensors J.* 12, 246–254. doi: 10.1109/JSEN.2011.2158416

Wu, Z., and McGoogan, J. M. (2020). Characteristics of and important lessons from the coronavirus disease 2019 (COVID-19) outbreak in China: summary of a report of 72 314 cases from the Chinese center for disease control and prevention. *JAMA* 323, 1239–1242. doi: 10.1001/jama.2020.2648

Wynants, L., Van Calster, B., Bonten, M. M., Collins, G. S., Debray, T. P., De Vos, M., et al. (2020). Prediction models for diagnosis and prognosis of COVID-19 infection: systematic review and critical appraisal. *BMJ* 369:m1328. doi: 10.1136/bmj.m1328

Xia, L., Malik, A. S., and Subhani, A. R. (2018). A physiological signal-based method for early mental-stress detection. *Biomed. Sign. Process. Control* 46, 18–32. doi: 10.1016/j.bspc.2018.06.004

Xiao, L., Greenstein, L. J., Mandayam, N. B., and Trappe, W. (2009). Channel-based detection of sybil attacks in wireless networks. *IEEE Trans. Inform. Forens. Secur.* 4, 492–503. doi: 10.1109/TIFS.2009.2026454

Xu, W., Trappe, W., Zhang, Y., and Wood, T. (2005). "The feasibility of launching and detecting jamming attacks in wireless networks," in *Proceedings of the 6th ACM International Symposium on Mobile Ad Hoc Networking and Computing* (Urbana-Champaign, IL), 46–57. doi: 10.1145/1062689.1062697

Zastrow, M. (2020). Coronavirus contact-tracing apps: can they slow the spread of COVID-19? *Nature*. doi: 10.1038/d41586-020-01514-2

Zhai, P., Ding, Y., Wu, X., Long, J., Zhong, Y., and Li, Y. (2020). The epidemiology, diagnosis and treatment of COVID-19. *Int. J. Antimicrob. Agents* 2020:105955. doi: 10.1016/j.ijantimicag.2020.105955

Zhang, K., Liang, X., Lu, R., and Shen, X. (2014). Sybil attacks and their defenses in the internet of things. *IEEE Intern. Things J.* 1, 372–383. doi: 10.1109/JIOT.2014.2344013

Zhang, Z.-K., Cho, M. C. Y., Wang, C.-W., Hsu, C.-W., Chen, C.-K., and Shieh, S. (2014). "IoT security: ongoing challenges and research opportunities," in *2014 IEEE 7th International Conference on Service-Oriented Computing and Applications*, (Matsue:IEEE). 230–234. doi: 10.1109/SOCA.2014.58

Zhen, R., Jin, Y., Hu, Q., Shao, Z., and Nikitakos, N. (2017). Maritime anomaly detection within coastal waters based on vessel trajectory clustering and naïve bayes classifier. *J. Navigat.* 70:648. doi: 10.1017/S0373463316000850

Zheng, Y.-Y., Ma, Y.-T., Zhang, J.-Y., and Xie, X. (2020). COVID-19 and the cardiovascular system. *Nat. Rev. Cardiol.* 17, 259–260. doi: 10.1038/s41569-020-0360-5

Conflict of Interest: The authors declare that the research was conducted in the absence of any commercial or financial relationships that could be construed as a potential conflict of interest.

frontiers in Robotics and AI

PERSPECTIVE
published: 14 April 2021
doi: 10.3389/frobt.2021.610677

Robotics and AI for Teleoperation, Tele-Assessment, and Tele-Training for Surgery in the Era of COVID-19: Existing Challenges, and Future Vision

Navid Feizi[1], *Mahdi Tavakoli*[2], *Rajni V. Patel*[1,3,4] *and S. Farokh Atashzar*[5,6]*

[1]Canadian Surgical Technologies and Advanced Robotics (CSTAR), London Health Sciences Centre, and School of Biomedical Engineering, University of Western Ontario, London, ON, Canada, [2]Department of Electrical and Computer Engineering, University of Alberta, Edmonton, AB, Canada, [3]Department of Electrical and Computer Engineering, University of Western Ontario, London, ON, Canada, [4]Department of Surgery, University of Western Ontario, London, ON, Canada, [5]Department of Electrical and Computer Engineering, New York University, New York, NY, United States, [6]Department of Mechanical and Aerospace Engineering, New York University, New York, NY, United States

The unprecedented shock caused by the COVID-19 pandemic has severely influenced the delivery of regular healthcare services. Most non-urgent medical activities, including elective surgeries, have been paused to mitigate the risk of infection and to dedicate medical resources to managing the pandemic. In this regard, not only surgeries are substantially influenced, but also pre- and post-operative assessment of patients and training for surgical procedures have been significantly impacted due to the pandemic. Many countries are planning a phased reopening, which includes the resumption of some surgical procedures. However, it is not clear how the reopening safe-practice guidelines will impact the quality of healthcare delivery. This perspective article evaluates the use of robotics and AI in 1) robotics-assisted surgery, 2) tele-examination of patients for pre- and post-surgery, and 3) tele-training for surgical procedures. Surgeons interact with a large number of staff and patients on a daily basis. Thus, the risk of infection transmission between them raises concerns. In addition, pre- and post-operative assessment also raises concerns about increasing the risk of disease transmission, in particular, since many patients may have other underlying conditions, which can increase their chances of mortality due to the virus. The pandemic has also limited the time and access that trainee surgeons have for training in the OR and/or in the presence of an expert. In this article, we describe existing challenges and possible solutions and suggest future research directions that may be relevant for robotics and AI in addressing the three tasks mentioned above.

Keywords: COVID-19, robotics, surgery, teleoperation, tele-examination, tele-training

OPEN ACCESS

Edited by:
Elena De Momi,
Politecnico di Milano, Italy

Reviewed by:
Selene Tognarelli,
Sant'Anna School of Advanced Studies, Italy
Riccardo Muradore,
University of Verona, Italy
Francesca Cordella,
Campus Bio-Medico University, Italy

***Correspondence:**
S. Farokh Atashzar
f.atashzar@nyu.edu

Specialty section:
This article was submitted to Biomedical Robotics, a section of the journal Frontiers in Robotics and AI

Received: *26 September 2020*
Accepted: *18 January 2021*
Published: *14 April 2021*

Citation:
Feizi N, Tavakoli M, Patel RV and Atashzar SF (2021) Robotics and AI for Teleoperation, Tele-Assessment, and Tele-Training for Surgery in the Era of COVID-19: Existing Challenges, and Future Vision. Front. Robot. AI 8:610677. doi: 10.3389/frobt.2021.610677

INTRODUCTION

The novel coronavirus has been declared a public health emergency of international concern by WHO in Jan 2020 (WHO, 2020). By the time of writing this paper, all countries are affected by the pandemic. The unprecedented shock wave of the virus spread has impacted regular health care service delivery. The extreme pressure on healthcare systems has exceeded capacity, and managing

the pandemic has become a global issue that has drastically influenced most aspects of the healthcare system. The performance of surgeries (most of which are categorized as elective surgeries), training for surgery, and assessments for surgery are aspects that have been significantly impacted.

Due to the chance of false negatives in the pre-surgery COVID-19 testing of patients, all patients have to be treated as suspect cases. Dealing with infected or suspected patients requires precautions such as consideration for anesthesiologists (Willer et al., 2020), limitation of staff exposure to patients, and wearing PPE, which poses difficulties to operating theatre (Kumar et al., 2020). However, these procedures cannot guarantee the safety of staff and patients. Moreover, since hospital staff is in contact with several people each day, cross-infection through staff should also be considered.

New regulations have recommended a moratorium on elective surgery to avoid virus spread in hospitals by minimizing personal interactions and expenditure of medical resources for infected patients who need intensive care. Deferring elective surgeries is based on opinions and has secondary consequences. Progression of the disease continues when the patient is waiting for surgery. This has a substantial impact on the life quality of patients (Fu et al., 2020), results in higher treatment costs (Reyes et al., 2019), and may cause unexpected death (Zafar, 2020). On the other hand, elective surgeries are not optional and must be performed eventually. Thus, there may be a need for performing a deferred surgery during the COVID-19 time frame. Moreover, catching up with the 2 million backlogged elective surgeries worldwide each week will impose a huge burden on the healthcare system when elective surgeries resume (Szklarski, 2020).

This unprecedented scenario not only has affected surgeries, but has also influenced surgery-related activities profoundly. Surgical education has been affected adversely by the pandemic. There has been a gradual reopening of activities, including schools, but with the anticipated rise in the rate of infection it is anticipated that there will be some levels of shut down again in this sector. Trainees are banished from wards, and residents have lost their access to practical OR training (Ferrario et al., 2020; Ferrel and Ryan, 2020). In addition, emergency and non-deferable surgeries are being done by senior surgeons without the presence of trainees to reduce operation time and risk of complications, and mitigate the risk of residents' exposure to COVID-19 (Bernardi et al., 2020). This situation has imposed mental anxiety and has slowed down the learning curve of residents and medical students, who will be needed in catching-up with deferred surgeries in the future (Ahmed et al., 2020).

Moreover, going into hospitals for pre- and post-surgery assessments is also a safety concern during the pandemic. There is always an infection risk for any minute that a non-COVID patient spends in a hospital. Consequently, hospitals try to discharge patients as soon as possible to reduce the risk of infection. Besides, the closure of medical offices has disturbed pre- and post-surgery assessments (Scaravonati et al., 2020).

Since there is no widely approved or sufficiently tested vaccine, there is a possible chance of second and third global waves in the Fall and Winter, and continuing lockdown regulations imposes an intolerable burden on the healthcare system. Several countries are therefore planning for a reopening guideline to resume safe delivery of surgical services (Dattani et al., 2020). However, it is not clear how the reopening phase will affect the quality of healthcare delivery and how the above-mentioned tasks should be performed safely while there is a lack of a clinically approved therapy for COVID-19. This perspective paper proposes robotics and artificial intelligence (AI) as a solution for the three above-mentioned tasks and investigates potential opportunities in the area to address the mentioned problems.

ROBOTICS-ASSISTED SURGERY

Minimally invasive surgery (MIS) has demonstrated superiority over open surgery. Less amount of blood loss, and shorter recovery and hospital stay are the main reasons for the preference of MIS when it is possible. Meanwhile, robotics-assisted MIS (RAMIS) has evolved and shown superhuman capabilities for teleoperation and has found its place in MIS. Teleoperation offers surgeons an ergonomically operating posture (Ballantyne, 2002), provides them with more dexterity than conventional laparoscopy (Moorthy et al., 2004), enhances the accuracy of motion beyond surgeons' natural ability, etc. Besides these benefits, the main virtue that distinguishes teleoperation in the COVID-19 era is providing the ability to separate the surgeon's console (leader robot) from the patient robot (follower robot) while keeping them connected through a communication interface (Challacombe et al., 2003).

Telesurgery affords physical separation of the surgeon from the patient, in a separate room avoiding bilateral infection transfer, which can be life-threatening. In addition, the number of bedside staff in RAMIS is less than in open surgery (Kimmig et al., 2020). This provides the safety of the patient and operating room by reducing inter-personal contacts to the lowest level possible. This performance has been shown experimentally. In the United States, a CorPath robotic intervention arm has been used in coronary intervention on a COVID patient to provide safety of the personnel (Tabaza et al., 2020).

Dealing with an infected or suspected patient requires a maximal level of protection (Liang, 2020). The physical disturbance caused by this level of protection has a negative influence on surgical performance. On the other hand, the COVID-19 situation increases the surgeon's mental stress, which critically affects the surgeon's performance. Elevated stress levels could likely be due to the fear of contracting the virus or spreading it to patients and the surgeon's family (Tan et al., 2020). Studies have shown that depression, anxiety, insomnia, and stress have increased, especially among front-line healthcare providers during the pandemic (Lin et al., 2020). High stress levels may result in inappropriate responses, such as poor decision making and impaired psychomotor performance (Wetzel et al., 2006; Arora et al., 2010). The elevated psychological stress levels among healthcare providers may sustain even one year after the outbreak as it happened in 2004 with SARS (Lee et al., 2007). Not only telesurgery reduces surgeon's stress by providing better ergonomics during surgery

(Berguer and Smith, 2006), but also, during the COVID era, robotics-assisted surgery significantly reduces stress levels by providing higher infection protection through physical distancing between the patient and the surgeon; also, it reduces the number of needed medical staff to be present in close proximity to the patient and each other during prolonged surgeries (which can increase the possibility of infection transfer between a patient and staff and between staff members). It should be highlighted that robotics assisted surgery does not make the aforementioned interactions zero as there is always the need for some format of interaction between a patient and staff. However, it reduces the duration and the number of interactions.

Recently, the concept of semi-autonomous and autonomous surgery has attracted a great deal of interest thanks to advancements in the area of machine intelligence especially when combined with computer vision (Moawad et al., 2020). When compared with teleoperated robotic surgery, AI-based autonomous and semi-autonomous robotic systems has not been fully exploited in the literature as these are newer topics of the field. In the language of surgery project, it has been shown that combining AI with teleoperation can provide a semi-automated system that can recognize and perform tasks automatically when there is a pre-trained model for the recognized task, allowing for faster and high accuracy procedures (Bohren et al., 2011). Semi-autonomous robots have been used for orthopedic surgery, such as MAKOplasty, when preoperative images are fused with intraoperative information to provide surgeons with an augmented sensorimotor capability through production of dynamic virtual fixture in time and space. More recently, fully-autonomous robotic surgery has been discussed in medical robotic communities and preliminary experiments on *ex-vivo* tissue have shown promising results. The performance and accuracy of semi-autonomous surgical robots have been proved clinically (Hampp et al., 2019). For example, the MAKO (Stryker, 2020) and NAVIO (Smith and Nephew, 2020) robots guide the surgeon in joint arthroplasty semi-autonomously and prevent excessive bone loss. This guarantees proper bone preparation and precise implantation. However, autonomous surgical robots, despite their great accuracy in comparison to manual procedures (Shademan et al., 2016), are still in the non-clinical development phase. In the context of remote operation, the use of autonomous robots can provide a higher degree of separation while providing some additional accuracy through processing of multimodal intraoperative information. However, this is a technologically challenging field which should be investigated to provide more autonomy regarding management of surgery during a crisis such as COVID-19.

The other benefit of RAMIS in the COVID-19 era is that it increases the availability of intensive care unit (ICU) beds. The smaller incision for RAMIS shortens patient's recovery time and hospital stay. This allows hospitals to dedicate more ICU beds to critically ill cases while handling surgeries. There is however a shortcoming in terms of the OR time usage for RAMIS as a result of the extra setting-up time and longer procedure times (Heemskerk et al., 2007; Cho et al., 2016; Lindfors et al., 2018). Nonetheless, a shorter post-surgery hospital stay is of paramount importance and outweighs the longer OR time, notably in the COVID-19 era. Moreover, deploying AI in robotic surgery has been shown to decrease soft tissue damage and consequently decrease recovery time (Wall and Krummel, 2020).

Due to abdominal pressure in laparoscopic surgery, there are some concerns about the possibility of aerosolization of viral particles and contamination through surgery smoke in laparoscopic surgery (Schwarz and Tuech, 2020; Van den Eynde et al., 2020). Although these methods of infection are not completely proved for COVID-19 yet, safety regulations should be considered to prevent possible infections. It should be noted that surgical smoke is also released in open surgeries; however, in RAMIS, it is easier to handle the smoke trapped in the patient's body. Safety precautions to prevent these issues are 1) lowering the electrocautery power to reduce the amount of smoke production (Mottrie, 2020); 2) smoke evacuation and abdominal deflation through ultra-low penetrating air (ULPA) filter (Kimmig et al., 2020); and 3) reducing abdominal pressure to the lowest possible. RAMIS surgeries are feasible to perform with lower abdominal pressure than conventional laparoscopic surgery (Kimmig et al., 2020). To summarize, RAMIS is safer than MIS and open surgery in terms of contamination through aerosolization of viral particles for bedside staff.

Telerobotic surgical systems have solved several issues associated with conventional MIS and also provided the surgeon with new capabilities. These features are 1) depth perception; 2) dexterity enhancement; 3) improved accuracy; 4) better hand-eye coordination; and 5) and multiple tools delivery through a single incision (Atashzar and Patel, 2018). Moreover, in teleoperation, information and operation data can be saved and used for training purposes both for AI supervision and training of novice surgeons (Zemmar et al., 2020). The problem of degraded haptic feedback in conventional laparoscopy has not been solved yet. Better tracking accuracy and improved surgical performances have been achieved using the haptic feedback in RAMIS (Talasaz et al., 2014), (Currie et al., 2017). Related to this, the lack of haptic feedback increases the risk of tissue damage due to large unintentional forces. Other modalities of feedback such as visual force feedback of the tool (Tavakoli et al., 2006), a tactile sensor and tactile ultrasound (tactUS) instrument for palpation and tumor localization (Trejos et al., 2009; Naidu et al., 2017a; Naidu et al., 2017b), and skin stretch feedback (Schorr et al., 2013) are influential in robotic surgery, but none of them can completely make up for the absence of haptic feedback. Thus, enabling telerobotic surgical systems with force sensing and force reflecting modules is of high importance, which increases the quality of teleoperated surgery (Talasaz and Patel, 2013; Talasaz et al., 2017). A machine learning algorithm has been deployed to estimate the elongation of suture from knot type, initial suture length, and surgical thread type data, and visual feedback has been used to warn the surgeon of the risk of suture breakage (Dai et al., 2019). In particular, considering a larger number of surgeries that can benefit from teleoperated procedures using robots, during the era of COVID, addressing this challenge should be accelerated. This topic has seen ongoing research, and unfortunately, the current trend does

not show a promise of an upcoming solution. With improving technology for haptic feedback, this can result in a major advance in the performance of teleoperated surgeries on a larger scale and can enlarge the domain of surgeries, which can be conducted teleoperatively, helping with the management of the current concerns regarding infection transfer during surgery in the time of COVID.

There are two characteristics associated with a good haptic teleoperation system: transparency and stability. In the last three decades, a significant amount of research has been done on developing a transparent control architecture. Four-Channel Lawrence (FCL) was proposed as the first transparent teleoperation system (Lawrence, 1993). It was modified to simpler architectures (Hashtrudi-Zaad and Salcudean, 2001), (Hashtrudi-zaad and Salcudean, 2002). Atashzar et al. proposed a simplified two-channel modified-ELFC (M-ELFC) architecture that provides a high degree of transparency (Atashzar et al., 2012). To deal with the stability issue, three categories of passivity-based controllers have been proposed: 1) the Wave Variable approach (Aziminejad et al., 2008); 2) Time Domain Passivity Approach (TDPA) (Ryu et al., 2010); and 3) Small-gain approach (Atashzar et al., 2017a). Both techniques stabilize the system; however, stabilization comes at the cost of compromising transparency. Considerable research has been done to improve the performance of teleoperation (Artigas et al., 2010; Chawda and Omalley, 2015; Atashzar et al., 2017b; Panzirsch et al., 2019; Singh et al., 2019), but the proposed stabilization methods are still far from ideal. The discussion above clarifies some of the technical challenges creating obstacles to realizing high-fidelity haptics-enabled teleoperated surgery. The potential of RAMIS in resolving the surgical issues caused by COVID-19 is calling for an accelerated trend of research and development, extending the performance of teleoperated surgical robotic systems for allowing more benefit of this technology in reducing the burden on the healthcare system during the pandemic and similar crises in the future.

Remark: AI has been extensively developed in the last decade and has revolutionized many industries. However, the application of AI in surgical procedures requires a significant amount of adaptation and consideration. Robotic surgery can take advantage of AI in the COVID era from three aspects; 1) increasing accuracy and reducing the risk of failure by providing shared and full autonomy in simple tasks (Rabinovich et al., 2020; Wall and Krummel, 2020); 2) allowing physical distancing by changing the surgeon's role from executive and continuous control to supervisory and intermittent control; and 3) increasing the average number of surgical procedures, which will be required to address the backlogged surgeries caused by the shutdown of elective surgeries over a long period of time, thereby reducing the load on surgeons and allowing after-hour surgeries (Zemmar et al., 2020).

TELE-EXAMINATION OF PATIENTS

Preoperative examination for surgery preplanning and post-operative patient examination in the recovery time is another matter of concern in the COVID-19 era. In-person visits increase the risk of virus contraction for the patient and the surgeon. Keeping personal interactions as low as possible is the key factor in dealing with the pandemic.

Post-operative examinations may include patient's assessment at home and ICU. Telepresence robots that are made for telehealthcare purposes allow physicians to interact with patients, and monitor patients' vital signs without the physical presence of the surgeon in the ICU (Laniel et al., 2017). These systems have been used in Italy at COVID-19 patients' bedside in the ICU (Bogue, 2020; Pullella, 2020). A similar robot has been used in Israel to communicate with quarantined patients (Marks, 2020). In terms of home healthcare, messages, phone, and video calls have been used for post-operative examination. It has been shown that telepresence robots could provide a stronger feeling of a person to person interaction for both users, in comparison to video and phone calls, and both physicians and patients have expressed satisfaction (Tavakoli et al., 2020), (Becevic et al., 2015).

Preoperative examinations have also been done with AI- and robotics-enabled telehealth, but applications are limited due to the lack of physical exams and the need for clinical imaging. However, it has been shown that for some specific conditions, diagnosis via telemedicine could be as accurate as an in-person diagnosis when examination through telemedicine is feasible subject to limitations (Asiri et al., 2018). For example, AI can be used for digital triage to direct patients to the most appropriate medical center based on the resources and their condition before they show up in emergency rooms (Lai et al., 2020). As another example, it has been shown that blood draw and injections can be done with portable robots using AI more accurately and faster than a manual procedure (Zemmar et al., 2020). Another example is the telerobotic system that has been used in China to perform cardiac and lung ultrasound on a COVID patient (Wang et al., 2020). These systems can help safeguard patients and staff by reducing the need for patient referral to hospital and physical distancing.

Robotics and AI have taken a step in the development of tele-examination of patients during pre- and post-operative phases. However, there is still room for adding new capabilities to tele-healthcare robots in order to lower the need for in-person examinations or patient referrals to hospital. Besides robots, focusing on smartphone-based or computer-based tele-examination systems would be useful because of their widespread use.

TELE-TRAINING OF SURGEONS

The outbreak of COVID-19 has severely affected surgical training procedures. The most significant components of surgical training are comprised of theoretical, pre-clinical, and hands-on clinical training, but the lockdown caused by the pandemic has severely limited the opportunities for students and residents to acquire surgical training (Puliatti et al., 2020), (Bernardi et al., 2020). High-quality and intense healthcare support, which would be needed during and after COVID-19, requires precise training.

Although some schools are in a gradual reopening phase, there would be some level of shut down again with the next wave of the pandemic.

In such extraordinary conditions, online learning, teleconferences, and webinars can be of benefit with regard to surgical education and fill the gap with regard to theoretical training issues (Dedeilia et al., 2020). The benefits of these online learning technologies have been shown prior to the COVID-19 pandemic.

On the other hand, robotics and AI could improve the quality of pre-clinical training. Pre-clinical training is conventionally performed through dry or wet lab practices. The use of robotic simulators based on virtual reality (VR) systems has shown a significant improvement in novice surgeons' skills (Tergas et al., 2013). Hands-on-Surgical Training (HoST) provided by augmented reality (AR), and dual-user teleoperated system with virtual fixtures are more advanced simulators that help the novice surgeon to navigate using haptics-enabled cues outside the OR (Shahbazi et al., 2013; Kumar et al., 2015). Xperience Team Trainer developed by Mimic Simulations allows teamwork training in the OR at the pre-clinical stage (Mimics, 2020). This technology provides simultaneous training for the novice surgeon and the bedside assistant to improve coordination between the surgeon and assistant.

The preservation of acquired skills is another important issue in the COVID time. Surgical skills including motor and cognitive skills decay when a surgeon goes through a long period of time without using the acquired skills (Perez et al., 2013). Simulation-based medical education may fill the gap in surgical practice and prevent the loss of surgical skills during a lockdown (Higgins et al., 2020). In addition, AI can be employed to interpret the data collected from simulations for surgeons' skill evaluation (Winkler-Schwartz et al., 2019).

Because the above-mentioned technologies provide high-quality training while keeping social distancing, they could be part of the solution for the educational gap in the COVID-19 era. An active line of research and development that can be accelerated would be to design and develop small, inexpensive, and portable sensorized robotic modules connected to cloud-based virtual reality surgical environments. A large number of trainee surgeons could then continue their hands-on practice/training when access to training facilities is significantly restricted. This is critical because sensorimotor learning is a continual process in the human brain, and a long pause before getting to the agency level can drastically result in fading of sensorimotor skills.

Theoretical and pre-clinical training may guide students to pass the cognitive phase of learning; however, the integration phase, which gives them appropriate motor skills to perform surgery, requires performing surgery under the supervision of an expert in the OR (Choi et al., 2020). Residents would have very limited access to this form of training due to cancelation of elective surgery (Imielski, 2020) or requirements of social distancing. For telesurgery which is more challenging for residents to perform than open surgery and requires specific training, a viable solution that can be achieved using existing systems can be developed using hand-over-hand haptic-enabled tele-training (realized by multilateral teleoperation systems). This would not only allow novice surgeons to perform surgery from a safe distance, but also give them the opportunity to be supervised by an expert at the same time (Shahbazi et al., 2018a; Shahbazi et al., 2018b). The dual console teleoperation system format shares the control of the operation between the expert and the trainee. Incorporating haptics-enabled feedback would then provide the trainee with real-time force feedback. This format of telesurgery training gives the resident experience through supervised surgery without jeopardizing the safety of the patient or the resident during the constraints imposed by COVID-19. Furthermore, these multilateral tele-training systems could also be set up to evaluate the motor skills of trainees based on their performance.

DISCUSSION AND CONCLUSION

The novel coronavirus has challenged the healthcare system across the globe. Social distancing has become a new normal and may remain for a significant length of time especially as a result of the lack of vaccine and treatment for a critical period of time. This has deeply impacted surgeries and surgically related activities which may revolutionize how future healthcare systems function. Canceling elective surgeries was an efficient policy to curb the spread of the virus; nevertheless, keeping to this plan could have a detrimental effect on the health of patients and the healthcare system. Currently, governments are working on reopening guidelines. In this unprecedented situation, robotics and AI could play an important role in the safe delivery of surgical services through the use of telesurgery, tele-examination, and tele-training environments. A summary of the existing technologies and required features is given in **Table 1**.

Regarding teleoperated robotic surgery, it should be noted that although there is a wide range of benefit for both patients and the surgeons, there still exist a spectrum of challenges which are open topics for research and development. Regarding benefits, in the context of laparoscopic surgery, it can be mentioned that besides reduced operation time, reduced blood loss, increased accuracy, and reduced recovery time, there are additional benefits that are more pronounced during the pandemic, including reduced time and frequency of interpersonal interaction between surgical staff, reduced number of staff, reduced interaction between patients and staff, all to reduce the risk of infection transfer and increase the safety of surgical procedures (Kimmig et al., 2020; Tavakoli et al., 2020). It should be noted that the current state of telesurgery and robotics-assisted surgery are advanced for abdominal surgery; however, for some categories such as orthopedic surgery, teleoperation has not been considered as a robust option. During the pandemic, any technology that reduces the duration of surgery directly or indirectly (for example, by increasing the accuracy which reduces the need for readjustments) can significantly reduce the chances of infection transmission. This is critical since, in general, surgeons operate on many patients in a short time, which can increase the risk of infection even between patients indirectly through their surgeon.

TABLE 1 | Existing technologies and required features in telesurgery, tele-examination, and tele-training.

	Current existing technologies translated into practice	Required missing features for performance improvement
Telesurgery	• Unidirectional teleoperation. pros: better ergonomy; physical separation; less bedside staff; shorter hospital stay; less abdominal pressure; simpler surgical smoke handling; automated data recording. cons: lack of force feedback in the loop; limited types of surgeries. • Visual and other modalities of force feedback. pros: better diagnosis in teleoperation and less tissue damage while avoiding instability. cons: not as effective as direct haptic feedback.	• Transparent direct haptic feedback. • Increased capability to include more types of surgeries. • Reduce the cost of robots to increase accessibility. • Development of shared autonomy between surgeons and robots. • Automating simple tasks using AI to augment the performance, fluency and consistency of the surgery while reducing the need for interpersonal interaction.
Tele-examination	• Telemedicine systems through voice and video conferencing. pros: no need for hospital attendance; minimizing the risk for patients to come into contact with the source of infection; minimizing the need for traveling to clinics enhancing the accessibility; allowing for more-frequent visits; better digital platform for tracking records and conditions. cons: not as effective as in-person examination in many cases due to limitations on conducting physical exams.	• Automated triage using AI. • Portable examination system for pre-and post-surgery. • Telepresence robots in ICU and patients' houses for tele-physical examination. • Advanced automated wearable systems for tracking patient's vital signs and physical ability.
Tele-training	• Online learning systems. pros: following up the theoretical aspects of surgical training during lockdown; minimize the need for in-person attendance. cons: lack of experimental training. • VR robotic surgery simulation systems. pros: effective experimental training for students while minimizing the risk of making mistakes in actual surgery and minimizing students risk of infection. cons: not as effective as actual wet lab training.	• Hands-on-Surgical Training through dual-console telesurgery systems. • A portable hands-on robotic module to provide consistency in surgical training. • Accurate surgical skill evaluation system using AI and actual saved telesurgery data.

However, it should be noted that there is a wide range of challenges which have not been addressed yet, especially in the context of teleoperated surgery, and these for the future direction of research. One of the major challenges is the stability and transparency of force-feedback teleoperated robotic systems (Aziminejad et al., 2008; Ryu et al., 2010; Atashzar et al., 2017a). Due to the concerns of safety the existing commercialized telerobotic surgical systems, such as the da Vinci surgical system, do not enable force reflection, even though it is known that force reflection can significantly increase the quality of surgery by providing a much higher situational awareness for surgeons. Although a number of stabilizers and control algorithms have been reported in the literature, the existing algorithms result in deviation of motion tracking and force reflection, which reduces the accuracy of surgery and is often not acceptable (Artigas et al., 2010; Chawda and Omalley, 2015; Atashzar et al., 2017b; Panzirsch et al., 2019; Singh et al., 2019). Besides stability, instrumentation is another challenge. Attaching inexpensive, disposable, biocompatible, and miniaturizable force sensors to surgical tools for measuring multidimensional forces for reflection through a teleoperation medium is a major instrumentation challenge and an open line of research (Atashzar and Patel, 2018). Technologies such as optical force sensors are promising options and are the front line of research in this regard.

In addition, the introduction of AI in telesurgery is a new field of research and development which has attracted a great deal of interest in order to enable parts of surgical tasks to be automated, thereby reducing some cognitive and physical burden for the surgical team with the potential for reducing the operation time, increasing accuracy and reducing the number of needed staff in the operating room. The accuracy resulting from using AI in industrial applications has been shown; however, more research is required to prove its performance and build up confidence in the medical area (Wall and Krummel, 2020). Dealing with soft tissue is the main challenge when involving AI in the context of robotic and telerobotic surgery.

Regarding tele-examination, telepresence robots have been effective in improving post-operative patient-surgeon interactions and monitoring patient's vital signs, mostly in ICUs. However, due to limitations, effective solutions for detailed pre- and post-operative tele-examination of patients have not been proposed in the literature. One of the main challenges in this area is the development of portable sensorized robots for detailed remote monitoring of patient's signs. On the other hand, AI would be particularly useful in automating tele-examination devices to reduce the need for in-person pre- and post-operative examinations.

As for tele-training, simulation-based training systems using AR and HoST have provided a context for pre-clinical training while ensuring the safety of trainees and experts. In addition, simulation-based training can be effective in ensuring skill levels of surgeons in the presence of long periods of surgical inactivity. However, there are open areas for research in this field. Hand-over-hand training using multilateral teleoperation is one of the future research areas that can profoundly improve the quality of clinical surgical tele-training. The stability of delayed multilateral teleoperation and effective methods for sharing control between an expert and a trainee are directions for future researches (Shahbazi et al., 2018a; Shahbazi et al., 2018b). Besides hand-over-hand training, employment of AI for surgical skill training and assessment are open research areas.

In this perspective article, we have provided our opinions on some existing technologies which can be adopted rapidly to help with the current unprecedented situation and have given a perspective of the technologies required in hospitals. The

intention in writing this article has been to initiate discussions between researchers, policymakers, and stakeholders to further investigate the use of robotic, telerobotic and AI-based solutions in a framework for enhancing the performance of surgery, surgical training, post-operative treatment, and monitoring under the severe restrictions imposed by COVID-19. The vision and opinions presented in this article are based on an extensive review of the literature concerning approaches through which Robotics and AI can play a significant role.

DATA AVAILABILITY STATEMENT

The original contributions presented in the study are included in the article/Supplementary Material, further inquiries can be directed to the corresponding author.

AUTHOR CONTRIBUTIONS

The four authors (NF, MT, RP, SA) collaborated on the conceptualization of this article, conduction of the literature review, technical and technological analysis, and writing and editing the paper.

FUNDING

The work of NF and RP was funded by the Natural Sciences and Engineering Research Council (NSERC) of Canada under grant #RGPIN-1345 (awarded to RP) and the Tier-1 Canada Research Chairs Program (RP). The work of SA is supported, by the National Science Foundation (Award Number: 2031594).

REFERENCES

Ahmed, H., Allaf, M., and Elghazaly, H. (2020). COVID-19 and medical education. *Lancet Infect. Dis.* 20 (7), 777–778. doi:10.1016/S1473-3099(20)30226-7

Arora, S., Sevdalis, N., Aggarwal, R., Sirimanna, P., Darzi, A., and Kneebone, R. (2010). Stress impairs psychomotor performance in novice laparoscopic surgeons. *Surg. Endosc.* 24 (10), 2588–2593. doi:10.1007/s00464-010-1013-2

Artigas, J., Ryu, J. H., and Preusche, C. (2010). "Position drift compensation in time domain passivity based teleoperation," in IEEE/RSJ 2010 international conference on intelligent robots and systems, Taipei, Taiwan, October 18–22, 2010 (IEEE), 4250–4256. doi:10.1109/IROS.2010.5652691

Asiri, A., AlBishi, S., AlMadani, W., ElMetwally, A., and Househ, M. (2018). The use of telemedicine in surgical care: a systematic review. *Acta Infor. Med.* 26 (3), 201–206. doi:10.5455/aim.2018.26.201-206

Atashzar, S. F., and Patel, R. V. (2018). Teleoperation for minimally invasive robotics-assisted surgery. *Biomed. Eng.* 4, 341–372. doi:10.1142/9789813232266_0012

Atashzar, S. F., Shahbazi, M., Talebi, H. A., and Patel, R. V. (2012). "Control of time-delayed telerobotic systems with flexible-link slave manipulators," in IEEE International Conference on Intelligent Robots and Systems, Vilamoura-Algarve, PT, October 7–12, 2012 (IEEE), 3035–3040. doi:10.1109/IROS.2012.6386170

Atashzar, S. F., Polushin, I. G., and Patel, R. V. (2017a). A small-gain approach for nonpassive bilateral telerobotic rehabilitation: stability analysis and controller synthesis. *IEEE Trans. Robot.* 33 (1), 49–66. doi:10.1109/TRO.2016.2623336

Atashzar, S. F., Shahbazi, M., Tavakoli, M., and Patel, R. V. (2017b). A passivity-based approach for stable patient-robot interaction in haptics-enabled rehabilitation systems: modulated time-domain passivity control. *IEEE Trans. Cont. Syst. Technol.* 25 (3), 991–1006. doi:10.1109/TCST.2016.2594584

Aziminejad, A., Tavakoli, M., Patel, R. V., and Moallem, M. (2008). Transparent time-delayed bilateral teleoperation using wave variables. *IEEE Trans. Cont. Syst. Technol.* 16 (3), 548–555. doi:10.1109/TCST.2007.908222

Ballantyne, G. H. (2002). Robotic surgery, telerobotic surgery, telepresence, and telementoring: review of early clinical results. *Surg. Endosc.* 16 (10), 1389–1402. doi:10.1007/s00464-001-8283-7

Becevic, M., Clarke, M. A., Alnijoumi, M. M., Sohal, H. S., Boren, S. A., Kim, S. M., et al. (2015). Robotic telepresence in a medical intensive care unit—clinicians' perceptions. *Perspect. Health Inf. Manag.* 12, 1–9.

Berguer, R., and Smith, W. (2006). An ergonomic comparison of robotic and laparoscopic technique: the influence of surgeon experience and task complexity. *J. Surg. Res.* 134 (1), 87–92. doi:10.1016/j.jss.2005.10.003

Bernardi, L., Germani, P., Del Zotto, G., Scotton, G., and de Manzini, N. (2020). Impact of COVID-19 pandemic on general surgery training program: an Italian experience. *Am. J. Surg.* 220 (5), 1361–1363. doi:10.1016/j.amjsurg.2020.06.010

Bogue, R. (2020). Robots in a contagious world. *Industrial Robot* 47 (5), 673–642. doi:10.1108/IR-05-2020-0101

Bohren, J., Guerin, K., Xia, T., Hager, G. D., Kazanzides, P., and Whitcomb, L. L. (2011). "Toward practical semi-autonomous teleoperation: do what i intend, not what i do," in Proceedings of IEEE workshop on advanced robotics and its social impacts, Menlo Park, CA, October 2–4, 2011 (IEEE), 20–23. doi:10.1109/ARSO.2011.6301974

Challacombe, B. J., Kavoussi, L. R., and Dasgupta, P. (2003). Trans-oceanic telerobotic surgery. *BJU Int.* 92 (7), 678–680. doi:10.1046/j.1464-410X.2003.04475.x

Chawda, V., and Omalley, M. K. (2015). Position synchronization in bilateral teleoperation under time-varying communication delays. *IEEE/ASME Trans. Mechatron.* 20 (1), 245–253. doi:10.1109/TMECH.2014.2317946

Cho, J. N., Park, W. S., Min, S. Y., Han, S. A., and Song, J. Y. (2016). Surgical outcomes of robotic thyroidectomy vs. conventional open thyroidectomy for papillary thyroid carcinoma. *World J. Surg. Oncol.* 14 (1), 1–7. doi:10.1186/s12957-016-0929-y

Choi, B., Jegatheeswaran, L., Minocha, A., Alhilani, M., Nakhoul, M., and Mutengesa, E. (2020). The impact of the COVID-19 pandemic on final year medical students in the United Kingdom: a national survey. *BMC Med. Edu.* 20 (1), 1–11. doi:10.1186/s12909-020-02117-1

Currie, M. E., Talasaz, A., Rayman, R., Chu, M. W. A., Kiaii, B., Peters, T., et al. (2017). The role of visual and direct force feedback in robotics-assisted mitral valve annuloplasty. *Int. J. Med. Robotics* 13 (3), 1–12. doi:10.1002/rcs.1787

Dai, Y., Abiri, A., Pensa, J., Liu, S., Paydar, O., Sohn, H., et al. (2019). Biaxial sensing suture breakage warning system for robotic surgery. *Biomed. Microdevices.* 21 (1), 5–10. doi:10.1007/s10544-018-0357-6

Dattani, R., Morgan, C., Li, L., Bennett-Brown, K., and Wharton, R. M. H. (2020). The impact of COVID-19 on the future of orthopaedic training in the UK. *Acta. Orthop.* 91 (6), 627–632. doi:10.1080/17453674.2020.1795790

Dedeilia, A., Sotiropoulos, M. G., Hanrahan, J. G., Janga, D., Dedeilia, P., and Sideris, M. (2020). Medical and surgical education challenges and innovations in the COVID-19 era: a systematic review. *In. Vivo* 34 (3), 1603–1611. doi:10.21873/invivo.11950

Ferrario, L., Maffioli, A., Bondurri, A. A., Guerci, C., Lazzarin, F., and Danelli, P., (2020). COVID-19 and surgical training in Italy: residents and young consultants perspectives from the battlefield. *Am. J. Surg.* 220 (4), 850–852. doi:10.1016/j.amjsurg.2020.05.036

Ferrel, M. N., and Ryan, J. J. (2020). The impact of COVID-19 on medical education. *Cureus* 12 (3), e7492. doi:10.7759/cureus.7492

Fu, S. J., George, E. L., Maggio, P. M., Hawn, M., and Nazerali, R. (2020). The consequences of delaying elective surgery: surgical perspective. *Ann. Surg.* 272 (2), e79–e80. doi:10.1097/SLA.0000000000003998

Hampp, E. L., Chughtai, M., Scholl, L. Y., Sodhi, N., Stoker, B. M., Jacofsky, D. J., et al. (2019). Robotic-arm assisted total knee arthroplasty demonstrated greater accuracy and precision to plan compared with manual techniques. *J. Knee Surg.* 32 (3), 239–250. doi:10.1055/s-0038-1641729

Hashtrudi-Zaad, K., and Salcudean, S. E. (2001). Analysis of control architectures for teleoperation systems with impedance/admittance master and slave manipulators. *Int. J. Robotics Res.* 20 (6), 419–445. doi:10.1177/02783640122067471

Hashtrudi-zaad, K., and Salcudean, S. E. (2002). Transparency in time-delayed systems and the effect of local force feedback for transparent teleoperation. *IEEE Trans. Robot. Automat.* 18 (1), 108–114. doi:10.1109/70.988981

Heemskerk, J., De Hoog, D. E. N. M., Van Gemert, W. G., Baeten, C. G. M. I., Greve, J. W. M., and Bouvy, N. D. (2007). Robot-assisted vs. conventional laparoscopic rectopexy for rectal prolapse: a comparative study on costs and time. *Dis. Colon Rectum* 50 (11), 1825–1830. doi:10.1007/s10350-007-9017-2

Higgins, M., Madan, C., and Patel, R. (2020). Development and decay of procedural skills in surgery: a systematic review of the effectiveness of simulated-based medical education interventions. *The Surgeon*. doi:10.1016/j.surge.2020.07.013

Imielski, B. (2020). The detrimental effect of COVID-19 on subspecialty medical education. *Surgery* 168 (2), 218–219. doi:10.1016/j.surg.2020.05.012

Kimmig, R., Verheijen, R. H. M., and Rudnicki, M. (2020). Robot assisted surgery during the COVID-19 pandemic, especially for gynecological cancer: a statement of the society of european robotic gynaecological surgery (SERGS). *J. Gynecol. Oncol.* 31 (3), e59. doi:10.3802/jgo.2020.31.e59

Kumar, A., Smith, R., and Patel, V. R. (2015). Current status of robotic simulators in acquisition of robotic surgical skills. *Curr. Opin. Urol.* 25 (2), 168–174. doi:10.1097/MOU.0000000000000137

Kumar, A., Taggarsi, M., and Selvasekar, C. R. (2020). Surgery during COVID-19 era-an overview. *Physi. Inter. J. Health* 6 (2), 3. doi:10.38192/1.6.2.3

Lai, L., Wittbold, K. A., Dadabhoy, F. Z., Sato, R., Landman, A. B., Schwamm, L. H., et al. (2020). Digital triage: novel strategies for population health management in response to the COVID-19 pandemic. *Healthcare* 8 (4), 100493. doi:10.1016/j.hjdsi.2020.100493

Laniel, S., Létourneau, D., Labbé, M., Grondin, F., Polgar, J., and Michaud, F. (2017). "Adding navigation, artificial audition and vital sign monitoring capabilities to a telepresence mobile robot for remote home care applications," in IEEE International Conference on Rehabilitation Robotics, London, UK, July 17–20, 2017 (IEEE), 806–811. doi:10.1109/ICORR.2017.8009347

Lawrence, D. A. (1993). Stability and transparency in bilateral teleoperation. *IEEE Trans. Robot. Automat.* 9 (5), 624–637. doi:10.1109/70.258054

Lee, A. M., Wong, J. G. W. S., McAlonan, G. M., Cheung, V., Cheung, C., Chua, S. E., et al. (2007). Stress and psychological distress among SARS survivors 1 year after the outbreak. *Can. J. Psychiatry* 52 (4), 233–240. doi:10.1177/070674370705200405

Liang, T. (2020). Handbook of COVID-19 prevention and treatment Compiled According to Clinical Experience. Hangzhou, Zhejiang: The First Affiliated Hospital, Zhejiang University School of Medicine

Lin, K., Yang, B. X., Luo, D., Liu, Q., Ma, S., Huang, R., et al. (2020). The mental health effects of COVID-19 on health care providers in china. *Am. J. Psychiatry* 177 (7), 635–636. doi:10.1176/appi.ajp.2020.20040374

Lindfors, A., Åkesson, Å., Staf, C., Sjöli, P., Sundfeldt, K, and Dahm-Kähler, P. (2018). Robotic vs open surgery for endometrial cancer in elderly patients: surgical outcome, survival, and cost analysis. *Int. J. Gynecol. Cancer* 28 (4), 692–699. doi:10.1097/IGC.0000000000001240

Marks, J. R. (2020). Sheba showcases future medtech used now for COVID-19. Available at: https://themedialine.org/life-lines/sheba-showcases-future-medtech-used-now-for-covid-19/. (Accessed May 27, 2020).

Mimics (2020). Xperience team TrainerTM. Mimic simulation technology. Available at: https://mimicsimulation.com/xperience/ (Accessed July 8, 2020).

Moawad, G. N., Elkhalil, J., Klebanoff, J. S., Rahman, S., Habib, N., and Alkatout, I. (2020). Augmented realities, artificial intelligence, and machine learning: clinical implications and how technology is shaping the future of medicine. *J. Clin. Med.* 9 (12), 3811. doi:10.3390/jcm9123811

Moorthy, K., Munz, Y., Dosis, A., Hernandez, J., Martin, S., F. Bello, F., et al. (2004). Dexterity enhancement with robotic surgery. *Surg. Endosc. Other Interv. Tech.* 18 (5), 790–795. doi:10.1007/s00464-003-8922-2

Mottrie, A. (2020). *ERUS (EAU robotic urology section) guidelines during COVID-19 emergency*. Available at: https://uroweb.org/wp-content/uploads/ERUS-guidelines-for-COVID-def.pdf. (Accessed May 11, 2020).

Naidu, A. S., Naish, M. D., and Patel, R. V. (2017a). A breakthrough in tumor localization: combining tactile sensing and ultrasound to improve tumor localization in robotics-assisted minimally invasive surgery. *IEEE Robot. Automat. Magaz.* 24 (2), 54–62. doi:10.1109/mra.2017.2680544

Naidu, A. S., Patel, R. V., and Naish, M. D. (2017b). Low-cost disposable tactile sensors for palpation in minimally invasive surgery. *IEEE/ASME Trans. Mechat.* 22 (1), 127–137. doi:10.1109/TMECH.2016.2623743

Panzirsch, M., Ryu, J. H., and Ferre, M. (2019). Reducing the conservatism of the time domain passivity approach through consideration of energy reflection in delayed coupled network systems. *Mechatronics* 58, 58–69. doi:10.1016/j.mechatronics.2018.12.001

Perez, R. S., Skinner, A., Weyhrauch, P., Niehaus, J., Lathan, C., Schwaitzberg, S. D., et al. (2013). Prevention of surgical skill decay. *Mil. Med.* 178 (10), 76–86. doi:10.7205/milmed-d-13-00216

Puliatti, S., Mazzone, E., and Dell'Oglio, P. (2020). Training in robot-assisted surgery. *Curr. Opin. Urol.* 30 (1), 65–72. doi:10.1097/MOU.0000000000000687

Pullella, P. (2020). Tommy the robot nurse helps keep Italy doctors safe from coronavirus. Available at: https://www.usnews.com/news/world/articles/2020-04-01/tommy-the-robot-nurse-helps-keep-italy-doctors-safe-from-coronavirus. (Accessed April 1, 2020).

Rabinovich, E. P., Capek, S., Kumar, J. S., and Park, M. S. (2020). Tele-robotics and artificial-intelligence in stroke care. *J. Clin. Neurosci.* 79, 129–132. doi:10.1016/j.jocn.2020.04.125

Reyes, C., Engel-Nitz, N. M., DaCosta Byfield, S., Ravelo, A., Ogale, S., and Bancroft, T. (2019). Cost of disease progression in patients with metastatic breast, lung, and colorectal cancer. *Oncologist* 24 (9), 1209–1218. doi:10.1634/theoncologist.2018-0018

Ryu, J. H., Artigas, J., and Preusche, C. (2010). A passive bilateral control scheme for a teleoperator with time-varying communication delay. *Mechatronics* 20 (7), 812–823. doi:10.1016/j.mechatronics.2010.07.006

Scaravonati, R., Diaz, E., Roche, S., Bertone, S., and Brandi, C. (2020). Strategies for follow up after hernia surgery during COVID 19 pandemia. *Int. J. Surg.* 79, 103–104. doi:10.1016/j.ijsu.2020.05.051

Schorr, S. B., Quek, Z. F., Romano, R. Y., Nisky, I., Provancher, W. R., and Okamura, A. M. (2013). "Sensory substitution via cutaneous skin stretch feedback," in IEEE International Conference on Robotics and Automation, Karlsruhe, Germany, May 6–10, 2013 (IEEE), 2341–2346. doi:10.1109/ICRA.2013.6630894

Schwarz, L., and Tuech, J. J. (2020). Is the use of laparoscopy in a COVID-19 epidemic free of risk? *Br. J. Surg.* 107 (7), e188. doi:10.1002/bjs.11649

Shademan, A., Decker, R. S., Opfermann, J. D., Leonard, S., Krieger, A., and Kim, P. C. W. (2016). Supervised autonomous robotic soft tissue surgery. *Sci. Translational Med.* 8 (337), 337ra64. doi:10.1126/scitranslmed.aad9398

Shahbazi, M., Atashzar, S. F., and Patel, R. V. (2013). "A dual-user teleoperated system with Virtual Fixtures for robotic surgical training," in Proceedings - IEEE International Conference on Robotics and Automation, Karlsruhe, Germany, May 6–10, 2013 (IEEE), 3639–3644. doi:10.1109/ICRA.2013.6631088

Shahbazi, M., Atashzar, S. F., and Patel, R. V. (2018a). A systematic review of multilateral teleoperation systems. *IEEE Trans. Hapt.* 11 (3), 338–356. doi:10.1109/TOH.2018.2818134

Shahbazi, M., Atashzar, S. F., Ward, C., Talebi, H. A., and Patel, R. V. (2018b). Multimodal sensorimotor integration for expert-in-the-loop telerobotic surgical training. *IEEE Trans. Robot.* 34 (6), 1549–1564. doi:10.1109/TRO.2018.2861916

Singh, H., Jafari, A., and Ryu, J. H. (2019). "Enhancing the force transparency of time domain passivity approach: observer-based gradient controller," in Proceedings - IEEE International Conference on Robotics and Automation, Montreal, QC, 20-24 May 2019 (IEEE), 1583–1589. doi:10.1109/ICRA.2019.8793902

Smithand Nephew, n. d. (2020). Using NAVIO in total knee arthroplasty. Available at: https://www.smith-nephew.com/professional/microsites/navio/total-knee-arthroplasty/navio-total-knee/ (Accessed December 10, 2020).

Stryker, n. d. (2020). Mako robotic-arm assisted surgery. Available at: https://www.stryker.com/us/en/portfolios/orthopaedics/joint-replacement/mako-robotic-arm-assisted-surgery.html. (Accessed November 30, 2020).

Szklarski, C. (2020). Canada's higher COVID-19 death rate tied to better chronic disease control. Available at: https://www.cbc.ca/news/health/covid-19-heart-stroke-1.5652003. (Accessed July 16, 2020).

Tabaza, L., Virk, H. U. H., Janzer, S., and George, J. C. (2020). Robotic-assisted percutaneous coronary intervention in a COVID-19 patient. *Catheterization and cardiovascular interventions* 97 (3), E343–E345. 10.1002/ccd.28982

Talasaz, A., and Patel, R. V. (2013). Integration of force reflection with tactile sensing for minimally invasive robotics-assisted tumor localization. *IEEE Trans. Hapt.* 6 (2), 217–228. doi:10.1109/TOH.2012.64

Talasaz, A., Trejos, A. L., Perreault, S., Bassan, H., and Patel, R. V. (2014). A dual-arm 7-degrees-of-freedom haptics-enabled teleoperation test bed for minimally invasive surgery. *J. Med. Devices.* 8 (4), 041004. doi:10.1115/1.4026984

Talasaz, A., Trejos, A. L., and Patel, R. V. (2017). The role of direct and visual force feedback in suturing using a 7-DOF dual-arm teleoperated system. *IEEE Trans. Hapt.* 10 (2), 276–287. doi:10.1109/TOH.2016.2616874

Tan, Y. Q., Chan, M. T., and Chiong, E. (2020). Psychological health among surgical providers during the COVID-19 pandemic: a call to action. *Br. J. Surg.* 107 (11), e459–e460. doi:10.1002/bjs.11915

Tavakoli, M., Aziminejad, A., Patel, R. V., and Moallem, M. (2006). Tool/tissue interaction feedback modalities in robot-assisted lump localization. *Conf Proc IEEE Eng Med Biol Soc* 2006, 3854–3857. doi:10.1109/IEMBS.2006.260672

Tavakoli, M., Carriere, J., and Torabi, A. (2020). Robotics, smart wearable technologies, and autonomous intelligent systems for healthcare during the COVID-19 pandemic: an analysis of the state of the art and future vision. *Adv. Intell. Syst.* 2 (7), 2000071. doi:10.1002/aisy.202000071

Tergas, A. I., Sheth, S. B., Green, I. C., and Giuntoli, R. L. (2013). A pilot study of surgical training using a virtual robotic surgery simulator. *JSLS.* 17 (2), 219–226. doi:10.4293/108680813X13654754535872

Trejos, A. L., Jayender, J., Perri, M. T., Naish, M. D., Patel, R. V., and Malthaner, R. A. (2009). Robot-assisted tactile sensing for minimally invasive tumor localization. *Int. J. Robotics Res.* 28 (9), 1118–1133. doi:10.1177/0278364909101136

Van den Eynde, J., De Groote, S., Van Lerberghe, R., Van den Eynde, R., and Oosterlinck, W. (2020). Cardiothoracic robotic assisted surgery in times of COVID-19. *J. Robotic Surg.* 14, 795–797. doi:10.1007/s11701-020-01090-7

Wall, J., and Krummel, T. (2020). The digital surgeon: how big data, automation, and artificial intelligence will change surgical practice. *J. Pediatr. Surg.* 55, 47–50. doi:10.1016/j.jpedsurg.2019.09.008

Wang, J., Peng, C., Zhao, Y., Ye, R., Hong, J., Huang, H., et al. (2020). Application of a robotic tele-echography system for COVID-19 pneumonia. *J. Ultrasound Med.* 40, 1–6. doi:10.1002/jum.15406

Wetzel, C. M., Kneebone, R. L., Woloshynowych, M., Nestel, D., Moorthy, K., Kidd, J., et al. (2006). The effects of stress on surgical performance. *Am. J. Surg.* 191 (1), 5–10. doi:10.1016/j.amjsurg.2005.08.034

Willer, B. L., Thung, A. K., Corridore, M., D'Mello, A. J., Schloss, B. S., Malhotra, P. S., et al. (2020). The otolaryngologist's and anesthesiologist's collaborative role in a pandemic: a large quaternary pediatric center's experience with COVID-19 preparation and simulation. *Int. J. Pediatr. Otorhinolaryngol.* 136, 110174. doi:10.1016/j.ijporl.2020.110174

Winkler-Schwartz, A., Yilmaz, R., Mirchi, N., Bissonnette, V., et al. (2019). Machine learning identification of surgical and operative factors associated with surgical expertise in virtual reality simulation. *JAMA Netw. Open* 2 (8), e198363. doi:10.1001/jamanetworkopen.2019.8363

WHO (2020). WHO Timeline - COVID-19. Available at: https://www.who.int/news-room/detail/27-04-2020-who-timeline—covid-19. (Accessed April 27, 2020).

Zafar, A. (2020). The unintended consequences of surgery delays during COVID-19. Available at: https://www.cbc.ca/news/health/covid-surgery-delay-unintended-consequences-1.5629360. (Accessed June 29, 2020).

Zemmar, A., Lozano, A. M., and Nelson, B. J. (2020). The rise of robots in surgical environments during COVID-19. *Nat. Machine Intelligence* 2 (10), 566–572. doi:10.1038/s42256-020-00238-2

Conflict of Interest: The authors declare that the research was conducted in the absence of any commercial or financial relationships that could be construed as a potential conflict of interest.

frontiers in Robotics and AI

ORIGINAL RESEARCH
published: 03 May 2021
doi: 10.3389/frobt.2021.611866

Design and Modelling of a Continuum Robot for Distal Lung Sampling in Mechanically Ventilated Patients in Critical Care

*Zisos Mitros[1,2], Balint Thamo[3], Christos Bergeles[1], Lyndon da Cruz[2], Kevin Dhaliwal[4] and Mohsen Khadem[3,4]**

[1] Robotics and Vision in Medicine (RViM) Lab, School of Biomedical Engineering & Imaging Sciences, King's College London, London, United Kingdom, [2] Wellcome/EPSRC Centre for Interventional and Surgical Sciences, University College London, London, United Kingdom, [3] School of Informatics, University of Edinburgh, Edinburgh, United Kingdom, [4] Translational Healthcare Technologies Group in the Centre for Inflammation Research, Queen's Medical Research Institute, Edinburgh, United Kingdom

In this paper, we design and develop a novel robotic bronchoscope for sampling of the distal lung in mechanically-ventilated (MV) patients in critical care units. Despite the high cost and attributable morbidity and mortality of MV patients with pneumonia which approaches 40%, sampling of the distal lung in MV patients suffering from range of lung diseases such as Covid-19 is not standardised, lacks reproducibility and requires expert operators. We propose a robotic bronchoscope that enables repeatable sampling and guidance to distal lung pathologies by overcoming significant challenges that are encountered whilst performing bronchoscopy in MV patients, namely, limited dexterity, large size of the bronchoscope obstructing ventilation, and poor anatomical registration. We have developed a robotic bronchoscope with 7 Degrees of Freedom (DoFs), an outer diameter of 4.5 mm and inner working channel of 2 mm. The prototype is a push/pull actuated continuum robot capable of dexterous manipulation inside the lung and visualisation/sampling of the distal airways. A prototype of the robot is engineered and a mechanics-based model of the robotic bronchoscope is developed. Furthermore, we develop a novel numerical solver that improves the computational efficiency of the model and facilitates the deployment of the robot. Experiments are performed to verify the design and evaluate accuracy and computational cost of the model. Results demonstrate that the model can predict the shape of the robot in <0.011s with a mean error of 1.76 cm, enabling the future deployment of a robotic bronchoscope in MV patients.

Keywords: surgical robot, robotic bronchoscope, mathematical modelling, steerable catheter, flexible robot

OPEN ACCESS

Edited by:
Ana Luisa Trejos, Western University, Canada

Reviewed by:
Luigi Manfredi, University of Dundee, United Kingdom
Cecilia Laschi, National University of Singapore, Singapore

***Correspondence:**
Mohsen Khadem
skhadem@ed.ac.uk

Specialty section:
This article was submitted to Biomedical Robotics, a section of the journal Frontiers in Robotics and AI

Received: *29 September 2020*
Accepted: *24 March 2021*
Published: *03 May 2021*

Citation:
Mitros Z, Thamo B, Bergeles C, da Cruz L, Dhaliwal K and Khadem M (2021) Design and Modelling of a Continuum Robot for Distal Lung Sampling in Mechanically Ventilated Patients in Critical Care. Front. Robot. AI 8:611866. doi: 10.3389/frobt.2021.611866

1. INTRODUCTION

Critically ill patients who develop respiratory failure and require mechanical ventilation (MV) suffer a high morbidity and mortality. Indeed, Covid-19 patients who require MV, have a mortality approaching 40% in some case series. Once MV, patients are at high risk of developing secondary infections and other secondary complications. Rapid and accurate sampling of the distal lung is an

important diagnostic procedure to guide therapeutic interventions. However, despite the high cost and attributable morbidity and mortality, diagnosis of diseases in the distal lung in MV patients is not standardised, lacks reproducibility and requires expert operators. Often, this leads to empirical treatments such as broad spectrum antibiotics which are then very difficult to deescalate, thus compounding the exposure of patients to non-targeted antimicrobials and promoting antimicrobial resistance. Pulmonary infiltrates in MV critically ill patients are a common occurrence and a major diagnostic challenge. Endobronchial secretions such as mucus and often hinder manually steered bronchoscopes, leading to poor sampling results. Hence, the aim of this paper is to develop a robotic bronchoscope that democratises sampling of the lung in MV ICU patients and enables non-skilled operators to safely sample disparate regions of the human lung to improve diagnostic accuracy and therapeutic interventions.

Bronchoscopy is a common diagnostic modality for the early detection of lung diseases (see **Figure 1**). During bronchoscopy, a thin tube (bronchoscope) is passed through the vocal cords into the airways to reach potential regions of the lung for directed sampling. Due to relatively large dimensions of the bronchoscope used for sampling ($>$ 5 mm), bronchoscopy of MV patients is challenging. Another major drawback of the current technology is reliance on manual insertion, which is difficult due to the limited Degrees of Freedom (DoFs) of the bronchoscope, i.e., rotation and insertion.

To address the aforementioned challenges, we have developed a miniaturised continuum robot for lung bronchoscopy. A continuum robot has a continuously elastic structure and can traverse tightly curved 3D paths in confined spaces and reach desired positions deep inside human cavities. Continuum robots retain force transmission capability and offer great dexterity, thus, enabling optimal therapies when deeply seated pathologies are targeted (Burgner-Kahrs et al., 2015). Continuum robots have been explored for various interventions including laparoscopy (Wu et al., 2019), cardiac surgery (Fagogenis et al., 2019), neurosurgery (Mattei et al., 2014), and eye surgery (Mitros et al., 2020).

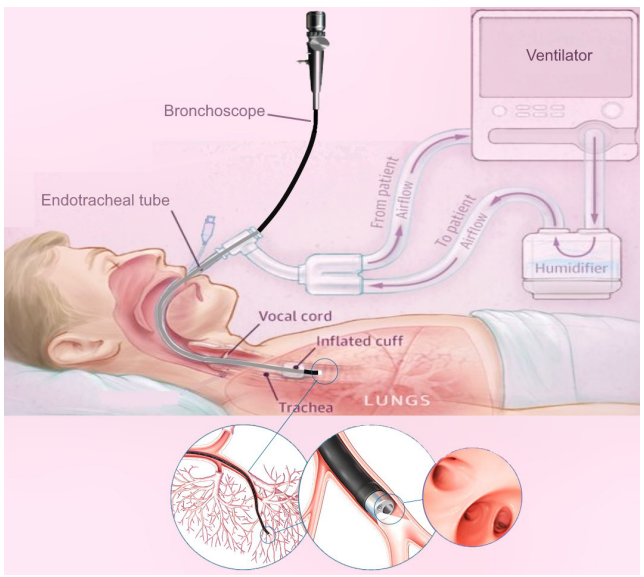

FIGURE 1 | A schematic of lung bronchoscopy in ICU, showcasing the insertion of the robotic bronchoscope through the mechanical ventilator and inside the lung.

The proposed bronchoscope is a continuum robot comprised of several parallel rods that can be bent via pushing/pulling of the rods. A continuum robot composed of several constrained push/pull rods is commonly known as a *multi-backbone robot*, first introduced in Gravagne and Walker (2000). Simaan et al. introduced the first surgical multi-backbone robot for dexterous tool manipulation in robotics surgery (Simaan et al., 2004; Ding et al., 2013). Xu et al. (2015) improved this design using a "dual continuum" actuation mechanism that increases modularity. Several researchers have explored the possibility of using a parallel multi-backbone approach without constraints, allowing more dexterous robots with increased DIFs per section (Bryson and Rucker, 2014; Wang et al., 2019). Multi-backbone robots have been commonly proposed for abdominal surgeries (Garbin et al., 2019; Riojas et al., 2019; Wu et al., 2019).

A major challenge in deployment of miniaturised continuum robots is real-time and precise modelling. There are several different kinematic and dynamic models presented in the literature (see Webster and Jones, 2010; Burgner-Kahrs et al., 2015 for a detailed review). The most common model for multi-backbone robots is a geometric model proposed in Simaan et al. (2004). The model has been used to control the motion of the robot as well as contact forces at the robot's tip (Bajo and Simaan, 2016). The geometric model assumes the robot curvature is constant and provides an accurate description of the robot's differential kinematics for large scale movements. However, due to the effects of unknown boundary conditions and the constant curvature assumption, the model's prediction of the robot shape and micro-scale movements are not accurate. To overcome this challenge, Del Giudice et al. (2017) proposed a method to improve micro-scale motion of a multi-backbone robot using modulation of the flexural rigidity of the rods. Another commonly method for modelling of multi-backbone robots is Cosserat rod theory (Bryson and Rucker, 2014; Wang et al., 2019). However, the Cosserat rod theory results in a relatively large boundary value problem (BVP) that should be solved for every rod in the robot and are computationally expensive. As a result, less accurate modelling methods are still attractive due to their low computational cost (Kaouk et al., 2014; Bajo and Simaan, 2016).

In this paper, we develop a bronchoscope using a miniaturised multi-backbone robot. The bronchoscope is mounted on a linear stage that can be used to automatically insert/retract the bronchoscope to reach targeted positions in the distal lung. Next, we develop a geometrically exact model of the robot that considers both the geometry of robot and mechanical properties of the backbones. The model results in a reduced order BVP and can be used to predict the shape of the bronchoscope without the constant curvature assumption. Furthermore, we develop a novel nonlinear observer that significantly improves the computational

efficiency of the model to estimate the solution of the proposed model in real-time. Finally, simulations and experiments are performed to validate the design and the modelling Theory.

In the next section, section 2.1, the robot architecture and bronchoscope design is presented. Section 2.2 details the model of the bronchoscope. Section 2.4 outlines the detail of the observer design. In section 3, simulations and experimental results are performed to evaluate the design and quantify the accuracy and computational efficiency of the model. Concluding remarks appear in section 4.

2. MATERIALS AND METHODS

2.1. System Design and Prototyping

This section describes the design and engineering of the robotic bronchoscope. The mechanical system design begins with DoFs discussion. To improve the dexterity of the bronchoscope, we propose a novel design that allows the robotic bronchoscope to bend in 3D at two points. The tip of the bronchoscope is composed of two segments shown in **Figure 2**. Each segment is actuated by 3 nitinol (NiTi) rods with an outer diameter of 0.475 mm which are passed through holes located on fixtures surrounding the bronchoscope. The circular fixtures are employed to avoid buckling of the rods. An additional silicone rod shown in blue in **Figure 2** is acting as the main backbone. It has an outer and inner diameters of 2.3 mm and 2 mm, respectively and is rigidly connected to the fixtures to ensure they cannot move relative to each other. The fixtures' outer and inner diameters are 4.5 and 2.4 mm, respectively. Length of proximal segment at the tip of the bronchoscope is 40 mm, length of the distal segment is 500 mm, and the overall length of the bronchoscope is 540 mm. The end-effector is actuated via the push-pull of the 6 rods. In contrast to the cable driven bronchoscopes, the proposed design employs in-compressible

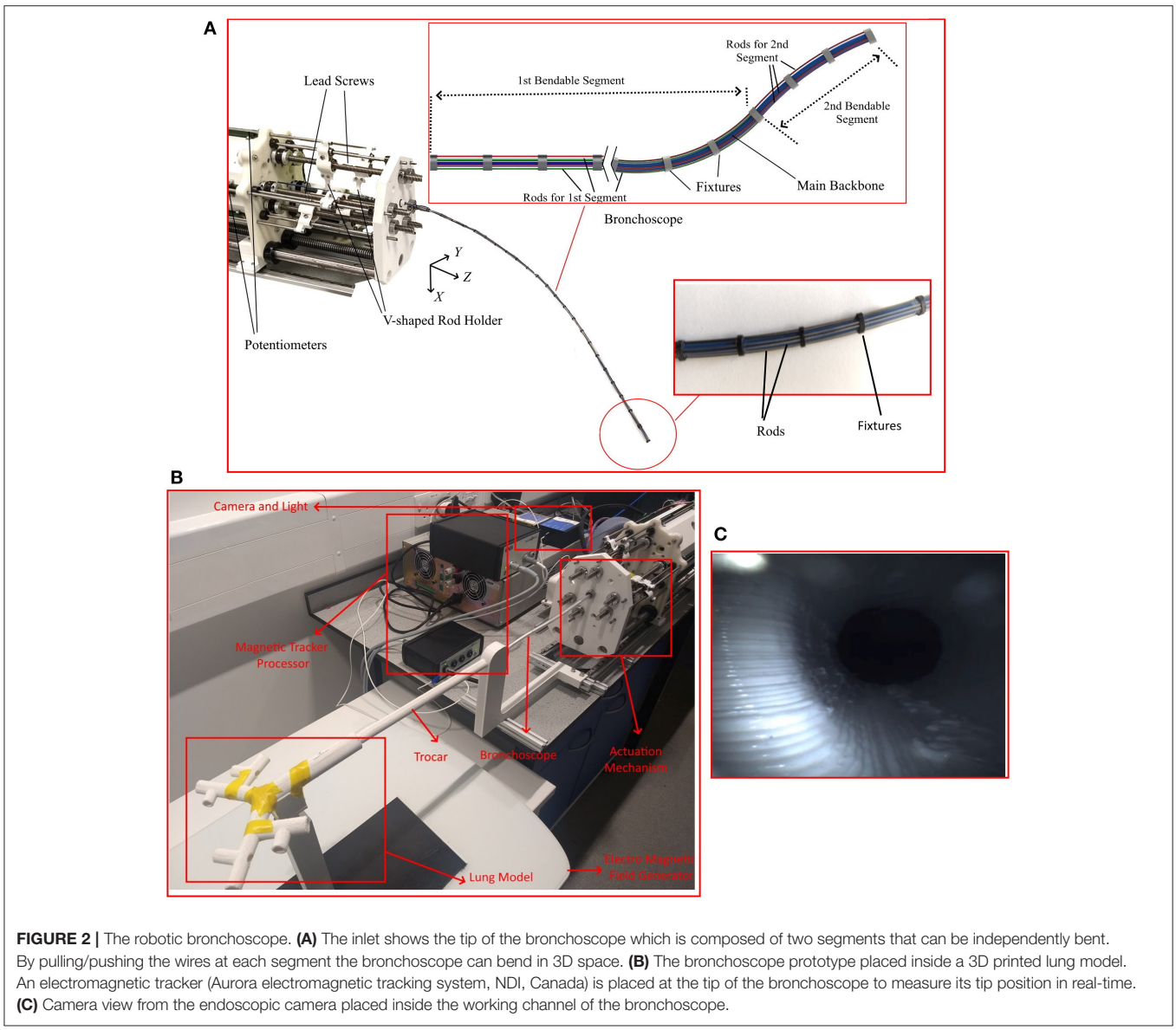

FIGURE 2 | The robotic bronchoscope. **(A)** The inlet shows the tip of the bronchoscope which is composed of two segments that can be independently bent. By pulling/pushing the wires at each segment the bronchoscope can bend in 3D space. **(B)** The bronchoscope prototype placed inside a 3D printed lung model. An electromagnetic tracker (Aurora electromagnetic tracking system, NDI, Canada) is placed at the tip of the bronchoscope to measure its tip position in real-time. **(C)** Camera view from the endoscopic camera placed inside the working channel of the bronchoscope.

Nitinol rods to offer more bending curvature via pushing of the rods. Furthermore, a 7th DoFs is employed for the insertion and retraction of the end-effector into the airways.

All DoFs are actuated by brushless DC motors (Maxon Motors) with a gearhead with a 150 : 1 reduction and a quadratic encoder. Each motor is controlled via a position controller module with a built in PID controller (EPOS4 Compact 50/5 CAN). The controllers employ the encoders feedback to accurately control the position of the motor shaft. The position controllers communicate with a PC via the CAN protocol. A CAN-to-USB interface (Kvaser Inc., CA, USA) is used to connect the position controllers to the PC.

The motors are connected to lead screws that convert the power generated by the motor into feed velocity for pulling/pushing the rods. The lead screws are carrying a v-shaped 3D printed part that is connected to the rods (shown in **Figure 2**) and travels along the lead screw to pull/push the rods. Additionally, 6 linear potentiometers are used to accurately measure the displacement of the rods.

Figure 2 shows the developed robot and an inlet showcases the different segments that the manipulator comprises.

2.2. Geometrically Exact Model of the Robot

We use the Cosserat-rod theory (Antman, 2005; Rucker et al., 2010) to model the robot. First, we present the model for a robot with one bendable segment. Next, we generalise the model to a robot with more segments. The following notation is used throughout the paper: x, x, and $\mathbf{X}$ denote a scalar, a vector, and a matrix, respectively. A complete summary of variables and operators is given in the Appendix. The symbols used are summarised in a nomenclature section.

A schematic of the robot is shown in **Figure 3**. The robot comprises a main backbone (shown in blue) rigidly connected to the fixtures and three NiTi rods (shown in red) fixed at the end fixture. The three rods can pass through the rest of the fixtures and have enough clearance to not create forces and moments but rather follow the curvature of the main backbone. The relative position of each rod with respect to the main backbone ($\boldsymbol{d}_i$, $i = 1, 2, 3$ in **Figure 3**) is given by

$$\boldsymbol{d}_i = [\delta\cos(\beta_i),\ \delta\sin(\beta_i),\ 0]^T, \tag{1}$$

where δ is the rods' distance from the robots centroid (see **Figure 3**) and β_i is the relative angular position of each rod with respect to the main backbone

$$\beta_i = \alpha + (i-1)\frac{2\pi}{3},\ \ i = 1, 2, 3, \tag{2}$$

with α shown in **Figure 3**.

The robot main backbone is modelled as a long, slender, one-dimensional Cosserat rod endowed with a Darboux frame attached to every point on its arc with the z axis of the frame tangent to the curve. The rod is under an external point force $[F(t)]$ and distributed constant load (f) simulating the weight of the fixtures. The configuration of the rod can be defined using a unique set of 3D centroids, $\mathbf{r}(s,t):[0,\ell]\times[0,\infty]\rightarrow\mathbb{R}^3\times[0,\infty]$, and a family of orthogonal transformations, $\mathbf{R}(s,t):[0,\ell]\times[0,\infty]\rightarrow so(3)\times[0,\infty]$. The position of the main backbone is defined by

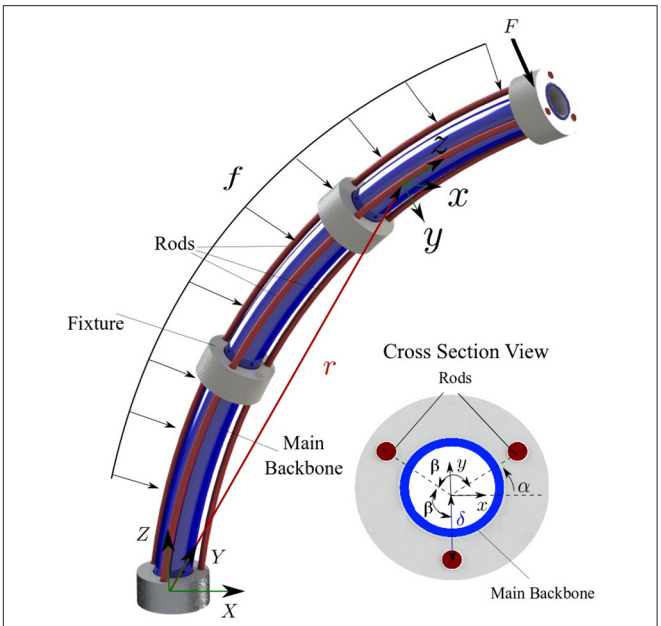

FIGURE 3 | A schematic of the continuum robot with one bent segment. The main backbone is modelled as a Cosserat rod under external point force (F) and distributed load (f). The cross section view shows the position of the rods with respect to the main backbone.

$$\boldsymbol{r}'(s,t) = \mathrm{R}(s,t)\boldsymbol{e}_3,\ \ \mathrm{R}'(s,t) = \mathrm{R}(s,t)[\mathrm{u}(s,t)]_\times, \tag{3}$$

where $\boldsymbol{u}(s,t) = [u_x(s,t), u_y(s,t), u_z(s,t)]^T$ is the curvature vector of the deformed backbone, $[.]_\times$ operator is the isomorphism between a vector in $\mathbb{R}^3$ and its skew-symmetric cross product matrix, and $\boldsymbol{e}_3 = [0,\ 0,\ 1]^T$ is the unit vector aligned with the z-axis of the global coordinate frame. Assuming the rods are made of linear elastic isotropic materials, we can derive the constitutive equations for calculating the instantaneous curvature of the rod (Rucker et al., 2010)

$$\begin{aligned}\boldsymbol{u}'(s,t) = -K^{-1}\Big[&[\mathrm{u}(s,t)]_\times K\boldsymbol{u}(s,t) + \\ &[\boldsymbol{e}_3]_\times \mathrm{R}^T(s,t)\big(\boldsymbol{F}(t) + (l-s)f\big)\Big],\end{aligned} \tag{4}$$

where l is the length of the main backbone and $\mathrm{K} = \mathrm{diag}(EI, EI, GJ)$ is the stiffness matrix for the whole robot; E is the robot's Young's modulus; I is the second moment of inertia; G is the shear modulus; J is the polar moment of inertia. It is assumed that the cross section of the robot is symmetric and the products of inertia are negligible (i.e., $I_{xy} = I_{xz} = I_{yz} \simeq 0$)

In practice, the robot curvature $\boldsymbol{u}(s,t)$ and position $\boldsymbol{r}(s,t)$ are unknown and should be estimated as the function of the length

of the three rods ($\ell_i,\ i = 1, 2, 3$). We can estimate each rod's total arc length as

$$\ell_i(t) = \int_0^l \|\boldsymbol{r}_i^{'}(s,t)\|\mathrm{d}s, \tag{5}$$

where $\|.\|$ denotes the ℓ_2-norm and $\boldsymbol{r}_i(s,t)$ is the position of ith rod given by

$$\boldsymbol{r}_i(s,t) = \boldsymbol{r}(s,t) + \mathrm{R}(s,t)\boldsymbol{d}_i. \tag{6}$$

Substituting (6) in (5) and simplifying the equations using (3) yields

$$\ell_i(t) = \int_0^l \|\boldsymbol{e}_3 + [\mathrm{u}(s,t)]_\times \boldsymbol{d}_i\|\mathrm{d}s, \tag{7}$$

Now, we can write the system of differential equations governing the motion of the robot using (3), (4), and (7)

$$\boldsymbol{r}^{'}(s,t) = \mathrm{R}(s,t)\boldsymbol{e}_3, \tag{8a}$$

$$\mathrm{R}^{'}(s,t) = \mathrm{R}(s,t)[\mathrm{u}(s,t)]_\times, \tag{8b}$$

$$\boldsymbol{u}^{'}(s,t) = -K^{-1}\Big[[\mathrm{u}(s,t)]_\times K\boldsymbol{u}(s,t) + [\boldsymbol{e}_3]_\times \mathrm{R}^T(s,t)\big(\boldsymbol{F}(t) + (l-s)f\big)\Big], \tag{8c}$$

$$\ell_i^{'}(s,t) = \|\boldsymbol{e}_3 + [\mathrm{u}(s,t)]_\times \boldsymbol{d}_i\|,\ i = 1, 2, 3, \tag{8d}$$

with the following boundary conditions

$$\boldsymbol{r}(0,t) = [0\ 0\ 0]^T, \tag{9a}$$

$$\mathrm{R}(0,t) = \mathrm{I}, \tag{9b}$$

$$u_z(0,t) = 0, \tag{9c}$$

$$\ell_i(0,t) = 0, \tag{9d}$$

$$\ell_i(l,t) = L_i(t),\ i = 1, 2. \tag{9e}$$

The model defined by (8) and (9) accepts the overall length of the first two rods $L_i,\ i = 1, 2$ as inputs and predicts the robot curvature $\boldsymbol{u}(s,t)$, position $\boldsymbol{r}(s,t)$, and length of the third rod $\ell_3(t)$. We note that the length of the third rod is always defined by the length of the first and second rod.

Additionally, (8) and (9) form a boundary value problem. In the absence of external torques, the initial curvature of the robot along z direction is zero (9c). However, the initial curvatures along x and y directions [i.e., $u_x(0,t)$ and $u_y(0,t)$] are unknown. In addition, the first and second rods' arc length $\ell_i(s,t),\ i = 1, 2$ are defined both at the base ($s = 0$) and the tip of the robot ($s = l$) by (9d, 9e).

Moreover, the model given in (8) is quasi-static and solved using the separation of variables. To solve the equations, it is assumed that at a given time, time-dependent variables are constant and the equations are solved in spatial domain (with respect to s) using standard methods such as the Runge-Kutta or Adams-Bashforth families of algorithms. Shooting methods can be used to solve the boundary value problem. A shooting method consists of using a nonlinear root-finding algorithm to iteratively converge on values for $u_x(0,t)$ and $u_y(0,t)$, in order to satisfy (9e). Next, the time-dependent variables are updated [i.e., $L_i(t)$], and the equations are solved again in the spatial domain.

2.3. Multi-Segment Robot

Here, we generalise the model given in (8) for a multi-backbone robot with multiple bending segments shown in **Figure 4**. It is assumed that the robot is composed of n segments with lengths of $l_j,\ j = 1, .., n$. Each segment is actuated via 3 parallel rods fixed at the end the segment. Thus, there are n rods and the jth segment contains $3 \times (n + 1 - j)$ rods.

To model the robot, we start from the 1st segment containing $n \times 3$ rods and use (8) to estimate the curvature, position of the main backbone, and the lengths of the cables up to the next segment. Next, at the junction where the segment ends (shown with dashed lines in **Figure 4**) we enforce the appropriate boundary conditions. The boundary conditions to be enforced across each transition point between sections are as follows: (1) The position and orientation of each tube must be continuous across the boundary, i.e.,

$$\boldsymbol{r}(s^-,t) = \boldsymbol{r}(s^+,t),\ \ \mathrm{R}(s^-,t) = \mathrm{R}(s^+,t), \tag{10}$$

(2) considering the static equilibrium and the fact that the rods apply no torque around z direction:

$$u_z(s^-,t) = u_z(s^+,t), \tag{11}$$

(3) at the distal end of each segment, we have a boundary condition for the length of the rods that end:

$$\ell_j(s,t) = L_j(t). \tag{12}$$

We repeat this process for the rest of the segments. We note that the curvatures along x and y at each break point are unknown. A shooting method must be used to iteratively converge on values for $\{u_x(0,t),\ u_y(0,t),\ u_x(l_1,t),\ u_y(l_1,t),..., u_x(\Sigma_{j=1}^n l_j, t),\ u_y(\Sigma_{j=1}^n l_j, t)\}$, in order to acquire the desired length for the rods. Solving the BVP numerically is computationally intensive. The computational cost of the model is a significant obstacle in deployment of such designs and more efficient numerical methods are needed. To this end, we study the design of a novel observer that can rapidly estimate the solution of robot's model without the need to solve the BVP.

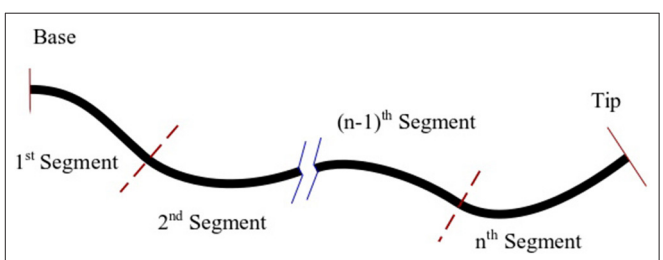

FIGURE 4 | A schematic of multi-backbone robot with multiple bending segments, dashed lines denote break points.

2.4. Rapid Solution of the Robot's Model

Our main goal in this section is to design an observer that employs measurements of $\ell_i(l,t)$ through time to estimate correct value of $u_y(0,t)$ and $u_x(0,t)$ and ensures the boundary conditions in (9) are satisfied without the need to solve the BVP iteratively. First, we transform the model in (8) into an observable form that simplifies the design of the observer. Next, we design an observer rule that guarantees exponential convergence of the solution of the observable model to the solution of the robot model given in by (8) and (9).

We define the vector of missing initial values as

$$\check{\boldsymbol{u}}(0,t) = [u_y(0,t),\ u_x(0,t)]^T. \tag{13}$$

To realise the effect of the missing initial value [i.e., $\check{\boldsymbol{u}}(0,t)$] on the solution of the equations, we define four auxiliary variables, namely,

$$\mathcal{A}_i(s,t) := \frac{\partial \ell_i(s,t)}{\partial \check{\boldsymbol{u}}(0,t)}, i = 1,2,3 \tag{14a}$$

$$\mathcal{B}(s,t) := \frac{\partial \boldsymbol{u}(s,t)}{\partial \check{\boldsymbol{u}}(0,t)}, \tag{14b}$$

$$\mathcal{C}(s,t) := \frac{\partial\big[\mathrm{R}^T(s,t)\big(\boldsymbol{F}(t) + (l-s)f\big)\big]}{\partial \check{\boldsymbol{u}}(0,t)}, \tag{14c}$$

$$\mathcal{D}(s,t) := \frac{\partial\big(\mathrm{R}^T(s,t)\boldsymbol{f}\big)}{\partial \check{\boldsymbol{u}}(0,t)}. \tag{14d}$$

Using the new variables defined by (14), one can derive the following generalised model of the multi-backbone robot (see the Appendix for derivation)

$$\boldsymbol{r}'(s,t) = \mathrm{R}(s,t)\boldsymbol{e}_3, \tag{15a}$$

$$\mathrm{R}'(s,t) = \mathrm{R}(s,t)[\mathrm{u}(s,t)]_\times, \tag{15b}$$

$$\boldsymbol{u}'(s,t) = -K^{-1}\Big[[\mathrm{u}(s,t)]_\times K\boldsymbol{u}(s,t) + [\boldsymbol{e}_3]_\times \mathrm{R}^T(s,t)\big(\boldsymbol{F}(t) + (l-s)f\big)\Big], \tag{15c}$$

$$\ell_i'(s,t) = \|\boldsymbol{e}_3 + [\mathrm{u}(s,t)]_\times \boldsymbol{d}_i\|,\ i = 1,2,3, \tag{15d}$$

$$\mathcal{A}_i'(s,t) = \frac{-(\boldsymbol{e}_3 + [\mathrm{u}(s,t)]_\times \boldsymbol{d}_i)^T[\boldsymbol{d}_i]_\times}{\|\boldsymbol{e}_3 + [\mathrm{u}(s,t)]_\times \boldsymbol{d}_i\|}\mathcal{B}(s,t),\ i = 1,2,3, \tag{15e}$$

$$\mathcal{B}'(s,t) = \mathrm{K}^{-1}\Big[[\mathrm{K}\boldsymbol{u}(s,t)]_\times \mathcal{B}(s,t) - [\boldsymbol{u}(s,t)]_\times \mathrm{K}\mathcal{B}(s,t) - [\boldsymbol{e}_3]_\times \mathcal{C}(s,t)\Big], \tag{15f}$$

$$\mathcal{C}'(s,t) = [\mathrm{R}^T(s,t)(\boldsymbol{F}(t) + (l-s)f)]_\times \mathcal{B}(s,t) - [\boldsymbol{u}(s,t)]_\times \mathcal{C}(s,t) - \mathcal{D}(s,t), \tag{15g}$$

$$\mathcal{D}'(s,t) = [\mathrm{R}^T(s,t)\boldsymbol{f}]_\times \mathcal{B}(s,t) - [\boldsymbol{u}(s,t)]_\times \mathcal{D}(s,t). \tag{15h}$$

Now, we provide a set of initial conditions for (15) that ensures the solution of the observer model in (15) exponentially converges to the solution of the boundary value problem defined by (8) and (9).

$$\boldsymbol{r}(0,t) = [0\ 0\ 0]^T, \tag{16a}$$

$$\mathrm{R}(0,t) = \mathrm{I}, \tag{16b}$$

$$u_z(0,t) = 0, \tag{16c}$$

$$\begin{bmatrix} u_x(0,t) \\ u_y(0,t) \end{bmatrix} = -\int_0^t \begin{bmatrix} \mathcal{A}_1^T(l,t) \\ \mathcal{A}_2^T(l,t) \end{bmatrix}^\dagger \mathrm{P} \begin{bmatrix} \ell_1(l,t) - L_1(t) \\ \ell_2(l,t) - L_2(t) \end{bmatrix} \mathrm{d}t, \tag{16d}$$

$$\ell_i(0,t) = 0, \tag{16e}$$

$$\mathcal{A}_i(0,t) = \boldsymbol{0},\ i = 1,2, \tag{16f}$$

$$\mathcal{B}(0,t) = [1\ 0\ 0;\ 0\ 1\ 0], \tag{16g}$$

$$\mathcal{C}(0,t) = 0, \tag{16h}$$

$$\mathcal{D}(0,t) = 0, \tag{16i}$$

where P is a symmetric positive definite matrix and † denotes the pseudo-inverse operator. We note that (16f-16i) are calculated based on the definition of the auxiliary variables in (14). (16d) is the main observer rule that guarantees the convergence of the observer (see the Appendix).

The observer given in (15) is quasi-static, similar to the robot's model in (8). However, instead of using an iterative BVP solver, it can be solved as an initial value problem using the initial values given in (16). At a given time t, time-dependent variables are assumed constant and the equations are solved in spatial domain. Next, the time-dependent variables are updated [i.e., $L_i(t)$, $u_x(0,t)$, $u_y(0,t)$]. The updated time-dependant variables are used to solve the equations in the spatial domain again. The observer can be generalised to a multi-segment robot following the approach discussed in section 2.3.

In the next section, series of simulation and experiments are performed to evaluate the model's accuracy and demonstrate the computational efficiency of the observer in comparison with common BVP numerical solvers.

3. RESULTS

Simulations and experiments are performed to evaluate the proposed design and modelling theory. The bronchoscopic robot used in the simulations and experiments consists of two bendable segments, shown in **Figure 2**. The length of the first segment is 500 mm, and the length of the second segment (at the tip) is 40 mm. The outer diameter of the robot is 4.5 mm and the inner diameter of the robot is 2 mm. Twenty-seven circular fixtures each weighting 5 g were equally spaced along the length of the bronchoscope and were rigidly fixed to the main backbone shown in blue in **Figure 2**.

We performed experiments to identify the developed model parameters and validate the model. First we performed experiments to identify the model parameters. For the identification phase, each rod was commanded to either push or pull the end disks by 5 mm, making the robot to randomly bend to 12 different positions. We estimated the 3D shape of the robot using calibrated stereo rig comprising two Logitech HD Pro C922 webcams. The cameras were running at

1,080p resolution. As identified through calibration using on average 30 views of a checkerboard, a single pixel corresponded to 0.25 × 0.25 mm on the image plane. Following calibration, the entry point of the robot, i.e., $s = 0$ was estimated in 3D space via triangulation. The robot coordinate frame was aligned to a planar calibration target always visible by the cameras during the experiments.

Furthermore, manual backbone segmentation established the base and shape of the bronchoscope relative to the aligned calibration grid. Matching backbone points were selected in both images, and then triangulated to provide the 3D point cloud. This process is shown in **Figure 5**. The mean error of the 3D triangulation algorithm was equal to 6 pixels corresponding to 1.5 mm. The extracted 3D backbones were used to identify for the robot model parameters, namely, Young's modulus, E and shear moduli G of the robot and initial displacement of the rods, $\delta\ell_i$, $i = 1, ..., 6$. The parameters were identified by fitting the kinematic model given in (8) to the shape of the robot estimated via the cameras at 12 different configurations. The identified parameters of the model and the known parameters of the model are given in **Table 1**.

In the next step, to validate the model accuracy we commanded the robot to move to 20 different positions. The shape of the robot was estimated using the calibrated cameras and was compared to the shape of the robot predicted by the identified model. **Figure 6** shows representative results. Results of the measurements including maximum, mean, and standard deviation of error of the model in predicting the robot tip position and the root-mean-squared error of the model in predicting robot shape are listed in **Table 2**. The root-mean-squared error is calculated as

$$\text{RMSE} = \sqrt{\frac{\sum_{j=1}^{m}(\|\hat{\boldsymbol{r}} - \boldsymbol{r}\|_j)^2}{m}}, \tag{17}$$

TABLE 1 | Physical parameters of the robot.

Known		Identified	
l_1	40 mm	E	92.13e9 GPa
l_2	500 mm	G	31e9 GPa
f	$[0.25, 0, 0]^T$ N	$\delta\ell_1$	6.03×10^{-14} m^4
α_1	15°	$\delta\ell_2$	0.23 mm
α_2	30°	$\delta\ell_3$	1.2 mm
δ	1.7 mm	$\delta\ell_4$	0 mm
I	2.13×10^{-12} m^4	$\delta\ell_5$	0 mm
J	2.72×10^{-12} m^4	$\delta\ell_6$	0.7 mm

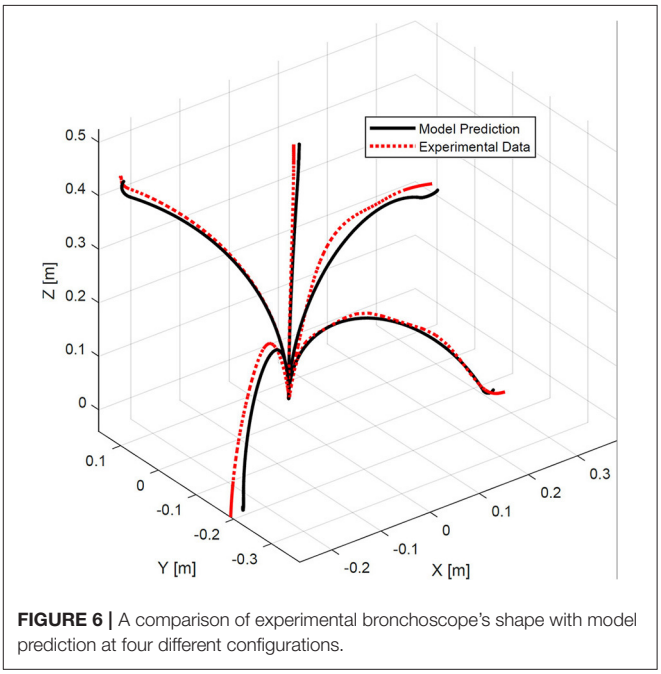

FIGURE 6 | A comparison of experimental bronchoscope's shape with model prediction at four different configurations.

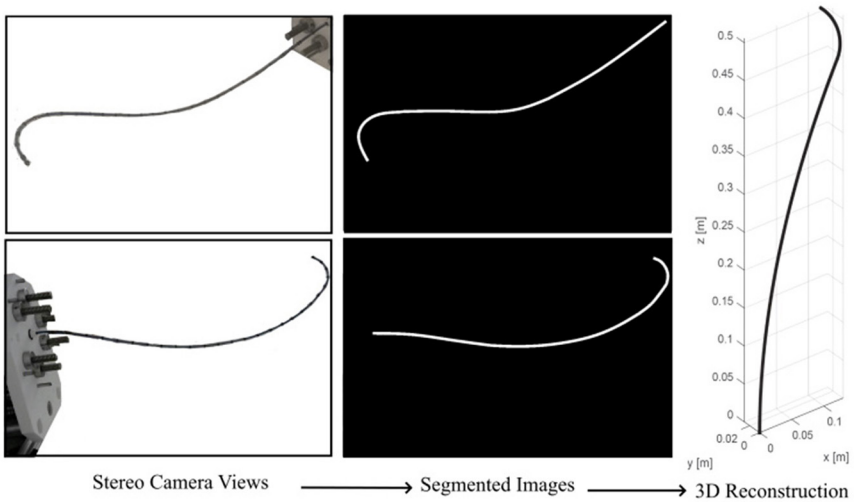

FIGURE 5 | Estimating robot's backbone shape using two calibrated cameras.

TABLE 2 | Experimental results.

e_{max} [mm]	e_{mean} [mm]	σ [mm]	RMSE [mm]
26.2	17.6	10.9	10.3

Maximum error of tip position (e_{max}), mean error of tip position (e_{mean}), standard deviation of error (σ), and root mean squared error (RMSE) are reported.

and is used as a measure of the differences between the actual shape of the robot, $\hat{\boldsymbol{r}}$, and the model predicted shape, i.e., $\boldsymbol{r}$, for $m = 30$ data points along the robot backbone.

In the experiments, the robot tip was capable of bending up to 100° with respect to its backbone (see **Figure 6**). The maximum error of the model in estimating the position of the robot tip is 26.2 mm, corresponding to 1.9% of the robot's length.

Finally, we performed simulations to compare the computational efficiency of the observer with various shooting methods used to solve BVPs. Shooting methods consists of using a nonlinear root-finding algorithm to iteratively converge on values for $u_x(0,t)$ and $u_y(0,t)$ for each segment, in order to satisfy the boundary conditions (9), i.e.,

$$\text{Minimize: } Error := \left\| \begin{bmatrix} \ell_1(l_1,t) - L_1(t) \\ \ell_2(l_1,t) - L_2(t) \\ \ell_4(l_1+l_2,t) - L_4(t) \\ \ell_5(l_1+l_2,t) - L_5(t) \end{bmatrix} \right\|, \qquad (18)$$

$$\text{w.r.t.} : u_x(0,t), u_y(0,t), u_x(l_1,t), u_y(l_1,t).$$

We compared the observer predictions with shooting method algorithms that employ three different root-finding algorithms, which to the best of authors knowledge, are the most commonly used BVP solvers. These solvers are:

1. Interior-point method (Byrd et al., 2000),
2. Quasi-Newton method with BFGS Hessian estimation (Curtis and Que, 2015),
3. Nelder-Mead method (Powell, 1973).

In the simulations, we pulled and pushed the cables from −5 to 5 mm at a frequency of $2\pi/10$ Hz. The simulation runs for 10 seconds at sampling frequency of 50 Hz. The observer gain P used in the simulations was set to $70 \times$ I, as this value was found to achieve the minimum prediction error. The optimally tolerance for all the algorithms were set to 10^{-6}. The simulations are performed in Matlab on an Intel Core i7 (2.93 GHz) machine with 16 GB memory.

Figure 7 shows the robot's trajectory estimated via different methods. The observer and the Nelder-Mead method gave the best accuracy. The other two methods, namely, interior-point and quasi-Newton, gave substantial error at two points across the robot trajectory. Also, it can be seen that the observer has an error at the first sampling time but rapidly converges to the correct solution.

Figure 8 shows the error of the solvers and the observer in satisfying the boundary conditions given in (18). The observer error is the same order as the BVP solvers. The BVP solvers occasionally fail in minimizing the error, while the observer

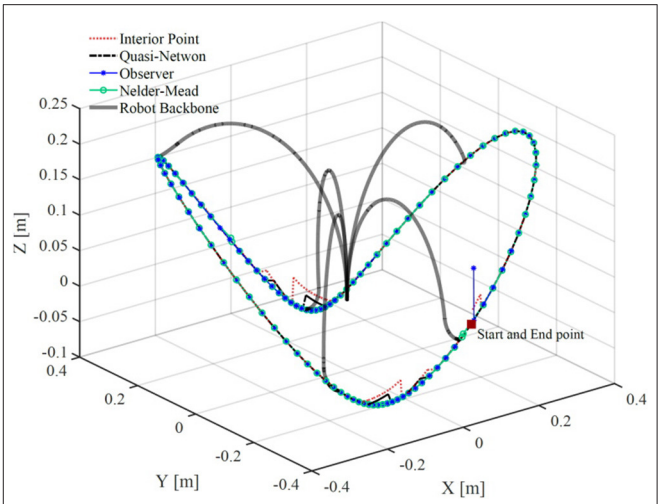

FIGURE 7 | A comparison of bronchoscope's tip trajectory calculated by solving the robot's model using four different methods. The bronchoscope's backbone is shown at several configurations along the trajectory.

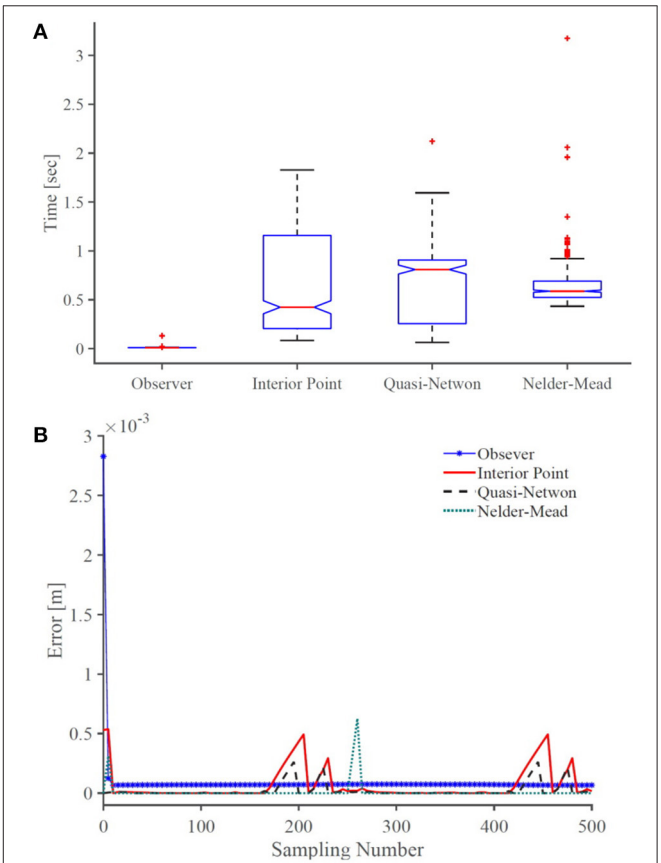

FIGURE 8 | A comparison of **(A)** accuracy and **(B)** computational efficiency of the observer with common BVP solvers. On each box in **(B)**, the central mark indicates the median, and the bottom and top edges of the box indicate the 25th and 75th percentiles, respectively. The whiskers extend to the most extreme data points and the outliers are plotted individually using plus symbol.

TABLE 3 | Experimental results.

	Observer	Interior-point	Quasi-Newton	Nelder-Mead
e_{mean} [mm]	8.05×10^{-5}	7.28×10^{-5}	2.53×10^{-5}	9.52×10^{-5}
σ_e [mm]	1.35×10^{-4}	1.39×10^{-4}	6.14×10^{-5}	6.04×10^{-5}
t_{mean} [sec]	0.011	0.52	0.62	0.64
σ_t [sec]	0.006	0.45	0.36	0.19

Mean error (e_{mean}), standard deviation of error (σ_e), average time to estimate the solution of the model (t_{mean}) for each method, and standard deviation of time σ_t are reported.

consistently maintains an error below 10^{-4} mm. **Figure 8** compares the computational efficiency of the BVP solvers and the observer in terms of the time that each method takes to compute the solution of the model at each sampling time. Evidently, the observer is much faster than the BVP solvers and has lower standard deviation. The average time that the observer takes to estimate the model's solution is 0.0108 s, which is significantly faster than other solvers. We performed 10 more simulations, where, the robots rods are pulled/pushed at frequencies between $\pi/5$ Hz and $\pi/50$. The results are summarised in **Table 3**. The results demonstrate that the observer maintain similar error as the BVP solvers, while exhibiting superior computational efficiency. The average time that the observer takes to estimate the model's solution is 47 times faster than the fastest BVP solver, namely, the interior-point method.

4. DISCUSSION

In this paper, we presented the concept for and the design of a continuum robot for pulmonary endoscopy in MV patients. MV patients are at high risk of developing secondary infections and there is a need for a reliable and controlled sampling of the distal lung to guide therapeutic interventions. Current methods for diagnosis of diseases in the distal lung in MV patients are not standardised, lack reproducibility and require expert operators. Here, we proposed a novel robotic bronchoscope that can be used to democratise lung sampling and improve the accuracy and reliability of distal lung sampling in MV patients. The proposed design of the system considers the limitations and constraints of current bronchoscopy, i.e., limited dexterity, low repeatability, and relatively large size of the bronchoscope.

One of the main challenges in current bronchoscopy is navigating the tightly curved architecture of bronchial tree. Several studies (Coppola et al., 1998; Ulusoy et al., 2016) have reported that bifurcation angles of the bronchial tree including sub-carinal angles and inter-bronchial angles vary between 30 and 100°. The experimentally measured maximum bending angle of the proposed robotic bronchoscope is 100° with respect to the robot's main backbone, which enables the robot to traverse the tightly curved structure of airways. We note that the maximum bending angle and curvature of the robot is a function of the robot's interaction with the environment. In the future, we will study the bending capability of the robot in lung models to fully verify the effectiveness of the robot in navigating the bronchial tree.

The external diameter of traditional bronchoscopes is generally 5–6 mm with a working channel with inner diameter of 2 mm (Vachani and Sterman, 2008). The developed prototype is comparable with current technology and has an outer diameter of 4.5 mm with a working channel with inner diameter of 2 mm. Moreover, the bronchoscope is highly dexterous and possesses 7 DoFs in total. The continuum manipulator is able to bend in 3D at 2 different points along its backbone thanks to 6 push/ pull NiTi rods. The extra dexterity offered by the proposed design can potentially extend the reach of the clinical bronchoscopy.

One of the aims of this research is to democratise bronchoscopy in MV patients in the ICU via automating the procedure. To this end, we have proposed a new theoretical framework to model the robot that can be used in closed-loop control of the bronchoscope motion. Our novel mechanics-based model of the robotic bronchoscope can predict the shape of the robotic bronchoscope under external forces with an accuracy corresponding to 1.9% of its arc-length. We note that for long, slender continuum robots, tip error is highly dependent on the total arc length (Rucker et al., 2010) and robot's backbone's interaction with its surrounding environment. We note that this error can be further reduced via closed-loop control of the robot tip. A closed-loop controller can employ sensory feedback from the robot tip position to minimise the bronchoscope error in navigating the lung. In practice, electromagnetic trackers are placed at the tip of the bronchoscope to measure its tip position in real-time. The proposed design offers a 2 mm working channel that can be used to place such trackers, allowing real-time monitoring of robot position for closed-loop control.

Furthermore, we have demonstrated that our numerical framework can estimate the model's solution 47 times faster than the fastest existing solvers, enabling applications in real-time robotic control. Future work will focus on developing a closed-loop control strategy that uses the model and the feedback of the robot tip position acquired with electromagnetic trackers, to minimise the error of the robot tip in following a desired trajectory for sampling.

DATA AVAILABILITY STATEMENT

The original contributions presented in the study are included in the article/supplementary material, further inquiries can be directed to the corresponding author/s.

AUTHOR CONTRIBUTIONS

MK conceived the study. ZM contributed to modelling and design of the robot. BT contributed to the experimental study. All authors contributed to manuscript writing, revision, and read and approved the submitted version.

FUNDING

This work was supported by the Medical Research Council [grants MR/T023252/1, and 8532390].

REFERENCES

Antman, S. (2005). *Nonlinear Problems of Elasticity, 2nd Edn*. Dordrecht: Springer.

Bajo, A., and Simaan, N. (2016). Hybrid motion/force control of multi-backbone continuum robots. *Int. J. Robot. Res.* 35, 422–434. doi: 10.1177/0278364915584806

Bryson, C. E., and Rucker, D. C. (2014). "Toward parallel continuum manipulators," in *IEEE International Conference on Robotics and Automation* (Hong Kong), 5264–5267. doi: 10.1109/ICRA.2014.6906943

Burgner-Kahrs, J., Rucker, D. C., and Choset, H. (2015). Continuum robots for medical applications: a survey. *IEEE Trans. Robot*. 31, 1261–1280. doi: 10.1109/TRO.2015.2489500

Byrd, R. H., Gilbert, J. C., and Nocedal, J. (2000). A trust region method based on interior point techniques for nonlinear programming. *Math. Prog.* 89, 149–185. doi: 10.1007/PL00011391

Coppola, V., Vallone, G., Coscioni, E., Coppola, M., Maraziti, G., Alfinito, M., et al. (1998). Normal value of the tracheal bifurcation angle and correlation with left atrial volume. *La Radiol. Med*. 95, 461–465.

Curtis, F. E., and Que, X. (2015). A quasi-Newton algorithm for nonconvex, nonsmooth optimization with global convergence guarantees. *Math. Prog. Comput*. 7, 399–428. doi: 10.1007/s12532-015-0086-2

Del Giudice, G., Wang, L., Shen, J., Joos, K., and Simaan, N. (2017). "Continuum robots for multi-scale motion: micro-scale motion through equilibrium modulation," in *IEEE/RSJ International Conference on Intelligent Robots and Systems* (Vancouver, BC), 2537–2542. doi: 10.1109/IROS.2017.8206074

Ding, J., Goldman, R. E., Xu, K., Allen, P. K., Fowler, D. L., and Simaan, N. (2013). Design and coordination kinematics of an insertable robotic effectors platform for single-port access surgery. *IEEE/ASME Trans. Mechatron.* 18, 1612–1624. doi: 10.1109/TMECH.2012.2209671

Fagogenis G, Mencattelli M, Machaidze Z, Rosa B, Price K, Wu F, et al. Autonomous robotic intracardiac catheter navigation using haptic vision. *Sci. Robot*. (2019) 4:eaaw1977. doi: 10.1126/scirobotics.aaw1977

Garbin, N., Wang, L., Chandler, J. H., Obstein, K. L., Simaan, N., and Valdastri, P. (2019). Dual-continuum design approach for intuitive and low-cost upper gastrointestinal endoscopy. *IEEE Trans. Biomed. Eng.* 66, 1963–1974. doi: 10.1109/TBME.2018.2881717

Gravagne, I. A., and Walker, I. D. (2000). "Kinematic transformations for remotely-actuated planar continuum robots," in *Proceedings 2000 ICRA, Millennium Conference, IEEE International Conference on Robotics and Automation, Symposia Proceedings (Cat. No.00CH37065), Vol. 1* (San Francisco, CA), 19–26. doi: 10.1109/ROBOT.2000.844034

Kaouk, J. H., Haber, G.-P., Autorino, R., Crouzet, S., Ouzzane, A., Flamand, V., et al. (2014). A novel robotic system for single-port urologic surgery: first clinical investigation. *Eur. Urol.* 66, 1033–1043. doi: 10.1016/j.eururo.2014.06.039

Mattei, T. A., Rodriguez, A. H., Sambhara, D., and Mendel, E. (2014). Current state-of-the-art and future perspectives of robotic technology in neurosurgery. *Neurosurg. Rev*. 37, 357–366; discussion: 366. doi: 10.1007/s10143-014-0540-z

Mitros, Z., Sadati, S., Seneci, C., Bloch, E., Leibrandt, K., Khadem, M., Cruz, L., et al. (2020). Optic nerve sheath fenestration with a multi-arm continuum robot. *IEEE Robot. Autom. Lett*. 5, 4874–4881. doi: 10.1109/LRA.2020.3005129

Powell, M. J. D. (1973). On search directions for minimization algorithms. *Math. Prog*. 4, 193–201. doi: 10.1007/BF01584660

Riojas, K. E., Anderson, P. L., Lathrop, R. A., Herrell, S. D., Rucker, D. C., and Webster, R. J. (2019). A hand-held non-robotic surgical tool with a wrist and an elbow. *IEEE Trans. Biomed. Eng.* 66, 3176–3184. doi: 10.1109/TBME.2019.2901751

Rucker, D. C., Jones, B. A., and Webster III, R. J. (2010). A geometrically exact model for externally loaded concentric-tube continuum robots. *IEEE Trans. Robot*. 26, 769–780. doi: 10.1109/TRO.2010.2062570

Simaan, N., Taylor, R., and Flint, P. (2004). "A dexterous system for laryngeal surgery," in *IEEE International Conference on Robotics and Automation, Vol. 1* (New Orleans, LA), 351–357. doi: 10.1109/ROBOT.2004.1307175

Ulusoy, M., Uysal, I. I., Kıvrak, A. S., Ozbek, S., Karabulut, A. K., Paksoy, Y., et al. (2016). Age and gender related changes in bronchial tree: a morphometric study with multidedector CT. *Eur. Rev. Med. Pharmacol*. Sci. 20, 3351–3357.

Vachani, A., and Sterman, D. H. (2008). "Chapter 12 – bronchoscopy," in *Clinical Respiratory Medicine, 3rd Edn*, eds R. K. Albert, S. G. Spiro, and J. R. Jett (Mosby, PA: Elsevier), 177–196. doi: 10.1016/B978-032304825-5.10012-1

Wang, J., Ha, J., and Dupont, P. E. (2019). "Steering a multi-armed robotic sheath using eccentric precurved tubes," in *2019 International Conference on Robotics and Automation (ICRA)* (Montreal, QC), 9834–9840. doi: 10.1109/ICRA.2019.8794245

Webster, R. J. III, and Jones, B. A. (2010). Design and kinematic modeling of constant curvature continuum robots: a review. *Int. J. Robot. Res.* 29, 1661–1683. doi: 10.1177/0278364910368147

Wu, Z., Li, Q., Zhao, J., Gao, J., and Xu, K. (2019). Design of a modular continuum-articulated laparoscopic robotic tool with decoupled kinematics. *IEEE Robot. Autom. Lett*. 4, 3545–3552. doi: 10.1109/LRA.2019.2927929

Xu, K., Zhao, J., and Fu, M. (2015). Development of the sjtu unfoldable robotic system (surs) for single port laparoscopy. *IEEE/ASME Trans. Mechatron*. 20, 2133–2145. doi: 10.1109/TMECH.2014.2364625

Conflict of Interest: The authors declare that the research was conducted in the absence of any commercial or financial relationships that could be construed as a potential conflict of interest.

A. NOMENCLATURE

t	Time.
s	Arc length.
$\dot{}$	Derivative with respect to time.
$'$	Derivative with respect to s.
$[\,]_\times$	Converts $\mathbb{R}^3$ in $so(3)$.
n	Number of bendable segments.
i	Number of rods in each segments.
$\boldsymbol{d}_i$	Position of rods with respect to the main backbone.
δ	Rods' distance from the robots centroid.
α_n	Angular position of 1st rod of n^{th} segment with respect to the main backbone.
β_i	Angular position of i^{th} rod with respect to the main backbone.
l	Overall length of the robot.
l_n	length of the n^{th} segment.
ℓ_i	Model predicted length of the i^{th} rod.
$\boldsymbol{r}(s,t)$	Position vector of the main backbone in the global reference frame.
$\boldsymbol{r}_i(s,t)$	Position vector of the i^{th} rod in the global reference frame.
$\mathrm{R}(s,t)$	Orientation matrix.
$\boldsymbol{u}(s,t)$	Vector of backbone curvatures.
$u_x(s,t)$	Curvature around x axis.
$u_y(s,t)$	Curvature around y axis.
$u_z(s,t)$	Curvature around z axis.
K	Stiffness matrix.
E	Young's modulus.
I	Second moment of inertia.
G	Shear modulus.
J	Polar moment of inertia.
$\boldsymbol{F}(t)$	External point force.
$\boldsymbol{f}$	External distributed force.
$\boldsymbol{e}_3$	Unit vector aligned with the z-axis of the global coordinate frame.
I	Identity matrix .
0	Zero matrix.
P	Observer gain.
$\mathcal{A}(s,t), \mathcal{B}(s,t), \mathcal{C}(s,t), \mathcal{D}(s,t)$	Auxiliary variables defined in (14).

APPENDIX

Derivation of Auxiliary Variables

Here, we derive the differential equations governing the evolution of auxiliary variables given in (14), beginning with (14a).

Using (8d) and the chain rule of differentiation we have

$$\mathcal{A}_i'(s,t) = \frac{\partial}{\check{\boldsymbol{u}}(0,t)}\left[(\boldsymbol{e}_3 + [\mathrm{u}(s,t)]_\times \boldsymbol{d}_i)^T(\boldsymbol{e}_3 + [\mathrm{u}(s,t)]_\times \boldsymbol{d}_i)\right]^{1/2} = \frac{-(\boldsymbol{e}_3 + [\mathrm{u}(s,t)]_\times \boldsymbol{d}_i)^T[\boldsymbol{d}_i]_\times}{\|\boldsymbol{e}_3 + [\mathrm{u}(s,t)]_\times \boldsymbol{d}_i\|}\mathcal{B}(s,t)$$

In deriving (15) we used the following identity

$$\frac{\partial([\boldsymbol{a}]_\times \boldsymbol{b})}{\partial \boldsymbol{c}} = -[\boldsymbol{b}]_\times \frac{\partial \boldsymbol{a}}{\partial \boldsymbol{c}} + [\boldsymbol{a}]_\times \frac{\partial \boldsymbol{b}}{\partial \boldsymbol{c}}.$$

We now use (8c) to derive the equations for calculating $\mathcal{B}(s,t)$.

$$\mathcal{B}'(s,t) = \frac{\partial \boldsymbol{u}'(s,t)}{\check{\boldsymbol{u}}(0,t)} = \mathrm{K}^{-1}\Big[[\mathrm{K}\boldsymbol{u}(s,t)]_\times \mathcal{B}(s,t) - [\boldsymbol{u}(s,t)]_\times \mathrm{K}\mathcal{B}(s,t) - [\boldsymbol{e}_3]_\times \mathcal{C}(s,t)\Big]$$

Furthermore, $\mathcal{C}(s,t)$ can be computed by taking the transpose of (8b), multiplying both sides by $\boldsymbol{F}(t) + (l-s)f$, subtracting $\mathrm{R}^T(s,t)\boldsymbol{f}$, and finally taking partial derivative of both sides with respect to $\check{\boldsymbol{u}}(0,t)$.

$$\mathcal{C}'(s,t) = [\mathrm{R}^T(s,t)(\boldsymbol{F}(t) + (l-s)f)]_\times \mathcal{B}(s,t) - [\boldsymbol{u}(s,t)]_\times \mathcal{C}(s,t) - \mathcal{D}(s,t).$$

We can calculate $\mathcal{D}(s,t)$ in a similar way. First, we take the transpose of (8b). Next, we multiply both sides by $\boldsymbol{f}$. Finally, taking partial derivative of both sides with respect to $\check{\boldsymbol{u}}(0,t)$ gives

$$\mathcal{D}'(s,t) = [\mathrm{R}^T(s,t)\boldsymbol{f}]_\times \mathcal{B}(s,t) - [\boldsymbol{u}(s,t)]_\times \mathcal{D}(s,t).$$

Proof of Convergence and Stability

The error of the observer in satisfying the robot's model's boundary condition in (9) (i.e., robot's rods' lengths) is

$$\boldsymbol{\epsilon}(t) = \begin{bmatrix}\ell_1(l,t)\\ \ell_2(l,t)\end{bmatrix} - \begin{bmatrix}L_1(t)\\ L_2(t).\end{bmatrix}$$

To prove that this error exponentially converges to zero, we select the following Lyapunov candidate

$$V = \frac{1}{2}\boldsymbol{\epsilon}^T\boldsymbol{\epsilon}. \tag{A1}$$

Taking the time derivative of V and replacing $\dot{\boldsymbol{\epsilon}}$ using (14a) we obtain

$$\dot{V} = \epsilon^T\dot{\epsilon} = \boldsymbol{\epsilon}^T\begin{bmatrix}\mathcal{A}_1^T(l,t)\\ \mathcal{A}_2^T(l,t)\end{bmatrix}\dot{\check{u}}(0,t).$$

Substituting $\dot{\check{u}}(0,t)$ using (16d) gives

$$\dot{V} = -\boldsymbol{\epsilon}^T\begin{bmatrix}\mathcal{A}_1^T(l,t)\\ \mathcal{A}_2^T(l,t)\end{bmatrix}\begin{bmatrix}\mathcal{A}_1^T(l,t)\\ \mathcal{A}_2^T(l,t)\end{bmatrix}^\dagger \mathrm{P}\boldsymbol{\epsilon} = -\boldsymbol{\epsilon}^T\mathrm{P}\boldsymbol{\epsilon}$$

In deriving the above equation we used the following identity

$$\mathrm{aa}^\dagger = \mathrm{aa}^T(\mathrm{aa}^T)^{-1} = \mathrm{I}.$$

P is symmetric positive definite. Thus, $\forall t > 0$, $\dot{V}$ is negative definite. Therefore, as $t \to \infty$, $\dot{\boldsymbol{\epsilon}}(t) \to 0$. Consequently, the solution of the observer converges to the solution of the model given in (8).

frontiers in Robotics and AI

ORIGINAL RESEARCH
published: 05 May 2021
doi: 10.3389/frobt.2021.612740

RoboEthics in COVID-19: A Case Study in Dentistry

Yaser Maddahi[1], *Maryam Kalvandi*[2], *Sofya Langman*[3,4], *Nicole Capicotto*[5] *and Kourosh Zareinia*[6]*

[1]Department of Research and Development, Tactile Robotics, Winnipeg, MB, Canada, [2]Manitoba Dental Association, Winnipeg, MB, Canada, [3]Department of Pathology and Laboratory Medicine, Faculty of Medicine, University of British Columbia, Vancouver, BC, Canada, [4]Department of Molecular Oncology, British Columbia Cancer Research Centre, Vancouver, BC, Canada, [5]Department of Biomedical Engineering, Faculty of Engineering and Architectural Science, Ryerson University, Toronto, ON, Canada, [6]Department of Mechanical and Industrial Engineering, Faculty of Engineering and Architectural Science, Ryerson University, Toronto, ON, Canada

The COVID-19 pandemic has caused dramatic effects on the healthcare system, businesses, and education. In many countries, businesses were shut down, universities and schools had to cancel in-person classes, and many workers had to work remotely and socially distance in order to prevent the spread of the virus. These measures opened the door for technologies such as robotics and artificial intelligence to play an important role in minimizing the negative effects of such closures. There have been many efforts in the design and development of robotic systems for applications such as disinfection and eldercare. Healthcare education has seen a lot of potential in simulation robots, which offer valuable opportunities for remote learning during the pandemic. However, there are ethical considerations that need to be deliberated in the design and development of such systems. In this paper, we discuss the principles of roboethics and how these can be applied in the new era of COVID-19. We focus on identifying the most relevant ethical principles and apply them to a case study in dentistry education. DenTeach was developed as a portable device that uses sensors and computer simulation to make dental education more efficient. DenTeach makes remote instruction possible by allowing students to learn and practice dental procedures from home. We evaluate DenTeach on the principles of data, common good, and safety, and highlight the importance of roboethics in Canada. The principles identified in this paper can inform researchers and educational institutions considering implementing robots in their curriculum.

Keywords: COVID-19, roboethics, dentistry, education, DenTeach

OPEN ACCESS

Edited by:
Simon DiMaio,
Intuitive Surgical, Inc., United States

Reviewed by:
Sreekanth Kumar Mallineni,
Majmaah University, Saudi Arabia
Sivakumar Nuvvula,
Narayana Dental College and Hospital, India

***Correspondence:**
Kourosh Zareinia
Kourosh.Zareinia@Ryerson.ca

Specialty section:
This article was submitted to Biomedical Robotics, a section of the journal Frontiers in Robotics and AI

Received: *30 September 2020*
Accepted: *21 April 2021*
Published: *05 May 2021*

Citation:
Maddahi Y, Kalvandi M, Langman S, Capicotto N and Zareinia K (2021) RoboEthics in COVID-19: A Case Study in Dentistry. Front. Robot. AI 8:612740. doi: 10.3389/frobt.2021.612740

INTRODUCTION

The coronavirus disease 2019 (COVID-19) pandemic has caused disturbances in all aspects of everyday life, including healthcare, commerce, manufacturing, and education. In Canada, the response to the COVID-19 pandemic included the shut-down of businesses and the reallocation of human resources to emergency functions (Detsky and Bogoch, 2020). Additionally, many companies asked personnel to work from home if possible. In order to slow down the spread of the SARS-CoV-2 virus, human interactions have to be limited, and people were asked to wear masks, avoid touching surfaces and their faces, and wash hands as often as possible. In a world where human

interaction is minimized, robotics and artificial intelligence can be invaluable tools in rebuilding the economy and resuming the "normal" life. Since the start of the COVID-19 pandemic, robots have been used to disinfect hospital rooms (Neustaeter, 2020) and provide comfort to Alzheimer's patients (Ryan, 2020). Robots can also potentially be used to deliver packages, track inventories, stock shelves and take temperatures. As health agencies are anticipating possible third and successive waves of COVID-19, a wider distribution of robots could alleviate the pressure on essential personnel and help minimize the spread of the virus. When considering a more significant implementation of robots in human life, ethical considerations must be made to ensure that robots are used for the betterment of humanity.

Ever since automatic machines have been invented, writers and directors have been dreaming up possible scenarios for robot technology to develop. Not surprisingly, many such attempts depict the end of the human race and the rise of machines. Discussion of robots in popular culture affects the public's view of robotics. In fact, over 70% of people say that sci-fi movies have influenced their attitude toward robots (El Mesbahi, 2015). In order to prevent these grim predictions from becoming a reality, and to appease the public's fears of a possible real-life Terminator scenario, ethical aspects of robotic development have to be considered, and strict rules of conduct are to be established. The relatively new field of roboethics, formally acknowledged since 2002, inspires the design, manufacturing, and use of robots (Veruggio, 2006). Roboethics shares some of its core ideas with information technology ethics, especially concerning the safe use of technology and fair access to technological resources. Robots pose a new challenge from the regulatory standpoint: if a robot commits a crime, who is liable? Would a company that built the robot be at fault when the robot's actions are unpredictable? Or how should the law tackle establish regulations that describe criminal intent in a machine (Pagallo, 2017; Bösl and Bode, 2018)? Roboethics helps to establish a structured way of dealing with moral dilemmas arising in robotics. If certain laws and moral principles are established for robotics research, that could facilitate the integration of robots in day-to-day life.

THE LAWS OF ROBOETHICS

The earliest rules of robotics were described by Isaac Asimov in 1942, when robots were more of a fiction than reality (Asimov, 1942). These Laws, including the Zeroth law added after the first three, are presented below:

1. A robot may not injure a human being under any conditions—and, as a corollary, must not permit a human being to be injured because of inaction on [the robot's] part."
2. A robot must follow all orders given by qualified human beings as long as they do not conflict with Rule 1.
3. A robot must protect [its] own existence, as long as that does not conflict with Rules 1 and 2.
4. (Zeroth law) No robot may harm humanity or, through inaction, allow humanity to come to harm.

The above Laws are generic and do not consider the wide spectrum of robotics applications. Since 1942 the field of robotics has evolved, and some of the resulting robots do function in accordance to the Laws. For example, combat robots have become a reality: robots are used to carry loads and other logistical support (Vincent, 2015) and help in bomb disposal (US Department of Homeland Security, 2020). However, it is not difficult to imagine a future in which robots will be able to carry firearms and assist in warfare. The latter would be in clear violation of Asimov's Laws as the harm to opposing humans would be imminent. On the other hand, the side that fights using robots is able to preserve the lives of its own soldiers. The dichotomy between ethical outcomes in the above situation is further amplified by a robot's potential inability to comprehend what "existence," "harm" or "humanity" is. If the robot has no sense of self, how can it act as an ethical agent?

In addition, Asimov's Laws are robot-centric and do not consider humans who design the robots. Since Asimov, many organizations and agencies have attempted to revise the Laws of Robotics to reflect both the complexity and the developments of robotics. As such, the field of roboethics can be divided into two fields: engineering ethics and machine ethics (Dodig Crnkovic and Çürüklü, 2012). Engineering ethics produce rules and bestow responsibility for robotic creations on engineers and computer scientists. Machine ethics suggests that internal ethical principles and moral decision-making patterns should be designed into robots, making them capable of autonomous ethical decision-making.

Murphy and Woods have proposed a revision for Asimov's Laws, shifting the attention from machine ethics to human design and responsibility (Murphy and Woods, 2009).

1. Human–robot work systems must comply with rigorous professional and legal standards for safety and ethics. Without such compliance, humans cannot utilize robots in a working system.
2. Robots must respond to humans only so far as determined by each robot's role.
3. Humans must provide robots with autonomous mechanisms for self-preservation. But those mechanisms must relinquish control as needed to comply with the previous two laws.

The revised Laws are in line with engineering ethics ideas but are still too general to be easily applicable to all robots, or to be written as a part of a government or industry policies. Across the globe, institutions have used the above Laws as a starting point for the development of their own sets of ethical standards for robotics.

TYPES OF ROBOETHICAL CONSIDERATIONS

There are several categories of ethical questions that must be considered before a robot becomes available to the public. These categories are not exclusive, and as the field develops further categories may be added.

Data

Today, data is becoming one of the most valuable commodities. Robots that have a capacity to record, store, and process data are thus working with a precious resource that must be carefully managed. With data that comes from the robot's operator, privacy is the topmost concern. A user should be able to consent to their data being recorded, but safety or ownership of that data is not inherent. Would a robot store data locally or on the cloud? Does the data, once recorded, belong to the user or the robotics company? Can that company guarantee the privacy of the data recorded? Is the data safe from possible breaches, and if leaked, can that data be used in harmful ways? If the company uses recorded data to further research or make a profit, should the primary source of data be compensated? If the company was funded through tax-dollars, should the generated data be available to the public? Questions of data ownership, integrity and accessibility should be considered at the design stage to ensure that human rights are not being violated, and the work contributes to the common good.

Common Good

With robots playing an increasingly larger role in day-to-day life, engineers and computer scientists who design robots will have to consider the broader impact of their work. Many robotics guidelines, such as the ones put up by the Institute of Electrical and Electronics Engineers (IEEE) and European Commission European Group on Ethics in Science and New Technologies, include clauses on the betterment of humanity and human well-being (European Group on Ethics in Science and New Technologies, 2018; The IEEE Global Initiative, 2019). As technologies develop, organizations, countries, and humanity should consider the impact such technologies will have in the future. With billions of dollars spent on military research, is artificial intelligence (AI) arms race something that should be prohibited at early stages? Can robots support human autonomy and prosperity? Would robot-generated benefits be accessible to anyone on the planet? If robots' expanded functionality makes certain professions obsolete, should there be a contingency plan to retrain workers? One could also ask how "common" is the common good—is contributing to the collective good instead of benefiting one's own interests something that organizations or countries are capable of?

Safety

Since Asimov proposed his Laws of Robotics, safety has been one of the main concerns for robotics. Ideally, a robot should never intentionally harm a human, but with the development of autonomous machines such as self-driving cars, the field of robotics has encountered the trolley problem[1] (Thomson, 1985). In case of an accident, should a car prioritize the life of its own passenger(s), or the bystander(s)? A machine would need to be able to decide in less than a second, and the decision algorithm is to be programmed in by an ethical computer scientist. The trolley problem can be solved in many ways depending on one's philosophical beliefs, so an overarching directive coming from a governing body would be necessary to unify the responses. In general, there is a need for a regulatory organization that would oversee the development of robotics to ensure human safety, system transparency and correct reporting, adherence to existing laws, and overall regard for humanity's future.

Robots' safety should also be considered here—if AI indeed reaches human-like intelligence levels, would it be ethical for humans to use robots in applications where they would be destroyed? Should the public be educated to treat robots with compassion and to prevent vandalism against robots, or should they be treated as utilitarian constructs built to serve as tools?

CURRENT STATE OF ROBOETHICS IN CANADA

There is currently no central agency that oversees roboethics in Canada. Universities and funding organizations have proposed some general guidelines, but don't have the authority to enforce them. One of the most comprehensive AI ethics manifests comes from scholars at the University of Montreal. They proposed the Montreal Declaration for Responsible Development of Artificial Intelligence in 2018 (The Forum on the Socially Responsible Development of AI, 2018). The main purpose of the Montreal Declaration is to establish an ethical framework for AI development that would benefit everyone in society. As such, the Montreal Declaration is addressed to any person who wishes to develop AI ethically, and to political representatives who may be able to contribute to AI development through lobbying or policymaking. The Montreal Declaration touches upon 10 ethical principles that should be followed when developing AI:

1. Well-being principle
2. Respect for autonomy principle
3. Protection of privacy and intimacy
4. Solidarity principle
5. Democratic participation principle
6. Equity principle
7. Diversity inclusion principle
8. Caution principle
9. Responsibility principle
10. Sustainable development principle

These principles fit under the data, common good, and safety considerations described in the previous section. However, these principles are largely human-centric, and do not account for super-intelligent AI systems.

The University of British Columbia has taken a more inquisitive approach to developing roboethics principles by establishing the N-Reasons Platform (Danielson, 2010). This

[1]The trolley problem refers to a series of thought experiments where one must decide between sacrificing one person to save several people. In the experiment, one imagines a trolley running on a track that ends with a several people tied up on the tracks, and the user has a choice to pull a lever to divert the trolley to a track with just one person tied up. Either choice will directly cause the death of one or several people respectively (Thomson, 1985).

survey-based platform asks the public to evaluate several types of robots and choose reasons for why they would approve/not approve of their development. Results can be used as an indicator for public perspectives on robotics and inform future policy development. Of note, when the N-Reasons survey was run in 2010, the public was largely supportive of bomb-disposing robots and therapeutic robot animals, but did not agree with the development of fully automated armed aircrafts (Danielson, 2010).

The science of robotics falls under the purvey of the Natural Sciences and Engineering Research Council of Canada (NSERC) funding agency. While there are no robotics-specific policies under their code of ethics, NSERC provides guidelines for ethical standards and values, conflicts of interest, decision-making, private interests, and confidentiality policies. NSERC provides a total funding capital of $1.2 billion dollars to natural science and engineering research, and as a result, has a large influence on determining the direction of innovation in Canada.

While there are no robotics-specific guidelines under the NSERC code of ethics, there are two robotics networks that function under its umbrella. The NSERC Canadian Field Robotics Network (NCFRN) was established to support collaboration between academic researchers, government, and industry partners to create outdoor-capable robotic systems (Natural Sciences and Engineering Research Council of Canada, 2018). Currently, NCFRN develops robots capable of working in land, water, air and human community environments. After NCFRN's success, the NSERC Canadian Robotics Network (NCRN) has been established (NSERC Canadian Robotics Network (NCRN), 2018). At this time, NCRN has two streams: Interactive Autonomy and Resilient Autonomy. Research in interactive autonomy aims to develop robots that are able to effectively interface and collaborate with humans. Robots developed under the latter category are designed to work in extreme environments for long-term missions. Both NCRN streams of research could contribute to development of robots useful during and after the COVID-19 pandemic.

ETHICAL CONSIDERATIONS FOR ROBOTICS RESEARCH AND DEVELOPMENT DURING COVID-19

The current economic system favors automation as a tool for faster product manufacturing and distribution. Robots and AI systems are becoming more popular in the service, healthcare, and education systems. As the field of robotics is developing, the resulting robots are becoming faster and more capable. Robotic intellect, usually powered by AI, must be considered when designing long-term roboethics politics or implementing robotic solutions in everyday life. It has been predicted that robots will reach human-like intelligence sometime in the 21st century (Kurzweil, 2005; Hibbard, 2008).

Since the start of the COVID-19 pandemic, robots were used as a solution for minimizing human-to-human contact. After the pandemic is contained, we may find that robots are playing a bigger role in our society than pre-COVID-19. Consequently, the field of robotics may consider revisiting ethical guidelines to ensure that newly deployed robots are benefiting society.

Bonds Between Humans and Robots

During the pandemic, vulnerable populations of elderly patients found themselves emotionally bonding with robots because they were unable to interact with their loved ones. Some elderly care homes provided Paro, a furry seal-looking robot, to their patients for stress-relief and comfort (Knibbs, 2020; Ryan, 2020). As a result, patients bonded with a robot, expressing feelings of love and excitement to it. We now should consider how ethical it is to let sometimes disoriented patients emotionally invest into a robot. In the past, such trust has sometimes turned unfortunate when robots were disabled by their parent company. Jibo was a robot developed by Jibo Inc.; it was the first intelligent speaker and was capable of learning new patterns as the users interacted with it (Camp, 2019). When Jibo Inc. was sold off and servers hosting source codes disabled, Jibo started glitching and eventually turned off forever. For users who spent months interacting with Jibo, it was a painful and distressing process. If robots are to become an integral part of a patient's life, its lifespan must be guaranteed. In a case of a company going bankrupt and turning off the servers, there could be a way to make the source code public so that any individual can host the code for their robot. In the culture of planned obsolescence, robots that form relationships or perform critical tasks cannot be allowed to slowly become non-functional for a company's profit. Guarantee of robot's function beyond a year-long trial period enforces the trust into robot's safety. Moreover, when that bond between the robot and a human (e.g., patient or elderly person) is established, companies can use that as a money-making function for their profit.

Loss of Jobs

Loss of jobs to automation is a hot topic for economists. Automation has played a critical role in the development of the current market: from the first assembly line to shipping, machines have increased productivity across the globe. As robots and AI develop, workers are facing changes in employment opportunities. Currently, it is estimated that in 6 out of 10 occupations, at least 30% of activities are automatable (Manyika et al., 2017). While up to 375 million people globally might need to switch their jobs by 2030, historically, automation has created employment opportunities. Some job sectors, like agriculture and manufacturing, have seen declining employment; however, completely new job positions have been created due to automation. Overall, a country's labor displacement by automation depends on many factors such as demographics, industry structure, and economic strategy. Due to the COVID-19 pandemic, many businesses were forced to close, and work positions that rely on human-to-human contact were especially affected. For some of those jobs, human employees were replaced with robot employees. Laid-off workers now have a choice of coming back to constricted job market or to go back to school to enter a new job market. For workers who are unable to do either, they are forced to join the gig economy, resulting in reduced wages and social stability. In line with the common good

principle, governments should consider the careers of workers whose positions are "automatable," providing them with post-graduate education opportunities and expanded job markets should come together with higher robot implementation.

ROBOETHICS AND EDUCATION PRE- AND POST-COVID-19

Exploration for the use of robotics in education has yielded many promising classroom robots such as Nao, a robot developed by Alderbaran robotics. Nao can be used to teach programming skills, motor skills (such as handwriting) and be a learning peer for autistic students (Shamsuddin et al., 2012; Hamamsy et al., 2019; Sandygulova et al., 2020). As this example suggests, robots can hold different roles in the educational process: they can act solely as tools, but they can also be social. Social educational robots can be further subdivided into teachers, peers, and novices (Belpaeme et al., 2018). Teaching robots are typically used to instill new skills, like teach new vocabulary to an elementary school student. This teaching type of robots has been around the longest. Teaching robots are successfully used as interactive practice tools, and as an alternative knowledge dissemination device. Interestingly, when robots establish an empathetic link with a student, student's results are observed to be better (Saerbeck et al., 2010). Further on, robots can act as tutors in one-on-one teaching sessions by personalizing their instructional approach to each individual student, thus improving their student's performance (Leyzberg et al., 2014). The application of tutor-robots in conjunction with online adaptive learning approaches is a promising area of development for dental education in particular (Alwadei et al., 2020). Peer robots are developed to form an empathetic bond with students, learn alongside human subjects, and collaborate with students to solve problems. Novice robots tap into a pedagogical method where a student must explain or teach a topic to a novice. Novice robots are programmed to be taught by students.

When considering the ethics of teaching, the effectiveness of the method is one of the chief concerns. Would a robot-teacher be as good at delivering material when a robot is unable (currently at least) to fully observe non-verbal cues coming from the students? For robot–teachers that have a capacity to automatically evaluate student's performance, their assessment should pass the following criteria (Kalu et al., 2005):

(1) Be accepted by the experts in the teaching community;
(2) Be reliable, and provide the same result when performed at various times;
(3) Be valid, thus measuring the skill being measured (instead of measuring skill tangential to skill being assessed).

To assess the validity of a particular teaching robot, we should consider how well the robot-delivered assessment reflects the real-life skill, predicts future performance, and compares to the existing gold-standard (Kalu et al., 2005; Holmboe et al., 2010).

Additionally, a big part of in-person school education is the development of social skills, and would a robot-based pedagogical team be able to support the same levels of social and emotional development in students? With COVID-19, schools were forced to shut down and largely transition to distance education. In an online classroom, it is harder for the instructor to observe or support their students. For schools where education revolves around practicums and labs, such as dental colleges, students are facing deferred classes and exams (Wu et al., 2020). Dental students have reported concerns about their clinical care education, but were open to other strategies such as simulation and teledentistry (Hung et al., 2020). Schools can hence adapt by using robots as tools for practicums, and in some cases, as instructors. The future of robot-centric education might be coming sooner than expected. It yet remains to be answered whether robotic educational tools would serve equally as well in training students as human instructors. As robotic tools often rely on the Internet to connect and run their respective programs, students located in areas with poor or nonexistent connections could be at a disadvantage. Additionally, depending on the level of education, students that pay high tuition prices might not be ready to pay for robot-centric education when there is no evidence of efficacy. There is much potential with robotics in education, and the COVID-19 pandemic might be helpful in providing more data and direction to educational robotics field.

DENTEACH FOR REMOTE DENTAL TEACHING AND LEARNING

The COVID-19 pandemic has paused both a dental practice and dental education. Because SARS-CoV-2 virus can be found in the saliva of infected patients, dental healthcare professionals are at a higher risk of exposure to the virus (Wyllie et al., 2020). Even after the first wave of the COVID-19 has subsided, dental practices are not able to return to the same patient numbers as pre-COVID, and dental schools are largely conducting instruction online. Dental clinics are able to continue working at reduced capacity until a vaccine is available by increasing preventative measures such as increased handwashing and the use of protective shields. However, dental colleges are not able to conduct any of the practical aspects of the curriculum due to classroom setup and instructors' capacity. This is a major source of concern for dental students, whose clinical education has been disrupted by the pandemic (Hung et al., 2020). Virtual educational systems and dental simulators have been previously tested in remote education settings and yielded promising results. Students reported positive attitudes toward virtual practice systems and VR-assisted dental simulators. Students also observed a significant increase in their practical skills performance (Liebermann and Erdelt, 2020; Liu et al., 2020; Murbay et al., 2020). However, previously developed dental training simulators are not widely adopted by dentistry schools because of the following concerns: affordability and portability. In addition, currently available simulators are not yet officially recommended for the assessment or training of students (Galibourg et al., 2020). The latter might change soon due to the necessity of remote dental education. To address the concerns of portability, Tactile Robotics has developed a haptic-enabled robotic platform for dental teaching, learning and practicing purposes. This platform, called DenTeach, is portable and affordable, making

TABLE 1 | Capabilities of DenTeach in both instructor and student workstations.

Instructor	Student
Evaluation of Performance	
Quantifying the students' skills during the performance of dental tasks using several KPIs[a] Evaluating students based on the performance index	Real-time quantitative evaluation of performing dental tasks using several KPIs Compare performance skill with instructor's KPIs
Instructional Experience	
Measuring kinematic and kinetic characteristics of the dental tool motion Communicating with students through a custom-made user interface Recording teaching sessions for future use, online education (e-learning) and case rehearsal	Follow along with a recorded video, audio and haptic feeling User-friendly augmented reality Available 24/7 No supervision required
Physical Setup	
Portable for use everywhere from school to home	

[a]*KPIs: Key Performance Indicators.*

remote practical dental education a possibility (Maddahi et al., 2020).

For dental educational institutions, DenTeach allows for continuous education through COVID-19, and aids in helping classrooms to become more efficient. DenTeach faithfully captures the environment in which a dental task is performed. It records both sounds, video, and drill vibrations during the procedure demonstrated by the instructor. This allows the student to better understand the task and facilitates the learning process. Additionally, DenTeach is supplied with an articulator that can mimic a patient's posture, thus training the student to perform the task in the most realistic position. Neither of these functions is widely available in a traditional classroom. As a result, DenTeach can increase teaching efficiency by accelerating skill acquisition by students, and removing limitations based on classroom size.

DenTeach provides extensive quantitative feedback and allows the student to learn and practice at a remote location, such as their home, with a minimal supervision of the instructor. The system uses a combination of sensory responses, and performance data to aid in the learning experience. During the instruction, the students experience how the tool feels during the performance of the task. Understanding proper dental tool handling is also made possible through sensors and actuators on dental tools and by providing an effective augmented reality environment. For the instructors, DenTeach supports an intuitive interface that allows the instructor to demonstrate the model procedure, review students' work, and provide them with assessments. Dental instructors can teach from a remote location, and the students are able to follow along with the procedure at their own workstation. Additionally, instructors can record a procedure that students can follow along later. This provides an opportunity to change the novice-expert apprenticeship model as an expert would not need to be present for instruction. The recorded material can be reused and could result in cost-benefits to educational institutions. A summary of the capabilities of the platform is listed in **Table 1**.

FIGURE 1 | (A) Instructor workstation. Instructor workstation comprises of a DT-Rightway dental articulator, a sensory system, 4 cameras covering 360° view coverage, a microphone to speak with students in real-time, a software that shows the performance and information of each student and allows the instructor to monitor them remotely. **(B)** Student workstation. Student workstation consists of the DT-Rightway dental articulator, a sensory system, two sets of RealFeel dental handpiece (slow-speed and high-speed) and a software that captures student's actions and provides performance metrics.

DenTeach Platform

DenTeach is a vibrotactile dental apparatus that can be situated to work in a wired or wireless setting. There are two types of DenTeach workstations available. The first setup is the instructor workstation that comprises a set of sensory systems attached to a commercially available dental drill. The sensors are able to measure the position,

orientation, velocities, accelerations, and jerk (vibrotactile characteristics) of the drill while it is in contact with a physical model of the tooth (**Figure 1A**). A robotic-based dental articulator is also included in the platform that allows the instructor to set the posture of the oral cavity in different orientations to emulate the patient's actual posture. The second type of setup is the student workstation. It includes a custom-designed training tool that has a set of sensory systems and a display showing the dental operation performed at the instructor workstation. A similar robotized dental articulator as the instructor helps the student follow the instructor's technique and to experience working on patient's posture in addition to the traditional tabletop technique (**Figure 1B**). The student workstation software quantifies student's performance and displays it as a set of key performance indices (KPIs) (Cheng et al., 2021). There is a total of 82 KPIs available through the DenTeach system, allowing for detailed analysis of student's performance. KPIs include metrics such as task completion time, tool handling smoothness and steadiness.

DenTeach in the Context of Learning Domains

The learning process and educational goals can be widely classified into three domains based on the Bloom's Taxonomy. These domains are 1) cognitive, 2) psychomotor and 3) affective (Bloom et al., 1956). The cognitive learning domain includes activities that train critical thinking skills, fact recollection, decision making, and general comprehension of the subject matter (Anderson et al., 2001; McHarg and Kay, 2009). The psychomotor domain includes learning technical skills such as procedural knowledge and accompanying adaptive thinking. Training in the psychomotor domain develops one's reflexes, dexterity and deliberate movement (Simpson, 1971; Anderson et al., 2001; McHarg & Kay, 2009). Educational goals classified under the affective learning domain typically emphasize skills related to emotional intelligence and personal values (Bloom et al., 1956; McHarg and Kay, 2009).

A successful dental school graduate should have the following characteristics after degree completion: technical competence, critical thinking, ethical and professional values, social responsibility, professionalism in the work environment, patient management, and capability for self-assessment (Schneider et al., 2014). Each of these characteristics correlates with certain learning domains identified above. When dental educators were asked to evaluate the types of skills that dental students train during their schooling, the two areas that received the highest rank were knowledge and technical skills (Hoskin et al., 2019). Critical thinking, decision making, and ethics were ranked highly as well under the same questionnaire (Hoskin et al., 2019). DenTeach is primarily intended for the practice of dental procedures, meaning the students would be engaging primarily in the practice of skills that fall under the psychomotor learning domain. When students are completing dental tasks using DenTeach, they are practicing operating the drill in an environment that emulates patient posture. This allows students to develop their motor skills in addition to spatial perception. The DenTeach system assumes that students already have prior theoretical knowledge of procedures, which was potentially acquired during lectures preceding dental tutorials. In the time of COVID-19, as dental education transitioned online, such theoretical knowledge would have been taught through e-learning tools such as Canvas (Iyer et al., 2020). Additionally, dental students have reported using YouTube to watch videos of dental procedures being performed even before the COVID-19 pandemic (Burns et al., 2020). This evidence suggests that the development of online tools can enhance dental education even after in-person education is resumed (Alwadei et al., 2020; Burns et al., 2020; Jeganathan and Fleming, 2020).

Ethical Aspects of DenTeach

As discussed in the above sections, when attempting to implement a new piece of technology into human life, we must consider the impact said technology will have. As an educational device, DenTeach's purpose is to benefit the current instruction model in dental colleges by making dental education accessible to students during and after the COVID-19 pandemic. In this section, we evaluate DenTeach on the principles of data, common good, and safety and discuss potential ethical considerations for DenTeach implementation.

Data Considerations: Privacy, Security, Longevity

DenTeach collects two kinds of data when in use: camera footage from an instructor's feed and sensor data from both students and instructor's workstations. This data, once recorded, would be processed by a data transmission system and is saved on a local server or on the cloud (depending on the institution's preference). After the data is saved, it is available on-demand for both students and instructors. To protect students' privacy, each student is only able to see their own performance, but the instructor has access to all student performance data. This system of information storage and protection is common among higher education institutions, but unfortunately, it is also common for universities and colleges to get hacked (Maranga and Nelson, 2019). With a device that is designed to fully rely on servers and cloud data backups, it is critical to highlight the importance of cybersecurity. Additionally, since remote learning instructors will only be able to base their assessments and marking on data provided by DenTeach, it is critical that this data is not tampered with both by external forces, and by students themselves.

One of the big advantages of DenTeach is the possibility of remote software upgrades. These upgrades can be done swiftly and applied during downtime, thus not impeding the education process. Additionally, Tactile Robotics offers a 4-years guarantee and 24/7 support for students who purchase and use DenTeach. Lastly, in order to access the instructor's data, install updates, and contact DenTeach for support, students will need to have a stable internet connection, which might not always be available. With expansion of services available online and technologies that require the Internet to function, internet access is starting to be viewed as a human right (Human Rights Council, 2016). While the Internet is reasonably ubiquitous in North America, other areas might not have a stable internet connection available, which

should be considered by dental schools accepting international students or situated abroad.

Common Good: Benefits of DenTeach

Over the years, there have been several attempts to create a simulation dental classroom. Most studies have found that new simulation classrooms did not have a big impact on the way dental pre-clinical procedures are taught (Buchanan, 2001). New generations of technology utilizing internet connection, virtual reality, 3D modeling and next-generation sensors are currently used to develop dental simulation devices that expand beyond what was previously possible. Still, many devices currently being used require supervision and real-life teaching in addition to being stationary and hence not suitable for remote teaching and learning. DenTeach is designed to support educators in the difficult time of COVID-19, but its potential use can extend beyond pandemic response. Professional education institutions, such as dental schools, require program standardization and objective evaluation (Quinn et al., 2003). DenTeach can provide unbiased quantitative feedback to students, and since instructors are able to upload procedures to the server, students are all exposed to the same material in the exact same way. This provides dental schools and education researchers with a unique opportunity to standardize the curriculum and evaluate the simulation classroom with only the experimental variable being the students. Tactile Robotics is currently conducting studies to comprehensively evaluate and compare student performance in DenTeach enabled and traditional classroom settings. The COVID-19 pandemic has challenged the current novice-expert apprenticeship model, and technology could be a useful tool in helping dental educational model evolve.

DenTeach allows students to practice dental procedures at any time, thus allowing for self-study and self-analysis–two important steps in mastering dental techniques. Because DenTeach is designed to be portable, it allows for schools to admit students located around the globe. Additionally, a standardized curriculum could make high-quality dental education available to students located in areas without dental schools, benefiting both the students, and the surrounding population. Further, to make DenTeach available to any dental school interested, Tactile Robotics has a flexible marketing plan for each country or client interested. This supports the principle of equitable access to technology.

Finally, DenTeach offers both right-hand and left-hand setups to enable students to practice in a way that would be most natural and comfortable for them. This emulates field conditions and is inclusive of all students who would be admitted to dental schools.

Safety

DenTeach could not reasonably cause harm to human beings–while it does have a dental drill, and weighs a few pounds, it would require a malicious intent from a human, or an unfortunate accident caused by a human for someone to sustain an injury from DenTeach. As such, safety is not a significant concern for DenTeach implementation.

CONCLUSION

The COVID-19 pandemic has stimulated the field of robotics to compensate for restrictions implemented to slow the spread of the SARS-Cov-2 virus. Robots were deployed to perform tasks that were too risky for humans, such as comforting at-risk elderly patients and sanitizing hospital spaces. Because of the urgency of the situation, more attention was focused on the rapid development of robots, and less on the ethical aspects of such robotic systems. The principles of data, the common good, and safety are of most relevance for the ethical implementation of robotic systems. This paper is specifically focused on ethical considerations in the design and development of robotic systems for healthcare education. Dental colleges were forced to shut down during the pandemic, and practical courses were delayed until the time it was safe to resume instruction. For students who are enrolled in dental schools during COVID-19 and are continuing to pay tuition fees, it is a dental college's ethical responsibility to deliver training, even in these challenging times. This created an opportunity for robots to be used to train students in practical dental skills. Previously there have been attempts to create portable dental simulators: both Simodont and IDEA can be used remotely to assist students in learning dental tasks (Luciano et al., 2009; Gal et al., 2011). DenTeach is a new-generation haptic-enabled dental simulator that can be used remotely to train dental tasks completed with a drill. When implementing DenTeach in the educational curriculum, data privacy and equal access should be considered a priority. We explore different aspects of such considerations and provide examples of real-life applications of robotic systems during the COVID-19 pandemic. This may provide some guidelines for engineers and researchers during the research and design process.

DATA AVAILABILITY STATEMENT

The original contributions presented in the study are included in the article/Supplementary Material, further inquiries can be directed to the corresponding author.

AUTHOR CONTRIBUTIONS

YM and SL worked on the ethics in robotics. YM, SL and NC prepared the first draft of the manuscript. YM and MK prepared the the section explaining the DenTeach technology. MK and SL worked on clinical aspects of the system. All authors reviewed and edited the manuscript.

REFERENCES

Alwadei, A. H., Tekian, A. S., Brown, B. P., Alwadei, F. H., Park, Y. S., Alwadei, S. H., et al. (2020). Effectiveness of an Adaptive eLearning Intervention on Dental Students' Learning in Comparison to Traditional Instruction. *J. Dent. Educ.* 84 (11), 1294–1302. doi:10.1002/jdd.12312

Anderson, L. W., Krathwohl, D. R., Airasian, P. W., Cruikshank, K. A., Mayer, R. E., Pintrich, P. R., et al. (2001). *A Taxonomy for Learning, Teaching, and Assessing: A Revision of Bloom's Taxonomy of Educational Objectives*. Boston: Addison Wesley Longman, Inc. Available at: https://www.uky.edu/~rsand1/china2018/texts/Anderson-Krathwohl.

Asimov, I. (1942). Runaround. *Astounding Science Fiction* 14, 59–93. doi:10.5749/j.ctt189tts8.3

Belpaeme, T., Kennedy, J., Ramachandran, A., Scassellati, B., and Tanaka, F. (2018). Social Robots for Education: A Review. *Sci. Robot.* 3 (21), eaat5954. doi:10.1126/scirobotics.aat5954

Bloom, B. S., Engelhart, M. D., Furst, E. J., Hill, W. H., and Krathwohl, D. R. (1956). The Classification of Educational Goals. *Taxonomy Educ. Object.* 14, 62–197.

Bösl, D. B. O., and Bode, M. (2018). "Roboethics and Robotic Governance—A Literature Review and Research Agenda," in ROBOT 2017: Third Iberian Robotics Conference. Editors A. Ollero, A. Sanfeliu, L. Montano, N. Lau, and C. Cardeira (Berlin: Springer International Publishing), 140–146. doi:10.1007/978-3-319-70833-1_12

Buchanan, J. A. (2001). Use of Simulation Technology in Dental Education. *J. Dental Edu.* 65 (11), 1225–1231. doi:10.1002/j.0022-0337.2001.65.11.tb03481.x

Burns, L. E., Abbassi, E., Qian, X., Mecham, A., Simeteys, P., and Mays, K. A. (2020). YouTube Use Among Dental Students for Learning Clinical Procedures: A Multi-institutional Study. *J. Dent. Educ.* 84 (10), 1151–1158. doi:10.1002/jdd.12240

Camp, J. V. (2019). My Jibo Is Dying and It's Breaking My Heart. Wired. Available at: https://www.wired.com/story/jibo-is-dying-eulogy/.

Cheng, L., Kalvandi, M., McKinstry, S., Maddahi, A., Chaudhary, A., and Maddahi, Y. (2021). Application of DenTeach in Remote Dentistry Teaching and Learning During the COVID-19 Pandemic: A Case Study. *Front. Rob. AI.* 7, 222.

Danielson, P. (2010). Designing a Machine to Learn about the Ethics of Robotics: The N-Reasons Platform. *Ethics Inf. Technol.* 12 (3), 251–261. doi:10.1007/s10676-009-9214-x

Detsky, A. S., and Bogoch, I. I. (2020). COVID-19 in Canada. *JAMA*. 324 (8), 743. doi:10.1001/jama.2020.14033

Dodig Crnkovic, G., and Çürüklü, B. (2012). Robots: Ethical by Design. *Ethics Inf. Technol.* 14 (1), 61–71. doi:10.1007/s10676-011-9278-2

El Mesbahi, M. (2015). "Human-Robot Interaction Ethics in Sci-Fi Movies: Ethics Are Not `There', We Are the Ethics!," in *Design, User Experience, and Usability: Design Discourse*. Editor A. Marcus (Berlin: Springer International Publishing). doi:10.21236/ad1001404

European Group on Ethics in Science and New Technologies (2018). *Artificial Intelligence, Robotics and 'Autonomous' Systems*. London: European Commission. doi:10.2777/531856

Gal, G. B., Weiss, E. I., Gafni, N., and Ziv, A. (2011). Preliminary Assessment of Faculty and Student Perception of a Haptic Virtual Reality Simulator for Training Dental Manual Dexterity. *J. Dental Educ.* 75 (4), 496–504. doi:10.1002/j.0022-0337.2011.75.4.tb05073.x

Galibourg, A., Maret, D., Monsarrat, P., and Nasr, K. (2020). Impact of COVID-19 on Dental Education: How Could Pre-clinical Training Be Done at Home? *J. Dent. Educ.* 84 (9), 949. doi:10.1002/jdd.12360

Hamamsy, L. El., Johal, W., Asselborn, T., Nasir, J., and Dillenbourg, P. (2019). "Learning by Collaborative Teaching: An Engaging Multi-Party CoWriter Activity," in 2019 28th IEEE International Conference on Robot and Human Interactive Communication, RO-MAN 2019, 048. doi:10.1109/roman46459.2019.8956358

Hibbard, B. (2008). The Technology of Mind and a New Social Contract. *J. Evol. Tech.* 17 (1), 13–22. doi:10.7551/mitpress/9780262035965.003.0009 Available at: http://jetpress.org/v17/hibbard.htm.

Holmboe, E. S., Sherbino, J., Long, D. M., Swing, S. R., and Frank, J. R. (2010). The Role of Assessment in Competency-Based Medical Education. *Med. Teach.* 32 (8), 676–682. doi:10.3109/0142159x.2010.500704

Hoskin, E. R., Johnsen, D. C., Saksena, Y., Horvath, Z., de Peralta, T., Fleisher, N., et al. (2019). Dental Educators' Perceptions of Educational Learning Domains. *J. Dental Edu.* 83 (1), 79–87. doi:10.21815/jde.019.010

Human Rights Council. (2016). Thirty-second Session, Agenda Item 3: Oral Revisions of 30 June. United Nations General Assembly, 10802(June), A/HRC/32/L.20. Available at: https://doi.org/10.1093/oxfordhb/9780199560103.003.0005.

Hung, M., Licari, F. W., Hon, E. S., Lauren, E., Su, S., Birmingham, W. C., et al. (2020). In an Era of Uncertainty: Impact of COVID-19 on Dental Education. *J. Dent. Educ.* 85, 148–156. doi:10.1002/jdd.12404

Iyer, P., Aziz, K., and Ojcius, D. M. (2020). Impact of COVID-19 on Dental Education in the United States. *J. Dent. Educ.* 84 (6), 718–722. doi:10.1002/jdd.12163

Jeganathan, S., and Fleming, P. S. (2020). Blended Learning as an Adjunct to Tutor-Led Seminars in Undergraduate Orthodontics: a Randomised Controlled Trial. *Br. Dent J.* 228 (5), 371–375. doi:10.1038/s41415-020-1332-1

Kalu, P. U., Atkins, J., Baker, D., Green, C. J., and Butler, P. E. M. (2005). How Do We Assess Microsurgical Skill? *Microsurgery* 25 (1), 25–29. doi:10.1002/micr.20078

Knibbs, K. (2020). There's No Cure for Covid-19 Loneliness, but Robots Can Help. Wired. Available at: https://www.wired.com/story/covid-19-robot-companions/.

Kurzweil, R. (2005). *The Singularity Is Near: When Humans Transcend Biology*. London: Viking. doi:10.1007/978-3-322-91896-3

Leyzberg, D., Spaulding, S., and Scassellati, B. (2014). Personalizing Robot Tutors to Individuals' Learning Differences. *ACM/IEEE Int. Conf. Human-Robot Interact.* 14, 423–430. doi:10.1145/2559636.2559671

Liebermann, A., and Erdelt, K. (2020). Virtual Education: Dental Morphologies in a Virtual Teaching Environment. *J. Dent. Educ.* 84 (10), 1143–1150. doi:10.1002/jdd.12235

Liu, L., Zhou, R., Yuan, S., Sun, Z., Lu, X., Li, J., et al. (2020). Simulation Training for Ceramic Crown Preparation in the Dental Setting Using a Virtual Educational System. *Eur. J. Dent Educ.* 24 (2), 199–206. doi:10.1111/eje.12485

Luciano, C., Banerjee, P., and DeFanti, T. (2009). Haptics-based Virtual Reality Periodontal Training Simulator. *Virtual Reality*. 13 (2), 69–85. doi:10.1007/s10055-009-0112-7

Maddahi, A., Bagheri, S., Mardan, M., Kalvandi, M., and Maddahi, Y. (2020). *Vibrotactile Method, Apparatus and System for Training and Practicing Dental Procedures*. Patent No. WO2020041879A1. doi:10.1145/3396339.3396381

Manyika, J., Lund, S., Chui, M., Bughin, J., Woetzel, J., Batra, P., et al. (2017). *Jobs Lost, Jobs Gained: Workforce Transitions in a Time of Automation*. New York: McKinsey Global Institute, 1–148.

Maranga, M. J., and Nelson, M. (2019). Emerging Issues in Cyber Security for Institutions of Higher Education. *IJCSN-International J. Comp. Sci. Netw.* 8 (4), 371–379. doi:10.1109/oi.2018.8535939

McHarg, J., and Kay, E. J. (2009). Designing a Dental Curriculum for the Twenty-First Century. *Br. Dent J.* 207 (10), 493–497. doi:10.1038/sj.bdj.2009.1011

Murbay, S., Chang, J. W. W., Yeung, S., and Neelakantan, P. (2020). Evaluation of the Introduction of a Dental Virtual Simulator on the Performance of Undergraduate Dental Students in the Pre-clinical Operative Dentistry Course. *Eur. J. Dent Educ.* 24 (1), 5–16. doi:10.1111/eje.12453

Murphy, R., and Woods, D. D. (2009). Beyond Asimov: The Three Laws of Responsible Robotics. *IEEE Intell. Syst.* 24 (4), 14–20. doi:10.1109/mis.2009.69

Natural Sciences and Engineering Research Council of Canada (2018). *NSERC Canadian Field Robotics Network*. Available at: https://www.nserc-crsng.gc.ca/Business-Entreprise/How-Comment/Networks-Reseaux/CFRN-RCRT_eng.asp.

Neustaeter, B. (2020). Canada's First Disinfection Robot Being Tested. CTV News. Available at: https://www.ctvnews.ca/health/coronavirus/canada-s-first-disinfection-robot-being-tested-1.4918668.

NSERC Canadian Robotics Network (NCRN) (2018). NSERC Canadian Robotics Network (NCRN). Available at: https://ncrn-rcrc.mcgill.ca/.

Pagallo, U. (2017). When Morals Ain't Enough: Robots, Ethics, and the Rules of the Law. *Minds Mach.* 27 (4), 625–638. doi:10.1007/s11023-017-9418-5

Quinn, F., Keogh, P., Mcdonald, A., and Hussey, D. (2003). A Study Comparing the Effectiveness of Conventional Training and Virtual Reality Simulation in the Skills Acquisition of Junior Dental Students. *J. Dental Edu.* 7, 164–169. doi:10.1034/j.1600-0579.2003.00309.x

Ryan, D. (2020). Robotic Seal Provides Emotional Support for Alzheimer's Patients at Vancouver General Hospital. Vancouver Sun. Available at: https://vancouversun.com/news/robotic-seal-provides-emotional-support-for-alzheimers-patients-at-vancouver-general-hospital.

Saerbeck, M., Schut, T., Bartneck, C., and Janse, M. D. (2010). Expressive Robots in Education: Varying the Degree of Social Supportive Behavior of a Robotic Tutor. *Conf. Hum. Factors Comput. Syst. Proc.* 3, 1613–1622. doi:10.1145/1753326.1753567

Sandygulova, A., Johal, W., Zhexenova, Z., Tleubayev, B., Zhanatkyzy, A., Turarova, A., et al. (2020). CoWriting Kazakh: Learning a New Script with a Robot. *ACM/IEEE Int. Conf. Human-Robot Interact.* 2016, 113–120. doi:10.1145/3319502.3374813

Schneider, G. B., Cunningham-Ford, M. A., Johnsen, D. C., Eckert, M. L., and Mulder, M. (2014). Outcomes Mapping: A Method for Dental Schools to Coordinate Learning and Assessment Based on Desired Characteristics of a Graduate. *J. Dental Edu.* 78 (9), 1268–1278. doi:10.1002/j.0022-0337.2014.78.9.tb05798.x

Shamsuddin, S., Yussof, H., Ismail, L. I., Mohamed, S., Hanapiah, F. A., and Zahari, N. I. (2012). Humanoid Robot NAO Interacting with Autistic Children of Moderately Impaired Intelligence to Augment Communication Skills. *Proced. Eng.* 41 (Iris), 1533–1538. doi:10.1016/j.proeng.2012.07.346

Simpson, E. J. (1971). Educational Objectives in the Psychomotor Domain. *Behav. Object. Curricul. Dev. Sel. Read. Bibliogr.* 60 (2), 1–35.

The Forum on the Socially Responsible Development of AI (2018). *Montreal Declaration for a Responsible Development of Artificial Intelligence*. Berlin: Springer, 1–21.

The IEEE Global Initiative (2019). Ethically Aligned Design: A Vision for Prioritizing Human Well-Being with Autonomous and Intelligent Systems, Version 2 (pp. 1–263). Available at: https://doi.org/10.1109/MCS.2018.2810458.

Thomson, J. J. (1985). The Trolley Problem. *Yale L. J.* 94 (6), 1395. doi:10.2307/796133

US Department of Homeland Security (2020). *US–Israeli Robot Accessory Arm Provides Enhanced Capabilities and Precise Manipulation*. New York, United States: Department of Homeland Security. Available at: https://www.dhs.gov/science-and-technology/news/2020/04/07/snapshot-us-israel-empower-bomb-squad-robots-second-arm.

Veruggio, G. (2006). "The EURON Roboethics Roadmap," in Proceedings of the 2006 6th IEEE-RAS International Conference on Humanoid Robots, HUMANOIDS, 612–617. Available at: https://doi.org/10.1109/ICHR.2006.321337

Vincent, J. (2015). *US Military Says Robotic Pack Mules Are Too Noisy to Use*. London: The Verge. Available at: https://www.theverge.com/2015/12/29/10682746/boston-dynamics-big-dog-ls3-marines-development-shelved.

Wu, D. T., Wu, K. Y., Nguyen, T. T., and Tran, S. D. (2020). The Impact of COVID-19 on Dental Education in North America-Where Do We Go Next? *Eur. J. Dent Educ.* 24 (4), 825–827. doi:10.1111/eje.12561

Wyllie, A. L., Fournier, J., Casanovas-Massana, A., Campbell, M., Tokuyama, M., Vijayakumar, P., et al. (2020). Saliva or Nasopharyngeal Swab Specimens for Detection of SARS-CoV-2. *N. Engl. J. Med.* 383 (13), 1283–1286. doi:10.1056/nejmc2016359

Conflict of Interest: YM is with Tactile Robotics, the company that holds intellectual property for DenTeach technology.

The remaining authors declare that the research was conducted in the absence of any commercial or financial relationships that could be construed as a potential conflict of interest.

frontiers in Robotics and AI

PERSPECTIVE
published: 05 May 2021
doi: 10.3389/frobt.2021.612415

Neurorehabilitation From a Distance: Can Intelligent Technology Support Decentralized Access to Quality Therapy?

Olivier Lambercy[1,2†], Rea Lehner[2,3†*], Karen Chua[2,4,5], Seng Kwee Wee[2,4,6], Deshan Kumar Rajeswaran[2,4], Christopher Wee Keong Kuah[2,4], Wei Tech Ang[2,5,7], Phyllis Liang[2,5], Domenico Campolo[2,7], Asif Hussain[2,7,8], Gabriel Aguirre-Ollinger[8], Cuntai Guan[2,9], Christoph M. Kanzler[1,2], Nicole Wenderoth[2,3] and Roger Gassert[1,2]*

[1]Rehabilitation Engineering Laboratory, Department of Health Sciences and Technology, ETH Zurich, Switzerland, [2]Future Health Technologies, Singapore-ETH Centre, Campus for Research Excellence and Technological Enterprise (CREATE), Singapore, Singapore, [3]Neural Control of Movement Laboratory, Department of Health Sciences and Technology, ETH Zurich, Switzerland, [4]Centre for Advanced Rehabilitation Therapeutics, Tan Tock Seng Hospital Rehabilitation Centre, Singapore, Singapore, [5]Rehabilitation Research Institute Singapore, Nanyang Technological University, Singapore, Singapore, [6]Singapore Institute of Technology (SIT), Singapore, Singapore, [7]School of Mechanical and Aerospace Engineering, Nanyang Technological University, Singapore, Singapore, [8]Articares Pte Ltd, Singapore, Singapore, [9]School of Computer Science and Engineering, Nanyang Technological University, Singapore, Singapore

Current neurorehabilitation models primarily rely on extended hospital stays and regular therapy sessions requiring close physical interactions between rehabilitation professionals and patients. The current COVID-19 pandemic has challenged this model, as strict physical distancing rules and a shift in the allocation of hospital resources resulted in many neurological patients not receiving essential therapy. Accordingly, a recent survey revealed that the majority of European healthcare professionals involved in stroke care are concerned that this lack of care will have a noticeable negative impact on functional outcomes. COVID-19 highlights an urgent need to rethink conventional neurorehabilitation and develop alternative approaches to provide high-quality therapy while minimizing hospital stays and visits. Technology-based solutions, such as, robotics bear high potential to enable such a paradigm shift. While robot-assisted therapy is already established in clinics, the future challenge is to enable physically assisted therapy and assessments in a minimally supervized and decentralized manner, ideally at the patient's home. Key enablers are new rehabilitation devices that are portable, scalable and equipped with clinical intelligence, remote monitoring and coaching capabilities. In this perspective article, we discuss clinical and technological requirements for the development and deployment of minimally supervized, robot-assisted neurorehabilitation technologies in patient's homes. We elaborate on key principles to ensure feasibility and acceptance, and on how artificial intelligence can be leveraged for embedding clinical knowledge for safe use and personalized therapy adaptation. Such new models are likely to impact neurorehabilitation beyond COVID-19, by providing broad access to sustained, high-quality and high-dose therapy maximizing long-term functional outcomes.

Keywords: neurorehabilitation, robot-assisted therapy (RAT), clinical intelligence, decentralized care, stroke

OPEN ACCESS

Edited by:
Ana Luisa Trejos, Western University, Canada

Reviewed by:
Hendrik Santosa, University of Pittsburgh, United States
Michelle Johnson, University of Pennsylvania, United States
Michael Sobrepera, University of Pennsylvania, United States, in collaboration with reviewer MJ

***Correspondence:**
Rea Lehner
rea.lehner@sec.ethz.ch
Olivier Lambercy
olivier.lambercy@hest.ethz.ch

[†]These authors have contributed equally to this work

Specialty section:
This article was submitted to Biomedical Robotics, a section of the journal Frontiers in Robotics and AI

Received: *30 September 2020*
Accepted: *20 April 2021*
Published: *05 May 2021*

Citation:
Lambercy O, Lehner R, Chua K, Wee SK, Rajeswaran DK, Kuah CWK, Ang WT, Liang P, Campolo D, Hussain A, Aguirre-Ollinger G, Guan C, Kanzler CM, Wenderoth N and Gassert R (2021) Neurorehabilitation From a Distance: Can Intelligent Technology Support Decentralized Access to Quality Therapy?. Front. Robot. AI 8:612415. doi: 10.3389/frobt.2021.612415

INTRODUCTION

Stroke is a leading cause of disability and morbidity globally, accounting for 132 million disability-adjusted life-years (DALYs) worldwide (GBD, 2018). Among others, the neurological damage resulting from a stroke can lead to severe upper limb sensorimotor impairment, affecting a person's ability to work and take part in activities of daily living. To date, there is no cure for stroke and patients rely on neurorehabilitation services long after their injury to at least partially recover sensorimotor function.

Currently, neurorehabilitation strongly relies on physical and occupational therapy sessions, which are primarily based on one-to-one interactions with healthcare practitioners either during an inpatient hospital stay (mostly during the acute to sub-acute phase) or as part of regular visits to specialized outpatient institutions (mostly during the sub-acute to chronic phase). This current model of care is highly resource demanding and already faces important challenges to cope with constantly increasing numbers of patients due to changing demographics, shortage of trained healthcare providers, and economic pressure to minimize healthcare costs. As a result, therapy dose is typically rather low at all stages of the continuum of care, despite the growing evidence that intensive high-dose neurorehabilitation positively impacts sensorimotor function even long after the injury (Daly et al., 2019; Ward et al., 2019).

The coronavirus (COVID-19) pandemic brought additional critical constraints to this already fragile ecosystem (Caso and Federico, 2020). Patients after stroke belong to the population at risk (Jordan et al., 2020) and essential care, such as neurorehabilitation services, was set to lower priority to avoid overloading the healthcare system. Furthermore, physical distancing measures and the cut-back on face-to-face consultations have led to a reduction in clinic and therapy stays/visits. As a result, several studies have reported that the quality of care in stroke patients has been impacted (Bersano et al., 2020; De Sousa et al., 2020; Richter et al., 2021). A recent survey revealed that a large majority of healthcare professsionals involved in stroke care (primarily neurologists, interventionalists and rehabilitation physicians) were concerned that this lack of care will have had a noticeable negative impact on long-term outcomes, and that rehabilitation is likely the most affected area of stroke care (De Sousa et al., 2020).

COVID-19 crystalizes the limitations of existing healthcare models and highlights the urgent need to rethink conventional neurorehabilitation so that high-quality therapy can be provided while the need for hospital stays and visits is minimized. In the last decade, the digital revolution has fueled the vision of new scalable technologies that provide higher doses of high-quality rehabilitation along the continuum of care and, in particular, in the home of patients (Galea, 2019). However, such solutions for "neurorehabilitation from a distance" still remain in their infancy (Dafer et al., 2020; De Sousa et al., 2020) and have so far only been investigated as separate elements (i.e., individual technologies and therapy concepts). This article aims to provide an overarching vision on how different existing technological solutions could be combined in the form of a connected RehabGym. The overall goal of such a framework is to promote recovery, maintain functional gains and maximize independence by optimally using the potential of rehabilitation technology. For this, we propose concrete considerations for the implementation of minimally supervized robot-assisted therapy as a possible approach to provide quality, high-dose neurorehabilitation solutions along the continuum of care. We argue that user-friendly, intelligent and robust technology could help transform the current hospital-centered model into a home-centered model of care that is potentially more resource- and cost-effective, and robust to extreme situations such as the COVID-19 pandemic.

NEUROREHABILITATION FROM A DISTANCE

From a Hospital-Centered Model to a Home-Centered Model of Neurorehabilitation

Neurorehabilitation after stroke often starts at the bedside early after the incident (e.g., after 2–3 days once the patient is stable), is then continued for 1–3 months in a rehabilitation clinic and later transitions to community-based rehabilitation treatment, for example, in an outpatient center (i.e., 5–6 weeks of intensive training). While such a model allows healthcare practitioners to closely monitor their patients and support them and their families (both physically and emotionally) throughout the recovery process, it heavily relies on physical access to medical facilities and sustained interactions with trained specialists (hospital-centered model, **Figure 1A**). This neurorehabilitation model is not only challenged by events such as the COVID-19 pandemic but also by changing demographics, which might lead to a shortage of human resources and non-sustainable costs. This ultimately affects the dose and quality of therapy patients receive, limiting rehabilitation to intense but relatively short and early time periods that might be insufficient to achieve functional recovery. After discharge, there is typically limited support for continued care management or to motivate patients to self-engage in physical activities or rehabilitation exercises at home, which are necessary for the maintenance of functional gains (Nicholson et al., 2013). This gap may explain the often observed decrease in functional ability or learned nonuse of the impaired limb (Taub et al., 2006; Hidaka et al., 2012).

To offer a more sustainable approach, there is a need to shift the existing hospital-centered model of care toward a more home-centered model (**Figure 1B**). In such a scheme, selected patients are discharged from hospital/outpatient centers earlier and provided with various solutions to perform high-quality therapy at home. This facilitates decreased dependence on hospital fixed schedules and limited resources, thereby bringing the promise of increasing the overall therapy dose patients may receive, provided that they engage in self-directed therapy.

While a home-centered approach to conventional therapy is not new and has been shown to be implementable in a cost-efficient

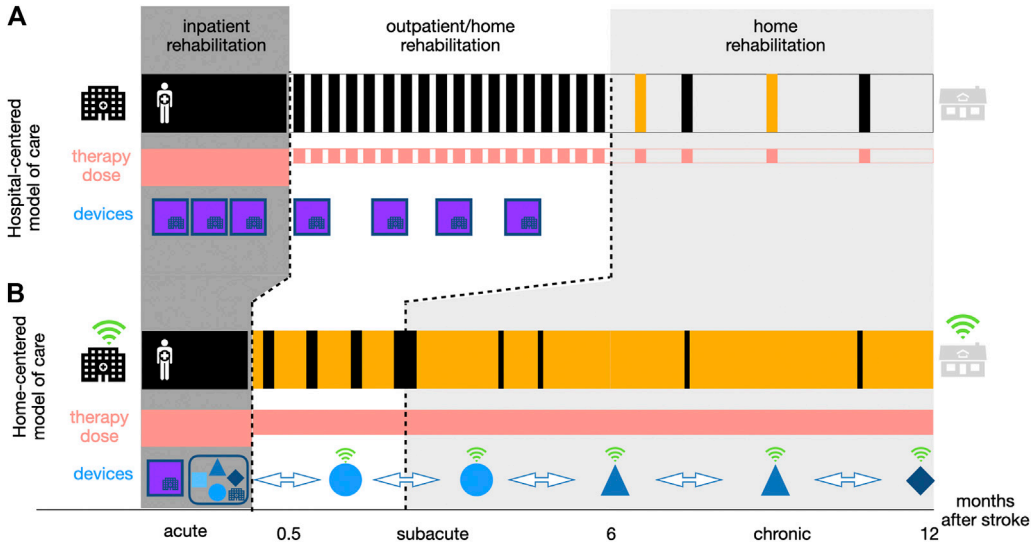

FIGURE 1 | Two approaches to neurorehabilitation along the continuum of care. Compared to the hospital-centered model of stroke rehabilitation (a), the home-centered model of care (b) aims to reduce the time a patient spends in a healthcare institution (depicted in black) physically visiting a rehabilitation professional. However, patients receive a similar or even potentially higher dose of therapy (depicted in red) due to continued self-directed training at home (depicted in yellow). This should be supported by different complementary mobile technology-based devices (e.g., robotics, wearables, virtual reality games) (blue shapes) introduced early in the inpatient rehabilitation (i.e., RehabGym), and that can, after a familiarization phase under therapist supervision, be taken home by patients to continue with a minimally supervized rehabilitation training (i.e., without the presence of a clinician or expert operator). These devices should be intelligent connected tools (depicted in green, more detail on a possible implementation in *Going Beyond COVID-19: Moving Towards Minimally-Supervised Robot-Assisted Therapy*) allowing for remote patient monitoring, while empowering and motivating patients to engage in high-quality therapy from a distance, which is not possible with traditional stationary neurorehabilitation technologies (purple blocks).

way (Mayo et al., 2000; Hillier and Inglis-Jassiem, 2010; Mayo, 2016), digital technologies and artificial intelligence have a key role to play in further establishing and supporting this model, as they could provide patients with intelligent connected tools empowering and motivating them to engage in quality therapy from a distance.

Technologies Supporting Neurorehabilitation From a Distance

A variety of technological approaches have been proposed to support the implementation of neurorehabilitation from a distance, and new developments emerged during the COVID-19 pandemic as possible answers to the limited access to medical facilities. Existing solutions span from simple webinars or mobile phone applications informing patients, to chatbots (i.e., artificial intelligent coaches (Argent et al., 2018; Tudor Car et al., 2020)) demonstrating and encouraging home-based exercises, or virtual reality (VR) exergames sometimes supported by passive instrumented tools (e.g., orthoses, gloves or objects to manipulate) (Nijenhuis et al., 2017). Telerehabilitation (or telemedicine) has already been widely studied as a method to support neurorehabilitation from a distance (Tyagi et al., 2018; Kuah et al., 2019; Laver et al., 2020) and has often been presented as a possible answer to meet neurorehabilitation needs during the COVID-19 pandemic (Chang and Boudier-Revéret, 2020; Turolla et al., 2020). In a typical telerehabilitation scenario, healthcare practitioners interact with patients over a live communication stream, offering the possibility to guide and encourage patients while monitoring their progress. Telerehabilitation approaches that go beyond video/audio support and offer additional connected hardware (e.g., USB-based wrist blood pressure cuff and mat with contact sensitive switches, gaming driving wheel with a special gripper, joysticks, etc.) have been proposed for stroke patients (Johnson et al., 2007; Dodakian et al., 2017; Johnson et al., 2017). Telerehabilitation using socially assistive robots (e.g., a humanoid robot with telepresence and computer vision under the supervision of a remote clinician) can also deliver emotional support and help to increase the patient's motivation (Fasola and Mataric, 2010; Pulido et al., 2019; Sobrepera et al., 2020). Nevertheless, the lack of physical assistance, an essential facilitator for movement therapy in patients with sensorimotor impairments, and the inability to actively measure physiological parameters for providing feedback to improve performance strongly limit such telehealth approaches. Also, most telerehabilitation applications still rely on the synchronous presence and supervision of a rehabilitation professional, thereby not solving the underlying issue of lacking resources for neurorehabilitation.

Active technologies such as robotics, which can guide and assist motion while collecting objective measures of movement quality, might be the key enabler providing access to quality therapy from a distance, without the need for constant supervision by a therapist or expert operator on site. Technology-assisted therapy has been established as a tool to complement conventional rehabilitation in the clinics, with the ability to safely deliver high therapy dose and intensity in suitably selected patients (Veerbeek et al., 2017; Gassert and Dietz, 2018;

Mehrholz et al., 2020). For the upper limb, there is increasing evidence demonstrating that robot-assisted therapy is at least as good as usual care (Ranzani et al., 2020) and provides the unique ability to actively assist patients with physical impairments and objectively monitor performance and engagement through objective sensor measurements. Nevertheless, most rehabilitation robots today remain complex systems (e.g., multi-degrees-of-freedom exoskeletons, or devices requiring precise attachment/positioning of the user, or systems relying on complex graphical user interface where input from an operator is required) that have so far been limited to supervised use in the clinic with close one-to-one monitoring and readily available technical assistance.

GOING BEYOND COVID-19: MOVING TOWARD MINIMALLY SUPERVIZED ROBOT-ASSISTED THERAPY

To fully exploit the potential of rehabilitation technologies such as robotics and truly revolutionize neurorehabilitation delivery, there is a need to move out of the research labs or clinical settings. While few pilot studies have demonstrated feasibility of home self-administered upper extremity training with robots (Sivan et al., 2014; Wolf et al., 2015), this translation remains a major challenge due to multiple key technical and clinical requirements imposed by minimally supervized use.

Technical Requirements and Usability

Realistically, for a rehabilitation robot to be adopted and regularly used by neurological patients in their home environment, it should be: intrinsically safe and user-friendly, portable for easy deployment in homes where available space might be scarce, robust so that little to no maintenance is needed over potentially long periods of use, and scalable (low-cost and relying on typically already available resources in patients' home such as standard electrical and internet connections). Of these technical aspects, ease of use in an independent way is probably the most critical point to ensure acceptance and adoption, and a point that has been so far rarely evaluated in existing robotic technologies for neurorehabilitation (Zhang et al., 2011; Catalan et al., 2018).

Usability considerations (e.g., in the form of user-centered design involving patients in the development process (Meyer et al., 2019)) should be taken into account not only at the level of the hardware (e.g., how to turn it on/off, how to don/doff a device, etc.) but also at the level of the software and graphical user interface, which should be intuitive and easy to navigate for non-experts in computer use, or patients with cognitive deficits (Ranzani et al., 2021). User archetypes created through data generated from actual target users might increase the potential for better design of technology-assisted interventions in stroke rehabilitation (Haldane et al., 2019). Along the same lines, robot-assisted exercises should be easily understandable to ensure safe use and the training of physiologically meaningful exercises.

Clinical Artificial Intelligence

Besides technical requirements, it is fundamental to integrate clinical knowledge into technologies to be used at home in a minimally supervized way. We define here clinical artificial intelligence (cAI) as a combination of medical, psychological and technical knowledge in the form of embedded algorithms analyzing and processing online the data generated by digital technologies. As such, cAI is expected to play a key role in clinical decision making, online adaptation of therapy exercises, and monitoring of progress through the extraction of validated assessment scores (Kanzler et al., 2020). For example, in a typical minimally supervized robot-assisted rehabilitation scenario, it is envisioned that an initial therapy plan (e.g., combination of exercises at a specific dose and intensity in order to achieve selected goals) is established by a therapist during the initial inpatient rehabilitation. However, this initial therapy plan should be able to adapt and evolve based on patients' progress without requiring the direct intervention of the therapist. Algorithms have been proposed, where cAI-based decisions regarding exercise selection were suggested to therapists during supervised rehabilitation in chronic stroke patients, showing strong agreement with therapist perception and decisions (Panarese et al., 2012). In a similar way, several assessment-driven therapy adaptation algorithms of various complexity (e.g., based on online extraction of performance biomarkers, or including machine learning models, etc.) have been proposed and evaluated with stroke patients to tailor rehabilitation exercises to the ability and needs of each patient. Several promising studies, under supervised use in the clinic, validated the feasibility of such algorithms to dynamically adapt difficulty and intensity of therapy exercises on a trial-per-trial basis, thereby ensuring that the therapy remains at an optimal level of challenge to maintain motivation for long term adoption (Metzger et al., 2014; Giang et al., 2020). Finally, cAI algorithms should as well monitor progress on a daily basis and detect potential decline in use and/or performance, with the possibility to feed this information back to the patients and caregivers. In a similar way, cAI should detect undesired symptoms that could lead to pain, increase in muscle tone, or upper limb compensatory movements, which could also be objectively extracted from the collected sensor data (Wittmann et al., 2016; Ranzani et al., 2019; Cai et al., 2020). When a severe abnormal deviation from the normal movement range/trajectories is detected, the cAI should initiate a safety procedure to prevent suboptimal rehabilitation outcomes or, in the worst case, an injury. It should be emphasized that the objective of cAI is not to replace healthcare practitioners, but to support a home-centered model of care where one-to-one presence of therapists is not viable. Communication channels should nevertheless be in place to asynchronously inform clinicians about therapy status and potential deviations e.g., via digital alerts, through the generation of daily reports, or via short digital questionnaires filled by patients/caregivers (de Jong et al., 2014; Hill & Breslin, 2016; Kowatsch et al., 2019). Once an unexpected event during minimally supervized training occurred, the cAI should alert the therapists in the hospital/clinic so that (tele)consultation can be arranged to evaluate the cause and to ensure that appropriate advice can be provided to the patient. These measures will aid in mitigating the risks of injuries.

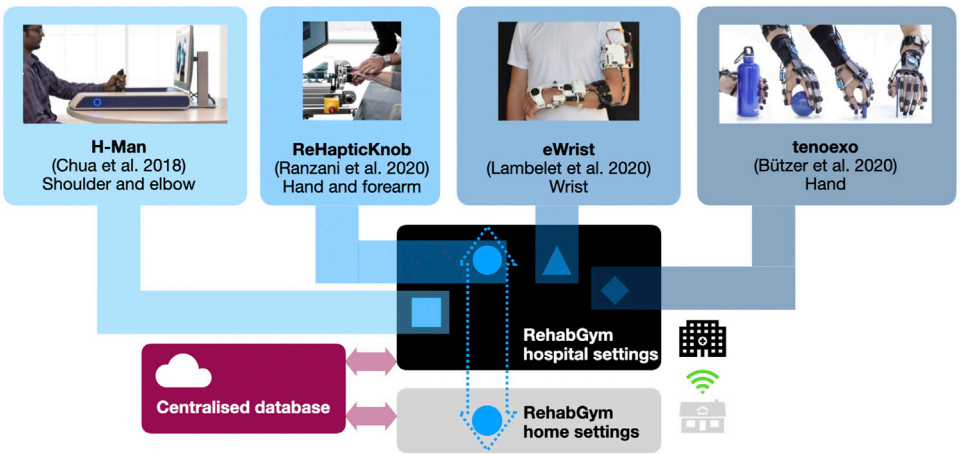

FIGURE 2 | Conceptual overview of a connected RehabGym, with examples of user-friendly and complementary (i.e., targeting all segments of the upper limb) mobile robotic technologies for minimally supervized neurorehabilitation. All technologies are first introduced during inpatient rehabilitation at the hospital, and selected technologies (e.g., the one(s) best adapted to the impairment level and rehabilitation goals of a patient) are taken home upon discharge. Connected devices ensure asynchronous (i.e., not online/real-time), remote communication with healthcare professionals for monitoring purposes.

Towards a Connected RehabGym

A robotic device for minimally supervized rehabilitation combined with cAI bears high potential for treating selected patients. However, as for any therapy, a more holistic approach is needed since patients with various impairment levels will have different needs and therapy goals that could hardly be met by a single device. The transition to a technology-supported home-centered model of care may therefore rely on a network of modular rehabilitation technologies that are complementary and interconnected within a common digital therapy platform. In this ideal concept of a connected "RehabGym", we foresee simple, dedicated, rehabilitation technologies targeting different body segments (e.g., shoulder/elbow, wrist, hand), motor function (e.g. reaching, grasping, haptic exploration) and impairment level (from hemiparetic to highly functional patients) being proposed as a battery of digital interventions available for the treatment of a patient. A common digital therapy platform offers the unique advantage of sharing user-interaction features between devices, to improve usability and help seamlessly transition from one device to the other (e.g., within a therapy session, or over the course of rehabilitation). **Figure 2** presents a possible set of selected user-friendly, mobile, complementary robotic systems targeting different components of the upper limb, that could be used as a basis to implement such a connected RehabGym concept (Chua et al., 2018; Butzer et al., 2020; Lambelet et al., 2020; Ranzani et al., 2020; Ranzani et al., 2021).

One possible implementation avenue would be to first deploy the RehabGym technologies in hospital settings, where a patient could familiarize with the use of each technology during the essential inpatient rehabilitation (under supervision), and where rehabilitation practitioners could identify which technologies are most likely to benefit a patient. This initial supervised step is certainly fundamental to ensure safe use of a robotic technology and adoption by the user. In the clinic, such a room equipped with multiple complementary devices could be operated with a single therapist supervising multiple patients, which should provide a cost-effective solution (Hesse et al., 2014; Bustamante Valles et al., 2016) and a compatible approach to minimized one-to-one interactions.

Upon discharge, a patient could then take home a selected rehabilitation technology to continue therapy in a minimally supervized manner. If available, the patient's caregiver(s)/family will also be instructed on how to operate the device(s) safely and how to optimally support the rehabilitation process (e.g., support setting up devices and promoting motivation and compliance). Caregivers and family could play an essential role in assisting patients who are not so familiar with handling devices or suffer from more severe impairments, thereby ensuring a successful transfer of the RehabGym to the home environment. Cloud computing should enable data exchange to a centralized database where patient profiles (e.g., data from all RehabGym technologies used by the patient, collected digital health biomarkers, as well as clinical assessment data) are stored and can be accessed remotely by a cAI concept shared by all devices of the connected RehabGym. It should be noted that the system should be operational even if the internet connection is slow or instable, which can be ensured by asynchronous data exchange and storage on the cloud. The cloud for the RehabGym should be securely hosted either within the hospital IT infrastructure or by a third party who is accountable for information security (e.g., data confidentially, integrity and availability). Algorithms should update therapy plans and other training parameters (e.g., suggest transfer to another RehabGym device/exercise), and inform on overall rehabilitation progress. Additionally, exercise adherence and motivation could be increased by integrating a conversational agent (i.e., chatbot) that educates users on relevant topics (e.g., healthy lifestyle) and provides personalized motivational messages, as well as real-time exercise support, monitoring, and feedback as previously shown for

physiotherapy patients and home exercise in a hands-free augmented reality environment (Kowatsch et al., 2021). Building a strong "virtual" working alliance between a chatbot interface and a patient might prove a promising tool to improve the acceptance of the connected RehabGym and avoid mental/social distress caused by isolation. However, it should certainly not replace regular in-person controls with healthcare practitioners if possible.

In controlled clinical settings (non-connected) RehabGym concepts with complementary upper limb robotic devices have proved feasible for stroke patients with moderate to severe upper limb impairment (Lo et al., 2010; Hesse et al., 2014; Bustamante Valles et al., 2016). These studies, however, did not directly investigate how to personalize therapy plans to best leverage on a set of complementary devices, nor did they investigate the feasibility of transferring such technologies to the home of patients. Building on our previous studies, we envision that moving to such a connected RehabGym to home settings and additionally targeting more distal upper limb components should be more suited for patients with mild to moderate upper limb impairment, and without severe cognitive deficit (Lambercy et al., 2011; Chua et al., 2018; Ranzani et al., 2020).

Potential Implementation Barriers

While promising, digital technologies will not solve all problems in the delivery of neurorehabilitation service, nor will they completely replace face-to-face visits. The idea of a connected RehabGym is to provide a new complementary model to existing rehabilitation approaches. The provision of minimally supervized therapy to neurological patients will raise a new set of questions that will need to be carefully addressed for successful implementation.

The selection of suitable patients and pairing with adequate technology-assisted therapies are necessary to ensure positive delivery and experiences of such a minimally supervized therapeutic model. Clinical considerations include patient impairment severity, medical fitness and motivation, desired rehabilitation goals, and available social supports. Certain groups of patients might find it difficult to accept this new paradigm of care, in particular the cognitively impaired, visually challenged, elderly and technologically non-savvy.

Ethical concerns may arise from patients and their families at several levels when a connected technology is introduced in the home environment, for example with respect to safety, access, privacy, data protection and respect for autonomy (Cavoukian et al., 2010). There would be anticipated needs to provide heightened cybersecurity infrastructure between healthcare institutions and technology providers, as patients' anonymized data may need to be accessed by remote servers for processing and continuous refinement of cAI algorithms. In general, ethical frameworks related to the use of cAI for decision making in the context of healthcare are still in their infancy, and should be carefully studied in view of the increasing amount of connected tools generating health-related data (Magrabi et al., 2019).

Finally, the adoption of technology in and out of clinic may not always hinge on hard evidence or clinical effectiveness, but rather technology robustness, subjective preferences, or technological proponents and partnerships (Backus et al., 2010; Turchetti et al., 2014; Chua and Kuah, 2017). Access to rehabilitation technology in low- and middle-income countries also needs to be considered and the proposed connected RehabGym would need to be adapted for low-resource environments with less robust infrastructure (e.g., power, internet) and limited access to rehabilitation services. Cost considerations, and in particular billing and reimbursement models for such novel means of neurorehabilitation delivery should also be carefully studied to ensure its viability on a large scale. In particular, possible device rental models should be explored to minimize the treatment costs for the individual and further promote flexibility in therapy plan adjustment.

CONCLUSION

Technology plays a key role in times of the COVID-19 pandemic for solving problems in essential healthcare delivery such as in neurorehabilitation. We proposed an approach to implement neurorehabilitation from a distance, through the use of digital connected interventions (e.g., minimally supervized robot-assisted therapy) that could accompany stroke patients along the continuum of care, from the hospital to their home.

For technology-based models of neurorehabilitation from a distance to become successful, three factors are crucial for their implementation: firstly, the technologies need to meet technical requirements such as robustness, safety and usability since patients train with at least one device at home (i.e., the most suitable device according to patients' needs). Secondly, rehabilitation technologies should be scalable (i.e., easily applicable to the increasing number of patients in need of such treatment, which implies social, technical, economical and infrastructure considerations) in order to be impactful. Thirdly, the implementation of artificial intelligence embedded in neurorehabilitation technologies needs to be clinically motivated and transparent to patients, caregivers and healthcare practitioners in order to increase the trust in technology-assisted rehabilitation in a home-centered model. All these aspects are essential to ensure that neurological patients accept rehabilitation technologies and actively self-engage in therapy (Neibling et al., 2021).

The proposed model of neurorehabilitation is likely to impact neurorehabilitation beyond the COVID-19 pandemic, by providing broad access to sustained, high-quality and high-dose therapy to maximize long-term functional outcomes and promote stroke survivors' independence and quality of life. Such a paradigm shift is bound to happen, and COVID-19 may act as an accelerator for the adoption by patients, caregivers and rehabilitation practitioners and for the market penetration of the proposed technology-assisted rehabilitation (Keesara et al., 2020). However, such a new approach to stroke rehabilitation can only become successful in the future if it is accompanied by a holistic digital transformation of healthcare systems, including appropriate responses by authorities, healthcare providers, and insurance companies.

DATA AVAILABILITY STATEMENT

The original contributions presented in the study are included in the article/Supplementary Material, further inquiries can be directed to the corresponding authors.

AUTHOR CONTRIBUTIONS

OL, RL, RG, and NW conceived the article's narrative; OL and RL wrote the manuscript text and prepared the figures; all authors read, corrected and approved the final manuscript.

FUNDING

This research is supported by the National Research Foundation, Prime Minister's Office, Singapore under its Campus for Research Excellence and Technological Enterprise (CREATE) program.

ACKNOWLEDGMENTS

The research was conducted at the Future Health Technologies program which was established collaboratively between ETH Zurich and the National Research Foundation Singapore.

REFERENCES

Argent, R., Daly, A., and Caulfield, B. (2018). Patient Involvement with Home-Based Exercise Programs: Can Connected Health Interventions Influence Adherence? *JMIR Mhealth Uhealth* 6 (3), e47. doi:10.2196/mhealth.8518

Backus, D., Winchester, P., and Tefertiller, C. (2010). Translating Research into Clinical Practice: Integrating Robotics into Neurorehabilitation for Stroke Survivors. *Top. Stroke Rehabil.* 17 (5), 362–370. doi:10.1310/tsr1705-362

Bersano, A., Kraemer, M., Touzé, E., Weber, R., Alamowitch, S., Sibon, I., et al. (2020). Stroke Care during the COVID-19 Pandemic: Experience from Three Large European Countries. *Eur. J. Neurol.* 27 (9), 1794–1800. doi:10.1111/ene.14375

Bustamante Valles, K., Montes, S., Madrigal, M. d. J., Burciaga, A., Martínez, M. E., and Johnson, M. J. (2016). Technology-assisted Stroke Rehabilitation in Mexico: a Pilot Randomized Trial Comparing Traditional Therapy to Circuit Training in a Robot/technology-Assisted Therapy Gym. *J. Neuroengineering Rehabil.* 13 (1), 83. doi:10.1186/s12984-016-0190-1

Butzer, T., Lambercy, O., Arata, J., and Gassert, R. (2020). Fully Wearable Actuated Soft Exoskeleton for Grasping Assistance in Everyday Activities. *Soft Robot* 8 (2), 128–143. doi:10.1089/soro.2019.0135

Cai, S., Li, G., Su, E., Wei, X., Huang, S., Ma, K., et al. (2020). Real-time Detection of Compensatory Patterns in Patients with Stroke to Reduce Compensation during Robotic Rehabilitation Therapy. *IEEE J. Biomed. Health Inform.* 24 (9), 2630–2638. doi:10.1109/JBHI.2019.2963365

Caso, V., and Federico, A. (2020). No Lockdown for Neurological Diseases during COVID19 Pandemic Infection. *Neurol. Sci.* 41 (5), 999–1001. doi:10.1007/s10072-020-04389-3

Catalan, J. M., Garcia, J. V., Lopez, D., Diez, J., Blanco, A., Lledo, L. D., et al. (2018). Patient Evaluation of an Upper-Limb Rehabilitation Robotic Device for Home Use. in 7th IEEE International Conference on Biomedical Robotics and Biomechatronics (Biorob). doi:10.1109/biorob.2018.8487201

Cavoukian, A., Fisher, A., Killen, S., and Hoffman, D. A. (2010). Remote Home Health Care Technologies: How to Ensure Privacy? Build it in: Privacy by Design. *Idis* 3 (2), 363–378. doi:10.1007/s12394-010-0054-y

Chang, M. C., and Boudier-Revéret, M. (2020). Usefulness of Telerehabilitation for Stroke Patients during the COVID-19 Pandemic. *Am. J. Phys. Med. Rehabil.* 99 (7), 582. doi:10.1097/phm.0000000000001468

Chua, K., Kuah, C., Ng, C., Yam, L., Budhota, A., Contu, S., et al. (2018). Clinical and Kinematic Evaluation of the H-Man Arm Robot for Post-stroke Upper Limb Rehabilitation: Preliminary Findings of a Randomised Controlled Trial. *Ann. Phys. Rehabil. Med.* 61, e95. doi:10.1016/j.rehab.2018.05.203

Chua, K. S. G., and Kuah, C. W. K. (2017). Innovating with Rehabilitation Technology in the Real World. *Am. J. Phys. Med. Rehabil.* 96 (10 Suppl. 1), S150–S156. doi:10.1097/phm.0000000000000799

Dafer, R. M., Osteraas, N. D., and Biller, J. (2020). Acute Stroke Care in the Coronavirus Disease 2019 Pandemic. *J. Stroke Cerebrovasc. Dis.* 29 (7), 104881. doi:10.1016/j.jstrokecerebrovasdis.2020.104881

Daly, J. J., McCabe, J. P., Holcomb, J., Monkiewicz, M., Gansen, J., and Pundik, S. (2019). Long-Dose Intensive Therapy Is Necessary for Strong, Clinically Significant, Upper Limb Functional Gains and Retained Gains in Severe/Moderate Chronic Stroke. *Neurorehabil. Neural Repair* 33 (7), 523–537. doi:10.1177/1545968319846120

de Jong, C. C., Ros, W. J., and Schrijvers, G. (2014). The Effects on Health Behavior and Health Outcomes of Internet-Based Asynchronous Communication between Health Providers and Patients with a Chronic Condition: a Systematic Review. *J. Med. Internet Res.* 16 (1), e19. doi:10.2196/jmir.3000

De Sousa, D. A., van der Worp, H. B., Caso, V., Cordonnier, C., Strbian, D., Ntaios, G., et al. (2020). Maintaining Stroke Care in Europe during the COVID-19 Pandemic: Results from an International Survey of Stroke Professionals and Practice Recommendations from the European Stroke Organisation. *Eur. Stroke J.* 5 (3), 230–236. doi:10.1177/2396987320933746

Dodakian, L., McKenzie, A. L., Le, V., See, J., Pearson-Fuhrhop, K., Burke Quinlan, E., et al. (2017). A Home-Based Telerehabilitation Program for Patients with Stroke. *Neurorehabil. Neural Repair* 31 (10-11), 923–933. doi:10.1177/1545968317733818

Fasola, J., and Mataric, M. J. (2010). *Robot Exercise Instructor: A Socially Assistive Robot System to Monitor and Encourage Physical Exercise for the Elderly*. Ieee Ro-Man, 416–421.

Galea, M. D. (2019). Telemedicine in Rehabilitation. *Phys. Med. Rehabil. Clin. North America* 30 (2), 473–483. doi:10.1016/j.pmr.2018.12.002

Gassert, R., and Dietz, V. (2018). Rehabilitation Robots for the Treatment of Sensorimotor Deficits: a Neurophysiological Perspective. *J. Neuroengineering Rehabil.* 15 (1), 46. doi:10.1186/s12984-018-0383-x

GBD (2018). Global, Regional, and National Disability-Adjusted Life-Years (DALYs) for 359 Diseases and Injuries and Healthy Life Expectancy (HALE) for 195 Countries and Territories, 1990-2017: a Systematic Analysis for the Global Burden of Disease Study 2017. *Lancet* 392 (10159), 1859–1922. doi:10.1016/S0140-6736(18)32335-3

Giang, C., Pirondini, E., Kinany, N., Pierella, C., Panarese, A., Coscia, M., et al. (2020). Motor Improvement Estimation and Task Adaptation for Personalized Robot-Aided Therapy: a Feasibility Study. *Biomed. Eng. Online* 19 (1), 33. doi:10.1186/s12938-020-00779-y

Haldane, V., Koh, J. J. K., Srivastava, A., Teo, K. W. Q., Tan, Y. G., Cheng, R. X., et al. (2019). User Preferences and Persona Design for an mHealth Intervention to Support Adherence to Cardiovascular Disease Medication in Singapore: A Multi-Method Study. *JMIR Mhealth Uhealth* 7 (5), e10465. doi:10.2196/10465

Hesse, S., Heß, A., Werner C, C., Kabbert, N., and Buschfort, R. (2014). Effect on Arm Function and Cost of Robot-Assisted Group Therapy in Subacute Patients with Stroke and a Moderately to Severely Affected Arm: a Randomized Controlled Trial. *Clin. Rehabil.* 28 (7), 637–647. doi:10.1177/0269215513516967

Hidaka, Y., Han, C. E., Wolf, S. L., Winstein, C. J., and Schweighofer, N. (2012). Use it and Improve it or Lose it: Interactions between Arm Function and Use in Humans Post-stroke. *Plos Comput. Biol.* 8 (2), e1002343. doi:10.1371/journal.pcbi.1002343

Hill, A. J., and Breslin, H. M. (2016). Refining an Asynchronous Telerehabilitation Platform for Speech-Language Pathology: Engaging End-Users in the Process. *Front. Hum. Neurosci.* 10, 640. doi:10.3389/fnhum.2016.00640

Hillier, S., and Inglis-Jassiem, G. (2010). Rehabilitation for Community-Dwelling People with Stroke: Home or Centre Based? A Systematic Review. *Int. J. Stroke* 5 (3), 178–186. doi:10.1111/j.1747-4949.2010.00427.x

Johnson, M. J., Feng, X., Johnson, L. M., and Winters, J. M. (2007). Potential of a Suite of Robot/computer-Assisted Motivating Systems for Personalized, Home-Based, Stroke Rehabilitation. *J. Neuroengineering Rehabil.* 4, 6. doi:10.1186/1743-0003-4-6

Johnson, M. J., Rai, R., Barathi, S., Mendonca, R., and Bustamante-Valles, K. (2017). Affordable Stroke Therapy in High-, Low- and Middle-Income Countries: From Theradrive to Rehab CARES, a Compact Robot Gym. *J. Rehabil. Assistive Tech. Eng.* 4, 205566831770873. doi:10.1177/2055668317708732

Jordan, R. E., Adab, P., and Cheng, K. K. (2020). Covid-19: Risk Factors for Severe Disease and Death. *BMJ* 368, m1198. doi:10.1136/bmj.m1198

Kanzler, C. M., Rinderknecht, M. D., Schwarz, A., Lamers, I., Gagnon, C., Held, J. P. O., et al. (2020). A Data-Driven Framework for Selecting and Validating Digital Health Metrics: Use-Case in Neurological Sensorimotor Impairments. *Npj Digit. Med.* 3, 80. doi:10.1038/s41746-020-0286-7

Keesara, S., Jonas, A., and Schulman, K. (2020). Covid-19 and Health Care's Digital Revolution. *N. Engl. J. Med.* 382 (23), e82. doi:10.1056/nejmp2005835

Kowatsch, T., Lohse, K.-M., Erb, V., Schittenhelm, L., Galliker, H., Lehner, R., et al. (2021). Hybrid Ubiquitous Coaching with a Novel Combination of Mobile and Holographic Conversational Agents Targeting Adherence to Home Exercises: Four Design and Evaluation Studies. *J. Med. Internet Res.* 23 (2), e23612. doi:10.2196/23612

Kowatsch, T., Otto, L., Harperink, S., Cotti, A., and Schlieter, H. (2019). A Design and Evaluation Framework for Digital Health Interventions. *Inf. Tech.* 61 (5-6), 253–263. doi:10.1515/itit-2019-0019

Kuah, C. W. K., Abdullah Huin, S. H., Chwee Ng, Y., Wee, S. K., Loh, Y. J., and Geok Chua, K. S. (2019). Post-stroke Outpatient and Home Tele-Rehabilitation with Jintronix System: a Feasibility Study in *CAREhab* (Singapore).

Lambelet, C., Temiraliuly, D., Siegenthaler, M., Wirth, M., Woolley, D. G., Lambercy, O., et al. (2020). Characterization and Usability Evaluation of a Fully Wearable Wrist Exoskeleton for Unsupervised Training after Stroke. *J. Neuroeng Rehabil.* 17 (1), 132. in press. doi:10.1186/s12984-020-00749-4

Lambercy, O., Dovat, L., Yun, H., Wee, S. K., Kuah, C. W., Chua, K. S., et al. (2011). Effects of a Robot-Assisted Training of Grasp and Pronation/supination in Chronic Stroke: a Pilot Study. *J. Neuroengineering Rehabil.* 8, 63. doi:10.1186/1743-0003-8-63

Laver, K. E., Schoene, D., Crotty, M., George, S., Lannin, N. A., and Sherrington, C. (2020). Telerehabilitation Services for Stroke. *Cochrane Database Syst. Rev.* 1, CD010255. doi:10.1002/14651858.CD010255.pub2

Lo, A. C., Guarino, P. D., Richards, L. G., Haselkorn, J. K., Wittenberg, G. F., Federman, D. G., et al. (2010). Robot-assisted Therapy for Long-Term Upper-Limb Impairment after Stroke. *N. Engl. J. Med.* 362 (19), 1772–1783. doi:10.1056/nejmoa0911341

Magrabi, F., Ammenwerth, E., McNair, J. B., De Keizer, N. F., Hyppönen, H., Nykänen, P., et al. (2019). Artificial Intelligence in Clinical Decision Support: Challenges for Evaluating AI and Practical Implications. *Yearb. Med. Inform.* 28 (1), 128–134. doi:10.1055/s-0039-1677903

Mayo, N. E. (2016). Stroke Rehabilitation at Home. *Stroke* 47 (6), 1685–1691. doi:10.1161/strokeaha.116.011309

Mayo, N. E., Wood-Dauphinee, S., Cote, R., Gayton, D., Carlton, J., Buttery, J., et al. (2000). There's No Place like Home. *Stroke* 31 (5), 1016–1023. doi:10.1161/01.str.31.5.1016

Mehrholz, J., Pollock, A., Pohl, M., Kugler, J., and Elsner, B. (2020). Systematic Review with Network Meta-Analysis of Randomized Controlled Trials of Robotic-Assisted Arm Training for Improving Activities of Daily Living and Upper Limb Function after Stroke. *J. Neuroengineering Rehabil.* 17 (1), 83. doi:10.1186/s12984-020-00715-0

Metzger, J.-C., Lambercy, O., Califfi, A., Dinacci, D., Petrillo, C., Rossi, P., et al. (2014). Assessment-driven Selection and Adaptation of Exercise Difficulty in Robot-Assisted Therapy: a Pilot Study with a Hand Rehabilitation Robot. *J. NeuroEngineering Rehabil.* 11, 154. doi:10.1186/1743-0003-11-154

Meyer, J. T., Schrade, S. O., Lambercy, O., and Gassert, R. (2019). User-centered Design and Evaluation of Physical Interfaces for an Exoskeleton for Paraplegic Users. *IEEE Int. Conf. Rehabil. Robot* 2019, 1159–1166. doi:10.1109/ICORR.2019.8779527

Neibling, B. A., Jackson, S. M., Hayward, K. S., and Barker, R. N. (2021). Perseverance with Technology-Facilitated Home-Based Upper Limb Practice after Stroke: a Systematic Mixed Studies Review. *J. Neuroengineering Rehabil.* 18 (1), 43. doi:10.1186/s12984-021-00819-1

Nicholson, S., Sniehotta, F. F., van Wijck, F., Greig, C. A., Johnston, M., McMurdo, M. E. T., et al. (2013). A Systematic Review of Perceived Barriers and Motivators to Physical Activity after Stroke. *Int. J. Stroke* 8 (5), 357–364. doi:10.1111/j.1747-4949.2012.00880.x

Nijenhuis, S. M., Prange-Lasonder, G. B., Stienen, A. H., Rietman, J. S., and Buurke, J. H. (2017). Effects of Training with a Passive Hand Orthosis and Games at Home in Chronic Stroke: a Pilot Randomised Controlled Trial. *Clin. Rehabil.* 31 (2), 207–216. doi:10.1177/0269215516629722

Panarese, A., Colombo, R., Sterpi, I., Pisano, F., and Micera, S. (2012). Tracking Motor Improvement at the Subtask Level during Robot-Aided Neurorehabilitation of Stroke Patients. *Neurorehabil. Neural Repair* 26 (7), 822–833. doi:10.1177/1545968311431966

Pulido, J. C., Suarez-Mejias, C., Gonzalez, J. C., Duenas Ruiz, A., Ferrand Ferri, P., Martinez Sahuquillo, M. E., et al. (2019). A Socially Assistive Robotic Platform for Upper-Limb Rehabilitation: A Longitudinal Study with Pediatric Patients. *IEEE Robot. Automat. Mag.* 26 (2), 24–39. doi:10.1109/mra.2019.2905231

Ranzani, R., Eicher, L., Viggiano, F., Engelbrecht, B., Held, J., Lambercy, O., et al. (2021). *Towards a Platform for Robot-Assisted Minimally-Supervised Therapy of Hand Function: Design and Pilot Usability Evaluation*. New Haven medRxiv, 2021. doi:10.1101/2021.01.12.21249685

Ranzani, R., Lambercy, O., Metzger, J.-C., Califfi, A., Regazzi, S., Dinacci, D., et al. (2020). Neurocognitive Robot-Assisted Rehabilitation of Hand Function: a Randomized Control Trial on Motor Recovery in Subacute Stroke. *J. Neuroengineering Rehabil.* 17 (1), 115. doi:10.1186/s12984-020-00746-7

Ranzani, R., Viggiano, F., Engelbrecht, B., Held, J. P. O., Lambercy, O., and Gassert, R. (2019). Method for Muscle Tone Monitoring during Robot-Assisted Therapy of Hand Function: A Proof of Concept. *IEEE Int. Conf. Rehabil. Robot* 2019, 957–962. doi:10.1109/ICORR.2019.8779454

Richter, D., Eyding, J., Weber, R., Bartig, D., Grau, A., Hacke, W., et al. (2021). Analysis of Nationwide Stroke Patient Care in Times of COVID-19 Pandemic in Germany. *Stroke* 52 (2), 716–721. doi:10.1161/strokeaha.120.033160

Sivan, M., Gallagher, J., Makower, S., Keeling, D., Bhakta, B., O'Connor, R. J., et al. (2014). Home-based Computer Assisted Arm Rehabilitation (hCAAR) Robotic Device for Upper Limb Exercise after Stroke: Results of a Feasibility Study in Home Setting. *J. NeuroEngineering Rehabil.* 11, 163. doi:10.1186/1743-0003-11-163

Sobrepera, M. J., Lee, V. G., and Johnson, M. J. (2020). *The Design of Lil'Flo, a Socially Assistive Robot for Upper Extremity Motor Assessment and Rehabilitation in the Community via Telepresence*. New Haven medRxiv. doi:10.1101/2020.04.07.20047696

Taub, E., Uswatte, G., Mark, V. W., and Morris, D. M. (2006). The Learned Nonuse Phenomenon: Implications for Rehabilitation. *Eura Medicophys* 42 (3), 241–256. doi:10.1037/0090-5550.50.1.34

Tudor Car, L., Dhinagaran, D. A., Kyaw, B. M., Kowatsch, T., Joty, S., Theng, Y.-L., et al. (2020). Conversational Agents in Health Care: Scoping Review and Conceptual Analysis. *J. Med. Internet Res.* 22 (8), e17158. doi:10.2196/17158

Turchetti, G., Lorenzoni, V., Bellelli, S., Pierotti, F., Rovai, D., Caselli, C., et al. (2014). Effectiveness and Costs of Different Strategies for the Diagnosis of Stable Coronary Artery Disease Results from the Evinci Study. *Value in Health* 17 (7), A474. doi:10.1016/j.jval.2014.08.1352

Turolla, A., Rossettini, G., Viceconti, A., Palese, A., and Geri, T. (2020). Musculoskeletal Physical Therapy during the COVID-19 Pandemic: Is Telerehabilitation the Answer? *Phys. Ther.* 100 (8), 1260–1264. doi:10.1093/ptj/pzaa093

Tyagi, S., Lim, D. S. Y., Ho, W. H. H., Koh, Y. Q., Cai, V., Koh, G. C. H., et al. (2018). Acceptance of Tele-Rehabilitation by Stroke Patients: Perceived Barriers and Facilitators. *Arch. Phys. Med. Rehabil.* 99 (12), 2472–2477. doi:10.1016/j.apmr.2018.04.033

Veerbeek, J. M., Langbroek-Amersfoort, A. C., van Wegen, E. E. H., Meskers, C. G. M., and Kwakkel, G. (2017). Effects of Robot-Assisted Therapy for the Upper Limb after Stroke. *Neurorehabil. Neural Repair* 31 (2), 107–121. doi:10.1177/1545968316666957

Ward, N. S., Brander, F., and Kelly, K. (2019). Intensive Upper Limb Neurorehabilitation in Chronic Stroke: Outcomes from the Queen Square Programme. *J. Neurol. Neurosurg. Psychiatry* 90 (5), 498–506. doi:10.1136/jnnp-2018-319954

Wittmann, F., Held, J. P., Lambercy, O., Starkey, M. L., Curt, A., Höver, R., et al. (2016). Self-directed Arm Therapy at Home after Stroke with a Sensor-Based Virtual Reality Training System. *J. Neuroengineering Rehabil.* 13 (1), 75. doi:10.1186/s12984-016-0182-1

Wolf, S. L., Sahu, K., Bay, R. C., Buchanan, S., Reiss, A., Linder, S., et al. (2015). The HAAPI (Home Arm Assistance Progression Initiative) Trial. *Neurorehabil. Neural Repair* 29 (10), 958–968. doi:10.1177/1545968315575612

Zhang, H., Austin, H., Buchanan, S., Herman, R., Koeneman, J., and He, J. (2011). Feasibility Studies of Robot-Assisted Stroke Rehabilitation at Clinic and Home Settings Using RUPERT. *IEEE Int. Conf. Rehabil. Robot* 2011, 5975440. doi:10.1109/ICORR.2011.5975440

Conflict of Interest: AH and DC hold equity positions in ARTICARES Pte. Ltd., a company that manufactures robotic devices for rehabilitation. AH is also the acting CEO of ARTICARES Pte. Ltd. GA-O is the acting Head of Research and Development at ARTICARES Pte. Ltd.

The remaining authors declare that the research was conducted in the absence of any commercial or financial relationships that could be construed as a potential conflict of interest.

frontiers in Robotics and AI

ORIGINAL RESEARCH
published: 07 May 2021
doi: 10.3389/frobt.2021.612855

A COVID-19 Emergency Response for Remote Control of a Dialysis Machine with Mobile HRI

*Hassam Khan Wazir, Christian Lourido, Sonia Mary Chacko and Vikram Kapila**

Mechatronics, Controls, and Robotics Laboratory, Mechanical and Aerospace Engineering Department, NYU Tandon School of Engineering, Brooklyn, NY, United States

Healthcare workers face a high risk of contagion during a pandemic due to their close proximity to patients. The situation is further exacerbated in the case of a shortage of personal protective equipment that can increase the risk of exposure for the healthcare workers and even non-pandemic related patients, such as those on dialysis. In this study, we propose an emergency, non-invasive remote monitoring and control response system to retrofit dialysis machines with robotic manipulators for safely supporting the treatment of patients with acute kidney disease. Specifically, as a proof-of-concept, we mock-up the touchscreen instrument control panel of a dialysis machine and live-stream it to a remote user's tablet computer device. Then, the user performs touch-based interactions on the tablet device to send commands to the robot to manipulate the instrument controls on the touchscreen of the dialysis machine. To evaluate the performance of the proposed system, we conduct an accuracy test. Moreover, we perform qualitative user studies using two modes of interaction with the designed system to measure the user task load and system usability and to obtain user feedback. The two modes of interaction included a touch-based interaction using a tablet device and a click-based interaction using a computer. The results indicate no statistically significant difference in the relatively low task load experienced by the users for both modes of interaction. Moreover, the system usability survey results reveal no statistically significant difference in the user experience for both modes of interaction except that users experienced a more consistent performance with the click-based interaction *vs.* the touch-based interaction. Based on the user feedback, we suggest an improvement to the proposed system and illustrate an implementation that corrects the distorted perception of the instrumentation control panel live-stream for a better and consistent user experience.

Keywords: COVID-19, interface, human-robot interaction, manipulation, remote interaction, robotics

OPEN ACCESS

Edited by:
Simon DiMaio,
Intuitive Surgical, Inc., United States

Reviewed by:
Xiao Xiao,
National University of Singapore, Singapore
Amol Dattatraya Mali,
University of Wisconsin–Milwaukee, United States

****Correspondence:***
Vikram Kapila
vkapila@nyu.edu

Specialty section:
This article was submitted to Biomedical Robotics, a section of the journal Frontiers in Robotics and AI

Received: *30 September 2020*
Accepted: *04 February 2021*
Published: *07 May 2021*

Citation:
Wazir HK, Lourido C, Chacko SM and Kapila V (2021) A COVID-19 Emergency Response for Remote Control of a Dialysis Machine with Mobile HRI. Front. Robot. AI 8:612855. doi: 10.3389/frobt.2021.612855

1 INTRODUCTION

Last few decades have witnessed widespread adoption of robotic solutions by several industries for operations that are considered difficult or dangerous for humans to perform (Trevelyan et al., 2008). In the automotive industry, for example, heavy-duty industrial manipulators form an integral part of the assembly line (Hägele et al., 2016) and one would be hard-pressed to find an automotive manufacturing facility that does not employ some sort of robotic assistance. Moreover, robots are actively being developed, examined, and used for inspection, decontamination, and

decommissioning of nuclear plants (Nagatani et al., 2013; Krotkov et al., 2017); search and rescue operations following natural, industrial, and man-made disasters (Murphy et al., 2008); and exploration in outer space (Yoshida and Wilcox, 2008). The above examples have one common thread, i.e., obviating the exposure to harm and risk to human safety. Thus, when operating in hazardous environments, in most cases the robots act as a physical extension of their human operators to enhance their dexterity, sensory experience, and cognition (Wang et al., 2015). Endowing a human operator with the ability to utilize the robot to its maximum potential requires the development of intuitive user interfaces for human-robot interaction (HRI). In recent years, several advancements have been made to render the HRI as seamless as it can be.

HRI is a rapidly advancing research field with several active areas of application that include human supervised control of robots, autonomous robot control, and human-robot social interaction (Sheridan, 2016). The human supervised control can be further divided into proximal *vs.* remote control, the latter of which includes teleoperation and telerobotics (Sheridan, 1992). In a hazard-prone, high-risk environment, the use of remotely controlled robots is preferable over proximally controlled robots because the human operator can perform the required tasks from a safe remote location. Varied HRI modalities for telerobotics have been developed over the years and each approach achieves a particular objective. Some early examples of HRI for telerobotics include using a joystick for teleoperation (Yamada et al., 2009), performing stroke gestures on a touchscreen (Sakamoto et al., 2008) and pointing gestures using a camera (Abidi et al., 2013), and using a wearable sleeve (Wolf et al., 2013). In recent years, as mobile devices (e.g., smartphones and tablets) have become ubiquitous in our personal and work environments, users have gained increased comfort in utilizing the rear-facing cameras of mobile devices to interact with their environments. Since mobile devices with well-endowed sensing, interaction, communication, and computing functionality are readily available to the common user, mobile mixed-reality interfaces have become greatly accessible and do not require research-grade devices to implement algorithms that were previously thought to be computationally expensive. Recent implementations of augmented reality (AR) based approaches include tracking a single or multiple fiducial markers on the robot (Hashimoto et al., 2011; Kasahara et al., 2013) or its surroundings (Frank et al., 2017a; Chacko and Kapila, 2019) to determine the pose of the robot or objects in its workspace. Other studies have used this approach for multi-robot tracking and control (Frank et al., 2017b). Although marker-based tracking has its merits, with the advent of markerless technologies, e.g., Google's AR Core (Lanham, 2018; Google, 2020), the tracking can be performed in even unstructured environments while using highly intuitive user interfaces. Studies such as Frank et al. (2017a) and Chacko and Kapila (2019) have explored the potential of directing a robot manipulator to perform pick-and-place tasks using virtual elements in a semi-autonomous manner with the aid of a human collaborator. Another study suggests the use of virtual waypoints to guide a robot along a path (Chacko et al., 2020). With telerobotics and HRI being used for myriad applications, we propose to use these approaches in a healthcare setting and show that telerobotics and intuitive HRI can obviate the need for patients and healthcare workers to be exposed to high-risk interactions during a pandemic.

Medical caregivers such as doctors and nurses share physical space and interact with patients routinely. These shared spaces have a higher concentration of pathogens, which makes their occupants particularly susceptible to contracting bacterial and viral infections. The situation is exacerbated in the case of an epidemic, or more importantly a pandemic, which can lead to a widespread shortage of personal protective equipment (PPE) and increase the risk of contagion for both the caregivers and patients in a medical facility. A contemporary, and still developing, example of this situation is the spread of the novel coronavirus pandemic across the world, including in the United States. Since the spring of 2020, there has been a massive global shortage of PPE, including face masks, eye protection, respirators, gloves, and gowns (Ranney et al., 2020). This PPE shortage has been a major barrier in responding effectively to the pandemic and in mitigating the resulting spread of Coronavirus Disease 2019 (COVID-19). Essential healthcare workers, such as first responders, nurses, and doctors have been forced to forgo or reuse PPE when working with patients with or without COVID-19 to preserve their limited stocks. Additionally, the novel coronavirus has been found to transmit asymptomatically, i.e., through infected patients who do not yet display any symptoms (Mizumoto et al., 2020), at a significant rate, thus markedly increasing the likelihood of cross-contamination during the treatment and care of all patients. Healthcare workers are additionally exposed to the risk of infection through interaction and contact with fomites, including medical devices or instrument panels, and subsequently transmitting the disease to coworkers (Klompas et al., 2020). Many healthcare providers caring for COVID-19 patients have become infected and even lost their lives due to a lack of sufficient access to PPE (Wang et al., 2020). In addition to increasing the strain on an already overloaded healthcare system, such a lack of protection poses a significant threat to the morale of healthcare workers and their families.

With the shortage of PPE, patients without COVID-19 who need critical and/or life-saving treatments also face increased risk in healthcare facilities (Naicker et al., 2020), including patients on dialysis. Such patients tend to be severely immunocompromised and are at a high risk of suffering serious complications if infected by the virus, as reported in China (Naicker et al., 2020). To minimize the risk of cross-contamination and infection, hospitals and dialysis centers have implemented strict protocols with multiple additional precautions in dialysis units for staff members, patients, and their family members (Naicker et al., 2020). However, dialysis centers have been plagued by staff, equipment, and PPE shortages. In fact, at the peak of the COVID-19 pandemic in New York City, a headline in the city's paper of record *The New York Times* declared that "Dialysis Patients Face Close-Up Risk From Coronavirus," (Abelson, 2020). During this period, healthcare workers sought to minimize visits with dialysis patients by using baby monitors and performing physical interaction with dialysis machines

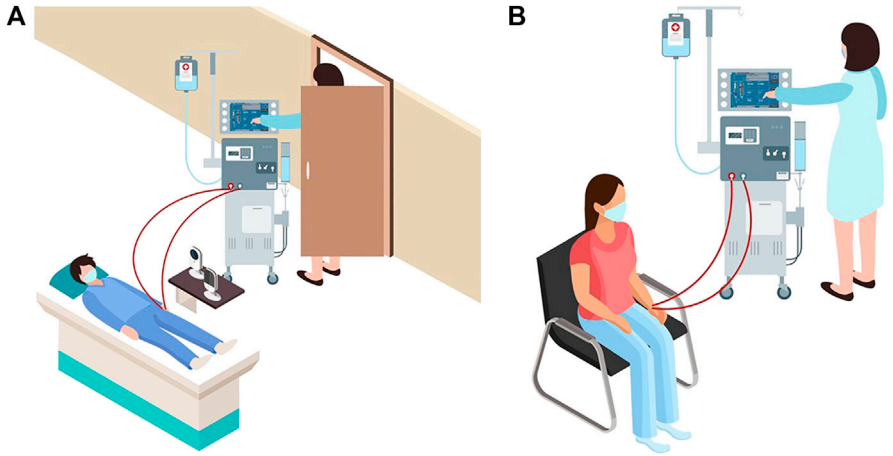

FIGURE 1 | (A) Schematic representation of a dialysis patient receiving treatment at a hospital during the COVID-19 pandemic. The image shows use of baby monitors and reluctance of healthcare workers in entering the patient room. **(B)** A typical schematic representation of a patient receiving treatment at a dialysis center.

without fully entering the patient rooms (see **Figure 1A**). To mitigate the plight of these patients and avoid healthcare worker exposure, concerned authorities, such as the Food and Drug Administration (FDA), have encouraged expanding the non-invasive remote monitoring of such patients (FDA, 2020). To remotely determine whether a specific patient requires help, many healthcare device manufacturers are rolling out Internet of Things (IoT) devices to remotely monitor bio-signals relating to their temperature, heart rates, respiration rates, etc., (Hale, 2020). These remote systems are important tools for avoiding the overcrowding of emergency rooms and hospitals and reducing the unnecessary exposure of vulnerable people to pathogens. Historically, most of the research around medical robotics has concentrated on surgical teleoperation robots such as the DaVinci robot (Intuitive Surgical, Mountain View, CA), and is more focused toward patient safety during surgical procedures by mitigating human error and promoting minimally invasive procedures. Other medical robotic approaches focus on augmenting the doctor's vision with virtual overlays to provide additional information (Liao et al., 2010; Wang et al., 2014). Some social and companion robots are available that target the elderly (Wada et al., 2005) or serve as emotional support (Logan et al., 2019), however there is a dearth of examples of telerobots that can be used to manipulate medical devices using intuitive HRI. There are autonomous robots that can deliver medications throughout hospitals (Murai et al., 2012), and a study explored the development of a tele-nursing robot (Li et al., 2017) that can navigate and interact with objects in the environment, but these solutions are either not relevant to this study or are cost prohibitive to be rapidly deployed in case of a pandemic.

In this paper, we propose to create an emergency, non-invasive remote monitoring and control response system that addresses the needs of a highly vulnerable population: patients with severe kidney diseases. A viable solution for remotely monitoring and controlling a dialysis machine's instrumentation panel poses several design challenges. Typically, dialysis centers consist of multiple reclining chairs or beds with attendant dialysis machines placed next to them (see **Figure 1B**). Potential solutions for remotely manipulating the dialysis machine's instrument panel include: (1) accessing embedded firmware of medical devices and (2) retrofitting the machine with a teleoperated robotic manipulator. As medical devices are sensitive instruments with proprietary firmware, varied software architectures, and individualized system requirements, it is not feasible to create a generalized framework to access the embedded firmware for remotely monitoring and controlling different medical instruments using smartphone/tablet-based third-party apps, especially as expeditiously as a pandemic emergency demands. Thus, retrofitting dialysis machines with teleoperated robotic arms, which can be easily mounted or removed as needed, is deemed as the most viable option. We envision a remote-monitoring-and-control framework wherein a camera-equipped robotic manipulator interacts with the instrument control panel of the dialysis machine, thus reducing the risk of COVID-19 exposure for both patients and healthcare providers. Our proposed solution can address the shortage of PPE in the heathcare facilities during a pandemic, enabling patients who require dialysis to continue receiving the life-saving treatment in isolation. At the same time, staff members in dialysis units can continue to provide high quality care with a relatively low risk of cross-contamination. This work's engineering merits involve piloting a framework to quickly retrofit available dialysis machines with robust off-the-shelf four degrees-of-freedom (DoF) robotic manipulators and supporting remote management of the device instrumentation panel with high fidelity. Thus, in the proof-of-concept study of this paper, we recreate and live-stream the instrument control panel touchscreen (ICPT) of a commonly used dialysis machine, the Gambro X-36 Phoenix (Baxter International Inc., Deerfield, IL) (see **Figure 2**), to replicate and access it on a remote user's tablet computer touchscreen (TCT). Moreover, we develop the control framework for the robot manipulator to achieve precise and accurate remote manipulation of the dialysis machine's ICPT. We test our intuitive smartphone/tablet-based interface with over

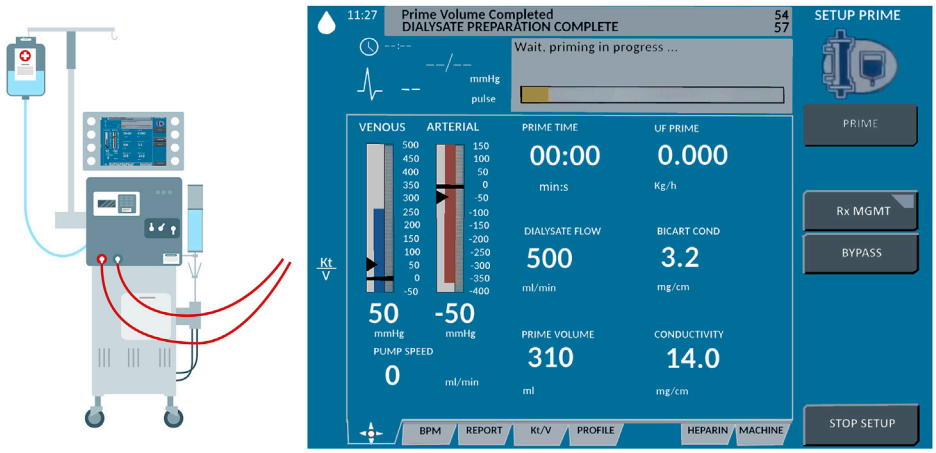

FIGURE 2 | Schematic representation of Gambro X-36 Phoenix dialysis machine and its touchscreen interface.

30 users. Our future work will investigate wider applications of this framework to diverse medical instruments in the post COVID-19 era.

The paper is organized as follows. **Section 2** elaborates on the materials and methods used in the study. This section provides details on the design of the robot manipulator and the user interface, the development of the communication architecture and marker detection, and the robot operation. **Section 3** explains the system evaluation metrics used in this study. These metrics include a quantitative study about the accuracy of the robot and the user interaction, as well as qualitative studies about the user experience while operating the robot remotely. Following this, the results of system evaluation are provided and discussed in **Section 4** and an improvement is suggested to render a distortion-free perception of the ICPT on the user TCT. Finally, **Section 5** provides concluding statements and discusses the future direction of the research.

2 MATERIALS AND METHODS

The method proposed in this paper uses an off-the-shelf four DoF robotic manipulator equipped with a USB camera. The robot base and camera stand are fixed on a board, making the system installation and operation simple, just requiring the user to properly locate the robot in front of its workspace and point the camera to a touchscreen (representing a dialysis machine ICPT) with which the robot manipulator is required to interact. The HRI user interface (UI) consisting of a mobile application (App) is connected to the same wireless network as the robot manipulator system. To identify the surface plane of action of the robot, the mobile App uses the camera's video-feed which includes a 2D image marker located in the plane of the ICPT, in front of the robot manipulator. The mobile App determines this plane of action (i.e., robot workspace) based on the dimensions of the robot and its *computed* position relative to the image marker. With the mobile App executing on a hand-held smartphone or tablet, when a user taps on the TCT at any location of the displayed surface of operation, an algorithm transforms the tapped location's pixel coordinates to a corresponding location coordinate in the workspace and frame of reference of the robot and sends it to the robot manipulator controller. Given this *commanded* position, another algorithm on the robot manipulator controller uses inverse kinematics to calculate a set of joint angles that can be used to attain the given position and orientation of the robot end effector and provides a solution to reach the specified location in space (Craig, 2018). Then, in a sequence of steps, the system plans a path, moves the robot manipulator to go to the desired location on the ICPT, taps on the desired location, and returns to its home position to wait for the next instruction. **Figure 3** illustrates the components and interconnections of the proposed dialysis machine HRI environment.

2.1 Robot Hardware

The robotic platform used in this study is a modified version of the Robotis OpenManipulator-X (Robotis, 2020). Based on the Robot Operating System (ROS) framework, this platform is open-source and open-hardware, i.e., its controllers and CAD models of most of its components are accessible and free to use (see **Figure 4A**). This robot platform's system configuration is a four DoF arrangement, with a pen holder tool holding a stylus pen (see **Figure 4B**), which interacts with the ICPT during operation. For the controller to function correctly, its program has been altered to account for the modified end effector, the number of actuators used, and each link's dimensions to accurately calculate the forward and inverse kinematics. The modified manipulator consists of four Dynamixel XL430-W250-T servomotors and two 3D-printed links made of polylactic acid (PLA) that are connected by means of metal brackets (see **Figure 4A**). The end effector is a PLA 3D-printed pen holder that holds the stylus pen to interact with the screen. The load capacity of the modified manipulator is conservatively estimated to be 160 g which can easily accommodate the 15 g end effector and 20 g stylus pen. A Raspberry Pi 4 (RPi4), with 4GB of RAM and with ROS Melodic

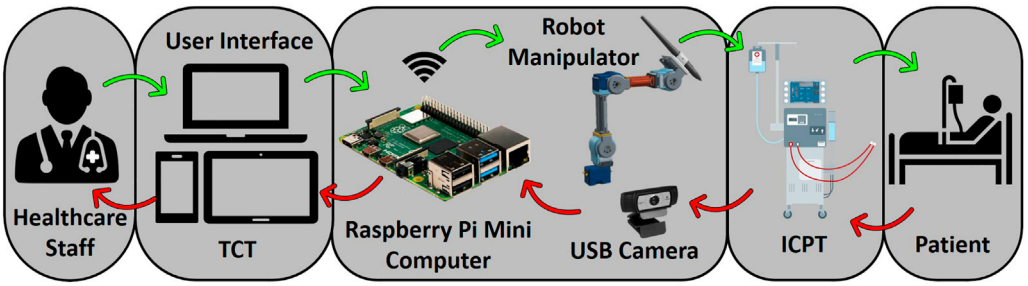

FIGURE 3 | Schematic of a remote monitoring and control system for medical instruments. A healthcare worker interacts with the video-feed from a camera on a user interface (UI) hosted on a tablet computer touchscreen (TCT). The user commands are processed to control a robot manipulator to interact with the instrument control panel touchscreen (ICPT) of a dialysis machine serving a patient.

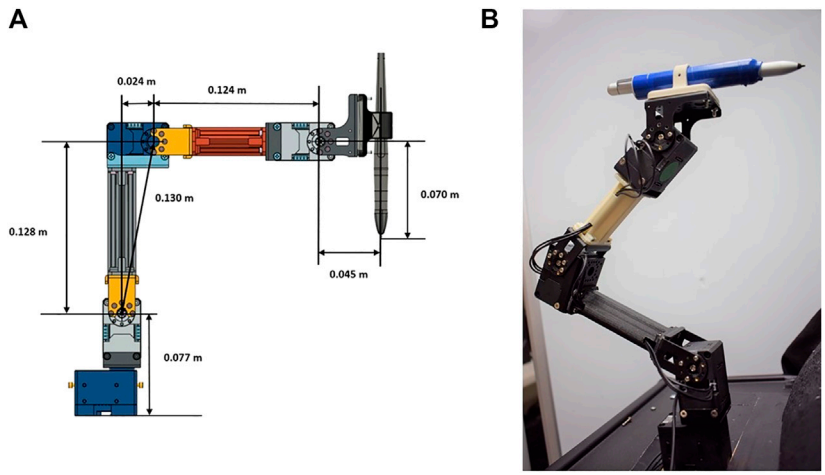

FIGURE 4 | Robot manipulator prototype **(A)** prototype CAD model and **(B)** built prototype.

installed on Raspbian-Buster OS, controls the robot manipulator using the ROS packages executing on it. Using this powerful and cost-effective single-board microcomputer gives the system sufficient capacity to control the robot and run computer vision algorithms without compromising the system's memory. Its small dimensions also make it simple to install and locate it near the system without interfering with the robot manipulator workspace.

To determine the workspace of the robot manipulator, the forward kinematics are first determined using the Denavit–Hartenberg (D–H) convention (Spong et al., 2006). Then, the Monte Carlo method is employed to generate the manipulator's work envelope using the forward kinematics equations along with random sampling of permissible joint angles (Jianjun et al., 2018). This method produces a graphical representation of the manipulator workspace (Guan and Yokoi, 2006) that in turn is used to determine the range of ideal positions to install the robot relative to the medical device ICPT monitor. The allowable maximum and minimum distances between the robot and the medical device ICPT are determined to be 0.27 m and 0.20 m, respectively. The maximum distance is determined as the maximum distance between the robot and the ICPT that ensures that the entirety of the ICPT lies within the estimated workspace of the robot. The minimum distance is obtained by placing the ICPT as close to the robot as possible while ensuring that all of the interactions and the fiducial marker on the ICPT remain visible to the camera (see **Figure 5**).

To establish the achievable accuracy and repeatability of the robot, tests are conducted by commanding it to move the end effector from its home position of ($x = 0.09$, $y = 0.0$, $z = 0.284$) m to a test position and then returning the end effector back to its home position. This test is conducted for five test positions, one at each corner of the ICPT and one at the center, with the position of each test point measured relative to the lower left corner of the ICPT. Moreover, the process is repeated 50 times for each test point and the computed accuracy and repeatability are provided in **Table 1**. Note that the accuracy represents the distance between the desired test position and the average of the achieved positions. Moreover, the repeatability represents the radius of the smallest circle that encompasses all of the achieved positions corresponding to a desired test position (Mihelj et al., 2019).

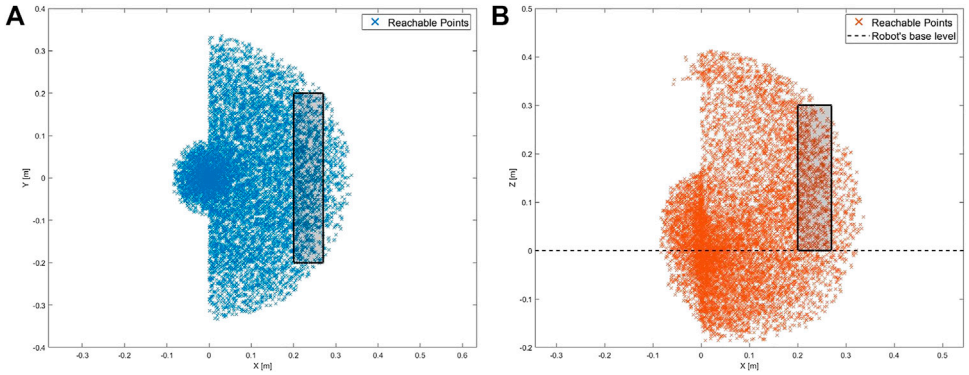

FIGURE 5 | Workspace of the robot with the rectangular regions showing the range of allowable positions for the ICPT **(A)** top-view of the workspace and **(B)** side-view of the workspace.

TABLE 1 | Robot accuracy and repeatability test results.

	P_1 (*u*, *v*)	P_2 (*u*, *v*)	P_3 (*u*, *v*)	P_4 (*u*, *v*)	P_5 (*u*, *v*)
Ideal (mm)	(128.5,84.3)	(55.1,151.6)	(206,151)	(204.5,18.1)	(56,20)
Accuracy (mm)	0.55	0.06	0.21	0.19	1.00
Repeatability (mm)	1.29	1.13	0.88	1.76	1.03

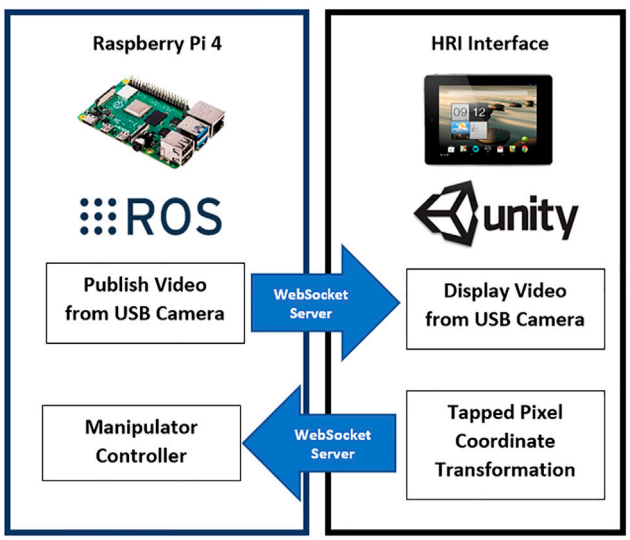

FIGURE 6 | Communication between RPi4 and App.

2.2 USB Camera and Camera Calibration

The USB camera used in this setup is a C920 HD Pro Webcam, configured to capture a 640×480 image. By executing the camera driver on ROS, the webcam capture is made available as a ROS topic and becomes accessible to any subscribing program. Next, we perform a one-time geometric camera calibration using a pattern on a planar surface (Zhang, 2000), allowing the system to correct the image for lens distortion and to detect and measure objects in world units by determining camera location in the scene. These calibration parameters are estimated using an available ROS package for camera calibration and are stored as a file, to be later used during operation by the HRI interface and estimate spatial coordinates.

2.3 Communication with HRI Interface

Using the built-in Wi-Fi adapter of the RPi4, the information generated and published by the nodes running on ROS is made accessible to all members of the network on which the microcomputer is connected. Using a WebSocket server node on ROS establishes a communication bridge and allows web interaction with the ROS topics using an IP address and a port number. Upon joining as a client, the mobile App used for the HRI interface communicates with the RPi4 server and accesses the information running on ROS. This mobile HRI interface, developed using the Unity Engine (Unity Technologies, San Francisco, CA) and a freely available ROS asset, lets the App publish and subscribe to ROS topics (see **Figure 6**). When the application first starts on the mobile device, it immediately looks for the IP address and port to establish communication with the RPi4 microcomputer. The RPi4 and the mobile HRI interface are connected to an *ad hoc* wireless network created using a Netgear Nighthawk X10 AD7200 Wi-Fi router. For the laboratory environment of this study, the maximum range of the wireless network is experimentally obtained to be 27 m.

2.4 Reference Marker Detection

The approaches initially considered for the design of the HRI user interface in this work can be distinguished by the number of reference markers affixed on the medical device ICPT monitor, i.e., (1) four markers approach and (2) single marker approach.

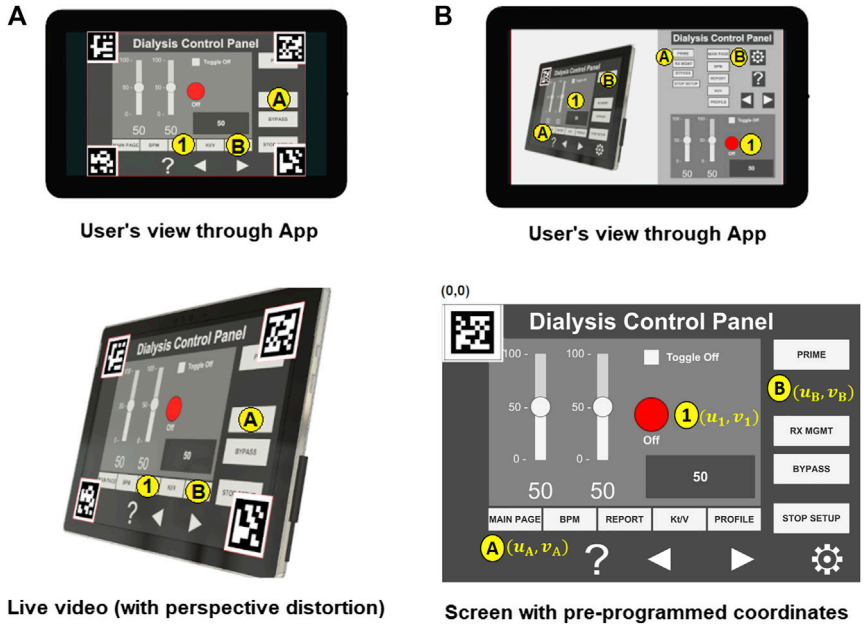

FIGURE 7 | Reference marker detection **(A)** four marker approach and **(B)** single marker approach.

2.4.1 Four Markers Approach

Using the projective transformation technique (Hartley and Zisserman, 2003), with four markers, allows the estimation of any location on the instrumentation control panel displayed in the video-feed on the touchscreen monitor. The four markers are placed on each corner of the ICPT monitor (see **Figure 7A**) and detected from the USB camera capture. The video-feed of the camera is used to estimate its real-world 3D pose (relative to the plane formed by the four markers) and subsequently to compute the pose of any point on the ICPT monitor relative to the camera's coordinate frame. In this approach, the user can select each button of the ICPT by touching the corresponding location of the button on the streaming video image shown on the UI of the TCT (see **Figure 7A**, top panel). Moreover, the markers' detected points are used to correct the perspective distortion caused by the placement of camera relative to the ICPT monitor and to scale the image to fit it on the UI of the TCT display. This method relies on two assumptions: (1) visual markers affixed to the ICPT monitor and interactive control elements (buttons and sliders) of the instrument control panel are on the same plane (coplanar points) and (2) the base location of robot relative to the camera position can be estimated (see **subsection 2.5**). Even though this approach can allow our system to interact with any medical machine with an ICPT, regardless of the ICPT function arrangements, placement of four markers on the same plane as the machine screen, in some cases, may block portions of the display containing important information for the machine functionality.

2.4.2 Single Marker Approach

This approach uses only one reference marker (see **Figure 7B**). The system localizes the robot relative to the marker's position using marker corners as correspondences to perform a projective transformation, but reducing the accuracy of the estimation (compared to the four markers approach) due to the lower number of correspondences detected. With this in mind, the robot control needs to be pre-programmed using the *a priori* knowledge about the locations of the on-screen control elements (buttons and sliders) relative to the attached marker to establish a one-to-one correspondence. For example, when the user touches button A on the UI of the TCT, the corresponding location (u_1, v_1) for the ICPT needs to be assigned automatically as the intended location. The UI executing on the TCT consists of a streaming video panel and a button panel. For each button on the medical device ICPT monitor, a corresponding button is available on the button panel of the UI on the TCT. This approach also assumes that the location of robot relative to the camera position can be estimated. However, requiring information about the arrangement of control elements on the ICPT to pre-program the UI of the TCT will limit the usability of this arrangement since the on-screen layouts of control panels may vary between machines of different manufacturers and specially for different medical machines. Moreover, not having the well-defined four corners of the surface plane of action (as in the four markers approach) limits the system's ability to accurately correct perspective distortion (see **Figure 7B**, top panel).

2.4.3 Hybrid Approach

In this paper, we present an early *proof-of-concept* that employs a hybrid approach by building on the two methods discussed above (see **Figure 8**). By subscribing to the image published by the camera driver node on ROS, the mobile App gains access to its video-feed that contains a single ArUco marker (Garrido-Jurado et al., 2016) placed on the top-left corner of the screen and detects it using the open-source ArUco module (Romero-Ramirez et al.,

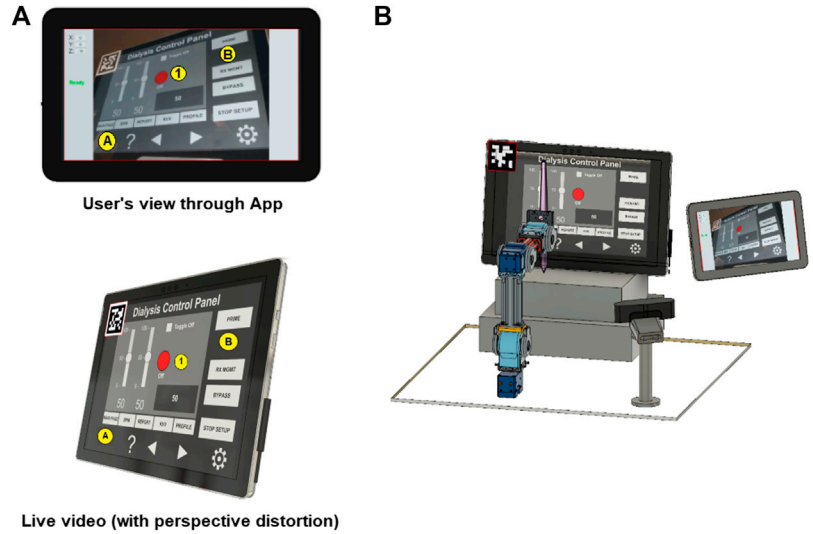

FIGURE 8 | Reference marker detection **(A)** hybrid marker detection approach and **(B)** complete setup with hybrid approach.

2018) of the Open Source Computer Vision Library (OpenCV). Instead of requiring a pre-programmed control panel on the UI of the TCT with known locations of the control elements on the ICPT (as in the single marker approach), the UI now detects the reference marker's corners, and an algorithm estimates the homography (Corke, 2013) between the camera image to the surface plane of the reference marker. With this transformation and the information from the camera calibration file, the mobile App maps coordinates of a user-selected pixel on the video streamed image on the UI of the TCT to a spatial coordinate on the ICPT in world units, relative to the camera's reference frame. As in the previous approaches, this approach assumes that the robot base location relative to the camera can be estimated. Its functionality is similar to the four markers approach, letting the user select a control element (button or slider) of the ICPT by touching its corresponding location on the UI's image on the TCT. However, its accuracy may be compromised due to the limited number of correspondences detected.

As described above, the usability of the hybrid approach benefits the system by not relying on the *a priori* knowledge of arrangement of the control elements on medical device ICPT or on risking portions of the ICPT being blocked by the placement of multiple markers, however it has less accuracy than the four markers approach. The hybrid approach will also not correct the captured image's perspective of the USB camera for the UI displayed on the TCT. In future research, we will test, compare, and contrast the usability and performance of the three approaches by conducting user tests to assess various parameters of UIs (such as intuitiveness, user-friendliness, perception, and remote operation workload) and the robotic device (such as accuracy and repeatability).

2.5 Camera Position and Robot Calibration

To allow the robot manipulator to interact with a point in its workspace (on ICPT) corresponding to any point selected by the user on the mobile App screen (on TCT), the robot controller requires the corresponding spatial coordinate specified in the robot's frame of reference (located on the center of the robot base). This necessitates imparting the system knowledge about the camera's pose relative to the robot frame of reference (${}^{R}T_{C}$). Thus, a calibration routine is created and implemented before the system starts any HRI operations. That is, this routine is run immediately after the camera's orientation has been established to capture the robot's workspace surface (i.e., the ICPT monitor).

We first locate the ArUco marker in a predefined pose relative to the robot's reference frame (see **Figure 9**). With this known pose (${}^{R}T_{M}$) and with the pose of the marker relative to the camera reference frame (${}^{C}T_{M}$), estimated by the mobile App, the calibration routine computes ${}^{R}T_{C}$ as follows

$$ {}^{R}T_{C} = {}^{R}T_{M}\left({}^{C}T_{M}\right)^{-1}. \tag{1} $$

Now ${}^{R}T_{C}$ is stored on and used by the mobile App to map pixel location of any point tapped by the user on the TCT to a spatial coordinate on the ICPT in the robot's reference frame. To achieve a mapping from the TCT to ICPT of any size, the user enters, in millimeters, the width and height of the ICPT, and the u and v offsets of the top left corner of ICPT from the center of the fiducial marker, into the App. This creates an interactive region on the TCT that is the size of the ICPT as seen on the video-feed on the TCT. Next, to map any desired point on the ICPT to the robot's workspace, we first locate the fiducial marker of known size (40 mm × 40 mm) on the ICPT surface. Based on the size and orientation of the marker obtained using computer vision, the App obtains the marker's pose relative to the camera position. It uses this information to map any pixel coordinate to a space coordinate relative to the camera frame. Finally, using the transformation matrix (${}^{R}T_{C}$) obtained in the calibration step, the desired interaction point on the ICPT is mapped to spatial coordinates in the robot arm's coordinate frame. This coordinate serves as the input to command the robot to move to the desired

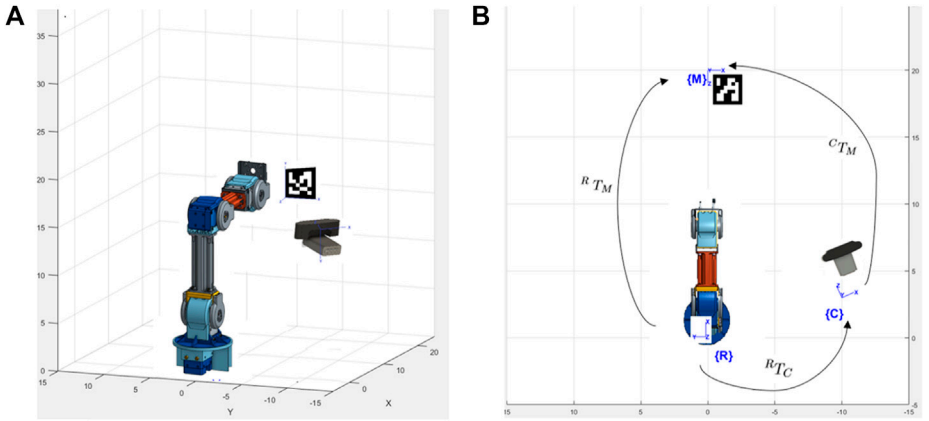

FIGURE 9 | System setup to estimate camera pose **(A)** isometric view and **(B)** top view.

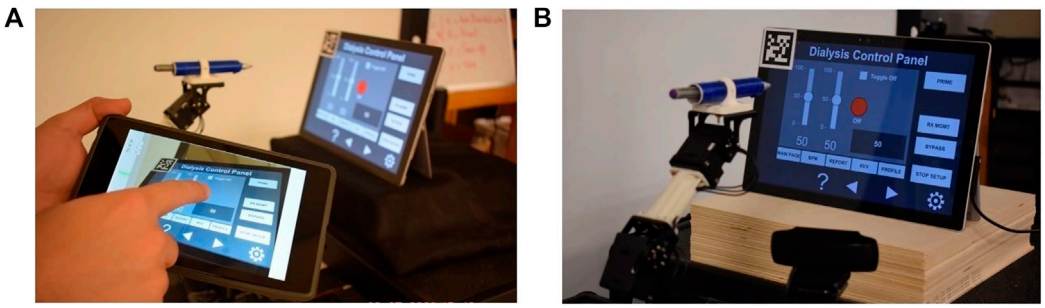

FIGURE 10 | (A) HRI interface and **(B)** complete robot system setup.

position. As long as the ICPT is located within the robot workspace and its entire screen (with the fiducial marker located on it) is visible to the camera, the robot can reach any desired point. Finally, once the App maps the TCT coordinate into a spatial coordinate, it is published to a ROS topic, making it available to the robot manipulator controller. However, even if the calculation of ${}^{R}T_{C}$ is accurate, there may be slight residual errors in the end effector's final position. To compensate for this, the second part of the calibration routine consists of commanding the robot to go to the center of the reference marker multiple times. The user moves the end effector's final position by tapping on the UI screen at preprogrammed buttons, which are displayed during the calibration routine, to manipulate the stylus pen's tip in the *X*, *Y*, and *Z* directions until it matches the marker's center as precisely as possible. The offset values needed to reach the actual desired position are stored and used to increase accuracy during the operation.

2.6 Robot Operation

A program on the RPi4 runs a ROS node that uses the information from the mobile App and uses the controller node of the manipulator robot to move it to the user-specified location. After performing the calibration routines, the system is ready to operate. The manipulator robot control program moves the robot to an initial position and waits for a user-specified coordinate to be available on the ROS topic where the mobile App publishes coordinates.

When the App starts, it immediately tries to communicate with the microcomputer. Once the communication is established, the touchscreen of the tablet device running the App will show the streaming video from the camera located next to the robot, capturing the images from the ICPT (see **Figure 10A**). With the detected 2D reference marker's information, the App will wait for the user to tap on the display of the TCT. The moment a new user-specified coordinate is received, using a sequence of events, the robot control program: (a) moves the robot manipulator to the desired location, just over the specified coordinate on the surface plane of the ICPT; (b) performs a tapping action that consists of moving slightly toward the ICPT until a contact occurs; and (c) returns to the initial position and waits for any new coordinates to be made available. This robot control program reads and responds to only one user-specified coordinate at a time and ignores any newly sent user coordinates while performing the sequence of operation for a previously received coordinate.

The complete system setup created for this proof-of-concept (see **Figure 10B**) uses a Microsoft Surface Pro 4 computer as the

ICPT, running an application that mimics the functions of a dialysis machine instrument control panel.

3 SYSTEM EVALUATION

An experimental study was conducted with participants to evaluate the performance and usability of the proposed system. The study was conducted with two groups of users, referred hereafter as the in-person and remote groups. In the in-person group, 17 participants performed the experiment in a room adjacent to the room housing the robot, camera, and ICPT monitor. Alternatively, in the remote group, 16 participants performed the experiment from a remote location via the internet. See http://engineering.nyu.edu/mechatronics/videos/mhrifordialysis.html for a video illustrating a user interacting with the prototype to complete a set of tasks. Prior to performing the experiment, participants in both groups were briefed individually on the purpose of the experiment, what it entails, and how do the interactions take place. They were informed that when the "Ready" prompt is shown on the TCT, the user can issue a command to the robot and when the "Busy" prompt is shown, it means that the robot is executing a task and will not accept any user command until the task is completed. No pretrial was conducted and each participant performed the experiment for only one time. This was done to ensure that the participants did not have any prior knowledge about the capabilities and the overall responsiveness of the system.

The participants who performed the experiment in-person were asked to use an Android tablet device with a touchscreen and interact with its screen using a stylus. During the experiment, the tablet device was connected to the same dedicated wireless network that the robot was connected to, and each user performed the experiment by staying in the same location in the room.

To test whether controlling the robot from a remote location has any influence over the system usability, system performance, and the task load of the user, an online study was conducted wherein the participants were asked to command the robot by assuming control of a computer connected to the dedicated wireless network shared by the robot. The participants were briefed in a similar manner to those in the in-person experiment, and no pretrial was conducted for this group either. The only major difference between the two groups was that the remote group of participants were interacting with the video-feed using a mouse pointer on their computer, whereas participants in the in-person group were interacting with a tablet device using a stylus to issue commands to the robot.

During the experiment, the participants were asked to read a set of instructions on a PDF document and perform the experiment accordingly. The PDF instruction document listed six numbered tasks and an accompanying annotated image of the user interface (see **Figure 11**), where the six tasks correspond to six different interactions that the users needed to perform. These tasks were designed to mimic a set of user interactions that a healthcare worker typically performs on a dialysis machine interface. The details of the interactions are as follows.

(1) Press the red ON/OFF button.
(2) Change the value of the left slider to '0' and the value of the right slider to '100'.
(3) Press the toggle button.
(4) Increase/decrease the value displayed in the gray box using the arrow buttons.
(5) Select the RX MGMT button.
(6) Return to the main display using the MAIN PAGE button.

After the participants performed the six tasks, they were asked to respond to two questionnaires that assessed their experience for qualitative evaluation. The first part of the evaluation required the participant to respond to the NASA-Task Load indeX (NASA-TLX) (Hart, 2006) to assess the workload experienced by the participants while using the system. The NASA-TLX is used to rate the perceived workload of an individual while performing a task. It is divided into six categories that include physical workload, mental workload, temporal workload, effort, frustration, and performance. In this study, the Raw TLX (RTLX) assessment was performed in which the TLX scores are unweighted and the overall load of the task is calculated as the average score of the six categories in the NASA-TLX. In the second part of the evaluation, the participants were asked to express their level of agreement on a System Usability Scale (SUS) (Brooke, 1996) questionnaire. The questionnaire consists of the following five positive and five negative statements with responses on a 5-point scale (1: strongly agree and 5: strongly disagree).

(1) I think that I would like to use this system frequently.
(2) I found the system unnecessarily complex.
(3) I thought the system was easy to use.
(4) I think that I would need the support of a technical person to be able to use this system.
(5) I found the various functions in this system to be well integrated.
(6) I thought there was too much inconsistency in this system.
(7) I imagine that most people would learn to use this system very quickly.
(8) I found the system to be very cumbersome to use.
(9) I felt very confident using the system.
(10) I needed to learn a lot of things before I could get going with this system.

The participants were provided Uniform Resource Locators (URL) to the NASA-RTLX and the SUS questionnaires and were asked to complete them on the spot immediately after completing the six-step interactive tasks provided above. The questionnaires were kept anonymous and no personal information was asked from the participants except their age group and their gender.

4 RESULTS

The performance and the user experience of the proposed system was evaluated by conducting a study with 33 participants, of whom 29 participants were either engineering students or professionals working in a STEM related field and the

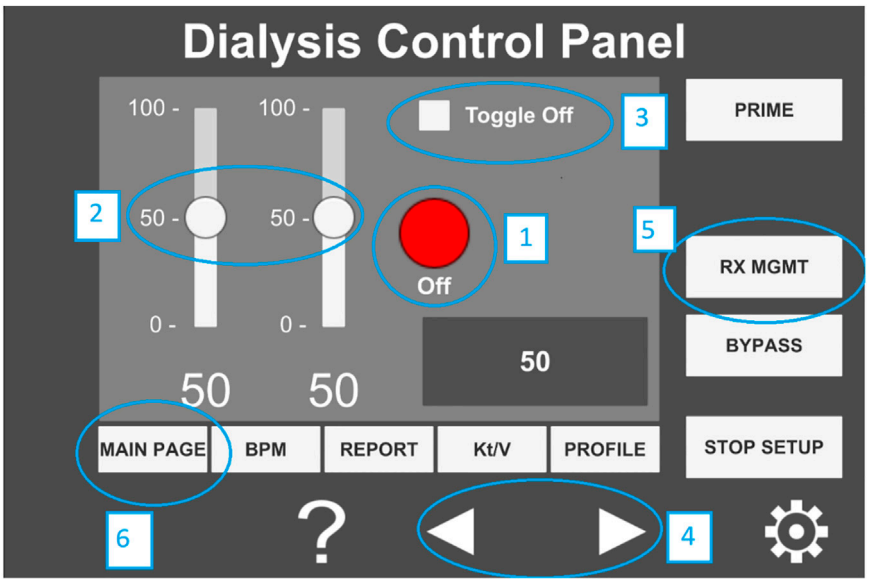

FIGURE 11 | Annotated image of the user interface hosted on the tablet computer.

remaining four were medical professionals. A majority of the participants (72.73%) had operated or programmed a robotic system while the rest 27.27% had neither operated nor programmed a robot prior to their participation in the study. Note that the four medical professionals were part of the remote group and only one of them reported to have programmed or operated a robotic system previously. Furthermore, qualitative data obtained from the SUS questionnaire contained two outliers and one participant from the remote group did not complete the NASA-RTLX self assessment. Thus, the data obtained from these three participants was not used for system evaluation and a total of 30 participants' data, 15 from each group, was used for the results reported below.

4.1 System Performance

First, the performance of the system was evaluated by validating the accuracy with which a user is able to select and interact with desired points on the ICPT monitor using the proposed HRI interface on the TCT. We considered five reference points on the ICPT. These points were located at the center ($P_1(u, v)$) and near the four corners ($P_i(u, v)$, $i = 2, \ldots,5$) of the screen. The experiment was conducted 50 times by a single user for each of the five reference points. The user input when interacting with TCT was recorded as pixel coordinates along the u and v axes and referred to as the *commanded* value. The point at which the robot interacted with the ICPT in response to the commanded value is referred to as the *measured* value and it was also stored as pixel coordinates along the u and v axes. The pixel coordinates for the commanded values were scaled up to the screen resolution of the ICPT so that a direct comparison with the measured values could be made. The performance of the HRI interface was evaluated by calculating the absolute difference between the commanded and measured values for each interaction. Then the average absolute error was calculated for both the u and v coordinates. This was done for all five reference points and the results are shown in **Table 2**. The results indicate that for all five reference points, the highest average absolute error was less than 18.54 pixels for the u coordinate and 26.98 pixels for the v coordinate. Given that the resolution of the screen used for the ICPT is 2,736 × 1,824, with a diagonal screen size of 12.3 inches (312.42 mm), the pixel-to-length ratio was found to be 10.5 pixels/mm. Thus, the maximum average absolute error was 2.56 mm in the v coordinate of the fifth reference point $P_5(u, v)$. It is important to note that there was a button located at each of the five reference points and all 50 tests conducted on each button were successful, i.e., the button was successfully pressed each time. The diameter of the buttons is 90 pixels which is approximately equal to 8.6 mm. This particular size of buttons is chosen because it is considerably smaller than all interactive elements on the touchscreen and the touch pad of a dialysis machine, and therefore proves to be a reliable indicator of the performance of the system.

The time taken by the robot to complete an interaction is determined by the task time programmed for the robot. In experimentation, it is measured as the difference between the time when the robot receives a command and the time when the robot returns to its home position after performing the interaction. The robot took 12.036 s to complete an interaction, without any significant difference in the times spent for different interactions. Next, the time it takes for a user to complete an interaction on the *ad hoc* wireless network is calculated as the difference between the time when the command is sent by the TCT and the time when the user receives the "Ready" prompt again on the TCT. For each of the following three scenarios, 15 tests were performed to measure the user interaction completion time.

TABLE 2 | Performance test results.

Values in pixels	P_1 (*u*, *v*)	P_2 (*u*, *v*)	P_3 (*u*, *v*)	P_4 (*u*, *v*)	P_5 (*u*, *v*)
Ideal	(1368,912)	(568,1612)	(2168,1612)	(2168,212)	(568,212)
Commanded (average)	(1367.4,912.1)	(569.7,1601.6)	(2166.9,1612.1)	(2163.2,211.4)	(595.9,215.9)
Measured (average)	(1385.9,905.7)	(565.8,1596.9)	(2162.6,1598.0)	(2173.6,215.9)	(599.8,189.1)

(1) The user holding the TCT and the robot are in the same room.
(2) The user holding the TCT and the robot are in different but adjacent rooms.
(3) The user holding the TCT is at the maximum working distance from the wireless router (27 m), with multiple rooms in between the user and the robot.

In all three scenarios, the average time to complete the user interaction showed no significant difference and was found to be 12.077 s. Finally, in the last time measurement experiment, we sought to determine the user interaction time when performing interactions with the robot over the internet. With a user located at a distance of approximately 1.5 mi from the robot, the average interaction time for 15 tests was obtained to be 12.56 s. Note that while the task completion time for the robot remains constant, the task completion time for the user and the maximum allowable interaction distance from the robot can change depending on user location and Wi-Fi signal strength, respectively.

4.2 User Experience

While the results obtained using the system performance test validated the utility of the proposed system from an accuracy and precision point of view, it is important to consider the overall user experience when the participants operate the system. Thus, three different methods were used to perform the qualitative analysis of the user experience. The first method involved measuring the task load of the experiment using the NASA-RTLX self-assessment. This was followed by administering a system usability questionnaire, and finally the verbal/written feedback given by the participants was reviewed.

4.2.1 Workload

The assessment of the workload was performed by analyzing the results obtained from the NASA-RTLX self-assessment for the in-person and the remote participant groups. All categories were scored on a scale of 0–100 and the overall score for each participant was computed as a mean of the score for the six categories.

The score for each category was averaged and these calculations were used to compute the mean overall workload for both groups. Since there was no overlap between both groups, and therefore both samples are independent, a Welch's unequal variances two-tailed *t*-test was performed on the individual categories of the NASA-RTLX scores from both groups and the tests yielded $p > 0.05$ for responses of in-person *vs.* remote experimenters. Thus, it was concluded that there was no statistically significant difference between the task loads experienced by the participants in the two groups. The combined average task load for both groups is computed and reported in **Figure 12A**.

The collective task load values for two groups (**Figure 12A**) and the raw data indicate that the frustration score was the highest for the two groups. The high frustration value can be attributed to the downtime that the participants experienced during the "Busy" phase of the robot movement, when the participants could not issue new commands to the robot. When we consider this factor with the slow speed at which the robot moves, it is plausible that the frustration value would increase as a result. Upon further examination of the raw task load data, it was observed that among the six categories, the effort scores exhibited a relatively high inter-group difference (in-person effort = 11.67, remote effort = 5.8). The difference between the effort values of both groups can be explained as a result of the type of interaction method with the robot. Participants in the remote group issued commands to the robot via a mouse pointer on a computer. This gave them very fine control with pixel perfect accuracy and a large screen size that definitely helped in the experiment. On the other hand, participants in the in-person group were asked to use a tablet device and a stylus to interact with the video-feed. The stylus requires extra pressure to be applied on the tablet computer screen to register a touch input and the smaller screen size required the users to pay more attention to where they were interacting with the screen of the tablet device.

4.2.2 System Usability

To gain an insight into the user experience of the participants, they were asked to complete a system usability questionnaire using a 5-point scale (1: strongly agree and 5: strongly disagree). The participants' individual responses were subjected to an unequal variances two-tailed *t*-test and the responses for the in-person group were compared with those of the remote group. Out of the 10 questions on the SUS questionnaire, three questions [(1), (5), and (6)] showed a statistically significant difference with $p = 0.03$, $p = 0.03$, and $p = 0.001$, respectively. Upon close examination of the data, two in-person group participants' responses were identified as outliers due to the large distance between their responses and the mean response for questions [(1), (3), (5), (7), and (9)]. Upon removing the outliers from the data, an unequal variances two-tailed *t*-test was performed again on the responses from the remaining 15 participants in the in-person and 15 participants in the remote groups. The results are shown in **Figures 12B**,**C**.

Out of the 10 questions, only question (6) showed a statistically significant difference with $p = 0.001$. Although all participants in the remote group disagreed or strongly disagreed

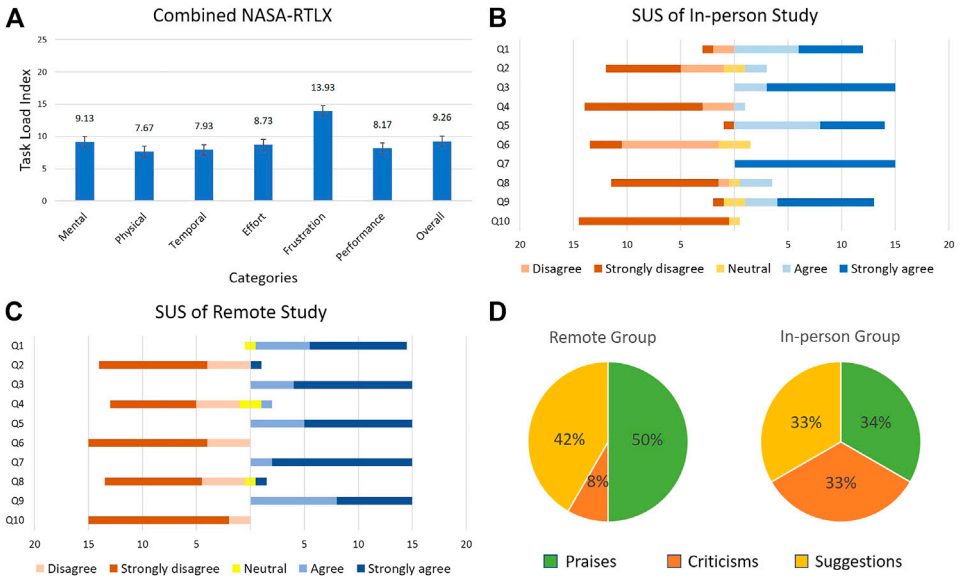

FIGURE 12 | User study results **(A)** NASA-RTLX **(B)** SUS in-person study **(C)** SUS remote study, and **(D)** user opinion.

that there was too much inconsistency in the system, some participants from the in-person group had neutral responses on this question. The neutral responses can be interpreted as participant reservations on the responsiveness of the tablet device when interacting with it using a stylus. Since the stylus used in this experiment had a relatively large tip, it is possible that some participants found inconsistencies when interacting with the tablet device if they did not pay close attention to where they touched the screen. This also explains why the participants in the remote group did not find any inconsistencies despite controlling the robot from a remote location. Since remote participants were using a mouse pointer on a comparatively larger screen (using a laptop or desktop computer), they could direct the robot more precisely, therefore reducing the human input error. A viable solution that would alleviate the problems faced by the in-person group would be to use a tablet device with a larger screen size, and/or use a stylus with a finer tip.

4.3 User Comments

From the participants who tested the prototype, remotely and locally, we obtained different insights about their experiences interacting with the system by reviewing their comments and feedback. A total of 33 individuals participated in this study, out of which 21 provided comments and suggestions about their experience in controlling the manipulator. Some of the comments praised the system as evidenced by the use of terms such as "helpful," "efficient," "easy-to-use," "pretty good," "requires very little experience," among others. Although several other participants did not express negatively biased comments, they expressed some reservation with the speed of the robot in executing the received commands, e.g., "the time taken by the robot to execute the command slows the process down." There were also criticisms from users who tested the prototype from a remote computer and on-site with a mobile device regarding the smoothness of the robot movements and the camera image shown in the HRI interface. Specifically, a participant who tested the prototype in-person using a tablet, suggested making the robot "more robust" and another participant who used the robot from a remote computer, advised "make the system more accurate and more stable [. . .] decrease the skew in the image from the camera."

Since this study proposes a solution to be used by heathcare workers, we also reached out to doctors who were willing to test the prototype and provide a review based on their experience working during the COVID-19 emergency. A total of four doctors remotely interacted with the proposed system and provided their feedback which included suggestions, criticisms, and compliments about the system and its utility as a viable solution for the control of dialysis machines during a pandemic. For example, one of the participant doctors, who used the prototype from a computer outside the United States, praised the system by commenting on its ease of understanding, use, sensitivity, absence of errors, ability to avoid contact with patient, etc. Another participant doctor offered insight into how this solution is perceived from a medical perspective, i.e., "interesting" and "of enormous use, especially when necessary to avoid physical contact." He also advised to improve the precision of robot because sometimes "it was necessary to select the same task until it was completed successfully." Additionally, another medical professional expressed his interest in how this system would perform in a real situation. This doctor provided a verbal review by stating that the system works very well but it will require testing on a real dialysis machine to see how it controls it.

We found that the difference in these reviewer experiences is partially explained by the variations of internet connection speeds available on each participant's respective location (when

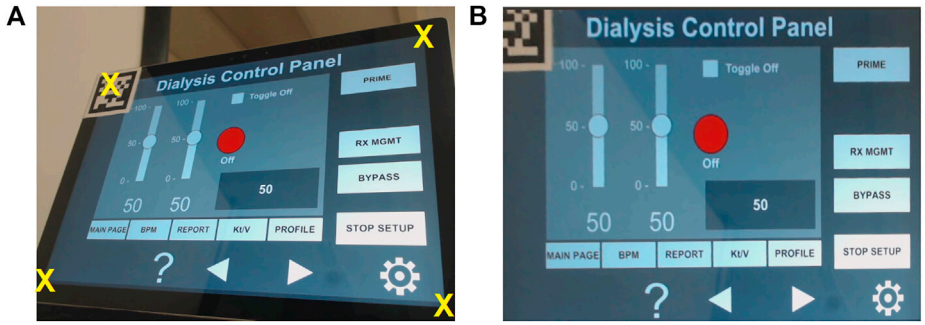

FIGURE 13 | (A) Raw image with corners selected by the user and **(B)** image with distortion corrected.

controlling the system from a remote computer, off-site). In some cases, this variable added delay to video streaming, which did not let the users monitor how the robot was performing the tasks.

Figure 12D presents the percentages of each type of comments provided by the participants using the proposed system. We categorized the comments into "praise", "suggestion", and "criticism" categories. Positively biased comments were categorized as praises and accounted for 34% of the commenters from the in-person group and 50% of the commenters from the remote group. We categorized as criticisms the comments that identified a shortcoming without providing a recommendation. These accounted for 33% of the commenters from the in-person group and 8% of the commenters from the remote group. Finally, comments that provided recommendations to improve the system were categorized as suggestions and accounted for 33% of the commenters from the in-person group and 42% of the commenters from the remote group. It is seen that most participants were affected enough by their participation in the study to leave meaningful comments. Moreover, a sizable portion of participants was satisfied enough to praise their experience in writing. We took these praises to confirm our arguments for integrating mobile hardware and software as an effective way to interact with medical machines remotely using robot systems, such as the one proposed in this study. Many of the praises expressed the satisfaction of completing a set of tasks remotely, either using a "click" on a computer screen or tapping a location on a mobile device screen.

On the other hand, criticisms gave us areas of opportunity on which we can focus to improve our prototype to deliver greater satisfaction in the use of HRI interfaces to control robots remotely and to meet the expectations of the system performance while executing a task. Observations regarding the smoothness of the robot movements and precision allow us to understand better how a system of this nature is perceived. Even if the users complete a set of tasks successfully, the speed while performing this task or lack of smoothness on the manipulator movements creates some distress. On the other hand, criticism about the skew of the camera view confirms that there is also some level of discomfort when a user perceives a distorted perspective of a surface (touch screen) with which interaction is required. While many of these suggestions for improvements will be considered in developing and testing future prototypes, below we offer one improvement to render a distortion-free perception of the ICPT on the TCT.

4.4 Suggested Improvement Based on User Tests

On the SUS questionnaire and in the comment section, several participants provided written (and verbal) feedback concerning the skewed perception of the camera video-feed. In response, we have explored the potential of including an additional feature to the hybrid approach of this study, which uses a single reference marker, to correct and improve the video-feed displayed on the TCT interface. Specifically, as previously, when the users run the mobile UI App on the tablet device, the raw live-stream of the ICPT is displayed on the TCT with a distorted perception. Next, the App prompts the user to touch (from the mobile device) or click (from the remote computer) the four corners on the video-feed of the surface plane of action of the ICPT in a clockwise manner, starting from the corner closest to the fiducial marker (see **Figure 13A**). These user-selected pixel coordinates, corresponding to the corners of the ICPT, are used to get a perspective transformation matrix and map the identified ICPT plane to fit the screen of the TCT by performing a perspective correction. This correction technique allows the user to be presented with a distortion-corrected view of the raw ICPT video-feed in the HRI interface (see **Figure 13B**). When the user interacts with the corrected image displayed on the TCT, the inverse of the perspective transformation matrix computed above can be used to map the pixel coordinates of the user interaction on the TCT to the original perspective view captured by the camera, allowing the application to work without any additional modifications. **Figure 13** illustrates that it is feasible to implement such a perspective correction approach, however a complete set of user-tests with this improved approach is beyond the scope of this study and will be considered in a broader study with the two alternative approaches suggested in **subsection 2.4**.

5 CONCLUSION

In this paper, we proposed a system for remote control of a dialysis machine with mobile HRI as part of COVID-19 emergency response. The proposed approach utilizes the capabilities of a smartphone/tablet device as a mode of interaction with a 4-DOF robot and explores the possibility of manipulating the robot to remotely interact with the instrument panel of a dialysis machine. This allows the medical professionals to maintain social distancing when treating dialysis patients, preventing potential exposure to pathogens for both the healthcare staff and the patients. Such a system will also help lower the use of PPE by doctors and nurses while performing routine, simple procedures that could be performed by a robot. To evaluate the proposed system, its performance, and the user experience, a user study was conducted in which participants remotely issued commands to a robot via a tablet device or a computer. The participants received a live streaming video of a mock dialysis machine ICPT that allowed them to command the robot to manipulate the UI elements of the ICPT by touching those elements on the video-feed on the TCT. Results of the study show that the participants were able to remotely access the UI elements of the ICPT and complete the tasks successfully. Based on the feedback received on the SUS questionnaire from the participants, an improvement to the proposed HRI interface was suggested and implemented which corrected the perspective distortion of the live-stream of ICPT and allowed the user to interact with the corrected image for a more intuitive exprience. Overall, the live streaming video of the instrument panel provides a very natural and intuitive mode of interaction for the user and does not require prior experience in programming or operating robots. Most importantly, there is no need to develop a custom UI for the TCT since the user directly interacts with the video-feed from the ICPT. This allows the proposed system to work with any touchscreen and the development of custom TCT interfaces that only work with their corresponding ICPT is not required. Finally, the proposed approach can be deployed very rapidly and requires minimum preparation work in case of an emergency, therefore saving valuable time and resources that can be directed elsewhere. Future work will incorporate force feedback control on the robot end effector and multiple fiducial markers on the ICPT to increase the accuracy of the robot. Furthermore, the possibility of a mobile robot platform will be explored, which will allow the user to interact remotely with multiple medical equipment in a given environment. Finally, additional intuitive modes of interaction involving wearable technologies and AR will be explored to enhance the user experience and user efficiency while minimizing the task load.

DATA AVAILABILITY STATEMENT

The raw data supporting the conclusions of this article will be made available by the authors, without undue reservation.

ETHICS STATEMENT

Ethical review and approval was not required for the study on human participants in accordance with the local legislation and institutional requirements. Written informed consent from the participants was not required to participate in this study in accordance with the national legislation and the institutional requirements.

AUTHOR CONTRIBUTIONS

HW is the main contributor in the research and development of the mobile App for HRI, mock-up instrument control panel for a dialysis machine, and their overall integration. CL is the main contributor in the research and development of the 4 DoF manipulator robot, computer vision, and the entire ROS integration. SC is the main contributor in the conceptual design of user studies and analysis of its results. HW and CL coordinated with all participants who performed in-person and remote user testing. VK supervised all aspects of research, including checking the accuracy of results and helping with the writing of the paper.

FUNDING

This work is supported in part by the National Science Foundation under RET Site Grant EEC-1542286, ITEST Grant DRL-1614085, and DRK-12 Grant DRL-1417769.

ACKNOWLEDGMENTS

VK acknowledges early conversations with and suggestions of Drs. Shramana Ghosh and Sai Prasanth Krishnamoorthy during the conception stages of this work in Spring 2020. The authors appreciate the time and effort of the individuals who participated in user studies and provided valuable feedback, specially the four medical professionals. The authors acknowledge the support of Dhruv Avdhesh for rendering the images of **Figures 1**, **2** and Drs. Ghosh and Krishnamoorthy for rendering an early version of **Figure 3**.

SUPPLEMENTARY MATERIAL

The Supplementary Material for this article can be found online at: https://www.frontiersin.org/articles/10.3389/frobt.2021.612855/full#supplementary-material.

REFERENCES

Abelson, R. (2020). Dialysis patients face close-up risk from coronavirus. *The New York Times*. (Accessed September 27, 2020).

Abidi, S., Williams, M., and Johnston, B. (2013). "Human pointing as a robot directive," in ACM/IEEE international conference on human–robot interaction (HRI), 67–68.

Brooke, J. (1996). "SUS: a quick and dirty usability scale," in *Usability evaluation in industry*. Editors P. W. Jordan, B. Thomas, I. L. McClelland, and B. Weerdmeester (London: Taylor and Francis), 189–194.

Chacko, S., Granado, A., and Kapila, V. (2020). "An augmented reality framework for robotic tool-path teaching," in Proceedings of CIRP conference on manufacturing systems, 93, 1218–1223.

Chacko, S. M., and Kapila, V. (2019). "Augmented reality as a medium for human-robot collaborative tasks," in 28th IEEE international conference on robot and human interactive communication (RO-MAN), 1–8.

Corke, P. (2013). *Robotics, vision and control: fundamental algorithms in MATLAB*. 1st edn. Berlin: Springer Publishing Company.

Craig, J (2018). *Introduction to robotics: mechanics and control*. New York, NY: Pearson.

FDA (2020). Enforcement policy for non-invasive remote monitoring devices used to support patient monitoring during the coronavirus disease 2019 (covid-19) public health emergency (revised). Tech. Rep., Food and Drug Administration. (Accessed September 27, 2020).

Frank, J. A., Krishnamoorthy, S. P., and Kapila, V. (2017a). Toward mobile mixed-reality interaction with multi-robot systems. *IEEE Robotics Autom. Lett.* 2, 1901–1908. doi:10.1109/LRA.2017.2714128

Frank, J. A., Moorhead, M., and Kapila, V. (2017b). Mobile mixed-reality interfaces that enhance human-robot interaction in shared spaces. *Front. Robot. AI* 4. doi:10.3389/frobt.2017.00020

Garrido-Jurado, S., Muñoz-Salinas, R., Madrid-Cuevas, F. J., and Medina-Carnicer, R. (2016). Generation of fiducial marker dictionaries using mixed integer linear programming. *Pattern Recognit.* 51, 481–491. doi:10.1016/j.patcog.2015.09.023

Google. (2020). ARCore. Available at: https://developers.google.com/ar/reference/

Guan, Y., and Yokoi, K. (2006). "Reachable space generation of a humanoid robot using the Monte Carlo method," in IEEE/RSJ international conference on intelligent robots and systems (IROS), 1984-1989.

Hägele, M., Nilsson, K., Pires, J. N., and Bischoff, R. (2016). *Industrial robotics*. Cham: Springer International Publishing, 1385–1422. doi:10.1007/978-3-319-32552-1_54

Hale, C (2020). Companies roll out remote covid-19 monitoring tools to free up hospital space. *Fierce Biotech*. (Accessed September 27, 2020).

Hart, S. G. (2006). NASA-Task Load Index (NASA-TLX); 20 years later. *Proc. Human Factors Ergon. Soc. Annu. Meet.* 50, 904–908. doi:10.1037/e577632012-009

Hartley, R., and Zisserman, A. (2003). *Multiple view geometry in computer vision*. 2nd edn. USA: Cambridge University Press.

Hashimoto, S., Ishida, A., Inami, M., and Igarashi, T. (2011). "Touchme: an augmented, reality based remote robot manipulation," in International conference on artificial reality and telexistence, 223–228.

Jianjun, Y., Xiaojie, S., Shiqi, Z., Ming, Y., and Xiaodong, Z. (2018). "Monte Carlo method for searching functional workspace of an underwater manipulator," in Chinese control and decision conference (CCDC), 6431–6435.

Kasahara, S., Niiyama, R., Heun, V., and Ishi, H. (2013). "exTouch: spatially-aware embodied manipulation of actuated objects mediated by augmented reality," in International conference on tangible, embedded and embodied interaction (ACM) 223–228.

Klompas, M., Morris, C. A., Sinclair, J., Pearson, M., and Shenoy, E. S. (2020). Universal masking in hospitals in the covid-19 era. *New Engl. J. Med.* 382, e63. doi:10.1056/NEJMp2006372

Krotkov, E., Hackett, D., Jackel, L., Perschbacher, M., Pippine, J., Strauss, J., et al. (2017). The DARPA robotics challenge finals: results and perspectives. *J. Field Robotics* 34, 229–240. doi:10.1002/rob.21683

Lanham, M. (2018). *Learn ARCore—fundamentals of Google ARCore: learn to build augmented reality apps for Android, Unity, and the web with Google ARCore 1.0*. London: Packt Publishing Ltd.

Li, Z., Moran, P., Dong, Q., Shaw, R. J., and Hauser, K. (2017). "Development of a tele-nursing mobile manipulator for remote care-giving in quarantine areas," IEEE international conference on robotics and automation (ICRA), 3581–3586.

Liao, H., Inomata, T., Sakuma, I., and Dohi, T. (2010). 3-d augmented reality for MRI-guided surgery using integral videography autostereoscopic image overlay. *IEEE Trans. Biomed. Eng.* 57, 1476–1486. doi:10.1109/tbme.2010.2040278

Logan, D. E., Breazeal, C., Goodwin, M. S., Jeong, S., O'Connell, B., Smith-Freedman, D., et al. (2019). Social robots for hospitalized children. *Pediatrics* 144. doi:10.1542/peds.2018-1511

Mihelj, M., Bajd, T., Ude, A., Lenarčič, J., Stanovnik, A., Munih, M., et al. (2019). *Robotics*. Cham, Switzerland: Springer.

Mizumoto, K., Kagaya, K., Zarebski, A., and Chowell, G. (2020). Estimating the asymptomatic proportion of coronavirus disease 2019 (covid-19) cases on board the Diamond Princess cruise ship, Yokohama, Japan, 2020. *Eur. Commun. Dis. Bull.* 25, 2000180–2000184. doi:10.2807/1560-7917.ES.2020.25.10.2000180

Murai, R., Sakai, T., Kawano, H., Matsukawa, Y., Kitano, Y., Honda, Y., et al. (2012). "A novel visible light communication system for enhanced control of autonomous delivery robots in a hospital," in IEEE/SICE international symposium on system integration (SII), 510–516. doi:10.1109/SII.2012.6427311

Murphy, R. R., Tadokoro, S., Nardi, D., Jacoff, A., Fiorini, P., Choset, H., et al. (2008). *Search and rescue robotics*. Berlin, Heidelberg: Springer, 1151–1173. doi:10.1007/978-3-540-30301-5_51

Nagatani, K., Kiribayashi, S., Okada, Y., Otake, K., Yoshida, K., Tadokoro, S., et al. (2013). Emergency response to the nuclear accident at the Fukushima Daiichi nuclear power plants using mobile rescue robots. *J. Field Robotics* 30, 44–63. doi:10.1002/rob.21439

Naicker, S., Yang, C.-W., Hwang, S.-J., Liu, B.-C., Chen, J.-H., and Jha, V. (2020). The novel coronavirus 2019 epidemic and kidneys. *Kidney Int.* 97, 824–828. doi:10.1016/j.kint.2020.03.001

Ranney, M. L., Griffeth, V., and Jha, A. K. (2020). Critical supply shortages-the need for ventilators and personal protective equipment during the covid-19 pandemic. *New Engl. J. Med.* 382, e41. doi:10.1056/NEJMp2006141

Robotis. (2020). OpenMANIPULATOR-X. Available at: https://emanual.robotis.com/docs/en/platform/openmanipulator_x/overview/

Romero-Ramirez, F. J., Muñoz-Salinas, R., and Medina-Carnicer, R. (2018). Speeded up detection of squared fiducial markers. *Image Vis. Comput.* 76, 38–47. doi:10.1016/j.imavis.2018.05.004

Sakamoto, D., Honda, K., Inami, M., and Igarashi, T. (2008). "Sketch and run: a stroke-based interface for home robots," in Proceedings of the SIGCHI conference on human factors in computing systems, 197–200.

Sheridan, T. B. (2016). Human–robot interaction: status and challenges. *Hum. Factors J. Hum. Factors Ergon. Soc.* 58, 525–532. doi:10.1177/0018720816644364

Sheridan, T. B. (1992). *Telerobotics, automation, and human supervisory control*. Cambridge, MA: MIT Press.

Spong, M. W., Hutchinson, S., and Vidyasagar, M. (2006). *Robot modeling and control*. Hoboken: John Wiley and Sons, Inc.

Trevelyan, J. P., Kang, S.-C., and Hamel, W. R. (2008). *Robotics in hazardous applications*. Berlin, Heidelberg: Springer, 1101–1126. doi:10.1007/978-3-540-30301-5_49

Wada, K., Shibata, T., Saito, T., Sakamoto, K., and Tanie, K. (2005). "Psychological and social effects of one year robot assisted activity on elderly people at a health service facility for the aged," in Proceedings of IEEE international conference on robotics and automation (ICRA), 2785–2790.

Wang, A., Ramos, J., Mayo, J., Ubellacker, W., Cheung, J., and Kim, S. (2015). "The Hermes humanoid system: a platform for full-body teleoperation with balance feedback," in IEEE-RAS 15th international conference on humanoid robots (Humanoids), 730–737.

Wang, J., Suenaga, H., Hoshi, K., Yang, L., Kobayashi, E., Sakuma, I., et al. (2014). Augmented reality navigation with automatic marker-free image registration using 3-d image overlay for dental surgery. *IEEE Trans. Biomed. Eng.* 61, 1295–1304. doi:10.1109/TBME.2014.2301191

Wang, J., Zhou, M., and Liu, F. (2020). Reasons for healthcare workers becoming infected with novel coronavirus disease 2019 (covid-19) in China. *J. Hosp. Infect.* 105, 100–101. doi:10.1016/j.jhin.2020.03.002

Wolf, M. T., Assad, C., Vernacchia, M. T., Fromm, J., and Jethani, H. L. (2013). "Gesture-based robot control with variable autonomy from the JPL BioSleeve," in IEEE International conference on robotics and automation (ICRA), 14, 1160–1165. doi:10.1109/icra.2013.6630718

Yamada, H., Tao, N., and DingXuan, Z. (2009). "Construction telerobot system with virtual reality," in IEEE conference on robotics, automation, and mechatronics, 36–40.

Yoshida, K., and Wilcox, B. (2008). *Space robots and systems*. Berlin, Heidelberg: Springer, 1031–1063. doi:10.1007/978-3-540-30301-5_46

Zhang, Z. (2000). A flexible new technique for camera calibration. *IEEE Trans. Pattern Anal. Mach. Intell.* 22, 1330–1334. doi:10.1109/34.888718

Conflict of Interest: The authors declare that the research was conducted in the absence of any commercial or financial relationships that could be construed as a potential conflict of interest.

frontiers in Robotics and AI

REVIEW
published: 24 May 2021
doi: 10.3389/frobt.2021.612834

Upper Limb Home-Based Robotic Rehabilitation During COVID-19 Outbreak

Hemanth Manjunatha[1], *Shrey Pareek*[2], *Sri Sadhan Jujjavarapu*[1], *Mostafa Ghobadi*[1], *Thenkurussi Kesavadas*[2] *and Ehsan T. Esfahani*[1]*

[1] Human in the Loop Systems Laboratory, Department of Mechanical and Aerospace Engineering, University at Buffalo, Buffalo, NY, United States, [2] Health Care Engineering Systems Center, University of Illinois Urbana-Champaign, Champaign, IL, United States

The coronavirus disease (COVID-19) outbreak requires rapid reshaping of rehabilitation services to include patients recovering from severe COVID-19 with post-intensive care syndromes, which results in physical deconditioning and cognitive impairments, patients with comorbid conditions, and other patients requiring physical therapy during the outbreak with no or limited access to hospital and rehabilitation centers. Considering the access barriers to quality rehabilitation settings and services imposed by social distancing and stay-at-home orders, these patients can be benefited from providing access to affordable and good quality care through home-based rehabilitation. The success of such treatment will depend highly on the intensity of the therapy and effort invested by the patient. Monitoring patients' compliance and designing a home-based rehabilitation that can mentally engage them are the critical elements in home-based therapy's success. Hence, we study the state-of-the-art telerehabilitation frameworks and robotic devices, and comment about a hybrid model that can use existing telerehabilitation framework and home-based robotic devices for treatment and simultaneously assess patient's progress remotely. Second, we comment on the patients' social support and engagement, which is critical for the success of telerehabilitation service. As the therapists are not physically present to guide the patients, we also discuss the adaptability requirement of home-based telerehabilitation. Finally, we suggest that the reformed rehabilitation services should consider both home-based solutions for enhancing the activities of daily living and an on-demand ambulatory rehabilitation unit for extensive training where we can monitor both cognitive and motor performance of the patients remotely.

Keywords: COVID-19, robotic rehabilitation, home-based monitoring, haptic, mental engagement, recovery

OPEN ACCESS

Edited by:
S. Farokh Atashzar, New York University, United States

Reviewed by:
Muhammad Ahmad Kamran, Pusan National University, South Korea
Yueling Lyu, Sun Yat-Sen University, China

***Correspondence:**
Ehsan T. Esfahani
ehsanesf@buffalo.edu

Specialty section:
This article was submitted to Biomedical Robotics, a section of the journal Frontiers in Robotics and AI

Received: *30 September 2020*
Accepted: *03 March 2021*
Published: *24 May 2021*

Citation:
Manjunatha H, Pareek S, Jujjavarapu SS, Ghobadi M, Kesavadas T and Esfahani ET (2021) Upper Limb Home-Based Robotic Rehabilitation During COVID-19 Outbreak. Front. Robot. AI 8:612834. doi: 10.3389/frobt.2021.612834

1. INTRODUCTION

COVID-19 has affected numerous sectors of society, particularly healthcare workers and patients. In this regard, stroke patients are no exception, about 4 million stroke survivors live in the United States today and as many as one-half struggles with chronic motor deficits (CDC, 2017). Nearly one-third of all stroke survivors have a significant residual disability, with older individuals generally experiencing slower functional recovery (Langhorne et al., 2011). These patients face challenges in continuing their physical therapy due to access barriers to quality rehabilitation

settings and services imposed by social distancing and stay at home orders due to COVID-19 outbreak.

Besides, 32% of patients recovering from COVID-19 already have comorbid conditions, such as stroke and some others suffer from post-intensive care syndrome (PICS) due to prolonged stay in ICU (Hermans and Van den Berghe, 2015; Sheehy, 2020). According to a systematic review performed on 18 Chinese studies and one Australian study, 20% of the infected patients required intensive care unit (ICU) admissions, out of which 33% suffered from acute respiratory distress syndrome and 13% suffer from acute cardiac injury (Rodriguez-Morales et al., 2020). Some of these patients show symptoms related to central and peripheral nervous system manifestations (Mao et al., 2020). Moreover, prolonged stay in ICU causes neuromuscular complications that affect limbs, respiratory muscles, and sensory nerves. These complications cause neurological impairments as well as muscular impairments, such as severe muscle weakness, reduced joint mobility, leading to the difficulties in performing activities of daily living (ADL) (Korupolu et al., 2020). These neuromuscular complications can be mitigated with the help of mobility and interventions, such as (1) passive, active-assisted, or resistive therapy; (2) repetitive therapeutic exercises; (3) functional mobility; and (4) occupational therapy for the activities of daily living (ADL) (Korupolu et al., 2020). Moreover, there is a significantly greater incidents of acute ischemic stroke in patient with COVID-19 infection compared to those without infection pointing the vulnerability of COVID-19 patients (Belani et al., 2020). Indeed, about 5% (Felten-Barentsz et al., 2020) of the admitted COVID-19 patients to the hospital may show severe symptoms and require extensive ICU stay.

However, the COVID-19 burden on the healthcare facilities worldwide is causing an early discharge of the existing patients, suspension of new patient admissions, and reduction in activities to reduce contact. For instance, in Europe alone, COVID-19 has affected access to rehabilitation services for about 2 million people (Andrenelli et al., 2020). The guideline offered by the World Health Organization for inpatient rehabilitation in COVID-19 requires daily health checks for personnel, continuous staff training on changing protocols/guidelines, use of personal protective equipment, cancellation of non-essential therapies, following proper hand hygiene instructions, and use of telecommunication for clinical interviews. Moreover, healthcare workers will be required to attend early discharged patients from acute care, decontaminate the shared equipment, prohibit group therapy, allocate a separate unit to all the patients, and provide one-on-one therapy (Bartolo et al., 2020; Sheehy, 2020). Even if inpatient rehabilitation is remodeled and available at a healthcare facility, the amount of time invested by the health care staff in practicing infection control measures decreases their work efficiency (Sheehy, 2020).

To reduce the burden on healthcare systems and provide a safe space for the patient to continue the therapy, the current rehabilitation programs should be transformed into telerehabilitation. Telerehabilitation refers to the therapy being conducted away from the hospital setting, mainly home-based or community based, which allows the users to perform a customized program of therapeutic activities. Almost, all research or review articles published in response to the physical therapy and rehabilitation needs during COVID-19 emphasize on the importance of the tele-rehabilitation and home exercise (Bettger and Resnik, 2020; Farzad et al., 2020; Zhu et al., 2020) and some even provide a guideline on how to approach staff training, patients evaluations, and discharge in such settings (Rosen et al., 2020). In this review article, we propose a hybrid model incorporating home-based telerehabilitation and inpatient treatments through ambulatory robotic rehabilitation services as a more effective solution during COVID-19 and similar pandemic that may accrue in future.

In telerehabilitation, an occupational therapist or a healthcare provider works closely with the patient and provides feedback and instructions through web interfaces. By monitoring the progress of the patient, they can also make necessary changes to the exercise regime. However, the therapists might not have enough time to monitor the patient's progress online due to the increased COVID hospitalizations. Nonetheless, thanks to the technological advancements in the last two decades, considerable effort has undergone toward building new physical platforms, such as robotic and orthotic systems (Brennan et al., 2009; Housley et al., 2018) to facilitate the telerehabilitation process and also improve the outcome of motor function recovery (**Figure 1**). In particular, using robots and orthotics equipped with haptic feedback or haptic assistance is viewed as an alternative solution to physical therapy (Krebs and Hogan, 2012; Linder et al., 2013). These systems can be effectively used to continue the rehabilitation procedure even during the COVID-19 pandemic in-home and community centers. For patients who face difficulties due to traveling disabilities or limited transportation (Holden, 2005), community-based rehabilitation can be extended to ambulatory robotic rehabilitation services.

Substituting the physical therapy with telerehabilitation approach requires four key components (**Figure 1**). First, *delivering assistance:* Since the therapists are not present to guide the patient physically, there is a need for low-cost devices that can provide necessary support (Frolov et al., 2018). In this regard, as discussed previously, haptic devices and robotic systems offer a promising solution. Second, *enhancing engagement and social support:* Even with repetitive support from robotic systems, the rehabilitation outcome may not be superior to physical therapy without patient's engagement (Blank et al., 2014). So, encouraging and maintaining patient's engagement in telerehabilitation is of paramount importance. Third, *assessing the progress:* As patients cannot access the hospital facilities frequently during COVID-19 restrictions, periodic assessment of functional status is impeded; thus, there is a requirement for remote assessment devices and metrics (Nordin et al., 2014; Frolov et al., 2018). Consequently, the telerehabilitation approach should support a wide array of low-cost sensors through which the therapist can assess the patient's recovery. Finally, *adaptation:* As the patient's needs vary throughout the rehabilitation regime, robotic/haptic systems' ability to adapt plays a vital role in delivering necessary rehabilitation assistance while adhering to social distancing norms during COVID-19 outbreak. With this backdrop, in the succeeding sections, we provide brief literature in these four critical areas in the context of upper limb rehabilitation.

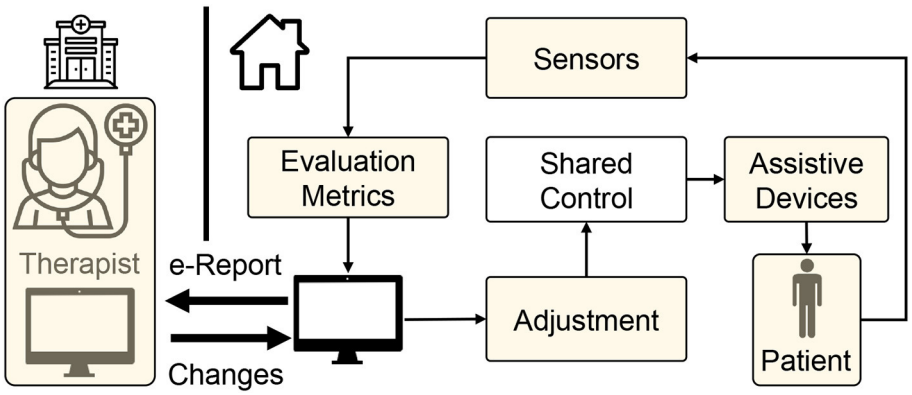

FIGURE 1 | Schematic of tele-rehabilitation where patients can continue their rehabilitation with the help of an assistive device while therapist can monitor the progress remotely.

In the subsequent sections, we will review the main components of telerehabilitation (home or community based) related to *delivering assistance*, *enhancing engagement and social support*, *assessing the progress*, and *providing adaptation* to provide successful therapy during COVID-19 outbreak.

2. ASSISTANCE DELIVERY

In the current pandemic, home environment serves as the best solution to deliver remote rehabilitation to patients. It reduces the burden on inpatient services and, at the same time, prevents the spread of disease to the patient. The main objectives of delivering therapy in such settings are to (1) facilitate repetitive task training with real-time feedback about performance, and (2) maintain high patient engagement during training (French et al., 2016).

2.1. Tele-Rehabilitation Framework

Tele-rehabilitation was first documented in 1959 when an interactive video was first used at the Nebraska Psychiatric Institute to deliver mental health services. With the advent of the Internet and the availability of large medical records, telerehabilitation/telemedicine received more attention in mid-1990s focusing on the proof of concept with few clinical trials. Since the early 2000, there has been a surge of tele-rehabilitation mainly focused on rural areas. By 2016, around 125,000 stroke patients were reported to have used telerehabilitation for treatment (Peretti et al., 2017). For years, researchers and practitioners utilized telerehabilitation to reduce inpatient hospitalization duration and reduce the cost of rehabilitation for patients. Cramer et al. (2019) has shown that the efficacy of upper limb home-based telerehabilitation is comparable to the therapy delivered in clinical settings. Many ADL skills, such as using a fork and spoon, twisting doorknobs, and being able to manipulate simple objects, require fine motor control of the patient's hand and are better suited for home-based therapy.

Rehabilitation therapy also requires the patient to perform high-intensity exercises and get periodic assessment from a therapist, which is not generally feasible in home environments due to the lack of equipment, thus, home-based rehabilitation should be combined with outpatient rehabilitation services offered by rehabilitation clinics and community rehabilitation centers. Ru et al. (2017) and Dean et al. (2018) have recently shown that patients participating in community-based rehabilitation programs, when coupled with home-based exercises, demonstrated enhanced motor function, daily activity, and social activity. Community rehabilitation centers or kiosks mentioned in the above studies use a video/audio communication channel to connect the therapist to the patient and allow a continuous exchange of information (**Figure 1**). Patients perform the physical exercise while being remotely monitored and assessed by a physiotherapist via video-conferencing. Such telerehabilitation services provide a cost-effective solution to deliver and monitor long-term therapeutic interventions. In this context, Holden et al. (2007) developed a telerehabilitation system that provides real-time interaction between a patient at home and a therapist located at a clinic. Reinkensmeyer et al. (2002) developed a web-based telerehabilitation system for the patient to practice simple movements using an adaptive joystick with force feedback. The therapist can track improvements in training. Another low-cost telerehabilitation platform is Habilis (Motus, 2020) developed for the Clinical Leading Environment for Assessment and Validation of Rehabilitation Protocols for Home Care (CLEAR) project under the European Union. At home, these telerehabilitation services can be accessed via mobile phones or tablets connected to the Internet. These technological devices provide an affordable solution to connect and directly interact with sensors (Ameer and Ali, 2017). Such devices also enable offline use of services, such as pre-recorded sessions by therapists and online services, such as video-conferencing. In the absence of such services, patients can follow some home exercise guides, such as one prepared by Ambrose et al. (2020).

The development of telerehabilitation requires a reliable communication network and tailored software systems to deliver rehabilitation support effectively. In this regard, Hosseiniravandi et al. (2020) provide a scoping review of different software systems designed to address the delivery problems of home-based telerehabilitation. The review included systems with

various functional features, such as exercise plan management, report generation, and task scheduling. On similar lines, Fiani et al. (2020) provide a review on the development, usage, and technological advances of telerehabilitation. The authors also provide suggestions on advancements of telerehabilitation during COVID-19. Additionally, the development of an effective telerehabilitation service requires identifying methods and material to evaluate patients' existing functional status such that the intensity of exercise can be modulated. The service should efficiently collect and document patient data to monitor exercise intensity and patients' progress during therapy. Tele-rehabilitation platforms, such as VidyoHealth^{TM}and Habilis^{TM}enable synchronous and asynchronous data collection. These services enable setting up automatic training schedules, recording patients' activity, evaluating their functional status, and manipulating the factors to vary the intensity of therapy based on their progress (Middleton et al., 2020).

In the remainder of this section, we will focus on the main components of telerehabilitation necessary to assist, evaluate the patient's state, assess the patient's engagement and compliance, and suggest adaptation based on the patient's functional status.

2.2. Robotic Devices

Robotic rehabilitation has shown promising results in lab environments. During clinical trials, their validation demonstrated huge potential in patients' recovery (Maciejasz et al., 2014) and can be used as an alternative to physical therapy. These robots sense the user's movement and use that information to provide force feedback or plan subsequent motions. The robot can interact with the patients in three possible ways: (1) passive (patient-driven), (2) active (robot drives), and (3) challenge (resist the forces applied by patients). In this regard, Frolov et al. (2018) provide a scoping review of different robotic devices used in rehabilitation. Even though much robotic rehabilitation systems are in use, only a few robots have been developed for home-based telerehabilitation. For instance, only robots, such as Hand Mentor, Foot Mentor (Motus Nova, 2020), and SCRIPT (Ates et al., 2017) have been successfully used in the home setting. The Hand and Foot Mentor devices provide active assistance to increase the range of motion in patients who have residual upper and lower extremity impairments. The patient completes a game-like training where the difficulty is modified depending on the progress. The device provides audio and video feedback along with remote monitoring through the clinician dashboard. Unlike Hand and Foot Mentor, SCRIPT provides passive assistance for finger and extension. This decreases the cost of deployment and simplifies the software algorithm design. Similar to Hand and Foot Mentor, SCRIPT provides an interactive game-like interface. To expand further, Brewer et al. (2007); Housley et al. (2018) provide a review of different telerehabilitation robotic (TRR) approaches and clinical outcomes in home-based settings. The review covers topics, such as ease of deployment, cost-effectiveness, involvement from the patients, intervention protocol, and dosing. The review concludes that future TRR design should consider the cost analysis for wide adaptation of TRRs in home-based settings.

However, most robotic rehabilitation setups are too expensive and require monitoring by a skilled operator, and are most suited for community-based rehabilitation centers and not home-based settings. In the last two decades, new low-cost haptic systems (e.g., Novint Falcon, 3dsystems Phantom, Quanzer Pantograph, and so on) have emerged and adopted for home-based rehabilitation. These haptic systems sense the user's movements and use them to assist subsequent motions by providing force feedback. Such continuous feedback is shown to enhance the rhythmic motor control by reducing the temporal variability in repeated movements (Ankarali et al., 2014). Thus, low-cost, ease of use, and low-maintenance haptic devices have attracted a lot of attention for home-based rehabilitation (Oblak et al., 2010; Piggott et al., 2016).

In addition to hardware, many researchers have studied how different force feedback strategies elicit better rehabilitation outcomes. The two most popular force feedback strategies are (1) *error-reduction (ER) strategy*, which decreases the performance error by providing active assistance to enable the patient to perform the rehabilitation tasks better; (2) *error-augmentation (EA) strategy* that increases the task difficulty to evoke a higher voluntary involvement of the patient to accomplish the goal (Israely and Carmeli, 2016). In a scoping review by Li et al. (2018) on the effect of EA and ER strategies on upper limb post-recovery showed that subjects under EA showed statistically significant motor performance improvement compared to the ER. In fact, the EA strategy aligns with the motor adaption principle, which suggests that kinematic errors generate neural signals that drive motor adaptation during movement (Schmidt et al., 2018). Even though EA and ER are widely used strategies, such therapy's outcomes will not be superior to manual therapy if the patient is not actively engaged in the therapy (Takeuchi and Izumi, 2013; Blank et al., 2014). Consequently, maintaining patients' engagement through virtual reality (VR) or augmented reality (AR) has gained significant traction.

2.3. Virtual Reality

VR in rehabilitation is explored as a modality to provide feedback and engage patients through immersive environments. VR refers to an artificial environment experienced through sensory stimuli (as sights and sounds) provided by a computer, and the user's actions partially determine what happens in the environment. In other words, any simulation on a computer screen may be considered VR (**Figure 2**). These systems cannot provide assistance/resistance to patient's movements and require a robotic or haptic system.

VR offers the capability of showing the trajectory of the patient's limb movements in real-time that enhances motor learning during rehabilitation (Pareek, 2020). Moreover, tasks designed using VR can be customized to patient's needs at different therapy levels, i.e., therapists can make the task easier or challenging according to the recovery status (**Figure 3**). Rose et al. (2018) provides a review on VR applications in rehabilitation aiming at (1) how VR is beneficial in the health outcomes, (2) how VR can influence the patients to adhere to the rehabilitation plans, and (3) influence of haptic feedback on the performance of an individual in the VR.

Display screens have been used for a long time to present virtual environments during rehabilitation. In recent years, head-mounted VR devices have attracted a lot of attention

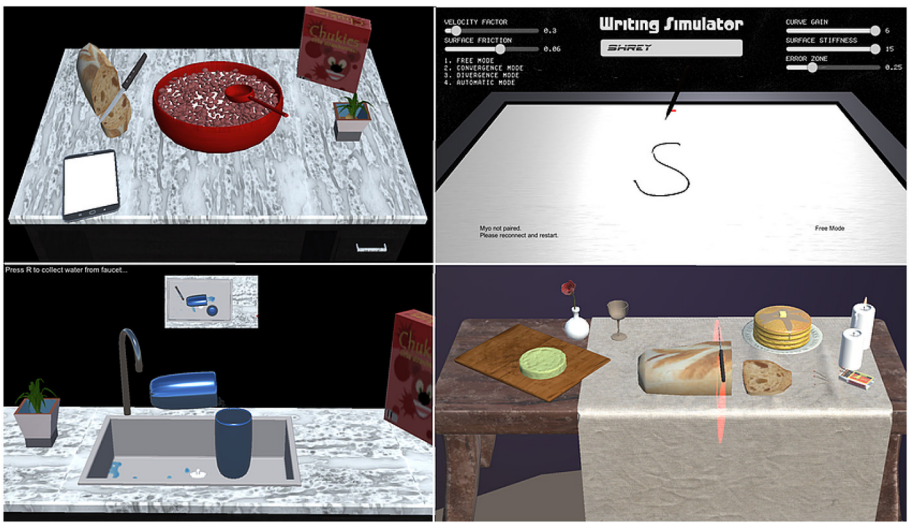

FIGURE 2 | Different virtual reality (VR) games that can emulate Activities of Daily Living (ADL), such as using a spoon (eating), pen (writing), knife (cutting), and glass (pouring) in clockwise order from top-left.

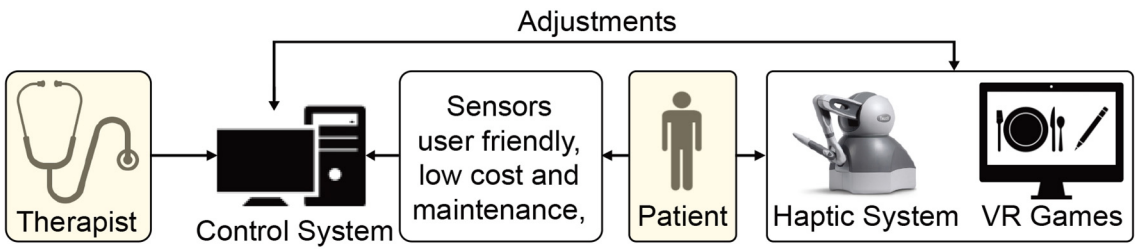

FIGURE 3 | Schematic demonstrating a haptic device and virtual reality (VR)-based home rehabilitation setup.

in rehabilitation. Commercially available VR headsets (Oculus Rift®, Microsoft HoloLens®, HTC Vive®, and the Samsung Gear VR®) have added additional dimensions and intuitiveness to the VR technology (Webster and Celik, 2014). Haptic interfaces can augment the virtual interaction forces in the real world and thus complement VR with force feedback during the therapy. Moreover, tasks designed using VR can be customized to the patient's needs to adaptively challenge them according to their progress and engage them in the therapy. Emerging companies, such as Neuro Rehab VR and Peili Vision have already developed VR stroke rehabilitation systems. These systems aim to increase patient engagement by making physical therapy more enjoyable. However, these systems currently rely on commercially available gaming hardware that is not tailored for stroke patients, which limit their practical use but promise a reliable framework for home-based therapy.

3. ENGAGEMENT AND SOCIAL SUPPORT

Maintaining motivation to adhere to the therapy is challenging for the patient during unsupervised therapy in home-based and community-based settings. A combination of VR and robotic systems can provide the necessary motivation by making the exercises more comfortable, less dangerous, engaging, and entertaining. Such customizability allows the therapist to make high-intensity and repetitive training exercises more motivating, engaging, and enjoyable for the patients (Rose et al., 2018). Specifically, VR-based therapy can increase patients' engagement by creating interactive and competitive tasks that provide frequent performance feedback during the exercise (Zimmerli et al., 2013). In addition to the VR visual feedback, multimodal feedback, such as auditory and haptics can enhance the patient's engagement during the exercise. One of the promising modalities is brain–computer interfaces (BCIs).

BCIs have proved to be a useful tool in evaluating patient's engagement during therapy. They can be used to objectively assess task performance, engagement, and voluntariness (Sullivan et al., 2017; Likitlersuang et al., 2018; Manjunatha et al., 2020). Concretely, BCIs have attracted a lot of attention in quantifying mental engagement as it directly measures the subject's cognition during rehabilitation (Berger et al., 2019). Such measures can adaptively change the robot/haptic parameters to desired levels (Bartur et al., 2017). The expense and setup procedure of BCIs

makes it challenging to be used in home-based environments. These sensors can be used in clinics or community-based setting where the patient's cognitive state can be monitored during his/her visit.

Another factor that impacts patients' participation in therapy is social support. Patients suffering from stroke or COVID-19 develop anxiety, depression, fatigue, and post-traumatic stress disorder. In addition to the physical or cognitive state, psychological health acts as an indicator of the surviving population's quality of living. For instance, a scoping review by Essery et al. (2017) revealed that social support is a strong predictor of home-exercise adherence. Along with social support, other main factors included self-motivation, intention, self-efficacy, and previous adherence. The study showed that social support would increase adherence by providing encouragement, boosting self-esteem, and buffering stress due to illness. Thus, as the patients are motivated to adhere to an exercise regime, the recovery is accelerated. The positive influence of social support on the outcome of patient's recovery is also in-line with previous adherence studies (DiMatteo, 2004; Jack et al., 2010).

Physical therapy and rehabilitation can improve neuromuscular functionality; however, the methods to prevent or treat depression or cognitive impairment are still lacking. Cognitive evaluation and behavioral therapy are slightly useful in improving the psychological and cognitive state. A more practical solution for enhancing psychological health is to provide motivation and emotional support to decrease their loneliness and coach them to compensate for diminished skills or lacking abilities.

In home-based therapy, family members are the primary caregivers who can provide social and moral support to the patient throughout the recovery process. Proffitt et al. (2011) indicated that activities incorporating family members might facilitate compliance and reduce patients' social isolation. The therapist can also provide additional social assistance through video-conferencing, virtual avatars (Borghese et al., 2013) designed in VR, indulging and entertaining VR games, and socially assistive robots (SAR).

3.1. Socially Assistive Robots

A social companion robot is defined as a robot that can assist humans in daily activities at home, workplace, and other environments (Dario et al., 2011) and possesses the skills to interact with the people socially. Social companion robots or SARs can benefit the elderly population, individuals with physical, neurocognitive impairments, and individuals suffering from depression (Lorenz et al., 2016). SAR provides a stimulating or motivating influence on individuals and reduces their loneliness. One of the main challenges of rehabilitation during COVID-19 is contact. In this regard, SAR creates a bridge between contact-based rehabilitation robotics and non-contact functionalities of the companion robotics. Therefore, SAR enables contact-free monitoring, coaching, and encouragement while also providing detailed assessments of the patient's progress.

Some popular SARs that fulfill the role of a pet are Paro (Shibata et al., 2001), NeCoRo (Libin and Libin, 2004), and Huggable (Stiehl et al., 2005). Similarly, SARs made for elderly care are Care-O-Bot (Graf et al., 2009), MobiNa, Hector (Schroeter et al., 2013), and Hobbit (Fischinger et al., 2016). These robots enable the independent living of the older population by helping them with household tasks. In addition to monitoring patients' progress and motivating them, SAR (Eriksson et al., 2005) and Clara (Kang et al., 2005) can help in rehabilitation. For example, Bandit (Eriksson et al., 2005) is a hands-off therapist robot that can navigate autonomously, demonstrate the task, monitor patients' arm activity, and remind them to follow a rehabilitation program. Clara (Kang et al., 2005) is another hands-off therapist robot that can assist patients in repetitive spirometry exercises; thus, it can be very useful for patients recovering from Acute Respiratory Distress Syndrome (ARDS).

The major challenge of SARs is to identify the social abilities from human and implementing them (Lorenz et al., 2013). SARs have to be adaptive as the interaction with a non-adaptive robot cannot result in movement synchronization (Lorenz et al., 2013). Synchronous behavior between the patient and a robot is essential for the emergence of compassion and positive emotions (Lorenz et al., 2016). In this context, Bethel and Murphy (2010) provided some measures to evaluate a robotic system in terms of interaction.

4. PROGRESS ASSESSMENT

While delivering remote rehabilitation, the therapist needs to monitor the functional progress of a patient to vary the intensity to the desired level. Sarfo et al. (2018) reviewed the commonly used metrics to monitor patients' progress during telerehabilitation interventions, of which *ABILHAND*, *Ashworth scale*, *Action Research Arm Test (ARAT)*, *Fugl-Meyer Motor scale for upper extremity (FMA-UE)*, *Grip strength*, *Nine-Hole Peg test (9-HPT)*, *Shoulder strength*, and *Wolf motor function test (WMFT)* are used to assess upper limb functionality. ABILHAND is a subjective measure of the ability to manage activities of daily living. Ashworth scale is a subjective score ranging from 0 to 4 based on the resistance to passive movement about a joint. ARAT requires a kit to test the grasp, grip, and pinch functionalities along with the gross movement capability of the upper limb. FMA-UE provides a quantitative measure for a range of functionalities involving the upper extremity, wrist, hand, coordination, speed, sensation, passive joint motion, and joint pain. 9-HPT is a standardized quantitative assessment to measure finger dexterity and requires a wooden board with nine holes and nine pegs. WMFT is a quantitative measure to assess time, functional ability, and upper extremity motor ability strength. These metrics have been extensively used for the remote assessment of upper limb functionality in chronic stroke and neuromuscular disorders, and can also provide a quantitative prior for assessing COVID-19 patients during telerehabilitation. In addition to these metrics, patients' satisfaction and cognitive

state should be examined to assess both mental and cognitive engagement as they are vital aspects in the success of remote rehabilitation (Pareek and Kesavadas, 2019).

In the absence of a therapist, sensors should measure and quantify patients' exercise in the home environment. Wearable sensors have been utilized to measure and assess a wide range of motor behaviors, such as fall detection, mobility characterization, and activity recognition. Moreover, the information from these sensors can act as biofeedback in automated training. The most common information used for assessing the upper limb functionality is the trajectory of the upper limb tracked by the robot's sensors. Moreover, inertial measurement units (IMUs) provide a portable and low-cost solution to physical activity detection (Wittmann et al., 2016). IMUs placed on the upper limb can be used to monitor movements during therapy, and when placed near the ankle, can be used to characterize patients' gait. On the other hand, IMUs in mobile phones provide low-cost alternatives to external IMUs. Force-sensitive sensors can be incorporated in wearable gloves (Polygerinos et al., 2015) and fabrics to detect grasp pressure during upper extremity exercises. Moreover, force-sensitive sensors incorporated in footware can measure ground reaction forces and provide better fall detection when used in combination with IMUs. IMUs and force sensors can be easily incorporated into home-based rehabilitation to detect voluntary forces from the patient. Moreover, the trajectories obtained from the haptic and VR systems are useful in tracking patients' progress.

Non-invasive physiological sensors, such as surface electromyography (sEMG) can also be used to assess changes in neuro-motor control during robotic intervention (Clark et al., 2010). A combination of sEMG sensors and IMUs has been used to monitor movement quality while assessing patients' muscle activity (Pareek et al., 2019). Such sensors provide a low-cost solution for differentiating voluntary contractions from spastic and enable automatic detection of functional ADLs, such as feeding, grooming, dressing, transferring, locomotion, and toileting in home-based therapy (Porciuncula et al., 2018). Additional physiological sensors used during therapy can record body temperature, respiratory rate, pulse rate, blood pressure, muscle activity, cognitive state, and so on (Chen et al., 2019). While these additional sensing technologies may seem redundant for the home-based setting, they may be used in the community-based rehabilitation center to provide additional insight into the patient's cognition.

New studies provide empirical evidence that closed-loop sensorimotor systems that use brain activity and haptics in robotic therapy improve the rehabilitation of upper limb (Frolov et al., 2018). Non-invasive BCIs introduce EEG signals as potential feedback capable of indicating the subject's intentions and providing his/her sophisticated cognitive state, such as the level of engagement. Popular metrics include event-related synchronization or desynchronization (ERS/ERD) (Jochumsen et al., 2013) and sensory-motor rhythms (SMR). For instance, Soekadar et al. (2015) suggested SMR as an ideal candidate for non-invasive BCI-training in stroke neuro-rehabilitation. This is because SMR is closely related to motor activities, accessible through EEG signals, and has a high signal-to-noise ratio (Soekadar et al., 2015). Moreover, studying motor learning after stroke is also possible with motor imagery measures in a passive setting (Meyer et al., 2012).

While the use of BCI in current clinical practice is viable, the remote operations may seem impractical due to setup and calibration requirements. The future generation of remote rehabilitation system can potentially use them as an alternative to traditional feedback in active rehabilitative platforms (Bamdad et al., 2015). In this regard, van Dokkum et al. (2015) conducted a literature review on different aspects of BCI application for neuro-rehabilitation. The study considered current methods useful for three applications: (1) providing feedback to adjust training tasks, (2) quantifying and measuring motor improvements, and (3) stimulating patients to encourage and make them optimize and correct themselves to execute their tasks. The authors recommended using BCI for motor rehabilitation purposes according to its adaptability to a large population and, at the same time, consider it necessary to study for more clinical results based on controlled designs to validate the impact of BCI on motor and functional recovery.

5. ADAPTIVE REHABILITATION

Due to the COVID-19 outbreak, the patient's rehabilitation should be shifted to a teleoperated home-based or community-based approach to reduce the therapists and inpatient facilities' burden. However, for such an approach, one of the major priorities is to devise a reliable decision-making algorithm as an alternative to the therapist (**Figure 4**). Such a decision-making algorithm must determine when, how, and to what degree the interventions must be modified and adapt accordingly to improve the patient's functional recovery. The adaptation should be based on the patients' existing state and recovery progress. For inferring the patient's state, physiological signals are an indispensable modality. For example, the physiological signals, such as EEG, EMG, and eye tracking can be used passively to understand the state of the patients and their level of engagement. They can also actively modify the rehabilitation parameters (e.g., assistance level provided by haptics/robotics system or VR game difficulty). Some modalities cannot be obtained in home-based settings as they desire low-cost sensors with a minimal setup procedure. However, various sensors ranging from EEG to IMUs can be used in the community or ambulatory rehabilitation. In this regard, significant measures have been adopted by researchers to implement adaptive rehabilitation services where VR and haptic devices can be adapted using physiological signals.

5.1. Adaptation of Virtual Reality Interfaces

VR has facilitated the implementation of adaptive rehabilitation approaches for two reasons. First, the relative ease and flexibility in developing VR environments compared to building physical interfaces in the real world. The VR systems can be easily adapted to both home, community, and ambulatory rehabilitation. Second, the patient's performance and progress can be measured easily with respect to the accomplishment of a mission through a series of tasks or games. Moreover, being involved in a game or even serious virtual tasks through an interactive

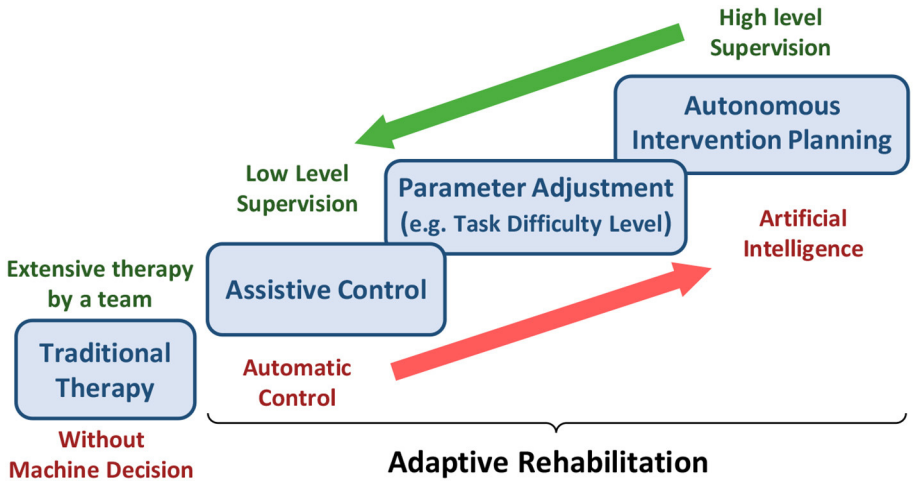

FIGURE 4 | The burden of assistance and decision-making shared between experts and machines from traditional therapy to adaptive rehabilitation.

environment can significantly increase cognitive engagement, which is traditionally provided by social communication between a patient and the rehabilitation team members.

In VR, the game difficulty can be easily adjusted depending on the patient's engagement and progress. In this category, Nirme et al. (2011) has designed a Rehabilitation Game System (RGS) based on VR. They developed two algorithms capable of controlling the task difficulty that an RGS user is exposed to and provide controlled variation in the therapy. In this regard, Hocine et al. (2015) have also recently studied related works in the adaptive adjustment of task difficulty. They hypothesized that a dynamic adaptation of task difficulty based on the subject's abilities and performance surpasses the other two methods reported in previous works, which make either an incremental or a random change in the task's difficulty level (Cameirao et al., 2010; Rabin et al., 2011). The results of their study demonstrated that the stroke patients under experiments with dynamic adaptation methods gained a higher amplitude of movement, which is considered a positive sign of recovery (Hocine et al., 2015).

An interesting result of the scoping review done by Bamdad et al. (2015) is that the work based on VR control (VRC) dedicates half of the research papers in BCI-based rehabilitation. Barzilay and Wolf (2013) have recently proposed an effective VR framework to improve triceps performance by designing a set of adaptive rehabilitation games that work with respect to some biofeedbacks. They provide these biofeedbacks through a learning system that estimates the biological model from raw data being acquired from hand motion and muscle activities. In this regard, Pirovano et al. (2012) have also developed a framework of self-adaptive games for rehabilitation at home. In such a framework, they have considered the game design to be (1) capable of being integrated into general-purpose rehabilitation stations, (2) consistent with the constraints posed by the clinical protocols, (3) inclusive of both effective and functional movements to reach the rehabilitation goals, and (4) adaptive to the patient's current status and his/her estimated progress. They utilized a fuzzy system to monitor the execution of exercises and a Bayesian adaptive approach to modify the gameplay with respect to the current performance and estimated progress of the patient as well as the exercise plan that is each time instructed by the therapist (Pirovano et al., 2012). This adaptive game engine is extended in a more recent research conducted by Pirovano et al. (2016), where they have also addressed how the adaptation of task difficulty can be performed with respect to the patient's performance as well as real therapist inputs to increase the level of engagement. To this end, a virtual therapist (Borghese et al., 2013) guarantees the patient to be properly challenged and, at the same time, motivated, safe, and supervised. Pirovano et al. (2016) also introduced a more independent autonomous rehabilitation game engine that provides a home-based framework needless of close supervision by a therapist. In a recent overview, Vaughan et al. (2016) presented state-of-the-art self-adaptive technologies within VR training.

Despite the recent advances in VR, its feasibility in the clinical rehabilitation setting is limited in terms of application, education, and research (Laver et al., 2011). Although many studies aiming at the development and evaluation of VR-based rehabilitation systems exist, very few have been evaluated outside laboratory settings. Three major limitations have been reported for the use of VR in rehabilitation, latency between input and output devices, underestimation of perceived distance in real world, and motion sickness (Morel et al., 2015). Latency is the delay between patient's action using input device and its corresponding reaction using output device in the virtual environment. Latency affects rehabilitation efficacy by delaying the timing of stimulus presented to the patient. Improper relation between the perceived distance in real and virtual environments, motion sickness, eye fatigue, headaches, nausea, and sweating caused due to prolonged exposure to head mounted displays limit the efficacy of VR systems (Laver et al., 2011; Yates et al., 2016; Park et al., 2019). Additionally, the cost of VR development, aggravated by the

poor reception of these technologies by older stroke patients, inhibits these systems' feasibility. However, these limitations should be evaluated using studies with larger sample sizes and post-intervention follow-up measures (Yates et al., 2016).

5.2. Adaptation of Haptic/Robotic System

The success of rehabilitation robots in physical therapy encourages the researchers to develop an adaptive robotic rehabilitation strategy (Mounis et al., 2019). For instance, Kan et al. (2011) proposed an automated rehabilitation robotic system that guides stroke patients through an upper limb reaching task. They used a decision-making algorithm to automatically modify exercise parameters, which account for different individuals' specific needs and abilities. They have also used these parameters to make appropriate decisions about the rehabilitation exercises.

Another common understanding of adaptive rehabilitation mainly used in robotic and haptic systems is to actively adapt the assistance provided to the patient by a robot. This assistance is provided as per the physical needs of the patient. Wolbrecht et al. (2008) researched to examine different hypotheses on how to maximize the participation of the motor system through robotic assistance. Their findings reveal that a minimally assistive intervention previously introduced by Cai et al. (2006) termed as "assist-as-needed" is an appropriate strategy that can be used as the core for many assistive robots. Surprisingly, the "assist-as-needed" strategy coincides with a motor learning principle realized by Hasson et al. (2012), explaining that a human evolves his/her motor skills by minimizing the required force to control dynamically complex objects. A hypothesis is that the way an experienced therapist assists a motor-impaired patient is very similar to how the patient deals with high dynamical complexity objects. Thereby, the "assist-as-needed" strategy is comparable to traditional therapies. This can be the main reason underlying the effectiveness of assistive robots working based on the "assist-as-needed" strategy. Krebs and Hogan (2012) has mentioned that robotic therapy (RT) is reaching its tipping point and that RT practices, particularly based on motor learning principles, such as the "assist-as-needed" strategy, have been successful.

TABLE 1 | Different adaptive rehabilitation approaches using virtual reality (VR) and robots.

Publication	Adaptive rehabilitation technique	Modalities used for adaptation		Rehabilitation interface	Upper (U)/Lower (L) body
		Feedback from human	Feedback to human		
Hocine et al. (2015)	Parameter adjustment	Estimation of task performance in terms of success rate of task completion Evaluation of subject's abilities in terms of maximum zone of 2D movements	Dynamic adjustment of task difficulty w.r.t. subject's ability and performance	Virtual Reality	U
Pehlivan et al. (2015)	Assistive control AAN (Assist-as-needed)	Subject performance	Modification of permissible error and assistance during movement execution	Robot	U
Perez-Ibarra et al. (2015)	Assistive control + Parameter adjustment	Estimation of force contribution and task performance using dynamic and kinematic feedback	Adjustment of level of assistance as well as the stiffness of impedance control	Robot	L
Squeri et al. (2014)	Assistive control	Subject's ability to keep up with target oscillations	Assistance adapted to residual capacities of motion while avoiding over-assistance	Robot	U
Barzilay and Wolf (2013)	Autonomous intervention planning	Estimation of task performance inferred by a trained neural network from biofeedback (EMG and Kinematic Info)	Planning rehabilitation tasks w.r.t. expectations of clinicians and feedbacks inferred from human	Virtual reality (Serious Games)	U
Pirovano et al. (2012)	Parameter adjustment	Estimation of task performance inferred by a fuzzy engine based on patients actions and Therapist's knowledge	Adjustment of task parameters, such as speed and range of motions+ Visual and voice effects are generated via an animated virtual therapist	Virtual reality (serious games)	U and L
Nirme et al. (2011)	Parameter adjustment	Estimation of the user model based on different parameters of task performance	Adjustment of task difficulty w.r.t. the estimated user model	Virtual Reality	U
Duff et al. (2010)	Autonomous intervention planning + Parameter adjustment	Estimation of task performance and recovery progress using kinematic feedback	Visual and musical stimulation are adapted by clinicians	Virtual reality (reaching task)	U

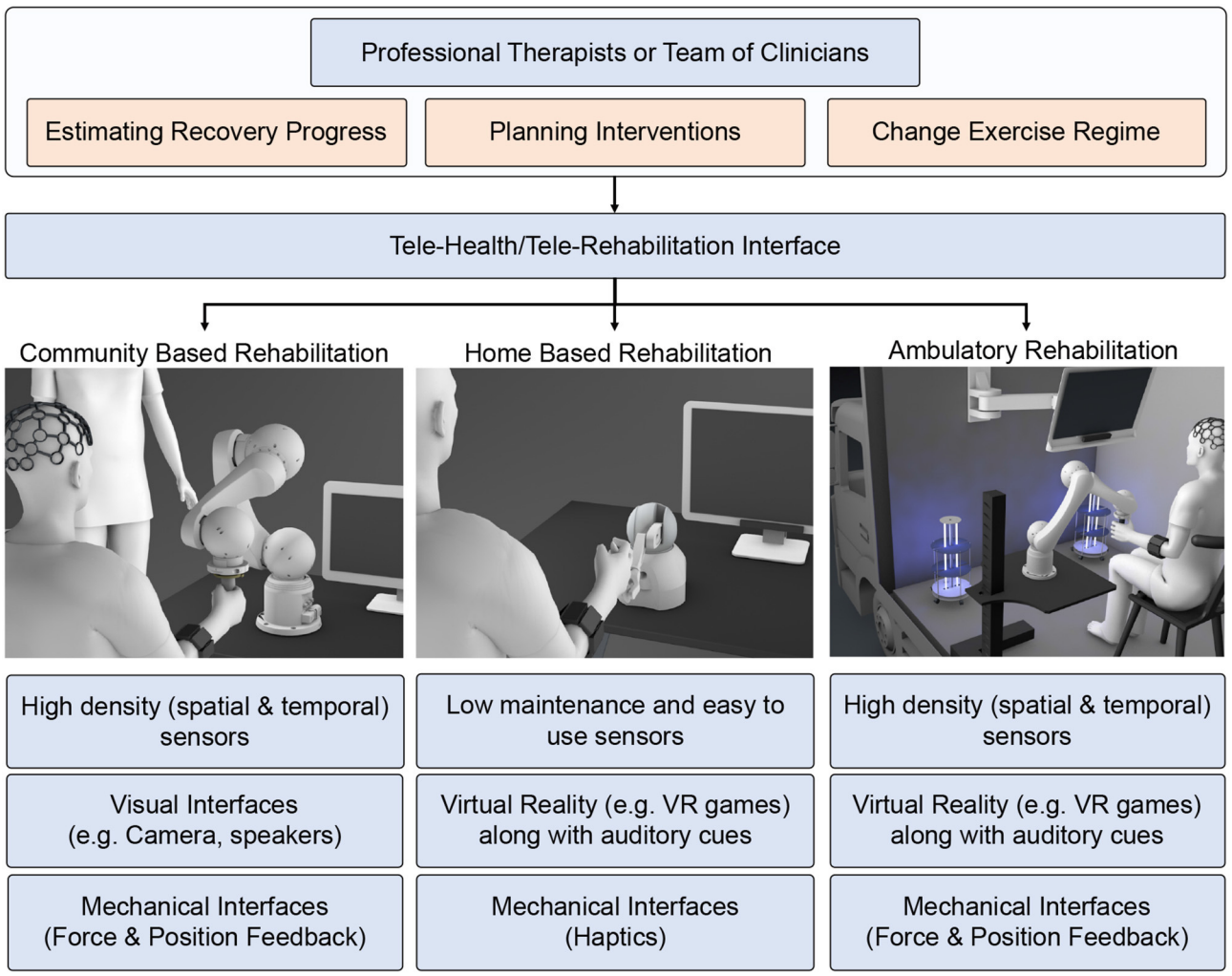

FIGURE 5 | Schematic showing the rehabilitation therapy in three different setups: (1) community-based, (2) home-based, and (3) ambulatory. Present robotic systems are geared toward hospital or home-based approaches. However, due to COVID pandemic, we need to modify and adapt the current system taking into account social distancing norms, emotional stress due to lockdown, and safety of health care workers and patients.

Most recently, Heuer and Lüttgen (2015) considered the assistive control strategies that work toward or against the motor recovery across trajectory and transformation learning skills. Their survey is accompanied by a classification of clinical results obtained from different strategies in terms of their effectiveness toward gaining certain motor skills. Maciejasz et al. (2014) adopted assistive control as one of the main high-level strategies of robotic therapy and added three more: challenge-based control, haptic stimulation, and couching control. To consolidate, **Table 1** provides an overview of different adaptive rehabilitation approaches.

6. DISCUSSION

In our opinion, the telerehabilitation procedure can serve as a safe and effective medium to continue the rehabilitation process while adhering to the safety guidelines during the COVID-19 outbreak. In teleoperated systems, patients and therapists interact through web-interfaces, and the clinical team can remotely monitor the progress of the patient and tune the system's parameters accordingly. Advances in robotic research have facilitated haptic devices that can sense the environment and adapt to it. Consequently, these devices can be used to collect the patient's information and provide necessary feedback effectively. This promotes lesser intervention from a clinical entity during the training process. Tele-rehabilitation can be conducted in-home, community, and as an ambulatory service catering to the needs of the patients (**Figure 5**).

Home-based rehabilitation has attracted many research studies in recent years due to its cost effectiveness and reliability. Moreover, patients can use it without any additional clinical assistance. Most of the therapy is concentrated in home environments to reduce the traffic toward clinical

facilities. The therapists can provide rehabilitation instructions synchronously (real-time feedback) or asynchronously (exercise regime evaluated periodically). For such a setup, the basic requirements are a mobile phone and an Internet connection. Other simple sensors like EMG, IMU, and Kinect can also collect physiological signals for assessment. However, the haptic therapy outcome need not be superior unless the patient is actively engaged in the therapy. In this context, VR acts as a successful medium to promote active patient participation. VR can be hosted in-home environment easily without requiring any expensive setup. The therapy can use VR to deliver game-based exercises that are highly engaging for the patients and provide emotional support. Under certain circumstances, the patients must participate in high-intensity therapy sessions that the home-based setups cannot provide.

Intensive robotic therapy sessions can be easily accessed by the patients in community-based robotic rehabilitation centers. Community-based centers can accommodate heavy and expensive robots for intensive therapy. Patients can access these rehabilitation setups following social distancing guidelines and under a clinician or a volunteer's supervision. Any of the accessed systems can be sanitized and kept ready for the next patient. When patients access these community centers, clinicians can record necessary physiological information, such as EEG to examine patients' cognitive state otherwise not feasible in home-based environments. This allows for high-level monitoring and the metrics calculated through telerehabilitation services. For patients who have travel difficulties, the community-based rehabilitation can be extended as an ambulatory vehicle service with an onboard therapist to emulate the similar intensive robotic therapy experience provided in the community-based robotic therapy. The ambulatory vehicle can be equipped with high-end assistive devices (robotic) along with high-density physiological sensors (EEG, EMG) to assess the patient's state. In terms of health-guidelines, the ambulatory vehicle can be sanitized using UV light between two consequent therapy sessions. These vehicles can be accessed periodically to assess the patient's functional state better and simultaneously deliver high-intensity exercises using the equipped larger bandwidth robotic devices.

However, most of the robotic systems are not adaptive as they do not directly record feedback from the subjects or assess the patient's state. Hence, they require the intervention of clinical teams or doctors who can assess the improvements in the patients' functional state, which is difficult during the COVID-19 outbreak. Thus, there is a need for an adaptive strategy that synergistically combines humans' intentions and robots' dynamics; inevitably, VR is a great resource for such applications. With recent advances in user experience, VR and AR technology had provided an immersive environment during rehabilitation. This approach increases the patients' willingness to take part in the rehabilitation process, thus speeding up the recovery. Adaptive rehabilitation provides required assistance as needed and is a chief strategy underlying successful robotic rehabilitation. Such an adaptive robotic rehabilitation framework should assess and consider the patient's state as one of the main factors for providing appropriate assistance. In this direction, physiological signals have attracted a lot of attention as a reliable modality to assess the patient's state. The physiological signals, such as EEG, EMG, and eye-tracking can be used passively or actively to understand the patients' condition and modify rehabilitation parameters.

7. CONCLUSION

This paper presented a brief review of different telerehabilitation services that can be effectively used during the COVID-19 or similar pandemic and can serve as a reliable alternative to physical therapy. However, the rehabilitation service will be successful if the patients adhere to the routine and are engaged with the exercise regime. For this purpose, telerehabilitation should consider a reliable and cost-effective approach to measure the patient's engagement. Finally, as the therapists cannot deliver one-on-one therapy to patients due to the threat of spreading the virus, an adaptive rehabilitation setup is required with minimal intervention to deliver quality remote care and simultaneously assess the patient's progress.

AUTHOR CONTRIBUTIONS

All authors listed have made a substantial, direct and intellectual contribution to the work, and approved it for publication.

REFERENCES

Ambrose, A. F., Bartels, M. N., Verghese, T. C., and Verghese, J., (2020). Patient and caregiver guide to managing COVID-19 patients at home. *J. Int. Soc. Phys. Rehabil. Med.* 3:53. doi: 10.4103/jisprm.jisprm_4_20

Ameer, K., and Ali, K. (2017). iPad use in stroke neuro-rehabilitation. *Geriatrics* 2:2. doi: 10.3390/geriatrics2010002

Andrenelli, E., Negrini, F., De Sire, A., Arienti, C., Patrini, M., Negrini, S., et al. (2020). Systematic rapid living review on rehabilitation needs due to COVID-19: update to May 31st 2020. *Eur. J. Phys. Rehabil. Med.* 56, 347–353. doi: 10.23736/S1973-9087.20.06329-7

Ankarali, M. M., Tutkun Sen, H., De, A., Okamura, A. M., and Cowan, N. J. (2014). Haptic feedback enhances rhythmic motor control by reducing variability, not improving convergence rate. *J. Neurophysiol.* 111, 1286–1299. doi: 10.1152/jn.00140.2013

Ates, S., Haarman, C. J., and Stienen, A. H. (2017). Script passive orthosis: design of interactive hand and wrist exoskeleton for rehabilitation at home after stroke. *Auton. Robots* 41, 711–723. doi: 10.1007/s10514-016-9589-6

Bamdad, M., Zarshenas, H., and Auais, M. A. (2015). Application of BCI systems in neurorehabilitation: a scoping review. *Disabil. Rehabil. Assist. Technol.* 10, 355–364. doi: 10.3109/17483107.2014.961569

Bartolo, M., Intiso, D., Lentino, C., Sandrini, G., Paolucci, S., Zampolini, M., et al. (2020). Urgent measures for the containment of the coronavirus (covid-19) epidemic in the neurorehabilitation/rehabilitation departments in the phase of maximum expansion of the epidemic. *Front. Neurol.* 11:423. doi: 10.3389/fneur.2020.00423

Bartur, G., Joubran, K., Peleg-Shani, S., Vatine, J. J., and Shahaf, G. (2017). An EEG tool for monitoring patient engagement during stroke rehabilitation: a feasibility study. *Biomed. Res. Int.* 2017:9071568. doi: 10.1155/2017/9071568

Barzilay, O., and Wolf, A. (2013). Adaptive rehabilitation games. *J. Electromyogr. Kinesiol.* 23, 182–189. doi: 10.1016/j.jelekin.2012.09.004

Belani, P., Schefflein, J., Kihira, S., Rigney, B., Delman, B., Mahmoudi, K., et al. (2020). Covid-19 is an independent risk factor for acute ischemic stroke. *Am. J. Neuroradiol.* 41, 1361–1364. doi: 10.3174/ajnr.A6650

Berger, A., Horst, F., Müller, S., Steinberg, F., and Doppelmayr, M. (2019). Current state and future prospects of EEG and fNIRS in robot-assisted gait rehabilitation: a brief review. *Front. Hum. Neurosci.* 13:172. doi: 10.3389/fnhum.2019.00172

Bethel, C. L., and Murphy, R. R. (2010). Review of human studies methods in HRI and recommendations. *Int. J. Soc. Robot.* 2, 347–359. doi: 10.1007/s12369-010-0064-9

Bettger, J. P., and Resnik, L. J. (2020). Telerehabilitation in the age of COVID-19: an opportunity for learning health system research. *Phys. Ther.* 100, 1913–1916. doi: 10.1093/ptj/pzaa151

Blank, A. A., French, J. A., Pehlivan, A. U., and O'Malley, M. K. (2014). Current trends in robot-assisted upper-limb stroke rehabilitation: promoting patient engagement in therapy. *Curr. Phys. Med. Rehabil. Rep.* 2, 184–195. doi: 10.1007/s40141-014-0056-z

Borghese, N. A., Pirovano, M., Lanzi, P. L., Wüest, S., and de Bruin, E. D. (2013). Computational intelligence and game design for effective at-home stroke rehabilitation. *Games Health J.* 2, 81–88. doi: 10.1089/g4h.2012.0073

Brennan, D. M., Mawson, S., and Brownsell, S. (2009). Telerehabilitation: enabling the remote delivery of healthcare, rehabilitation, and self management. *Stud. Health. Technol. Inform.* 145, 231–248.

Brewer, B. R., McDowell, S. K., and Worthen-Chaudhari, L. C. (2007). Poststroke upper extremity rehabilitation: a review of robotic systems and clinical results. *Top. Stroke Rehabil.* 14, 22–44. doi: 10.1310/tsr1406-22

Cai, L. L., Fong, A. J., Otoshi, C. K., Liang, Y., Burdick, J. W., Roy, R. R., et al. (2006). Implications of assist-as-needed robotic step training after a complete spinal cord injury on intrinsic strategies of motor learning. *J. Neurosci.* 26, 10564–10568. doi: 10.1523/JNEUROSCI.2266-06.2006

Cameirao, M. S., Bermudez i Badia, S., Duarte Oller, E., and Verschure, P. F. M. J. (2010). Neurorehabilitation using the virtual reality based rehabilitation gaming system: methodology, design, psychometrics, usability and validation. *J. Neuroeng. Rehabil.* 7:48. doi: 10.1186/1743-0003-7-48

CDC (2017). Available online at: http://www.cdc.gov/stroke/ (accessed May 3, 2021).

Chen, Y., Abel, K. T., Janecek, J. T., Chen, Y., Zheng, K., and Cramer, S. C. (2019). Home-based technologies for stroke rehabilitation: a systematic review. *Int. J. Med. Inform.* 123, 11–22. doi: 10.1016/j.ijmedinf.2018.12.001

Clark, D. J., Ting, L. H., Zajac, F. E., Neptune, R. R., and Kautz, S. A. (2010). Merging of healthy motor modules predicts reduced locomotor performance and muscle coordination complexity post-stroke. *J. Neurophysiol.* 103, 844–857. doi: 10.1152/jn.00825.2009

Cramer, S. C., Dodakian, L., Le, V., See, J., Augsburger, R., McKenzie, A., et al. (2019). Efficacy of home-based telerehabilitation vs in-clinic therapy for adults after stroke: a randomized clinical trial. *JAMA Neurol.* 76, 1079–1087. doi: 10.1001/jamaneurol.2019.1604

Dario, P., Verschure, P. F., Prescott, T., Cheng, G., Sandini, G., Cingolani, R., et al. (2011). Robot companions for citizens. *Proc. Comput. Sci.* 7, 47–51. doi: 10.1016/j.procs.2011.12.017

Dean, S. G., Poltawski, L., Forster, A., Taylor, R. S., Spencer, A., James, M., et al. (2018). Community-based rehabilitation training after stroke: results of a pilot randomised controlled trial (retrain) investigating acceptability and feasibility. *BMJ Open* 8:e018409. doi: 10.1136/bmjopen-2017-018409

DiMatteo, M. R. (2004). Social support and patient adherence to medical treatment: a meta-analysis. *Health Psychol.* 23:207. doi: 10.1037/0278-6133.23.2.207

Duff, M., Yinpeng Chen, Attygalle, S., Herman, J., Sundaram, H., Gang Qian, Jiping He, and Rikakis, T. (2010). An adaptive mixed reality training system for stroke rehabilitation. *IEEE Trans. Neural Syst. Rehabil. Eng.* 18, 531–541. doi: 10.1109/TNSRE.2010.2055061

Eriksson, J., Mataric, M. J., and Winstein, C. J. (2005). "Hands-off assistive robotics for post-stroke arm rehabilitation," in *9th International Conference on Rehabilitation Robotics 2005. ICORR 2005* (Chicago, IL), 21–24.

Essery, R., Geraghty, A. W., Kirby, S., and Yardley, L. (2017). Predictors of adherence to home-based physical therapies: a systematic review. *Disabil. Rehabil.* 39, 519–534. doi: 10.3109/09638288.2016.1153160

Farzad, M., Ashrafi, M., and Farhoud, A. R. (2020). Considerations in upper limb rehabilitation during covid-19 crisis. *Arch. Bone Jt Surg.* 8, 315–316. doi: 10.22038/abjs.2020.47699.2338

Felten-Barentsz, K. M., van Oorsouw, R., Klooster, E., Koenders, N., Driehuis, F., Hulzebos, E. H., et al. (2020). Recommendations for hospital-based physical therapists managing patients with covid-19. *Phys. Ther.* 100, 1444–1457. doi: 10.1093/ptj/pzaa114

Fiani, B., Siddiqi, I., Lee, S. C., and Dhillon, L. (2020). Telerehabilitation: development, application, and need for increased usage in the covid-19 era for patients with spinal pathology. *Cureus* 12:e10563. doi: 10.7759/cureus.10563

Fischinger, D., Einramhof, P., Papoutsakis, K., Wohlkinger, W., Mayer, P., Panek, P., et al. (2016). Hobbit, a care robot supporting independent living at home: first prototype and lessons learned. *Robot. Auton. Syst.* 75, 60–78. doi: 10.1016/j.robot.2014.09.029

French, B., Thomas, L. H., Coupe, J., McMahon, N. E., Connell, L., Harrison, J., et al. (2016). Repetitive task training for improving functional ability after stroke. *Cochrane Database Syst. Rev.* 11:CD006073. doi: 10.1002/14651858.CD006073.pub3

Frolov, A., Kozlovskaya, I., Biryukova, E., and Bobrov, P. (2018). Use of robotic devices in post-stroke rehabilitation. *Neurosci. Behav. Physiol.* 48, 1053–1066. doi: 10.1007/s11055-018-0668-3

Graf, B., Reiser, U., Hägele, M., Mauz, K., and Klein, P. (2009). "Robotic home assistant Care-O-bot3–product vision and innovation platform," in *2009 IEEE Workshop on Advanced Robotics and Its Social Impacts* (Berlin; Heidelberg), 139–144. doi: 10.1109/ARSO.2009.5587059

Hasson, C. J., Hogan, N., and Sternad, D. (2012). "Human control of dynamically complex objects," in *2012 4th IEEE RAS & EMBS International Conference on Biomedical Robotics and Biomechatronics (BioRob)* (Rome: IEEE), 1235–1240. doi: 10.1109/BioRob.2012.6290911

Hermans, G., and Van den Berghe, G. (2015). Clinical review: intensive care unit acquired weakness. *Crit. Care* 19, 1–9. doi: 10.1186/s13054-015-0993-7

Heuer, H., and Lüttgen, J. (2015). Robot assistance of motor learning: a neuro-cognitive perspective. *Neurosci. Biobehav. Rev.* 56, 222–240. doi: 10.1016/j.neubiorev.2015.07.005

Hocine, N., Gouaïch, A., Cerri, S. A., Mottet, D., Froger, J., and Laffont, I. (2015). Adaptation in serious games for upper-limb rehabilitation: an approach to improve training outcomes. *User Model. User Adapt. Interact.* 25, 65–98. doi: 10.1007/s11257-015-9154-6

Holden, M. K. (2005). Virtual environments for motor rehabilitation: review. *Cyberpsychol. Behav.* 8, 187–211. doi: 10.1089/cpb.2005.8.187

Holden, M. K., Dyar, T. A., and Dayan-Cimadoro, L. (2007). Telerehabilitation using a virtual environment improves upper extremity function in patients with stroke. *IEEE Trans. Neural Syst. Rehabil. Eng.* 15, 36–42. doi: 10.1109/TNSRE.2007.891388

Hosseiniravandi, M., Kahlaee, A. H., Karim, H., Ghamkhar, L., and Safdari, R. (2020). Home-based telerehabilitation software systems for remote supervising: a systematic review. *Int. J. Technol. Assess. Health Care* 36, 113–125. doi: 10.1017/S0266462320000021

Housley, S. N., Fitzgerald, K., and Butler, A. J. (2018). "Telerehabilitation robotics: overview of approaches and clinical outcomes," in *Rehabilitation Robotics*, eds R. Colombo and V. Sanguineti (Elsevier), 333–346. doi: 10.1016/B978-0-12-811995-2.00026-6

Israely, S., and Carmeli, E. (2016). Error augmentation as a possible technique for improving upper extremity motor performance after a stroke-a systematic review. *Top. Stroke Rehabil.* 23, 116–125. doi: 10.1179/1945511915Y.0000000007

Jack, K., McLean, S. M., Moffett, J. K., and Gardiner, E. (2010). Barriers to treatment adherence in physiotherapy outpatient clinics: a systematic review. *Manual Ther.* 15, 220–228. doi: 10.1016/j.math.2009.12.004

Jochumsen, M., Niazi, I. K., Mrachacz-Kersting, N., Farina, D., and Dremstrup, K. (2013). Detection and classification of movement-related cortical potentials associated with task force and speed. *J. Neural Eng.* 10:56015. doi: 10.1088/1741-2560/10/5/056015

Kan, P., Huq, R., Hoey, J., Goetschalckx, R., and Mihailidis, A. (2011). The development of an adaptive upper-limb stroke rehabilitation robotic system. *J. Neuroeng. Rehabil.* 8:33. doi: 10.1186/1743-0003-8-33

Kang, K. I., Freedman, S., Mataric, M. J., Cunningham, M. J., and Lopez, B. (2005). "A hands-off physical therapy assistance robot for cardiac patients," in *9th International Conference on Rehabilitation Robotics 2005. ICORR 2005* (Chicago, IL), 337–340.

Korupolu, R., Francisco, G. E., Levin, H., Needham, D. M., et al. (2020). Rehabilitation of critically ill COVID-19 survivors. *J. Int. Soc. Phys. Rehabil. Med*. 3:45. doi: 10.4103/jisprm.jisprm_8_20

Krebs, H. I., and Hogan, N. (2012). Robotic therapy: the tipping point. *Am. J. Phys. Med. Rehabil*. 91:S290. doi: 10.1097/PHM.0b013e31826bcd80

Langhorne, P., Bernhardt, J., and Kwakkel, G. (2011). Stroke rehabilitation. *Lancet* 377, 1693–1702. doi: 10.1016/S0140-6736(11)60325-5

Laver, K., George, S., Ratcliffe, J., and Crotty, M. (2011). Virtual reality stroke rehabilitation-hype or hope? *Aust. Occup. Ther. J*. 58, 215–219. doi: 10.1111/j.1440-1630.2010.00897.x

Li, Y., Lamontagne, A., et al. (2018). The effects of error-augmentation versus error-reduction paradigms in robotic therapy to enhance upper extremity performance and recovery post-stroke: a systematic review. *J. Neuroeng. Rehabil*. 15:65. doi: 10.1186/s12984-018-0408-5

Libin, A. V., and Libin, E. V. (2004). Person-robot interactions from the robopsychologists' point of view: the robotic psychology and robotherapy approach. *Proc. IEEE* 92, 1789–1803. doi: 10.1109/JPROC.2004.835366

Likitlersuang, J., Koh, R., Gong, X., Jovanovic, L., Bolivar-Tellería, I., Myers, M., et al. (2018). EEG-controlled functional electrical stimulation therapy with automated grasp selection: a proof-of-concept study. *Top. Spinal Cord Injury Rehabil*. 24, 265–274. doi: 10.1310/sci2403-265

Linder, S. M., Reiss, A., Buchanan, S., Sahu, K., Rosenfeldt, A. B., Clark, C., et al. (2013). Incorporating robotic-assisted telerehabilitation in a home program to improve arm function following stroke. *J. Neurol. Phys. Ther*. 37, 125–132. doi: 10.1097/NPT.0b013e31829fa808

Lorenz, T., Mörtl, A., and Hirche, S. (2013). "Movement synchronization fails during non-adaptive human-robot interaction," in *2013 8th ACM/IEEE International Conference on Human-Robot Interaction (HRI)*, 189–190. doi: 10.1109/HRI.2013.6483565

Lorenz, T., Weiss, A., and Hirche, S. (2016). Synchrony and reciprocity: key mechanisms for social companion robots in therapy and care. *Int. J. Soc. Robot*. 8, 125–143. doi: 10.1007/s12369-015-0325-8

Maciejasz, P., Eschweiler, J., Gerlach-Hahn, K., Jansen-Troy, A., and Leonhardt, S. (2014). A survey on robotic devices for upper limb rehabilitation. *J. Neuroeng. Rehabil*. 11:3. doi: 10.1186/1743-0003-11-3

Manjunatha, H., Pareek, S., Memar, A. H., Kesavadas, T., and Esfahani, E. T. (2020). Effect of haptic assistance strategy on mental engagement in fine motor tasks. *J. Med. Robot. Res.* 5:2041004. doi: 10.1142/S2424905X20410044

Mao, L., Wang, M., Chen, S., He, Q., Chang, J., Hong, C., et al. (2020). Neurological manifestations of hospitalized patients with COVID-19 in Wuhan, China: a retrospective case series study. *medRxiv*. doi: 10.2139/ssrn.3544840

Meyer, T., Peters, J., Brtz, D., Zander, T. O., Scholkopf, B., Soekadar, S. R., et al. (2012). "A brain-robot interface for studying motor learning after stroke," in *2012 IEEE/RSJ International Conference on Intelligent Robots and Systems* (Vilamoura-Algarve: IEEE), 4078–4083. doi: 10.1109/IROS.2012.6385646

Middleton, A., Simpson, K. N., Bettger, J. P., and Bowden, M. G. (2020). COVID-19 pandemic and beyond: considerations and costs of telehealth exercise programs for older adults with functional impairments living at home—lessons learned from a pilot case study. *Phys. Ther*. 100, 1278–1288. doi: 10.1093/ptj/pzaa089

Morel, M., Bideau, B., Lardy, J., and Kulpa, R. (2015). Advantages and limitations of virtual reality for balance assessment and rehabilitation. *Neurophysiol. Clin*. 45, 315–326. doi: 10.1016/j.neucli.2015.09.007

Motus Nova (2020). *Motus Nova–Stroke Rehabilitation Technology Designed for at Home Use*. Motus Nova. Available online at: https://motusnova.com/

Motus, S. (2020). *Habilis Europe: A New Concept for Telerehabilitation*. Available online at: https://www.habiliseurope.com/

Mounis, S. Y. A., Azlan, N. Z., and Sado, F. (2019). Assist-as-needed control strategy for upper-limb rehabilitation based on subject's functional ability. *Meas. Control.* 52, 1354–1361. doi: 10.1177/0020294019866844

Nirme, J., Duff, A., and Verschure, P. F. M. J. (2011). "Adaptive rehabilitation gaming system: on-line individualization of stroke rehabilitation," in *Conference Proceedings: Annual International Conference of the IEEE Engineering in Medicine and Biology Society. IEEE Engineering in Medicine and Biology Society. Annual Conference 2011* (Boston, MA), 6749–6752. doi: 10.1109/IEMBS.2011.6091665

Nordin, N., Xie, S. Q., and Wünsche, B. (2014). Assessment of movement quality in robot-assisted upper limb rehabilitation after stroke: a review. *J. Neuroeng. Rehabil*. 11:137. doi: 10.1186/1743-0003-11-137

Oblak, J., Cikajlo, I., and Matjacic, Z. (2010). Universal haptic drive: a robot for arm and wrist rehabilitation. *IEEE Trans. Neural Syst. Rehabil. Eng*. 18, 293–302. doi: 10.1109/TNSRE.2009.2034162

Pareek, S. (2020). *iART: an intelligent assistive robotic therapy system for home-based stroke rehabilitation* (Ph.D. thesis), University of Illinois at Urbana Champaign, Champaign, IL, United States.

Pareek, S., and Kesavadas, T. (2019). iART: Learning from demonstration for assisted robotic therapy using lstm. *IEEE Robot. Autom. Lett*. 5, 477–484. doi: 10.1109/LRA.2019.2961845

Pareek, S., Manjunath, H., Esfahani, E. T., and Kesavadas, T. (2019). Myotrack: realtime estimation of subject participation in robotic rehabilitation using sEMG and IMU. *IEEE Access* 7, 76030–76041. doi: 10.1109/ACCESS.2019.2922325

Park, M. J., Kim, D. J., Lee, U., Na, E. J., and Jeon, H. J. (2019). A literature overview of virtual reality (VR) in treatment of psychiatric disorders: recent advances and limitations. *Front. Psychiatry* 10:505. doi: 10.3389/fpsyt.2019.00505

Pehlivan, A. U., Sergi, F., and OMalley, M. K. (2015). A subject-adaptive controller for wrist robotic rehabilitation. *IEEE/ASME Trans. Mechatron*. 20, 1338–1350. doi: 10.1109/TMECH.2014.2340697

Peretti, A., Amenta, F., Tayebati, S. K., Nittari, G., and Mahdi, S. S. (2017). Telerehabilitation: review of the state-of-the-art and areas of application. *JMIR Rehabil. Assist. Technol*. 4:e7. doi: 10.2196/rehab.7511

Perez-Ibarra, J. C., Siqueira, A. A. G., and Krebs, H. I. (2015). "Assist-as-needed ankle rehabilitation based on adaptive impedance control," in *2015 IEEE International Conference on Rehabilitation Robotics (ICORR)* (Ponta Delgada: IEEE), 723–728. doi: 10.1109/ICORR.2015.7281287

Piggott, L., Wagner, S., and Ziat, M. (2016). Haptic neurorehabilitation and virtual reality for upper limb paralysis: a review. *Crit. Rev. Biomed. Eng*. 44, 1–32. doi: 10.1615/CritRevBiomedEng.2016016046

Pirovano, M., Mainetti, R., Baud-Bovy, G., Lanzi, P. L., and Borghese, N. A. (2012). "Self-adaptive games for rehabilitation at home," in *2012 IEEE Conference on Computational Intelligence and Games (CIG)* (Granada: IEEE), 179–186. doi: 10.1109/CIG.2012.6374154

Pirovano, M., Surer, E., Mainetti, R., Lanzi, P. L., and Alberto Borghese, N. (2016). Exergaming and rehabilitation: a methodology for the design of effective and safe therapeutic exergames. *Entertain. Comput*. 14, 55–65. doi: 10.1016/j.entcom.2015.10.002

Polygerinos, P., Galloway, K. C., Savage, E., Herman, M., Donnell, K. O., and Walsh, C. J. (2015). "Soft robotic glove for hand rehabilitation and task specific training," in *2015 IEEE International Conference on Robotics and Automation (ICRA)* (Seattle, WA), 2913–2919. doi: 10.1109/ICRA.2015.7139597

Porciuncula, F., Roto, A. V., Kumar, D., Davis, I., Roy, S., Walsh, C. J., et al. (2018). Wearable movement sensors for rehabilitation: a focused review of technological and clinical advances. *PM&R* 10, S220–S232. doi: 10.1016/j.pmrj.2018.06.013

Proffitt, R. M., Alankus, G., Kelleher, C. L., and Engsberg, J. R. (2011). Use of computer games as an intervention for stroke. *Top. Stroke Rehabil*. 18, 417–427. doi: 10.1310/tsr1804-417

Rabin, B., Burdea, G., Hundal, J., Roll, D., and Damiani, F. (2011). "Integrative motor, emotive and cognitive therapy for elderly patients chronic post-stroke a feasibility study of the brightarm^{TM}rehabilitation system," in *2011 International Conference on Virtual Rehabilitation* (Zurich), 1–8. doi: 10.1109/ICVR.2011.5971852

Reinkensmeyer, D. J., Pang, C. T., Nessler, J. A., and Painter, C. C. (2002). Web-based telerehabilitation for the upper extremity after stroke. *IEEE Trans. Neural Syst. Rehabil. Eng*. 10, 102–108. doi: 10.1109/TNSRE.2002.1031978

Rodriguez-Morales, A. J., Cardona-Ospina, J. A., Gutiérrez-Ocampo, E., Villamizar-Peña, R., Holguin-Rivera, Y., Escalera-Antezana, J. P., et al. (2020). Clinical, laboratory and imaging features of COVID-19: a systematic review and meta-analysis. *Travel Med. Infect. Dis*. 34:101623. doi: 10.1016/j.tmaid.2020.101623

Rose, T., Nam, C. S., and Chen, K. B. (2018). Immersion of virtual reality for rehabilitation-review. *Appl. Ergon*. 69, 153–161. doi: 10.1016/j.apergo.2018.01.009

Rosen, K., Patel, M., Lawrence, C., and Mooney, B. (2020). Delivering telerehabilitation to COVID-19 inpatients:a retrospective chart review suggests it is a viable option. *HSS J*. 16, 64–70. doi: 10.1007/s11420-020-09774-4

Ru, X., Dai, H., Jiang, B., Li, N., Zhao, X., Hong, Z., et al. (2017). Community-based rehabilitation to improve stroke survivors' rehabilitation participation and functional recovery. *Am. J. Phys. Med. Rehabil*. 96, e123–e129. doi: 10.1097/PHM.0000000000000650

Sarfo, F. S., Ulasavets, U., Opare-Sem, O. K., and Ovbiagele, B. (2018). Tele-rehabilitation after stroke: an updated systematic review of the literature. *J. Stroke Cerebrovasc. Dis*. 27, 2306–2318. doi: 10.1016/j.jstrokecerebrovasdis.2018.05.013

Schmidt, R. A., Lee, T., Winstein, C., Wulf, G., and Zelaznik, H. (2018). *Motor Control and Learning 6E*. Human Kinetics.

Schroeter, C., Mueller, S., Volkhardt, M., Einhorn, E., Huijnen, C., van den Heuvel, H., et al. (2013). "Realization and user evaluation of a companion robot for people with mild cognitive impairments," in *2013 IEEE International Conference on Robotics and Automation* (Karlsruhe), 1153–1159. doi: 10.1109/ICRA.2013.6630717

Sheehy, L. M. (2020). Considerations for postacute rehabilitation for survivors of COVID-19. *JMIR Public Health Surveill*. 6:e19462. doi: 10.2196/19462

Shibata, T., Mitsui, T., Wada, K., Touda, A., Kumasaka, T., Tagami, K., et al. (2001). "Mental commit robot and its application to therapy of children," in *2001 IEEE/ASME International Conference on Advanced Intelligent Mechatronics. Proceedings (Cat. No.01TH8556)* (Como), Vol. 2, 1053–1058.

Soekadar, S. R., Birbaumer, N., Slutzky, M. W., and Cohen, L. G. (2015). Brain–machine interfaces in neurorehabilitation of stroke. *Neurobiol. Dis*. 83, 172–179. doi: 10.1016/j.nbd.2014.11.025

Squeri, V., Masia, L., Giannoni, P., Sandini, G., and Morasso, P. (2014). Wrist rehabilitation in chronic stroke patients by means of adaptive, progressive robot-aided therapy. *IEEE Trans. Neural Syst. Rehabil. Eng*. 22, 312–325. doi: 10.1109/TNSRE.2013.2250521

Stiehl, W. D., Lieberman, J., Breazeal, C., Basel, L., Lalla, L., and Wolf, M. (2005). "Design of a therapeutic robotic companion for relational, affective touch," in *ROMAN 2005. IEEE International Workshop on Robot and Human Interactive Communication 2005* (Nashville, TN), 408–415. doi: 10.1109/ROMAN.2005.1513813

Sullivan, J. L., Bhagat, N. A., Yozbatiran, N., Paranjape, R., Losey, C. G., Grossman, R. G., et al. (2017). "Improving robotic stroke rehabilitation by incorporating neural intent detection: preliminary results from a clinical trial," in *2017 International Conference on Rehabilitation Robotics (ICORR)* (London: IEEE), 122–127. doi: 10.1109/ICORR.2017.8009233

Takeuchi, N., and Izumi, S. I. (2013). Rehabilitation with poststroke motor recovery: a review with a focus on neural plasticity. *Stroke Res. Treat*. 2013:128641. doi: 10.1155/2013/128641

van Dokkum, L. E. H., Ward, T., and Laffont, I. (2015). Brain computer interfaces for neurorehabilitation–its current status as a rehabilitation strategy post-stroke. *Ann. Phys. Rehabil. Med*. 58, 3–8. doi: 10.1016/j.rehab.2014.09.016

Vaughan, N., Gabrys, B., and Dubey, V. N. (2016). An overview of self-adaptive technologies within virtual reality training. *Comput. Sci. Rev*. 22, 65–87. doi: 10.1016/j.cosrev.2016.09.001

Webster, D., and Celik, O. (2014). Systematic review of kinect applications in elderly care and stroke rehabilitation. *J. Neuroeng. Rehabil*. 11:108. doi: 10.1186/1743-0003-11-108

Wittmann, F., Held, J. P., Lambercy, O., Starkey, M. L., Curt, A., Höver, R., et al. (2016). Self-directed arm therapy at home after stroke with a sensor-based virtual reality training system. *J. Neuroeng. Rehabil*. 13:75. doi: 10.1186/s12984-016-0182-1

Wolbrecht, E. T., Chan, V., Reinkensmeyer, D. J., and Bobrow, J. E. (2008). Optimizing compliant, model-based robotic assistance to promote neurorehabilitation. *IEEE Trans. Neural Syst. Rehabil. Eng*. 16, 286–297. doi: 10.1109/TNSRE.2008.918389

Yates, M., Kelemen, A., and Sik Lanyi, C. (2016). Virtual reality gaming in the rehabilitation of the upper extremities post-stroke. *Brain Injury* 30, 855–863. doi: 10.3109/02699052.2016.1144146

Zhu, Y., Wang, Z., Zhou, Y., Onoda, K., Maruyama, H., Hu, C., et al. (2020). Summary of respiratory rehabilitation and physical therapy guidelines for patients with COVID-19 based on recommendations of world confederation for physical therapy and national association of physical therapy. *J. Phys. Ther. Sci*. 32, 545–549. doi: 10.1589/jpts.32.545

Zimmerli, L., Jacky, M., Lünenburger, L., Riener, R., and Bolliger, M. (2013). Increasing patient engagement during virtual reality-based motor rehabilitation. *Arch. Phys. Med. Rehabil*. 94, 1737–1746. doi: 10.1016/j.apmr.2013.01.029

Conflict of Interest: The authors declare that the research was conducted in the absence of any commercial or financial relationships that could be construed as a potential conflict of interest.

frontiers in Robotics and AI

ORIGINAL RESEARCH
published: 25 May 2021
doi: 10.3389/frobt.2021.652685

Modelling the Impact of Robotics on Infectious Spread Among Healthcare Workers

Raul Vicente[1,2], Youssef Mohamed[2], Victor M. Eguíluz[3], Emal Zemmar[4], Patrick Bayer[4], Joseph S. Neimat[4], Juha Hernesniemi[1], Bradley J. Nelson[5] and Ajmal Zemmar[1,4]**

[1]Department of Neurosurgery, Henan Provincial People's Hospital, Henan University People's Hospital, Henan University School of Medicine, Zhengzhou, China, [2]Institute of Computer Science, University of Tartu, Tartu, Estonia, [3]Instituto de Fisica Interdisciplinar y Sistemas Complejos IFISC (CSIC-UIB), Palma de Mallorca, Spain, [4]Department of Neurosurgery, University of Louisville, School of Medicine, Louisville, KY, United States, [5]Multi-Scale Robotics Laboratory, Swiss Federal Institute of Technology (ETH) Zurich, Zurich, Switzerland

The Coronavirus disease 2019 (Covid-19) pandemic has brought the world to a standstill. Healthcare systems are critical to maintain during pandemics, however, providing service to sick patients has posed a hazard to frontline healthcare workers (HCW) and particularly those caring for elderly patients. Various approaches are investigated to improve safety for HCW and patients. One promising avenue is the use of robots. Here, we model infectious spread based on real spatio-temporal precise personal interactions from a geriatric unit and test different scenarios of robotic integration. We find a significant mitigation of contamination rates when robots specifically replace a moderate fraction of high-risk healthcare workers, who have a high number of contacts with patients and other HCW. While the impact of robotic integration is significant across a range of reproductive number R_0, the largest effect is seen when R_0 is slightly above its critical value. Our analysis suggests that a moderate-sized robotic integration can represent an effective measure to significantly reduce the spread of pathogens with Covid-19 transmission characteristics in a small hospital unit.

Keywords: robotics, COVID-19, epidemiology, healthcare, biomedical robots

OPEN ACCESS

Edited by:
Patrick M. Pilarski, University of Alberta, Canada

Reviewed by:
Luis Gomez, University of Las Palmas de Gran Canaria, Spain
Ioannis Georgilas, University of Bath, United Kingdom

****Correspondence:***
Ajmal Zemmar
ajmal.zemmar@gmail.com
Raul Vicente
raulvicente@gmail.com

Specialty section:
This article was submitted to Biomedical Robotics, a section of the journal Frontiers in Robotics and AI

Received: *12 January 2021*
Accepted: *07 May 2021*
Published: *25 May 2021*

Citation:
Vicente R, Mohamed Y, Eguiluz VM, Zemmar E, Bayer P, Neimat JS, Hernesniemi J, Nelson BJ and Zemmar A (2021) Modelling the Impact of Robotics on Infectious Spread Among Healthcare Workers. Front. Robot. AI 8:652685. doi: 10.3389/frobt.2021.652685

INTRODUCTION

The Coronavirus disease 2019 (Covid-19) pandemic has had a devastating impact on global healthcare and economy. The rapid global spread of the Severe Acute Respiratory Syndrome Coronavirus (SARS-CoV-2) is owed to its high transmissibility (van Doremalen et al., 2020), transmission prior to symptom onset (Tindale et al., 2020), and infectious spread through asymptomatic carriers (Bai et al., 2020). These features have posed significant challenges in various sectors, especially essential services such as the healthcare sector. Several measures are taken to reduce infectious spread for patients and healthcare worker (HCW) protection while maintaining healthcare services (The Lancet, 2020). Nevertheless, infection rates of up to 20% among HCW are reported in certain countries (Remuzzi and Remuzzi, 2020). As of October 2020, 7,000 HCW have died of Covid-19 worldwide (https://www.amnesty.org/en/latest/news/2020/09/amnesty-analysis-7000-health-workers-have-died-from-covid19/), of which 1,077 deaths and almost 80,000 HCW positive cases have been confirmed within the United States (https://www.washingtonpost.com/graphics/2020/health/healthcare-workers-death-coronavirus/), where various

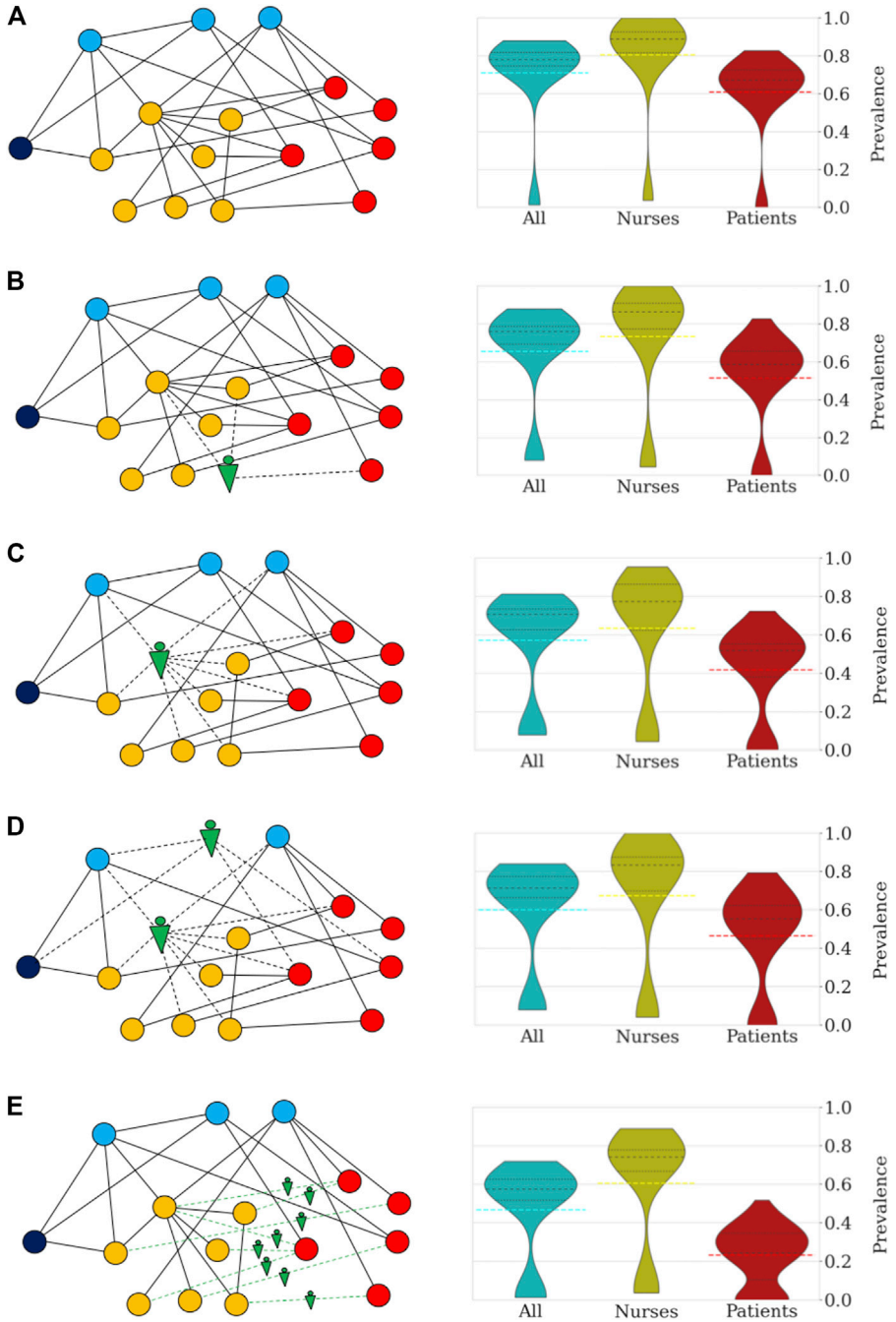

FIGURE 1 | Robotization scenarios and their impact on the probability of pathogen spread through the network and number of infected individuals ($R_0 = 4.4$). The networks on the left side depict sketches of the networks of close contacts at the geriatric ward under different scenarios. The colors indicate the categories: patients (red), nurses (orange), doctors (blue), administration (dark blue), and robots (green). **(A)** In scenario (i) no robotic assistance is provided and the network of close contacts remains intact. **(B)** Scenario (ii) is illustrated by a random nurse being replaced by a robot. **(C)** In scenario (iii) high-risk nurses are being replaced. **(D)** Scenario (iv) is illustrated by the robotic replacement of a high-risk nurse and a random doctor. **(E)** In scenario (v) the robotization affects the interactions between nurses and patients. The right side of each panel shows the distribution of prevalence of infection (percentage of individuals infected) under the different scenarios. All simulations were repeated 100 times to obtain the distributions shown in the violin plots and percentile statistics. For each violin plot, the dashed black lines indicate the different quartiles of the distribution while dashed color lines mark the mean. **(A)** In the absence of robotic intervention, the distribution of the number of infected cases is bimodal with 10% of trials in which the infection does not spread. Across all trials, an average of 71% of the personnel and patients become eventually infected. In general, the nurses and doctors are more vulnerable to becoming infected than patients and administrative workers. **(B)** Random replacement of five nurses increases the percentage of non-spreading trials to 16%. This intervention has the effect of decreasing the average number of infected individuals (66%). **(C)** The situation improves further when the five nurses are selected according to the number of contacts. In this case, the probability that the infection does not spread increases to 21% (more than doubling the case

(*Continued*)

FIGURE 1 | without robotization). Patients and nurses benefit from the targeted intervention with an increase in the number of non-infected cases when the infection spreads. On average, the fraction of infected individuals decreases to 57%. **(D)** Replacement of high-risk nurses and random doctors resulted in a similar probability of no propagation through the network (22%), while resulting in an average of 60% infected individuals. **(E)** Interaction replacement led to a probability that the infection does not spread in 23% of the trials, and an average of only 47% of individuals being infected. For patients the impact is most significant with the majority of simulations predicting that less than 25% of patients of the geriatric unit become eventually infected.

infection control measures including a lockdown, social distancing and personal protective equipment (PPE) have been implemented. In another study, 50% of HCW have reported their work setting as the single source of exposure (Burrer et al., 2020). Among patients, the elderly generation in geriatric units and nursing homes has been primarily affected by the pandemic. Prolonged close contact between patients and HCW, e.g., assistance in patient care and daily needs such as eating, bathing, walking or lifting, are among the prevailing causes that expose the elderly community and their caregivers to increased risk of contamination (McMichael et al., 2020).

The use of robotics as a shielding layer between patients and caregivers is a promising approach to reduce infectious spread in healthcare (Yang et al., 2020). While some hospitals have started to use robotic technology to combat the pandemic and one ward was entirely staffed by robots (O'Meara, 2020), modelling data in real-hospital scenarios is lacking to investigate the efficiency and timing of robotic implementation for reduction of pathogen contamination (Heesterbeek et al., 2015). Here, we utilized a temporally and spatially precise dataset of close personal contacts of 29 patients and 46 HCW in a geriatric unit (Vanhems et al., 2013). We identify nodes of high contact representing increased contagion risk, replace these high-risk nodes and model contamination rates. The model demonstrates that strategically placed robotic assistance to high-risk HCW can significantly reduce and delay the number of infections in a hospital unit in diseases with similar transmissibility to Covid-19. In the studied scenario, robotic integration is shown to be effective across a wide range of reproductive number R_0 from slightly above 1 to at least 4.4.

RESULTS

Effects of Robotic Replacement of Healthcare Workers

Robots can be utilized to assist HCW in a variety of tasks (**Supplementary Table S1**) and hence, to reduce the number and duration of interactions among different types of HCW and patients. To effectively mitigate pathogen contamination and operate cost-efficient, it is critical to determine high-risk groups of individuals and interactions and deploy robotic assistance specifically to these nodes. In a previous study, nurse-to-patient interactions accounted for 21.1% and nurse-nurse interactions resulted in 39.2% of the total number of close contacts (>20 s and <1.5 m) in a geriatric unit (Vanhems et al., 2013). Data from the same study shows that five nurses were responsible for 36.1% of all close contacts with patients. Based on these observations, we focused on replacing nurses with robots and simulate pathogen transmission in a geriatric unit with a model tailored to the state, transmissibility, and latency of SARS-CoV-2 (Ivorra et al., 2020; Eguíluz et al., 2020). Infectious spread was modelled under five scenarios: (i) no robotic assistance, and four scenarios in which robots replaced five random nurses (ii), the top five high-risk nurses (iii), the top 3 high-risk nurses and 2 random medical doctors (iv) and finally, when robots replaced all interactions between nurses and patients (v) (**Figure 1**). The model was run for 100 trials, results were averaged. Each simulation describes the pathogen spreading over the network and timing of close contacts in a geriatric unit, while we collect statistics of the transmission for the curse of an outbreak, which often lasted more than 90 days. A non-spreading state was defined when less than 10% of the individuals become infected within a single trial, whereas a spreading state was defined when more than 10% of individuals become infected. Without use of robotic technology, only 10 of 100 trials (10%) resulted in a non-spreading case. (**Figure 1A**). The probability of a non-spreading dynamics is augmented by 6% (i.e. from 10 to 16%) if five random nurses are replaced by robots (**Figure 1B**). In scenarios iii, iv and v, a strategic process was used by first identifying the nurses with the highest number of contacts (i.e. high-risk nurses) and selectively replacing them with robots. When robots replaced the five high-risk nurses (iii) (**Figure 1C**), the probability to contain the virus was 22%, or in other words, the probability of non-spreading dynamics increased by 110% when compared to the baseline scenario (i) without any robotic assistance (from 10 to 22%). To compare the impact of the five high-risk nurses with other medical staff, we replaced the top 3 high-risk nurses and 2 random medical doctors (MD) with robots, which resulted in a 21% probability to contain the virus (scenario iv, **Figure 1D**). In the last scenario, robotic assistance was applied to all interactions between nurses and patients, i.e., no nurse had direct contact with a patient, but nurses can still interact with other staff. This measure resulted in a 23% probability not to spread the pathogen (**Figure 1E**). Detailed numerical results of these and other measures of infection are collected in **Supplementary Table S2**.

Temporal Evolution of Infectious Spread

The temporal evolution of the infectious spread is also a key aspect for the management of an outbreak. For example, the speed of propagation and the peak number of active infected cases are important challenges to the limited reaction time and capacity for a response to the outbreak. Here, we focus on how pathogen contamination propagates across the network in the geriatric unit and describe how the different robotic assistance scenarios affect the temporal dynamics of the infectious spread. We measured the number of days from outbreak onset until the 10th infection occurs (T_{10}), and the number of infections on the 30th day from outbreak onset (I_{30}). As observed in **Figure 2**, no robotic

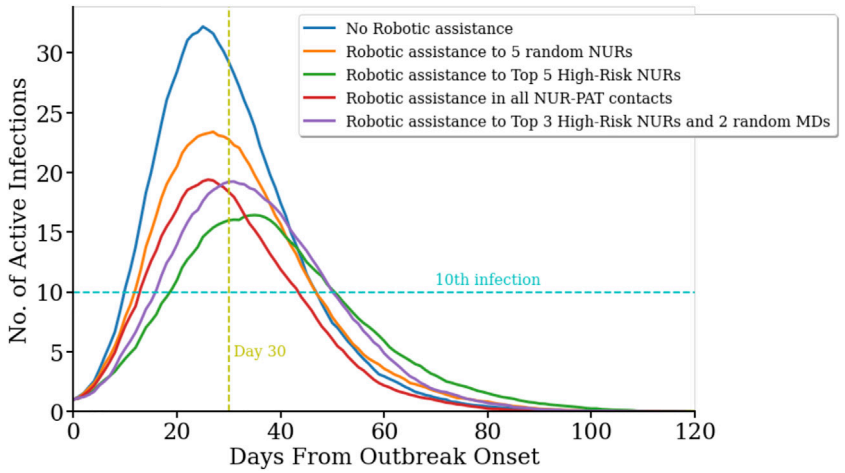

FIGURE 2 | Temporal evolution of infection spread across the network for difference scenarios.(R_0 = 4.4). Number of active infected cases in five different scenarios as a function of the days passed since the first infection in the population on day zero. No robotic integration (blue line) yields in the fastest onset and highest number of active infected cases. In contrast, robotic replacement of the five nurses with the highest number of contacts with other Health Care Workers (HCW) and patients results in the slowest increase and the overall lowest number of active cases (green line). Replacing five random nurses with robots leads to more peak active cases and a steeper slope (orange curve). Replacing all nurse-to-patient contacts (red line) and the top three high-risk nurses and two random medical doctors (purple line) resulted in a similar peak for active cases.

TABLE 1 | Measures of the temporal evolution of infection spreading for a baseline case of R_0 = 4.4.

Scenario	R_0 after intervention	Individuals infected	T10	I30
Reproductive number (R_0 = 4.4)				
No robotic assistance	4.4 ± 0.3	71 ± 2.4	10.1 ± 0.7	32.5 ± 0.8
Assist rand 5 NUR	3.8 ± 0.3	63 ± 0.7	11.9 ± 0.8	26.8 ± 1.0
Assist top 5 NUR	2.7 ± 0.2	54 ± 2.9	17.1 ± 0.8	19.2 ± 1.0
Assist top 3 NUR-Rand 2 MD	3.2 ± 0.3	57 ± 3.0	14.2 ± 0.7	24.3 ± 0.9
Assist all NUR-PAT contacts	3.1 ± 0.2	47 ± 2.5	12.0 ± 0.7	23.8 ± 0.7

The measures consist of the effective R_0 for each robotic implementation scenario, the total number of individuals infected by the end of the outbreak, the number of days until the 10th infection occurs (T_{10}), and the number of active infections on the 30th day of the outbreak (I_{30}).

assistance leads to the highest and earliest peak in the number of infected cases, with T_{10} = 10.1 ± 0.7 days (average ± s.e.m., n = 100), and I_{30} = 32.5 ± 0.8 active infected cases (average ± s.e.m., n = 100). Robotic replacement of the top five high-risk nurses leads to a significant delay of 1 week to reach the 10th infection in the population (T_{10} = 17.1 ± 0.8 days, n = 100; p_{val} = 0, permutation test for statistical difference with T_{10} without robotic assistance), and also results in a significant reduction of the number of active infected cases by day 30 (I_{30} = 19.2 ± 1.0 cases, n = 100; p_{val} = 0, permutation test for statistical difference with I_{30} without robotic assistance). Strikingly, this scenario shows both, the slowest initial growth of infection propagation and the slowest final decay, and hence it produces the largest flattening of the curve of active infections (**Figure 2**, green line). Robotic replacement of all nurse-patient interactions results in the earliest termination of the outbreak, while its rise time is not significantly different from the baseline scenario without any robotic implementation (**Figure 2**, red curve; T_{10} = 12.0 ± 0.7 days, p_{val} = 0.074, permutation test). **Table 1** and **Supplementary Table S3** contain more details on the temporal evolution of active infections for each robotic scenario.

The Impact of the Basic Reproductive Number R_0

Another important factor for infectious spread prediction is the basic reproductive number R_0. During the first wave of Covid-19, R_0 ranged between 2 and 6 considering all countries (Sanche et al., 2020), values of 3.2–3.4 were reported for China (Alimohamadi et al., 2020), Austria, Switzerland (Karnakov et al., 2020), Italy, Korea (Zhuang et al., 2020) and Germany (Dehning et al., 2020). Measures including the use of personal protective equipment (PPE), social distancing and frequent sanitization have reduced the basic reproductive to values as low as 0.6 (Fisman et al., 2020). After investigating the role of robotic integration for pathogen spread, we analyzed how different reproductive numbers R_0 affect these measures. To this end, we simulated the virus spread in the above-mentioned scenarios for different R_0 values. R_0 values around 3.15 were reported in a meta-analysis from China (He et al., 2020). R_0 values around 1.1–1.2 are estimated after the first wave of Covid-19 infections (Karnakov et al., 2020) (**Figure 3**). Basic reproductive numbers between 1.2 and 0.6 have also been used to model the effect of using personal protective equipment,

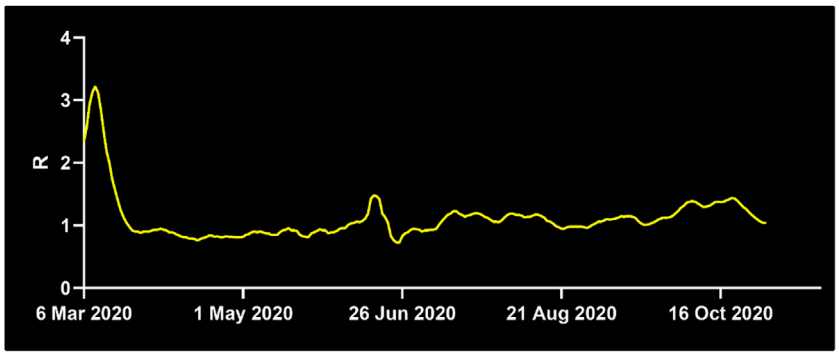

FIGURE 3 | Development of the basic reproductive number R_0 in Germany. While R_0 was at 1.3 on April 7th, 2020, it decreased below the critical value of $R_0 = 1$ shortly after April 7th until June 21st, where it surged to 2.03. For the majority of time thereafter, R_0 stayed above 1, at the time of writing it is 1.22. Source: Reprinted with permission from Robert-Koch-Institute.

TABLE 2 | Results for the probability of pathogen spread across the network for different reproductive numbers.

Scenario	Reproductive number R_0			
	4.4	**3.4**	**1.2**	**0.6**
Ratio of non-spreading trials				
No robotic assistance	0.1	0.22	0.67	0.92
Assist rand 5 NUR	0.16	0.2	0.83	1.0
Assist top 5 NUR	0.22	0.28	0.96	1.0
Assist top 3 NUR-Rand 2 MD	0.21	0.24	0.96	0.99
Assist all NUR-PAT contacts	0.23	0.27	0.75	0.96

such as masks, depending on the compliance and viral reduction rate provided. Therefore, in the model, we have focused on fitting the basic reproductive numbers of 3.4, 1.2, and 0.6, respectively, and studied the impact of robotic implementation under each of these epidemiological conditions. For $R_0 = 3.4$, the targeted scenarios of replacing high-risk nurses or the interactions between nurses and patients result in the largest non-spreading probability (see **Table 2** and **Supplementary Figure S1**). These two scenarios also lead to the smallest number of infected individuals by the end of the outbreak. The impact of robots on $R_0 = 3.4$ is thus qualitatively similar to that obtained when $R_0 = 4.4$. On the other hand, the benefit of robotic integration is limited when $R_0 = 0.6$ since the baseline case (i.e. no robotic intervention) already results in 92% of non-spreading trials. However, we note that in some robotic scenarios the pathogen propagation can be stopped in 100% of the trials. It is also important to note that when $R_0 < 1$, each infected individual infects less than 1 other individual on average and therefore, pathogen spread is relatively well controlled. Interestingly, basic reproductive numbers near the critical value of 1, such as $R_0 = 1.2$, provide the largest gain for robotic scenarios, even more than for larger R_0 that we have considered (i.e., 3.4 and 4.4). The probability not to spread the virus increased from 67% at baseline to 96% with targeted robotic replacement. Overall, these results indicate that the qualitative effects of robotic scenarios are robust across a range of basic reproductive numbers with significant benefit occurring at regimes with a relatively large value of R_0, and specially with R_0 slightly above its critical value of 1.

DISCUSSION

Our model investigates whether robotic assistance to a moderate number of HCW influences the pathogen spread rate in a geriatric ward. We find that targeted robotic replacement of nurses with the largest number of personal close contacts results in the largest effect to control infectious spread. This scenario not only decreases the probability of viral spread but also slows down its outbreak. The most optimal R_0 to integrate robots into clinical use is when the reproductive number is slightly higher than the critical value of $R_0 = 1$, while significant effects are still observed for relatively high values (at least up to 4.4).

Limitations and Shortcomings of the Model

The present model is limited in several aspects. First, it only considers pathogen spread due to close personal contact. However, growing evidence suggests that aerosol and fomite transmission are additional routes of infection of Covid-19 (Lu et al., 2020; Shen et al., 2020). Detailed models simulating the physics of aerosol and fomite transmission have been applied to hospital infrastructures during outbreaks of other diseases such as influenza (Kraay et al., 2018; Wong et al., 2010), and could be integrated to refine our basic model on the impact of robotic scenarios on pathogen spread. Robots such as for example those used as companion robots can be in frequent contact with several patients and thus also be a source of pathogen contagion *via* fomite transmission. Maintenance and cleaning of robots,

including disinfection robots, are other potential sources of transmission for healthcare and maintenance personnel. These effects can also be modeled for an accurate balance of the effect of robotic integration in the spread of infectious diseases with surface contact as a major *via* of transmission. Second, our spreading model runs on real proximity contact data obtained from a geriatric unit during a non-pandemic state. While we considered a range of values of the reproductive number that occurred at different stages of the Covid-19 pandemics, it will be necessary to also test the model with contact data obtained at such stages. Third, detailed proximity contact data of HCW and patients are not publicly available for larger healthcare infrastructures such as entire hospitals. How the predictions of the effects of robotic assistance scale to larger nursing homes and geriatric units will require further data. Fourth, modeling a specific robotic system integration within the real network of proximity contacts would require a refined annotation of the activity conducted during each contact to determine which interactions can be replaced by specific types of robot and tasks. Our model abstracted from the specific robotic system including the network of specific personnel and patients, and assumed that robotic integration operated at the level of an effective number of node replacement or removal of interactions.

Overall, we believe that the present model is a step in modeling the potential impact of robotic assistance in pathogen spread, and that new data will make possible models tailored to specific situations and robotic systems.

Yield, Timing and Cost of Robotic Integration Into Clinical Use

Robots have been utilized to assist humans in a variety of hazardous tasks, including visual aid (Xing et al., 2017) for firefighters (Tuffield and Elias, 2003), in nuclear environments and in mountain rescue (Sugiyama et al., 2013). The use of robots for infectious diseases has come into the spotlight with the Covid-19 pandemic. Acquisition of new robotic technology considers two major factors for hospital administrations: Yield and cost. Our study suggests that robots can significantly reduce infectious spread to protect healthcare workers and patients. Our data points out that the determination of HCW with a high number of contacts and targeted replacement of these HCW yields the most effective reduction in pathogen spread. While robots have been used during Covid-19 to employ an entire unit of a hospital (https://hbr.org/2020/04/how-hospitals-are-using-ai-to-battle-covid-19. https://www.medicaldevice-network.com/features/coronavirus-robotics/), our results demonstrate that integration of a smaller number of robots focused on high-risk HCW can significantly reduce cost and effectively decrease spreading probability. The basic reproductive number R_0 also plays an important role in the efficiency of robotic implementation. During times, when R_0 is below the critical number of 1, application of robots does not have a significant value, whereas with R_0 values just above one or higher, robots can reduce infectious spread effectively. Thus, monitoring of R_0 (**Figure 3**) and selection of appropriate time windows is a critical factor. Another important consideration is the use of personal protective equipment (PPE). PPE shortage has been a key concern during the Covid-19 pandemic, creating competition between governments and prioritizing certain countries over others. The integration of robots reduces the need for PPE since less HCW work within the unit. This can alleviate pressure during PPE shortage. In addition, robots can serve at maximum capacity to meet the increased need during extraordinary times.

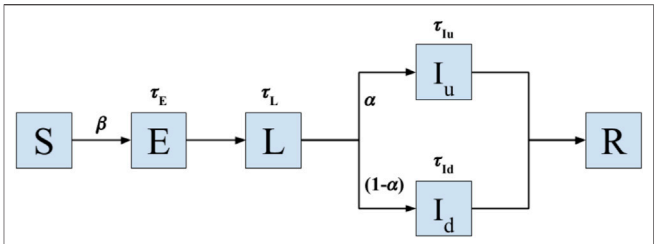

FIGURE 4 | Model of Covid-19 transmission. Transition model used to simulate the spread of infectious disease with epidemiological characteristics of Covid-19 on a real sequence of contact data in a geriatric unit. Upon close contact with a latent (L) or infected case (I_u and I_d stand for infected asymptomatic and diseased states, respectively), an individual in susceptible state (S) will transition to the state of exposed (E) with probability β, which controls the transmissibility of the disease. The individuals in the E state remain in such a state for a time interval τE before entering into the latent state (L). After a duration τL an individual in the latent state will transition with probability α to an infected undetected (or asymptomatic) state (I_u), and with probability 1-α to an infected diseased (I_d) state. Each infected individual remains in its infected state for latencies τI_u and τI_d, respectively, before being effectively removed from the spreading population after becoming removed or recovered (R). The model operates until all individuals belong to either the S or R states, the moment in which the local outbreak ends. All latencies are probabilistically sampled from Gamma distributions fitted for the dynamics of Covid-19 (Lauer et al., 2020).

METHODS

Simulation of Infectious Spread

For pathogen spread, we consider a model with six states according to the disease status of the individual: Susceptible (S), exposed (E), latent (L), infected undetected (I_u), infected diseased (I_d), and recovered (R) (Ivorra et al., 2020). See **Figure 4** for the graphical depiction of the model and transitions between states. The model is a recent variation of the well-established Susceptible-Exposed-Infected-Recovered (SEIR) model, adapted to the epidemiological characteristics of Covid-19, including the latencies (Eguíluz et al., 2020; Flaxman et al., 2020; Bi et al., 2020; Lauer et al., 2020) and the reported large fraction of asymptomatic cases occurring in this disease (Ivorra et al., 2020). All individuals start with a susceptible status. Upon close contact with an infected or latent case, an individual in susceptible state (S) will transition to the state of exposed (E) with probability β, which controls the transmissibility of the disease.

An individual will remain in the E state for a time interval of duration τE before entering into the latent state (L). After a duration τL an individual in the latent state will transition with probability α to an infected undetected (or asymptomatic) state (I_u), and with probability 1-α to an infected diseased (I_d) state. Each infected individual remains in its infected state for latencies τI_u and τI_d, respectively, before being effectively removed from the spreading population after becoming removed or recovered (R).

Under different scenarios, we quantify the infectious spread occurring from a single individual. The model is based on a real sequence of close proximity contacts obtained from a geriatric unit as described in the section *Proximity contact dataset*.

The proximity contact network is critical to simulate the model in a real setting and avoid the assumption of random or homogeneous mixing of individuals in a population that is characteristic of models used at larger scales. As the propagation of Covid-19 takes longer than 4 days (duration of the recordings of the real sequence of close contacts), we repeat the interaction sequence in a loop when running the infectious spread model.

For each scenario simulated, we randomly select one nurse to become infected at day zero and run the spread model until all individuals eventually belong to the S or R state. That is, the spread and simulation stop when only susceptible and recovered individuals remain. We repeat each simulation 100 times to account for the variability of the spread dynamics (measured by the standard error of the mean; s.e.m.) and collect averaged statistics. The average computer running time for the 100 trials was 8 h per scenario on Google Collab (on machines that use single core hyper-threaded Xeon processors running at 2.3 GHz). The simulations are implemented in python as interactive python notebooks and can be found at the repository: https://github.com/Mo-youssef/Robotic-Impact-Simulation.git.

Incubation Period and Latencies

The incubation period, which includes the E and L compartments, is estimated at around 6 days (Bi et al., 2020) Specifically, the incubation period considers an average latency of 2 days in exposed (E compartment) and 4 days in the latent state (L compartment), in which the infected person is undetected but still contagious. All latencies are randomly sampled from Gamma distributions (Flaxman et al., 2020). The Gamma distributions have a shape parameter of 3, and we fit their scale parameter to adjust the mean of the distribution to the reported values. All default model parameters are described in **Supplementary Table S4**.

Proximity Contact Dataset

Infectious spread is modelled based on real data of personal contacts among patients, as well as between patients and HCW in a geriatric unit (Vanhems et al., 2013). The dataset was obtained using unobstructive wearable badges embedded with small active radiofrequency devices that could exchange ultra-low-power radio packets when facing another tag within a distance of 1.5 m. The dataset includes proximity contact data for 29 patients (PAT) and 46 HCW. Out of these 46 HCWs, there are 27 nurses (NUR), eleven doctors (MD) and eight administrators (ADM). A contact was recorded when two individuals faced each other for more than 20 s. The contacts were recorded during 4 days and four nights. There was a total of 14,037 contacts in this period, including contacts extending 20 s, for a total of 10,808 min of contact.

Scenarios

We study the effect of robotic assistance by simulating four scenarios and comparing them to the case without robotics intervention.
In total, the five scenarios are:

1. No robotic assistance.
2. Assistance to five random nurses.
3. Assistance to Top 5 high-risk nurses.
4. Assistance to Top 3 high-risk nurses and 2 random medical doctors.
5. Assistance in all interactions between nurses and patients.

In all cases, it is assumed that the robotics assistance allows interactions of the specific HCW being assisted to not be of a close-contact type and hence, to not lead to contagion by personal proximity with an infected individual.

Measures Used to Characterize the Infectious Spread

R_0. R_0 is the basic reproduction number and is calculated as the average number of people who are directly infected by one person with the disease.

Number of susceptible cases. It refers to the number of subjects remaining in the susceptible state, i.e. who have not been infected by the end of the outbreak episode.

Propagating trials. We define the infection dynamics as propagating when the spread is such that the fraction of susceptible individuals by the end of the episode is less than 90% of the total population. For the scenarios described above, we report the fraction of trials in which the spread dynamics are propagating and the average percentage of infected individuals.

I_{30}. I30 is calculated as the number of active infection cases (individuals in states E, L, I_u or I_d) on day 30 after the first infection among the population.

T_{10}. T_{10} is the number of days elapsed from the first to the 10th infection in the population.

In all cases, we always report the values for these metrics as their mean value over 100 trials together with their respective standard error of the mean.

Calibrating the Probability of Disease Transmission Upon Proximity Contact

The probability of disease transmission of disease upon close contact (β) is the main parameter controlling the spread of infection in the model. To determine a reasonable estimate for this parameter, we scanned a range of values of β from 0.0001 to 0.0095 at steps of 0.001. For each value of β, we repeat 10 simulations of the model for 50 days to determine the basic reproductive number. We determine

that the range of β between 0.0001 and 0.0025 results in spreading simulations displaying a basic reproductive number R_0 in the most frequent ranges reported along the pandemic for Covid-19 (Flaxman et al., 2020).

DATA AVAILABILITY STATEMENT

The original contributions presented in the study are included in the article/**Supplementary Material**, further inquiries can be directed to the corresponding authors.

AUTHOR CONTRIBUTIONS

RV designed research, conducted research, analyzed data and wrote the manuscript, YM conducted research and analyzed data, VE designed research, conducted research, analyzed data, wrote the manuscript, EZ conducted research and analyzed data, PB conducted research and analyzed data, JN designed research and wrote the manuscript, JH designed research and wrote the manuscript, BN designed research and wrote the manuscript, AZ designed research, conducted research, analyzed data and wrote the manuscript.

FUNDING

RV thanks the financial support from the Estonian Center of Excellence in IT (EXCITE) funded by the European Regional Development Fund, through the research grant TK148. This research was funded by "la Caixa" Foundation's Social Research Call 2021 under the project code SR20-00386 to VME, and by grants from the Heidi Demetriades Foundation, the ETH Zurich Foundation, and the Henan Provincial People's Hospital Outstanding Talents Founding Grant Project to AZ.

SUPPLEMENTARY MATERIAL

The Supplementary Material for this article can be found online at: https://www.frontiersin.org/articles/10.3389/frobt.2021.652685/full#supplementary-material

REFERENCES

Alimohamadi, Y., Taghdir, M., and Sepandi, M. (2020). Estimate of the Basic Reproduction Number for COVID-19: A Systematic Review and Meta-Analysis. *J. Prev. Med. Public Health* 53, 151–157. doi:10.3961/JPMPH.20.076

Bai, Y., Yao, L., Wei, T., Tian, F., Jin, D.-Y., Chen, L., et al. (2020). Presumed Asymptomatic Carrier Transmission of COVID-19. *Jama* 323, 1406. doi:10.1001/jama.2020.2565

Bi, Q., Wu, Y., Mei, S., Ye, C., Zou, X., Zhang, Z., et al. (2020). Epidemiology and Transmission of COVID-19 in 391 Cases and 1286 of Their Close Contacts in Shenzhen, China: a Retrospective Cohort Study. *Lancet Infect. Dis.* doi:10.1016/S1473-3099(20)30287-5

Burrer, S. L., de Perio, M. A., Hughes, M. M., Kuhar, D. T., Luckhaupt, S. E., McDaniel, C. J., et al. (2020). Characteristics of Health Care Personnel with COVID-19 — United States, February 12–April 9, 2020. *MMWR. Morb. Mortal. Wkly. Rep.* doi:10.15585/mmwr.mm6915e6

Dehning, J., Zierenberg, J., Spitzner, F. P., Wibral, M., Neto, J. P., Wilczek, M., et al. (2020). Inferring Change Points in the Spread of COVID-19 Reveals the Effectiveness of Interventions. *Science* 369, eabb9789. doi:10.1126/science.abb9789

Eguíluz, V. M., Fernández-Gracia, J., Rodríguez, J. P., Pericás, J. M., and Melián, C. (2020). *Risk of Secondary Infection Waves of COVID-19 in an Insular Region: The Case of the Balearic Islands, Spain. Front. Med.* 7, 563455. doi:10.3389/fmed.2020.563455

Fisman, D. N., Greer, A. L., and Tuite, A. R. (2020). Bidirectional Impact of Imperfect Mask Use on Reproduction Number of COVID-19: A Next Generation Matrix Approach. *Infect. Dis. Model.* 5, 405–408. doi:10.1016/j.idm.2020.06.004

Flaxman, S., Mishra, S., Gandy, A., Juliette Unwin, H. T., Mellan, T. A., Coupland, H., et al. (2020). Estimating the Effects of Non-pharmaceutical Interventions on COVID-19 in Europe Mélodie Monod 1, Imperial College COVID-19 Response Team*, Azra C. *Nature* 584, 257–261. doi:10.1038/s41586-020-2405-7

He, W., Yi, G. Y., and Zhu, Y. (2020). Estimation of the Basic Reproduction Number, Average Incubation Time, Asymptomatic Infection Rate, and Case Fatality Rate for COVID-19: Meta-Analysis and Sensitivity Analysis. *J. Med. Virol.* 92, 2543–2550. doi:10.1002/jmv.26041

Heesterbeek, H., Anderson, R. M., Andreasen, V., Bansal, S., De Angelis, D., Dye, C., et al. (2015). Modeling Infectious Disease Dynamics in the Complex Landscape of Global Health. *Science* 347, aaa4339. doi:10.1126/science.aaa4339

Ivorra, B., Ferrández, M. R., Vela-Pérez, M., and Ramos, A. M. (2020). Mathematical Modeling of the Spread of the Coronavirus Disease 2019 (COVID-19) Taking into Account the Undetected Infections. The Case of China. *Commun. Nonlinear Sci. Numer. Simulation* 88, 105303. doi:10.1016/j.cnsns.2020.105303

Karnakov, P., Arampatzis, G., Kii, I., Wermelinger, F., Wlchli, D., Papadimitriou, C., et al. (2020). Data-driven Inference of the Reproduction Number for COVID-19 before and after Interventions for 51 European Countries. *Swiss Med. Wkly.* doi:10.4414/smw.2020.20313

Kraay, A. N. M., Hayashi, M. A. L., Hernandez-Ceron, N., Spicknall, I. H., Eisenberg, M. C., Meza, R., et al. (2018). Fomite-mediated Transmission as a Sufficient Pathway: a Comparative Analysis across Three Viral Pathogens. *BMC Infect. Dis.* 18. doi:10.1186/s12879-018-3425-x

The Lancet, COVID-19: Protecting Health-Care Workers. *Lancet* (2020). 395, 922. doi:10.1016/S0140-6736(20)30644-9

Lauer, S. A., Grantz, K. H., Bi, Q., Jones, F. K., Zheng, Q., Meredith, H. R., et al. (2020). The Incubation Period of Coronavirus Disease 2019 (CoVID-19) from Publicly Reported Confirmed Cases: Estimation and Application. *Ann. Intern. Med.* 172, 577–582. doi:10.7326/M20-0504

Lu, J., Gu, J., Li, K., Xu, C., Su, W., Lai, Z., et al. (2020). COVID-19 Outbreak Associated with Air Conditioning in Restaurant, Guangzhou, China, 2020. *Emerg. Infect. Dis.* 26, 1628–1631. doi:10.3201/eid2607.200764

McMichael, T. M., Clark, S., Pogosjans, S., Kay, M., Lewis, J., Baer, A., et al. (2020). COVID-19 in a Long-Term Care Facility - King County, Washington, February 27-March 9, 2020. *MMWR Morb. Mortal. Wkly. Rep.* 69, 339–342. doi:10.15585/mmwr.mm6912e1

O'Meara, S. (2020). Meet the Engineer behind China's First Robot-Run Coronavirus ward. *Nature* 582, S53. doi:10.1038/d41586-020-01794-8

Remuzzi, A., and Remuzzi, G. (2020). COVID-19 and Italy: what Next? *Lancet* 39. doi:10.1016/S0140-6736(20)30627-9

Sanche, S., Lin, Y. T., Xu, C., Romero-Severson, E., Hengartner, N., and Ke, R. (2020). High Contagiousness and Rapid Spread of Severe Acute Respiratory Syndrome Coronavirus 2. *Emerg. Infect. Dis.* 26, 1470–1477. doi:10.3201/eid2607.200282

Shen, Y., Li, C., Dong, H., Wang, Z., Martinez, L., Sun, Z., et al. (2020). Community Outbreak Investigation of SARS-CoV-2 Transmission Among Bus Riders in

Eastern China. *JAMA Intern. Med.* 180, 1665. doi:10.1001/jamainternmed.2020.5225

Sugiyama, H., Tsujioka, T., and Murata, M. (2013). Real-time Exploration of a Multi-Robot rescue System in Disaster Areas. *Adv. Robotics* 27, 1313–1323. doi:10.1080/01691864.2013.838333

Tindale, L. C., Stockdale, J. E., Coombe, M., Garlock, E. S., Lau, W. Y. V., Saraswat, M., et al. (2020). Evidence for Transmission of Covid-19 Prior to Symptom Onset. *Elife* 9. doi:10.7554/eLife.57149

Tuffield, P., and Elias, H. (2003). The Shadow Robot Mimics Human Actions. *Ind. Robot* 30, 56–60. doi:10.1108/01439910310457715

van Doremalen, N., Bushmaker, T., Morris, D. H., Holbrook, M. G., Gamble, A., Williamson, B. N., et al. (2020). Aerosol and Surface Stability of SARS-CoV-2 as Compared with SARS-CoV-1. *N. Engl. J. Med.* 382, 1564–1567. doi:10.1056/NEJMc2004973

Vanhems, P., Barrat, A., Cattuto, C., Pinton, J.-F., Khanafer, N., Régis, C., et al. (2013). Estimating Potential Infection Transmission Routes in Hospital Wards Using Wearable Proximity Sensors. *PLoS One* 8, e73970. doi:10.1371/journal.pone.0073970

Wong, B. C. K., Lee, N., Li, Y., Chan, P. K. S., Qiu, H., Luo, Z., et al. (2010). Possible Role of Aerosol Transmission in a Hospital Outbreak of Influenza. *Clin. Infect. Dis.* 51, 1176–1183. doi:10.1086/656743

Xing, Y., Vincent, T. A., Cole, M., Gardner, J. W., Fan, H., Bennetts, V. H., et al. (2017). Mobile Robot Multi-Sensor Unit for Unsupervised Gas Discrimination in Uncontrolled Environments. *Proc. IEEE Sensors*. doi:10.1109/icsens.2017.8234440

Yang, G.-Z., J. Nelson, B., Murphy, R. R., Choset, H., Christensen, H., H. Collins, S., et al. (2020). Combating COVID-19-The Role of Robotics in Managing Public Health and Infectious Diseases. *Sci. Robot.* 5, eabb5589. doi:10.1126/scirobotics.abb5589

Zhuang, Z., Zhao, S., Lin, Q., Cao, P., Lou, Y., Yang, L., et al. (2020). Preliminary Estimates of the Reproduction Number of the Coronavirus Disease (COVID-19) Outbreak in Republic of Korea and Italy by 5 March 2020. *Int. J. Infect. Dis.* 95, 308–310. doi:10.1016/j.ijid.2020.04.044

Conflict of Interest: The authors declare that the research was conducted in the absence of any commercial or financial relationships that could be construed as a potential conflict of interest.

frontiers in Artificial Intelligence

ORIGINAL RESEARCH
published: 25 May 2021
doi: 10.3389/frai.2021.598932

COVID-FACT: A Fully-Automated Capsule Network-Based Framework for Identification of COVID-19 Cases from Chest CT Scans

*Shahin Heidarian[1], Parnian Afshar[2], Nastaran Enshaei[2], Farnoosh Naderkhani[2], Moezedin Javad Rafiee[3], Faranak Babaki Fard[4], Kaveh Samimi[5], S. Farokh Atashzar[6,7], Anastasia Oikonomou[8], Konstantinos N. Plataniotis[9] and Arash Mohammadi[2]**

[1]Department of Electrical and Computer Engineering, Concordia University, Montreal, QC, Canada, [2]Concordia Institute for Information Systems Engineering (CIISE), Concordia University, Montreal, QC, Canada, [3]Department of Medicine and Diagnostic Radiology, McGill University Health Center-Research Institute, Montreal, QC, Canada, [4]Biomedical Sciences Department, Faculty of Medicine, University of Montreal, Montreal, QC, Canada, [5]Department of Radiology, Iran University of Medical Science, Tehran, Iran, [6]Department of Electrical and Computer Engineering, New York University, New York, NY, United States, [7]Department of Mechanical and Aerospace Engineering, New York University, New York, NY, United States, [8]Department of Medical Imaging, Sunnybrook Health Sciences Centre, University of Toronto, Toronto, ON, Canada, [9]Department of Electrical and Computer Engineering, University of Toronto, Toronto, ON, Canada

OPEN ACCESS

Edited by:
Jun Deng,
Yale University, United States

Reviewed by:
Shailesh Tripathi,
Tampere University of Technology, Finland
Yuliang Huang,
Peking University Cancer Hospital, China

***Correspondence:**
Arash Mohammadi
arash.mohammadi@concordia.ca

Specialty section:
This article was submitted to Medicine and Public Health, a section of the journal Frontiers in Artificial Intelligence

Received: *10 July 2020*
Accepted: *09 February 2021*
Published: *25 May 2021*

Citation:
Heidarian S, Afshar P, Enshaei N, Naderkhani F, Rafiee MJ, Babaki Fard F, Samimi K, Atashzar SF, Oikonomou A, Plataniotis KN and Mohammadi A (2021) COVID-FACT: A Fully-Automated Capsule Network-Based Framework for Identification of COVID-19 Cases from Chest CT Scans. Front. Artif. Intell. 4:598932. doi: 10.3389/frai.2021.598932

The newly discovered Coronavirus Disease 2019 (COVID-19) has been globally spreading and causing hundreds of thousands of deaths around the world as of its first emergence in late 2019. The rapid outbreak of this disease has overwhelmed health care infrastructures and arises the need to allocate medical equipment and resources more efficiently. The early diagnosis of this disease will lead to the rapid separation of COVID-19 and non-COVID cases, which will be helpful for health care authorities to optimize resource allocation plans and early prevention of the disease. In this regard, a growing number of studies are investigating the capability of deep learning for early diagnosis of COVID-19. Computed tomography (CT) scans have shown distinctive features and higher sensitivity compared to other diagnostic tests, in particular the current gold standard, i.e., the Reverse Transcription Polymerase Chain Reaction (RT-PCR) test. Current deep learning-based algorithms are mainly developed based on Convolutional Neural Networks (CNNs) to identify COVID-19 pneumonia cases. CNNs, however, require extensive data augmentation and large datasets to identify detailed spatial relations between image instances. Furthermore, existing algorithms utilizing CT scans, either extend slice-level predictions to patient-level ones using a simple thresholding mechanism or rely on a sophisticated infection segmentation to identify the disease. In this paper, we propose a two-stage fully automated CT-based framework for identification of COVID-19 positive cases referred to as the "COVID-FACT". COVID-FACT utilizes Capsule Networks, as its main building blocks and is, therefore, capable of capturing spatial information. In particular, to make the proposed COVID-FACT independent from sophisticated segmentations of the area of infection, slices demonstrating infection are detected at the first stage and the second stage is responsible for classifying patients into COVID and non-COVID cases. COVID-FACT detects slices with infection, and identifies positive

COVID-19 cases using an in-house CT scan dataset, containing COVID-19, community acquired pneumonia, and normal cases. Based on our experiments, COVID-FACT achieves an accuracy of 90.82%, a sensitivity of 94.55%, a specificity of 86.04%, and an Area Under the Curve (AUC) of 0.98, while depending on far less supervision and annotation, in comparison to its counterparts.

Keywords: capsule networks, COVID-19, computed tomography scans, fully automated classification, deep learning

1 INTRODUCTION

The recent outbreak of the novel coronavirus infection (COVID-19) has sparked an unforeseeable global crisis since its emergence in late 2019. Resulting COVID-19 pandemic is reshaping our societies and people's lives in many ways and caused more than half a million deaths so far. In spite of the global enterprise to prevent the rapid outbreak of the disease, there are still thousands of reported cases around the world on daily bases, which raised the concern of facing a major second wave of the pandemic. Early diagnosis of COVID-19, therefore, is of paramount importance, to assist health and government authorities with developing efficient resource allocations and breaking the transmission chain.

Reverse Transcription Polymerase Chain Reaction (RT-PCR), which is currently the gold standard in diagnosing COVID-19, is time-consuming and prone to high false-negative rate (Fang et al., 2020). Recently, chest Computed Tomography (CT) scans and Chest Radiographs (CR) of COVID-19 patients, have shown specific findings, such as bilateral and peripheral distribution of Ground Glass Opacities (GGO) mostly in the lung lower lobes, and patchy consolidations in some of the cases (Inui et al., 2020). Diffuse distribution, vascular thickening, and fine reticular opacities are other commonly observed features of COVID-19 reported in (Bai et al., 2020; Chung et al., 2020; Ng et al., 2020; Shi et al., 2020). Although imaging studies and their results can be obtained in a timely fashion, such features can be seen in other viral or bacterial infections or other entities such as organizing pneumonia, leading to misclassification even by experienced radiologists.

With the increasing number of people in need of COVID-19 examination, health care professionals are experiencing a heavy workload reducing their concentration to properly diagnose COVID-19 cases and confirm the results. This arises the need to distinguish normal cases and non-COVID infections from COVID-19 cases in a timely fashion to put a higher focus on COVID-19 infected cases. Using deep learning-based algorithms to classify patients into COVID and non-COVID, health care professionals can exclude non-COVID cases quickly in the first step and allow for paying more attention and allocating more medical resources to COVID-19 identified cases. It is worth mentioning that although the RT-PCR, as a non-destructive diagnosis test, is commonly used for COVID-19 detection, in some countries with high number of COVID-19 cases, CT imaging is widely used as the primary detection technique. Therefore, there is an unmet need to develop advanced deep learning-based solutions based on CT images to speed up the diagnosis procedure.

1.1 Literature Review

Convolutional Neural Networks (CNNs) have been widely used in several studies to account for the human-centered weaknesses in detecting COVID-19. CNNs are powerful models in related tasks and are capable of extracting distinguishing features from CT scans and chest radiographs (Yamashita et al., 2018). In this regard, many studies have utilized CNNs to identify COVID-19 cases from medical images. The study by (Wang and Wong, 2020), is an example of the application of CNN in COVID-19 detection, where CNN is first pre-trained on the ImageNet dataset (Krizhevsky et al., 2017). Fine-tuning is then performed using a CR dataset. Results show an accuracy of 93.3% in distinguishing normal, non-COVID-19 pneumonia (viral and bacterial), and COVID-19 infection cases (Sethy et al., 2020). have also explored the same problem with the difference that the CNN is followed by a Support Vector Machine (SVM), to identify positive COVID-19 cases. Their obtained results show an overall accuracy of 95.38%, sensitivity of 97.29% and specificity of 93.47%. Another study by (Mahmud et al., 2020) proposed a CNN-based model utilizing depth-wise convolutions with varying dilation rates to extract more diversified features from chest radiographs. They used a pre-trained model on a dataset of normal, viral, and bacterial pneumonia patients followed by additional fine-tuned layers on a dataset of COVID-19 and other pneumonia patients, obtaining an overall accuracy of 90.2%, sensitivity of 89.9%, and specificity of 89.1%.

Chest radiograph acquisition is relatively simple with less radiation exposure than CT scans. However, a single CR image fails to incorporate details of infections in the lung and cannot provide a comprehensive view for the lung infection diagnosis. CT scan, on the other hand, is an alternative imaging modality that incorporates the detailed structure of the lung and infected areas. Unlike CR images, CT scans generate cross-sectional images (slices) to create a 3D representation of the body. Consequently, there has been a surge of interest on utilizing 2D and 3D CT images to identify COVID-19 infection. For instance (Yang et al., 2020), proposed a DenseNet-based model to classify manually selected slices with COVID-19 manifestations and pulmonary parenchyma into COVID-19 and normal classes. The underlying study achieved an accuracy of 92% on the patient-level classification by averaging slice-level probabilities followed by a threshold of 0.8 on the averaged values. Furthermore, the dataset used to train and test the model does not include other types of pneumonia. *Identified Drawback 1*: Such methods require manual selecting slices demonstrating infection to feed the model, which makes the overall process time-consuming and only partially automated. To extract features from all CT slices (Li et al., 2020), first segmented

the lung regions using a U-net based segmentation method (Ronneberger et al., 2015), and then used them to fine-tune a ResNet50 model, which was pre-trained on natural images from the ImageNet dataset (Deng et al., 2009). Extracted features are then combined using a max-pooling operation followed by a fully connected layer to generate probability scores for each disease type. Their proposed model achieved sensitivities of 90%, 87%, and 94% for COVID-19, Community Acquired Pneumonia (CAP), and non-pneumonia cases respectively. *Identified Drawback 2:* Such methods combine extracted features from all slices of a patient, with or without infection, which potentially results in lower accuracy as there are numerous slices without evidence of infection in a volumetric CT scan of an infected patient.

In the study by (Hu et al., 2020), segmented lungs are fed into a multi-scale CNN-based classification model, which utilizes intermediate CNN layers to obtain classification scores, and aggregates scores generated by intermediate layers to make the final prediction. Their proposed method achieves an overall accuracy of 87.4% in the three-way classification (Zhang et al., 2020). proposed a two-stage method consisting of a Deeplabv3-based lung-lesion segmentation model (Chen et al., 2017) followed by a 3D ResNet18 classification model (Hara et al., 2017) to identify lung lesions and abnormalities and use them to classify patients into COVID-19, community acquired pneumonia, and normal findings. They manually annotated chest CT scans into seven regions to train their lung segmentation model, which is a time-consuming and sophisticated task requiring high level of thoracic radiology expertise to accomplish. Their proposed method achieves the overall accuracy of 92.49% in both three-way and binary (COVID-19 vs. others) classifications.

1.2 Problem Statement

At one hand, we aim to address the two identified drawbacks of the aforementioned methods. More specifically, existing solutions either require a precise annotation/labeling of lung images, which is time-consuming and error-prone, especially when we are facing a new and unknown type of disease such as COVID-19, or assign the patient-level label to all the slices. On the other hand, CNN, which is widely adopted in COVID-19 studies, suffers from an important drawback that reduces its reliability in clinical practice. CNNs are required to be trained on different variations of the same object to fully capture the spatial relations and patterns. In other words, CNNs, commonly, fail to recognize an object when it is rotated or transformed. In practice, extensive data augmentation and/or adoption of huge data resources are needed to compensate for the lack of spatial interpretation. As COVID-19 is a relatively new phenomenon, large datasets are not easily accessible, especially due to strict privacy preserving constraints. Furthermore, most COVID-19 cases have been reported with a specific infection distribution in their image (Bai et al., 2020; Chung et al., 2020; Ng et al., 2020; Shi et al., 2020), which makes capturing spatial relations in the image highly important.

1.3 Contributions

As stated previously, structure of infection spread in the lung for COVID-19 is not yet fully understood given its recent and abrupt emergence. Furthermore, COVID-19 has a particular structure in affecting the lung, therefore, picking up those spatial structures are significantly important. Capsule Networks (CapsNets) (Hinton et al., 2018), in contrast to CNNs, are equipped with routing by agreement process enabling them to capture such spatial patterns. Even without a large dataset, capsules interpret the object instantiation parameters, besides its existence, and by reaching a mutual agreement, higher-level objects are developed from lower-level ones. The superiority of Capsule Networks over their counterparts has been shown in different medial image processing problems (Afshar et al., 2018; Afshar et al., 2019a; Afshar et al., 2019b; Afshar et al., 2020b; Afshar et al., 2020d; Afshar et al., 2020c). Recently, we proposed a Capsule Network-based framework (Afshar et al., 2020a), referred to as the COVID-CAPS, to identify COVID-19 cases from chest radiographs, which achieved an accuracy of 98.3%, a specificity of 98.6%, and a sensitivity of 80%. As stated previously, CT imaging is superior for COVID-19 detection and diagnosis purposes when compared to chest radiographs. However, as in the case of CT imaging, we are dealing with 3D inputs and several slices per patient (compared to one chest radiograph per patient), the learning process is significantly more challenging. As such, accuracies of deep models trained over CT scans cannot be directly compared with those obtained based on chest radiographs.

Following our previous study on chest radiographs, in the present study, we take one step forward and propose a fully automated two-stage Capsule Network-based framework, referred to as the COVID-FACT, to identify COVID-19 patients using chest CT images. Based on our in-house dataset, COVID-FACT achieves an accuracy of 90.82%, sensitivity of 94.55%, specificity of 86.04%, and Area Under the Curve (AUC) of 0.98. We developed two variants of the COVID-FACT, one of which is fed with the whole chest CT image, while the other one utilizes the segmented lung area as the input. In the latter case, instead of using an original chest CT image, first a segmentation model (Hofmanninger et al., 2020) is applied to extract the lung region, which is then provided as input to the COVID-FACT. This will be further clarified in **Section 3**. Experimental results show that the model coupled with lung segmentation achieves the same overall accuracy compared to the other COVID-FACT variation working with original images. However, using the segmented lung regions increases the sensitivity and AUC from 92.72% and 0.95 to 94.55% and 0.98, respectively, while slightly decreasing the specificity from 88.37% to 86.04%.

COVID-FACT benefits from a two-stage design, which is of paramount importance in COVID-19 detection using CT scans, as a CT examination is typically associated with hundreds of slices that cannot be analyzed at once. At the first stage, the proposed COVID-FACT detects slices demonstrating infection in a 3D volumetric CT scan to be analyzed and classified at the next stage. At the second stage, candidate slices detected at the previous stage are classified into COVID and non-COVID (community acquired pneumonia and normal) cases and a voting mechanism is applied to generate the classification scores in the patient level. COVID-FACT's two-stage architecture has the advantage of being trained by even weakly labeled dataset,

as errors at the first stage can be compensated at the second stage. As a result, COVID-FACT does not require any infection annotation or a very precise slice labeling, which is a valuable asset due to the limited knowledge and experience on the novel COVID-19 disease. In fact, manual annotation is completely removed from the COVID-FACT. The only information required from the radiologists to train the first stage is the slices containing evidence of infection. In other words, COVID-FACT is not dependent on the manual delineation of specific infected regions in the slices, which is a complicated and time-consuming task compared to only identifying slices with the evidence of infection. This issue is more critical in the case of a novel disease such as COVID-19, which requires comprehensive research to identify the disease manifestations. It is worth noting that the pre-trained lung segmentation model used as the pre-processing step in our study is related to the well-studied lung segmentation task, which is totally different from the infection segmentation. As a final note, we would like to mention that the radiologist's input is not required in the test phase of the COVID-FACT and the trained framework is fully automated.

The reminder of the paper is organized as follows: **Section 2** describes the dataset and imaging protocol used in this study. **Section 3** presents a brief description of Capsule Networks and explains the proposed COVID-FACT in details. Experimental results and model evaluation are presented in **Section 4**. Finally, **Section 5** concludes the work.

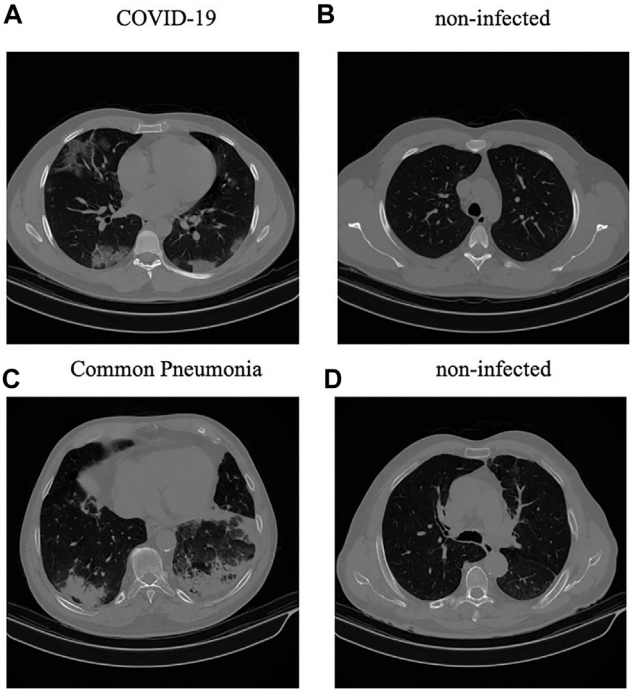

FIGURE 1 | (**A**,**B**): Infected and non-infected sample slices in a COVID-19 case; **(C**,**D)**: Infected and non-infected sample slices in a non-COVID Pneumonia case.

2 MATERIALS AND EQUIPMENT

In this section, we will explain the in-house dataset used in this study, along with the associated imaging protocol.

2.1 Dataset

The dataset used in this study, referred to as the "COVID-CT-MD" Afshar et al. (2021), contains volumetric chest CT scans of 171 patients positive for COVID-19 infection, 60 patients with Community Acquired Pneumonia (CAP), and 76 normal patients acquired from April 2018 to May 2020. The average age of patients is 50 ± 16 including 183 men and 124 women. This dataset and the related annotations are publicly available through Figshare at https://figshare.com/s/c20215f3d42c98f09ad0.

Diagnosis of COVID-19 infection is based on positive real-time reverse transcription polymerase chain reaction (rRT-PCR) test results, clinical parameters, and CT scan manifestations by a thoracic radiologist, with 20 years of experience in thoracic imaging. CAP and normal cases were included from another study and the diagnosis was confirmed using clinical parameters, and CT scans. A subset of 55 COVID-19, and 25 community acquired pneumonia cases were analyzed by the radiologist to identify and label slices with evidence of infection as shown in **Figure 1**. This labeling process focuses more on distinctive manifestations rather than slices with minimal findings. The labeled subset of the data contains 4,962 number of slices demonstrating infection and 18,447 number of slices without infection. The data is then used to train and validate the first stage of our proposed COVID-FACT model to extract slices demonstrating infection from volumetric CT scans to be used in the second classification stage. We have randomly divided this subset into three separate components for training, validation, and testing. 60% of the labeled data is used for training, 10% for validation, and 30% for the test. The unlabeled subset is also randomly divided with the same proportion and used along with the labeled data to develop the second stage of the COVID-FACT model and evaluate the overall method. The data leakage between the train and test sets has been prevented. In other words, all slices related to a patient are included either in the train or the test dataset. This research work is performed based on the policy certification number 30013394 of Ethical acceptability for secondary use of medical data approved by Concordia University. Furthermore, informed consent is obtained from all the patients. Finally, the dataset is complied with the DICOM supplement 142 (Clinical Trial De-identification Profiles) DICOM Standards Committee, Working Group 18 Clinical Trials (2011), indicating that all CT studies are de-identified by either removing or obfuscating the patient and center-related information such as names, UIDs, dates, times, and comments based on the directions specified in DICOM Standards Committee, Working Group 18 Clinical Trials (2011).

2.2 Imaging Protocol

All CT examinations have been acquired using a single CT scanner with the same acquisition setting and technical parameters, which are presented in **Table 1**, where kVP (kiloVoltage Peak) and Exposure Time affect the radiation exposure dose, while Slice Thickness and Reconstruction

TABLE 1 | Imaging device and settings used to acquire the in-house dataset.

Scanner manufacturer and model	Slice thickness (mm)	Image type	kVP (kV)	Exposure time (ms)	Reconstruction matrix	Window center	Window width
SIEMENS, SOMATOM scope	2	Axial	110	600	512 × 512	(50, –600)	(350, 1200)

Matrix represent the axial resolution and output size of the images, respectively Raman et al. (2013). Next, we describe the proposed COVID-FACT framework followed by the experimental results.

3 METHODS

The COVID-FACT framework is developed to automatically distinguish COVID-19 cases from other types of pneumonia and normal cases using volumetric chest CT scans. It utilizes a lung segmentation model at a pre-processing step to segment lung regions and pass them as the input to the two-stage Capsule Network-based classifier. The first stage of the COVID-FACT extracts slices demonstrating infection in a CT scan, while the second stage uses the detected slices in first stage to classify patients into COVID-19 and non-COVID cases. Finally, the Gradient-weighted Class Activation Mapping (Grad-CAM) localization approach (Selvaraju et al., 2017) is incorporated into the model to highlight important components of a chest CT scan, that contribute the most to the final decision.

In this section, different components of the proposed COVID-FACT are explained. First, Capsule Network, which is the main building block of our proposed approach, is briefly introduced. Then the lung segmentation method is described, followed by the details related to the first and second stages of the COVID-FACT architecture. Finally, the Grad-CAM localization mapping approach is presented.

3.1 Capsule Networks

A Capsule Network (CapsNet) is an alternative architecture for CNNs with the advantage of capturing hierarchical and spatial relations between image instances. Each Capsule layer utilizes several capsules to determine existence probability and pose of image instances using an instantiation vector. The length of the vector represents the existence probability and the orientation determines the pose. Each Capsule i consists of a set of neurons, which collectively create the instantiation vector $\boldsymbol{u}_i$ for the associated instance. Capsules in lower layers try to predict the output of Capsules in higher levels using a trainable weight matrix $\boldsymbol{W}_{ij}$ as follows

$$\hat{u}_{j|i} = \boldsymbol{W}_{ij}\boldsymbol{u}_i, \tag{1}$$

where $\hat{\boldsymbol{u}}_{j|i}$ is the predicted output of Capsule j in the next layer by the Capsule i in the lower layer. The association between the prediction $\hat{\boldsymbol{u}}_{j|i}$ and the actual output of Capsule j, denoted by $\mathbf{v}_j$, is determined by taking the inner product of $\hat{\boldsymbol{u}}_{j|i}$ and $\boldsymbol{v}_j$. The higher the inner product, the more contribution of the lower level capsules to the higher level one. The contribution of Capsule i to the output of the Capsule j in the next layer is determined by a coupling coefficient c_{ij}, trained over a course of few iterations known as the "Routing by Agreement" given by

$$a_{ij} = \boldsymbol{v}_j \,.\, \hat{\boldsymbol{u}}_{j|i}, \tag{2}$$

$$b_{ij} = b_{ij} + a_{ij}, \tag{3}$$

$$c_{ij} = \frac{\exp\left(b_{ij}\right)}{\sum_k \exp\left(b_{ik}\right)}, \tag{4}$$

$$s_j = \sum_i c_{ij}\hat{u}_{j|i}, \tag{5}$$

and

$$\boldsymbol{v}_j = \frac{\left\|\boldsymbol{s}_j\right\|^2}{1 + \left\|\boldsymbol{s}_j\right\|^2}\frac{\boldsymbol{s}_j}{\left\|\boldsymbol{s}_j\right\|}, \tag{6}$$

where a_{ij} is referred to as the agreement coefficient between the prediction and actual output, and b_{ij} denotes the log prior of the coupling coefficient c_{ij}. Vector $\boldsymbol{s}_j$ denotes the Capsule output before applying the squashing function. As the length of output vectors represents probabilities, the ultimate output of Capsule j ($\boldsymbol{v}_j$) is obtained by squashing $\boldsymbol{s}_j$ between 0 and 1 using the squashing function defined in **Eq. 6**. In order to update weight matrix $\boldsymbol{W}_{ij}$ through a backward training process, the loss function is calculated for each Capsule k as follows

$$l_k = T_k \max\left(0, m^+ - ||v_k||\right)^2 + \lambda\left(1 - T_k\right)\max\left(0, ||v_k|| - m^-\right)^2, \tag{7}$$

where T_k is 1 when the class k is present and 0 otherwise. m^+, m^-, and λ are hyper parameters of the model and are originally set to 0.9, 0.1, and 0.5, respectively. The overall loss is the summation of all losses calculated for all Capsules.

3.2 Proposed COVID-FACT

The overall architecture of the COVID-FACT is illustrated in **Figure 2**, which consists of a lung segmentation model at the beginning followed by two Capsule Network-based models and an average voting mechanism coupled with a thresholding approach to generate patient-level classification results. The three components of the COVID-FACT are as follows:

- Lung Segmentation: The input of the COVID-FACT is the segmented lung regions identified by a U-net based segmentation model (Hofmanninger et al., 2020), referred to as the "U-net (R231CovidWeb)", which has been initially trained on a large and diverse dataset including multiple pulmonary diseases, and fine-tuned on a small dataset of COVID-19 images. The Input of the U-net (R231CovidWeb) model is a single slice with the size of 512 × 512. The output is the lung tissues, which will be normalized between 0 and 1 to

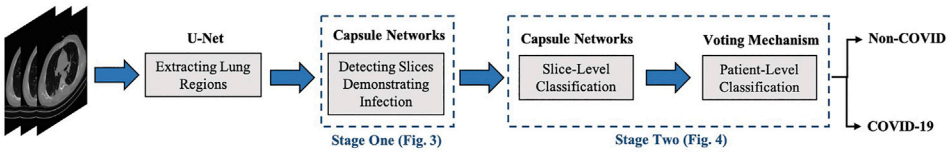

FIGURE 2 | The two-stage architecture of the proposed COVID-FACT.

generalize the features and help the model to perform more effectively. Following the literature (Hu et al., 2020; Zhang et al., 2020), we down-sampled the output from 512 × 512 to 256 × 256 size to reduce the complexity and memory allocation without losing any significant information. Slices with no detected lung regions are removed and the remaining are fed into the first stage of the COVID-FACT model.

- COVID-FACT's Stage One: The first stage of the COVID-FACT, shown in **Figure 3** is responsible to identify slices demonstrating infection (by COVID-19 or other types of pneumonia). Using this stage, we discard slices without infection and focus only on the ones with infection. Intuitively speaking, this process is similar in nature to the way that radiologists analyze a CT scan. When radiologists review a CT scan containing numerous consecutive cross-sectional slices of the body, they identify the slices with an abnormality in the first step, and analyze the abnormal ones to diagnose the disease in the next step. Existing CT-based deep learning processing methods either use all slices as a 3D input to a classifier, or classify individual slices and transform slice-level predictions to the patient-level ones using a threshold on the entire slices (Rahimzadeh et al., 2021). Determining a threshold on the number or percentage of slices demonstrating infection over the entire slices is not precise, as most pulmonary infections have different stages with involvement of different lung regions (Yu et al., 2020). Furthermore, a CT scan may contain different number of slices depending on the acquisition setting, which makes it impossible to find such a threshold. In most methods passing all slices as a 3D input to the model, the input size is fixed and the model is trained to assign higher scores to slices demonstrating infection. However, the performance of such models will be reduced when testing on a dataset other than the dataset on which they are originally trained (Zhang et al., 2020).

The model used in stage one of the proposed COVID-FACT is adapted from the COVID-CAPS model presented in our previous work (Afshar et al., 2020a), which was developed to identify COVID cases from chest radiographs. The first stage consists of four convolutional layers and three capsule layers. The first and second layers are convolutional ones followed by a batch-normalization. Similarly, the third and fourth layers are convolutional ones followed by a max-pooling layer. The fourth layer, referred to as the primary Capsule layer, is reshaped to form the desired primary capsules. Afterwards, three capsule layers perform sequential routing processes. Finally, the last Capsule layer represents two classes of infected and non-infected slices. The input of stage one is set of CT slices corresponding to a patient, and the output is slices of the volumetric CT scan demonstrating infection. The output of stage one may vary in size for each patient due to different areas of lung involvement and phase of infection.

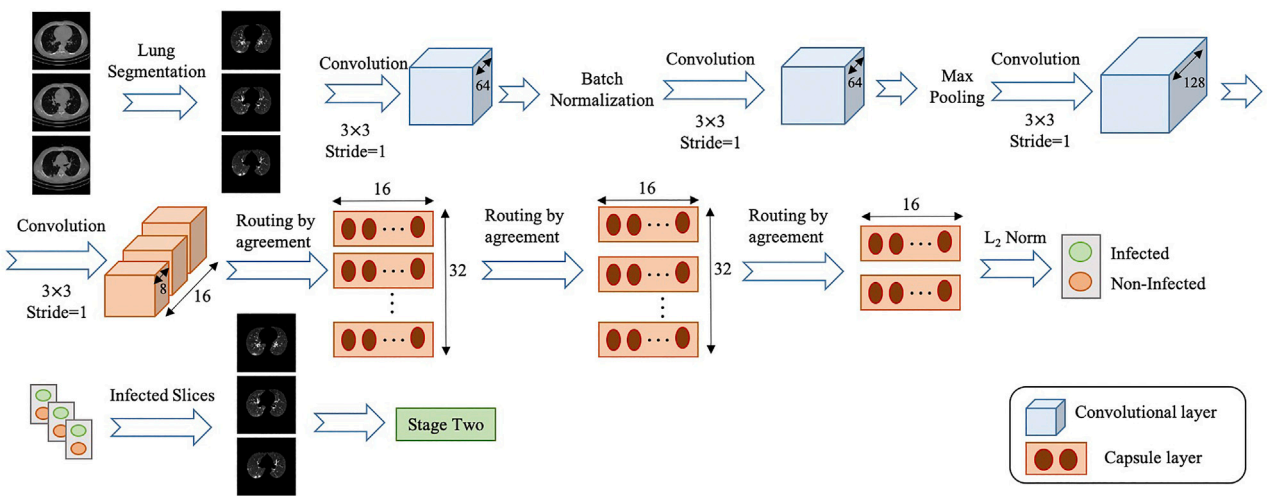

FIGURE 3 | Architecture of the COVID-FACT at stage one.

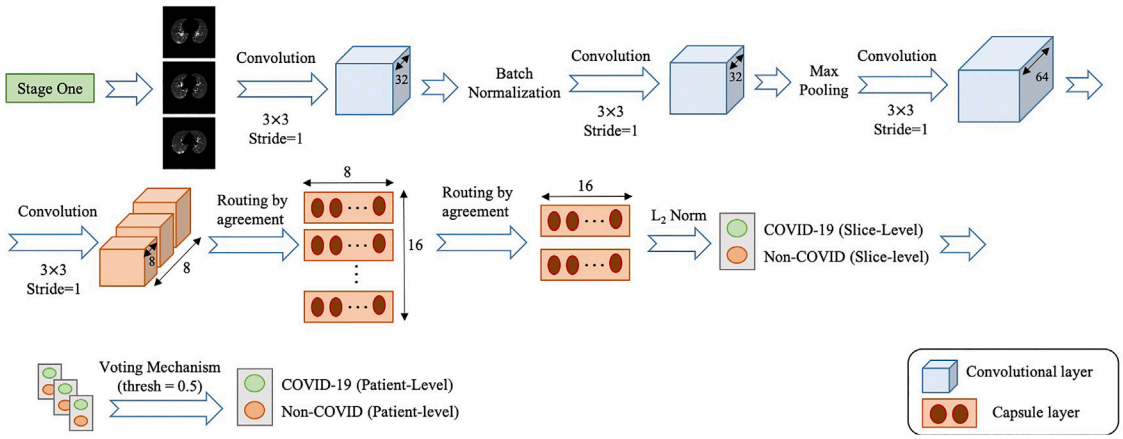

FIGURE 4 | Architecture of the COVID-FACT at stage two.

In order to cope with our imbalanced training dataset, we modified the loss function, so that a higher penalty rate is given to the false positive (infected slices) cases. The loss function is modified as follows

$$loss = \frac{N^+}{N^+ + N^-} \times loss^- + \frac{N^-}{N^+ + N^-} \times loss^+, \tag{8}$$

where N^+ is the number of positive samples, N^- is the number of negative samples, $loss^+$ denotes the loss associated with positive samples, and $loss^-$ denotes the loss associated with negative samples.

- COVID-FACT's Stage Two: As mentioned earlier, we need to apply classification methods on a subset of slices demonstrating infection rather than on the entire slices in a CT scan. It is worth noting that, lung segmentation (i.e., extracting lung tissues) is performed in one of the variants of the COVID-FACT as a pre-processing step. The first stage of the COVID-FACT, on the other hand, is tasked with this specific issue of extracting slices demonstrating infections.

The second stage of the COVID-FACT takes candidate slices of a patient detected in stage one as the input, and classifies them into one of COVID-19 or non-COVID (including normal and pneumonia) classes, i.e., we consider a binary classification problem. Stage two is a stack of four convolutional and two capsule layers shown in **Figure 4**. The output of the last capsule indicates classification probabilities in the slice-level. An average voting function is applied to the classification probabilities, in order to aggregate slice-level values and find the patient-level predictions as follows

$$P(p_k \in c) = \frac{1}{L_k} \sum_{i=1}^{L_k} P\left(s_i^k \in c\right), \tag{9}$$

where $P(p_k \in c)$ refers to the probability that patient k belongs to the target class c (e.g., COVID-19), L_k is the total number of slices detected in stage one for patient k, and $P(s_i^k \in c)$ refers to the probability that the i^{th} slice detected for patient k belongs to the target class c. It is worth noting that while, initially, the COVID-FACT performs slice-level classification in its second stage, the output is patient-level classification (through its voting mechanism), which is on par with other works that COVID-FACT is compared with. As a final note to our discussion, we would like to add that, corona virus infection is, typically, distributed across the lung volume as such manifests itself in several CT slices. Therefore, having a single slice identified as COVID-19 infection can not necessarily lead to a positive COVID-19 detection.

Similar to stage one, the loss function modification in **Eq. 8** is used in the training phase of Stage two. The default cut-off probability of 0.5 is chosen in Stage two to distinguish COVID-19 and non-COVID cases. However, it is worth mentioning that the main concern in the clinical practice is to have a high sensitivity in identifying COVID-19 positive patients, even if the specificity is not very high. As such, the classification cut-off probability can be modified by physicians using the ROC curve shown in **Figure 5** in order to provide a desired balance between the sensitivity and the specificity (e.g., having a high sensitivity while the specificity is also satisfying). In other words, physicians can decide how much certainty is required to consider a CT scan as a COVID-19 positive case. By choosing a cut-off value higher than 0.5, we can exclude those community acquired pneumonia cases that contain highly overlapped features with COVID-19 cases. On the other hand, by selecting a lower cut-off value, we will allow more cases to be identified as a COVID-19 case.

To further improve the ability of the proposed COVID-FACT model to distinguish COVID-19 and non-COVID cases and attenuate effects of errors in the first stage, we classify all patients with less than 3% of slices demonstrating infection in the entire volume as a non-COVID case. These cases are more likely normal cases without any slices with infection. The few slices with infection identified for these cases might be due to the model error in the first stage, non-infectious abnormalities such as pulmonary fibrosis, or motion artifacts in the original images, which will be covered by this threshold. Based on (Yu et al., 2020), it can be interpreted that 4% lung involvement is the

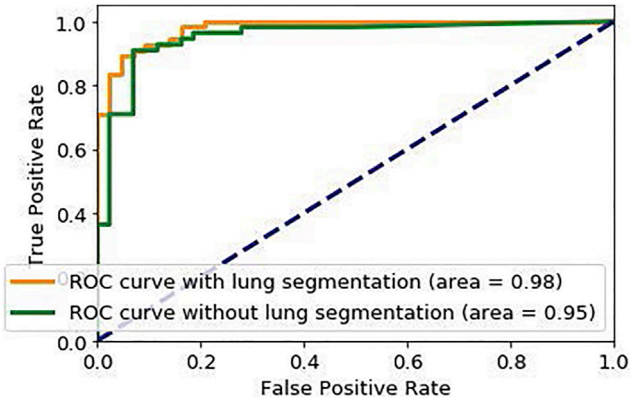

FIGURE 5 | ROC curve of the proposed COVID-FACT.

minimum percentage for COVID-19 positive cases. In addition, the minimum percentage of slices demonstrating infection detected by the radiologist in our dataset is 7%, and therefore 3% would be a safe threshold to prevent mis-classifying infected cases as normal.

As a final note, it is worth mentioning that the role of Stage 1 is critical to achieving a fully automated framework, which does not require any input from the radiologists, especially when an early and fast diagnosis is desired. However, the COVID-FACT framework is completely flexible and Stage 1 can be skipped if the slices demonstrating infections have already been identified by the radiologists, meaning that the normal cases are already identified in this case and Stage 2 merely separates COVID-19 and CAP cases.

- Grad-CAM: Using the Grad-CAM approach, we can visually verify the relation between the model's prediction and the features extracted by the intermediate convolutional layers, which ultimately leads to a higher level of interpretability of the model. Grad-CAM's outcome is a weighted average of the feature maps of a convolutional layer, followed by a Rectified Linear Unit (ReLU) activation function, i.e.,

$$L^{c}_{Grad-CAM} = ReLU\left(\sum_{k} \alpha^{c}_{k} A^{k}\right), \tag{10}$$

where $L^{c}_{Grad-CAM}$ refers to the Grad-CAM's output for the target class c; α^{c}_{k} is the importance weight for the feature map k and the target class c, and; A^{k} refers to the feature map k of a convolutional layer. The weights α^{c}_{k} are obtained based on the gradients of the probability score of the target class with respect to an intermediate convolutional layer followed by a global average pooling function as follows

$$\alpha^{c}_{k} = \frac{1}{Z}\sum_{i}\sum_{j}\frac{\partial y^{c}}{\partial A^{k}_{ij}}, \tag{11}$$

where y^{c} is the prediction value (probability) for target class c, and Z refers to the total number of feature maps in the convolutional layer.

4 EXPERIMENTAL RESULTS

The proposed COVID-FACT is tested on the in-house dataset described earlier in **Section 2**. The testing set contains 53 COVID-19 and 43 non-COVID cases (including 19 community acquired pneumonia and 24 normal cases). We used the Adam optimizer with the initial learning rate of $1e-4$, batch size of 16, and 100 epochs. The model with the minimum loss value on the validation set was selected to evaluate the performance of the model on the test set. The proposed COVID-FACT method achieved an accuracy of 90.82%, sensitivity of 94.55%, specificity of 86.04%, and AUC of 0.97. The obtained ROC curve is shown in **Figure 5**. The training and validation loss curves are also illustrated in **Figure 6**.

In a second experiment, we trained our model using the complete CT images without segmenting the lung regions. The obtained model reached an accuracy of 90.82%, sensitivity of 92.72%, specificity of 88.37%, and AUC of 0.95. The corresponding ROC curve is shown in **Figure 5**. This experiment indicates that segmenting lung regions in the first step will increase the sensitivity and AUC from 92.72% and 0.95 to 90.82% and 0.98 respectively, while slightly decreases the specificity from 88.37% to 86.04%. Although the numerical results show a slight improvement achieved by segmenting the lung regions, further investigating the sources of errors demonstrates the superiority of using segmented lung regions over the original CT scans. In the COVID-FACT model using lung segmented regions, none of COVID-19 and community acquired pneumonia cases have been mis-classified as a normal case by the 3% thresholding after the first stage, and 95.84% (23/24) of normal cases have been identified correctly using this threshold, while for the model without the lung segmentation, there is one mis-classification of a COVID-19 case by the 3% thresholding, and 91.66% (22/24) of normal cases were identified correctly using this threshold.

Furthermore, we compared performance of the Capsule Network-based framework of COVID-FACT with a CNN-based alternative to demonstrate the effectiveness of Capsule Networks and their superiority over CNN in terms of number of trainable parameters and accuracy. In other words, the CNN-based alternative model has the same front-end (convolutional layers) as that of COVID-FACT in both stages. However, the Capsule layers are replaced by fully connected layers including 128 neurons for intermediate layers and two neurons for the last layer at each stage. The last fully connected layer in each stage is followed by a sigmoid activation function and the remaining modifications and hyper-parameters are kept the same as used in COVID-FACT. The CNN-based COVID-FACT achieved an accuracy of 71.43%, sensitivity of 81.82%, and specificity of 58.14%. The COVID-FACT performance, and number of trainable parameters for examined models are presented in **Table 2**. It is worth noting that in designing the CNN-based COVID-FACT described above, the complexity and structure have been kept similar to its capsule-based version. The goal is to evaluate and illustrate potential advantages of capsule network design over its CNN-based counterpart. Alternative models using CNN architecture and fully connected layers such as the DenseNet model (Yang et al., 2020), however, consist of several convolutional layers and a high degree of complexity,

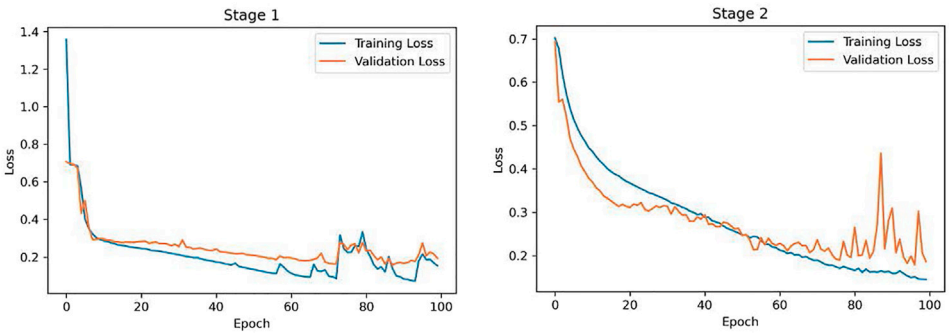

FIGURE 6 | Training and Validation loss curves obtained for the COVID-FACT stage one and stage two.

TABLE 2 | Results obtained from COVID-FACT and the alternative CNN-based model.

Method	Accuracy	Sensitivity	Specificity	AUC	Trainable parameters
COVID-FACT with lung segmentation	90.82	94.55	86.04%	0.98	406,880
COVID-FACT without lung segmentation	90.82	92.72%	88.37	0.95	406,880
CNN-based COVID-FACT	71.43%	81.82%	58.14%	0.67	365, 806, 660

as such it is expected from such complex models to outperform the CNN-based COVID-FACT.

As mentioned earlier, the ROC curve provides physicians with a precious tool to modify the sensitivity/specificity balance based on their preference by changing the classification cut-off probability. To elaborate this point, we changed the default cut-off probability from 0.5 to 0.75 and reached an accuracy of 91.83%, a sensitivity of 90.91%, and a specificity of 93.02%. Further increasing the cut-off probability to 0.8 results in the same accuracy of 91.83%, a lower sensitivity of 89.01%, and a higher specificity of 95.34%. On the other hand, decreasing the cut-off probability from 0.5 to 0.35 will increase the accuracy and the sensitivity to 91.83% and 98.18% respectively, while slightly decreases the specificity to 83.72%. The performance of the COVID-FACT for different values of cut-off probability are presented in **Table 3**.

TABLE 3 | Performance of COVID-FACT for different values of cut-off probability.

Cut-off probability	0.35	0.5	0.6	0.7	0.75	0.8
Accuracy (%)	91.83	90.82	91.83	90.82	91.83	91.83
Sensitivity (%)	98.18	94.55	92.73	90.91	90.91	89.01
Specificity (%)	83.72	86.04	90.70	90.70	93.02	95.34

While performance of the COVID-FACT is evaluated by its final decision made in the second stage, the first stage plays a crucial role in the overall accuracy of the model. As such, performance of the COVID-FACT in the first stage is also reported in **Table 4**. As shown in **Table 4**, $\sim 91\%$ of the slices demonstrating infection are identified correctly by the COVID-FACT at the first stage, while there are some mis-classified slices that will be passed to the next stage as the infectious slices. It is also evident that the CNN-based model cannot properly identify infectious slices, which in turn led to the low performance of the second stage. It is worth mentioning that stage one is only responsible to detect candidate slices, while stage two classifies the slices into COVID and non-COVID categories. The second stage is followed by an aggregation mechanism, which takes all the slices of a patient into account and consequently decreases the impact of mis-classified slices at the first stage. We have also investigated the performance of the model when the commonly used focal loss function (Lin et al., 2017) is utilized to train the model. The COVID-FACT framework trained by the focal loss function ($\gamma = 2$, $\alpha = 0.25$) achieved the same patient-level performance compared to our proposed model while the performance of the first stage was lower with the accuracy of 92.79%, sensitivity of 87.69%, and the specificity of 97.03%. The lower sensitivity in the first stage shows benefits of using the modified loss function as the role of the first stage in the pipeline is to detect slices with the evidence of infection to be analyzed in the second stage. As such, the model, which is trained using our modified loss function has been selected as the final model due to its higher accuracy and sensitivity in detecting slices demonstrating infection.

As another experiment, performance of stage two is evaluated without applying the first stage to provide a better comparison of the models used in the second stage. More specifically, the stage two model is trained based on the infectious slices identified by the radiologist and evaluated on the labeled test set including 17 COVID-19 and 8 CAP cases. The numbers of correctly predicted cases in this experiment are presented in **Table 5**. The experimental results obtained by the COVID-FACT framework using the lung segmentation achieved quite a similar performance compared to the case in which the model was trained based on the outputs of stage one. This result further demonstrates that the Capsule Network and the aggregation mechanism used in stage two can cope with errors in the previous stage and achieve desirable performance. It is worth

TABLE 4 | The performance of stage one in diagnosis of slices demonstrating infection.

Method (stage one)	Accuracy (%)	Sensitivity (%)	Specificity (%)	AUC
COVID-FACT with lung segmentation	93.14	90.75	94.01%	0.96
COVID-FACT without lung segmentation	92.78%	87.59%	94.36	0.96
CNN-based COVID-FACT	79.74%	33.00%	91.28%	0.64

mentioning that this experiment was performed using only the labeled dataset, which consequently provided a smaller dataset to train the model.

The localization maps generated by the Grad-CAM method are illustrated in **Figure 7** for the second and fourth convolutional layers in the first stage of the COVID-FACT. It is evident in **Figure 7** that the COVID-FACT model is looking at the right infectious areas of the lung to make the final decision. Due to the inherent structure of the Capsule layers, which represent image instances separately, their outputs cannot be superimposed over the input image. Consequently, in this study, the Grad-CAM localization maps are presented only for convolutional layers.

4.1 K-Fold Cross-Validation

We have evaluated the performance of the COVID-FACT and its variants based on the 5-fold cross-validation (Stone, 1974) to provide more objective assessments. In this experiment, the COVID-FACT achieves the accuracy of 87.61 ± 2.00%, the sensitivity of 88.30 ± 3.22%, and specificity of 86.75 ± 1.91%. Using the same 5-fold cross-validation technique, the COVID-FACT without using the segmented lung areas achieves the accuracy of 87.31 ± 3.37%, sensitivity of 88.32 ± 5.00%, and specificity of 86.03 ± 3.18%. Finally, the CNN-based COVID-FACT achieves the accuracy of 64.49 ± 1.61%, sensitivity of 79.58 ± 6.61%, and specificity of 46.67 ± 8.48%. The results confirm the superiority of the COVID-FACT using the segmented lung areas over its variants as was demonstrated in the previous experiments based on randomly selected test dataset. Moreover, similar to the previous experiments, modifying the cut-off probability is beneficial in the cross-validation case to adjust the capability of the model to focus on COVID or non-COVID cases depending on radiologists' priorities. More specifically, in the aforementioned 5-fold cross-validation, decreasing the cut-off probability to 0.35 increases the sensitivity to 92.97 ± 2.96% while the overall accuracy remains the same. Increasing the cut-off probability to 0.6, on the other hand, increases the specificity to 91.16 ± 3.73% and provides the same accuracy similar to the previous case.

TABLE 5 | Correctly predicted cases using only stage two without applying the first stage.

Model	COVID-19	CAP
Stage 2 with lung segmentation	94.1% (16/17)	87.5% (7/8)
Stage 2 without lung segmentation	88.2% (15/17)	62.5% (5/8)
Stage 2 CNN-based	82.4% (14/17)	25% (2/8)

5 DISCUSSION

In this study, we proposed a fully automated Capsule Network-based framework, referred to as the COVID-FACT, to diagnose COVID-19 disease based on chest CT scans. The proposed framework consists of two stages, each of which containing several layers of convolutional and Capsule layers. COVID-FACT is augmented with a thresholding method to classify CT scans with zero or very few slices demonstrating infection as non-COVID patients, and an average voting mechanism coupled with a thresholding approach is embedded to extend slice-level classification into patient-level ones. Experimental results indicate that the COVID-FACT achieves a satisfactory performance, in particular a high sensitivity with far less trainable parameters, supervision requirements, and annotations compared to its counterparts.

We further investigated mis-classified cases to determine the limitations and possible improvements. **Table 6** shows the number of the mis-classified cases for each type of the input disease (COVID-19, CAP, normal) obtained at stage two, as well as the number of normal cases that were not identified correctly by the 3% threshold after the first stage. The low rate of errors obtained by the 3% threshold in the first stage demonstrates the capability of COVID-FACT to identify normal cases in the first stage, which is very helpful for physicians and radiologists to exclude normal cases at the very beginning of their study.

As in the case of highly contagious diseases such as COVID-19, the False-Negative-Rate (FNR) is of utmost importance, we have further analyzed such errors to explore the possible sources of the mis-classification. As shown in **Table 6** there are 3/55 COVID-19 cases that are mis-classified by the COVID-FACT framework. We found that one mis-classified COVID-19 case contains unifocal infection manifestation with consolidation predominance rather than GGO, which are more common in CAP cases rather than COVID-19 ones. One other case of error was identified as an incomplete CT scan with missing slices, which has consequently made the correct identification difficult for the framework. In addition, we have reviewed the aforementioned errors in the case of image quality and lung segmentation as other potential causes of the error. The assessment results showed that the image qualities are adequate and the segmentation model performed well without removing or cropping the infection manifestations. Therefore, some errors are likely to be caused by the similarities between the infection patterns in CAP and COVID-19 cases. It is worth noting that decreasing the cut-off probability from 0.5 to 0.35, as shown in **Table 3**, will result in the correct classification of the two false-negative cases, which contain similar characteristics to other

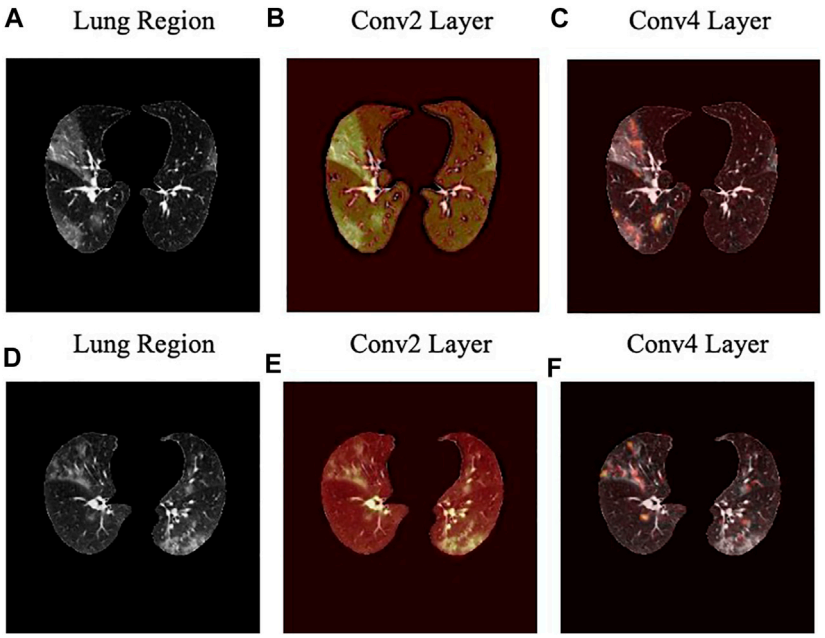

FIGURE 7 | Localization heatmaps for the second and forth convolutional layers of the first stage obtained by the Grad-CAM for two slices.

infections. This can be considered as a remedy, when FNR is of the main concern.

We also identified that errors in stage one are mainly caused by non-infectious abnormalities such as pulmonary fibrosis and artifacts. In this regard, we have further explored slices with the evidence of artifact where no infection manifestation presents. In some cases, the motion artifact or the artifacts caused by the presence of metallic components inside the body have generated some components in the image that were mis-classified as infectious slices. **Figure 8** illustrates 4 samples of such slices in which images A) and B) belong to a mis-classified normal case while images C) and D) are related to two CAP cases, where classified correctly in the second stage. It is worth mentioning that, the number of such slices is negligible especially when they appear in cases that have multiple infectious slices (caused by CAP or COVID-19). In those cases, the influence of such slices with the evidence of artifact will be diminished by the second stage and the following aggregation mechanism. Motion artifact reduction algorithms can be investigated as a future work to cope with undesired impacts of the artifacts on the final result. It is worth mentioning that during the labeling process accomplished by the radiologist to detect slices demonstrating infection, we noticed that in some cases the abnormalities are barely visible with the standard visualization setting (window center and window width). Those abnormalities have been detected by changing the image contrast (by adjusting the window center and width) manually by the radiologist. This limitation will arise the need to research on the optimal contrast and window level use in future studies. As another limitation, we can point to the retrospective study used in the data collection part of this research. Although the provided dataset is acquired with the utmost caution and inspection, a retrospective data collection might add inappropriate cases to the study at hand. The potential improvement to address this limitation could be the collaboration of more radiologists in analyzing and labeling the data to assess if the interobserver agreement is satisfying or not.

As a side note to our discussion, we would like to mention that while both CT and CR can decrease the false negative rate at the admission and discharge times, the CR is less sensitive, and less specific compared to CT. Some studies such as Reference (Wong et al., 2020) report that CR often shows no lung infection in COVID-19 patients at early stages resulting in a low sensitivity of 69% for diagnosis of COVID-19. Therefore, chest CT has a key role for diagnosis of COVID-19 in the early stages of the infection and also to set up a prognosis. Furthermore, a single CR image fails to incorporate details of infections in the lung and cannot provide a comprehensive view for the lung infection diagnosis. Unlike CR images, CT scans generate cross-sectional images (slices) and create a 3D representation of the body (i.e., each patient is associated with several 2D slices). As a result, CT images can show detailed structure of the lung and infected areas. Consequently, CT is considered as the preferred modality for grading and evaluation of imaging manifestations for COVID-19 diagnosis. It is worth adding that as CT scans are 3D images, as

TABLE 6 | The number of the mis-classified cases for each type of the input disease and the number of cases that were not identified correctly by. the 3% threshold.

Input	Errors (thresholding)	Errors (stage two)
COVID-19	0/55	3/55
CAP	0/19	5/19
Normal	1/24	1/24

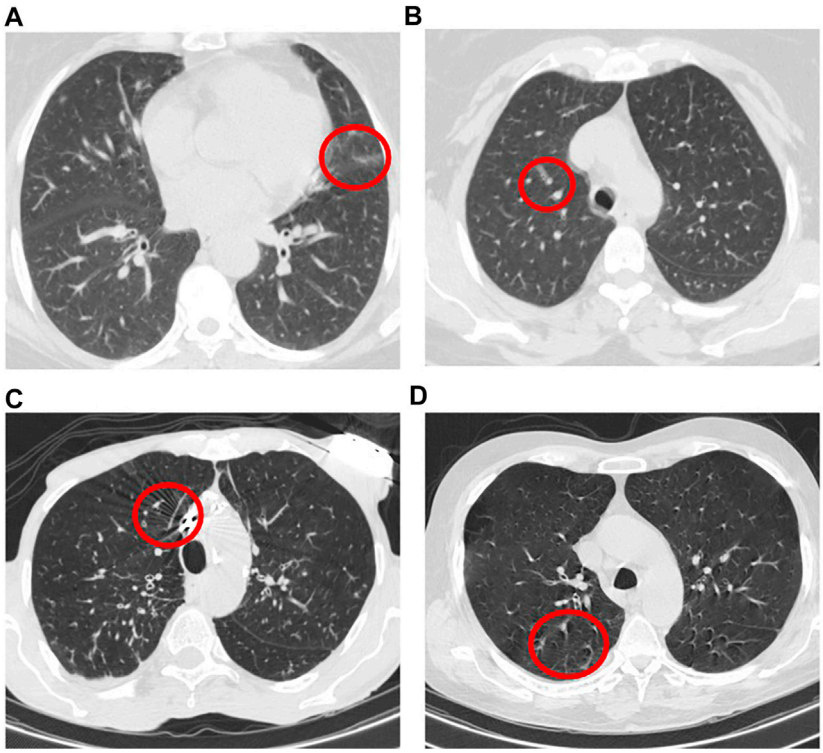

FIGURE 8 | Example of slices with the evidence of artifact where no infection manifestation presents.

opposed to 2D chest radiographs, they are more difficult to be processed using ML and DL techniques, as the currently available resources cannot efficiently process the whole volume at once. As such, slice-level and thresholding techniques are utilized to cope with such limitations, leading to a reduced performance compared to the models working with CR (e.g., the COVID-CAPS (Afshar et al., 2020d), which deals with 2D chest radiographs). The focus of our ongoing research is to further enhance performance of CT-based COVID-19 diagnosis models to fill the gap between the radiologists' performance and that of volumetric-based DL techniques.

As a final note, unlike our previous work on the chest radiographs (Afshar et al., 2020a), where we used a more imbalanced public dataset, the dataset used in this study contains a substantial number of COVID-19 confirmed cases making our results more reliable. Upon receiving more data from medical centers and collaborators, we will continue to further modify and validate the COVID-FACT by incorporating new datasets.

DATA AVAILABILITY STATEMENT

Publicly available datasets were analyzed in this study. This data can be found here: Figshare, https://figshare.com/s/c20215f3d42c98f09ad0.

ETHICS STATEMENT

The studies involving human participants were reviewed and approved by Concordia University. The patients/participants provided their written informed consent to participate in this study.

AUTHOR CONTRIBUTIONS

SH, PA, and NE implemented the deep learning models. SH and PA drafted the manuscript jointly with AM and FN. FB, KS, and MR supervised the clinical study and data collection. FB and MR annotated the CT images. AO contributed to interpretation analysis and edited the manuscript. SA and KP edited the manuscript, AM, FN, and MR directed and supervised the study. All authors reviewed the manuscript.

FUNDING

This work was supported by the Natural Sciences and Engineering Research Council (NSERC) of Canada through the NSERC Discovery Grant RGPIN-2016-04988. Atashzar's efforts were supported by US National Science Foundation, Award # 2031594.

REFERENCES

Afshar, P., Heidarian, S., Enshaei, N., Naderkhani, F., Rafiee, M. J., Oikonomou, A., et al. (2021). *COVID-CT-MD: COVID-19 Computed Tomography (CT) Scan Dataset Applicable in Machine Learning and Deep Learning*. Nature Scientific Data. In Press.

Afshar, P., Heidarian, S., Naderkhani, F., Oikonomou, A., Plataniotis, K. N., and Mohammadi, A. (2020a). COVID-CAPS: A Capsule Network-Based Framework for Identification of COVID-19 Cases from X-Ray Images. *Pattern Recognition Lett.* 138, 638–643. doi:10.1016/j.patrec.2020.09.010

Afshar, P., Mohammadi, A., and Plataniotis, K. N. (2020c). "BayesCap: A Bayesian Approach to Brain Tumor Classification Using Capsule Networks," in Submitted to IEEE International Conference on Image Processing (ICIP) (IEEE), 2024–2028. doi:10.1109/LSP.2020.3034858

Afshar, P., Mohammadi, A., and Plataniotis, K. N. (2018). "Brain Tumor Type Classification via Capsule Networks," in 2018 25th IEEE International Conference on Image Processing (ICIP) (IEEE), 3129–3133. doi:10.1109/ICIP.2018.8451379

Afshar, P., Oikonomou, A., Naderkhani, F., Tyrrell, P. N., Plataniotis, K. N., Farahani, K., et al. (2020b). 3D-MCN: A 3D Multi-Scale Capsule Network for Lung Nodule Malignancy Prediction. *Sci. Rep.* 10, 7948. doi:10.1038/s41598-020-64824-5

Afshar, P., Plataniotis, K. N., and Mohammadi, A. (2020d). "BoostCaps: A Boosted Capsule Network for Brain Tumor Classification," in *Accepted in IEEE Engineering in Medicine and Biology Society (EMBC)* (IEEE), 20–24. doi:10.1109/EMBC44109.2020.9175922

Afshar, P., Plataniotis, K. N., and Mohammadi, A. (2019a). "Capsule Networks for Brain Tumor Classification Based on MRI Images and Coarse Tumor Boundaries," in ICASSP 2019 - 2019 IEEE International Conference on Acoustics, Speech and Signal Processing (ICASSP) (IEEE), 1368–1372. doi:10.1109/ICASSP.2019.8683759

Afshar, P., Plataniotis, K. N., and Mohammadi, A. (2019b). "Capsule Networks' Interpretability for Brain Tumor Classification via Radiomics Analyses," in 2019 IEEE International Conference on Image Processing (ICIP) (IEEE), 3816–3820. doi:10.1109/ICIP.2019.8803615

Bai, H. X., Hsieh, B., Xiong, Z., Halsey, K., Choi, J. W., Tran, T. M. L., et al. (2020). Performance of Radiologists in Differentiating COVID-19 from Non-COVID-19 Viral Pneumonia at Chest CT. *Radiol.* 296, E46–E54. doi:10.1148/radiol.2020200823

Chen, L. C., Papandreou, G., Schroff, F., and Adam, H. (2017). Rethinking Atrous Convolution for Semantic Image Segmentation *ArXiv: 1706.05587*.

Chung, M., Bernheim, A., Mei, X., Zhang, N., Huang, M., Zeng, X., et al. (2020). CT Imaging Features of 2019 Novel Coronavirus (2019-nCoV). *Radiol.* 295, 202–207. doi:10.1148/radiol.2020200230

Deng, J., Dong, W., Socher, R., Li, L. J., Kai Li, Kai., and Li Fei-Fei, Li. (2009). "ImageNet: A Large-Scale Hierarchical Image Database," in 2009 IEEE Conference on Computer Vision and Pattern Recognition (IEEE), 248–255. doi:10.1109/CVPR.2009.5206848

DICOM Standards Committee, Working Group 18 Clinical Trials (2011). *Supplement 142: Clinical Trial De-identification Profiles*. Rosslyn, VI, United States: DICOM Standard, 1–44.

Fang, Y., Zhang, H., Xie, J., Lin, M., Ying, L., Pang, P., et al. (2020). Sensitivity of Chest CT for COVID-19: Comparison to RT-PCR. *Radiol.* 296, E115–E117. doi:10.1148/radiol.2020200432

Hara, K., Kataoka, H., and Satoh, Y. (2017). "Learning Spatio-Temporal Features with 3D Residual Networks for Action Recognition," in Proceedings - 2017 IEEE International Conference on Computer Vision Workshops, Venice, Italy (ICCVW), 3154–3160. doi:10.1109/ICCVW.2017.373

Hinton, G., Sabour, S., and Frosst, N. (2018). "Matrix Capsules with EM Routing," in 6th International Conference on Learning Representations, ICLR 2018 - Conference Track Proceedings, 1–29.

Hofmanninger, J., Prayer, F., Pan, J., Rohrich, S., Prosch, H., and Langs, G. (2020). *Automatic Lung Segmentation in Routine Imaging Is a Data Diversity Problem, Not a Methodology Problem*, 1–10.

Hu, S., Gao, Y., Niu, Z., Jiang, Y., Li, L., Xiao, X., et al. (2020). Weakly Supervised Deep Learning for COVID-19 Infection Detection and Classification from CT Images. *IEEE Access* 8, 118869–118883. doi:10.1109/ACCESS.2020.3005510

Inui, S., Fujikawa, A., Jitsu, M., Kunishima, N., Watanabe, S., Suzuki, Y., et al. (2020). Chest CT Findings in Cases from the Cruise Ship Diamond Princess with Coronavirus Disease (COVID-19). *Radiol. Cardiothorac. Imaging* 2, e200110. doi:10.1148/ryct.2020200110

Krizhevsky, A., Sutskever, I., and Hinton, G. E. (2017). ImageNet Classification with Deep Convolutional Neural Networks. *Commun. ACM* 60, 84–90. doi:10.1145/3065386

Li, L., Qin, L., Xu, Z., Yin, Y., Wang, X., Kong, B., et al. (2020). Using Artificial Intelligence to Detect COVID-19 and Community-Acquired Pneumonia Based on Pulmonary CT: Evaluation of the Diagnostic Accuracy. *Radiol.* 296, E65–E71. doi:10.1148/radiol.2020200905

Lin, T.-Y., Goyal, P., Girshick, R., He, K., and Dollár, P. (2017). *Focal Loss for Dense Object Detection*. doi:10.1109/iccv.2017.324

Mahmud, T., Rahman, M. A., and Fattah, S. A. (2020). CovXNet: A Multi-Dilation Convolutional Neural Network for Automatic COVID-19 and Other Pneumonia Detection from Chest X-Ray Images with Transferable Multi-Receptive Feature Optimization. *Comput. Biol. Med.* 122, 103869. doi:10.1016/j.compbiomed.2020.103869

Ng, M.-Y., Lee, E. Y. P., Yang, J., Yang, F., Li, X., Wang, H., et al. (2020). Imaging Profile of the COVID-19 Infection: Radiologic Findings and Literature Review. *Radiol. Cardiothorac. Imaging* 2, e200034. doi:10.1148/ryct.2020200034

Rahimzadeh, M., Attar, A., and Sakhaei, S. M. (2021). A fully automated deep learning-based network for detecting COVID-19 from a new and large lung CT scan dataset *Biomed. Signal Process. Control*. 68, 102588. doi:10.1016/j.bspc.2021.102588

Raman, S. P., Mahesh, M., Blasko, R. V., and Fishman, E. K. (2013). CT Scan Parameters and Radiation Dose: Practical Advice for Radiologists. *J. Am. Coll. Radiol.* 10, 840–846. doi:10.1016/j.jacr.2013.05.032

Ronneberger, O., Fischer, P., and Brox, T. (2015). *U-Net: Convolutional Networks for Biomedical Image Segmentation*, 234–241. doi:10.1007/978-3-319-24574-4_28

Selvaraju, R. R., Cogswell, M., Das, A., Vedantam, R., Parikh, D., and Batra, D. (2017). "Grad-CAM: Visual Explanations from Deep Networks via Gradient-Based Localization," in 2017 IEEE International Conference on Computer Vision (ICCV) (IEEE), 618–626. doi:10.1109/ICCV.2017.74

Sethy, P. K., Behera, S. K., Ratha, P. K., and Biswas, P. (2020). Detection of Coronavirus Disease (COVID-19) Based on Deep Features. *Int. J. Math. Eng. Manag. Sci.* 5, 643–651. doi:10.20944/preprints202003.0300.v1

Shi, H., Han, X., Jiang, N., Cao, Y., Alwalid, O., Gu, J., et al. (2020). Radiological Findings from 81 Patients with COVID-19 Pneumonia in Wuhan, China: a Descriptive Study. *Lancet Infect. Dis.* 20, 425–434. doi:10.1016/S1473-3099(20)30086-4

Stone, M. (1974). Cross-Validatory Choice and Assessment of Statistical Predictions. *J. R. Stat. Soc. Ser. B (Methodological)* 36, 111–133. doi:10.1111/j.2517-6161.1974.tb00994.x

Wang, L., and Wong, A. (2020). *COVID-Net: A Tailored Deep Convolutional Neural Network Design for Detection of COVID-19 Cases from Chest X-Ray Images*.

Wong, H. Y. F., Lam, H. Y. S., Fong, A. H.-T., Leung, S. T., Chin, T. W.-Y., Lo, C. S. Y., et al. (2020). Frequency and Distribution of Chest Radiographic Findings in Patients Positive for COVID-19. *Radiol.* 296, E72–E78. doi:10.1148/radiol.2020201160

Yamashita, R., Nishio, M., Do, R. K. G., and Togashi, K. (2018). Convolutional Neural Networks: an Overview and Application in Radiology. *Insights Imaging* 9, 611–629. doi:10.1007/s13244-018-0639-9

Yang, S., Jiang, L., Cao, Z., Wang, L., Cao, J., Feng, R., et al. (2020). Deep Learning for Detecting Corona Virus Disease 2019 (COVID-19) on High-Resolution Computed Tomography: a Pilot Study. *Ann. Transl Med.* 8, 450. doi:10.21037/atm.2020.03.132

Yu, N., Shen, C., Yu, Y., Dang, M., Cai, S., and Guo, Y. (2020). Lung Involvement in Patients with Coronavirus Disease-19 (COVID-19): a Retrospective Study Based on Quantitative CT Findings. *Chin. J. Acad. Radiol.* 3, 102–107. doi:10.1007/s42058-020-00034-2

Zhang, K., Liu, X., Shen, J., Li, Z., Sang, Y., Wu, X., et al. (2020). Clinically Applicable AI System for Accurate Diagnosis, Quantitative Measurements, and Prognosis of COVID-19 Pneumonia Using Computed Tomography. *Cell* 181, 1423–1433. doi:10.1016/j.cell.2020.04.045

Conflict of Interest: The authors declare that the research was conducted in the absence of any commercial or financial relationships that could be construed as a potential conflict of interest.

frontiers in Robotics and AI

ORIGINAL RESEARCH
published: 02 June 2021
doi: 10.3389/frobt.2021.612746

Expectations and Perceptions of Healthcare Professionals for Robot Deployment in Hospital Environments During the COVID-19 Pandemic

*Sergio D. Sierra Marín[1], Daniel Gomez-Vargas[1], Nathalia Céspedes[1], Marcela Múnera[1], Flavio Roberti[2], Patricio Barria[3], Subramanian Ramamoorthy[4], Marcelo Becker[5], Ricardo Carelli[2] and Carlos A. Cifuentes[1]**

[1] Department of Biomedical Engineering, Colombian School of Engineering Julio Garavito, Bogota, Colombia, [2] Institute of Automatics, National University of San Juan, San Juan, Argentina, [3] Club de Leones Cruz del Sur Rehabilitation Center, Punta Arenas, Chile, [4] School of Informatics, University of Edinburgh, Edinburgh, United Kingdom, [5] Department of Mechanical Engineering, São Carlos School of Engineering, University of São Paulo, São Carlos, Brazil

OPEN ACCESS

Edited by:
S. Farokh Atashzar,
New York University, United States

Reviewed by:
Muhammad Ahmad Kamran,
Pusan National University,
South Korea
Calin Vaida,
Technical University of Cluj-Napoca,
Romania

***Correspondence:**
Carlos A. Cifuentes
carlos.cifuentes@escuelaing.edu.co

Specialty section:
This article was submitted to Biomedical Robotics, a section of the journal Frontiers in Robotics and AI

Received: 30 September 2020
Accepted: 31 March 2021
Published: 02 June 2021

Citation:
Sierra Marín SD, Gomez-Vargas D, Céspedes N, Múnera M, Roberti F, Barria P, Ramamoorthy S, Becker M, Carelli R and Cifuentes CA (2021) Expectations and Perceptions of Healthcare Professionals for Robot Deployment in Hospital Environments During the COVID-19 Pandemic. Front. Robot. AI 8:612746. doi: 10.3389/frobt.2021.612746

Several challenges to guarantee medical care have been exposed during the current COVID-19 pandemic. Although the literature has shown some robotics applications to overcome the potential hazards and risks in hospital environments, the implementation of those developments is limited, and few studies measure the perception and the acceptance of clinicians. This work presents the design and implementation of several perception questionnaires to assess healthcare provider's level of acceptance and education toward robotics for COVID-19 control in clinic scenarios. Specifically, 41 healthcare professionals satisfactorily accomplished the surveys, exhibiting a low level of knowledge about robotics applications in this scenario. Likewise, the surveys revealed that the fear of being replaced by robots remains in the medical community. In the Colombian context, 82.9% of participants indicated a positive perception concerning the development and implementation of robotics in clinic environments. Finally, in general terms, the participants exhibited a positive attitude toward using robots and recommended them to be used in the current panorama.

Keywords: robotics, healthcare professionals' expectations, COVID-19, hospital environments, robot applications, UV robot, telemedicine, survey

1. INTRODUCTION

The recent outbreak of COVID-19, caused by the new severe acute respiratory syndrome coronavirus 2 (SARS-CoV-2), has spread globally in an unprecedented way around the world (World Health Organization, 2020c). In the last months, the number of infections and deaths worldwide was alarming. Thus, the efforts of most countries were focused on containing and mitigating the effects of the pandemic (United Nations Development Programme, 2020; World Health Organization, 2020c). Given the transmission rate of the virus, the World Health Organization (WHO) recommended several strategies, such as physical distancing to prevent the transmission of COVID-19 (World Health Organization, 2020a). However, some countries are now

resuming economic activities, and compliance with bio-safety protocols is still necessary to prevent the spread of the virus (Center for Disease Control and Prevention, 2020; Favero et al., 2020). In this context, to mitigate the effects of the COVID-19 pandemic, different public health measures have been adopted around the world with multiple impacts on the social, economic, and political sectors (Douglas et al., 2020; The World Bank, 2020; World Health Organization, 2020b).

Regarding the health sector, all levels and stakeholders of the world's health systems have been mainly committed to provide medical care during the pandemic (Barroy et al., 2020; Government of Canada, 2020; World Health Organization, 2020b). Hence, numerous challenges have arisen, such as (1) the vulnerability and overloading of healthcare professionals, (2) the decongestion and reduction of the risk of contagion in intra-hospital environments, (3) the availability of biomedical technology, and (3) the sustainability of patient care (Chatterjee and Kagwe, 2020; Government of Canada, 2020; Yang et al., 2020). Under this scenario, multiple strategies have been proposed to address such challenges. For instance, robotics that is a promising solution to help control and mitigate the effects of the COVID-19 pandemic (Boston Dynamics, 2020; EuRobotics, 2020; Javaid et al., 2020; Yang et al., 2020). Historically, robotics has assisted humans in a large number of fields, given its ability to execute tasks with precision, carry out industrial operations efficiently, interact in hostile environments, and execute highly complex works (Siciliano and Khatib, 2016; Cresswell et al., 2018; Nayak et al., 2020). Therefore, the applicability of robotics in society has been evident and is significantly growing (Siciliano and Khatib, 2016).

Overall, as multiple experts have discussed, robotics are potentially applicable in hospital environments during the pandemic for: (1) disinfection and sterilization of facilities, (2) handling and delivery of drugs, food, and waste, (3) telemedicine and remote assistance, as well as (4) detection and identification of new cases (Cresswell et al., 2018; Aymerich-Franch, 2020; Demaitre, 2020; Yang et al., 2020). For the first application, the implemented robot types commonly use ultraviolet (UV) lights, vaporization techniques, and vacuuming to guarantee disinfection or sterilization. This way, those devices show advantages in pathogen elimination and cleaning places, which could result in reduction of contagion risk (Yang et al., 2020).

Within the logistics and service context, robotic devices mainly apply mobile and aerial systems in delivery and supply production tasks (Yang et al., 2020). However, aerial robots could be unworkable for hospital environments. On the other hand, devices based on manipulators and hybrid systems (i.e., mobile base and manipulators) can also work in this application, focusing on these same tasks and supporting patient management (Yang et al., 2020). In telemedicine and telepresence applications, social robots and virtual agents are commonly implemented (Aymerich-Franch, 2020; Yang et al., 2020). Thus, these robotic systems allow providing benefits in aspects, such as accompanying, monitoring, and patrolling (Yang et al., 2020). Finally, for the detection and control applications, the motivation lies in monitoring of vital signs for clinical environments (Yang et al., 2020). Therefore, devices focused on this application covers hybrid mechanisms, aerial systems, or social robots.

Table 1 summarizes the most common types of robotic applications mentioned above applied to clinical environments and their potential benefits during the COVID-19 pandemic.

Despite the above, only a few studies have been focused on measuring the perception and acceptance of healthcare providers toward robotic tools in the COVID-19 pandemic (Betriana et al., 2020; Miner et al., 2020; Viswanathan et al., 2020). Several studies analyzing the acceptability and adherence of technology in healthcare, such as home healthcare robots and information systems, have shown that more than 40% of these technologies have failed or have been abandoned in the last two decades (Alaiad and Zhou, 2014; Greenhalgh et al., 2017). One of the primary adoption barriers is an inadequate understanding of the socio-technical aspects of the technology, as well as users' knowledge and perception (Aarts, 2004). Due to this reason, different methods to measure attitudes and perceptions have been implemented (Krägeloh et al., 2019). Measuring such parameters, robot developers and engineering teams can understand the users' needs and expectations (Macdonald, 2009), as well as to have an initial insight into the usability of robot applications within the involved scenarios (Shinohara, 2012; Riek, 2017).

Accordingly, the current study aims to measure clinicians' knowledge and perception toward healthcare robotics for the COVID-19 pandemic. It is expected that a positive perception/attitude toward robotics and a high level of knowledge might promote better acceptability, adherence, and adoption of robots. Hence, a Knowledge, Attitudes, and Practices (KAP) questionnaire was developed. This questionnaire collects the data on the knowledge (i.e., what is known), attitudes (i.e., what is perceived), and practices (i.e., what is done) of a particular population (World Health Organization, 2014). In this case, 41 healthcare professionals (e.g., nurses, doctors, biomedical engineers, among others) participated in the study, assessing three categories: (DIS) Disinfection and cleaning robots, (ASL) Assistance, Service, and Logistics robots, and (TEL) Telemedicine and Telepresence robots 1.

The remainder of this work is organized as follows. Section 2 describes multiple robotic devices that have been reported in the literature to be useful for disinfection, assistance, and telemedicine. Section 3 outlines the experimental protocol and the perception questionnaires carried out in the study. Section 4 and 5 describes the primary outcomes of this study and the discussion. Finally, section 6 shows the main findings of this work.

2. ROBOTICS FOR COVID-19 PANDEMIC

As described in **Table 1**, robotics for COVID-19 in hospital environments covers a wide range of possibilities. In this sense, multiple research groups worldwide have focused their efforts on developing strategies against the pandemic (Boston Dynamics, 2020; EuRobotics, 2020; Maxon Motors Inc., 2020; Robotnik, 2020; SoftBank Robotics, 2020), as the following sections show. Mainly, reported solutions vary from the design of new robots,

TABLE 1 | Medical robotics applications that are potentially useful in combating the spread of COVID-19.

Application	Robot type	Benefits	Suitable for hospitals?	Category in this study
Disinfection, and cleaning	UV	Pathogen elimination.	Yes	DIS
	Vaporization	Reduction of the risk of contagion.	Yes	DIS
	Vacuuming	Cleaning	Yes	–
Logistics and service	Mobile	Waste and/or sample management. Delivery of food and medicines. Delivery of instrumentation.	Yes	ASL
	Aerial		No	–
	Manipulator	Supply production. Waste and/or sample management.	Yes	–
	Hybrid	Supply production. Waste and/or sample management. Delivery of food and medicine Delivery of instrumentation. Patient management	Yes	ASL
Telemedicine and telepresence	Virtual agents	Accompanying. Remote monitoring.	Yes	TEL
	Social	Accompanying. Remote monitoring.	Yes	TEL
	Hybrid	Patrolling and awareness.	Yes	TEL
Detection and control	Hybrid	Vital signs monitoring Patrolling and awareness	Yes	ASL
	Social		Yes	–
	Aerial		No	–

TEL stands for Telemedicine, DIS stands for Disinfection and Cleaning, and ASL stands for Assistance, Service, and Logistics.

the adaption of existing devices for different purposes, to the implementation of commercial robotic platforms. Overall, the primary goal of those groups consists of providing efficient tools, exploiting the advantages of applying robotics or technology in the context of the COVID-19 pandemic (Brohi et al., 2020). This work focuses on three main categories (see **Figure 1**), which mainly seek to avoid propagating the virus, support the clinical staff, and ensure clean areas for both clinicians and patients.

2.1. Disinfection and Cleaning (DIS) Robots

Considering the high level of COVID-19 spread risk, the development and deployment of robots for clinical environment disinfection and decontamination have increased lately. The leading causes of infection in these areas include aspects as prolonged periods of exposure (unavoidable for clinical staff), conventional methods for cleaning (i.e., ineffective chemical inputs and human error), survivance of pathogens for long periods, and transmission through the hands between coworkers (Kramer et al., 2006; Otter et al., 2014; Boyce, 2016).

In this way, the inclusion of systems based on no-touch automated room disinfection (NTD) seeks to reduce the infection risk, removing human error, improving the effectiveness of the cleaning, and optimizing the disinfection times (Otter et al., 2013; Boyce, 2016; Marra et al., 2018). Robotic solutions of both commercial industries and research groups take strength in this period employing two cleaning principles: (1) spraying of chemicals and (2) ultraviolet (UV) light (Otter et al., 2013; Marra et al., 2018).

In the commercial context, specific-designed robots for disinfection and decontamination can be found, such as UVD Robot (UVD Robots, Odense, Denmark), Indoor Disinfection RoboCop (Milagrow Robotics, Gurgaon, India), SEIT-UV (Milvus Robotics, Ankara, Turkey), Anscer UVDR ALPHA (Anscer, Bangalore, India), ARIS-K2 (YOUIBOT, Shenzhen, China), CONNOR UVC Disinfection Robot (RobotLAB, San Francisco, USA), WDR01A (Wellwit Robotics, Shenzhen, China), LightStrike Germ-Zapping (Xenex, San Antonio, USA), Glosair 400 (Glosair, Champigny-sur-Marne, France), or Bioquell ProteQ (Bioquell, Andover, UK).

Robotic solutions have also been developed in scientific institutions, based on previous developments of mobile platforms and coupling disinfection mechanism as spraying or radiation. Moreover, although the interest in implementing those solutions has recently increased (e.g., XDBOT developed by the Nanyang Technological University), this field had previously presented significant advances in robotic systems (Andersen et al., 2006; Couto et al., 2017; Kovach et al., 2017; Yang et al., 2019).

For the Latin American autonomous robots, e.g., EXO-Andes UV-72 (EXO, Buenos Aires, Argentina), UVR-bot (UVRobotics, Buenos Aires, Argentina), Robot-UV (NFM Robotics, Callao, Peru), LD OMRON (Asahi, Aguascalientes, Mexico), RSD (Gesedic, Ciudad de Mexico, Mexico), and Thalon UV (Millenium BPO, Bogotá, Colombia) are also supporting the disinfection process. Furthermore, research projects in the region are providing robotic systems like the device developed by the Institute of Physics of Sao Carlos at the University of São Paulo for air decontamination.

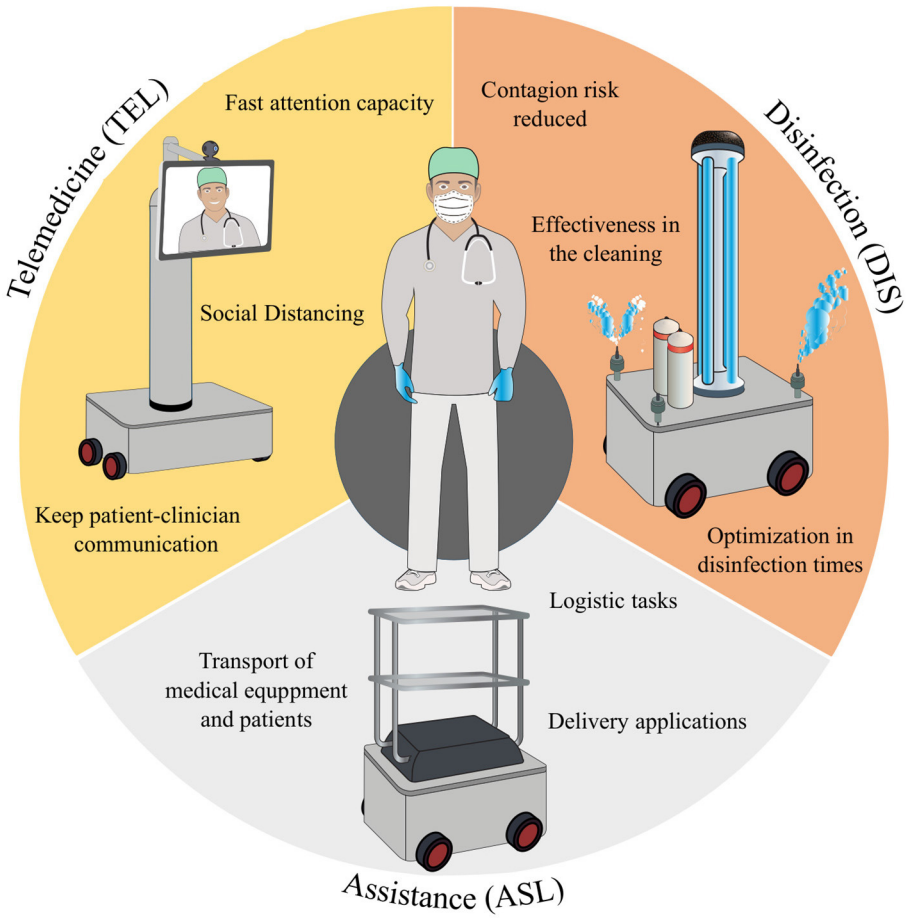

FIGURE 1 | Categories of robotics application considered in this study: (1) Telemedicine (TEL), Disinfection (DIS), and Assistance (ASL). The exhibited characteristics refer to the main advantages of using robots of the corresponding category (i.e., the yellow section for TEL, orange for DIS, and gray for ASL) in clinic environments.

2.2. Assistance, Service, and Logistics (ASL) Robots

Scenarios focused on assisting the clinical staff implies the use of robotics profiting characteristics as weight support capacity, smart navigation for mobile platforms, and precision in task execution, to name a few (Cremer et al., 2016). Recently, the development of robots for this application has not been very popular within the scientific community, resulting in the use of industrial platforms or social robots to support those tasks (Bloss, 2011).

Among the robotic tools that support the clinical staff in hospital environments for assistive applications, the following examples are found: Techi Buter (Techmetics Robotics, Santa Clara, USA), MiR100 (Mobile Industrial Robots, Odense, Denmark), TUG robot (Aethon, Pittsburgh, USA), RB-1 (Robotnik, Valencia, Spain), and Robotino (Festo, Esslingen am Neckar, Germany). Moreover, several studies have reported the use of these robots for logistic tasks, such as medication and food delivery (Kirschling et al., 2009; Takahashi et al., 2010, 2012; Bloss, 2011; Sermeus et al., 2016), patients transportation (Hu et al., 2011), medical equipment transportation (Wang et al., 2009; Ilias et al., 2014), environmental monitoring (Cremer et al., 2016; Mahdy et al., 2018), among others.

Regarding the Latin American context, few robotic applications for ASL have been reported. In Colombia, a food delivery startup is using a fleet of Kiwibot mobile robots (Kiwibot, Medellín, Colombia) to provide contactless deliveries (Meisenzahl, 2020). Although these robots are not being used in hospital environments, they can be easily adapted for healthcare support, as they are already equipped with sensing technologies for semi-autonomous navigation (Meisenzahl, 2020). Likewise, multipurpose robots are being implemented in this environment, such as RSD (Gesedic, Ciudad de Mexico, Mexico), whose mobile platform can be used in disinfection and assistance applications.

In the pre-pandemic period, the primary motivations consisted of delegating irrelevant activities to the robots to optimize the clinicians' time in patients' attention and executing heavy-weight tasks. Nevertheless, reducing the direct interaction of people with positive cases is also an attractive characteristic to implement this technology nowadays.

2.3. Telemedicine and Telepresence (TEL) Robots

Telemedicine is a general concept that encompasses any medical activity involving an element of distance (Wootton, 2001). Thus, this concept uses technology to provide a wide variety of clinical services through robots, the Internet, wireless devices, satellite, and telephone media (Achenbach, 2020). The expected benefits of telemedicine are mainly related to the faster access to health professionals, leading to optimization and improvement of the clinician's attention capacity (Hjelm, 2005; Achenbach, 2020). However, telemedicine takes hold in this pandemic time, changing a previously known drawback in its most significant advantage: the social distancing.

Different social robots are being adapted and applied to the telemedicine concept with significant growth in this period (Khan et al., 2020). Renowned platforms, such as Pepper (SoftBank Robotics, Tokyo, Japan) heads the list of robots to be called to keep the patient-clinician communication, even without representing a contagion risk (Podpora et al., 2020). This task is not unknown by the platform, since several studies have shown the potential of Pepper working in this application (Pandey and Gelin, 2018; Stock and Merkle, 2018).

In general terms, the common factor in the use of telemedicine robots involves mobile platforms integrated with videoconferencing hardware, such as RP-7 (Petelin et al., 2007; Rincon et al., 2012; Bettinelli et al., 2015; Garingo et al., 2016), RP-Vita (Sucher et al., 2011), Telepresence (Dao et al., 2019), Robotino (Tonin et al., 2011; Dobrev et al., 2018), BESSY (Murray et al., 2014). Similarly, humanoid-type robots are also found within this category, such as Stevie (McGinn et al., 2020), XR-1 (CloudMinds, Cayman Islands), Roy the robot (Smith et al., 2005), SCITOS (Hebesberger et al., 2017), among others.

Furthermore, Latin American initiatives, e.g., RED (Gesedic, Ciudad de Mexico, Mexico), RoomieBot COVID-19 (Roomie IT Services, Ciudad de Mexico, Mexico), as well as collaborative projects like EVA (PwC—RoboticsLab, Chile), have high potential and they are already being used in Telemedicine applications in this pandemic time. Similarly, a higher education institution of the Colombian government has developed a mobile robot to assist isolated patients due to COVID-19 (SENA, 2020). The robot of the National Learning Service (SENA) allows temperature taking and videoconferencing with family members and health professionals (SENA, 2020).

3. MATERIALS AND METHODS

According to the above, this work presents the design and implementation of a perception questionnaire to assess healthcare providers' level of acceptance and education toward robotic solutions for the COVID-19 pandemic. In particular, several questionnaires were proposed to evaluate the perception of medical robotics, as well as of three types of robotics platforms for COVID-19 mitigation and control: (DIS) Disinfection and cleaning robots, (ASL) Assistance, Service, and Logistic robots; and (TEL) Telemedicine and Telepresence robots. This section describes the designed questionnaires and the experimental protocol.

3.1. Perception Assessment

A qualitative survey-based study was designed to assess health professionals' concepts, ideas, perceptions, and attitudes toward robotics in the management of the COVID-19 pandemic. The proposed surveys and questions are described below.

3.1.1. Knowledge, Attitude, and Practice (KAP) Questionnaire

A quantitative questionnaire was developed to gather information on what health professionals know, how they feel and how they behave about disinfection (DIS), assistance (ASL), and telemedicine (TEL) robotic tools. In this sense, this study was based on the formulation of questions about the knowledge, attitudes, and practices of health care professionals regarding robotic tools for COVID-19 pandemic management and control. The first part of the survey was designed using knowledge-oriented questions. These questions measure the level of awareness and understanding that healthcare professionals have regarding robotic tools for DIS, ASL, and TEL. The second part was designed using attitude-oriented questions. These questions measure how healthcare professionals feel about robotic tools for DIS, ASL, and TEL, as well as any preconceived ideas or beliefs they may have about this topic. The third part was designed using practice-oriented questions. These questions provide insight into how healthcare professionals apply their knowledge and attitudes regarding robotic tools for DIS, ASL and TEL through their everyday actions.

Table 2 describes the proposed questions for the Knowledge, Attitude, and Practice (KAP) survey. Remarkably, *yes* or *no* questions were rated using 1 and −1 scores, respectively. Regarding the questions asking to rate experience or knowledge about a topic, a 5-point Likert scale was used, which were then converted to a scale from −2 to 2 points. Finally, questions formulated as statements were also evaluated using 5-point likert scales, and then they were converted to a scale from −2 to 2. **Table 2** also illustrates the minimum and maximum score for each type of question.

3.1.2. Perception Toward Robotics for COVID-19 in Colombia

To assess healthcare professionals' perceptions of the possibilities and scope of robotics for pandemic management in Colombia, an additional short questionnaire was proposed. The purpose of this questionnaire was to determine whether participants considered Colombia to have potential capabilities to develop robotic solutions for disinfection, care and telemedicine, or whether there are barriers to the development of these platforms.

Table 3 describes the proposed questions. These questions were formulated as statements and participants were asked to respond at what level they agreed with them, using a 5-point Likert scale. These questions were then converted to a scale from −2 to 2.

TABLE 2 | Designed questions for the Knowledge, Attitude, Perception (KAP) survey used in this study.

Category	Question	Type of robot	Minimum score	Maximum score
K	Have you ever heard of medical robotics?	ROB	−1	1
	Have you ever seen a health care robot?	ROB	−1	1
	Have you ever interacted with a health care robot?	ROB	−1	1
	Did you know about cleaning and disinfection robots?	DIS	−1	1
	Rate your experience with robots for cleaning and disinfection.	DIS	−2	2
	Rate your knowledge about the benefits of cleaning and disinfecting robots.	DIS	−2	2
	Did you know the robots for assistance and logistics?	ASL	−1	1
	Rate your experience with robots for assistance and logistics.	ASL	−2	2
	Did you know the robots for telemedicine?	TEL	−1	1
	Rate your experience with telemedicine robots	TEL	−2	2
	Rate your knowledge about the benefits of robots for telemedicine.	TEL	−2	2
A	In general, robots are useful.	ROB	−2	2
	I consider robots to be useful in medicine and health care.	ROB	−2	2
	I think robots in medicine and health care could replace people.	ROB	2	−2
	I think robots in medicine and health care improve service delivery.	ROB	−2	2
	I believe that disinfection and cleaning robots can mitigate and control the effects of the COVID-19 pandemic.	DIS	−2	2
	I believe that robotic assistance and logistics in hospital settings can mitigate and control the effects of the COVID-19 pandemic.	ASL	−2	2
	I believe that telemedicine robots can mitigate and control the effects of the COVID-19 pandemic.	TEL	−2	2
P	How often do you discuss about health robots in your work?	ROB	−2	2
	How often do you use or interact with robots for disinfection and cleaning?	DIS	−2	2
	I would recommend robotic tools for disinfecting and cleaning in my work.	DIS	−2	2
	How often do you use or interact with robots for assistance and logistics?	ASL	−2	2
	I would recommend robotic tools for assistance and logistics in my work.	ASL	−2	2
	How often do you use or interact with robots for telemedicine?	TEL	−2	2
	I would recommend robotic tools for telemedicine in my work	TEL	−2	2

ROB stands for questions oriented to assess robotics in general. DIS stands for questions oriented to assess disinfection and cleaning robots. ASL stands for questions oriented to assistance and logistics robots. TEL stands for questions oriented to telemedicine and telepresence robots.

TABLE 3 | Proposed questions to assess the perception of healthcare providers toward medical robotics for COVID-19 in Colombia.

Tag	Question	Minimum score	Maximum score
QCOL1	I believe that Colombia can develop robots to mitigate and control the effects of the COVID-19 pandemic	−2	2
QCOL2	In the case of Colombia, I believe that there are barriers to implement the robots that are in the international market	2	−2
QCOL3	I believe that robotic tools for disinfection, assistance and telemedicine should be acquired in Colombia	−2	2

3.1.3. Open Questions

Finally, three additional open questions were designed to identify the functionalities that clinicians consider useful and necessary in DIS, ASL, and TEL robots. **Table 4** describes the proposed questions.

3.2. Experimental Protocol

This section describes the designed experimental procedure to apply the questionnaires for perception assessment in a group of healthcare professionals. Similarly, this section summarizes the session environment and the

demographic information of the volunteers who took part in this study.

3.2.1. Session Environment

This study was carried out in two private healthcare institutions in the city of Bogotá D.C., Colombia. The two clinics were selected because they have been treating patients with COVID-19 since the beginning of the pandemic. Additionally, selecting the clinics for this study also required professionals working in intensive care units.

3.2.2. Session Procedure

Participants were asked to virtually fill out the perception questionnaires, using the Google Forms online tool. At the beginning of the form, participants were presented with the informed consent, which they had to read carefully and accept before proceeding with the form. Afterward, participants were asked for demographic information about their profession and their work environment. Preceding the questionnaires, a brief description of each type of robot was presented (i.e., DIS, ASL, and TEL), to homogenize the definition of such devices among the participants. **Table 5** describes the definitions that were used with the participants. Moreover, the questionnaire also included the visual description presented in **Figure 1**. Finally, the questionnaires were applied.

TABLE 4 | Proposed open questions to identify key functionalities of disinfection, assistance, and telemedicine robots.

Tag	Question
QO1	Briefly describe the features that you think a cleaning and disinfection robot should have.
QO2	Briefly describe the features that you think a robot should have for assistance and logistics.
QO3	Briefly describe the features that you think a telemedicine robot should have.

3.2.3. Participants Recruitment

Before the recruitment of volunteers, this study was approved by the Escuela Colombiana de Ingeniería Julio Garavito ethics committee. The subjects were all formally recruited to participate in this study voluntarily, and provided their signed consent form. The informed consent clarified that participants would not have any repercussions on their job because of the responses collected. Moreover, the data was stored without any identifier to determine the source of the answers.

The inclusion criteria were as follows: adults over 18 years old, healthcare professionals working in hospital environments can read and sign the informed consent form. The exclusion criteria were as follows: subjects with declared conflicts of interest with this study.

From the two clinics, 41 healthcare professionals voluntarily participated in this study, who were contacted by email. This sample size follows the criteria reported in previous studies that involve the use of surveys Vasileiou et al. (2018). **Table 6** summarizes the demographic information of the subjects. In particular, 20 women and 21 men with an average age of 35.39 $\pm$ 8.48 years were involved in the study. Approximately 83% of the participants indicated a work experience of more than 2 years. Additionally, 43.9% of participants indicated that they work in intensive care units or surgery, and 70% of participants responded that their daily work activities implied contact with COVID-19 patients.

3.3. Data Analysis

All data was virtually collected and then processed using Microsoft Excel and R Studio software. In relation to the KAP questionnaire, quantitative indicators related to the scores obtained by each participant were estimated. To determine if there were differences between participants with positive and negative knowledge levels about robotics, all scores were separated and compared between these two conditions. To assess the existence of significant differences the non-parametric Mann-Whitney *U* test was used. This test was selected, considering that it has been reported to have minimal

TABLE 5 | Brief description of the different robot categories that were used in the study.

Tag	Category name	Description provided to participants
TEL	Telemedicine and telepresence robots	During this survey, robots for telemedicine will be understood as those robots that allow accompanying patients who are in isolation, monitoring patient's vital signs remotely, and performing patrol and awareness tasks. This category does not include surgical robots.
DIS	Cleaning and disinfection robots	During this survey, cleaning and disinfection robots will be understood as those devices that allow the decontamination, sterilization and elimination of pathogens in different environments. Generally, these robots use ultraviolet light technology, chemical spraying systems or cleaning systems with disinfectant substances.
ASL	Assistance and logistics robots	During this survey, robots for assistance and logistics will be understood as those devices that allow the distribution of medicines in an automated way, automated catering or food distribution, sample and/or waste management, delivery of medical instruments and patient management.

This information was provided to the participants prior to the fulfillment of the questionnaires.

TABLE 6 | Demographic data of the healthcare personnel who participated in the study.

Participants	**41**	
Gender	20 female	21 male
Age, mean (SD)	35.39 (8.48) years	
Healthcare profession		
- Physiatrist	4.87%	
- Physical therapist	14.64%	
- Occupational therapist	9.75%	
- Biomedical engineer	9.75%	
- Health technologist	4.87%	
- Nursing auxiliary	7.31%	
- Surgical instrumentalist	4.87%	
- Anesthesiologist	19.57%	
- Respiratory therapist	19.57%	
- Nurse/Medical intensivist	4.86%	
Experience		
- 0–2 years	17.07%	
- 3–5 years	24.39%	
- 6–7 years	24.39%	
- 8–10 years	9.75%	
- Over 11 years	24.39%	
Educational level		
- Bachelor's degree	48.78%	
- Master's degree	2.43%	
- Post-graduate studies	36.58%	
- Technologist	12.19%	
Healthcare working area		
- Rehabilitation	21.95%	
- Hospitalization	9.75%	
- Imageology	4.87%	
- Surgery	21.95%	
- Sterilization	4.87%	
- Intensive care	21.95%	
- NA	14.65%	

type I error rates, as well as, equivalent power with *t*-test for Likert scales (Joost and Dodou, 2010). Likewise, for small sample sizes this test presents better results than *t*-test (Blair and Higgins, 1980).

4. RESULTS

A total of 41 surveys were satisfactorily fulfilled, with all participants completing the proposed form. No survey was discarded and all participants reported that the questions were clear and understandable. As a further result, none of the participants reported being infected with SARS-CoV-2. The data of this results are available in a public repository at https://doi.org/10.6084/m9.figshare.13373741. This section describes and illustrates the primary outcomes of this study.

4.1. Knowledge, Attitude, and Practice (KAP) Questionnaire

Regarding the KAP survey, **Figure 2** summarizes the primary outcomes of the proposed questions. For each type of robot (i.e., ROB, DIS, ASL, and TEL), the questions were grouped into three categories: knowledge-oriented questions, attitude-oriented questions, and practice-oriented questions. Moreover, considering the maximum and minimum scores described in **Table 2**, the scores obtained for questions of the same category and type of robot were averaged for each participant. The data was normalized through the maximum and minimum values that can be obtained in each question, being inverted for questions formulated negatively. Finally, an overall normalized score was obtained by averaging the scores of all the participants. In **Figure 2**, the normalized scores are displayed between −1 and 1, indicating a negative to positive perception scale. For analysis purposes, such an scale was equally divided into three zones, namely negative, neutral, and positive perception.

Moreover, to assess if there was a difference in perceptions between those participants who reported a negative knowledge about robotics and those who reported a positive one, a comparison of the average scores obtained with the KAP survey was performed between these conditions. **Table 7** illustrates the comparison between the scores for all participants, the scores for participants with negative knowledge, and the scores for participants with positive knowledge about robotics. Furthermore, to determine the existence of significant differences between these conditions, the non-parametric Mann-Whitney *U* test was performed. Thus, **Table 7** also describes the obtained *p*-values with this test.

4.2. Robotics for COVID-19 in Colombia

To identify the perceptions of the healthcare professionals about the scope of medical robotics during COVID-19 in Colombia, the questions presented in **Table 3** were applied. **Figure 3** summarizes the average score for each question.

4.3. Open Questions

Finally, **Figure 4** presents the results of the open questions proposed in **Table 4**.

5. DISCUSSION

All the subjects successfully completed the online questionnaires, and no cases of misunderstanding were reported. The outcomes from the KAP survey, the Colombian context, and the open questions are discussed as follows.

5.1. Knowledge, Attitude, and Practice (KAP) Questionnaire

Regarding the KAP survey, several outcomes related to the three constructs of the questionnaire can be assessed (i.e., knowledge, attitude and practice). First, it can be established that there is a positive level of knowledge about medical robotics in general for the surveyed population. However, concerning robots for disinfection (DIS), assistance (ASL), and telemedicine (TEL), participants indicated that they have a low level of knowledge and

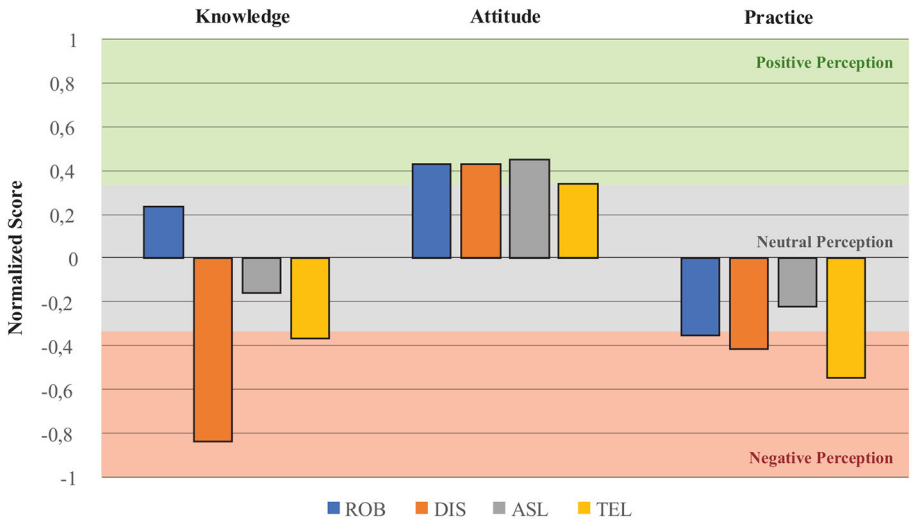

FIGURE 2 | Results of the Knowledge, Attitude, and Practice (KAP) survey. The scores for each type of robot were grouped and normalized to identify the overall perception. ROB stands for questions oriented to medical robotics. DIS stands for questions oriented to disinfection robots. ASL stands for questions oriented to assistance, service, and logistics robots. TEL stands for telemedicine and telepresence robots. The data standardization used the possible maximum and minimum values of each question, being inverted the values for questions formulated negatively.

TABLE 7 | Comparison of average scores obtained for the participants with a negative knowledge about robotics (ROB) and the participants with a positive knowledge about robotics (ROB).

Category	Type of robot	Scores			Negative vs. Positive *p*-value
		All (*n* = 41)	Negative knowledge (*n* = 16)	Positive knowledge (*n* = 25)	
K	ROB	0.24	−0.38	0.63	**0.00001**
	DIS	−0.84	−0.75	−0.90	**0.04136**
	ASL	−0.16	−0.34	−0.05	**0.02144**
	TEL	−0.37	−0.53	−0.26	0.20766
A	ROB	0.43	0.40	0.45	0.55520
	DIS	0.43	0.50	0.38	0.38430
	ASL	0.45	0.41	0.48	0.62414
	TEL	0.34	0.34	0.34	0.96012
P	ROB	−0.35	−0.81	−0.06	**0.00022**
	DIS	−0.41	−0.28	−0.50	**0.05486**
	ASL	−0.22	−0.39	−0.11	**0.01140**
	TEL	−0.55	−0.63	−0.50	**0.03078**

P-values in bold indicate significant differences ($p < 0.05$) between participants with negative and positive knowledge.

experience with these types of robots. This result may imply that although professionals recognize medical robotics as a potential tool to assist their work, they do not have sufficient awareness or education about robots' functions and features for DIS, ASL, and TEL.

Conversely, although the level of awareness was low, participants reported a positive attitude toward robots' usefulness and benefits in managing and controlling the COVID-19 pandemic. In particular, one of the attitude-oriented questions sought to determine whether health professionals believed robotics could replace them. If participants responded that they agreed with the statement, it was considered to be a negative attitude. In this case, 60.9% of the participants answered "neither agree nor disagree," and only 29.3% responded that they disagreed with the statement. This result may imply that it is necessary to carry out education and awareness processes in the medical community (Goh and Sandars, 2020), to strengthen the idea that robots can enhance and improve their work, but they cannot replace the healthcare professionals fundamental activities. For instance, Coombs (2020) recommends performing a familiarization stage based on culture theory to understand individuals' social practices when interacting with the technology

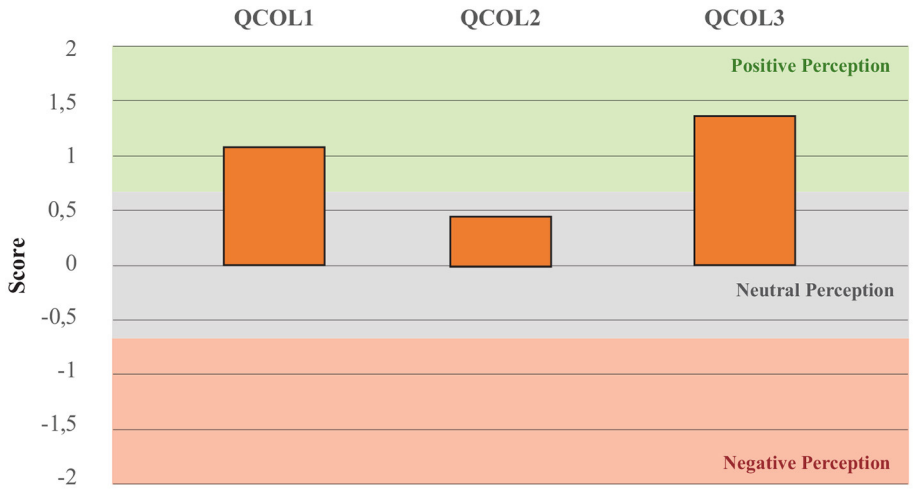

FIGURE 3 | Results of the perception questions toward the scope of Robotics for COVID-19 in Colombia. QCOL1 assess the perception of the potential to develop robotic solutions in Colombia. QCOL2 assess the perception of barriers to implement robotic solutions. QCOL3 assess the need for robotic solutions for disinfection, assistance and telemedicine during COVID-19 pandemic.

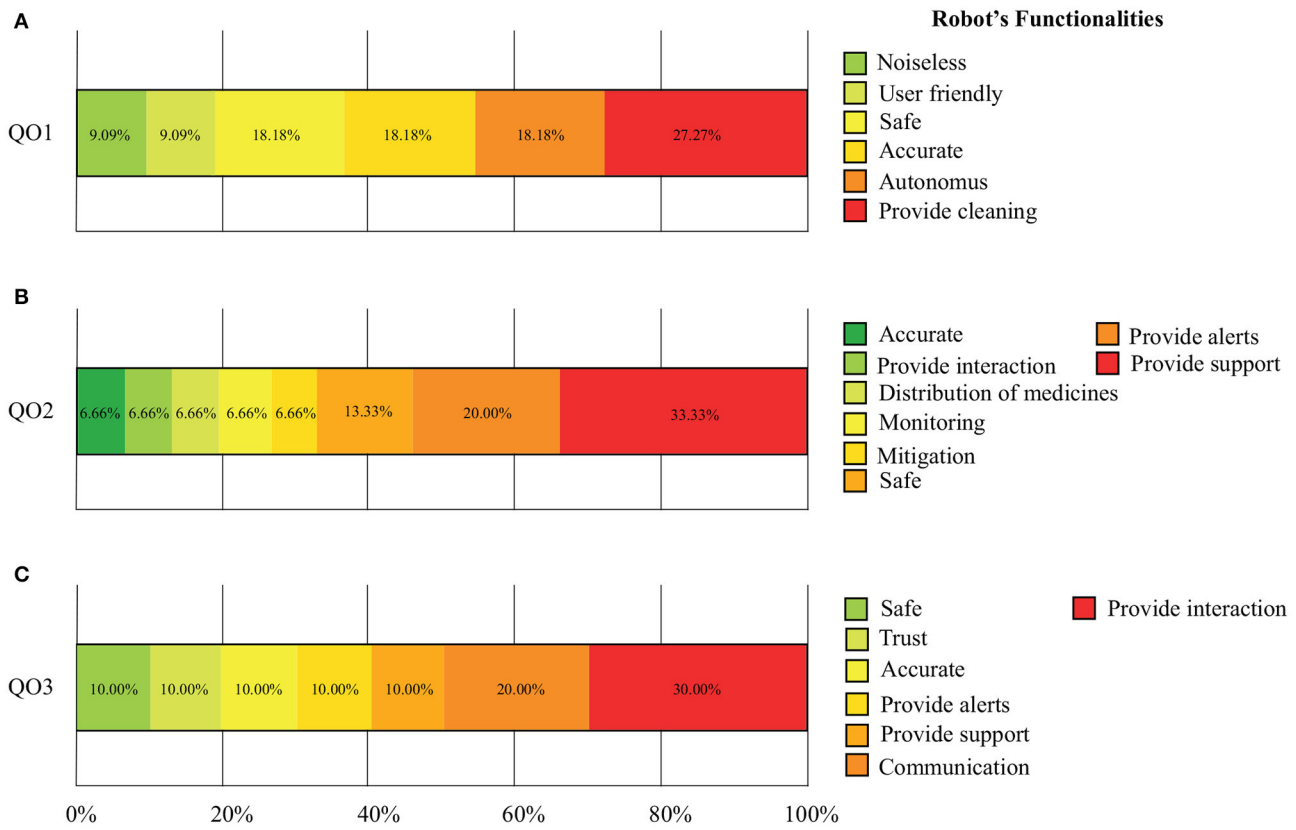

FIGURE 4 | Results of the proposed open questions to identify key functionalities of disinfection, assistance, and telemedicine robots. **(A)** Disinfection and Cleaning Robots. **(B)** Assistance, Service, and Logistics Robots. **(C)** Telemedicine and Telepresence Robots.

and their preferences within its usages. This culture theory will increase their motivation and trust toward technology, such as medical robotics. Additionally, following design methods, such as Design Thinking and Design Sprint can be useful to create user-friendly applications, and more acceptable devices within the medical community (White et al., 2020).

Regarding practice-oriented questions, the common denominator among the participants' answers indicates that healthcare professionals do not frequently use nor interact with robots in their work. An interesting result was obtained regarding whether participants would recommend using robots for DIS, ASL and TEL in their work. In particular, for disinfection (DIS) robots, only 19.5% of the participants agreed to recommend them in their work. For assistance, service, and logistics (ASL) robots, 65.8% of participants agreed to recommend them in their work. However, for telemedicine (TEL) robots, 48.8% of participants did not agree to recommend them in their work. These outcomes follow the ideas highlighted by some researches in the use of robotics mostly to assist the patients through platforms that could navigate in hostile clinical environments (Yang et al., 2020), and perform medical delivery tasks (Feil-Seifer et al., 2020). Furthermore, to reduce the reluctance to DIS and TEL robotics platforms is essential to include healthcare personnel in training programs to elucidate robots' importance and capabilities during the pandemic. Also, a challenge could be DIS and TEL comprehensive tools that can integrate features of ASL platforms.

Finally, to evaluate if there were differences in the perceptions of participants with positive (61%) and negative (39%) knowledge about robotics, the results of the KAP survey were separated and compared accordingly. For analysis purposes, the participants that reported positive knowledge will be referred to as the *positive group*, and the participants that reported negative knowledge will be referred to as the *negative group*. As presented in **Table 7**, comparing the knowledge scores (K) for disinfection (DIS) and assistance (ASL) robots, significant differences were found between negative and positive groups. Regarding DIS robots, Although the positive group scored more negatively than the whole group, this result may be explained by the fact that health professionals, who have notions of robotics, have commonly worked with or seen robots related to surgery, rather than robots associated with disinfection tasks. Conversely, regarding ASL robots, the positive group reported a neutral knowledge about them, whilst the negative group reported more negative scores than the whole group, as expected.

In relation to the attitude questions, no significant differences were found between the positive and negative groups for any type of robot. This result can be explained because in spite of the level of knowledge and conscientiousness of the health professionals, their attitude remains positive, as they recognize the robotics' usefulness and benefits in hospital environments.

In relation to the practice questions, significant differences were found for all types of robots between the positive and negative groups. For robotics in general (ROB), the positive group reported neutral scores, similar to the whole group. However, the negative group reported very negative scores, indicating that owing to the little knowledge about robotics, robots are not commonly used in their daily activities. Regarding DIS robots, the positive group reported negative scores, while the negative group reported neutral scores. This result suggests that regardless of knowledge about robotics in general, the level of awareness and in healthcare professionals about the benefits of robots for disinfection (DIS) is still low. With regards to ASL robots, the positive group exhibited a neutral distribution, similar to the whole group. In contrast, the negative group consequently reported the absence of practices and use of ASL robots in their daily tasks. Lastly, both the positive and negative groups reported poor practices related to TEL robots; however the scores from the negative group were slightly more negative.

5.2. Robotics for COVID-19 in Colombia

With regards to the perception of the participants toward the capacities and needs for robotics amid the COVID-19 in Colombia, several aspects were identified. First, question QCOL1 was aimed at determining if the participants considered that Colombia has enough technological advances to develop robotic solutions for the COVID-19 pandemic. In particular, 82.9% of participants indicated that they agreed that Colombia could develop such robotic solutions. Second, question QCOL2 was intended to determine if the participants considered barriers to the deployment of robotic platforms available in the international market. In this case, a slightly positive perception was obtained, where 40% of the participants indicated that they disagreed that there were barriers to the implementation of robots from the international market for the COVID-19 pandemic. Finally, question QCOL3 sought to identify if participants considered that robotic tools for DIS, ASL and TEL should be acquired in Colombia. In this case, 87.8% of participants agreed with this statement.

There are few publications related to robotic-tools for the COVID-19 pandemic in Colombia. Some of the applications, propose the use of robotic arms to sustain physical distancing between patients and doctors (Guerra et al., 2020), disinfection robots to support clinical neurophysiology studies (San-Juan et al., 2020), and teleoperation robots to monitor patients and connect doctors (Forbes Staff, 2020). Thus, the opportunities for developing robotics tools in Colombia during and after the pandemic are increasing to answer the healthcare sector needs.

5.3. Open Questions

Finally, this study also sought to provide insights into the features that robots should have for COVID-19 management, according to the opinions of healthcare professionals. Particularly, question QO1 was focused on identifying the expectations regarding the functionalities of disinfection robots. As it can be seen, the healthcare personnel answered that the robot must provide cleaning tasks, be safe and accurate. In a lower percentage, the clinicians recommended that the device has to be noiseless and user friendly. On the other hand, Question QCOL2 was intended to assess the clinicians' expectations regarding assistance and logistics robots. The healthcare personnel highlighted the importance of these robots, to support clinicians' tasks, and to trigger alerts as advice for emergency or important events. Finally, Question QCOL3 was focused on evaluating the clinician's opinions regarding the telemedicine and telepresence robots for the COVID-19 pandemic. The outcomes showed that the healthcare staff expects that these robots can socially interact within hospital environments, and communicate with users, connecting patients and doctors.

Overall, the healthcare personnel seeks for safe and accurate robotic systems. Therefore, the efforts of deploying robotics for COVID-19 have to be focused on optimizing and building tools with high precision, and increase safety strategies (Otter et al., 2013; Marra et al., 2018). Similarly, the work by (Tavakoli et al., 2020) remarked the features that robotics should have (i.e., autonomy, monitor, provide support and interaction) to collaborate in healthcare scenarios, not only to manage the adverse effects of the COVID-19 pandemic but also to support prevention processes.

5.4. Final Remarks

In this work, the sample size might be considered as small, however it follows the criteria reported in previous studies that involve the use of surveys (Vasileiou et al., 2018). Moreover, although the participants were only recruited from two healthcare institutions in Bogotá D.C., Colombia, this is the first study that describes the perceptions and expectations of healthcare professionals toward robotics for COVID-19 in Colombia. Particularly, several KAP surveys on COVID-19 have been reported in literature; however, they were aimed at assessing the overall perception toward COVID-19 in patients and survivors, and they did not evaluate robotics perception for COVID-19 outbreak management (Ferdous et al., 2020; IFRC Turkish Red Crescent, 2020; REACH, 2020).

6. CONCLUSIONS

This paper presented clinician's perception toward DIS, ASL, and TEL robots amidst the COVID-19 pandemic. A total of 41 participants completed an online KAP (i.e., Knowledge, Attitudes, and Perception) survey, as well as two short questionnaires about medical robotics.

In general, the outcomes showed that participants have a positive level of knowledge regarding medical robots in general. However, the clinicians' experience and knowledge regarding DIS, ASL, and TEL platforms are shallow. Consequently, their awareness and education have to be increased in order to understand the opportunities, functions, and features of these tools. Furthermore, as reported in the literature, a familiarization stage in the first instance is recommendable to increase healthcare personnel's trust and motivation. This stage will achieve the successful adaptation of the technology during the COVID-19 pandemic and after the outbreak.

Despite this level of awareness, participants elucidate a positive attitude toward robots in managing and mitigating the effects of the COVID-19 pandemic. In particular, 65.8% of clinicians recommend using ASL robots in the pandemic, which remark the clinicians' preferences for platforms capable of supporting logistic tasks, medication and food delivery, and monitoring the environment. In the case of DIS and TEL platforms a lower perception was presented. Hence, the efforts concerning these technologies have to be in increase the clinicians' trust and develop comprehensive platforms capable of providing assistance and disinfection or teleoperation.

Additionally, a very encouraging result is the healthcare positive perception regarding the capabilities in Colombia to develop these tools. Although few studies propose the development of robotic platforms to assist medical procedures in Colombia, the opportunity to increase the research and advances regarding DIS, ASL, and TEL robots are very high.

Regarding the robot's functionalities. The participants highlight the importance of building safe and accurate systems in general. For DIS robots, the healthcare staff's primary characteristic is that the robot provides reliable cleaning and autonomy. In the ASL robots case, the significant features were to provide support and provide alerts to attend emergency events. Finally, for TEL the results suggest that the main capabilities are to provide interaction and communication. Concluding, these results demonstrate that DIS, ASL and TEL platforms hold the promising potential to be a feasible approach to support COVID-19 pandemic from different approaches. One last interesting result of this work is related to the fear in health professionals to be replaced by robots. In particular, the participants' opinions were not very conclusive since ∼60% of the participants assumed a neutral position when asked if they considered that they could be replaced. However, when relating the findings of the functionalities that robots should provide to improve health service, participants agreed that robots should perform repetitive and non-critical tasks, such as transporting medications and cleaning. In this sense, it can be stated that "being replaced" by a robot does not necessarily imply a negative perception if robots assist in less essential tasks.

Future works will address the validation and implementation of this survey in multiple Latin American countries to provide a more deep comparison and assessment of healthcare providers' perception. Moreover, future studies will also be focused on identifying the specific opinions of healthcare professionals toward existing DIS, ASL, and TEL robotic platforms in both national and international markets.

DATA AVAILABILITY STATEMENT

The datasets presented in this study can be found online at: https://doi.org/10.6084/m9.figshare.13373741.

ETHICS STATEMENT

The studies involving human participants were reviewed and approved by the ethics committee at the Colombian School of Engineering Julio Garavito. The patients/participants provided their written informed consent to participate in this study.

AUTHOR CONTRIBUTIONS

DG-V, FR, PB, SR, MB, and RC performed the literature review. SS, DG-V, MM, and CC designed the methodology. SS and DG-V conducted the experimental sessions. SS and NC performed the data curation and processing. SS, DG-V, and NC wrote the original manuscript. MM, FR, PB, SR, MB, RC, and CC reviewed and edited the manuscript. MM and CC supervised the study and

managed the funding resources. All authors contributed to the conceptualization of the study.

FUNDING

This work was supported by the COVIBOT Project: Robotic Strategies for Monitoring and Disinfection of COVID-19 environments (EXPP2021\1\183) funded by the Royal Academy of Engineering (Grant: Pandemic Preparedness Phase 1), and internal funding from the Colombian School of Engineering Julio Garavito.

ACKNOWLEDGMENTS

The authors would like to thank the members of the Center for Biomechatronics for supporting this research. Likewise, we were grateful to participants, without whom this work would not have been possible.

REFERENCES

Aarts, J. (2004). IT in health care: sociotechnical approaches "To Err is System". *Int. J. Med. Inform*. 76, 6–8. doi: 10.1016/S1386-5056(07)00078-0

Achenbach, S. J. (2020). Telemedicine: benefits, challenges, and its great potential. *Health Law Policy Brief* 14:1. Available online at: https://digitalcommons.wcl.american.edu/hlp/vol14/iss1/

Alaiad, A., and Zhou, L. (2014). The determinants of home healthcare robots adoption: an empirical investigation. *Int. J. Med. Inform*. 83, 825–840. doi: 10.1016/j.ijmedinf.2014.07.003

Andersen, B. M., Rasch, M., Hochlin, K., Jensen, F. H., Wismar, P., and Fredriksen, J. E. (2006). Decontamination of rooms, medical equipment and ambulances using an aerosol of hydrogen peroxide disinfectant. *J. Hosp. Infect*. 62, 149–155. doi: 10.1016/j.jhin.2005.07.020

Aymerich-Franch, L. (2020). Why it is time to stop ostracizing social robots. *Nat. Mach. Intell*. 2:364. doi: 10.1038/s42256-020-0202-5

Barroy, H., Wang, D., Pescetto, C., and Kutzin, J. (2020). *How to Budget for COVID-19 Response? A Rapid Scan of Budgetary Mechanisms in Highly Affected Countries. Health Systems Governance and Financing & COVID-19*. Available online at: https://www.who.int/publications/m/item/how-tobudget-for-covid-19-response

Betriana, F., Tanioka, T., Locsin, R., Malini, H., and Lenggogeni, D. P. (2020). Are indonesian nurses ready for healthcare robots during the covid-19 pandemic? *Belit. Nurs. J*. 6, 63–66. doi: 10.33546/bnj.1114

Bettinelli, M., Lei, Y., Beane, M., Mackey, C., and Liesching, T. N. (2015). Does robotic telerounding enhance nurse-physician collaboration satisfaction about care decisions? *Telemed. e-Health* 21, 637–643. doi: 10.1089/tmj.2014.0162

Blair, R. C., and Higgins, J. J. (1980). A comparison of the power of Wilcoxon's rank-sum statistic to that of student's t statistic under various nonnormal distributions. *J. Educ. Stat*. 5:309. doi: 10.2307/1164905

Bloss, R. (2011). Mobile hospital robots cure numerous logistic needs. *Ind. Robot* 38, 567–571. doi: 10.1108/01439911111179075

Boston Dynamics (2020). *Boston Dynamics COVID-19 Response*. Available online at: https://www.bostondynamics.com/resources/COVID-19

Boyce, J. M. (2016). Modern technologies for improving cleaning and disinfection of environmental surfaces in hospitals. *Antimicrob. Resist. Infect. Control* 5, 1–10. doi: 10.1186/s13756-016-0111-x

Brohi, S. N., Jhanjhi, N., Brohi, N. N., and Brohi, M. N. (2020). *Key Applications of State-of-the-Art Technologies to Mitigate and Eliminate Covid-19*. doi: 10.36227/techrxiv.12115596

Center for Disease Control and Prevention (2020). *Reopening Guidance for Cleaning and Disinfecting Public Spaces, Workplaces, Businesses, Schools, and Homes*. Available online at: https://stacks.cdc.gov/view/cdc/87297

Chatterjee, S., and Kagwe, M. (2020). "Health workers are the frontline soldiers against Covid-19. Let's protect them | Africa renewal," in *Africa Renewal–Special Edition on COVID-19* (New York, NY), 1.

Coombs, C. (2020). Will COVID-19 be the tipping point for the intelligent automation of work? A review of the debate and implications for research. *Int. J. Inform. Manage*. 55:102182. doi: 10.1016/j.ijinfomgt.2020.102182

Couto, B. R. G. M., Alvim, A. L. S., da Silva, I. L. A., Horta, M. M. B., da Cunha Júnior, J. J., and Starling, C. E. F. (2017). "Using ozires, a humanoid robot, to continuing education of healthcare workers: a pilot study," in *CSEDU* (Vila Nova de Gaia), 293–299.

Cremer, S., Doelling, K., Lundberg, C. L., McNair, M., Shin, J., and Popa, D. (2016). "Application requirements for robotic nursing assistants in hospital environments," in *Sensors for Next-Generation Robotics III*, Vol. 9859 (Baltimore, MD: International Society for Optics and Photonics), 98590E. doi: 10.1117/12.2229241

Cresswell, K., Cunningham-Burley, S., and Sheikh, A. (2018). Health care robotics: qualitative exploration of key challenges and future directions. *J. Med. Internet Res*. 20:e10410. doi: 10.2196/10410

Dao, N., Hai, X., Huu, L., Nam, T., and Thinh, N. T. (2019). "Remote healthcare for the elderly, patients by tele-presence robot," in *2019 International Conference on System Science and Engineering (ICSSE)* (Dong Hoi: IEEE), 506–510.

Demaitre, E. (2020). *Coronavirus Response Growing From Robotics Companies*. Available online at: https://www.therobotreport.com/coronavirusresponse-growing-robotics-companies/

Dobrev, Y., Gulden, P., and Vossiek, M. (2018). An indoor positioning system based on wireless range and angle measurements assisted by multi-modal sensor fusion for service robot applications. *IEEE Access* 6, 69036–69052. doi: 10.1109/ACCESS.2018.2879029

Douglas, M., Katikireddi, S. V., Taulbut, M., McKee, M., and McCartney, G. (2020). Mitigating the wider health effects of covid-19 pandemic response. *BMJ* 369:m1557. doi: 10.1136/bmj.m1557

EuRobotics (2020). *10 Ways Robots Fight Against the COVID-19 Pandemic*. Available online at: https://www.eurobotics.net/eurobotics/newsroom/press/robotsagainst-covid-19.html?changelang=1

Favero, C. A., Ichino, A., and Rustichini, A. (2020). Restarting the economy while saving lives under COVID-19. *SSRN Electron. J*. 1–5. doi: 10.2139/ssrn.3580626

Feil-Seifer, D., Haring, K. S., Rossi, S., Wagner, A. R., and Williams, T. (2020). Where to next? The impact of COVID-19 on human-robot interaction research. *ACM Trans. Hum. Robot Interact*. 10, 1–7. doi: 10.1145/3405450

Ferdous, M. Z., Islam, M. S., Sikder, M. T., Mosaddek, A. S. M., Zegarra-Valdivia, J. A., and Gozal, D. (2020). Knowledge, attitude, and practice regarding COVID-19 outbreak in Bangladesh: an online-based cross-sectional study. *PLoS ONE* 15:e0239254. doi: 10.1371/journal.pone.0239254

Forbes Staff (2020). *El Sena presenta un robot para atender pacientes contagiados de coronavirus–Forbes Colombia*. Forbes Colombia Magazine.

Garingo, A., Friedlich, P., Chavez, T., Tesoriero, L., Patil, S., Jackson, P., et al. (2016). "Tele-rounding" with a remotely controlled mobile robot in the neonatal intensive care unit. *J. Telemed. Telec*. 22, 132–138. doi: 10.1177/1357633X15589478

Goh, P. S., and Sandars, J. (2020). A vision of the use of technology in medical education after the COVID-19 pandemic. *MedEdPublish* 9, 1–8. doi: 10.15694/mep.2020.000049.1

Government of Canada (2020). *COVID-19 Pandemic Guidance for the Health Care Sector*. Available online at: https://www.canada.ca/en/publichealth/services/diseases/2019-novel-coronavirusinfection/health-professionals/covid-19-pandemicguidance-health-care-sector.html

Greenhalgh, T., Wherton, J., Papoutsi, C., Lynch, J., Hughes, G., A'Court, C., et al. (2017). Beyond adoption: a new framework for theorizing and evaluating nonadoption, abandonment, and challenges to the scale-up, spread, and sustainability of health and care technologies. *J. Med. Internet Res*. 19:e367. doi: 10.2196/jmir.8775

Guerra, J., Fabian, Y., and Gamba, S. (2020). *Dise˜no* de brazo robótico remoto para reducir crisis en el campo médico promoviendo el distanciamiento social en el

marco de la contingencia sanitaria del COVID-19. Universidad Santo Tomás. doi: 10.15332/dt.inv.2020.01258

Hebesberger, D., Koertner, T., Gisinger, C., and Pripfl, J. (2017). A long-term autonomous robot at a care hospital: a mixed methods study on social acceptance and experiences of staff and older adults. *Int. J. Soc. Robot*. 9, 417–429. doi: 10.1007/s12369-016-0391-6

Hjelm, N. (2005). Benefits and drawbacks of telemedicine. *J. Telemed. Telec*. 11, 60–70. doi: 10.1258/1357633053499886

Hu, J., Edsinger, A., Lim, Y. J., Donaldson, N., Solano, M., Solochek, A., et al. (2011). "An advanced medical robotic system augmenting healthcare capabilities-robotic nursing assistant," in *2011 IEEE International Conference on Robotics and Automation* (Shanghai: IEEE), 6264–6269. doi: 10.1109/ICRA.2011.5980213

IFRC Turkish Red Crescent (2020). *Knowledge, Attitudes and Practices (KAP) Assessment on COVID-19–Community Based Migration Programme, September 2020 [EN/TR]–Turkey | ReliefWeb*. Available online at: https://reliefweb.int/report/turkey/knowledgeattitudes-and-practices-kap-assessment-covid-19-community-based-migration

Ilias, B., Nagarajan, R., Murugappan, M., Helmy, K., Awang Omar, A. S., and Abdul Rahman, M. A. (2014). Hospital nurse following robot: hardware development and sensor integration. *Int. J. Med. Eng. Inform*. 6, 1–13. doi: 10.1504/IJMEI.2014.058521

Javaid, M., Haleem, A., Vaishya, R., Bahl, S., Suman, R., and Vaish, A. (2020). Industry 4.0 technologies and their applications in fighting COVID-19 pandemic. *Diabet. Metab. Syndr. Clin. Res. Rev*. 14, 419–422. doi: 10.1016/j.dsx.2020.04.032

Joost, C. F., and Dodou, D. (2010). Five-Point Likert Items: *t*-test versus Mann-Whitney-Wilcoxon. *Pract. Assess. Res. Eval*. 15, 1–16. doi: 10.7275/bj1p-ts64

Khan, Z. H., Siddique, A., and Lee, C. W. (2020). Robotics utilization for healthcare digitization in global covid-19 management. *Int. J. Environ. Res. Public Health* 17:3819. doi: 10.3390/ijerph17113819

Kirschling, T. E., Rough, S. S., and Ludwig, B. C. (2009). Determining the feasibility of robotic courier medication delivery in a hospital setting. *Am. J. Health Syst. Pharm*. 66, 1754–1762. doi: 10.2146/ajhp080184

Kovach, C. R., Taneli, Y., Neiman, T., Dyer, E. M., Arzaga, A. J. A., and Kelber, S. T. (2017). Evaluation of an ultraviolet room disinfection protocol to decrease nursing home microbial burden, infection and hospitalization rates. *BMC Infect. Dis*. 17:186. doi: 10.1186/s12879-017-2275-2

Krägeloh, C. U., Bharatharaj, J., Sasthan Kutty, S. K., Nirmala, P. R., and Huang, L. (2019). Questionnaires to measure acceptability of social robots: a critical review. *Robotics* 8:88. doi: 10.3390/robotics8040088

Kramer, A., Schwebke, I., and Kampf, G. (2006). How long do nosocomial pathogens persist on inanimate surfaces? A systematic review. *BMC Infect. Dis*. 6:130. doi: 10.1186/1471-2334-6-130

Macdonald, E. B. R. S. B. (2009). Acceptance of healthcare robots for the older population: review and future directions. *Int. J. Soc. Robot*. 1, 319–330. doi: 10.1007/s12369-009-0030-6

Mahdy, L. N., Ezzat, K. A., and Hassanien, A. E. (2018). "Integrated multi-sensor monitoring robot for inpatient rooms in hospital environment," in *International Conference on Advanced Intelligent Systems and Informatics* (Cairo: Springer), 117–126. doi: 10.1007/978-3-319-99010-1_11

Marra, A. R., Schweizer, M. L., and Edmond, M. B. (2018). No-touch disinfection methods to decrease multidrug-resistant organism infections: a systematic review and meta-analysis. *Infect. Control Hosp. Epidemiol*. 39, 20–31. doi: 10.1017/ice.2017.226

Maxon Motors Inc. (2020). *COVID-19: Drive Technology and Physical Distancing*. Available online at: https://drive.tech/en/streamcontent/covid-19-drive-technology-and-physicaldistancing

McGinn, C., Bourke, E., Murtagh, A., Donovan, C., Lynch, P., Cullinan, M. F., et al. (2020). Meet stevie: a socially assistive robot developed through application of a "design-thinking" approach. *J. Intell. Robot. Syst*. 98, 39–58. doi: 10.1007/s10846-019-01051-9

Meisenzahl, M. (2020). *Softbank-Backed Delivery Startup Rappi Is Testing Out Robots for Contactless Delivery—Take a Look*. Available online at: https://www.businessinsider.com/delivery-startupusing-robots-in-colombia-to-avoid-coronavirus-2020-4

Miner, H., Fatehi, A., Ring, D., and Reichenberg, J. S. (2020). Clinician telemedicine perceptions during the covid-19 pandemic. *Telemed. e-Health*. 1–48. doi: 10.1089/tmj.2020.0295

Murray, C., Ortiz, E., and Kubin, C. (2014). Application of a robot for critical care rounding in small rural hospitals. *Crit. Care Nurs. Clin*. 26, 477–485. doi: 10.1016/j.ccell.2014.08.006

Nayak, J., Balas, V. E., Favorskaya, M. N., Choudhury, B. B., Rao, S. K. M., and Naik, B. (Eds.). (2020). *Applications of Robotics in Industry Using Advanced Mechanisms, Volume 5 of Learning and Analytics in Intelligent Systems*. Cham: Springer International Publishing. doi: 10.1007/978-3-030-30271-9

Otter, J., Yezli, S., Perl, T., Barbut, F., and French, G. (2014). "A guide to no-touch automated room disinfection (NTD) systems," in *Decontamination in Hospitals and Healthcare* (Elsevier), 413–460. doi: 10.1533/9780857096692.2.413

Otter, J. A., Yezli, S., Perl, T. M., Barbut, F., and French, G. L. (2013). The role of 'no-touch' automated room disinfection systems in infection prevention and control. *J. Hosp. Infect*. 83, 1–13. doi: 10.1016/j.jhin.2012.10.002

Pandey, A. K., and Gelin, R. (2018). A mass-produced sociable humanoid robot: pepper: the first machine of its kind. *IEEE Robot. Autom. Mag*. 25, 40–48. doi: 10.1109/MRA.2018.2833157

Petelin, J., Nelson, M., and Goodman, J. (2007). Deployment and early experience with remote-presence patient care in a community hospital. *Surg. Endosc*. 21, 53–56. doi: 10.1007/s00464-005-0261-z

Podpora, M., Gardecki, A., Beniak, R., Klin, B., Vicario, J. L., and Kawala-Sterniuk, A. (2020). Human interaction smart subsystem—extending speech-based human-robot interaction systems with an implementation of external smart sensors. *Sensors* 20:2376. doi: 10.3390/s20082376

REACH (2020). *COVID-19 Knowledge, Attitudes and Practices (KAP) Survey: Northwest Syria–August–September 2020 (Round 4)–Syrian Arab Republic | ReliefWeb*. Available online at: https://reliefweb.int/report/syrian-arabrepublic/covid-19-knowledge-attitudes-and-practiceskap-survey-northwest-syria-4

Riek, L. D. (2017). Healthcare robotics. *Communications of the ACM* 60, 68–78. doi: 10.1145/3127874

Rincon, F., Vibbert, M., Childs, V., Fry, R., Caliguri, D., Urtecho, J., et al. (2012). Implementation of a model of robotic tele-presence (RTP) in the neuro-ICU: effect on critical care nursing team satisfaction. *Neurocrit. Care* 17, 97–101. doi: 10.1007/s12028-012-9712-2

Robotnik (2020). *The Importance of Collaborative Robotics in the Fight Against COVID-19*. Available online at: https://robotnik.eu/collaborative-roboticsin-the-fight-against-covid-19/

San-Juan, D., Ramos, C., Ximenez, C., Cruz-Reyes, L., Aguirre, E., Ramos, G., et al. (2020). *Guía para la realización de estudios de neurofisiología clínica durante la pandemia de COVID-19*. Available online at: https://www.acmfr.org/blog/comunicados/guia-parala-realizacion-de-estudios-de-neurofisiologia-clinicadurante-la

SENA (2020). *Investigadores e instructores del Sena crearon robot que ayuda al personal médico en la atención de pacientes con Covid-19*. Available online at: https://id.presidencia.gov.co/Paginas/prensa/2020/Investigadores-instructores-Sena-crearon-robot-que-ayudaal-personal-medico-en-la-atencion-de-pacientes-concovid-19-200430.aspx#:~:text=Investigadores%20e%20instructores%20del%20Centro,familia%20y%20personal%20de%20salud

Sermeus, W. (2016). "Robotic assistance in medication management: development and evaluation of a prototype," in *Nursing Informatics* (New York, NY), 422.

Shinohara, K. (2012). "A new approach for the design of assistive technologies," in *ACM SIGACCESS Accessibility and Computing* (New York, NY), 45–48. doi: 10.1145/2140446.2140456

Siciliano, B., and Khatib, O. (Eds.). (2016). *Springer Handbook of Robotics, 2nd Edn*. Cham: Springer International Publishing.

Smith, A. C., Coulthard, M., Clark, R., Armfield, N., Taylor, S., Goff, R., et al. (2005). Wireless telemedicine for the delivery of specialist paediatric services to the bedside. *J. Telemed. Telec*. 11, 81–85. doi: 10.1258/135763305775124669

SoftBank Robotics (2020). *COVID-19: Our Response and Actions*. Available onine at: https://www.softbankrobotics.com/emea/en/covid-19-our-response-and-actions

Stock, R. M., and Merkle, M. (2018). "Can humanoid service robots perform better than service employees? A comparison of innovative behavior cues," in *Proceedings of the 51st Hawaii International Conference on System Sciences* (Waikoloa Village, HI), 1056–1065. doi: 10.24251/HICSS.2018.133

Sucher, J. F., Todd, S. R., Jones, S. L., Throckmorton, T., Turner, K. L., and Moore, F. A. (2011). Robotic telepresence: a helpful adjunct that is viewed favorably by critically ill surgical patients. *Am. J. Surg.* 202, 843–847. doi: 10.1016/j.amjsurg.2011.08.001

Takahashi, M., Moriguchi, T., Tanaka, S., Namikawa, H., Shitamoto, H., Nakano, T., et al. (2012). Development of a mobile robot for transport application in hospital. *J. Robot. Mechatron.* 24, 1046–1053. doi: 10.20965/jrm.2012.p1046

Takahashi, M., Suzuki, T., Shitamoto, H., Moriguchi, T., and Yoshida, K. (2010). Developing a mobile robot for transport applications in the hospital domain. *Robot. Auton. Syst.* 58, 889–899. doi: 10.1016/j.robot.2010.03.010

Tavakoli, M., Carriere, J., and Torabi, A. (2020). Robotics, smart wearable technologies, and autonomous intelligent systems for healthcare during the COVID–19 pandemic: an analysis of the state of the art and future vision. *Adv. Intell. Syst.* 2:2000071. doi: 10.1002/aisy.202000071

The World Bank (2020). *World Bank Group and COVID-19 (Coronavirus)*. Available online at: https://www.worldbank.org/en/who-weare/news/coronavirus-covid19

Tonin, L., Carlson, T., Leeb, R., and Millán, J. R. (2011). "Brain-controlled telepresence robot by motor-disabled people," in *2011 Annual International Conference of the IEEE Engineering in Medicine and Biology Society* (Boston, MA: IEEE), 4227–4230. doi: 10.1109/IEMBS.2011.6091049

United Nations Development Programme (2020). *COVID-19 Pandemic: Humanity Needs Leadership and Solidarity to Defeat the Coronavirus*. Available online at: https://www.undp.org/content/undp/en/home/coronavirus.html

Vasileiou, K., Barnett, J., Thorpe, S., and Young, T. (2018). Characterising and justifying sample size sufficiency in interview-based studies: systematic analysis of qualitative health research over a 15-year period. *BMC Med. Res. Methodol.* 18:148. doi: 10.1186/s12874-018-0594-7

Viswanathan, R., Myers, M. F., and Fanous, A. H. (2020). Support groups and individual mental health care via video conferencing for frontline clinicians during the covid-19 pandemic. *Psychosomatics* 61, 538–543. doi: 10.1016/j.psym.2020.06.014

Wang, J., Wei, B., Zhang, Y., and Chen, H. (2009). "Design of an autonomous mobile robot for hospital," in *2009 IEEE International Symposium on IT in Medicine & Education*, Vol. 1 (Jinan: IEEE), 1181–1186. doi: 10.1109/ITIME.2009.5236275

White, P., Marston, H. R., Shore, L., and Turner, R. (2020). Learning from COVID-19: design, age-friendly technology, hacking and mental models. *Emerald Open Res.* 2:21. doi: 10.35241/emeraldopenres.13599.1

Wootton, R. (2001). Telemedicine. *BMJ* 323, 557–560. doi: 10.1136/bmj.323.7312.557

World Health Organization (2014). *Knowledge, Attitudes, and Practices (KAP) Surveys During Cholera Vaccination Campaigns: Guidance for Oral Cholera Vaccine Stockpile Campaigns "Working Copy"*. Technical Report June, World Health Organization.

World Health Organization (2020a). *Coronavirus Disease (COVID-19) Outbreak*. Available online at: http://www.euro.who.int/en/healthtopics/health-emergencies/coronavirus-covid-19

World Health Organization (2020b). *Strengthening and Adjusting Public Health Measures Throughout the COVID-19 Transition Phases*. Available online at: http://www.euro.who.int/en/healthtopics/health-emergencies/coronavirus-covid-19/technical-guidance/2020/strengthening-andadjusting-public-health-measures-throughout-thecovid-19-transition-phases.-policy-considerations-forthe-who-european-region,-24-ap

World Health Organization (2020c). *WHO Coronavirus Disease (COVID-19) Dashboard*. Available online at: https://covid19.who.in

Yang, G. Z., J. Nelson, B., Murphy, R. R., Choset, H., Christensen, H., H. Collins, S., et al. (2020). Combating COVID-19—the role of robotics in managing public health and infectious diseases. *Sci. Robot.* 5:eabb5589. doi: 10.1126/scirobotics.abb5589

Yang, J. H., Wu, U. I., Tai, H. M., and Sheng, W. H. (2019). Effectiveness of an ultraviolet-C disinfection system for reduction of healthcare-associated pathogens. *J. Microbiol. Immunol. Infect.* 52, 487–493. doi: 10.1016/j.jmii.2017.08.017

Conflict of Interest: The authors declare that the research was conducted in the absence of any commercial or financial relationships that could be construed as a potential conflict of interest.

frontiers in Robotics and AI

ORIGINAL RESEARCH
published: 09 June 2021
doi: 10.3389/frobt.2021.648485

A Computational Framework Towards the Tele-Rehabilitation of Balance Control Skills

*Kubra Akbas and Carlotta Mummolo **

Department of Biomedical Engineering, New Jersey Institute of Technology, Newark, NJ, United States

Mobility has been one of the most impacted aspects of human life due to the spread of the COVID-19 pandemic. Home confinement, the lack of access to physical rehabilitation, and prolonged immobilization of COVID-19-positive patients within hospitals are three major factors that affected the mobility of the general population world-wide. Balance is one key indicator to monitor the possible movement disorders that may arise both during the COVID-19 pandemic and in the coming future post-COVID-19. A systematic quantification of the balance performance in the general population is essential for preventing the appearance and progression of certain diseases (e.g., cardiovascular, neurodegenerative, and musculoskeletal), as well as for assessing the therapeutic outcomes of prescribed physical exercises for elderly and pathological patients. Current research on clinical exercises and associated outcome measures of balance is still far from reaching a consensus on a "golden standard" practice. Moreover, patients are often reluctant or unable to follow prescribed exercises, because of overcrowded facilities, lack of reliable and safe transportation, or stay-at-home orders due to the current pandemic. A novel balance assessment methodology, in combination with a home-care technology, can overcome these limitations. This paper presents a computational framework for the in-home quantitative assessment of balance control skills. Novel outcome measures of balance performance are implemented in the design of rehabilitation exercises with customized and quantifiable training goals. Using this framework in conjunction with a portable technology, physicians can treat and diagnose patients remotely, with reduced time and costs and a highly customized approach. The methodology proposed in this research can support the development of innovative technologies for smart and connected home-care solutions for physical therapy rehabilitation.

Keywords: telehealth, physical rehabilitation, balance assessment, margins of balance, balanced region, center of mass, balance perturbation, biped stability

OPEN ACCESS

Edited by:
S. Farokh Atashzar, New York University, United States

Reviewed by:
Selene Tognarelli, Sant'Anna School of Advanced Studies, Italy
Nick Obradovich, Max Planck Institute for Human Development, Germany

***Correspondence:**
Carlotta Mummolo
cmummolo@njit.edu

Specialty section:
This article was submitted to Biomedical Robotics, a section of the journal Frontiers in Robotics and AI

Received: *31 December 2020*
Accepted: *14 May 2021*
Published: *09 June 2021*

Citation:
Akbas K and Mummolo C (2021) A Computational Framework Towards the Tele-Rehabilitation of Balance Control Skills. Front. Robot. AI 8:648485. doi: 10.3389/frobt.2021.648485

INTRODUCTION

The COVID-19 pandemic and subsequent stay-at-home orders put in place have caused a general reduction in physical mobility among countries across the globe (World Health Organization, 2020a; World Health Organization, 2020b; World Health Organization, 2020c). The fundamentally altered daily routine of the healthy young, adult, and elderly populations has been preventing them from performing the usual daily motor exercise. A direct effect of home confinement is the alteration of

normal muscle activation during daily motion, which can cause muscular atrophy and other problems in motor function in otherwise healthy people of all ages. The negative impact that this reduction in mobility due to the COVID-19 pandemic has on muscles, neuromuscular junctions, and nerves has been especially stressed (Narici et al., 2020). As a secondary effect, the pandemic has made it particularly difficult for the pathological populations needing regular physical therapy and rehabilitation sessions to receive treatment. This can cause a deterioration of physical health in low-mobility patients, leading them to be more prone to falls and injuries (Visser et al., 2008; Levinger et al., 2017; Gandolfi et al., 2018). In addition, COVID-19 has also caused prolonged immobilization of patients within the hospital environment, leading researchers and medical professionals to brainstorm proper treatment protocols for these "secondary" mobility ailments (Iannaccone et al., 2020). The physical rehabilitation during this bedridden stage takes on passive and active modes, including resistance training and both static and dynamic balance training exercises (Iannaccone et al., 2020). In summary, sedentarism due to stay-at-home orders, lack of access to proper physical therapy, and prolonged immobilization during COVID-19-positive hospitalizations are the three main factors causing reduced mobility of various populations during COVID-19. These circumstances will continue to impact mobility in the medium/long term after the pandemic and motivate the need for alternative solutions for the delivery of physical therapy and rehabilitation in remote settings.

The use of telehealth and telerehabilitation can help counteract the above-mentioned challenges. Many benefits exist within switching to remote care: increased access to healthcare, reduction in overall cost, increased interaction with providers and patient engagement, the ability to provide both synchronous and asynchronous treatment, and the eventual generation of large datasets for broader scientific investigation and impact. Though many approaches to telemedicine currently exist (Ruiz et al., 2020; Seshadri et al., 2020), proper telemedicine for use in motor rehabilitation requires more functional components in combination with a computational framework that can systematically quantify specific aspects of motor performance, such as balance control skills.

Within the circumstances caused by the pandemic, there is a focus on restoring motor function in the following areas: deconditioning, strength, balance, and the ability to perform daily activities (Iannaccone et al., 2020). In particular, static and dynamic balance training must be performed to help restore the compromised postural stability due to the reduced exercise and exposure to proprioceptive stimuli (Iannaccone et al., 2020; World Health Organization, 2020b; World Health Organization, 2020c). Balance is influenced by many subsystems of the body (i.e., musculoskeletal, vestibular, ocular). This interconnectedness is why balance assessment within motor rehabilitation is critical to understanding the components of falling and how to prevent injury due to falls. Poor balance capabilities are among the leading causes for falls in the elderly (Visser et al., 2008; Levinger et al., 2017; Gandolfi et al., 2018), often resulting in limited mobility and reduced engagement in physical activities. Balance assessment methods are useful in helping practitioners determine the proper customized rehabilitation plan for their patients and allow researchers to develop better technology to conduct these assessments. Currently used methods range from subjective observations performed by medical professionals to more quantitative approaches, using medical devices specifically designed for computerized dynamic posturography (CDP) analysis. While many balance exercises are qualitatively designed and assessed in the clinical setting (e.g., Berg Balance Scale (Stevenson, 2001), Balance Error Scoring System (Bell et al., 2011), Activities Balance Confidence Scale (Raad et al., 2013), Y Excursion Balance Test (Kinzey and Armstrong, 1998), Star Excursion Balance Test (Glave et al., 2016)), the score subjectivity and variance across physical therapists can lead to inconsistencies in the rehabilitation outcomes. Furthermore, this qualitative approach is less feasible in a home-care setting, where the physical presence of a therapist is removed. Many clinics use CDP to determine a patient's progress based on a quantitative type of assessment. For example, the NeuroCom SMART Balance Master can score a user's performance through the sensory organization test of equilibrium and motor control test (Wagner et al., 2016). The sensory organization test evaluates postural stability under various sensory conditions, where the visual, proprioceptive, and vestibular senses are altered (Wagner et al., 2016; Olchowik and Czwalik, 2020). A final "equilibrium score" based on the center of gravity sway is associated to the sensory organization test to evaluate postural stability. Additionally, the motor control test uses a "latency score" to quantify the user's postural response time in reaction to platform perturbations (Wagner et al., 2016).

Although the existing CDP devices are considered to be the best currently available technologies, these machines are too costly and substantial in size for in-home use, and they require a trained clinician to supervise the machine setup and operation. Technologies for home care rehabilitation must be portable, compact, and must have a user-friendly interface so that the general patient can operate the device with minimal training. Commercial balance training technologies aimed for the home environment are typically presented as "exergames" (exercise games), which utilize the body's motion as a method of controlling gameplay and were developed to encourage activity through fun activities. For example, Wii Fit uses the body's weight distribution on the balance board as a proxy indicator of balance (Wikstrom, 2012); the Kinect's balance training games, based on body motion tracking, can provide a low-cost and accessible form of rehabilitation (Sápi et al., 2019); Neofect's Smart Balance technology uses virtual environments and other visualizations to aid in stroke recovery by measuring center of pressure (COP), center of mass (COM), pressure distribution, and the traveled path during walking (Neofect, 2020); the Togu Challenge Disc made by MFT Bodyteamwork uses games and visual targets to train balance and tracks the general motion of the user (MFT Bodyteamwork, 2020); the Boditrak2 Balance Assessment System also uses games to assist with training and tracks balance through pressure mapping. These platforms have been proposed as portable solutions for increasing physical activity and for balance assessment and training (Kennedy et al., 2011; Goble

et al., 2014; Sápi et al., 2019). However, they have limitations in both their technology (e.g., sensor quality, resolution, processing power) and assessment approach (e.g., simple tracking of body motion and pressure distribution as proxies for the evaluation of balance control). Research efforts are being made to develop more accurate portable and wearable technologies for quantitative balance assessment (Conforti et al., 2020; Torricelli et al., 2020) by including, for instance, inertial measurement units or electromyographic devices (Zampogna et al., 2020).

The limitations on the CDP and exergames technologies prevent simultaneous balance assessment and training from being properly performed at home. Specifically, existing assessment metrics and testing protocols need to be improved to better understand the mechanisms that affect postural control (Keshner and Fung, 2019). The theoretical/computational framework employed in any given technology to quantify rehabilitation outcomes must be both specific and comprehensive enough to capture the balance skills across multiple subjects and multiple exercises. At the same time, the systematic outcomes evaluation must not be too computationally intensive. Current balance assessments focus on selected specific measures, which provide only partial information on human balance control and may omit important components of balance related to the risk of falls (Sibley et al., 2015). Few specific indicators are typically captured in CDP or exergames (i.e., reaction time, movement velocity, endpoint excursion, COM and COP sway), whose deviation from a baseline only partially and indirectly characterizes the balance control ability of a subject (Chaudhry et al., 2004; Ganesan et al., 2015). Each of these mechanical indicators alone do not capture the state of balance of a system (i.e., whether the subject is balanced or not) nor do they characterize the overall capability of the subject to recover from general perturbations. As a result, the perspectives of quantification of human balance have not yet reached a golden standard (Sibley et al., 2015) and identifying a comprehensive set of quantifiable and customized targets for balance rehabilitation remains a challenge. Furthermore, the existing assessment metrics and technologies pose a limit to the type of movements that can be analyzed. In typical CDP protocols, movements are restricted to the device's narrow platform and postural stability is assessed during periods of quiet standing (Glave et al., 2016). While numerous stability analyses have been proposed during general movements (e.g., sit-to-stand (Holmes et al., 2020), walking (Young et al., 2012), stair climbing (Herman et al., 2009), etc.), these have not been translated into a unified approach for the design of exercise protocols (and associated technology) involving multiple motor tasks. Assessment sessions typically analyze balance during the upright standing posture (postural stability) and tend to be independent from the physical therapy training sessions, which usually involve different types of dynamic motor tasks (Bayouk et al., 2006; Marioni et al., 2013; Levinger et al., 2017). For effective rehabilitation, assessment and training protocols should be simultaneously performed and combined into a unified technology-based framework for a broad range of balance exercises with quantifiable custom targets.

Recent studies have addressed the limited scope of quantification of existing balance assessment methods by addressing the stability of biped systems from a dynamic system perspective. In this context, balance is defined as the ability to maintain the state of a dynamic system inside a defined desired region of the state space (Pratt et al., 2017). The quantification of balance capabilities consists in the evaluation of a balanced region in the state space (Mummolo et al., 2017), also called basin of attraction or viability kernel (Aubin et al., 2011; Koolen et al., 2012; Zaytsev et al., 2015; Smith et al., 2017). The resulting balance stability criterion is a threshold that can discriminate between the conditions of balance and imbalance of a given biped system (Koolen et al., 2012; Mummolo et al., 2017; Koolen, 2019) by considering all possible factors that could lead to a loss of balance. These are more comprehensive approaches for monitoring the state of balance of a system and predicting fall, as opposed to tracking individual balance-related indicators. Furthermore, they can be generalized to various movements and translated into a broader range of static and dynamic exercise goals for simultaneous balance assessment and training.

In this study, a state-space balance criterion (Mummolo et al., 2017) is used to formulate metrics of balance that can serve as quantitative outcomes, as well as customized goals for the simultaneous assessment and training of balance control skills. This computational framework can be customized for a given patient in a rehabilitation regimen that involves multiple motor exercises. The evaluation of the proposed balance performance metrics relies on computational models of the human subject and associated balanced regions and requires capturing the subject's COM motion and foot stance during the performed balance exercise. Based on these requirements, the proposed framework has the potential to be integrated with an affordable portable technology solution for customized tele-rehabilitation needs, in which the novel performance metrics can be evaluated on- and off-line to visually guide the patient during the balance exercises. The outcome of this research can contribute to tackling the issue of compromised mobility and motor performance of people living at the time of the COVID-19 pandemic.

SIMULTANEOUS BALANCE ASSESSMENT AND TRAINING METHOD

A computational framework is proposed in which novel balance performance measures are formulated and implemented in exercises for simultaneous balance assessment and training. The use of the balance performance measures is twofold: 1) they are used as quantitative outcomes for general balance assessment and 2) they define customized and quantifiable balance training goals across multiple exercises. This novel rehabilitation paradigm requires the integration of the following components: 1) the theoretical formulation of the novel balance performance measures, 2) the design of exercises for which the balance performance is quantified, 3) a computationally tractable model of the user (human subject).

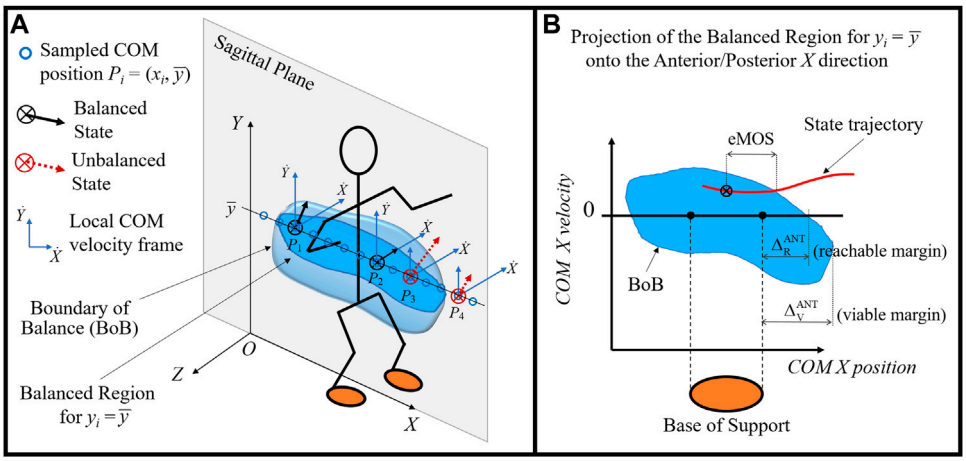

FIGURE 1 | (A) Illustration of the balanced region concept (blue volume) and its boundary (BoB) in the sagittal plane of a biped system. At each sampled COM position (circles), the maximum feasible range of COM velocitiy perturbations are calculated and shown with respect to local velocity frames. Examples of balanced states at positions P_1 and P_2 and unbalanced states at positions P_3 and P_4 are shown, whose COM velocities fall inside and outside of the BoB, respectively. **(B)** The BoB is projected onto the $(X, \dot{X})$ plane to illustrate the concepts of viable and reachable boundary margins and their relationship with the base of support. The instantaneous state margin (eMOS) is also illustrated.

Theoretical Formulation of Balance Performance Measures

A stability criterion based on the concept of balanced regions in the COM state space (Mummolo et al., 2017) is adopted in this study for the formulation of two categories of balance performance measures. This criterion uses nonlinear optimization for the numerical construction of a balance threshold in the state space of biped systems; it can be applied to general bipeds in various stance configurations, as well as to generic three-dimensional dynamic motor tasks.

The *balanced region* is the set of all possible COM balanced states from which a given subject can reach an upright rest state, while avoiding a change in foot stance (Mummolo et al., 2017). The *balance stability criterion* states that a COM state located within the balanced region, i.e., balanced state, is the necessary condition for dynamic balance in generic biped models (Mummolo et al., 2017). A COM state outside of this region is defined as unbalanced and it predicts an inevitable change in foot stance at some time in the future. The boundary of the balanced region, called *boundary of balance* (BoB), represents the maximum limits of balance recovery of a subject while maintaining a given foot stance and is quantified in terms of maximum feasible range of COM velocity perturbations. The BoB is formed by the COM velocity extrema (minimum and maximum) calculated iteratively at various COM sampled positions, P_i, $i = 1, \ldots, N$, and along any specified direction; hence the balanced region is a partition of the six-dimensional state space of COM Cartesian position and velocity. For practical analysis and visualization, the BoB can be evaluated for a specified plane (e.g., sagittal plane) and projected onto a single direction of interest (e.g., anterior/posterior) (**Figure 1**).

The BoB is generated numerically by solving a series of constrained optimization problems. For each sampled COM initial position P_i, optimization finds the limiting balance recovery trajectories in the joint space that drive the biped system from its extreme initial conditions (i.e., sampled COM initial position and minimum/maximum COM initial velocity) to a rest state, without a change in foot stance. The extremized COM initial state of each trajectory solution represents a point of the BoB. From any point of the BoB, there exists at least one controlled trajectory from which the subject can reach upright quiet stance without changing contacts. Alternatively, if the optimization finds no solution at a given P_i, the feasible range of COM initial velocity that guarantees the COM will return to a stationary upright position without altering foot stance is null; in this case, any COM state at that specified P_i is unbalanced, i.e., outside of the BoB. The balancing trajectories generated from each point of the BoB satisfy the following constraints: 1) a final rest state (e.g., upright static posture), 2) various system and physics constraints (e.g., joint and torque limits, COP constraints), and 3) the preservation of the original stance (i.e., base of support). The resulting BoB is a stance-specific threshold that is customized using subject-specific body and joint parameters in the modeling, capturing the balance capabilities of a subject as predicted by the model. Details of the numerical optimization algorithm and its solution via sequential quadratic programming can be found in previous work (Mummolo et al., 2018b). The construction method of the balance threshold has been demonstrated for the study of gait and posture stability of human, robot, and exoskeleton systems (Mummolo et al., 2017; Mummolo et al., 2018a; Mummolo et al., 2018b; Mummolo and Vicentini, 2020; Mummolo et al., 2021).

In this study, the BoB is constructed point by point, by calculating the feasible range of COM velocity at various COM positions P_i sampled in the sagittal plane at a selected COM height, i.e., $P_i = (x_i, \overline{y})$ (**Figure 1A**). The COM initial velocity is extremized along the anterior/posterior direction of interest (X)

and the BoB results into the following set of limiting COM initial conditions in the sagittal plane: $(x_i, \overline{y}, \dot{x}_{i,\mathrm{lim}}^{\mathrm{ANT/POS}}, \dot{y}_i^{\mathrm{ANT/POS}})$, for $i = 1{-}N$. The three-dimensional BoB can then be projected onto the state space of COM X position and velocity (**Figure 1B**) for practical analysis.

Two categories of balance performance metrics are formulated in the COM state space, based on the balanced region concept described above:

1) *Boundary Margins* are numerical indicators that characterize the dimension of a balance region relative to the base of support (**Figure 1B**). These indicators include the reachable (Δ_R) and viable (Δ_V) boundary margins, which quantify the capability of a subject in a given stance to recover from internal and external perturbations, respectively, along a specified direction. Similar to the balanced region, both boundary margins do not depend on a specific motor task but are a property of the selected models for both the subject's body and the desired stance configuration.

The reachable boundary margin Δ_R is the distance between the point of the BoB with zero velocity and the edge of the base of support, measured in both anterior and posterior directions. It predicts how far the body can displace its COM outside of the footprint and then invert its motion (hence, zero velocity) to recover balance without any external impulse or change of contact. This margin identifies a limit to the amount of self-induced perturbations (i.e., internal) that a subject can sustain from a given stance; hence it is analogous to a maximum voluntary COM sway in dynamic conditions (i.e., out of the base of support (Mummolo et al., 2013)).

The viable boundary margin Δ_V is the distance between the point of the BoB with maximum COM position and the edge of the base of support, measured in both anterior and posterior directions. It quantifies the range of COM positions outside of the footprint for which a feasible COM velocity exists. The balanced states included in between the reachable and the viable margins cannot be attained through the body internal dynamics alone, but they are viable initial conditions resulting from an external impulse. Therefore, the viable margin identifies a limit to the amount of externally induced perturbations that a subject can sustain while in a given stance.

2) *State Margins* are numerical indicators that characterize the instantaneous state of balance for a given trajectory, by measuring its relative distance to the BoB. Depending on how this distance is measured in the state space, these indicators can include position, velocity, or mixed margins. In this study, the extended Margin of Stability (eMOS) (Mummolo et al., 2021) is used as a position margin that quantifies the distance from a given state to the BoB along the position coordinate of the state space (**Figure 1B**). The eMOS is equivalent to the Margin of Stability (MOS) for a linear inverted pendulum (LIP) model (Hof et al., 2005; Mummolo et al., 2021), but it can be applied to any generic biped system. This indicator, unlike the boundary margin, is specific to the motor task performed by the subject in a given stance, allowing for the continuous evaluation of the COM state of balance.

Design of Balance Assessment and Training Exercises

The application of the balanced region and balance performance measures within the rehabilitation context is presented. The two categories of balance performance measures are used as design criteria for rehabilitation exercises in which balance performance is simultaneously quantified and trained. For a given subject and foot stance, the balanced region and boundary margins predicted by the optimization-based algorithm provide a reference map for defining customized target states across multiple exercises.

The intersections of the BoB with the edges of the base of support and the boundary margins in both anterior and posterior directions identify three partitions of the balanced region (**Figure 2**):

1) The portion of the balanced region characterized by a COM ground projection within the edges of the base of support (Mummolo et al., 2013) is the set of statically balanced states: a state in this partition can be driven to a static equilibrium configuration by controlling the COP position within the given base of support and/or through the regulation of whole-body linear and angular momentum. From a statically balanced state the motion could in theory be stopped instantaneously without causing the system to lose balance.

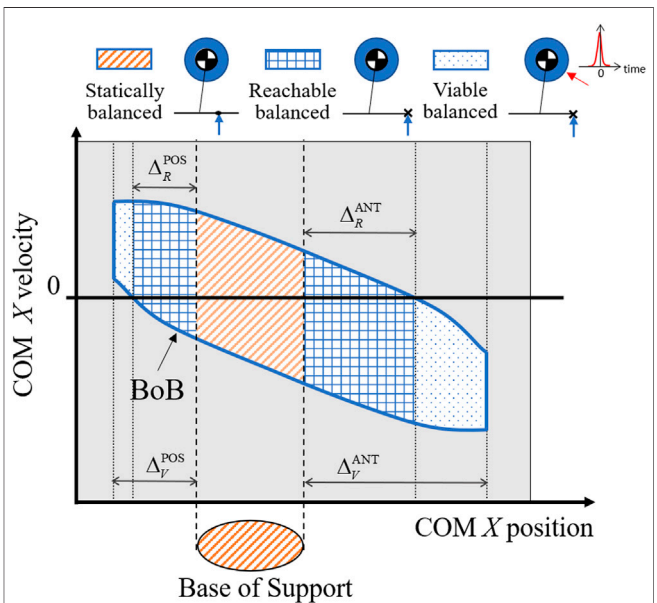

FIGURE 2 | The reachable and viable boundary margins in both the anterior (ANT) and posterior (POS) directions divide the balanced region into three partitions, each identifying a type of balanced states: statically, reachable, and viable balanced states. For each type of balanced state, an illustration of the corresponding balance control strategy is shown using a simple legged system with a point mass, flywheel, and foot link.

2) The portion of balanced region included within the reachable margins is the set of reachable balanced states: each of these states has a COM position outside of the footprint, hence is dynamically balanced. Because this partition contains both positive and negative COM velocity, the COM can enter it from a statically balanced state using internal dynamics and then invert its motion to recover balance. Balance recovery from reachable balanced states is only possible through the rotation of multiple body segments about the COM that generates a stabilizing angular momentum and its derivative, similar to the effect of a flywheel. Within this partition, the COP cannot be controlled and balancing must rely on a combination of favorable (i.e., balanced) COM initial conditions and whole-body inertial effects over a finite interval of time.
3) The portion of balanced region characterized by COM positions that are outside of the reachable margins, but within the viable margins, is the set of viable balanced states: similar to the reachable states, they are also dynamically balanced and must rely on favorable initial conditions and whole-body inertial effects in order to reach a static equilibrium within a finite interval of time. The difference from reachable states is that the system's COM can enter this partition only through externally imposed perturbations, e.g., external impulse. However, once the COM state is inside this partition (i.e., it becomes viable) the external push can cease and the system in the given stance can recover balance by means of its initial conditions and actuation capacity.

The above partition-based analysis of the balanced region provides a reference map that characterizes the different stability nature and means of control for a COM state within each partition (**Figure 2**). Statically, reachable, and viable balanced states are three categories of exercises targets that can be assigned to the subject's COM during a rehabilitation exercise. The amount of sustainable perturbations and recovery strategy associated with each target category is known a priori; this constitutes a novel approach to the design of balance exercise as compared to traditional balance perturbation experiments, in which there is no a priori knowledge of the effects of a given perturbation on the COM stability, hence no clear and meaningful balance target can be established.

Two types of balance exercises (perturbation-based and motor task-based) are proposed in which the requirements of a desired user's motion are imposed in terms of COM initial, target, and final states. For each exercise, the final state is a statically balanced state, while the initial and target states are assigned to the different partitions of the balanced region, based on the exercise desired outcome. In addition, each exercise has a prescribed foot contact (or sequence of contacts), used to evaluate the associated contact-dependent balanced region.

The first type of balance exercise consists in perturbation experiments guided by target states placed progressively closed to the boundaries of the balanced region (i.e., the BoB) (Targets A and B, **Figure 3**). This exercise has the purpose of determining the amount of internal and external perturbations that can be attained by the subject in experimental conditions (i.e., experimental reachable and viable margins), where internal perturbations are the impulses generated by the subject when initiating or performing a movement, whereas external perturbations require the impulse generated through contact with another object, such as pushing off from a wall or the ground. The experimental boundary margins are then compared with the exercise targets, i.e., the margins predicted by the simulated numerical boundary (i.e., numerical boundary margins).

Two examples of perturbation-based balance exercises during standing posture are described:

1) Example training exercise to reject internal perturbations from upright stance—Starting from rest, the subject is asked to initiate a forward/backward motion, come as close as possible to reachable Target A, and then invert its motion to reach a final rest state, all while maintaining a double stance configuration. Experimental reachable margins resulting from this exercise are quantified as the maximum anterior/posterior position reached by the subject's COM before inverting its motion. The experimental and numerical reachable margins are compared to have a relative measure of the subject's maximal COM sway capacity along a specific direction.
2) Example training exercise to reject external perturbations from upright stance—Starting from rest, the subject is asked to perform a pre-balancing task in which the COM should attain initial conditions as close as possible to viable Target B using the external impulse generated, for instance, by a hand-push on a fixed handle. The subject's state at the end of the push-off motion is recorded as the initial viable state of the balancing motion, which will terminate at upright equilibrium with no change in foot stance. The most extreme viable initial state that can be successfully attained by the subject gives the experimental viable margin, which is compared with the numerical counterpart to have a relative measure of the subject's limits of recovery from external perturbations.

This first type of perturbation-based exercises aims at simultaneously quantifying and training the general perturbation rejection capability of a subject relative to a given stance. Using the reference map, specific portions of the balanced region can be targeted for a given patient, to enhance a particular type and direction of balance control.

The second type of balance exercise is specific for a motor task and focuses on quantifying the balance performance of a specific trajectory. Multiple target states are assigned either inside or outside (e.g., Target C, **Figure 3**) of the BoB, as via-points of a desired motor task placed at selected distances from the boundary as quantified by the state margin eMOS. Throughout the exercise, the state margin is also utilized to quantify a subject's instantaneous level of balance/imbalance. As the subject's COM state trajectory remains within the boundary (i.e., balanced), the resulting eMOS values are positive, while states that exit the boundary result in negative eMOS values, leading to an inevitable foot contact change in the future. Given the general applicability of the BoB, the motor tasks for this type of exercise can be selected among common daily lives activities, including standing, frontal and lateral stepping, walking, and sit-to-stand actions.

In summary, the boundary and state margins are used in the proposed exercises as balance targets relative to the overall subject's

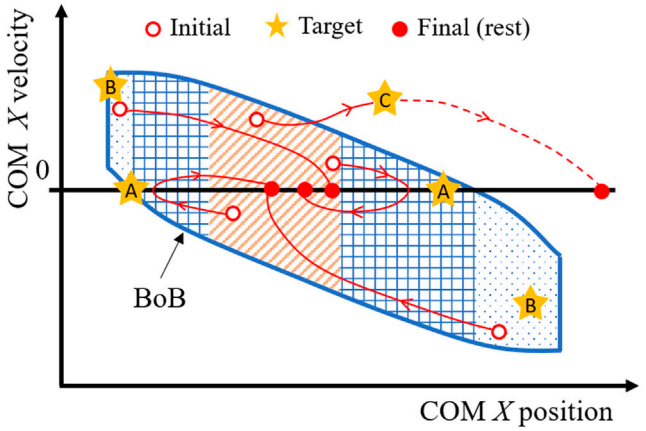

FIGURE 3 | Design of motor task for balance exercises (perturbation-based and motor task-based), where the COM is guided through initial, target, and final states. Targets A are selected progressively close to the reachable boundary margin, to find the experimental maximum COM sway of a given subject, i.e., the capacity of withstanding internal perturbations. Targets B are selected progressively close to the viable boundary margin, to find the experimental limits of external perturbations that a subject can withstand. Targets C are selected to drive a motor task at a known distance either inside or outside of the BoB and determine in real time the instantaneous state margin throughout the motion.

balance capabilities quantified by the balanced regions. At the same time, the experimental boundary/state margins are evaluated as balance performance outcomes of a given exercise and compared to the respective numerical values predicted by the model, to assess a patient's relative level of balance performance in a given stance and during a specific motor task, respectively.

When implementing these exercises within tele-rehabilitation settings, the desired and current COM state and foot stance information must be recorded and visualized by the patient. The patient's COM motion can be captured by existing methods (Lafond et al., 2004) and will be visually guided by targets prescribed within the different partitions of a balanced region (i.e., statically balanced, reachable, and viable). Meanwhile the COM state and foot stance information can be displayed as an overlay on the subject's balanced region. This would allow the patient and the physician to receive visual feedback on their balance performance during the exercises, in which a change in foot stance and/or a COM state crossing the BoB will signal an unbalanced motion. Additionally, the physician (remotely) could adjust the initial, final, and target states with respect to the balanced region maps, according to the patient's training status and needs.

Human Subject Modeling Approach

The theoretical/computational framework described above can be applied to any generic human body model, ranging from whole-body (Mummolo et al., 2019) to reduced-order (Mummolo et al., 2015b) biped mechanisms, and to various contact configurations between the feet and the environment (Mummolo et al., 2018b). The balance criterion and performance indicators can therefore be implemented in a broad range of balance rehabilitation protocols, including static, dynamic, and multi-stance exercises.

The construction of a subject's BoB via the optimization-based algorithm previously described requires the establishment of the dynamic model of the subject's body. Links' length and mass distribution, joint strengths and range of motions, ground contact modeling, and stance-specific constraints are specified and the subject's dynamics can then be described using common robotic modeling approaches for floating-base robotic systems with multiple degrees-of-freedom (DOF) (**Figure 4A**). The dynamics and stability of systems in multi-contact stances is usually more challenging to describe (Del Prete et al., 2018; Orsolino et al., 2020), given the indeterminacy in the system's foot reactions when the legs form a closed loop with the ground (Mummolo et al., 2015a). Different modeling choices (e.g., number of DOF, single vs. double stance, planar vs. three-dimensional) lead to different BoB and balanced regions. The complexity of the established biped model should reflect a good balance between the accuracy in the numerical prediction of the subject's balanced region and the computational performance of the BoB algorithm. In practice, when a balance region is sought for a specific motor task, a task-oriented modeling approach can be pursued for higher computational efficiency. Depending on the motor task requirements of a given exercise (e.g., range of desired COM displacement, anatomical plane and direction of interest, and expected foot contacts), the simplest model that fits those criteria should be selected.

In this study, balance exercises during standing posture are considered for demonstration purposes, which are characterized by a symmetric double stance, small variation of COM height, and significant COM perturbations in the sagittal plane along the anterior/posterior direction. Three increasingly complex models of human body that satisfy the exercise requirements are implemented in the balance assessment framework: a 1-DOF linear inverted pendulum (LIP) model, with a single mass and a flat foot (**Figure 4C**); a 4-DOF model with upper and lower body segments and a rigid foot (i.e., without metatarsal joint; **Figure 4B**); a 5-DOF model with upper and lower body segments and a two-link foot (i.e., with metatarsal joint; **Figure 4B**). All three models are in the sagittal plane and are reasonable candidates to analyze dynamic balance in the anterior-posterior direction. The balanced regions and their margins provide a systematic approach to evaluate the effects of each modeling assumption on the predictive capability of the model's balance stability. An accurate model would result in a balanced region that encompasses all experimental COM state trajectories resulting from the exercises in which balance is preserved.

DEMONSTRATIVE RESULTS AND DISCUSSION

The novel paradigm for simultaneous balance assessment and training is demonstrated with the results of balanced regions and balance performance measures calculated for different models of human standing posture. Experimental balance recovery trajectories extracted from published literature (Patton et al., 1999) are used to exemplify the proposed perturbation-based and motor task-based exercises and associated margins calculation.

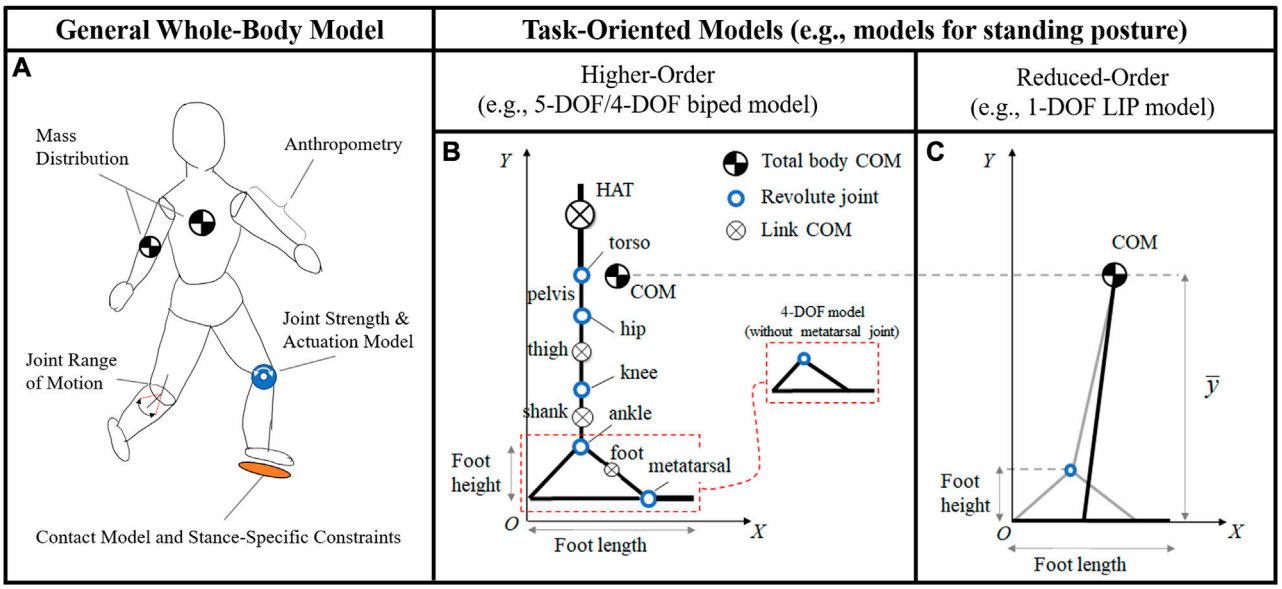

FIGURE 4 | (A) General human body models take into consideration individual anthropomorphic parameters, joint strengths and actuations, mass distributions, range of motions, ground contact modeling, and stance-specific constraints. Whole-body models are valid for the representation of any general motor task, although their simulation can be computationally intractable. In practice, task-oriented models can give a practical computation of the balanced region for the specific task considered. For balance stability during standing posture, both higher- and reduced-order models in the sagittal plane can be established. The higher-order models **(B)** include more detailed subject-specific parameters at the link and joint level, upper and lower body segments, as well as multi-segment feet (5-DOF model), as described in previous work (Mummolo and Vicentini, 2020). The LIP model **(C)** constrains the motion of the COM at a fixed height $\bar{y}$, equal to the *Y*-coordinate of the body's COM while standing and does not include joint-level design parameters.

Nondimensional Balanced Regions and Boundary Margins for Standing Posture

The balanced region results are presented for three increasingly complex models of a human subject in the sagittal plane, i.e., the LIP, 4-DOF, and 5-DOF models, to illustrate the effects of body and foot modeling choices on the predicted range of allowable perturbations during standing posture (**Figure 5A**). The anthropometric parameters and joint angle/torque limits of the reference subject are from the literature (Winter 2005; Mummolo and Vicentini, 2020). The LIP and the 4-DOF models have a rigid foot link with no metatarsal joint, which is assumed to maintain a fixed contact with the ground at all times; the 5-DOF model includes a two-link foot, where a metatarsal joint and a multimodal foot-ground interaction model (Mummolo et al., 2021) allow the foot to rotate about its heel and metatarsal. All models have a total foot length $fl = 0.23$ m.

For the higher-order models, the BoB is numerically constructed using the proposed algorithm. The COM velocity extrema are calculated along the anterior ($+X$) and posterior ($-X$) direction, by sampling the COM initial positions at a constant height $\bar{y} = 1.12$ m, corresponding to the subject's COM *Y*-coordinate in the upright standing configuration. The BoB of the LIP model can be found analytically using the linear inequalities that limit the position of the extrapolated center of mass ($XCoM = x + \dot{x}/\omega$) within the base of support $[0, fl]$ (Mummolo et al., 2021), i.e., $-\omega x \leq \dot{x} \leq -\omega x + fl\omega$, where x and $\dot{x}$ are the COM position and velocity, respectively, $\bar{y}$ and $\omega = \sqrt{g/\bar{y}}$ are the pendulum's length and natural frequency.

Fitted models of the BoB and enclosed balanced regions are obtained in the nondimensional COM state space for each of the three biped models considered (**Figure 5B**), where the COM position and velocity are normalized with respect to fl and $fl\omega$, respectively. The nondimensional formulation of the BoB provides a general characterization of the balanced regions for upright standing posture in three different subject modeling approaches. These nondimensional linear models can used for multiple individuals, with different anthropometric parameters, when adopted in a home-care rehabilitation context.

The three balanced regions are representative of the different balance control strategies that can be employed by each biped model. This is demonstrated quantitatively through the calculation of the nondimensional boundary margins (**Table 1**), which give a relative measure of maximum balanced COM displacement as a percentage of foot size. The only means of balance control for the LIP model is the regulation of the COP within the limits of its flat foot; as a result, the LIP reachable boundary margins are zero, indicating that the COM sway cannot exceed the base of support in order to preserve balance, according to this reduced-order model predictions. In addition, the linear inequalities for the *XCoM* do not provide limits to the range of feasible COM positions, therefore the LIP viable margins are undefined. On the other hand, the higher-order models show a greater range of sustainable COM velocity perturbation for a given COM position and along both anterior and posterior directions. The 4-DOF and 5-DOF models have posterior reachable boundary margins equal to 11 and 28.8% of the foot size, respectively, predicting that the COM sway can

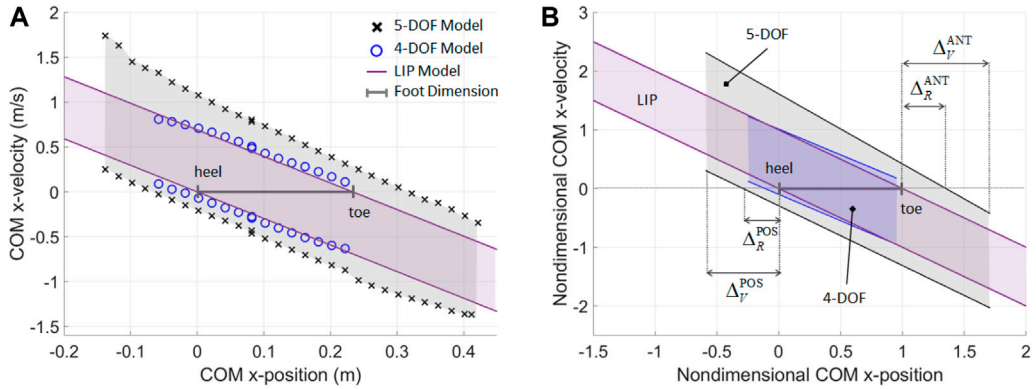

FIGURE 5 | (A) Numerical construction of the BoB for a reference subject in upright stance, when the subject's body is modeled with a 5-DOF mechanism with a two-link foot, a 4-DOF mechanism with a rigid foot, and a 1-DOF LIP with flat foot. **(B)** Nondimensional fitted lines provide a general model of BoB for the three types of biped mechanism considered ($R^2 > 0.99$). The nondimensional upper and lower BoB limits are $-x \leq \dot{x} \leq -x + 1$ (LIP), $-0.89x - 0.099 \leq \dot{x} \leq -0.88x + 1.01$ (4-DOF), and $-1.02x - 0.29 \leq \dot{x} \leq -1.19x + 1.61$ (5-DOF).

TABLE 1 | Anterior (ANT) and posterior (POS) nondimensional boundary margins of the general linear models of BoB calculated for the reduced- and higher-order body models.

	Reachable boundary margin		*Viable boundary margin*	
	Δ_R^{POS}	Δ_R^{ANT}	Δ_V^{POS}	Δ_V^{ANT}
5-DOF MODEL two-link foot	0.288	0.352	0.591	0.808
4-DOF MODEL rigid foot	0.110	−0.047	0.248	−0.047
LIP MODEL rigid foot	0.0	0.0	n.a.	n.a.

exceed the rear edge of the base of support while retaining the ability to invert its motion thanks to angular momentum inertial effects. The posterior viable margins in both higher-order models quantify the range of viable negative COM positions at which an external impulse can be applied to stabilize the system. The anterior reachable margin for the 5-DOF model predicts that the COM sway can exceed the front edge of the base of support by 35.2% of foot size, and then recover balance. The negative values for the anterior boundary margins in the 4-DOF model indicate that the set of reachable and viable balanced states is null in the anterior direction, due to the kinematic restrictions of a rigid foot, which do not allow significant COM displacement at the given COM height $\overline{y}$.

The greater perturbation rejection capability predicted by the higher-order models is due to the multiple balancing strategies that can be employed by a multi-DOF system (e.g., ankle, hip, upper-body, and general angular momentum regulation) in addition to COP control. In particular, the largest boundary margins are for the 5-DOF model, due to the presence of a two-link foot that enables the additional balancing strategy of heel-to-toe foot rocking, which increases the range of feasible COM positions and velocity perturbations.

The above boundary margins values predicted by the three models of human posture can be used as both targets and outcomes in COM perturbation experiments in tele-rehabilitation settings, to simultaneously assess and train a subject's overall balance performance ability to reject internal and external perturbations.

Use of Boundary and State Margins during Balance Exercises

To showcase the role of boundary margins in a balance rehabilitation exercise, empirical data relative to push recovery exercises published in the literature (Patton et al., 1999) is partially extracted and adapted to the proposed framework. In the experiments of the reference study (Patton et al., 1999), subjects were asked to pull on a horizontal handle, targeting various percentages of their maximum pulling force in order to attain perturbed COM initial conditions in the posterior direction. At the end of the pull, the balancing trajectories of the subjects' COM as they recovered balance while standing on two feet were recorded. It should be noted that, although derived from a different study, the experimental data illustrated is the result of perturbation-based balancing exercises analogous to those proposed in this framework, with the difference that the experiments in (Patton et al., 1999) are guided by force-based targets, while the proposed experiments would be conducted using the viable and reachable margins as novel balance-related targets.

Here, 35 perturbed COM states for one subject of the reference study are extracted, normalized, and represented against the nondimensional balanced regions (**Figure 6A**). The most

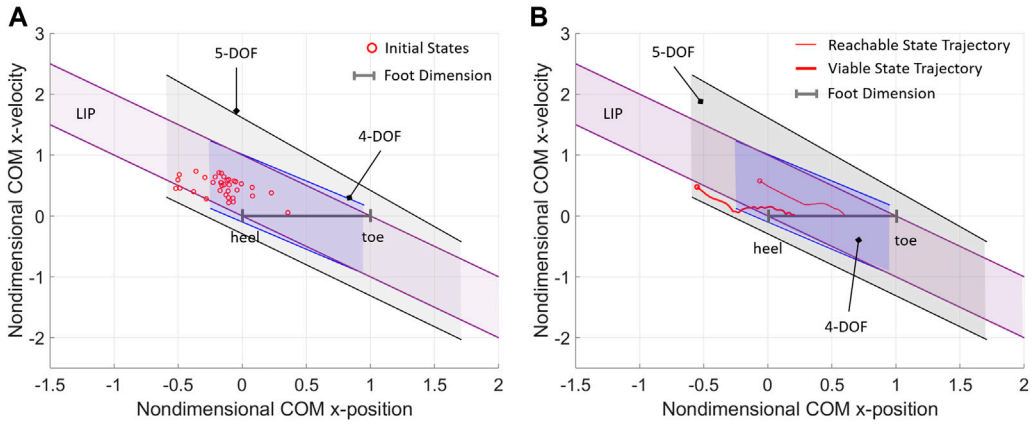

FIGURE 6 | (A) A collection of initial states of a subject during externally-imposed perturbation experiments (Patton et al., 1999), compared with the nondimensional models of balanced region for standing posture. **(B)** Two experimental balance recovery trajectories extracted from (Patton et al., 1999), where the subject standing on two feet recovers balance and reaches static equilibrium after receiving an external impulse the subject standing on two feet recovers balance and reaches static equilibrium after receiving an external impulse.

extreme COM initial state is used to estimate the subject's experimental viable margin in the posterior direction (0.519), which is closely predicted by the posterior viable margin of the 5-DOF model (0.591). The 4-DOF posterior viable margin fails to enclose eight highly dynamic initial states, hence the model underestimates the subject's balance performance in terms of rejection of external perturbations. Four initial states are either outside or on the boundary of the LIP balanced region; while this indicates that the reduced order model predicts balance in about 88% of the selected initial states, it should be noted that the LIP analytical boundaries did not provide quantifiable target viable states. These results demonstrate how the balance performance of a subject can be assessed and trained based on perturbation experiments and the evaluation of experimental boundary margins. In the current results and reference study, no data is available to demonstrate the experimental evaluation of reachable margins, which is left to future work.

Lastly, the evaluation of balance performance in the motor task-based exercise is illustrated by two example trajectories extracted from the reference study (Patton et al., 1999), which exemplify the analysis of a generic balancing trajectory with respect to the balanced regions of the subject (**Figure 6B**). In both experimental trajectories, the subject was able to recover upright static equilibrium without altering the double foot stance. The reachable balanced trajectory starts from initial conditions within the reachable boundary margins of the higher-order models and well within the LIP balanced region. The first half of the reachable balanced trajectory starts from a dynamic reachable state (with COM outside of the base of support) and reaches an upright statically stable state (with COM approximately aligned with the ankle joint); this segment of trajectory appears close to the linear passive dynamics of the LIP, suggesting that the first part of the balancing motion may rely mostly on the favorable initial conditions, while angular momentum effects may not be relevant. Conversely, the viable balanced trajectory starts from initial conditions outside of all reachable boundary margins and even outside of the LIP and 4-DOF balanced regions; however, the initial state is viable with respect to the boundary margins predicted by the 5-DOF model, which is an indication that the balancing motion must rely on multiple strategies, including the angular momentum and foot rocking strategy, in addition to the favorable initial conditions. These results suggest that for such a highly dynamic balancing motion, a higher-order mechanism with a multi-segment foot model gives a better prediction of an individual's balance performance, as compared to biped models with lower DOF and rigid foot.

The state margin eMOS is calculated for the two example trajectories to evaluate their instantaneous level of balance or imbalance (**Figure 7**). The nondimensional eMOS quantifies the distance from a given state of the trajectory with respect to both the upper and lower bounds of each balance threshold, measured along the position coordinate; here, the smallest distance from either lower (dashed lines, **Figure 7**) and upper (solid lines, **Figure 7**) bounds is shown, since it represents the most critical balance condition. A positive eMOS value indicates that the trajectory is within a balanced region, where a greater eMOS absolute value corresponds to a greater balance safety margin, while a smaller eMOS absolute value indicates a closer proximity to the unbalanced region; the opposite is true for negative eMOS. When the LIP is used the eMOS coincides with the MOS (Mummolo et al., 2021), and its positive values range from 0 to 1.

The eMOS of the reachable trajectory indicate that all three biped models correctly predict a balanced trajectory that is closer to the lower BoB boundaries for approximately 65% of the motion, after which the COM state results closer to the upper BoB lines (**Figure 7**; left). Throughout the reachable trajectory, the BoB of the 4-DOF and LIP models underestimate the instantaneous margin of balance, as compared to the 5-DOF model, hence predicting a smaller level of balance throughout the motion. The eMOS of the viable trajectory indicates that only the 5-DOF model correctly predict a balanced motion, with a state margin always closer to the lower BoB limits (**Figure 7**; right). The 4-DOF and LIP models present negative eMOS values at the beginning of the viable

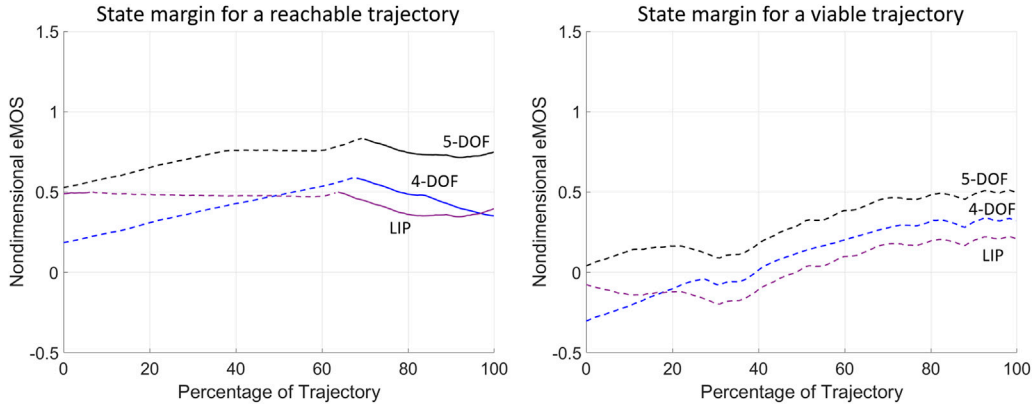

FIGURE 7 | The instantaneous state margin (eMOS) is calculated throughout the balancing motion of the two example trajectories from (Patton et al., 1999). The eMOS values are calculated for the normalized trajectories and BoB of each biped model considered, where the solid and dashed lines correspond to state margins relative to the upper and lower BoB lines, respectively.

trajectory, which would wrongly predict the subject's inability to recover balance from those initial conditions, without external help and without changing foot stance.

The above analysis of balanced regions, boundary and state margins demonstrates an objective method of assessing a patient's progress throughout treatment. The nondimensional boundary margins have highlighted the differences between the different modeling approaches of human standing posture: the inclusion of a multi-segment foot can lead to a more accurate balance characterization in real human subjects. Boundary margins allow the selection of customized and quantifiable targets for training balance recovery from internal and external perturbations, while state margins provide a numerical benchmark of the subject's balance capabilities during a particular trajectory. All proof-of-concept results demonstrate the benefits of having a balance criterion that can be extended to higher-order models that can more accurately predict dynamic stability, as compared with reduced-order models.

CONCLUSIONS AND FUTURE WORK

This study proposed a novel balance training and assessment computational technique, illustrated through an example subject performing a postural stability exercises obtained from a reference study (Patton et al., 1999). By using the balanced regions as reference maps, new balance exercises can also be developed for the furthering of current physical rehabilitation approaches. The application of the proposed framework to home-care rehabilitation, which is essential during and after the COVID-19 pandemic, is briefly discussed. The balance performance indicators are proposed as both targets and outcomes of balance exercises that require only tracking and visual feedback of desired vs. current COM motion and foot stance, as opposed to, for example, the measurement of COP, ground reactions, and external impulse forces profiles, which may not be easily integrated into an affordable and portable device. For this reason, the proposed theoretical/computational framework could be a promising initial step for the development of innovative devices for the remote assessment and rehabilitation of balance performance in patients affected by reduced mobility. The integration of the presented criterion for quantitative balance assessment with a portable instrumented platform would contribute to the advancement of postural stability analysis in three ways: first, it would allow patients and the general population to participate in highly customized in-home physical therapy treatment plans to prevent or treat mobility disorders while also being systematically evaluated; second, it could open the way for clinicians to design and test balance exercises that can include dynamic stance changes and other general motor tasks; third, it has the capability to generate a unified benchmarking dataset of significant volume across multiple populations (e.g., of different ages and pathological conditions), which would boost further investigation on the medium/long term effects of COVID-19 on people's balance ability and the associated fall risk.

DATA AVAILABILITY STATEMENT

The raw data supporting the conclusions of this article can be made available by the authors, upon request.

AUTHOR CONTRIBUTIONS

KA contributed to the design of balance exercises and processed all the data relative to the balance performance indicators. CM developed the theoretical and computational framework and supervised the entire work. Both authors contributed to writing and editing the paper.

FUNDING

This research has been funded by New Jersey Institute of Technology, Newark School of Engineering.

REFERENCES

Aubin, J. P., Bayen, A. M., and Saint-Pierre, P. (2011). *Viability Theory: New Directions*. Springer-Verlag Berlin Heidelberg: Springer Science & Business Media.

Bayouk, J.-F., Boucher, J. P., and Leroux, A. (2006). Balance Training Following Stroke: Effects of Task-Oriented Exercises With and Without Altered Sensory Input. *Int. J. Rehabil. Res.* 29 (1), 51–59. doi:10.1097/01.mrr.0000192100.67425.84

Bell, D. R., Guskiewicz, K. M., Clark, M. A., and Padua, D. A. (2011). Systematic Review of the Balance Error Scoring System. *Sports Health* 3 (3), 287–295. doi:10.1177/1941738111403122

Chaudhry, H., Findley, T., Quigley, K. S., Bukiet, B., Ji, Z., Sims, T., et al. (2004). Measures of Postural Stability. *J. Rehabil. Res. Dev.* 41 (5), 713–720. doi:10.1682/jrrd.2003.09.0140

Conforti, I., Mileti, I., Del Prete, Z., and Palermo, E. (2020). Measuring Biomechanical Risk in Lifting Load Tasks Through Wearable System and Machine-Learning Approach. *Sensors* 20 (6), 1557. doi:10.3390/s20061557

Del Prete, A., Tonneau, S., and Mansard, N. (2018). Zero Step Capturability for Legged Robots in Multicontact. *IEEE Trans. Robot.* 34 (4), 1021–1034. doi:10.1109/tro.2018.2820687

Gandolfi, M., Geroin, C., Picelli, A., Smania, N., and Bartolo, M. (2018). *Assessment of Balance Disorders, Advanced Technologies for the Rehabilitation of Gait and Balance Disorders*. Cham, Switzerland: Springer, 47–67.

Ganesan, M., Kanekar, N., and Aruin, A. S. (2015). Direction-Specific Impairments of Limits of Stability in Individuals With Multiple Sclerosis. *Ann. Phys. Rehabil. Med.* 58 (3), 145–150. doi:10.1016/j.rehab.2015.04.002

Glave, A. P., Didier, J. J., Weatherwax, J., Browning, S. J., and Fiaud, V. (2016). Testing Postural Stability: Are the Star Excursion Balance Test and Biodex Balance System Limits of Stability Tests Consistent? *Gait Posture* 43, 225–227. doi:10.1016/j.gaitpost.2015.09.028

Goble, D. J., Cone, B. L., and Fling, B. W. (2014). Using the Wii Fit as a Tool for Balance Assessment and Neurorehabilitation: The First Half Decade of "Wii-Search". *J. Neuroeng. Rehabil.* 11, 12. doi:10.1186/1743-0003-11-12

Herman, T., Inbar-Borovsky, N., Brozgol, M., Giladi, N., and Hausdorff, J. M. (2009). The Dynamic Gait Index in Healthy Older Adults: The Role of Stair Climbing, Fear of Falling and Gender. *Gait Posture* 29 (2), 237–241. doi:10.1016/j.gaitpost.2008.08.013

Hof, A. L., Gazendam, M. G. J., and Sinke, W. E. (2005). The Condition for Dynamic Stability. *J. Biomech.* 38 (1), 1–8. doi:10.1016/j.jbiomech.2004.03.025

Holmes, P. D., Danforth, S. M., Fu, X.-Y., Moore, T. Y., and Vasudevan, R. (2020). Characterizing the Limits of Human Stability During Motion: Perturbative Experiment Validates a Model-Based Approach for the Sit-to-Stand Task. *R. Soc. Open Sci.* 7 (1), 191410. doi:10.1098/rsos.191410

Iannaccone, S., Castellazzi, P., Tettamanti, A., Houdayer, E., Brugliera, L., de Blasio, F., et al. (2020). Role of Rehabilitation Department for Adult Covid-19 Patients: The Experience of the San Raffaele Hospital of Milan. *Arch. Phys. Med. Rehabil.* 101 (9), 1656–1661. doi:10.1016/j.apmr.2020.05.015

Kennedy, M. W., Schmiedeler, J. P., Crowell, C. R., Villano, M., Striegel, A. D., and Kuitse, J. (2011). "Enhanced Feedback in Balance Rehabilitation Using the Nintendo Wii Balance Board," in IEEE 13th International Conference on e-Health Networking, Applications and Services, June 13–15, 2011, (Columbia MO: IEEE), 162–168.

Keshner, E. A., and Fung, J. (2019). Editorial: Current State of Postural Research - Beyond Automatic Behavior. *Front. Neurol.* 10, 1160. doi:10.3389/fneur.2019.01160

Kinzey, S. J., and Armstrong, C. W. (1998). The Reliability of the Star-Excursion Test in Assessing Dynamic Balance. *J. Orthop. Sports Phys. Ther.* 27 (5), 356–360. doi:10.2519/jospt.1998.27.5.356

Koolen, F. A. (2019). Balance Control and Locomotion Planning for Humanoid Robots Using Nonlinear Centroidal Models. Doctoral dissertation. Cambridge MA: Massachusetts Institute of Technology.

Koolen, T., De Boer, T., Rebula, J., Goswami, A., and Pratt, J. (2012). Capturability-Based Analysis and Control of Legged Locomotion, Part 1: Theory and Application to Three Simple Gait Models. *Int. J. Robot. Res.* 31 (9), 1094–1113. doi:10.1177/0278364912452673

Lafond, D., Duarte, M., and Prince, F. (2004). Comparison of Three Methods to Estimate the Center of Mass during Balance Assessment. *J. Biomech.* 37 (9), 1421–1426. doi:10.1016/s0021-9290(03)00251-3

Levinger, P., Dunn, J., Bifera, N., Butson, M., Elias, G., and Hill, K. D. (2017). High-Speed Resistance Training and Balance Training for People With Knee Osteoarthritis to Reduce Falls Risk: Study Protocol for a Pilot Randomized Controlled Trial. *Trials* 18 (1), 1–11. doi:10.1186/s13063-017-2129-7

Marioni, G., Fermo, S., Zanon, D., Broi, N., and Staffieri, A. (2013). Early Rehabilitation for Unilateral Peripheral Vestibular Disorders: A Prospective, Randomized Investigation Using Computerized Posturography. *Eur. Arch. Otorhinolaryngol.* 270 (2), 425–435. doi:10.1007/s00405-012-1944-4

MFT Bodyteamwork (2020). MFT Challenge Disc. Available at: https://www.challenge-disc.com/en/ (Accessed April 10, 2021).

Mummolo, C., Akbas, K., and Carbone, G. (2021). State-Space Characterization of Balance Capabilities in Biped Systems With Segmented Feet. *Front. Robot. AI* 8, 613038. doi:10.3389/frobt.2021.613038

Mummolo, C., Mangialardi, L., and Kim, J. H. (2015a). "Concurrent Contact Planning and Trajectory Optimization in One Step Walking Motion," in ASME 2015 International Design Engineering Technical Conferences and Computers and Information in Engineering Conference, August 2–5, 2015, Boston, MA: American Society of Mechanical Engineers Digital Collection.

Mummolo, C., Mangialardi, L., and Kim, J. H. (2015b). "Identification of Balanced States for Multi-Segmental Legged Robots Using Reduced-Order Model," in IEEE-RAS 15th International Conference on Humanoid Robots (Humanoids), November 3–5, 2015, (Seoul, Korea: IEEE), 914–919.

Mummolo, C., Mangialardi, L., and Kim, J. H. (2013). Quantifying Dynamic Characteristics of Human Walking for Comprehensive Gait Cycle. *J. Biomech. Eng.* 135 (9), 91006. doi:10.1115/1.4024755

Mummolo, C., Mangialardi, L., and Kim, J. H. (2017). Numerical Estimation of Balanced and Falling States for Constrained Legged Systems. *J. Nonlinear Sci.* 27 (4), 1291–1323. doi:10.1007/s00332-016-9353-2

Mummolo, C., Peng, W. Z., Agarwal, S., Griffin, R., Neuhaus, P. D., and Kim, J. H. (2018a). Stability of Mina V2 for Robot-Assisted Balance and Locomotion. *Front. Neurorobot.* 12, 62. doi:10.3389/fnbot.2018.00062

Mummolo, C., Peng, W. Z., Gonzalez, C., and Kim, J. H. (2018b). Contact-Dependent Balance Stability of Biped Robots. *J. Mech. Robot.* 10 (2), 021009. doi:10.1115/1.4038978

Mummolo, C., Peng, W. Z., and Kim, J. H. (2019). "Whole-Body Balancing Criteria for Biped Robots in Sagittal Plane," in International Design Engineering Technical Conferences and Computers and Information in Engineering Conference, August 18–21, 2019, Anaheim, CA: American Society of Mechanical Engineers (ASME).

Mummolo, C., and Vicentini, G. (2020). "Limits of Dynamic Postural Stability with a Segmented Foot Model," In: Editors Ateshian, G., Myers, K., and Tavares, J.Computer Methods, Imaging and Visualization in Biomechanics and Biomedical Engineering. CMBBE 2019. Lecture Notes in Computational Vision and Biomechanics. 36, (Cham, Switzerland: Springer), 256–270. doi:10.1007/978-3-030-43195-2_21

Narici, M., De Vito, G., Franchi, M., Paoli, A., Moro, T., Marcolin, G., et al. (2020). Impact of Sedentarism Due to the COVID-19 Home Confinement on Neuromuscular, Cardiovascular and Metabolic Health: Physiological and Pathophysiological Implications and Recommendations for Physical and Nutritional Countermeasures. *Eur. J. Sport Sci.* 21 (4), 614–635. doi:10.1080/17461391.2020.1761076

Neofect (2020). Smart Balance. Available at: https://www.neofect.com/us/smart-balance (Accessed April 10, 2021).

Olchowik, G., and Czwalik, A. (2020). Effects of Soccer Training on Body Balance in Young Female Athletes Assessed Using Computerized Dynamic Posturography. *Appl. Sci.* 10 (3), 1003. doi:10.3390/app10031003

Orsolino, R., Focchi, M., Caron, S., Raiola, G., Barasuol, V., Caldwell, D. G., et al. (2020). Feasible Region: An Actuation-Aware Extension of the Support Region. *IEEE Trans. Robot.* 36 (4), 1239–1255. doi:10.1109/tro.2020.2983318

Patton, J. L., Pai, Y.-C., and Lee, W. A. (1999). Evaluation of a Model that Determines the Stability Limits of Dynamic Balance. *Gait Posture* 9 (1), 38–49. doi:10.1016/s0966-6362(98)00037-x

Pratt, J., Ott, C., Hyon, S. H., Goswami, A., and Vadakkepat, P. (2017). "Introduction to Humanoid Balance," in *Humanoid Robotics: A Reference*. Editors Goswami, A., and Vadakkepat, P. (Dordrecht, Netherlands: Springer). 1315–1321.

Raad, J., Moore, J., Hamby, J., Rivadelo, R. L., and Straube, D. (2013). A Brief Review of the Activities-Specific Balance Confidence Scale in Older Adults. *Arch. Phys. Med. Rehabil.* 94 (7), 1426–1427. doi:10.1016/j.apmr.2013.05.002

Ruiz, I., Contreras, J., and Garcia, J. (2020). Towards a Physical Rehabilitation System Using a Telemedicine Approach. *Comput. Methods Biomech. Biomed. Eng. Imaging Vis.* 8 (6), 671–680. doi:10.1080/21681163.2020.1795929

Sápi, M., Domján, A., Fehérné Kiss, A., and Pintér, S. (2019). Is Kinect Training Superior to Conventional Balance Training for Healthy Older Adults to Improve Postural Control?. *Games Health J.* 8 (1), 41–48. doi:10.1089/g4h.2018.0027

Seshadri, D. R., Davies, E. V., Harlow, E. R., Hsu, J. J., Knighton, S. C., Walker, T. A., et al. (2020). Wearable Sensors for COVID-19: A Call to Action to Harness Our Digital Infrastructure for Remote Patient Monitoring and Virtual Assessments. *Front. Digit. Health* 2, 8. doi:10.3389/fdgth.2020.00008

Sibley, K. M., Beauchamp, M. K., Van Ooteghem, K., Straus, S. E., and Jaglal, S. B. (2015). Using the Systems Framework for Postural Control to Analyze the Components of Balance Evaluated in Standardized Balance Measures: A Scoping Review. *Arch. Phys. Med. Rehabil.* 96 (1), 122–132. doi:10.1016/j.apmr.2014.06.021

Smith, V. A., Lockhart, T. E., and Spano, M. L. (2017). Basins of Attraction in Human Balance. *Eur. Phys. J. Spec. Top.* 226 (15), 3315–3324. doi:10.1140/epjst/e2016-60345-4

Stevenson, T. J. (2001). Detecting Change in Patients With Stroke Using the Berg Balance Scale. *Aust. J. Physiother.* 47 (1), 29–38. doi:10.1016/s0004-9514(14)60296-8

Torricelli, D., Rodriguez-Guerrero, C., Veneman, J. F., Crea, S., Briem, K., Lenggenhager, B., et al. (2020). Benchmarking Wearable Robots: Challenges and Recommendations From Functional, User Experience, and Methodological Perspectives. *Front. Robot. AI* 7, 168. doi:10.3389/frobt.2020.561774

Visser, J. E., Carpenter, M. G., van der Kooij, H., and Bloem, B. R. (2008). The Clinical Utility of Posturography. *Clin. Neurophysiol.* 119 (11), 2424–2436. doi:10.1016/j.clinph.2008.07.220

Wagner, D. R., Saunders, S., Robertson, B., and Davis, J. E. (2016). Normobaric Hypoxia Effects on Balance Measured by Computerized Dynamic Posturography. *High Alt. Med. Biol.* 17 (3), 222–227. doi:10.1089/ham.2016.0040

Wikstrom, E. A. (2012). Validity and Reliability of Nintendo Wii Fit Balance Scores. *J. Athl. Train.* 47 (3), 306–313. doi:10.4085/1062-6050-47.3.16

Winter, D. A. (2005). *Biomechanics and Motor Control of Human Movement*. 3rd ed. New York, NY: Wiley.

World Health Organization (2020b). #BeActive for the UN International Day of Sport for Development and Peace. Available at: https://www.who.int/news-room/detail/06-04-2020-beactive-for-the-un-international-day-of-sport-for-development-and-peace (Accessed July 27, 2020).

World Health Organization (2020c). #HealthyAtHome - Physical Activity. Available at: https://www.who.int/news-room/campaigns/connecting-the-world-to-combat-coronavirus/healthyathome/healthyathome—physical-activity (Accessed September 6, 2020).

World Health Organization (2020a). Coronavirus. Available at: https://www.who.int/health-topics/coronavirus (Accessed September 26, 2020).

Young, P. M. M., Wilken, J. M., and Dingwell, J. B. (2012). Dynamic Margins of Stability During Human Walking in Destabilizing Environments. *J. Biomech.* 45 (6), 1053–1059. doi:10.1016/j.jbiomech.2011.12.027

Zampogna, A., Mileti, I., Palermo, E., Celletti, C., Paoloni, M., Manoni, A., et al. (2020). Fifteen Years of Wireless Sensors for Balance Assessment in Neurological Disorders. *Sensors* 20 (11), 3247. doi:10.3390/s20113247

Zaytsev, P., Hasaneini, S. J., and Ruina, A. (2015). "Two Steps is Enough: No Need to Plan Far Ahead for Walking Balance," in IEEE International Conference on Robotics and Automation (ICRA), 26-30 May 2015, (Seattle, WA: IEEE), 6295–6300.

Conflict of Interest: The authors declare that the research was conducted in the absence of any commercial or financial relationships that could be construed as a potential conflict of interest.

frontiers in Robotics and AI

ORIGINAL RESEARCH
published: 22 June 2021
doi: 10.3389/frobt.2021.612331

Robotic Home-Based Rehabilitation Systems Design: From a Literature Review to a Conceptual Framework for Community-Based Remote Therapy During COVID-19 Pandemic

Aylar Akbari[†], *Faezeh Haghverd*[†] *and Saeed Behbahani* *

Department of Mechanical Engineering, Isfahan University of Technology, Isfahan, Iran

During the COVID-19 pandemic, the higher susceptibility of post-stroke patients to infection calls for extra safety precautions. Despite the imposed restrictions, early neurorehabilitation cannot be postponed due to its paramount importance for improving motor and functional recovery chances. Utilizing accessible state-of-the-art technologies, home-based rehabilitation devices are proposed as a sustainable solution in the current crisis. In this paper, a comprehensive review on developed home-based rehabilitation technologies of the last 10 years (2011–2020), categorizing them into upper and lower limb devices and considering both commercialized and state-of-the-art realms. Mechatronic, control, and software aspects of the system are discussed to provide a classified roadmap for home-based systems development. Subsequently, a conceptual framework on the development of smart and intelligent community-based home rehabilitation systems based on novel mechatronic technologies is proposed. In this framework, each rehabilitation device acts as an agent in the network, using the internet of things (IoT) technologies, which facilitates learning from the recorded data of the other agents, as well as the tele-supervision of the treatment by an expert. The presented design paradigm based on the above-mentioned leading technologies could lead to the development of promising home rehabilitation systems, which encourage stroke survivors to engage in under-supervised or unsupervised therapeutic activities.

Keywords: home based rehabilitation, stroke rehabilitaiton, COVID 19 pandemic, conceptual framework, rehabilitation robotics

OPEN ACCESS

Edited by:
Ana Luisa Trejos,
Western University, Canada

Reviewed by:
Dhaval S. Solanki,
Indian Institute of Technology Gandhinagar, India
Yue Zhou,
Western University, Canada

***Correspondence:**
Saeed Behbahani
behbahani@cc.iut.ac.ir

[†]*These authors have contributed equally to this work and share first authorship*

Specialty section:
This article was submitted to Biomedical Robotics, a section of the journal Frontiers in Robotics and AI

Received: *30 September 2020*
Accepted: *01 June 2021*
Published: *22 June 2021*

Citation:
Akbari A, Haghverd F and Behbahani S (2021) Robotic Home-Based Rehabilitation Systems Design: From a Literature Review to a Conceptual Framework for Community-Based Remote Therapy During COVID-19 Pandemic. Front. Robot. AI 8:612331. doi: 10.3389/frobt.2021.612331

INTRODUCTION

Coronavirus disease 2019 (COVID-19) is an infectious disease with serious public health risk declared a global pandemic by WHO on March 11, 2020. In the present time of the COVID-19 pandemic, the lives of individuals have been drastically affected due to the imposed restrictions such as social distancing, curfews, and travel restrictions. This situation has had a considerable impact on the lives of certain more vulnerable groups on a larger scale, namely people living with chronic diseases such as stroke. In a pooled data analysis published in the International Journal of Stroke (IJS), Aggarwal et al. emphasized that COVID-19 puts post-stroke patients at a greater risk of developing complications and death. In fact, the odds of severe COVID-19

infection increase by 2.5 times in patients with a history of cerebrovascular disease (Aggarwal et al., 2020). This calls for consideration of extra safety precautions for this vulnerable population to protect them from infected environments, namely strictly abiding by the quarantine rules and social distancing, as breaking them could prove fatal (Markus and Brainin, 2020).

Stroke is accounted one of the dominant causes of severe and long-term disability. It leads to a total or partial loss of aptitude to trigger muscle activation to perform any activity (Borboni et al., 2016). The broad spectrum of induced disabilities includes a reduced range of motion (ROM), strength of the affected limb, and abnormal inter-joint coordination (Chen J. et al., 2017). The sensitive/motor deficits impede the performance of activities of daily living (ADLs), such as reaching, grasping, and lifting objects, as well as walking, etc., in the surviving individuals (Chen J. et al., 2017; Heung et al., 2019). Patients must be subjected to rehabilitative treatment to help them regain the ability to perform daily activities independently. As Martinez-Martin et al. stated, "Rehabilitation can be defined as the step-by-step process designed to reduce disability and to optimize functioning in individuals with health conditions, enabling them to better interact with their environment." (Martinez-Martin and Cazorla, 2019). In the post-stroke rehabilitation process, the period between the first and the sixth months after stroke, known as the post-stroke sensitive period, has been proved to bear the maximum recovery impact, both spontaneous and intervention-mediated. Indeed, according to the statistics presented in Krakauer et al. article, during the first four weeks of rehabilitation, failure of reaching an arm Fugl-Meyer score of at least 11 would indicate only a 6% possibility of regaining dexterity at six months (Krakauer 2006). Regarding the aforementioned issues, in the current restrictive climate of COVID-19, the crucial question to be addressed for post-stroke patients would be how to use this critical and limited window of time to achieve the best possible recovery.

Robot-mediated therapy for post-stroke rehabilitation offers highly repetitive, high-dosage, and high-intensity alternatives, while reducing labor intensity and the manual burden on therapists. Hence, myriads of studies have focused on exploring robotics technologies for post-stroke rehabilitation. An increasing amount of research has investigated the efficiency of different types of robotic rehabilitation systems and found that these interventions can effectively complement conventional physical therapy, e.g., Mehrholz et al. and Bertani et al. investigated the effects of robot-assisted gait and upper-limb training, respectively, and both concluded that using robotic technologies positively affects post-stroke recovery (Bertani et al., 2017; Mehrholz et al., 2020). To tackle the recent rising issues associated with restrictions caused by the pandemic, there is a need to speed up the process of providing autonomous and affordable care that can be transferred out of inpatient or out-patient facilities into home environments. This study reviews the existing home-based robotic rehabilitation interventions and proposes reliable concepts that can be used to confront the discussed problems.

Home-based rehabilitation systems can be considered viable options capable of promoting care delivery while adhering to physical distancing measures and reducing the potential exposure to the infectious virus along with protecting vulnerable stroke survivors. Besides, even prior to this pandemic, the demand for home-based rehabilitation far exceeded its availability, further emphasizing the importance of this form of rehabilitation as a sustainable solution. According to WHO, demand for rehabilitation is approximately ten times that of the capacity of the service that the current healthcare system can provide, in terms of both rehabilitation professionals and rehabilitative tools (Gupta et al., 2011; World Health Organization, 2017). This poses a clear priority on further extension of home-based rehabilitation, which could prove to be a better alternative than conventional care by maintaining physical distancing and ameliorating the saturated health service.

Home-based systems offer a platform for unsupervised or under-supervised therapy, in which the need for the physical presence of a therapist is reduced. Rehabilitative treatments need to be intensive with long duration to improve functional outcomes and motor recovery (Bütefisch et al., 1995). Compared to clinical therapy, home therapy potentially augments standard care and enables consistent treatment by increasing the frequency and duration of training sessions. Performing rehabilitation at home provides patients with a comfortable setting. It gives them a sense of control of therapy as it reduces their reliance on external assistance (Chen et al., 2019). This can result in the patients demonstrating enhanced motivation and engagement (Borghese et al., 2013). In terms of the associated costs, home-based therapy reduces the expenses compared with clinical-based therapy; for example, in statistics provided by Housley et al., a saving of $2,352 (64.97%) was reported (Housley et al., 2016).

However, deployment in the unsupervised context of home-based rehabilitation poses risks to patients. Therapists perceive risks to patients regarding the training/acquisition of harmful movements when unsupervised at home—abnormal movement can be damaging or slow recovery (Borghese et al., 2014). Careful system design and deployment measures need to be taken, such as providing adequate feedback on proper task execution, to preclude these movements. On the other hand, in robotic medical devices the occurrence of errors that cannot be accounted for or predicted during device design leads to patient injuries and more severe incidents in some cases (Kim, 2020), e.g., crashes in device operability, both in hardware and software, and errors induced by contextual barriers in patients home environment. In clinical settings, in case of such incidents, the physical presence of healthcare professionals could mitigate the risk, yet such an option is not available at home.

Due to the benefits mentioned above, robot-mediated home therapy has gained attraction in recent years. Its feasibility has been evaluated through several studies using state-of-the-art home robots. The literature surveys indicated the feasibility of self-administered treatment at home using rehabilitation robots in terms of functional outputs, training duration, user acceptance,

TABLE 1 | Summary of state-of-the-art robotic systems for home-based upper-limb rehabilitation.

Device	Main features and drawbacks	Control strategy	DOF	Supported movements	Weight (kg)	Stroke severity	Outcome measures	Time after stroke
HandSOME Brokaw et al. (2011); Chen and Lum (2016b); Chen et al. (2017a)	Only assists with extension; adjustable hard stops to limit ROM; assists with hand opening, grasp, grip, pinch, and gross movements	Extension passive assistance	11-Passive	5 fingers E	0.22 (version 1) and 0.128 (version 2)	Moderate to severe	FM; MAS; MAL; ARAT	>6 months after stroke
HandMATE Sandison et al. (2020)	Customizable 3D printed components; both manual and automated calibration sequence options for a facilitated home-use; using force sensitive resistors (FSR) for intention detection; android app with 4 customized game	Passive assistance; triggered passive assistance	11-(One actuator for each finger)	5 fingers FE	0.34	Moderate to severe	N/A	Chronic
X-glove Fischer et al. (2016); Ghassemi et al. (2018)	Facilitated two-component donning; custom GUI; multi-user VR exercises; haptic feedback	Passive assistance; partial assistance; resistance	N/A	5 fingers E (assisted)/F (resisted)	N/A	Severe	CMSA-H; FMUE; ARAT; CAHAI-9 GWMFT-func; GWMFT-time; EXT; FMUE; GS; LPS (N); PPS; MMAS; MAL QOM	Subacute phase
My-HERO Yurkewich et al. (2020)	EMG-based intention detection; automated calibration	Triggered passive assistance	2 actuators	5 fingers FE	0.377	Severe	FMA-UE; FMA-Hand; CAHAI-13	>6 months post stroke
HERO Yurkewich et al. (2019)	Ease of donning/doffing (3/1 minutes with assistance)	Passive assistance	1 actuator	5 fingers FE	0.192	Broad range of severe hand impairments	MMAS; MTS; BBT; CAHAI	Acute and chronic
IOTA Aubin et al. (2013)	Targeting pediatric population; portable control box	Passive assistance; triggered passive assistance	2	Thumb FE; thumb add-abduction	0.23	N/A	N/A	N/A
Grasping rehabilitation device Park et al. (2013)	Pressure sensors for intention detection	Passive assistance; triggered passive assistance; partial assistance	2 actuators	N/A	N/A	N/A	N/A	N/A
Vanderbilt Gasser et al. (2017)	Bidirectional under-actuated tendon system; simultaneous fingers actuation; adjustable thumb design	Passive assistance	1-Active	4 fingers FE	0.4	N/A	N/A	N/A
WearME Zhou et al. (2019)	Performing resistive motion tasks	Resistance	3 actuators	Wrist FE; finger opposition	0.5	N/A	N/A	Chronic
Soft robotic exomusculature glove Delph et al. (2013)	sEMG-based intention detection; moving weight off hand by housing actuating components in a backpack	Partial assistance; resistance	5 actuators	5 fingers FE	6	N/A	N/A	N/A

(Continued on following page)

TABLE 1 | (*Continued*) Summary of state-of-the-art robotic systems for home-based upper-limb rehabilitation.

Device	Main features and drawbacks	Control strategy	DOF	Supported movements	Weight (kg)	Stroke severity	Outcome measures	Time after stroke
BCI-controlled pneumatic glove Coffey et al. (2014)	Adaptable BCI-based controller	BCI-based passive assistance	1 actuator/ 15 DOF	Finger E	2	N/A	N/A	N/A
Soft robotic glove Polygerinos et al. (2015)	Size customizable; easy to don/doff; minimal ADL interference	Partial assistance	3 per finger	5 fingers FE	0.285	N/A	N/A	N/A
Anthropomorphic soft exosuit Klug et al. (2019)	sEMG-based intention detection; cascade control	Passive assistance; triggered passive assistance	4 actuators	4 fingers FE	0.13	N/A	N/A	N/A
Exo-glove (in et al., 2015)	Bend sensors for intention detection; extremely lightweight; soft tendon routing system designed for zero pretension of the tendons; introduced a slack prevention mechanism; pinch and grasping assistance/training	Triggered passive assistance	3 actuators/ 9 DOF	Index, middle finger and thumb FE	0.194	N/A	N/A	N/A
Wrist rehabilitation device Ambar et al. (2017)	Android-based game application; mouse-like joystick suitable for patients with grasping difficulties	N/A	3-Passive	Wrist FE; wrist add-abduction; forearm PS	N/A	N/A	N/A	N/A
e-Wrist Lambelet et al. (2020)	Easy one-handed donning/doffing	Partial assistance (AAN)	1-Active	Wrist FE	Distal module 0.238 Proximal module 0.224	N/A	N/A	Acute or subacute
SCRIPT Amirabdollahian et al. (2014); Nijenhuis et al. (2015); Ates et al. (2017)	Easy don/doffing; motivational game environment based on AD; a tele-robotic support platform with a reach and user-friendly user-interfaces	Triggered passive assistance	6-Passive (1-unactuated for thumb ab-adduction)	Wrist FE; 5 fingers FE	0.65	Mild to severe	FM; ARAT; MAL; SIS	Chronic (>6 months post-stroke)
Ambidexter Wai et al. (2018)	IoT-enabled; aesthetically appealing; 3D printed standard components; offers gamification	Passive assistance; partial assistance	3 DOF	Hand opening/ closing; forearm PS; wrist FE	3	N/A	N/A	N/A
(HAL-SJ) Hyakutake et al. (2019)	Hybrid control algorithm, both for voluntary and autonomous control; interactive biofeedback	Passive assistance; triggered passive assistance	1-Active	Elbow FE	1.3	Mild	MAL; FMA-UE; ARAT	Chronic (>6 months post-stroke)
A home-based bilateral rehabilitation system Liu et al. (2020); Liu et al. (2018)	Bilateral rehabilitation; sEMG-based real-time stiffness control	Triggered passive assistance	1-Active 3-Passive	Elbow FE (active); shoulder add-abduction; shoulder FE; shoulder IE rotation	3.1	N/A	N/A	N/A
Soft robotic elbow sleeve Koh et al. (2017)		Passive assistance;	1-Active	Elbow FE	N/A	N/A	N/A	N/A

(Continued on following page)

TABLE 1 | (*Continued*) Summary of state-of-the-art robotic systems for home-based upper-limb rehabilitation.

Device	Main features and drawbacks	Control strategy	DOF	Supported movements	Weight (kg)	Stroke severity	Outcome measures	Time after stroke
	EMG for intention detection; motion capture system	triggered passive assistance						
SpringWear Chen and Lum (2018)	Spring operated	Passive assistance	5 DOF	Shoulder F; elbow E; forearm PS Shoulder Horizontal abd-adduction; shoulder IE rotation	1.2	N/A	Shoulder FE ROM; elbow FE ROM; forearm PS ROM	Chronic (>6 months post-stroke)
PACER Alamdari and Krovi (2015)	Various control modes; parallel platform; 3D workspace	Passive assistance; partial assistance; resistance	N/A	Arm FE, add-abduction, medial/lateral rotation; elbow FE, forearm PS; wrist FE, and wrist add-abduction	N/A	N/A	N/A	N/A
HomeRehab Díaz et al. (2018); Catalan et al. (2018)	Cloud-based communication system; VR and gamification; wearable devices to record the physiological state of the user	Partial assistance (AAN); resistance	3-Active	Shoulder FE; shoulder Horizontal abd-adduction; elbow FE	7	N/A	N/A	N/A
ArmAssistJung et al. (2013); Perry et al. (2012); Tomić et al. (2017); Butler et al. (2017); Perry et al. (2016)	Portable device table; interactive games operating on a web-based platform; a global position and orientation detection mat; visual and auditory feedback; grasp and pinch exercises	Partial assistance (AAN)	4 DOF	Shoulder Horizontal abd-adduction; elbow FE; wrist PS	N/A	Moderate to severe	FMA-UE; BI; WMFT	Subacute
Active therapeutic device (ATD) Westerveld et al. (2014)	Arm weight support; 3D end-point manipulator; functional training of reaching tasks; inherently safe design	Passive assistance; resistance	N/A	N/A	25	N/A	N/A	N/A
PaRRo Washabaugh et al. (2019)	Inherently safe due to using passive actuators: eddy current brakes; adjustable resistance	Resistance	4 actuators	Planar 2D motions	N/A	N/A	N/A	N/A
RUPERT Zhang et al. (2011); Huang et al., 2016)	VR; GUI for remote supervision; size adjustable; built-in safety mechanism	Passive assistance; partial assistance	5 DOF	Shoulder FE; humeral IE rotation; elbow FE; forearm PS; wrist FE	N/A	Mild to moderate	FMA; WMFT	Chronic

motivation, and safety concerns. Remotely supervised participants of these studies exhibited increased motivation and autonomy in completing the prescribed task with no adverse events or edema. They also self-reported increased mobility, improved mood, and an outlet for physical and mental tension and anxiety (Sivan et al., 2014; Nijenhuis et al., 2015; Cherry et al., 2017; Bernocchi et al., 2018; Catalan et al., 2018). Catalan et al. compared the performance of a commercialized clinical upper-limb rehabilitation device and its newly developed home-based counterpart, which showed that functional outcomes of treatment are similar for home users and clinic patients (Catalan et al., 2018). This suggests that, although both groups would reach the task's goals similarly in terms of session numbers, due to the higher frequency of home-based therapy, users are able to master tasks in a shorter timespan (Godlove et al., 2019).

TABLE 2 | Summary of commercialized robotic systems for home-based upper-limb rehabilitation.

Device	Main features and drawbacks	Control strategy	DOF	Supported movements	Weight (kg)	Stroke severity	Outcome measures	Time after stroke
Saebo SaeboVR 2017; Adams et al. (2018); Doucet and Mettler (2018); Franck et al. (2019); Runnalls et al. (2019)	Fine motor skills, grasp, grip, pinch and release training; virtual world-based rehabilitation software for ADL; provides various additional treatment kits; arm weigh support; non-slip surface	N/A	N/A	Wrist FE and PS; 5 fingers FE	N/A	Mild to severe	WMFT; FMUE; ROM; ARAT; SIS	Subacute to chronic
WeReha Bellomo et al. (2020)	Simultaneously stimulating the cognitive aspect; fine movement training of the hand	N/A	N/A	Shoulder F; elbow FE; forearm PS; wrist PS	N/A	Mild to moderate	BBS; BI; FM; mRS	Chronic
SEM glove Osuagwu et al. (2020); Nilsson et al. (2012)	Pressure sensor for intention detection logic; tactile sensor and force sensor; power unit backpack	Partial assistance	3 Actuators/ 9 DOF	3 fingers F	0.7	N/A	N/A	N/A
IronHand Radder et al. (2019); Radder et al. (2018)	Pressure sensors for intension detection logic; assistive and therapeutic platform; motivating game-like environment	Partial assistance	9 DOF	3 or 5 fingers F	0.07	N/A	Use time; SUS; BBT; JTHFT; maximal pinch strength; maximal handgrip strength	N/A
Gloreha lite Bernocchi et al. (2018)	3D animations for simulated preview of the movement; dynamic arm supports; grasping, reaching and picking tasks; audio and visual feedback	Passive assistance; partial assistance	5-Active	5 fingers F	0.25	N/A	FIM; MAS	N/A
The motus hand Wolf et al. (2015); Butler et al. (2014); Linder et al. (2013a); Linder et al. (2013b)	Visual biofeedback; offers gamification; FDA class 1 device	Partial assistance	N/A	Wrist and fingers FE	control box: 6.37	Mild to severe	FMA; WMFT; ARAT; SIS; MAS	Subacute to chronic

This article is intended to be used as a general guideline for developing robotic home-based rehabilitation systems. For this purpose, first, the authors conducted a comprehensive review on developed home-based rehabilitation technologies of the last 10 years (2011–2020), categorizing them into upper and lower limb devices and considering both commercialized and state-of-the-art realms. The literature review analyzes and synthesizes the current knowledge of home-based robotic systems. This aims to provide a categorized comparison among reviewed literature leading to a classified roadmap to help guide current research and propose recommendations for advancing research development in this field. By addressing current challenges and shortcomings, three main aspects are considered in the proposed design paradigm, i.e., mechatronics, control, and user interface. While existing reviews take a generalized approach on home-based rehabilitation solutions—e.g., Chen et al. provided a systematic review based on the utilized technology types (Chen et al., 2019)—we focus and expand on robotic devices. In contrast to solutions relying solely on VR and game-based technologies, this paper addresses robotics-based technologies to cover the need for a significantly wider range of post-stroke patients, including patients who require external assistance reflecting the therapist's role in unsupervised settings. In the end, a conceptual community-based robotic rehabilitation framework, offering smart rehabilitation, is also introduced.

HOME-BASED REHABILITATION SYSTEMS

Over the last decade, researchers have been addressing existing challenges and requirements to design and develop rehabilitation robots suitable for home therapy. As a result, many at-home rehabilitation devices have been designed within the research realm, and some have been commercialized (**Tables 1–4**). In the following subsections, a comprehensive review of developed home-based rehabilitation technologies of the last ten years (2011–2020) is presented.

We conducted a literature review in the PubMed search engine. The search included the following terms: "Rehabilitation Robotics," "Home-Based Rehabilitation," and "Stroke Rehabilitation." Secondary references and citations of the resultant articles were checked to further identify relevant literature and other available sources providing information on commercially available solutions. Reviewers screened the abstracts of the collected articles for extracting those satisfying the eligibility criteria. Studies were excluded if they were not

TABLE 3 | Summary of state-of-the-art robotic systems for home-based lower-limb rehabilitation.

Device	Main features and drawbacks	Control strategy	DOF	Supported movements	Weight (kg)	Stroke severity	Outcome measures	Time after stroke
Soft robotic sock Low et al. (2018); Low et al. (2019)	Not size adjustable; not customizable for treatment parameters; offers early bedside care; improves venous flow during inpatient usage (fabric-based form factor and silicone-rubber-based actuator design provide a greater chance of user acceptance due to its compliant nature)	Pneumatic-actuated assistance	N/A	Ankle PD	N/A	Severe	Ankle ROM	Acute and subacute
Wearable ankle rehabilitation robotic device Ren et al. (2017)	Size adjustable; progressive augmented real-time feedback; sensory stimulus	Triggered passive assistive; partially assistive (AAN); resistive (active assistive training; resistance training; passive stretching)	1-Active	Ankle PD	N/A	N/A	FMLE; MAS	Acute
Motorized ankle stretcher (MAS) Beom-Chan et al. (2017); Yoo et al. (2019)	Equipped with a customized software	Passive assistance	2-Active per leg	Ankle PD and eversion/ inversion	N/A	N/A	Ankle ROM, gait parameters	At least 6 months post stroke
EMG-controlled Knee exoskeleton Lyu et al. (2019)	Provides multisensory feedback; EMG record for intention detection; customized gaming; ensures safety at software, electrical and mechanical levels; simplified setup process with setup time of around 1 minute	Triggered passive assistance	2-Active per leg	Hip FE; Knee FE	20 (total including the electronic components and battery),0.92 (the exoskeleton's lower leg)	N/A	N/A	Tested on healthy subjects
Lower limb rehabilitation wheelchair system Chen et al. (2017b)	Equipped with a tele-doctor; patient interaction module including user interfaces for both patients and therapist; customized virtual reality game	Passive assistance	N/A	Knee FE-standing/lying (movement of back)	N/A	N/A	N/A	N/A
Lower limb rehabilitation robot (LLR-Ro) Feng et al., 2017)	Intelligent human-machine cooperative control system; mechanical, electrical, and software safety features	Passive assistance	3-Active per leg	Hip FE; Knee FE; ankle PD	N/A	N/A	N/A	Early phase of
i-Walker Morone et al., 2016)	Used either for training or as an assistive device	Partial assistance (AAN); progressive assistance	N/A	N/A	N/A	Mild to moderate	Tineti's scal-MAS- BI-6MWT-10MWT	Subacute <90 days
Curara® Mizukami et al. (2018); Tsukahara et al. (2017)	Non-exoskeletal structure	Synchronization-based assistance	2-Active for each leg	Hip FE; Knee FE	5.8	N/A	N/A	N/A
	Highly repetitive without fatigue;	Triggered assistance	2-Active per leg	Hip FE; Knee FE	25 (including battery)	Mild	FMAS-BBS-TUGT-SPPB	Mean 1 year after

(Continued on following page)

TABLE 3 | (*Continued*) Summary of state-of-the-art robotic systems for home-based lower-limb rehabilitation.

Device	Main features and drawbacks	Control strategy	DOF	Supported movements	Weight (kg)	Stroke severity	Outcome measures	Time after stroke
WA-H Moon et al. (2017); Sung et al. (2017)	facilitates weight shifting by passive hip joints in coronal plane							
GEMS-H Hwang-Jae Lee et al. (2019); su-Hyun Lee et al. (2020)	Flexible exoskeleton	Partial assistance (AAN)	1-Active (per leg) 2-Passive	Hip FE	2.8	Mild to moderate	FMA, BBS, K-FES	Chronic stroke
Eddi current braking knee brace Washabaugh and Krishnan (2018); Washabaugh et al., 2016)	Inherently safe due to utilization of passive actuators: eddy current brakes	Resistance	1-Passive	Knee FE	1.6	Mild to moderate	10MWT	Chronic

TABLE 4 | Summary of commercialized robotic systems for home-based lower-limb rehabilitation.

Device	Main features and drawbacks	Control strategy	DOF	Supported movements	Weight (kg)	Stroke severity	Outcome measures	Time after stroke
Stride management assist (SMA) (by Honda) Buesing et al. (2015)	Single-charge operation time of 2 hours; not size adjustable but available 3 sizes: M, L and XL; only provides assistance in sagittal plane; one functional upper limb side is required for putting it on	Uses a mutual rhythm scheme to generates assist torques at specific instances during the gait cycle to regulate the user's walking pattern	1-Active per leg	Hip FE	2.8	N/A	N/A	Chronic (more than one year)
ReWalk ReStore™ (by ReWalk robotics) Awad et al. (2020)	Offers an optional textile component for patients who require medio-lateral ankle support; a hand-held real-time monitoring device with a graphical interfaces; some adverse events involving pain in lower extremity and skin abrasions were reported by users	Partial assistance	1-Active per leg	Ankle plantarflexion/ Dorsiflexion	5	N/A	10MWT	> two weeks
EksoNR (by ekso bionics) Carlan and singleorigin (2020)	Variable assistance modes	N/A	3-Active per leg	Hip FE and knee FE	N/A	N/A	N/A	N/A
HAL(by CYBERDYNE inc.) Nilsson et al. (2014); Kawamoto et al. (2013); Kawamoto et al. (2009)	Hybrid control algorithm, both for voluntary and autonomous control	Passive assistance; triggered passive assistance	3-Active per leg	Hip FE; Knee FE; ankle PD	14 (double leg model)	N/A	10MWT; BBS; TUGT; FM-LE; FES; BI; FIM	Early onset; chronic (more than a year)
AlterG bionic leg Wright et al. (2020); Iida et al. (2017); Stein et al. (2014)	Auditory and sensory feedback; easy and fast donning and doffing (approximately of 2 minutes); standardized overground functional tasks including sit to stand transfer	Partial assistance	1-Active	N/A	3.6	N/A	10MWT; 6MWT; TUGT; DGI; BBS; mRS;; accelerometry	Chronic stroke (>3 months since stroke diagnosis)

implemented and/or did not demonstrate implementation potential in home settings, based on the criteria introduced by authors in the following subsections.

Approximately 70% of stroke patients experience impaired arm function (Intercollegiate Working Party for Stroke, 2012). Hemiparesis is prevalent in up to 88% of post-stroke patients, which mostly leads to gait and balance disorders, that even persists in almost one-third of patients even after rehabilitation interventions, leaving them with the inability in independent walking (Gresham et al., 1995; Duncan et al., 2005; Díaz et al., 2011; Morone et al., 2016). Lower-limb devices face critical challenges for home use, making the upper-limb the primary focus of early efforts in this field. The following subsections were set to cover both state-of-the-art and commercialized devices by categorizing based on the upper or lower targeted limb.

Upper-Limb

State-of-the-Art: Systems in the Literature

Due to the significant results of active participation between patients and robots in functional improvement, the majority of current rehabilitative robots are equipped with electrical or pneumatic motors (Pehlivan et al., 2011). However, the inherent considerable weight of mounted motors precludes the device from being used during daily activities, since proximal arm weakness is prevalent among individuals with stroke. Thus, to allow hand rehabilitation during the performance of ADLs, HandSOME (Brokaw et al., 2011), a passive lightweight wearable device has been developed. The design is based on the concepts of patient-initiated repetitive tasks to rehabilitate and assist during ADL performance by increasing assistive torque with increasing extension angle. To help with opening the patient's hand and assisting with finger and thumb extension movements, HandSOME uses a series of elastic cords, as springs, to apply extension torques to the finger joint. For safety precautions, adjustable hard stops are used to control the ROM. Studies demonstrated that HandSOME could benefit stroke patients with ROM improvement. While patients commented that the device was generally comfortable for use at home (Chen J. et al., 2017), there is a need to develop a remote communication system instead of weekly clinical visits. Yet, one of the disadvantages of the device is its inability of assistance level adaptation to patient performance. Addressing this issue, Sandison et al. built a wearable motorized hand exoskeleton, HandMATE, upon HandSOME. This device benefits from 3D printing technology for manufacturing the components; hence it can be optimally adjustable and customizable to fit the patients' physiological parameters (Sandison et al., 2020). Combining hand orthosis with serious gaming, Ghasemi et al. have integrated eXtention Glove (X-Glove) actuated glove orthosis with a VR system to augment home-based hand therapy. For a facilitated donning, the device design allows for being put on by two separate components (Ghassemi et al., 2018). The glove provides both stretching therapy and extension assistance for each digit independently while allowing free movements and interaction with real-world objects (Fischer et al., 2016). Gasser et al. presented compact and lightweight hand exoskeleton Vanderbilt intended to facilitate ADLs for post-stroke hand paresis. The design includes an embedded system and onboard battery to provide a single degree of freedom (DOF) actuation that assists with both opening and closing of a power grasp (Gasser et al., 2017).

The Hand Extension Robot Orthosis (HERO) Glove is another wearable rehabilitation system that provides mechanical assistance to the index and middle fingers and thumb (Yurkewich et al., 2019). Linear actuators control the artificial tendons embedded into the batting glove's fingers for finger extension and grip assistance. Yurkewich et al. proceeded with their research by introducing My-HERO, a battery-powered, myoelectric untethered robotic glove. The new glove benefits from forearm electromyography for sensing the user's intent to grasp or release objects and provides assistance to all five fingers (Yurkewich et al., 2020). Addressing the pediatric disorders, such as stroke, causing thumb deformation, lightweight hand-mounted rehabilitation exoskeleton, the Isolated Orthosis for Thumb Actuation (IOTA), offers 2 degrees of freedom thumb rehabilitation at home while allowing for significant flexibility in the patient's wrist (Aubin et al., 2013). The device is patient-specific and can be securely aligned and customized to the patient's hand. The portable control box of the design enhances user freedom and allows rehabilitation exercises to be executed virtually anywhere. For recovering hand grasp function, Park et al. developed a robotic grasp rehabilitation device integrated with patient intention detection utilizing handle-embedded pressure sensors (Park et al., 2013). The device was designed for home use by being small in size, portable, and inexpensive. As one of the first wearable robots performing resistive training, Wearable Mechatronics-Enabled (WearME) glove was developed coupled with an associated control system for enabling the execution of functional resistive training. The soft-actuated cable-driven mechanism of the power actuation allows for applying resistive torque to the index finger, thumb, and wrist independently (Zhou et al., 2019).

Targeting individuals with functional grasp pathologies, Delph et al. developed an sEMG-based cable-driven soft robotic glove that can independently actuate all five fingers to any desired position between open and closed grip using position or force control and simultaneously regulate grip force using motor current (Delph et al., 2013). Coffey et al. integrated a soft pneumatic glove with a novel EEG-based BCI controller for an increased motor-neurorehabilitation during hand therapy at home (Coffey et al., 2014). In contrast to clinical BCI-mediated solutions, it is an inexpensive and simplified alternative for training the subject's wrist and fingers at home together with a haptic feedback system. Polygerinos et al. presented a portable soft robotic glove that combines assistance with ADL and at-home rehabilitation (Polygerinos et al., 2015). Hydraulically actuated multi-segment soft actuators using elastomers with fiber reinforcements induce specific bending, twisting, and extending trajectories when pressurized. The soft actuators are able to replicate the finger and thumb motions suitable for many typical grasping motions, to match and support the range of motion of individual fingers. Furthermore, the device has an open palm design in which the

actuators are mounted to the dorsal side of the hand. This provides an open-palm interface, potentially increasing user freedom as it does not impede object interaction. The entire compact system can be packaged into one portable waist belt pack that can be operated for several hours on a single battery charge. Gross and fine functional grasping abilities of the robotic glove in free-space and interaction with daily life objects were qualitatively evaluated on healthy subjects. Compared to other robotic rehabilitation devices, the soft robotic glove potentially increases independence, as it is lightweight and portable. An electrically actuated tendon-driven soft exosuit was developed for supporting and training hand's grasp function. The device offers versatile rehabilitation exercises covering motion patterns, including both power and precision grip, on each independently actuated finger (Klug et al., 2019). The Exo-Glove, a soft wearable robot using a glove interface for hand and finger assistance, developed by In et al., employs a soft tendon routing system and an underactuated adaptive mechanism (In et al., 2015). Inspired by the human musculoskeletal system, Exo-Glove transmits the tension of the tendons routed around the index and middle finger at the palm and back sides to the body to induce flexion and extension motions of the fingers.

The majority of upper-limb devices are dedicated to wrist rehabilitation due to its importance for peoples' daily work and life (Wang and Xu, 2019). By combining sensing technology with an interactive computer game, Ambar et al. aimed at developing a portable device for wrist rehabilitation (Ambar et al., 2017). To consider difficulties of stroke patients in firm grasping, the design was based on a single-person mouse-like joystick. The third DOF is considered for forearm pronation/supination, adding to standard flexion/extension and adduction-abduction movements for wrist rehabilitation. Clinical trials on healthy subjects using the device have shown task completion through a smooth recorded trajectory. In 2020, they also developed an android-based game application to enable patients to use the rehabilitation device at home or anywhere while making the therapy systematic and enjoyable (Ail et al., 2020). Lambelet et al. developed a fully portable sEMG-based force-controlled wrist exoskeleton offering extension/flexion assistance, eWrist. Given the prominence of the donning aspects of rehabilitation robots in unsupervised settings, the device was iteratively designed emphasizing attachment mechanism and distal weight reduction to enable one-hand and independent donning of the device (Lambelet et al., 2020).

One of the first projects dedicated to enabling home rehabilitation is the SCRIPT project. SCRIPT project—Supervised Care, and Rehabilitation Involving Personal Tele-robotics—is based on designing a passive finger, thumb, and wrist orthosis for stroke rehabilitation (Amirabdollahian et al., 2014). SPO-F, the final design, is equipped with novel actuation mechanisms at the fingers and wrist and a motivational game environment based on ADL, combined with remotely monitored consistent interfaces (Ates et al., 2017). To make the devices inherently safe and integrable to home environment, a dynamic but passive mechanism is implemented, providing adaptable and compliant extension assistance. The device is targeted at patients who are able to generate some residual muscle control. Also, it utilizes physical interfaces developed by Saebo Inc. due to its proven track record in providing safe and comfortable interaction. An evaluation study on post-stroke patients using the device training with virtual reality games indicated the feasibility of home training using SPO-F, providing reports on the compliance and improvement of hand function after training (Nijenhuis et al., 2015) (**Figure 1**).

Liu et al. integrated a powered variable-stiffness elbow exoskeleton device with an sEMG-based real-time joint stiffness control to offer bilateral rehabilitation to patients suffering from hemiparesis (Liu et al., 2021). For a patient-specific approach ensuring human-like behavior patterns and facilitated coordinated movements, the device mirrors the dynamic movement captured from the unaffected side to generate stiffness-adapted motion to the contralateral side (Liu et al., 2018). The device also benefits from five passive DOFs for providing natural range of motion and minimizing misalignments between the robot and hand joints. Koh et al. introduced a soft robotic elbow sleeve for enabling flexion and extension of the elbow through passive and intent-based assisted movement execution. Further investigation is required to assess the efficiency of the device in neuro-muscular training (Koh et al., 2017).

Motivated by their prior research with HandSOME, Chen et al. attempted to target another population of patients with arm weakness instead of grasping impairment and developed a spring-operated wearable upper limb exoskeleton, called SpringWear, for potential at-home arm rehabilitation (Chen and Lum, 2018). With a total of five DOFs, SpringWear applies angle-dependent assistance to the forearm supination, elbow extension, and shoulder extension while incorporating passive joints for two other shoulder movements to allow complex and lifelike multi-joint movement patterns (Chen J. P. S. and Lum P. S., 2016). Over a ten-year iterative research cycle, Zhang et al. developed the wearable exoskeleton RUPERT—Robotic Upper Extremity Repetitive Trainer—for both clinical and in-home post-stroke upper-extremity therapy that incorporates five degrees of freedom of shoulder, humeral, elbow, forearm, and wrist (Zhang et al., 2011). Each DOF is supported by a compliant and safe pneumatic muscle (Huang et al., 2016). The device employs adaptive sensory feedback control algorithms with associated safety mechanisms. The developers claim that easiness in donning and operating the device and its graphic user interface excludes the need for the presence of a physical therapist.

As the end-effector of the human body, the hand takes the lead of ADL (Ates et al., 2017). Hence, improving the ability to perform ADLs is regarded as one of the main goals of physical/occupational therapy. To this end, Ambidexter, an end-effector type three DOF robotic device, has been developed for training hand opening/closing, forearm pronation/supination, and wrist flexion/extension (Wai et al., 2018). To meet the essential requirements for home systems, the cost was reduced while maintaining the effectiveness, the set-up process is easy and fast—taking less than one minute—and compactness and aesthetics were practiced carefully during the

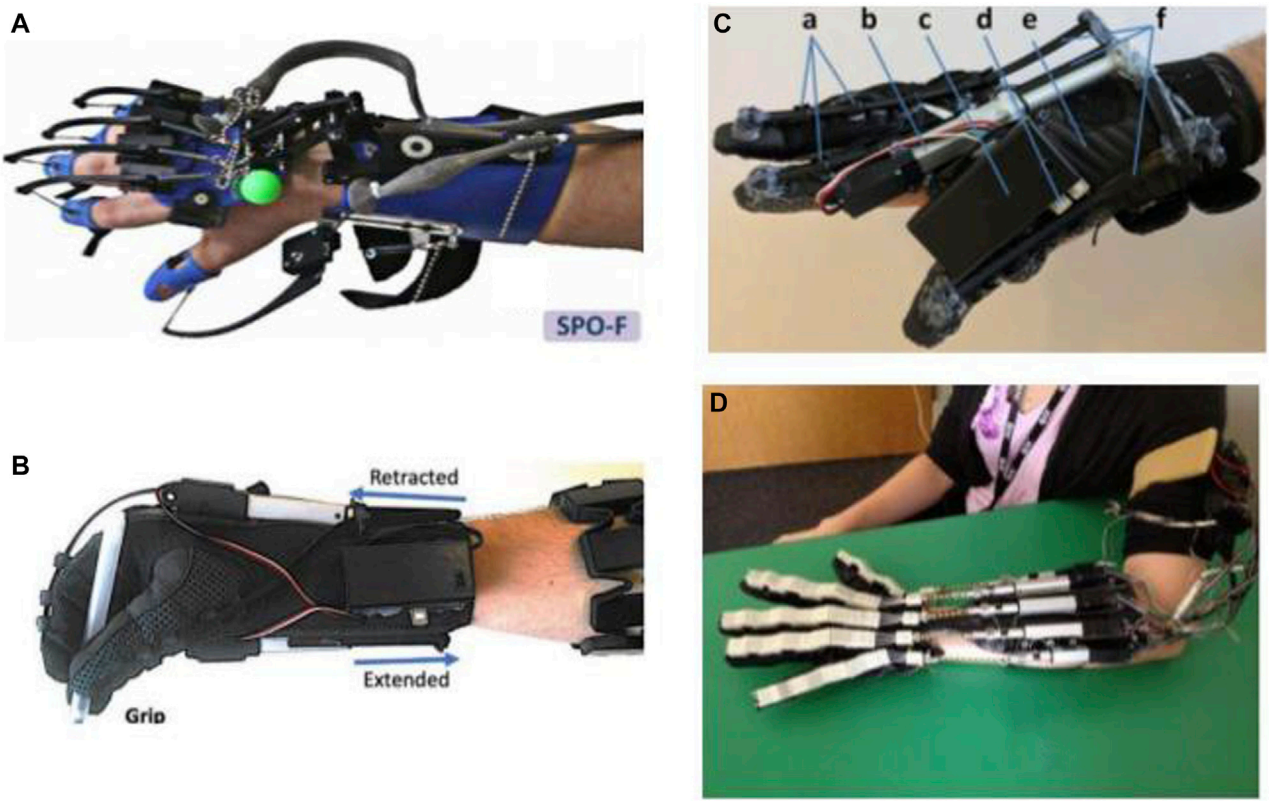

FIGURE 1 | Robotic gloves and exoskeleton devices for home-based hand rehabilitation: **(A)** SCRIPT project (Ates et al., 2017), **(B)** My-HERO (Yurkewich et al., 2020), **(C)** HERO (Yurkewich et al., 2019), and **(D)** X-Glove (Triandafilou, 2014).

design process. A universal and ambidextrous grip is utilized to allow both left- and right-hand usage and to be adjustable to different hand sizes without changing the attachment. Both active and passive motion assistance in a game context is provided based on the ability of the user. Also, automatic customization is allowed by receiving user information from a mobile interfacethrough an integrated internet of things (IoT) network to monitor and communicate with the therapist. Ambidexter is lighter and smaller compared to its commercial counterparts, ReachMan and ReachMan2.

A novel home-based End-effector-based Cable-articulated Parallel Robot, PACER—Parallel articulated-cable exercise robot—, was developed by Alamdari et al. for post-stroke rehabilitation (Alamdari and Krovi, 2015). The device features a modular and reconfigurable design and is easy to assemble/disassemble. The device is able to assist and train the muscles involved in arm, forearm, and wrist motions. In 2018, Díaz et al. (2018) conducted research on converting a large pneumatic commercialized device, which had been designed for clinical therapy, into an electric and compact system for home rehabilitation by making it smaller, lighter, and cheaper, but maintaining the functionality (Díaz et al., 2018). It resulted in the development of HomeRehab, a desktop-type 2DOF robotic system intended to improve ROM and strength of the paretic hand in stroke patients. Designed for the home environment, all the components are concentrated in a small portable box, and the device can easily be placed on a home table. VR and gamification are also enabled through a standard PC communication and a novel low-cost force sensor. Force feedback allowed both assistive—the assist-as-needed approach—and resistive scenarios to be implemented during the therapy, depending on the therapist's assigned task. Remote management is enabled by using wearable devices to record patient's biosignals and providing a cloud-based communication system. A comparison between PupArm, a commercialized rehabilitation device for clinical settings, and HomeRehab indicated that, while offering similar outcomes, the latter is significantly lighter; 80 vs. 7 kg (Catalan et al., 2018) (**Figure 2**).

ArmAssist (Tecnalia R&I, Spain) is a portable, modular, easy-to-use, low-cost robotic system consisting of a tabletop module using omni-wheels, an arm, and hand gravity compensator orthosis aimed at post-stroke shoulder and elbow rehabilitation. Also, at the University of Idaho, add-on modules for wrist prono-supination and hand grasping training have been presented. Over the years, the device has been iteratively redesigned based on the updated requirements gained from clinical interviews, expert focus groups, and pilot tests with patients and therapists (Perry et al., 2012; Jung et al., 2013; Perry et al., 2016; Butler et al., 2017; Tomić et al., 2017).

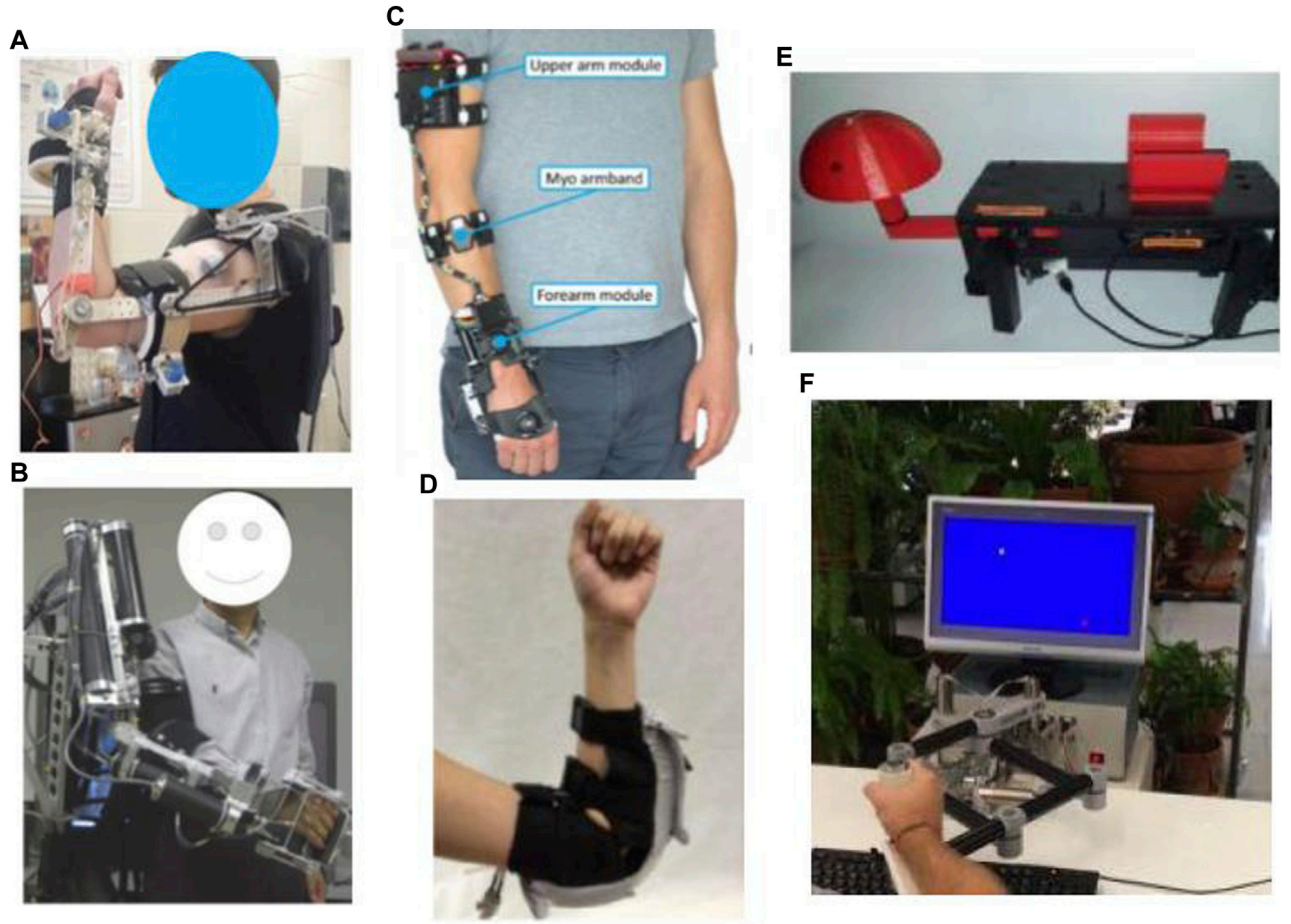

FIGURE 2 | Robotic exoskeleton and end-effector devices for home-based upper-limb rehabilitation: **(A)** SpringWear (Chen and Lum, 2018), **(B)** RUPERT (Tu et al., 2017), **(C)** eWrist (Lambelet et al., 2020), **(D)** Soft robotic elbow sleeve (Koh et al., 2017), **(E)** Portable device for wrist rehabilitation (Ambar et al., 2017), and **(F)** HomeRehab (Díaz et al., 2018).

As an intermediate step between high-power active and passive assistive robots, Westerveld et al. developed a low-power three-dimensional damper-driven end-point robotic manipulator, called active therapeutic device (ATD) (Westerveld et al., 2014). ATD provides a combination of passive arm weight support and assistance for functional reaching training. Increasing its potential for home-based therapy, the device deployed an inherently safe and compact system design. Washabaugh et al. designed a planar passive rehabilitation robot, PaRRo, that is fully passive yet provides multi-directional functional resistance training for the upper-limb (Washabaugh et al., 2019). This happens through integrating eddy current brakes with a portable mechanical layout that incorporates a large reachable workspace for a patient's planar movements. The considered kinematic redundancies of the layout allow for posing direct resistance to the patients' trajectories.

Commercially Available Devices

Based on the premise that the best way to reacquire the capability to perform a task is to practice that task repeatedly, Saebo Inc. proposed SaeboVR, a non-immersive VR rehabilitation system incorporating motivating games. These games are designed to simulate activities of daily living (ADL) and engage patient's impaired arm in meaningful tasks aiming to evoke functional movements (Recover From Your Stroke With Saebo, 2017). The goal of the customizable tasks is to test and train user's cognitive and motor skills such as endurance, speed, range of motion, coordination, timing, and cognitive demand, e.g., visual-spatial planning, attention, or memory, under the supervision of a medical professional in a home setting. The device includes a Provider Dashboard application that enables the medical professional to view patient performance metrics and participation history while providing audiovisual feedback and graphic movement representation for patients.

To target a specific group of patients with various treatment options, this device can be upgraded with additional technologies, e.g., SaeboMas, SaeboRejoyce, or SaeboGlove, which can be integrated into the virtual environment. SaeboGlove, a functional hand orthosis, combined with electrical stimulation, has been shown to be beneficial for functional use of moderately

to severely impaired hands in sub-acute stroke patients (Franck et al., 2019). SaeboMAS, a zero-gravity upper extremity dynamic mobile arm support device, provides the necessary weight support in a customizable manner, facilitating exercise drills and functional tasks for the individuals who have arm weaknesses (Runnalls et al., 2019). The usage of this technology will potentially allow patients with proximal weakness to reach a larger anterior workspace and engage in more versatile functional tasks and exercises that would have otherwise been difficult or impossible. The SaeboReJoyce is an upper extremity rehabilitation computerized workstation that includes pre-installed neurogaming software and offers task-oriented and customizable games. The workstation is composed of two components. A lightweight height-adjustable and portable gross motor component makes the device useful for sitting, standing, and lying positions and enables the execution of exercises and tasks in all directions and planes. A fine motor component aims at improving necessary dexterity for daily tasks by incorporating various grip and pinch patterns, such as spherical grasp, grip strength, wrist flexion/extension, tip to tip pinch, and pronation/supination, among others. Several studies have been conducted to prove the efficacy and results of Saebo products (Adams et al., 2018; Doucet and Mettler, 2018; Runnalls et al., 2019).

Another home rehabilitation device for post-stroke patients is WeReha, which is intended to be used for hand impairments with the possible remote supervision of physiotherapists (Bellomo et al., 2020). The primary purpose of this device's invention is to train the fine movements of the hand and simultaneously stimulate the cognitive aspect, exploiting the biofeedback technology. It can track patient movements with the 3D printed "smart" objects equipped with inertial sensors while transmitting data via Bluetooth to the software. The software processes the data and produces visual-auditory feedback to guide the patient. Such guidance enables the patients to correctly execute various motor tasks through the exercises in the specially designed and studied video games that allow them to exercise the grip of finer or larger objects. Moreover, simple and effective gamification is based on indexes of rotation, flexion-extension, and prono-supination of the upper-limb.

The soft extra muscle (SEM) Glove by Bioservo Technologies AB, Sweden (BIOSERVO, n.d.), was developed to improve the hand's grasping capacity by providing additional finger flexion strength. This novel technical solution simultaneously mimics a biological solution and functions in symbiosis with the biological system that excludes the need for an external mechanical structure to achieve controlling and strengthening effects. The servo device uses artificial tendons connected to electrical motors that actuate finger movements by creating pulling forces. The device features intention detection to apply proportional finger flexion strength facilitating grip or object manipulation, benefitting from control algorithms that are based on tactile sensor signals located on the tip of fingers. The efficacy of SEM Glove has been evaluated for improving gross and fine hand motor functions for at-home rehabilitation for people with impaired hand function after high-level spinal cord injury, yet further investigation is required for its efficiency for post-stroke rehabilitation (Nilsson et al., 2012; Osuagwu et al., 2020). Based on the SEM Glove technology and with the aim of extending its application for stroke rehabilitation at home, Radder et al. designed IronHand, a lightweight and easy-to-use soft robotic glove that thanks to the soft and flexible materials used for its fabrication, accommodates wearable applications (Radder et al., 2019). The IronHand, formerly known as HandinMind (HiM) project, offers an easy-to-use combination of assistive functionality during ADL and therapeutic functionality through a training context within a motivating game-like environment (Prange-Lasonder et al., 2017). They allow individuals with reduced hand function to use their hand(s) during a large variety of functional activities. The therapeutic functionality of the device incorporates a therapeutic software platform for patient assessment and database and it covers therapy goals of simultaneous finger coordination, hand strength and sequential finger coordination (Radder et al., 2018). The assistive functionality provides extra strength to the grip of fingers after the active contribution of the user's grip force, and an intention detection logic ensures that extra force proportional to that of the user is activated. IronHand is one of the first user trials that applied and tested a fully wearable robotic system in an unsupervised home setting to support hand function during an extended period of multiple weeks. Findings from this extensive trial indicated improvements in unsupported handgrip strength and pinch strength (Radder et al., 2019).

In an attempt to transfer Gloreha—Hand Rehabilitation Glove—Professional, a wearable hand rehabilitation hospital device, to a home setting, Gloreha Lite has been miniaturized and specifically designed for home use in a safe and feasible way for hand rehabilitation (Bernocchi et al., 2018). Gloreha Lite is a portable, lightweight, and space-saving glove-brace (Aggogeri et al., 2019). The robotic glove represents a relevant adjunct intervention to intensify activity-based therapy, integrating the principle of neuroplasticity with the intensity of treatment (Proulx et al., 2020). It provides computer-controlled passive mobilization of the fingers. Before each exercise drill, a 3D-simulated preview of the movement is presented on the monitor, and during the performance of the movement, a simultaneous 3D simulation of the movement is displayed as it is being performed. Bernocchi et al. evaluated and demonstrated the feasibility and safety of the device for in-home therapy and indicated improvement of functional capacity of the paretic hand. They also demonstrated that the acquired benefits on strength and dexterity were maintained over time. The majority of patients completed the entire course of the program while performing all the prescribed home exercises.

The Motus Hand (Motus Nova, n.d.) (https://motusnova.com/hand), previously known as Hand Mentor Pro, is a portable robotic device designed to enhance active flexion and extension movements of wrist and fingers along with motor control of the distal upper limb. The device deploys pneumatic artificial muscles for simulating dorsal muscle contraction and relaxation. The Motus Hand has been classified as an FDA class 1 device presenting non-significant risk (NSR). Several clinical trials investigated and supported the clinical efficiency, feasibility, and user-friendliness of the Motus Hand for in-home

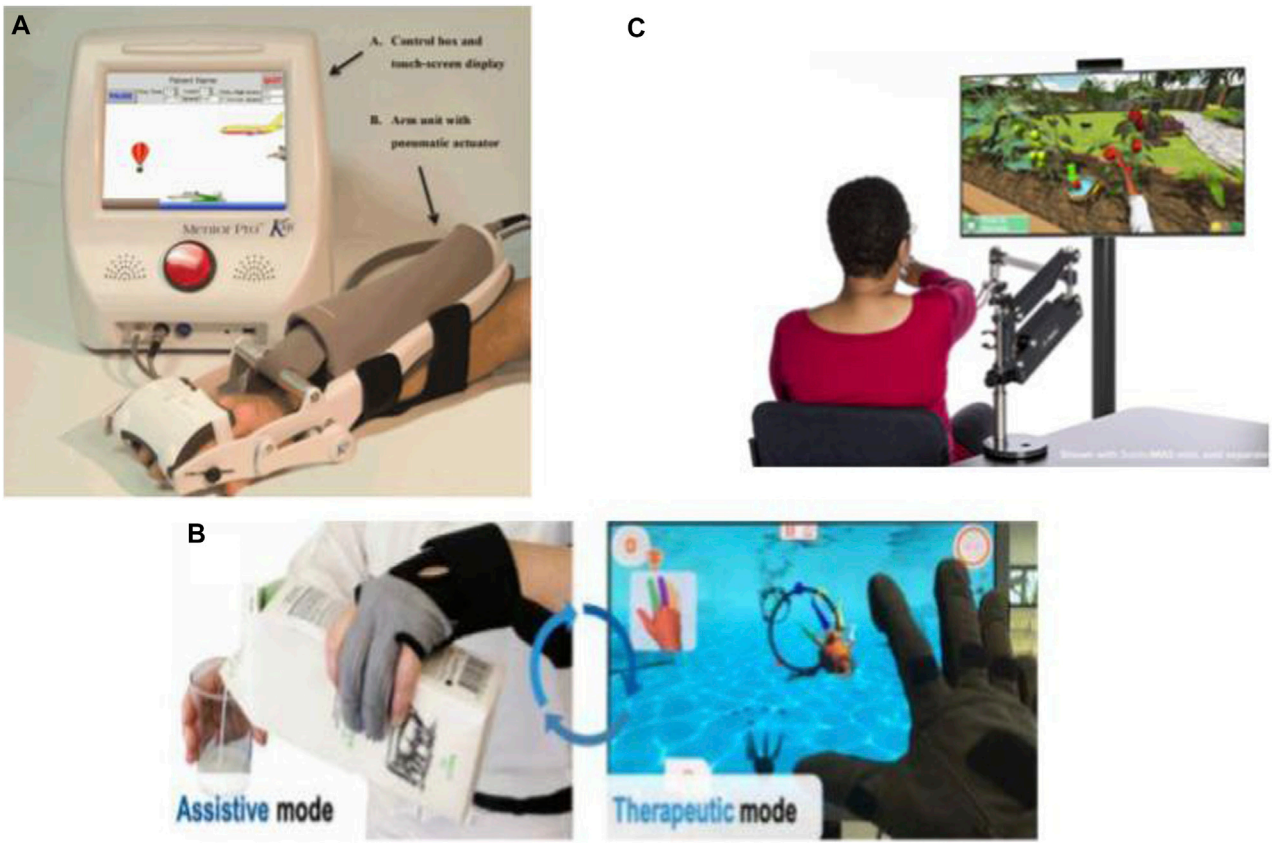

FIGURE 3 | Commercialized robotic devices for home-based upper-limb rehabilitation: **(A)** The Motus Hand (Butler et al., 2014), **(B)** IronHand (Radder et al., 2019), and **(C)** SaeboVR (Recover From Your Stroke With Saebo 2017).

telerehabilitation among subacute to chronic post-stroke (Linder et al., 2013a; Linder et al., 2013b; Butler et al., 2014; Wolf et al., 2015) (**Figure 3**).

Hyakutake et al. investigated the efficiency and feasibility of home-based rehabilitation involving the single-joint hybrid assistive limb (HAL-SJ) (Hyakutake et al., 2019). Drawing on the "interactive biofeedback" theory, HAL-SJ is a lightweight power-assisted exoskeleton on the elbow joint triggered by biofeedback for assisting the patient in the voluntary movements of the affected upper limb.

Lower-Limb

State-of-the-Art: Systems in the Literature

Many developed lower-limb robotic systems offer rehabilitation in sitting/lying positions for stroke patients who cannot stand or walk safely (Eiammanussakul and Sangveraphunsiri, 2018). In this approach, the patients may exercise more independently with no safety concerns like falling. Therefore, compared to the other lower-limb rehabilitation principles, such as treadmill gait trainers, this kind of lower-limb device shows considerable potential for in-home therapy. Moreover, these robots are potentially suitable for home environments, as they can be smaller, lighter, and portable.

Spasticity of the limbs is one of the most common impairments ensuing onset of stroke. It puts patients at a high risk of developing foot deformity. Hence, treating the spasticity of lower extremities to prevent any deformity and facilitate ankle muscle activities during the acute phase and even after the long bedridden period is of utmost importance. In order to reduce or prevent the occurrence of spasticity at later stages, Low et al. developed a soft robotic sock, which can provide compliant actuation to simulate natural ankle movements in the early stage of stroke recovery. The soft robotic sock controls the internal pneumatic pressure of the soft extension actuators to assist the patient in ankle dorsiflexion and plantarflexion (Low et al., 2018; Low et al., 2019). For the same purpose, Ren et al. also developed a wearable ankle rehabilitation robotic device capable of delivering in-bed stroke rehabilitation in three training modes, active assistive training, resistance training, and passive stretching (Ren et al., 2017). These aforementioned devices mainly target people with acute stroke; Nonetheless, to treat chronic stroke survivors who have already developed ankle-foot deformities or imbalanced ankle muscles, Lee et al. developed a relatively small, lightweight, and user-friendly rehabilitative system, called Motorized Ankle Stretcher (MAS) (Beom-Chan et al., 2017; Yoo et al., 2019). The MAS consists of two linear in-line actuators, each connected to a platform for generating ankle dorsiflexion and eversion. The system requires patients to perform exercises in the standing position, with a walker

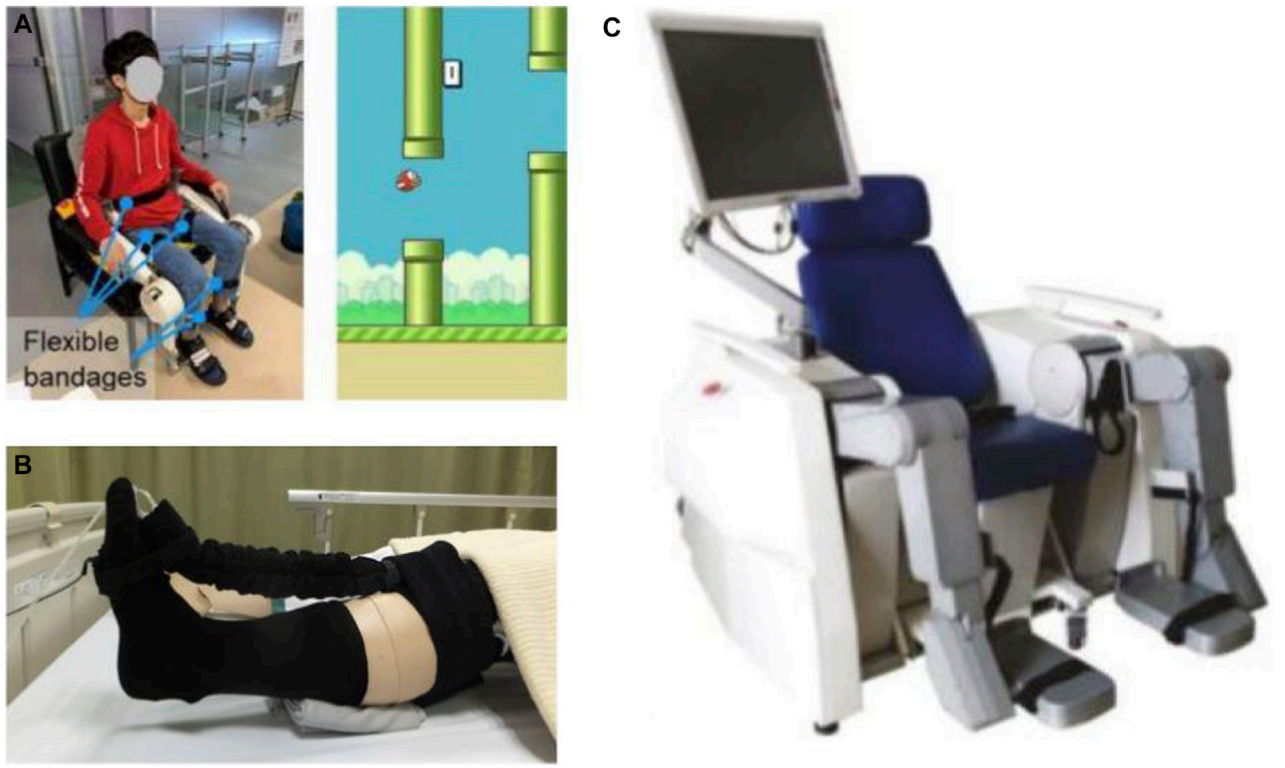

FIGURE 4 | Robotic devices for sitting/lying home-based lower-limb rehabilitation: **(A)** EMG-Controlled Knee Exoskeleton (Lyu et al., 2019), **(B)** Soft Robotic Sock (Low et al., 2019), and **(C)** LLR-Ro (Feng et al., 2017).

positioned in front of them for safety concerns. The above-mentioned devices have not yet been implemented in home-setting but are deemed potentially feasible by the authors in terms of safety, size, portability, complexity, and user-friendliness. However, the clinical efficiency of these devices for in-home treatment requires further investigation.

As one of the first home-based EMG-controlled systems, Lyu et al. (2019) developed a knee exoskeleton within a game context to be used while the subject was seated on the chair wearing the exoskeleton. Utilizing four active DOF at both hip and knee, the exoskeleton improves knee joint movement stability and accuracy by strengthening anti-gravity knee extensor muscles. The robot can be generally considered a successful effort at designing a home-based system by being adjustable to the wearer's leg length, with a quick setup time of approximately 1 min, and considering safety cautions in all stages of software, electrical, and mechanical. Initial testing on healthy subjects represented promising results on the possibility of carrying out early rehabilitation by this device, the amount of muscle activation by the participants, and the timing of that activation.

Another example of lower-limb devices is a multi-posture electric wheelchair developed by Chen et al. with a lower-limb training function. Combined with virtual reality games and a tele-doctor–patient interaction, this device forms an intelligent rehabilitation system suitable for home therapy (Chen S. et al., 2017). Apart from rehabilitation training, it can be used as an everyday wheelchair. This hybrid nature of the design has made it economically efficient. The wheelchair is equipped with four linear motors to carry out the training function and the lying/standing process, and is controlled by a cell phone interface. The system also benefits from a communication platform through web-based interfaces for patients and doctors. As another genre of lower-limb rehabilitation robots seemingly viable for home implementation, a sitting/lying Lower Limb Rehabilitation Robot (LLR-Ro) was developed containing a moveable seat and bilaterally symmetrical right and left leg mechanism modules, each comprising the hip, knee, and ankle joints. This device benefits from mechanical, electrical, and software safety features and an amendment impedance control strategy to realize good compliance (Feng et al., 2017) (**Figure 4**).

One of the most prevalent lower-limb impairments following hemiplegia in post-stroke patients is asymmetric gait patterns and balance dysfunction. These impairments can adversely affect the quality of life as they lead to compensatory movement patterns, slowed gait speed, limited functional mobility, which results in reduced performance of the activities of daily living and increased risk of experiencing falls. Therefore, regaining autonomous gait and improving independent walking ability should be among the top priorities of rehabilitation interventions post-stroke. Aimed at improving stability and walking capacity, Morone et al. introduced i-Walker, a robotic walker for overground training with embedded intelligence that provides asymmetrical assistance as needed by detecting the imposed force by the user to adjust the amount of help to the impaired side (Morone et al., 2016).

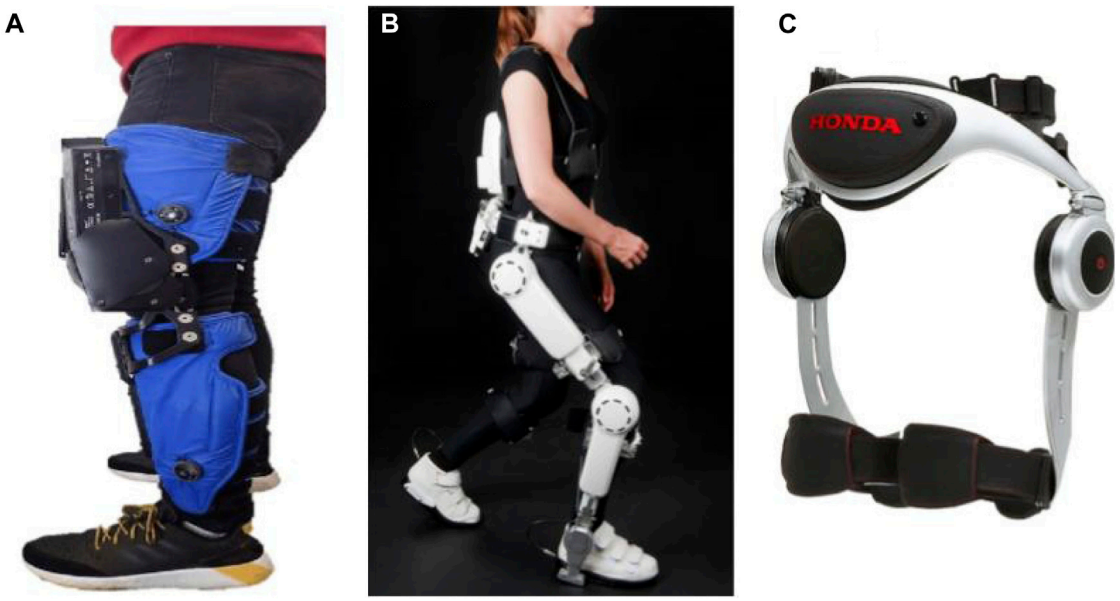

FIGURE 5 | Robotic devices for in-home walking training: **(A)** AlterG Bionic Leg (Wright et al., 2020), **(B)** HAL lower-limb exoskeleton (Anneli Nilsson et al., 2014), and **(C)** SMA (Buesing et al., 2015).

Developing wearable robots for lower-limb treatments has increasingly gained traction for their capability to facilitate ambulatory rehabilitation delivery. Among them, Gait Exercise Assist Robot (GEAR), proposed by Hirano et al. in collaboration with Toyota Motor Corporation, is a wearable knee-ankle-foot robot (only for the paralyzed leg) integrated with a low floor treadmill and a safety suspending device (Hirano et al., 2017; Tomida et al., 2019). The Lokomat (Hocoma AG, Volketswil, Switzerland) is a commercial widely used exoskeleton-type robot for gait training worn over both lower extremities, consisting of a combination of adjustable orthoses, a dynamic bodyweight support system, and virtual reality for providing sensory-motor stimulation (van Kammen et al., 2017). Although the clinical efficacy of wearable devices for lower extremity is supported by a growing body of evidence (Hidler et al., 2009; Tomida et al., 2019; Mehrholz et al., 2020), only a number of them are realizable in a home setting with modifications addressing various factors, e.g., safety issues, size, weight, portability, complexity, and cost. Among robotic rehabilitation devices of the past ten years, those provisioned for home therapy only requiring further investigation validating their clinical efficiency at home are presented.

Walking Assist for Hemiplegia (WA-H) is a portable, lightweight, modular, and wearable exoskeletal robot supporting the hip and knee joint movements that, by providing customized gait training, can be used in various environments depending on the degree of impairment in patients. WA-H has an inherently safe design in which all robot joints mechanically limit the movements occurring beyond the natural range of motion. The device features a passive joint simulating the weight shift occurring during walking in the hip joint in the coronal plane (Moon et al., 2017; Sung et al., 2017).

As both rehabilitation and welfare robot, Curara® is a wear robot that assists hip and knee joints in both impaired and unaffected legs simultaneously with no rigid connection between joint frames, resulting in a higher degree of freedom. Prioritizing user-friendliness in terms of ease in don/doffing and minimizing the restraining stress against the natural human movement, Mizukami et al. adopted a non-exoskeletal structure coupled with a synchronization-based control system, introducing the ability to feel what natural movement would be like. Due to the absence of any rigid connection between joint frames, the device provides a high degree of freedom for patient movement (Tsukahara and Hashimoto, 2016; Tsukahara et al., 2017; Mizukami et al., 2018). Lee et al. developed a smart wearable hip-assist robot for restoring the locomotor function, the Gait Enhancing and Motivating System (GEMS, Samsung Advanced Institute of Technology, Suwon, South Korea). GEMS is equipped with an assist-as-needed algorithm for delivering active-assistance in hip extension and flexion (Lee et al., 2019; Lee et al., 2020) (**Figure 5**).

Interposed between active and passive training robots, Washabaugh et al. proposed their eddy current braking device on a knee brace as a wearable passive alternative that provides functional resisted gait training while adhering to features required for home-based devices (Washabaugh et al., 2016; Washabaugh and Krishnan, 2018).

Commercially Available Devices

There are several commercially available lower-extremity rehabilitation robots, and those exhibiting potential for home therapy are presented. The wear overground robotic Stride

Management Assist (SMA®) is developed and available for purchase (Honda Global, 2020) by Honda that assists hip joint movements for increasing walking performance independence (Buesing et al., 2015). The ReWalk ReStore™ is a soft exosuit designed and introduced by ReWalk (2019) for actively assisting paretic ankle plantarflexion and dorsiflexion for the propulsion and ground clearance walking subtasks (Awad et al., 2020). ReWalk Robotics also proposed the ReWalk Personal 6.0 System as a customizable exoskeleton with motors at the hip and knee joints specifically designed for all day home-use (ReWalk, 2015). EksoNR is an FDA-cleared ambulatory exoskeleton featuring adaptive gait training and posture support, yet it is currently being tested in a clinical trial with stroke patients for evaluating its clinical efficiency (Carlan and singleorigin, 2020) (https://eksobionics.com/eksonr/).

Different exoskeletons have been developed based on the HAL's technology to offer active motion support systems with a hybrid control algorithm, Cybernic Voluntary Control for providing physical support associated with the patients' voluntary muscles activity and Cybernic Autonomous Control that utilizes characterized movements of healthy subjects and adopts the motion patterns in accordance. One such device has been described in the prior section for elbow rehabilitation. Kawamoto et al. also, based on this technology, developed the single-leg version of the HAL, an exoskeleton-based robotic suit for independent supporting of the ankle, knee and hip joints (Kawamoto et al., 2009). Kawamoto et al. and then Nilsson et al. investigated the efficiency of this exoskeleton for intensive gait training for chronic and acute, respectively, hemiparetic patients (Kawamoto et al., 2013; Nilsson et al., 2014). The device is commercially available in Japan (Cyberoyne, 2021).

The AlterG Bionic Leg (AlterG, 2015; AlterG, n.d), a portable dynamic battery-operated over-ground wearable lower extremity orthosis, provides adjustable progressive mobility training by supplementing existing muscle strength, providing audio-sensory feedback and mobility assistance during rehabilitation (Stein et al., 2014; Iida et al., 2017; Wright et al., 2020). This dynamic orthosis supports knee mobility when standing or walking by providing external support to the lower extremity and assisting the patient in aid of weight shifts and knee movement and can be worn in a manner similar to an orthopedic knee brace.

DESIGN PARADIGM

The interdisciplinary field of rehabilitation requires the simultaneous employment of a range of expertise, including engineering, medicine, occupational therapy, and neuroscience, especially due to the lack of enriched research in motor learning principles for optimized post-stroke motor recovery (Krakauer, 2006; Brewer et al., 2007). A successful home rehabilitation device can be designed within a certain sequence of steps that incorporate all of the aforementioned expertise, as skipping one could prevent achieving optimum outcomes.

Mechatronic home-based systems for post-stroke therapy are based on four basic components: 1) a mechatronic device delivering rehabilitation intervention, 2) a control system ensuring proper performance of the system, 3) interactive interfaces for patients and medical professionals who provide remotely supervised therapy, 4) a communication system gluing the whole system together.

To provide a classified roadmap for assisting researchers who aim at further developing this field, a design paradigm is proposed to form a guideline on developing each component based on the engineering design process.

Post-Stroke Rehabilitation and Treatment Interventions

Among different post-stroke symptoms, motor deficits are the most commonly recognized impairments that affect the face, arm, and leg motor functions. These impairments result in various manifestations, including impaired motor control, muscle weakness or contracture, changes in muscle tone, joint laxity, spasticity, increased reflexes, loss of coordination, and apraxia (Basteris et al., 2014; Hatem et al., 2016). To recover lost function and aid motor recovery, many rehabilitation interventions have been developed based on neurorehabilitation principles (Basteris et al., 2014). So as to develop a robot-assisted therapy that offers maximal motor function recovery, it is essential to employ interdisciplinary research on the broad spectrum of post-stroke disabilities and their corresponding rehabilitation protocols. The outcomes could help create a clear picture of the target users, establish target and rehabilitation program specifications, and derive requirements from the needs of all stakeholders, the largest being the therapists and the patients. Note that it is essential for the device to be accepted by medical professionals. From the therapists' point of view, the crucial features for iterative design and modification of each rehabilitation robot must be surveyed and practiced carefully.

Engineers should develop the rehabilitation system based on multiple contributing factors, including the part of the limb being trained, the targeted stage of recovery, the severity of initial motor deficit, range of movements in the paretic limb, grade of spasticity, age, and individual patient's characteristics. Depending on the patient, it is known that motor impairments can induce disabilities in several functions, such as range of motion, speed, coordination, cadence (steps/minute), balance, precision, the ability to regulate forces, muscle strength, and energy efficiency (Perry et al., 2011). Physiological measurements during rehabilitation, i.e., heart rate, blood pressure, body temperature, etc., assist in sensing the patient's status during therapy and their capability to do exercise, and in turn, offer a foundation for determining the dosage of assigned tasks based on one's capability (Solanki et al., 2020). Monitoring physiological parameters could also be utilized for detecting the user's psychological state, in terms of mood, motivation, engagement, etc., and lead to modification of the course of therapy accordingly (Novak et al., 2010). It is important to tailor treatment strategies to the goals of improving one or a combination of these functional disabilities. Current robotic rehabilitation systems incorporate a variety of neurorehabilitation strategies. These strategies include

constraint-induced movement therapy (CIMT), repetitive movement training, impairment-oriented training, explicit learning paradigms such as bilateral training, implicit training, and functional task paradigms (Brewer et al., 2007). Given training goals as guidelines, a combination of these interventions can be utilized in order to develop a reasonable user-specific program with respect to the aforementioned critical factors (Hatem et al., 2016), as different types of tasks are necessary to retrain all lost function.

Recovery would benefit if scientific principles behind post-stroke motor learning were incorporated into the design of the rehabilitation device. Under the assumption that performance improvement is dependent on the amount of practice, most current mechatronic devices for post-stroke therapy are solely based on the repetition of a single task, termed "massed practice" (Brewer et al., 2007). It is important to note that, although repetition is the key to improving within-session performance, other critical factors must be considered while scheduling rehabilitation protocols. As Krakour et al. state, there are two crucial questions to ask before developing any rehabilitation system: "whether gains persist for a significant period after training and whether they generalize to untrained tasks" (Krakauer, 2006; Kitago and Krakauer, 2013). There is evidence that "distributed practice," which means inserting more extended rest periods between repetitions, e.g., increasing the number of sessions while decreasing session duration, promotes retention (Krakauer, 2006; Kitago and Krakauer, 2013). While limitations of clinical therapy preclude the proper implementation of this method, home-based therapy provides the opportunity of distributed task scheduling in a way that it can always be at the patients' disposal.

For rehabilitation interventions to be meaningful, learned tasks must generalize to new tasks or contexts, especially real-world tasks. Introducing variability to training sessions, though worsening the patients' performance in the short term, improves their performance in retention sessions and also increases generalization by representing each task as a problem to be solved rather than just memorized and repeated (Krakauer, 2006; Kitago and Krakauer, 2013). Contextual interference is a concept used to introduce variability to the task by random ordering between several existing tasks. Moreover, recovery of function to increase patient autonomy is another important aspect of rehabilitation. It seeks to consider training for true recovery, as well as, compensatory mechanisms—respectively accomplishing task goals by recruiting the affected muscles or alternative muscles (Krakauer, 2006; Kitago and Krakauer, 2013). Nevertheless, when establishing goals for rehabilitation interventions, there has to be a clear distinction in mind between these two, true or compensatory recovery, as they may make differential contributions to the treatment plan.

Mechatronic System

Once the target group and treatment plan have been identified, the design criteria, including requirements and constraints, need to be established and prioritized to fit the need. Since the device is being designed for the home setting, certain factors are introduced, and some others become more prominent—safety, adaptability to the home setting, the autonomy of patients, aesthetic appeal, affordability, to name a few (Carbone et al., 2018; Chen et al., 2019).

Design Criteria for Home-Use

In addition to the general criteria, the adoption of each home rehabilitation solution requests specific features of the device itself. For example, in the case of exoskeletons, besides absolute safety when worn, lightness, wearing ease, comfortability, and smoothness, there should be an absence of friction and allergenic factors as it is in contact with the skin. So the device should guarantee a high tunability and reliability (Borboni et al., 2016). Considering all of the factors and criteria, a solution has to be adopted, which offers a satisfactory compromise to each of the existing issues and requests of all parties involved, as all of the requirements affect the device's structure. Also, there are some optional and preferable criteria, among which expandability and upgradability are favorable to cover a wide range of disabilities and possible treatment methods. To this end, modularization benefits both manufacturers and customers for it increases diversity and a variety of available options and enables interchangeability and compatibility. This way, various gadgets could be developed to be integrated into a wide range of existing home-based devices, which in turn enhances both acceptability and functionality. For example, Amirabdollahian et al. in the SCRIPT project and Kutlu et al. in their home-based FES rehabilitation system utilized commercialized Saebo module, SaeboMAS arm support (Amirabdollahian et al., 2014; Kutlu et al., 2017). Moreover, the donning aspect of robotic devices in an unsupervised context should be underlined. Therefore, attachment mechanisms should be designed to enable facilitated and independent donning and doffing of the device by the patient. In this regard, Lambelet et al. designed the eWrist to offer easy and fast donning/doffing to enable single-handed mounting of the device for hemiparetic patients, significantly promoting the autonomy of the patient were they to train independently (Lambelet et al., 2020). Equivalently, Fischer et al. realized facilitated donning of X-Glove by means of adopting a two-separate component design, a zipper on the palmar side, and a flexed wrist posture (Fischer et al., 2016). It should be flexible to be used in different positions, such as sitting/lying for bedridden or chaired individuals, and also light enough to be easily transportable. Another criterion that needs to be taken into account is that the device's functioning noise must be as low as possible to be acceptable by the patient (Borboni et al., 2016).

Mechanism Type

Having design criteria and target functionality in mind, the designer has to decide the mechanism type. The type of the mechanism and the treatment options are correlated; for example, additional movement protocols can be utilized based on the number of arms. In general, human limb rehabilitation robots are divided into two groups based on the target limbs: upper-limb rehabilitation devices and lower-limb rehabilitation devices, each divided into several subgroups. Based on motion systems, upper-limbs are categorized into exoskeletons or end-

effector devices. Based on the patient's posture, lower-limb devices can be designed to be used in sitting/lying positions or standing positions with the help of body and robot weight support.

In his study in 2019, Aggogeri et al. categorize robotic rehabilitation technologies into end-effector or exoskeleton devices based on design concepts (Aggogeri et al., 2019). End-effector devices, also known as endpoint control, determine the joint level movements by recreating dynamic environments corresponding to ADL. End-effector devices may be dedicated to hand rehabilitation or integrated into more complex structures for arm recovery. Attached to the user's limbs, exoskeletons are wearable robots aiming at enhancing their movements. Focusing on the patient's anatomy, each degree of freedom of the device is aligned with the corresponding human joint. Exoskeletons should be compliant with the user's movements and deliver part of the power required by the movements. Therefore, the mechanical axes of exoskeleton joints and anatomical joints should be aligned to prevent patient discomfort and not obstruct natural limb movement (Fischer et al., 2016). In designing exoskeletons, the high sensitivity of stroke survivors to the applied mechanical load on their paretic limb makes the weight of the device an important factor to be considered. Reducing the applied load on the impaired limb can be achieved through locating the components not directly involved in actuation—e.g., battery and controller—on more proximal rather than distal body parts. For example, Fischer et al. provided an upper arm module for locating the battery and electronics, resulting in the reduced weight of the forearm module located on the distal part of the arm (Fischer et al., 2016). Equivalently, in the ReWalk Restore lower-limb exosuit, the actuation pack is worn at the waist so that the larger proportion of device weight is located proximally (Awad et al., 2020).

Comparing these two different approaches, end-effector robots are more flexible than exoskeleton devices in fitting the different sizes, require less setup time, and increase the usability for new patients. Besides, end-effector mechanisms are also generally ambidextrous. On the contrary, exoskeletons should be fully user-adjustable and therefore require more complex control systems. While both distal and proximal joints are constrained in exoskeleton devices, end-effector robots merely constrain the distal joints (Aubin et al., 2013). Therefore, explicit control of each individual joint is only possible with exoskeleton devices. The limited control of end-effector robots could result in abnormal movement patterns in patients. In contrast, due to the direct controllability of individual joints in exoskeletons, these abnormal postures or movements are minimized (Aggogeri et al., 2019).

In conventional exoskeleton mechanisms, the rigidity of the frames and fixed straps poses an issue on their wearability and usability. The heaviness and bulkiness of such frames result in high energy cost and also affects the natural gait dynamic and kinematics of the patient. Hence, soft orthotic systems have been developed as an alternative to traditional rigid exoskeletons (Lee et al., 2019). In this regard, soft robots have shown promising potential to be adopted for at-home rehabilitation. In their study, Polygerinos et al. argue that soft wearables could further advance home-based rehabilitation in that they provide safer human-robot interaction due to the use of soft and compliant materials, a larger range of motion and degrees of freedom, and increased portability. The materials used for the fabrication of these robots are inexpensive, making these devices affordable. Also, soft material makes these devices inherently lighter and, therefore, more suitable for rehabilitation purposes. Another advantage of soft robotic devices over conventional rehabilitation robots is that they can be fully adapted to the patient's anatomy offering a more customizable actuation (Polygerinos et al., 2015).

In rehabilitation devices, it is essential to improve physical human-robot interaction (pHRI). For each type of rehabilitation device, the recruitment of different engineering methods is required for such improvements. This interaction is fundamentally affected by the mechanisms that should be designed by taking sophisticated biological features and activities into account. By considering the compliance/stiffness factor, modes of actuation and transmission need to be selected in a systematic way. Control methods also affect pHRI (Gull et al., 2020).

Degrees of Freedom

The number of active and passive DOFs determines the system's functionality. They condition the workspace in which the joints are capable of moving, indicating the assistance/rehabilitation, which is needed to be delivered to each joint (Shen et al., 2020). Patients' anatomy should be incorporated into the design when determining a reachable workspace based on anthropometric norms of the end-user (Washabaugh et al., 2019). By reviews on upper and lower-limb devices, it can be figured out that the majority of the developed devices profit from certain degrees of freedom that are compatible with the human body's anatomy. Anatomically speaking, in the upper extremity, often simplified to have seven degrees of freedom, the shoulder is simplified as three rotary joints achieving extension/flexion, adduction/abduction, and internal/external rotation. Elbow and forearm are simplified to provide extension/flexion and pronation/supination movements, respectively. Lastly, the wrist achieves extension/flexion and radial/ulnar deviations. The seventh DOF in the upper extremity's joint space poses challenging complications since the maximum DOFs in the task space is six. Not only does this require us to have a firm understanding of how a human resolves this redundancy issue, but also such understanding must be taken into consideration when designing rehabilitation device mechanisms (Shen et al., 2020). Furthermore, fingers are simplified as joints capable of achieving flexion/extension and abduction/adduction movements.

In the lower extremity, the hip is simplified as three rotary joints to achieve flexion/extension, abduction/extension, and internal/external rotation. The knee achieves pure sagittal rotation and flexion/extension. And finally, the ankle, simplified into three rotation joints, achieves plantar/dorsiflexion, eversion/inversion, and internal/external rotation (Shi et al., 2019). The kinematic models should be developed by considering the anthropometric and morphology of human body structure in accordance with the command-and-control possibilities of actuated joints (Dumitru et al., 2018; Cardona and Garcia Cena,

2019). Joint movements during upper and lower-limb movements cause misalignments between the exoskeletal and human joint axes that need to be adjusted and fit to the position of joints. Some exoskeletal devices have addressed this issue by providing passive joints to trace the joint movements to enable of the wearer's natural range of motion. For example, Sung et al. equipped WA-H with passive hip joints in the coronal plane to enable weight shifting during walking (Sung et al., 2017). Also, Liu et al. incorporated three passive shoulder joints in their design to minimize the misalignments (Liu et al., 2021).

Modeling Tools

Modeling tools are of paramount importance in the design of rehabilitation devices for both robot and musculoskeletal modeling. Rigid body simulation programs or general-purpose simulation software such as Adams, Matlab, and Modelica can be used to evaluate the mechanics and control aspects. Also, computer-aided design software, such as CATIA and SOLIDWORKS, could be used to design, simulate, and analyze these robotic mechanisms. To simulate and control soft robots, SOFA, an open-source framework, can be used. It provides an interactive simulation of the mechanical behavior of the robot and its interactive control. It is also possible to model a robot's environment to be able to simulate their mechanical interaction.

On the other hand, the heavy dependence of design parameters upon the targeted application requires careful analysis of the human body anatomy to design the device by considering the end-user application (Gull et al., 2020). In turn, programs such as OpenSim and AnyBody can evaluate and predict the effect of the device on the human musculoskeletal system for any given motion. For example, in order to generate a digital exoskeleton model, Bai et al. exported the designed exoskeleton in CAD, SolidWorks, to AnyBody (Bai and Rasmussen, 2011). When it comes to musculoskeletal systems, software tools can significantly facilitate the process of derivation of the motion equations to model muscle force and path. Various musculoskeletal software packages are commercially available such as SIMM, OpenSim, AnyBody, and MSMS. Among these software packages, OpenSim is free and open-source software, and MSMS is a free software (Cardona and Garcia Cena, 2019). Muscle activation and muscular contraction dynamics of musculoskeletal models can also be used as a reference input signal for real-time controlling methods. For example, Liu et al. utilized an s-EMG-driven musculoskeletal model to adjust the stiffness control based on the patient's physical status and assigned task requirements (Liu et al., 2018).

Two commonly used dynamic modeling methods are Newton-Euler and Lagrange's methods. In the Newton Euler method, by solving the Newton-Euler equation, the robot's internal and external forces are extracted. In Lagrange's method, which is based on the system's energy, the external driving force/torque of the system can be calculated. In 2019 Zhang et al. drew a comparison between these two methods and provided a table to demonstrate the differences between these methods. Derivation analysis in the Newton-Euler method is more complicated than the Lagrange method, but calculations in the Newton-Euler method are large and heavier to compile, while in the Lagrange method, are easily compiled. In the Newton-Euler method, in addition to the driving force/moment, internal forces can be obtained (Zhang et al., 2019). Dynamic simulation can be carried out in Adams environment while theoretical calculations are performed in MATLAB. Zhang et al. use these simulations to provide a basis for the optimal design of the structure and the selection of the motor (Zhang et al., 2019).

Actuation and Transmission

The design of the device, further completed and integrated with the detailed design of chosen actuators, the transmission system, and the sensing system, should be presented at the next step. As there are myriad options to choose from, the designer has to weigh his/her options against the design criteria and their allocated importance and priority.

Efficient actuator design is important for home-based rehabilitation systems since these systems should be compact. Therefore, as the main powering elements, small-sized actuators that have a high power-to-weight ratio are required as they are capable of producing high torques with precise movement (Gull et al., 2020). Actuators should be chosen based on the target application. Three main categories of actuators are electric motors, hydraulic/pneumatic actuators, and linear actuators.

Electric motors are used for their quick responses and capability of providing high controllability and controlled precision. However, they have a low power-to-mass ratio and are usually expensive. Pneumatic actuators can yield high torques but could save self-weight. Nevertheless, by using these types of actuators, the portability of the system is compromised due to the accompanying inherent components such as pump, regulators, valves, and reservoirs. Another factor that makes these types of actuators unsuitable for home-based systems is that they require maintenance since lubricant/oil leakages could be problematic for users. In hydraulic and pneumatic actuators, control is less precise, and hence the safety cannot be ensured. According to Shen et al. and Gul et al., these actuators are not suitable for providing assistance or therapy or for rehabilitation purposes due to their possessing high impedances; however, some studies utilize them because of their ability to provide high power. Ultimately, based on the studies done by Gull et al., Series Elastic Actuators (SEAs) by reducing inertia and user interface offer a safe pHRI and can achieve stable force control (Gull et al., 2020). Tuning the stiffness of the transmission system is one of the approaches to achieve a specific level of compliance. In this regard, Jamwal et al. suggest using variable/adjustable stiffness actuators for rehabilitation purposes since these actuators offer safer human-robot interaction due to their ability to minimize large forces caused by shocks (Jamwal et al., 2015). Especially, employing SEA in lower-limb robots offers the advantage of a facilitated control-based disturbance rejection by improving tolerance to mechanical shocks, e.g., resulting from foot-ground impacts (Simonetti et al., 2018). According to Hussain et al., compliant actuators enable lightweight design with low endpoint impedance for wrist rehabilitation, while electromagnetic actuators are bulky and have high endpoint impedance (Hussain et al., 2020). Also, based on the study done by Chen et al., in 2016, compliant actuators are regarded as safe and

human-friendly. These actuators are preferable over stiff actuators for various reasons. For example, such systems can deliver controlled force with back-drivability and low output impedance and are tolerant against shock and impacts. Chen et al. suggest using SEAs for assistive and rehabilitation robots (Chen et al., 2016).

On the other hand, passive robots must be equipped with passive actuators to enable scalable resistance and assistance based on the patient's mobility status. There are various types of passive actuators such as friction brakes, viscous dampers, and elastic springs to name a few (Washabaugh et al., 2019).

Power transmission may be realized through the utilization of direct drive, gear, linkages, or cable-driven methods. Cable-driven transmission means allow for a more lightweight and compliant design. Backlash and transmission losses render the control of such systems challenging (Fischer et al., 2016). Sanjuan et al. classify cable-driven transmission into two categories of open-ended cables and closed-loop cables (Sanjuan et al., 2020). According to this study, open-ended cable systems exert forces in one direction, while close-ended cable systems exert friction forces (Sanjuan et al., 2020).

Sensing

In order to provide proper guidance for the device's movement to execute the required tasks, the system should utilize sensing methods as input signals. Generally, four main sensors are used in rehabilitation devices, namely Motion and Position sensors, Force/Torque sensors, Electromyograms (EMG), and Electroencephalogram (EEG) (Shen et al., 2020). Since the rehabilitation devices are directly in contact with the human body, they should be reliable and highly accurate to provide the control system with real-time feedback of moving components (Zheng et al., 2005; Porciuncula et al., 2018).

The spatial configuration of the device is needed in order to analyze its kinematics and dynamics. For this purpose, position sensors are used to measure and indicate this spatial configuration. Among the sensors used for this purpose are: encoders, potentiometers, flex sensors, and transducers. For haptic applications like rehabilitation in VR, force/torque sensors are required. Usually, extra force/torque sensors are added to the system to provide additional safety levels. Gyro and acceleration sensors can be mounted on the mechanical structure for measuring the patient's posture, for example, in HAL (Kawamoto et al., 2013).

Moreover, EMG and EEG could be used for measurements in noninvasive ways. The received signals in these two methods are often noisy and thus require further processing. Also, sensor fusion, in which the data from multiple sensors are merged, could provide a safer and more stable intention detection for the system.

Safety Measures

Last but not least, in the unsupervised context of home-based rehabilitation, safety is the most crucial criterion to be considered. Multiple redundant safety features must be incorporated in different modules of the device. In designing the mechanism stage, the device could be designed to offer intrinsic mechanical safety so as not to transfer excessive force to the patient's body. Also, abnormal reactions of the patient should not be transferred to the actuator. For example, in Gloreha, these eventual reactions are absorbed by the mechanical transmission (Borboni et al., 2016). In "Design Issues for an Inherently Safe Robotic Rehabilitation Device," Carbone et al. maintain that there are three major aspects that significantly affect the safety of the rehabilitation device, namely operation ranges, operation modes (speed, accelerations, paths), and operation force/torque (Carbone et al., 2018). Other measures could be taken to ensure safety; for example, Kim et al. utilized emergency stop buttons for both the user and the operator, hard stops at every joint, and also at the software level added safety features limiting the ROM and joint velocity and stopping the robot in case of excessive force/torque interaction (Kim and Deshpande, 2017). Feng et al. designed LLR-Ro to tackle the safety issue in three levels, i.e., mechanical limit, the electrical limit, and the software protection, to fully guarantee the limb safety of the patient in the whole training process (Feng et al., 2017). The device took advantage of inherent mechanical joint range of motion limits and limit switches placed on joint extreme positions to effectuate electrical limits and realizes the software protection according to the recorded patient information. Biomechanical, physiological, and even psychological information of patients can be utilized at software level safety checks to limit forces, motion, speed, and user adjustments to control parameters (Van der Loos and Reinkensmeyer, 2008).

Ultimately, at the end of each step, following the suit of the engineering design process, iterative optimization is needed to redefine the design process based on the predefined criteria. All of these design steps are highly interconnected and, therefore, should be considered from different aspects (Kruif et al., 2017). The HERO Glove was iteratively modified and redesigned based on evaluations and feedbacks from occupational therapists, specialized in stroke therapy, engineers, and stroke survivors (Yurkewich et al., 2019).

Control System

After considering the mechatronic aspects, the control system has to be developed to ensure the proper behavior of the device (Desplenter et al., 2020). From the hierarchy point of view, it is suggested to group the control system into three levels, mission planning, trajectory planning, and state space control, where the state space control can itself be in two levels of supervisory control and low-level control. The mission planning level is responsible for task assignment and completion. Task assignment includes enabling the therapist or task planning algorithms on the therapy control unit to customize task details such as treatment strategy, initial angles and positions, movement period and dwell, movement velocities, motion patterns, number of repetitions, range of motion, to name a few. At this level, IoT technology can be utilized to provide proper feedback from the treatment and identification of muscloskeletal parameters for the therapist, as well as therapist supervision. To this end, a mission planning module must be developed proposing a wide variety of options applicable to the mechatronic design; including multiple modalities and training protocols can increase the chance of adoption by medical professionals (Desplenter and Trejos, 2020).

According to the specified task, the trajectory planning level plans the kinematic and kinetic parameters of the motion to meet the objectives of the planned mission. For example, if the robot is supposed to provide a motion from an initial to a final configuration, the trajectory planning level designs the detailed variation of position, velocity and acceleration of the joints at each moment. If a force control mission is given, the force trajectory to be given to the control level is designed in the trajectory planning level. In the last level, the planned mechanical motion has to be implemented via the state space control level. Since the robot dynamic equations are normally nonlinear with unknown parameters and considerable uncertainties, a high-level supervisory control may be required to adaptively tune the control parameters recursively. This requirement can be handled easily by fuzzy logic or neural network schemes (Lin and Lee, 1991; Bai et al., 2018). The low-level control can then be a model-based control, where the computed torque method (CTM) is one of the most effective and convenient method for this level (Yıldırım, 2008).

During the last two decades, many solutions have been proposed to provide motion tasks suitable for post-stroke motor recovery. Priotteti et al. categorized existing global strategies for robotic-mediated rehabilitation into three groups of assistive, corrective, and resistive controllers (Proietti et al., 2016).

Passive assistance, where the device moves a muscle rigidly along the desired path by adopting different techniques, is the most common treatment strategy for acute patients due to the unresponsiveness of the paretic limb at early post-stroke stages. As soon as patients regain some degrees of mobilization, switching to other assistive solutions, such as triggered passive, where the patient initiates the assistance, or partial assistance, where the device assists the patient as needed (AAN), as utilized by Díaz et al. in HomoRehab (Díaz et al., 2018), may lead to better functional outcomes. Wai et al. provided a combination of the two mentioned assistive strategies in Ambidexter (Wai et al., 2018). Active initiation and execution of movements are the cornerstones of these strategies due to their proven effectiveness in stimulating neuroplasticity to enhance functional therapy.

The corrective mode is linked to the rehabilitation situation in which the patient is not performing the movement correctly, and the robot intervenes by forcing the impaired limb to the correct orthogonal direction. However, it is not easy to clearly differentiate assistive and corrective techniques. Hence, combined assistive-corrective controllers are mostly recurrent among existing controllers (Proietti et al., 2016).

When patients have recovered enough motor capacity, undergoing resistive therapies, which make tasks more difficult in some ways, may result in more significant rehabilitation gains (Ali et al., 2016). Added to the assistive controller, HomoRehab is also equipped with a resistive controller (Díaz et al., 2018). Resistive control, also termed as "challenge-based control," can be achieved by merely applying constant resistance to the movement or error-based methods such as error augmenting and error amplification strategies (Ali et al., 2016). Existing devices mostly provide a combination of these three categories to offer a span variety of motion tasks adaptable to the patient's degree of rehabilitation and the targeted impairment (Proietti et al., 2016). The control system of HAL exoskeletons is based on a hybrid control algorithm, consisting of two subsystems; one for voluntary control according to the patient's voluntary muscles activity and another for autonomous control, which provides predefined physical passive assistance when patients are not able to generate required voluntary signals (Kawamoto et al., 2013). For asymmetrical gait rehabilitation, Curara® employed a synchronization-based assistance control strategy using neural oscillators based on a central pattern generator network. The synchronization-based controller detects the user's movement and measures the mutual gap between the user and the device, and then achieves a desired joint angle trajectory to be synchronized with human movements (Mizukami et al., 2018). Ren et al. proposed three different control strategies in their in-bed wearable ankle rehabilitation robotic device, namely triggered passive assistance for the early stages of recovery, and partial assistance and resistance when the patient gained some mobility (Ren et al., 2017). Their robot-guided rehabilitation protocol is capable of automatically switching between the control modes based on the patient situation and recovery status during the therapy.

Different control strategies can be realized by different methods and algorithms, such as position control, force control, force/position hybrid control, impedance/admittance control, or other control methods (Zhang et al., 2018). Due to their ability to provide natural, comfortable, and safe interaction between robots and patients, impedance control and its dual admittance control are two of the most common control algorithms currently used for rehabilitation exoskeletons, mostly for active training approaches (Proietti et al., 2016).

The difficult task of translating physiotherapist's experience in manipulating the paretic limb into the desired trajectory for rehabilitative devices has made trajectory planning one of the issues for researchers in this field (Proietti et al., 2016). Proietti et al. summarized three main methods for defining reference trajectories, teach/record-and play (Pignolo et al., 2012), motion intention detection (Lyu et al., 2019), and optimization algorithms (Su et al., 2014).

Considering the type of human-machine interaction, control system inputs can be divided into bioelectric signals, e.g., EMG, and biomechanical signals, e.g., joint position, or a combination of these two types of signals (Desplenter et al., 2020). Biomechanical signals provide an accurate and stable interaction, especially for patients with high-level impairment, while biosignals are used for their potential in intention detection and neurological clinical applications due to their favorable effects on nerve rehabilitation treatment (Zhang et al., 2018).

Given the underlying significance of the control system in motor control recovery, some characteristics must be carefully practiced during design steps. Especially when designing for the home setting, providing an appropriately shared control between the device and the patient is of paramount importance. Such control enables a favorable autonomous therapy, including predictable behaviors for patients and never taking control when undesired by the user (Beckerle et al., 2017). It is also

required for addressing neurorehabilitation issues not to suppress or hinder patients' motor capabilities (JarrassÃ© et al., 2014).

Regarding the safety concerns of home therapy due to the absence of the therapist, highly adaptive control systems need to be developed to consider the differences of the human bodies, the motion tasks during the recovery process for each patient, and the nature of the injury between patients (Desplenter and Trejos, 2020). The control solution has to show an adequate amount of active compliance to avoid hurting the patient in the case of trajectory errors due to abnormal or excessive muscle contraction, spasticity, or other pathological synergies (Proietti et al., 2016). Impedance-based control schemes provide a dynamic relationship between force and position and could be utilized for adopting a safe, compliant, and flexible human-machine relationship. In this regard, LLR-Lo benefits from an amendment impedance control based on position control to realize motion compliance for patients in case of patient's discomfort, which leads to aching movement of their leg while the mechanism leg is still moving (Feng et al., 2017). Analyzing the kinesthetic biomechanical capabilities of the target limb is also necessary for developing safe human-robot interaction (Atashzar et al., 2017). Compared to conventional therapy, relying on time or position-dependent trajectories can restrict rehabilitation therapy from the generalization of learning to new tasks. Thus, targeting goal-independent strategies would increase therapy's efficacy, as patients are not constrained by following rigidly planned trajectories (Proietti et al., 2016).

As control system development tools, there are software frameworks designed to provide developers with a platform for the design and implementation of the control system, (e.g., Tekin et al., 2009; Coevoet et al., 2017; Desplenter and Trejos, 2020). The use of such frameworks supports the idea of standardization across different studies and devices. This enables a more efficient evolution and comparison of control systems, reduces the current ambiguity in classification, and neuters existing poor attention in documenting the control strategy of developed devices (Basteris et al., 2014), all assisting in identifying which strategy provides better results. WearMECS is a recently developed control software design and implementation tool available as an open-source software library. The framework provides a foundation for regulating the motion behavior of therapeutic mechatronic devices by considering three main control functionality groups, i.e., task-level control, estimation-level control, and actuation-level control (Desplenter and Trejos, 2020).

User-Interfaces

The concept of remote supervision is entangled in home-rehabilitation. Developing a platform for tele-patient-doctor interaction is the key enabling factor for home-based therapy, in which the interaction of three parties of the patient, the therapist, and the device is provided (Desplenter et al., 2019). Harmonious completion of the rehabilitation program relies on the interaction between each of these parties, which takes place through two main user interfaces of the therapist and the patient. Therapists need to have access to the interface to prescribe treatment regimens and monitor patient's progress in a scheduled plan through detailed reports containing the qualitative and quantitative evaluation of exercises. Patients also would have access to the prescriptions in their interface and move forward through the exercises. In the interface, the correct execution of motions should be displayed (Pereira et al., 2019). Before each exercise, visual and auditory descriptions need to be provided for the patient regarding how he/she is supposed to carry out the activity. The patient's interface must provide feedback on the correctness of the performed activities, as well as a qualitative evaluation of his/her movement. All measurements and relevant data are collected, processed, and stored during each session and are remotely available. For example, in PAMAP the data is stored in the user's electronic health record (EHR) (Martinez-Martin and Cazorla, 2019). In the end, IoT technologies can be utilized to connect the entire system together. These IoT-enabled software interfaces enable the therapist to remotely monitor a patient's progress and tailor a customized treatment plan for him/her (Agyeman and Al-Mahmood, 2019).

Due to differences in patient demographics, needs, and characteristics of the target group must be carefully mapped to a set of general design principles. So as for considering the common cognitive impairments resulting from stroke or normal aging, there are certain factors to have in mind. These factors include ensuring clear directions, providing larger letters and numbering for improved readability, and avoiding vagueness, complexity, and involvement of what Egglestone et al. introduce as abstract thought (Egglestone et al., 2009; Cavuoto et al., 2018). Also, people with other pre-existing disabilities should also be taken into account, e.g., a text to speech component could be added to the interface for people with vision problems and sign language for people with hearing problems (Gomez-Donoso et al., 2017b).

To successfully replace the direct involvement of a therapist with a virtual one, the interfaces should provide options resembling those of traditional methods. Each interface has to be designed to replicate the traditional rehabilitation in a clinical setting, which means the therapist should be able to track the patient's movements, assess his/her performance and analyze his/her progress to be able to prescribe the right treatment plan. Therefore, there is a need for careful evaluation of all of the steps that a therapist takes in a traditional setting to identify the parameters he needs to access. Once these parameters have been identified, user interface software through graphical interfaces (GUIs) provides access for displaying and editing stored data. This provides a base for therapists upon which they can make more educated decisions and choose the best treatment plan for their patients. Also, it is possible to add reminders to the system for notifying the patient to do his/her daily practices. In the end, the system uses this information to adapt the treatment program focusing on the parts that require more recovery to increase therapeutic value.

There are some other crucial principles to be considered for offering software interfaces that assist home-based systems in providing structured training sessions. A user-friendly interface in terms of environment and layout of features and components is the starting point of having a well-established interaction between

patients and the device. This friendliness arises from patients', as well as their caregivers', ability to interact easily with the device in a familiar environment and to have quick and straightforward access to the training and monitoring components (Amirabdollahian et al., 2014). Enabling the patient to personalize the user interface environment, for example, in terms of shape or size of components or layout of different parts and modules, may increase the user-friendliness and create a sense of comfort and control.

For patients to be engaged and challenged during home rehabilitation in the physical absence of the therapist, there is a significant need for careful study and practice of motivational scenarios and features that ensure patient's adherence to the treatment program. The most commonly identified and mentioned barriers to motivation are that rehabilitation scenarios are inherently repetitive and boring, having in mind that stroke patients themselves are prone to depression due to several factors such as social isolation and fatigue that is common among them (Egglestone et al., 2009; Borghese et al., 2013). The intrinsic entertaining characteristic of *Virtual/Augmented Reality (VR, AR)* and gaming present an alternative world in which mundane rehabilitation exercises are disguised in the shape of appealing fantasies. Integrating these methods into home rehabilitation is a common practice aimed at encouraging motivation in patients. The score-based nature of gaming further motivates patients—by rewarding points, coins, and badges as immediate feedback—and reinforces confidence and positivity through achievements (Hatem et al., 2016). VR, AR, and gaming offer plausible environments for versatile game design. Tuning the game content to the interests and needs of users (Egglestone et al., 2009), introducing variability and unpredictability to the tasks, e.g., by contextual interface concept, and programming real-world tasks by simulating real-life objects and events (Martinez-Martin and Cazorla, 2019), may encourage motivation even further. Another great feature of these methods, which makes them preferable to traditional ones, is that during therapy, the enjoyable experience distracts the patients from the prevalent potential pain induced by stroke (Gama et al., 2016). However, an important question remains regarding the efficacy and generalization of this virtual recovery to real world activities. Several studies have been conducted addressing this issue and found that training in a virtual environment offers equal, if not better, motor recovery compared to real-life training (Rose et al., 2005). According to Gama et al. (2016), AR might be more effective than VR, for it provides auto visualization during task execution and this, in turn, can improve patient corporal conscience and potentially engage additional visuospatial networks of the cortex; hence, it leads to more precision and accuracy respectively during interactive exercises and path traveling.

Designing games specifically for rehabilitation purposes, serious games, requires the incorporation of both entertaining and therapeutic goals. Games should offer fully customizable task options and hierarchical order of difficulty for each task. During the recovery process, patients' mental and functional abilities improve, and tasks must be adapted to this variability to keep patients motivated by challenging yet achievable tasks at each stage of the recovery. In other words, by careful modification of the current skill level of the patient and challenge posed by the game, e.g., tuning assistance level and therapy intensity and difficulty, patients may go through a flow-like experience which in turn could potentially increase their active participation (Egglestone et al., 2009). In order to create a unified experience for the patient, it is preferable to develop games around a resonant theme, like Egglstone et al. approach, rather than unrelated minigames. In this approach, the systems do not merely offer video games but complete environments (Agyeman, Al-Mahmood, et al., 2019; Egglestone et al., 2009). It is also suggested to design flexible systems to have the capacity to integrate and support various devices. For example, audio-visual and haptic interfaces will enable the therapists to customize interaction mechanisms and to choose the proper device to deliver the best treatment regime with optimum efficacy for covering the wide range of disabilities, be it upper or lower. In this regard, Egglestone et al. developed a game that could be played by feet, hands, or whole body (Egglestone et al., 2009). In this way, a standardized game platform could be proposed to the entire community of therapists.

Training in home settings requires interface developers to design meaningful and consistent feedback, which should be similar to therapists' clinical feedback—both on the quality of movement and their progress in performing tasks and achieving long-term and personal goals. Providing clear and customized feedback is another way of increasing engagement and motivation in patients, positively affecting retention and recovery (Kitago and Krakauer, 2013). Indeed, creating awareness in patients of their progress and offering a progress tracking module is one crucial approach toward stimulating internal motivation (Chen et al., 2019). Designing both immediate feedback during the therapy and after-session/long-term feedback must be taken into consideration as well. According to Guadagnoli et al., the immediacy of the feedback should be proportional to the task difficulty, i.e., the easier the task, the less frequent the feedback (Guadagnoli et al., 1996). Most current devices, as seen in the previous section, provided immediate visual, auditory, and haptic feedback to the patient (Lyu et al., 2019), which showed improved motivation, for example, by congratulation alarms after each correctly performed task, as well as educating and correcting task performances. Should the patient execute an exercise incorrectly, the system warns the patient and provides graphical help to guide the patient to perform it correctly. For instance, Gloreha provides a 3D simulated preview of the movement on the monitor as well as when the exercise is being performed (Bernocchi et al., 2018), PHAROS provides audio-visual descriptions (Martinez-Martin and Cazorla, 2019), and Lyu et al. generated haptic feedback through vibrating motors as punishment (Bernocchi et al., 2018; Lyu et al., 2019).

Daily and long-term summaries of patient records are another critical form of feedback, termed "knowledge of results" by Schmidt and Lee (1999), and it is a major source of motivation for patients. According to Chen et al. review study, a number of developers of home-based devices described how

patients came motivated to proceed with therapy when they found themselves recovering (Chen et al., 2019). Progress tracking and visual feedback are better provided by graphical representation such as bar or pie charts, rather than numerical or analytical representation, to make a clearer sense of change at first glance. This can be particularly useful when the patients are mostly among elderlies, and it may be difficult for them to analyze the results. Note that patients' dependence on feedback is not favorable, and to avoid that, it is suggested to lower the feedback frequency over time (Kitago and Krakauer, 2013).

When designing for home use, particularly due to the absence of a medical professional, it is essential to consider therapeutic and clinical requirements from the therapists' perspective. Based on the premise that adoption of mechatronic rehabilitation devices heavily relies on the acceptability of the device from the therapist's point of view, Despleneter et al.surveyed Canadian therapists to extract design features that successfully convey the needs of the therapists. Then they mapped the derived data into software requirements for an enhanced therapist-device relationship (Desplenter et al., 2019). A good therapist-device relationship is desirable for equipping therapists with an extensive data set of patient history to be assessed and analyzed toward optimized and educated planning of treatment strategies. Participants mentioned the five areas of patient history, pain, motion, activities, or strength as their most favorable data to be tracked over time for patients' assessment. Desplenter et al. concluded that the designed software system should have features such as standard data records, treatment plan templates, and patient evaluation scales. The user should also be able to design and customize these templates and scales to meet the needs of a particular treatment strategy, both qualitative and quantitative. For this purpose, time-stamped data should be collected, and numerical analyses and visualizations should be generated based on the quantitative data to provide reports. Visualization, particularly in graphs and tables, facilitates data assessment, and puts them into perspective for the therapists. Eventually, a cumulative report must be provided in the therapist's interface in which session history, the patient's history, and progress tracker are among its most important components.

CONCEPTUAL FRAMEWORK

In the previous sections, some of the existing home-based rehabilitation devices were briefly reviewed, and after a general analysis of current challenges and shortcomings, a guideline for designing the components of these systems, in particular for utilizing new advanced technologies, was discussed. As described before, there is a need for a telerehabilitation platform that concerns remote supervision implementation by interconnecting all described modules. To this end, reviewed home-based systems have leveraged different approaches. For example, HomeRehab benefited from a cloud service for exchanging performance and therapy information between the patient and the therapist (Díaz et al., 2018). Amirabdollahian et al. utilized a tele-robotic support platform in their SCRIPT project consisting of a replicated database, a healthcare professional web portal, and a decision support system (Amirabdollahian et al., 2014). Chen et al. also benefited from a web server for the Tele-Doctor-Patient Interaction module in their proposed rehabilitation wheelchair system (Chen S. et al., 2017). Ambidexter provides remote rehabilitation through IoT technologies (Wai et al., 2018). While the aforementioned systems undoubtedly help with remote supervision and patient-therapist interaction, most of them are case-specific for their device and do not offer an interoperable platform allowing for supporting other devices. On the other hand, telehealth platforms for in-home interventions, which need more supervision, information exchange, and online communication, have gained significant traction over the recent years, (e.g., Wang et al., 2017; Kouris et al., 2018; Hilty et al., 2019; Tun et al., 2020; Tsiouris et al., 2020). Among existing telehealth frameworks, they either do not specifically and comprehensively address post-stroke robotic rehabilitation interventions or do not cover the beyond-physical-rehabilitation demands of this population. Therefore, to address the aforementioned limitations as well as to cover the real-life needs of post-stroke individuals, we propose a versatile conceptual framework for community-based robotic in-home rehabilitation. Our proposed framework conceptually provides a unified interoperable solution for interconnecting various rehabilitation robots, lays a foundation for in-home rehabilitation and supports beyond-rehabilitation needs of the post-stroke community—like the need for socialization and assisting in gaining independence for daily activities like shopping, especially during pandemics. Our framework offers a comprehensive solution addressing the multi-faceted needs of involved parties in post-stroke rehabilitation, including patients, healthcare professionals and researchers. To this end, some existing telehealth frameworks, e.g., HOLOBALANCE (Tsiouris et al., 2020), could potentially be modified and adapted for implementing our conceptual framework.

This framework's central concept is based on the development of a multi-agent IoT communication system in which patients, therapists, and administrators each represent an agent of their community interacting with each other over the provided platform (**Figure 6**). This interaction utilizes cloud-based methods for computation, storage and analysis of data collected from each agent. The acquired data is initially processed before being transmitted to cloud and fog servers, where they form a large data set. According to Sahu et al. (2020), due to the sensitive nature of medical data, security, privacy, and confidentiality, as well as the integrity of these data, are of critical importance. Hence, to monitor these concerns, precautionary safety measures must be developed in advance. Also, policies and rules, defining and authorizing the access level of each agent, need to be carefully established and implemented in order to ensure and enhance the security and privacy of the system (Sahu et al., 2020).

The acquired data can be initially processed before being transmitted to cloud and fog servers, where they form a large data set. For example, online identification of musculoskeletal parameters and their variation during treatment can be conducted and plotted in the smartphone, PC, or any other

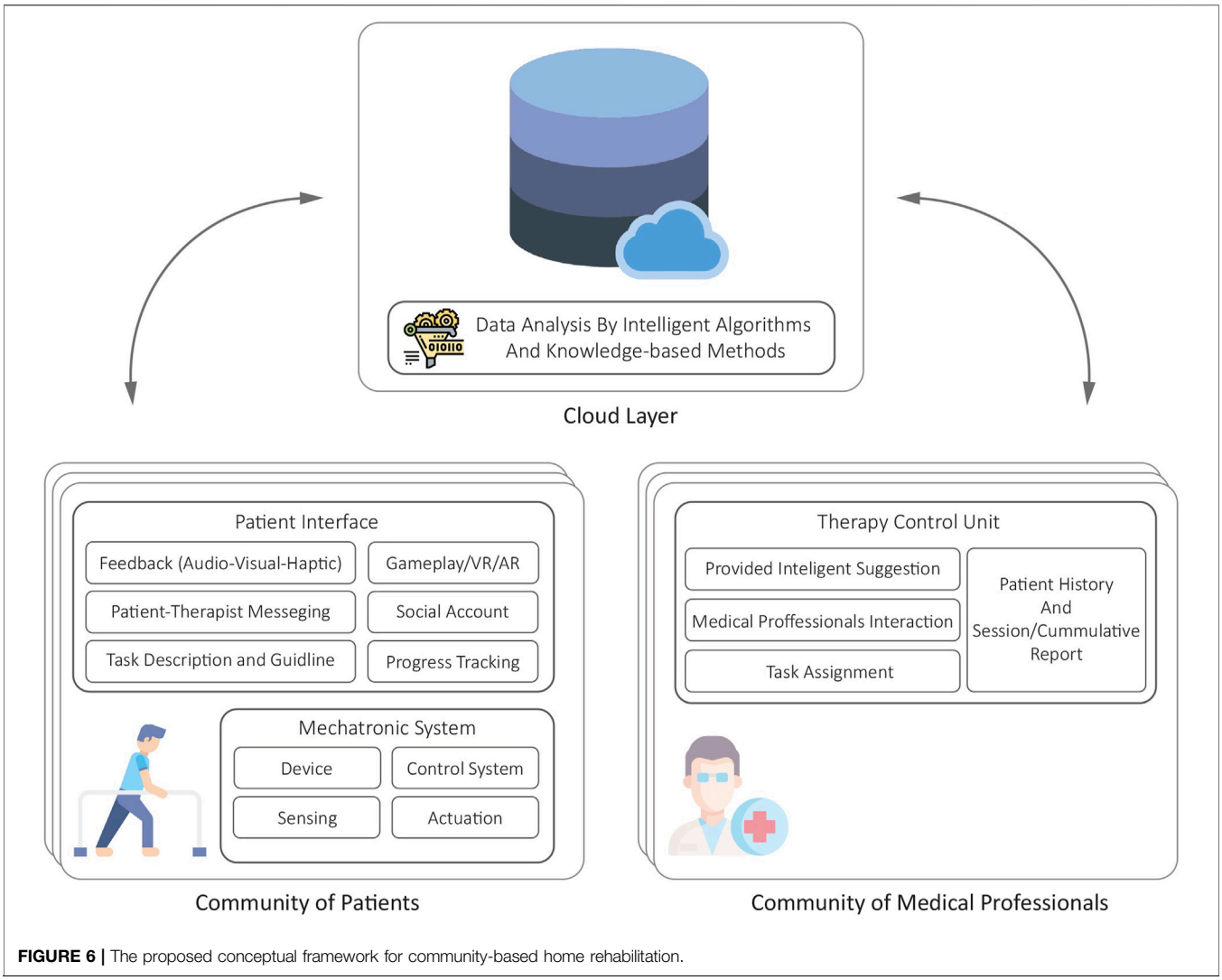

FIGURE 6 | The proposed conceptual framework for community-based home rehabilitation.

digital processor which is connected to the rehabilitation robot. These preprocessing features can be based on either model-based approaches, or artificial intelligence (AI) algorithms such as artificial neural networks. Although training of such systems can be computationally very demanding for these processors, the training process is performed mostly offline. Applying the trained AI feature and even its required recursive update does not involve significant computation, and can be easily handled on the processor of a smartphone, PC, or any other available digital processor.

Acquired data from agents should be comparable with each other, and therefore it is critical to bring the collected data into a common format which occurs through data standardization. By providing internally consistent data with the same content and format, any confusion and ambiguity are avoided. This ensures that all parties involved have mutual understanding, and view the results in the same way which leads to reliable measurements and decision plans. Standardized quantitative and qualitative data should be collected for reliable and educated assessment of patients' performance through evaluation forms and outcome measurements. From a therapist's point of view, the prescribed tasks, reports, and evaluations should be offered in a standard format. To do so, there needs to be a predetermined data extraction on which the community of healthcare professionals has reached a consensus. However, in case of any ambiguity or to provide further details and explanations, therapists should have the option of attaching notes to the data (Desplenter et al., 2019).

The proposed community-based rehabilitation framework facilitates knowledge sharing and provides comprehensive data to ensure educated judgment regarding the best treatment regimen yielding the best recovery outcome. This massive pool of information—both from recorded data and also normalized datasets from already existing medical center repositories—generates big data. By applying machine learning, meaningful information from these large data sets can be extracted. This extensive database can be beneficial for various applications, one of which could be providing a research base enabling further studies in fields of neurorehabilitation, engineering, and occupational/physical therapists. Thus, in this IoT-enabled rehabilitation system, data analysis is performed by

intelligent algorithms and knowledge-based methods to provide intelligent suggestions to the therapists, creating a basis for the best treatment plan assignment.

In the framework, the capability of communication among agents of each community is also feasibly provided. The interaction of healthcare professionals gives them the opportunity to clarify any issues or ambiguities, gain additional expertise, discuss possible treatments, and share their knowledge. The provided platform can also enable socialization among patients. Social restrictions imposed by stroke and exacerbated by the COVID-19 pandemic, have adversely affected patients' lives. Therefore, any means of social interaction could potentially improve their quality of life, which in turn could further motivate them to adhere to the therapy (Egglestone et al., 2009). This community-based rehabilitation allows the possibility of performing rehabilitation in the connected groups, for example, through multiplayer gaming. By optional assignment of a social media profile to each patient ID, they could also share their achievements and support each other.

We suggest an alternative approach in which the purpose of the framework goes beyond rehabilitation to contribution to society and household chores. The virtual environment tasks should be designed so that, along with rehabilitation, they can offer patients the opportunity to learn real-life and daily living skills—cooking, gardening, and housekeeping, to name a few. For example, learning the cooking skill takes place in a virtual kitchen where all of the ingredients and utensils are available along with cooking instructions in the form of video and audio to enable the patient to learn and practice simultaneously. The theme-based free world gameplay would be one of the best options as it can be flexible enough to reflect various aspects of daily life. For example, Saebo Inc. has developed a virtual reality environment in which in the cooking scenario, should the virtual kitchen lack any of the ingredients or utensils required to complete the task, the game enables the patient to go grocery shopping; this way through a comprehensive experience, patient not only goes through therapy but gets to enhance his/her life skills. Integrating this free world environment with our suggested community-based framework adds an additional social layer where patients can teach and learn these skills from each other. For instance, if a patient knows a particular recipe, she/he can teach and share it with the patient community. This provides the patients with a sense of control over their treatment and fosters a sense of usefulness, purpose, and contribution to society. Also, in this time of COVID-19, where everybody, especially elders, feels disconnected from the world, this will excite the feelings of inclusion and connection, which in turn will further motivate the patients to partake more frequently and actively in their treatment sessions.

To go one step further, this virtual environment could be linked to existing online shops allowing the patient to contribute to household chores by purchasing the required and essential items for the house and facilitating the acquisition of his/her own necessities. According to Brenner and Clarke (2019), shopping difficulty is one of the most common self-reported difficulties with daily activities among individuals with disabilities. Thus, the enhanced autonomy and independence in patients alleviates the prevalent feeling of being a burden to their family which in turn promotes a sense of achievement and self-worth. The suggested alternative approaches and rehabilitation are not mutually exclusive, as maintaining engagement in daily life activities is critical for functional and motor recovery (Brenner and Clarke, 2019). As of 2020, due to restrictions caused by the COVID-19 Pandemic and the importance of adhering to social distancing measures, online shopping has become ubiquitous, making this option ever-increasingly plausible.

Finally, the framework has the capacity to incorporate an ambient assisted living ecosystem that can provide patients, specifically elders, with personalized options. These options include remote monitoring, assessment, and support based on their unique profiles and surrounding context. The purpose of such options is to enhance the independence of elderly or disabled individuals in their own secure and convenient space of living (Al-Shaqi et al., 2016; Sahu et al., 2020; Stavropoulos et al., 2020).

Rehabilitation programs, even in the clinical setting, are often not fully supported by public health systems, and hence not all post-stroke patients can afford this option, and due to the enormous socioeconomic impact and high costs, not just on the patient but also on their families, patients opt to drop out (Borghese et al., 2014). Additionally, implementing the proposed framework for post-stroke telerehabilitation, imposes extra costs to the patients for providing the required hardware and software basis of the telehealth framework. For home-based rehabilitation to be acceptable by all end-users involved (patients, clinicians, therapists, and health administrators), these challenges and limitations need to be addressed both by healthcare providers and technology developers. Burden and strain potentially imposed on caregivers are other limiting concerns. However, implementation of the proposed telerehabilitation framework could offer valuable functional outcomes for motor recovery of the wide range of the post-stroke population. Future work should focus on evaluating the proposed telerehabilitation framework for community-based remote therapy during and beyond the pandemic, in terms of different use dimensions, technological acceptance by the stakeholders, clinical efficacy of the system and its economic efficiency.

CONCLUSION

Early-stage post-stroke rehabilitation, a crucial phase of rehabilitation, could be a direct indicator of the possibility of motor recovery. In the current restrictive climate of the COVID-19, due to the restrictions associated with social distancing and limitations for commuting, it has become more difficult for patients to use this sensitive window of time for rehabilitation treatments. In this context, home-based rehabilitation can be a solution.

Several home-based rehabilitation devices have been developed in recent years, both at the research and commercial levels. Although there are some challenges in the research and development of these devices, based on a technical evaluation of aspects such as mechatronics, the control system, and software, these devices can be tuned to be suitable for home-based rehabilitation therapy. Eventually, such systems can be

utilized in a framework aiming at creating a comprehensive network for therapists, patients, engineers, and researchers. To this end, standardization in every aspect of home-based systems, from design criteria to performance evaluation, is required.

The COVID-19 pandemic has proved the necessity of further deploying the power of the internet and computers, not only for the purpose of communication but also for big data analysis. Such technologies can be feasibly integrated with mechatronic systems such as rehabilitation robots to enable new applications such as remote home-based therapies. The outcome of such an interconnected framework would be significantly vital for the recovery of post-stroke patients, promoting the quality of their lives, and eventually reducing the associated burdens on the healthcare system in the long term.

DATA AVAILABILITY STATEMENT

The original contributions presented in the study are included in the article/Supplementary Material, further inquiries can be directed to the corresponding author.

AUTHOR CONTRIBUTIONS

FH and AA equally performed the reviewing of the literature, analyzing the reviewed studies, and writing the draft of the manuscript. SB performed the conception of the order of the paper. All authors contributed to manuscript revision, read, and approved the submitted version.

REFERENCES

Adams, R. J., Lichter, M. D., Ellington, A., White, M., Armstead, K., Patrie, J. T., et al. (2018). Virtual Activities of Daily Living for Recovery of Upper Extremity Motor Function. *IEEE Trans. Neural Syst. Rehabil. Eng.* 26 (1), 252–260. doi:10.1109/tnsre.2017.2771272

Aggarwal, G., Lippi, G., and Michael Henry, B. (2020). Cerebrovascular Disease Is Associated with an Increased Disease Severity in Patients with Coronavirus Disease 2019 (COVID-19): A Pooled Analysis of Published Literature. *Int. J. Stroke* 15 (4), 385–389. doi:10.1177/1747493020921664

Aggogeri, F., Mikolajczyk, T., and O'Kane, J. (2019). Robotics for Rehabilitation of Hand Movement in Stroke Survivors. *Adv. Mech. Eng.* 11 (4), 168781401984192. doi:10.1177/1687814019841921

Agyeman, M. O., and Al-Mahmood, A. (2019). "Design and Implementation of a Wearable Device for Motivating Patients with Upper And/or Lower Limb Disability via Gaming and Home Rehabilitation," in 2019 Fourth International Conference on Fog and Mobile Edge Computing (FMEC). doi:10.1109/fmec.2019.8795317

Agyeman, M. O., Al-Mahmood, A., and Hoxha, I. (2019). "A Home Rehabilitation System Motivating Stroke Patients with Upper And/or Lower Limb Disability," in Proceedings of the 2019 3rd International Symposium on Computer Science and Intelligent Control. doi:10.1145/3386164.3386168

Ail, N. L. M., Ambar, R., Wahab, M. H. A., Idrus, S. Z. S., and Jamil, M. M. A. (2020). Development of a Wrist Rehabilitation Device with Android-Based Game Application. *J. Phys. Conf. Ser.* 1529, 022110. doi:10.1088/1742-6596/1529/2/022110

Al-Shaqi, R., Mourshed, M., and Rezgui, Y. (2016). Progress in Ambient Assisted Systems for Independent Living by the Elderly. *Springer Plus* 5, 624. doi:10.1186/s40064-016-2272-8

Alamdari, A., and Krovi, V. (2015). "Modeling and Control of a Novel Home-Based Cable-Driven Parallel Platform Robot: PACER," in 2015 IEEE/RSJ International Conference on Intelligent Robots and Systems (IROS). doi:10.1109/iros.2015.7354281

Ali, A., Ahmed, S. F., Joyo, M. K., Malik, A., Ali, M., Kadir, K., et al. (2016). *Control Strategies for Robot Therapy*. Sindh University Research Journal (Science Series) SURJ.

AlterG (2015). AlterG Bionic Leg User Manual. https://www.who.int/news-room/fact-sheets/detail/e-coli (Accessed April 10, 2021).

AlterG (n.d). https://www.alterg.com/ (Accessed May 5, 2021).

Ambar, R., Yusof, Y., Jamil, M. M. A., Sharif, J. M., and Ngadi, M. A. (2017). *Design of Accelerometer Based Wrist Rehabilitation Device*. International Journal of Electrical and Computer Engineering (IJECE). doi:10.1109/ict-ispc.2017.8075342

Amirabdollahian, F., Ates, S., Basteris, A., Cesario, A., Buurke, J., Hermens, H., et al. (2014). *Design, Development and Deployment of a Hand/wrist Exoskeleton for Home-Based Rehabilitation after Stroke - SCRIPT Project*. Robotica.

Atashzar, S. F., Shahbazi, M., Tavakoli, M., and Patel, R. V. (2017). A Grasp-Based Passivity Signature for Haptics-Enabled Human-Robot Interaction: Application to Design of a New Safety Mechanism for Robotic Rehabilitation. *Int. J. Robotics Res.* 36 (5–7), 778–799. doi:10.1177/0278364916689139

Ates, S., Haarman, C. J. W., and Stienen, A. H. A. (2017). *SCRIPT Passive Orthosis: Design of Interactive Hand and Wrist Exoskeleton for Rehabilitation at Home after Stroke*. Autonomous Robots.

Aubin, P. M., Sallum, H., Walsh, C., Stirling, L., and Correia, A. (2013). A Pediatric Robotic Thumb Exoskeleton for at-home Rehabilitation: the Isolated Orthosis for Thumb Actuation (IOTA). *IEEE Int. Conf. Rehabil. Robot* 2013, 6650500. doi:10.1109/ICORR.2013.6650500

Awad, L. N., Esquenazi, A., Francisco, G. E., Nolan, K. J., and Jayaraman, A. (2020). The ReWalk ReStore Soft Robotic Exosuit: a Multi-Site Clinical Trial of the Safety, Reliability, and Feasibility of Exosuit-Augmented post-stroke Gait Rehabilitation. *J. Neuroengineering Rehabil.* 17 (1), 80. doi:10.1186/s12984-020-00702-5

Bai, S., and Rasmussen, J. (2011). "Modelling of Physical Human-Robot Interaction for Exoskeleton Designs," in Proceedings of the ECCOMAS Thematic Conference on Multibody Dynamics, Belgium.

Bai, S., Virk, G. S., and Sugar, T. G. (2018). *Wearable Exoskeleton Systems: Design, Control and Applications, Control*. Robotics and Sensors, 408.

Basteris, A., Nijenhuis, S. M., Stienen, A. H., Buurke, J. H., Prange, G. B., and Amirabdollahian, F. (2014). Training Modalities in Robot-Mediated Upper Limb Rehabilitation in Stroke: A Framework for Classification Based on a Systematic Review. *J. NeuroEngineering Rehabil.* 11, 111. doi:10.1186/1743-0003-11-111

Beckerle, P., Salvietti, G., Unal, R., Prattichizzo, D., Rossi, S., Castellini, C., et al. (2017). A Human-Robot Interaction Perspective on Assistive and Rehabilitation Robotics. *Front. Neurorobot.* 11, 24. doi:10.3389/fnbot.2017.00024

Bellomo, R. G., Paolucci, T., Saggino, A., Pezzi, L., Bramanti, A., Cimino, V., et al. (2020). The WeReha Project for an Innovative Home-Based Exercise Training in Chronic Stroke Patients: A Clinical Study. *J. Cent. Nerv Syst. Dis.* 12, 117957352097986. doi:10.1177/1179573520979866

Beom-Chan, L., Dae-Hee, K., Younsun, S., Kap-Ho, S., Sung Ho, P., Dongyual, Y., et al. (2017). Development and Assessment of a Novel Ankle Rehabilitation System for Stroke Survivors. *IEEE Eng. Med. Biol. Soc.* 2017, 3773–3776. doi:10.1109/EMBC.2017.8037678

Bernocchi, P., Mulè, C., Vanoglio, F., Taveggia, G., Luisa, A., and Scalvini, S. (2018). Home-based Hand Rehabilitation with a Robotic Glove in Hemiplegic Patients after Stroke: A Pilot Feasibility Study. *Top. Stroke Rehabil.* 25 (2), 114–119. doi:10.1080/10749357.2017.1389021

Bertani, R., Melegari, C., De Cola, M. C., Bramanti, A., Bramanti, P., and Calabrò, R. S. (2017). Effects of Robot-Assisted Upper Limb Rehabilitation in Stroke Patients: A Systematic Review with Meta-Analysis. *Neurol. Sci.* 38 (9), 1561–1569. doi:10.1007/s10072-017-2995-5

BIOSERVO (). Keeping People Strong Healthy and Motivated. https://www.bioservo.com (Accessed May 5, 2021).

Borboni, A., Mor, M., and Faglia, R. (2016). Gloreha—Hand Robotic Rehabilitation: Design, Mechanical Model, and Experiments. *J. Dynamic Syst. Meas. Control.* 138, 11. doi:10.1115/1.4033831

Borghese, N. A., Alberto Borghese, N., Murray, D., Paraschiv-Ionescu, A., Bruin, E. D., Bulgheroni, M., et al. (2014). *Rehabilitation at Home: A Comprehensive Technological Approach*. Virtual, Augmented Reality and Serious Games for Healthcare, 1.

Borghese, N. A., Mainetti, R., Pirovano, M., Lanzi, P. L., and Lanzi, P. L. (2013). "An Intelligent Game Engine for the at-Home Rehabilitation of Stroke Patients," in 2013 IEEE 2nd International Conference on Serious Games and Applications for Health (SeGAH). doi:10.1109/segah.2013.6665318

Brenner, A. B., and Clarke, P. J. (2019). Difficulty and Independence in Shopping Among Older Americans: More Than Just Leaving the House. *Disabil. Rehabil.* 41 (2), 191–200. doi:10.1080/09638288.2017.1398785

Brewer, B. R., McDowell, S. K., and Worthen-Chaudhari, L. C. (2007). Poststroke Upper Extremity Rehabilitation: A Review of Robotic Systems and Clinical Results. *Top. Stroke Rehabil.* 14 (6), 22–44. doi:10.1310/tsr1406-22

Brokaw, E. B., Black, I., Holley, R. J., and Lum, P. S. (2011). Hand Spring Operated Movement Enhancer (HandSOME): A Portable, Passive Hand Exoskeleton for Stroke Rehabilitation. *IEEE Trans. Neural Syst. Rehabil. Eng.* 19 (4), 391–399. doi:10.1109/tnsre.2011.2157705

Buesing, C., Fisch, G., O'Donnell, M., Shahidi, I., Thomas, L., Mummidisetty, C. K., et al. (2015). Effects of a Wearable Exoskeleton Stride Management Assist System (SMA) on Spatiotemporal Gait Characteristics in Individuals after Stroke: a Randomized Controlled Trial. *J. Neuroengineering Rehabil.* 12, 69. doi:10.1186/s12984-015-0062-0

Bütefisch, C., Hummelsheim, H., Denzler, P., and Mauritz, K.-H. (1995). Repetitive Training of Isolated Movements Improves the Outcome of Motor Rehabilitation of the Centrally Paretic Hand. *J. Neurol. Sci.* 130 (1), 59–68. doi:10.1016/0022-510x(95)00003-k

Butler, A. J., Bay, C., Wu, D., Richards, K. M., and Buchanan, S. (2014). Expanding Tele-Rehabilitation of Stroke through in-home Robot- Assisted Therapy. *Int. J. Phys. Med. Rehabil.* 2, 184. doi:10.4172/2329-9096.1000184

Butler, N. R., Goodwin, S. A., and Perry, J. C. (2017). "Design Parameters and Torque Profile Modification of a Spring-Assisted Hand-Opening Exoskeleton Module, IEEE," in International Conference on Rehabilitation Robotics: [proceedings], 591–596.

Carbone, G., Gherman, B., Ulinici, I., Vaida, C., and Pisla, D. (2018). *Design Issues for an Inherently Safe Robotic Rehabilitation Device*. Advances in Service and Industrial Robotics.

Cardona, M., and Garcia Cena, C. E. (2019). *Biomechanical Analysis of the Lower Limb: A Full-Body Musculoskeletal Model for Muscle-Driven Simulation*. IEEE Access.

Carlan, A.Singleorigin (2020). EksoNR - the Next Step in NeuroRehabilitation - Ekso Bionics. https://eksobionics.com/eksonr/ (Accessed May 5, 2021).

Catalan, J. M., Garcia, J. V., Lopez, D., Diez, J., Blanco, A., Lledo, L. D., Badesa, F. J., Ugartemendia, A., Diaz, I., Neco, R., and Garcia-Aracil, N. (2018). "Patient Evaluation of an Upper-Limb Rehabilitation Robotic Device for Home Use," in 2018 7th IEEE International Conference on Biomedical Robotics and Biomechatronics (Biorob). doi:10.1109/biorob.2018.8487201

Cavuoto, L. A., Subryan, H., Stafford, M., Yang, Z., Bhattacharjya, S., Xu, W., et al. (2018). "Understanding User Requirements for the Design of a Home-Based Stroke Rehabilitation System," in Proceedings of the Human Factors and Ergonomics Society Annual Meeting.

Chen, G., Qi, P., Guo, Z., and Yu, H. (2016). *Mechanical Design and Evaluation of a Compact Portable Knee–Ankle–Foot Robot for Gait Rehabilitation*. Mechanism and Machine Theory.

Chen, J., and Lum, P. S. (2018). Pilot Testing of the Spring Operated Wearable Enhancer for Arm Rehabilitation (SpringWear). *J. Neuroengineering Rehabil.* 15 (1), 13. doi:10.1186/s12984-018-0352-4

Chen, J., Nichols, D., Brokaw, E. B., and Lum, P. S. (2017). Home-based Therapy after Stroke Using the Hand Spring Operated Movement Enhancer (HandSOME). *IEEE Trans. Neural Syst. Rehabil. Eng.* 25 (12), 2305–2312. doi:10.1109/tnsre.2017.2695379

Chen, J. P. S., and Lum, P. S. (2016a). Spring Operated Wearable Enhancer for Arm Rehabilitation (SpringWear) after Stroke. *Annu. Int. Conf. IEEE Eng. Med. Biol. Soc.* 2016, 4893–4896. doi:10.1109/EMBC.2016.7591824

Chen, S., Fu, F.-F., Meng, Q.-L., and Yu, H.-L. (2017). *Development of a Lower Limb Rehabilitation Wheelchair System Based on Tele-Doctor–Patient Interaction*. Wearable Sensors and Robots.

Chen, T. P. S., and Lum, P. S. (2016b). "Hand Rehabilitation after Stroke Using a Wearable, High DOF, Spring Powered Exoskeleton," in Annual International Conference of the IEEE Engineering in Medicine and Biology Society, 578–581. doi:10.1109/EMBC.2016.7590768

Chen, Y., Abel, K. T., Janecek, J. T., Chen, Y., Zheng, K., and Cramer, S. C. (2019). Home-based Technologies for Stroke Rehabilitation: A Systematic Review. *Int. J. Med. Inform.* 123, 11–22. doi:10.1016/j.ijmedinf.2018.12.001

Cherry, C. O. B., Chumbler, N. R., Richards, K., Huff, A., Wu, D., Tilghman, L. M., et al. (2017). Expanding Stroke Telerehabilitation Services to Rural Veterans: a Qualitative Study on Patient Experiences Using the Robotic Stroke Therapy Delivery and Monitoring System Program. *Disabil. Rehabil. Assistive Tech.* 12 (1), 21–27. doi:10.3109/17483107.2015.1061613

Coevoet, E., Morales-Bieze, T., Largilliere, F., Zhang, Z., Thieffry, M., Sanz-Lopez, M., et al. (2017). *Software Toolkit for Modeling, Simulation, and Control of Soft Robots*. Advanced Robotics.

Coffey, A. L., Leamy, D. J., and Ward, T. E. (2014). "A Novel BCI-Controlled Pneumatic Glove System for home-based Neurorehabilitation," in Conference Proceedings: IEEE Engineering in Medicine and Biology Society. Conference, 3622–3625. doi:10.1109/EMBC.2014.6944407

Cyberoyne (2021). Hall for Well Being (Lower Limb Type). https://www.cyberdyne.jp/english/products/fl05.html (Accessed April 10, 2021).

Delph, M. A., 2nd, Fischer, S. A., Gauthier, P. W., Luna, C. H. M., Clancy, E. A., and Fischer, G. S. (2013). A Soft Robotic Exomusculature Glove with Integrated sEMG Sensing for Hand Rehabilitation. *IEEE Int. Conf. Rehabil. Robot* 2013, 6650426. doi:10.1109/ICORR.2013.6650426

Desplenter, T., Chinchalkar, S., and Trejos, A. L. (2019). "Enhancing the Therapist-Device Relationship: Software Requirements for Digital Collection and Analysis of Patient Data," in 2019 IEEE 16th International Conference on Rehabilitation Robotics (ICORR). doi:10.1109/icorr.2019.8779528

Desplenter, T., and Trejos, A. L. (2020). *A Control Software Framework for Wearable Mechatronic Devices*. Journal of Intelligent & Robotic Systems.

Desplenter, T., Zhou, Y., Edmonds, B. P., Lidka, M., Goldman, A., and Trejos, A. L. (2020). Rehabilitative and Assistive Wearable Mechatronic Upper-Limb Devices: A Review. *J. Rehabil. Assistive Tech. Eng.* 7, 205566832091787. doi:10.1177/2055668320917870

Díaz, I., Catalan, J. M., Badesa, F. J., Justo, X., Lledo, L. D., Ugartemendia, A., et al. (2018). Development of a Robotic Device for Post-Stroke Home Tele-Rehabilitation. *Adv. Mech. Eng.* 10 (1), 168781401775230. doi:10.1177/1687814017752302

Díaz, I., Gil, J. J., and Sánchez, E. (2011). Lower-Limb Robotic Rehabilitation: Literature Review and Challenges. *J. Robotics* 2011, 1. doi:10.1155/2011/759764

Doucet, B. M., and Mettler, J. A. (2018). *Pilot Study Combining Electrical Stimulation and a Dynamic Hand Orthosis for Functional Recovery in Chronic Stroke*. American Journal of Occupational Therapy.

Dumitru, S., Copilusi, C., and Dumitru, N. (2018). *A Leg Exoskeleton Command Unit for Human Walking Rehabilitation*. Advanced Engineering Forum. doi:10.1109/aqtr.2018.8402732

Duncan, P. W., Zorowitz, R., Bates, B., Choi, J. Y., Glasberg, J. J., Graham, G. D., et al. (2005). Management of Adult Stroke Rehabilitation Care. *Stroke* 36 (9), e100–143. doi:10.1161/01.str.0000180861.54180.ff

Egglestone, S. R., Axelrod, L., Nind, T., Turk, R., Wilkinson, A., Burridge, J., Fitzpatrick, G., Mawson, S., Robertson, Z., Hughes, A. M., Ng, K. H., Pearson, W., Shublaq, N., Probert-Smith, P., Rickets, I., and Rodden, T. (2009). "A Design Framework for a Home-Based Stroke Rehabilitation System: Identifying the Key Components," in Proceedings of the 3d International ICST Conference on Pervasive Computing Technologies for Healthcare. doi:10.4108/icst.pervasivehealth2009.6049

Eiammanussakul, T., and Sangveraphunsiri, V. (2018). A Lower Limb Rehabilitation Robot in Sitting Position with a Review of Training Activities. *J. Healthc. Eng.* 2018, 1–18. doi:10.1155/2018/1927807

Feng, Y., Wang, H., Yan, H., Wang, X., Jin, Z., and Vladareanu, L. (2017). Research on Safety and Compliance of a New Lower Limb Rehabilitation Robot. *J. Healthc. Eng.* doi:10.1155/2017/1523068

Fischer, H. C., Triandafilou, K. M., Thielbar, K. O., Ochoa, J. M., Lazzaro, E. D. C., Pacholski, K. A., et al. (2016). Use of a Portable Assistive Glove to

Facilitate Rehabilitation in Stroke Survivors with Severe Hand Impairment. *IEEE Trans. Neural Syst. Rehabil. Eng.* 24 (3), 344–351. doi:10.1109/tnsre.2015.2513675

Franck, J. A., Smeets, R. J. E. M., and Seelen, H. A. M. (2019). Evaluation of a Functional Hand Orthosis Combined with Electrical Stimulation Adjunct to Arm-Hand Rehabilitation in Subacute Stroke Patients with a Severely to Moderately Affected Hand Function. *Disabil. Rehabil.* 41 (10), 1160–1168. doi:10.1080/09638288.2017.1423400

Gama, A. E. F. D., Da Gama, A. E. F., Chaves, T. M., Figueiredo, L. S., Baltar, A., Meng, M., et al. (2016). MirrARbilitation: A Clinically-Related Gesture Recognition Interactive Tool for an AR Rehabilitation System. *Comp. Methods Programs Biomed.* 135, 105–114. doi:10.1016/j.cmpb.2016.07.014

Gasser, B. W., Bennett, D. A., Durrough, C. M., and Goldfarb, M. (2017). "Design and Preliminary Assessment of Vanderbilt Hand Exoskeleton," in IEEE International Conference on Rehabilitation Robotics: [proceedings], 1537–1542.

Ghassemi, M., Ochoa, J. M., Yuan, N., Tsoupikova, D., and Kamper, D. (2018). "Development of an Integrated Actuated Hand Orthosis and Virtual Reality System for Home-Based Rehabilitation," in Conference Proceedings: IEEE Engineering in Medicine and Biology Society. Conference, 1689–1692. doi:10.1109/EMBC.2018.8512704

Godlove, J., Anantha, V., Advani, M., Des Roches, C., and Kiran, S. (2019). Comparison of Therapy Practice at Home and in the Clinic: A Retrospective Analysis of the Constant Therapy Platform Data Set. *Front. Neurol.* 10, 140. doi:10.3389/fneur.2019.00140

Gomez-Donoso, F., Orts-Escolano, S., Garcia-Garcia, A., Garcia-Rodriguez, J., Castro-Vargas, J. A., and Ovidiu-Oprea, S. (2017b). *A Robotic Platform for Customized and Interactive Rehabilitation of Persons with Disabilities*. Pattern Recognition Letters, 105–113.

Gresham, G. E., Duncan, P. W., Stason, W. B., Adams, H. P., Adelman, A. M., Alexander, D. N., et al. (1995). *Post-stroke Rehabilitation: Clinical Practice Guidelines*. Rockville: U.S. Department of Health and Human Services.

Guadagnoli, M. A., Dornier, L. A., and Tandy, R. D. (1996). Optimal Length for Summary Knowledge of Results: The Influence of Task-Related Experience and Complexity. *Res. Q. Exerc. Sport* 67 (2), 239–248. doi:10.1080/02701367.1996.10607950

Gull, M. A., Bai, S., and Bak, T. (2020). *A Review on Design of Upper Limb Exoskeletons*. Robotics.

Gupta, N., Castillo-Laborde, C., and Landry, M. D. (2011). *Health-Related Rehabilitation Services: Assessing the Global Supply of and Need for Human Resources*. BMC Health Services Research.

Hang Zhang, H., Austin, H., Buchanan, S., Herman, R., Koeneman, J., and Jiping He, J. (2011). Feasibility Studies of Robot-Assisted Stroke Rehabilitation at Clinic and Home Settings Using RUPERT. *IEEE Int. Conf. Rehabil. Robot* 2011, 5975440. doi:10.1109/ICORR.2011.5975440

Hatem, S. M., Saussez, G., Della Faille, M., Prist, V., Zhang, X., Dispa, D., et al. (2016). Rehabilitation of Motor Function after Stroke: A Multiple Systematic Review Focused on Techniques to Stimulate Upper Extremity Recovery. *Front. Hum. Neurosci.* 10, 442. doi:10.3389/fnhum.2016.00442

Heung, K. H. L., Tang, Z. Q., Ho, L., Tung, M., Li, Z., and Tong, R. K. Y. (2019). Design of a 3D Printed Soft Robotic Hand for Stroke Rehabilitation and Daily Activities Assistance. *IEEE Int. Conf. Rehabil. Robot* 2019, 65–70. doi:10.1109/ICORR.2019.8779449

Hidler, J., Nichols, D., Pelliccio, M., Brady, K., Campbell, D. D., Kahn, J. H., et al. (2009). Multicenter Randomized Clinical Trial Evaluating the Effectiveness of the Lokomat in Subacute Stroke. *Neurorehabil. Neural Repair* 23 (15–13), 5–13. doi:10.1177/1545968308326632

Hilty, D. M., Chan, S., Torous, J., Luo, J., and Boland, R. J. (2019). A Telehealth Framework for Mobile Health, Smartphones, and Apps: Competencies, Training, and Faculty Development. *J. Tech. Behav. Sci.* 4, 1. doi:10.1007/s41347-019-00091-0

Hirano, S., Saitoh, E., Tanabe, S., Tanikawa, H., Sasaki, S., Kato, D., et al. (2017). The Features of Gait Exercise Assist Robot: Precise Assist Control and Enriched Feedback. *Nre* 41 (1), 77–84. doi:10.3233/nre-171459

Honda Global (2020). Honda Walking Assist Device. https://global.honda/products/power/walkingassist.html (Accessed May 5, 2020).

Housley, S. N., Garlow, A. R., Ducote, K., Howard, A., Thomas, T., Wu, D., et al. (2016). Increasing Access to Cost Effective Home-Based Rehabilitation for Rural Veteran Stroke Survivors. *Austin J. Cerebrovasc. Dis. Stroke* 3 (21–11), 1–11. 28018979

Huang, J., Tu, X., and He, J. (2016). Design and Evaluation of the RUPERT Wearable Upper Extremity Exoskeleton Robot for Clinical and in-Home Therapies. *IEEE Trans. Syst. Man. Cybern, Syst.* 46 (7), 926–935. doi:10.1109/tsmc.2015.2497205

Hussain, S., Jamwal, P. K., Van Vliet, P., and Ghayesh, M. H. (2020). State-of-the-Art Robotic Devices for Wrist Rehabilitation: Design and Control Aspects. *IEEE Trans. Human-Machine Syst.* 99, 1–12. doi:10.1109/THMS.2020.2976905

Hyakutake, K., Morishita, T., Saita, K., Fukuda, H., Shiota, E., Higaki, Y., et al. (2019). Effects of Home-Based Robotic Therapy Involving the Single-Joint Hybrid Assistive Limb Robotic Suit in the Chronic Phase of Stroke: A Pilot Study. *Biomed. Res. Int.* 2019, 1–9. doi:10.1155/2019/5462694

Iida, S., Kawakita, D., Fujita, T., Uematsu, H., Kotaki, T., Ikeda, K., et al. (2017). Exercise Using a Robotic Knee Orthosis in Stroke Patients with Hemiplegia. *J. Phys. Ther. Sci.* 29, 1920–1924. doi:10.1589/jpts.29.1920

In, H., Kang, B. B., Sin, M., and Cho, K.-J. (2015). Exo-glove: A Wearable Robot for the Hand with a Soft Tendon Routing System. *IEEE Robot. Automat. Mag.* 22, 97–105. doi:10.1109/mra.2014.2362863

Intercollegiate Working Party for Stroke (2012). *Stroke Association (Great Britain) and Royal College of Physicians of London, National Clinical Guideline for Stroke*, 208.

Jamwal, P. K., Hussain, S., and Xie, S. Q. (2015). Review on Design and Control Aspects of Ankle Rehabilitation Robots. *Disabil. Rehabil. Assistive Tech.* 10 (2), 93–101. doi:10.3109/17483107.2013.866986

JarrassÃ©, N., Proietti, T., Crocher, V., Robertson, J., Sahbani, A., Morel, G., et al. (2014). Robotic Exoskeletons: A Perspective for the Rehabilitation of Arm Coordination in Stroke Patients. *Front. Hum. Neurosci.* 8, 947. doi:10.3389/fnhum.2014.00947

Je Hyung Jung, J. H., Valencia, D. B., Rodríguez-de-Pablo, C., Keller, T., and Perry, J. C. (2013). Development of a Powered Mobile Module for the ArmAssist Home-Based Telerehabilitation Platform. *IEEE Int. Conf. Rehabil. Robot* 2013, 6650424. doi:10.1109/ICORR.2013.6650424

Jian, H., Tu, X., and He, j. (2016). Design and Evaluation of the RUPERT Wearable Upper Extremity Exoskeleton Robot for Clinical and in-Home Therapies. *IEEE Trans. Syst. Man, Cybernetics: Syst.* 46 (7), 926–935. doi:10.1109/tsmc.2016.2645026

Kawamoto, H., Hayashi, T., Sakurai, T., Eguchi, K., and Sankai, Y. (2009). Development of Single Leg Version of HAL for Hemiplegia. *Conf. Proc. IEEE Eng. Med. Biol. Soc.* 2009, 5038–5043. doi:10.1109/IEMBS.2009.5333698

Kawamoto, H., Kamibayashi, K., Nakata, Y., Yamawaki, K., Ariyasu, R., Sankai, Y., et al. (2013). Pilot Study of Locomotion Improvement Using Hybrid Assistive Limb in Chronic Stroke Patients. *BMC Neurol.* 13, 141. doi:10.1186/1471-2377-13-141

Kim, B., and Deshpande, A. D. (2017). An Upper-Body Rehabilitation Exoskeleton Harmony with an Anatomical Shoulder Mechanism: Design, Modeling, Control, and Performance Evaluation. *Int. J. Robotics Res.* 36, 414–435. doi:10.1177/0278364917706743

Kim, T. (2020). *Factors Influencing Usability of Rehabilitation Robotic Devices for Lower Limbs*. Sustainability.

Kitago, T., and Krakauer, J. W. (2013). Motor Learning Principles for Neurorehabilitation. *Neurol. Rehabil.* 110, 93–103. doi:10.1016/B978-0-444-52901-5.00008-3

Klug, F., Hessinger, M., Koka, T., Witulla, P., Will, C., Schlichting, T., et al. (2019). An Anthropomorphic Soft Exosuit for Hand Rehabilitation. *IEEE Int. Conf. Rehabil. Robot* 2019, 1121–1126. doi:10.1109/ICORR.2019.8779481

Koh, T. H., Cheng, N., Yap, H. K., and Yeow, C.-H. (2017). Design of a Soft Robotic Elbow Sleeve with Passive and Intent-Controlled Actuation. *Front. Neurosci.* 11, 597. doi:10.3389/fnins.2017.00597

Kouris, I., Sarafidis, M., Androutsou, T., and Koutsouris, D. (2018). HOLOBALANCE: An Augmented Reality Virtual Trainer Solution Forbalance Training and Fall Prevention. *Annu. Int. Conf. IEEE Eng. Med. Biol. Soc.* 2018, 4233–4236. doi:10.1109/EMBC.2018.8513357

Krakauer, J. W. (2006). Motor Learning: Its Relevance to Stroke Recovery and Neurorehabilitation. *Curr. Opin. Neurol.* 19 (1), 84–90. doi:10.1097/01.wco.0000200544.29915.cc

Kruif, B. J., Schmidhauser, E., Stadler, K. S., and O'Sullivan, L. W. (2017). Simulation Architecture for Modelling Interaction between User and Elbow-Articulated Exoskeleton. *J. Bionic Eng.* 14, 706–715. doi:10.1016/S1672-6529(16)60437-7

Kutlu, M., Freeman, C., Hughes, A.-M., and Spraggs, M. (2017). A Home-Based FES System for Upper-Limb Stroke Rehabilitation with Iterative Learning Control. *IFAC-PapersOnLine* 50, 12089–12094. doi:10.1016/j.ifacol.2017.08.2153

Lambelet, C., Temiraliuly, D., Siegenthaler, M., Wirth, M., Woolley, D. G., Lambercy, O., et al. (2020). Characterization and Wearability Evaluation of a Fully Portable Wrist Exoskeleton for Unsupervised Training after Stroke. *J. Neuroengineering Rehabil.* 17 (1), 132. doi:10.1186/s12984-020-00749-4

Lee, H.-J., Lee, S.-H., Seo, K., Lee, M., Chang, W. H., Choi, B.-O., et al. (2019). Training for Walking Efficiency with a Wearable Hip-Assist Robot in Patients with Stroke. *Stroke* 50 (12), 3545–3552. doi:10.1161/strokeaha.119.025950

Lee, S.-H., Lee, H.-J., Shim, Y., Chang, W. H., Choi, B.-O., Ryu, G.-H., et al. (2020). Wearable Hip-Assist Robot Modulates Cortical Activation during Gait in Stroke Patients: A Functional Near-Infrared Spectroscopy Study. *J. Neuroengineering Rehabil.* 17 (1), 145. doi:10.1186/s12984-020-00777-0

Lin, C.-T., and Lee, C. S. G. (1991). *Neural-Network-Based Fuzzy Logic Control and Decision System*. IEEE Transactions on Computers.

Linder, S. M., Reiss, A., Buchanan, S., Sahu, K., Rosenfeldt, A. B., Clark, C., et al. (2013a). Incorporating Robotic-Assisted Telerehabilitation in a Home Program to Improve Arm Function Following Stroke. *J. Neurol. Phys. Ther.* 37, 125–132. doi:10.1097/NPT.0b013e31829fa808

Linder, S. M., Rosenfeldt, A. B., Reiss, A., Buchanan, S., Sahu, K., Bay, C. R., et al. (2013b). The Home Stroke Rehabilitation and Monitoring System Trial: A Randomized Controlled Trial. *Int. J. Stroke* 8, 46–53. doi:10.1111/j.1747-4949.2012.00971.x

Liu, Y., Guo, S., Hirata, H., Ishihara, H., and Tamiya, T. (2018). Development of a Powered Variable-Stiffness Exoskeleton Device for Elbow Rehabilitation. *Biomed. Microdevices* 20 (3), 64. doi:10.1007/s10544-018-0312-6

Liu, Y., Guo, S., Yang, Z., Hirata, H., and Tamiya, T. (2021). A Home-Based Bilateral Rehabilitation System with sEMG-Based Real-Time Variable Stiffness. *IEEE J. Biomed. Health Inform.* 25, 1529–1541. doi:10.1109/JBHI.2020.3027303,

Low, F.-Z., Lim, J. H., Kapur, J., and Yeow, R. C.-H. (2019). Effect of a Soft Robotic Sock Device on Lower Extremity Rehabilitation Following Stroke: A Preliminary Clinical Study with Focus on Deep Vein Thrombosis Prevention. *IEEE J. Transl. Eng. Health Med.* 7, 1–6. doi:10.1109/JTEHM.2019.2894753

Low, F.-Z., Lim, J. H., and Yeow, C.-H. (2018). Design, Characterisation and Evaluation of a Soft Robotic Sock Device on Healthy Subjects for Assisted Ankle Rehabilitation. *J. Med. Eng. Tech.* 42 (1), 26–34. doi:10.1080/03091902.2017.1411985

Lyu, M., Chen, W.-H., Ding, X., Wang, J., Pei, Z., and Zhang, B. (2019). Development of an EMG-Controlled Knee Exoskeleton to Assist Home Rehabilitation in a Game Context. *Front. Neurorobotics* 13, 67. doi:10.3389/fnbot.2019.00067

Markus, H. S., and Brainin, M. (2020). COVID-19 and Stroke-A Global World Stroke Organization Perspective. *Int. J. Stroke* 15 (4), 361–364. doi:10.1177/1747493020923472

Martinez-Martin, E., and Cazorla, M. (2019). Rehabilitation Technology: Assistance from Hospital to Home. *Comput. Intell. Neurosci.* 2019, 1431509. doi:10.1155/2019/1431509

Mehrholz, J., Thomas, S., Kugler, J., Pohl, M., and Elsner, B. (2020). Electromechanical-Assisted Training for Walking after Stroke. *Cochrane Database Syst. Rev.* 10, CD006185. doi:10.1002/14651858.CD006185.pub5

Mizukami, N., Takeuchi, S., Tetsuya, M., Tsukahara, A., Yoshida, K., Matsushima, A., et al. (2018). Effect of the Synchronization-Based Control of a Wearable Robot Having a Non-exoskeletal Structure on the Hemiplegic Gait of Stroke Patients. *IEEE Trans. Neural Syst. Rehabil. Eng.* 26 (5), 1011–1016. doi:10.1109/tnsre.2018.2817647

Moon, S. B., Ji, Y.-H., Jang, H.-Y., Hwang, S.-H., Shin, D.-B., Lee, S.-C., et al. (2017). *Gait Analysis of Hemiplegic Patients in Ambulatory Rehabilitation Training Using a Wearable Lower-Limb Robot: A Pilot Study*. International Journal of Precision Engineering and Manufacturing.

Morone, G., Annicchiarico, R., Iosa, M., Federici, A., Paolucci, S., Cortés, U., et al. (2016). Overground Walking Training with the I-Walker, a Robotic Servo-Assistive Device, Enhances Balance in Patients with Subacute Stroke: A Randomized Controlled Trial. *J. Neuroengineering Rehabil.* 13 (1), 47. doi:10.1186/s12984-016-0155-4

Motus Nova (n.d.). Motus Nova Stroke Rehab Recovery at Home. https://motusnova.com/hand (Accessed April 10, 2021).

National University of Singapore (2015). *Robotic Sock Designed to Prevent Blood Clots*.

Nijenhuis, S. M., Prange, G. B., Amirabdollahian, F., Sale, P., Infarinato, F., Nasr, N., et al. (2015). Feasibility Study into Self-Administered Training at Home Using an Arm and Hand Device with Motivational Gaming Environment in Chronic Stroke. *J. Neuroengineering Rehabil.* 12, 89. doi:10.1186/s12984-015-0080-y

Nilsson, A., Vreede, K. S., Häglund, V., Kawamoto, H., Sankai, Y., and Borg, J. (2014). Gait Training Early after Stroke with a New Exoskeleton – the Hybrid Assistive Limb: a Study of Safety and Feasibility. *J. Neuroengineering Rehabil.* 11, 92. doi:10.1186/1743-0003-11-92

Nilsson, M., Ingvast, J., Wikander, J., and von Holst, H. (2012). "The Soft Extra Muscle System for Improving the Grasping Capability in Neurological Rehabilitation," in 2012 IEEE-EMBS Conference on Biomedical Engineering and Sciences. doi:10.1109/iecbes.2012.6498090

Novak, D., Ziherl, J., Olenšek, A., Milavec, M., Podobnik, J., Mihelj, M., et al. (2010). Psychophysiological Responses to Robotic Rehabilitation Tasks in Stroke. *IEEE Trans. Neural Syst. Rehabil. Eng.* 18 (4), 351–361. doi:10.1109/tnsre.2010.2047656

Osuagwu, B. A. C., Timms, S., Peachment, R., Dowie, S., Thrussell, H., Cross, S., et al. (2020). Home-based Rehabilitation Using a Soft Robotic Hand Glove Device Leads to Improvement in Hand Function in People with Chronic Spinal Cord Injury:a Pilot Study. *J. Neuroengineering Rehabil.* 17 (1), 40. doi:10.1186/s12984-020-00660-y

Pehlivan, A. U., Celik, O., and O'Malley, M. K. (2011). Mechanical Design of a Distal Arm Exoskeleton for Stroke and Spinal Cord Injury Rehabilitation. *IEEE Int. Conf. Rehabil. Robot* 2011, 5975428. doi:10.1109/ICORR.2011.5975428

Pereira, A., Folgado, D., Nunes, F., Almeida, J., and Sousa, I. (2019). "Using Inertial Sensors to Evaluate Exercise Correctness in Electromyography-Based Home Rehabilitation Systems," in 2019 IEEE International Symposium on Medical Measurements and Applications (MeMeA). doi:10.1109/memea.2019.8802152

Perry, J. C., Trimble, S., Castilho Machado, L. G., Schroeder, J. S., Belloso, A., Rodriguez-de-Pablo, C., et al. (2016). Design of a Spring-Assisted Exoskeleton Module for Wrist and Hand Rehabilitation. *Annu. Int. Conf. IEEE Eng. Med. Biol. Soc.* 2016, 594–597. doi:10.1109/EMBC.2016.7590772

Perry, J. C., Ruiz-Ruano, J. A., and Keller, T. (2011). Telerehabilitation: Toward a Cost-Efficient Platform for Post-Stroke Neurorehabilitation. *IEEE Int. Conf. Rehabil. Robotics* 2011. doi:10.1109/icorr.2011.5975413

Perry, J. C., Zabaleta, H., Belloso, A., Rodriguez-de-Pablo, C., Cavallaro, F. I., and Keller, T. (2012). "ArmAssist: Development of a Functional Prototype for at-Home Telerehabilitation of Post-Stroke Arm Impairment," in 2012 4th IEEE RAS & EMBS International Conference on Biomedical Robotics and Biomechatronics (BioRob). doi:10.1109/biorob.2012.6290858

Pignolo, L., Dolce, G., Basta, G., Lucca, L. F., Serra, S., and Sannita, W. G. (2012). "Upper Limb Rehabilitation after Stroke: ARAMIS a "Robo-mechatronic" Innovative Approach and Prototype," in 2012 4th IEEE RAS & EMBS International Conference on Biomedical Robotics and Biomechatronics (BioRob). doi:10.1109/biorob.2012.6290868

Polygerinos, P., Galloway, K. C., Sanan, S., Herman, M., and Walsh, C. J. (2015). *EMG Controlled Soft Robotic Glove for Assistance during Activities of Daily Living*. Robotics and Autonomous Systems. doi:10.1109/icorr.2015.7281175

Porciuncula, F., Roto, A. V., Kumar, D., Davis, I., Roy, S., Walsh, C. J., et al. (2018). Wearable Movement Sensors for Rehabilitation: A Focused Review of Technological and Clinical Advances. *PM&R* 10, S220–S232. doi:10.1016/j.pmrj.2018.06.013

Prange-Lasonder, G. B., Radder, B., Kottink, A. I. R., Melendez-Calderon, A., Buurke, J. H., and Rietman, J. S. (2017). Applying a Soft-Robotic Glove as Assistive Device and Training Tool with Games to Support Hand Function after Stroke: Preliminary Results on Feasibility and Potential Clinical Impact. *IEEE Int. Conf. Rehabil. Robot* 2017, 1401–1406. doi:10.1109/ICORR.2017.8009444

Proietti, T., Crocher, V., Roby-Brami, A., and Jarrasse, N. (2016). Upper-Limb Robotic Exoskeletons for Neurorehabilitation: A Review on Control Strategies. *IEEE Rev. Biomed. Eng.* 9, 4–14. doi:10.1109/rbme.2016.2552201

Proulx, C. E., Beaulac, M., David, M., Deguire, C., Haché, C., Klug, F., et al. (2020). Review of the Effects of Soft Robotic Gloves for Activity-Based Rehabilitation in Individuals with Reduced Hand Function and Manual Dexterity Following a Neurological Event. *J. Rehabil. Assistive Tech. Eng.* 7, 205566832091813. doi:10.1177/2055668320918130

Radder, B., Prange-Lasonder, G. B., Kottink, A. I. R., Holmberg, J., Sletta, K., Dijk, M. V., et al. (2019). Home Rehabilitation Supported by a Wearable Soft-Robotic Device for Improving Hand Function in Older Adults: A Pilot Randomized Controlled Trial. *PLOS ONE* 14, e0220544. doi:10.1371/journal.pone.0220544

Radder, B., Prange-Lasonder, G., Kottink, A., Melendez-Calderon, A., Buurke, J., and Rietman, J. (2018). Feasibility of a Wearable Soft-Robotic Glove to Support Impaired Hand Function in Stroke Patients. *J. Rehabil. Med.* 50 (7), 598–606. doi:10.2340/16501977-2357

Recover From Your Stroke With Saebo (2017). https://www.saebo.com (Accessed May 5, 2021).

Ren, Y., Wu, Y.-N., Yang, C.-Y., Xu, T., Harvey, R. L., and Zhang, L.-Q. (2017). Developing a Wearable Ankle Rehabilitation Robotic Device for In-Bed Acute Stroke Rehabilitation. *IEEE Trans. Neural Syst. Rehabil. Eng.* 25 (6), 589–596. doi:10.1109/tnsre.2016.2584003

ReWalk (2019). ReStore™ Soft Exo-Suit for Stroke Rehabilitation - ReWalk Robotics. https://rewalk.com/restore-exo-suit/ (Accessed May 5, 2021).

ReWalk (2015). ReWalk™ Personal 6.0 Exoskeleton. https://rewalk.com/rewalk-personal-3/ (Accessed May 5, 2021).

Rose, F. D., David Rose, F., Brooks, B. M., and Rizzo, A. A. (2005). *Virtual Reality in Brain Damage Rehabilitation: Review*. CyberPsychology & Behavior.

Runnalls, K. D., Ortega-Auriol, P., McMorland, A. J. C., Anson, G., and Byblow, W. D. (2019). Effects of Arm Weight Support on Neuromuscular Activation during Reaching in Chronic Stroke Patients. *Exp. Brain Res.* 237 (12), 3391–3408. doi:10.1007/s00221-019-05687-9

Sahu, M. L., Atulkar, M., and Ahirwal, M. K. (2020). "Comprehensive Investigation on IoT Based Smart HealthCare System," in 2020 First International Conference on Power, Control and Computing Technologies (ICPC2T). doi:10.1109/icpc2t48082.2020.9071442

Sandison, M., Phan, K., Casas, R., Nguyen, L., Lum, M., Pergami-Peries, M., et al. (2020). HandMATE: Wearable Robotic Hand Exoskeleton and Integrated Android App for at Home Stroke Rehabilitation. *Annu. Int. Conf. IEEE Eng. Med. Biol. Soc.* 2020, 4867–4872. doi:10.1109/EMBC44109.2020.9175332

Sanjuan, J. D., Castillo, A. D., Padilla, M. A., Quintero, M. C., Gutierrez, E. E., Sampayo, I. P., et al. (2020). *Cable Driven Exoskeleton for Upper-Limb Rehabilitation: A Design Review*. Robotics and Autonomous Systems.

Schmidt, R. A., and Lee, T. D. (1999). *Motor Control and Learning: A Behavioral Emphasis*. Human Kinetics Publishers, 495.

Shen, Y., Ferguson, P. W., and Rosen, J. (2020). *Upper Limb Exoskeleton Systems—Overview*. Wearable Robotics.

Shi, D., Zhang, W., Zhang, W., and Ding, X. (2019). A Review on Lower Limb Rehabilitation Exoskeleton Robots. *Chin. J. Mech. Eng.* 32, 74. doi:10.1186/s10033-019-0389-8

Simonetti, D., Tagliamonte, N. L., Zollo, L., Accoto, D., and Guglielmelli, E. (2018). *Biomechatronic Design Criteria of Systems for Robot-Mediated Rehabilitation Therapy*. Rehabilitation Robotics, 29–46. doi:10.1016/b978-0-12-811995-2.00032-1

Sivan, M., Gallagher, J., Makower, S., Keeling, D., Bhakta, B., O'Connor, R. J., et al. (2014). Home-based Computer Assisted Arm Rehabilitation (hCAAR) Robotic Device for Upper Limb Exercise after Stroke: Results of a Feasibility Study in Home Setting. *J. NeuroEngineering Rehabil.* 11, 163. doi:10.1186/1743-0003-11-163

Solanki, D., Kumar, S., Shubha, B., and Lahiri, U. (2020). Implications of Physiology-Sensitive Gait Exercise on the Lower Limb Electromyographic Activity of Hemiplegic Post-Stroke Patients: A Feasibility Study in Low Resource Settings. *IEEE J. Transl. Eng. Health Med.* 8, 12100709–9. doi:10.1109/JTEHM.2020.3006181

Stavropoulos, T. G., Papastergiou, A., Mpaltadoros, L., Nikolopoulos, S., and Kompatsiaris, I. (2020). IoT Wearable Sensors and Devices in Elderly Care: A Literature Review. *Sensors* 20, 2826. doi:10.3390/s20102826

Stein, J., Bishop, L., Stein, D. J., and Wong, C. K. (2014). Gait Training with a Robotic Leg Brace after Stroke. *Am. J. Phys. Med. Rehabil./ Assoc. Acad. Physiatrists* 93 (11), 987–994. doi:10.1097/phm.0000000000000119

Su, C.-J., Chiang, C.-Y., and Huang, J.-Y. (2014). *Kinect-Enabled Home-Based Rehabilitation System Using Dynamic Time Warping and Fuzzy Logic*. Applied Soft Computing.

Sung, J., Choi, S., Kim, H., Lee, G., Han, C., Ji, Y., et al. (2017). Feasibility of Rehabilitation Training with a Newly Developed, Portable, Gait Assistive Robot for Balance Function in Hemiplegic Patients. *Ann. Rehabil. Med.* 41 (2), 178–187. doi:10.5535/arm.2017.41.2.178

Tekin, O. A., Babuska, R., Tomiyama, T., De Schutter, B., and De Schutter, B. (2009). "Toward a Flexible Control Design Framework to Automatically Generate Control Code for Mechatronic Systems," in 2009 American Control Conference. doi:10.1109/acc.2009.5160184

Tomić, T. J. D., Savić, A. M., Vidaković, A. S., Rodić, S. Z., Isaković, M. S., Rodríguez-de-Pablo, C., et al. (2017). ArmAssist Robotic System versus Matched Conventional Therapy for Poststroke Upper Limb Rehabilitation: A Randomized Clinical Trial. *Biomed. Res. Int.* 2017, 1–7. doi:10.1155/2017/7659893

Tomida, K., Sonoda, S., Hirano, S., Suzuki, A., Tanino, G., Kawakami, K., et al. (2019). Randomized Controlled Trial of Gait Training Using Gait Exercise Assist Robot (GEAR) in Stroke Patients with Hemiplegia. *J. Stroke Cerebrovasc. Dis.* 28 (9), 2421–2428. doi:10.1016/j.jstrokecerebrovasdis.2019.06.030

Triandafilou, K. M. (2014). *Effect of Static versus Cyclical Stretch on Hand Motor Control in Subacute Stroke*. International Journal of Neurorehabilitation.

Tsiouris, K. M., Gatsios, D., Tsakanikas, V., Pardalis, A. A., Kouris, I., Androutsou, T., et al. (2020). *Designing Interoperable Telehealth Platforms: Bridging IoT Devices with Cloud Infrastructures*. Enterprise Information Systems. doi:10.1109/embc44109.2020.9176082

Tsukahara, A., and Hashimoto, M. (2016). "Pilot Study of Single-Legged Walking Support Using Wearable Robot Based on Synchronization Control for Stroke Patients," in 2016 IEEE International Conference on Robotics and Biomimetics (ROBIO). doi:10.1109/robio.2016.7866436

Tsukahara, A., Yoshida, K., Matsushima, A., Ajima, K., Kuroda, C., Mizukami, N., et al. (2017). Evaluation of Walking Smoothness Using Wearable Robotic System Curara for Spinocerebellar Degeneration Patients. *IEEE Int. Conf. Rehabil. Robot* 2017, 1494–1499. doi:10.1109/ICORR.2017.8009459

Tu, X., Han, H., Huang, J., Li, J., Su, C., Jiang, X., et al. (2017). Upper Limb Rehabilitation Robot Powered by PAMs Cooperates with FES Arrays to Realize Reach-To-Grasp Trainings. *J. Healthc. Eng.* 2017. doi:10.1155/2017/1282934

Tun, S. Y. Y., Madanian, S., and Mirza, F. (2020). Internet of Things (IoT) Applications for Elderly Care: A Reflective Review. *Aging Clin. Exp. Res.* 33, 855–867. doi:10.1007/s40520-020-01545-9

Van der Loos, H. F. M., and Reinkensmeyer, D. J. (2008). "Rehabilitation and Health Care Robotics," in *Springer Handbook of Robotics* (Berlin, Heidelberg: Springer Berlin Heidelberg), 1223–1251. doi:10.1007/978-3-540-30301-5_54

van Kammen, K., Boonstra, A. M., van der Woude, L. H. V., Reinders-Messelink, H. A., and den Otter, R. (2017). Differences in Muscle Activity and Temporal Step Parameters between Lokomat Guided Walking and Treadmill Walking in Post-Stroke Hemiparetic Patients and Healthy Walkers. *J. Neuroengineering Rehabil.* 14 (1), 32. doi:10.1186/s12984-017-0244-z

Wai, C. C., Leong, T. C., Gujral, M., Hung, J., Hui, T. S., and Wen, K. K. (2018). "Ambidexter: A Low Cost Portable Home-Based Robotic Rehabilitation Device for Training Fine Motor Skills," in 2018 7th IEEE International Conference on Biomedical Robotics and Biomechatronics (Biorob). doi:10.1109/biorob.2018.8487204

Wang, J., Qiu, M., and Guo, B. (2017). Enabling Real-Time Information Service on Telehealth System over Cloud-Based Big Data Platform. *J. Syst. Architecture* 72. doi:10.1016/j.sysarc.2016.05.003

Wang, Y., and Xu, Q. (2019). "Design of a New Wrist Rehabilitation Robot Based on Soft Fluidic Muscle," in IEEE/ASME International Conference on Advanced Intelligent Mechatronics (AIM). doi:10.1109/aim.2019.8868626

Wanjoo Park, W., Wookjin Jeong, W., Gyu-Hyun Kwon, G. H., Yun-Hee Kim, Y. H., and Laehyun Kim, L. (2013). A Rehabilitation Device to Improve the Hand Grasp Function of Stroke Patients Using a Patient-Driven Approach. *IEEE Int. Conf. Rehabil. Robot* 2013, 6650482. doi:10.1109/ICORR.2013.6650482

Washabaugh, E. P., Claflin, E. S., Gillespie, R. B., and Krishnan, C. (2016). A Novel Application of Eddy Current Braking for Functional Strength

Training during Gait. *Ann. Biomed. Eng.* 44 (9), 2760–2773. doi:10.1007/s10439-016-1553-2

Washabaugh, E. P., Guo, J., Chang, C.-K., Remy, C. D., and Krishnan, C. (2019). A Portable Passive Rehabilitation Robot for Upper-Extremity Functional Resistance Training. *IEEE Trans. Biomed. Eng.* 66 (2), 496–508. doi:10.1109/tbme.2018.2849580

Washabaugh, E. P., and Krishnan, C. (2018). A Wearable Resistive Robot Facilitates Locomotor Adaptations during Gait. *Rnn* 36 (2), 215–223. doi:10.3233/rnn-170782

Westerveld, A. J., Aalderink, B. J., Hagedoorn, W., Buijze, M., Schouten, A. C., and Kooij, H. v. d. (2014). A Damper Driven Robotic End-Point Manipulator for Functional Rehabilitation Exercises after Stroke. *IEEE Trans. Biomed. Eng.* 61 (10), 2646–2654. doi:10.1109/tbme.2014.2325532

Wolf, S. L., Sahu, K., Curtis Bay, R., Buchanan, S., Reiss, A., Linder, S., et al. (2015). The HAAPI (Home Arm Assistance Progression Initiative) Trial. *Neurorehabil. Neural Repair* 29 (10), 958–968. doi:10.1177/1545968315575612

World Health Organization (2017). *The Need to Scale up Rehabilitation*. World Health Organization. WHO/NMH/NVI/17.1.

Wright, A., Stone, K., Martinelli, L., Fryer, S., Smith, G., Lambrick, D., et al. (2020). Effect of Combined Home-Based, Overground Robotic-Assisted Gait Training and Usual Physiotherapy on Clinical Functional Outcomes in People with Chronic Stroke: A Randomized Controlled Trial. *Clin. Rehabil.* 2020, 026921552098413. doi:10.1177/0269215520984133

Yoo, D., Kim, D.-H., Seo, K.-H., and Lee, B.-C. (2019). The Effects of Technology-Assisted Ankle Rehabilitation on Balance Control in Stroke Survivors. *IEEE Trans. Neural Syst. Rehabil. Eng.* 27 (9), 1817–1823. doi:10.1109/tnsre.2019.2934930

Yurkewich, A., Hebert, D., Wang, R. H., and Mihailidis, A. (2019). Hand Extension Robot Orthosis (HERO) Glove: Development and Testing with Stroke Survivors with Severe Hand Impairment. *IEEE Trans. Neural Syst. Rehabil. Eng.* 27 (5), 916–926. doi:10.1109/tnsre.2019.2910011

Yurkewich, A., Kozak, I. J., Ivanovic, A., Rossos, D., Wang, R. H., Hebert, D., et al. (2020). Myoelectric Untethered Robotic Glove Enhances Hand Function and Performance on Daily Living Tasks after Stroke. *J. Rehabil. Assistive Tech. Eng.* 7, 205566832096405. doi:10.1177/2055668320964050

Yıldırım, Ş. (2008). *A Proposed Hybrid Neural Network for Position Control of a Walking Robot*. Nonlinear Dynamics.

Zhang, K., Chen, X., Liu, F., Tang, H., Wang, J., and Wen, W. (2018). System Framework of Robotics in Upper Limb Rehabilitation on Poststroke Motor Recovery. *Behav. Neurol.* 2018, 1–14. doi:10.1155/2018/6737056

Zhang, M., Guo, Y., and He, M. (2019). "Dynamic Analysis of Lower Extremity Exoskeleton of Rehabilitation Robot," in Proceedings of the 2019 4th International Conference on Robotics, Control and Automation - ICRCA 2019. doi:10.1145/3351180.3351207

Zheng, H., Black, N. D., and Harris, N. D. (2005). Position-Sensing Technologies for Movement Analysis in Stroke Rehabilitation. *Med. Biol. Eng. Comput.* 43 (4), 413–420. doi:10.1007/bf02344720

Zhou, Y., Desplenter, T., Chinchalkar, S., and Trejos, A. L. (2019). A Wearable Mechatronic Glove for Resistive Hand Therapy Exercises. *IEEE Int. Conf. Rehabil. Robot* 2019, 1097–1102. doi:10.1109/ICORR.2019.8779502

Conflict of Interest: The authors declare that the research was conducted in the absence of any commercial or financial relationships that could be construed as a potential conflict of interest.

GLOSSARY

MAL Motor activity log

MAL QOM Motor activity log (quality of movement)

BBS Berg balance scale

FMAS Fugl-Meyer assessment scale

FMUE or FMA-UE The Fugl-Meyer assessment for motor recovery after stroke for the upper extremity

FMA-Hand The Fugl-Meyer assessment for hand

FMLE or FM-LE The Fugl-Meyer assessment for motor recovery after stroke for the lower extremity

FM Fugl-Meyer assessment of motor recovery

TUGT Timed up and go test

SPPB Short physical performance battery

DGI Dynamic Gait index

mRS Modified Rankin scale

CMSA-H Chedoke McMaster stroke assessment stage

FES(S) Falls-efficacy scale Swedish version

BI Barthel index

FIM Functional independence measure

ARAT Action research arm test

WMFT Wolf motor function test

GWMFT or GWMFT-func The graded wolf motor function test

GWMFT-time Graded wolf motor function test (completion time)

CAHAI The Chedoke arm and hand inventory

MAS The motor assessment scale

MMAS The modified Modified ashworth scale

EXT Finger extension force

GS Grip strength

LPS Lateral pinch strength

PPS Palmar pinch strength

MTS Modified Tardieu scale

SIS Stroke impact scale

SUS System usability scale

BBT Box and blocks test

JTHFT Jebsen-Taylor hand function test

10MWT 10 minute walk test

6MWT 6 minute walk test

K-FES Korean falls-efficiency scale

FE Flexion/Extension

F Flexion

E Extension

PS Pronation/Supination

IE Inversion/Eversion

PD Plantarflexion/Dorsiflexion

frontiers in Robotics and AI

ORIGINAL RESEARCH
published: 24 June 2021
doi: 10.3389/frobt.2021.612964

Telerobotic Operation of Intensive Care Unit Ventilators

*Balazs P. Vagvolgyi[1], Mikhail Khrenov[2], Jonathan Cope[3], Anton Deguet[1], Peter Kazanzides[1], Sajid Manzoor[3], Russell H. Taylor[1] and Axel Krieger[1,2]**

[1]*Laboratory for Computational Sensing and Robotics, Whiting School of Engineering, Johns Hopkins University, Baltimore, MD, United States,* [2]*Department of Mechanical Engineering, A. James Clark School of Engineering, University of Maryland, College Park, MD, United States,* [3]*Anaesthesia and Critical Care Medicine, Johns Hopkins Hospital, Baltimore, MD, United States*

Since the first reports of a novel coronavirus (SARS-CoV-2) in December 2019, over 33 million people have been infected worldwide and approximately 1 million people worldwide have died from the disease caused by this virus, COVID-19. In the United States alone, there have been approximately 7 million cases and over 200,000 deaths. This outbreak has placed an enormous strain on healthcare systems and workers. Severe cases require hospital care, and 8.5% of patients require mechanical ventilation in an intensive care unit (ICU). One major challenge is the necessity for clinical care personnel to don and doff cumbersome personal protective equipment (PPE) in order to enter an ICU unit to make simple adjustments to ventilator settings. Although future ventilators and other ICU equipment may be controllable remotely through computer networks, the enormous installed base of existing ventilators do not have this capability. This paper reports the development of a simple, low cost telerobotic system that permits adjustment of ventilator settings from outside the ICU. The system consists of a small Cartesian robot capable of operating a ventilator touch screen with camera vision control *via* a wirelessly connected tablet master device located outside the room. Engineering system tests demonstrated that the open-loop mechanical repeatability of the device was 7.5 mm, and that the average positioning error of the robotic finger under visual servoing control was 5.94 mm. Successful usability tests in a simulated ICU environment were carried out and are reported. In addition to enabling a significant reduction in PPE consumption, the prototype system has been shown in a preliminary evaluation to significantly reduce the total time required for a respiratory therapist to perform typical setting adjustments on a commercial ventilator, including donning and doffing PPE, from 271 to 109 s.

Keywords: robotics, telerobotics and teleoperation, coronavirus (2019-nCoV), intensive care unit, ventilator, personal protective equipment, visual servoing, touch screen

OPEN ACCESS

Edited by:
Mahdi Tavakoli, University of Alberta, Canada

Reviewed by:
Xiao Xiao, Southern University of Science and Technology, China
Selene Tognarelli, Sant'Anna School of Advanced Studies, Italy

****Correspondence:***
Axel Krieger
axel@jhu.edu

Specialty section:
This article was submitted to Biomedical Robotics, a section of the journal Frontiers in Robotics and AI

Received: *01 October 2020*
Accepted: *07 June 2021*
Published: *24 June 2021*

Citation:
Vagvolgyi BP, Khrenov M, Cope J, Deguet A, Kazanzides P, Manzoor S, Taylor RH and Krieger A (2021) Telerobotic Operation of Intensive Care Unit Ventilators. Front. Robot. AI 8:612964. doi: 10.3389/frobt.2021.612964

1 INTRODUCTION

Since the first reports of a novel coronavirus (SARS-CoV-2) in December 2019, over 33 million people have been infected worldwide and approximately 1 million patients across age groups worldwide have died from the disease caused by this virus (COVID-19) according to the World Health Organization (2020). COVID-19 is a respiratory viral disease with transmission *via* respiratory aerosols and micro-droplets. This places clinicians and nurses at risk of contracting the virus when caring for patients infected with COVID-19. The primary morbidity and mortality of COVID-19 is related to pulmonary involvement, and according to data from the United States

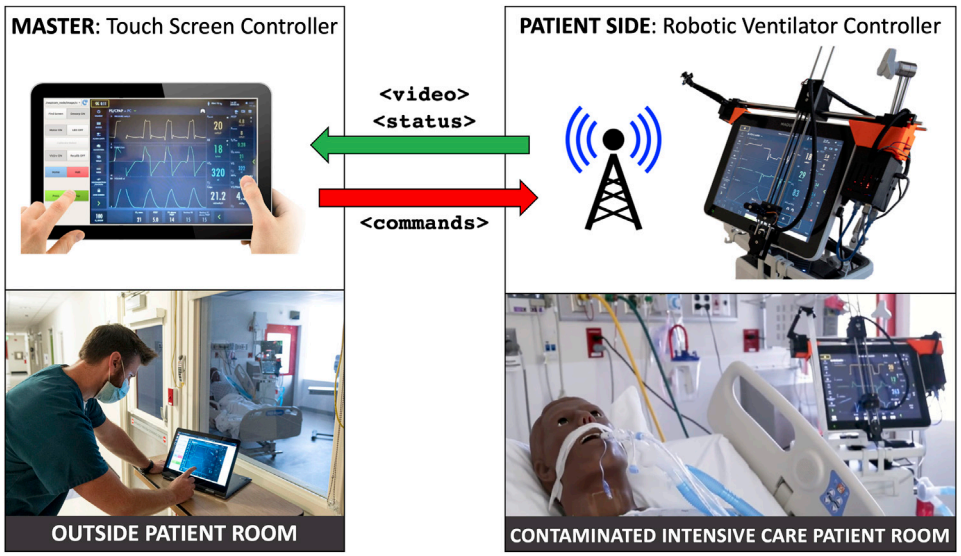

FIGURE 1 | System overview: ventilator-mounted camera streams video to master touchscreen; healthcare worker outside patient room presses buttons on video displayed on master touchscreen, which sends commands to ventilator-mounted robot to move to and press buttons on the actual ventilator touchscreen.

Centers for Disease Control and Prevention (2020), pneumonia was the primary cause of death in 45.2% of COVID-19 cases between February 1, 2020 and September 26, 2020 in the United States. 8.5% of patients who develop COVID-19 will require ventilation in an intensive care unit (ICU) at some point during their illness according to a recent meta-analysis by Chang et al. (2020).

This pandemic has shown that the scarcest resources necessary to fight COVID-19 are personal protective equipment (PPE), ventilators to combat poor oxygenation, and trained clinical staff. The infection risk for staff and the strain on PPE resources is exacerbated by the fact that for an infectious disease such as COVID-19, healthcare workers must don and doff PPE every time they enter an ICU, even if only to perform a simple task such as changing a setting on a ventilator. Most ICU ventilator patients will require some sort of manipulation of the ventilator touchscreen between 3 and 12 times per 12-h shift. Depending on the patient needs, many of these can be done without physical interaction with the patient. Patient response to minor ventilator setting changes can be safely assessed by ventilator waveforms and measured parameters, as well as the patient vital signs monitor. There will still be occasions that require physical presence in the room to assess the patient or care for them, such as endotracheal suctioning, airway care, or other respiratory treatments, but this is generally the minority of the visits to a patient room for ventilator management. Although ICU equipment may eventually be controlled remotely through an in-ICU network, this is not currently the case, and the installed equipment base is not amenable to this solution.

Medical robots can play a key role in reducing the infectious risk for staff by reducing the amount of close encounters with patients. A recent paper by Yang et al. (2020b) categorizes the role of robotics in combating infectious diseases like COVID-19 in four areas, including clinical care, logistics, reconnaissance, and continuity of work/maintenance of socioeconomic functions. Since the beginning of the pandemic, companies and researchers proposed several such robotic systems for automated temperature screening, Gong et al. (2020), remote cardiopulmonary imaging, Ye et al. (2020), taking nasal swabs, Li et al. (2020) and Biobot Surgical Pte Ltd. (2020), autonomous vascular access, Chen et al. (2020), facilitating rapid COVID-19 testing, IGI Testing Consortium (2020), addressing mental health challenges and supplementing distanced education, Scassellati and Vázquez (2020), promoting social well-being, Henkel et al. (2020), and for general telepresence with bimanual teleoperation in ICUs, Yang et al. (2020a). However, none of the current robotic systems are capable of converting the existing installed base of ventilators and other ICU equipment to remote operation.

The goal of this work is to develop a rapidly deployable solution that will allow healthcare workers to remotely operate and monitor equipment from outside the ICU room, saving valuable time and PPE resources, as operators will not need to don, wear, and doff PPE while remotely operating medical devices, enabling the clinician to spend more time seeing patients rather than donning and doffing. As shown in **Figure 1**, these robots are controlled from outside the ICU room by a healthcare worker *via* a tablet, using encrypted communications to ensure security and patient privacy. Tablet computers are ideal for the healthcare settings because they can be easily cleaned with well-defined infection-control procedures, according to Hollander and Carr (2020). To meet the urgency of the crisis we prioritized the development and deployment of a remote controlled Cartesian robot dedicated to the most prevalent touchscreen controlled ventilator at Johns Hopkins Hospital (JHH), the Maquet Servo-U (Getinge AB, Gothenburg, Sweden), with plans to then expand capabilities and robots to other ventilators and infusion pumps. The proposed robotic device is not designed for portability, as it

requires expert installation by a trained professional. However, its affordability would allow hospitals to mount a separate unit on each ventilator.

The Servo-U comprises approximately 75% of the standard ventilator fleet at JHH. In surge conditions more Hamilton (Hamilton Medical Inc., Reno, NV, United States) models are used, which may reduce the ratio of Servo-U usage to closer to 60%. The Hamilton C1, Hamilton G5, and the Carefusion Avea (CareFusion Inc., San Diego, CA, United States, no longer in business) all use a combination of touchscreen and rotating dial. According to Morita et al. (2016), the Servo-U is one of the market leading ventilators used in many health systems around the world due to its safety and user experience. Many hospitals only have only one brand of ICU ventilator, so their entire fleet may be a fit for the current design. However, other ICU equipment, like infusion pumps also have physical buttons, therefore, in order to support a wider range of devices, the proposed robotic system will have the added capability to interact with physical controls in the future.

Robotic control of touch screens is not unprecedented, but the application of these existing systems is exclusively for touch screen reliability testing in an industrial setting. Such systems include MATT by mattrobot. ai (Bucharest, Romania), SR-SCARA-Pro by Sastra Robotics (Kochi, Kerala, India), and Tapster by Tapster Robotics (Oak Park, IL, United States). All of these systems use a capacitive stylus to interact with the touch screen, but the robot kinematic structures are different from the Cartesian design of our system, utilizing either a delta or SCARA configuration, and completely enveloping the screen they are intended to manipulate. The existing touchscreen testing robots are primarily designed for testing screens laid down flat, and so are generally tall in design, and meant for horizontal mounting. For the purposes of this work, it was important that the touchscreen remain vertically mounted and be minimally obstructed for any manual or emergency operation by a respiratory therapist. If we were to use a delta type robot, mounting it on the Servo-U ventilator screen would result in a large protruding mass, cantilevered on the screen. This would exert a significant bending load on the mounting system, while also interfering with manual operation. The Cartesian layout we chose and developed keeps the robot as close in to the screen horizontally as possible, minimizing any mounting loads, while also leaving the screen easily accessible for conventional manual operation.

The primary contributions of this work consist of a custom Cartesian robot designed to interact with a touch sensitive display and a computer vision-based teleoperation method that together effectively enable the replication of the direct interaction scheme with a touch screen on a master tablet console. Further contributions include thorough evaluation of this robotic system with a series of engineering system tests determining open-loop repeatability, closed-loop visual servoing accuracy, and test deployment in an ICU environment. As described in **Section 4**, additional actuator modules that enable the interaction with other physical controls, such as buttons and knobs, have the potential to broaden the range of replicable control interfaces. Applications of such systems range from the safe teleoperation of medical devices in infectious environments to remote management of industrial assembly lines.

2 MATERIALS AND METHODS

The teleoperated ventilator controller system consists of a custom robotic *patient side* device and a touch based *master* console. Computer vision tasks that enable the intuitive user interface and accurate robot control are executed on the *master*. Communication between *master* and *patient side* is implemented in a component-based architecture using the Robot Operating System (ROS), as described by Quigley et al. (2009).

2.1 Ventilator-Mounted Cartesian Robot

The main component of the robot teleoperation system is the robot itself. While Cartesian robots are nothing new, those available on the market are not optimized for the ventilator touch screen control application. Existing robots are primarily designed for manufacturing or plotting tasks, both of which are performed on steady, horizontal surfaces. As ventilator screens are vertical and liable to be moved in operation, a significantly different design is necessary. Said design must be suitable to the unique mounting situation and optimized for weight, cost, and ease of handling by ICU staff, while still providing suitable accuracy and precision for ventilator manipulation. We have successfully designed and built a lightweight Cartesian robot that attaches to a ventilator screen and enables button pushing through a mechanized robotic finger.

This design consists of a two-axis gantry and a mechanized end-effector finger, with the ends of the horizontal (X) axis used to secure the robot to the desired screen. The vertical (Y) axis assembly is cantilevered on the X axis and translates along it. A roller at the bottom of the Y axis engages the screen bezel and prevents unexpected touch interactions. The two axes are driven by a pair of 45 Ncm NEMA 17 stepper motors *via* GT2 timing belts. The use of timing belts and stepper motors for the axes allows the robot to translate quickly to the requested positions and to be easily back-driven by an operator in the case of emergencies. The total stroke of the X and Y axes is approximately 400 mm by 280 mm, respectively. The resolution for both axes is 0.2 mm using a 20 tooth GT2 pulley, 200 steps per revolution of the motor, and no microstepping. This can be increased, if needed, with microstepping. The Servo-U ventilator features a 15 TFT LCD capacitive touchscreen with an aspect ratio of 4:3.

The end-effector finger (**Figure 2D**) is spring-loaded and controlled by a compact servo turning an eccentric retaining cam. As such, to perform a tap the finger follows a sinusoidal linear motion, with the cam rotating 110° at 0.5°/ms, stopping after the end-effector tip touches the screen, dwelling for 20 ms, and returning at the same rate. If commanded to press and hold, the finger will perform the first half of the motion and maintain the downwards position until commanded to release, at which point it will retract.

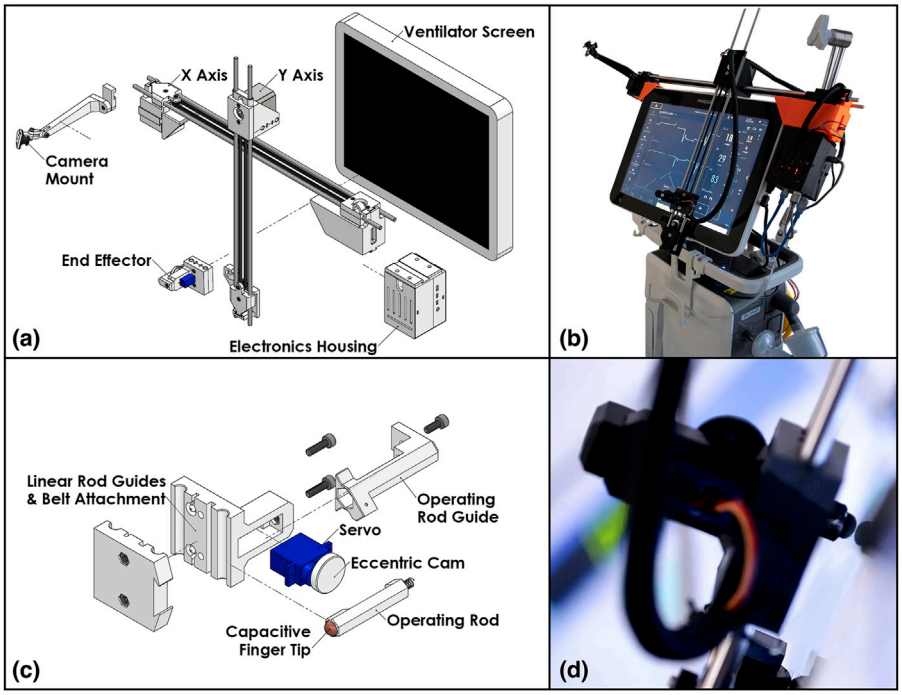

FIGURE 2 | The patient side robotic ventilator controller: **(A)** exploded view drawing of the robotic system, **(B)** photo of the robotic system installed on a Maquet Servo-U ventilator, **(C)** detailed exploded view drawing of the end effector assembly, **(D)** close-up photo of the end effector operating a Servo-U ventilator.

An inexpensive wide-angle camera observes the ventilator screen and Cartesian robot from an adjustable mount attached to the far side of the X axis. This is used to provide immediate feedback to the operator and robot control system on the state of the visual status indicators and notifications displayed on the screen of the ventilator and the position of the end-effector.

Control for the motors and servo is supplied by an ATmega328 microcontroller alongside TMC2130 stepper motor drivers. The local device firmware, written in C++, takes advantage of the TMC2130 drivers' current sensing capability to perform automatic homing without the use of limit switches and to detect possible collisions with an operator or foreign objects. The microcontroller is connected over a serial port (UART-USB) to a Raspberry Pi microcomputer which provides all the local computing needed in a very light and compact package. **Figures 2A,C** show an isometric exploded-view engineering drawing of the design and the assembled robot mounted on a Maquet Servo-U ventilator, while **Figure 3** illustrates the various communication channels between all hardware components. The Raspberry Pi is connected to the aforementioned camera and provides the network connection needed for the remote controller to drive the robot and monitor the ventilator screen. The maximum operation distance is difficult to estimate as a host of confounding variables can affect the reach of the wireless network, however, in our testing, we were able to easily connect to a robot some 20 m within an ICU on the other side of a wall. The video feed of the teleoperation system presently experiences latency of approximately 1 s. Parts were bought stock or manufactured *via* consumer-grade FFF 3D-printing, minimizing weight, cost, and complexity.

2.2 Intuitive Robot Control and Visual Servoing

Operators of the proposed system are medical professionals, nurses, respiratory therapists, and physicians with little or no experience with teleoperated robotic systems. Our goal is to make the system easy to operate with very little training by providing a remote-control device with a familiar and intuitive user interface for both setup and operation. We therefore propose a graphical user interface on the remote controller that replicates—as much as possible—the appearance of the ventilator's user interface and the way users typically interact with it.

To achieve this, the remote controller device features a large screen on which the live image of the ventilator's control panel is displayed. The live image is captured by a camera placed adjacent to the ventilator inside the ICU. The optimal angle for the live camera view of the control panel would be provided by a camera mounted directly in front of the ventilator screen (*front-view*). This is not practical, however, because the camera would obscure manual operation of the device and likely interfere with, or be obstructed by, robot motion. It is therefore necessary to mount a camera on the side of the ventilator and use computer vision methods to create an image that replicates the front-view. For some ventilators, it may be possible to obtain the front-view image *via* an external video output connector, but the side-mounted camera is still required for visual servoing.

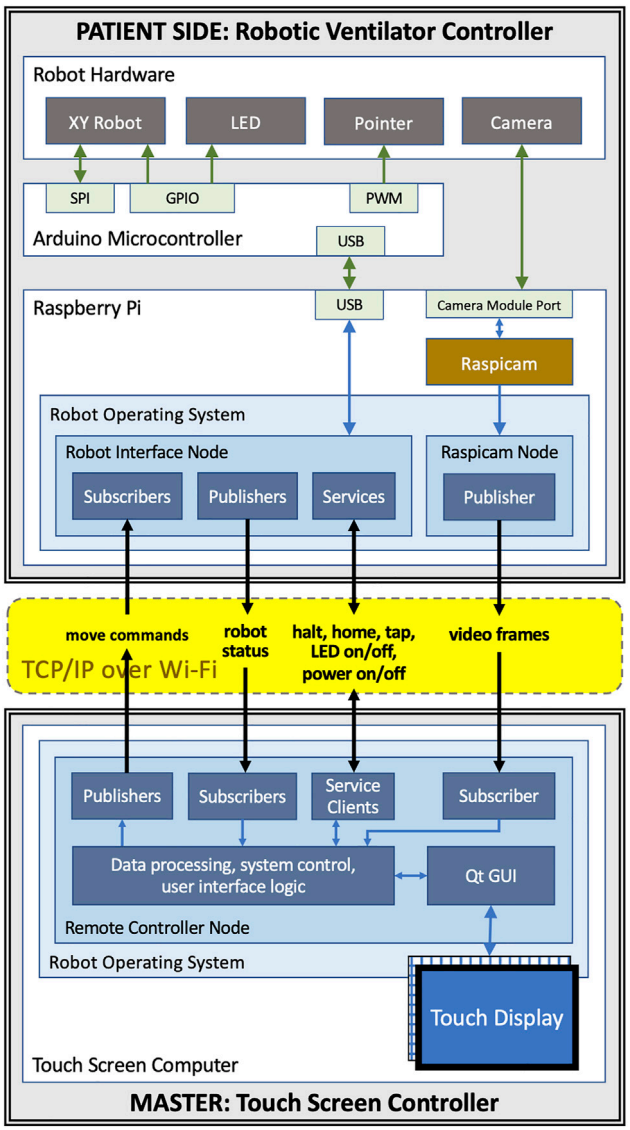

FIGURE 3 | Communication channels between components of the teleoperated system: the master and patient side devices communicate with each other using ROS topics and services over WiFi; the patient side Raspberry Pi is connected to the Arduino that controls the motors, the end-effector, and the LED using USB; the camera is connected to Raspberry Pi using the Pi's camera module port.

For a human user directly operating the ventilator, the brain manages the coordination of hand motions with respect to the visual field. Conversely, in a robotic remote control system this hand-eye coordination is handled by the robot control algorithm that requires vision feedback to ensure that the robot moves to the correct location and a calibration of the spatial relationships between the camera, the robot, and the ventilator screen.

Our development mainly focused on ventilator models that are controlled exclusively through a touch screen interface, such as the Maquet Servo-U, but in the Discussion (**Section 4**) we describe how the system can be modified to accommodate other physical controls, such as buttons and knobs.

2.2.1 Components for Vision Based Processing

In the following, we describe the components of the vision-based robot control system, all of which, except camera capture, are executed on the remote controller device. **Figure 4** illustrates the screen registration method that enables the generation of the front-view, the processing steps performed before displaying a camera frame on the remote controller's screen, and the robot control system's actions in response to a touch event.

Image capture: The camera is mounted on the robot's frame near the upper-left corner of the ventilator screen. Its mounting bracket holds it at 12 cm distance from the image plane, as shown in **Figures 2A,B**. The current prototype hardware uses an 8-megapixel Raspberry Pi camera module that is configured to capture color images at 10 frames per second in 1,920 × 1,440 image resolution. The images are compressed in JPEG format by the ROS *image_transport* node and sent to the remote controller over a ROS image topic. This particular image resolution was chosen because it provides a reasonable trade-off between spatial fine-detail fidelity, frame-rate, compression time, and bandwidth required. Image quality and framerate were evaluated by a clinical respiratory therapist and were found to be adequate. The intrinsic parameters of the camera were calibrated off-line, which enables the elimination of radial distortion in the first step of vision processing.

Visual tracking of robot end-effector: Live camera images are used by the robot control system to track the robot's position. Knowing the location of the robot's end-effector on video frames enables robot-to-camera calibration and high accuracy robot control by visual servoing. The visual tracking algorithm is designed to localize a single white light emitting diode (LED) on a dark background and was optimized for real-time performance on a tablet computer when processing a 2.8 megapixel resolution input video stream acquired from the camera. While the camera may see parts of the patient room and other medical equipment in its wide field-of-view, LED localization is only performed inside the area of the detected screen of the ventilator, therefore other devices and light sources cannot directly affect localization performance, although it is possible that reflections of external lights show up in the region of interest. The tracking algorithm first performs image thresholding and connected component analysis to identify large dark areas on the video frames, then uses template matching to find LED candidates in these dark regions. We only search for the LED in dark image regions because the end-effector, on which the LED is mounted, is a black piece of plastic. The template is a 2D Gaussian function that matches the typical size and appearance of the LED on the images. Of the LED candidates, the one with the highest peak intensity relative to its surrounding is selected. There are three special cases that are considered: 1) If the robot is already calibrated to the camera, as described in the next paragraph, then the system assumes that the robot-to-camera calibration is reasonable, which can be used to predict the position of the LED on the image from robot kinematics, and it only looks for the LED on the image in a

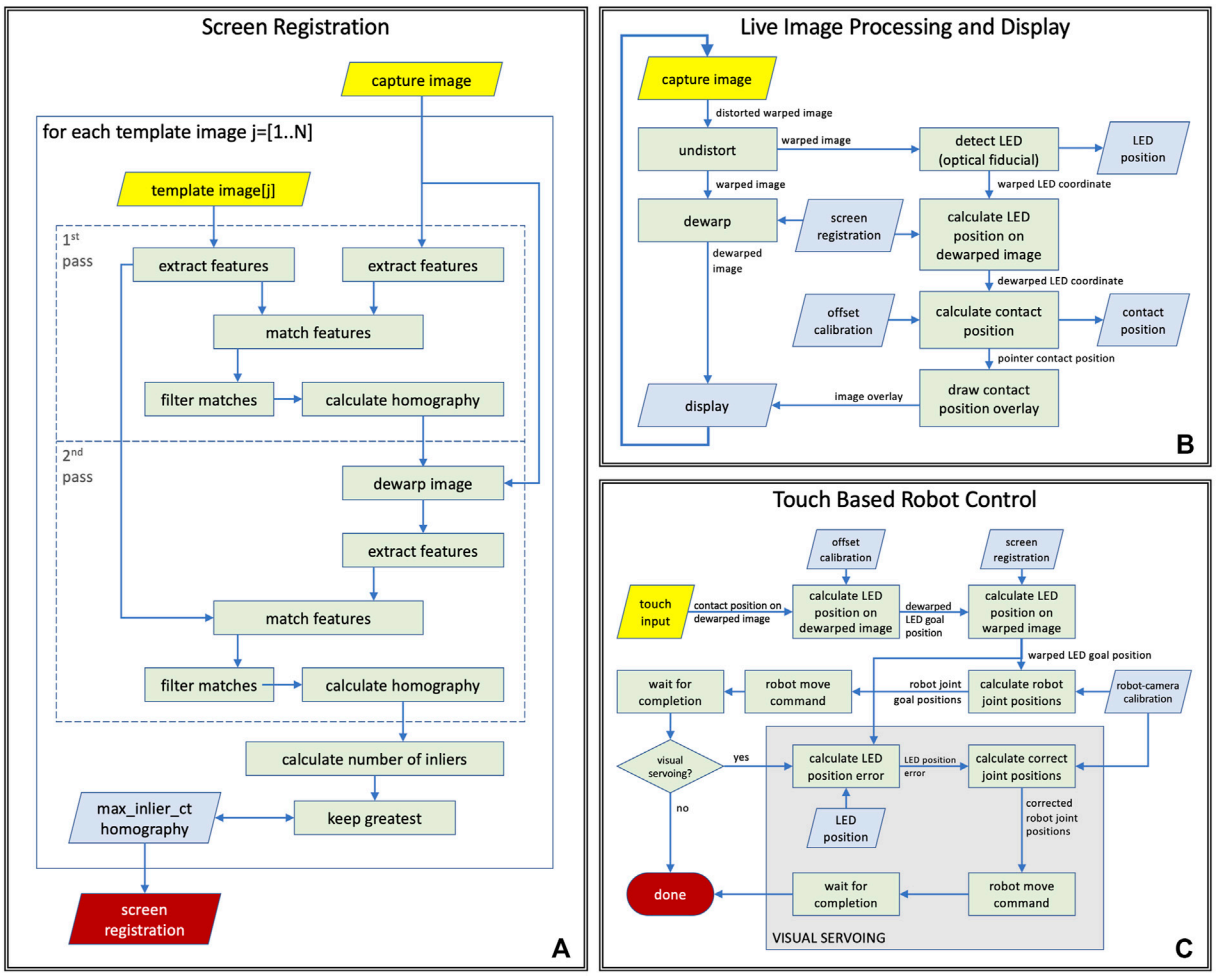

FIGURE 4 | Computer vision tasks performed during **(A)** ventilator screen registration, **(B)** live teleoperation, **(C)** touch based robot control logic with and without visual servoing.

small neighborhood of the predicted position. This results in a faster and more robust detection. 2) If the two best LED candidates on the image are in a spatial configuration where one of the candidates could be interpreted as a reflection of the LED on the ventilator's screen, then the algorithm will select the candidate that is not the reflection, even if that candidate has a lower peak intensity. 3) If the LED's position is predicted from kinematics to lie outside the visible area, then visual tracking is disabled.

Robot-to-camera calibration: For accurate teleoperation of the system using the remote live view, the robot must be calibrated to the camera, which is done as part of the auto-calibration process of the system. The calibration method moves the robot's end-effector to 4 or more locations with known joint positions, while the system uses a computer vision method to track the optical fiducial mounted on the end-effector in the camera frames. As the Cartesian frame of the robot is aligned with the ventilator screen, the fiducial will also move along a plane near and parallel to the screen. During the calibration process, the system stores the end-effector joint positions with the corresponding image coordinates and calculates a homography between the robot and the image coordinates. A homography is suitable for modeling this transformation because the robot's XY joints are prismatic and their scales are linear. The resulting homography enables the mapping between robot joint positions and image coordinates of the optical fiducial in the camera image. The robot calibration does not require operator interaction, takes less than 30 s to complete, and is valid as long as the relative position of the camera and the robot is unchanged. The robot calibration process can be executed remotely without entering the ICU. Under normal circumstances the calibration needs to be completed only when the robot is first turned on, after which, so long as the camera is not disturbed, the robot can continue to use the same calibration information. Recalibration would only be necessary if the robot lost power, the camera moved, or the system needs to be reset for some unforeseen reason. In case of an emergency, the recalibration process should take a comparable or lesser amount of time compared to donning the necessary PPE to enter the ICU room.

Fiducial offset calibration: The location where the LED is mounted on the end-effector was selected to provide good

visibility in any allowed end-effector position. Since its position is fixed on the end-effector, it moves rigidly with the capacitive touch device (mechanical finger), but knowing the LED's position in image coordinates is not sufficient to determine where the pointer will touch the screen. In order to be able to calculate that for any end-effector position, a fiducial offset calibration is performed offline, before mounting the robot on the ventilator. Luckily, all input values are coordinates on planes observed under perspective projection, therefore this calibration can also be modeled by a homography. The offset calibration is carried out using a different capacitive touch sensitive display of the same resolution and dimensions as the Servo-U screen, further discussed in **Section 3**. This display—just like the ventilator screen—has a completely flat glass surface. The identical setup enables us to use the same offset transformation calculated with the calibration display on the ventilator screen. During calibration, we send the robot to predetermined positions in joint space, while tracking the optical fiducial, then we command the robot to touch the screen and record the detected touch coordinates and the corresponding fiducial image coordinates for each position. Finally we calculate the calibration: the homography that describes the transformation between the two sets of coordinates and can also be applied to convert between other touch and fiducial coordinates.

Image dewarping to generate front-view image: The placement of the camera provides an oblique view of the screen that needs to be *dewarped* to a rectangular view before displaying it on the remote-control device's screen. The dewarping can be modeled as a perspective transform, which is described by a homography. The homography is calculated during the auto-calibration process of the system, by registering the camera image showing the ventilator screen to reference images of the ventilator screen. Since the screen of the ventilator is dynamically changing (it displays plots, numbers, icons, etc.), the reference images are generated from ventilator screen shots by manually masking out non-static regions. As shown in **Figure 4A**, the screen registration process—that is repeated for every reference image—is a two pass method that carries out the following processing steps in each pass: 1) it extracts ORB image features, as described in Rublee et al. (2011), on both the reference image and the camera image, 2) calculates the matches between these feature sets, 3) uses RANSAC, by Fischler and Bolles (1981), to find the homography that best describes the matches. The steps of processing are identical in the two passes but the parameters for the matching algorithm are different so that the first pass performs a quick coarse alignment, while the second pass performs fine-tuning on the results. In the case of multiple reference images, the match with the highest number of inliers is selected as the best match. The resulting homography is used to convert image coordinates between warped (camera) and dewarped (front) views, and to pre-calculate a dewarping look-up table (LUT) that enables efficient dewarping of every camera frame before displaying on the remote controller's screen. While the position and orientation of the camera are adjustable during installation, they remain fixed during use, therefore robot control methods may assume that the position of the ventilator's screen in camera images remains static during operation. However, if the camera is moved or reoriented intentionally or unintentionally, the screen registration needs to be recalculated, which takes a fraction of a second and can be done with a single button press on the remote controller.

Visual servoing: The proposed robot control system is designed for robustness by incorporating visual servoing, as illustrated in **Figure 4C**. During operation, the vision system continuously tracks the position of the end-effector in the live camera video and measures the difference between the robot's tracked position and the expected position calculated from calibration and robot kinematics. Every time the robot reaches the goal position after a move command, the system compares the visually tracked end-effector position to the goal position and calculates the amount of correction necessary for accurate positioning. If the error is larger than a given threshold, a move command is sent to the robot to execute the correction. The system also integrates the correction in the robot-to-camera calibration to provide better estimates for subsequent moves.

2.2.2 Vision Based Processes

Live image display: The system continuously captures images from the camera mounted on the robot, and each image is processed by a series of image processing and computer vision methods before getting displayed on the display of the remote controller, as illustrated in **Figure 4B**. In the first step (*undistort*), the radial distortion of the image is corrected based on camera calibration parameters that were calculated offline. The resulting image shows the screen of the ventilator as the camera sees it from the top left corner of the screen, but without the optical distortions of the lens (*warped image*). The *warped image* is then *dewarped* to create a simulated front-view (*dewarped image*), which is displayed on the remote controller. In the same time, the LED on the end-effector is tracked (*detect LED*) on the *warped image* by the system, and the resulting *warped LED coordinates* are then converted into *dewarped LED coordinates* using the *screen registration*. Using the parameters of the offline fiducial *offset calibration*, the corresponding *pointer contact position* is then calculated from the *dewarped LED coordinates*, and displayed as an overlay on the *dewarped image* on the remote controller's display.

Touch based robot control: When the operator taps the live image display on the remote controller, a chain of processing steps are initiated that, upon completion, results in the robot moving to the corresponding position on the screen of the ventilator. A flow chart of the process is shown in **Figure 4C**. First, the operator's tap *position on the dewarped image* is converted to *dewarped LED (goal) position* using the inverse fiducial *offset calibration*, from which then the system calculates the *warped LED goal position* using the inverse *screen registration*. The *robot-camera calibration* enables computing the corresponding *robot joint goal positions* from the *warped LED goal positions*. Next, the system issues a *robot move command* to the robot goal position and waits until the move is finished. If visual servoing is enabled, the system then *calculates the LED position error* by comparing the current *LED position* on the *warped image* to the *warped LED goal position* that enables the

FIGURE 5 | Evaluation of the ventilator controller system on a human body phantom in the Johns Hopkins Hospital's biocontainment unit (BCU). **(A)** Robot mounted on the screen of a Maquet Servo-U ventilator, **(B)** respiratory therapist using the remote controller software on a tablet computer outside the BCU, **(C)** remote controller user interface layout, with the setup group of controls indicated in green and the control group in red.

computation of corrected joint positions using the *robot-camera calibration* to which the robot is then moved by issuing another move command.

2.3 User Interface for Teleoperation

The remote controller of the robotic system is a software designed to be run on a tablet-style computer equipped with a touch screen. In our prototype, we use a Dell Inspiron 14 5000 2-in-1 Laptop that features a 14″ touch screen and a keyboard that can be folded behind the screen for tablet-style use. The computer communicates with the robot hardware wirelessly, enabling a completely untethered operation. During teleoperation, the software's graphical user interface (GUI) fills the remote controller's screen, as shown in **Figure 5C**, with the camera's live image occupying the entire right side, and Graphical User Interface (GUI) elements located on the left side. As the aspect ratio of the prototype tablet's screen is 16:9 while that of the camera image is 4:3, when the image is scaled to fill the entire height of the screen, there is still room left on the side for the GUI elements without occluding the image. The right side of the user interface, where the front-view live image of the camera is displayed, shows the screen of the ventilator. To move the robotic pointer to a particular position on the ventilator screen, the operator taps the same location on the live image of the remote controller's screen.

In the prototype remote controller software, the user interface elements on the left side can be divided into two groups: a *setup group* and a *control group*. The *setup group* includes buttons to initiate robot-to-camera calibration, register the ventilator's screen, and switches to enable/disable dewarping, turn the LED on/off, enable/disable visual servoing, and turn motors on/off. The *setup group*'s GUI elements are primarily used for debugging and as such, will be moved into a separate configuration panel or will be hidden from users in the production version of the device. The *control group* contains the buttons that are the most relevant for operators. The most frequently used button is the Tap button, which sends a command to the robot to perform a single tap action, as described in **Section 2.1**. The Press/Release button has two states and enables touch-and-hold actions by dividing the forward and backward motions of the pointer into two separate commands. This interaction style was chosen for safety reasons. We separated the motion of the pointer and the action of the pointer to two separate interactions so that the operator has a chance to visually confirm the positioning of the end-effector before committing to a touch action. The *control group* also contains the Halt button to cancel the current motion of the robot and the Home button to move the robot to a side position where it does not interfere with direct operator access to the ventilator screen.

2.4 Software and Communication

A teleoperated system relies on the communication method between the master and the patient side device. In a healthcare setting, the success of the entire concept relies on the communication channels being safe, reliable and secure. In the proposed system, the connection also needs to be wireless, as routing a cable out from within an isolated room may not be feasible. This wireless connection must not interfere with existing wireless hospital systems, and since a hospital may want to install multiple instances of the remote controller in a unit, the additional wireless links should not interfere with each other either.

In our design, we chose to use industry standard WiFi (IEEE 802.11g-2003 or IEEE 802.11n-2009) connections with built-in WPA2 authentication (IEEE 802.11i-2004). Each instance of the remote controlled system uses its own dedicated WiFi network with only the master and the patient side device being part of the network. This communication method is safe, as it is compatible with hospitals' own wireless systems, secure and highly reliable. It is also easy to deploy and WiFi support is already built into most modern computers. Having the UDP and TCP protocols available on WiFi networks enabled us to use the Robot Operating System (ROS) for establishing data connections between the master and patient side device. The ROS middleware provides a communication software library and convenient software tools for robotics and visualization. ROS communication is not secure in itself but channeling its network traffic through a secure WiFi network makes our system secure. The communication channels between the components of the teleoperated system are shown in **Figure 3**.

Both the master and the patient side of our system run on the Linux operating system. The patient side Raspberry Pi runs Raspbian Buster while the master runs Ubuntu 18.04. Both systems have ROS Melodic installed. The GUI software on the master is implemented in C++ using RQT, a Qt based GUI software library with access to the ROS middleware. The patient side software is also implemented in C++. Computer vision methods were implemented using the OpenCV software library, Bradski (2000).

3 RESULTS

To quantify the effectiveness of the robotic teleoperation system, four experiments were carried out, intended to measure the open-loop repeatability, the closed-loop visual servoing accuracy, relative time needed to operate a ventilator with the system, and the qualitative user experience of the teleoperation system. Under ideal circumstances, without restrictions affecting access to health care facilities, personnel, and equipment, a rigorous human subject experiment would be done to evaluate the usability and efficacy of the proposed robotic system. However, in the middle of the COVID-19 pandemic, we did not have the opportunity to perform a time consuming rigorous study using clinical ventilators.

As, due to the COVID-19 pandemic, access to mechanical ventilators for testing was precious and limited, a "mock ventilator" was constructed to perform the tests, which did not necessitate exact replication of a clinical environment. This mock ventilator consisted of a commercially available point-of-sale capacitive touch screen monitor, selected to match the Servo-U screen size and resolution, connected to a laptop computer running test software written in JavaScript. The software was programmed to display screen captures from the Servo-U ventilator, record the location of any touch interactions in screen pixel coordinates, and emulate three commonly used features of the Servo-U: changing the oxygen concentration, activating the oxygen boost maneuver, and changing the respiratory rate alarm condition.

3.1 Mechanical Repeatability Testing

In order to quantify the open-loop mechanical repeatability of the robotic system, we performed a positional repeatability test according to ISO 9283:1998 (1998) (*Manipulating industrial robots—Performance criteria and related test methods*). The robot was commanded to move in sequence to five positions in joint space distributed across the screen, performing the sequence a total of 50 times. At each position, the robot paused and tapped the screen, with each touch location on the screen being registered in pixel coordinates by the test software. Given the measured dimensions of the screen and its defined resolution (1,024 by 768 pixels), the pixel width and height were both found to be approximately 0.3 mm, which enabled the conversion of pixel coordinates to position coordinates in millimeters.

Figure 6 shows the location data from the 5 groups of 50 taps, re-centered about their respective barycenter. As can be seen, the distributions were uniform and practically indistinguishable across the five locations. The pose repeatability (RP), is defined by ISO 9283:1998 (1998) as $RP = \bar{l} + 3S_l$, for $\bar{l}$ average euclidean distance to barycenter, and S_l standard deviation of euclidean distances to barycenter. For the 250 position measurements taken from the robotic prototype, RP was found to be 7.5 mm. While these results are far from high precision positioning, given that the smallest button on the Servo-U ventilator needed for setting adjustment is 21 mm by 21 mm, it is appropriate for the task at hand.

The one notable feature of the data was that the spread was significantly greater in the X (horizontal) direction than the Y (vertical) direction, ranging ±5 mm in X and only ±1.5 mm in Y. The reason for this was readily apparent: due to its low-cost and lightweight construction, the prototype design omitted linear bearings, with the two axis frames riding directly on the linear rods with a loose 3D-printed slip-fit cylindrical feature. Due to the play in this feature and the cantilevered design, the Y axis arm could swing a small angle, inducing errors. Due to the arm's length and the small degree of the swept angle, this issue's impact on the Y repeatability was minimal (as it was of order $cos(\theta) \approx 1$), but the impact in the X direction was detectable ($sin(\theta) \approx \theta$). This issue could be resolved in future prototypes with the use of close-fitting linear bearings.

3.2 Visual Servoing Accuracy Testing

In order to quantify the accuracy of visual servoing, 40 uniformly distributed positions were generated across the

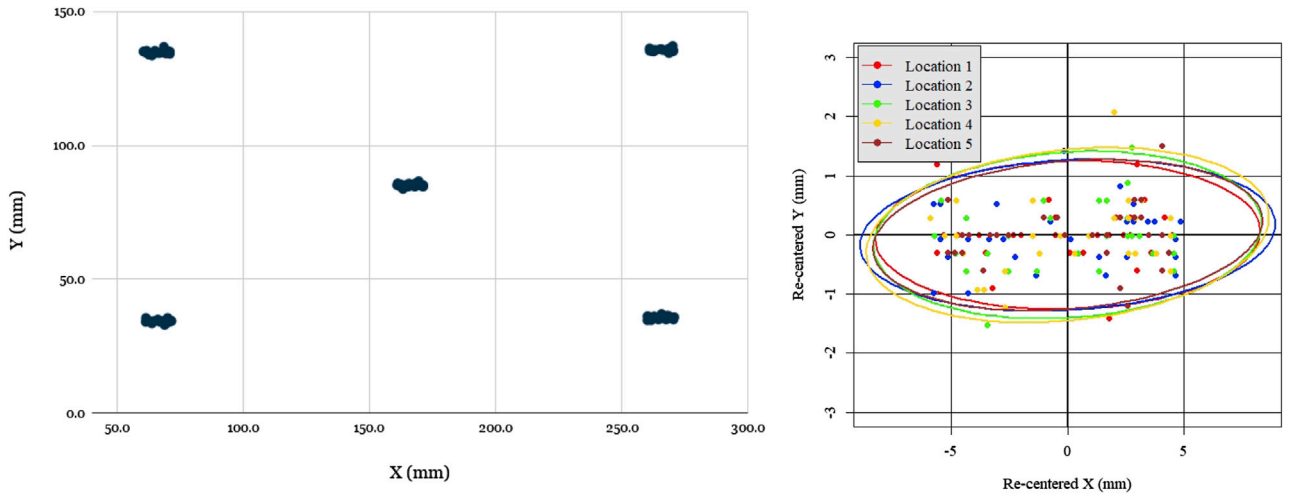

FIGURE 6 | Evaluation of robot open loop repeatability: scatter plot of open-loop recorded taps for five locations distributed across the screen **(left)**, scatter plot of all tap locations re-centered with respect to each barycenter with 95% confidence covariance ellipses for each location. Notably, the spread of re-centered locations is approximately the same across all locations, as evidenced by the covariance ellipse overlap, but spread is greater in X than in Y.

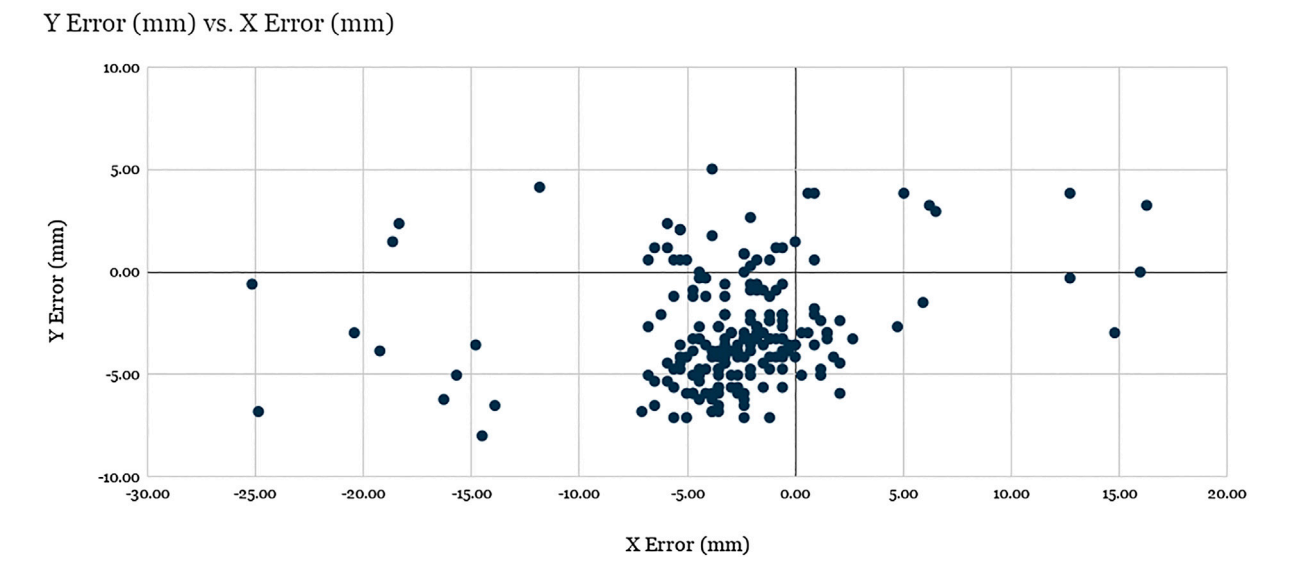

FIGURE 7 | Evaluation of robot positioning accuracy: Scatter plot of visual servoing recorded tap location errors for the 40 target locations spanning the screen across the 5 experimental runs (200 total points). See discussion.

ventilator screen. In a random sequence, each of these locations was displayed on the mock ventilator screen by means of a thin black crosshair on a white background. The experimenter, using the teleoperation interface, would then command the robot to move (with visual servoing enabled) to the center of the cross-hair, using a mouse to ensure precise selection. Upon arriving at its destination, the robot would be commanded to tap, with the resulting pixel coordinates being recorded by the test software of the mock ventilator. This sequence was repeated 5 times, each time using a different screenshot taken directly from the Servo-U ventilator for screen registration. The raw errors for all 40 locations across the 5 runs are shown in **Figure 7**.

The X average error and Y average error were found to be −2.87 and −2.89 mm, respectively, with standard deviations of 5.31 and 2.71 mm. The average Euclidean error was found to be 5.94 mm with a standard deviation of 4.19 mm, where 89.5% of the data points (179 of 200) are clustered around the barycenter within 2σ radius, with the remaining points considered outliers. The analysis of the results suggest that the factors responsible for the errors for the data points within the cluster are related to mechanical precision, system calibration, and screen registration

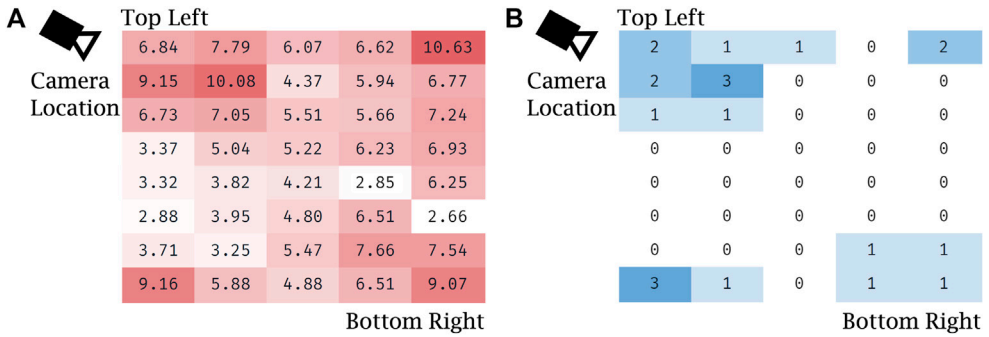

FIGURE 8 | Evaluation of robot positioning accuracy with visual servoing: **(A)** heat map of Euclidean error (in mm) for visual servoing for each of the 40 locations spanning the screen, averaged over the five trials, **(B)** heat map of the number of outliers with respect to Euclidean error for each of the same locations spanning the screen, summed over the five trials.

inaccuracies, while the outliers were produced as a result of failed vision-based tracking of the optical fiducial.

Notably, the error of visual servoing is not uniform across the screen. **Figure 8** shows the heatmaps of error (a) and the number of outliers (b) across the 40 uniformly distributed spanning locations. Error is overall greatest near the corners and the edges of the screen that are farthest from the view of the left-side mounted camera. Outliers are clustered near the corners, which shows that the vision-based tracker often failed to detect the optical fiducial when the LED was far from the center of the screen. This failure is particularly apparent in the top left corner, nearest the camera, which suggests that in that particular configuration the LED detection algorithm often confused the LED with another nearby bright spot in the camera's image. The larger errors in the other three corners, farther from the camera, are partially due to the lower spatial fidelity of the image at those locations, which leads to significantly higher errors when measured as projections on the image plane.

While an average 5.94 mm of Euclidean positioning error is significant, it is sufficient for the teleoperation tasks required of the prototype given the aforementioned 21 mm minimum feature size. Controls on medical equipment, such as buttons, knobs, and switches are designed for easy and safe manual operation even while the operator is wearing two layers of nitrile gloves. Similarly, touch screen-based ventilators, like the Maquet Servo-U, also feature large on-screen buttons generously spaced from each other. During our evaluation the accuracy of our remote controlled robot prototype proved to be sufficient for easy and safe teleoperation. Nevertheless, further planned improvements for the visual servoing system are discussed later in this text (**Section 4**).

3.3 Manual Operation vs. Teleoperation Setting Change Time Comparison

To verify the usability and utility of the device, the prototype teleoperated Cartesian ventilator robot was mounted on the mock ventilator. Experimenters were asked to perform three tasks representative of routine setting changes, manually and *via* teleoperation: increasing the oxygen concentration setting by five percentage points, activating the O2 boost maneuver, and lowering the respiratory rate alarm condition by three increments. The experiments were recorded and timed from the first interaction to the confirmation of the last setting change. **Table 1** shows the results for three such experiments performed on the mock ventilator, and one experiment performed on an actual Servo-U.

TABLE 1 | Experimental data for manual and teleoperation performance of three routine setting change tasks.

Test equipment	Manual operation time (s)	Teleoperation time (s)
Mock ventilator	20	74
Mock ventilator	18	60
Mock ventilator	15	67
Servo-U ventilator	28	109

The data showed that, on average, operators were able to complete the three tasks in 18 s manually and in 67 s *via* teleoperation, using a mock ventilator screen. They were able to complete the same tasks in 28 s manually vs. 109 s using a clinical ventilator, a ratio of approximately 3.8 in terms of additional time needed using the robot. However, the protocol of manual ventilator operation for infectious patients requires the healthcare worker to don new PPE before entering the ICU room and doff it after exiting. Seeing how the proper donning and doffing of PPE is of essential importance to the safety of personnel and infection control, it is a process that inherently takes time to be done correctly. For teleoperated ventilator operation, there are no PPE requirements since the operator never enters the patient room. A co-investigator with clinical expertise performed the full don/doff sequence that would be required and recorded the times as being 170 s to don and 73 s to doff, not including time to clean equipment post-doff. Thus, in total, including donning and doffing, manual operation of the Maquet Servo-U ventilator for these tasks would have taken 271 s compared to only 109 s for teleoperation with our prototype Cartesian ventilator robot, leading to a significant net time savings, in addition to reducing the amount of PPE consumed and the risk of infection to the

respiratory therapist. Due to limited time and access to hospital resources during pandemic conditions, we have only a single data point for donning and doffing times and for teleoperation times with the clinical ventilator, therefore our results are not yet conclusive. However, our clinical collaborators confirmed that these times are representative of typical ventilator operation and PPE donning and doffing times.

3.4 Qualitative System Evaluation in Biocontainment Unit

We took the teleoperated ventilator controller system to the Johns Hopkins Hospital's Biocontainment Unit (BCU) for qualitative evaluation in maximally accurate conditions. The tests were carried out by a clinical respiratory therapist (RT) while the patient side robotic manipulator was mounted on a Maquet Servo-U mechanical ventilator, as shown in **Figure 5A**. The ventilator was connected to a human body respiratory phantom to enable the simulation of realistic usage scenarios. Before evaluation, the camera and robot were calibrated using the system's remote controller, after which the RT spent approximately 2 h using the system for making typical adjustments on the ventilator from outside of the BCU bay (**Figure 5B**). The wireless signal easily penetrated into the BCU bay resulting in reliable communication between the remote controller and robot.

During and after the evaluation, the RT provided invaluable feedback regarding the system. His feedback is summarized by topic in the following:

Image quality: The quality of the live front-view camera image was assessed to be adequate to read numerical information and plots displayed on the ventilator's screen. The respiratory therapist found no issues with the frame rate of 10 frames per second provided on the remote controller's screen. He suggested that since the most relevant information on the ventilator's display is on the right side, the remote controller would be able to provide a higher definition view of that information if the camera was moved from the top left to the top right corner. He found the current video latency of approximately 1 s distracting, and recommended that it should be reduced in a production version of the system.

Robot: The RT emphasized that the robot may not yet be physically robust enough to be used in a healthcare setting and would need to be ruggedized. He also asked us to investigate if the robot being mounted on the ventilator screen can potentially affect the range of motion of the ventilator's swiveling display and whether the robot's mounting points are compatible with other ventilator models with different screen thickness.

Graphical user interface (GUI) of the remote controller: The current prototype remote controller's graphical user interface contains buttons and switches that are for debugging purposes, which the RT suggested should be hidden or moved into a dialog box. He also mentioned that the current user interface is inconvenient for right-handed operation and we should add an option for switching between left and right-handed layouts. The most significant feedback regarding the GUI we received is that the location of the Tap button is unintuitive in the current fixed position and it would be preferred to have it move together with the robot's end-effector near the touch point. He suggested that the Tap button should be merged with the Press/Release button.

Robot control and visual servoing: According to the RT, controlling the robot by touch on the remote controller's interface is intuitive and visual servoing seemed to make a positive impact, but due to the video latency of approximately 1 s, visual servoing adds an additional delay that should be reduced.

On handling multiple systems in a single unit: The patient identifier should be clearly shown on the remote controller. Currently, ventilator screens do not show patient identifying information, but a remote controller unit that can work from a distance must have the patient ID prominently shown in order to make sure the right ventilator settings are entered for the correct patients.

With the help of the RT, as previously mentioned in **Section 3.3** we also measured the time required to don and doff personal protective equipment (PPE) for a healthcare worker to access a negative-pressure intensive care patient room or a BCU from outside. As shown in **Figure 9**, it took 170 s for the RT to don and 73 s to doff the PPE during the one trial we had a chance to observe. The required PPE included two pairs (two layers) of nitrile disposable gloves, a respirator device with the attached mask, and a plastic gown.

4 DISCUSSION

This paper reports the development of a simple, low cost telerobotic system that allows adjustment of ventilator settings from outside the ICU. Our experiences with our initial prototype are very encouraging and provide a basis for further development. Engineering system tests demonstrated that open-loop position repeatability was 7.5 mm and that the average positioning error of the robotic finger under visual servoing control was 5.94 mm. Successful usability tests in a simulated ICU environment were also reported. Preliminary evaluation highlighted the system's potential to save significant time and PPE for hospitals and medical staff. In one evaluation where we compared the time required to make an adjustment on the ventilator using the proposed teleoperated system to the time required for a respiratory therapist to don PPE, enter the patient room, make the change directly on the ventilator, then leave the room and doff the PPE, we found that the RT managed to make the adjustment in a significantly shorter time (109 s) using teleoperation than without (271 s). We also received positive feedback during qualitative evaluation in a clinical setting. The respiratory therapist who performed the evaluation emphasized that the system can be a force-multiplier for respiratory teams by freeing up valuable resources. This robotic system has the potential to reduce the infection risk for healthcare workers, reduce usage of PPE, and reduce the total time required to adjust a ventilator setting.

One limitation of the current prototype robotic system hindering clinical usability is the difficulty to adequately clean

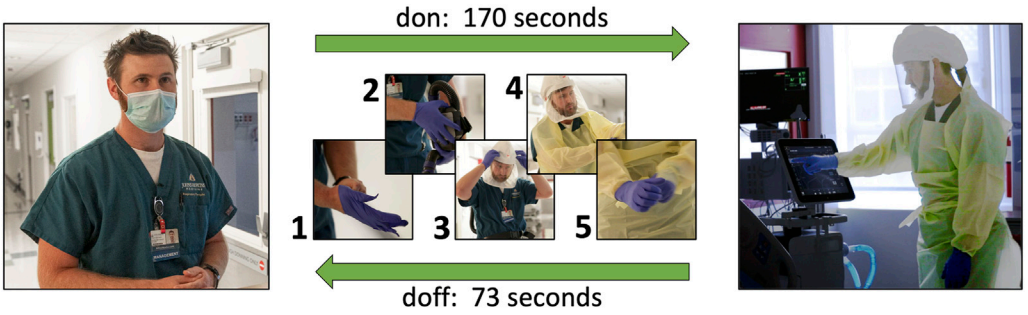

FIGURE 9 | During our qualitative system evaluation in the biocontainment unit of the Johns Hopkins Hospital, it took 170 s for a respiratory therapist to don his personal protective equipment (1: a pair of disposable nitrile gloves, 2: respirator device, 3: mask, 4: plastic gown, 5: a second pair of disposable nitrile gloves) and 73 s for doffing.

and disinfect the Cartesian robot. A future clinical grade device will be encased in an acrylic cover to protect recessed features and components from contamination, thus facilitating easier cleaning by wiping down the convex outer surface. Disinfection of the device will follow the CDC's Environmental Cleaning strategy, WB4224, which requires disinfecting the device with EPA-registered hospital disinfectant during regular cleaning cycles, between patients, and before removing it from the room.

A second limitation of the reported study was the frequent large position error under visual servoing. 17 of the 200 test taps had an Euclidean error >10 mm, which would result in a miss when tapping small features on the ventilator, which have a minimal size of 21 mm. While any setting changes on the ventilator require tapping a confirmation button, which prevents accidental parameter adjustments, this high fail rate reduced usability and confidence in the prototype system. There were three contributing factors to the errors that will be addressed in a future clinical system: 1) The mechanical play in the system created an unintended swing of the end-effector, contributing to the error in the X direction. This error can be easily reduced by using linear bearings. 2) The visual servoing control did not work robustly due to missed detections of the optical fiducial on the end-effector, which was the root cause of outliers in the visual servoing evaluation results. We found that the detection of a single LED mounted on the end-effector sometimes proved challenging as the LED detection method occasionally detected a different bright spot in the image (e.g., the LED's reflection on the screen, a similar sized bright dot shown on the ventilator screen, or metallic reflection from a robot component), therefore in the next version of the prototype we will replace the single LED with a small cluster of LEDs arranged in a unique pattern that is distinguishable from its mirror image. With the use of multiple LEDs we aim to achieve better than 99.5% success rate in unambiguously determining the end-effector position. While it would be desirable to achieve 100% detection rate, occasionally missed detections do not invalidate the system as the operator can always manually correct for robot positioning inaccuracies before giving a tap command. 3) Calibration and screen registration inaccuracies contributed to an error of approximately 4 mm in the visual servoing experiments. This error manifested itself as a consistent offset in touch positions. While this offset alone would not significantly impact system performance, considering the large size of buttons on the ventilator screen, we will reduce the introduced offset by improving the fiducial offset calibration process and screen registration.

During qualitative evaluation of the system in a BCU, our clinical collaborators uncovered usability issues in the graphical user interface of the remote controller software that will be addressed in the next versions of the system. These improvements include the relocation of the interaction buttons, Tap and Press/Release, adding an image zoom feature, and adding an option to allow switching between right-handed and left-handed layouts.

Our current system is capable of transmitting the live image of the ventilator's screen to the remote controller, however in certain cases it may be required to transmit audible alerts as well. This was not a priority in our design because most ICU ventilators are also connected to the central nurse call and alarm management system, therefore audible alerts are already relayed to the healthcare staff outside patient rooms.

A system used in a clinical setting will also need to properly address patient identification. Currently mechanical ventilators do not require patient identifying information during setup and operation because the device is placed near the patient and it is always entirely unambiguous to which patient the ventilator is connected. However, in a remote controlled scenario, particularly in the situation when there are multiple remote controlled systems used simultaneously with different patients, a lack of patient ID could lead to confusion where adjustments are made to the wrong patients by mistake. We will address this critical issue by adding a patient identifier to the remote controller's graphical user interface and make the entering of patient ID a mandatory step in the system setup process.

To broaden the pool of ventilators that the robot can control, we are planning to incorporate a sub-system to turn an adjustment knob. Both the Hamilton ventilator series, which represent the second largest install base at Johns Hopkins Hospital after the Maquet Servo-U, and the

GE (General Electric Healthcare Inc., Chicago, IL, United States) ventilators have an integrated knob. The system will use a stepper-driven, spring-loaded friction wheel, which will run along and turn the setting adjustment knob, while the robotic finger will be used to push the confirmation button on the touch screen.

Our team of clinicians and engineers came together during an extraordinarily challenging time, at the beginning of a global pandemic, to leverage our expertise and experience in assistance of frontline healthcare workers. Team members were geographically separated as a result of social distancing, which made some aspects of system integration and evaluation particularly difficult. Software developers never got to see the hardware in person that they were developing for, and none of the people participating in implementation were able to be present for the system evaluation in the Biocontainment Unit. Despite the difficulties, our initial prototype performed well during evaluation and received mainly positive feedback from clinical professionals. Our team is committed to carry on and make the system sufficiently robust for controlled clinical studies in the near future.

DATA AVAILABILITY STATEMENT

The raw data supporting the conclusions of this article will be made available by the authors, without undue reservation.

ETHICS STATEMENT

Written informed consent was obtained from the individual(s) for the publication of any potentially identifiable images or data included in this article.

AUTHOR CONTRIBUTIONS

BV developed the computer vision and visual servoing algorithms, along with the robot control software and user interface used in this system. MK performed the detailed design and construction of the prototype robot, wrote the local controller firmware, and conducted the engineering system validation. JC provided key insights into system requirements and conducted the usability evaluation. AD provided key elements of the system software implementation. PK contributed to the system design. SM provided expert advice on mechanical ventilation and PPE, as well as key insights into the system requirements. RT coordinated the overall effort and contributed to all phases of the design and evaluation discussions. AK led the development of the in-ICU robot and robot integration, designed the system evaluation studies, and performed the manual vs. teleoperation comparison and BCU studies. All authors contributed to the article and approved the submitted version.

FUNDING

The reported work was supported by Johns Hopkins University internal funds and University of Maryland internal funds.

ACKNOWLEDGMENTS

We thank Brian Garibaldi and the BCU team for access and support for the BCU evaluation; Sarah Murthi and Michelle Patch for early discussions on clinical needs and physician perspectives; Anna Goodridge for early design consultation; and Lidia Al-Zogbi and Kevin Aroom for participating in the evaluation of the robotic system.

REFERENCES

Biobot Surgical Pte Ltd (2020). *SwabBot - the World's First Patient-Controlled Nasopharyngeal Swab Robot*. Singapore: Biobot Surgical Pte Ltd.

Bradski, G. (2000). The OpenCV Library. *Dr. Dobb's J. Softw. Tools* 25 (11), 120–125.

Chang, R., Elhusseiny, K. M., Yeh, Y.-C., and Sun, W.-Z. (2020). *COVID-19 ICU and Mechanical Ventilation Patient Characteristics and Outcomes - A Systematic Review and Meta-Analysis.* medRxiv. doi:10.1101/2020.08.16.20035691

Chen, A. I., Balter, M. L., Maguire, T. J., and Yarmush, M. L. (2020). Deep Learning Robotic Guidance for Autonomous Vascular Access. *Nat. Mach Intell.* 2, 104–115. doi:10.1038/s42256-020-0148-7

Fischler, M. A., and Bolles, R. C. (1981). Random Sample Consensus. *Commun. ACM* 24, 381–395. doi:10.1145/358669.358692

Gong, Z., Jiang, S., Meng, Q., Ye, Y., Li, P., Xie, F., et al. (2020). SHUYU Robot: An Automatic Rapid Temperature Screening System. *Chin. J. Mech. Eng.* 33, 38. doi:10.1186/s10033-020-00455-1

Henkel, A. P., Čaić, M., Blaurock, M., and Okan, M. (2020). Robotic Transformative Service Research: Deploying Social Robots for Consumer Well-Being during COVID-19 and beyond. *Josm* 31, 1131–1148. doi:10.1108/JOSM-05-2020-0145

Hollander, J. E., and Carr, B. G. (2020). Virtually Perfect? Telemedicine for Covid-19. *N. Engl. J. Med.* 382, 1679–1681. doi:10.1056/NEJMp2003539

IGI Testing Consortium (2020). Blueprint for a Pop-Up SARS-CoV-2 Testing Lab. *Nat. Biotechnol.* 38, 791–797. doi:10.1038/s41587-020-0583-3

ISO 9283 1998 (1998). *Manipulating Industrial Robots – Performance Criteria and Related Test Methods. Standard*. Geneva, CH: International Organization for Standardization.

Li, S.-Q., Guo, W.-L., Liu, H., Wang, T., Zhou, Y.-Y., Yu, T., et al. (2020). Clinical Application of an Intelligent Oropharyngeal Swab Robot: Implication for the COVID-19 Pandemic. *Eur. Respir. J.* 56, 2001912. doi:10.1183/13993003.01912-2020

Morita, P. P., Weinstein, P. B., Flewwelling, C. J., Bañez, C. A., Chiu, T. A., Iannuzzi, M., et al. (2016). The Usability of Ventilators: a Comparative Evaluation of Use Safety and User Experience. *Crit. Care* 20, 263. doi:10.1186/s13054-016-1431-1

Quigley, M., Conley, K., Gerkey, B., Faust, J., Foote, T. B., Leibs, J., et al. (2009). "ROS: an Open-Source Robot Operating System," in ICRA Workshop on Open Source Software. Kobe, Japan.

Rublee, E., Rabaud, V., Konolige, K., and Bradski, G. (2011). "ORB: An Efficient Alternative to SIFT or SURF," in 2011 International Conference on Computer Vision. Barcelona, Spain, 2564–2571.

Scassellati, B., and Vázquez, M. (2020). The Potential of Socially Assistive Robots during Infectious Disease Outbreaks. *Sci. Robot.* 5, eabc9014. doi:10.1126/scirobotics.abc9014

United States Centers for Disease Control and Prevention (2020). *COVID-19 Death Data and Resources, Daily Updates of Totals by Week and State*. Atlanta, GA: United States Centers for Disease Control and Prevention.

World Health Organization (2020). *Coronavirus Disease (COVID-19) Dashboard*. Geneva, Switzerland: World Health Organization.

Yang, G.-Z., J. Nelson, B. B., Murphy, R. R., Choset, H., Christensen, H., H. Collins, S. S., et al. (2020b). Combating COVID-19-The Role of Robotics in Managing Public Health and Infectious Diseases. *Sci. Robot.* 5, eabb5589. doi:10.1126/scirobotics.abb5589

Yang, G., Lv, H., Zhang, Z., Yang, L., Deng, J., You, S., et al. (2020a). Keep Healthcare Workers Safe: Application of Teleoperated Robot in Isolation Ward for COVID-19 Prevention and Control. *Chin. J. Mech. Eng.* 33, 47. doi:10.1186/s10033-020-00464-0

Ye, R., Zhou, X., Shao, F., Xiong, L., Hong, J., Huang, H., et al. (2021). Feasibility of a 5G-Based Robot-Assisted Remote Ultrasound System for Cardiopulmonary Assessment of Patients with Coronavirus Disease 2019. *Chest* 159, 270–281. doi:10.1016/j.chest.2020.06.068

Conflict of Interest: The authors declare that the research was conducted in the absence of any commercial or financial relationships that could be construed as a potential conflict of interest.

frontiers in Artificial Intelligence

PERSPECTIVE
published: 20 July 2021
doi: 10.3389/frai.2021.590189

AI-Assisted CT as a Clinical and Research Tool for COVID-19

Zion Tsz Ho Tse[1†], Sierra Hovet[1†], Hongliang Ren[2], Tristan Barrett[3], Sheng Xu[4], Baris Turkbey[4] and Bradford J. Wood[4]*

[1]Department of Electronic Engineering, The University of York, York, United Kingdom, [2]Department of Electronic Engineering, The Chinese University of Hong Kong, Hong Kong, China, [3]Department of Radiology, University of Cambridge School of Clinical Medicine, Cambridge, United Kingdom, [4]Center for Interventional Oncology, Radiology and Imaging Sciences, National Institutes of Health, Bethesda, MD, United States

There is compelling support for widening the role of computed tomography (CT) for COVID-19 in clinical and research scenarios. Reverse transcription polymerase chain reaction (RT-PCR) testing, the gold standard for COVID-19 diagnosis, has two potential weaknesses: the delay in obtaining results and the possibility of RT-PCR test kits running out when demand spikes or being unavailable altogether. This perspective article discusses the potential use of CT in conjunction with RT-PCR in hospitals lacking sufficient access to RT-PCR test kits. The precedent for this approach is discussed based on the use of CT for COVID-19 diagnosis and screening in the United Kingdom and China. The hurdles and challenges are presented, which need addressing prior to realization of the potential roles for CT artificial intelligence (AI). The potential roles include a more accurate clinical classification, characterization for research roles and mechanisms, and informing clinical trial response criteria as a surrogate for clinical outcomes.

Keywords: COVID-19, computed tomography, RT-PCR, artificial intelligence, diagnosis

OPEN ACCESS

Edited by:
Patrick M Pilarski, University of Alberta, Canada

Reviewed by:
Maria F. Chan, Memorial Sloan Kettering Cancer Center, United States
Sunyoung Jang, Princeton Radiation Oncology Center, United States

****Correspondence:***
Zion Tsz Ho Tse
zion.tse@york.ac.uk

†Co-first author

Specialty section:
This article was submitted to Medicine and Public Health, a section of the journal Frontiers in Artificial Intelligence

Received: *10 August 2020*
Accepted: *19 May 2021*
Published: *20 July 2021*

Citation:
Tse ZTH, Hovet S, Ren H, Barrett T, Xu S, Turkbey B and Wood BJ (2021) AI-Assisted CT as a Clinical and Research Tool for COVID-19. Front. Artif. Intell. 4:590189. doi: 10.3389/frai.2021.590189

INTRODUCTION

Computed tomography (CT) is not being used to its full potential toward a better understanding of COVID-19. The reverse transcription polymerase chain reaction (RT-PCR) test is the current gold standard for diagnosing COVID-19 through the detection of nucleic acid present in SARS-CoV-2, the virus that causes COVID-19 (Ai et al., 2020). One of the main disadvantages with RT-PCR testing is that the results may take several hours to several days to obtain. Another disadvantage is that RT-PCR test kits are a finite resource. In many instances, test kits have become temporarily limited in areas experiencing outbreaks as the demand has spiked. Moreover, in low- and middle-income countries, it has been a struggle to access test kits altogether or in the quantity needed (Peplow, 2020). Any hospital equipped with a CT scanner could potentially use CT in conjunction with RT-PCR to address these problems. In specific high-prevalence settings early in the pandemic, the sensitivity of chest CT for detecting COVID-19 has been reported as high as 97–98%, compared to 71–85% for early real-time reverse transcriptase polymerase chain reaction (rRT-PCR) (Ai et al., 2020; Bernheim et al., 2020; Kanne, 2020; Xie et al., 2020). There has been much debate over the ability to generalize such high performance numbers, which are highly dependent on background prevalence in the community or screening population, clinical suspicion, and the performance of specific RT-PCR methodologies, which has improved over the past year.

To complement the use of standard chest CT for COVID-19 characterization and to further contribute to the body of knowledge for combating the pandemic, artificial intelligence (AI) could be utilized to improve the ability of CT to swiftly and accurately flag CTs for immediate interpretation, characterize COVID-19 for clinical research, such as response to medical countermeasures, and potentially increase patient safety by optimizing radiation exposure.

THE ROLE OF CT IN THE COVID-19 PANDEMIC

Using CT in Conjunction With RT-PCR for COVID-19 Diagnosis

To address the aforementioned weaknesses of RT-PCR (namely, the delay in results and fluctuating availability), CT could be used in conjunction with RT-PCR in selected target populations with a high risk for COVID-19, such as at the point of care (POC) in an outbreak setting. In such a POC setting, CT could be used to identify possible cases, and RT-PCR would be used to confirm conclusive diagnosis. CT might solve the problem of delayed results because CT results with or without AI models are obtained more quickly compared to RT-PCR. CT scanners are widely available and offer reliable daily accessibility. Moreover, CT has been shown to assist with detecting possible cases of COVID-19, even among asymptomatic patients, which may be important given the public health conundrum of presymptomatic and asymptomatic transmission (Apostolopoulos and Bessiana, 2003; Narin et al., 2003; Wang and Wong, 2003; Bernheim et al., 2020; Kanne, 2020; Liang, 2020; Xie et al., 2020). Some studies have touted the sensitivity of chest CT (vs. RT-PCR) for detecting COVID-19 in super-acute high-prevalence early epidemic outbreak settings (Ai et al., 2020; Liu et al., 2020). Another study found that RT-PCR and CT together may miss fewer patients than CT alone or RT-PCR alone (Inui et al., 2020).

Certain high-risk patients who undergo CT in an outbreak setting or after a high dose exposure might be identified by CT and isolated or quarantined while they await RT-PCR results, thus reducing the risk of transmission (Amalou et al., 2020). CT scans for other indications, performed in asymptomatic patients, might also identify and isolate patients prior to risking transmission to a busy clinic POC setting. This is important because many people infected with SARS-CoV-2 have mild symptoms or no symptoms at all. Additionally, peak viral shedding occurs at or just before the onset of symptoms (Zou et al., 2020), so it is common for asymptomatic people to unknowingly transmit the disease and those patients may have CT opacities (Varble et al., 2021). CT should not replace RT-PCR for the diagnosis of SARS-CoV-2/COVID-19, so its use might be tightly linked to RT-PCR availability, and the risk-to-benefit ratios of the radiation risk vs. the risk to the population of not diagnosing or isolating a particular patient. CT might also be proposed as an epidemiology tool to assess spread or focus on a target population who has exposure history, such as a cruise ship.

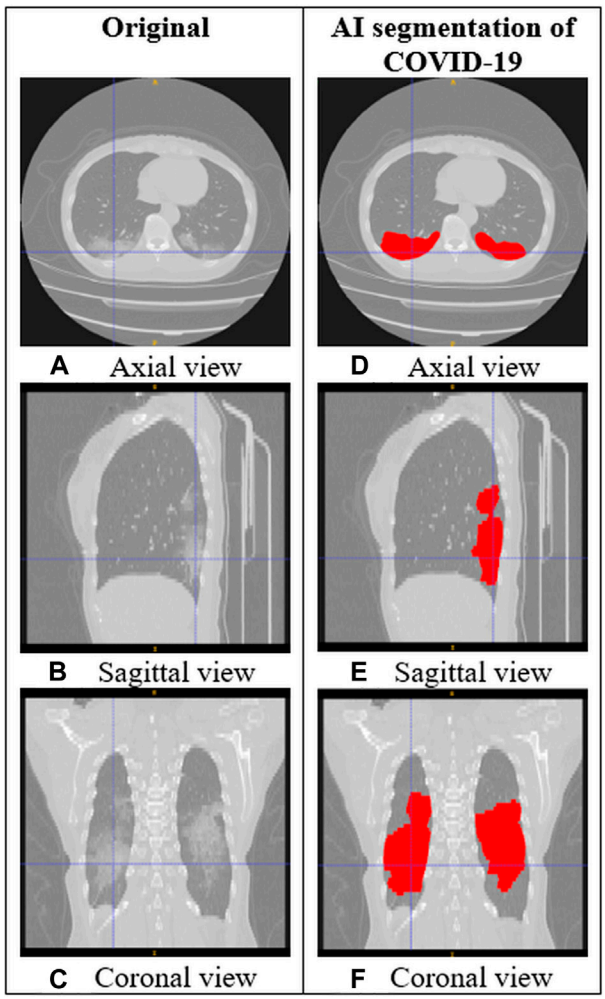

FIGURE 1 | CT images of the lungs in a subject with COVID-19. **(A–C)** Original CT images. **(D–F)** CT images with AI segmentation of COVID-19 lung opacities.

Precedent

There is a precedent for widening the role of chest CT in COVID-19 evaluation. Although some US and UK guidelines have recommended against using chest CT for screening (NHCotPsRo, 2019; Long et al., 2020), other countries have applied chest CT to specific outbreak settings with a more widespread, targeted, and strategic use of chest CT. In Chinese outbreak settings, for example, chest CT of high-risk populations, alongside of strict public health containment strategies, may have contributed to successful containment and low mortalities. In the US and Europe, chest CT has mainly been used to examine patients later in the disease cycle, such as to screen for complications or superinfections. In contrast, chest CT was used frequently along with RT-PCR for acute diagnosis in "fever clinics" in Hubei Province, China (Liang, 2020). For a brief and transient period during a high outbreak setting, COVID-19 diagnoses were made based on positive CT and a recent high-risk travel or possible exposure, even when the

patients' RT-PCR results were initially negative (NHCotPsRo, 2019). Thus, CT has been aggressively applied alongside of RT-PCR in an outbreak setting as an epidemiology tool for optimized contact tracing.

Furthermore, early in the pandemic, the United Kingdom provided intercollegiate guidelines stating that patients undergoing elective surgery required chest CT beforehand if the procedures were high risk or if the patients were expected to require admission to the intensive therapy unit or high dependency unit postoperatively (Standards and Clinical Gu, 2020). Additionally, for patients presenting with abdominal symptoms and undergoing CT evaluation of the abdomen and pelvis, CT coverage of the chest also was recommended early in the pandemic (Bullock et al., 2020).

Potential Roles of Artificial Intelligence in CT Optimization

AI is a promising tool to increase the potential suitability of chest CT for COVID-19 screening, detection, monitoring, and research in certain highly constrained settings. AI has already been applied in many technologies developed in response to the emergence of COVID-19 (Bullock et al., 2020), including lung and infection segmentation, COVID-19 quantification, and techniques for clinical classification, detection, assessment, and monitoring. **Figure 1** shows an example of how AI segmentation models for COVID-19 can be applied to chest CT.

Currently, a common recommendation among medical and public health organizations is that CT should not be used for screening, and it should only be used for COVID-19 in patients with moderate to severe symptoms of COVID-19, worsening respiratory status, or indications of cardiopulmonary complications, and only when RT-PCR is unavailable or RT-PCR access is highly limited. Despite the high sensitivity of chest CT for COVID-19 in high-prevalence settings, one reason why chest CT is not more widely recommended for COVID-19 diagnosis is that the imaging findings are nonspecific, overlapping with many other diseases such as influenza, H1N1, SARS, MERS, and pneumonias with underlying causes other than SARS-CoV-2 (A. C. O. Radiology, 2020; C. F. D. C. A. Prevention, 2020). One study found that two standardized grading systems for determining the suspicion level of COVID-19 pneumonia based on chest CT had good inter-reader agreement among experienced readers but only moderate inter-reader agreement among less experienced readers (Sushentsev et al., 2020). To increase specificity and reduce the analytical burden on radiologists, AI could be utilized to learn the unique characteristics of chest CT in COVID-19 compared to other diseases (Roberts et al., 2021). This would be especially useful for smaller medical centers that lack dedicated, experienced radiologists and for out-of-hours scanning. Standardized AI initial interpretations might also reduce the subjectivity or interobserver variability of a subsequent radiologist review.

Lin et al. (2021) investigated differences in CT characteristics, some of which were determined by AI software, between patients with COVID-19 pneumonia and influenza virus pneumonia. Although they identified four CT characteristics with statistical differences, they concluded it might still be difficult to differentiate between the two causes of pneumonia in clinical practice.

In a particularly promising study by Harmon et al. (2020), a series of deep learning algorithms were used to assist chest CT in distinguishing between COVID-19 pneumonia and non-COVID-19 pneumonia. The algorithms were trained in a cohort of 1,280 patients and tested in an independent set of 1,337 patients. The resulting classification of COVID-19 pneumonia had an accuracy of >90%, sensitivity of 84%, and specificity of 93%. Among 140 patients with laboratory confirmed non-COVID-19 pneumonia in the test set, the false positive rate of the AI-assisted chest CT was 10%.

However, the overall pool of research on AI-assisted chest CT is at a very early stage, with many limitations, generalizations, overfit models, and reproduction of similar models. Image-based AI models abound that lack external validation, clinical metadata and relevant clinical labs, phase of disease parameters, or background prevalence data. Two separate reviews on this research topic have highlighted the shortcomings. One was a systematic review on machine learning literature related to the use of CT and CXR imaging for COVID-19 diagnosis and prognosis (Roberts et al., 2021). It did not find any articles that satisfied all three key criteria for clinical translation of research: sufficiently documented and reproducible methods, methods adhering to best practices for machine learning model development, and proper external validation. The other review was on the use of AI with chest CT to diagnose COVID-19 (Ozsahin et al., 2020). It found that the majority of studies on this topic were not peer-reviewed. Additionally, some studies had extremely limited data and some used data from different institutions and scanners, but did not carry out the necessary preprocessing of the data to increase the consistency across data from different sources. Furthermore, some studies lacked sufficient demographic or clinical information for the patients. The two review articles agree that larger and higher quality datasets will be of the utmost importance for future studies in the field. COVID-Net aims to accelerate research in the field by releasing open-source, open-access deep learning models and networks created for AI-assisted chest CT for various COVID-19 related tasks (e.g., screening and treatment monitoring) as well as large, diverse datasets (Wong, 2020). Federated learning incentivizes and facilitates data sharing by removing certain privacy barriers, which have variable rules and processes throughout the world. With federated learning, the deep learning model weights can be shared without actual data exchange, without compromising the AI training process (Yang et al., 2021).

One of the risks associated with CT imaging is radiation exposure. Regarding patient safety, AI-based estimations of body region thickness could calculate optimal X-ray exposure parameters and AI-generalized adversarial networks could facilitate low-dose imaging. The population risks of more broadly using chest CT scans for enhanced indications in COVID-19 remain to be defined or fully justified for specific settings and remain a concern.

Looking forward, AI could be used to improve the sensitivity and efficiency of chest CT for detecting COVID-19 and to increase the effectiveness of CT as a disease response or a monitoring tool for both research and clinical practice. AI could further enhance the ability of CT to provide quantification of objective biomarkers of response to experimental treatment programs for specific cohorts of patients. AI could also help optimize the CT image quality through the development of automated, high-precision Iso-centering and scan range determination.

CT AI might provide a standardized measure and surrogate biomarker metric for lung disease. Speculative uses of CT AI include the measurement of clinical response to therapeutics like steroids, monoclonal antibodies, or anti-inflammatory medications. It is unknown whether CT AI could help identify chronic lung changes in chronic COVID-19 breathlessness, variant-specific features, or early detection of at-risk phases of disease exacerbations (either primary infectious opacities or immune or inflammatory phase reactions). We have a lot to learn and CT AI adds a tool to the discovery toolbox.

CONCLUSION

In conclusion, there are compelling reasons to be attracted toward studying chest CT as a tool for developing a better understanding of COVID-19. Clinical public health and research goals for COVID-19 might be enlightened by a targeted application of chest CT and CT AI to seeking answers for specific clinical and research questions in specific outbreak or therapeutic settings. Additional research and data are required to determine the exact roles of chest CT in early detection, classification, and triage of resource-limited therapies, and its potential role as an epidemiology tool in limited targeted populations. The pandemic has proved to be an "AI-instigator"; however, AI-assisted CT tools will require more rigorous academic development, broader clinical metadata, and more thorough critical review in hopes of more generalized tools with clinical or research relevance. We can do better. The times demand it.

DATA AVAILABILITY STATEMENT

The original contributions presented in the study are included in the article; further inquiries can be directed to the corresponding author.

AUTHOR CONTRIBUTIONS

ZT, SH, and HR wrote the article. TB, SX, and BW conceived the ideas and edited the article.

FUNDING

This study was supported in part by the Royal Society Wolfson Fellowship, the National Institutes of Health (NIH) Bench-to-Bedside Award, the NIH Center for Interventional Oncology Grant, the National Science Foundation (NSF) I-Corps Team Grant (1617340), NSF REU site program 1359095, the UGA-AU Inter-Institutional Seed Funding, the American Society for Quality Dr. Richard J. Schlesinger Grant, the PHS Grant UL1TR000454 from the Clinical and Translational Science Award Program, the NIH National Center for Advancing Translational Sciences, the NIH Center for Interventional Oncology (Grant ZID# BC011242 and CL040015), the Intramural Research Program of the National Institutes of Health, and the Intramural Targeted Anti-COVID (ITAC) Program of the National Institute of Allergy and Infectious Diseases.

REFERENCES

A. C. O. Radiology (2020). ACR Recommendations for the Use of Chest Radiography and Computed Tomography (CT) for Suspected COVID-19 Infection. Available: https://www.acr.org/Advocacy-and-Economics/ACR-Position-Statements/Recommendations-for-Chest-Radiography-and-CT-for-Suspected-COVID19-Infection (Accessed March 31, 2021).

Ai, T., Yang, Z., Hou, H., Zhan, C., Chen, C., Lv, W., et al. (2020). Correlation of Chest CT and RT-PCR Testing for Coronavirus Disease 2019 (COVID-19) in China: A Report of 1014 Cases. *Radiology* 296 (2), E32–E40. doi:10.1148/radiol.2020200642

Amalou, A., Türkbey, B., Sanford, T., Harmon, S., Türkbey, E. B., Xu, S., et al. (2020). Targeted Early Chest CT in COVID-19 Outbreaks as Diagnostic Tool for Containment of the Pandemic- A Multinational Opinion. *Diagn. Interv. Radiol.* 26 (4), 04–24. doi:10.5152/dir.2020.20231

Apostolopoulos, I. D., and Bessiana, T. (2003). *Covid-19: Automatic Detection from X-Ray Images Utilizing Transfer Learning with Convolutional Neural Networks*. arXiv, 11617.

Bernheim, A., Mei, X., Huang, M., Yang, Y., Fayad, Z. A., and Zhang, N. (2020). Chest CT Findings in Coronavirus Disease-19 (COVID-19): Relationship to Duration of Infection. *Radiology* 295, 200463.

Bullock, J., Luccioni, A., Pham, K. H., Lam, C. S. N., and Luengo-Oroz, M. (2020). *Mapping the Landscape of Artificial Intelligence Applications against COVID-19*. arXiv:2003.11336.

C. F. D. C. A. Prevention (2020). Interim Clinical Guidance for Management of Patients with Confirmed Coronavirus Disease (COVID-19). Available: https://www.cdc.gov/coronavirus/2019-ncov/hcp/clinical-guidance-management-patients.html (Accessed March 31, 2021).

Harmon, S. A., Sanford, T. H., Xu, S., Turkbey, E. B., Roth, H., Xu, Z., et al. (2020). Artificial Intelligence for the Detection of COVID-19 Pneumonia on Chest CT Using Multinational Datasets. *Nat. Commun.* 11 (1), 4080. doi:10.1038/s41467-020-17971-2

Inui, S., Fujikawa, A., Jitsu, M., Kunishima, N., Watanabe, S., Suzuki, Y., et al. (2020). Chest CT Findings in Cases from the Cruise Ship Diamond Princess with Coronavirus Disease (COVID-19). *Radiol. Cardiothorac. Imaging* 2 (2), e200110. doi:10.1148/ryct.2020200110

Kanne, J. P. (2020). Chest CT Findings in 2019 Novel Coronavirus (2019-nCoV) Infections from Wuhan, China: Key Points for the Radiologist. *Radiology* 295, 16–17.

Liang, T. (2020). *Handbook of COVID-19 Prevention and Treatment: The First Affiliated Hospital*. Zhejiang University School of Medicine.

Lin, L., Fu, G., Chen, S., Tao, J., Qian, A., Yang, Y., et al. (2021). CT Manifestations of Coronavirus Disease (COVID-19) Pneumonia and Influenza Virus

Pneumonia: A Comparative Study. *Am. J. Roentgenology* 216 (1), 71–79. doi:10.2214/ajr.20.23304

Liu, J., Yu, H., and Zhang, S. (2020). The Indispensable Role of Chest CT in the Detection of Coronavirus Disease 2019 (COVID-19). *Eur. J. Nucl. Med. Mol. Imaging* 47, 1638–1639. doi:10.1007/s00259-020-04795-x

Long, C., Xu, H., Shen, Q., Zhang, X., Fan, B., Wang, C., et al. (2020). Diagnosis of the Coronavirus Disease (COVID-19): rRT-PCR or CT? *Eur. J. Radiol.* 126, 108961. doi:10.1016/j.ejrad.2020.108961

Narin, A., Kaya, C., and Pamuk, Z. (2003). *Automatic Detection of Coronavirus Disease (COVID-19) Using X-ray Images and Deep Convolutional Neural Networks*. arXiv, 10849.

NHCotPsRo, C. (2019). Diagnosis and Treatment Protocols of Pneumonia Caused by a Novel Coronavirus (Trial Version 5). Available: http://www.nhc.gov.cn/yzygj/s7653p/202002/3b09b894ac9b4204a79db5b8912d4440.shtml.

Ozsahin, I., Sekeroglu, B., Musa, M. S., Mustapha, M. T., and Uzun Ozsahin, D. (2020). Review on Diagnosis of COVID-19 from Chest CT Images Using Artificial Intelligence. *Comput. Math. Methods Med.* 2020, 1–10. doi:10.1155/2020/9756518

Peplow, M. (2020). *Developing Countries Face Diagnostic Challenges as the COVID-19 Pandemic Surges*. Chemical & Engineering News. Available: https://cen.acs.org/analytical-chemistry/diagnostics/Developing-countries-face-diagnostic-challenges/98/i27 (Accessed April 11, 2021).

Roberts, M., Driggs, D., Thorpe, M., Gilbey, J., Yeung, M., Ursprung, S., et al. (2021). Common Pitfalls and Recommendations for Using Machine Learning to Detect and Prognosticate for COVID-19 Using Chest Radiographs and CT Scans. *Nat. Mach Intell.* 3 (3), 199–217. doi:10.1038/s42256-021-00307-0

Standards and Clinical Guidelines (2020). British Society of Gastrointestinal and Abdominal Radiology and British Society of Thoracic Imaging - Covid-19: BSTI/BSGAR Decision Tool for Chest Imaging in Patients Undergoing CT for Acute Surgical Abdomen. Available: https://www.bsti.org.uk/media/resources/files/BSGAR_BSTI_joint_decision_tool_for_CT_v1_FINAL_25.03.20_CM7VQla.pdf.

Sushentsev, N., Bura, V., Kotnik, M., Shiryaev, G., Caglic, I., Weir-McCall, J., et al. (2020). A Head-To-Head Comparison of the Intra- and Interobserver Agreement of COVID-RADS and CO-RADS Grading Systems in a Population with High Estimated Prevalence of COVID-19. *BJR open* 2 (1), 20200053. doi:10.1259/bjro.20200053

Varble, N., Blain, M., Kassin, M., Xu, S., Turkbey, E. B., Amalou, A., et al. (2021). CT and Clinical Assessment in Asymptomatic and Pre-symptomatic Patients with Early SARS-CoV-2 in Outbreak Settings. *Eur. Radiol.* 31 (5), 3165–3176. doi:10.1007/s00330-020-07401-8

Wang, L., and Wong, A. (2003). *COVID-net: A Tailored Deep Convolutional Neural Network Design for Detection of COVID-19 Cases from Vhest Radiography Images*. arXiv, 09871.

Wong, A. S. (2020). COVID-net. Available: https://alexswong.github.io/COVID-Net/ (Accessed May 14, 2021).

Xie, X., Zhong, Z., Zhao, W., Zheng, C., Wang, F., and Liu, J. J. R. (2020). Chest CT for Typical 2019-nCoV Pneumonia: Relationship to Negative RT-PCR Testing. *Radiology* 296, E41–E45.

Yang, D., Xu, Z., Li, W., Myronenko, A., Roth, H. R., Harmon, S., et al. (2021). Federated Semi-supervised Learning for COVID Region Segmentation in Chest CT Using Multi-National Data from China, Italy, Japan. *Med. image Anal.* 70, 101992. doi:10.1016/j.media.2021.101992

Zou, L., Ruan, F., Huang, M., Liang, L., Huang, H., Hong, Z., et al. (2020). SARS-CoV-2 Viral Load in Upper Respiratory Specimens of Infected Patients. *N. Engl. J. Med.* 382, 1177–1179. doi:10.1056/NEJMc2001737

Disclaimer: The content of this manuscript does not necessarily reflect the views, policies, or opinions of the U.S. Department of Health and Human Services nor the National Institutes of Health. The mention of commercial products, their source, or their use in connection with material reported herein is not to be construed as an actual or implied endorsement of such products by the United States government. Opinions expressed are those of the authors, not necessarily the NIH. NIH has a cooperative research and development agreement with Philips, Siemens, and Canon Medical. Canon Medical and NIH have a licensing agreement for a software algorithm related to classification of COVID-19 on chest CT.

Conflict of Interest: The authors declare that the research was conducted in the absence of any commercial or financial relationships that could be construed as a potential conflict of interest.

frontiers in Artificial Intelligence

REVIEW
published: 21 July 2021
doi: 10.3389/frai.2021.612914

AI-Empowered Computational Examination of Chest Imaging for COVID-19 Treatment: A Review

Hanqiu Deng[1,2] *and Xingyu Li*[1]*

[1]Department of Electrical and Computer Engineering, University of Alberta, Edmonton, AB, Canada, [2]School of Aerospace Engineering, Beijing Institute of Technology, Beijing, China

Since the first case of coronavirus disease 2019 (COVID-19) was discovered in December 2019, COVID-19 swiftly spread over the world. By the end of March 2021, more than 136 million patients have been infected. Since the second and third waves of the COVID-19 outbreak are in full swing, investigating effective and timely solutions for patients' check-ups and treatment is important. Although the SARS-CoV-2 virus-specific reverse transcription polymerase chain reaction test is recommended for the diagnosis of COVID-19, the test results are prone to be false negative in the early course of COVID-19 infection. To enhance the screening efficiency and accessibility, chest images captured *via* X-ray or computed tomography (CT) provide valuable information when evaluating patients with suspected COVID-19 infection. With advanced artificial intelligence (AI) techniques, AI-driven models training with lung scans emerge as quick diagnostic and screening tools for detecting COVID-19 infection in patients. In this article, we provide a comprehensive review of state-of-the-art AI-empowered methods for computational examination of COVID-19 patients with lung scans. In this regard, we searched for papers and preprints on bioRxiv, medRxiv, and arXiv published for the period from January 1, 2020, to March 31, 2021, using the keywords of COVID, lung scans, and AI. After the quality screening, 96 studies are included in this review. The reviewed studies were grouped into three categories based on their target application scenarios: automatic detection of coronavirus disease, infection segmentation, and severity assessment and prognosis prediction. The latest AI solutions to process and analyze chest images for COVID-19 treatment and their advantages and limitations are presented. In addition to reviewing the rapidly developing techniques, we also summarize publicly accessible lung scan image sets. The article ends with discussions of the challenges in current research and potential directions in designing effective computational solutions to fight against the COVID-19 pandemic in the future.

Keywords: chest imaging, image analysis, severity assessment, COVID-19, prognosis prediction, ROI segmentation, diagnostic model, machine learning

OPEN ACCESS

Edited by:
Simon DiMaio,
Intuitive Surgical, Inc., United States

Reviewed by:
Mehdi Moradi,
IBM Research Almaden, United States
Wei Zhao,
Central South University, China

***Correspondence:**
Xingyu Li
xingyu.li@ualberta.ca

Specialty section:
This article was submitted to Medicine and Public Health, a section of the journal Frontiers in Artificial Intelligence

Received: *02 October 2020*
Accepted: *23 June 2021*
Published: *21 July 2021*

Citation:
Deng H and Li X (2021) AI-Empowered Computational Examination of Chest Imaging for COVID-19 Treatment: A Review. Front. Artif. Intell. 4:612914. doi: 10.3389/frai.2021.612914

1 INTRODUCTION

COVID-19, caused by severe acute respiratory syndrome coronavirus 2 (SARS-CoV-2), was noted to be infectious to humans in December 2019 in Wuhan, China. Afterward, it swiftly spread to most countries around the world. People infected with COVID-19 present with have fever, cough, difficulty in breathing, and other symptoms, while there are also asymptomatic infectious patients (Bai et al., 2020).

For COVID-19 diagnosis, on the one hand, the reverse transcription polymerase chain reaction (RT-PCR) is a specific and simple qualitative analysis method for the detection of COVID-19 (Tahamtan and Ardebili, 2020). Despite its high sensitivity and strong specificity, the RT-PCR test has several limitations. First, false-negative results for the SARS-CoV-2 test are very common in clinical diagnosis of COVID-19 due to various factors, e.g., an insufficient amount of virus in a sample (Xiao et al., 2020). Second, the RT-PCR test provides a yes/no answer without any indication of disease progression. On the other hand, clinical studies have discovered that most COVID-19 patients, even in the early course of infection or without showing any clinical symptoms, possess common features in their lung scans (Hao and Li, 2020; Long et al., 2020; Salehi et al., 2020; Wong et al., 2020; Zhou et al., 2020a). These patterns in lung images are believed to be a complement to the RT-PCR test and thus form an alternative important diagnostic tool for the detection of COVID-19. Particularly, among various non-invasive techniques to view and examine internal tissues and organs in chest, ultrasound (US) does not depict the differences between COVID-19 and other viral types of pneumonia well and magnetic resonance imaging (MRI) suffers from long scan times and high costs. Consequently, CT scans and chest X-ray (CXR) are the widely used techniques in lung scans for the clinical diagnosis of COVID-19 (Vernuccio et al., 2020; Dong et al., 2021). Currently, chest imaging has been used for preliminary/emergency screening, monitoring, and follow-up check-ups in COVID-19 treatment in China and Italy.

AI-empowered computational solutions have been successfully used in many medical imaging tasks. Particularly to combat COVID-19, computational imaging technologies include, but are not limited to, lung and infection region segmentation, chest image diagnosis, infection severity assessment, and prognosis estimation. Compared to physician's examination, computational solutions are believed to be more consistent, efficient, and objective. In literature, early works on chest image examination for COVID-19 patients have usually adopted the paradigm of supervised learning to build an image analysis model. These learning algorithms range from support vector machine (SVM), K-nearest neighbor, random forest, decision tree to deep learning. Lately, to improve learning models' generalization, transfer learning, multi-task learning, and weakly supervised learning have become popular.

In this article, we review the state-of-the-art AI diagnostic models particularly designed to examine lung scans for COVID-19 patients. To this end, we searched for papers and preprints on bioRxiv, medRxiv, and arXiv published for the period from January 1, 2020, to March 31, 2021, with keywords of COVID, lung scans, and AI. After quality inspection, 96 papers were included in this article, among which most are peer-reviewed and published in prestigious venues. We also included a small portion of reprints in this review due to their methodology innovations. Particularly, this review presents in-depth discussions on methodologies of region-of-interest (ROI) segmentation and chest image diagnosis in Segmentation of *Region of Interest in Lung Scans and COVID-19 Detection and Diagnosis*, respectively. Infection severity assessment and prognosis prediction from COVID-19 lung scans are closely related and thus presented together in *COVID-19 Severity Assessment and Prognosis Prediction*. Since AI solutions are usually data-driven, *Public COVID-19 Chest Scan Image Sets* lists primary COVID-19 lung image sets publicly accessible to researchers. Limitations and future directions on AI-empowered computational solutions to COVID-19 treatment are summarized at the end of this article.

Several review papers have been published on AI solutions to combat COVID-19. Pham et al. (2020) and Latif et al. (2020) have emphasized the importance of artificial intelligence and big data in responding to the COVID-19 outbreak and preventing the severe effects of the COVID-19 pandemic, but computational medical imaging was not their focus. (Dong et al. (2021) and Roberts et al. (2021) have broadly covered the use of various medical imaging modalities for COVID-19 treatment and Shi et al. (2021) overviewed all aspects along the chest imaging pipeline, from imaging data acquisition to image segmentation and diagnosis. This article constitutes the latest technical review (up to March 31, 2021) of AI-based lung scan screening for the COVID-19 examination. In contrast to previous review papers, this review particularly focuses on the AI-driven techniques for COVID-19 chest image analysis. We present an in-depth discussion on various AI-based methods, from their motivations to specific machine learning models and architectures. The specific scope and updated, in-depth review of technology distinguish this article from previous works.

2 SEGMENTATION OF REGION OF INTEREST IN LUNG SCANS

The region of interest in lung scans is usually lung fields, lesions, or infection regions. As a prerequisite procedure, obtaining accurate segmentation of lung field or other ROIs in chest images is essential. It helps avoid the interference of non-lung regions in subsequent analysis (Majeed et al., 2020). This section provides a comprehensive review of AI-driven solutions for ROI segmentation for COVID-19 treatment. We will start with performance metrics for segmentation evaluation. Then, computational solutions are grouped based on image modalities (first with CXR, followed by CT). Note that though many studies have focused on lung segmentation, this article surveys publications directly related to COVID-19 treatment.

2.1 Performance Metrics

Dice coefficient is the most common metric used to evaluate segmentation methods. It quantifies the agreement between

ground truth mask and segmentation results. Specifically, Dice coefficient is defined as follows:

$$Dice(X, Y) = \frac{2|A \cap B|}{|A| + |B|}, \quad (1)$$

where A and B are ground truth and segmented regions, respectively; $\cap$ denotes the operation to obtain the overlap regions between A and B; $|\cdot|$ calculates the number of pixels in an image. In addition to Dice coefficient, accuracy, sensitivity, and precision can also be used as evaluation criteria (Yan et al., 2020).

2.2 Methodologies

Among various machine learning methods for ROI segmentation, the encoder-decoder architecture such as U-Net (Ronneberger et al., 2015) is the common backbone model. The encoder extracts numerical representations from a query image and the decoder generates a segmentation mask in the query image size. To boost the performance of U-Net shape models, different deep learning strategies are investigated to address unique challenges that exist in lung scans of COVID-19 patients. We specify these novel algorithms and models as follows.

2.2.1 Region-of-Interest Segmentation in Chest X-Ray

Chest X-ray images from COVID-19 patients usually suffer from various levels of opacification. This opacification masks the lung fields in CXRs and makes accurate segmentation of lung fields difficult. To tackle this problem, Selvan et al. (2020) have proposed a weak supervision method that fuses a U-Net and a variational autoencoder (VAE) to segment lungs in high-opacity CXRs. The novelty in their method is the use of VAE for data imputation. In addition, three data augmentation techniques are attempted to improve the generalization of the proposed method.

2.2.2 Region-of-Interest Segmentation in Computed Tomography Scans

In the literature, many studies have proposed improvements for ROI segmentation in lung CT images. For instance, an attention mechanism is often deployed for segmentation recently. For automated segmentation of multiple COVID-19 infection regions, Chen X. et al. (2020) have applied the soft attention mechanism to improve the capability of U-Net to detect a variety of symptoms of the COVID-19. The proposed aggregated residual transformation facilitates the generation of a robust and descriptive feature representation, further improving the segmentation performance. Inf-Net (Fan et al., 2020) is a semi-supervised segmentation framework based on a randomly selected propagation strategy. It utilizes implicit reverse attention and explicit edge attention to enhance abstract representations and model boundaries of lung infection regions, respectively. Similar to Inf-Net, COVID-SegNet proposed by Yan et al. (2020) introduces two attention layers in a novel feature variation (FV) block for lung infection segmentation. The channel attention handles confusing boundaries of COVID-19 infection regions, and the spatial attention in the FV block optimizes feature extraction in the encoder model.

Alternatively, multi-task learning is used to leverage useful information in multiple related tasks to boost the performance of both segmentation and classification (Amyar et al., 2020). In this study, a common encoder is shared by two decoders and one classification layer for COVID-19 infection segmentation, lung image reconstruction, and CT image binary classification (i.e., COVID-19 and non-COVID-19). Similarly, Wu et al. (2021) have designed a joint classification and segmentation framework, which used a decoder to map the combined features from the classification network and an encoder to the segmentation results.

In addition to the development of advanced deep learning models, several studies have tried to improve the segmentation performance by either synthesizing CT image samples or massaging image labels. For instance, Liu et al. (2020) have proposed using GAN to synthesize COVID-19 opacity on normal CT images. To address data scarcity, Zhou. et al. (2020) have created a CT scan simulator that expands the data by fitting variations in the patient's chest images at different time points. Meanwhile, they have transformed the 3D model into three 2D segmentation tasks, thus not only reducing the model complexity but also improving the segmentation performance. On the other hand, instead of generating new, "fake" CT images for training, Laradji et al. (2020) have built an active learning model for image labeling. The active image labeling and infection region segmentation are iteratively performed until performance converges. Wang et al. (2020) have introduced a noise-robust Dice loss to improve the robustness of the model against noise labels. In addition, an adaptive self-ensembling framework based on the teacher-student architecture was incorporated to further improve noise-label robustness in image segmentation.

3 COVID-19 DETECTION AND DIAGNOSIS

Pneumonia detection from lung images is a key part of an AI-based diagnostic system for fast and accurate screening of COVID-19 patients. In this regard, machine learning methods, especially discriminative convolutional neural networks (CNN), are deployed for COVID-19 detection (binary classification of COVID-19 and non-COVID-19) and multi-category diagnosis (classification of normal, bacterial, COVID-19, and other types of viral pneumonia).

3.1 Performance Metrics

The widely used measurement metrics for image classification are accuracy, precision, sensitivity, specificity, and F1 score. The areas under the ROC curve (AUC) were also reported in some studies. ROC curve describes the performance of a classification model at various classification thresholds and AUC measures the area underneath the obtained ROC curve.

$$Accuracy = \frac{T_P + T_N}{T_P + T_N + F_P + F_N}, \quad (2)$$

$$Precision = \frac{T_P}{T_P + F_P}, \quad (3)$$

TABLE 1 | Summary of COVID-19 detection from CXR images in the literature (%). If multiple models are used in a study, we report the best-performance model here.

Literature	Task	Method	Acc	Sens	Spec	Pre	F1	AUC
Wang et al. (2020a)	Multi-class	COVID-net	93.3	91.0	-	98.9	-	-
Asif et al. (2021)	Multi-class	InceptionV3	96.0	-	-	-	-	
Asnaoui and Chawki (2020)	Multi-class	InceptionResnetV2	92.18	92.11	96.06	92.38	92.07	-
Rajaraman and Antani (2020)	Two classes	VGG-16	93.08	97.11	86.49	92.16	94.57	95.65
Moutounet-Cartan (2020)	Multi-class	VGG-16	84.1	87.7	-	-	-	97.4
Albahli (2020)	Multi-class	Resnet	89	-	-	-	-	-
Eldeen et al. (2021)	Multi-class	Alexnet	87.1	-	-	91.67	89.53	-
Punn and Agarwal (2021)	Multi-class	NASNetLarge	95	90	92	95	90	94
Ozcan (2020)	Multi-class	Resnet50	97.69	97.26	97.90	95.95	96.60	-
Kumar et al. (2020)	Two classes	DeQueezeNet	94.52	96.15	-	90.48	-	-
Goodwin et al. (2020)	Two classes	Ensemble learning	89.4	80	-	53.3	64.0	-
Chatterjee et al. (2020)	Multi-class	Ensemble learning	88.9	85.1	-	-	86.9	-
Shibly et al. (2020)	Two classes	Faster R-CNN	97.36	97.65	95.48	99.29	98.46	-
Fakhfakh et al. (2020)	Two classes	ProgNet	92.4	93.9	-	93.0%	93.4	-
Li et al. (2020)	Multi-class	DCSL	97.01	97.09	-	97.00	96.98	-
Yamac et al. (2020)	Multi-class	CSEN	95.9	98.5	95.7	-	-	-
Al-karawi et al. (2020)	Multi-class	SVM	94.43	95.00	93.86	-	-	-
Khuzani et al. (2020)	Multi-class	CNN	94.05	100	-	96	98	-
Medhi et al. (2020)	Two classes	CNN	93	-	-	-	-	-
Abbas et al. (2021a)	Multi-class	4S-DT	97.54	97.88	97.15	-	-	99.58
Zhang et al. (2021)	Two classes	CAAD	72.77	71.7	73.83	-	-	83.61
Ahishali et al. (2021)	Two classes	CSEN	95.66	97.28	95.52	-	-	-
Zabirul-Islam et al. (2020)	Multi-class	LSTM	99.4	99.3	99.2	-	98.9	99.9
Narayan Das et al. (2020)	Multi-class	Xception	97.41	97.09	97.30	-	96.97	-
Khan et al. (2020)	Two classes	Xception	99.0	-	98.6	98.3	98.5	-
Abbas et al. (2021b)	Multi-class	VGG19	93.1	100	-	-	-	-
Apostolopoulos and Mpesiana (2020)	Multi-class	MobileNet V2	96.78	98.66	96.46	-	-	-
Minaee et al. (2020)	Multi-class	ResNet	-	98.0	90.7	86.9	-	98.9
Afshar et al. (2020)	Multi-class	CAPS	98.3	80	98.6	-	-	-
Toğaçar et al. (2020)	Multi-class	Ensemble learning	98.25	99.32	99.37	99.66	-	-
Apostolopoulos et al. (2020)	Multi-class	MobileNet V2	87.66	97.36	99.42	-	-	-

Acc, accuracy; AUC, area under the ROC curve; F1, F-score; Pre, precision; Sens, sensitivity and Spec, specificity.

TABLE 2 | Summary of COVID-19 detection from lung CT slides in the literature (%). If multiple models are used in a study, we report the best-performance model here.

Literature	Task	Method	Acc	Sens	Spec	Pre	F1	AUC
Soares et al. (2020)	Two classes	xDNN	97.38	95.53	-	99.16	97.31	97.36
Anwar and Zakir (2020)	Multi-class	EfficientNetB4	89.7	-	-	-	89.6	89.5
Han et al. (2020)	Multi-class	AD3D-MIL	94.3	90.5	-	95.9	92.3	98.8
Rahimzadeh et al. (2020)	Two classes	ResNet50V2	98.49	94.96	98.7	81.26	-	-
He et al. (2020a)	Multi-class	DenseNet3D	87.62	89.07	91.13	85.94	87.48	89.8
Javaheri et al. (2021)	Multi-class	CovidCTNet	87.5	87.5	93.85	-	-	95
Di et al. (2021)	Two classes	UVHL	89.79	93.27	84.00	90.65	-	-
Chao et al. (2021)	Two classes	Random forest	88.4	84.3	-	-	-	88.0
He et al. (2020b)	Two classes	DenseNet-169	86	-	-	-	85	94
Jin et al. (2020)	Multi-class	ResNet152	-	90.19	95.76	-	-	97.17
Zhang et al. (2020)	Multi-class	Two-stage model	92.49	94.93	91.13	-	-	97.97
Aslan et al. (2021)	Multi-class	BiLSTM	98.70	-	99.33	98.77	98.76	99.00
Wang et al. (2021b)	Two classes	Inception	82.5	75.0	86.0	-	-	-
Song et al. (2021)	Two classes	DRE-net	86	96	-%	79	87	95

Acc, accuracy; AUC, area under the ROC curve; F1, F-score; Pre, precision; Sens, sensitivity and Spec, specificity.

$$Sensitivity = \frac{T_P}{T_P + F_N}, \tag{4}$$

$$Specificity = \frac{T_N}{T_N + F_P}, \tag{5}$$

$$F1\ score = \frac{2T_P}{2T_P + F_N + F_P}, \tag{6}$$

where T_P is true positive, T_N is true negative, F_P is false positive, and F_N is false negative.

3.2 Methodologies

The biggest challenge in the problem of COVID-19 detection from chest images is data scarcity. To address this issue, early

works have usually designed diagnostic systems following the handcraft engineering paradigm. Moreover, solutions based on transfer learning, ensemble learning, multi-task learning, semi-supervised learning, and self-supervision have been proposed in recent publications. For ease of comparison, we summarize the reviewed methods for CXRs and CT scans in **Table 1** and **Table 2**, respectively.

3.2.1 COVID-19 Detection/Diagnosis From Chest X-Ray

Handcrafted engineering is believed to be effective when prior knowledge of the problem is known. It is also preferred over deep learning when a training set is small. To solve the problem of COVID-19 diagnosis from chest X-ray images, Al-karawi et al. (2020) have proposed manually extracting image texture descriptors (LBP, Gabor features, and histograms of oriented gradient) for downstream SVM classification. Similarly, Khuzani et al. (2020) have suggested extracting numerical features from both spatial domain (Texture, GLDM, and GLCM) and frequency domain (FFT and Wavelet). Instead of SVM, a multi-layer neural network was designed for triple classification (normal, COVID-19, and other pneumonia). In the diagnostic pipeline introduced by Medhi et al. (2020), a CXR image is first converted to the grayscale version for image thresholding. Then, the obtained binary images are passed to a shallow net to distinguish normal images and COVID-19 cases. Chandra et al. (2021) have proposed extracting 8,196 radiomic texture features from lung X-ray images and differentiated different pneumonia types by multi-classifier voting.

Recently, with the increase in the collections of CXR images from COVID-19 patients, deep learning methods have become a major technique. Wang L. et al. (2020) have designed a lightweight diagnostic framework, namely, COVID-Net, for triple classification (i.e., no infection, non-COVID-19 infection, and COVID-19 viral infection). The tailored deep net makes heavy use of a residual projection-expansion-projection-extension (PEPX) design pattern and enhances representational capacity while maintaining relatively low computational complexity. Zabirul-Islam et al. (2020) have introduced an interesting hybrid deep CNN-LSTM network for COVID-19 detection. In this work, deep features of a CXR scan are extracted from a tailored CNN and passed to a long short-term memory (LSTM) unit for final classification. Since LSTM replaces a fully connected layer in the CNN-LSTM model, the number of trainable parameters in the model is reduced due to the parameter sharing property of LSTM.

Among the large volume of literature, transfer learning is one of the most common strategies in deep learning to combat data scarcity. It retrains a deep model on large-scale datasets and fine-tunes it on target COVID-19 image sets (Ahishali et al., 2021; Apostolopoulos et al., 2020; Apostolopoulos and Mpesiana, 2020; Asnaoui and Chawki, 2020; Khan et al., 2020; Moutounet-Cartan, 2020; Narayan Das et al., 2020; Ozcan, 2020; Ozturk et al., 2020; Punn and Agarwal, 2021; Abbas et al., 2021b; Asif et al., 2021; Eldeen et al., 2021). These models include, but are not limited to, Inception, ResNet, VGG-16, NASNet, and AlexNet. To further leverage the discriminative power of different models, ensemble learning is deployed, where multiple deep nets are used to vote for the final results. For example, DeQueezeNet, proposed by Kumar et al. (2020), ensembles DenseNet and SqueezeNet for classification. Similar models were proposed by Goodwin et al. (2020); Chatterjee et al. (2020); Shibly et al. (2020); Minaee et al. (2020); Toğaçar et al. (2020) Alternatively, Afshar et al. (2020) haveintroduced a capsule network-based model for CXR diagnosis, where transfer learning is exploited to boost the performance. To "open" the black box in a deep learning-based model, Brunese et al. (2020) have introduced an explainable detection system where transferred VGG-16 and class activation maps (CAM) (Zhou et al., 2016) were leveraged to detect and localize anomalous areas for COVID-19 diagnosis. Furthermore, Majeed et al. (2020) have performed a comparison study on pretrained CNN models and deployed CAM to visualize the most discriminating regions. Based on the experimental results, Majeed et al. (2020) have recommended performing ROI segmentation before diagnostic analysis for reliable results. The study by Hirano et al. (2020) focused on the vulnerability of deep nets against universal adversarial perturbation (UAP) with the application of detecting COVID-19 cases from chest X-ray images. The experimentation suggests that deep models are vulnerable to small UAPs and that adversary training is a necessity.

Since direct transfer across datasets from different domains may lead to poor performance, researchers have developed various strategies to mitigate the effects of domain difference on transfer performance. Li et al. (2020) have proposed a discriminative cost-sensitive learning (DCSL) model for a triple-category classification between normal, COVID-19, and other types of pneumonia. It uses a pre-trained VGG16 as the backbone net, where the first 13 layers are transferred and the two top dense layers are refined using an auxiliary conditional center loss to decrease the intra-class variations in representation learning. Convolution Support Estimation Network (CSEN) (Ahishali et al., 2021; Yamac et al., 2020) targets bridging the gap between model-based methods and deep learning approaches. It takes the numerical representations from pre-trained ChXNet as input and innovates a non-iterative mapping for sparse representation learning. In addition, Zhou et al. (2021) have considered the problem of COVID-19 CXR image classification in a semi-supervised domain adaptation setting and proposed a novel domain adaptation method, namely, semi-supervised open set domain adversarial network (SODA). It aligns data distributions in different domains through domain adversarial training (Ganin et al., 2016). To address highly imbalanced image sets, Zhang et al. (2021) have formulated the task of differentiating viral pneumonia in lung scans into a one-class classification-based anomaly detection problem and proposed a confidence-aware anomaly detection model (CAAD). CAAD consists of a shared feature extractor derived from a pre-trained EfficientNet, an anomaly detection module, and a confidence prediction module. A sample is detected as a COVID-19 case if it has a large anomaly score or a small confidence score.

Another strategy to tackle the data scarcity issue is data augmentation. For instance, offline augmentation strategies,

such as adjusting noise, shear, and brightness, are adopted to solve the data imbalance problem by Ucar and Korkmaz (2020). To further address the shortage of COVID-19 CXR images, Albahli (2020) and Waheed et al. (2020) have proposed using GAN to synthesize CXR images directly. To leverage a large amount of unlabeled data in COVID-19 CXR detection, Rajaraman and Antani (2020) have introduced a semi-supervised model to generate pseudo-annotation for unlabeled images. Then, recognizing COVID-19 pneumonia opacities is achieved based on these "newly" labeled samples. Similarly, Abbas et al. (2021a) have introduced a self-supervision method to generate pseudo-labels. With abstract representations generated by the bottleneck layer of an autoencoder, unlabeled samples are clustered for downstream training.

3.2.2 Detecting COVID-19 From Lung Computed Tomography Slides

Transfer learning is still the most common technique among the diverse methods to detect COVID-19 from lung CT images (Anwar and Zakir, 2020; He et al., 2020b; Chowhury et al., 2020; Soares et al., 2020; Wang S. et al., 2021). Particularly, previous studies (He et al., 2020a; Ardakani et al., 2020) have built a benchmark to evaluate state-of-the-art 2D and 3D CNN models (e.g., DenseNet and ResNet) for lung CT slides classification. It is worth mentioning that in the study of Wang S. et al. (2021), the model also performed re-detection on the results of the nucleic acid testing. According to this study, fine-tuned deep models can detect false-negative results. In addition, a lightweight 3D network optimized by neural architecture search was introduced for comparison in the proposed benchmark. To address the issue of large domain shift between source data and target data in transfer learning, He et al. (2020b) have proposed a self-supervised transfer learning approach called Self-Trans. By integrating contrastive self-supervision (Chen T. et al., 2020) in the transfer learning process to adjust the network weights pre-trained on source data, the bias incurred by source data is reduced in the target task. Aslan et al. (2021) have introduced a hybrid pre-trained CNN model and BiLSTM architecture to form a detection framework to improve the diagnosis performance.

In addition to transfer learning, diagnostic solutions based on weak supervision, multi-instance learning, and graphic learning were proposed in the literature. Rahimzadeh et al. (2020) have introduced a deep model that combined ResNet and the feature pyramid network (FPN) for CT image classification. ResNet is used as the backbone network and FPN generates a feature hierarchy from the backbone net's features at different scales. The obtained feature hierarchy helps detect COVID-19 infection in different scales. DRE-Net proposed by Song et al. (2021) has a similar architecture that combines ResNet and FPN to achieve detail relation extract for image-level prediction. This study also implements Grad-CAM on ResNet layers for main lesion region visualization. Javaheri et al. (2021) have introduced a multi-step pipeline of a deep learning algorithm, namely, CovidCTNet, to detect COVID-19 from CT images. Using controlled CT slides as a reference, the dual function of BCDU-Net (Azad et al., 2019) in terms of anomaly detection and noise cancellation was exploited to differentiate COVID-19 and community-acquired pneumonia anomalies. An attention-based deep 3D multiple instance learning (AD3D-MIL) was proposed for accurate and interpretable screening of COVID-19 with weak labels (Han et al., 2020). In the AD3D-MIL model, a bag of raw CT slides is transformed to multiple deep 3D instances. Then, an attention-based pool layer is utilized to generate a Bernoulli-distributed bag label. COVID-19 and community-acquired pneumonia (CAP) have very similar clinical manifestations and imaging features in CT images. To differentiate the confusing cases in these two groups, Di et al. (2021) have designed an uncertainty vertex-weighted hypergraph learning (UVHL) method to identify COVID-19 from CAP. In this method, a hypergraph structure is constructed where each vertex corresponds to a sample and hyperedges connect neighbor vertices that share common features. Hypergraph learning is repeated till the hypergraph is converged.

Alternatively, instead of directly detecting COVID-19 from CT scans using one deep model, some researchers have proposed AI-based diagnosis systems that consist of multiple deep models, each completing one sub-task in sequential order. For example, Jin et al. (2020) have introduced an AI system that consisted of five key parts: 1) lung segmentation network, 2) slice diagnosis network, 3) COVID-infectious slice locating network, 4) visualization module for interpreting the attentional region of deep networks, and 5) image phenotype analysis module for explaining the features of the attentional region. By sequentially completing the key tasks, the whole system achieves 97.17% AUC on an internal large CT set. Zhang et al. (2020) have innovated a two-stage model to distinguish novel coronavirus pneumonia (NCP) from other types of pneumonia and normal controls in CT scans. Particularly, a seven-category lung-lesion segmentation model is deployed for ROI mask and the obtained lung-lesion map is fed to a deep model for COVID-19 diagnosis. Similarly, Wang B. et al. (2021) have introduced a diagnosis system consisting of a segmentation model and a classification model. The segmentation model detects ROI from lung scans and then the classification model determines if it is associated with COVID-19 for each lesion region.

4 COVID-19 SEVERITY ASSESSMENT AND PROGNOSIS PREDICTION

Though most works on COVID-19 focus on ROI segmentation and chest image diagnosis, severity assessment and prognosis prediction are of significance. Severity assessment facilitates monitoring the COVID-19 infection course. Furthermore, it is closely related to prognosis outcomes (Fang et al., 2021), and detection of high-risk patients with early intervention is highly important to lower the fatality rate of COVID-19. Thus, we reviewed AI algorithms and models proposed for COVID-19 severity assessment and prognosis prediction in one section. Note that though it is closely related to severity assessment, prognosis prediction is a very difficult and challenging task. It requires

monitoring patients' outcomes over time, spanning from several days to several weeks. Given this challenge in data collection, the research on prognosis prediction relatively lags behind compared to COVID-19 detection and diagnosis.

4.1 COVID-19 Severity Assessment

4.1.1 Performance Metrics

To evaluate the quality of COVID-19 severity estimation, we used Spearman's rank correlation coefficient between the ground truth and prediction as the evaluation metric. Spearman's ρ is defined as follows:

$$\rho\left(\mathrm{y}^{true}, \mathrm{y}^{pred}\right) = \frac{cov\left(rg\left(\mathrm{y}^{true}\right), rg\left(\mathrm{y}^{pred}\right)\right)}{\sigma\left(rg\left(\mathrm{y}^{true}\right)\right) \cdot \sigma\left(rg\left(\mathrm{y}^{pred}\right)\right)}, \tag{7}$$

where y^{true} is the ground truth of infected fractions, y^{pred} is the predicted fractions, cov $(\cdot,\cdot)$ is a sample covariance, $\sigma(\cdot)$ is a sample standard deviation, and $rg(\cdot)$ is the rank vector of the input.

4.1.2 Severity Assessment From Chest X-Ray

To assess the pneumonia severity in a CXR, Signoroni et al. (2020) have proposed a novel end-to-end scheme deploying U-Net++ as the backbone net. With the lung segmentation network (i.e., U-Net++), feature maps that come from different CNN layers of the encoder are masked with segmentation results and fed to a global average pooling layer with a SoftMax activation for final severity score. Cohen et al. (2020) have proposed a transfer learning-based method for assessing the severity of COVID-19 infection. With a pre-trained DenseNet as the backbone architecture, the convolutional layers transform an input image into a 1,024-dimensional vector and the dense layers serve as task prediction layers to detect 18 medical evidences for COVID-19 diagnosis. Finally, a linear regression model is deployed to fuse the 1024D features and 18 evidences for COVID-19 infection prediction.

4.1.3 Severity Assessment From Computed Tomography Images

The severity of COVID-19 can be measured by different quantities. Goncharov et al. (2020) have proposed using infected lung percentage as an indicator of COVID-19 severity. In this regard, the study has deployed multi-task learning to detect COVID-19 samples and estimate the percentage of infected lung areas simultaneously. Since the method requires lung segmentation, U-Net is used as the backbone in the proposed multi-task learning. In the work proposed by Chao et al. (2021), an integrative analysis pipeline for accurate image-based outcome prediction was introduced. In the pipeline, patient metadata, including both imaging and non-imaging data, is passed to a random forest for outcome prediction. Besides, to address the challenges of weak annotation and insufficient data in COVID-19 severity assessment with CT, Li et al. (2021) have proposed a novel weak multi-instance learning framework for severity assessment, where instance-level augmentation was adopted to boost the performance.

4.2 COVID-19 Prognosis Prediction

Due to the complexity of prognosis estimation, previous studies usually fused lung ROI segmentation, COVID-19 diagnosis results, and patient's metadata for a prognosis outcome. Note that in contrast to other tasks that follow similar evaluation protocols, AI-based prognosis prediction models are usually evaluated by different metrics in the literature. Depending on the specific setup and context, either classification accuracy or regression error can be used as model evaluation quantities. Thus, instead of summarizing the prognosis performance metrics in one sub-section independently, we will specify the evaluation protocols for each reviewed study in the following section.

4.2.1 Prognosis Estimation From Chest X-Ray

To evaluate the COVID-19 course in patients for prognosis analysis, a deep model that leverages RNN and CNN architectures to assess the temporal evolution of images was proposed by Fakhfakh et al. (2020). The multi-temporal classification of X-ray images, together with clinical and radiological features, is considered as the foundation of prognosis and assesses COVID-19 infection evolution in terms of positive/negative evolution. Since this study formulates the prognosis prediction as a binary classification problem, conventional classification metrics, including accuracy, precision, recall, and F1 score, are reported.

4.2.2 Prognosis Prediction From Computed Tomography Scans

Prior models of COVID-19 prognosis prediction from lung CT volume can be roughly categorized into two different scenarios. In the first scenario, prognosis prediction is formulated as a classification problem and the output is a classification result from a predefined outcome set (Meng et al., 2020; Chao et al., 2021; Shiri et al., 2021). For instance, Meng et al. (2020) have proposed a 3D DenseNet-similar prognosis model, namely, De-COVID19-Net, to predict a patient's death. In this study, CT images are first segmented using a threshold-based method and the detected lung regions are fed into De-COVID19-Net. Before the final classification layer, clinic metadata and the obtained numerical features in De-COVID-Net are fused for the final prediction. Similarly, Shiri et al. (2021) have introduced an XGBoost classifier to predict patient's survival based on radiomic features in lung CT scans and clinical data. Moreover, Chao et al. (2021) have implemented a prognosis model using a random forest to identify high-risk patients who need ICU treatment. Following a similar data processing flow from lung region segmentation, CT scan feature learning, metadata fusion to classification, a binary classification outcome in terms of ICU admission prediction is generated. For prognosis prediction models belonging to the first scenario, conventional classification evaluation metrics such as AUC and sensitivity are used.

In the second scenario, prognosis estimation is formulated by a regression problem (Wang S. et al., 2020; Zhang et al., 2020; Lee

et al., 2021). Specifically, Zhang et al. (2020) have defined the prognosis output by the time in days that critical care demands are needed after hospital admission. In this regard, a light gradient boosting machine (LightGBM) and Cox proportional-hazards (CoxPH) regression model are built. The Kaplan–Meier analysis in model evaluation suggests that incorporating lung lesions and clinical metadata boosts prognosis prediction performance. Alternatively, Wang S. et al. (2020) have defined the prognostic event as the hospital stay time until discharge and proposed using two deep nets, one for lung region segmentation and the other for CT feature learning, for a multivariate Cox proportional hazard regression. In this study, Kaplan–Meier analysis and log-rank test are used to evaluate the performance of the proposed prognostic analysis. Under the same prognosis regression setting in (Wang S. et al., 2020), Lee et al. (2021) have developed a deep learning convolutional neural network, namely, Deep-COVID-DeteCT (DCD), for prognosis estimation based on the entire chest CT volume and experimentally demonstrates that multiple scans during hospitalization provide a better prognosis.

5 PUBLIC COVID-19 CHEST SCAN IMAGE SETS

Machine learning is one of the core techniques in AI-driven computational solutions. Data are the stepstone to develop any machine learning-based diagnostic system. This section includes primary COVID-19 chest image sets that are publicly accessible to researchers. We will start with CXR datasets, followed by chest CT image sets. Note that when a dataset contains both X-ray images and CT scans, it will be summarized in the CXR section.

5.1 COVID-19 Chest X-Ray Datasets

COVID-19 CXR image data collection (Cohen et al., 2020) is an open public dataset of chest X-ray images collected from patients who are positive or suspected of COVID-19 or other types of viral and bacterial pneumonia (including MERS and SARS). The collection contains 589 chest X-ray images (542 frontal and 47 lateral views) from 282 people over 26 countries, among which 176 patients are male and 106 are female. Of the frontal views, 408 images are taken with standard frontal PA/AP (posteroanterior/anteroposterior) position and the other 134 are AP Supine (anteroposterior laying down). In addition to CXR, the dataset also provides clinical attributes, including survival, ICU stay, intubation events, blood tests, and location, and is free from clinical notes for each image/case.

BIMCV COVID-19 + (Vayá et al., 2020) is a large dat set with 1,380 chest X-ray images and 163 full-resolution CT scans from 1,311 patients in the Valencian Region Medical Image Bank (BIMCV). All samples are labeled as COVID-19 infection, no infection, and other infection and stored as 16-bit PNG format images. Along with chest images, metadata including radiographic findings, pathologies, polymerase chain reaction, IGG and IGM diagnostic antibody tests, and radiographic reports are also provided. In addition, ten images in this dataset are annotated by a team of eight radiologists from the Hospital Universitario de San Juan de Alicante to include semantic segmentation of radiographic findings.

COVID-19 Radiography Database (Chowhury et al., 2020) consists of 219 COVID-19 positive CXR images, 1,341 normal images, and 1,345 viral pneumonia images. All images are stored in grayscale PNG format with a resolution of 1024 by 1024 pixels.

5.2 COVID-19 Computed Tomography Scan Sets

COVID-CT-dataset (Yang et al., 2020) provides 349 CT scans with clinical characteristics of COVID-19 from 216 patients and 463 non-COVID-19 CTs. Images in this set are collected from COVID19-related papers from medRxiv, bioRxiv, NEJM, JAMA, and Lancet and thus in different sizes. The number of CT scans that a patient has ranges from 1 to 16, with an average of 1.6 per patient. The utility of these samples is confirmed by a senior radiologist who has been diagnosing and treating COVID-19 patients since the outbreak of the COVID-19 pandemic. Meta-information, including patient ID, patient information, DOI, and image caption, is available in this dataset.

COVID-CTset (Rahimzadeh et al., 2020) is a large CT images dataset that collected 15,589 COVID-19 images from 95 patients and 48,260 normal images from 282 persons from the Negin Medical Center located at Sari in Iran. The patient's private information is removed and each image is stored in 16-bit grayscale TIFF format with 512*512-pixel resolution.

MosMedData (Morozov et al., 2020) contains 1,100 lung CT scans from municipal hospitals in Moscow, Russia, between March 1, 2020, and April 25, 2020. Among the 1,100 images, 42% are of male and 56% of female, with the rest 2% unknown. The dataset groups samples into five categories (i.e., zero, mild, moderate, severe, and critical) based on the severity of lung tissue abnormalities related to COVID-19, where the sample ratios of the five categories are 22.8, 61.6, 11.3,4.1, and 0.2%, respectively. In addition to severity labels, a small subset with 50 cases in MosMedData is annotated with binary ROI masks in the pixel level, which localizes the ground-class opacifications and regions of consolidations in CT images.

CC-CCII CT image set (Zhang et al., 2020) consists of a total of 617,775 CT images from 4,154 patients in China to differentiate between NCP due to SARS-CoV-2 virus infection, common pneumonia incurred by viral, bacterial, or mycoplasma, and normal controls. Each image is accompanied by corresponding metadata (patient ID, scan ID, age, sex, critical illness, liver function, lung function, and time of progression). Furthermore, 750 CT slices from 150 COVID-19 patients are manually annotated at the pixel level and classified into four classes: background, lung field, ground-glass opacity, and consolidation.

COVID-19 CT segmentation dataset (Jenssen, 2020) consists of 100 axial CT images associated with confirmed COVID-19 cases from the Italian Society of Medical and Interventional Radiology. Each image is segmented by a radiologist using three labels: ground-glass (mask value =1), consolidation (=2),

and pleural effusion (=3) and stored in a single NIFTI file with a size of $512 \times 512 \times 110$.

SARS-CoV-2 CT scan dataset (Soares et al., 2020) contains 1252 CT scans that are positive for SARS-CoV-2 infection and 1,230 images from non-COVID-19 patients from hospitals in Sao Paulo, Brazil. This dataset is used to develop artificial intelligence methods to identify if a person is infected by SARS-CoV-2 through the analysis of his/her CT scans.

6 SUMMARY AND DISCUSSIONS ON FUTURE WORKS

AI and machine learning have been applied in the fight against the COVID-19 pandemic. In this article, we reviewed the state-of-the-art solutions to lung scan examination for COVID-19 treatment. Though promising results have been reported, many challenges still exist that should be discussed and investigated in the future.

First, when studying these publications, we find it very challenging to compare their performance. Prior works have usually evaluated model performance on either their private dataset or a combination of several public image sets. Furthermore, the use of different evaluation protocols (e.g., binary classification vs. multi-category classification) and various performance metrics makes the comparison very difficult. We argue that the lack of benchmark hinders the development of AI solutions based on state of the art. With more chest images being available, we expect a comprehensive benchmark for fair comparison among different solutions in the near future.

Second, AI-based methods, especially deep learning, usually require a huge amount of training data with quality annotations. It is always more difficult and expensive to collect medical images to collect natural image samples. Compared to the model sizes, which are easily up to millions of training parameters, the sample size in the current public lung scan image sets is relatively small. This observation is more noticeable in the literature of prognosis estimation. Consequently, the generalizability of the state-of-the-art models on unseen data is in question. In addition, since current lung scan image sets contain many images from heavily or critically ill patients, there is a debate on if AI can differentiate nuances between mild/moderate COVID-19 and other lower respiratory illnesses in real clinical settings. The data bias in training data would greatly harm model's generalizability. Without tackling these data bias issues, data-driven solutions are hardly ready for deployment clinically. There are two possible solutions to address this issue. On the one hand, collecting large image sets that cover a variety of COVID-19 cases is demanding. On the other hand, methods based on self-supervision anomaly detection can help mitigate data bias in data-driven solutions. Specifically, it is relatively easier to collect a large number of lung scans from healthy subjects. By studying the normal patterns in these negative cases, AI-based anomaly detection methods are expected to detect positive chest images by identifying any abnormal patterns that do not follow the normal patterns.

Third, in COVID-19 treatment, examination based on data from one modality is usually not sufficient. For instance, some COVID-19 patients do not experience fever and cough, while others have no symptoms in their chest images. To tackle this problem, omni-modality learning capable of holistically analyzing patients' clinical information, for example, blood test results, age, chest images, and RT-PCR test, is highly desired for COVID-19 treatment. We have witnessed the trend of including multi-modality data in prognosis estimation. However, from the technical aspect, current multi-modality data fusion methods are too simple. How to effectively combine the lung scans with patients' clinical records is still an open question.

Last but not least, despite the promising results reported in prior arts, the issue of explainability in these AI models is less addressed. Decision-making in a medical setting can have serious health consequences; it is often not enough to have a good decision-making or risk-prediction system in the statistical sense. Conventional medical diagnosis and prognosis usually are concluded with evidence. However, such evidence is usually missed in current AI-based methods. We argue that this limitation of explainability is another hurdle in deploying AI technology on lung scans for COVID-19 examination. A desirable system should not only indicate the existence of COVID-19 (with yes/no) but also be able to identify what structures/regions in images are the basis for its decision.

AUTHOR CONTRIBUTIONS

All authors listed have made a substantial, direct, and intellectual contribution to the work and approved it for publication.

REFERENCES

Abbas, A., Abdelsamea, M., and Gaber, M. (2021a). 4S-DT: Self Supervised Super Sample Decomposition for Transfer Learning with Application to COVID-19 Detection. *IEEE Trans. Neural Netw. Learn. Syst.* 32 (7), 2798–2808. doi:10.1109/TNNLS.2021.3082015

Abbas, A., Abdelsamea, M. M., and Gaber, M. M. (2021b). Classification of COVID-19 in Chest X-ray Images Using DeTraC Deep Convolutional Neural Network. *Appl. Intell.* 51, 854–864. doi:10.1007/s10489-020-01829-7

Afshar, P., Heidarian, S., Naderkhani, F., Oikonomou, A., Plataniotis, K. N., and Mohammadi, A. (2020). COVID-CAPS: A Capsule Network-Based Framework for Identification of COVID-19 Cases from X-ray Images. *Pattern Recognition Lett.* 138, 638–643. doi:10.1016/j.patrec.2020.09.010

Ahishali, M., Degerli, A., Yamac, M., Kiranyaz, S., Chowdhury, M., Hameed, K., et al. (2021). *A Comparative Study on Early Detection of COVID-19 from Chest X-ray Images*. *IEEE Access* 9, 41052–41065. doi:10.1109/ACCESS.2021.3064927

Al-karawi, D., Al-Zaidi, S., Polus, N., and Jassim, S. (2020). Artificial Intelligence-Based Chest X-Ray Test of COVID-19 Patients. *Int. J. Comput. Inform. Engg.*, 14 (10).

Albahli, S. (2020). Efficient GAN-based Chest Radiographs (CXR) Augmentation to Diagnose Coronavirus Disease Pneumonia. *Int. J. Med. Sci.* 17, 1439–1448. doi:10.7150/ijms.46684

Amyar, A., Modzelewski, R., Li, H., and Ruan, S. (2020). Multi-task Deep Learning Based CT Imaging Analysis for COVID-19 Pneumonia: Classification and Segmentation. *Comput. Biol. Med.* 126, 104037. doi:10.1016/j.compbiomed.2020.104037

Anwar, T., and Zakir, S. (2020). Deep Learning Based Diagnosis of COVID-19 Using Chest CT-scan Images. In IEEE International Multitopic Conference

(INMIC), Bahawalpur, Pakistan, 5-7 Nov. 2020. IEEE. doi:10.1109/INMIC50486.2020.9318212

Apostolopoulos, I. D., Aznaouridis, S. I., and Tzani, M. A. (2020). Extracting Possibly Representative COVID-19 Biomarkers from X-ray Images with Deep Learning Approach and Image Data Related to Pulmonary Diseases. *J. Med. Biol. Eng.* , 1, 1, 8. doi:10.1007/s40846-020-00529-4

Apostolopoulos, I. D., and Mpesiana, T. A. (2020). COVID-19: Automatic Detection from X-ray Images Utilizing Transfer Learning with Convolutional Neural Networks. *Phys. Eng. Sci. Med.* 43, 635–640. doi:10.1007/s13246-020-00865-4

Ardakani, A. A., Kanafi, A. R., Acharya, U. R., Khadem, N., and Mohammadi, A. (2020). Application of Deep Learning Technique to Manage COVID-19 in Routine Clinical Practice Using CT Images: Results of 10 Convolutional Neural Networks. *Comput. Biol. Med.* 121, 103795. doi:10.1016/j.compbiomed.2020.103795

Asif, S., Wenhui, Y., Jin, H., Tao, Y., and Jinhai, S. (2021). Classification of COVID-19 from Chest X-ray Images Using Deep Convolutional Neural Networks, Proceedings of International Conference on Computer and Communications.

Aslan, M. F., Unlersen, M. F., Sabanci, K., and Durdu, A. (2021). CNN-based Transfer Learning-BiLSTM Network: A Novel Approach for COVID-19 Infection Detection. *Appl. Soft Comput.* 98, 106912. doi:10.1016/j.asoc.2020.106912

Asnaoui, K. E., and Chawki, Y. (2020). Using X-ray Images and Deep Learning for Automated Detection of Coronavirus Disease. *J. Biomol. Struct. Dyn.* 5, 1–12. doi:10.1080/07391102.2020.1767212

Azad, R., Asadi, M., Fathy, M., and Escalera, S. (2019). Bi-Directional ConvLSTM U-Net with Densley Connected Convolutions. Proceedings of the IEEE/CVF International Conference on Computer Vision (ICCV) Workshops. doi:10.1109/ICCVW.2019.00052

Bai, Y., Yao, L., Wei, T., Tian, F., Jin, D.-Y., Chen, L., et al. (2020). Presumed Asymptomatic Carrier Transmission of COVID-19. *JAMA* 323, 1406–1407. doi:10.1001/jama.2020.2565

Brunese, L., Mercaldo, F., Reginelli, A., and Santone, A. (2020). Explainable Deep Learning for Pulmonary Disease and Coronavirus COVID-19 Detection from X-Rays. *Computer Methods Programs Biomed.* 196, 105608. doi:10.1016/j.cmpb.2020.105608

Chandra, T. B., Verma, K., Singh, B. K., Jain, D., and Netam, S. S. (2021). Coronavirus Disease (COVID-19) Detection in Chest X-ray Images Using Majority Voting Based Classifier Ensemble. *Expert Syst. Appl.* 165, 113909. doi:10.1016/j.eswa.2020.113909

Chao, H., Fang, X., Zhang, J., Homayounieh, F., Arru, C. D., Digumarthy, S. R., et al. (2021). Integrative Analysis for COVID-19 Patient Outcome Prediction. *Med. Image Anal.* 67, 101844. doi:10.1016/j.media.2020.101844

Chatterjee, S., Saad, F., Sarasaen, C., Ghosh, S., Khatun, R., Radeva, P., et al. (2020). Exploration of Interpretability Techniques for Deep COVID-19 Classification Using Chest X-ray Images. *arXiv:2006,02570* [Epub ahead of print].

Chen, T., Kornblith, S., Norouzi, M., and Hinton, G. (2020a). A Simple Framework for Contrastive Learning of Visual Representations. International Conference on Machine Learning. ICML.

Chen, X., Yao, L., and Zhang, Y. (2020b). Residual Attention U-Net for Automated Multi-Class Segmentation of COVID-19 Chest CT Images. *arXiv:2004.05645* [Epub ahead of print].

Chowhury, M., Rahman, T., Khandakar, A., Mazhar, R., Kadir, M., Mahbub, Z., et al. (2020). Can AI Help in Screening Viral and COVID-19 Pneumonia? *IEEE Access*, 8, 132665- 132676. doi:10.1109/ACCESS.2020.3010287

Cohen, J., Morrison, P., Dao, L., Roth, K., Duong, T., and Ghassemi, M. (2020). COVID-19 Image Data Collection: Prospective Predictions Are the Future. *J. Mach. Learn.*

Cohen, J. P., Dao, L., Roth, K., Morrison, P., Bengio, Y., Abbasi, A. F., et al. (2020). Predicting COVID-19 Pneumonia Severity on Chest X-ray with Deep Learning. *Cureus* 12, e9448. doi:10.7759/cureus.9448

Di, D., Shi, F., Yan, F., Xia, L., Mo, Z., Ding, Z., et al. (2021). Hypergraph Learning for Identification of COVID-19 with CT Imaging. *Med. Image Anal.* 68, 101910. doi:10.1016/j.media.2020.101910

Dong, D., Tang, Z., Wang, S., Hui, H., Gong, L., Lu, Y., et al. (2021). The Role of Imaging in the Detection and Management of COVID-19: a Review. *IEEE Rev. Biomed. Eng.* 14, 16–29. doi:10.1109/rbme.2020.2990959

Eldeen, N., Smarandache, F., and Loey, M. (2021). A Study of the Neutrosophic Set Significance on Deep Transfer Learning Models: An Experimental Case on a Limited COVID-19 Chest X-ray Dataset. *Cognit. Comput.* 4, 1–10. doi:10.1007/s12559-020-09802-9

Fakhfakh, M., Bouaziz, B., Gargouri, F., and Chaari, L. (2020). ProgNet: COVID-19 Prognosis Using Recurrent and Convolutional Neural Networks. *Open Med. Imaging J.* 12. doi:10.2174/1874347102012010011

Fan, D.-P., Zhou, T., Ji, G.-P., Zhou, Y., Chen, G., Fu, H., et al. (2020). Inf-net: Automatic COVID-19 Lung Infection Segmentation from CT Images. *IEEE Trans. Med. Imaging.* 39, 2626 – 2637. doi:10.1109/tmi.2020.2996645

Fang, X., Kruger, U., Homayounieh, F., Chao, H., Zhang, J., Digumarthy, S. R., et al. (2021). Association of AI Quantified COVID-19 Chest CT and Patient Outcome. *Int. J. CARS.* 16, 435–445. doi:10.1007/s11548-020-02299-5

Ganin, Y., Ustinova, E., Ajakan, H., Germain, P., Larochelle, H., Laviolette, F., et al. (2016). Domain-adversarial Training of Neural Networks. *J. Machine Learn. Res.* 17, 2096–2030.

Goncharov, M., Pisov, M., Shevtsov, A., Shirokikh, B., Kurmukov, A., Blokhin, I., et al. (2020). CT-based COVID-19 Triage: Deep Multitask Learning Improves Joint Identification and Severity Quantification. *arXiv:2006.01441*. [Epub ahead of print].

Goodwin, B., Jaskolski, C., Zhong, C., and Asmani, H. (2020). *Intra-model Variability in COVID-19 Classification Using Chest X-ray Images*. eprint arXiv. 2005, 02167. [Epub ahead of print].

Han, Z., Wei, B., Hong, Y., Li, T., Cong, J., Zhu, X., et al. (2020). Accurate Screening of COVID-19 Using Attention-Based Deep 3D Multiple Instance Learning. *IEEE Trans. Med. Imaging* 39, 2584–2594. doi:10.1109/tmi.2020.2996256

Hao, W., and Li, M. (2020). Clinical Diagnostic Value of CT Imaging in COVID-19 with Multiple Negative RT-PCR Testing. *Trav. Med Infect Dis. Infect. Dis.* 34, 101627. doi:10.1016/j.tmaid.2020.101627

He, X., Wang, S., Shi, S., Chu, X., Tang, J., Liu, X., et al. (2020a, *Benchmarking Deep Learning Models and Automated Model Design for COVID-19 Detection with Chest CT Scans*. eprint medRvix: doi:10.1101/2020.06.08.20125963

He, X., Yang, X., Zhang, S., Zhao, J., Zhang, Y., Xing, E., et al. (2020b). *Sample-efficient Deep Learning for COVID-19 Diagnosis Based on CT Scans*. eprint medRxiv: doi:10.1101/2020.04.13.20063941

Hirano, H., Koga, K., and Takemoto, K. (2020). *Vulnerability of Deep Neural Networks for Detecting COVID-19 Cases from Chest X-ray Images to Universal Adversarial Attacks*. *PLoS ONE* 15 (12). doi:10.1371/journal.pone.0243963

Javaheri, T., Homayounfar, M., Amoozgar, Z., Reiazi, R., Homayounieh, F., Abbas, E., et al. (2021). CovidCTNet: An Open-Source Deep Learning Approach to Identify COVID-19 Using CT Image. *Npj Digit. Med.* 4. doi:10.1038/s41746-021-00399-3

Jenssen, H. (2020). COVID-19 CT Segmentation Dataset. Availableat: https://medicalsegmentation.com/about/.

Jin, C., Chen, W., Cao, Y., Xu, Z., Tan, Z., Zhang, X., et al. (2020). Development and Evaluation of an Artificial Intelligence System for COVID-19 Diagnosis. *Nat. Commun.* 11, 5088. doi:10.1038/s41467-020-18685-1

Khan, A. I., Shah, J. L., and Bhat, M. M. (2020). CoroNet: A Deep Neural Network for Detection and Diagnosis of COVID-19 from Chest X-ray Images. *Computer Methods Programs Biomed.* 196, 105581. doi:10.1016/j.cmpb.2020.105581

Kumar, S., Mishra, S., and Singh, S. K. (2020). *Deep Transfer Learning-Based Covid-19 Prediction Using Chest X-Rays*. eprint medRxiv: doi:10.1101/2020.05.12.20099937

Laradji, I., Rodriguez, P., Branchaud-Charron, F., Lensink, K., Atighehchian, P., Parker, W., et al. (2020). A Weakly Supervised Region-Based Active Learning Method for COVID-19 Segmentation in CT Images. *arXiv:2007.07012* [Epub ahead of print].

Latif, S., Usman, M., Manzoor, S., Iqbal, W., Qadir, J., Tyson, G., et al. (2020). Leveraging Data Science to Combat COVID-19: A Comprehensive Review. *IEEE Trans. Artif. Intelligence* 1, 85–103. doi:10.1109/TAI.2020.3020521

Lee, E. H., Zheng, J., Colak, E., Mohammadzadeh, M., Houshmand, G., Bevins, N., et al. (2021). Deep COVID DeteCT: an International Experience on COVID-19 Lung Detection and Prognosis Using Chest CT. *NPJ Digit Med.* 4, 11. doi:10.1038/s41746-020-00369-1

Li, T., Han, Z., Wei, B., Zheng, Y., Hong, Y., and Cong, J. (2020). Robust Screening of COVID-19 from Chest X-ray via Discriminative Cost-Sensitive Learning. *arXiv. 2004, 12592* [Epub ahead of print].

Li, Z., Zhao, W., Shi, F., Qi, L., Xie, X., Wei, Y., et al. (2021). A Novel Multiple Instance Learning Framework for COVID-19 Severity Assessment via Data Augmentation and Self-Supervised Learning. *Med. Image Anal.* 69. doi:10.1016/j.media.2021.101978

Liu, S., Georgescu, B., Xu, Z., Yoo, Y., Chabin, G., Chaganti, S., et al. (2020). *3D Tomographic Pattern Synthesis for Enhancing the Quantification of COVID-19*. eprints arXiv:2005.01903.

Long, C., Xu, H., Shen, Q., Zhang, X., Fan, B., Wang, C., et al. (2020). Diagnosis of the Coronavirus Disease (COVID-19): rRT-PCR or CT? *Eur. J. Radiol.* 126, 108961. doi:10.1016/j.ejrad.2020.108961

Majeed, T., Rashid, R., Ali, D., and Asaad, A. (2020). Problems of Deploying Cnn Transfer Learning to Detect COVID-19 from Chest X-Rays. *medRxiv*[Epub ahead of print]. doi:10.1101/2020.05.12.20098954

Medhi, K., Jamil, M., and Hussain, I. (2020). Automatic Detection of COVID-19 Infection from Chest X-ray Using Deep Learning. *medRxiv* [Epub ahead of print]. doi:10.1101/2020.05.10.20097063

Meng, L., Dong, D., Li, L., Niu, M., Bai, Y., Wang, M., et al. (2020). A Deep Learning Prognosis Model Help Alert for COVID-19 Patients at High-Risk of Death: A Multi-center Study. *IEEE J. Biomed. Health Inform.* 24, 3576–3584. doi:10.1109/JBHI.2020.3034296

Minaee, S., Kafieh, R., Sonka, M., Yazdani, S., and Jamalipour Soufi, G. (2020). Deep-COVID: Predicting COVID-19 from Chest X-ray Images Using Deep Transfer Learning. *Med. Image Anal.* 65, 101794. doi:10.1016/j.media.2020.101794

Morozov, S., Andreychenko, A., Pavlov, N., Vladzymyrskyy, A., Ledikhova, N., Gombolevskiy, V., et al. (2020). *MosMedData: Chest CT Scans with COVID-19 Related Findings Dataset*. arXiv.2005, 06465. doi:10.1101/2020.05.20.20100362

Moutounet-Cartan, P. (2020). *Deep Convolutional Neural Networks to Diagnose COVID-19 and Other Pneumonia Diseases from Posteroanterior Chest X-Rays*. arXiv. 2005, 00845. [Epub ahead of print].

Narayan Das, N., Kumar, N., Kaur, M., Kumar, V., and Singh, D. (2020). Automated Deep Transfer Learning-Based Approach for Detection of COVID-19 Infection in Chest X-Rays. *IRBM: Biomed. Eng. Res.* 10. doi:10.1016/j.irbm.2020.07.001

Ozcan, T. (2020). A Deep Learning Framework for Coronavirus Disease (COVID-19) Detection in X-ray Images. [Epub ahead of print]. doi:10.21203/rs.3.rs-26500/v1

Ozturk, T., Talo, M., Yildirim, E. A., Baloglu, U. B., Yildirim, O., and Rajendra Acharya, U. (2020). Automated Detection of COVID-19 Cases Using Deep Neural Networks with X-ray Images. *Comput. Biol. Med.* 121, 103792. doi:10.1016/j.compbiomed.2020.103792

Pham, Q., Nguyen, D., Huynh-The, T., Hwang, W.-J., and Pathirana, P. (2020). Artificial Intelligence (AI) and Big Data for Coronavirus (COVID-19) Pandemic: A Survey on the State-Of-The-Arts. *IEEE Access* 8. doi:10.1109/access.2020.3009328

Punn, N., and Agarwal, S. (2021). Automated Diagnosis of COVID-19 with Limited Posteroanterior Chest X-ray Images Using fine-tuned Deep Neural Networks. *Appl. Intell.* 51, 2689–2702. doi:10.1007/s10489-020-01900-3

Rahimzadeh, M., Attar, A., and Sakhaei, S. M. (2020, *A Fully Automated Deep Learning-Based Network for Detecting COVID-19 from a New and Large Lung CT Scan Dataset*. medRxiv: doi:10.1101/2020.06.08.20121541

Rajaraman, S., and Antani, S. (2020). Weakly Labeled Data Augmentation for Deep Learning: A Study on COVID-19 Detection in Chest X-Rays. *Diagnostics* 10, 358. doi:10.3390/diagnostics10060358

Roberts, M., Driggs, D., Driggs, D., Thorpe, M., Gilbey, J., Yeung, M., et al. (2021). Common Pitfalls and Recommendations for Using Machine Learning to Detect and Prognosticate for COVID-19 Using Chest Radiographs and CT Scans. *Nat. Mach Intell.* 3, 199–217. doi:10.1038/s42256-021-00307-0

Ronneberger, O., Fischer, P., and Brox, T. (2015). U-net: Convolutional Networks for Biomedical Image Segmentation. In *Medical Image Computing and Computer-Assisted Intervention*. 234–241. doi:10.1007/978-3-319-24574-4_28

Salehi, S., Abedi, A., Balakrishnan, S., and Gholamrezanezhad, A. (2020). Coronavirus Disease 2019 (COVID-19): A Systematic Review of Imaging Findings in 919 Patients. *Am. J. Roentgenology* 215, 87–93. doi:10.2214/ajr.20.23034

Selvan, R., Dam, E., Detlefsen, N., Rischel, S., Sheng, K., Nielsen, M., et al. (2020). Lung Segmentation from Chest X-Rays Using Variational Data Imputation. ICML Workshop on the Art of Learning with Missing Values . ICML.

Shi, F., Wang, J., Shi, J., Wu, Z., Wang, Q., and Tang, Z., and (2021). Review of Artificial Intelligence Techniques in Imaging Data Acquisition, Segmentation and Diagnosis for COVID-19. *IEEE Rev. Biomed. Eng.* 14, 4–15. doi:10.1109/rbme.2020.2987975

Shibly, K., Dey, S., Islam, M., and Rahman, M. (2020). COVID Faster R-CNN: A Novel Framework to Diagnose Novel Coronavirus Disease (COVID-19) in X-ray Images. *Inform. Med. Unlocked.* 20. doi:10.1016/j.imu.2020.100405

Shiri, I., Sorouri, M., Geramifar, P., Nazari, M., Abdollahi, M., Salimi, Y., et al. (2021). Machine Learning-Based Prognostic Modeling Using Clinical Data and Quantitative Radiomic Features from Chest CT Images in COVID-19 Patients. *Comput. Biol. Med.* 132. doi:10.1016/j.compbiomed.2021.104304

Signoroni, A., Savardi, M., Benini, S., Adami, N., Leonardi, R., Gibellini, P., et al. (2020). End-to-end Learning for Semiquantitative Rating of COVID-19 Severity on Chest X-Rays. *arXiv:2006.04603* [Epub ahead of print].

Soares, E., Angelov, P., Biaso, S., Froes, M. H., and Abe, D. K. (2020). *SARS-CoV-2 CT-scan Dataset: A Large Dataset of Real Patients CT Scans for SARS-CoV-2 Identification*. medRxiv. doi:10.1101/2020.04.24.20078584

Song, Y., Zheng, S., Li, L., Zhang, X., Zhang, X., Huang, Z., et al. (2021). Deep Learning Enables Accurate Diagnosis of Novel Coronavirus (COVID-19) with CT Images. *IEEE/ACM Trans. Comput. Biol. Bioinform.* , 1. doi:10.1109/tcbb.2021.3065361

Tahamtan, A., and Ardebili, A. (2020). Real-time RT-PCR in COVID-19 Detection: Issues Affecting the Results. *Expert Rev. Mol. Diagn.* 20, 453–454. doi:10.1080/14737159.2020.1757437

Toğaçar, M., Ergen, B., and Cömert, Z. (2020). COVID-19 Detection Using Deep Learning Models to Exploit Social Mimic Optimization and Structured Chest X-ray Images Using Fuzzy Color and Stacking Approaches. *Comput. Biol. Med.* 121, 103805.

Ucar, F., and Korkmaz, D. (2020). COVIDiagnosis-Net: Deep Bayes-Squeezenet Based Diagnosis of the Coronavirus Disease 2019 (COVID-19) from X-ray Images. *Med. Hypotheses* 140, 109761. doi:10.1016/j.mehy.2020.109761

Vayá, M. I., Saborit, J., Montell, J., Pertusa, A., Bustos, A., Cazorla, M., et al. (2020). *BIMCV COVID-19+: a Large Annotated Dataset of RX and CT Images from COVID-19 Patients*. arXiv:2006.01174.

Vernuccio, F., Giambelluca, D., Cannella, R., Lombardo, F., Panzuto, F., Midiri, M., et al. (2020). Radiographic and Chest CT Imaging Presentation and Follow-Up of COVID-19 Pneumonia: a Multicenter Experience from an Endemic Area. *Emerg. Radiol.* 27, 623–632. doi:10.1007/s10140-020-01817-x

Waheed, A., Goyal, M., Gupta, D., Khanna, A., Al-Turjman, F., and Pinheiro, P. R. (2020). CovidGAN: Data Augmentation Using Auxiliary Classifier GAN for Improved COVID-19 Detection. *IEEE Access* 8, 91916–91923. doi:10.1109/ACCESS.2020.2994762

Wang, B., Jin, S., Yan, Q., Xu, H., Luo, C., Wei, L., et al. (2021a). Ai-assisted CT Imaging Analysis for COVID-19 Screening: Building and Deploying a Medical AI System. *Appl. Soft Comput.* 98, 106897. doi:10.1016/j.asoc.2020.106897

Wang, G., Liu, X., Li, C., Xu, Z., Ruan, J., Zhu, H., et al. (2020). A Noise-Robust Framework for Automatic Segmentation of COVID-19 Pneumonia Lesions from CT Images. *IEEE Trans. Med. Imaging* 39, 2653–2663. doi:10.1109/tmi.2020.3000314

Wang, L., Lin, Z. Q., and Wong, A. (2020a). COVID-net: A Tailored Deep Convolutional Neural Network Design for Detection of COVID-19 Cases from Chest X-ray Images. *Sci. Rep.* 10, 19549. doi:10.1038/s41598-020-76550-z

Wang, S., Kang, B., Ma, J., Zeng, X., Xiao, M., Guo, J., et al. (2021b). A Deep Learning Algorithm Using Ct Images to Screen for corona Virus Disease (Covid-19). *Eur. Radiol.* doi:10.1007/s00330-021-07715-1

Wang, S., Zha, Y., Li, W., Wu, Q., Li, X., Niu, M., et al. (2020b). A Fully Automatic Deep Learning System for COVID-19 Diagnostic and Prognostic Analysis. *Eur. Respir. J.* 56. doi:10.1183/13993003.00775-2020

Wong, H., Lam, H., Fong, A., Leung, S., Chin, T., Lo, C., et al. (2020). Frequency and Distribution of Chest Radiographic Findings in COVID-19 Positive Patients. *Radiology* 269, E72–E78. doi:10.1148/radiol.2020201160

Wu, Y., Gao, S., Mei, J., Xu, J., Fan, D., Zhang, R., et al. (2021). JCS: An Explainable COVID-19 Diagnosis System by Joint Classification and Segmentation. *IEEE Trans. Image Process.* 30, 3113–3126. doi:10.1109/tip.2021.3058783

Xiao, A., Tongn, Y., and Zhang, S. (2020). Profile of RT-PCR for SARS-CoV-2: a Preliminary Study from 56 COVID-19 Patients. *Clin. Infect. Dis.* 71, 2249–2251. doi:10.1093/cid/ciaa460

Yamac, M., Ahishali, M., Degerli, A., Kiranyaz, S., Chowdhury, M., and Gabbouj, M. (2020). *Convolutional Sparse Support Estimator Based COVID-19 Recognition from X-ray Images*. arXiv. 2005. 04014.

Yan, Q., Wang, B., Gong, D., Luo, C., Zhao, W., Shen, J., et al. (2020). *COVID-19 Chest CT Image Segmentation – a Deep Convolutional Neural Network Solution*. arXiv. 2004, 10987.

Yang, X., He, X., Zhao, J., Zhang, Y., Zhang, S., and Xie, P. (2020). *COVID-CT-Dataset: A CT Scan Dataset about COVID-19*. arXiv. 2003, 13865.

Zabirul-Islam, M., Milon-Islam, M., and Asraf, A. (2020). A Combined Deep CNN-LSTM Network for the Detection of Novel Coronavirus (COVID-19) Using X-ray Images. *Inform. Med. Unlocked* 20, 100412. doi:10.1016/j.imu.2020.100412

Zargari Khuzani, A., Heidari, M., and Shariati, A. (2020). *COVID-classifier: An Automated Machine Learning Model to Assist in the Diagnosis of COVID-19 Infection in Chest X-ray Images*. medRxiv: doi:10.1101/2020.05.09.20096560

Zhang, J., Xie, Y., Liao, Z., Pang, G., Verjans, J., Li, W., et al. (2021). Viral Pneumonia Screening on Chest X-ray Images Using Confidence-Aware Anomaly Detection. *IEEE Trans. Med. Imaging* 40, 879–890. doi:10.1109/tmi.2020.3040950

Zhang, K., Liu, X., Shen, J., Li, Z., Sang, Y., Wang, X., et al. (2020). Clinically Applicable AI System for Accurate Diagnosis, Quantitative Measurements, and Prognosis of COVID-19 Pneumonia Using Computed Tomography. *Cell* 181, 1423–1433. doi:10.1016/j.cell.2020.04.045

Zhou, B., Khosla, A., Lapedriza, A., Oliva, A., and Torralb, A. (2016). Learning Deep Features for Discriminative Localization. *Conf. Computer Vis. Patter Recognition* , 2921–2929.

Zhou, J., Jing, B., and Wang, Z. (2021). SODA: Detecting COVID-19 in Chest X-Rays with Semi-supervised Open Set Domain Adaptation. *IEEE/ACM Trans. Comput. Biol. Bioinform.*

Zhou, L., Li, Z., Zhou, J., Li, H., Chen, Y., Huang, Y., et al. (2020a). A Rapid, Accurate and Machine-Agnostic Segmentation and Quantification Method for CT-based COVID-19 Diagnosis. *IEEE Trans. Med. Imaging* 39, 2638–2652. doi:10.1109/tmi.2020.3001810

Zhou, S., Wang, Y., Zhu, T., and Xia, L. (2020b). CT Features of Coronavirus Disease 2019 (COVID-19) Pneumonia in 62 Patients in Wuhan, china. *AJR. Am. J. Roentgenol.* 214, 1287–1294. doi:10.2214/ajr.20.22975

Conflict of Interest: The authors declare that the research was conducted in the absence of any commercial or financial relationships that could be construed as a potential conflict of interest.

frontiers in Robotics and AI

ORIGINAL RESEARCH
published: 12 August 2021
doi: 10.3389/frobt.2021.612949

Applications of Haptic Technology, Virtual Reality, and Artificial Intelligence in Medical Training During the COVID-19 Pandemic

Mohammad Motaharifar[1,2], Alireza Norouzzadeh[1], Parisa Abdi[3], Arash Iranfar[4], Faraz Lotfi[1], Behzad Moshiri[4,5], Alireza Lashay[3], Seyed Farzad Mohammadi[3] and Hamid D. Taghirad[1]**

[1]Advanced Robotics and Automated Systems (ARAS), Industrial Control Center of Excellence, Faculty of Electrical Engineering, K. N. Toosi University of Technology, Tehran, Iran, [2]Department of Electrical Engineering, University of Isfahan, Isfahan, Iran, [3]Translational Ophthalmology Research Center, Farabi Eye Hospital, Tehran University of Medical Sciences, Tehran, Iran, [4]School of Electrical and Computer Engineering, University College of Engineering, University of Tehran, Tehran, Iran, [5]Department of Electrical and Computer Engineering, University of Waterloo, Waterloo, ON, Canada

OPEN ACCESS

Edited by:
S. Farokh Atashzar,
New York University, United States

Reviewed by:
Beom-Chan Lee,
University of Houston, United States
Pete Culmer,
University of Leeds, United Kingdom
Soroosh Shahtalebi,
Montreal Institute for Learning Algorithm (MILA), Canada

***Correspondence:**
Seyed Farzad Mohammadi
sfmohammadi@tums.ac.ir
Hamid D. Taghirad
taghirad@kntu.ac.ir

Specialty section:
This article was submitted to Biomedical Robotics, a section of the journal Frontiers in Robotics and AI

Received: 01 October 2020
Accepted: 29 July 2021
Published: 12 August 2021

Citation:
Motaharifar M, Norouzzadeh A, Abdi P, Iranfar A, Lotfi F, Moshiri B, Lashay A, Mohammadi SF and Taghirad HD (2021) Applications of Haptic Technology, Virtual Reality, and Artificial Intelligence in Medical Training During the COVID-19 Pandemic. Front. Robot. AI 8:612949. doi: 10.3389/frobt.2021.612949

This paper examines how haptic technology, virtual reality, and artificial intelligence help to reduce the physical contact in medical training during the COVID-19 Pandemic. Notably, any mistake made by the trainees during the education process might lead to undesired complications for the patient. Therefore, training of the medical skills to the trainees have always been a challenging issue for the expert surgeons, and this is even more challenging in pandemics. The current method of surgery training needs the novice surgeons to attend some courses, watch some procedure, and conduct their initial operations under the direct supervision of an expert surgeon. Owing to the requirement of physical contact in this method of medical training, the involved people including the novice and expert surgeons confront a potential risk of infection to the virus. This survey paper reviews recent technological breakthroughs along with new areas in which assistive technologies might provide a viable solution to reduce the physical contact in the medical institutes during the COVID-19 pandemic and similar crises.

Keywords: COVID-19 pandemic, medical training, haptic, virtual reality, artificial intelligence

1 INTRODUCTION

After the outbreak of COVID-19 virus in Wuhan, China at the end of 2019, this virus and its mutations has rapidly spread out in the world. In view of the fact that no proven treatment has been so far introduced for the COVID-19 patients, the prevention policies such as staying home, social distancing, avoiding physical contact, remote working, and travel restrictions has strongly been recommended by the governments. As a consequence of this global problem, universities have initiated policies regarding how to keep up teaching and learning without threatening their faculty members and students to the virus. Thus, the majority of traditional in-class courses have been substituted to the online courses. Notwithstanding the fact that the emergency shift of the classes have reduced the quality of education during the COVID-19 pandemics Hodges et al. (2020), some investigators have proposed ways for rapid adaption of the university faculty and the students to the situation and improve the quality of education Zhang et al. (2020).

Nevertheless, the case of remote learning is different in the medical universities as the learning process in the medical universities is not just rely on the in-class courses. As an illustration, the

medical training in the traditional way is accomplished by a medical student through attending some training courses, watching how the procedure is performed by a trainer, performing the procedure under supervision of a trainer, and at the final stage, independently performing the procedure. In fact, the traditional method of surgery training relies on excessive presence of students in the hospital environments and the skill labs to practice the tasks on the real environments such as physical phantoms, cadavers, and patients and that is why medical students are called "residents". Thus, the aforementioned traditional surgery training methodology requires a substantial extent of physical contact between medical students, expert surgeons, nurses, and patients, and as a result, the risk of infection is high among those people. On the other hand, the assistive technologies based on virtual reality and haptic feedback have introduced alternative surgical training tools to increase the safety and efficiency of the surgical training procedures. Nowadays, the necessity of reducing the physical contact in the hospital environments seems to make another motivation for those assistive technologies. Therefore, it is beneficial to review those technologies from COVID-19 motivation aspect.

In this paper, the existing assistive technologies for medical training are reviewed in a COVID-19 situation. While there are several motivations for those technologies such as increasing the safety, speed, and efficiency of training, the new motivations created for those technologies during the COVID-19 pandemic are the specific focus of this paper. In spite of the existing literature on COVID-19, our main focus is surgery training technologies that help to reduce physical contact during this and other similar pandemics. Notably, a number of those studies have analyzed systemic and structural challenges applicable to medical training programs with little emphasis on technological aspects of the subject Sharma and Bhaskar (2020), Khanna et al. (2020). On the other hand, the methods of remote diagnostics and remote treatment have received a great deal of attention after COVID-19 pandemic and a massive body of literature have covered those topics Tavakoli et al. (2020), Feizi et al. (2021), Akbari et al. (2021). In contrast, less studies have given special attention on remote training and remote skill assessment which is the subject of this paper. For this reason, this paper addresses scientific methods, technologies and solutions to reduce the amount of physical contact in the medical environments that is due to training reasons.

Relevant literature was chosen from articles published by IEEE, Frontiers, Elsevier, SAGE, and Wiley with special attention to the well-known interdisciplinary journals. The search was preformed using the keywords "remote medical training," "skill assessment in surgery," "virtual and augmented reality for medical training," "medical training haptic systems," and "artificial intelligence and machine learning for medical training" until June 30, 2021. The literature was examined to systematically address key novel concepts in remote training with sufficient attention to the future direction of the subject. Finally, it is tried to review the problem in the COVID-19 context in a way that the discussed materials are distinct from similar literature in a conventional non-COVID context.

The rest of this paper is organized as follows: The clinical motivations of the training tools are discussed in **Section 2**. The virtual and augmented reality and the related areas of utilization for medical training are described in **Section 3**. **Section 4** explains how haptic technology may be used for medical training, while **Section 5** describes some data-based approaches that may be used for skill assessment. Then, the machine vision and its relevant methods used for medical training are presented in **Section 6**. Finally, concluding remarks are stated in **Section 7**.

2 THE CLINICAL MOTIVATION

The process of skill development among medical students have always been a challenging issue for the medical universities, as the lack of expertise may lead to undesired complications for the patients Kotsis and Chung (2013). Moreover, owing to the rapid progress of minimal invasive surgeries during the past decades, the closed procedures have been becoming a method of choice over traditional open surgeries. In the minimal invasive surgery, the instruments enter the body through one or more small incisions, while this type of surgery is applicable to a variety of procedures. The foremost advantage of this technique is the minimal affection to healthy organs, which leads to less pain, fewer post-operative complications, faster recovery time, and better long-term results.

However, the closed surgery technique is more challenging from the surgeon's point of view since the surgeon does not have a complete and direct access on the surgical site and the tiny incisions limit the surgeon's accessibility. Owing to the limited access, some degrees of freedom are missing and surgeon's manipulation capability is considerably reduced. Furthermore, there is fulcrum effect at the entry point of the instrument, i.e., the motion of the tip of the instrument, which is placed inside the organ, and the external part of the instrument, which is handled by the surgeon, are reversed. This results in more difficult and even awkward instrument handling and requires specific and extensive surgical training of the surgeon. As a result, the minimal invasive surgeries demands advanced expertise level, the lack of which might cause disastrous complications for the patient. These conditions are equally important in many medical interventions, especially in minimally invasive surgeries. Here a number of specific areas of surgical operation are expressed in order to address complications that might occur during the training procedures.

- Eye surgery:

An important category of medical interventions which need a very high skill level is intraocular eye surgical procedures. Notably, the human eye is a delicate and highly complex organ and the required accuracy for the majority of intraocular surgeries is in the scale of 50–100 microns. The closed type of surgery is applicable to a number of eye surgeries such as the Cataract surgery in the anterior segment as well as the vitro-retinal surgical procedures in the posterior segment. Notably, some complications such as Posterior Capsule

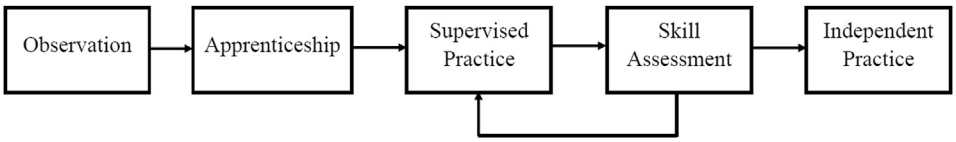

FIGURE 1 | Process of procedural skill development in medical training and surgery.

Rupture (PCR) for cataract surgery and retina puncture for the vitro-retinal surgical procedures are among the relatively frequent complications that might happen, due to the surgeon's lack of surgical skills and dexterity. It is shown in a study on ophthalmic residents that the rate of complications such as retinal injuries is higher for the residents with less skills Jonas et al. (2003).

- Laparoscopic Cholecystectomy

Another example is Laparoscopic Cholecystectomy (LC) which is now the accepted standard procedure across the world and is one of the most common general and specialist surgical procedures. However, it can be prone to an important complication that is bile duct injury (BDI). Although BDI is uncommon but it is one of the most serious iatrogenic surgical complications. In extreme BDI cases, a liver resection or even liver transplantation becomes necessary. BDI is considered as an expensive medical treatment and its mortality rate is as high as 21% Iwashita et al. (2017).

- Neurosurgery

Neurosurgery is another field that deals with complex cases and requires high accuracy and ability in the surgeon's performance. In a prospective study of 1,108 neurosurgical cases, 78.5% of errors during neurosurgery were considered preventable Stone and Bernstein (2007). The most frequent errors reported were technical in nature. The increased use of endoscopy in neurosurgery introduces challenges and increases the potential for errors because of issues such as indirect view, elaborate surgical tools, and a confined workspace.

- Orthopedic surgery

In the field of orthopedics, knee and shoulder arthroscopic surgeries are among the most commonly performed procedures worldwide. There is a steep learning curve associated with arthroscopic surgery for orthopaedic surgery trainees. Extensive hands-on training is typically required to develop surgical competency. The current minimum number of cases may not be sufficient to develop competency in arthroscopic surgery. It is estimated that it takes about 170 procedures before a surgeon develops consultant-level motor skills in knee arthroscopic surgery Yari et al. (2018). With work-hour restrictions, patient safety concerns, and fellows often taking priority over residents in performing cases, it is challenging for residents to obtain high-level arthroscopic skills by the end of their residency training.

The above motivation shows the importance of skill development among the medical students. The standard process of procedural skill development in medicine and surgery is shown as a diagram in **Figure 1**. In the observation stage, the medical students need to attend a clinical environment and watch how the procedure is performed by a trainee. Then, the medical students get involved in the operation as an apprentice, while the actual procedure is performed by the trainer. Later, the medical students practice the operation under direct supervision of the trainer, while the trainer assesses the skill level of the medical students. The supervised practice and skill assessment steps are repeated as long as the trainee does not have enough experience and skill to conduct the procedures without supervision of the trainer. Finally, after obtaining sufficient skill level, the trainee is able to independently perform the operation.

Remarkably, a learning curve is considered for each procedure, which means that performance tends to improve with experience. This concept applies for all of the medical procedures and specialties, but complex procedures, surgery in particular, are more likely to gradual learning curves, which means that improvement and expertise is achieved after longer training time. Some of the important factors in the learning curve are manual dexterity of the surgeon, the knowledge of surgical anatomy, structured training and mentoring and the nature of the procedure. The learning curve is longer for minimally invasive procedures than that for open surgical procedures. The learning curve is also influenced by the experience of the supporting surgical team. Besides, learning curves depend on the frequency of procedures performed in a specified period. Many studies suggest that complication rates are inversely proportional to the volume of surgical workload.

Notably, the above mentioned process of skill development require a considerable extent of physical contact between the trainees, the expert surgeons, the nurses, and the patients, while this shall be reduced in the COVID-19 pandemic. In addition to the high risk of infection in the medical universities with the conventional medical training approaches, the majority of the health-care capacity is focused on fighting the COVID-19 virus and consequently, the education requirements of medical universities are failed to be entirely fulfilled. As a result, the training efficiency of medical universities will be reduced, provided that they just rely on the conventional training approaches. This will have possible side-effects on the future performance of the health-care system mainly due to the

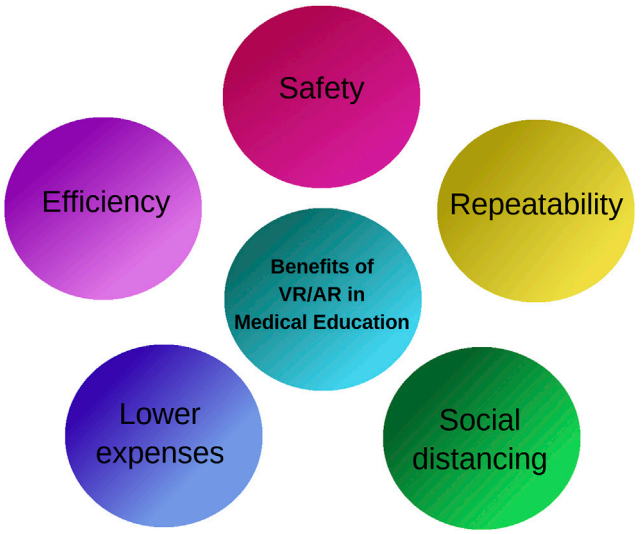

FIGURE 2 | VR/AR advantages in medical training.

insufficient number of recently graduated students with adequate expertise level.

On the other hand, traditional education takes place in hospitals and on real patients, which face several problems during the COVID-19 pandemic: the hospital environment is contaminated with the virus, hospital staff and physicians are very busy and tired and have less training capacity, prolonged hospital stays of patients to train students put them at greater risk for exposure to the virus, especially if complication occurs by a resident who does not have gained sufficient skills during the training procedure. Therefore, training with assistive devices outside the hospital may play an effective role in this situations. The highlighted factors can significantly be improved by assisted learning, especially in minimally invasive procedures. In more complex surgeries, the complications becomes more serious, the learning curve will be longer, and the role of assisted learning becomes more prominent.

To solve the above mentioned problems, assistive training tools provide a variety of solutions through which the medical universities are able to continue their education procedures, while the risks enforced by the COVID-19 outbreak are reduced. In the following sections, the main assistive training tools including the haptic systems, virtual reality, machine vision, and data mining are reviewed and the areas in which those technologies facilitate the training process during the COVID-19 pandemic are detailed. The aim of these technologies is to have the training efficiency higher or at least equal to that of the conventional training methods without risk of infection of the involved parties to the virus.

3 VIRTUAL AND AUGMENTED REALITY

Virtual Reality is employed to create an immersive experience for various applications such as visualization, learning and education. In virtual reality, a computer generated graphical presence is visualized using a head mounted display and the user can interact with 3D objects located in the virtual world. In addition to VR, the Augmented Reality (AR) is developed to add 3D objects to the real world creating a different experience by adding digital information to the real objects in the surrounding environment. Although experiencing the 3D objects in VR scenes is far from the interaction with real objects, the VR experience is getting closer to the real world environments by the help of more realistic computer graphics and full-body haptics suits.

The virtual reality (VR) and augmented reality (AR) are getting more interest as a training technique in the medical fields, unlocking significant benefits such as safety, repeatability and efficiency Desselle et al. (2020). Furthermore, during the COVID-19 pandemic, remote training and consulting are considered as vital advantages of VR/AR based training methods (Singh et al., 2020).

Some advantages of using VR/AR in medical training are depicted in **Figure 2**. Safety is the first and the most important benefit of VR/AR employment in medical education. Complex medical operations may be performed in a simulated environment based on VR with complete safety and without putting the patient's life into danger. Repeatability is the second advantage of using VR as any simulation scenario in the field of medical training can be repeated over and over until the trainee is completely satisfied. During the COVID-19 pandemic it is vital to practice social distancing which is delivered by VR/AR employment in medical education. Medical training and surgery simulation by computer graphics in VR/AR virtual environments results in reduced training costs as no material except than a computer, a VR headset and a haptic device is required. Since medical training by VR/AR is performed using a computer, the surgery simulation is always in hand as soon the computer and VR headset are ready to be used. Therefore, the efficiency of medical training is increased as no time is required for either preparation of an operation room or getting a patient ready.

VR/AR techniques are employed in various applications in surgical training as it can be seen in **Figure 3**. The first application of AR/VR in surgical training is surgical procedure diagnosis and planning. Using AR/VR, the real surgical operation is simulated ahead without putting the patient's life into danger. The AR/VR is used in surgical education and training which is mentioned as the second application. Simulation based environments are developed for training of medical students by virtual human anatomy 3D models. Another application of AR/VR is robotic and tele-surgery, by which surgical consulting becomes possible even from a far distance. The last application of AR/VR in surgical training is sensor data and image visualization during the surgical operation which makes the effective usage of patient's medical data possible.

It is shown that the learning curve of hip arthroscopy trainees is significantly improved using a virtual reality simulator (Bartlett et al., 2020). In this study, a group of twenty five inexperienced students were chosen to perform seven arthroscopies of a healthy virtual hip joint weekly. The experimental results indicated that average total time decreased by nearly 75% while the number of

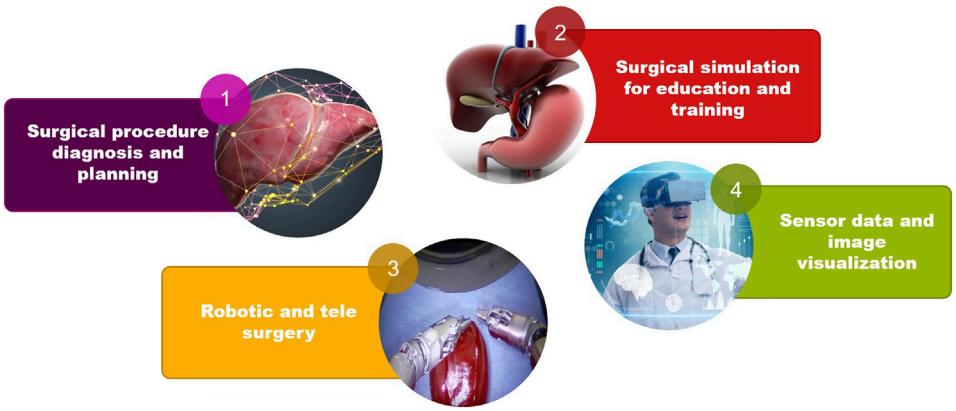

FIGURE 3 | VR/AR applications in surgical training.

collisions between arthroscope and soft-tissues decreased almost by 90%.

VR is also employed in orthopedic surgical training, where 37 residents participated in a study to obtain an understanding of the LISS[1] plating surgical process (Cecil et al., 2018). The developed virtual surgical environment is equipped with a haptic device to perform various activities such as assembling LISS plate, placing the assembled LISS plate correctly inside the patient's leg, and attaching the LISS plate to the fractured bone. The test was divided into pre–test where the students get familiar with the surgery process and the post–test which is devoted to the actual evaluation phase. The participants had 1 h to finish both the pre–and post–tests which resulted in improvement of learning the LISS plating surgical process.

The applicability and effectiveness of VR based training in orthopedic education is evaluated in (Lohre et al., 2020), where nineteen orthopedic surgical residents cooperated in this study. The surgical residents performed a glenoid exposure module on a VR based simulator using a haptic device as the input controller. The result of training of residents using VR simulator has been compared to the conventional surgery training methods. Considering the learning time, repeating 3 to 5 VR based surgery experiments by the residents, resulted in 570% training time reduction. Additionally, VR based surgical training helped the residents to finish glenoid exposure significantly faster than the residents trained by conventional education methods.

Orthognathic surgery is another surgery field considered for VR based training as it is one of the complex surgical procedures (Medellin-Castillo et al., 2020). While conventional OSG[2] learning techniques are dependent to cadavers or models and experienced surgeons are trained after several years of experiments in operating rooms, employment of VR in surgical training can reduce the learning time and the education cost at the same time. In this study, three cases are considered for evaluation of VR in OSG, cephalometry training, osteotomy training and surgery planning to be precise. The experimental results indicated that the combination of haptics and VR is effective in skill improvement of trainees and surgery time reduction. Furthermore, the surgery errors and mistakes are reduced by using haptic feedback to recreate the sense of touch as trainees can detect landmarks more precisely in comparison to conventional techniques.

In conjunction with VR, the AR technology has also been used in various medical fields for training such as neurosurgical training (Si et al., 2019). Anatomical information and other sensory information can be visualized to the surgeons more properly, and therefore, more accurate decision can be made during a surgery. Although this study is only applicable to the simulated environments because of registration problem, the experiment indicated the effectiveness of the simulator in skill improvement of surgeons.

While key features of VR/AR have led to improved training specially in surgical training, there are some limitations that should be considered (kumar Renganayagalu et al., 2021). The first limitation of VR simulators is the cost of VR content production, and therefore, most of simulators are made for very specific type of simulation in a limited context. The second limitation is the immaturity of interaction devices for VR simulations, which has a great affect on the user experience. Another limitation of VR usage in medical training is the inability of using VR devices for long period of time as the VR devices are made for entertainment and not for a long training session.

It can be concluded that in spite of some limitations, VR/AR based simulators equipped with a haptic device can be used in medical surgery training in order to achieve skill improvement and training time reduction. Furthermore, during the isolation requirements due to COVID-19 pandemic, VR/AR based techniques can be well employed for medical training.

4 TELEOPERATED HAPTIC SYSTEMS

Haptic systems provide the sense of touch with remote objects without the need of actual contact. It also provides collaboration between several operators without the need of any physical

[1]Less invasive stabilization system
[2]Orthoganthic surgery

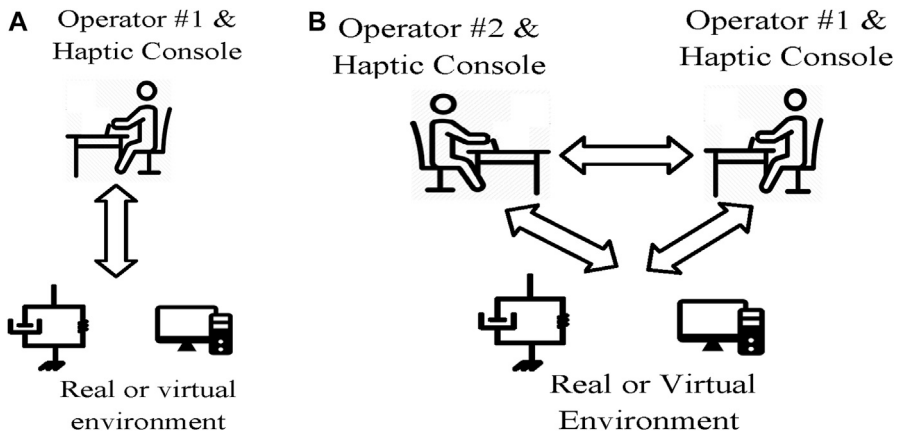

FIGURE 4 | Single user vs. dual user haptic systems. **(A)** Single user haptic system. **(B)** Dual user haptic system.

contact. As depicted in **Figure 4**, based on the number of the operators, the haptic systems may be classified into single user, dual-user or multi-user haptic systems. Single user haptic systems enable a single human operator to interact with a remote or virtual environment, whereas dual-user or multi-user haptic systems provide a mechanism for collaboration of two or multiple human operators. The medical training applications of those systems is presented here.

4.1 Single User Haptic Systems

Single user haptic systems extend the abilities of human operators to interact with remote, virtual, and out-of-reach environment. In the field of surgery training, a number of investigations have proposed haptic training simulators for training of minimally invasive surgery (MIS) Basdogan et al. (2004), dental procedures Wang et al. (2014), sonography Tahmasebi et al. (2008), and ocular therapies Spera et al. (2020). As shown in **Figure 4A**, a typical single-user haptic simulator system consists of a human operator, a haptic interface, a graphical interface, and a reference model for the virtual object. Notably both the graphical interface and the haptic interface utilize the reference model to provide necessary feedback for the operator. While the graphical interface provides a visual feedback of the environment, the haptic interface provides the kinesthetic feedback of the interaction between the tool and the surgical field. Indeed, the role of haptic feedback is to recreate the sense of contact with the virtual environment for the operator. As a result, the circumstances of actual operation is provided for the medical students, while the need of physical presence in the clinical environments is eliminated. Indeed, through haptic technology, the medical students are able to practice on a virtual environment without the need of presence at the clinical environment. Thus, the risk of infection during the COVID-19 pandemic is effectively reduced.

4.2 Dual User Haptic Systems

The cooperative and joint conduction of an operation either for the purpose of collaboration or training, as a fundamental clinical task, cannot be provided by single user haptic systems. In order to make the cooperation of two surgeons possible, the system should be upgraded to a dual user haptic system by adding another haptic console. A dual user haptic system is a more recent advancement in haptic technology, and it consists of two haptic consoles, one for the trainer and one for the trainee Shahbazi et al. (2018a). Remarkably, the traditional collaboration methods require direct physical contact of the persons conducting the operation, whereas the haptic-based collaboration approach eliminates the physical contact of the collaborators. As a result of removing the need of physical contact, the involved people are no longer in the risk of the Corona virus. A commercial dual user haptic system developed by intuitive Surgical Inc.® is the da Vinci Si Surgical System which supports training and collaboration during minimally invasive surgery. The da Vinci Si System builds on the existing da Vinci technology, where it has a number of enabling features such as leading-edge 3D visualization, advanced motion technology, and sufficient dexterity and workspace. However, the da Vinci Si does not provide active supervision and intervention of the trainer on the trainee's actions. As an illustration, in the case that the trainee controls the procedure, the trainer does not have the possibility to guide the trainee during the procedure.

The issue of supervision and intervention of the trainer during the operation in dual user haptic systems have been a topic of active investigation during the past years. A number of studies have utilized the concept of *dominance factor* to determine the task dominance of each operator Nudehi et al. (2005), Khademian and Hashtrudi-Zaad (2012), Shahbazi et al. (2014b), Motaharifar et al. (2016). In those approaches, the trainee is given a partial or full task authority by the trainer based on his/her level of expertise. Notably, the task authority provided by these control architectures is supposed to be fixed during the operation. Thus, changing the authority of the surgeons and specially blocking the trainee's commands is not possible in the middle of the operation. This might lead to undesired operative complications specially in the case that the trainee makes a sudden unpredictable mistake.

Fortunately, a number of investigations have developed control architectures to address the above shortcoming of the previously proposed haptic architectures Motaharifar et al. (2019b), Shahbazi et al. (2014a), Motaharifar and Taghirad (2020). As a case in point, an S-shaped function is proposed in Motaharifar et al. (2019b) for the adjustment of the corrective feedback in order to shape the trainee's muscle memory. In fact, the training approach behind the presented architecture is based on allowing the trainee to freely experience the task and be corrected as needed. Nevertheless, through the above scheme, the trainee is just granted the permission to receive the trainer's motion profile; that is, the trainee is deprived of any realistic contribution to the surgical procedure. In contrast, several investigations have proposed mechanisms for adjusting the task dominance, through which the trainee is granted partial or full contribution to the task Shahbazi et al. (2014a), Motaharifar and Taghirad (2020), Liu et al. (2015), Lu et al. (2017), Liu et al. (2020). Remarkably, the above approaches require both the trainer and the trainee to completely perform the operation on their haptic devices, and the actual task authority is determined based on the position error between the trainer and the trainee Shahbazi et al. (2014a), Motaharifar and Taghirad (2020), Liu et al. (2015), Lu et al. (2017), Liu et al. (2020). This constitutes an important limitation of the above architectures, since the trainer is enforced to be involved in every detail of each operation and even the trivial ones. Notably, the trainer's obligation to precisely perform every part of the surgical procedure has little compatibility with the trainer's responsibilities in terms of supervisory assistance and interference. In fact, by grabbing the idea from the conventional training programs of the medical universities, the haptic architecture should be developed in such a manner that the trainer is able to intervene only in order to prevent a complication to the patient due to the trainee's mistake. The issue of trainer's supervisory assistance and interference is addressed in Motaharifar et al. (2019a) by adjusting the task authority based on the trainer's hand force Motaharifar et al. (2019a). That is, the trainer is able to grant the task authority to the trainer by holding the haptic device loosely or overrule the trainee's action by grasping the haptic device tightly. Therefore, the active supervision and interference of the trainer is possible without the need of any physical contact between the trainer and the trainee.

Although the above investigations address the essential theoretical aspects regarding dual user haptic systems, the commercialization of collaborative haptic system needs more attention. In the past years, some research groups have developed pilot setups of dual user haptic system with the primal clinical evaluation that have the potential of commercialization. For instance, the ARASH-ASiST system provides training and collaboration of two surgeons and it is preliminary designed for Vitreoretinal eye surgical procedures ARASH-ASiST (2019). It is expected that the commercialization and widespread utilization of those assistive surgery training tools is considerably beneficial to the health-care systems in order to decrease the physical contact during the COVID-19 pandemic, and to increase the safety and efficiency of training programs during and after this crisis.

Notwithstanding the fact that teleoperated haptic systems provide key benefits for remote training during COVID-19 pandemic, they face a number of challenges that inspire perspectives of future investigations. First, the haptic modality is not sufficient to recreate the full sense of actual presence at the surgical room near an expert surgeon. To overcome this challenge and increase the operators telepresence, the haptic, visual, and auditory components are augmented to achieve a multi–modal telepresence and teleaction architecture in Buss et al. (2010). The choice of control structure and clinical investigation of the above multi–modal architecture is still an area of active research Shahbazi et al. (2018b), Caccianiga et al. (2021). On the other hand, the on-line communication system creates another challenge for the haptic training systems. Notably, owing to the high-bandwith requirement for an appropriate on-line haptic system, the majority of existing haptic architectures in applications such as collaborative teleopertion, handwriting and rehabilitation cover off-line communication Babushkin et al. (2021). However, due to the complexity, uncertainty, and diversity of the surgical procedures, the online feedback from the expert surgeon is necessary for a safe and efficient training. The advent of 5G technology with faster and more robust communication network may provide enough bandwidth for an effective real-time remote surgery training.

5 DATA DRIVEN SCORING

A vital element of a training program is how to evaluate the effectiveness of exercises by introducing a grading system based on participants' performance. The conventional qualitative skill assessment methods require physical contact between the trainer and the trainee since they are based on direct supervision of the trainer. On the other hand, the systematic approaches for skill assessment are based on collecting the required data using appropriate instruments and analyzing the obtained data, while they eliminate the requirement of physical contact between the trainer and the trainee. Thus, reviewing the systematic data-based methods is of utmost importance, as they can be utilized to reduce the physical contact during the COVID-19 Pandemic. In this section, some of the state of the art methods in surgical skill evaluation are reviewed. Following the trend of similar research in the context of surgical skill evaluation, we categorize the reviewed methods by two criteria. The first is the type of data, and the method uses for grading the participant. The second criterion is the features extraction techniques that are used during the evaluation stage.

Generally speaking, two types of data may be available in Robotic-Assisted surgery; kinematic and video data. Kinematic data is available when a robot or haptic device is involved. The most common form of capturing kinematic information is using IMUs, encoders, force sensors, magnetic field positioning sensors, etc. The video is generally recorded in all minimally invasive surgeries using endoscopy procedures.

Kinematic data are more comfortable to analyze because the dimensionality of kinematic data is lower than video data. Moreover, Kinematic information is superior to video in

TABLE 1 | Summery of different sources of data and different feature extraction techniques.

	Data type		
	Kinematic	**Video**	**Experts' opinion**
Pros	Lower dimensionality	Convenient to capture	Higher semantic level
	Actual 3D trajectories	Info. of the surroundings	
Cons	Needs tools	Higher dimensionality	Quantitative
	No info. of the surrounding	Estimated 3D trajectories	
		Occlusion, Clutter, etc.	
	Feature extraction technique		
	Hand-engineered	Automatic	
Pros	Interpretable	End to end solution	
	Easy to calculate	Case independent	
Cons	Hard to define	Requires a big dataset	
	Case dependent	Computational cost	

measuring the actual 3D trajectories, and 3D velocities Zappella et al. (2013). On the other hand, video data is more convenient to capture since no additional equipment and sophisticated sensors are needed to be attached to the surgical tool. Additionally, video data reflects the contextual semantic information such as the presence or absence of another surgical instrument, which can not be derived from the kinematic data Zappella et al. (2013). To use the video data effectively, one should overcome some common obstacles like occlusion and clutter. Using multiple cameras, if possible, can greatly assist in this procedure Abdelaal et al. (2020). In conclusion, it can be said that each type of data has its own merits and limitations, and using kinematic data as well as the video may result in a richer dataset.

Other than the kinematic and video data, another source of information is often disregarded in the literature. The expert surgeon who conducts the training program can evaluate the trainee's performance and provide useful feedback regarding his/her performance. This type of information, which is at another semantic level compared to the sensory data, is called soft data. The hard and soft information fusion methods can merge the expert's opinion with the kinematic and video data (hard data) to accomplish a better grading system.

Most surgical skill evaluation methods utilize a feature extraction technique to classify the participant's skill level after acquiring the data, like expert, intermediate, and novice. The classification problem can be solved by employing some hand-engineered features or features that are automatically extracted from the data. Hand-engineered features are interpretable and easy to obtain. However, hand-engineered features are hard to define. Specifically, defining a feature that represents the skill level regardless of the task is not trivial. Therefore, the states of the art methods are commonly based on automatic feature extraction techniques. An end-to-end deep neural network is used to unfold the input data's spatial and temporal features and classify the participant in one of the mentioned skill levels in an automated feature extraction procedure. While, **Table 1** summarizes the topic of different data types and feature extraction techniques, we are going to cover some of the reviewed methods in the next sections.

The most convenient hand-engineered features are those introduced by descriptive statistics Anh et al. (2020). In a skill rating system proposed by Brown et al. (2016), eight values of mean, standard deviation, minimum, maximum, range, root-mean-square (RMS), total sum-of-squares (TSS), and time integral of force and acceleration signals are calculated. Together with time features like task completion time, these values are used as inputs for a random forest classifier to rate the peg transfer score of 38 different participants. In Javaux et al. (2018), metrics like mean/maximum velocity and acceleration, tool path length, depth perception, maximum and integral of planar/vertical force, and task completion time are considered as a baseline for skill assessment Lefor et al. (2020). Another commonly used method in the literature is to use statistical tests such as Mann-Whitney test Moody et al. (2008), Kruskal–Wallis test Javaux et al. (2018), Pearson or Spearman correlation Zendejas et al. (2017), etc. These tests are utilized to classify the participants directly Moody et al. (2008) or automatically calculate some of the well-known skill assessment scores like GOALS and FLS Zendejas et al. (2017).

Since many surgical tasks are periodic by nature, the data frequency domain analysis proves to be effective Zia et al. (2015). For periodic functions like knot tying and suturing Zia et al. (2015) suggests that transforming the data into time series and performing a Discrete Fourier Transform (DFT) and Discrete Cosine Transform (DCT) on the data extracts features, will assist the skill level classification task. The results show that such an approach outperforms many machine-learning-based methods like Bag of Words (BoW) and Sequential Motion Texture (SMT). In another work by the same author, symbolic features, texture features, and frequency features are employed for the classification. A Sequential Forward Selection (SFS) algorithm is then utilized to reduce the number of elements in the feature vector and remove the irrelevant data Zia et al. (2016). Hojati et al. (2019) suggests that since Discrete Wavelet Transform (DWT) is superior to DFT and DCT in a sense that it offers simultaneous localization in time and frequency domain, DWT is a better choice for feature extraction in surgical skill assessment tasks.

As it is mentioned before, hand-engineered features are task-specific. For example, the frequency domain analysis discussed in

the previous section is only viable when the task is periodic. Otherwise, the frequency domain features should be concatenated with other features. Moreover, perceiving the correct features that reflect participants' skill levels in different surgical tasks requires an intensive knowledge of the field. As a result, developing a method in which the essential features are identified automatically is advantageous.

With the recent success of Convolutional Neural Networks (CNN) in classification problems like image classification, action recognition, and segmentation, it is safe to assume that CNN can be used in skill assessment problems. However, unlike image classification, improvement brought by end-to-end deep CNN remains limited compared to hand-engineered features for action recognition Wang et al. (2018). Similarly, using conventional CNN does not contribute too much to the result in surgical skill evaluation problems. For example, Fawaz et al. (2018) proposed a CNN-based approach for dry-lab skill evaluation tasks such as needle passing, suturing, and knot-tying. However, a hand-engineered-based method with a set of features introduced as holistic features (SMT, DFT, DCT, and Approximate Entropy (ApEn)) suggested by Zia and Essa (2018) reaches the same accuracy as the CNN-based method in the needle passing and suturing tasks and outperforms the CNN-based method in the knot-tying task.

Wang et al. (2018) suggests that conventional CNN falls short compared to traditional hand-crafted feature extraction techniques because it only considers the appearances (spatial features) and ignores the data's temporal dynamics. In Wang and Fey (2018), a parallel deep learning architecture is proposed to recognize the surgical training activity and assess trainee expertise. A Gated recurrent unit (GRU) is used for temporal feature extraction, and a CNN network is used to extract the spatial features. The overall accuracy calculated for the needle passing, suturing, and knot tying tasks is 96% using video data. The problem of extracting spatiotemporal features is addressed with 3D ConvNets in Funke et al. (2019). In this method, inflated convolutional layers are responsible for processing the video snippets and unfolding the classifier's input data.

To the best of our knowledge, all of the proposed methods in the literature have used single classifier techniques in their work. However, methods like classifier fusion have proved to be useful in the case of medical-related data. In Kazemian et al. (2005) an OWA-based fusion technique is used to combine multiple classifiers and improve the accuracy. For a more advanced classifier fusion technique, one can refer to the proposed method in Kazemian et al. (2010) where more advanced methods such as Dempster's Rule of Combination (DCR) and Choquet integral are compared with more basic techniques. Activity recognition and movement classification is another efficient way to calculate metrics representing the surgical skill automatically Khan et al. (2020). Moreover, instrument detection in a video and drawing centroid based on the orientation and movement of the instruments can reflect the focus and ability to plan moves in a surgeon. Utilizing these centroids and calculating the radius, distance, and relative orientation can aid with the classification based on skill level Lavanchy et al. (2021).

In conclusion, the general framework illustrated in **Figure 5** can summarize the reviewed techniques. The input data, either kinematic and video, is fed to a feature extraction block. A fusion block Naeini et al. (2014) can enrich the semantic of the data using expert surgeon feedback. Finally, a regression technique or a classifier can be employed to calculate a participant's score based on his/her skill level or represent a label following his/her performance.

6 MACHINE VISION

The introduction of new hardware capable of running deep learning methods with acceptable performance led artificial intelligence to play a more significant role in any intelligent system Han (2017). It is undeniable that there is a huge potential in employing deep learning methods in a wide range of various applications Weng et al. (2019), Antoniades et al. (2016), Lotfi et al. (2018), Lotfi et al. (2020). In particular, utilizing a camera along with a deep learning algorithm, machines may precisely identify and classify objects by which either performing a proper reaction or monitoring a process may be realized automatically. For instance, considering a person in a coma, any tiny reaction is crucial to be detected, and since it is not possible to assign a person for each patient, a camera can solve the problem satisfactorily. Regarding the COVID-19 pandemic situation, artificial intelligence may be used to reduce both physical interactions and the risk of a probable infection especially when it comes to a medical training process. Considering eye surgery as an instance, not only should the novice surgeon closely track how the expert performs but also the expert should be notified of a probable mistake made by the novice surgeon during surgery. In this regard, utilizing computer vision approaches as an interface, the level of close interactions may be minimized effectively. To clarify, during the training process, the computer vision algorithm may act as both the novice surgeon looking over the expert's hand and the expert monitoring and evaluating how the novice performs. This kind of application in a medical training process may easily extend to other cases. By this means, the demand for keeping in close contact is met properly.

Not needing a special preprocessing, deep convolutional neural networks (CNNs) are commonly used for classifying images into various distinct categories. For instance, in medical images, this may include probable lesions Farooq et al. (2017), Chitra and Seenivasagam (2013). Moreover, they can detect intended objects in the images which can be adopted not only to find and localize specific features but also to recognize them if needed. Since most of the medical training tasks require on-line and long-term monitoring, by utilizing a camera along with these powerful approaches, an expert may always keep an eye on the task assigned to a trainee. Besides, methods based on CNNs are capable of being implemented on graphics processor units (GPUs) to process the images with an applicable performance in terms of both speed and accuracy Chetlur et al. (2014), Bahrampour et al. (2015). This will reduce the

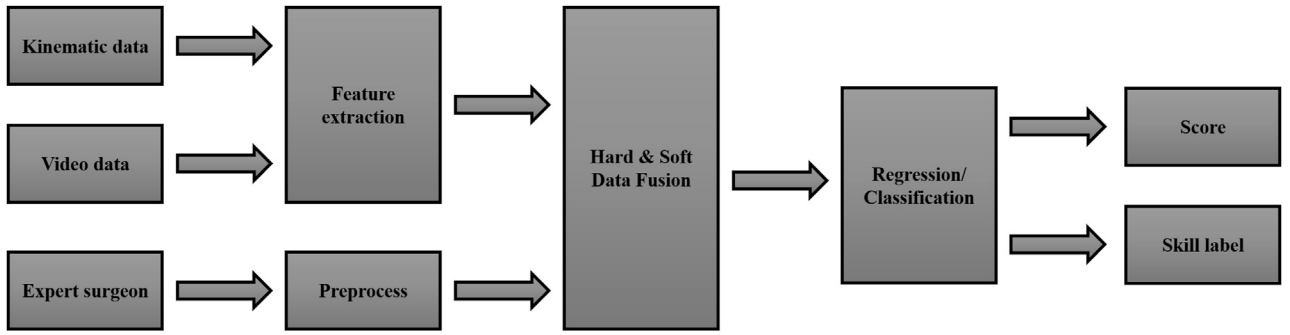

FIGURE 5 | A general framework for surgical skill assessment.

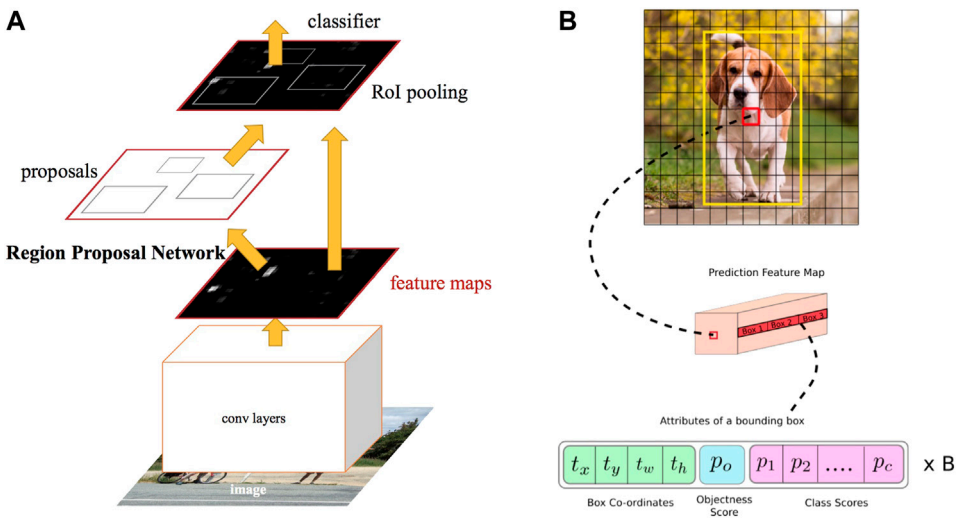

FIGURE 6 | Example of two-stage and single-stage detectors Kathuria (2021). **(A)** Two-stage detector (RCNN). **(B)** Single-stage detector (YOLO).

probable latency and makes it possible for the trainer to be notified on time and correct the trainee remotely.

There are numerous researches carried out in the field of image processing based on CNNs. These methods are mainly divided into two single-stage and two-stage detectors. The former is known to be fast while the latter results in higher accuracy. In **Figure 6** the difference between a two-stage and a single-stage detector is illustrated. Considering single-stage detectors and starting with the LeCun et al. (1998) as one of the earliest networks, plenty of different approaches have been presented in the literature among which single-shot multi-box detector (SSD) Liu et al. (2016), RetinaNet Lin et al. (2017), and you only look once (YOLO) Redmon and Farhadi (2018) may be counted as nominated ones. Some of these approaches have been proposed with several structures including simpler and more complex structures to be employed depending on whether the speed is of high importance or accuracy. Mainly, training and the test are two phases when utilizing these methods. While it is crucial to define a proper optimization problem in the first phase, it is indispensable to implement the trained CNN optimally. Coming up with various solutions, methods like Krizhevsky et al. (2012), Simonyan and Zisserman (2015), Szegedy et al. (2015), and Szegedy et al. (2016) suggest utilizing specific CNN models to obtain better outcomes. On the other hand, to further improve the accuracy, in two-stage detectors like Girshick et al. (2014), it is suggested to first determine a region of interest (ROI) then identify probable objects in the related area. As a representative, Uijlings et al. (2013), which is known as selective search, is designed to propose $2k$ proposal regions, while a classifier may be employed for the later stage. Dealing with some challenging problems in these detectors, He et al. (2015), Girshick (2015), and Ren et al. (2015) are proposed to enhance the results in terms of both accuracy and speed.

To put all in a nutshell, when dealing with critical situations such as the current COVID-19 epidemic, it is highly recommended to employ artificial intelligence techniques in image processing namely deep CNNs for medical training tasks. By this means, neither is a close physical interaction

TABLE 2 | The main tools and approaches that help to reduce physical contact in medical training.

Training tool or technology	Approach	Some investigations
Virtual Reality	VR Based surgical training system	Bartlett et al. (2020), Cecil et al. (2018), Lohre et al. (2020), Medellin-Castillo et al. (2020)
	AR Based surgical training system	Si et al. (2019)
Haptic Technology	Single haptic simulators	Tahmasebi et al. (2008), Wang et al. (2014), Spera et al. (2020)
	Dual haptic with fixed authority	Nudehi et al. (2005), Khademian and Hashtrudi-Zaad (2012), Shahbazi et al. (2014b), Motaharifar et al. (2016), Motaharifar et al. (2019b)
	Dual haptic with variable authority	Shahbazi et al. (2014a), Motaharifar et al. (2019a), Motaharifar and Taghirad (2020), Liu et al. (2020)
Data Driven Scoring	DDS using hand-engineered features	Brown et al. (2016), Javaux et al. (2018), Hojati et al. (2019), Lefor et al. (2020)
	DDS using automated feature extraction	Wang and Fey (2018), Funke et al. (2019), Khan et al. (2020), Lavanchy et al. (2021)
	Fusion techniques	Naeini et al. (2014), Kazemian et al. (2010)
Machine Vision	Single-Stage Detectors	Redmon and Farhadi (2018), Liu et al. (2016), Lotfi et al. (2018), Lotfi et al. (2020)
	Two-Stage Detectors	Girshick (2015), Ren et al. (2015)
	Classifiers	Simonyan and Zisserman (2015), Szegedy et al. (2016)

between the expert and novice necessary, nor the quality of the training is reduced adversely due to the limitations. In fact, the computer vision approach acts as an interface making it possible both to learn from the expert and to evaluate the novice, remotely.

7 CONCLUSION AND FUTURE PROSPECTS

The faculty members and the students of the medical universities are classified in the high-risk category due to the potential exposure to coronavirus through direct contact and aerosol-generating procedures. As a result, many medical schools have suspended their clinical programs or implemented social distancing in their laboratory practices. Furthermore, the current fight against the COVID-19 virus have used nearly all capacity of health-care systems, and some less urgent and less emergent medical services including the education issues are limited or even paused. Therefore, unless some assistive training tools are utilized to support the educational procedures, the training efficiency of medical universities will be reduced and it have future consequences for the world health-care system.

Practicing medical tasks with current lock-down policies can be solved utilizing state of the art techniques in haptics, virtual reality, machine vision, and machine learning. Notably, utilization of the above technologies in medical education has been researched actively within the past years in order to increase the safety and efficiency of the surgical training procedures. Nowadays, another motivation is created for those assistive technologies owing to the COVID-19 pandemic. In this paper, the existing assistive technologies for medical training are reviewed in the COVID-19 context and a summary of them is presented in **Table 2**.

It is reviewed that a surgical simulator system including a VR/AR based graphical interface and a haptic interface is able to provide the circumstances of actual surgical operation for the medical students, without the necessity of attending the hospital environments. Furthermore, through augmenting the system with another haptic console and having a dual user haptic system, the opportunity of collaboration with and receiving guidance cues from an expert surgeon in a systematic manner is given to the trainees. In contrast to the traditional collaboration methodologies, the haptic-based collaboration does not require the physical contact between the involved people and the risk of infection is reduced. Assessment of the expertise level of the medical students is another element of each training program. The necessity of reducing physical contact during the COVID-19 pandemic have also affected the skill assessment methodologies as the traditional ways of skill assessment are based on direct observation by a trainer. In contrast, data-based analysis may be utilized as a systematic approach for skill assessment without any need of physical contact. In this paper, some of the ongoing methods in surgical skill evaluation have been reviewed.

Biomedical engineering technology has progressed by leaps and bounds during the past several decades and advancements in remote diagnostics and remote treatment have been considered as a leading edge in this field. For instance, the tele-surgery robotic-assisted da Vinci system have received a great deal of attention in the healthcare marketplace with more than 5 million surgeries in the last 2 decades DaVinci (2021). However, the rate of advancement in medical training, which usually follows traditional methods, has been considerably less than the other aspects of medical field, and modern training technologies have received fewer attention during the past several decades. While remote training and remote skill assessment technologies make relatively lower risk to the patient than remote diagnostics and remote treatment, the reason behind fewer attention to the former is the lack of sufficient motivations. It is hoped that the motivations created for those advanced medical training methods during the COVID-19 crisis are strong enough to continuously increase their utilization among the medical universities. Although wide utilization of those technologies needs a considerable extent of time, effort, and investment, immediate and emergent decisions and actions are required to widely utilize those potential techniques. Notably, all of the presented approaches and techniques are targeted to be utilized in the normal situations without any pandemic in order to provide safer and more efficient medical training. Therefore, even after the world recovers from this crisis, these

techniques, tools, and approaches deserve more attention, recognition, investigation, and utilization. There needs to be a global awareness among the medical universities that haptic technology and virtual reality integrated with machine learning and machine vision provides an excellent systematic medical training apparatus that ensures the requirements of health-care systems to enhance the safety, efficiency, and robustness of medical training.

DATA AVAILABILITY STATEMENT

The original contributions presented in the study are included in the article/supplementary material, further inquiries can be directed to the corresponding authors.

AUTHOR CONTRIBUTIONS

Conceptualization, HT, SFM, and MM; original draft preparation MM, AN, PA, AI, and FL; review and editing, HT, SFM, BM, and AL.

FUNDING

This work was supported in part by the National Institute for Medical Research Development (NIMAD) under Grant No. 942314, in part by Tehran University of Medical Sciences, Tehran, Iran under Grant No. 35949-43-01-97, and in part by K. N. Toosi University of Technology, Tehran, Iran Research Grant.

REFERENCES

Abdelaal, A. E., Avinash, A., Kalia, M., Hager, G. D., and Salcudean, S. E. (2020). A Multi-Camera, Multi-View System for Training and Skill Assessment for Robot-Assisted Surgery. *Int. J. CARS* 15, 1369–1377. doi:10.1007/s11548-020-02176-1

Akbari, M., Carriere, J., Meyer, T., Sloboda, R., Husain, S., Usmani, N., et al. (2021). Robotic Ultrasound Scanning with Real-Time Image-Based Force Adjustment: Quick Response for Enabling Physical Distancing during the Covid-19 Pandemic. *Front. Robotics AI* 8, 62. doi:10.3389/frobt.2021.645424

Anh, N. X., Nataraja, R. M., and Chauhan, S. (2020). Towards Near Real-Time Assessment of Surgical Skills: A Comparison of Feature Extraction Techniques. *Comput. Methods Programs Biomed.* 187, 105234. doi:10.1016/j.cmpb.2019.105234

Antoniades, A., Spyrou, L., Took, C. C., and Sanei, S. (2016). "Deep Learning for Epileptic Intracranial Eeg Data," in 2016 IEEE 26th International Workshop on Machine Learning for Signal Processing (MLSP), Vietri sul Mare, Salerno, Italy, September 13–16, 2016 (IEEE), 1–6. doi:10.1109/mlsp.2016.7738824

ARASH-ASiST (2019). Dataset. Aras Haptics: A System for EYE Surgery Training. Available at: https://aras.kntu.ac.ir/arash-asist//. (Accessed 08 05, 2020).

Babushkin, V., Jamil, M. H., Park, W., and Eid, M. (2021). Sensorimotor Skill Communication: A Literature Review. *IEEE Access* 9, 75132–75149. doi:10.1109/access.2021.3081449

Bahrampour, S., Ramakrishnan, N., Schott, L., and Shah, M. (2015). Comparative Study of Caffe, Neon, Theano, and Torch for Deep Learning. *CoRR*. arXiv: 1511.06435. Available at: http://arxiv.org/abs/1511.06435.

Bartlett, J. D., Lawrence, J. E., Yan, M., Guevel, B., Stewart, M. E., Audenaert, E., et al.fnm (2020). The Learning Curves of a Validated Virtual Reality Hip Arthroscopy Simulator. *Arch. Orthopaedic Trauma Surg.* 140 (6), 761–767. doi:10.1007/s00402-020-03352-3

Basdogan, C., De, S., Kim, J., Muniyandi, M., Kim, H., and Srinivasan, M. A. (2004). Haptics in Minimally Invasive Surgical Simulation and Training. *IEEE Comput. Graphics Appl.* 24, 56–64. doi:10.1109/mcg.2004.1274062

Brown, J. D., O'Brien, C. E., Leung, S. C., Dumon, K. R., Lee, D. I., and Kuchenbecker, K. J. (2016). Using Contact Forces and Robot Arm Accelerations to Automatically Rate Surgeon Skill at Peg Transfer. *IEEE Trans. Biomed. Eng.* 64, 2263–2275. doi:10.1109/TBME.2016.2634861

Buss, M., Peer, A., Schauß, T., Stefanov, N., Unterhinninghofen, U., Behrendt, S., et al. (2010). Development of a Multi-Modal Multi-User Telepresence and Teleaction System. *Int. J. Robot. Res.* 29, 1298–1316. doi:10.1177/0278364909351756

Caccianiga, G., Mariani, A., de Paratesi, C. G., Menciassi, A., and De Momi, E. (2021). Multi-Sensory Guidance and Feedback for Simulation-Based Training in Robot Assisted Surgery: A Preliminary Comparison of Visual, Haptic, and Visuo-Haptic. *IEEE Robot. Autom. Lett.* 6, 3801–3808. doi:10.1109/lra.2021.3063967

Cecil, J., Gupta, A., and Pirela-Cruz, M. (2018). An Advanced Simulator for Orthopedic Surgical Training. *Int. J. Comput. Assist. Radiol. Surg.* 13, 305–319. doi:10.1007/s11548-017-1688-0

Chetlur, S., Woolley, C., Vandermersch, P., Cohen, J., Tran, J., Catanzaro, B., et al. (2014). cuDNN: Efficient Primitives for Deep Learning. *CoRR*. arXiv: 1410.0759. Available at: http://arxiv.org/abs/1410.0759.

Chitra, R., and Seenivasagam, V. (2013). Heart Disease Prediction System Using Supervised Learning Classifier. *Bonfring Int. J. Softw. Eng. Soft Comput.* 3, 01–07. doi:10.9756/bijsesc.4336

DaVinci (2021). Dataset. Enabling Surgical Care to Get Patients Back to what Matters. Available at: https://www.intuitive.com/en-us/products-and-services/da-vinci. (Accessed 202107 04.

Desselle, M. R., Brown, R. A., James, A. R., Midwinter, M. J., Powell, S. K., and Woodruff, M. A. (2020). Augmented and Virtual Reality in Surgery. *Comput. Sci. Eng.* 22, 18–26. doi:10.1109/mcse.2020.2972822

Farooq, A., Anwar, S., Awais, M., and Rehman, S. (2017). "A Deep Cnn Based Multi-Class Classification of Alzheimer's Disease Using Mri," in 2017 IEEE International Conference on Imaging systems and techniques (IST) (IEEE), Beijing, China, October 18–20, 2017, 1–6. doi:10.1109/ist.2017.8261460

Fawaz, H. I., Forestier, G., Weber, J., Idoumghar, L., and Muller, P.-A. (2018). "Evaluating Surgical Skills from Kinematic Data Using Convolutional Neural Networks," in International Conference on Medical Image Computing and Computer-Assisted Intervention, Granada, Spain, September 16–20, 2018 (Springer), 214–221. doi:10.1007/978-3-030-00937-3_25

Feizi, N., Tavakoli, M., Patel, R. V., and Atashzar, S. F. (2021). Robotics and Ai for Teleoperation, Tele-Assessment, and Tele-Training for Surgery in the Era of Covid-19: Existing Challenges, and Future Vision. *Front. Robot. AI* 8, 610677. doi:10.3389/frobt.2021.610677

Funke, I., Mees, S. T., Weitz, J., and Speidel, S. (2019). Video-based Surgical Skill Assessment Using 3d Convolutional Neural Networks. *Int. J. Comput. Assist. Radiol. Surg.* 14, 1217–1225. doi:10.1007/s11548-019-01995-1

Girshick, R., Donahue, J., Darrell, T., and Malik, J. (2014). "Rich Feature Hierarchies for Accurate Object Detection and Semantic Segmentation," in Proceedings of the IEEE conference on computer vision and pattern recognition, Columbus, OH, June 23–28, 2014, 580–587. doi:10.1109/cvpr.2014.81

Girshick, R. (2015). "Fast R-Cnn," in Proceedings of the IEEE international conference on computer vision, Boston, MA, June 7–12, 2015, 1440–1448. doi:10.1109/iccv.2015.169

Han, S. (2017). *Efficient Methods and Hardware for Deep Learning*. Stanford University.

He, K., Zhang, X., Ren, S., and Sun, J. (2015). Spatial Pyramid Pooling in Deep Convolutional Networks for Visual Recognition. *IEEE Trans. pattern Anal. machine intell.* 37, 1904–1916. doi:10.1109/tpami.2015.2389824

Hodges, C., Moore, S., Lockee, B., Trust, T., and Bond, A. (2020). The Difference between Emergency Remote Teaching and Online Learning. Boulder, CO. *Educause Rev.* 27 (1), 1–9.

Hojati, N., Motaharifar, M., Taghirad, H., and Malekzadeh, A. (2019). "Skill Assessment Using Kinematic Signatures: Geomagic Touch Haptic Device," in 2019 7th International Conference on Robotics and Mechatronics (ICRoM), Tehran, Iran, November 20–22, 2019 (IEEE), 186–191. doi:10.1109/icrom48714.2019.9071892

Iwashita, Y., Hibi, T., Ohyama, T., Umezawa, A., Takada, T., Strasberg, S. M., et al. (2017). Delphi Consensus on Bile Duct Injuries during Laparoscopic Cholecystectomy: an Evolutionary Cul-De-Sac or the Birth Pangs of a New Technical Framework? *J. Hepato-Biliary-Pancreatic Sci.* 24, 591–602. doi:10.1002/jhbp.503

Javaux, A., Joyeux, L., Deprest, J., Denis, K., and Vander Poorten, E. (2018). Motion-based Skill Analysis in a Fetoscopic Spina-Bifida Repair Training Model. In *CRAS*, Date: 2018/09/10-2018/09/11, London, United Kingdom.

Jonas, J. B., Rabethge, S., and Bender, H.-J. (2003). Computer-assisted Training System for Pars Plana Vitrectomy. *Acta Ophthalmol. Scand.* 81, 600–604. doi:10.1046/j.1395-3907.2003.0078.x

Kathuria, A. (2021). Dataset. *Tutorial on Implementing yolo V3 from Scratch in Pytorch*. Available at: https://blog.paperspace.com/how-to-implement-a-yolo-object-detector-in-pytorch/. (Accessed on 01 07, 2021).

Kazemian, M., Moshiri, B., Nikbakht, H., and Lucas, C. (2005). "Protein Secondary Structure Classifiers Fusion Using Owa," in International Symposium on Biological and Medical Data Analysis, Aveiro, Portugal, November 10–11, 2005 (Springer), 338–345. doi:10.1007/11573067_34

Kazemian, M., Moshiri, B., Palade, V., Nikbakht, H., and Lucas, C. (2010). Using Classifier Fusion Techniques for Protein Secondary Structure Prediction. *Int. J. Comput. Intell. Bioinf. Syst. Biol.* 1, 418–434. doi:10.1504/ijcibsb.2010.038225

Khademian, B., and Hashtrudi-Zaad, K. (2012). Dual-user Teleoperation Systems: New Multilateral Shared Control Architecture and Kinesthetic Performance Measures. *Ieee/asme Trans. Mechatron.* 17, 895–906. doi:10.1109/tmech.2011.2141673

Khan, A., Mellor, S., King, R., Janko, B., Harwin, W., Sherratt, R. S., et al. (2020). Generalized and Efficient Skill Assessment from Imu Data with Applications in Gymnastics and Medical Training. New York, NY, *ACM Trans. Comput. Healthc.* 2 (1), 1–21.

Khanna, R. C., Honavar, S. G., Metla, A. L., Bhattacharya, A., and Maulik, P. K. (2020). Psychological Impact of Covid-19 on Ophthalmologists-In-Training and Practising Ophthalmologists in india. *Indian J. Ophthalmol.* 68, 994. doi:10.4103/ijo.ijo_1458_20

Kotsis, S. V., and Chung, K. C. (2013). Application of See One, Do One, Teach One Concept in Surgical Training. *Plast. Reconstr. Surg.* 131, 1194. doi:10.1097/prs.0b013e318287a0b3

Krizhevsky, A., Sutskever, I., and Hinton, G. E. (2012). "Imagenet Classification with Deep Convolutional Neural Networks," in Advances in neural information processing systems, Lake Tahoe, NV, December 3–6, 2012, 1097–1105.

kumar Renganayagalu, S., Mallam, S. C., and Nazir, S. (2021). Effectiveness of Vr Head Mounted Displays in Professional Training: A Systematic Review. *Technol. Knowl. Learn*. (Springer), 1–43. doi:10.1007/s10758-020-09489-9

Lavanchy, J. L., Zindel, J., Kirtac, K., Twick, I., Hosgor, E., Candinas, D., et al. (2021). Automation of Surgical Skill Assessment Using a Three-Stage Machine Learning Algorithm. *Scientific Rep.* 11, 1–9. doi:10.1038/s41598-021-88175-x

LeCun, Y., Bottou, L., Bengio, Y., and Haffner, P. (1998). Gradient-based Learning Applied to Document Recognition. *Proc. IEEE* 86, 2278–2324. doi:10.1109/5.726791

Lefor, A. K., Harada, K., Dosis, A., and Mitsuishi, M. (2020). Motion Analysis of the Jhu-Isi Gesture and Skill Assessment Working Set Using Robotics Video and Motion Assessment Software. *Int. J. Comput. Assist. Radiol. Surg.* 15, 2017–2025. doi:10.1007/s11548-020-02259-z

Lin, T.-Y., Goyal, P., Girshick, R., He, K., and Dollár, P. (2017). "Focal Loss for Dense Object Detection," in Proceedings of the IEEE international conference on computer vision, 2980–2988. doi:10.1109/iccv.2017.324

Liu, F., Lelevé, A., Eberard, D., and Redarce, T. (2015). "A Dual-User Teleoperation System with Online Authority Adjustment for Haptic Training," in 2015 37th Annual International Conference of the IEEE Engineering in Medicine and Biology Society (EMBC), Milan, Italy, August 25–29, 2015, 1168–1171. doi:10.1109/embc.2015.7318574

Liu, W., Anguelov, D., Erhan, D., Szegedy, C., Reed, S., Fu, C.-Y., et al. (2016). "Ssd: Single Shot Multibox Detector," in European conference on computer vision (Springer), 21–37. doi:10.1007/978-3-319-46448-0_2

Liu, F., Licona, A. R., Lelevé, A., Eberard, D., Pham, M. T., and Redarce, T. (2020). An Energy-Based Approach for N-Dof Passive Dual-User Haptic Training Systems. *Robotica* 38, 1155–1175. doi:10.1017/s0263574719001309

Lohre, R., Bois, A. J., Athwal, G. S., and Goel, D. P. (2020). Improved Complex Skill Acquisition by Immersive Virtual Reality Training: a Randomized Controlled Trial. *JBJS* 102, e26. doi:10.2106/jbjs.19.00982

Lotfi, F., Ajallooeian, V., and Taghirad, H. D. (2018). "Robust Object Tracking Based on Recurrent Neural Networks," in 2018 6th RSI International Conference on Robotics and Mechatronics (IcRoM), 507–511. doi:10.1109/icrom.2018.8657608

Lotfi, F., Hasani, P., Faraji, F., Motaharifar, M., Taghirad, H., and Mohammadi, S. (2020). "Surgical Instrument Tracking for Vitreo-Retinal Eye Surgical Procedures Using Aras-Eye Dataset," in 2020 28th Iranian Conference on Electrical Engineering (ICEE) (IEEE), 1–6. doi:10.1109/icee50131.2020.9260679

Lu, Z., Huang, P., Dai, P., Liu, Z., and Meng, Z. (2017). Enhanced Transparency Dual-User Shared Control Teleoperation Architecture with Multiple Adaptive Dominance Factors. *Int. J. Control. Autom. Syst.* 15, 2301–2312. doi:10.1007/s12555-016-0467-y

Medellin-Castillo, H. I., Zaragoza-Siqueiros, J., Govea-Valladares, E. H., de la Garza-Camargo, H., Lim, T., and Ritchie, J. M. (2020). Haptic-enabled Virtual Training in Orthognathic Surgery. *Virtual Reality* 25, 53–67. doi:10.1007/s10055-020-00438-6

Moody, L., Waterworth, A., McCarthy, A. D., Harley, P. J., and Smallwood, R. H. (2008). The Feasibility of a Mixed Reality Surgical Training Environment. *Virtual Reality* 12, 77–86. doi:10.1007/s10055-007-0080-8

Motaharifar, M., and Taghirad, H. D. (2020). A Force Reflection Robust Control Scheme with Online Authority Adjustment for Dual User Haptic System. *Mech. Syst. Signal Process.* 135, 106368. doi:10.1016/j.ymssp.2019.106368

Motaharifar, M., Bataleblu, A., and Taghirad, H. (2016). "Adaptive Control of Dual User Teleoperation with Time Delay and Dynamic Uncertainty," in 2016 24th Iranian conference on electrical engineering (ICEE), Shiraz, Iran, May 10–12, 2016 (IEEE), 1318–1323. doi:10.1109/iraniancee.2016.7585725

Motaharifar, M., Taghirad, H. D., Hashtrudi-Zaad, K., and Mohammadi, S. F. (2019a). Control of Dual-User Haptic Training System with Online Authority Adjustment: An Observer-Based Adaptive Robust Scheme. *IEEE Trans. Control. Syst. Technol.* 28 (6), 2404–2415. doi:10.1109/tcst.2019.2946943

Motaharifar, M., Taghirad, H. D., Hashtrudi-Zaad, K., and Mohammadi, S.-F. (2019b). Control Synthesis and ISS Stability Analysis of Dual-User Haptic Training System Based on S-Shaped Function. *IEEE/ASME Trans. Mechatron.* 24 (4), 1553–1564. doi:10.1109/tmech.2019.2917448

Naeini, M. P., Moshiri, B., Araabi, B. N., and Sadeghi, M. (2014). Learning by Abstraction: Hierarchical Classification Model Using Evidential Theoretic Approach and Bayesian Ensemble Model. *Neurocomputing* 130, 73–82. doi:10.1016/j.neucom.2012.03.041

Nudehi, S. S., Mukherjee, R., and Ghodoussi, M. (2005). A Shared-Control Approach to Haptic Interface Design for Minimally Invasive Telesurgical Training. *IEEE Trans. Control. Syst. Technol.* 13, 588–592. doi:10.1109/tcst.2004.843131

Redmon, J., and Farhadi, A. (2018). Yolov3: An Incremental Improvement. *CoRR abs/1804.02767*. Available at: http://arxiv.org/abs/1804.02767.

Ren, S., He, K., Girshick, R., and Sun, J. (2015). "Faster R-Cnn: Towards Real-Time Object Detection with Region Proposal Networks," in Advances in neural information processing systems, Montreal, Quebec, Canada, December 7–12, 2015, 91–99.

Shahbazi, M., Atashzar, S. F., Talebi, H. A., and Patel, R. V. (2014a). An Expertise-Oriented Training Framework for Robotics-Assisted Surgery. *Proc. IEEE Int. Conf. Rob. Autom.*, 5902–5907. doi:10.1109/icra.2014.6907728

Shahbazi, M., Atashzar, S. F., Talebi, H. A., and Patel, R. V. (2014b). Novel Cooperative Teleoperation Framework: Multi-Master/single-Slave System. *IEEE/ASME Trans. Mechatron.* 20, 1668–1679. doi:10.1109/tmech.2014.2347034

Shahbazi, M., Atashzar, S. F., and Patel, R. V. (2018a). A Systematic Review of Multilateral Teleoperation Systems. *IEEE Trans. Haptics* 11, 338–356. doi:10.1109/toh.2018.2818134

Shahbazi, M., Atashzar, S. F., Ward, C., Talebi, H. A., and Patel, R. V. (2018b). Multimodal Sensorimotor Integration for Expert-In-The-Loop Telerobotic Surgical Training. *IEEE Trans. Robot.* 34, 1549–1564. doi:10.1109/tro.2018.2861916

Sharma, D., and Bhaskar, S. (2020). Addressing the Covid-19 burden on Medical Education and Training: the Role of Telemedicine and Tele-Education during and beyond the Pandemic. *Front. Public Health* 8, 838. doi:10.3389/fpubh.2020.589669

Si, W.-X., Liao, X.-Y., Qian, Y.-L., Sun, H.-T., Chen, X.-D., Wang, Q., et al. (2019). Assessing Performance of Augmented Reality-Based Neurosurgical Training. *Vis. Comput. Industry, Biomed. Art* 2, 6. doi:10.1186/s42492-019-0015-8

Simonyan, K., and Zisserman, A. (2015). "Very Deep Convolutional Networks for Large-Scale Image Recognition," in International Conference on Learning Representations, San Diego, CA, May 7–9, 2015.

Singh, R. P., Javaid, M., Kataria, R., Tyagi, M., Haleem, A., and Suman, R. (2020). Significant Applications of Virtual Reality for Covid-19 Pandemic. *Diabetes Metab. Syndr. Clin. Res. Rev.* 14 (4), 661–664. doi:10.1016/j.dsx.2020.05.011

Spera, C., Somerville, A., Caniff, S., Keenan, J., and Fischer, M. D. (2020). Virtual Reality Haptic Surgical Simulation for Sub-retinal Administration of an Ocular Gene Therapy. *Invest. Ophthalmol. Vis. Sci.* 61, 4503. doi:10.1039/d0ay90130j

Stone, S., and Bernstein, M. (2007). Prospective Error Recording in Surgery: an Analysis of 1108 Elective Neurosurgical Cases. *Neurosurgery* 60, 1075–1082. doi:10.1227/01.neu.0000255466.22387.15

Szegedy, C., Liu, W., Jia, Y., Sermanet, P., Reed, S., Anguelov, D., et al. (2015). "Going Deeper with Convolutions," in Proceedings of the IEEE conference on computer vision and pattern recognition, Boston, MA, June 7–12, 2015, 1–9. doi:10.1109/cvpr.2015.7298594

Szegedy, C., Vanhoucke, V., Ioffe, S., Shlens, J., and Wojna, Z. (2016). "Rethinking the Inception Architecture for Computer Vision," in Proceedings of the IEEE conference on computer vision and pattern recognition, Las Vegas, NV, June 27–30, 2016, 2818–2826. doi:10.1109/cvpr.2016.308

Tahmasebi, A. M., Hashtrudi-Zaad, K., Thompson, D., and Abolmaesumi, P. (2008). A Framework for the Design of a Novel Haptic-Based Medical Training Simulator. *IEEE Trans. Inf. Technol. Biomed.* 12, 658–666. doi:10.1109/titb.2008.926496

Tavakoli, M., Carriere, J., and Torabi, A. (2020). Robotics, Smart Wearable Technologies, and Autonomous Intelligent Systems for Healthcare during the Covid-19 Pandemic: An Analysis of the State of the Art and Future Vision. *Adv. Intell. Syst.* 2, 2000071. doi:10.1002/aisy.202000071

Uijlings, J. R., Van De Sande, K. E., Gevers, T., and Smeulders, A. W. (2013). Selective Search for Object Recognition. *Int. J. Comput. Vis.* 104, 154–171. doi:10.1007/s11263-013-0620-5

Wang, Z., and Fey, A. M. (2018). "Satr-dl: Improving Surgical Skill Assessment and Task Recognition in Robot-Assisted Surgery with Deep Neural Networks," in In 2018 40th Annual International Conference of the IEEE Engineering in Medicine and Biology Society (EMBC), Honolulu, HI, July 17–21, 2018 (IEEE), 1793–1796. doi:10.1109/EMBC.2018.8512575

Wang, D., Shi, Y., Liu, S., Zhang, Y., and Xiao, J. (2014). Haptic Simulation of Organ Deformation and Hybrid Contacts in Dental Operations. *IEEE Trans. Haptics* 7, 48–60. doi:10.1109/toh.2014.2304734

Wang, L., Xiong, Y., Wang, Z., Qiao, Y., Lin, D., Tang, X., et al. (2018). Temporal Segment Networks for Action Recognition in Videos. *IEEE Trans. pattern Anal. machine intell.* 41, 2740–2755. doi:10.1109/TPAMI.2018.2868668

Weng, J., Weng, J., Zhang, J., Li, M., Zhang, Y., and Luo, W. (2019). "Deepchain: Auditable and Privacy-Preserving Deep Learning with Blockchain-Based Incentive," in IEEE Transactions on Dependable and Secure Computing. doi:10.1109/tdsc.2019.2952332

Yari, S. S., Jandhyala, C. K., Sharareh, B., Athiviraham, A., and Shybut, T. B. (2018). Efficacy of a Virtual Arthroscopic Simulator for Orthopaedic Surgery Residents by Year in Training. *Orthopaedic J. Sports Med.* 6, 2325967118810176. doi:10.1177/2325967118810176

Zappella, L., Béjar, B., Hager, G., and Vidal, R. (2013). Surgical Gesture Classification from Video and Kinematic Data. *Med. image Anal.* 17, 732–745. doi:10.1016/j.media.2013.04.007

Zendejas, B., Jakub, J. W., Terando, A. M., Sarnaik, A., Ariyan, C. E., Faries, M. B., et al. (2017). Laparoscopic Skill Assessment of Practicing Surgeons Prior to Enrollment in a Surgical Trial of a New Laparoscopic Procedure. *Surg. Endosc.* 31, 3313–3319. doi:10.1007/s00464-016-5364-1

Zhang, W., Wang, Y., Yang, L., and Wang, C. (2020). Suspending Classes Without Stopping Learning: China's Education Emergency Management Policy in the Covid-19 Outbreak. Multidisciplinary digital publishing institute, *J. Risk Finan. Manag.* 13 (3), 1–6.

Zia, A., and Essa, I. (2018). Automated Surgical Skill Assessment in Rmis Training. *Int. J. Comput. Assist. Radiol. Surg.* 13, 731–739. doi:10.1007/s11548-018-1735-5

Zia, A., Sharma, Y., Bettadapura, V., Sarin, E. L., Clements, M. A., and Essa, I. (2015). "Automated Assessment of Surgical Skills Using Frequency Analysis," in International Conference on Medical Image Computing and Computer-Assisted Intervention, Munich, Germany, October 5–9, 2015 (Springer), 430–438. doi:10.1007/978-3-319-24553-9_53

Zia, A., Sharma, Y., Bettadapura, V., Sarin, E. L., Ploetz, T., Clements, M. A., et al. (2016). Automated Video-Based Assessment of Surgical Skills for Training and Evaluation in Medical Schools. *Int. J. Comput. Assist. Radiol. Surg.* 11, 1623–1636. doi:10.1007/s11548-016-1468-2

Conflict of Interest: The authors declare that the research was conducted in the absence of any commercial or financial relationships that could be construed as a potential conflict of interest.

Publisher's Note: All claims expressed in this article are solely those of the authors and do not necessarily represent those of their affiliated organizations, or those of the publisher, the editors and the reviewers. Any product that may be evaluated in this article, or claim that may be made by its manufacturer, is not guaranteed or endorsed by the publisher.

Advantages of publishing in Frontiers

OPEN ACCESS
Articles are free to read for greatest visibility and readership

FAST PUBLICATION
Around 90 days from submission to decision

HIGH QUALITY PEER-REVIEW
Rigorous, collaborative, and constructive peer-review

TRANSPARENT PEER-REVIEW
Editors and reviewers acknowledged by name on published articles

Frontiers
Avenue du Tribunal-Fédéral 34
1005 Lausanne | Switzerland

Visit us: www.frontiersin.org
Contact us: frontiersin.org/about/contact

REPRODUCIBILITY OF RESEARCH
Support open data and methods to enhance research reproducibility

DIGITAL PUBLISHING
Articles designed for optimal readership across devices

FOLLOW US
@frontiersin

IMPACT METRICS
Advanced article metrics track visibility across digital media

EXTENSIVE PROMOTION
Marketing and promotion of impactful research

LOOP RESEARCH NETWORK
Our network increases your article's readership